3.3.5 Number of books and chapters in edited volumes/books published and papers in national/ international conference-proceedings per teacher during last five years

Name of the teacher	Title of the book/chapters published	Title of the paper	Name of the conference	National / International	Year of publication	ISBN number of the proceeding	Affiliating Institute at the time of publication	Name of the publisher	Relavant link
T Kumaragurubaran	Nil	RCOHP-SM A Rules Generation and Clustering based uncovering hidden patterns in Social Media	Cluster Computing	International	2018	clus-D - 18-00882	MSEC, Kilakarai	Cluster Computing	https://docs.google.com/uc?export=download&id=1MO3kj7eS3PsnTshTM3SF8anCoHyFWP-G
Mr K Sakthikumar	Nil	Synthesis, Spectroscopic, Thermogravimetric kinetics, Antioxidant, Antimicrobial, DNA-BSA Interaction and Cytotoxicity Studies	2nd International conference on Recent Trends in Analytical	International	2018	978-93-85374-82-1	MSEC, Kilakarai	Dept of Analytical Chemistry, University of Madras, Chennai-25	https://docs.google.com/uc?export=download&id=1oORsM6zP7G9n8m5j4if_N3DfcGyfcYtd
H Mohamed Mohaideen	Nil	The ac impedance spectroscopy and antibacterial studies on NiO nanoparticles	International Conference On Momentous role of nanomaterials in	International	2018	978-81-934473-2-1	MSEC, Kilakarai	Department of Physics, Alagappa University, Karaikudi-03, Tamil Nadu, India	https://docs.google.com/uc?export=download&id=1gl9dtyPaEQAXAONvozAsNnKbOjWDyAHU
P Victor	Nil	Connectivity of the Product of S-valued Graphs	International Conference on Algebra and Discrete Mathematics(ICADM-	International	2018	2048-6600	MSEC, Kilakarai	International Journal of Computer Science	https://docs.google.com/uc?export=download&id=10tCA9aJAEUR4rc44O48uj_lZ-3SH7aSu
P Victor	Nil	Lexicographic product of S-valued Graphs	International conference on Pure and Applied Mathematics(ICPAM-	International	2018	978-93-86435-53-8 (or) 2278-8697	MSEC, Kilakarai	Mathematical Sciences International Research Journal	https://docs.google.com/uc?export=download&id=1MVzOdF3GR-chVUVXtkQEf7FDRwXw8uby
H Peer Oli,Dr S Senthamarai Kannan	Nil	Certain investigation on gabor filter based facial expression recognition viewed automatically	IJPPA- International Journal of Printing , Packaging & Applied	International	2018	2320-4387	MSEC, Kilakarai	IJPPA- International Journal of Printing , Packaging & Applied sciences	https://docs.google.com/uc?export=download&id=1OW5gAoJsalZmK5Q55LFZ_Sbu70Uoak-X
S Venkatesh Babu, C Ravichandran	Nil	Power Efficient probabilistic multiplier for digital image processing	(IJET) - International Journal of Engineering & Technology	International	2018	0975-4024	MSEC, Kilakarai	(IJET) - International Journal of Engineering & Technology	https://docs.google.com/uc?export=download&id=1Qs8o4M_WhFuu54zX4LDSMBS0RXMnYKhV
K Ramaraj	Stability of Ships	Stability of Ships	Nil	Nil	2018	81-7874-099-0	MSEC, Kilakarai	Eswar Publisher, Chennai	https://docs.google.com/uc?export=download&id=1LzGPa6HT_RiHFnSDvt6nPN4S3zSj2JWD
T Sheik yousuf	Nil	Integrated Wireless Sensor Network for Medical Data Transmission Using Gsrm And Hebm	International Journal Of Advanced Research In Basic Engineering	International	2018	1743-8195 (online) 1743-8187(Print)	MSEC, Kilakarai	IJARBEST Scientific Publishers	https://docs.google.com/uc?export=download&id=1k4awuINXR3IIDjhZJ9AGPjUIy8qmYfcY
R Karthikeyan		Novel Power Reduction Framework for Enhancing Cloud Computing by Integrated GSNN Scheduling	Cluster Computing - Springer	International	2017	1386-7857	Mohamed Sathak Engineering college	Cluster Computing Springer	https://docs.google.com/uc?export=download&id=1VTkVk2HeI5x_w00yvZ5j84HWk1LsH9j
C Saifudeen	Nil	The impact of today's English communication for Engineering Students in TamilNadu	Enhancing learning English through effective teaching	National	2017	978-93-86146-38-0	MSEC, Kilakarai	Department of English, AnandaCollege, Devakottai, Karaikudi, TamilNadu	https://docs.google.com/uc?export=download&id=1shseqn3V732HngrIoHpO5HL0LnHpVqAV
M Sundar, P Victor, M Chandramouleeswaran	Nil	Publickey Cryptography- Key sharing With Semiring Action	International journal of Math Sci&Engg Appls	International	2017	0973 9424	MSEC, Kilakarai	International journal of Math Sci&Engg Appls	https://docs.google.com/uc?export=download&id=1f_fLgQzX3xi2nkZgxvRqaqEQonsFLUHZ
P Victor, M Chandramouleeswaran	Nil	Categorical Product of two S-valued Graphs	International journal of Math Sci&Engg Appls	International	2017	0973 9424	MSEC, Kilakarai	International journal of Math Sci&Engg Appls	https://docs.google.com/uc?export=download&id=1oLJbZbFrAlpSdOQW5MS3ZVuKMl1dFGfU
Dr J Rajesh	Nil	Structural, Optical and Fluorescence properties of Azo Schiff based metal complexes	10th International conference on Science, Technology and	International	2017	2319-8354	MSEC, Kilakarai	International Journal of Advance Research Science and Engineering	https://docs.google.com/uc?export=download&id=1rFtH0GE6ntYy8YwfQqy2j4hE1vcmkVa0
H I		Studies on the Synthesis and Characterization structured NiO for Biomedical tion	National Conference on Advanced Materials Processing and	National	2017	978-93-86724-04-5	MSEC, Kilakarai	Excel India Publishers, 91 A, Ground Floor, Pratick Market, Munirka, New Delhi-110 067	https://docs.google.com/uc?export=download&id=1R33iCIUu2nfW4YkM1adTgS394ExzSR2r
		m in sashiDeshPande's Novel *Hut fence*	Insights into Women's Liberaration in Third World Literature	National	2017	819077880-3	MSEC, Kilakarai	Literati Journals	https://docs.google.com/uc?export=download&id=10EkUTnWLw18WA-Zi2nTQgAOA5KXkwF6t
Dr		ic experience in JhumbaLahiri's Novel *me Sake*	Insights into Women's Liberaration in Third World Literature	National	2017	819077880-3	MSEC, Kilakarai	Literati Journals	https://docs.google.com/uc?export=download&id=1GH8D8R-rlYkU6juzqqpHQRkRtwSEum_I

TRUE COPY ATTESTED

PRINCIPAL
MOHAMED SATHAK ENGINEERING COLLEGE
KILAKARAI-623806.

MOHAMED SATHAK ENGINEERING COLLEGE KILAKARAI 623806

Name of the teacher	Title of the book/chapters published	Title of the paper	Name of the conference	National / International	Year of publication	ISBN number of the proceeding	Affiliating Institute at the time of publication	Name of the publisher	Relavant link
Dr A Gowri Manohari	Nil	Irrationality and injustice in Domestic And Social Life of women in Arundhati Roy's Novel *The God of Small Things*	Insights into Women's Liberaration in Third World Literature.	National	2017	819077880-3	MSEC, Kilakarai	Literati Journals	https://docs.google.com/uc?export=download&id=1UYF7Ox_xXeBAYDp3Eg_jAqaBZlwyvjF
M D Durai murugan Alias Saravanan	Nil	BioDiesel Production & Optimisation from prosopis Julifera Oil- A Three step Method	International Journal for Advanced Research in Engineering and	International	2016	ISSN0976-3945	MSEC, Kilakarai	Mohamed Sathak Engineering College	https://docs.google.com/uc?export=download&id=1vcNktE3uAH48MddPrU6X-CfXe-8KVz6k
S Sheik Fareed	Nil	α-Fe_2O_3 Nanoparticles As A Byproduct From The Thin Film (SILAR) Deposition Process. A Study On The Product	International Conference on Smart Engineering Materials ICSEM '16	International	2016	2214-7853	MSEC, Kilakarai	Materials Today: Proceeding.	https://docs.google.com/uc?export=download&id=1exyPuDzq19DTiRiMoJQagSAld3O1IPp2
S Sheik Fareed	Nil	Influence of PVA addition on the structural and optical properties of SILAR deposited thin films	GravitateApplications In Nanotechnology (GAIN '16)	National	2016	978-93-80173-56-6	MSEC, Kilakarai	Albert Einstein Association, Department Of Physics, E.R.K Arts and Science college, Dharmapuri-636 905, Tamil	https://docs.google.com/uc?export=download&id=1iDJShV3qqT6rwFT6arvL8Ajo4wy5hyd-
Dr N Mythili	Nil	A study on the structural and morphological properties of boehmitenano flakes prepared by Sol-Gel method	GravitateApplications In Nanotechnology (GAIN '16)	National	2016	978-93-80173-56-6	MSEC, Kilakarai	Albert Einstein Association, Department Of Physics, E.R.K Arts and Science college, Dharmapuri-636 905, Tamil	https://docs.google.com/uc?export=download&id=1ujRDBYIOV9Yv1O1IgMB1DhomVOp0A9D8
M Mohamed Yaseen	Nil	Effect of complexing agents on the synthesis of Iron oxide nanoparticles by chemical method	GravitateApplications In Nanotechnology (GAIN '16)	National	2016	978-93-80173-56-6	MSEC, Kilakarai	Albert Einstein Association, Department Of Physics, E.R.K Arts and Science college, Dharmapuri-636 905, Tamil	https://docs.google.com/uc?export=download&id=10XN-h2Uy7UVxU2qKYTZ8Ulj2WLIJHU4w
S Sabeena Begam	Nil	Structural analysis of Al_2O_3 nanoparticles on The effect of temperature by chemical method	GravitateApplications In Nanotechnology (GAIN '16)	National	2016	978-93-80173-56-6	MSEC, Kilakarai	Albert Einstein Association, Department Of Physics, E.R.K Arts and Science college, Dharmapuri-636 905, Tamil	https://docs.google.com/uc?export=download&id=14KgVYkfVVVCRjeVCvHouFvmlFUqx3F-
C Alagesan	Nil	Suffereings of Downtrodden in mulkrajanand *"Untouchable"*	The Literature of the Marginalized	National	2016	978-93-81992-22-7	MSEC, Kilakarai	Department of English, Sir sevuganannamalai College, Devakottai, Karaikudi, Tamilnadu	https://docs.google.com/uc?export=download&id=1mTvEMwFTjNIjazt1_erIhdztgYI3KG6g
A Gowrimanohari	Nil	Human predicament in arun joshi's the apprentice	Literary Endeavour	National	2016	0976 299X	MSEC, Kilakarai	Literary Endeavour	https://docs.google.com/uc?export=download&id=1xHDM9nYBpZQ6yGQCnLMhJR4s8DH90BA3
M Rekha	Nil	Alientation in arun joshi's the foreigner	Literary Endeavour	National	2016	0976 299X	MSEC, Kilakarai	Literary Endeavour	https://docs.google.com/uc?export=download&id=137FUCu0n_E5W_eKgpsVCsFzEsQ-yD7u0
Dr J Rajesh	Nil	Synthesis,Characterisation & Biological activity of Zn(II) Complexes with Dibasic TridendateONS Donor Ligand	Asian Journal of Chemistry.	International	2016	2487-2494	SIT	Asian Journal of Chemistry.	https://docs.google.com/uc?export=download&id=1SYglVkttR_fxqQraL_O1RWB_SEK586CB
Dr A Abdul Brosekhan	NIL	Factors Influencing Consumer Buying Behavior	National Conference on Emeging Trends on Entrepreneurial	National	2016	2321-4643	MSEC, Kilakarai	Caussannel Colleg of Arts and science, Muthupettai	https://docs.google.com/uc?export=download&id=1K_S4FiA2o2uWc4bpmIF8QrH3P8faTP45
Ms S Santhana Jeyalakshmi	Nil	challenges facing by women entrepreneur	Shanlax International Journal Publisher	International	2016	2321-4643	MSEC, Kilakarai	Caussannel Colleg of Arts and science, Muthupettai	https://docs.google.com/uc?export=download&id=1yHTGqMXpqPoh0wXEOIKyThfoPdo-dkln
Ms C Shalini	Nil	Entrepreneurial Success of McDonald -A critical Strategic Analytical Approach	Shanlax International Journal Publisher	International	2016	2321-4643	MSEC, Kilakarai	Caussannel Colleg of Arts and science, Muthupettai	https://docs.google.com/uc?export=download&id=1SYzgRgYsFPaRIRsS3k6Nzmfq3OaifBIy
Mr M		Impact of Self Help Group in Entrepreneurial nent	Shanlax International Journal Publisher	International	2016	2321-4643	MSEC, Kilakarai	Caussannel Colleg of Arts and science, Muthupettai	https://docs.google.com/uc?export=download&id=1sJ74TxIBm3Q64v3jp4SqCWIDKUlYpomr
Dr I		es facing by women entrepreneur	Shanlax International Journal Publisher	International	2016	2321-4643	MSEC, Kilakarai	Caussannel Colleg of Arts and science, Muthupettai	https://docs.google.com/uc?export=download&id=1hRz6nwhJcx8GHigY04rXIUUG7GcPmx8i
Ms Sa		uality Management- A Literature	Shanlax International Journal Publisher	International		2321-4643	MSEC, Kilakarai	Shanlax International Journal Publisher	https://docs.google.com/uc?export=download&id=1d-axf3oDagarFSZgsuOgwWfgHLYNRzpG
Jeyalakshmi	nil	Gap Analysis - Distance Education Services	Challenges in Reinventing the Business Process	National		4643	MSEC, Kilakarai	Arehers & Elevators Publishing House	https://docs.google.com/uc?export=download&id=1_NTTWXaAuY8wSPPLpajNQxR5C_codVIM

TRUE COPY ATTESTED

PRINCIPAL
MOHAMED SATHAK ENGINEERING COLLEGE
KILAKARAI-623806.

MOHAMED SATHAK ENGINEERING COLLEGE ★ KILAKARAI 623806

Name of the teacher	Title of the book/chapters published	Title of the paper	Name of the conference	National / International	Year of publication	ISBN number of the proceeding	Affiliating Institute at the time of publication	Name of the publisher	Relavant link
Dr P Sathees Kumar	Nil	Apllication of Remote Sensing And GIS In Land Resource Management	Geospatial technologies for rural development	National	2016	978-81-933316-3-7	MSEC, Kilakarai	The Gandhigram Rural Institue, Dindigul	https://docs.google.com/uc?export=download&id=1sYK_0072jx_r4PXkJE4JKXcR42He9fBA
A Jevapradha and J Abbas Mohaideen	Nil	Removal of Hazardous Metals from Waste Printed Circuit Boards by Chemical and Biological Methods	Research Journal of Pharmaceutical, Biological and Chemical	International	2015	0975 8585	Maamallan Institute of Tech, Chennai	Research Journal of Pharmaceutical, Biological and Chemical Sciences	https://docs.google.com/uc?export=download&id=1jSG8hf4dG2box3bSE81Eawvsn3ka705f
G GAJALAKSHMI, DR J ABBAS MOHAIDEEN, DR A R	Nil	Analysis of Harmonic Behaviour of Human Rhythmic Activity in A RCC Roof Slab	International Journal of Innovative Science,Engineering and	International	2015	2348-7968	Maamallan Institute of Tech, Chennai	International Journal of Innovative Science,Engineering and Technology	https://docs.google.com/uc?export=download&id=113DWmGk0nFnIGBMf_HIrfiD5fqvjqpGT
Siji thomas and J Abbas Mohaideen	Nil	Determination of some heavy metals in fish, water and sediments from Bay of Bengal	International Journal of Chemical Sciences	International	2015	0972-768X	Maamallan Institute of Tech, Chennai	International Journal of Chemical Sciences	https://docs.google.com/uc?export=download&id=1J4DGrYCXoX8Vq_iYUBpZgdZ_24XuEhIj
V R Sathish kumar	Nil	Light Weight Hash function for scalable data sharing in cloud storage	International Conference on Advanced Communication	International	2015	978-93-80757-74-2	MSEC, Kilakarai	International Conference on Advanced Communication Technology 2015	https://docs.google.com/uc?export=download&id=1A4JelbtctlYtz0lal2OWjulYu6oHTDvS
Dr M Vadivel	Nil	Development and corrosion performance of 3-aminopropyltriethoxysilane grafted epoxidized ethylene-propylene-dieneterpolymer rubber	National Conference On Recent Trends And Developments In	National	2015	0974-2115	MSEC, Kilakarai	Journal of Chemical and Pharmaceutical Sciences	https://docs.google.com/uc?export=download&id=1L3jVX5VZWJ4CoGzK9boj8dB99C5HDG7g
H Mohamed Mohaideen	Nil	Effect of sulfur concentration on the physical properties of the ZnS thin film deposited by SILAR method	Recent Trends In Nano Materials And Thin Film Research (RTNMTR-	National	2015	978-93-81521-65-6	MSEC, Kilakarai	Jayam Publication, Trichirappalli-620 023, Tamil Nadu, India.	https://docs.google.com/uc?export=download&id=1JCD563tSEeagSikRmoiydJ0dEmnA2UDo
M Rekha	Nil	Diasporic Elements and Identity crisis in *Bharati Mukherjee's Novel Jasmine*	Self-relevation of the writers in post-colonial Literature	National	2015	978-93-81992-36-4	MSEC, Kilakarai	Today's graphics, Chennai	https://docs.google.com/uc?export=download&id=1O5cev8d2t65VMMsBBHCl4RR_kreWQ5Sq
Dhaveethu Raja, J , Senthilkumar G S , Vedhi, C , Vadivel, M	Nil	"Synthesis, structural characterization, electrochemical, biological, antioxidant and nuclease activities of 3-morpholinopropyl	J Chem Pharm Res ,	International	2015	0975 7384	MSEC, Kilakarai	J Chem Pharm Res ,	https://docs.google.com/uc?export=download&id=1IEKX9V4LgwmNsmZCjBnEuQImu-AZcCkf
Dhaveethu Raja, J , Jevaveeramadhavi, S , Vedhi, C , Sankarganesh	Nil	"Novel schiff base metal complexes from morpholine derivatives as potent antioxidant and DNA interacting agents"	J Chem Pharm Res ,	International	2015	0975 7384	MSEC, Kilakarai	J Chem Pharm Res ,	https://docs.google.com/uc?export=download&id=12A8XGEa2OLhqcoDG5w14m-ewrtbQfw2M
Dhaveethu Raja, J , Sakthikumar K	Nil	"Synthesis of water soluble transition metal(II) complexes from morpholine condensed tridentate schiff base Structural elucidation,	J Chem Pharm Res ,	International	2015	0975 7384	MSEC, Kilakarai	J Chem Pharm Res ,	https://docs.google.com/uc?export=download&id=1LC6EpUQWud9941ZpjIPW7tOUT9VSJfE2
Dhaveethu Raja J , LeebanonPoonkuil, N	Nil	"A study on invitro antioxidants, antimicrobial, antileukemia activities of Cocosnucifera (coconut) female flowers"	J Chem Pharm Res ,	International	2015	0975 7384	MSEC, Kilakarai	J Chem Pharm Res ,	https://docs.google.com/uc?export=download&id=130L9Gxi6HQ1nCprDwzsBAORcOmFx0d1S
Dhaveethu Raja, J , ShahulhameedSukkurSaleem, KaruruganathanSakthiku	Nil	"Synthesis of transition metal(II) complexes from piperonal condensed Schiff base Structural elucidation, antimicrobial,	J Chem Pharm Res ,	International	2015	0975 7384	MSEC, Kilakarai	J Chem Pharm Res ,	https://docs.google.com/uc?export=download&id=1ajlZ-DWyN7IbbrjAF8ngpUux8m0mxtQA
Haneefa Mohamed Mohaideen , Kandasamy Saravanakumar	Nil	"The studies on optical and structural properties of zinc sulfide thin films deposited by SILAR method"	J Chem Pharm Res ,	International	2015	0975 7384	MSEC, Kilakarai	J Chem Pharm Res ,	https://docs.google.com/uc?export=download&id=1H-bUlssXTYwG5ZTGbVPkQqZQN3rrq6x7
Vadivel, M , Suresh Chandi... Vedhi, C		Development and corrosion performance of 3-...ltriethoxysilane grafted epoxidized ...opylene-dieneterpolymer rubber	International Journal of Chemical Sciences	International	2015	0974 2115	MSEC, Kilakarai	International Journal of Chemical Sciences	https://docs.google.com/uc?export=download&id=1xqm0ZwzP8cqh0dwWwwNHsenGr9W8UpBr
M Vadi... Chand... Dhave...		...nd Morphology Studies of ...Expoxidized Ethylene-Propylene-...lymer"	International Journal of Chemical Science	International	2015	0972 768 X	MSEC, Kilakarai	International Journal of Chemical Science	https://docs.google.com/uc?export=download&id=1mbR36UknfAd5v_4d-EYbPNwOzY29RGmX
A Girija and N...		...ow-cost Ion -Exchangers	Journal of Chemical and Pharmaceutical Reseach	International	2015	...5 7384	MSEC, Kilakarai	Journal of Chemical and Pharmaceutical Reseach	https://docs.google.com/uc?export=download&id=1pzzsZYJemsXGsYreQfBrNlgrG8nle2vK
Fareed... Mohamed Ganikalyathee, Jeyaraj Dhaveethu Raja	Nil	...on optical and structural properties of zinc sulfide thin films deposited by SILAR method	Journal of Chemical and Pharmaceutical Research	International	2015	...5 7384	MSEC, Kilakarai	Journal of Chemical and Pharmaceutical Research	https://docs.google.com/uc?export=download&id=1a21GgDDyefJIb4PUU7dpPiVCDBSRfUkW

TRUE COPY ATTESTED

PRINCIPAL
MOHAMED SATHAK ENGINEERING COLLEGE
KILAKARAI-623806.

MOHAMED SATHAK ENGINEERING COLLEGE
KILAKARAI
623806

Name of the teacher	Title of the book/chapters published	Title of the paper	Name of the conference	National / International	Year of publication	ISBN number of the proceeding	Affiliating Institute at the time of publication	Name of the publisher	Relavant link
K Rajam, M Chandramouleeswaran	Nil	L-Fuzzy -Ideals of -Algerbas	International Mathematical Forum	International	2015	1312 7594	MSEC, Kilakarai	International Mathematical Forum	https://docs.google.com/uc?export=download&id=19EGXBhcSeYZH1qSddgkntvSuxIIR5T38
K Rajam, M Chandramouleeswaran	Nil	L-Fuzzy T-ideals of -Algebras	Applied mathematical Sciences	International	2015	1312 885X	MSEC, Kilakarai	Applied mathematical Sciences	https://docs.google.com/uc?export=download&id=1SrKqXbPUVFsgmDIzOp6r36vLd5Nmv3IS
S Tharmar	Nil	Soft Expert Generalized Closed sets with respect to soft expert ideals	International Journal of Mathematics and its Applications	International	2015	2347 1557	MSEC, Kilakarai	International Journal of Mathematics and its Applications	https://docs.google.com/uc?export=download&id=1EsJrF6IDE9OqV74YTvPmgWx9eDi8kxNx
Jeyaraj Dhaveethu Raja, Karunganathan Sakthikumar	Nil	Synthesis of water soluble transition metal(II) complexes from morpholine condensed tridentate schiff base Structural elucidation,	Journal of Chemical and Pharmaceutical Research	National	2015	0975 7384	MSEC, Kilakarai	Journal of Chemical and Pharmaceutical Research	https://docs.google.com/uc?export=download&id=1tAJUav6r_vIUam88emtjMaQgMIDUGjBP
K M Alaaudeen ,S Vengatesh kumar	Nil	A Ultra Low Power Router Design for Network on ChipFull Text	International journal of Applied Control, Electrical &Electronics	International	2015	2394-6237	MSEC, Kilakarai	International journal of Applied Control, Electrical &Electronics Engineering	https://docs.google.com/uc?export=download&id=1SjUbEMSG1gMR9WhkK2tiQzryrlHy_LI
S A Fatima Nuvairah, K Monisha	Nil	Real Time HD video Segmentation using WAVGMM with Shadow elimination	Coimbatore Institute of Information Technology	National	2015	0974-9586	MSEC, Kilakarai	Coimbatore Institute of Information Technology	https://docs.google.com/uc?export=download&id=1frbIGOUsD9BnBevabT2xwJREfBxDF48z
Mr I Sheik Arafath,N B Balamurugan, • S Bismillah Khan	Nil	Influence of scattering in near ballistic silicon nano wired metal - oxide semiconductor field effect transistor	Journal of Nanoscience & Nanotecnology	International	2015	0369-8203	MSEC, Kilakarai	Journal of Nanoscience & Nanotecnology	https://docs.google.com/uc?export=download&id=1vNvmZP8gARjMRKxogoxBmZVBaEOE-gnP
S Boobalan, Dr R Dhanasekaran	Nil	Improving power quality of renewable energy source by using UPQC based on cascaded multilevel topology	International Journal of Control theory and applications.	International	2015	0974-5572	MSEC, Kilakarai	International Journal of Control theory and applications	https://docs.google.com/uc?export=download&id=1s_S6ME7qrH1mDLowpsM6LIKTREtANRCH
R Niraimathi, R Seyezhai	Nil	Investigation of Multilevel DcC link inverter to solve partial shading	Middle East journal of Scientific research	International	2015	1990-9233	MSEC, Kilakarai	Middle East journal of Scientific research	https://docs.google.com/uc?export=download&id=14VrkAc8S687eC5BhbJSqw2_yUA7LWsL
Dr M Abbas Malik	Nil	Marketing of Hospital Services in Ramanthapuram District	National Conference on Entrepreneurial Opportunities and	International	2015	2320-4168-Vol 3	MSEC, Kilakarai	Shanlax International Journal Publisher	https://docs.google.com/uc?export=download&id=1nhJvxkRtpkMzhXyCDz8dkCnqKxU6HjSg
Ms Santhana Jeyalakshmi	Nil	Role Of Higher ducation in Promoting Entrepreneurship	Shanlax International Journal Publisher	International	2015	2321-4643	MSEC, Kilakarai	Shanlax International Journal Publisher	https://docs.google.com/uc?export=download&id=1C981aNrLJDYstlzY5bpIOf4d3Vma40D0
S Sajithabanu	Nil	Enhanced Efficient Information Sharing In Cloud Environment Using EERA	International Conference on Trends in Technology for	International	2015	2229-5518	MSEC, Kilakarai	AVS Engineering College	https://docs.google.com/uc?export=download&id=1HzWrjJEno4Dn2zK_6kXgNRwMhK9r0mMy
M Rajeshwaran	Nil	Biodiesel Production And Optimization From Prosopis Julifera Oil A Three Step Method	International Journal for Advanced Research in Technology	International	2015	0976-3945	MSEC, Kilakarai	International Journal for Advanced Research in Technology	https://docs.google.com/uc?export=download&id=1LKwwNA5FrLFMzT-TNNOTVVr4MxMHg71Y
Dr J Abbas Mohaideen, Dr S Ramachandran,	Environmental Science	Nil		International	2015	978-93-84893-06-4	Maamallan Institute of Tech, Chennai	Airwalk Publications	https://docs.google.com/uc?export=download&id=1-G7KjeaCYIEdz0RVNjekpPg1ymQ4aJjn
S P Shanmughapriya	Nil	An Overview on Removable of Heavy Metals trokinetic Remediation Process	International Conference on Green Technologies for Energy Management	International	2015	0973-4562	MSEC, Kilakarai	Mohamed Sathak Engineering College	https://docs.google.com/uc?export=download&id=1hx-KjQi0MKvjDjpTz6I-t45yI-cmfEIQ
Dr J Al Dr S Ra			Nil	International	2015	978-93-84893-06-4	Maamallan Institute of Tech, Chennai	Airwalk Publications	https://docs.google.com/uc?export=download&id=1t4abG6Xqho5DEbjsInAl9evreSISqvp9
S		and analysis of three phase common symmetric cascaded multilevel	Second international conference on green technologies for power	International	2015	0973-4562	MSEC, Kilakarai	St Peter's University, Chennai	https://docs.google.com/uc?export=download&id=10uhecBUIPAv2_5NVGMvA4ZscwUqhz1u
Sujith Mohaideen	Nil	tion of Lead in fish, water and sediment	IOSR Journal of Environmental Science, Toxicology and Food	International	2014	eISSN 2319-2402, pISSN 2319- 2399 ISBN-978-93-83409	Maamallan Institute of Tech, Chennai	www.iosrjournals.org	https://docs.google.com/uc?export=download&id=1zdEqN0WIIJOcJI9ZZosgqLGVM3vdiqd1

TRUE COPY ATTESTED

PRINCIPAL
MOHAMED SATHAK ENGINEERING COLLEGE
KILAKARAI-623806.

MOHAMED SATHAK ENGINEERING COLLEGE * KILAKARAI

Name of the teacher	Title of the book/chapters published	Title of the paper	Name of the conference	National / International	Year of publication	ISBN number of the proceeding	Affiliating Institute at the time of publication	Name of the publisher	Relavant link
M.D. Duraimurugan alias Saravanan, S.P. Shanmuga Priya,	Nil	Electro-kinetic remediation to evaluate and enhance the removal of arsenic from cultivated soil and red soil	International Conference on Emerging Trends in Engineering and	International	2014	0973 4562	MSEC, Kilakarai	International journal of Applied Engineering research	https://docs.google.com/uc?export=download&id=1PDjdbXuGIC4URMzRSQm5SoR8IyBKit3X
G.Gajalakshmi1, Dr. J. Abbas Mohaideen2, Prof. A.R. Santhakumar	Nil	State of the art on Dynamic Behavior of Structures under Human Induced Activities	National Journal on Advances in Building Sciences & Mechanics	national	2014	ISSN 0975-7317	Maamallan Institute of Tech, Chennai	Sathyabama institute of science and technology	https://docs.google.com/uc?export=download&id=1nz88Z0vmB_MIPMaFoN1YGKk4zuUzfoL8
siji thomas and J Abbas Mohaideen	Nil	"Determination of Cadmium in Water, Sediment and Spotted Seer Fish"	INTERNATIONAL JOURNAL OF LATEST TRENDS IN	International	2014	2278-621X	Maamallan Institute of Tech, Chennai	INTERNATIONAL JOURNAL OF LATEST TRENDS IN ENGINEERING AND TECHNOLOGY	https://docs.google.com/uc?export=download&id=1Q6WuiMt5Yuv4NXbTpyom4BYXuFgAcs_5
Siji thomas and Abbas J Mohaideen	Nil	Analysis of Heavy Metals in fish, water and sediment from Bay of Bengal"	International Journal of Engineering Science Invention	International	2014	2319 – 6726	Maamallan Institute of Tech, Chennai	International Journal of Engineering Science Invention	https://docs.google.com/uc?export=download&id=1A_CNkVUaRPB_RDyQQ9JsFCwrsrCDb5UN
G.GAJALAKSHMI, DR.J.ABBAS OHAIDEEN, PROF. A.R.	Nil	A Study on Transient Behaviour of A RCC Floor Slab	International Jouranl of Latest Trends in Engineering and	International	2014	2319-1058	Maamallan Institute of Tech, Chennai	International Jouranl of Latest Trends in Engineering and Technology	https://docs.google.com/uc?export=download&id=1u-PYJeAatKOkWgczU8RVmfmYx3TPXTtz
M.D. Duraimurugan alias Saravanan, D.K. Shanmugapriya, P.	Nil	'Cloud point extraction of Phenol using TX-100 as non-ionic surfactant'	International Journal of Scientific & Engineering Research,	International	2014	2229-5518	MSEC, Kilakarai	International Journal of Scientific & Engineering Research,	https://docs.google.com/uc?export=download&id=1q7Hmp7GYmGfRSPfsSkb5L5fwHYo3c6yH
M.D. Duraimurugan alias Saravanan	Nil	Antimicrobial activity and phytochemical screening of cynodon dactylon and carica papaya	Research in bio-technology	International	2014	ISSN 2229-791X	MSEC, Kilakarai	https://www.researchgate.net/publication/277567426	https://docs.google.com/uc?export=download&id=1DGYiNrFKUI01guvy6MhOwNvD2ig961bd
Dr. J. Dhaveethu Raja	Nil	PCR amplication and cloning of PPE41 of mycobacterium tuberculosis in *E.Coli*"	Indo Global Journal of Applied Engineering	International	2014	2321-5267	MSEC, Kilakarai	Indo Global Journal of Applied Engineering	https://docs.google.com/uc?export=download&id=1XhS9ZjZ5zDJCtuBxX8mi8IQzXYaGkbOE
Dr. J. Dhaveethu Raja	Nil	DNA Binding, Oxidative Cleavage Studies of Pyrimidine with Morpholine derivative Ligands and its Gold, Copper, Platinum and Zinc	TEQIP II Sponsored International Conference on Chemistry and	International	2014	978-93-81521-49-6	MSEC, Kilakarai	Bharathidasan Institute of Technology (BIT) Campus, Anna University, Trichirappalli	https://docs.google.com/uc?export=download&id=1ipsHAVf-FIQRh-5dGNNYSh7OWnqWUdtZ
Dr. J. Dhaveethu Raja	Nil	Synthesis, Structural, Characterization, Antibacterial, DNA cleavage and Binding study of Pyrimidine Derivative Schiff Base metal	International conference on Advances in New materials [ICAN 2014]	International	2014	978-81-89843-57-1	MSEC, Kilakarai	Dept of Inorganic Chemistry, University of Madras, Chennai-25	https://docs.google.com/uc?export=download&id=1mp08fA4VwT8L-9RBjgGVuvIv-6FMHfZ6
Muthumari, G., Nasar Ali, R., Dhaveethu Raja, J.	Nil	Comparative Study on Stabilizaiton of Expansive Soil using Cement Kiln Dust And Ceramic Dust	Journal of Geotechnical Engineering,	International	2014	23941987	MSEC, Kilakarai	Journal of Geotechnical Engineering,	https://docs.google.com/uc?export=download&id=1mSTdFS2f6UlbG3j8itCd7DwQsudSAetj
Dhaveethu Raja, J., Angeline, S.	Nil	"Study on Synthesis, Structural Elucidation of Biologically Active Schiff Base Transition Metal Complexes"	International Journal of Innovative Research in Science & Engineering	International	2014	2347 3207	MSEC, Kilakarai	International Journal of Innovative Research in Science & Engineering	https://docs.google.com/uc?export=download&id=1k2MMnw4fC7k56C0pvyO5T64EOjlVvhWB
Revathi, N., Dhaveethu Raja, J.	Nil	"Synthesis, Structural Characterization, Antibacterial Activity, DNA Cleavage and Binding Study of Pyrimidine Derivative Schiff	International Journal of Innovative Research in Science & Engineering	International	2014	2347 3207	MSEC, Kilakarai	International Journal of Innovative Research in Science & Engineering	https://docs.google.com/uc?export=download&id=1s0HMEVJg8PoaVGeyZmPaYK7oZuXnmFd-
D.Ragavan, A.Girija, B.Kathreen, R.K.Seenivasan	Nil	Synthesis,Characterisation and Application of Phenol-Formaldehyde Resin Blended with Sulphonated TerminaliaBellerica.	International Journal of Innovative Research in Science & Engineering	International	2014	2278 0211	MSEC, Kilakarai	International Journal of Innovative Research in Science & Engineering	https://docs.google.com/uc?export=download&id=1c5W6865CTJetgEPaM-gy1cAN9XIzwUwG
Mr.I.Sheik Arafath,N.B. B...	Nil	Roll- off Discrete Dopants in carrier transport of near Balistic silicon nano wired metal - ...conductor field effect transistor	Jokull Jornal	International	2014	4490576	MSEC, Kilakarai	Jokull Jornal	https://docs.google.com/uc?export=download&id=12ENh4RK5Id1Y53n7PfTM2u4ldkfjZ2Li
Mr.I.Sh...		...oughnesss scattering in carrier ...near balistic silicon nanowire	Applied Mechanics & Materials	International	2014	1662-7482	MSEC, Kilakarai	Applied Mechanics & Materials	https://docs.google.com/uc?export=download&id=1m8gecjWJWbIOqIfpVkUzI3MCITlRF0qJ
I... Arafath...		...of future nano transistor	International journal on Application of Information &	International	2014	2394-6237	MSEC, Kilakarai	International journal on Application of Information & Communication Engineering	https://docs.google.com/uc?export=download&id=1V3TWyQs17gFFOIXaoeJLPv67rITL5tKK
I. Sure... Manoharan		...sensitivity analysis in potential area ...one hybrid renewable energy in tamilnadu, india	Applied mechanics and materials	International	2014	1662-7482	MSEC, Kilakarai	Applied mechanics and materials	https://docs.google.com/uc?export=download&id=17eejbwTitm8VfVIfq3W4S4UVjSUpZXks

TRUE COPY ATTESTED

PRINCIPAL
MOHAMED SATHAK ENGINEERING COLLEGE
KILAKARAI-623806.

MOHAMED SATHAK ENGINEERING COLLEGE * KILAKARAI 623806

Name of the teacher	Title of the book/chapters published	Title of the paper	Name of the conference	National / International	Year of publication	ISBN number of the proceeding	Affiliating Institute at the time of publication	Name of the publisher	Relavant link
U Suresh kumar, Dr P S Manoharan	Nil	optimization and cost of energy of renewable energy system in health clinic building for a coastal area in tamilnadu India using Homer	Research journal applied science and Engineering technology	International	2014	2040-7459	MSEC, Kilakarai	Research journal applied science and Engineering technology	https://docs.google.com/uc?export=download&id=1NzzRUrpBg212KucTdxa-87vVOqMfJkNJ
R Niramathi, R Seyezhai	Nil	MATLAB simulation of PV based asymmetric multilevel inverter	International Journal of Industrial Electronics and Electrical	International	2014	2347-6982	MSEC, Kilakarai	International Journal of Industrial Electronics and Electrical Engineering	https://docs.google.com/uc?export=download&id=1HzcBaQO-4XD5xuBa8N5fws95QOQBByM4
Dr M Abbas Malik	Nil	Recent Trends in Insurance Services in Tamilnadu	National Conference on Entrepreneurial Opportunities and	International	2014	2321-4643	MSEC, Kilakarai	Shanlax International Journal Publisher	https://docs.google.com/uc?export=download&id=1Oboj4Lo0w5I489M-46EUAyZnj5xyvqIX
Dr N Shankar	Nil	Effect of Social Factors,Entrepreneurial Behaviour towards Entrepreneurial intention among Law Graduates	International Journal on Management Research and Reeview	International	2014	2249-7196	MSEC, Kilakarai	Shanlax International Journal Publisher	https://docs.google.com/uc?export=download&id=10FqyxnPAN8AhJpyiP5mStNs2043t_efo
Dr A Abdul Brosekhan	Nil	Rapid change in consumer buying behaviour - A big challenge for sustainable growth of todays business	Samzodhana Journal of Management Resarch	National	2014	2321-4643	MSEC, Kilakarai	St Michael College of Engineering & Tech, Kalaiyarkoil, Sivagangai District	https://docs.google.com/uc?export=download&id=1vaTC9S6IX5ZBQWE0rqThM3btCOdM_kUA
Dr N Shankar	Nil	Competency Analysis of Tamilnadu Newsprints and Paper Limited(TNPL) - An Emerging Success Among Public Sector	Golden Research thoughts	National	2014	2231-5036	MSEC, Kilakarai	Lakshmi Book Publication, Maharashtra	https://docs.google.com/uc?export=download&id=1FNwOiBJoFuCVbnwM5zxavHYiFUY4DPI4
N Bala Subramanivan, B Deeba, M Sabari Ramachandran	Nil	Mobile Commerce Explorer for Personal Mobile Commerce Pattern Mining and Prediction	International Journal for Advanced Research in Engineering and Technology	International	2014	0976-6480	MSEC, Kilakarai	International Journal for Advanced Research in Engineering and Technology	https://docs.google.com/uc?export=download&id=12v0wvPWpLe24Fto5NIS44PzSzCcNOyC3
V Mayilvel Nathan	Nil	Experimented Analysis Of Nano Enhanced Latent Heat Thermal Energy Storage System	Journal of the Chinese Society of Mechanical Engineers	National	2014	0257-9731	MSEC, Kilakarai	Sardar Raja College Of Engineering, Alaganguam, Tirunelveli, Tamilnadu	https://docs.google.com/uc?export=download&id=12N5Gr-3inqFH6edOX7sZz7d5oAPcLX8_
S P Shanmuga priva, J Rohan	Nil	Arsenic pollution in India an overview	National conference on Advances In Process Engineering	national	2014	0975-7384	MSEC, Kilakarai	Sastra University STUDENT CHAPTER OF THE INDIAN INSTITUTE OF CHEMICAL ENGINEERING	https://docs.google.com/uc?export=download&id=1H26Ld8bkfp1ecTHHW0OP9EGNpk6yIXr9
Sijt thomas and J Abbas Mohaideen	Nil	Seasonal variation in heavy metal distribution near Ennore sea shore, Chennai	International congress on environmental and bio technology and chemistry engineering	international	2014	2010-4618	Maamallan Institute of Tech, Chennai	International congress on Environmental, Biotechnology & Chemistry Engineering	https://docs.google.com/uc?export=download&id=18t_SJyoQn9Saoc6HmRJUXSV-ESvU9SdR
N I Haroon Rashid	Nil	Effect of pitch angelon blade- tower interference on HAWT	Asia Pacific Internal National Conference in Wind Engineering	International	2013	978-98107-8011-1	MSEC, Kilakarai	Research Publishing, Singapore	https://docs.google.com/uc?export=download&id=1qU5MgTc8UkjSDIFqmNVdhZ6r7RI5Spx8
A Girija	Nil	A Study on Cation Exchange Capacity using Resorcinol-Formaldehyde Resin blended with low Cost Plant Material	Recent Advances in Surface Science	National	2013	2394-9759	MSEC, Kilakarai	Bonfring International Journal	https://docs.google.com/uc?export=download&id=1MLtDPaDIA7rDvI3r_e4mvd2MDnR_YoUd
A Girija, R K Seenivasan	Nil	Synergism Modified ion-Exchange Process of Selective Metal ions and its binary mixtures by using low-cost ion exchange resin and its Binary mixture	RasayanJ Chem	International	2013	0976 0083	MSEC, Kilakarai	RasayanJ Chem	https://docs.google.com/uc?export=download&id=1kCpeIqT1Kzr3pAfdT3o-62sWaXrdSdLD
Dr N Shankar	Nil	Lawpreneurship and Opportunities	National Conference on Entrepreneurial Opportunities and Challenges	International	2013	2321-788X	MSEC, Kilakarai	Shanlax International Journal Publisher	https://docs.google.com/uc?export=download&id=1aN_doUjN66TMFSBtAs2WhmqSII5p1HnF
Dr A		s consumer and Decision Maker - al Framework	National Conference on Entrepreneurial Opportunities and Challenges	International	2013	2321-788X	MSEC, Kilakarai	Shanlax International Journal Publisher	https://docs.google.com/uc?export=download&id=1-80K91oJYixfUQqDFLVAwBiMp1CWF6GU

TRUE COPY ATTESTED

PRINCIPAL
MOHAMED SATHAK ENGINEERING COLLEGE
KILAKARAI-623806.

MOHAMED SATHAK ENGINEERING COLLEGE ★ KILAKARAI 623806

TRUE COPY ATTESTED

PRINCIPAL
MOHAMED SATHAK ENGINEERING COLLEGE
KILAKARAI

The Eighth Asia-Pacific Conference on Wind Engineering, December 10-14, 2013, Chennai, India

EFFECT OF PITCH ANGLE ON BLADE - TOWER INTERFERENCE ON HAWT

N. I. Haroon Rashid[1], S. Nadaraja Pillai[2], C. Senthil Kumar[3].

[1]*Research Scholar,Department of Aerospace Engineering, MIT Campus, Anna University Chennai, TN, India,* aeroharoonrashid@gmail.com

[2]*Department of Aeronautical Engineering, J. J. College of Engineering & Technology, Tiruchirapalli, TN, India,* aeropillai@gmail.com

[3]*Department of Aerospace Engineering, Madras Institute of Technology, Anna University, Chennai, TN, India,* cskumar@annauniv.edu

ABSTRACT

In the wind turbine, the distribution of wind is altered by the presence of the tower. For upwind rotors, the flow of wind in front of the tower is redirected thereby reduces the torque at each blade. The performance of the wind turbine is affected by such influence of interference. Hence, it is important to understand the flow interference between blade and tower. In this research, the wind turbine blade with various pitch angles has been studied both computationally and experimentally. The result shows that the influence of interference leads to negative pressure region on the tower where the blade interference occurs. Hence this leads a slowdown of rotor locally for every 120 degree, this in turn affect the power performance and decrease the structural stability.

Keywords: Tower Shadow, Interference, HAWT, pitch angle

Introduction

For horizontal axis wind turbine, the interaction between the tower and the blade creates flow complexity and leads to reduced power performance. Even though various unsteady effects in the wind turbines such as atmospheric boundary layer, turbulence intensity of the upstream flow, yaw effect of the nacelle, wake of the neighboring turbines, upstream blockage effect dominates; this has been discussed by many researchers. However the interference between the wind turbine blade and its tower and also the influence of the blade pitch angle interaction needs further more research attention. This effect is discussed widely as tower shadow and most of the effect on downwind turbine wake model is discussed by Wang and Coton. Also they concluded that the discrepancies arise when the angle of attack of the blade experiences higher value. Experimental study by Orlando et al., found that there is 35% of velocity reduction in the anemometer reading the anemometer is in the downstream of the turbine tower.

Chattot studied with vortex model for the simulation of the tower shadow and its effect on the blade working conditions as analyzed with the blade root flap bending moment. The importance of rotor in the upwind and downwind configurations and its importance is discussed by chattot. Amada et al., showed the decrease in power output by around 6% due to the various effect including tower shadow. Dolan and Lehn discussed about the normalized s effect in terms of wind shear and the tower shadow effect. They found low and wind shear combinely reduce 6% of the power output. In this e model has been made both computationally and experimentally in order

to study the interaction between tower and blade. Leishman studied about the induced velocity field produced by the vortical wake behind the turbine, the various unsteady aerodynamic issues associated with the blade sections, and the intricacies of dynamic stall. Anemometer in the wind turbine is kept in the nacelle part where the most of the blade rotation wake influences. Lubitz studied about the tower shadow influence on the anemometer data. Various research has been done in wind turbine and the component influence on aerodynamics of wind turbine, however there are limited study carried out in the area of interference or the effect of rotor with various parameters needs a extensive study. The issue on pitch angle of the blade and its influence on interference between blade and the tower is discussed in this paper.

Computational Model Geometry and Flow conditions

The computational domains for the blade, hub, and tower are created and meshed. Mesh is carefully checked so that there is no discrepancy which leads to the discontinuity. To generate the volume mesh for the three bladed rotors, the 120 degrees periodicity of the rotor is exploited by only meshing the volume around the blades. The computational domain created using tetrahedral elements, extending in the axial direction roughly 4 diameters upstream and 8 diameters downstream of the turbine.

In the plane of the rotor, the domain diameter is 4 times that of the turbine. Second stage involves creating the meshing element. One of the major difficulties in CFD modeling is to mesh the flow domain near the rotor. The grid should be fine enough to capture the details of geometry and flow field at these locations, but not too large to handle and then the succeeded meshing models are exported for the analysis.

HAWT geometry with 108m tower height and 46m blade height has been created computationally. The model is surrounded by the fluid elements of tetrahedral shape with more than 1 million elements. The model rotor boundary condition is set as rotating reference frame in order to create the required rpm. The rotor has been rotated to 5, 10, 15, 20, 25 rpm corresponding to the wind speed. The computational turbulence model used is $k - \varepsilon$, because it is more general and predicts well in general. The model made computationally and the domain created for flow analysis is shown in Figs. 1 & 2.

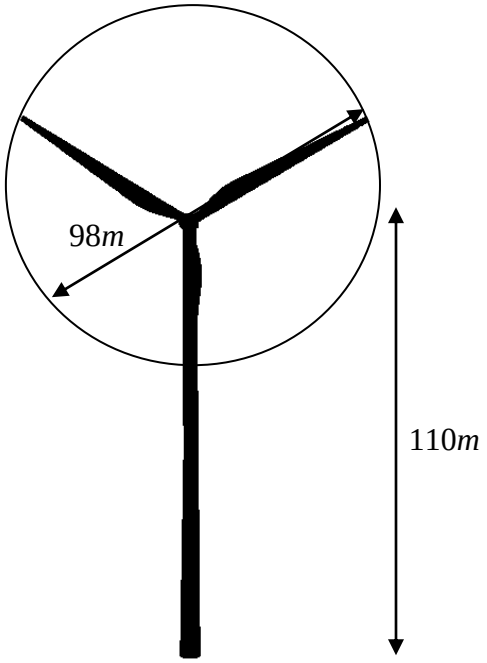

Fig. 1 Wind turbine model and its dimensions considered for the present study.

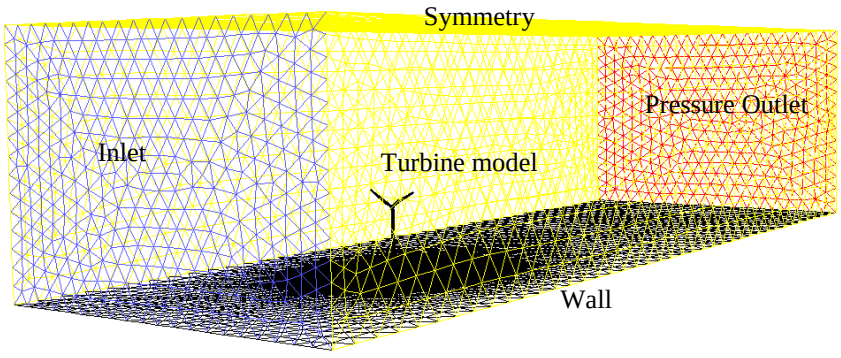

Fig. 2 Computational domain for the flow analysis (rotational boundary condition is given for the rotor).

Experimental Study

The experiments were carried out using low speed wind tunnel at MIT for the test section velocities of 10 m/s, 20 m/s and 30m/s. The size of the test section is 3 ft^x 4ft x 6ft, where the turbine model is scale down to 1:333. 64 channel pressure scanner is (DTC-Initium) used to measure the pressure on the tower surfaces of the wind turbine model. There were 32 pressure tapings in the wind turbine model tower and it is shown in fig. 3. The pressure tapings are connected to the pressure scanners and to capture the pressure distribution on the surface of the tower.

Fig-3 Experimental Model in Wind Tunnel

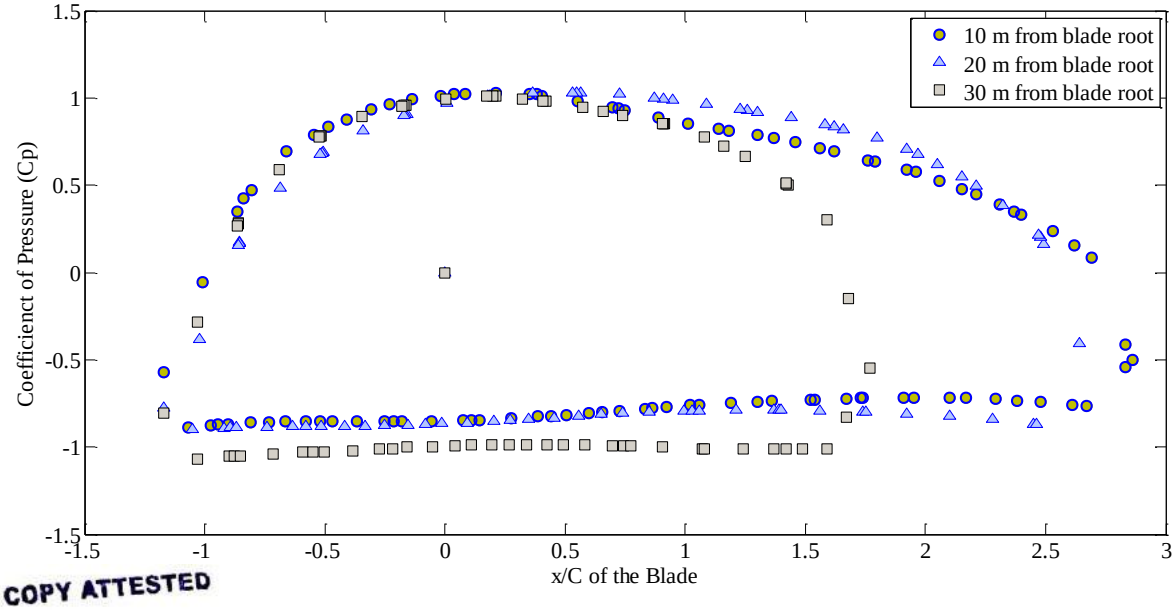

oefficient of Pressure (Cp) at various cross section of the blade.

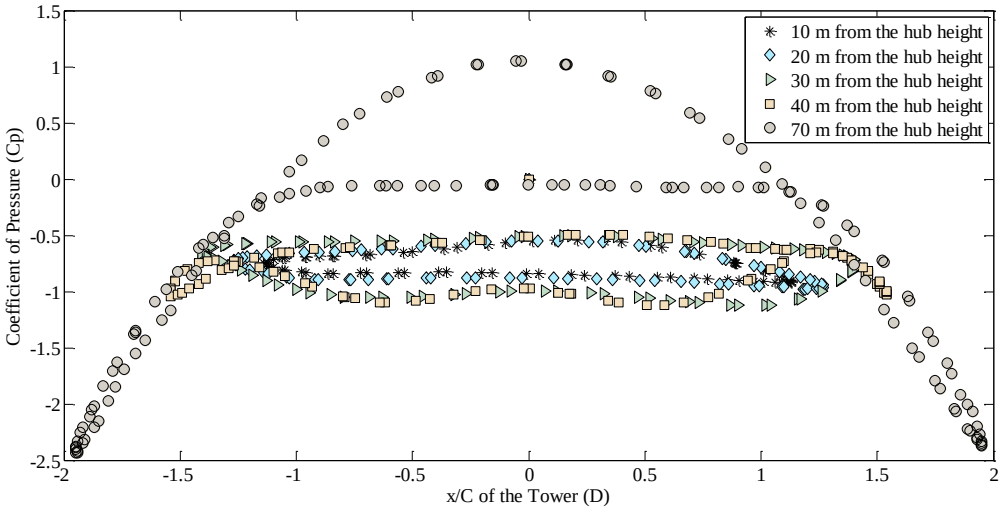

Fig. 5 Coefficient of Pressure (Cp) at various cross section of the Turbine tower

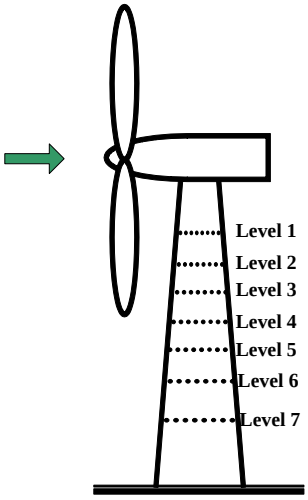

Fig. 6 Schematic representation of Wind Turbine with pressure tapings at different levels

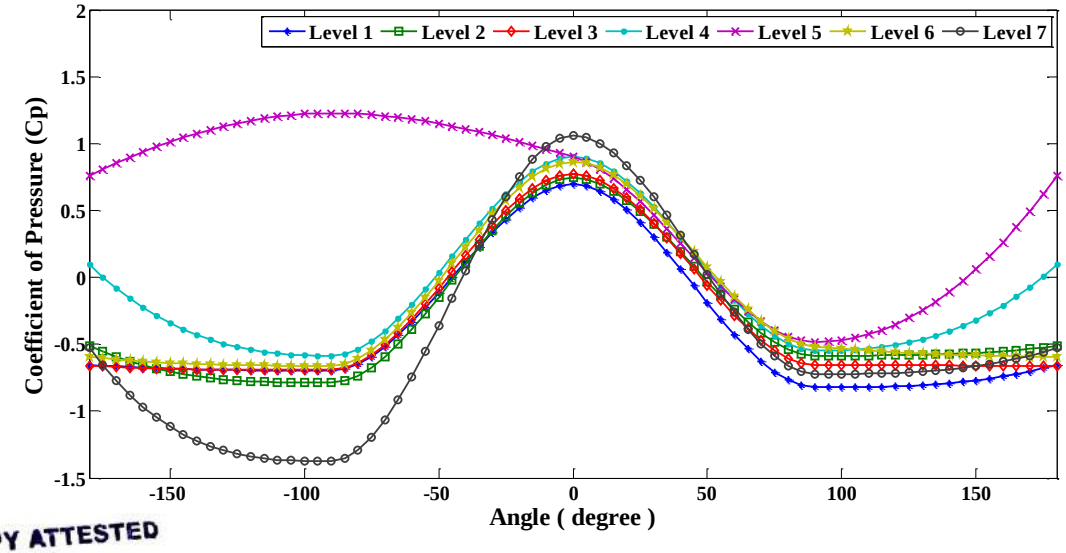

imental Pressure distribution (Cp) value at different levels of fig. 6

Results and Discussions

From the computational study the results for the coefficient of pressure has been obtained for the various blade cross section at the locations 10, 20, 30m from the blade root shown in Fig. 4. The pressure distribution for the aerofoil on the pressure side and suction side are shown in the Fig 4. The suction side pressure is very well constant and this could be due to the influence of tower. In the other case where the pressure coefficient for various locations of the tower geometry from 10, 20, 30, 40, 70m has been obtained and shown in Fig. 5. For 70m location there is no influence of the blade and tower interaction, hence the pressure distribution looks like normal circular cylinder. For other cases like 10 to 40m tower height from the hub height, the influence is clearly shown. Here the pressure difference created is small and also all are in the negative pressure region. Even though the pressure difference causes a force but it is very small.

Fig. 6 shows the schematic representation of the wind turbine model kept in the wind tunnel with pressure tapings. The pressure distribution (Cp) of the different levels shown in Fig. 7. It shows that the effect of the tower is visible at the levels 4, 5 and 7. In the levels 1, 2 , 3 shows the similar value or pattern whose value is different from levels below. Cp affected by the blade influence in the tower and the one which is not affected from the interference is shown in fig.7. The extensive study in the wind tunnel is needed much more to get the information about the interferences.

References

[1]Tongguang Wang, Frank N. Coton, "A high resolution tower shadow model for downwind wind turbines" Journal of Wind Engineering and Industrial Aerodynamics 89 (2001) 873–892.

[2]Stephen Orlando, Adam Bale, David A. Johnson, "Experimental study of the effect of tower shadow on anemometer readings" Journal of Wind Engineering and Industrial Aerodynamics 99 (2011) 1–6.

[3]Jean-Jacques Chattot, "Tower shadow modelization with helicoidal vortex method", Computers & Fluids 37 (2008) 499–504.

[4]J. Gordon Leishman, "Challenges in Modeling the Unsteady Aerodynamics of Wind Turbines", 21*st* ASME Wind Energy Symposium and the 40th AIAA Aerospace Sciences Meeting, Reno, NV.

5 Joaquín Mur-Amada, Ángel A. Bayod-Rújula, "Pace of Tower Shadow Fluctuation in a Wind Farm", 9th International Conference, Electrical Power Quality and Utilization, Barcelona, 9 – 11, October, 2007.

6 Dale S. L. Dolan, Peter W. Lehn, "Simulation Model of Wind Turbine 3p Torque Oscillations due to Wind Shear and Tower Shadow", IEEE Transactions On Energy Conversion, Vol. 21, No. 3, September 2006.

7 M.C. Robinson, M.M. Hand, D.A. Simms, S.J. Schreck, "Horizontal Axis Wind Turbine Aerodynamics: Three- Dimensional, Unsteady, and Separated Flow Influences" 3rd ASME/JSME Joint Fluids Engineering Conference, San Francisco, California, July 18-23, 1999.

8 William David Lubitz, "Effects of Tower Shadowing on Anemometer Data", 11th Americas Conference on Wind Engineering, San Juan, PR, USA, June 22-26, 2009

GEOSPATIAL TECHNOLOGIES FOR RURAL DEVELOPMENT

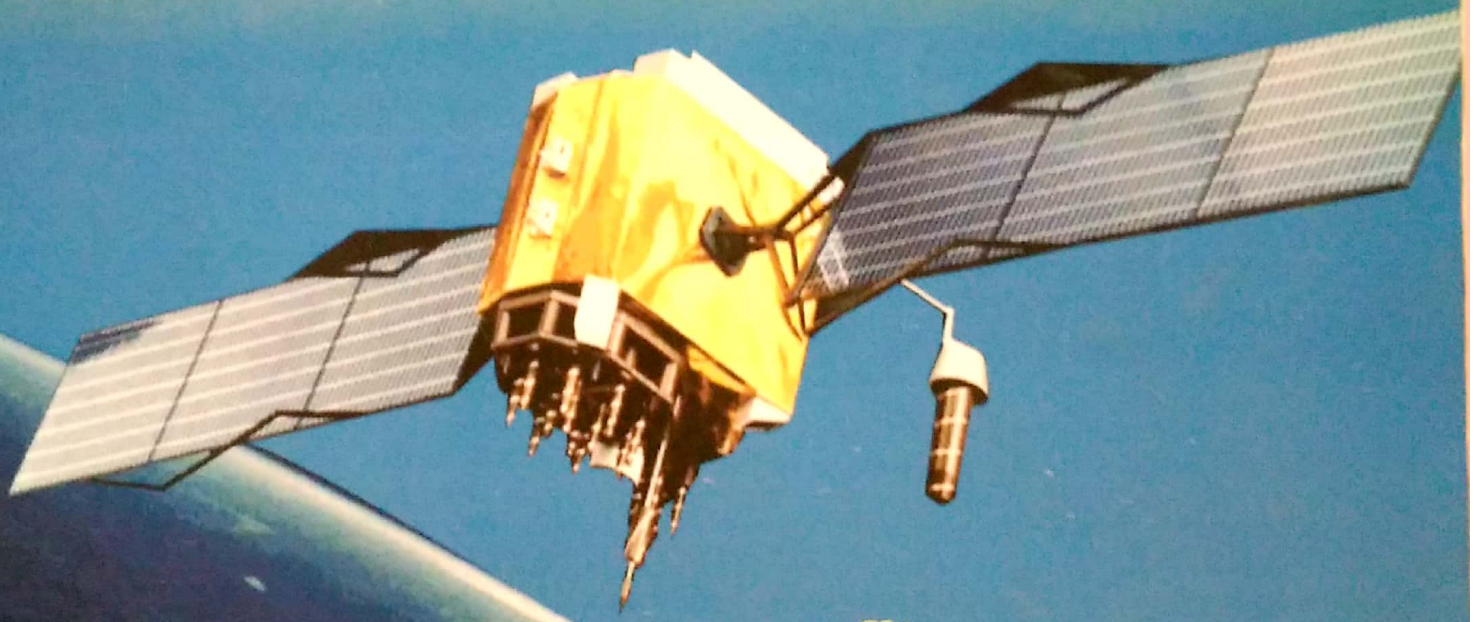

Editor

Dr.M.Muthukumar

Department of Rural Development

Faculty of Rural Development

The Gandhigram Rural Institute-Deemed University

Re-accredited by NAAC with 'A' Grade (3rd Cycle)

...ram – 624302, Dindigul District, Tamil Nadu, India

ज्ञान-विज्ञान विमुक्तये

Sponsored by

UGC, New Delhi

APPLICATION OF REMOTE SENSING AND GIS IN LAND RESOURCE MANAGEMENT

Sathees Kumar[1], Syed Ibrahim Sahib[2] & Nazeer Khan[3]
[1]Associate Professor, [2,3]Student,
Department of Civil Engineering, Mohamed Sathak Engineering College, Kilakarai-623 806, India

Abstract- *Land use Land cover (LU/LC) mapping serve as a basic information for land resource study. Detecting and analysing the quantitative changes along the earth's surface has become necessary and advantageous because it can result in proper planning which would ultimately result in improvement in infrastructure development, economic and industrial growth. The LU/LC pattern of Madurai city, Tamil Nadu, has undergone a significant change over past two decades due to accelerated urbanization. In this study, LU/LC change dynamics were investigated by the combined use of satellite remote sensing and geographical information system. To understand the LU/LC change in Madurai city, the different land use categories and their spatial as well as temporal variability has been studied over a period of seven years (1999-2006), from the analysis of LANDSAT images for the years 1999 and 2006 respectively, using ArcGIS 9.3 and ERDAS Imagine 9.1 software. This result shows that Geospatial technology is able to effectively capture the spatio-temporal trend in the landscape pattern associated with urbanization for this region.*

*Keywords – **GIS, LANDSAT, Land use Land cover, Remote Sensing.***

1. Introduction

Planning and development of urban areas with infrastructure, utilities, and services has its legitimate importance and requires extensive and accurate LU/LC classification. Information on changes in land resource classes, direction, area and pattern of LU/LC classes form a basis for future planning. It is also essential that this information on LU/LC be available in the form of maps and statistical data as they are very vital for spatial planning, management and utilization of land. However, LU/LC classification is a time consuming and expensive processes. In recent years, the significance of spatial data technologies, especially the application of remotely sensed data and geographic information systems (GIS) has greatly increased. Now-a-days, remote sensing technology is offering one of the quick and effective approaches to the classification and mapping of LU/LC changes over space and time. The satellite remote sensing data with their repetitive nature have proved to be quite useful in mapping LU/LC patterns and changes

Quantifying the anthropogenic or human activity that governs the LU/LC changes has become a key concept in the town planning profession. A major objective of planning analysis is to determine how much space and what kind of facilities a community will need for activities, in order to perform its functions. An inventory of land uses will show the kind and amount of space used by the urban system.

LU/LC study with the use of remote sensing technology is emerging as a new concept and has become a crucial item of basic tasks in order to carry through a series of important works, processes such as the prediction of land-use change, prevention and management of natural disaster, and protection of environment, etc and most importantly analysing the present development and future scope of development of the nation. In the recent years, with the enhancement of more advanced Remote Sensing technology and Geo-Analysis models, monitoring the status and dynamical change of LU/LC thoroughly using remotely sensed digital data has become one of the most rapid, credible and effectual methods.

The main aim of this paper is to assess the LU/LC changes, and to observe the growth of various urban classes over a period of seven years along Madurai City, by using remote sensing and GIS technology. For this purpose, multispectral, multi-temporal LANDSAT images were downloaded from USGS Earth Resources Observation Systems data centre. The classification, identification and graphical representation of the changes detected in the classes defined for the study area were done using ERDAS Imagine 9.1 software and ArcGIS 9.2 software. The paper focuses on the analyses and discussions of the results including the pattern of changes in LU/LC studied from year 1999 to 2006.

2. Study Area

The study area is Madurai city, Tamil Nadu (Fig.1), one of the famous historical and cultural cities in India. It is located in South Central Tamil Nadu, is the second largest city after Chennai and is the headquarters of Madurai District. In 2011, the jurisdiction of the Madurai Corporation was expanded from 72 wards to 100 wads covering area 151 Sq.Km, dividing into four regions Zone I, II, III,

International Journal of Applied Engineering Research, ISSN 0973-4562 Vol. 10 No.77 (2015)

A Overview on the Removal of Heavy Metals Using Electrokinetic Remediation Process

Mrs.Shanmuga Priya [1]
Chemical engineering
Mohamed Sathak Engineering College
Kilakarai
chemical_priya@yahoo.co.in

M.D.Duraimurugan alias saravanan[2]
Chemical engineering
Mohamed Sathak Engineering College
Kilakarai
durai_sar2003@yahoo.co.in

Dr.D.Alagia Meenal[3]
Civil Engineering
Mohamed Sathak Engineering College
Kilakarai

I.Kaja bahurdeen[4]
Chemical Engineering
Mohamed Sathak Engineering College
Kilakarai
ihaja78@gmail.com

G.Leo suraj[5]
Chemical Engineering
Mohamed Sathak Engineering College
Kilakarai

Abstract— Heavy Metal Contamination of soil and groundwater is a widespread problem nowadays. The presence of heavy metal in the soil will toxic to living organisms in higher concentration. The contamination of heavy metal will also affect the ecosystem and make the Environmental Issues. Several research work are undertaken for the removal of heavy metals. Electro-kinetic remediation method is found to be suitable technique for the removal of heavy metals where other common remediation technologies typically fail. This method is a promising technology for the removal of heavy metals by the application direct current to electrodes. Heavy metals are large group of elements which are having higher density. Several heavy metals like Lead Cadmium, Arsenic, Zinc, and Mercury contaminate the quality of soil and ground water .This paper is a survey work on the removal of heavy metals in the soil and ground water using electro-kinetic Process. This comparative study will provide review about the possible sources, chemistry, potential biohazards and best available remedial strategies for a number of heavy metals (lead, chromium, arsenic, zinc, cadmium, copper, mercury and nickel) commonly found in contaminated soils.

Keywords— Heavy metals, Contamination, Remediation, Electrokinetic process, Biohazards.

I. INTRODUCTION

Soil is a crucial component of rural and urban environments, and in both places land management is the key to soil quality. This series of technical notes examines the urban activities that cause soil degradation, and the management practices that protect the functions urban societies demand from soil. This technical note focuses on heavy metal soil contamination.

In general, soil contamination is placing human health at a great risk. Soil contamination is becoming a key environmental issue, due to its importance in ecosystems, and the influence it has on the quality of ground water, plants and food. Spills and leaks can contaminate both the soil above the water table as well as the aquifer itself. Excavation of such sites may not be cost effective or politically acceptable. Some of the most common and most damaging types of soil contaminants are metals. Generally, during routine operations or accidental spills in industry soil may be contaminated with metals. Once metal contaminates the soil, it can have complex interactions with natural binders that can lead to both short (delaying the normal hydration reaction) and long (release of the heavy metals in groundwater) term problems. Presence of heavy metals in soil has great concern with respect to human health and safety.

II. HEAVY METALS

A. AVAILABLE HEAVY METALS IN SOIL

Mining, manufacturing, and the use of synthetic products (e.g. pesticides, paints, batteries, industrial waste, and land application of industrial or domestic sludge) can result in heavy metal contamination of urban and agricultural soils. Heavy metals also occur naturally, but rarely at toxic levels. Potentially contaminated soils may occur at old landfill sites (particularly those that accepted industrial wastes), old orchards that used insecticides containing arsenic as an active ingredient, fields that had past applications of waste water or municipal sludge, areas in or around mining waste piles and tailings, industrial areas where chemicals may have been dumped on the ground, or in areas downwind from industrial sites.

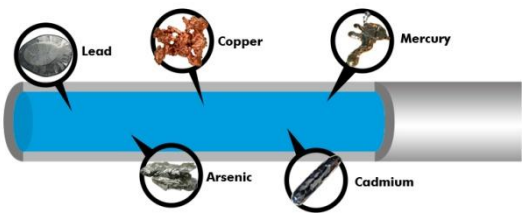

Figure 1. *Important Most Toxic Heavy Metals*

B. PROBLEMS DUE TO HEAVY METALS IN SOIL

Excess heavy metal accumulation in soils is toxic to humans and other animals. Exposure to heavy metals is normally chronic (exposure over a longer period of time), due to food chain transfer.

Acute (immediate) poisoning from heavy metals is rare through ingestion or dermal contact, but is possible. Chronic problems associated with long-term heavy metal exposures are:

- Lead - mental lapse.
- Cadmium - affects kidney, liver, and GI tract.
- Arsenic - skin poisoning, affects kidneys and central nervous system.

The most common problem causing cationic metals (metallic elements whose forms in soil are positively charged cations e.g., Pb2+) are mercury, cadmium, lead, nickel, copper, zinc, chromium, and manganese.

The most common anionic compounds (elements whose forms in soil are combined with oxygen and are negatively charged e.g., Mo042-) are arsenic, molybdenum, selenium, and boron.

Table 1. *Maximum permissible concentration of metals in soil*

Metal	***Max limit in Soil (mg/kg)*** *US-EPA*
Arsenic (As)	*14*
Selenium (Se)	*1.6*
Nickel (Ni)	*32*
Cobalt (Co)	*20*
Cadmium (Cd)	*1.6*
Chromium(Cr)	*120*
Copper (Cu)	*100*
Lead (Pb)	*60*
Mercury (Hg)	*0.5*
Zinc (Zn)	*220*

III. ELECTROKINETIC REMEDIATION

Electro kinetic remediation is one possible technique for in situ removal of such contaminants from both saturated and unsaturated soils. To understand Electrokinetic remediation, it is necessary to know the governing equations of the transport phenomena. The two most important transport mechanisms for electro kinetics are Electro migration and electro osmosis. This section discusses the two transport equations for a typical soil and compares them to determine the dominant Electrokinetic transport process. In electro kinetic remediation, electrodes are implanted in the soil, and a direct current is imposed between the electrodes. The ionic species and charged particles in the soil water will migrate to the oppositely charged electrode (electro migration and electrophoresis), and along with this migration, a bulk flow of water is induced, usually toward the cathode (electro-osmosis) The combination of these phenomena leads to a movement of contaminants toward the electrodes Contaminants arriving at the electrodes may potentially be removed from the soil in several ways including electroplating or adsorption onto the electrode, precipitation or co-precipitation at the electrode, pumping water near the electrode, or complexing with ion-exchange resins. Application of Electrokinetic process for the removal of contaminant may vary mainly due to the variation in soil type and type of contaminant in the soil.

The first Electrokinetic phenomenon was observed at the beginning of the 19th Century, when Reuss applied a direct current to a clay water mixture. However, Helmholtz and Smoluchowski were the first scientists to propose a theory dealing with the electro-osmotic velocity of a fluid and the zeta potential under an imposed electric gradient. Electrokinetic remediation, variably named as electrochemical soil processing, Electro-migration, Electrokinetic decontamination or electro reclamation uses electric currents to extract radionuchdes, heavy metals, certain organic compounds, or mixed inorganic species and some organic wastes from soils and slurries.

The application of electric current has several effects:

(1) It produces an acid in the anode compartment that is transported across the soil and desorbs contaminants from the surface of soil particles;

(2) It initiates Electro migration of species available in the pore fluid and those introduced at the electrodes;

(3) It establishes an electric potential difference which may lead to Electro osmosis generated flushing of different species.

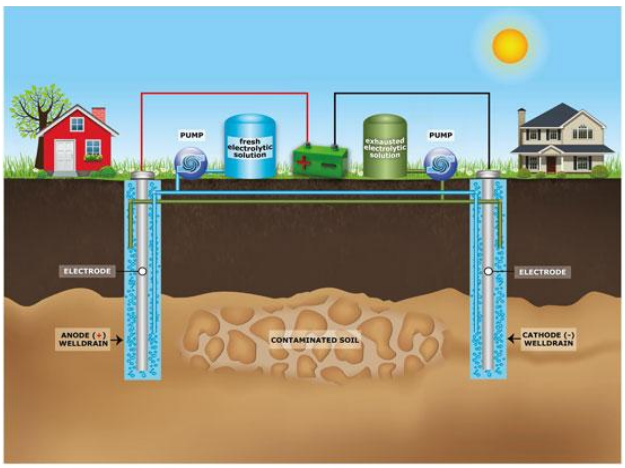

Figure 2. *Electrokinetic Remediation Process*

IV.LEAD

In the human body, lead accumulates mainly in the kidneys. At high levels, it can reach a critical threshold and can lead to serious kidney failure. Recent studies have shown that kidney effects may be reversible at low exposures once lead exposure is reduced or removed. Maximum contaminant level (MCL) of metals that could be present in soil is presented in Table 1. It can be seen

from Table 1 that permissible concentration limits for metals in soil is very low which, in turn, reflects the toxicity level and hazards associated with these metals [2, 17].

Author Utchimuthu done an experimental on Electrokinetic remediation for removing Lead. He uses Electrokinetic experiments were conducted using same type of clay soil taken from the site. Initial total concentrations of lead (II) maintained at 1000mg/kg for each process. The clay soils were to a voltage gradient of 1VDC/cm for over 24hrs, 36hrs and 48hrs.In a porous compact matrix of surface charged particles such as soil, the ion containing pore fluid may be made to flow to collection sites under the applied field. The work presented here describes part of the effort undertaken to investigate the electro kinetically enhanced transport of soil contaminants (lead) in synthetic systems. The result of his experiment indicate that Electrokinetic enhancement of contaminant transport in clay soils with different durations, increased duration (48hrs) is best removal efficiency for comparing the other durations (24hrs and 36hrs).He concluded with his as further research is need to understand the effects of characteristics for further increasing the removal efficiency.

V.CADMIUM

Cadmium is a non-essential heavy metal pollutant of the environment resulting from various agricultural, mining and industrial activities and also from the exhaust gases of automobiles. It was first discovered 1817 as a by-product of the zinc refining process. In the human body, cadmium accumulates mainly in the kidneys. At high levels, it can reach a critical threshold and can lead to serious kidney failure. Recent studies have shown that kidney effects may be reversible at low exposures once cadmium exposure is reduced or removed.

In this study, the effectiveness of introducing chelating agents to enhance the removal of cadmium from kaolinite in the region of neutral pH by ionic migration is examined. The chelating agents selected were ethylenediaminetetraacetic acid (EDTA) and citric acid. The investigation was carried out in a laboratory scale column containing kaolinite contaminated with cadmium .Cadmium migrates toward the anode, indicating that cadmium is indeed solubilized by EDTA and citric acid as negative charged chelates. The dissolved chelates migrate toward the anode by ionic migration and are successfully removed at the anode reservoir. The effectiveness soft EDTA and citric acid for removing cadmium was also investigated and it was found that EDTA was more effective than citric acid reserved.

IV. NATURAL METHODS FOR REMOVAL OF HEAVY METALS IN SOIL

A. Traditional Remediation of Contaminated soil

Once metals are introduced and contaminate the environment, they will remain. Metals do not degrade like carbon-based (organic) molecules. However, in general it is very difficult to eliminate metals from the environment.

Traditional treatments for metal contamination in soils are expensive and cost prohibitive when large areas of soil are contaminated. Treatments can be done in situ (on-site), or ex situ (removed and treated off-site). Both are extremely expensive. Some treatments that are available include:

1. High temperature treatments (produce a vitrified, granular, non-leachable material).
2. Solidifying agents (produce cement-like material).
3. Washing process (leaches out contaminants).

B. Management of Contaminated soil

Soil and crop management methods can help prevent uptake of pollutants by plants, leaving them in the soil. The soil becomes the sink, breaking the soil-plant- animal or human cycle through which the toxin exerts its toxic effects

The following management practices will not remove the heavy metal contaminants, but will help to immobilize them in the soil and reduce the potential for adverse effects from the metals

1. Increasing the soil pH to 6.5 or higher.
2. Draining wet soils.
3. Applying phosphate.
4. Carefully selecting plants for use on metal-contaminated soils

C. Plants for Environmental Cleanup

Research has demonstrated that plants are effective in cleaning up contaminated soil by the author Wenzel et al.,in 1999. Phytoremediation is a general term for using plants to remove, degrade, or contain soil pollutants such as heavy metals, pesticides, solvents, crude oil, polyaromatic hydrocarbons, and landfill leacheates

C.1 Plants for Treating Metal Contaminated soils

Plants have been used to stabilize or remove metals from soil and water. The three mechanisms used are

1. Phytoextraction
2. Rhizofiltration
3. PhytoStabilization

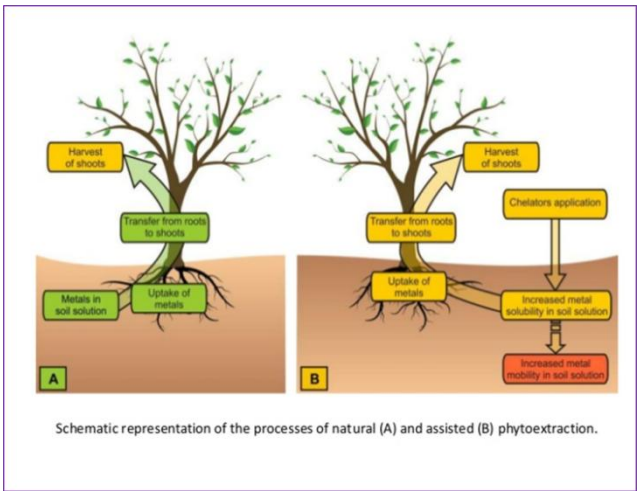

Schematic representation of the processes of natural (A) and assisted (B) phytoextraction.

Figure 3. **Phytoextraction Process**

Rhizofiltration is the adsorption onto plant roots or absorption into plant roots of contaminants that are in solution surrounding the root zone. Rhizofiltration is used to decontaminate groundwater. In Chernobyl, Ukraine, sunflowers were used in this way to remove radioactive contaminants from groundwater.

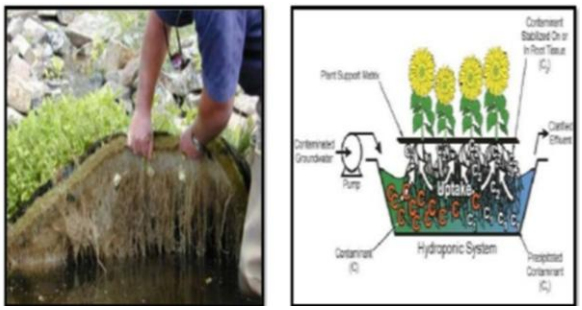

Figure 4. *Rhizofilteration Process*

PhytoStabilization is the use of perennial, non-harvested plants to stabilize or immobilize contaminants in the soil and groundwater. Metals are absorbed and accumulated by roots, adsorbed onto roots, or precipitated within the rhizosphere.PhytoStabilization reduces the mobility of the contaminant and prevents further movement of the contaminant into groundwater or the air and reduces the bioavailability for entry into the food chain.

Phytoextraction is the process of growing plants in metal contaminated soil. Plant roots then translocate the metals into aboveground portions of the plant. After plants have grown for some time, they are harvested and incinerated or composted to recycle the metals. Several crop growth cycles may be needed to decrease contaminant levels to allowable limits.

CONCLUSION

This paper describes the information regarding heavy metal contamination to soil and ground water. The problems associated with the heavy metals are clearly explained with several literature review. The method to remove the heavy water is explained with its own experimental setup given by several authors. And this paper not only deals with the theoretical concept but it also force every individual to manage the heavy metal on our own towards soil contamination and ground water spills.

REFERENCES

[1]. Kedziorek, M. A. M. and Bourg, A. C. M., Solubilization of lead and cadmium during the percolation of EDTA through a soil polluted by smelting activities. Journal of Contaminant Hydrology, 2000, 40(4), 381 –392.
[2]. Niinae, M., Aoe, T., Kishi, W., Sugano, T., Numerical analysis for distributions of weak acid concentration onelectrokinetic soil remediation. Journal of the Mining and Materials Processing Institute of Japan, 1998,114(11), 801 – 806.
[3]. Niinae, M., Ogawa, H., Sugano, T., Aoki, K., Removal of Pb and Cd from artificially contaminated clay soilswith chelating agents. Journal of the Mining and Materials Processing Institute of Japan, 1999, 115(11),825 – 829.
[4]. Niinae, M., Aoe, T., Sugano, T., Aoki, K., Distributions of cadmium on electrokinetic soil remediation undercondition of constant applied voltage. Journal of the Mining and Materials Processing Institute of Japan,2000, 116, (10), 855 – 860.
[5]. Niinae, M., Aoe, T., Sugano, T., Aoki, K., Removal of cadmium from soil by electrokinetic method undercondition of catholyte pH. Journal of the Mining and Materials Processing Institute of Japan, 2001a,117(2), 127 – 132.
[6]. Shapiro, A. P. and Probstein, R. F., Removal of contaminants from saturated clay by electroosmosis. Environmental Science and Technology, 1993, 27(2), 283 – 291.
[7]. Wong, J. S., Hicks, R. E., Probstein, R. F., EDTA - enhanced electroremediation of metal - contaminated soils. Journal of Hazardous Materials, 1997, 55, 61 – 79.
[8]. Yeung, A. T., Hsu, C., Menon, R. M., EDTA - enhanced electrokinetic extraction of lead. Journal of Geotechnical Engineering, 1996, 122(8), 666 – 673.
[9]. Suantak Kamsonlian, Chandrajit Balomajumder and Shri Chand., Removal of As (III) from AqueousSolution by Biosorption onto Maize (Zea mays) Leaves Surface: Parameters Optimization, SorptionIsotherm, Kinetic and Thermodynamics Studies, Res. J. Chem. Sci., 1(5), 73-79 (2011)

For B.E. / B.Tech - Common to all branches

Environmental Science and Engineering

With Part-A Questions & Answers

Dr.J.ABBAS MOHAIDEEN
Dr. S.RAMACHANDRAN
Prof. K. PANDIAN

AIR WALK PUBLICATIONS
Ph: 044 - 24661909, 9444 08 1904

ENVIRONMENTAL SCIENCE AND ENGINEERING

(As per latest Anna University and UGC Syllabus)

Dr. J. Abbas Mohaideen

Dr. S. Ramachandran

Prof. K. Pandian

AIR WALK PUBLICATIONS
(Near All India Radio)
80, Karneeshwarar Koil Street,
Mylapore, Chennai - 600 004.
Ph.: 2466 1909, 94440 81904
Email: aishram2006@gmail.com
www.airwalkpublications.com

First Edition: Sep., 2005
Second Edition: June 2014
Third and Revised Edition: July 2015

Price : **Rs. 300/-**

ISBN: 978-93-84893-06-4

ISBN:978-93-84893-06-4

9 789384 893064

Books will be door delivered after payment into **AIR WALK PUBLICATIONS** A/c No. 801620100001454 (IFSC: BKID0008016) Bank of India, Santhome branch, Mylapore, Chennai - 4 (or)

S.Ramachandran, A/c.No.482894441 (IFSC:IDIB000S201), Indian Bank, Sathyabama University Branch, Chennai - 600119.

...sharan muthu salayam, Chennai – 18. Ph.: 044-2436 4303

Int. J. Chem. Sci.: 13(1), 2015, 53-62
ISSN 0972-768X
www.sadgurupublications.com

DETERMINATION OF SOME HEAVY METALS IN FISH, WATER AND SEDIMENTS FROM BAY OF BENGAL

SIJI THOMAS[*] and J. ABBAS MOHAIDEEN[a]

Research Scholar, Sathyabama University, CHENNAI (T.N.) INDIA
[a]Maamallan Institute of Technology, CHENNAI (T.N.) INDIA

ABSTRACT

Concentrations of five heavy metals, arsenic (As), cadmium (Cd), chromium (Cr), lead (Pb) and mercury (Hg) were determined in water, sediments and in marine species, the Indo-Pacific king mackerel popularly known as Spotted Seer fish (Scomberomorus Guttus). The samples were collected near the seashore of the Bay of Bengal from five different locations in North Tamilnadu Pulicat, Ennore, Marina, Mahabalipuram and Kalpakkam during the period September-November 2012. The maximum concentrations of heavy metals observed in fish were arsenic (0.382 mg/Kg-Pulicat), cadmium (0.441 mg/Kg-Ennore), chromium (0.711- mg/Kg-Marina), lead (0.673 mg/Kg-Marina), and mercury (0.08 mg/Kg-Kalpakkam). Maximum heavy metal concentrations in water are arsenic (0.03 mg/L-Kalpakkam), cadmium (0.022 mg/L-Ennore), chromium (0.046 mg/L-Ennore), lead (0.015 mg/L-Pulicat) and mercury (0.016 mg/L-Marina). Highest concentrations of arsenic (2.518 mg/Kg), cadmium (1.815 mg/Kg), chromium (3.082 mg/Kg) and lead (1.273 mg/Kg) in sediment was observed in samples collected from Ennore, while mercury was found in the highest concentration (0.668 mg/Kg) from Marina.

Key words: Heavy metals, Concentration, Atomic absorption spectrophotometer (AAS), Chennai, Spotted seer fish.

INTRODUCTION

Heavy metals occur naturally in the ecosystem with larger variations in the concentration. Eventhough some heavy metals form the part of our daily life activities, they are subjected to potent toxics, contaminating ecosystems. Some heavy metals like iron, cobalt, copper, manganese, molybdenum, and zinc are essential to the human body to maintain the metabolism, but its excessive levels can be damaging to the organism. Unlike other pollutants, such as petroleum hydrocarbons and wastes that invade the environment, heavy metals accumulate surreptitiously, eventually reaching toxic levels. The problems associated with the contamination by heavy metals was first highlighted in the industrially

[*]Author for correspondence; E-mail: sijithomas76@yahoo.com

advanced countries because of their large industrial spills, especially after accidents caused by the pollution of metals like mercury and cadmium. Iron, cobalt, copper, manganese, zinc, etc. are required by humans, but excessive levels can cause a grave damage to the organism[1]. It is the estuary of the Seine[2], an ecological association and a representative of the water police that bring their testimony to this worrying situation. However, there has been a growing awareness of the need for sound management of water resources[3] and in particular to control the dumping of waste in the environment. With industrialization and urban activities happening at a faster pace, the study of heavy metal contamination becomes more relevant in this regard. Heavy metals such as mercury, plutonium and lead are toxic[4] and their accumulation, over a period of time in the bodies of animals can cause serious illness. In natural aquatic ecosystems, metals are found at lower concentrations, typically in the nanogram or microgram. However, the presence of heavy metal contaminants[5], especially higher than natural filler metal concentrations, has become an issue of increasing concern. Heavy metal toxicity can result in damaged or reduced mental and central nervous function, lower energy levels, and damage to blood composition, lungs, kidneys, liver and other vital organs.

The elevated heavy metal contamination rate can be attributed to rapid population growth, increased urbanization, expansion of industrial activities, exploration and exploitation of natural resource. Factors such as expansion of irrigation, spread of other modern agricultural practices and the absence of environmental regulations have also contributed to the increased contamination. Long-term exposure[6] may affect in the physical, muscular, and neurological degenerative processes. For the sound management and control of water pollution, a detailed study of the inputs, distribution and fate of contaminants, including heavy metals from a land flowing into aquatic ecosystems become relevant. It is particularly important to study the quantity and quality characteristics, and the routes they travel when they disperse their destiny and their effects. Many of our rivers, lakes, and oceans have been contaminated by pollutants. The natural sources such as volcanic activity, weathering of rocks and forest fires, also contribute in contamination. The contribution of volcanoes can be in the form of large, but sporadic emissions from explosive activity, or continuous emission of low volume, resulting in particular, from geothermal activity and magma degassing. Over the past decade[7,] sampling and analytical techniques applied to heavy metals have also improved considerably.

These advances, coupled with the realization of international intercalibration exercises brought together more reliable data. Efforts have been made in this document, to collect and analyze the available information on the presence of heavy metals in marine waters, in order to contribute to the sound development policies for managing water

resources. Some of these pollutants are directly discharged by industrial plants and municipal sewage treatment plants, others come from polluted runoff in urban and agricultural areas, and some are the result of historical contamination. The decision to review the data on marine water comes from the need to adopt a holistic approach, which can inspire future strategies. The pollutants that enter the water cause undesirable changes, which affect the ecological balance of the environment. Among all the pollutants, accumulation of heavy metals is of global importance due to its adverse impact on human health. Fish is a valuable food item and source of protein. The concentration of heavy metals in aquatic organisms is higher than that present in water through the effect of bio concentration and bio magnification and eventually threaten the health of human by sea food consumption[8]. Fishes are widely used as bio indicators of marine pollution by metals[9]. Heavy metals cant enter the aquatic environment from both natural sources and anthropogenic sources. Their input can be the result either of spills made directly in marine ecosystems and freshwater, or an indirect path as in the case of dry and wet landfills and agricultural runoff. So the determination of heavy metal concentration in fishes is very important as far as human health is concerned. The objective of this study is to determine the concentration of some trace metals in Seer fish, water and sediments collected from Bay of Bengal in North Tamilnadu.

Literature survey

In the last twenty years, many studies have been devoted to metal toxicity[10]; on the basis of these results, several international and national organizations have developed criteria for water quality for aquatic life. Some heavy metals such as Zn, Cu, Mn and Fe[11] are essential to the growth and well-being of living organisms, including humans. It might nevertheless be expected to have toxic effects when organisms are exposed to concentration levels higher than they normally require. Other elements, such as Pb, Hg and Cd, are not essential for metabolic activities and exhibit toxic properties. The contamination of the aquatic environment[12] by metals from localized sources can have deleterious effects, on aquatic life within the area concerned. The published data so far on the effects of metals on aquatic organism indicate, that these adverse effects occur at higher than those typically found in environmental concentrations. The metals can be absorbed in an inorganic form or organic form. For some elements, such as arsenic and copper, inorganic form is the most toxic. For others, such as Hg, Pb and Sn, organic forms are the most toxic. The main routes of absorption of heavy metals by man are food, water and air.

One of the sources through which mercury and arsenic enters the human system is through consumption of fish. Several methods have been used to find the elements present as

traces in environmental matrices. Data on dissolved metals in inland water bodies (lakes and rivers) and in marine and coastal areas were presented. As already mentioned, most studies on the levels and distribution of heavy metals focused on urban and industrial areas. The method[13] most commonly used for the determination of heavy metals is the atomic absorption spectrophotometry (AAS). It has the advantage of being rapid, sensitive, simple and can help analyze complex mixtures without prior separation. For some heavy metals, atomization using graphite furnace or cold vapour is done for better accuracy. In view of the importance of fish as a human diet, it is necessary that biological monitoring of the water and fish meant for consumption should be done regularly to ensure continuous safety of the seafood. Safe disposal of domestic sewage and industrial effluents should be practiced and where possible, recycled to avoid these metals and other contaminants from going into the environment. Laws enacted to protect our environment should be enforced.

EXPERIMENTAL

Methodology

Study area

The study area consists of 5 different locations (Pulicat, Ennore, Marina, Mahabalipuram and Kalpakkam) along the coast of Bay of Bengal in North Tamilnadu.

Pulicat (Pazhaverkadu) is a historic seashore town in Thiruvallur District, of Tamil Nadu. It is about 60 km north of Chennai and 3 km from Elavur, on the barrier island of Sriharikota, which separates Pulicat Lake from the Bay of Bengal.

Ennore is situated on a peninsula and is bounded by the Korttalaiyar River, Ennore creek and the Bay of Bengal. The creek separates Ennore from the Ennore Port. Ennore creek carries a high load of heavy metals. The treated effluents of the Madras Refinery Ltd., through the Buckingham canal and the Madras Fertilizers Ltd.[14-16], through the Red Hills surplus channel, reach the Ennore backwater[17].

Marina beach is an urban beach in the city of Chennai, India, along the Bay of Bengal, part of the Indian ocean. The beach runs from near Fort St. George in the north to Besant Nagar in the south, a distance of 13 Kms, making it the longest urban beach in the country and the world's second longest.

Mahabalipuram lies on the Coromandel Coast which faces the Bay of Bengal. It is around 60 Km south from the city of Chennai. It is an ancient historic town and was a bustling seaport during the time of Periplus (1st century CE) and Ptolemy (140 CE).

Kalpakkam is a small town in Tamil Nadu, situated on the Coromandel Coast 70 kilometers south of Chennai Nuclear facilities. The Madras Atomic Power Station is located at Kalpakkam. It is a comprehensive nuclear power production, fuel reprocessing, and waste treatment facility that includes plutonium fuel fabrication for fast breeder reactors (FBRs). It is also India's first fully indigenously constructed nuclear power station. It has two units of 220 MW capacity each[18-20].

Materials and methods

The water, sediment and spotted seer fish samples were collected during September – November 2012 from all the 5 locations within 500 meters from the seashore. The physico-chemical parameters like temperature, pH, salinity and dissolved oxygen are measured. The fish samples were washed thoroughly with distilled water to remove the sediments and debris. The length and weight of each sample were measured. Then the edible parts were separated and frozen at -20^{o} for the analysis. The fish samples were thawed, and then dried in a hot air oven at 60^{o}C. After removing the moisture content, the weight was taken again.

Digestion procedure for fish samples

15 g of fish sampled was taken and the ashing was done at 500^{o}C for 16 hrs. After cooling, 2 mL of nitric acid (HNO_3) and 10 mL of 1 molar hydrochloric acid (HCl) were added. After digestion, samples were filtered using Whatman filter paper No. 41, and the filtrate is made up to 25 mL with distilled water.

Digestion procedure for water samples

For As, Cd, Cr and Pb: 100 mL water sample was taken in a beaker and 0.5 mL nitric acid (HNO_3) and 5 mL hydrochloric acid (HCl) were added. Then it is kept in a hot plate for digestion. After digestion, it was made up to 10 mL. Heavy metal concentrations were determined by Atomic Absorption Spectrophotometer (AAS).

For Hg: 100 mL water sample was taken in a beaker and 5 mL sulphuric acid (H_2SO_4), 2.5 mL nitric acid (HNO_3) and 15 mL potassium permanganate ($KMnO_4$) were added. Then it was placed on a hot plate for 15 min for digestion. Then 8 mL potassium persulphate ($K_2S_2O_8$) was added and heated in 100^{0}C water bath for 2 hrs.

After cooling, 6 mL sodium chloride hydroxylamine sulphate was added. After decoloration, 5 mL stannous chloride ($SnCl_2$) was added.

Digestion procedure for sediment samples

2 g of dry sediment was taken in a digestion vessel, 10 mL of 1:1 nitric acid (HNO_3) was added and covered with a watch glass. It was heated at 95 ± 5^oC for 10-15 min without boiling. After cooling, 5 mL concentrated HNO_3 was added and refluxed for 30 mins. The step was repeated until no brown fumes come. The solution was allowed to evaporate to nearly 5 mL by heat without boiling. After the sample has cooled, 2 mL of water and 30% H_2O_2 were added. Heated until effervescence subsides and the vessel was cooled. 30% H_2O_2 was added in 1 mL aliquots with warm until the effervescence is minimal. The sample was covered with a ribbed watch glass and continued until the volume has been reduced to 5 mL. 10 mL HCl was added and refluxed for 15 min at 95 ± 5^0C. The digest was filtered through Whattman filter paper No. 41 and was collected in 100 mL standard flask. Heavy metal concentrations were determined by Atomic Absorption Spectrophotometer (AAS).

RESULTS AND DISCUSSION

Fish

The maximum and minimum concentrations of selected heavy metals (H. M.) in fish caught from different locations are given in Table 1 and the graphical representation of the maximum concentration in Fig. 1. It is observed that the maximum concentration of arsenic (0.382 mg/Kg), cadmium (0.441 mg/Kg) and lead (0.673 mg/Kg) are observed in fish samples collected from Pulicat, Ennore and Kalpakkam, respectively. The maximum concentrations of chromium (0.711 mg/Kg), and mercury (0.08 mg/Kg) are observed in samples collected from Marina.

Water

The concentrations of heavy metals in water collected from 5 different locations are given in Table 2 and the graphical representation in Fig. 2. The maximum concentration of arsenic (0.03 mg/L), lead (0.015 mg/L) and mercury (0.016 mg/L) are observed in water samples collected from Kalpakkam, Pulicat and Marina, respectively. Maximum concentration of cadmium (0.022 mg/L) and chromium (0.046 mg/L) are observed in samples collected from Ennore.

Sediment

The concentrations of heavy metals in sediments collected from 5 different locations are given in Table 2 and the graphical representation in Fig. 3.

Table 1: Concentrations (Minimum and maximum values) of H. M. in fish caught from different locations (mg/Kg)

Location	As		Cd		Cr		Pb		Hg	
	Min	Max	Min	Max	Min	Max	Min	Max	Min	Max
Pulicat	BDL	0.382	0.083	0.417	0.036	0.518	BDL	0.368	BDL	0.064
Ennore	BDL	0.247	BDL	0.441	BDL	0.463	BDL	0.375	BDL	0.06
Marina	BDL	0.24	0.032	0.423	BDL	0.711	BDL	0.203	BDL	0.08
Mahabalipuram	BDL	0.334	BDL	0.417	BDL	0.465	BDL	0.286	BDL	0.062
Kalpakkam	BDL	0.358	BDL	0.308	BDL	0.415	0.071	0.673	BDL	0.072

Table 2: Concentration of H. M. in water and sediment collected from different locations

HM/ Location	Water (mg/L)					Sediment (mg/Kg)				
	As	Cd	Cr	Pb	Hg	As	Cd	Cr	Pb	Hg
Pulicat	0.02	0.021	0.032	0.015	0.008	1.548	0.831	1.387	1.083	0.286
Ennore	0.029	0.022	0.046	0.014	0.007	2.518	1.815	3.082	1.273	0.483
Marina	0.01	0.012	0.02	0.006	0.016	0.572	1.034	1.664	0.574	0.668
Mahabalipuram	0.01	0.011	0.022	0.012	0.012	0.926	0.872	0.423	0.952	0.386
Kalpakkam	0.03	0.015	0.02	0.013	0.007	1.351	1.147	0.736	0.904	0.242

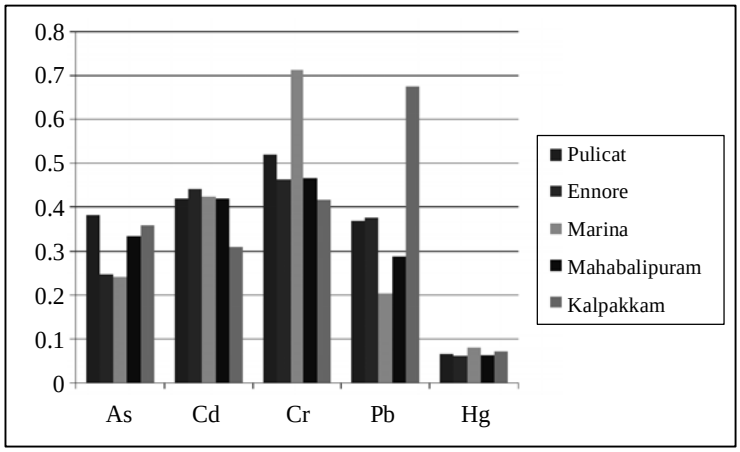

Fig. 1: Maximum concentration of H. M. in fish caught from different locations (mg/Kg)

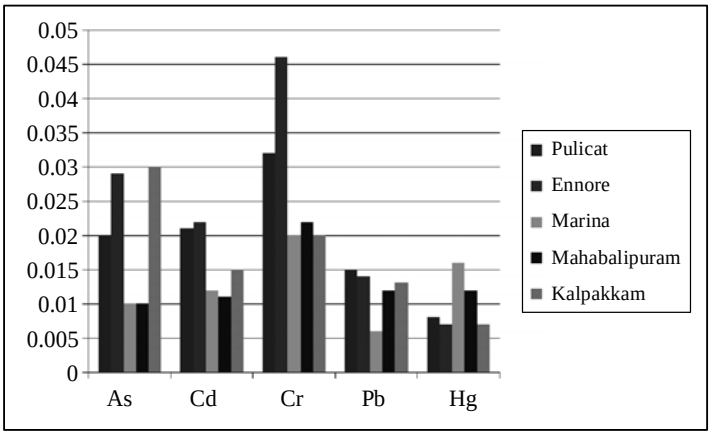

Fig. 2: Concentration of H. M. in water collected from different locations (mg/L)

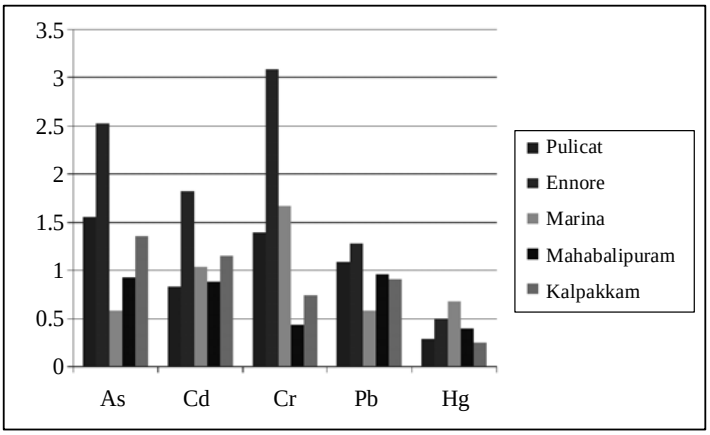

Fig. 3: Concentration of H. M. in sediment collected from different locations (mg/Kg)

The maximum concentration of arsenic (2.518 mg/Kg), cadmium (1.815 mg/Kg), chromium (3.082 mg/Kg) and lead (1.273 mg/Kg) is observed in sediment samples collected from Ennore. Maximum concentration of mercury (0. 668 mg/Kg) is observed in samples collected from Marina.

CONCLUSION

It is observed from this study, that the maximum concentrations of all the five heavy metals in the fish and water are observed in samples collected from different locations. But, the maximum concentrations of four heavy metals (arsenic, cadmium, chromium and lead) in sediment are observed in samples collected from Ennore. It may be due to the discharge of untreated effluent from various industries located near Ennore. As far as the importance of fish

in the human diet is concerned, it is necessary that the biological monitoring of water and fish should be done periodically to ensure the safety of seafood consumption. The safe disposal of industrial effluents and domestic sewage should be practiced to avoid such contamination. Also, the laws enacted to protect the environment should be enforced effectively.

REFERENCES

1. S. Martin and W. Griswold, Human Health Effects of Heavy Metals, Center for Hazardous Substance Research, Kansas State University, 15 (2009).
2. O. Chabrerie, I. Poudevigne, F. Bureau, M. Vinceslas-Akpa, S. Nebbache, M. Aubert and D. Alard, Biodiversity and Ecosystem Functions in Wetlands: A Case Study in the Estuary of the Seine River, France, Estuaries, **24(6)**, 1088-1096 (2001).
3. C. Pahl-Wostl, Transitions Towards Adaptive Management of Water Facing Climate and Global Change, Water Res. Manag., **21(1)**, 49-62 (2007).
4. R. U. Ayres,. Toxic Heavy Metals: Materials Cycle Optimization, Proceedings of the National Academy of Sciences, **89(3)**, 815-820 (1992).
5. T. Duxbury, Ecological Aspects of Heavy Metal Responses in Microorganisms, In Advances in Microbial Ecology, Springer US (1985) pp. 185-235.
6. K. E. Giller, E. Witter and S. P. Mcgrath, Toxicity of Heavy Metals to Microorganisms and Microbial Processes in Agricultural Soils: A Review, Soil Biol. Biochem., **30(10)**, 1389-1414 (1998).
7. A. L. Martin-Del Pozzo, F. Aceves, R. Espinasa, A. Aguayo, S. Inguaggiato, P. Morales and E. Cienfuegos, Influence of Volcanic Activity on Spring Water Chemistry at Popocatepetl Volcano, Mexico. Chemical Geology, **190(1)**, 207-229 (2002).
8. I. S. Eneji, R. Sha'Ato and P. A. Annune, Bioaccumulation of Heavy Metals in Fish (Tilapia Zilli and Clarias Gariepinus) Organs from River Benue, North–Central Nigeria, Pakistan J. Analytical Environ. Chem., **12**, 25-31 (2011).
9. E. Padmini and M. Kavitha, Contaminant Induced Stress Impact on Biochemical Changes in Brain of Estuarine Grey Mullets, Poll. Res., **24(3)**, 647-651 (2005).
10. W. Wang, Literature Review on Duckweed Toxicity Testing, Environ. Res., **52(1)**, 7-22 (1990).
11. S. P. McGrath and C. H. Cunliffe, A Simplified Method for the Extraction of the Metals Fe, Zn, Cu, Ni, Cd, Pb, Cr, Co and Mn from Soils and Sewage Sludges, J. Sci. Food Agri., **36(9)**, 794-798 (1985).

12. J. P. Sumpter and S. Jobling, Vitellogenesis as a Biomarker for Estrogenic Contamination of the Aquatic Environment, Environ. Health Perspectives, 103 (Suppl 7), 173 (1995).

13. S. Vellaichamy and K. Palanivelu, Preconcentration and Separation of Copper, Nickel and Zinc in Aqueous Samples by Flame Atomic Absorption Spectrometry after Column Solid-Phase Extraction onto MWCNTs Impregnated with D2EHPA-TOPO Mixture, J. Hazard. Mater., **185(2)**, 1131-1139 (2011).

14. M. Jayaprakash, S. Srinivasalu, M. P. Jonathan and V. R. Mohan, A Baseline Study of Physico-chemical Parameters and Trace Metals in Waters of Ennore Creek, Chennai, India, Marine Pollution Bulletin, **50(5)**, 583-589 (2005).

15. E. Padmini and B. Geetha, A Comparative Seasonal Pollution Assessment Study on Ennore Estuary with Respect to Metal Accumulation in the Grey Mullet, Mugil Cephalus, Oceanological and Hydrobiological Studies, **36(4)**, 91-103 (2007).

16. J. S. I. Rajkumar, M. C. John Milton and T. Ambrose, Distribution of Heavy Metal Concentrations in Surface Waters from Ennore Estuary, Tamil Nadu, India, Int. J. Curr. Res., **3(3)**, 237-244 (2011).

17. V. Shanthi and N. Gajendran, The Impact of Water Pollution on the Socio-economic Status of the Stakeholders of Ennore Creek, Bay of Bengal (India): Part I, Indian J. Sci. Technol., **2(3)**, 66-79 (2009).

18. B . P. D. Batvari, S. Kamala Kannan, K. Shanthi, R. Krishnamoorthy, K. J. Lee and M. Jayaprakash, Heavy Metals in Two Fish Species (Carangoidel m Alabaricus and Belones Tronglurus) from Pulicat Lake, North of Chennai, South East Coast of India, Environ. Monitoring Assess., **145**, 167-175 (2008).

19. M. K. Ahmad, S. Islam, M. S. Rahman, M. R. Haque and M. M. Islam, Heavy Metals in Water, Sediment and Some Fishes of Buriganga River, Bangladesh, Int. J. Environ. Res., **4(2)**, 321-332 (2010).

20. R. K. V. Murthy and B. K. Rao, Survey of Meiofauna in the Gautami-Godavari Estuary, J. Mar. Biol. Assoc. India, **29**, 37-44 (1987).

Accepted : 27.11.2014

ISSN: 0975-8585

Research Journal of Pharmaceutical, Biological and Chemical Sciences

Removal of Hazardous Metals from Waste Printed Circuit Boards by Chemical and Biological Methods.

A Jayapradha[1]*, and J Abbas Mohaideen[2].

[1]Sathyabama University, Department of Chemical Engineering, Chennai, Tamil Nadu, India.
[2]Mamallan Institute of Technology, Sriperumbudur, Chennai, Tamil Nadu, India.

ABSTRACT

A printed circuit board, or PCB, is used to mechanically support and electrically connect various electronic components by using conductive tracks etched from copper sheets laminated on to a non-conductive substrate. The material composition of PCB is 40% of metals, 30% of ceramics and 30% of plastics. Since the PCB contains higher percentage of metals which are hazardous when discarded to the ecosystem the metals must be removed. The objective of the study is to remove hazardous metals from PCB by biological and chemical treatment methods. PCBs are collected from waste electrical and electronic equipment. The study is carried out for both economic and ecological reasons. The biological study involves the removal of hazardous metals by biological leaching process by using the fine powder obtained from the seed of "Persia Americana" commonly called as AVOCADO (butter fruit). The seed is powdered and processed which is used for removing the hazardous metals present in the waste PCB. In chemical method, the fine powder of discarded PCB is leached with mixed acids for the removal of hazardous metals from PCB. Thus both the methods were studied to achieve an eco-friendly technique.

Keywords*:* Printed Circuit Boards (PCB's), Metals, Mixed Acid Leaching, Biological leaching.

ISSN: 0975-8585

INTRODUCTION

Electronic Waste (E-Waste)

"Electronic waste" (E-waste) may be defined as discarded electrical and electronic equipment. They may be discarded computers, office electronic equipment, entertainment devices, mobile phones, television sets and refrigerators. Rapid changes in technology, change in trend, changes in media (tapes, software, MP3) and falling prices have resulted in a fast-growing surplus of electronic waste around the globe. Display units (CRT, LCD, and LED monitors), Processors (CPU chips), memory (RAM), and audio components have different useful lives. Processors are most frequently out-dated (by software) and are more likely to become "e-waste", while display units are most often replaced while working without repair attempts, due to changes in technology.

An estimated 50 million tons of E-waste are produced each year. The USA discards 30 million computers each year and 100 million phones are disposed of in Europe each year [1]. The Environmental Protection Agency (EPA) estimates that only 15-20% of e-waste is recycled, the rest of these electronics go directly into landfills and incinerators. Asia itself disposes around 12 million metric tons of E-Waste. With increase in population, urbanization, capacity, economic growth and lifestyle orientation the developing countries will produce three times the amount of E-Waste producing right now in the next few years.

The amount of e-waste being produced - including mobile phones and computers - could rise by as much as 500 percent over the next decade in some countries, such as India. The United States is the world leader in producing electronic waste, tossing away about 3 million tons each year. China already produces about 2.3 million tons (2010 estimate) domestically, second only to the United States. And despite having banned e-waste imports, China remains a major e-waste dumping ground for developed countries.

Electrical waste contains hazardous but also valuable and scarce materials. Up to 60 elements can be found in complex electronics. In the United States, an estimated 70% of heavy metals in landfills come from discarded electronics. The two most commonly employed disposal techniques are Land filling and Incineration. Land filling technique is the most commonly employed technique throughout the India and it is the cheapest one. The waste are dumped in open pits and covered with soil. This may cause pollution to the nearby water bodies and agricultural fields because of the leaching behaviour of the heavy metals with the soil. Incineration is costlier than Land filling and does not cause much pollution. They use large furnace called Incinerators operating @ 9000C. If any untreated vapours are released to the atmosphere it can cause pollution [2-3].

Instead of disposing the equipment as waste, they can be dismantled and the various components in them can be recycled or reused in many ways. This not only reduces the cost involved in purchase or in the demand of raw materials but also reduces the hazardous caused because of disposing E-Waste.

Today the electronic waste recycling business is in all areas of the developed world as a large and rapidly consolidating business. Here equipment is reverted to a raw material form. This diversion is achieved through reuse and refurbishing. The environmental and social benefits of reuse include diminished demand for new products and raw materials, larger quantities of pure water and electricity for manufacturing and diminished use of landfills. Many outdated equipments are recycled in these days for the above merits. Audio-visual components, televisions, VCRs, stereo equipment, mobile phones, other handheld devices, and computer components contain valuable elements and substances suitable for reclamation, including lead, copper, and gold.

Printed Circuit Boards (PCB)

Printed Circuit Boards (PCB) is one of the most widely used components in making of electrical and electronic equipments. It is used in connecting electrical and electronic components using conductive pathways etched from copper. Today PCB's are virtually present in all electronic gadgets. So when equipments te, PCB's are also present in it. The PCB's contains almost 40% of metals. Some of the PCB's are Copper (being the most around 30% by mass), Iron, Lead, Nickel, Aluminium,

ISSN: 0975-8585

One of the major challenges is recycling the printed circuit boards from the electronic wastes. The circuit boards contain such precious metals as gold, silver, platinum, etc. and such base metals as copper, iron, aluminium, etc. Conventional method employed is mechanical shredding and separation but the recycling efficiency is low.

An alternative technology for removal of hazardous metals from waste PCB's is Hydrometallurgy. Magnetic separation is another one that is widely used for removal of ferromagnetic metals from non-ferrous metals and other non-magnetic waste. There are various electrical methods like Ion Exchange, Electro deposition, Electrostatic Separator also available but only the removal of Copper is given importance.

The material composition of 4 random PCB samples is given in Table 1

Table 1: Material Composition of various samples of PCB's

Materials	Sample A	Sample B	Sample C	Sample D
METALS Max 40%				
Copper (Cu)	20	26.8	17.85	23.47
Aluminium (Al)	2	4.7	4.78	1.33
Lead (Pb)	2	-	4.19	0.99
Zinc (Zn)	1	1.5		1.51
Nickel (Ni)	2	0.47	1.63	2.35
Iron (Fe)	8	5.3	2	1.22
Tin (Sn)	4	1	5.28	1.54
Au/ppm	1000	80	350	570
Pt/ppm	-	-	4.6	30
Ag/ppm	2000	3300	1300	3301

These when disposed by the conventional methods like land filling and incineration, the metals present in them may contaminate in the nearby lands or water bodies and pose risk to biotic and abiotic components. Thus the study suggests a suitable way for removing the hazardous metals by chemical and biological methods.

MATERIALS AND METHODS

PULVERIZING PCB'S

The PCB's are dismantled from the electrical and electronic devices. Then they are pulverized to fine powder. Crushing is done less than 2mm size. But crushing to 0.5mm size is preferable. This PCB is subjected to a series of crushers to obtain a fine powder. Particle of size 0.5mm preferred. The crushers used are Jaw Crusher, Ball Mill and Drop Weight Crusher. This crushing is carried for almost 30 minutes. The sequence of crushing is shown in figure 1.

Figure 1: Equipment used for crushing PCB's

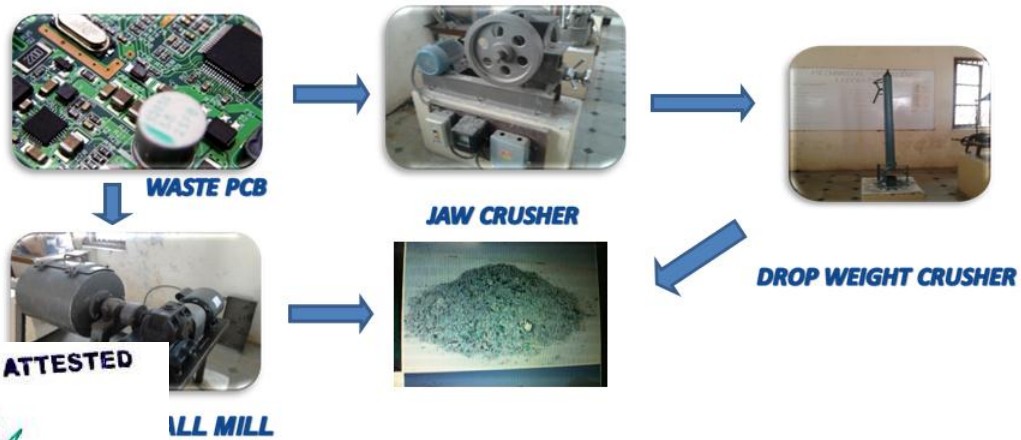

ISSN: 0975-8585

Chemical Treatment

The mixed acid is prepared by mixing equivalent volumes of sulphuric acid, Nitric acid and Hydrochloric Acid of equal normality. Here mixed acids of three different normalities (4N, 6N, 8N) are prepared i.e. mixing Sulphuric acid, Nitric acid and Hydrochloric Acid of 4N, 6N and 8N separately. In each case 10ml of each acid of same normality is mixed well to give the corresponding "Mixed Acid". Figure 2 gives the steps involved in the process of mixed acid leaching.

Figure 2: Steps involved in Process of mixed acid leaching

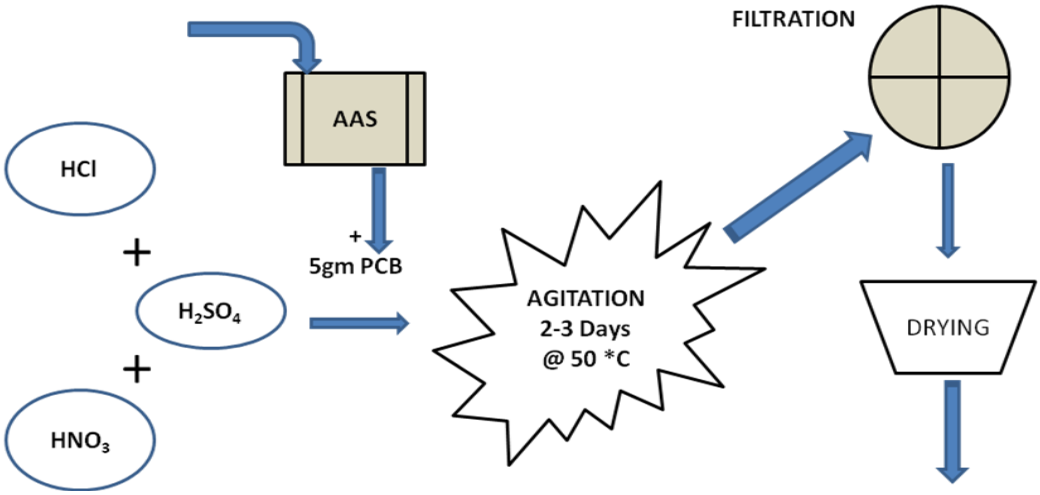

10ml of each acid of same normality are mixed in which 5grams of pulverized PCB's is added. The mixture is then subjected to agitation in a shaker with temperature and rpm controller. The agitation is carried out at 500C. The agitation is carried for 2 days and 3 days separately. The shaker is set to 200-300 rpm. After the period of agitation is over the contents are cooled in a water bath. The contents are then subjected to filtration where the resultant mass is separated off from the liquid. To clear the contents off completely from the vessel distilled water is used and they are filtered. The filtered mass is then dried in a Tray Dryer @ 1000C for 15-20 min. The drier is checked for every 5 minutes to prevent any burning. The sample of pulverized PCB's before treatment and the reacted PCB's that are filtered after treatment are subject to elemental analysis to find the percentage of hazardous metals present. Elemental analysis is done by AAS (Atomic Absorption Spectroscopy) technique [4-5].

Biological Treatment

Persea Americana seed used for creating the solvent for biological treatment is shown in figure 3

Figure 3: *Persea Americana* seeds used for creating the solvent for biological treatment

In biological treatment leaching process is carried out by using "Avocado" commonly called as Butter Fruit whose seeds are used as the raw material. The scientific name of Avocado is "Persea Americana". The aching is prepared as follows. The Avocado seeds in the form of activated carbon are in biological treatment [6]

ISSN: 0975-8585

The Avocado seeds are cut to pieces and sundried for 3-4 days to remove the moisture as much as possible. The dried seeds are removed off the debris and cleaned. Then it is again subjected to drying. The dried seeds are then subjected to crushing. The crushed powder is then subjected to screening where Mesh no 4 is used these are now taken in a Porcelain Crucible (withstands temperature of 12000C) and kept in a Muffle Furnace to convert into char. The Muffle Furnace is operated @ 5000C for 1 hour. After 1 hour we obtain char from the muffle furnace. It is cooled for nearly 1 hour and then taken in a Mortar where it is crushed using a pestle. The finely crushed activated char is taken in a beaker and then kept in an Autoclave @ 1300C for 3 hours, during the time duration constant pressure is maintained by regulating the release valve. Thereby we obtain activated carbon from Avocado seeds [7], [9-10].

Sequence of steps involved in the process of bio-solvent leaching is shown in figure 4

Figure 4: Steps involved in Process of process of bio-solvent leaching

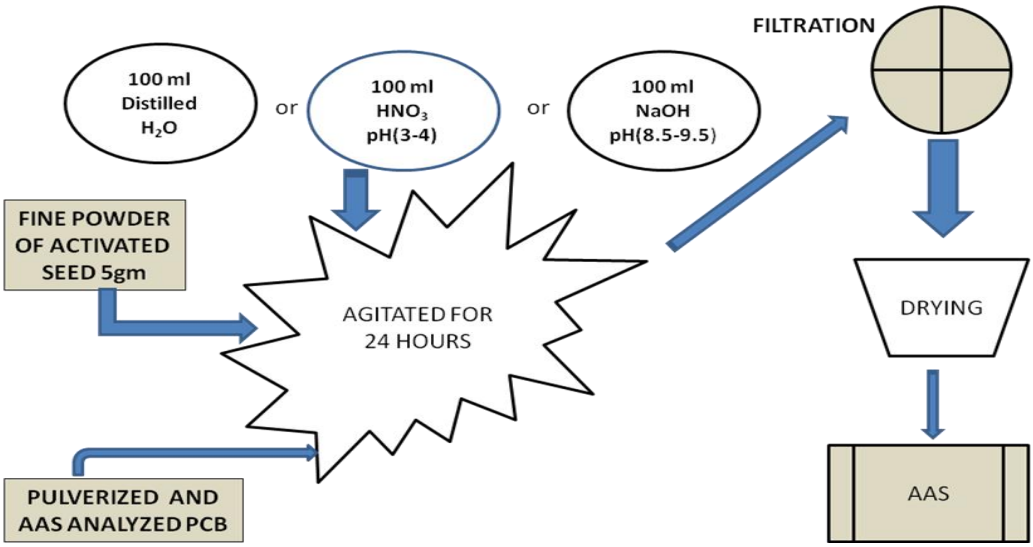

The activated carbon from above is used as the raw material. The biological treatment is carried out in three different pH conditions acidic (pH 3-4), basic (pH 8.5-9.5) and neutral (pH 7).

Initially 10gm of activated carbon is mixed with Nitric Acid / Sodium Hydroxide/ Distilled water mediums whose pH are adjusted by adding either base or an acid to the distilled water to get required values. To this mixture 5gm of PCB is added. The resultant mixture above is agitated for 24 hrs. in a shaker at room temperature (30*C). The shaker is set to 200-300 rpm. After the period of agitation is over the contents are subjected to filtration where the resultant mass is separated off from the resultant liquid. To clear the contents off completely from the vessel distilled water is used and they are filtered [8]. The resultant mass is then dried in a Tray Dryer @ 100*C for 15-20 minutes. The resultant is subjected to elemental analysis to find the percentage of hazardous metals present in it by weight. The results obtained are compared and thereby the most effective procedure for biological treatment is concluded. And finally compare whether biological treatment or chemical treatment is the effective one.

RESULTS AND DISCUSSION

Chemical Treatment

The leaching process was carried out using 4N, 6N and 8N “Mixed Acids” for 48 hours. The results obtained are shown in Table 2, 3and 4

ISSN: 0975-8585

Table 2: Percentage of metals removed by leaching with 4N mixed acid

S. No	Hazardous Metals	Initial Composition (%)	Final Composition (%)	Removal Efficiency (%)
1	Copper(Cu)	4.65	0.18	96.13
2	Lead (Pb)	0.46	0.09	80.43
3	Iron (Fe)	0.36	0.016	95.55

Table 3: Percentage of metals removed by leaching with 6N mixed acid

S. No	Hazardous Metals	Initial Composition (%)	Final Composition (%)	Removal Efficiency (%)
1	Copper(Cu)	4.65	0.062	98.67
2	Lead (Pb)	0.46	0.059	87.17
3	Iron (Fe)	0.36	0.023	93.61

Table 4: Percentage of metals removed by leaching with 8N mixed acid

S. No	Hazardous Metals	Initial Composition (%)	Final Composition (%)	Removal Efficiency (%)
1	Copper(Cu)	4.65	0.06	98.71
2	Lead (Pb)	0.46	0.024	94.78
3	Iron (Fe)	0.36	0.019	94.72

Figure 5: Percentage of metals removed by Chemical methods

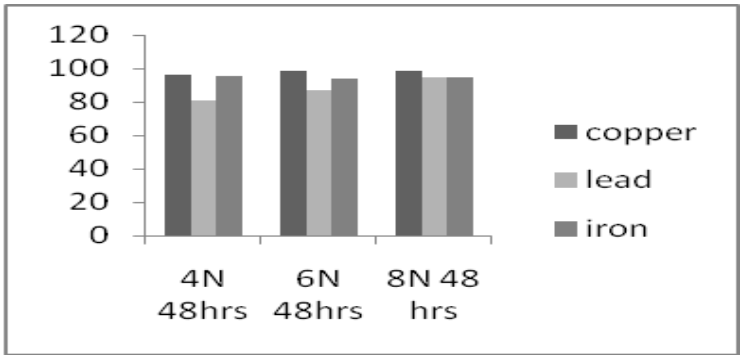

From the above results it is clear that 8N Mixed Acid Leaching is more effective in removing Iron, Lead and Copper with a removal efficiency above 90% for all the metals.

Biological Treatment

The leaching process was carried out using a solvent prepared from a biological agent and reacted under acidic, neutral and basic pH conditions for 48 hours. The PCB sample was then dried and analysed in AAS. The results obtained are tabulated in Table 5, 6, 7.

Table 5: Percentage of metals removed by leaching with bio-solvent under acidic pH conditions

S. No	Hazardous Metals	Initial Composition (%)	Final Composition (%)	Removal Efficiency (%)
1	Copper(Cu)	5.28	2.14	59.47
2	Lead (Pb)	0.75	0.1	86.67
3	Iron (Fe)	0.36	0.046	87.22

Table 6: Percentage of metals removed by leaching with bio-solvent under neutral pH conditions

S. No	Hazardous Metals	Initial Composition (%)	Final Composition (%)	Removal Efficiency (%)
1	Copper(Cu)	5.28	5.28	0
2	Lead (Pb)	0.75	0.75	0
	n (Fe)	0.36	0.18	50

ISSN: 0975-8585

Table 7: Percentage of metals removed by leaching with bio-solvent under basic pH conditions

S. No	Hazardous Metals	Initial Composition (%)	Final Composition (%)	Removal Efficiency (%)
1	Copper(Cu)	5.28	2.14	52.08
2	Lead (Pb)	0.75	0.1	0
3	Iron (Fe)	0.36	0.046	76.11

Figure 6: Percentage of metals removed by Biological method

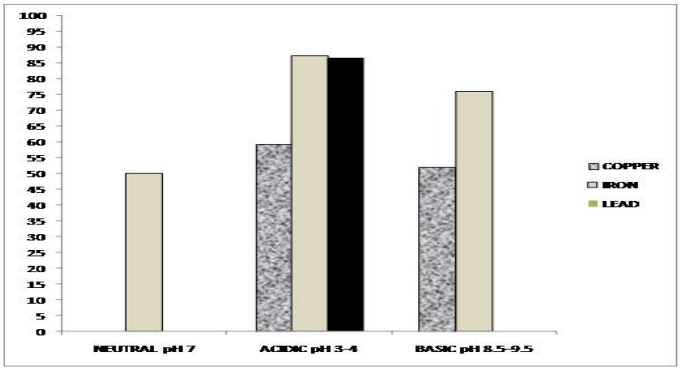

From the above results it is clear that Leaching in acidic pH is more effective in removing Iron, Lead and Copper with higher removal efficiency for all the metals.

CONCLUSION

When hazardous elements present in PCBs are disposed by the conventional methods like land filling and incineration, the metals present in them may pollute the land or water bodies and pose environmental risks to biotic and abiotic components

Chemical Treatment using 8N Mixed Acid Leaching was effective when compared to other Chemical Treatments (using 4N, 6N Acid Leaching) and more effective than Biological Treatments (using biological solvents under neutral pH, acidic pH and basic pH conditions).

The study suggests a suitable way for removing the hazardous metals by chemical and biological methods which is safe and economically viable.

ACKNOWLEDGEMENTS

The authors would like to thank Sathyabama University for providing an opportunity to carry out this research work.

REFERENCES

[1] Junaidah Ahmad Kalana. Int J Environ Sci 2010; 1: 132-136
[2] Olowu, Dejo, J LEAD, 2012; 8: 59-65
[3] Jha MK, Jae-chun Lee. J Metall Mater Sci 2006; 48: 117-128
[4] Ogunniyi, Vermaak MKG, Groot DR. 2009; 29: 2140-2146
[5] Oliveira C, Marta Cabral, Charters Taborda F, Margarido F. J Electronics & Battery Recycling '09, Proceedings. 2nd Intern. Conference, Toronto, 2009; 2
[6] Nilanjana Das, Vimala R, Karthikha. P. Indian J Biotechnol 2008; 7: 159-169
[7] Wan Nagh WS, Hanafiah MAKM, Bioresour Technol 2007; 99: 3935-3948
[8] Yakubu MK, Gumel MS, Abdulaahi AM. African J Sci Technol 2009; 9: 39-49
[9] Williams P. J Waste Biomass Valoriz 2010;1: 107-120
J Hazard Mater 2008; 158: 228-256

IJISET - International Journal of Innovative Science, Engineering & Technology, Vol. 2 Issue 5, May 2015.
www.ijiset.com

ISSN 2348 – 7968

Analysis of Harmonic Behaviour of Human Rhythmic Activity in A RCC Roof Slab

[1]G.Gajalakshmi, [2]Dr.J.Abbas Mohaideen, [3]Dr.A.R.Santha Kumar

[1] Asst.Prof., Department of Civil Engineering,Sathyabama university.

[2]Principal, Maamallan Institute of Technology, Sriperumbudur.

[3] Former Dean, Anna University. Chennai.

Abstract

Floor vibration is a natural phenomenon of a floor system in response to dynamic forces due to people activities like jumping, walking, dancing applied directly to the floor system. All suspended floors vibrate irrespective of the floor type whether steel or concrete or wood. The research related to vibration is not new and it is a complex phenomena. This paper is concerned with the dynamic study of a RCC floor slab of size7mx 7.5m. The analysis is done using ANSYS. The human rhythmic activity is been conducted on the slab and the modal and Harmonic analysis are done. The results are compared with IS 800 recommendations.

Key words: Vibration, rhythmic,Modal,Harmonic,Frequency,Amplitude,ANSYS

Introduction

The vibration is a general problem related to the dynamic movements of human rhythmic activities like jumping,dancing(Bachmann and Ammann 1987, Murray and Howard 1998, Silva et al. 2003). The modern construction concentrate on slender floor with high strength materials. This slender slab creates unwanted vibration. This excessive floor vibration can make people feel insecure and uncomfortable. Sometimes, the vibration can create people get afraid of a structural failure also. The fear, of course is unwarranted since the displacement and stress induced by floor vibration are generally small in view of the design criteria for structural safety.

This research is related to the dynamic response of human concerned with rhythmic activity slab. The aim is to i) analyse the RCC floor slab of size 7mx 7.5m using compare the result with IS 800-2007.

ISSN 2348 – 7968

Mathematical Equation from Faisca

Faisca (2003) considered the dynamic loads, based on results achieved through a long series of experimental tests made with individuals carrying out rhythmic and non-rhythmic activities. These dynamic loads, generated by human activities, are described such as jumps with and without stimulation, aerobics, soccer, rock concert audiences and dancing. The load modeling is able to simulate human activities like aerobic gymnastics, dancing and free jumps.

The mathematical representation of the human dynamic loading is described by the following equation .This expression requires some parameters like the activity period T, contact period with the structure Tc, period without contact with the model Ts, impact coefficient Kp, and phase coefficient CD.

$$F(t) = CD\left\{K_p P\left[0.5 - 0.5\cos\left(\frac{2\pi}{T_c}t\right)\right]\right\}, \text{for } t \le T_c$$

$$F(t) = 0, \text{for } T_c < t \le T$$

Where:

F (t): dynamic loading, in (N);

t: time, in (s);

T: activity period (s);

Tc: activity contact period (s);

P: weight of the individual (N);

Kp: impact coefficient;

CD: phase coefficient.

STRUCTURAL FLOOR DETAILS

The composite floor system consisted of span 7mx 7.5m .

RC Beam Details: 8"x 18"

Slab Thickness: 8"

ISSN 2348 – 7968

The concrete slab had a 25N/mm^2 specified compression strength and a 2.4x10^4 N/mm^2 Young's Modulus (Faisca).

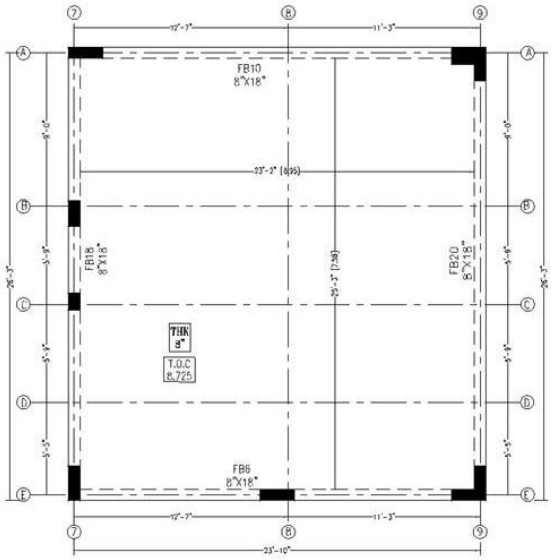

Fig.1 Layout of the floor plan.

Finite Element Analysis using ANSYS

The proposed computational model, developed for the RCC floor dynamic analysis, adopted the usual mesh refinement techniques present in finite element method simulations implemented in the ANSYS program (ANSYS, 11). In the present computational model, the floor beams are represented by three-dimensional beam elements (BEAM44), tension, compression, bending and torsion capabilities. The floor slab is represented by shell finite elements (SHELL63).

In this investigation, it is considered that materials (beam and slab) presented total interaction and have an elastic behaviour.

ANALYSES OF FLOOR MODEL

LOADING SCHEME

The individual person weight is equal to 70kg(0.8kN- Bachmann &Amman, 1987).The assumed Damping ratio is equal to 2%(ξ = 0.02(IS 800- 2007).

ıan-induced dynamic action is applied to the dancing area, as shown in Fig. :e floor dynamical response, are obtained on the nodes A and B to verify the

ISSN 2348 – 7968

influence of the dynamical loads on the adjacent slab floor, as shown Fig. 2. In the current investigation, the human rhythmic dynamic loads are applied to the structural model corresponding to the effect of 2, 4, 8, 10, 12,14,16 and 18 individuals practicing aerobics. Hence 18 individual practicing is the full load condition for the numerical model.

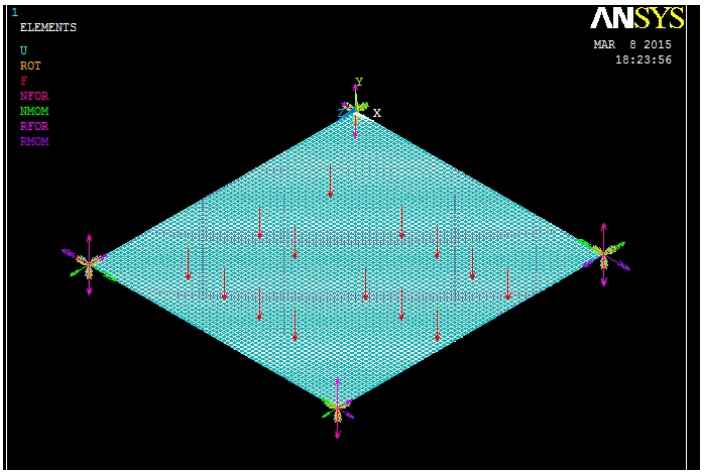

Fig.2 Load distribution Scheme associated to fourteen individuals

METHODS OF ANALYSIS

The following analysis are performed for the numerical model,

- Model Analysis
- Harmonic analysis

MODAL ANALYSIS

The concrete floor's natural frequencies is determined with the aid of the numerical simulations. The structural system vibration mode shapes and the natural frequency values are tabulated. It is starting point for more detailed dynamic analysis, such as harmonic response analysis, transient dynamic analysis.

HARMONIC ANALYSIS

The FE model composite floor is subjected to human activities such as human rthymicactivity(jumping). The mode-superposition method available in ANSYS computer ted for the Harmonic analysis, which is advantageous in tracing the harmonic The FE Model subjected to the forcing frequency of range 0 to 50Hz and

ISSN 2348 – 7968

corresponding Amplitudes are measured. The dynamic response of FE model floor Amplitudes are compared by varying number of person's activities.

Results and Discussions.

Modal Analysis:

The first six mode shapes are considered and the corresponding natural frequencies are tabulated.

Table1. Mode Shape and its Natural Frequency

Mode shape	1	2	3	4	5	6
Natural frequency	9.055	16.913	17.983	21.302	29.645	37.621

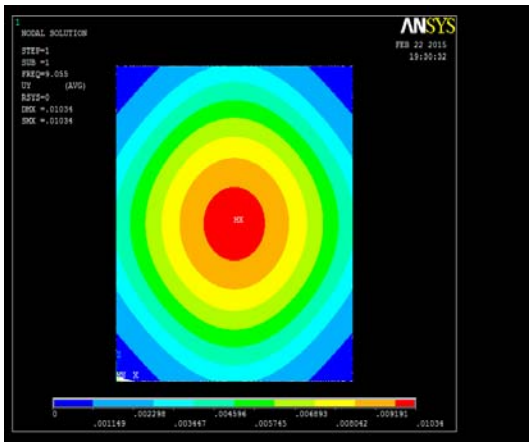

Fig.3 Mode shape 1 with natural frequency 9.055 Hz.

ISSN 2348 – 7968

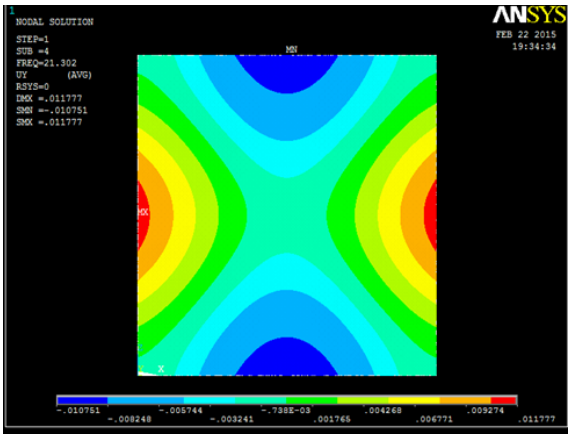

Fig.4 Mode shape 4 with natural frequency 21.302Hz.

Harmonic Analysis:

The results of 2,4,6,8,10,12,16 &18 persons rhythmic movements of Harmonic analysis are tabulated below.

Table 2.maximum amplitude values

No of Persons	Maximum.Freq		Maximum Amplitude	
	Point A	Point B	Point A	Point B
2	9.05	9.05	0.12	0.147
4	9.05	9.05	0.251	0.305
6	9.05	9.05	0.375	0.46
8	9.05	9.05	0.49	0.599
10	9.05	9.05	0.639	0.778
12	9.05	9.05	0.732	0.891
14	9.05	9.05	0.851	1.039
16	9.05	9.05	0.981	1.19
18	9.05	9.05	1.09	1.334

ISSN 2348 – 7968

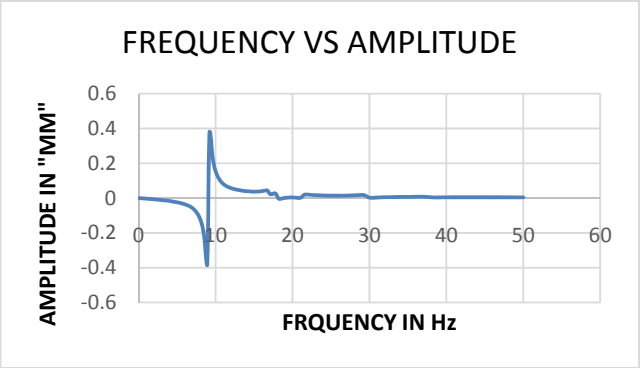

Fig.5 SIX PERSONS LOADING AT POINT A

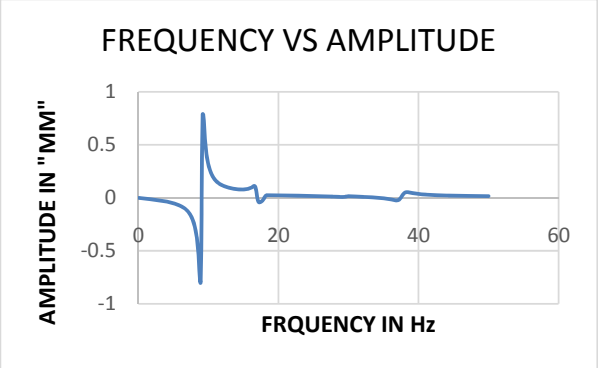

Fig.6 TEN PERSONS LOADING AT POINT B

Discussions:

IS 800-2007 quotes that" In the frequency range of 2 to 8Hz in which people are most sensitive to vibration"

The first natural frequency which is obtained from analysis is 9.05Hz. This value is closer to the value suggested by IS 800. The floor slab may be in the critical place for dynamic activities like jumping.

Two points A & B are selected on which the response like modal analysis and Harmonic analysis are obtained.

The first six mode shapes are considered for such dynamic activities. The amplitudes are measured at point A and B. The human induced loads by jumping on the respective node two persons are allowed to jump. Consecutively it is by 4,6,8,10,12,16,18 lues are comparatively lesser in point A to Point B.

ISSN 2348 – 7968

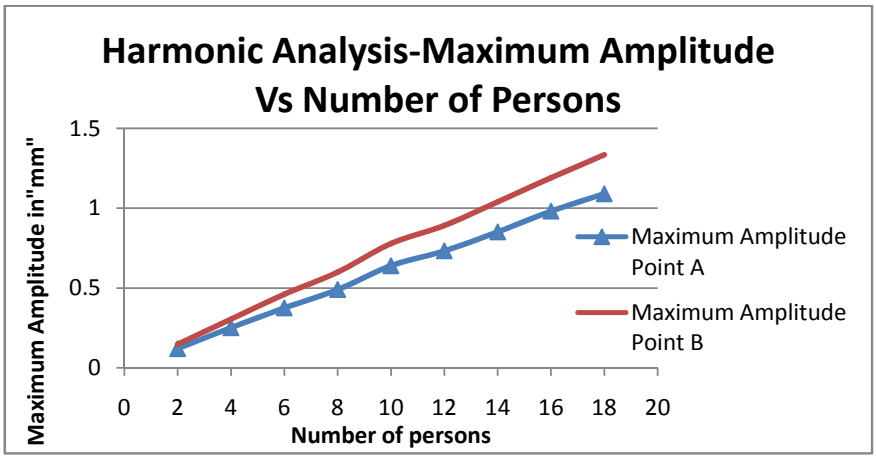

*Fig. 7*Harmonic Analysis-Maximum Amplitude Vs Number of Persons

Conclusion:

The RC concrete floor slab is analysed using ANSYS. The first natural frequency is obtained as 9.05 Hz. As per IS 800, " Natural frequency of the floor vibration corresponding to the lowest mode of vibration, damping characteristics are important characteristics in floor vibration". Since the frequency value is to the value of 8Hz(IS 800-2007), it advise able to make floor with more stiffness. The designer should know the occupancy usage of floor before construction. This will make the structure under dynamic activities like human rhythmic activity more stiffener at the initial stage itself.

Reference:

1. Allen ,D.E et al(1985) Vibration criteria for assembly occupancies, Canadian journal of Civil engineering, vol.12, pp. 617 – 623.

2. Allen ,D.E (1990) Building vibration from human activities, ACI concrete International -Design and Construction.

3. Bachmann,H (1992) Case studies of structures with man induced vibration , Journal of Structural Engineering,vol-118,No:3.

lingwood,M and Andrew Tallin (1984) Structural Serviceability -Floor ı, Journal of Structural Engineering, vol.110,No.2,ISSN 0733-9445.

ISSN 2348 – 7968

5. Da Silva, J.G.S. et al(2006) Dynamical response of composite steel deck floors, Latin American Journal of Solids and Structures, 3 .

6. Da Silva, J.G.S. et al(2008) Vibration Analysis of orthotropic composite floors for human rhythmic activities, Journal of Brazilian Society of Mechanical Sciences and Engineering, pp. 56 – 65, 2008.

7. Da Silva, J.G.S. et al(2011) Vibration Analysis of long span joist floors submitted to Human Rhythmic Activities, State University of Ride janeiro , ISBN 978-953-307-209-8, pp. 231 – 244, 2011.

8. Faisca, R.G. (2003)Caracterização de cargasdinâmicasgeradasporatividadeshumanas (Characterization of Dynamic Loads due to Human Activities), PhD Thesis (in Portuguese), COPPE/UFRJ, Rio de Janeiro, RJ, Brazil, pp. 1-240

9. IS 800:2007, Indian standard general construction in steel – code of practice- third revision

10. Murray,T.M et al (2003) Floor vibrations due to human activity, Steel design guide series by American institute of steel Construction.

IOSR Journals
International Organization
of Scientific Research

International Organization
of Scientific Research
Community of Researchers

Is hereby honoring this certificate to

Abbas.J.Mohaideen

In recognition of the Publication of Manuscript entitled

Determination of Lead in fish, water and sediment

Published in IOSR Journal of Environmental Science, Toxicology and Food Technology

Vol. 8, Issue 9, September 2014

TRUE COPY ATTESTED

PRINCIPAL
MOHAMED SATHAK ENGINEERING COLLEGE
KILAKARAI-623806.

Editor-In-C
IOSR-JES

E-mail id : ***iosrjestft@gmail.com***
Web.: ***www.iosrjournals.org***

International Journal of Applied Engineering Research, ISSN 0973-4562 Vol. 10 No.2 (2015) pp. 1243-1245
 http://www.ripublication.com/ijaer.htm

Electro-Kinetic Remediation To Evaluate And Enhance The Removal Of Arsenic From Cultivated Soil And Red Soil

M.D. Duraimurugan alias Saravanan [1,*], S.P. Shanmuga Priya[1], T. Boobalan [1], A. Arunagiri [2]

[1]Department of Chemical Engineering, Mohamed Sathak Engineering College, Kilakarai, Ramanathapuram, Tamil nadu - 623 806, India

[2]Department of Chemical Engineering, National Institute of Technology, Tiruchirappalli - 620015, India

* Corresponding author: durai_sar2003@yahoo.co.in

Abstract: **Electro-kinetic remediation is a relatively new technique examined to evaluate and enhance removal of the arsenic residues from cultivated soil and red soil. Short duration 10 hours treatment approach is initiated for this purpose. Laboratory 1-D column tests are performed on cultivated soil and red soil under the influence of a DC electric field. Mobilized charged species, causing ions and water to move toward the electrodes. Metal ions and positively charged compounds move toward the cathode. NaOH and tap water are purged through the direction of electro osmotic flow to enhance arsenic remediation. Configuration of electrodes/reactor setup is also adjusted to improve the removal efficiency of the arsenic chemicals by inducing buoyancy with electro-osmotic flow. Interesting results are obtained showing up to 54% of arsenic removal by purging Sodium hydroxide (NaOH). Also the applications of this electro kinetic technique are dewatering, ground water purification, and detection of metallic minerals and manipulation of bio-particles.**

Keywords: Electro kinetic technique, Arsenic, Electro-osmotic flow Ground water purification.

INTRODUCTION

Electro kinetics is a developing technology that is intended to separate and extract heavy metals, radionuclides, and organic contaminants from saturated or unsaturated soils, sludge and sediments, and groundwater. In recent years there has been considerable interest in the application of electro kinetic processes, especially for the remediation of low permeability contaminated soils, and ground water (1). The demand to develop innovative, cost-effective remediation technologies in waste management provided the impetus to exploit the conductive properties of soils, and using an electric field to remove chemical species from soils (2, 3). Electroosmosis is the movement of soil moisture or groundwater from the anode to the cathode of an electrolytic cell. Electromigration is the transport of ion complexes to the electrode of opposite charge. Electrophoresis is the transport of charged particles or colloids under the influence of an electric field: contaminants bound to mobile particulate matter can be transported in this manner (4).

MATERIALS AND METHODS

Material and chemicals

Saturated /partially saturated cultivated soil and red soil samples have been collected from the Mayakulam land Mohamed Sathak Engineering College campus. And these samples have the various sizes. Then these soil samples have been sieved into the size of 300µm and below. All the chemicals and sol-vents used in the experiments were obtained from Sigma (St. Louis, MO), Super Religare Laboratories (SRL).

2.2. METHODOLOGY

Experimental Design

This experimental program consist of series of 1-D column trials designed to determine the feasibility of remediation of the arsenic compound and to find a suitable purging chemical for the efficient desorption of contaminants. A total of four electro-kinetic experiments were conducted on cultivated soil and red soil. Two tests were performed in Series-1 to study remediation of arsenic in the cultivated soil. Series-2 has also two tests performed to decontaminate arsenate in the red soil. Table 1- shows details of the testing chart. In all investigations, an applied electric field induced electro-osmotic flow moved the pore fluid through the soil from anode towards cathode. All tests were accomplished in the experimental reactor shown in Figure 1 which was exclusively built for this study. Soil was contaminated with 50 mg/kg of arsenic. In series-1, the first experiment (EK-1) was conducted as a baseline, where tap water was purged as an enhancement solution. And the next test (EK-2) was conducted in the presence of enhancing chemical NaOH (0.1N) used for the purging with the goal of increase arsenic decontamination. In series-2, the first experiment (EK-3) was conducted with tap water as an enhancement solution. And the next test (EK-4) was conducted in the presence of enhancing chemical NaOH (0.1N) used for the purging with the goal of increase arsenic decontamination.

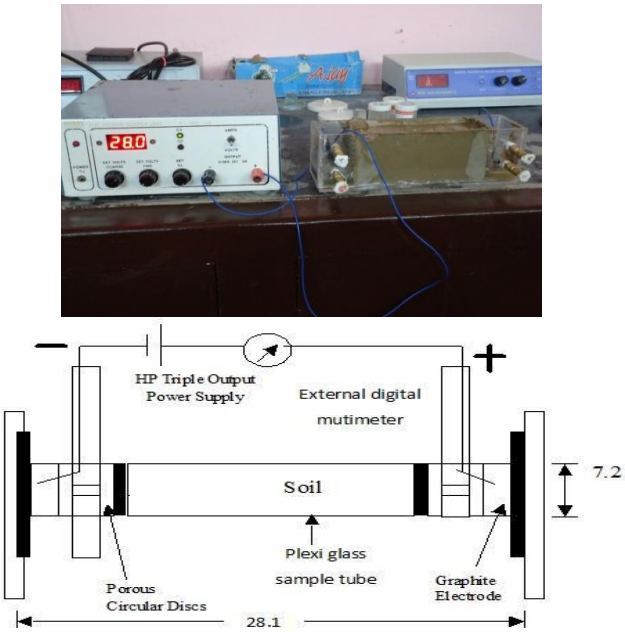

Figure 1. Experimental reactor for electro kinetic tests cultivated soil and red soil

2.2.2. Contaminated soil preparation

The cultivated and red soil was artificially contaminated in all electro-kinetic tests. Dry clean soil of 550 g was spiked with the standard solutions prepared using As2O3. The standard solution was added in such a way that the desired concentration (as mentioned in Table 1) was achieved. De-ionized water was added to the spiked soil to fix the water content. Soil was mixed thoroughly; contaminated soil was poured in the electro-kinetic reactor in 2-inch layers.

2.2.3. Electro-kinetic Reactor Setup

The electro-kinetic cell was fabricated using a Plexiglas tube having a length of 28.1 cm and height of 7.2 cm. The actual length of the soil specimen was 18.1cm. The spiked soil specimen was placed in the cell in 2-inch layers and was then allowed to equilibrate for 10 hr as shown in Figure 1, filter papers, porous disk and graphite electrodes are placed at the both end soil column. The porous discs were used to separate the soil from the electrodes at each end of the soil column. This space constituted a small fluid compartment at the cathode and anode. Depending on the test, these fluid compartments were filled with water or chemicals. Fluid levels at cathode and anode compartments were maintained at almost the same level to avoid any hydraulic gradient. The electrodes were connected to a dc electric power supply. A constant voltage gradient of 1DV/cm was applied to the soil sample. At the beginning of the tests soil was partially saturated with water content ranging 34% to 35%. But after 2 to 3 hours it was observed to be fully saturated when steady outflow (effluent) starts.

2.2.4. Test procedure

The current across the soil sample was measured during the experiment using the instrument Regulated Power Supply. Also pH and conductivity of the aqueous solutions in both the anode and the cathode reservoirs was monitored throughout the duration of experiments (10 hour). Conductivity was measured by conductivity cell; pH was measured using a differential electrode. The inflow and outflow through the electrode compartment was also be monitored to determine the electro-osmotic flow.

2.2.5. Post electro-kinetic treatment

At the end of the test, aqueous solutions from both the cathode (catholite) and anode (anolite) compartments and reservoirs were collected and volume measurements were made. The reservoirs and the electrode assemblies were carefully disconnected. For every 2 hours pH and conductivity of the samples have been taken. Treated soil was extruded from the cell and 10 g of soil was taken and mixed with 10 ml of de-ionized water in a glass beaker. The mixture was shaken thoroughly by hand and the solids were allowed to settle. The pH and conductivity of the soil as well as that of the aqueous solutions from the electrodes were measured using the above-mentioned apparatus.

2.2.6. Metal analysis

Water samples have been collected from electro-osmotic flow, anode and cathode reservoir were digested and the final concentration of arsenic have been determined by using UV spectrophotometer.

2.2.7. Contaminant concentration in soil

Precautions were taken in order to ensure the accuracy and repeatability of the test results. These precautions included. Soaking the apparatus, electrodes, porous stones and tubing in dilute acid solution for 24 h and rinsing with tap water followed by de-ionized water to avoid cross contamination between experiments. Each sample was check UV spectrophotometer performing a mass balance analysis for each test.

RESULTS AND DISCUSSION

Results from tests EK-1, EK-2, EK-3 and EK-4 are grouped in Series 1 and series 2. The objective of these tests was to evaluate remediation of arsenic from cultivated soil and red soil with different purging solutions .Soils in these experiments were contaminated by arsenic with a concentration of 50 mg/kg .In series-1 (cultivated soil) and in series 2 (red soil), the experiments (EK-1), (EK-2) (EK-3) (EK-4) was conducted with tap water and NaOH (0.1N) as purge solutions respectively.

Table 2 presents a summary of the experimental program of series-1 and series-2. Results for pH and conductivity of anolyte and catholyte which indicate the soil environment are shown. At the end of experiment, soil pH and conductivity were measured. Finally, concentration of arsenic of the treated soil was determined to get the clear idea of contaminant migration and remediation.

Treated Soil

At the end of the electro-kinetic treatment, 10g of soil was taken. Soil pH and conductivity were measured to get the idea of soil environment and contaminant migration. Finally arsenic concentration of the treated soil was determined to determine arsenic migration and remediation.

pH profiles

Table 2 shows the initial pH of cultivated soil ranged from 5.6 to 8.0. A sharp drop of pH from anode to cathode was observed in all tests. Treated soil pH near the anode ranged 2.1-3.5, and pH in cathode region ranged 4.9-11.3. As mentioned in previous section, the main reason for low pH at anode zone was generation of H+ at anode. Enhancement solution NaOH in EK-2 was probably not able to control the soil pH near the anode and it remained lower than expected.

Conductivity

Table 2 shows the conductivity profile of the treated cultivated and red soil specimen. Conductivity ranged between 0.35-43.3 mhoS/cm at the anode and 1.73-40 mhoS/cm at the cathode. Slightly higher conductivity was observed near the anode indicating higher accumulation of ionic species.

Table 1. Test plan

Tests	Test title	Target contaminant	Spike soil concentration (mg/kg)	Chemicals purged	Initial water content
Series-1	EK-1	AS	50	Tap water	35%
	EK-2	AS	50	NaOH 0.1N)	35%
Series-2	EK-3	AS	50	Tap water	35%
	EK-4	AS	50	NaOH 0.1N)	35%

Table 2. Experimental program for arsenic remediation (Series-1 and series 2)

Parameters	Tests			
Initial soil pH	EK-1	EK-2	EK-3	EK-4
	8.26	8.6	6.67	9.17
Initial soil conductivity mho S/cm	1.777	2.62	9.27	17.5
Voltage gradient DV/cm	1	1	1	1
Purging solution	Tap water	NaOH	Tap water	NaOH

Table 3. Efficiency for cultivated soil and red soil with their purge solutions

Series	Tests	Initial concentration of arsenic (mg/kg)	Concentration of arsenic (mg/kg)			Removal efficiency
			Anode	Cathode	Soil	
1	EK-1	50	2.7	8.8	38.5	23%
	EK-2	50	7	16.5	26.5	47%
2	EK-3	50	3.9	11.6	34.5	31%
	EK-4	50	9.2	17.8	23	54%

CONCLUSION

The main features of electro-kinetics, which makes it particularly attractive for remediation of hazardous waste sites, is as follows: It is less risky from the point of view of health hazard. Contaminant migration is independent of soil pore size; therefore this technology is applicable in low permeable soils, where pressure driven techniques are prone to flow channeling through cracks or soil rupture. It is applicable to inaccessible sites, because of the easy placement of electrodes. This study has examined the suitability of an electro-kinetic remediation system for the efficient removal of residual of the arsenic from cultivated soil and red soil. Recovery in series-1 where main goal was arsenic remediation ranged from 23% to 47% (Table 3). In series-2, arsenic recovery was 31% to 54%. Low mass recovered were in EK-3 (arsenic recovery 31%), EK- 4 (arsenic recovery 54%) These differences may be due to the non-uniform contaminant distribution within the selected soil sample for chemical analysis and adsorption of contaminants onto the electrodes and porous stones. Applying 0.1 N NaOH purging solution can lead to 47% arsenic removed from the soil in 10 hours. These indicate that alkaline chemicals can enhance the remediation of these chemicals. Since contaminant migration/removal depends on various factors such as soil pH, conductivity, sorption-disorption, ionic mobility of contaminants, the possible enhanced removal could be achieved if these factors can be controlled. The other possible enhancement of removal could be associated with the particulate position of the reactor (position of the electrodes in the soil, if performed at the field). The targeted modification of electro-kinetic technique that would allow enhancement of the buoyancy force could adapt this technique to removal of hydrocarbons (petroleum products, benzene, phenol, and different acetates), or even for creation of hydrodynamic barrier to prevent subsurface contamination.

ACKNOWLEDGEMENTS

The authors are thankful to the Principal and Management, Mohamed Sathak Engineering College, Kilakarai-Ramanathapuram, for providing the necessary laboratory facilities.

REFERENCES

[1] Danuta, L., and Hafiz, A., 2006, "Toxic elements in soil and groundwater: short-time study on electro kinetic removal of arsenic in the presence of other ions," Int. J. Environ. Res. Public Health, 3(2), 196-201.

[2] Hafiz, A., 2004, "Evaluation and enhancement of electro-kinetic technology for remediation of chromium copper arsenic from clayey soil," The Florida State University College of Engineering.

[3] Utchimuthu, N., Saravanakumar, K., and Joshua, A.D., 2012, "Removal or reducing heavy metal (lead) from soil by electro kinetic process," Int. J. Eng. Res. App. 2(3), 2248-9622.

[4] Reddy, K.R., and Supraja, C., 2004, "Enhanced electro kinetic remediation of heavy metals in glacial till soils using different electrolyte solutions," J. Environ. Eng., 130(4), 442–455.

Available online www.jocpr.com

Journal of Chemical and Pharmaceutical Research, 2015, 7(10S):174-177

Review Article

ISSN : 0975-7384
CODEN(USA) : JCPRC5

Arsenic pollution in India–An overview

Shanmugapriya S. P.[1*], Rohan J.[1] and Alagiyameenal D.[2]

[1]*Mohamed Sathak Engineering College, Kilakarai, Ramanathapuram, Tamilnadu*
[2]*Department of Civil Engineering, MSEC, Kilakarai*

ABSTRACT

There is general notion that most of the arsenic were from Himalayan Mountains and are then deposited in alluvial deposits. Higher proportions of arsenic are to be found in sedimentary rocks than that of igneous and volcanic rocks. Arsenic contamination has recently received worldwide attention because of the nature of its health effects Arsenic poisoning in India is more than 50 µg/L covering almost 7 states becoming the biggest natural groundwater calamity to the human beings. Exposure to arsenic through inhalation causes both acute and chronic problems resulting in severe damage of brain and nervous systems as well as peripheral nervous systems. Oral exposure to arsenic results in skin related disorders or even liver and kidney disorders. This paper discusses the multiple sources and effects of arsenic compounds in eastern parts of India, where the impacts on water quality and public health are seen in disastrous proportions. They are 6 of 17 districts in West Bengal, 20 of 70 districts in Uttra Pradesh, 13 districts in Bihar, 20 of 24 districts in Assam, 3 of 4 districts in Tripura, 6 of 13 districts in Arunachal Pradesh, 2 of 8 districts in Nagaland and 1 of 9 districts in Manipur.

Key words: Arsenic Compounds. Pollution effects, sources, contamination, India

---

INTRODUCTION

Arsenic's history in science, medicine, and technology has been overshadowed by its notoriety as a poison in homicides. It is viewed as being synonymous with toxicity. Arsenic contamination in water supplies continues to increase in many countries, especially in developing nations, thereby creating both environmental and health hazard and often referred to as a 20th, 21 st century calamities. High arsenic concentrations have been reported recently from China, Chile, Bangladesh, India, Taiwan, Mexico, Argentina, Poland, Canada, Hungary and Japan. Among 21 countries in different parts of world affected by ground water arsenic contamination, the largest population at risk is in Bangladesh followed by west Bengal in India.

Arsenic and its forms in environment:
Arsenic is a metalloid widely distributed in the earth's crust at an average concentration of 2 mg/kg and appears in Group 15 (V) of the periodic table, below nitrogen and phosphorus. Elemental arsenic, which is also referred to as metallic arsenic, (As 0)) normally, occurs as the α-crystalline metallic form, which is a steel gray and brittle solid. The β-form is a dark gray amorphous solid. Other allotropic forms of arsenic may also exist. In compounds, arsenic typically exists in one of three oxidation states, -3, +3, and +5 . Arsenic compounds can be categorized as inorganic, compounds without an arsenic-carbon bond, and organic, compounds with an arsenic-carbon bond. Over 200 arsenic-containing minerals have been identified, with approximately 60 per cent being arsenates, 20 per cent sulphides and sulphosalts, and the remaining 20 per cent including arsenides, arsenates and oxides. The most rm is arseno pyrite, an iron arsenic sulphide associated with many types of mineral deposits luding sulphide mineralization

1.1 Sources of arsenic:
Arsenic can be released into the atmosphere and water in the following ways:
1. natural activities, such as volcanic activity, dissolution of minerals (particularly into groundwater), exudates from vegetation and wind-blown dusts;
2. human activities, such as mining, metal smelting, combustion of fossil fuels, agricultural pesticide production and use, and timber treatment with preservatives;
3. remobilization of historic sources, such as mine drainage water;
4. Mobilization into drinking-water from geological deposits by drilling of tube wells.

It has been estimated that about one-third of the atmospheric flux of arsenic is of natural origin. Volcanic action is the most important natural source of arsenic, followed by low-temperature volatilization. Inorganic arsenic of geological origin is found in groundwater used as drinking-water in several parts of the world, for example Bangladesh. Organic arsenic compounds such as arsenobetaine, arseno- choline, tetramethylarsonium salts, arsenosugars and arsenic- containing lipids are mainly found in marine organisms although some of these compounds have also been found in terrestrial species. Elemental arsenic is produced commercially from arsenic trioxide. Arsenic trioxide is a by-product of metal smelting operations. It has been estimated that 70% of the world arsenic production is used in timber treatment as copper chrome arsenate (CCA), 22% in agricultural chemicals like pesticides, and the remainder in glass, pharmaceuticals and non-ferrous alloys

1.2 Applications of arsenic compounds:
Arsenic was used in some medicinal applications until the 1970s. Inorganic arsenic was used in the treatment of leukaemia, psoriasis, and chronic bronchial asthma, and organic arsenic was used in antibiotics for the treatment of spiro- chetal and protozoal disease (ATSDR, 2007).after that Arsenic compounds are used in making special types of glass, as a wood preservative and, lately, in the semiconductor gallium arsenade, which has the ability to convert electric current to laser light. .Because of its high electron mobility, as well as light-emitting, electromagnetic and photovoltaic properties, gallium arsenide is used in high-speed semiconductor devices, high- power microwave and millimetre-wave devices, and opto-electronic devices, including fibre- optic sources and detectors .Arsine gas AsH3, has become an important dopant gas in the microchip industry, although it requires strict guidelines regarding its use because it is extremely toxic. During 1990– 2002, approximately 4% of arsenic produced was used in the manufacture of glass, and 1–4% was used in the production of non-ferrous alloys.

1.3 Effects of arsenic on human health
There are different pathways through which arsenic enters human systems: drinking water, inhalation and dermal uptake. . The problem is severe in South Asia, particularly in Bangladesh and eastern parts of India, where the impacts on water quality and public health are seen in disastrous proportions. While the World Health Organization (WHO) suggest a standard of 50 micrograms per litre (mg l-1) (WHO, 1993), scientific studies advise a much lower value of 10 ppb (WHO, 1999).

The order of toxicity of arsenicals is :

MMA (lll) > Arsenite (lll) > Arsenate (V) > MMA (V) = DMA (V)

Several studies have also shown that inorganic arsenic can increase the risk of lung, skin, bladder, liver, kidney and prostate cancers. Arsenic can cause cancer, blindness and fetal malformations in other mammals and amphibians. Various adverse health effects including cancer have been reported from the districts in West Bengal which are associated with prolonged arsenic exposure. Blackfoot disease is more prevalent in developing countries, particularly among the poor, because the process of detoxification of arsenic may not take place in their bodies as a result of nutritional inadequacies.

Arsenic is also associated with the growth retardation in children. The height of children might be affected by the arsenic in drinking water. The children who have high arsenic concentration in their hair had less height than the children with low arsenic.(Nrashant Singh,2007)

2. ARSENIC PERIL IN INDIA
In India seven states have so far been reported by arsenic contamination in ground water above the permissible limit of 10 microgram per litre. As of 2008, West Bengal, Jharkhand, Bihar, Uttar Pradesh in flood plain of Ganga River; Assam and Manipur in flood plain of Brahamaputra and Imphal rivers, and Rajnandgaon village in Chhattisgarh xposed to drinking arsenic contaminated hand tube-wells water. The area and population of km2 & approx. 360 million respectively, in which 88688 km2 and approximately 50 million ected vulnerable to groundwater arsenic contamination. Almost all the identified arsenic

affected areas in the Gangetic plains except areas in Chhattisgarh and 3 districts in Bihar namely, Darbhanga, Purnea and Kishanganj, are in a linear tract on either side of the River Ganga in UP, Bihar They are 6 of 17 districts in West Bengal, 20 of 70 districts in Uttra Pradesh, 13 districts in Bihar, 20 of 24 districts in Assam, 3 of 4 districts in Tripura, 6 of 13 districts in Arunachal Pradesh, 2 of 8 districts in Nagaland and 1 of 9 districts in Manipur.

2.1 West Bengal:

Since groundwater arsenic contamination was first reported in year 1983 from 33 affected villages in four districts in West-Bengal, the number of villages has increased to 3417 in 111 blocks in nine districts till 2008 in West Bengal alone. There can be several other lists of arsenic affected areas prepared by different organizations, which may differ from one to another, because of number of reasons, e.g.,(i) number of samples analyzed, and different sampling locations (ii) compilation of information may be different, etc. However, the fact is that during last 25 years, with every additional survey, an increasing number of contaminated villages and more affected people have been identified. In the last 18 years of survey, we analyzed 140,150 water samples from hand-tube wells in West Bengal and found that 48.2% had arsenic concentrations of >10 µg/L and 23.9% had >50 µg/L. Nine of 19 districts were severely affected (50 µg/L), five each were in the mildly-affected (most of them had concentrations of <50 µg/L) and safe categories (<10 µg/L). We found that 3,500 villages from 90 blocks were arsenic-affected. The area and population of the nine arsenic-affected districts are 38,865 sq km and 50 mil- lion respectively.

2.2 Bihar

In 2002, groundwater arsenic contamination first surfaced in two villages, Barisban and Semaria Ojhapatti in the Bhojpur district of Bihar in the Middle Ganga Plain. The area is located in the flood-prone belt of Sone-Ganga inter-fluve region. Investigations by Central Ground Water Board and Public Health Engineering Department, Bihar indicated contamination as high as .178 µg/L in the surrounding villages, affecting the hand pumps, which are generally at 20-40 m below ground surface. With ongoing study, more and more contaminated districts have surfaced. It was reported (CGWB, 2008) that by the year 2008, out of 38 districts, 15 districts covering 57 blocks are exposed to groundwater arsenic contamination above 50 µg/L. These districts are: i) Buxar ii) Bhojpur, iii) Patna, iv) Lakhisarai v) Saran, vi) Vaishali vii) Begusarai, Samastipur, ix) Munger, x) Khagaria, xi) Bhagalpur xii) Darbhanga, xiii) Purnea xiv) Katihar xv) Kishanganj (Figure-2.7). These districts are mostly distributed along the course of the river Ganga in Bihar except three; (i) Darbhanga, (ii) Purnea and (iii) Kishanganj, which are in isolated and scattered places showing no distinct routes of connection to one-another gravel, etc.

2.3 Uttra Pradesh

Groundwater arsenic contamination in UP was first exposed in 2003 by SOES from survey of 25 villages in Ballia district. Thereafter, with continued survey two more districts, Gazipur and Varanasi were detected for arsenic groundwater contamination. As of 2008, 3 districts covering 69 villages in 7 blocks in Uttar Pradesh were found affected by arsenic groundwater contamination and people suffering from arsenical skin lesions. The used to drink water of hand pump operated tube wells. All those tube wells tap groundwater from shallow aquifer below about 20-30 m.

2.4 Jharkhand

During 2003-2004, groundwater arsenic contamination above 50 µg/L was first reported by SOES in the Sahibganj district of the Jharkhand, in the middle Ganga plain. Later on (2006-07), it was confirmed by CGWB through detailed investigation. Arsenic contamination is close to the Ganga River and in those areas from where the Ganga River shifted during recent past. The hand pump tube-wells of depth range 25-50 m were reported to be contaminated, and the affected areas had similar geological formations as in adjacent Bihar and West Bengal

2.5 Assam & Manipur in North Eastern Hill states

There are seven states in North Eastern Hills. They are Manipur, Mizoram, Assam, Tripura, Arunachal Pradesh, Nagaland, and Meghalaya. Groundwater arsenic contamination was reported from Assam and Manipur states. A preliminary survey indicated that hand tube-well water in flood plains of these two states had some arsenic contamination above 50 µg/ L and the magnitude was much less compared to Ganga-Padma- Meghna plain. Recently UNICEF reported arsenic contamination from Assam and found arsenic contamination in 18 out of 23 districts of Assam above 50 µg/L.Recently SOES reported groundwater arsenic contamination situation from Manipur state. Mainly valley districts of Manipur are arsenic contaminated. These districts are Kakching, Imphal east, Imphal west, Bishnupur. The area of these 4 districts is 10% of total area of Manipur but about 70% of total population lives in these 4 districts. In Manipur at present people are not using hand tube- wells water for drinking, cooking and agricultural purposes.

hand tube-well water samples from all these 7 states for arsenic detection by School of Jadavpur University (SOES, JU) reported presence of arsenic in 45.96% and 22.94% of the

water samples more than 10 µg/L (WHO guideline value of arsenic in drinking water) and 50µg/L (Indian standard of arsenic in drinking water), respectively. Importantly, 3.3% of the analyzed tube-wells had been found arsenic concentrations above 300µg/L, the concentration predicting overt arsenical skin lesions.

3. REMEDIATION

Technological options to combat arsenic menace, in groundwater, to ensure supply of arsenic free water, in the affected areas, can be one of the followings or a combination of all:

I. In-situ remediation of arsenic from aquifer system,
II. Ex-situ remediation of arsenic from tapped groundwater by arsenic removal technologies like chemical coagulation,reverse osmosis ,membrane filtration etc.
III. Use of surface water source as an alternative to the contaminated groundwater source,
IV. Tapping alternate safe aquifers for supply of arsenic free groundwater.
V. Innovative technologies, such as permeable reactive barriers, phytoremediation, biological treatment and electrokinetic treatment, are also being used to treat arsenic- water, waste water and soil

Instead of this, point-of-entry (POE) or point-of-use (POU) treatment options may be acceptable treatment alternatives, which offer ease of installation, simplify operation and maintenance, and generally have lower capital costs (Fox, 1989).Location- specific research, combined with a combination of technology, incentive and self-protection policies could be used to address the problem of arsenic contamination worldwide.

CONCLUSION

Arsenic sources and effects are multiple and diffused in nature and it requires detailed assessment and policy. Innovation in low cost technologies offers possibilities for reducing abatement cost and for economic efficiency. To reduce arsenic in water resources, incentive policies such as taxing and subsidizing can be used to reduce arsenic levels in point sources through creation of appropriate incentives. Creating awareness among the people in the arsenic affected states in India will decrease the contamination level in water resources.

REFERENCES

[1]Amitava Mukherjee, Mrinal Kumar Sengupta, M. Amir Hossain, Sad Ahamed, Bhaskar Das1, Bishwajit Naya, Dilip Lodh, Mohammad Mahmudur Rahman, and Dipankar Chakrabort *J Health Popul Nutr* **2006** Jun;24(2):142-163

[2] Mitigation and Remedy of Groundwater Arsenic Menace in India: A Vision Document by National Institute of Hydrology, Roorkee Central Ground Water Board, New Delhi

[3]Arsenic Contamination in Water: A Conceptual Framework of Policy Options, Zareena Begum,january **2012**

[4] Peter Ravenscroft, Predicting the global distribution of arsenic in ground water, Royal Geographical Society Annual International Conference **2007**

[5] Nrashant Singh, Deepak Kumar and Anand P. Sahu , *Journal of Environmental Biology* April **2007**, 28(2) 359-365 (**2007**)

[6] N. C. Ghosh & Scientist F & R.D. Singh, Groundwater Arsenic Contamination in India: Vulnerability and scope for remedy, National Institute of Hydrology, Roorkee

State of the art on Dynamic Behavior of Structures under Human Induced Activities

G.Gajalakshmi[1], Dr. J. Abbas Mohaideen[2], Prof. A.R. Santhakumar[3],

[1]Dept. of Civil Engineering, Sathyabama University, Chennai,
[2] Maamallan Institute of Technology, Sriperumbudur,
[3]Former Dean, Anna University.
gajalakshmidhran@gmail.com

Abstract-

Traditionally, buildings constructed with concrete floors have performed well in concern with vibration serviceability. This is due to heavy weight with high mass stiffness of floors. Modern building designs are concentrated on light weight floor system, efficient structures with high strength materials. Such system of designing compromises strength as well as span length. This light weight floor and decreased mass with long and slender spans along with minimum partitions leads vibration problems in buildings. This phenomenon is often visualized in structures subjected to dynamic loads. Dynamic loads are generally generated by human activities such as aerobics, dancing, sporting events and free jumps.

Key words: Vibration, dynamic loads, acceleration, frequency, displacement.

I. PREVIOUS RESEARCH DETAILS

Many researchers made attempts in finding the solution for these vibration problems. Starting from Reiher 1931(Ellingwood, 1983), he developed the tolerance limits for steady state excitation. In 1983, Ellingwood modifiedthe concept of Reiher to account for the transient type of excitation using limit state. He suggested that large amplitude of transient motion which will be dissipated within few cycles can be accepted easily when compared to the steady state motion. His analysis confirms the observation, communicated to the writers by several practicing engineers, that no particular problems have been encountered with several floor systems that would be classified as unacceptable according to a heel drop test. Thus, the use of realistic force functions is important in assessing the sensitivity of floors to disturbing dynamic motion. He has pointed out two options from his analysis: One being low level vibrations that occur frequently and the other, a large transient vibration that occur infrequently. He also extended that force-time relationship against dynamic effects was not supporting at that time. He mentioned stiffness and mass are the criteria responsible for dynamic effects in which if

ot the solution for reducing
ime there is a possibility for
ss is increased for reducing

dynamic responses, the solution suggested by him was to provide topping of concrete with minimal thickness. In his conclusion he mentioned maximum permissible deflection or increased span to depth ratio are not sufficient to meet the problems against vibration.

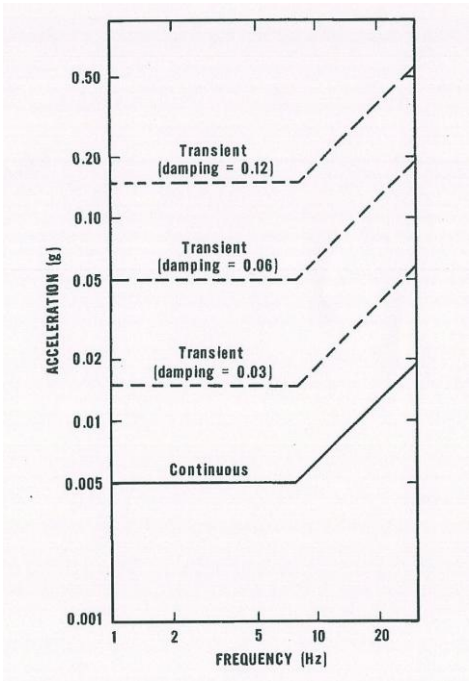

Fig.1 Frequency Vs Acceleration

Allen (1987), made several research on human induced vibration on building structures. Up to his period it was concluded that dynamic actions from human body motions were simulated by a simple harmonic function with a frequency equal to the activity rate. After few years later it was found that upper harmonics also (as part of the Fourier decomposition of the forcing function) may be critical for the dynamic design of a structure.

Table-1 Recommended acceleration limits for vibration due to rhythmic activities

Occupancies affected by the vibration	Acceleration limit, percent gravity
Office and residential	0.4 to0.7
Dining,Dancing,Weight-lifting	1.5 to 2.5
Aerobics,rhythmic activities only	4 to 7
Mixed use occupancies housing aerobics	2

Table-2 Minimum recommended natural assembly floor frequencies, Hz.

Type of floor construction	Dance floors*, Gymnasia**	Stadia, Arenas**
Composite (steel-concrete)	9	6
Solid concrete	7	5
wood	12	8

* Limiting peak acceleration 0.02 g.
** Limiting peak acceleration 0.05 g.

Natural assembly floor frequencies, Hz3.Floors*, stadia,

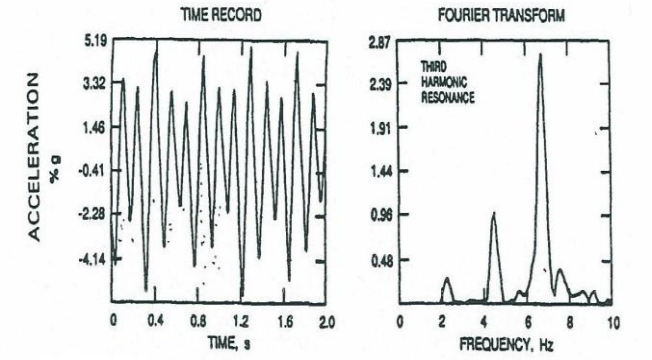

oor due to aerobics at 2.25 Hz :

ics- Time Vs Acceleration

$$\frac{a}{g} = \frac{1.3\,\alpha\, w_p/w \cdot \sin 2\pi ft}{\sqrt{\left[\left(\frac{f_o}{f}\right)^2 - 1\right]^2 + \left[2\beta\frac{f_o}{f}\right]^2}} \quad (1)$$

$$f_o \geq f\sqrt{1 + \frac{1.3}{a_o/g}\cdot\frac{\alpha\, w_p}{w}} \quad (2)$$

Bachmann considered the above studies and has examined many case studies such as that of footbridges, gymnasiums and sports halls, dancehalls and concert halls without fixed seating, concert halls with fixed seating, and high-diving platforms. With these structures he studied the dynamic behavior, fundamental frequency range, forced vibration and acceleration values. He compared these values with available standards, and suggested that the structure needs to be modified in a planning stage or in the existing stage also. He adopted a method for frequency tuning of the structure. The above said cases has corrected the vibration problems and concluded that in normal cases, frequency tuning of a structure is a useful countermeasure to reduce excessive vibrations.

Later on, the necessity for check against vibration was realized. Based on this requirement along with the revision of National Building Code of Canada by Allen (1990), Farzad Naeim (1991) published Design practice to prevent floor vibration. Floor vibration under rhythmic activities is a topic under this guidance. It is mentioned that for rhythmic activities, first harmonic natural frequency is sufficient. In case of aerobics and jumping exercises, the 2nd and 3rd harmonics play a significant role which is the important part to be considered. He developed a design procedure to prevent floor vibration from rhythmic activities. He solved some problems related to the different structural properties under different usage by incorporating the design parameters from NBC.

Table 3 Recommended Natural Frequencies of Structures with man-induced Vibrations

Structure type (1)	Construction Type			
	Reinforced Concrete (2)	Prestressed concrete (3)	Composite steel-concrete (4)	Steel 5
Gymnasiums and sports halls	>7.5	>8.0	>8.5	>9.0
Dance halls and concert halls without fixed seating Concert halls, theaters, and spectator galleries with fixed seating	>6.5	>7.0	>7.5	>8.0
With classical concerts or “soft” pop music concerts	>3.4	>3.4	>3.4	>3.4
with “hard” pop music concerts	>6.5	>6.5	>6.5	>6.5
In horizontal direction	>2.5	>2.5	>2.5	>2.5
Note: Footbridges: Avoidance of 106-2.4 Hz(with Low Damping also 3.5-4.5 Hz)				

For aerobics and jumping exercises, the first three harmonics of the forcing frequency should be considered. However, since these harmonics add together, the factor 1.3 in [15] should be increased to 2.0. Hence, the governing criterion for aerobics becomes:

Ellis (1994) described his research by comparing the analytical results of dynamic response with Finite Element and also by comparing analytical with Experimental values. This research has-been undertaken by keeping in mind that in UK the knowledge about vibration activities induced by human was there, but there was no such standards for vibration problems.

He considered dance type loading system induced by human. He concentrated on resonance response by sixth multiple of dance frequency. He concluded that based on his numerical values related to potential resonance almost verified with experiments and confirmed that significant accelerations could occur on a relatively stiff dance floor which cause serviceability problems (F11>10). He has also extended that this design criteria cannot be applicable for all types of floors based on simply supported beam. It is suggested that the considered as 1.62 instead

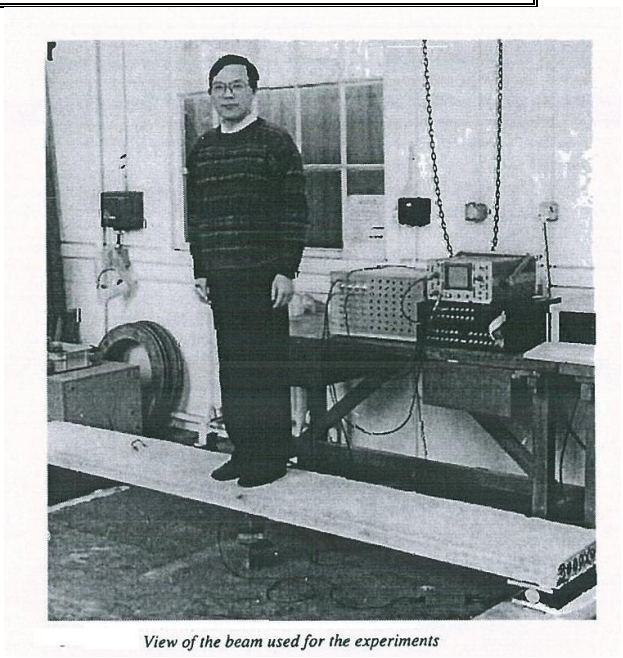
View of the beam used for the experiments

Fig.3 Experimental study

In the year 1997, a cover story was published under the title "Annoying floors- Help coming to keep floors from being too flexible for comfort" in Building Design on May-19th-ENR 33. The cover page is about vibration shaking of the Ballroom under synchronized dancing. For this incident, many researchers and Engineers have come out

with their ideas and comments like too flexible floors may get collapsed if the damping values are low and with low stiffness. The comment of Thomas Murray was "Floor serviceability design is still a development ". It was concluded by experts that columns or posts can be added, so that in future such types of problems can be avoided. If the floor is with Theatre or Gymnasium hall, they adopted Thornton-Tomasetti devise systems of TMD.

For floor vibration, the human tolerance side of the equation by Thomsan Murray providing the comparison of tolerance criteria of North American and Europeans, has started with Tregold 1828 in his paper.

For longer spans, it should be made deeper to avoid vibration problems. Later he has mentioned so many authors view in applying parameters like Acceleration limits, natural frequency for different structural configuration and the allowance of damping. He concluded that the European criteria against human tolerance are very strict and severe than North American Criteria.

In the year 1998, under the updating article of control of vibration by D.E. Allen and G.Pernica it is suggested to counteract resonance due to rhythmic activity, the floor must be designed to have natural frequency greater than the forcing frequency of the highest significant harmonic.

He mentioned the vibration limits in terms of acceleration as percentage of gravity. In this paper they said that the vibration impact not only depend on the nature of material of the floor, its thickness and span but also depend on the nature of activity of the people. For example, people sitting or lying down in offices or residences find distinctly perceptible vibration (accelerations of about 0.5% g) unacceptable, whereas those taking part in an activity such as aerobics will accept much greater vibration (about 10% g). People dining beside a dance floor or standing in a shopping mall will find vibrations that fall between these two extremes (about 2% g) acceptable. He has pointed out that the collapse failure due to overloading the NBC requires the design against structure of natural frequency less than

e natural floor frequency (fn
a simple formula, in (3)

$$fn\ (Hz) = 18/ D\ (mm) \quad (3)$$

Where D is the total deflection of the floor structure due to the weight supported by all its members (joists, girders and columns). For example, if the floor deflects 9 mm, the natural frequency is 6 Hz. To get a natural frequency of 9 Hz, the floor must deflect only 4 mm, which is practically impossible for floors supported on very long members to achieve.

2007-AVA Mello et al described the dynamic behavior of composite structures with steel beams and concrete slab of span varying from 5m to 10m. They have considered four load human induced models like jumping, walking, running, and sitting activities. In the first load model only one resonant harmonic of the load was applied on the highest modal amplitude of the floor. In the second loading model, phase angle is included. In third model the position of the dynamic loading with respect to individual position and the general time function has a space and time description. In the fourth model, human heel effect has also been considered. The structural model is analysed using ANSYS. The results obtained from the four loading models are compared with design codes of AISC and ISO to evaluate the possible occurrence of unwanted excessive vibration levels and human discomfort. In conclusion part, the

First and second load models are in good design critical compared to codes AISC and ISC. The third and fourth load models incorporate a more realistic load in which the position of the dynamic action is changed according to the individual position. On the other hand, the AISC recommendations considered only one harmonic applied in the middle of the main span of the pedestrian footbridge, without varying the load position.

According to Russell (2008) A. Parnell the fundamental frequency, static deflection and acceleration were experimentally found and compared with ATC, AISC and SCH design guides. He concluded that the reliable method is ATC and suggested the most efficient way to increase fundamental frequency is to increase the moment of inertia of the joists, which adds bending stiffness and relatively little mass. He concluded that the ATC procedure is more accurate for floor systems without a topping and ceiling, which is relevant in single occupancy residential construction. Based on the

prediction of static deflection, the ATC method, in its current state, is the best option for designers. This recommendation has the added benefit of requiring one design method for calculating static condition. Several recommendations for modifying the ATC design method were made so that it will be more accurate and applicable to the materials used for cold-formed steel floor systems. The following modifications can be made to the calculation procedure:

They use design damping ratios presented in Table 4-9 when calculating dynamic response, and reduce limiting acceleration based on ISO limiting curve when fundamental frequency is above 8 Hz.

Fig.4 Human Dynamic Loading- Jumping

Silva et al obtained the dynamic loads from Faisca 2003 whereas he conducted experiments based on rhythmic andnon-rhythmic activities. Faisca concluded with the mathematical representation with human dynamic loading with weight if the person, contact period is as below

By utilizing this equation, the authors conducted analysis of 14m long span of composite floor using Finite element Method-ANSYS. They compared their results with ISO 2631-2, 1989. They concluded that results were not satisfied with the recommended codalprovisions. Such fact shows that these rhythmic activities may that violated design criteria

The present investigation also indicated that these dynamic loads can even be generated with considerable perturbations on adjacent areas, where there is no human rhythmic activity of such kind present. Despite this fact there is still a surpassing of the associated human comfort criteria

M. Feldman et al in 2009 Design of floor structures for human induced vibrations states that for ultimate limit state verifications and for the determination of deflections design codes provide sufficient rules. However, the calculation and assessment of floor vibrations in the design stage has still a number of uncertainties. The uncertainties are associated to a suitable design model including the effects of frequencies, damping, displacement amplitudes, velocity and acceleration to predict the dynamic response of the floor structure with sufficient reliability in the design stage are,

- the characterisation of boundary conditions for the model,

- the shape and magnitude of the excitation,

- the judgement of the floor response in light of the type of use of the floor and acceptance of the user.

They formulated design charts based on modal mass and Eigen frequency for respective damping ratios varying from 1% to9%. This report gives a procedure for the determination and assessment of floor responses to walking of pedestrians which on one side takes account of the complexity of the mechanical vibrations problem, but on the other side leads by appropriate working up-to easy-to-use design charts.

S. Sandun De Silva, David P. Thambiratnam (2009) states that steel deck composite floor with increased displacements and acceleration cause discomfort to the occupants. They analysed the composite slab system under FEM with four damping values as 1.6%, 3%, 6% and 12%.They have plotted the results one with forcing frequency Vs Dynamic amplification and second is with frequency Vs Acceleration with four damping values. Loads are applied as four different loads that could be excited with multi-modal vibration in the structural system. They concluded that load intensity alone is not responsible for vibration, the higher harmonics (2nd and 3rd) modes also cause vibration of the floor. Vibration assessment in terms of deflections and accelerations

need to be considered together. The dynamic amplification in deflection and the acceleration response of the floors are

Table.4- Performance Requirement Table.

Class	$OS\text{-}RMS_{90}$ Lower Limit	$OS\text{-}RMS_{90}$ Upper Limit	Function of floor: Critical Workspace	Health	Education	Residential	Office	Meeting	Retail	Hotel	Prison	Industrial	Sport
A	0.0	0.1											
B	0.1	0.2											
C	0.2	0.8											
D	0.8	3.2											
E	3.2	12.8											
F	12.8	51.2											

Recommended
Critical
Not recommended

Recommendations for performance requirements

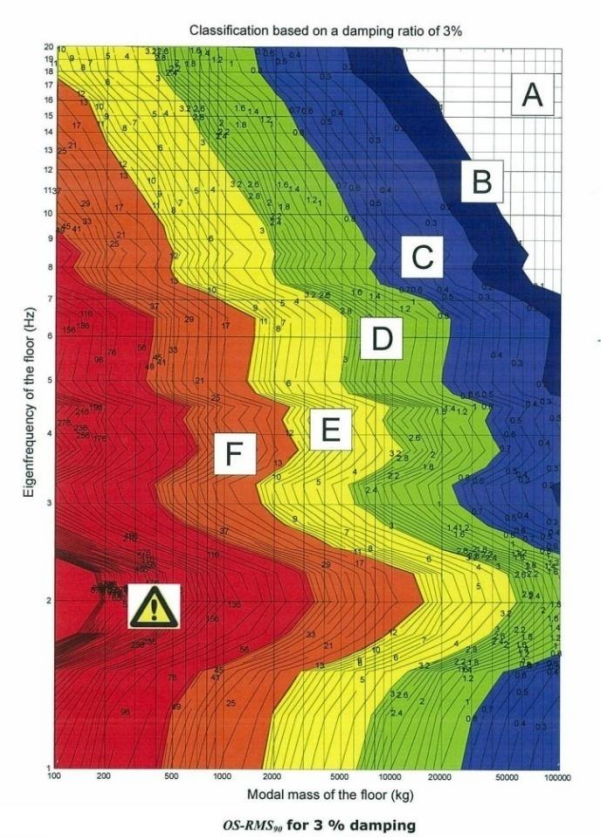

$OS\text{-}RMS_{90}$ for 3 % damping

Fig.5-RMS for 3% Damping

significantly influenced by the type of activity or foot contact ratio, with lower contact ratios giving higher responses.

Pia Johansson (2009) analysed the vibration of hollow core concrete elements induced by walking. In this paper, he tells that in Sweden, the hollow core elements are widely used due to its light weight and longer span structure. But the people who are walking over such structures are experiencing the impacts of vibration and they had started to give complaints generally in office buildings. Even Swedish Design code does not provide any general rules with respect to vibration, but some advices for wooden floors under vibration. In the current ISO standard concerning whole-body vibration in buildings, no guidance values regarding acceptable magnitudes of vibration are included since their possible range is too widespread to be reproduced in an International Standard. They conducted a test to investigate the dynamic response under different conditions by considering the topping of concrete. This sensitivity to the frequency content of the applied load means that it is difficult to draw any clear conclusions based on the three different load functions that were used in this study. For instance, another choice of load function may result in higher magnitudes of acceleration.

Therefore, as a suggestion for further work, and when designing for vibration serviceability, it is recommended that many different load functions may be tested, and the one that results in the highest acceleration magnitudes be chosen to be the governing load case. Another approach would be to design a load function that contains the natural frequencies of the floor structure, for instance by using Fourier series. Of course, the constructed load function must be within reasonable limits compared to results from measurements of the reaction force time history of gait loading. Because of the limited time frame of this paper it was not possible to try these approaches.

Author D.Varela, Rolando C Battista (2011) suggests the usage of passive control system for the lack of damping against vibration problem. They considered TMDs-tuned Mass Dampers which is economical, low maintenance, and considerably efficient. It can be designed in different shapes and sizes as per the requirement. They conducted tests over the composite

floor deck induced by six volunteers walking. Volunteers are allowed to walk over the slab and finally they gave their feel during walking and one may feel by standing and others are allowed to walk and with different probable situations were made. All of the volunteers changed their opinion positively on the vibration level when the TMDs were in full operation as compared to the situation when the TMDs were locked .When the TMDs were locked, half of the volunteers felt uncomfortable, and the other half could not tolerate the vibrations. When the TMDs were released, four of the six volunteers classified the vibrations as only perceptible, one of the other two classified them as imperceptible, and only one still classified them as uncomfortable. Moreover, better results could be achieved with extra units of the same TMD, that is, by increasing the ratio between the TMD mass and the structural modal mass. They have proved that using such type of passive control system reduces the vibration impacts and it is improving the dynamic response of the structure which can be recommend in any type of usage.

They developed a numerical model using FEM SAP 2000 for the effect of change in various floor parameters on vibration performance of timber floors. The parametric study under this research involves varying the joist spacing, joist depth, sheathing thickness and nail spacing. The corresponding fundamental frequency, modal separation factors and Rms acceleration values are obtained and tabulated. They concluded human induced activity like footsteps loading cannot be isolated as it is the main source of floor vibration especially if made of timber. It is advised to consider the vibration analysis during design process itself.

The author from his study found that under human induced activity like walking, jumping which creates vibration problems are consistent with that. To control such vibration problems they investigated the dynamic performance of an innovative Hybrid Composite Floor Plate System (HCFPS). It is made of Polyurethane (PU) core, outer layers of Glass–fiber Reinforced Cement (GRC) and steel laminates at tensile regions. They conducted experiments using Finite Element (FE) modeling, included heel impact and walking tests for anels. Their results were d BS 6472 and concluded frequency of HCFPS floor system is greater than 10 Hz and hence HCFPS can be categorized as a high frequency floor system. The maximum possible fourth harmonic of the walking frequency (2.4 Hz) is lower than the first mode natural frequency and this makes resonant vibration a rarity.

Human - structure interaction system has been analyzed

by Nicholas Noss. They concluded saying that it is expected that the crowd characteristics, including size, density, distribution, and posture, will affect the dynamic properties of the empty structure, including natural frequency, damping ratio, and possibly mode shapes.

II. CONCLUSION

From the above literature study, it is observed that the understanding of the human interaction to the structure is a complex phenomenon. All researchers arrived some equations and formula from their input data based on the corresponding activities from human. Even current designs guide uses the natural frequency for assessing the vibration serviceability. But the dynamic interface between passive occupants and the structure can alter the natural frequency of thee system. The dynamic response are depending upon the posture of the occupants , the dynamic properties of the structure and the mass of the people inducing activities like jumping, walking, aerobics . There is no straight calculation available for fundamental frequency under human rhythmic activities. Even if a single person is doing any type of activity, it may generate perceptible levels of vibration in many floors. The results obtained from previous researchers are noteworthy, but are limited in their application because the data is sparse, disjointed, and lack continuity.

REFERENCES

[1] Abbas,F et al (2012) Dynamic Response of low frequency Profiled Steel Sheet Dry Board with Concrete infill (PSSDBC) floor system under human walking load, Latin American Journal of Solids and Structures, pp. 21 – 41.

[2] Allen ,D.E et al(1985) Vibration criteria for assembly occupancies, Canadian journal of Civil engineering, vol.12, pp. 617 – 623.

[3] Allen, D.E (1990) Building vibration from human activities, ACI concrete International -Design and Construction.

[4] Bachmann, H (1992) Case studies of structures with man induced vibration, Journal of Structural Engineering, vol-118, No: 3.

[5] Bruce Ellingwood, M and Andrew Tallinn (1984) Structural Serviceability -Floor vibration, Journal of Structural Engineering, vol.110, No.2, ISSN 0733-9445.

[6] Da Silva, J.G.S. et al (2006) Dynamical response of composite steel deck floors, Latin American Journal of Solids and Structures, 3.

[7] Da Silva, J.G.S. et al(2008) Vibration Analysis of orthotropic composite floors for human rhythmic activities, Journal of Brazilian Society of Mechanical Sciences and Engineering, pp. 56 – 65, 2008.

[8] Da Silva, J.G.S. et al (2011) Vibration Analysis of long span joist floors submitted to Human Rhythmic Activities, State University of Ride janeiro , ISBN 978-953-307-209-8, pp. 231 – 244, 2011.

[9] Faisca, R.G. (2003)Caracterização de cargas dinâmicas geradas por atividades humanas (Characterization of Dynamic Loads due to Human Activities), PhD Thesis (in Portuguese), COPPE/UFRJ, Rio de Janeiro, RJ, Brazil, pp. 1-240

[10] IS 800:2007, Indian standard general construction in steel – code of practice- third revision

[11] Murray, T.M et al (2003) Floor vibrations due to human activity, Steel design guide series by American institute of steel Construction.

[12] McGrath and Foote ,D(1981)What happened at the Hyatt?", Newsweek, National Affairs, Unitedstates edition, pg. 26, http://www.me.utexas.edu/me179/topics/lessons/case2artcles/case2article2.html

Determination of Cadmium in water, sediment and Spotted Seer fish

Siji Thomas
Research scholar
Sathyabama University, Chennai, Tamilnadu, India

J.Abbas Mohaideen
Principal, Maamallan Institute of Technology
Sriperumpudur, tamilnadu, India

Abstract- The objective of the study is to determine the concentration of Cadmium in water, sediment and the marine species Indo-Pacific king mackerel popularly known as spotted seer fish (Scomberomorus guttus) collected near seashore of Bay of Bengal from 5 locations (Pulicat, Ennore, Marina, Mahabalipuram and Kalpakkam) in North Chennai in 4 different seasons (Summer, Monsoon, Post-Monsoon, and Winter). The concentrations of Cadmium in each sample were determined using AAS method. The study shows that the higher concentration of Cadmium in fish is observed in fish collected from Ennore during Post-Monsoon season. Also, the higher concentration of cadmium in water and sediments are found in Pulicat in Monsoon season and Ennore in Post-Monsoon season respectively.

Keywords – Heavy metals, concentration, Atomic Absorption Spectrophotometer(AAS), Chennai, spotted seer fish, Cadmium, fish, sediment, water

I. INTRODUCTION

Cadmium is an extremely toxic metal commonly found in industrial workplaces. Due to its low permissible exposure limit, overexposures may occur even in situations where trace quantities of cadmium are found. Cadmium is used extensively in electroplating, although the nature of the operation does not generally lead to overexposures. Cadmium is also found in some industrial paints and may represent a hazard when sprayed. Operations involving removal of cadmium paints by scraping or blasting may pose a significant hazard. Cadmium is also present in the manufacturing of some types of batteries. Exposures to cadmium are addressed in specific standards for the general industry, shipyard employment, construction industry, and the agricultural industry. Food is another source of cadmium. Plants may only contain small or moderate amounts in non-industrial areas, but high levels may be found in the liver and kidneys of adult animals. Cigarettes are also a significant source of cadmium exposure. Although there is generally less cadmium in tobacco than in food, the lungs absorb cadmium more efficiently than the stomach. Acute exposure to cadmium fumes may cause flu like symptoms including chills, fever, and muscle ache sometimes referred to as "the cadmium blues." Inhaling cadmium-laden dust quickly leads to respiratory tract and kidney problems which can be fatal (often from renal failure). Ingestion of any significant amount of cadmium causes immediate poisoning and damage to the liver and the kidneys. Fish is a valuable food item and source of protein. The concentration of heavy metals in aquatic organisms is higher than that present in water due to the effect of bio concentration and bio accumulation and eventually threaten the health of human by sea food consumption. Also Fishes are widely used as bio indicators of marine pollution by metals (Evans et al. 1993). So determination of heavy metal concentration in fishes is very important as far as human health is concerned. The samples (Spotted Seer fish, water and sediments) were collected in the seasons Summer (March-May, 2012), Monsoon (June – August, 2012), Post-Monsoon (September – November, 2012) and Winter (December 2012 – February 2013) from Pulicat, Ennore, Marina, Mahabalipuram and Kalpakkam. The aim of the study was to determine the concentration of Cadmium in fish muscle, water and sediment and to analyze it with respect to the seasons and locations.

II. METHODOLOGY

A. Study Area

The study consists of 5 different locations (Pulicat, Ennore, Marina, Mahabalipuram and Kalpakkam) along the Bay of Bengal in North Tamilnadu.

Pulicat (Pazhaverkadu) is a historic seashore town in Thiruvallur District, of Tamil Nadu. It is about 60 km north of Chennai and 3 km from Elavur, on the barrier island of Sriharikota, which separates Pulicat Lake from the Bay of Bengal.

Ennore is a suburb in Chennai, India. Ennore is situated on a peninsula and is bounded by the Korttalaiyar River, Ennore creek and the Bay of Bengal. The creek separates Ennore from the Ennore Port. Ennore creek carries high load of heavy metals (Kannan et al., 2007). The treated effluents of the Madras Refinery Ltd, through the Buckingham canal and the Madras Fertilizers Ltd, through the Red Hills surplus channel, reach the Ennore backwater (Sreenivasan and Franklin, 1975).

Marina Beach is an urban beach in the city of Chennai, India, along the Bay of Bengal, part of the Indian Ocean. The beach runs from near Fort St. George in the north to Besant Nagar in the south, a distance of 13 km, making it the longest urban beach in the country and the world's second longest.

Mahabalipuram lies on the Coromandel Coast which faces the Bay of Bengal. It is around 60 km south from the city of Chennai. It is an ancient historic town and was a bustling seaport during the time of Periplus and Ptolemy.

Kalpakkam is a small town in Tamil Nadu, situated on the Coromandel Coast 70 kilometres south of ChennaiNuclear facilities. Madras Atomic Power Station is located at Kalpakkam. It is a comprehensive nuclear power production, fuel reprocessing, and waste treatment facility that includes plutonium fuel fabrication for fast breeder reactors (FBRs). It is also India's first fully indigenously constructed nuclear power station. It has two units of 220 MW capacities each.

B. Materials and Methods

The spotted seer fish samples (minimum 10 number of samples), water and sediment were collected from all the 5 locations in 4 different seasons, Summer (March-May, 2012), Monsoon (June – August, 2012), Post-Monsoon (September – November, 2012) and Winter (December 2012 – February 2013) within 500 meters from the seashore. The physiochemical parameters like Temperature, pH, Salinity and Dissolved oxygen were measured.

The fish samples were washed thoroughly with distilled water to remove the sediments and debris. The length and weight of each sample were measured. Then the edible parts were separated and frozen at -20^{o} for the analysis. The fish samples were thawed, and then dried in a hot air oven at 60^{o}C. After removing the moisture content, the weight was taken again. 15 gm of fish sample was taken and the ashing was done at 500^{o}C for 16 hours. After cooling, 2 ml of Nitric Acid (HNO_3) and 10 ml of 1 molar Hydrochloric Acid (HCl) were added. After digestion, samples were filtered using Whatman filter paper No. 41, and the filtrate is made up to 25 ml with distilled water.

100 ml water sample was taken in a beaker and 0.5 ml Nitric Acid (HNO_3) and 5 ml Hydrochloric Acid (HCl) were added. Then it is kept in a hot plate for digestion. After digestion, it was made up to 10 ml. Cadmium concentration was determined by Atomic Absorption Spectrophotometer (AAS).

2 gm of dry sediment was taken in a digestion vessel, 10 ml of 1:1 Nitric acid (HNO_3) was added and covered with watch glass. It was heated at 95±5 degree C for 10-15 min without boiling. After cooling, 5 ml concentrated HNO_3 was added and refluxed for 30 minutes. The step was repeated until no brown fumes come. The solution was allowed to evaporate to nearly 5 ml by heat without boiling. After the sample has cooled, 2 ml of water and 30% H_2O_2 were added. Heated until effervescence subsides and vessel was cooled. 30 % H_2O_2 was added in 1 ml aliquots with warming until the effervescence is minimal. The sample was covered with a ribbed watch glass and continued until the volume has been reduced to 5 ml. 10 ml HCL was added and refluxed for 15 min at 95±5 degree C. The digestate was filtered through Whatman filter paper No.41 and was collected in 100 ml standard flask. Cadmium concentration was determined by Atomic Absorption Spectrophotometer (AAS).

III. Results and Discussions

A. Fish

The concentrations of Cadmium in Spotted Seer fish caught from 5 different locations in 4 different seasons are given in table 1 and the graphical representation of the maximum concentration in Figure 1. It is observed that the maximum concentration of Cadmium (Cd) in Ennore(0.441 mg/kg), Marina(0.423 mg/kg) and mahabalipuram (0.417 mg/kg) are observed in Post-Monsoon season. Maximum concentration in Pulicat(0.426 mg/kg), and kalppakkam (0.407 mg/kg) are is observed in Winter and Monsoon seasons respectively.

of Cadmium in water collected from 5 different locations in 4 different seasons are given in
al representation in Figure 2. It is observed that the maximum concentration of Cadmium (Cd)

in Pulicat (0.028 mg/l), Ennore(0.027 mg/l), Mahabalipuram (0.013 mg/l) and Kalpakkam (0.023 mg/l) are observed in Monsoon season. Maximum concentration in Marina (0.014 mg/l) is observed in Summer season.

.

C. Sediment

The concentrations of Cadmium in sediments collected from 5 different locations in 4 seasons are given in Table 3 and the graphical representation in Figure 3. The maximum concentration of Cadmium in Pulicat (1.317 mg/kg) and Kalpakkam (1.247 mg/kg) are observed in Monsoon season. Concentrations of Cd in Marina (1.246 mg/kg) and Mahabalipuram (0.878 mg/kg) are observed in summer season and that in Ennore (1.815 mg/kg) is observed in Post-Monsoon season.

TABLE I. MINIMUM AND MAXIMUM VALUES CONCENTRATIONS OF CADMIUM IN FISH CAUGHT FROM DIFFERENT LOCATIONS IN DIFFERENT SEASONS (MG/KG)

	Pulicat		Ennore		Marina		Mahabalipuram		Kalpakkam	
Season	***Min***	***Max***	***Min***	***Max***	***Min***	***Max***	***Min***	***Max***	***Min***	***Max***
Summer	0.032	0.423	0.042	0.383	BDL	0.382	BDL	0.368	BDL	0.321
Monsoon	0.032	0.382	0.034	0.418	BDL	0.368	BDL	0.312	BDL	0.407
Post-Monsoon	0.083	0.417	BDL	0.441	0.032	0.423	BDL	0.417	BDL	0.308
Winter	BDL	0.426	BDL	0.364	BDL	0.418	BDL	0.268	BDL	0.241

TABLE II. CONCENTRATION OF CADMIUM IN WATER COLLECTED FROM DIFFERENT LOCATIONS IN DIFFERENT SEASONS (MG/L)

Seasons	**As**	**Cd**	**Cr**	**Pb**	**Hg**
Summer	0.018	0.02	0.014	0.01	0.017
Monsoon	0.028	0.027	0.012	0.013	0.023
Post-Monsoon	0.021	0.022	0.012	0.011	0.015
Winter	0.015	0.018	0.01	0.01	0.012

TABLE III. CONCENTRATION OF CADMIUM IN SEDIMENT COLLECTED FROM DIFFERENT LOCATIONS IN DIFFERENT SEASONS (MG/KG)

Seasons	**As**	**Cd**	**Cr**	**Pb**	**Hg**
Summer	1.184	1.12	1.246	0.878	1.096
Monsoon	1.317	1.374	1.067	0.564	1.247
Post-Monsoon	0.831	1.815	1.034	0.872	1.147
Winter	1.293	1.613	0.948	0.783	1.041

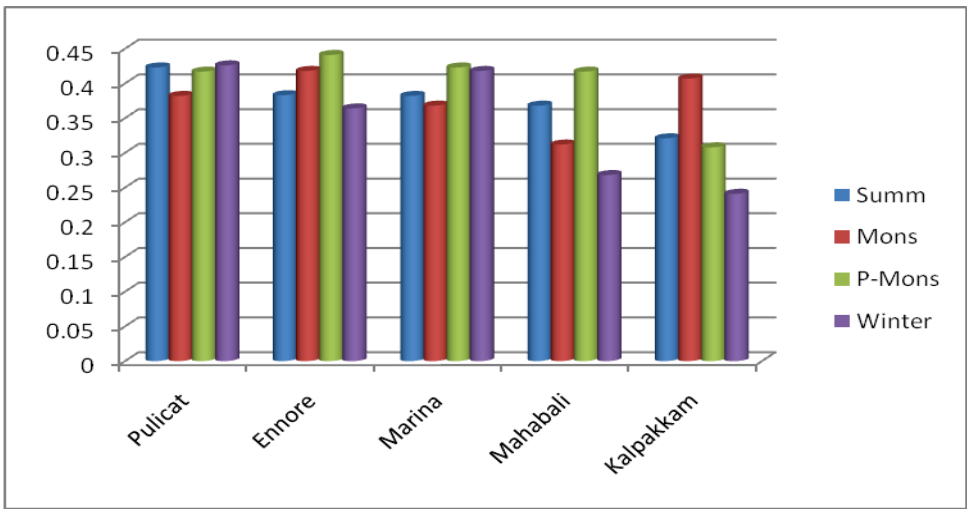

Figure 1. Maximum Concentration of Cadmium in fish caught from different locations in different seasons (mg/kg)

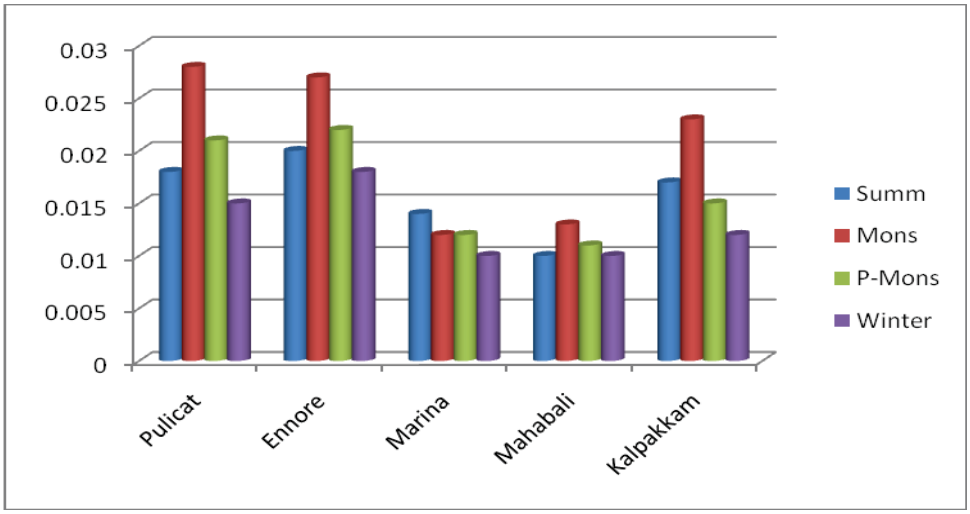

Figure 2. Concentration of Cadmium in water collected from different locations in different seasons (mg/l)

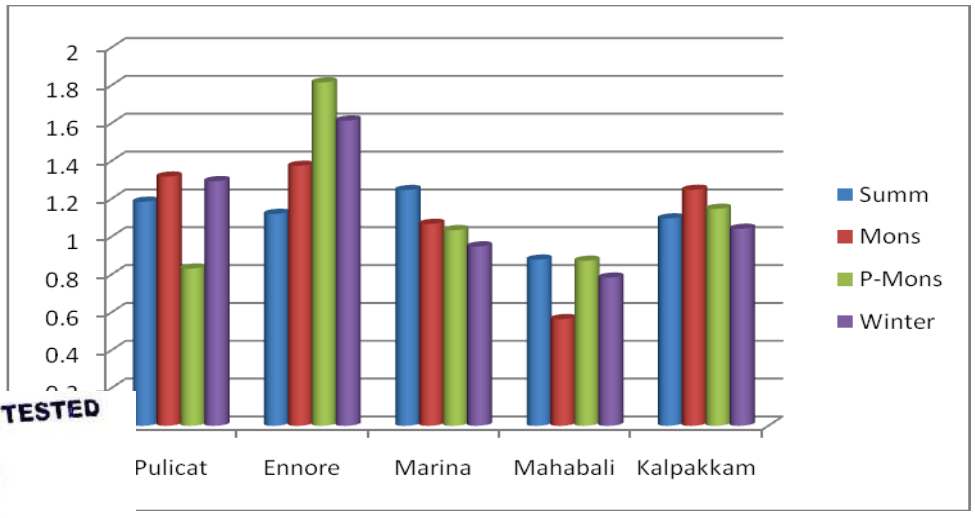

Figure 3. Concentration of Cadmium in sediment collected from different locations in different seasons (mg/kg)

IV.CONCLUSION

It is observed from this study that there is no much seasonal variation in concentrations of the Cadmium in fish samples, however the concentration in three locations are higher in Post-Monsoon season. The higher concentrations of Cd in water in most of the locations are observed in monsoon season. This may be mainly due to the run off during the monsoon. The maximum concentrations of Cd in sediment are observed in various seasons in different locations. Maximum Cd concentration in fish and sediment are observed in Ennore in Post-Monsoon season. This shows the higher concentration of Cd in the effluents discharged from various industries located near Ennore.

REFERENCES

[1] Jayaprakash, M., Srinivasalu, S., Jonathan, M.P., and Mohan, V. 2005. A baseline study of physicochemical parameters and trace metals in water of Ennore Creek, Chennai, India. Mar. Poll. Bull., 50: 583-589.

[2] Kannan, K.S. and Krishnamoorthy, R. 2006. Isolation of mercury resistant bacteria and influence of abiotic factors on bioavailability of mercury-A case study in Pulicat Lake north of Chennai, South East India. Sci. Tot. Environ., 367: 341-363.

[3] Kannan, K.S., Lee, K.J. Krishnamoorthy, R., Purusothaman, A., Shanthi, K. and Rao, R. 2007. Aerobic chromium reducing Bacillus cereus isolated from the heavy metal contaminated Ennore Creek sediment, North of Chennai, Tamilnadu, South East India. Res. J. Microbiol., 2(2): 130-140.

[4] Padmini, E. and Kavitha, M. 2005a. Contaminant induced stress impact on biochemical changes in brain of estuarine grey mullets. Poll. Res., 24: 647-651.

[5] Varma, P. U. and Reddy, C. V. G., Seasonal variation of the hy-drological conditions of the Madras coastal waters. Indian J. Fish., 1959, 6, 298–305.

[6] Murthy, RKV. & Rao BK. (1987).Survey of meiofauna in the Gautami-Godavari estuary. J Mar Biol Assoc India, 29, 37-44.

[7] Nammalwar, P. (1992). Fish bioassay in the Cooum and Adyar estuaries for environmental management, In K.P. Singh & U.J.S Singh (Eds), Tropical ecosystems Ecology and management (359-370). Delhi, India : Wiley Eastern.

[8] Nieboer, E. & Richardson DHS. (1980). The replacement of the nondescript term 'heavy metals' by a biologically and chemically significant classification of metal ions. Environ Poll Bull, 1, 3-26.

[9] Batvari, B . P. D., K amala Kannan, S., Shanthi , K., K rishnamoorthy, R., Lee, K. J., & Jayaprakash, M. (2008). Heavy metals in two fish species (Carangoidel m alabaricus and Belones tronglurus) from Pulicat Lake, North of Chennai, South east coast of India. Environmental Monitoring and Assessment, 1 45, 167–17 5.

[10] Ahmad, M. K., Islam, S. , Rahman, S. , Haque, M. R. and Islam, M. M. Heavy Metals in Water, Sediment and Some Fishes of Buriganga River, Bangladesh Int. J. Environ. Res., 4(2):321-332,Spring 2010

[11] Murthy, RKV. & Rao BK. (1987).Survey of meiofauna in the Gautami-Godavari estuary. J Mar Biol Assoc India, 29, 37-44.

[12] Nammalwar, P. (1992). Fish bioassay in the Cooum and Adyar estuaries for environmental management, In K.P. Singh & U.J.S Singh (Eds), Tropical ecosystems Ecology and management (359-370). Delhi, India : Wiley Eastern.

[13] Nieboer, E. & Richardson DHS. (1980). The replacement of the nondescript term 'heavy metals' by a biologically and chemically significant classification of metal ions. Environ Poll Bull, 1, 3-26.

International Journal of Engineering Science Invention
ISSN (Online): 2319 – 6734, ISSN (Print): 2319 – 6726
www.ijesi.org Volume 3 Issue 8 ǁ August 2014 ǁ PP.41-46

Analysis of Heavy Metals in fish,water and sediment from Bay of Bengal

Siji Thomas [1], Abbas.J.Mohaideen [2]
[1](Research Scholar, Department of Chemical Engineering
Sathyabama University, Chennai, India)
[2](Principal, Maamallan Institute of Technology, Chennai, India)

ABSTRACT : *The Concentrations of 5 heavy metals Arsenic (As), Cadmium (Cd), Chromium (Cr), Lead (Pb) and Mercury (Hg) were determined in water, sediment and marine species Indo-Pacific King Mackerel popularly known as Spotted Seer fish (Scomberomorus Guttus). The samples were collected near seashore of Bay of Bengal from 5 different locations in North Tamilnadu like Pulicat, Ennore, Marina, Mahabalipuram and Kalpakkam during the period June-August 2012. The maximum concentrations of heavy metals in fish Arsenic (0.429 mg/kg), Cadmium (0.418 mg/kg), Chromium (0.713 mg/kg), Lead (0.716 mg/kg), and Mercury (0.078 mg/kg) were observed in samples collected from Ennore. Maximum heavy metal concentrations in water are Arsenic (0.034 mg/l - Ennore), Cadmium (0.028 mg/l- Pulicat), Chromium (0.063 mg/l - Ennore), Lead (0.016 mg/l- Kalpakkam) and Mercury (0.019 mg/l - Marina). Highest concentrations of Arsenic (1.841 mg/kg), Cadmium (1.374 mg/kg) and Lead (1. 814 mg/kg) in sediment were observed in samples collected from Ennore and that of Chromium (1.569 mg/kg) and Mercury (0. 673 mg/kg) in Marina.*

KEY WORDS : *Atomic Absorption Spectrophotometer (AAS), Concentration, Chennai, Heavy metals, Spotted Seer fish*

I. INTRODUCTION

There are more definitions for the word ”Heavy metal”, but none has obtained widespread acceptance. The different criteria used to define “heavy metal” are density, atomic weight, atomic number and position in the periodic table [1]. The definitions for “heavy metal” in terms of density (specific gravity) is “metal whose density is approximately 5.0 or higher” [2] .In terms of atomic weight (relative atomic mass), it is defined as “the metallic element with high atomic weight (e.g., mercury, chromium, cadmium, arsenic, and lead) which can damage living things at low concentrations and tends to accumulate in the food chain” [3].“Any element with an atomic number greater than 20” is the definition of “heavy metal” in terms of atomic number [4].Heavy metals are found naturally in the earth, and become concentrated as a result of human caused activities. Common natural sources of heavy metals are volcanic activities, forest fires, erosion of rocks etc. The anthropogenic sources of heavy metals are mining and industrial wastes, lead –acid batteries, vehicle emission, fertilizers, paints and treated woods. Some heavy metals like Iron, cobalt, copper, manganese, zinc etc. are required by humans, but excessive levels can be damaging to the organism. Some other heavy metals such as mercury and lead are highly toxic and their accumulation over time in the bodies of animals can cause serious illness [5]. Generally, humans are exposed to these metals by ingestion (drinking or eating) or inhalation (breathing). Working or living in and around the industrial area will increase the risk of exposure to heavy metals. Heavy metal toxicity can result in various ill health effects in humans. Inorganic arsenic is carcinogen and can cause cancer of skin, lungs, liver and bladder.

Ingestion of very high levels may result in death. Cadmium and cadmium compounds are also known human carcinogens. Breathing high levels of cadmium may cause severe damage to the lungs. Ingestion of high level severely irritates the stomach causing vomiting and diarrhea. Long term exposure to Chromium can cause damage to liver, kidney circulatory and nerve tissues, as well as skin irritation. Exposure to high levels of Mercury can permanently damage the brain, kidneys, and developing fetuses. Exposure to high levels of lead can severely damage the brain and kidneys and ultimately cause death. [6]Many of our rivers, lakes, and oceans have been contaminated by pollutants. Some of these pollutants are directly discharged from industrial plants and municipal sewage treatment plants, some come from polluted runoff in urban and agricultural areas, and some are the result of historical contamination. The pollutants that enter the water cause undesirable changes ical balance of the environment. Among all the pollutants, accumulation of heavy metals because of its adverse impact on environment and human health. Fish is a valuable food source of protein.

The concentration of heavy metals in aquatic organisms is higher than that present in water through the effect of bio concentration and bio magnification and eventually threaten the health of human by sea food consumption [7]. Fishes are widely used as bio indicators of marine pollution by metals [8]. So determination of heavy metal concentration in fishes is very important as far as human health is concerned. The objective of this study is to determine the concentration of some trace metals in Spotted Seer fish, water and sediments collected from Bay of Bengal from 5 different locations in North Tamilnadu (Pulicat, Ennore, Marina, Mahabalipuram and Kalpakkam) during the period June-August 2012

II. METHODOLOGY

2.1. Study Area

The study area consists of 5 different locations (Pulicat, Ennore, Marina, Mahabalipuram and Kalpakkam) along the coast of Bay of Bengal in North Tamilnadu. A map showing the study area is given in Fig.1.

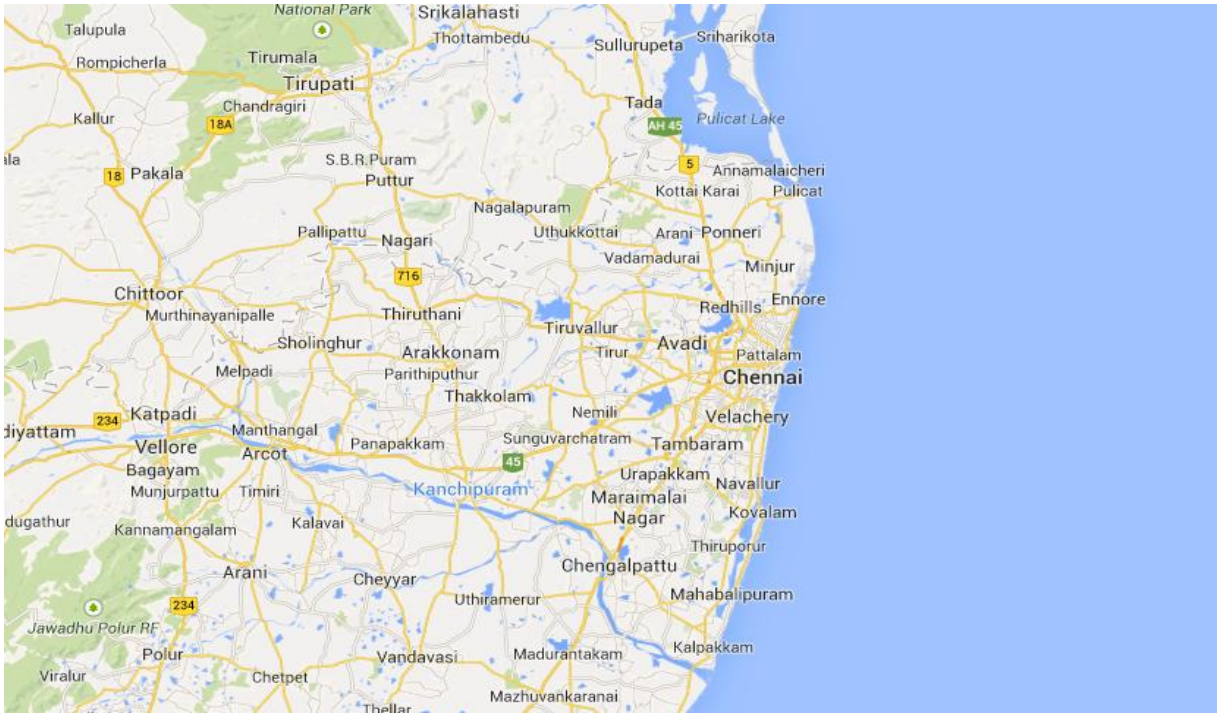

Figure 1. Map showing the study area

Figure 2.

Pulicat (Pazhaverkadu) is a historic seashore town in Thiruvallur District, of Tamil Nadu. It is about 60 km north of Chennai and 3 km from Elavur, on the barrier island of Sriharikota, which separates Pulicat lake from the Bay of Bengal. It is the second leading brackish lagoon in India–covering a total area of 720 sq km of which 84% comes in Andhra Pradesh and 16% in Tamil Nadu, which once nurtured rich flora and fauna. But, in recent years, the discharge of effluent from various industries imparted severe stress on its ecosystem. Several studies have already been conducted related to the heavy metal contamination in this area. [9] [10] [11]. Ennore is situated on a peninsula and is bounded by the Korttalaiyar River, Ennore creek and the Bay of Bengal. The creek separates Ennore from the Ennore Port. Ennore creek carries high load of heavy metals. [12] [13 [14] The treated effluents of the Madras Refinery Ltd, through the Buckingham canal and the Madras Fertilizers Ltd, through the Red Hills surplus channel, reach the Ennore backwater[15].

Marina Beach is an urban beach in the city of Chennai, Tamilnadu, India, along the Bay of Bengal, part of the Indian Ocean. The beach runs from near Fort St.George in the north to Besant Nagar in the south, a distance of 13 km (8.1 mi), making it the longest urban beach in the country and the world's second longest. Mahabalipuram lies on the Coromandel Coast which faces the Bay of Bengal. It is around 60 km south from the city of Chennai. It is an ancient historic town and was a bustling seaport during the time of Periplus and s a small town in Tamil Nadu, situated on the Coromandel Coast 70 kilometres south of ies.

Madras Atomic Power Station is located at Kalpakkam. It is a comprehensive nuclear power production, fuel reprocessing, and waste treatment facility that includes plutonium fuel fabrication for fast breeder reactors (FBRs). It is also India's first fully indigenously constructed nuclear power station. It has two units of 220 MW capacities each.

Materials and Methods : The water, sediment and spotted seer fish samples were collected during June – August 2012 from all the 5 locations within 500 meters from the seashore. The physico-chemical parameters like Temperature, pH, Salinity and Dissolved oxygen were measured. The fish samples were washed thoroughly with distilled water to remove the sediments and debris. The length and weight of each sample were measured. Then the edible parts were separated and frozen at -20^o for the analysis. The fish samples were thawed, and then dried in a hot air oven at 60^{o}C. After removing the moisture content, the weight was taken again.

Digestion procedure for fish samples : 15 gm of fish sample was taken and the ashing was done at 500^{o}C for 16 hours. After cooling, 2 ml of Nitric Acid (HNO_3) and 10 ml of 1 molar Hydrochloric Acid (HCl) were added. After digestion, samples were filtered using Whatman filter paper No. 41, and the filtrate was made up to 25 ml with distilled water.

Digestion procedure for water samples : For As, Cd, Cr and Pb: 100 ml water sample was taken in a beaker and 0.5 ml Nitric Acid (HNO_3) and 5 ml Hydrochloric Acid (HCl) were added. Then it was kept in a hot plate for digestion. After digestion, it was made up to 10 ml. Heavy Metal concentrations were determined by Atomic Absorption Spectrophotometer (AAS).For Mercury (Hg): 100ml water sample was taken in a beaker and 5 ml Sulphuric Acid (H_2SO_4), 2.5 ml Nitric Acid (HNO_3) and 15 ml Pottassium Permanganate ($KMNO_4$) were added. Then it was placed in a hot plate for 15 minutes for digestion. Then 8 ml Pottassium Persulphate ($K_2S_2O_8$) was added and heated in 100^{0}C water bath for 2 hours. After cooling, 6 ml Sodium Chloride Hydroxylamine Sulphate was added. After discoloration, 5 ml stannous chloride (SnCl2) was added.

Digestion procedure for sediment samples : 2 gm of dry sediment was taken in a digestion vessel, 10 ml of 1:1 Nitric acid (HNO_3) was added and covered with watch glass. It was heated at 95±5 degree C for 10-15 min without boiling. After cooling, 5 ml concentrated HNO_3 was added and refluxed for 30 minutes. The step was repeated until no brown fumes come. The solution was allowed to evaporate to nearly 5 ml by heat without boiling. After the sample has cooled, 2 ml of water and 30% H_2O_2 were added. Heated until effervescence subsides and vessel was cooled. 30 % H_2O_2 was added in 1 ml aliquots with warming until the effervescence is minimal. The sample was covered with a ribbed watch glass and continued until the volume has been reduced to 5 ml. 10 ml HCL was added and refluxed for 15 min at 95±5 degree C. The digestate was filtered through Whattman filter paper No.41 and was collected in 100 ml standard flask. Heavy Metal concentrations were determined by Atomic Absorption Spectrophotometer (AAS).

III. RESULTS AND DISCUSSIONS

Fish : The maximum and minimum concentrations of selected heavy metals in fish caught from different locations are given in Table 1 and the graphical representation of the maximum concentration in Fig.2. It is observed that the maximum concentration of Arsenic (0.429 mg/kg), Cadmium (0.418 mg/kg), Chromium (0.713 mg/kg), Lead (0.716 mg/kg), and Mercury (0.078 mg/kg) were observed in Ennore.

Table 1. Concentrations (Minimum and maximum values) of H.M. in fish caught from different locations (mg/kg)

	As		Cd		Cr		Pb		Hg	
Location	Min	Max	Min	Max	Min	Max	Min	Max	Min	Max
Pulicat	BDL	0.42	0.032	0.382	0.03	0.585	BDL	0.521	BDL	0.072
Ennore	BDL	0.429	0.034	0.418	0.112	0.713	BDL	0.716	BDL	0.078
Marina	BDL	0.302	BDL	0.368	0.033	0.518	BDL	0.616	BDL	0.064
Mahabalipuram	BDL	0.264	BDL	0.312	0.031	0.411	BDL	0.318	BDL	0.06
Kalpakkam	BDL	0.254	BDL	0.407	BDL	0.308	BDL	0.486	BDL	0.064

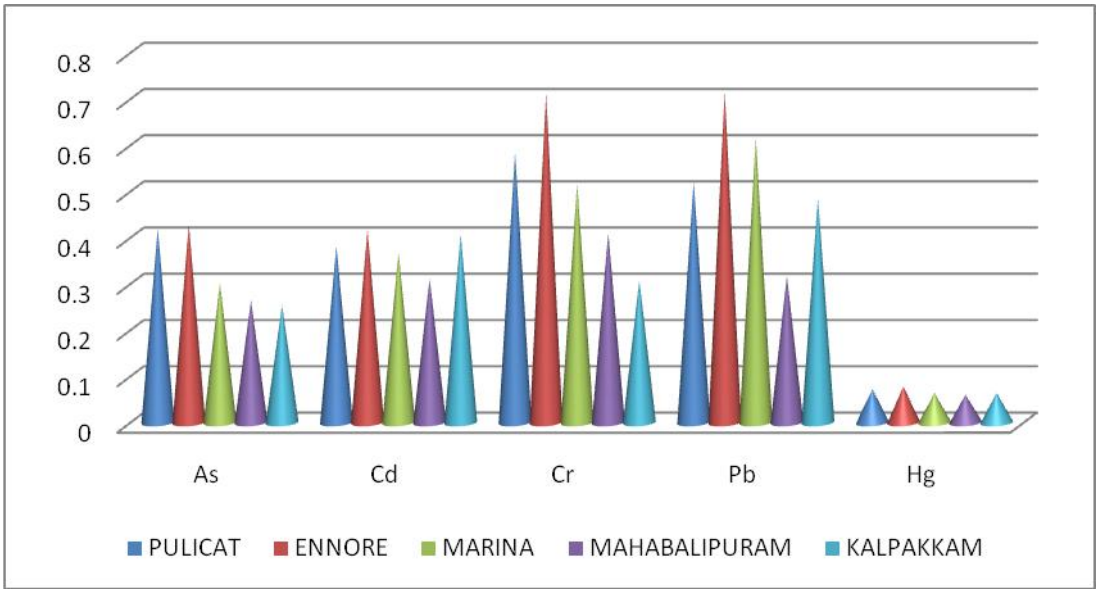

Figure 3. Maximum concentration of H.M. in fish caught from different locations (mg/kg)

Water : The concentrations of heavy metals in water collected from 5 different locations are given in Table 2 and the graphical representation in Fig.3. The maximum concentration of Arsenic (0.034 mg/l), and Chromium (0.063 mg/l) were observed in Ennore. Maximum concentration of Cadmium (0.028 mg/l), Lead (0.016 mg/l) and Mercury (0.019 mg/l) were observed in Pulicat, Kalpakkam and Marina respectively.

Table 2. Concentrations of H.M. in water collected from different locations (mg/lit)

Location	As	Cd	Cr	Pb	Hg
Pulicat	0.024	0.028	BDL	0.014	0.01
Ennore	0.034	0.027	0.063	0.015	0.009
Marina	0.016	0.012	0.022	0.012	0.019
Mahabalipuram	0.013	0.013	0.026	0.014	0.009
Kalpakkam	0.012	0.023	0.02	0.016	0.01

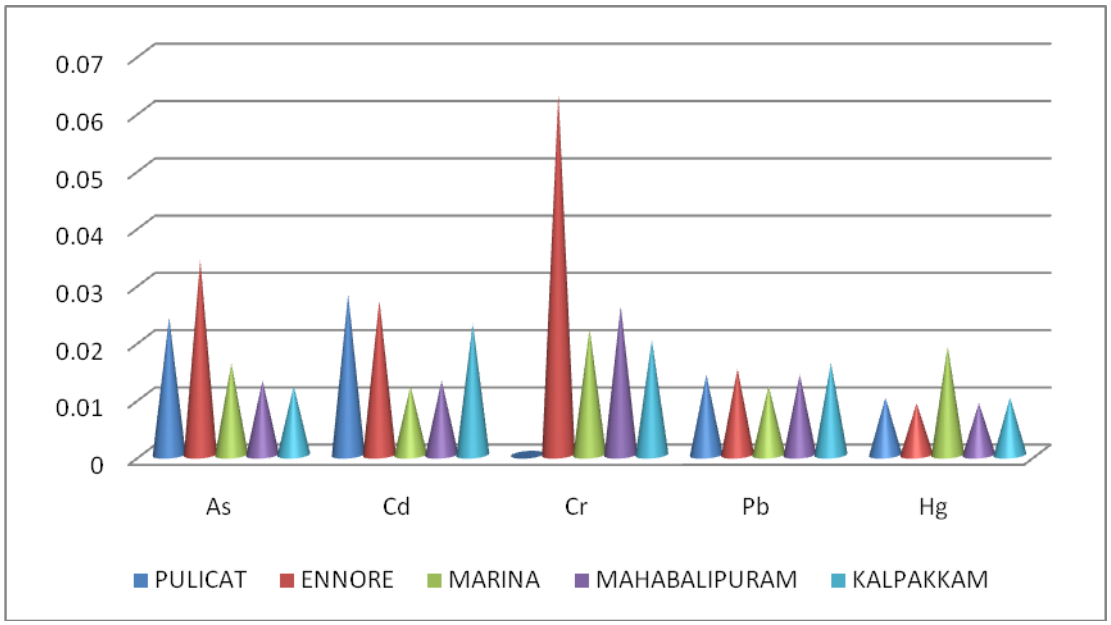

Concentration of H.M. in water collected from different locations (mg/lit)

Sediment L: The concentrations of heavy metals in sediments collected from 5 different locations are given in Table 3 and the graphical representation in Fig.4. The maximum concentration of Arsenic (1.841 mg/kg), Cadmium (1.374 mg/kg) and Lead (1. 814 mg/kg) were observed in Ennore. Maximum concentration of Chromium (1.569 mg/kg) and Mercury (0. 736 mg/kg) were observed in Marina.

Table3. Concentrations of H.M. in sediment collected from different locations (mg/kg)

Location	As	Cd	Cr	Pb	Hg
Pulicat	1.18	1.317	1.113	0.468	0.284
Ennore	1.841	1.374	1.157	1.481	0.394
Marina	0.508	1.067	1.569	0.363	0.673
Mahabalipuram	0.636	0.564	0.919	0.412	0.318
Kalpakkam	0.518	1.247	0.542	0.241	0.194

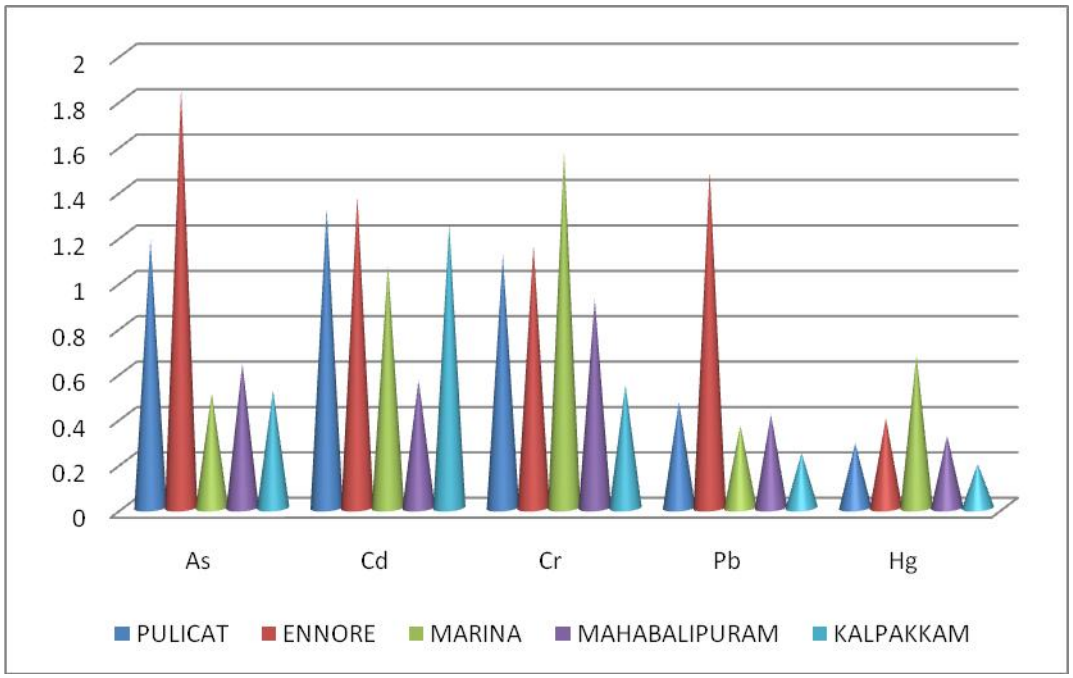

Figure 5. Concentration of H.M. in sediment collected from different locations (mg/kg)

IV. CONCLUSION

It is observed from this study that the maximum concentrations of all the five heavy metals in the fish are high in samples collected from Ennore. Maximum concentrations of two heavy metals (Arsenic and Chromium) in water and 3 heavy metals (Arsenic, Cadmium and Lead) in sediment are observed in Ennore. It may be due to the discharge of untreated effluent from various industries located near Ennore. As far as the importance of fish in human diet is concerned, it is necessary that the biological monitoring of water and fish should be done periodically to ensure the safety of sea food consumption. The safe disposal of industrial effluents and domestic sewage should be practiced to avoid such contamination. Also, the laws enacted to protect the environment should be enforced effectively.

REFERENCES

[1] Duffus.J.H (Heavy Metal-A Meaningless Term?. Pure and Applies Chemistry, Vol.74, No.5, Pages 793-8072002)
[2] S.P.Parker, Dictionary of Scientific and Technical Terms 4th Edition, Mc Graw Hill New York (1989).
[3] Drinking water Glossary, A Dictionary of Technical and Legal Terms Related to Drinking water. World Water Rescue Foundation.
[4] Hawkes.S.J. What is a Heavy Metal?. Journal of Chemical Education, Vol 74, No.11, Page-1374(1997).
[5] 200. Reena Sinhh, Neethu Gautam and Rajiv Gupta, Heavy Metals and Living Systems, Indian Journal of Pharmacology, 2011, May-June 43(3), Pages 246-253
[6] Wendy Griswold, Human Health Effects of Heavy Metals. Environmental Science and Technology Briefs for 15, March 2009.
[7] ShaíAto and P. A. Annune. Bioaccumulation of Heavy Metals in Fish (Tilapia Zilli and Clarias Gariepinus) enue, North ñ Central Nigeria. Pak. J. Anal. Environ. Chem. Vol. 12, No. 1 & 2Pages. 25-31. (2011)

[8] Padmini, E. and Kavitha, M. 2005a. Contaminant induced stress impact on biochemical changes in brain of estuarine grey mullets. Poll. Res., 24: 647-651.
[9] Batvari, B . P. D., K amala Kannan, S., Shanthi, K.K rishnamoorthy, R., Lee, K. J., & Jayaprakash, M. Heavy metals in two fish species (Carangoidel m alabaricus and Belones tronglurus) from Pulicat Lake, North of Chennai, South east coast of India. Environmental Monitoring and Assessment, 1 45, Pages.167–17 5. (2008).
[10] Prabhu Dass Batvari.B, Sivakumar.S, Shanthi.K, Lee.K.J, Oh.B.T, Krishnamurthy.R, Kamalakanna.S. Heavy metals accumulation in crab and shrimps from Pulicat lake, North Chennai coastal region, Southeast coast of India. Toxicolo Ind Health 2013 Jan 23.
[11] Seralathan Kamala-Kanna, B.Prabhu Dass Batvari, Kui Jae Lee, R.Krishnamoorthy, K.Shanthi, M.Jayaprakash. Assessment of heavy metals (Cd, Cr, and Pb) in water, sediment and seaweed (Ulvalactuca) in the Pulicat lake, South East India. Chemoshere Volume 71, Issue 7, Pages 1233-1240. April 2008,
[12] Jayaprakash,.M., Srinivasalu. S.Jonathan.M.P. and Mohan.V.. A baseline study of physicochemical parameters and trace metals in water of Ennore Creek, Chennai, India. Mar. Poll. Bull., 50: Pages:583-589.(2005)
[13] E.Padmini and B.Vijaya Geetha, A comparative seasonal pollution assessment study on Ennore Estuary with respect to metal accumulation in the grey mullet, Mugil cephalus. Oceanological and Hydrobiological Studies. Volume 36, Issue 4, Pages 91–103.
[14] Rajkumar, J.S.I., John Milton, M.C and Ambrose, T. Distribution of heavy metal concentrations in surface waters from Ennore Estuary, Tamil Nadu, India, International Journal of Current Research, Vol.3, Issue.3, Pages 237-244, March,2011.
[15] V.Shanthi1 and N. Gajendran. The impact of water pollution on the socio-economic status of the stakeholders of Ennore Creek,Bay of Bengal (India): Part I. Indian Journal of Science and Technology Vol.2 No 3 (Mar. 2009).

A Study on Transient Behaviour of A RCC Floor Slab

G.Gajalakshmi
Assistant professor, department of civil engineering
Sathyabama University, Chennai, Tamil Nadu, India

Dr. J. Abbas Mohaideen
Principal, Maamallan institute of technology, Sriperumbudur, Tamilnadu, India

Prof. A.R. Santhakumar
Professor and Former Dean, Anna University, Chennai, Tamilnadu, India

Abstarct - Modern construction systems use slender floor construction with high strength materials. The slender floor construction creates vibration problems. Vibration creates discomfort to the occupants. The usage of any floors should be recognized by the designer at the initial stage before construction. Nowadays the human activities are carried out in any of the floors under multi storied building. Based on such activities the analysis should be made prior and the effects should be handled in a safer manner before construction process. Human activities like jumping, dancing, walking create vibration. This paper analyse the dynamic behaviour of a RCC floor slab. The RCC floor slab size is 7mx 7.5m. The human rhythmic study is carried over the slab and the transient analysis is being done to know the behaviour study of the slab. ANSYS, a finite element method is used for the dynamic analysis. The rhythmic activities are created by making people to jump over the slab in the order of 2, 8, 12 & 18. Point A and B are selected over which the observations are made. Through transient analysis, Acceleration and Amplitude parameters are obtained. The results of maximum acceleration values are compared with I.S -800:2007 recommendations and the suggestion is provided.

Key words: vibration, acceleration, frequency, ANSYS, amplitude, time.

I. INTRODUCTION

The modern trend of construction technologies guide the structural Engineers to build with fast erection methods, light weight structures, large spans with minimum columns enabling greater construction space. These slender structures are made with the reduction of the structural elements cross section. The slender structure is more vulnerable to vibration problems. Generally, study of vibration and its effects are complex phenomena. The structures are with low natural frequencies which are closer to the frequency range associated with human rhythmic activities. Such vibration creates discomfort to the occupants.

The above matters lead a consistent structural analysis of the floor dynamic behaviour. These analysis make the structural Engineer to verify the stability of the structural systems and to reduce the human activities vibration problems.

The objective of the present study is to analyse the transient behaviour of a RCC floor slab when subjected to human rhythmic activities and to compare the maximum acceleration values with I.S800-2007 recommendation.

II. HUMAN INDUCED ACTIVITIES

In 1983, Ellingwood modified the concept of Reiher to account for the transient type of excitation using limit state. He suggested that large amplitude of transient motion which will be dissipated within few cycles can be accepted easily when compared to the steady state motion. He also extended that force-time relationship against dynamic effects was not supporting at that time. He mentioned stiffness and mass are the criteria responsible for dynamic effects in which if stiffness is increased, it is not the solution for reducing acceleration but at the same time there is a possibility for reducing the resonance. He concluded that maximum permissible deflection or increased span to depth ratio is not sufficient to meet the problems against vibration.

Allen (1987), made several research on human induced vibration on building structures. He concluded that dynamic actions from human body motions were simulated by a simple harmonic function with a frequency and rate.

Occupancies affected by the vibration	Acceleration limit, percent gravity
Office and residential	0.4 to0.7
Dining, Dancing, Weight-lifting	1.5 to 2.5
Aerobics, rhythmic activities only	4 to 7
Mixed use occupancies housing aerobics	2

Table-1. Recommended acceleration limits for vibration due to rhythmic activities

D.E. Allen and G.Pernica (1998) suggested how to counteract resonance due to rhythmic activity, the floor must be designed to have natural frequency greater than the forcing frequency of the highest significant harmonic. He mentioned the vibration limits in terms of acceleration as percentage of gravity. In this paper they said that the vibration impact not only depend on the nature of material of the floor, its thickness and span but also depend on the nature of activity of the people.

Silva et al obtained the dynamic loads from Faisca 2003 whereas he conducted experiments based on rhythmic and non-rhythmic activities. Faisca concluded with the mathematical representation with human dynamic loading.

III. MATHEMATICAL EQUATION FROM FAISCA

Faisca (2003) considered the dynamic loads, based on results achieved through a long series of experimental tests made with individuals carrying out rhythmic and non-rhythmic activities. These dynamic loads, generated by human activities, are described such as jumps with and without stimulation, aerobics, soccer, rock concert audiences and dancing. The load modelling is able to simulate human activities like aerobic gymnastics, dancing and free jumps.

The mathematical representation of the human dynamic loading is described by the following equation(1) .This expression requires some parameters like the activity period T, contact period with the structure Tc, period without contact with the model Ts, impact coefficient Kp, and phase coefficient CD.

$$F(t) = CD\left\{K_p P\left[0.5 - 0.5\cos\left(\frac{2\pi}{T_c}t\right)\right]\right\}, \text{for } t \le T_c$$

$$F(t) = 0, \text{for } T_c < t \le T \qquad \text{----------(1)}$$

Where:

F (t): dynamic loading, in (N); t: time, in (s); T: activity period (s); Tc: activity contact period (s); P: weight of the individual (N); Kp: impact coefficient; CD: phase coefficient.

IV. STRUCTURAL FLOOR DETAILS

The composite floor system consisted of span 7mx 7.5m .

RC Beam Details: 8"x 18"

RC Roof Slab Thickness: 8"

The concrete slab had a 25N/mm2 specified compression strength and a 2.4x104 N/mm2 Young's Modulus (Faisca).

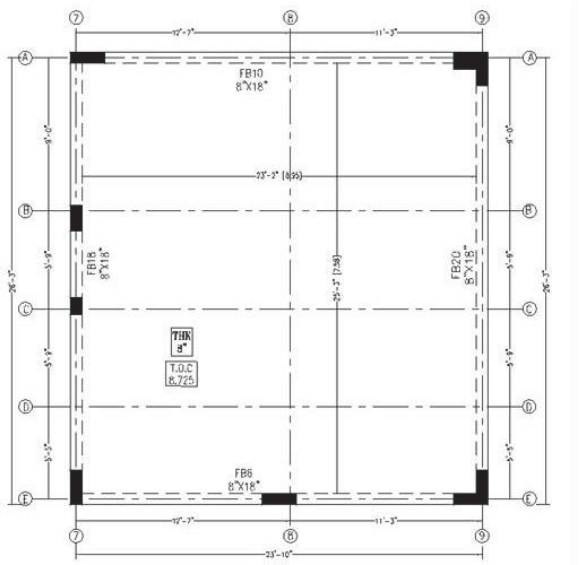

Fig.1 Layout of the floor plan.

V. FINITE ELEMENT ANALYSIS USING ANSYS

The proposed computational model, developed for the RCC floor dynamic analysis, adopted the usual mesh refinement techniques present in finite element method simulations implemented in the ANSYS program (ANSYS, 11). In the present computational model, the floor beams are represented by three-dimensional beam elements (BEAM44), tension, compression, bending and torsion capabilities. The floor slab is represented by shell finite elements (SHELL63).

In this investigation, it is considered that materials (beam and slab) presented total interaction and have an elastic behaviour.

VI. ANALYSES OF FLOOR MODEL

The individual person weight is equal to 70kg(0.8kN- Bachmann & Amman, 1987).The assumed Damping ratio is equal to 2%(ξ = 0.02(IS 800- 2007).

The human-induced dynamic action is applied to the dancing area, as shown in Fig.2. The composite floor dynamical response, are obtained on the nodes A and B to verify the influence of the dynamical loads on the adjacent slab floor. In the current investigation, the human rhythmic dynamic loads are applied to the structural model corresponding to the effect of 2, 8, 12, and 18 individuals practicing aerobics. Hence 18 individual practicing is the full load condition for the numerical model.

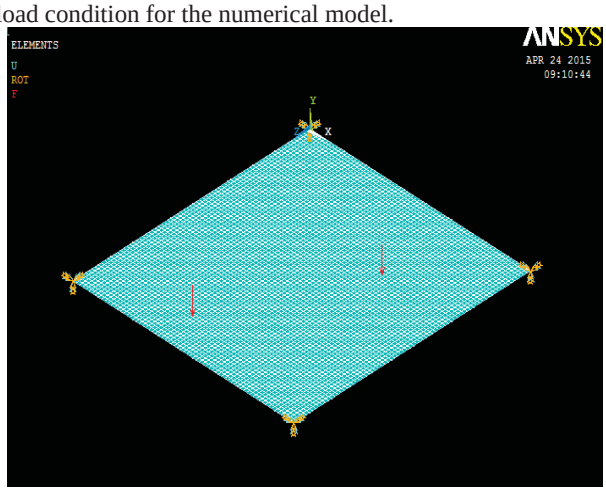

Fig.2 Load distribution Scheme associated to two persons

VII. TRANSIENT METHOD OF ANALYSIS

The following figures, 3,4,5,6,7,8,9,&10 present Acceleration versus Time graphs for the analyzed RCC floor slab at measuring point A and B, the person load is acting on the structural Model as human rhythmic activity.

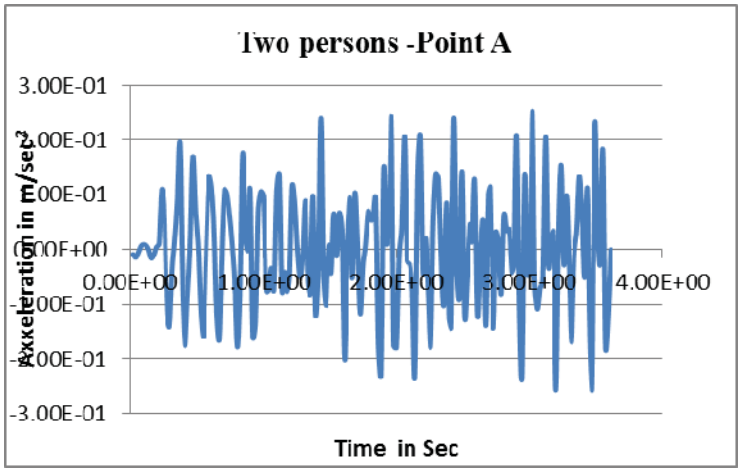

Fig.3- Acceleration Vs Time for 2 persons loading at Point A

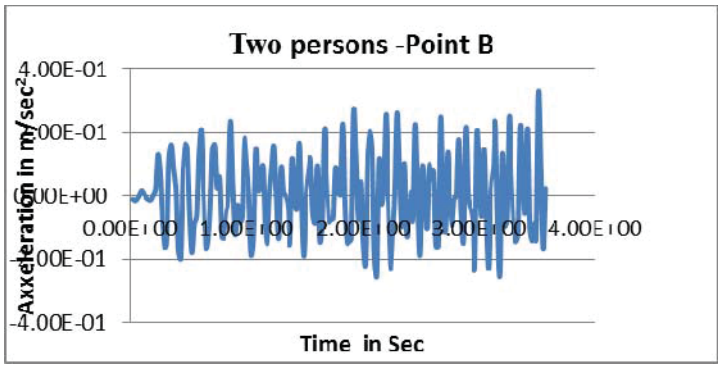

Fig.4- Acceleration Vs Time for 2 persons loading at Point B

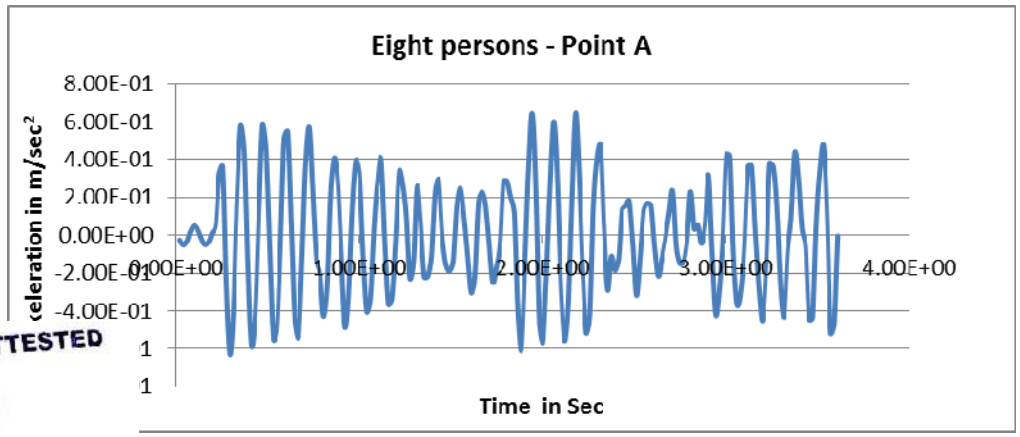

Fig.5 - Acceleration Vs Time for 8 persons loading at Point A

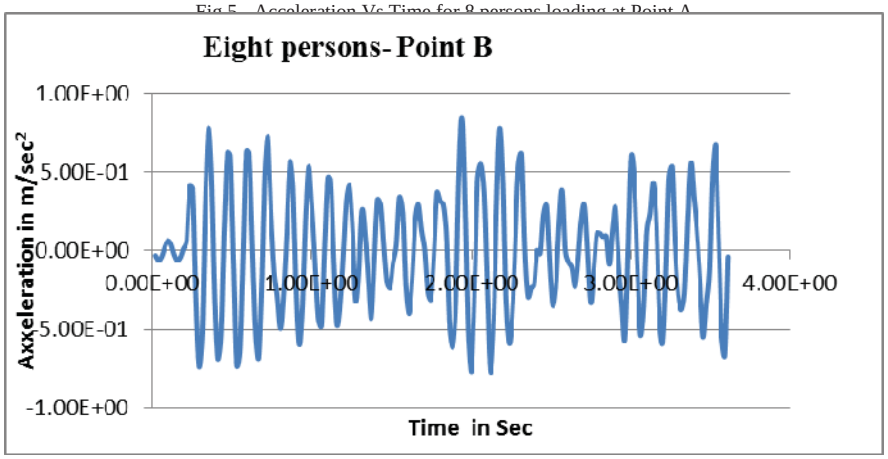

Fig.6- Acceleration Vs Time for 8 persons loading at Point B

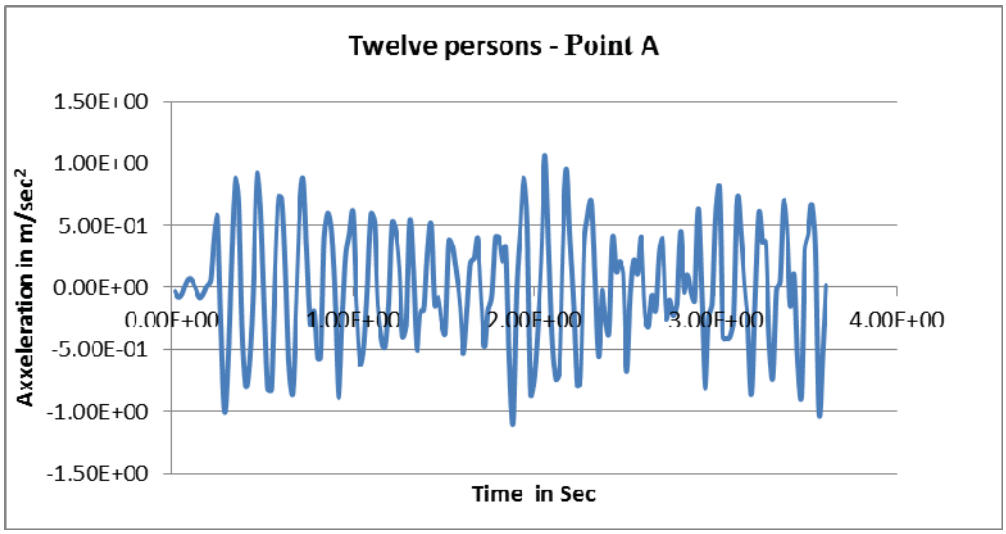

Fig.7- Acceleration Vs Time for 12 persons loading at Point A

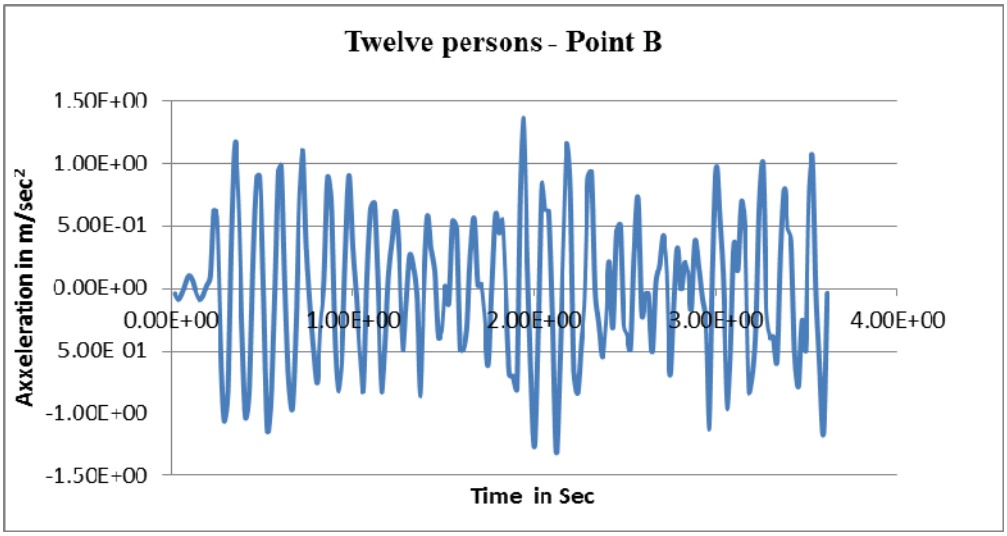

Fig.8- Acceleration Vs Time for 12 persons loading at Point B

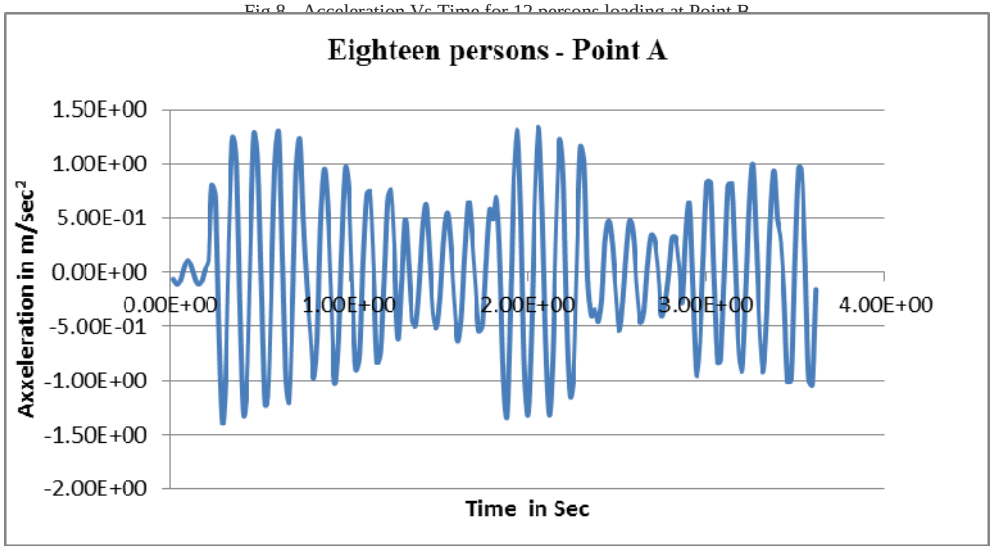

Fig.9- Acceleration Vs Time for 18 persons loading at Point A

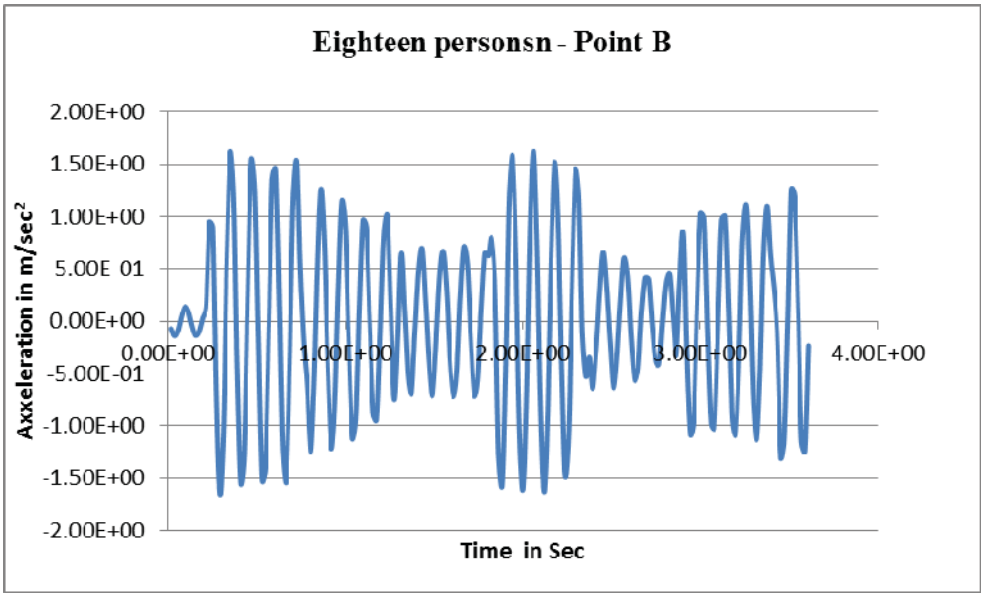

Fig.10-Acceleration Vs Time for 18 persons loading at Point B

Table-2: Maximum Amplitude values

No of Persons	Maximum Amplitude	
	Point A	Point B
2	0.062	0.068
8	0.21	0.263
12	0.32	0.39
18	0.47	0.58

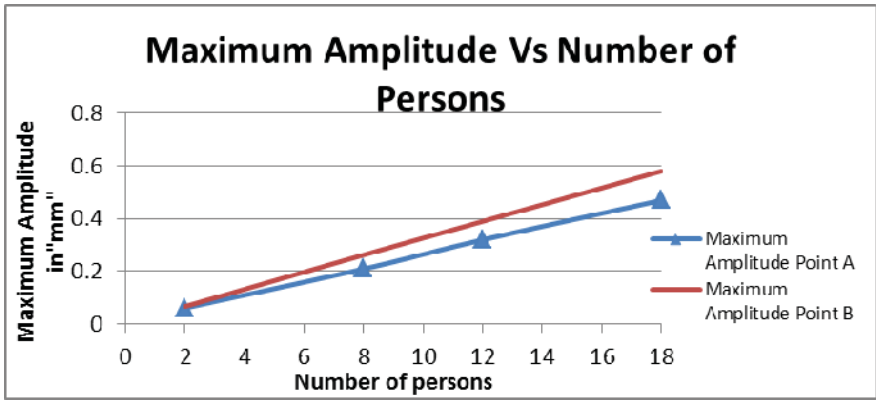

Fig.11-Maximum Amplitude comparison between Point A and B

VIII. DISCUSSIONS

A. Comparison of values between point A and point B .

1. From the result, it is observed that peak acceleration value is increased nearly 22% in point A when compare to point B for 2 persons loading with the acceleration values are 0.254 m/sec2 & 0.324 pectively.

ons loading, it is observed that peak acceleration value is increased nearly 24% in point A pare to point B with the acceleration values are 0.646 m/sec2& 0.846 m/sec2respectively.

mum acceleration values is increased nearly 21% in point A when compare to point B for 12 ading with the values are 1.07 m/sec2& 1.35 m/sec2 respectively.

4. For full loading condition, peak the acceleration value is increased nearly 15% for point B when compare with point A.
5. Nearly 1/4th of the values are increased in point B when compare to point A for 2,8 and 12 persons loading.
6. For 18 persons loading condition only one seventh of value is increased at point B than point A.

B. Comparison of Maximum acceleration values with Threshold limit.

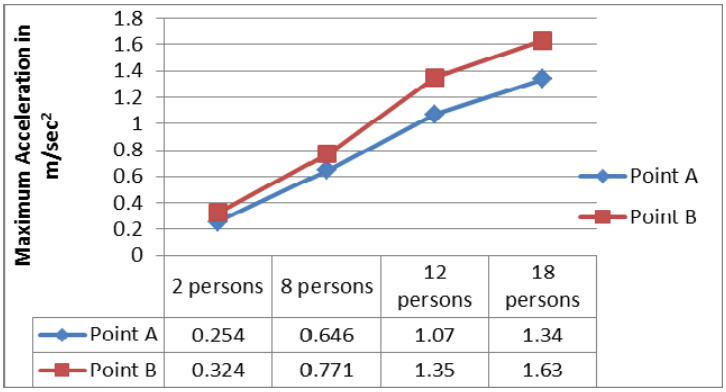

	2 persons	8 persons	12 persons	18 persons
Point A	0.254	0.646	1.07	1.34
Point B	0.324	0.771	1.35	1.63

Fig.12- Maximum acceleration values

The maximum values of acceleration observed at point A and B for two persons loading are 0.254 & 0.324 respectively. The present code of practice in steel (IS 800-2007) limits the maximum acceleration levels to a value of 0.5% g =0.05m/sec 2 which is a very stringent vibration criteria.

IX. CONCLUSION

1. It is concluded that for maximum loading condition ,number of persons are scattered throughout the slab at the maximum level. On account of this, the vibration effects are also scattered fully over the floor slab. Therefore the observations at point A & B are nearly closer with the values of maximum acceleration as 1.39 and 1.63 for 18 persons loading. In this case ,17% increase value is observed at point B when compare with point A whereas for 2,8 and 12 persons loading 22-23% difference is observed.

2. The maximum vertical response acceleration at critical measurement points in the floor system are found to be in the range of 0.254-1.39m/sec2 in point A and 0.324-1.63m/sec2 in point B for 2,8,12 &18 persons loading condition. This shows that, there is not a substantial increase due to cumulative loading of number of persons simultaneously jumping on the floor as compared to single person or a couple jumping. There is a non-linear relationship found from the study between the maximum peak response acceleration versus number of persons inducing dynamic excitation.

However it is concluded and cautioned that even for the two persons generally the rhythmic activity response acceleration is for higher than what is permitted in I.S 800-2007 as the governing maximum acceleration. Hence, it is suggested that suitable stiffening or enhanced damping shall be available for floor system meant for these kinds of rhythmic activities.

REFERENCES

[1] Allen ,D.E et al(1985) Vibration criteria for assembly occupancies, Canadian journal of Civil engineering, vol.12, pp. 617 – 623.
[2] Allen ,D.E (1990) Building vibration from human activities, ACI concrete International -Design and Construction.
[3] Bachmann. H (1992) Case studies of structures with man induced vibration, Journal of Structural Engineering, vol-118,No:3.
[4] Bruce Ellingwood. M and Andrew Tallin (1984) Structural Serviceability- Floor vibration, Journal of Structural Engineering, vol.110, No.2, ISSN 0733-9445.
[5] Da Silva, J.G.S. et al(2006) Dynamical response of composite steel deck floors, Latin American Journal of Solids and Structures, 3 .
[6] Da Silva, J.G.S. et al(2008) Vibration Analysis of orthotropic composite floors for human rhythmic activities, Journal of Brazilian Society of Mechanical Sciences and Engineering, pp. 56 – 65, 2008.
[7] Da Silva, J.G.S. et al(2011) Vibration Analysis of long span joist floors submitted to Human Rhythmic Activities, State University of
N 978-953-307-209-8, pp. 231 – 244, 2011.
3) Caracterização de cargas dinâmicas geradas por atividades humanas (Characterization of Dynamic Loads due to
, PhD Thesis (in Portuguese), COPPE/UFRJ, Rio de Janeiro, RJ, Brazil, pp. 1-240
n standard general construction in steel – code of practice- third revision
2003) Floor vibrations due to human activity, Steel design guide series by American institute of steel Construction.

International Journal of Scientific & Engineering Research, Volume 5, Issue 1 2, December-2014 18

ISSN 2229-5518

Cloud point extraction of Phenol using TX-100 as non-ionic surfactant

M.D. Duraimurugan alias Saravanan 1, D.K. Shanmugapriya 1, P.Kalaichelvi 1, A.Arunagiri 1,*

1 Department of Chemical engineering, National Institute of Technology, Tiruchirappalli -620015, Tamil nadu, India. email: durai_sar2003@yahoo.co.in

Abstract - Cloud point extraction is one of the surfactant-based separation technologies based on the clouding phenomenon of non-ionic surfactants. In this study, the experiments are carried out to study the effect of non-ionic surfactant concentration and additives concentration on Cloud point of non-ionic surfactant which is one of the design parameter for the cloud point extraction system. The effect of surfactant concentration, solute concentration, electrolytes concentration and operating temperature on the vital parameters of the system such as phase volume ratio (RV), pre-concentration factor (fC), solute distribution coefficient (Kd) and extraction efficiency (η %) has been studied. In the present study, Triton X-100 and phenol are used as non-ionic surfactant and solute respectively. In order to study electrolyte effects, NaCl and Na2SO4 are used for salting-out effect and NaI and NH4SCN are used for salting-in effect.

Index Terms - Non-ionic surfactants, Cloud point, Cloud point extraction, Phenol,

1 INTRODUTION

The removal of aromatic compounds is paid more attention recently, due to their carcinogenic and mutagenic characteristics. The amount of this type of compounds discharged into the environment is increasing day by day, especially in hydrosphere. Phenol is one of the major pollutants which have toxic effects on human health. The ingestion of phenol polluted water in the human body causes proteins degeneration, tissue erosion and paralysis of the central nervous system and also damages the kidney, liver and pancreas. Hence, it is necessary to remove the phenol from effluents before discharging into the water stream. However, because of their low solubility in water, common separation methods are inefficient in its acquirement and for its analysis. In treatment of water containing aromatics, traditional methods, such as coagulating sedimentation, adsorption, oxidation or biodegradation methods, are inefficient or costly in time or money [1], [2]. Hence, it is necessary to identify the new separation technique. Even there are different separation techniques are available; recently the CPE (micelle mediated separation process systems) is identified as one of the potential separation system [3].

1.1. Cloud Point Extraction(CPE)

Aqueous solutions of non-ionic surfactants turn cloudy at a definite temperature on heating and this temperature is referred to as the Cloud Point temperature (CP). This clouding phenomenon is caused by the decreased solubility
of a surfactant in aqueous media as a result of weakening of hydrogen bonding between a water molecule and the hydrophilic moiety of the surfactant due to heating. By allowing the solution to settle at a temperature above the cloud point, phase separation takes place. The smaller phase contains most of the surfactant and usually sinks to the bottom, some cases at the top called as surfactant rich phase. This unique surfactant solution phase separation phenomenon has been utilized in the design of some creative extraction, pre concentration and purification schemes. This is known as Cloud Point Extraction (CPE) [3].

2 EXPERIMENTAL

2.1 Materials

Triton X-100 is used as non-ionic surfactant. It is an octylphenol ethoxylate consisting of 9 to 10 moles of ethylene oxide and abbreviated as TX-100. It is a high purity and water-soluble liquid. Phenol is used as solute. K_2HPO_4 and KH_2PO_4 are used for the preparation of phosphate buffer. Ammonia is used to maintain the pH of the solution. 4-amino antipyrene and potassium ferricyanide are used as coloring agent. The electrolytes used are Sodium chloride and Sodium sulfate, Ammonium thiosulphate and Sodium iodide

2.1.1 Apparatus

nts was carried out in a water-bath with a good temperature control within 0.1□C. The phase separation can

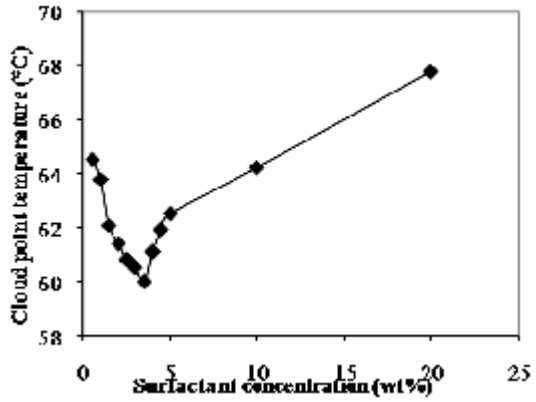

for 15 min at 3000rpm. After centrifugation, both phases become transparent with a clear phase boundary. The phenol concentration in the dilute phase was measured using UV-visible spectrophotometer wavelength at 530 nm.

2.2 Methods

2.2.1 Determination of Cloud point and CPE

The cloud point of aqueous surfactant solution was determined by heating 10 ml of such micellar solution in graduated glass tubes. The rate of temperature increase in the water bath is set at 1ºC per min. The cloud point is determined by visual observation at the temperature at which the solution became obviously turbid. The measurement of cloud point temperature is reproducible within ± 0.2ºC. The same procedure is repeated for aqueous nonionic surfactant micellar solution with addition of phenol and electrolytes. When the solution is heated above the cloud point temperature, it will accelerate the phase separation. After centrifugation, the volumes of both phases have been noticed. The amount of phenol in the dilute phase can be determined by 4-aminoantipyrene methods using UV-visible spectrophotometer.

3 RESULTS AND DISCUSSIONS

3.1 Effect of surfactant concentration on Cloud point

The variation of cloud point with the surfactant concentration is shown in Fig.1. The cloud point temperature of aqueous solutions of TX-100 decreases up to
3.5% (by wt) and then increases with increases in TX-100 concentration. The micelles concentration increases with increase in TX-100 concentration. Because of this, the cloud point of aqueous solutions of TX-100 decreases up to 3.5% (by wt). At higher surfactant concentration, the cloud point continues to increase due to the presence of structured water-surfactant system and the water molecules might act as buffers between micelles also observed the same trend [4].
Fig. 1 Effect of Triton-X 100 concentration on cloud Point

3.2 Effect of phenol concentration on Cloud point

Fig. 2 shows the change in cloud point temperature for different concentration of Phenol. Phenol concentration varied from 0.1 to 0.5% (wt %). The cloud point temperature decreases with increase in phenol concentration. When phenol is added to the aqueous non- ionic surfactant solutions, the decrease in cloud point may be due to the decreased hydrophilic (water-liking) character of the surfactant micelle [5]. It may be also due to the decrease in hydrophilic nature of the nearest ethylene oxide units, which results in a loss of some hydration. Due to the loss of hydration, the ethylene oxide chain should be shorter observed the similar results [6].

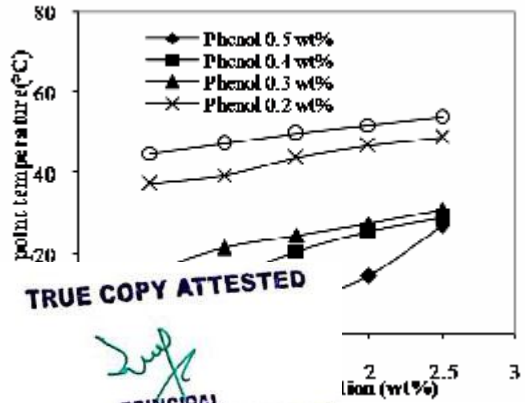

oint of TX-100

3.3 Effect of electrolytes on cloud point

In order to study the effect of electrolytes on cloud point, four different salts were used for the present study to consider both salting-in and salt out effect. When small amount of salt is added to nonionic surfactant solutions, the cloud point remains constant. Salting in effect salts

IJSER © 2014 http://www.ijser.org/

International Journal of Scientific & Engineering Research, Volume 5, Issue 1 2, December-2014 20

ISSN 2229-5518

(NH_4SCN, NaI) increase the critical micelle concentration and raise the cloud point. In contrast, salting out salts (NaCl, Na_2SO_4) can decrease the cloud point. The cloud point changes of the aqueous TX-100 solution in presence of electrolytes are shown in Fig. 3. The cloud point changes of the aqueous TX-100 solution in presence of solute and electrolytes are shown in Fig. 4. In the following sections, the salting in and salting out effects is explained.

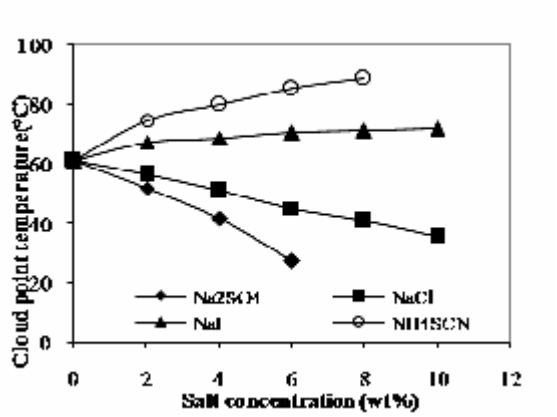

Fig. 3 Effect of electrolytes on cloud point of TX-100

3.3.1 Salting-out effect

The addition of most neutral electrolytes such as chlorides sulfates and carbonates typically depress the cloud point due to their salting-out effect in proportion to their concentration. In Fig. 3, it is shown that the cloud point decreases with increase in NaCl and Na_2SO_4 concentration for Triton X-100. In Fig. 4, it is shown that the cloud point decreases with increase in NaCl and Na_2SO_4 concentration and it decreases further with concentration of solute for Triton X-100. The addition of salts such as Cl^-, SO_4^{2-} to the non-ionic surfactant solution can depress the cloud point temperature by decreasing the availability of non associated water molecules to hydrate the ether oxygen's of the poly (ethylene) chains [7]. It is also observed that the depression of cloud point is more for Na_2SO_4 than NaCl [7], [8].

3.3.2 Salting-in effect

Salting-in effect salts such as iodides, thiocyanates and nitrates typically increase the cloud point. Fig. 3 shows the cloud point of aqueous TX-100 solution increases with increase in NH_4SCN and NaI concentration. Fig. 4 shows the cloud point of aqueous TX-100 solution decreases linearly because of the solute present in the solution as compared to Fig. 3. The increase in cloud point is more for NH_4SCN compared to NaI. The positive charge of NH_4SCN

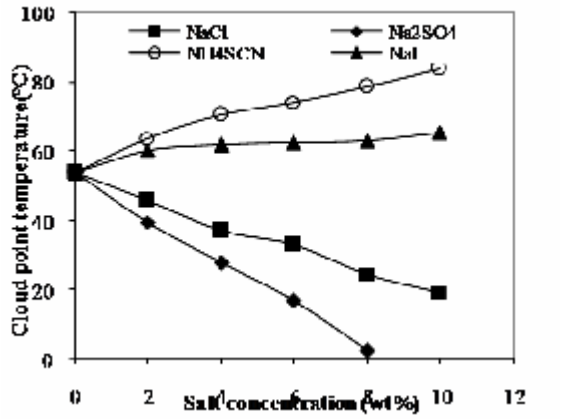

since it breaks the water structure. When NH_4SCN and NaI are added to the aqueous non-ionic surfactant been formed. If the concentration of NH_4SCN and NaI increases, then mixed micellar charge density also ar size. The charge density depends on the micellar size and it does not depend on the concentration of salts

lytes on cloud point of

3.4 Effect of concentration of surfactant, solute and operating temperature on CPE

The effects of surfactant concentration, solute concentration and operating temperature on CPE are discussed. The concentration of surfactant is varied from 0.5 to 2.5% (by wt) and solute concentration is varied from 0.1 to 0.5% (by wt). All the experiments have been conducted at three different temperatures such as 50, 60 & 70ºC. These operating temperatures have been selected based on the Cloud point temperatures.

3.5 Effect of surfactant and solute concentration on

R_V and f_C

3.5.1 Phase volume ratio

The phase volume ratio, R_V, is defined as the ratio of the volume of the surfactant-rich phase to that of the volume of the aqueous phase. The volumes of the two phases are measured using graduated centrifuged tubes

$R_V = V_S / V_W$ (1)

Where V_S and V_W are the volumes of the surfactant-rich phase and the aqueous phase respectively.

International Journal of Scientific & Engineering Research, Volume 5, Issue 1 2, December-2014 21

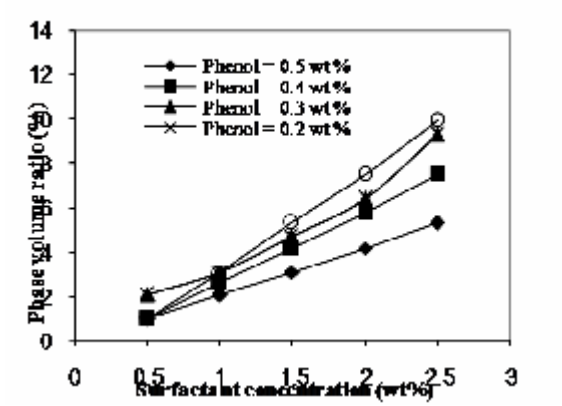

ISSN 2229-5518

Fig. 5 Effect of solute and surfactant in phase volume ratio

Fig.5 shows the effect of surfactant and solute concentration in phase volume ratio. From the figure it is observed that the phase volume ratio increases with increase in surfactant concentration and it decreases with increase in solute concentration. The phase volume ratio increases because of increasing volume of surfactant-rich phase. It is due to the distribution of surfactant increases in the surfactant rich phase. The low phase volume ratio for higher concentration of solute shows that the amount of phenol in surfactant-rich phase would be high [9].

3.5.2 Pre-concentration factor

The pre concentration factor f_C is defined as the ratio of the volume of bulk solution before phase separation to that of the surfactant-rich phase after phase separation.

Fig. 6 shows the effect of surfactant and solute concentration on pre-concentration factor. It is observed that the pre-concentration factor decreases with increase in surfactant concentration and decreases with solute concentration. The high solubility of solute in the surfactant micelles and the solute concentration in the surfactant-rich phase was very high. Because of high solubility of solute shows the decreasing pre-concentration factor due to increase in surfactant concentration and decrease in solute concentration also observed the similar result [9], [10].

3.6 Effect of Operating Temperature

3.6.1 Distribution Coefficient

The distribution coefficient or equilibrium partition coefficient K_d or K_p is defined as the ratio of the concentration of solute in surfactant-rich phase to that of the concentration of solute in dilute phase.

$K_d = C_S / C_W$ (3)

Where C_S and C_W are the concentration of solute in the surfactant-rich phase and the dilute phase respectively.

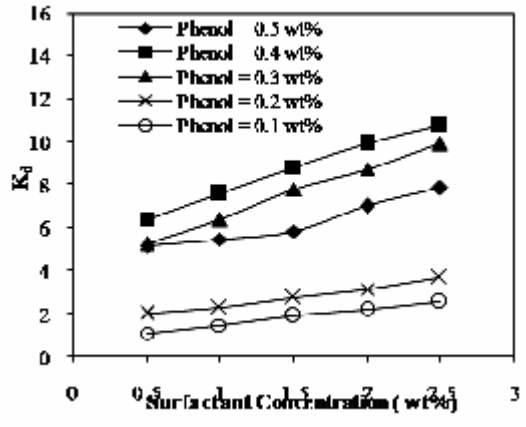

(2)

Where V_t and V_s are the volumes of the bulk solution before

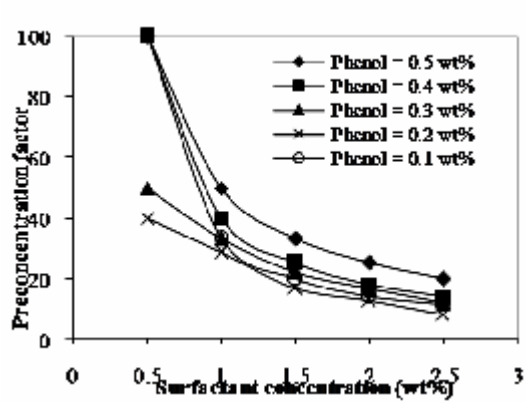

phase separation and the surfactant-rich phase respectively.

Fig. 6 Effect of solute and surfactant in pre-concentration factor

Fig. 7 Effect of operating temperature at 60ºC on distribution coefficient

Fig.7 shows the effect of operating temperature at 60ºC on distribution coefficient. The same pattern is observed for 50ºC & 70ºC. It increases with increase in both surfactant and solute concentration. The distribution of solute depends on the specific solute-water interaction. If the interaction is more, then distribution coefficient will be high. The distribution coefficient increases with increase in operating temperature is shown in Fig. 8 for the phenol concentration of 0.4% (by wt) and three different temperatures. The observations made by are similar to the present experimental observation [10], [11].

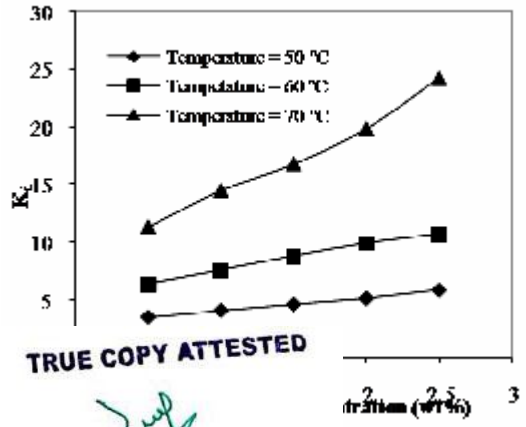

ure at phenol concentration of 0.4% (by wt) on distribution coefficient

The recovery efficiency of solute, η, can be characterized as the percentage of solute extracted from the bulk solution into the surfactant-rich phase.

$$CoVt \square Cw(Vt \square Vs)$$

hydrophilic (Phenol has a short hydrophobic portion (benzene ring) and a highly polar hydroxyl group) and then the extraction efficiency is low at 50ºC. The extraction efficiency is high, when the system is at higher operating temperature. The increase in recovery at elevated temperatures may be due to an increase in solubility of the solutes in the micellar phase [11].

3.7 Effect of Electrolyte Concentration and Operating

Temperature on CPE

The following section deals on the effect of electrolytes concentration and operating temperatures on phase volume ratio, pre-concentration factor, distribution coefficient and the extraction efficiency. Both salting-in and salting-out effects are studied with three different operating temperatures which is selected based on their cloud point. NaCl and Na_2SO_4 are used as salting-out effect salts and all the experiments have been conducted at three different temperatures. For NaCl, the experiments are conducted at
50, 60 & 70ºC. For Na_2SO_4, the experiments are conducted at
50, 55 & 60ºC. NaI and NH_4SCN is used to study the salting-in effect and all the experiments have been conducted at three different temperatures i.e. 80, 82.5 &
85□C. All the experiments are conducted for the surfactant

$$\eta\ \% = \frac{CoVt}{} *100 \quad (4)$$

concentration and solute concentration 2.5% (by wt) and
0.1% (by wt) respectively. The salt concentration is varied
Where C_0 is the initial concentration of solute in the micellar solution and C_w is the concentration of solute in dilute phase.

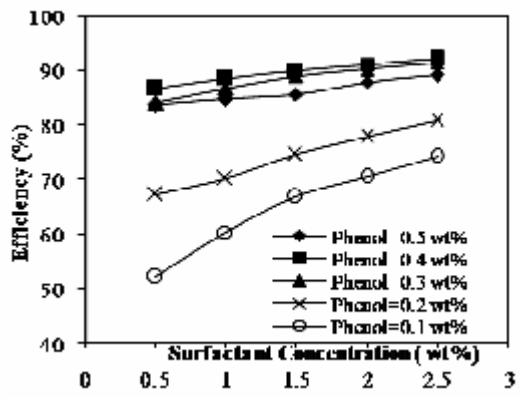

Fig. 9 Effect of operating temperature at 60ºC on efficiency
(%)
Fig. 9 shows the effect of temperature at 60ºC on the extraction efficiency. For temperature 50 and 70ºC, the observed trend is similar to 60ºC. It increases with increase in surfactant concentration and also increases with increase in operating temperatures. The nature of solute is more from 0 to 10% (by wt).

3.7.1 Salting-out effect

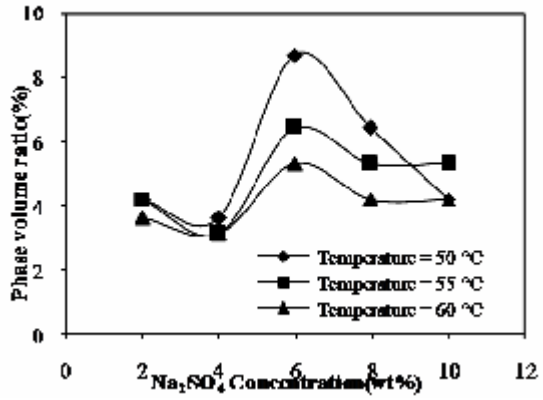

The effect of Na_2SO_4 concentration and operating temperature on the phase volume ratio is shown in Fig. 10. The phase volume ratio increases with increase in Na_2SO_4 concentration and it decreases with increase in operating temperature. The addition of electrolyte would compress the volume of surfactant-rich phase from 0.9 ml to 0.25 ml because of the dehydration process.

IJSER © 2014 http://www.ijser.org/

International Journal of Scientific & Engineering Research, Volume 5, Issue 1 2, December-2014 23

ISSN 2229-5518

Fig.10 Effect of Na_2SO_4 and operating temperature on phase volume ratio

The effect of Na_2SO_4 concentration and operating temperature on the pre-concentration factor is shown in Fig.11. The pre-concentration factor was obtained in the CPE process for 0.1% (by wt) of phenol and 2.5% (by wt) of TX-100 without any electrolyte is 11. The addition of electrolyte may compress the surfactant-rich phase volume and the pre-concentration factor for the same concentration of solute and surfactant in presence of salt fall down from

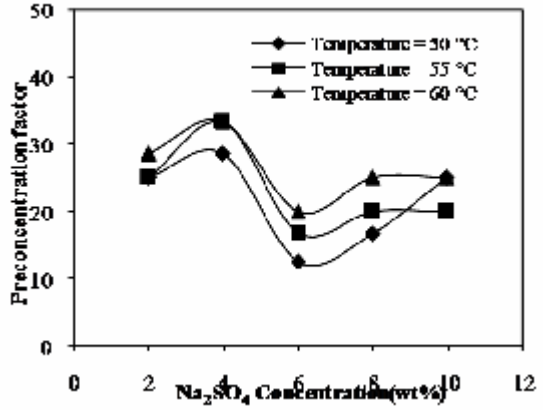

40 to 10 at three different operating temperatures [12].

Fig. 11 Effect of Na_2SO_4 and operating temperature on pre- concentration factor

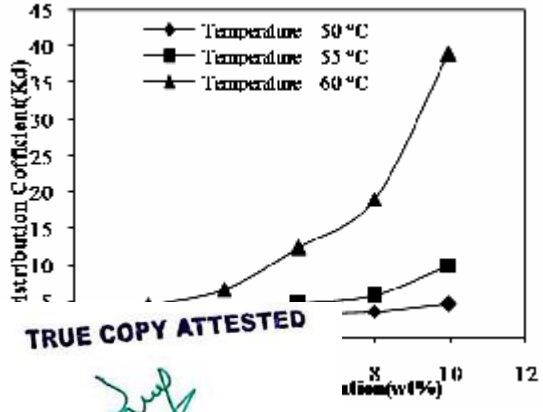

and operating temperature on distribution coefficient is shown in Fig.12. The distribution coefficient concentration and also it increases with increase in operating temperatures. The addition of electrolyte factant-rich phase (V_S); due to low V_S, the amount of solute in surfactant-rich phase is very high. Because of o found as high value [12].

Fig. 12 Effect of Na_2SO_4 and operating temperature on distribution coefficient

Fig.13 illustrates the effect of Na_2SO_4 concentration and operating temperature on the recovery of phenol. The efficiency increases with increase in concentration of Na_2SO_4 and operating temperature. An efficient change in the recovery is observed at the different salt concentrations. Recovery of phenol depends on the micellar concentration. Increasing salt concentration could lead to greater recovery efficiency. For example, the recovery of phenol for sodium sulfate increases up to 98% at the operating temperature of 60°C. At the higher operating temperature, the recovery of phenol increases due to an increase in solubility of the

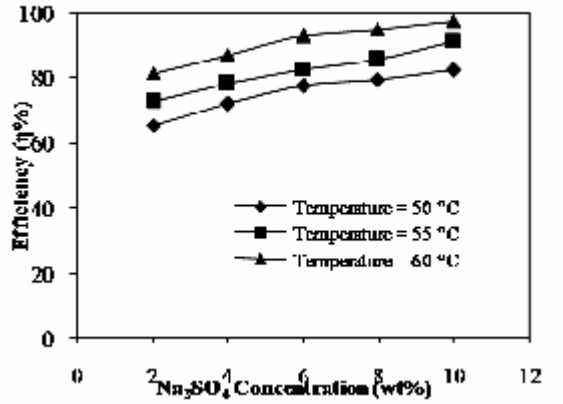

analyses in the micellar phase [13]. The above said parameters are studied for NaCl at the three different temperatures such as 50, 60 & 70ºC and the similar trend is observed.

Fig. 13 Effect of Na_2SO_4 and operating temperature on extraction efficiency

3.7.2 Salting-in effect

The following figures illustrate the results obtained for the effect of NaI concentration and operating temperature on above mentioned parameters. The influence of NaI concentration and operating temperature on phase volume ratio is shown in Fig.14. In this case the phase volume ratio attained high value such as salting-out at 6% (by wt) of electrolyte concentration and then decreases with increase in electrolyte concentration. The pre-concentration factor is obtained as high as 67, because of added electrolytes would compress the V_S. This result has shown in Fig. 15. Distribution coefficient decreases with increase in concentration of NaI and at operating temperatures it increases.

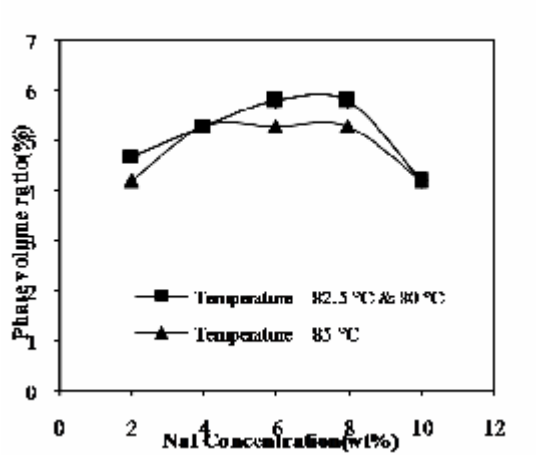

ISSN 2229-5518

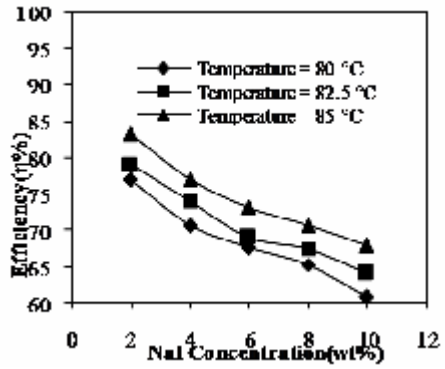

Fig. 14 Effect of NaI and operating temperature on phase volume ratio

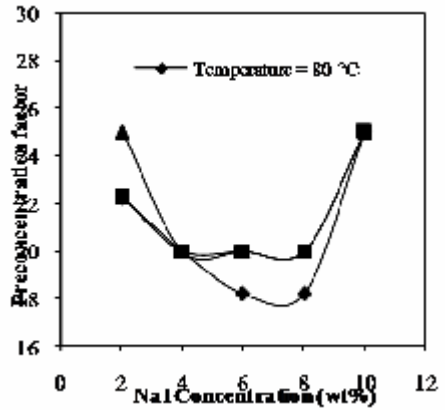

Fig. 15 Effect of NaI and operating temperature on pre- concentration factor

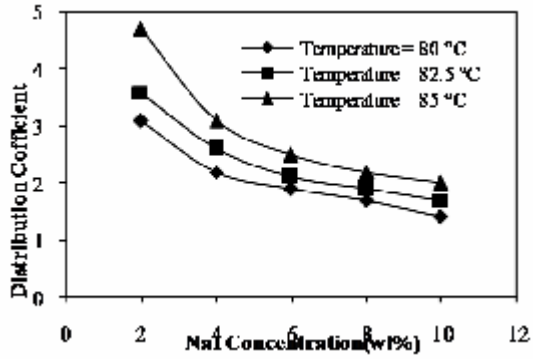

The distribution coefficient decreases with increase in solute hydrophobicity (the hydrophobicity of phenol increases with increase in phenol concentration).It is probably due to the increase in the water solubility of the hydrocarbon compounds. It is shown in Fig. 16.

Fig. 16 Effect of NaI and operating temperature on distribution coefficient

Fig. 17 Effect of NaI and Operating temperature on extraction efficiency

The recovery of phenol decreases with increase in concentration of NaI and it increases with operating temperatures. The recovery of solute decreases, because of solute hydrophobicity. The result is shown in Fig. 17. The above said parameters are studied for NH_4SCN at the same set of temperature conditions.

4 CONCLUSIONS

CPE using Triton X-100 as non-ionic surfactant can extract phenol without using organic solvents. The effect of nonionic surfactant concentration (TX-100) on cloud point was studied. The cloud point temperature decreases up to
3.5% (by wt) with the increase in Triton X-100 concentration
and then it increases with increase in concentration. The cloud point temperature decreases with increase in phenol concentration, NaCl and Na_2SO_4 concentration (salting out effect). The cloud point temperature increases for NH_4SCN and NaI due to its salting-in effect.

se volume ratio, pre-concentration factor, and distribution coefficient and extraction efficiency are studied
ant, solute and electrolyte concentration and for different set of operating temperatures. The distribution
y are increases with increase in surfactant and solute concentration for without electrolytes. For added
creases with increasing operating temperature. Pre- concentration factor varies between 10 and 67. The
tion efficiency increases with increasing in operating temperature and NaCl and Na_2SO_4 concentration for
coefficient and extraction efficiency decreases with increasing in NH_4SCN and NaI concentration.

International Journal of Scientific & Engineering Research, Volume 5, Issue 1 2, December-2014 25

ISSN 2229-5518

REFERENCES

[1] www.osha.gov, “Occupational safety and Health Guideline for phenol”. *OSHA, Washington, DC, U.S*. Department of labour.

[2] Pollution Control Department, *Ministry of Natural Resources and Environment*, Thailand.

[3] L. Willie and P. Edmondo, “A Critical Review of Surfactant- Mediated Phase Separations (Cloud-Point Extractions): Theory and Applications”. *Critical reviews in analytical chemistry*, Vol. 24, pp. 133-177 (1993) .

[4] L. Koshy, A. H. Saiyad and A. K. Rakshit, “The effects of

various foreign substances on the cloud point of Triton X

100 and Triton X 114”. *J. Colloid Polym Sci*., Vol. 274, pp. 582-

587 (1996).

[5] H. Saito and K. Shinoda, “The solubilization of hydrocarbons in aqueous solutions of nonionic surfactants”. *J. Colloid Sci.* Vol. 24, pp. 10-15 (1967).

[6] N. M. William “Factors affecting the solubility of nonionic emulsifiers”. *J. Colloid Sci.* Vol. 11, pp. 272-285 (1956).

[7] D. Bai, J. Li, S. B. Chen, and B.H. Chen, “A Novel Cloud- Point Extraction Process for Preconcentrating Selected Polycyclic Aromatic Hydrocarbons in Aqueous Solution”. *Environ. Sci. Technol*. Vol. 35, pp. 3936-3940 (2001).

[8] B. Haddou, J.P. Canselier and C. Gourdon, “Cloud point extraction of phenol and benzyl alcohol from aqueous stream”. *Sep. Purif. Tech*. Vol. 50, pp. 114-121 (2006).

[9] Y. Bingjia, Y. Li, H. Qiong and S. Akita, “Cloud Point Extraction of Polycyclic Aromatic Hydrocarbons in Aqueous Solution with Silicone Surfactants”. *Chin. J. Chem. Eng*. Vol. 15 (4), pp. 468-473 (2007).

[10] D. Sicilia, S. Rubio and D. Pérez-Bendito, “Evaluation of

the factors affecting extraction of organic compounds based on the acid-induced phase cloud point approach”. *Analytica Chimica Acta*. Vol. 460, pp. 13-22 (2002).

[11] Q. Fang, H. W. Yeung, H. W. Leung and C. W. Huie, “Micelle-mediated extraction and preconcentration of ginsenosides from Chinese herbal medicine”. *J. Chromatography A*. Vol. 904, pp. 47-55 (2000).

[12] L. Jing-Liang and C. Bing-Hung, “Equilibrium partition of polycyclic aromatic hydrocarbons in a cloud-point extraction process”. *J. Colloid Sci.* Vol. 263, pp. 625-632 (2003).

[13] S. R. Sarath, B. R. John and P. G. Donald, “Quantification

of Polycyclic Aromatic Hydrocarbons and Polychlorinated Dibenzo- p -dioxins in Human Serum by Combined Micelle-Mediated Extraction (Cloud-Point Extraction) and HPLC”. *Anal. Chem*. Vo. 68, pp. 1556-1560 (1996).

ENVIRONMENTAL ENGINEERING

As per Anna University New Syllabus
For Ist Year B.E /B.Tech Students

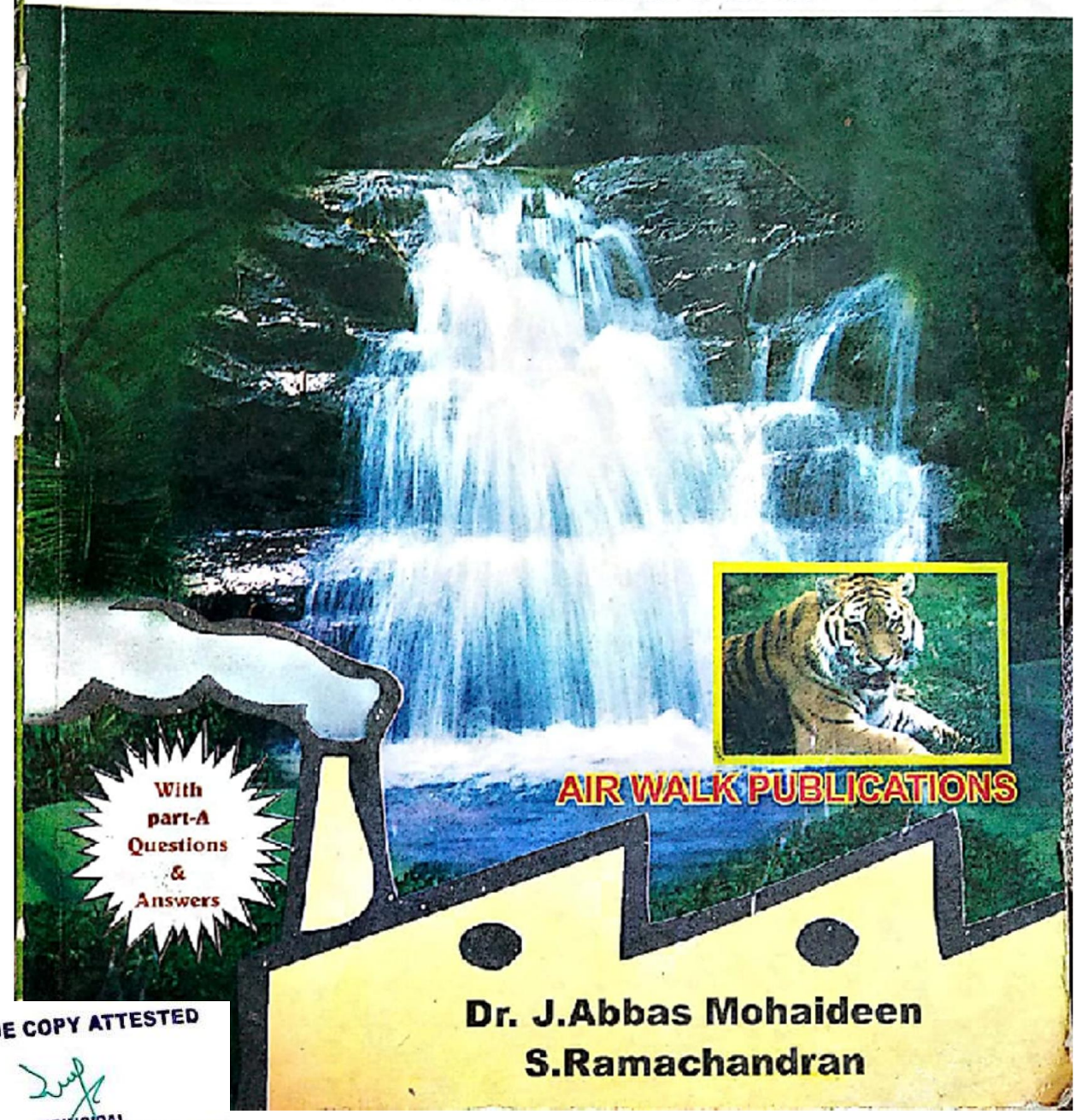

With part-A Questions & Answers

AIR WALK PUBLICATIONS

Dr. J.Abbas Mohaideen
S.Ramachandran

Environmental Engineering

(For I Year B.E. / B.Tech. - common to all branches)

(As per Anna University New Syllabus)

Dr. J. ABBAS MOHAIDEEN
M.Tech., Ph.D
Prof. & HOD,
Department of Chemical and
Environmental Engineering

S. RAMACHANDRAN,
M.E., M.B.A., (Ph.D)
Assistant Professor

Sathyabama Deemed University
Jeppiaar Nagar, Chennai - 600 119

AIR WALK PUBLICATIONS

First Edition: 2004

Price : **Rs. 120/-**

Dedicated to Our Parents

Copies can be had from :
AIR WALK PUBLICATIONS
(Near All India Radio)
28-A, I Floor, Karneeshwarar Pagoda Street,
Mylapore, Chennai - 600 004.
Ph.: 2466 1909, Cell: 3101 8887

Typeset by:
AKSHARA, Chennai - 18. Ph.: 2436 4303

Printed at:
Abinayaram Printers, Chennai - 4. **Ph.: 2467 0703, 2466 1909**

PREFACE

I have great pleasure and satisfaction in presenting this book titled "**Environmental Engineering**" to Ist year B.E. / B.Tech Sathyabama Deemed University students. This book will make it easier, for the students to understand the basic concepts. This book is based on lecture notes prepared for teaching the under graduate students.

Two marks and 12 marks questions and answers of each unit are also included.

I express my sincere gratitude to our revered Chairman **Thiru. Jeppiaar,** M.A., B.L., Chancellor, Sathyabama Institute of Science and Technology (Deemed University).

I sincerely thank to our Secretary and Correspondent **Thiru. P. Chinnadurai,** M.A., M.Phil., M.Ed., I also express my sincere thanks to **Dr. B. Babu Manoharan,** M.A., M.B.A., Ph.D., and **Tmt. Sheila Babu Manoharan,** M.A., B.L., Directors, St.Joseph's College of Engineering for their constant encouragement to bring out this book.

I express my sincere thanks to **Thiru. N. Marie Johnson,** B.E., and **Tmt. Mariazeena Johnson,** B.E., Directors, Sathyabama Institute of Science and Technology for their encouragement to bring out this book. I also express my sincere thanks to **Thiru. N. Marie Wilson,** B.Tech., and **Tmt. Rageena Wilson,** B.Tech., Directors, Jeppiaar Engineering College for their constant encouragement and support.

I express my great appreciation to **Mrs. R. Parameshwari,** M.Com., Air Walk Publications for her continuous encouragement, technical support and patience during the preparation of this book.

Any errors, omissions and suggestions for the improvement of this book, brought to my notice will be thankfully acknowledged and incorporated in the next edition.

– Author

Antimicrobial activity and phytochemical screening of Cynodon dactylon and Carica papaya

Article *in* Research journal of biotechnology · February 2014

CITATIONS
0

READS
336

1 author:

Arumugam Nagarajan
Indian Institute of Technology Madras
25 PUBLICATIONS **22** CITATIONS

SEE PROFILE

Research in Biotechnology, 5(5): 21-31, 2014 ISSN: 2229-791X
www.researchinbiotechnology.com

Regular Article

Antimicrobial activity and phytochemical screening of *Cynodon dactylon* and *Carica papaya*

Arumugam N[1*], T. Boobalan[2], P. Raja Rajeswari[3] & M D. Duraimurugan[2]

[1*] Department of Biology, Gandhigram Rural Institute – Deemed University, Dindigul – 624 302, Tamil Nadu India
[2]Department of Chemical Engineering, Mohamed Sathak Engineering College, Kilakarai-623 806, Tamil Nadu, India
[3]Department of Biochemistry, St., Mary's College (Autonomous), Thoothukudi-628 001, Tamil Nadu, India
Corresponding author Email: aarumugham83@gmail.com

Presence of various phytochemical compounds in C*ynodon dactylon* and C*arica papaya* was qualitatively and quantitatively determined by various standard method of analysis. The suitable extraction method was identified for phytochemical compound extraction in above selected plants. The present study revealed that ethanol is a suitable solvent system which showed the presence of high percentage in the range of 0.01 to 1.46 and 0.02 to 10.0 percentage of phytochemicals compared to other solvent extracts. The moderate percentage 0.01 to 1.0 and 0.00 to 0.7 percentages is obtained in chloroform extraction system and least is 0.00 to 1.04 and 0.01 to 0.64 percentage of constituents in acetone extract, very lowest percentage of phytochemical constituents was observed in the range of 0.00 to 0.03 and 0.00 to 0.04 percentage in hot water extraction system. These extracted various phytochemical constituents antimicrobial activity were tested against *E.coli* and *Salmonella sps.*, Ethanol, Chloroform and Acetone extractions showed inhibitory activity against *E.Coli* and *Salmonella sps.*, The selected plants has wide range of phytochemical constituents, hence further structural elucidation of such bioactive compounds is essential to study their traditional use and readily available food preservative agents against above bacterial food contamination.

Keywords: Phytochemical screening, Medicinal plant, *Cynodon dactylon, Carica papaya.*

Plants have always been a source of natural products for the treatment of various diseases (Newman and Cragg, 2005). Around 70 to 80% of the world populations, particularly in developing countries, rely on non-conventional medicine in their primary healthcare as reported by the World Health O forum 1993). Plant based advantage over synthetic ow human toxicity. In addition, chemical diversity of secondary plant metabolites that result from plant evolution is equal or superior to that found in synthetic combinatorial chemical libraries (Cosa *et al*., 2006).

Plants have their own chemical constituents and medicinal value that may alter certain physiologic actions in the human body. The most important of these bioactive constituents of plants are terpenes, alkaloids,

flavonoids and phenolic compounds. Terpenes are used as insecticides and their pharmacological properties include antibacterial, antifungal, antihelmintic, antimalarial and molluscicidal (Nisar Ahmad et *al*., 2011). Similarly phenolic compounds have a wide range of pharmaceutical activities such as anti-inflammatory, analgesics, antitumor, anti-HIV, anti-infective, vasodilatory, immunostimulant and antiulcerogenic (Walsh and Edward O'Farrell, 1961).

Recently, flavonoids have attracted interest due to the discovery of their pharmacological activities. Alkaloids are pharmaceutically significant and are used as analgesic, antimalarial, antiarrythmic, antispasmodic, the treatment of coughs and pain, the treatment of gout, and as pupil dilatin (Fehling, 1984). Hence, the last five decades, plants derived bioactive compounds and allied research have been focused more. The present study is to investigate the qualitative phytochemical analysis of two temperate regional plants. *C.dactylon* is an important ingredient in various ayurvedic preparations such as Anabolic, Antiseptic, Astringent, Cyanogenetic, Demulcent, Depurative, Laxative, Diuretic and Emollient. A decoction of the root is used as a diuretic in the treatment of dropsy and secondary syphilis etc., a whole plant has medicinal property. In recent years, leafs of *C.papaya (*an evergreen shrub or small tree) extract have been recommend by physicians for the treatment of dengue fever (a viral fever) orally. Hence, the identification and screening of active chemical constituents in selected plant extracts as potential recommendable medicine for various human illnesses. The different uses of selected plants in traditional medicine are reviewed in (Table 1). The selected plants for phytochemicals studies are well grown in temperate regions where the preliminary research work was carried out.

Table 1: Review of the Selected Plants of *Cynodon dactylon & Carica papaya* Medicinal Use

S.No	Species	Family	Traditional use	Reference
1	*Cynodon dactylon*	Poaceae	Anti inflammatory	Sindhu *et al*., 2009
			Cardio protective	Garjani *et al*., 2009
			Anti diabetic	Jarald *et al*., 2008
			Anti arrhythmic	Santosh Kumar Singh *et al*., 2008
			Diuretic	Sadki *et al*., 2010
			Antioxidant	Albert-Baskar *et al*., 2009
			Immunomodulatory & DNA protective	Mangathayaru *et al*., 2009
			Chemo preventive	Albert-Baskar *et al*., 2009
			Protection from ionizing radiation cytogenetic damage	Rao *et al*., 2008
			Nephrolithiasis (Kidney stone removal)	Atmani *et al*., 2009
2	*Carica papaya*	Caricaceae	Treatment for malaria	Titanji and Zofou *et al*., 2008
			Treatment for dengue fever	Subenthiran and Choon *et al*., 2013
			Antioxidant potential	Okoko and Ere *et al*., 2012
			Anti cancer activity	Nguyen *et al*., 2013
			Anti inflammatory activity	Gupta *et al* ., 1992
			Anti diabetic activity	Oboh *et al*., 2013
			Wound healing activity	Mahmood et *al*., 2005
			Anti microbial activity	Anibijuwon and Udeze *et al*., 2009
			Anti sicking activity	Imaga and Gbenle *et al*., 2009

Materials and Methods

Plant preparation

Fresh and disease-free shoots of *C.dactylon* and leaves of *C.papaya* were collected. The collected leaves were cleaned, washed with water and dried for 15 days under shade and at room temperature. Leaves were powdered and preserved in clean plastic containers, away from light, heat and moisture until use.

Preparation of plant extraction

Extraction in Hot water

5gm of powdered plant material was suspended in 200ml of distilled water. This mixture was heated with continuous stirring at 30°C to 40°C for 20min.The water extract was filtered through What man No.1 filter paper and the filtrate was used for the phytochemical analysis.

Table 2: Physical appearance of *Cynodon dactylon* and *Carica papaya* extract in different Solvents

S.No	Extracts	*Cynodon dactylon*		*Carica papaya*	
	Solvent used	Color	Texture	Color	Texture
1.	Acetone	Green	Gummy	Dark green	Hard
2.	Choloroform	Green	Gummy	Green	Gummy
3.	Ethanol	Green	Gummy	Green	Gummy
4.	Hot water	Green	Hard	Green	Hard

Solvent extraction

Plant samples were extracted with various organic solvents (Chloroform, Acetone & Ethanol) and hot water in the order to enhance the polarity nature and finally with distilled water. 5gms of dry powder was suspended in 25ml of chloroform and kept for 48 hours incubation with continuous shake. After 48 hrs the suspension was filtered with Whatman No.1 filter paper. The solvent filtrate was centrifuged at 5000 rpm for 5 min. This process was repeated three times and supernatant were collected and pooled together. Residual plant material left over after filtration was air-dried to evaporate the chloroform completely. The residues were treated with acetone for extraction. This acetone extraction process was repeated three times. The above process was applied with ethanol and water and their respective solvent supernatants were collected for phytochemical analysis and their physical nature was observed (Table.2).

s of phytochemical

cal test for the presence of constituents in *C. dactylon* and C. papaya plant studies were carried out in different solvent extracts using the standard procedures.

Qualitative analysis of total proteins

The presence of protein was carried out by Millions test (5ml of Millions reagent) and Ninhydrin test (5ml Ninhydrin reagent) were performed separately to the solvent extract of *C. dactylon* and *C. papaya* followed by gentle heating gives development of light blue color developed (Walsh and Edward O'Farrell *et al*., 1961).

Qualitative analysis of carbohydrates

The presence of carbohydrates in solvent extracts was determined by different methods such as, Fehling's test, Benedict's test, Molisch's test and iodine test.

a) **Fehling's test**: equal volume of Fehling's reagent A and B mixed together and 2ml of mixture was added to crude plant extracts followed gentle heat, the mixture turned brick red color (Fehling, 1984).

(b) **Benedict's test**: 2ml of Benedict's solution were added to crude plant extracts followed gentle boiling gives reddish brown precipitate (Benedict, 1909).

(c) **Molisch's test**: 2ml of Molisch's reagent were added in plant extract followed addition of H_2SO_4 develops the appearance of violet ring in the interphase.
(d) **Iodine test**, 2ml of iodine solution was added in plant extract gives development of dark blue. Simultaneously, presence of phenols and tannins were tested: 2 ml of 2% of $FeCl_3$ solution were added in the plant extracts, development of dark green for phenolic compounds and black color for presence of tannins (Segelman *et al.,* 1969).

Qualitative analysis of Flavonoids

2ml of 2% NaOH were added in plant extract, which gives intense yellow color, which disappeared on standing for few min. further additions of few drops of 1% aluminum solution added in each filtrate turns reappearance of yellow color indicates the presence of flavonoids (Edeoga *et al.,* 2005).

Qualitative analysis of Flavonoids by Bohm and Kocipai- Abyazan method

The flavonoid was tested with 10gms of the plant sample was extracted repeatedly with 100 ml of 80% aqueous methanol at room temperature. The whole solution was filtered through Whatman filter paper No 42 (125 mm). The filtrate was later transferred into a crucible and evaporated into dryness over a water bath and measured to a constant weight (Bohm, and Kocipai-Abyazan, 1994).

Qualitative analysis of Saponin by Obadoni and Ochuko method

5ml of plant extracts were mixed with equal volume of distilled water and mixed vigorously for 3 to 5min gives intense stable foam development. In addition of 3ml of olive oil mixed vigorously, observed the development of emulsion (Edeoga *et al.,* 2005).

Qualitative analysis of Glycoside by Keller-
l

:oform, 2 ml of acetic acid
nt extract and allowed to cool, followed by addition of 2ml of concentrated H_2SO_4 changes the violet to blue then green, indicates the presence of steroidal nucleus that is glycone portion of glycoside, steroidal ring that is glycone portion of glycoside, (Siddiqui and Ali *et al.,* 1997).In another way, the available cardiac glycosides are tested by addition of 1-2 drops of glacial acetic acid and 2% of $FeCl_3$ solution in crude plant extract followed by 2ml of H_2SO_4, gives brown ring at the interphase indicates the presence of cardiac glycosides.

Qualitative analysis of Steroids

Plant extracts mixed in 2ml of chloroform and Conc. H_2SO_4 were added gently, which leads to the development of red color in the lower chloroform layer indicating the presence of steroid, and was further confirmed with addition of acetic acid which develops the greenish color formation.

Qualitative analysis of Terpenoids by Salkowski test method

Presence of terpenoids in plant extract was determined according to Salkowski method (Singh *et al*., 2004). 5 ml (1 mg/ml) of fraction was combined with few drops chloroform, and 3 ml of concentrated H_2SO_4. Change of reddish brown color revealed the presence of terpenoids (Siddiqui and Ali, 1991).

Qualitative analysis of Alkaloids by Phenonthroline method

Alkaloids in plant extract were detected according to Phenonthroline method (Singh *et al*., 2004). Plant extract was added with 8 ml of HCl (1%), warmed and filtered. 2ml of each filtrate was titrated separately by means of (a) potassium mercuric iodide (Mayer's reagent) and (b) potassium bismuth (Dragendroff's reagent). Turbidity of precipitation indicated the presence of alkaloid.

Preparation of Maeyer's reagent

0.355gms of mercuric chloride was dissolved in 60ml of distilled water. 5gms of

potassium iodide was dissolved in 20ml of distilled water. Both solutions were mixed and volume was raised to 100ml with distilled water.

Preparation of Dragendorff's reagent

Solution A: 1.7gms of basic bismuth nitrate and 20gms of tartaric acid were dissolved in 80ml of distilled water. Solution B: 16gms of potassium iodide was dissolved in 40ml of distilled water. Both solutions (A and B) were mixed in1:1 ratio.

Qualitative analysis of Napthoquinone by Dam - Karrer test method

The presence of napthoquinone was identified by addition of few drops of 10% KOH solution in plant extract, which gives blue color (Siddiqui and Ali, 1997).

Qualitative analysis of Anthocyanins

The presence of Anthocyanins, were tested by addition of 2ml of HCl and ammonia with 2ml of aqueous plant extract, gives the development of pink red turn to violet color (Kokate *et al.*, 2007).

Qualitative analysis of Leuco anthocyanins:

The leucoanthocyanins were tested by adding equal volume of plant extract and isoamyl alcohol, which leads to the development of red color (Julian *et al.*, 2005).

Qualitative analysis of Coumarins

5ml of the moistened solvent plant extract was taken in a test tube. The mouth of the tube was covered with filter paper treated with 1N NaOH solution. Test tube was placed for few minutes in boiling water and then the filter paper was removed and examined under the UV light for yellow fluorescence indicated the presence of coumarins (Maique *et al.*, 2003).

Qualitative analysis of Phenols and Tannins

Crude extract was mixed with 2ml of 2% solution of $FeCl_3$. A blue-green or black [illegible] the presence of phenols

Qualitative analysis of Total Phenols by spectrophotometric method

The fat free sample was boiled with 50 ml of ether for the extraction of the phenolic component for 15min. 5ml of the extract was pipette into a 50ml flask, then 10ml of distilled water was added. 2ml of ammonium hydroxide solution and 5ml of concentrated amylalcohol were also added. The samples were made up to mark and left to react for 30min for color development. The spectrophotometric absorbance wavelength measured at 505nm.

Quantitative analysis of phytochemicals from plant extracts (*C. dactylon* and *C.papaya*) Quantitative analysis of Alkaloid by Harborne method

The residual sample of *C.dactylon* and *C.papaya* plant extract was measured 10gms separately in each case, taken in 250ml beaker and 200ml of 10%acetic acid in ethanol was added. Beaker was covered and allowed to stand for 4hrs. The content was filtered through Whatman No:1 filter paper and the extract was concentrated on a rotator water bath to one quarter of its original volume concentration NH_3OH was added drop wise to the plant extract until the precipitation was complete. The whole solution was allowed to stand till settlement. The precipitate was collected from the solution and was washed with dilute NH_3OH and filtered. The residue was the alkaloid that weighed after complete dryness and the percentage were calculated.

Quantitative analysis of Tannin by Van-Burden and Robinson method

The residual sample of *C.dactylon* and *C.papaya* plant extract was measured for 10gms in each case were taken in a schotduran bottle, and 50ml of distilled water was added. It was in shaker for 1hr, and filtered in a 50ml volumetric flask made up to the mark. 5ml of the filtrate was pipette out into the test tube and mixed with 2ml of 0.1M $FeCl_3$ in 0.1N HCl and 0.008M $K_4Fe(CN)_6$.

The absorbance wavelength measured at 120nm with in 10min.

Quantitative analysis of Saponin by Obadoni and Ochuko method

10gms of well air dried sample residual filtrate of each case was taken into a conical flask and 20% of 15ml of aqueous ethanol was added. Then the flask was heated on a hot water bath for 4hrs with constant stirring at about 55°C. The mixture sample filtered and the residue was again extracted with another 200ml 20% ethanol. The combined extract was reduced to 40ml on a hot water bath at about 90°C. The concentrate was transferred into a 250ml separatory funnel, added 20ml diethyl ether followed by mixed vigorous. The aqueous layer was recovered while the ether layer was discarded. The purification process was repeated. 60ml of n-butanol was added. The combined n-butanol extracts were washed twice with 10ml of 5% aqueous sodium chloride. The remaining solution was heated in a water bath. After evaporation the samples were dried in oven, measured and saponin content was calculated as percentage.

Quantitative analysis of total phenols by spectrophotometric method

10gms of each plant sample solvent residual filtrate was defatted with the help of 100ml of diethyl ether using a soxhlet apparatus for 2hrs. The fat free sample was boiled with 50ml of ether for 15min for the extraction of phenolic component. 5ml of the extract was pipette into a 50ml flask and 10ml distilled water was added. 2ml of ammonium hydroxide solution and 5ml of concentrated amylalcohol were also added in it. The samples were made up to mark and left to react for 30min. Color was developed and its absorbance wavelength measured at 505nm.

Quantitative analysis of flavonoid by Bohm ...an method

...ch solvent residual sample ...ed with 100 ml of acetone, chloroform, ethanol and hot water separately in each case, repeatedly at room temperature. The whole solution was filtered through Whatman filter paper 42 (125 mm). The filtrate was later transferred into a crucible and evaporated into dryness over a water bath, the measured of the material and percentage quantity was calculated.

Quantitative analysis of Coumarin by dry basis method

10gms of each solvent residual plant extracts mixed with add 10ml of 5N NaOH then boiled at 80^0C for 30min, then cool at room temperature and add 2ml of 5N H_2SO_4 mixed thoroughly, add 0.25gms of anhydrous $NaHCO_3$, mixed well and transfer the content to the extractor. Extractor volume is made up to 50ml with petroleum ether. Extract immediately for 3hours with petroleum ether, add 20ml. of water to the petroleum ether extract and carefully evaporate the ether by swirling the flask in a water bath 50^0C to 55^0C. Transfer the aqueous solution to a 50 ml volumetric flask, make up 30ml volume with dis.H_2O, pipette out 25ml of aliquot into a test-tube. Add 5ml of 1% Na_2CO_3 solution, heat in a water bath at 85^0C for 15min, and cooled at room temperature. Add 5ml of the diazonium solution make up 50ml with dis. H_2O, mixed well and let stand 2hours, the sediment was dried and calculate the percentage of coumarin to the dry basis.

Quantitative analysis of Cardiac glycosides by Baljet's reagent method

The quantitative estimation of glycosides residual of *C. dactylon and C. papaya* plant extract was evaluated using reagent, (95ml of aqueous picric acid and 5 ml of 10 aqueous NaOH). The presence of glycosides developed an orange – red color with Baljet's reagent. The intensity of the color produced is proportional to the concentration of the glycosides. This color formation is made use for the quantitiave estimation of glycoside present in the samples. 10gms of each sample extracted

residue with soaking overnight with 10ml of 70% alcohol and filtered. The extracts were there purified using lead acetate and Na_2HPO_4 solution. The intensity of the color produced was measured using a spectrophotometric absorbance wavelength at 495nm. Water and reagent act as a Blank. The intensity of the color produced is proportional to the concentration of the glycoside.

Quantitative analysis of Steroids by Liberman-Burchard method

10gms of residual solvent filtrate of plant extract samples was taken separately, which was made free from solvents. 2ml of reagent was added followed by addition of gradient volume of chloroform. The tubes were cover with black paper and incubated in dark for 15min, all the samples were measured absorbance wavelength at 640nm against blank. A standard graph was plotted for percentage calculation of presence of steroids.

Quantitative analysis of Terpinoids by Ferguson method

10gms of residual filtrate of each plant extract samples was taken separately and soaked in alcohol for 24 hours. Then filtered, the filtrate was extracted with petroleum ether; the ether extract was treated as total terpenoids.

Antimicrobial activity studies of extracted Compounds

Panel of Microorganisms

A board of organisms comprising 2 Gram-negative bacteria, *Escherichia* and *Salmonella sps.,* water borne pathogens was selected to test the extracts of *C. dactylon and C. papaya* ability to inhibit the growth. Each of the bacteria strains were cultured onto nutrient agar plates and incubated for 18 to 24 h at 37deg C to obtain colonies.

ity

ity was perfomed using method (Franklin R. Cockerill 2012). The plant extracts were tested on Nutrient agar plates to detect the presence of antibacterial activity. All plates were inoculated with the test bacterium, a sterile cotton swab was dipped into the suspension, rotated several times, and pressed firmly on the inside wall of the tube above the fluid level removing excess inoculum. The surface of the agar plate was streaked over the entire sterile agar surface rotating the plate to ensure an even distribution of inoculum with a final swab around the rim. The plates are allowed 3 to 5min to dry the excess moisture. 50 uL of each solvent extract were dispensed into each well after the inoculation of the plates with bacteria. The wells were made in 5 mm dia using sterile borer. The same extract was used on each plate, with a total of three plates used for each extract for selecting bacterium. After 24 hours of incubation of plates at 37 deg C, each plate was examined for inhibition zones.

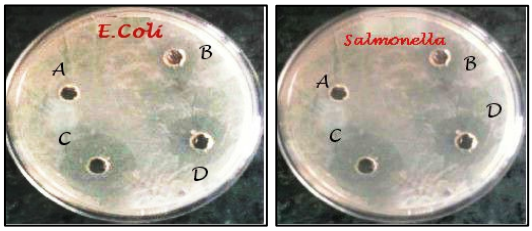

Fig: 1 Antibiotic sensitivity test of E.Coli and Salmonella; well A)Hot water, B)Acetone, C)Ethanol D) Chloroform extracts of *C.dactylon* and *C.papaya*

Results and Discussion

The present studies for the selected temperate plants revealed the presence of various phytochemical constituents. Presence of various phytochemical constituents in *C.dactylon* and *C.papaya* are furnished below (in Table 3). The extraction of which showed the presence of high percentage in the range of 0.01 to 1.46 and 0.02 to 10.0 percentage of phytochemicals compared to other solvent extracts. Moderate percentage 0.01 to 1.0 and 0.00 to 0.7

percentages is obtained in chloroform extraction system and least is 0.00 to 1.04 and 0.01 to 0.64 percentage of constituents in acetone extract, very lowest percentage of phytochemical constituents was observed in the range of 0.00 to 0.03 and 0.00 to 0.04 percentage in hot water extraction system in Table 4 (A & B).

The table (1 & 2) clearly shows the ideal solvent system for the extraction of desired phytochemicals from selected medicinal plants. Results of table 4 (a) & 4(b) clearly showing the Ethanol is the ideal solvent system for extraction of Phytochemicals in *cynodon dactylon* shoot extract and *carica papaya* leaf extract. Further research investigation on identification and structural elucidation of each and every constitution in the shoot portion extract of *C.dactylon* and leaf part of *C.papaya* need to be explore more in molecular level approach against various illnesses.

Table 3: Qualitative Analysis of the Phytochemicals in *Cynodon dactylon* and *Carica papaya*

Plants	Proteins	Carbohydrate	Flavnoids	Saponins	Glycosides	Steroids	Terpinoids	Alkaloids	Coumarins	Phenol	Tannins	Napthoquinone	Anthrocyanin	Leucoanthocyanin
Cynodon dactylon	+	-	+	+	-	+	-	-	-	+	+	+	+	-
Carica papaya	+	-	+	+	+	+	+	+	+	+	+	-	+	+

Table 4(a): Percentage of phytochemical constituents in different solvents extract of *cynodon dactylon* shoot extract the data represents mean of three replicates

Solvent Extraction Mg/10 Gm Residue	Flavonoids	Saponins	Glycosides	Steroids	Terpinoids	Alkaloids	Coumarin	Phenol	Tannin
Acetone	0.23 ±0.10	1.04± 0.29	0.3± 0.20	0.6± 0.01	0.03± 0.04	0.02± 0.01	ND	0.08± 0.40	0.78± 0.10
Chloroform	0.21± 0.08	0.5± 0.15	1.0± 0.45	0.8± 0.03	0.02± 0.10	0.01± 0.00	0.04± 0.0	0.99± 0.10	0.89± 0.0
Ethanol	1.0 ± 0.15	1.5± 0.50	0.9± 0.10	1.2± 0.12	0.97± 0.40	0.09± 0.00	0.01± 0.00	1.46± 0.01	1.20± 0.10
Hot water	0.01± 0.05	0.03± 0.01	ND	0.01± 0.03	0.01± 0.00	0.01± 0.00	0.021± 0.00	ND	0.030± 0.00

ND: Not Deducted

The phytochemical screening and percentage estimation (quantitative) of various solvent crude extracts yields in shoot and leaf part studies showed the presence of ins, Glycosides, Steroids, quinones, Anthrocyanin, marins, Phenols And Tannins. They were known to show medicinal activity as well as physiological activity (Dhandapani and Sabna, 2008). Proteins are found in all part of the plants, which is essential and associated with polyphenols (Rambourg and Monties, 1983). Flavanoid contents are almost equally

present in both plant crude extracts, which is essential for pigmentation and also act as a UV filtration unit. Saphonins function as an anti-feedant, present in shoot and leaf of selected plants (Ahmad Faizal and Danny Geelen, 2013 and Dharmarathna *et al*., 2013).

Table 4(b): Percentage of phytochemical constituents in different solvents extract of C*arica papaya* leaf extract the data represents mean of three replicates

Solvent Extraction Mg/10 Gm Residue	Flavonoids	Saponins	Glycosides	Steroids	Terpinoids	Alkaloids	Coumarin	Phenol	Tannin
Acetone	0.21± 0.12	0.04± 0.11	0.3± 0.10	0.4± 0.00	0.6± 0.00	0.02± 0.00	0.31± 0.00	0.64± 0.10	0.24± 0.00
Chloroform	0.22± 0.00	0.4± 0.05	1.6± 0.10	0.30± 0.00	0.7± 0.30	0.54± 0.01	0.21± 0.00	0.56± 0.12	0.25± 0.00
Ethanol	10.0± 0.11	0.8± 0.50	0.7± 0.10	0.6± 0.11	0.9± 0.00	0.6± 0.00	0.6± 010	0.8± 0.00	0.7± 0.00
Hot water	0.0.± 0.04	0.04± 0.12	0.01± 0.00	ND	0.01± 0.00	0.01± 0.00	0.01± 0.00	0.02± 0.00	0.01± 0.00

ND: Not Deducted

Cardiac glycosides, Terpinoids, Leucoanthocyanins and Cumarin are absent in *C.dactylon* but present in leaf extract of *C.papaya*. The untraceable level of such phyto constitutes is estimated qualitatively. Crude leaf extract of the *C.papaya* does not have Napthoquinone. Glycosides act as medications. Both phenols and tannins are present in the shoot and leaf extracts, which is mainly used for plant defense mechanisms against various infections. The presence of Steroids and terpinoids in *C.dactylon* and *C.papaya* has been reported by researchers and was widely used as herbal medicines. The plants identified for this study are potential sources of useful phytochemicals; the plants studied here can be seen as a potential source of useful drugs. The present antimicrobial activity studies stated the extracts of extraction of ethanol, Chloroform, Acetone showed the positive inhibitory effects in for the selected tested organisms. Further focus on these plants to isolate, identify and characterize and elucidate the bioactive compounds is necessary. The antimicrobial activities of these plants for the treatments of multidrug resistance against the pathogenic bacteria as claimed by traditional healers and much more research need to extract the value added food preservative agents for selected microbes are being investigated.

Acknowledgements

The authors are thankful to the Principal and Management, Mohamed Sathak Engineering College, Kilakarai- Ramnad, for providing the necessary laboratory facilities. The authors express their thanks to the Assistant professor. P.U.Mahalingam and Head Department of Biology, Gandhigram Rural Institute- Deemed University for their support for carry out the preliminary study.

References

Albert-Baskar A, Ignacimuthu S. 2009; Chemo preventive effect of *Cynodon dactylon* (L.) Pers. extract against DMH-induced colon carcinogenesis in experimental animals. *J. Exp. Toxicol. Pathol*., 62; 423–431.

Atmani F, Sadki C, Aziz M, Mimouni M, Hacht B. 2009; *Cynodon dactylon* extract as a preventive and curative agent in experimentally induced nephrolithiasis. *J Urol Res.*, 37:75–82.

Anibijuwon I.I. and Udeze A.O. 2009; Antimicrobial Activity of *Carica papaya* (Pawpaw Leaf) on Some Pathogenic Organisms of Clinical Origin from South-Western Nigeria. *Afr. J. Ethnobot.*, 13: 850-864.

Ahmad Faizal and Danny Geelen. 2013; Saponins and their role in biological processes in plants. *J. Phytochem. Rev*., 12: 877–893.

Benedict S R., 1909; Reagent for the Detection of Reducing Sugars. *J. Biol. Chem*., 5 (4):485–487.

Bohm BA, Kocipai- Abyazan R., 1994; Flavonoid and condensed tannins from the leaves of *Vaccinum raticulation* and *Vaccinum calcyimium*. *J. Pacific Sci*., 48(3): 458-463.

Cosa P, Vlietinck AJ, Berghe, Maes DV., 2006; Anti-infective potential of natural products: How to develop a stronger in vitro 'proof-of-concept'. *J Ethnopharma*., 9 (2):290-295.

Dhandapani R and Sabna B. 2008; Phytochemical constituents of some Indian medicinal plants. *Anc. Sci. Life.*, 27(5):1-8.

Dharmarathna SL, Wickramasinghe S, Waduge RN, Rajapakse RP, Kularatne SA.. 2013; Does *Carica papaya* leaf-extract increase the platelet count? An experimental study in a murine model. *Asian Pac. J. Trop. Biomed*., 3(1):720-724.

Edeoga HO, Okwuand DE, Mbaebie BO., 2005; Phytochemical constituents of some Nigerian medicinal plants. *Afr. J. Biotechnol*., 4 (1):685-688

Fehling H. 1984; The quantitative determination of sugar and starch-by l. *J Chemie and Pharmacia*.,

Franklin R. Cockerill 2012; Clinical and Laboratory Standards Institute, "Performance Standards for antimicrobial susceptibility testing," Nineteenth informational supplement M100-S19, Clinical and Laboratory Standards Institute, Wayne, Pa, USA.

Garjani, A and frooziyan, A. 2009; Protective effects of hydro alcoholic extract from rhizomes of *Cynodon dactylon* on compensated right heart failure in rats. *J. BMC. Comp & Alt Med.*, 28; 1 – 9.

Gupta OP, Sharma N, Chand D.1992; A sensitive and relevant model for evaluating anti-inflammatory activity-papaya latex-induced rat paw inflammation. *J. Pharma. Toxicol. Met.*, 28: 15-9.

Imaga NA, Gbenle GO, Okochi VI, et al., 2010; Phytochemical and antioxidant nutrient constituents of *Carica papaya* and *Parquetina nigrescens* extracts. *Sci. Res. Essays.* 5(16): 2201-2205.

Jarald EE, SB Joshi. 2008; Anti diabetic activity of aqueous extract and non polysaccharide fraction of *Cynodon dactylon. J. exp bio.,* 46; 660-667.

Julian C, Verdonk Michel, Haring A, Arjenvan Tunen T, Robert C, Schuurink., 2005; ODORANT1 Regulates Fragrance Biosynthesis in Petunia Flowers. *Plant cell*., 17(2):1612–1624.

Kokate CK, Purohit AP, Gokhale SB. 2007; *Hand Book of Pharmacognosy 2nd edition*, Wiley Publisher Ltd. pp. 25-30.

Mahmood A A, Sidik & Salmah I, 2005; Wound Healing activity of *Caracia Papaya* L. Aqueous Leaf Extract in Rats. *Int. J Mol. med. Adv. Sci.*, 1(4); 398-401.

Maique W, Biavatti Cesar A, Koerich, Carlos H, Henck, Enderson Zucatelli, Fernanda H, Martineli, Tania B, Bresolin, Silvana N, Leite., 2003; Coumarin Content and Physicochemical Profile of *Mikaniala evigata* Extract, coumarin extraction protocol. *J Pharmacol*., 1(4):20-25.

Mangathayaru K, Uma devi M and Umamaheswara reddy C, 2009; Evaluation of the immunomodulatory and DNA protective activities of the shoots of *Cynodon dactylon*. *J. Ethanopharma.*, 123(1); 181-4.

Newman D.J., Cragg G.M. 2005; In: Drug Discovery, Therapeutics, and Preventive Medicine. Zhang L., Fleming A., Demain A.L., editors. Humana Press; Totowa, NJ, USA.

Nisar Ahmad L, Hina Fazal P, Muhammad, 2011; Dengue fever treatment with *Carica papaya* leaves extracts. *Asian Pac. J. Trop Biomed*., 1(2):330-336.

Nguyen, T. T. T., Shaw, P. N., Parat, M.-O. and Hewavitharana A.K. 2013; Anti-cancer activity of *Carica papaya*: A review. *J. Mol. Nutr. Food Res*., 57: 153–164.

Oboh G, Olabiyi AA, Akinyemi AJ, 2013; Inhibition of key enzymes linked to type 2 diabetes and sodium nitro prusside-induced lipid peroxidation in rat pancreas by water-extractable phytochemicals from unripe pawpaw fruit (*Carica papaya). J Basic Clin Physiol Pharmacol*., 30:1-14.

Okoko T, Ere D, 2012; Reduction of hydrogen peroxide–induced erythrocyte damage by *Carica papaya* leaf extract. *Asian Pac. J. Trop. Biomed*. 2, (6): 449–453.

Rambourg JC, Monties B., 1983; Determination of polyphenolic compounds in leaf protein concentrates of lucerne and their effect on the nutritional value. *J Qual Plant Foods Hum Nutr.* 33(2):169–172.

Rao BS, Upadhya D, Adiga SK, 2008; Protection of ionizing radiation-induced cytogenetic damage by hydro alcoholic extract of *Cynodon dactylon* in Chinese hamster lung fibroblast cells and human peripheral blood lymphocytes. *J Environ Pathol Toxicol Oncol*., 27(2):101-112.

Sadki C, Hacht B, Souliman A, Atmani F. 2010; Acute diuretic activity of aqueous flowers and *Cynodon dactylon* rhizomes extracts in rats. *J Ethanopharma*., 128:352-356.

Santosh Kumar Singh F, Prashant Kumar Rai V, Dolly Jaiswal, and Geeta Watal.2008; Evidence based Critical Evaluation of Glycemic Potential of *Cynodon dactylon. J Alternat Med.,* 5; 415–420.

Segelman AB, Farnsworth NR, Quimby MD., 1969; False-Negative saponins test results induced by the presence of tannins. *J Biol Chem*., 32(2):52 – 58.

Sindhu, G. and Ratheesh. J. 2009; Inhibitory effects of *Cynodon dactylon* L. on inflammation and oxidative stress in adjuvant treated rats. *J Immunopharmacol & Immunotoxicol*., 31, 647–653.

Siddiqui AA, Ali M., 1997; *Practical Pharmaceutical chemistry*. CBS Publishers and distributors, New Delhi, India. pp.126-131.

Singh DK, Srivastva B, Sahu A., 2004; Spectrophotometric determination of Rauwolfia alkaloids, estimation of reserpine in pharmaceuticals. *J. Anal. Sci*., 20(2):571-573.

Subenthiran S, Choon TC, Cheong KC, Thayan R, Teck MB, Muniandy PK, Afzan A, Abdullah NR, Ismail Z. 2013; Carica papaya Leaves Juice Significantly Accelerates the Rate of Increase in Platelet Count among Patients with Dengue Fever and Dengue Haemorrhagic Fever. *J Comp & Alt Med.,* 1(5): 18-25.

Titanji PK, Zofou D, Ngemenya NM, 2008; The Antimalarial potential of Medicinal plants used for the treatment of Malaria in Cameroonian Folk Medicine. *Afr. J. Tradit. Complement. Altern. Med.* 5(3): 302–321.

Walsh, Edward O'Farrell 1961; *An Introduction to Biochemistry*. The English Universities Press Ltd. London.

World Health Forum 1993; Controller of Publication, United States of America, *Ministry of Health Sciences forum, WHO*, 14(6):390-396.

Research Paper

BIODIESEL PRODUCTION AND OPTIMIZATION FROM *PROSOPIS JULIFERA* OIL – A THREE STEP METHOD

M. Rajeshwaran[1], K. Raja[2,], P.Marimuthu[3]and M.D. Duraimurugan alias Saravanan[4]

Address for Correspondence

[1]Department of Mechanical Engineering, Mohamed Sathak Engineering College, Kilakarai, Ramanathapuram 623 806, Tamil Nadu, India.

[2]Department of Mechanical Engineering, Anna University, University college of Engineering Dindigul - 624005, Tamil Nadu, India.

[3]Principal, Syed Ammal Engineering College, Ramanathapuram-623502, Tamil Nadu, India,

[4]Department of Chemical Engineering, National Institute of Technology, Tiruchirappalli – 620015, Tamil nadu, India.

ABSTRACT

The production of Biodiesel by the method of transesterification has been admired in the recent years due to the anxiety in the conservation of fossil fuels and due to the price hike in conventional fuel. *Prosopis Julifera* is a non edible feedstock found in the arid and semi-arid regions. Oil from *Prosopis Julifera* was extracted by the method of solvent extraction. The present work mainly concentrates on the three step process of biodiesel production from *Prosopis Julifera* oil .Initially the acid value of *Prosopis Julifera* oil was reduced below 1% from 21.85% (43.7 mg KOH/gm) by the two step pretreatment process using acid catalyst 1% v/v H_2SO_4. The second step is the esterification process of the product obtained from pretreatment using alkaline catalyst. The parameters such as methanol to *Prosopis Julifera* oil molar ratio, amount of catalyst used, reaction time and reaction temperature were studied. For the efficient conversion of *Prosopis Julifera* oil to methyl ester gas chromatography was used to analyse the Fatty acid methyl esters. The optimum reaction conditions of Methanol/oil molar ratio of 9:1v/v, reaction temperature of 60^0C, reaction time of 2 hrs and 1% w/v of NaOH usage were determined. In the acid transesterification process, the main objective for process optimization was the reduction of acid value. The process optimization was done using Response surface Methodology technique (RSM). The methyl ester obtained from the previous step was refined to produce biodiesel in the third step. The fuel properties of *Prosopis Julifera* methyl ester (PJME) such as viscosity, cetane number, flash point, acid value, etc were determined. The values thus found experimentally were compared according to the ASTM standards.

KEYWORDS: *Prosopis Julifera*; Acid Esterification; Transesterification; Process optimization.

1. INTRODUCTION

As there is the increase in population, there is the rapid increase in the energy demand. The depletion of fossil fuel reserves and conventional energy sources has stimulated the interest in the alternative energy sources. While considering the environmental concerns, the alternative fuel source must be eco friendly in nature [8].This led the researchers to propose biodiesel to be the ideal choice among all the alternative fuels. In the recent years, world market for biodiesel has expanded rapidly. Though various research works, evaluations, tests and certifications from large number of countries, researchers have confirmed as clean alternative fuel having self combustion properties with lower carbon emission, no sulfur and no aromatics [9].Wide ranges of traditional oil seed crops such as ground nut, mustard, rape seed, sunflower, safflower, linseed, soybean, palm etc were used for the biodiesel production [29]. Though there is the production of large volume of oils, India is not self sufficient in producing edible oils [7]. If the edible oils were used for biodiesel production, then there will be the world food crisis [8].Human rights activists and social reformers have called for a ban on the production of biodiesel from food crops for several years and hence resolved the food versus fuel conflict. Waste cooking oil, Tallow and animal fat have replaced the edible oils in the production of Biodiesel [30].Though they can be afforded at the lowest price, the disposal of these materials constitutes a major problem.

For the production of biodiesel, non edible vegetable oil sources have become more attractive now a day. Thus the dependence of biodiesel production non iced to a greater extent [18]. toxic components in the non suitable for having as food. btained from the plants grown Non edible oils like Jatropha obacco[14], Rubber seed[21], *sativa* [25], Rice bran [10] etc. are found to be the cheapest feedstock for biodiesel production.

Prosopis Julifera is one such cheapest feedstock which acts as a source of fuel, vegetative fence for protection and increased fertility to the arid and semi arid zones of India. The shrubs of drought resistant *Prosopis Julifera* can grow in highly saline areas, alkaline soils, areas near sea, and corrupted grasslands [4].

The species *Prosopis Julifera* is widespread all over the world. It consists of 44 species, having mostly thorny trees and shrubs. Different species of *Prosopis Julifera* and *Acacia Nilotica* have been predicted to occupy some 3.1million sq.km in the world [1].India covers an area of about 3.29 million sq.km. Over 40% of the country's total land surface constitutes the arid and semi-arid regions. Nearly it covers 10 states of India (DFID). Prosopis Julifera grow up abundantly in India [1].It is commonly known as Mesquite in English, Algarroba in Spanish. In India it is called as Vilayati babul, Vilayati khejra, Gando baval, Vilayati kikar. The genus *Prosopis Julifera* seems to be originated before the separation of the African and South African continents, approximately about the million years ago. The history of the first introduction of *Prosopis Julifera* into India is about 130 years old [1].

According to the Department of land resources (DOLR), GOI about 63.9 million hectare of land is lying waste in India. Since these lands are unsuitable for cultivation, they are termed as "Waste lands". Waste lands are said to be characterized by sandy soils, rocky soils, saline soils etc [5]. About 23 million hectare land (10 million hectare salt affected region and 13 hectare arid and semi arid region) is found to be lying waste [45] in India. The current strategy is cultivation of Jatropha, sweet sorghum, and castor, Pongamia in these waste lands [32]. The oils obtained from these plants are non-edible oils. Though these plants grow in diverse agro-climate conditions, withstand pest attack and drought, the

yield of the seed, oil content and nutrient requirements are found to be critical. This leads to the less chance for plantation of these plants in the waste lands [6].

Hence the afforestation of the waste lands can be done with *Prosopis Julifera, Acacia Nilotica* etc. These species require only less amount of water and is found to be more suitable for dry and arid waste lands.

Prosopis Julifera has been recommended as the "Wonder tree" for dry saline areas. *Prosopis Julifera* is found to be abundantly used in various fields and new research is going on in making new drugs and pesticides from the same [1]. Oils obtained from non edible feedstock can be converted into Biodiesel using four standard techniques namely blending, Pyrolysis, Transesterification and micro-emulsification [24].Among these four methods, Transesterification resolves the problem of oils having high viscosity. This process has the advantage of reducing the viscosity of oil thereby increasing the fuel properties [36]. Transesterification is a chemical reaction to produce mono ester by reacting triglycerides with short chain alcohol in the presence of catalysts. Methanol, ethanol, propanol, butanol are the commonly used short chain alcohols. Methanol is widely used alcohol due to its lowest price [10].The triglyceride in the vegetable oil or animal fat react with alcohol to form a mixture of glycerol and fatty acid methyl ester called biodiesel [19].

Transesterification reaction can be a carried out with the help of one or more than one catalyst. Depending on the FFA content, the reaction is either one step or two step process. When comparing edible oils with non-edible oils, edible oils are found to contain large amount of FFA [11, 13, 23]. Base catalysed transesterification of non edible oils produces high quality biodiesel in a shorter reaction time. This usage of base catalyst has the disadvantage of reduction in the yield of biodiesel due to soap formation [35]. NaOH and KOH are the catalysts used in most of the processes. The use of acid catalyst in the transesterification process has the advantage of tolerance and less sensitivity towards high FFAs. However the rate of reaction using acid catalyst is slow. Commonly used acid catalysts are H_2SO_4 and [10, 21] .The advantages of both acid and base catalysts are combined to form 2 step acid (acid/base) process for production of biodiesel from non edible oils having high FFA content [28]. In the first step, the FFA value was reduced below 1% using acid catalysed transesterification. In the next step, biodiesel of *Prosopis Julifera* is produced using an alkaline catalyst[25].This two step transesterification is influenced by reaction time, reaction temperature, and quantity of catalyst [14,25].In acid catalysed and base catalysed reactions,to get the faster yield of FAME, methanol was used as the alcohol when compared with ethanol [6].

nvolving factors affecting the onse surface methodology uitable tool. Comparing RSM information obtained is very shorter time period. The main e Methodology is to identify n be thought of as a surface over the variables experimental space. The explanatory variables use an experimental design like central-composite design CCD to fit full second-order polynomial model. In general, a CCD coupled with a full second-order polynomial model, is considered to be a very powerful combination providing an adequate representation of most continuous response surfaces. For the investigation of complex processes, RSM is proved to be the effective statistical technique giving enough information in the reduced number of experimental runs. Most of the research regarding optimization of Biodiesel production is carried out by RSM only [21].In the present study, RSM was used to optimize and to study the maximum biodiesel conversion of Prosopis Julifera.

The literatures from the recent years show that non-edible oil is the best for the production of biodiesel when compared with the edible oils. In some of the review papers, authors have suggested different techniques to reduce the FFA content of non edible oils using acid and base catalysed transesterification [6, 10]. The high viscosity found in the non edible vegetable oil creates serious problem if it is used directly used in the diesel engines [33].The transesterification process makes biodiesel as a suitable fuel for CI engine [34].

Based on the above literature, there is no detailed work regarding the extraction of oil from the non edible feedstock-*Prosopis Julifera* oil which has a huge potential for biodiesel Production. Also optimization of the oil extracted from *Prosopis Julifera* was not yet reported so far.

The main aim of this paper is to discover a new and powerful non edible feedstock that produces biodiesel for the future use. Also, the transesterification processes, and optimization techniques are taken much care for the improvement of FAME.

2. MATERIALS AND METHODS

2.1 Materials

The genus *Prosopis Julifera* fit into the Botanical family Leguminosae (Fabaceae), sub-family Mimosoideae [1]. The form of the tree and its size vary between the species. *Prosopis Julifera* normally reaches a maximum height of 12m and can also reach upto 20m.The wood of *Prosopis Julifera* is diffusely porous in structure[3]. The tree has thorns which vary in number and size. It may be present in some branches or may be absent.

The size of the leaflets varies greatly, 2.5-23 mm long and 1-7 mm wide [1]. The flowers are small which are densely gathered together on cylindrical, spike-like inflorescences. Flowers are 4-6mm long and are generally straw yellow in colour [2]. The plant flowers almost any time of the year except from hot summer to mid rainy season.

The pods of *Prosopis Julifera* are flattened and straight. The pods are 6-30cm long, 5-16mm wide and 4-9mm thick. The aged pods will swell and become pulpy and will look yellowish brown in colour. The number of pods produced per inflorescence will vary with 1-16 fruit per inflorescence. Seeds are upto 6.5mm long and weigh approximately 0.25 to 0.3g (25000-30000 seed/kg) [1].The production of pods approximately vary from 5 kg to 40 kg/tree depending on the climatic conditions and habitat[44]. Also, 2300 Kg/ha pods

can be produced with *Prosopis Julifera* planted with a density of 20 Kg/tree [45].

The dried fruits of *Prosopis Julifera* were gathered from the waste lands of Ramnad district in Tamil Nadu. Prosopis Julifera collected during the seasonal period were then cleaned and dried for removal of moisture content. The dried pods are crushed and powdered. From the powdered pods, PJO was extracted using the soxhlet apparatus. Polar and non-polar solvents such as Petroleum Ether (68.7^{0}C), n-Pentane (35-37^{0}C), Ethyl acetate (76-78^{0}C), Iso-propanol (81-83^{0}C), Hexane (60-80^{0}C), Methanol (65^{0}C), and Ethanol (78.36^{0}C) were used and the amount of oil extracted with these solvents ranged from 10-37%. Since, maximum oil yield was obtained with methanol, oil from *Prosopis Julifera* was extracted using methanol as the solvent.

The unrefined oil of *Prosopis Julifera* oil was dark brown in colour. Gas chromatography analysis was made and the fatty acid composition of *Prosopis Julifera* oil was found. Based on Triglycerides, the vegetable oil has different grades of Fatty acid and variation in fatty acid is based on hydrocarbon chain length and number of double bonds. Percentage compositions of fatty acids differ based on the flora species and growth conditions. Table [1] provides the properties of oils produced from non edible feedstock.

The saturated (palmitic, stearic) fatty acids and unsaturated (oleic, linoleic) fatty acids present in PJO was 23% and 68% respectively. The PJO had an acid value of about (39-43.7) mg KOH/gm, which corresponds to a fatty acid value of 21.85%.For the agreeable transesterification reaction using acid catalyst, the FFA value should be 1%.Since the FFA value obtained was far away from the limits, the transesterification process became complicated forming soap .The formation of soap prevented the separation of Biodiesel from Glycerin. Hence, the FFAs were initially converted into ester in a pre-treatment process, using an acid catalyst like 1% (v/v) H_2SO_4.In this pretreatment process, the acid value of PJO can be reduced below a FFA value of 1%.

TABLE 1. PROPERTIES OF OIL PRODUCED FROM NON-EDIBLE FEEDSTOCKS

properties	Jatropha oil [6][23]	Rubber seed oil [11][21]	Rice Bran oil[10]	Mahua oil [15][28]	Karanja oil[12]	*Camelina Sativa* oil[25]	Waste cooking oil[29]	Tobacco oil[14]	*Prosopis Julifera* oil(PJO)
Density, Kg/m^3	913	910	922	960	909	910	920	923	967-971
Viscosity at 40^{0}C(mm^2/sec)	40.4	76.4	43.5	24.9	27.84	14.03	28.8	27	38-41.2
Calorific value(MJ/kg)	38.65	37.5	--	36	--	44.5	44.44	--	38-41
Flash point(^{0}C)	240	198	316	232	232	--	--	--	202-212
Acid value (mg KOH/g of oil)	28	34	40	38	12.27	3.163	17.41	36.6	39-43.7
Saponification value (mg KOH/g of oil)	195	206	--	--	165.5	193.31	166.3	--	180-186
Iodine value (I_2g100/g of oil)	101	135.3	108	--	89	--	--	130.2	102-112

2.2 Apparatus

Fig [1], the apparatus used for transesterification consists of constant temperature water bath, reaction flask with condenser and digital rpm. Digital rpm is used for controlling the Mechanical stirrer. The agitation speed of the mechanical stirrer was maintained as 600rpm for all the transesterification processes. The glass reactor consists of three necks, one for stirrer, and others for condenser. The volume of the glass reactor measured 500ml.The reaction temperature was measured using a temperature indicator.

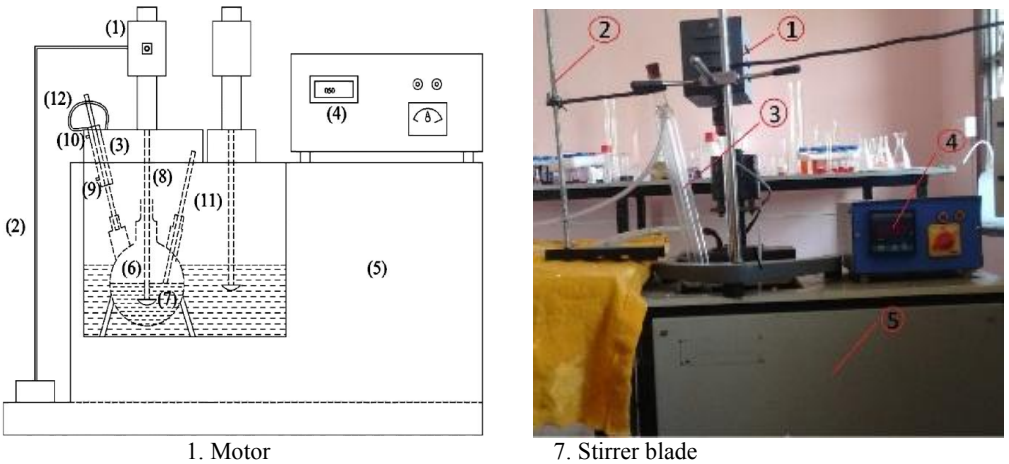

1. Motor
2. Motor stand
3. Lie beg condenser
4. Temperature controller
5. Constant temperature Water bath
6. Three neck round bottom flask
7. Stirrer blade
8. Stirrer rod
9. Water in
10. Water out
11. Thermocouple
12. Tube

hematic diagram and photographic view of constant temperature water bath

oil obtained from *Prosopis* wo steps. The influence of methanol /oil molar ratio,(3,5,6,7and 9) v/v, and reaction time (0.5,0.75,1,1.25,1.5,2,2.5 hours) on the acid value of PJO in each step of pretreatment were

studied. In this pretreatment process, whatever may be the methanol/oil molar ratio and reaction time, the amount of H_2SO_4 used was 1% v/v only [10]. 100gm of PJO was taken and poured into a flask which was kept in a water bath. The water bath was retained hot by keeping at the temperature 110^0C for 30 minutes to eliminate moisture and the PJO was preheated [18].To this preheated oil, sulfuric acid methanol solution was added and the mixture was stirred at the same rate for few minutes. After the completion of this reaction, the end product was poured into a separating funnel to separate the excess methanol. The excess methanol along with H_2SO_4 and impurities moved to the top surface and it was then removed .Using standard ASTM method, the acid value of the product separated at the bottom surface was measured at standard intervals. In a minimum reaction time, the product having an acid value of 8.6mg KOH/gm and very little amount of methanol was utilized as raw material for the second step. For to investigating the influences of methanol/oil molar ratio and reaction times and the acid value of the raw material obtained the same experimental procedure as above was repeated. For the transesterification reaction, the product having 2.7mgKOH/gm and with lowest amount of methanol in minimum reaction time was used. Rubber seed oil having acid values of 35mgKOH/gm was reduced to 3.8mg KOH/gm and 40mg KOH/gm was reduced to 0.9mg KOH/gm in Rice bran oil [10]. Similarly in Jatropha oil an acid value of 28mg KOH/gm was reduced to 2mg KOH/gm [17]. The final reaction mixture was poured into a separating funnel. The mixture was separated by centrifugal process was then washed with distilled water and then dried with anhydrous sodium sulphate and was used for additional processing.

2.4 Transesterification

The experimental setup for this process was the same as utilized in the pretreatment process using acid as catalyst. Before starting the reaction, PJO was preheated to the desired temperature to maintain the catalytic activity and to avoid the moisture absorbance, NaOH-methanol solution was prepared newly. The methanolic solution was then added to the already present PJO in the reaction flask and from that point, time was noted. The product obtained after transesterification was poured into a separating funnel. The esters present in the lower aqueous glycerol were then separated by gravity. The esters thus separated were then washed twice with distilled water. In a rotary evaporator, the washed esters were dried under vacuum and were stored for further analysis.

Fatty acid methyl ester composition of *Prosopis Julifera* oil was analysed by means of Gas chromatography attached with a flame ionization detector (GC FID). Gas chromatography analysis was performed in Central Electrochemical Research Institute (CECRI) - CSIR Lab, located at Karaikudi, in Tamil nadu. Gas Chromatograph used was Agilent Technologies, model 7980A with split-spiltless injector. This Gas chromatograph used a capillary column of dimension (30 x 250µm x0.25 µm) Helium was used as a carrier gas at velocity of 36.445 cm/s .The split ratio was maintained at 1:10.The initial temperature of the oven was kept at 50^0C for 1 minute then, 10^0C for 1minute to 300^0C for 3minutes and the run time as a total of 28 minutes. The lipids and other components composed in extracted oils were quantitatively and qualitatively analyzed using AOAC norms. Methyl esters obtained from *Prosopis Julifera* contain 16% saturated fatty acids like Palmitic and stearic acids. Table [2] shows the fatty acid composition of *Prosopis Julifera* oil. The percentage of unsaturated fatty acids such as Oleic, Linoleic and linolenic acids present in oil was 78.1% .The proportion of fatty acid present in the Biodiesel extracted from *Prosopis Julifera* pods is as follows: Palmitic acid (10.6%), oleic acid (34.7%), linoleic acid (43.4%), Lauric acid (0.2%), Myristic acid (0.1%), Arachidice acid (0.13%), Behenic acid (0.1%) and Stearic acid (5.2%).

TABLE 2. FATTY ACID COMPOSITION OF PROSOPIS JULIFERA OIL

Fatty Acids	Formula	Systematic name	Structure	Net (%)
Lauric acid	$C_{12}H_{24}O_2$	Dodecanoic acid	C_{12}	0.2
Myristic acid	$C_{14}H_{28}O_2$	Tetradecanoic acid	C_{14}	0.1
Palmitic acid	$C_{16}H_{32}O_2$	Hexadecanoic acid	C_{16}	10.6
Stearic acid	$C_{18}H_{38}O_2$	Octadecanoic acid	C_{18}	5.2
Oleic acid	$C_{18}H_{34}O_2$	Cis-9- Octadecanoic acid	$C_{18:1}$	34.7
Linoleic acid	$C_{18}H_{32}O_2$	Cis-9-cis12-Octadecanoic acid	$C_{18:2}$	43.4
Arachidice acid	$C_{20}H_{40}O_2$	Eicosanoic acid	C_{20}	0.13
Behenic acid	$C_{22}H_{44}O_2$	Docosanoic acid	C_{22}	0.1

3. RESULTS AND DISCUSSION

3.1. Pretreatment

Pretreatment is found to be the best method for the reduction of acid values below 1mg KOH/gm as all the non-edible oils have an acid values in the range 20 to 45mgKOH/gm[10,11,17].Important variables which affect the acid value were type of feedstock and alcohol, alcohol: oil molar ratio, concentration of catalyst, reaction time and reaction temperature. From figure [2], it can be seen that the reaction was and became very slow in the research, the rate of reaction ratio and reaction time. With atio, the acid value decreased ion rate were found to be ce due to the effect of water terification of FFA, the supplementary reaction may be put off and the reaction rate was nearly identical [14]. If the FFA should be 1mgKOH/gm after the second pretreatment step, then FFA of 5mgKOH/gm should be obtained in the first step [11, 15].The optimum condition of 9:1v/v methanol/oil ratio and 2 hours minimum reaction time was selected for reducing the acid value from 43.7mg KOH/gm to 8.6mgKOH/gm. In the second step pretreatment also, the same tendency was followed similar to the first step. This can be shown from the figure [3].The combination of 9:1v/v methanol/oil molar ratio and reaction time of 2 hours was found to be optimum value which reduced acid value from 8.6mgKOH/gm to 2.7mg KOH/gm. With the increase in the Methanol/oil ratio and the reaction time, there was a decrease in the acid value.

Transesterification of PJO with methanol was performed after this pre-treatment process.

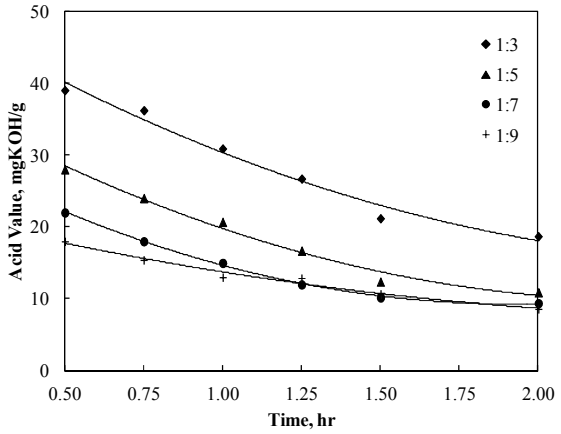

Fig. 2 Effect of methanol /oil molar ratio and reaction time on reduction of acid value of PJO during the first step pretreatment of biodiesel production. Initial acid value was 43.7mg KOH/g of oil.

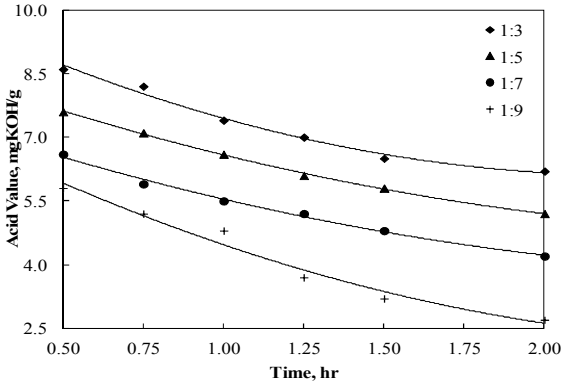

Fig. 3 Effect of methanol /oil molar ratio and reaction time on reduction of acid value of PJO during the second step pretreatment of biodiesel production. Initial acid value was 8.6mg KOH/g of oil.

3.2. Alkaline catalysed transesterification

The reaction product obtained from acid catalyzed pretreatment was used for this alkali catalysed transesterification. The experiments were carried out at different molar ratios, catalyst amount, reaction temperature and reaction time and optimum condition was noted down.

3.2.1 Effect of molar ratio on conversion efficiency

Three moles of alcohol and one mole of triglyceride reacts to yield 3 moles of fatty acid alkyl esters and one mole of glycerol [35].Methanol to oil ratio is an important parameter in the conversion of fatty acid alkyl esters [22]. Surplus amount of alcohol is needed to impel reaction products to right side of equilibrium reactions.

In the present work molar ratios of 3:1, 5:1, 7:1, 9:1, 12:1 v/v were used. From the test, it was found that the molar/oil ratio had no effect on acid, peroxide, saponification and iodine values of methyl ester [10]. Figure [4] shows the conversion efficiency at different molar ratios. With the increase in the addition of methanol, the conversion efficiency showed proportional increase in the initial stage and

rsion efficiency was very less molar ratio was above 9:1v/v. fered with the separation of creased solubility. Amount of he solution drove the reaction t side of equilibrium, and thus of low amount of esters. An optimum value of methanol was chosen carefully. From the literatures, the methanolysis reaction of non-edible oils was carried out with the molar ratio from 6:1 to 18:1 for both the steps irrespective of the catalyst. The molar ratio increased from 3:1 to 6:1, showed improved results on the ester yield. In the first step, when the methanol/oil molar ratio increased, the acid value reduced stridently, then slowly decreased and was constant at the final step [24]. More amount of triglycerides would be produced if the molar ratio was increased further and the reaction will also be incomplete if the molar ratio is less than 6:1.Aslo mixing of the reactants during transesterification will be insufficient for molar ratio < 6:1. The end product will be diluted if the molar ratio is greater than 6:1 and if it is increased further than 6:1, the methanol added will not have any effect on the yield of esters [35].

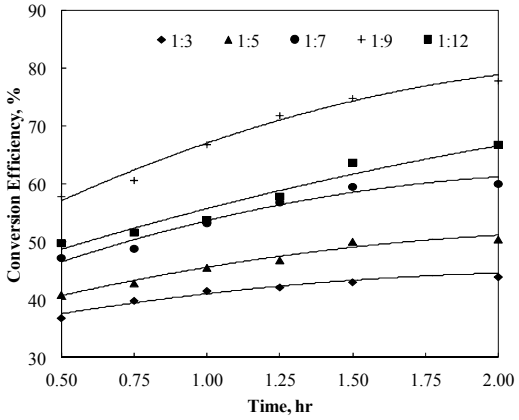

Molar Ratio Vs Time

Fig 4. Influence of molar ratio (methanol /oil) on the yield of PJME (NaOH 1%, temperature 60^{0}C, rate of stirring 600 rpm).

The present study revealed that the better yield of methyl esters of about 81% was at an optimum methanol/oil molar ratio of 9:1.Also, it was inferred that the yield of methyl esters gradually increased from 42 % to 81%.This gradual increase was noticed for the ratios from 3:1 to 9:1.After that methyl ester yield decreased. The transparency of biodiesel and the oil yield decreases if the molar ratio is increased from 7:1 to11:1. Abundant quantity of methanol used for the reaction leads to the difficulty in the separation of glycerol from biodiesel [22]. For the molar ratio above 13:1, unreacted methanol in the top level, ester in the middle level and glycerin at the bottom will be obtained [20].

3.2.2 Effect of catalyst amount on conversion efficiency

A set of experiments were conducted by changing the amount of NaOH from 0.25%to 1.5% w/v figure [5] shows the conversion efficiency with different catalyst amounts. The maximum yield of ester was obtained during the esterification of PJO with the catalyst 1% w/v NaOH. It was observed that the lowest catalytic concentration (0.25%) was not sufficient to complete the reaction. Increasing the amount of catalyst above 1.25%w/v did not increase the conversion efficiency. With the enhancement in the concentration of catalyst beyond 1.25%w/v, the methyl ester yield diminished and the quality of ester yield was based on the formation of glycerol and soap. The ester yield efficiency reduced with the increase in the amount of catalyst added. Excess amount of catalyst used led to the formation of

emulsion which increased the viscosity and formation of gels and at last the reaction ceased. From the experimental work, it was found that, for an efficient transesterification reaction, 1%w/v of NaOH was the optimum amount of catalytic concentration. The yield of methyl ester for Rapseed oil, Tobacco seed oil and *Pongamia pinnata* was 95-96% ,98% and 97-98% using 1%NaOH[6].Catalytic concentration of 1.33% yielded 89.9% of Karanja oil and 86.2% *Jatropha curcas* oil was obtained using 1% NaOH [24].

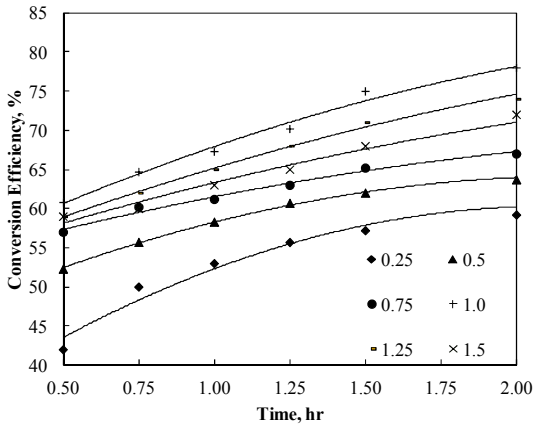

Catalyst Vs Reaction Time

Fig.5 Influence of NaOH concentration on the yield of PJME (methanol /oil molar ratio 9:1, temperature 60^{0}C, rate of stirring 600 rpm).

3.2.3 Effect of reaction temperature on conversion efficiency

The influence of reaction temperature on conversion efficiency is shown in the figure [6] keeping 9:1 molar ratio and 1%w/v NaOH catalytic concentration. For the yield of esters, reaction temperatures of 55^{0}C, 60^{0}C, 65^{0}C, 70^{0}C were used. The conversion efficiency was 71% for the temperature of 55^{0}C and at the reaction temperature of 60^{0}C, and 2.5 hrs, maximum ester yield of 81% was obtained. Similar results have been reported by earlier researchers using non edible oils [20]. In general for the base catalysed transesterification reaction, the temperature was set based on the type of alcohol used [24]. The methyl ester yield efficiency reduced when there was the rise in temperature. When the temperature was further increased from 65^{0}C -70^{0}C, PJ biodiesel yield and purity was decreased. At the high reaction temperature, loss of methanol accelerates saponification of glycerol by alkaline catalyst and the ester yield will be attained earlier than the completion of alcoholysis. Bubbles produced due to the vaporization of methanol obstructed the alcoholysis reaction though condensation system was used in the experiment. Hence the reaction temperature must not exceed the boiling point of methanol (65^{0}C) and reaction at higher temperature must be avoided. The findings from the experimental results of most of the researchers conclude that almost all the experiments were conducted near the boiling point of methanol

er yield was observed in the om 50 to 60^{0}C.95- 99% of ıed for Jatropha oil, Mahua ın oil [10], *Pongamia pinnata* ılepia syiraca* oil[40] ,*croton* reaction temperature of 60^{0}C

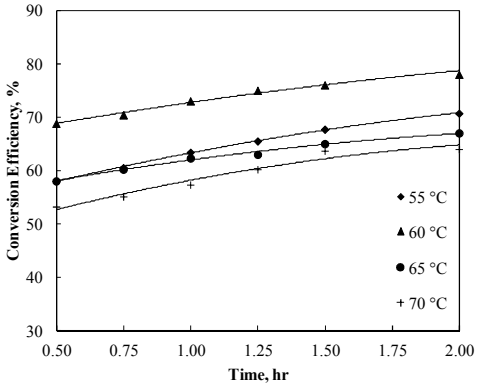

Reaction Temperature Vs Time

Fig 6. Influence of Reaction Temperature on the yield of PJME (methanol /oil) 9:1, Catalyst NaOH 1%, rate of stirring 600 rpm).

3.2.4 Effect of reaction time on conversion efficiency

The ester conversion was carried out at the reaction time such as 0.5, 0.75, 1, 1.25, 1.5, 1.75,2 and 2.5 hours keeping 9:1v/v molar ratio, 1%w/v NaOH catalytic concentration and 60^{0}C reaction temperature. The conversion efficiency can be improved by stirring the chemical reagents and oil at constant rate [11]. drawn between the biodiesel yield and reaction time, it was observed that reaction time extremely influenced the yield of esters. When the reaction time was enhanced from 1.5 to 2.5 hrs, there was the rise in the conversion efficiency of PJME. The conversion procedure is considered to be the best if it achieves maximum conversion within a shortest time period. The data obtained from the current experiments indicate that the reaction time of 2 hours was sufficient for the completion of the reaction and also it was found to be the optimum value. The ester conversion of *Prosopis Julifera* oil with this time was found to be 81%. If the oil is kept too long under the reaction time than the optimal value, the appearance of the oil becomes dark in colour. The yield of Jatropha biodiesel was 95% and 98% for Soybean and castor oil for a reaction time of 2 hours[42].In general, on edible oils can be analysed by further increasing the reaction time above 2 hours. Neem oil when reacted at 6.5to 8 hrs yielded 88 to 94% biodiesel[43] and Mahua oil produced 99% of ester yield after undergoing a chemical reaction of 3hours[15].

3.2.5 Fuel Properties of Methyl esters of *Prosopis Julifera* oil

Based on the Biodiesel ASTM standards, the fuel properties of Methyl esters *Prosopis Julifera* oil are summed up in Table 3. Most of the properties of Prosopis Julifera Biodiesel match the values as prescribed in the ASTM standard D6751-02.

Oxygen content present in Biodiesel helps in complete combustion. The calorific value of *Prosopis Julifera* Biodiesel was lower than that of diesel and that is due to the presence of oxygen content in Biodiesel. The Cetane number was found to be slightly greater than the regular diesel fuel. Also viscosity value was noticed to be a little bit greater than diesel. This implies that the biodiesel is having good ignition properties and there is the need to do slight engine modification. Density was very much greater than the diesel. The flash point and cloud point observed was confined as per the ASTM D6751-02 and DIN EN 14214 standards.

TABLE 3. PROPERTIES OF BIODIESEL PRODUCED FROM NON-EDIBLE FEEDSTOCKS

Properties	Test Procedure	Biodiesel-standard ASTM D6751-02	DIN EN 14214	Diesel	Diesel Prosopis Julifera oil-Biodiesel(PJME)
Density, Kg/m^3	ASTM D4052	875-900	860–900	847	893
Viscosity at $40^0C(mm^2/sec)$	ASTM D445	1.9–6.0	3.5–5.0	2.85	4.9
Calorific value(MJ/kg)	ASTM D240			43.4	39
Cetane number	D613	47 min	51 min	46	49
Flash point(^0C)	ASTM D4052	>130	>120	68	120
Cloud point (^0C)	ASTM D2500	-3 to 12	--	--	4
Acid value (mg KOH/g of oil)	ASTM D4052	>0.8	>0.50	0.35	2.7
Saponification value (mg KOH/g of oil)	--	--	--	--	92
Iodine value (I_2g100/g of oil)	--	--	--	--	87

3.2.6 Optimization of transesterification process

To evaluate the effect of process parameters on acid value in the first step of Transesterification, Central composite design (CCD) was used. The model significance and suitability was tested by analysis of variance (ANOVA) based on the alkaline value (response).The process parameters level for the optimization of transesterification process is given in Table no[4].The statistical analysis of experimental data was done using Deign expert 7.1.5 trial software.

3.2.7 Optimization of alkaline-esterification process parameters

After reducing the FFA value of the *Prosopis Julifera* oil by Acid transesterification process, Biodiesel was produced by Alkaline Transesterification.

Analysis of variance was then carried out to test the model significance. The ANOVA table is given in Table no [6].

TABLE 4. PROCESS PARAMETERS LEVEL FOR THE OPTIMIZATION OF TRANSESTERIFICATION PROCESS

Factors	Process Parameters	Lower level(-1)	Middle level (0)	Upper level (+1)	Std. Dev.
A	Methanol/oil (v/v)	3:1	6	9:1	2.32379
B	NaOH (w/v)	0.25	0.8583	1.5	0.470741
C	Extraction temperature (deg C)	55^0C	62.5^0C	70^0C	5.809475
D	Extraction time (min)	30	75	120	34.85685

TABLE 5. EXPERIMENTAL DESIGN WITH PROCESS DATA AND THE RESPONSE FOR TRANSESTERIFICATION PROCESS MODEL

Std	Run	Methanol/ (v/v)	NaOH (w/v)	Temperature deg C	Time (min)	Yield of Methyl Ester (%)
1	1	3	0.25	55	30	42
2	2	9	0.25	55	30	51
3	3	3	1.5	55	30	43.7
4	4	9	1.5	55	30	53
9	5	3	0.25	55	120	59.1
10	6	9	0.25	55	120	79.9
11	7	3	1.5	55	120	61.4
12	8	9	1	55	120	81
21	9	6	0.875	55	75	60.3
17	10	3	0.875	62.5	75	52
18	11	9	0.875	62.5	75	72.5
19	12	6	0.25	62.5	75	57.4
20	13	6	1.5	62.5	75	62.5
23	14	6	0.875	62.5	30	44.7
24	15	6	0.875	62.5	120	77.2
25	16	6	0.875	62.5	75	62
26	17	6	0.875	62.5	75	62
27	18	6	0.875	62.5	75	62
28	19	6	0.875	62.5	75	62
29	20	6	0.875	62.5	75	62
30	21	6	0.875	62.5	75	62
5	22	3	0.25	70	30	43.2
	23	9	0.25	70	30	55
	24	3	1.5	70	30	60.3
	25	9	1.5	70	30	58
	26	3	0.25	70	120	57
	27	9	0.25	70	120	76
	28	3	1.5	70	120	54
	29	9	1.5	70	120	73
22	30	6	0.875	70	75	62.3

TABLE 6. ANOVA RESULT FOR METHYL ESTER YIELD BY TRANSESTERIFICATION METHOD

Source	Sum of Squares	df	Mean Square	Value	p-value Prob > F	
Model	2867.982	10	286.7982	20.11568	< 0.0001	Significant
A-Methanol/oil (v/v)	862.0208	1	862.0208	60.46111	< 0.0001	
B-NaOH	33.40525	1	33.40525	2.343004	0.1423	
C-Temperature	4.226698	1	4.226698	0.296456	0.5924	
D-Time	1518.303	1	1518.303	106.492	< 0.0001	
AB	13.81237	1	13.81237	0.968783	0.3374	
AC	5.950516	1	5.950516	0.417362	0.5260	
AD	149.384	1	149.384	10.47762	0.0043	
BC	3.29608	1	3.29608	0.231183	0.6361	
BD	41.28586	1	41.28586	2.895741	0.1051	
CD	135.1723	1	135.1723	9.480824	0.0062	
Residual	270.8914	19	14.25744			
Lack of Fit	242.6781	14	17.33415	3.071978	0.1107	not significant
Pure Error	28.21333	5	5.642667			
Cor Total	3138.874	29				

The investigation of process parameters methanol/oil volume ratio (factor A), amount of sodium hydroxide (factor B), reaction temperature (factor C) and reaction time (factor D) with respect to methyl ester yield(Y) was analysed with the help of the following equation.

$$Y = +60.24 + 6.97 * A + 1.44 * B + 0.48 * C + 9.24 * D - 0.96 * A * B - 0.62 * A * C + 3.08 * A * D + 0.46 * B * C - 1.67 * B * D - 2.93 * C * D$$

The model using Response surface methodology with central-composite design (CCD) for the methyl ester yield had an F-value of 20.65 and a p-value of 0.0001 which show that the model is significant with a chance of 0.01% and the Model-F value happened due to noise. In this RSM model, methanol/oil volume ratio (factor A) was the important resolving factor in the Biodiesel yield and the main aim is to increase the yield. This was validated by the high F-value of 109.44 for factor A. Other than this, the parameters like amount of alkaline catalyst, sodium hydroxide (factor B) also had significant impact on the biodiesel yield and the effect of temperature has not much deviation in the methyl ester yield. The two process variable namely methanol/oil volume ratio (factor A) and amount of sodium hydroxide (factor B) had an interactive effect as observed from the p-value of 0.3417 which was less than 0.05. R squared & adj R squared values found using RSM were 0.915744 and 0.8714 respectively is shown in Table [7].Figure [a] shows the normal distribution of the data which help to confirm the ANOVA results. The RSM based predicted and actual methyl ester yield and perturbation chart is shown in the figure [b] and [c].

The Perturbation chart showed a negative non-linear steep curvature for methanol/oil volume ratio and the methyl ester yield. The chart also depicts that the (factor A) was the most important process parameter when compared with other variables. The other process parameters such as sodium hydroxide, time and temperature showed a plateau shaped curves in the Perturbation chart indicating their less odiesel yield. The response ester yield comparing (factors in figure [d] and the other kept at middle level. The ximum when the methanol/oil ot minimum 3:1v/v and the d were also minimum.

The percentage of yield can be given by the empirical formula

Yield Of Methyl Ester = - 17.14458 + 2.77394 * Methanol/oil(v/v) + 3.74168 * NaOH + 0.79556 * Temperature + 0.66313* Time - 0.50977 * Methanol/oil (v/v) * NaOH-0.027478 * Methanol/oil (v/v) * Temperature + 0.022820* Methanol/oil (v/v) * Time + 0.097240* NaOH * Temperature - 0.059318* NaOH * Time - 8.68369E - 003 * Temperature * Time

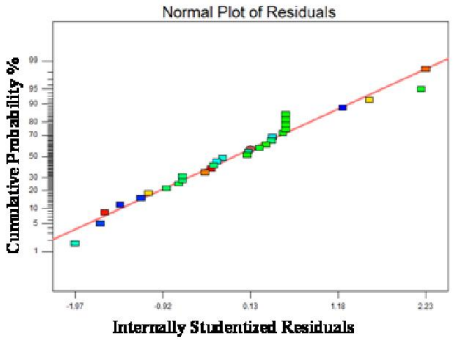

Fig (a) Normal Probability Plot of Residuals

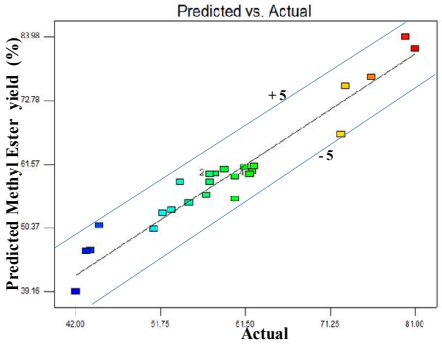

Fig(b) Predicted and Actual Methyl Ester Yield (%)

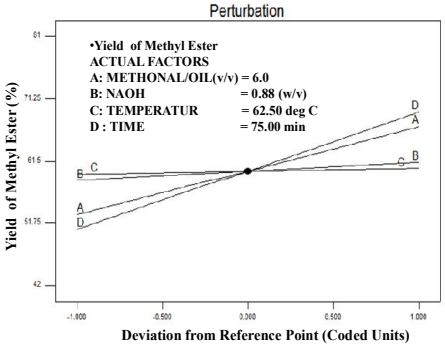

Fig (c) Perturbation of Transesterification for Percentage Yield of Methyl Ester

Table 7. R-squared results for methyl ester yield

Factor	Optimum value	Factor	Optimum value
Std. Dev.	3.726169	R-Squared	0.915744
Mean	60.28333	Adj R-Squared	0.871399
C.V. %	6.181094	Pred R-Squared	0.679232
PRESS	1004.313	Adeq Precision	19.84067

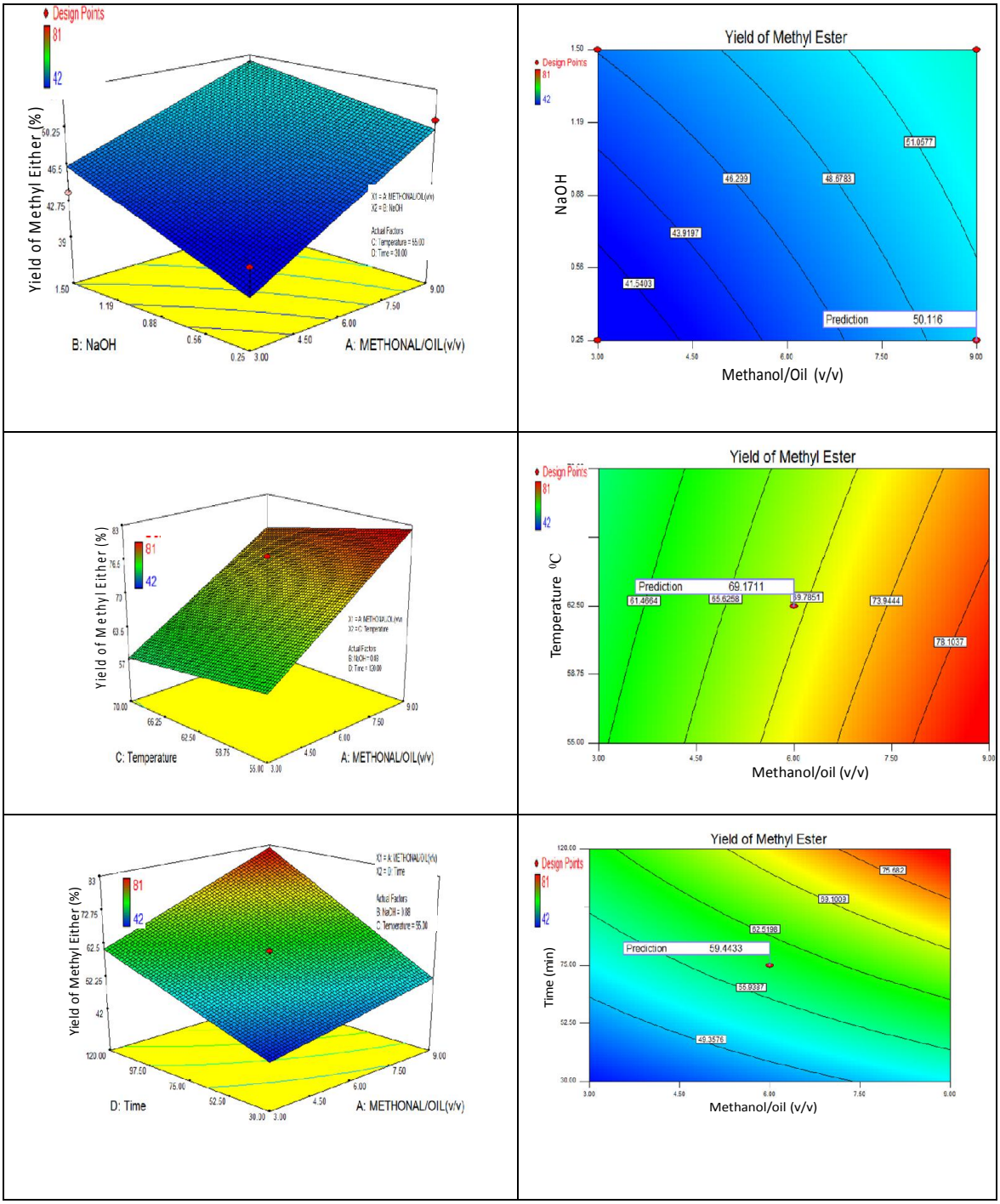

Fig (d) Response Surface and contour plots of methyl ester as function relationship of AB, AC, AD base on the second order polynomial equation.

4. Conclusion

There is 10 million hectare of salt affected land and 13 million hectare of arid and semi-arid zones which are suitable for the growth of trees like *Prosopis* Hence, 23 million hectare of for the plantation of *Prosopis* amount of 6.3 million litres an be produced from about 1 ion of *Prosopis Julifera.* By *rosopis Julifera* oil to methyl amount of 5 million litres of biodiesel can be produced. Hence, the species Prosopis Julifera found abundant in our country can do wonders if utilized in a useful manner.

Biodiesel from *Prosopis Julifera* oil was obtained by acid catalysed transesterification reaction using various catalyst concentration, methanol/oil molar ratios, reaction temperature and reaction time. The following points are concluded from the present work.

- In a two step acid esterification process using 1% v/v H_2SO_4 and9:1v/v methanol/oil ratio and 2 hours minimum reaction time, the FFA level of *Prosopis Julifera* oil was decreased from

43.7mgKOH/gm to 8.6mgKOH/gm and then finally it was reduced to 2.7mgKOH/gm.

- The optimum condition for transesterification was found to be using NaOH as catalyst, 1%w/v catalytic concentration, 9:1v/v molar ratio,60^{0}C reaction temperature and 2 hours reaction time.
- The ester conversion efficiency with these parameters is 81%.
- Using Response surface methodology, optimum conditions of 9:1v/v methanol/oil molar ratio, 1% w/v sodium hydroxide, at an extraction temperature of 55^{0}C and an extraction time of 120 min produced 82.27% of methyl ester yield.
- The properties of refined biodiesel such as cetane number, kinematic viscosity, Acid value, calorific value after transesterification agrees well with the ASTM standards.
- The biodiesel obtained in this process could be the best suitable alternative fuel for direct injection diesel engines.

REFERENCES

1. Pragnesh N. Dave, International Journal of Chemical Studies, 2321-4902.
2. Controlling and/or using *Prosopis Julifera* in spate irrigation system.
3. "A Technical manual on Managing *prosopis Julifera*", Department or International development, Foretsry Research programme.
4. P. Felker," Review of Applied aspects of *Prosopis*", Center for semi-Arid Forest Resources,Texas A&M University,Kingsville,Texas78363,U.S.A.
5. Deepak Rajagpoal, " Rethinking current strategies for biofuel Production in India".
6. E. Atabani., Non-edible Vegetable Oils: A Critical Evolution of Oil Extraction, Fatty Acid Compositions, Biodiesel Production, Characteristics, Engine Performance and Emission Production. Renewable and Sustainable Energy Reviews 18: (2013); 211-245.
7. Mambully Chandraekaran Gopinathan, Biofuels: Opportunities and Challenges in India, Springer-In vitro cell. Dev. Biol-plant 45 ;(2009):350-371.
8. Palligarnai T. Vasudevan, Bioiesel production-current state of the art and challenges. Springer-J Ind Microbiol Biotechnol 35;(2008):421-430.
9. Bryan R. Moser ,Biodiesel production, properties and feed stocks, Springer-In vitro cell. Dev. Biol-. plant 45; (2009):229-266.
10. Lin Lin., Dong Ying., Sumpun Chaitep., Saritporn Vittayapaung., Biodiesel production from crude rice bran oil and properties as fuel, Applied energy 86;(2009):681-688.
11. A. S. Ramadhas, S. Jayaraj, C. Muraleedharan Biodiesel production from high FFA rubber seed oil, Fuel 84; (2005):335–340.
12. Junhua Zhang , Lifeng Jiang Acid-catalyzed esterification of *Zanthoxylum bungeanum* seed oil with high free fatty acids for biodiesel production, Bioresource Technology 99 ;(2008): 8995–8998.
13. Hanny Johanes Berchmans a, Shizuko Hirata b, Biodiesel production from crude *Jatropha curcas* L. seed oil with a high content of free fatty acids, Bioresource Technology 99; (2008): 1716–1721.
14. V.B. Veljkovic, S. H. Lakic´evic, O.S. Stamenkovic, Z. B. Todorovic, M.L. Lazic Biodiesel production from tobacco (*Nicotiana tabacum* L.) seed oil with a high content of free fatty acids, Fuel 85; (2006): 2671–2675.
15. Shashikant Vilas Ghadge, Hifjur Raheman Biodiesel production from mahua (*Madhuca indica*) oil having high free fatty acids, Biomass and Bioenergy 28;(2005):601–605.
16. gadaravi, J. Nandagopal, P. '. Sathya Selva Bala, S. Sivanesan, sterification of karanja (*Pongamia* high free fatty acids for biodiesel 3;(2012): 1–4.
17. ri, Akhilesh Kumar, Hifjur Raheman tion from jatropha oil (*Jatropha* h free fatty acids: An optimized and Bioenergy 31; (2007):569–575.
18. Rui Wang, Wan-Wei Zhou , Milford A. Hanna , Yu-Ping Zhang , Pinaki S. Bhadury , Yan Wanga, Bao-An Song , Song Yang. Biodiesel preparation, optimization, and fuel properties from non-edible feedstock, *Datura stramonium* L. Fuel 91; (2012): 182–186.
19. Venu Babu Borugadda, Vaibhav V. Goud Biodiesel production from renewable feedstocks: Status and opportunities, Renewable and Sustainable Energy Reviews 16 ;(2012): 4763–4784.
20. B.K. Venkanna, C. Venkataramana Reddy, Biodiesel production and optimization from *Calophyllum inophyllum linn oil* (honne oil) – A three stage method, Bioresource Technology 100 ;(2009): 5122–5125.
21. D.F. Melvin Jose, R. Edwin Raj, B. Durga Prasad, Z. Robert Kennedy, A. Mohammed Ibrahim A multi-variant approach to optimize process parameters for biodiesel extraction from rubber seed oil, Applied Energy 88; (2011):2056–2063.
22. Mehdi Atapour, Hamid-Reza Kariminia, Characterization and transesterification of Iranian bitter almond oil for biodiesel production, Applied Energy 88;(2011):2377–2381.
23. Feng Guo, Zhen Fang , Xiao-Fei Tian, Yun-Duo Long, Li-Qun Jiang, ''One-step production of biodiesel from Jatropha oil with high-acid value in ionic liquids'' Bioresource Technology 140;(2013):447–450.
24. Ivana B. Bankovi´ c´-ll', Olivera S. Stamenkovi´, Vlada B. Veljkovi´, Biodiesel production from non-edible plant oils, Renewable and Sustainable Energy Reviews 16;(2012):3621– 3647.
25. Patil P, Gude VG, Deng S. Biodiesel production from *Jatropha curcas*, waste cooking and *Camelina sativa oils*. Ind Eng Chem Res 48; (2009): 8:10850–6.
26. Tiwari AK, Kumar A, Raheman H. Biodiesel production from jatropha oil (*Jatropha curcas*) with high free fatty acids: an optimized process. Biomass Bioenergy 31 ;(2007):569–75.
27. Naik M, Meher LC, Naik SN, Das LM. Production of biodiesel from high free fatty acid karanja (*Pongamia pinnata*) oil. Biomass Bioenergy 32 ;(2008):354–7.
28. Ghadge SV, Raheman H. Biodiesel production from mahua (*Madhuca indica*) oil having high free fatty acids. Biomass Bioenergy 28 ;(2005):601–5.
29. Mustafa Balat. Potential alternatives to edible oils for biodiesel production – A review of current work. Energy Conversion and Management 52; (2011): 1479–1492.
30. Singh D, Singh SP. Low cost production of ester from non edible oil of *Argemone mexicana*. Biomass Bioenergy 2010; 34:545–9.
31. Phan AN, Phan TM. Biodiesel production from waste cooking oils. Fuel 87 ;(2008):3490–6.
32. Pradip Kumar Biswas, Sanjib Pohit, RajeshKumar. Biodiesel from jatropha: Can India meet the 20% blending target?. Energy Policy 38 ;(2010):1477–1484.
33. Raheman H, Ghadge S V. Performance of diesel engine with biodiesel at varying compression ratio and ignition timing Fuel, 87(12); (2008): 2659–66.
34. Anand K, Sharma R ,Mehta P S. Experimental investigations on combustion, performance and emissions characteristics of neat karanji biodiesel and its methanol blend in a diesel engine. Biomass and Bioenergy 35(1);2011: 533–41.
35. Umar Rashid, Farooq Anwar, Gerhard Knothe. Evalution of biodiesel obtained from cotton seed oil. Fuel processing Technology 90; (2009):1157-1163.
36. Mustafa Balat , Havva Balat. Progress in biodiesel processing. Applied Energy 87 ;(2010): 1815–1835.
37. Mustafa Balat , Havva Balat. Progress in biodiesel processing. Applied Energy 87; (2010): 1815–1835.
38. Parlak A, Karabas H, Ayhan V, Yasar H, Soyhan HS, Ozsert I. Comparison of the variables affecting the yield of tobacco seed oil methyl ester for KOH and NaOH catalysts. Energy Fuels 23 ;(2009):1818–24.
39. Kamath HV, Regupathi I, Saidutta MB. Optimization of two step karanja biodiesel synthesis under microwave irradiation. Fuel Process Technology 92 ;(2011):100–5.
40. Wang R, Hanna MA, Zhou WW, Bhadury PS, Chen Q, Song BA, et al. Production and selected fuel properties of biodiesel from promising non-edible oils: *Euphorbia lathyris* L., *Sapium sebiferum* L. and *Jatropha curcas* L. Bioresour Technol 102;(2011):1194–9.
41. Pinzi S, Garcia IL, Gimenez FJL, Castro MDL, Dorado G, Dorado MP. The ideal vegetable oil-based biodiesel

composition: a review of social, economical and technical implications. Energy & Fuels 23; (2009): 2325–41.
42. Kafuku G, Mbarawa M. Biodiesel production from Croton megalocarpus oil and its process optimization. Fuel 89(9);(2010): 2556–60.
43. Barbosa DC, Serra TM, Meneghetti SMP, Meneghetti MR. Biodiesel production by ethanolysis of mixed castor and soybean oils. Fuel 89 ; (2010): 3791–4.
44. Barbosa DC, Serra TM, Meneghetti SMP, Meneghetti MR. Biodiesel production by ethanolysis of mixed castor and soybean oils. Fuel 89;2010: 3791–4.
45. Nabi MdN, Hustad JE, Kannan D. First generation biodiesel production from non-edible vegetable oil and its effect on diesel emissions. In: Proceedings of the 4th BSME–ASME international conference on thermal engineering, 2008.
46. L. N. Harsh and J. C. Tewari, Prosopis in the arid regions of India: some important aspect of research and development - central Arid Zone research Institute, Jodhpur, India.
47. Saxena, S.K and J. Venkateswaralu, Mesquite: an ideal tree for desert reclamation and fuel wood production 41 ;(1991):15-21.

2014 1st International Congress on Environmental, Biotechnology, and Chemistry Engineering
IPCBEE vol.64 (2014) © (2014) IACSIT Press, Singapore
DOI: 10.7763/IPCBEE. 2014. V60. 4

Seasonal Variation of Heavy Metal Distribution in Ennore Sea Shore, Chennai

Siji Thomas [1] and J.Abbas Mohaideen [2]

[1] Research Scholar, Sathyabama University, Chennai, India

[2] Principal, Maamallan Institute of Technology, Chennai, India

Abstract. The objective of the study is to reveal the seasonal variations of heavy metal concentrations in fish, water and sediment collected near seashore of Bay of Bengal in Ennore located in North Chennai, Tamilnadu. The concentrations of 5 heavy metals (Arsenic (As), Cadmium (Cd), Chromium (Cr), Lead (Pb) and Mercury (Hg)), were determined in water, sediment and marine species Indo-Pacific king mackerel popularly known as Spotted Seer fish (Scomberomorus Guttus) from Ennore in 4 different seasons. The concentrations of heavy metals in each sample were determined using AAS method. The study shows that the concentrations of most of the heavy metals in fish are higher in summer season and that in water and sediments are higher in monsoon and post-monsoon seasons respectively.

Keywords: Heavy metals, concentration, Atomic Absorption Spectrophotometer(AAS), Chennai, spotted seer fish, Ennore, sediment, water

1. Introduction

Heavy metals occur naturally in the ecosystem with large variations in concentration. Living organisms require varying amounts of "heavy metals". Iron, cobalt, copper, manganese, molybdenum, and zinc are required by humans, but excessive levels can be damaging to the organism.[1] Other heavy metals such as mercury, plutonium, and lead are toxic metals and their accumulation over time in the bodies of animals can cause serious illness. Heavy metal toxicity can result in damaged or reduced mental and central nervous function, lower energy levels, and damage to blood composition, lungs, kidneys, liver, and other vital organs. Long-term exposure may result in slowly progressing physical, muscular, and neurological degenerative processes that mimic Alzheimer's disease, Parkinson's disease, muscular dystrophy, and multiple sclerosis. Fish is a valuable food item and source of protein. The concentration of heavy metals in aquatic organisms is higher than that present in water through the effect of bio concentration and bio magnification and eventually threaten the health of human by sea food consumption [2]. Fishes are widely used as bio indicators of marine pollution by metals [3]. So determination of heavy metal concentration in fishes is very important as far as human health is concerned.

2. Methodology

2.1. Study area

The samples were collected from the fish catchment area nearby Ennore sea shore of Bay of Bengal in North Chennai, India. Ennore is situated on a peninsula and is bounded by the Korttalaiyar River, Ennore creek and the Bay of Bengal. The creek separates Ennore from the Ennore Port. Ennore creek carries high load of heavy metals. [4] [5] [6] The treated effluents of the Madras Refinery Ltd, through the Madras Fertilizers Ltd, through the Red Hills surplus channel, reach the

nethods

The water, sediment and spotted seer fish samples were collected during the period March 2012 to February 2013 in 4 seasons; Summer, Monsoon, Post-Monsoon and Winter within 500 meters from the seashore.[8][9] The physiochemical parameters like Temperature, pH, Salinity and Dissolved oxygen are measured. The fish samples were washed thoroughly with distilled water to remove the sediments and debris. The length and weight of each sample were measured. Then the edible parts were separated and frozen at -20^{o} for the analysis. The fish samples were thawed, and then dried in a hot air oven at 60^{o}C. After removing the moisture content, the weight was taken again. 15 gm of fish sample was taken and the ashing was done at 500^{o}C for 16 hours. After cooling, 2 ml of Nitric Acid (HNO_3) and 10 ml of 1 molar Hydrochloric Acid (HCl) were added. After digestion, samples were filtered using Whatman filter paper No. 41, and the filtrate is made up to 25 ml with distilled water.

100 ml water sample was taken in a beaker and 0.5 ml Nitric Acid (HNO_3) and 5 ml Hydrochloric Acid (HCl) were added. Then it is kept in a hot plate for digestion. After digestion, it was made up to 10 ml. Heavy Metal concentrations were determined by Atomic Absorption Spectrophotometer (AAS).

2 gm of dry sediment was taken in a digestion vessel; 10 ml of 1:1 Nitric acid (HNO_3) was added and covered with watch glass. It was heated at 95±5 degree C for 10-15 min without boiling. After cooling, 5 ml concentrated HNO_3 was added and refluxed for 30 minutes. The step was repeated until no brown fumes come. The solution was allowed to evaporate to nearly 5 ml by heat without boiling. After the sample has cooled, 2 ml of water and 30% H_2O_2 were added. Heated until effervescence subsides and vessel was cooled. 30 % H_2O_2 was added in 1 ml aliquots with warming until the effervescence is minimal. The sample was covered with a ribbed watch glass and continued until the volume has been reduced to 5 ml. 10 ml HCL was added and refluxed for 15 min at 95±5 degree C. The digestate was filtered through Whatman filter paper No.41 and was collected in 100 ml standard flask. Heavy Metal concentrations were determined by Atomic Absorption Spectrophotometer (AAS) [10].

3. Results and Discussions

3.1. Fish

The concentrations of heavy metals in spotted seer fish caught in 4 different seasons are given in table 1 and the graphical representation of the maximum concentration in Figure 1. It is observed that the maximum concentration of Arsenic (As), Cadmium (Cd), Chromium (Cr), Lead (Pb), and Mercury (Hg), are in summer (0.523 mg/kg), post-monsoon (0.441 mg/kg), monsoon (0.713 mg/kg), summer (0.722 mg/kg) and summer (0.082 mg/kg) respectively.

TABLE I. MINIMUM AND MAXIMUM CONCENTRATIONS OF H.M. IN FISH CAUGHT IN DIFFERENT SEASONS (MG/KG)

	As		Cd		Cr		Pb		Hg	
Season	***Min***	***Max***	***Min***	***Max***	***Min***	***Max***	***Min***	***Max***	***Min***	***Max***
Summer	BDL	0.523	0.042	0.383	0.036	0.631	0.08	0.722	BDL	0.082
Monsoon	BDL	0.429	0.034	0.418	0.112	0.713	BDL	0.716	BDL	0.078
Post-Monsoon	BDL	0.247	BDL	0.441	BDL	0.463	BDL	0.375	BDL	0.06
Winter	BDL	0.304	BDL	0.364	0.035	0.605	BDL	0.524	BDL	0.063

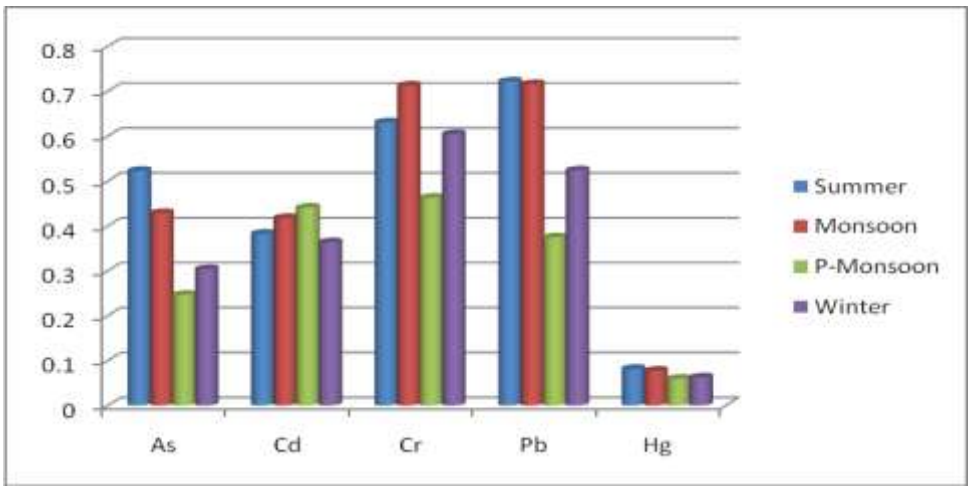

Fig 1. Maximum concentration of H.M. in fish collected in different seasons (mg/kg)

3.2. Water

The concentrations of heavy metals in water collected in 4 seasons are given in Table 2 and the graphical representation in Figure 2. The maximum concentration of Arsenic (0.043 mg/l) is observed in summer season. The Maximum concentration Cadmium (0.027 mg/l), Chromium (0.063 mg/l), Lead (0.015 mg/l) and Mercury (0.009 mg/l) are observed in monsoon season.

TABLE II. CONCENTRATION OF H.M. IN WATER COLLECTED IN DIFFERENT SEASONS (MG/L)

Seasons	As	Cd	Cr	Pb	Hg
Summer	0.043	0.02	0.048	0.011	0.006
Monsoon	0.034	0.027	0.063	0.015	0.009
Post-Monsoon	0.029	0.022	0.046	0.014	0.007
Winter	0.025	0.018	0.041	0.013	0.008

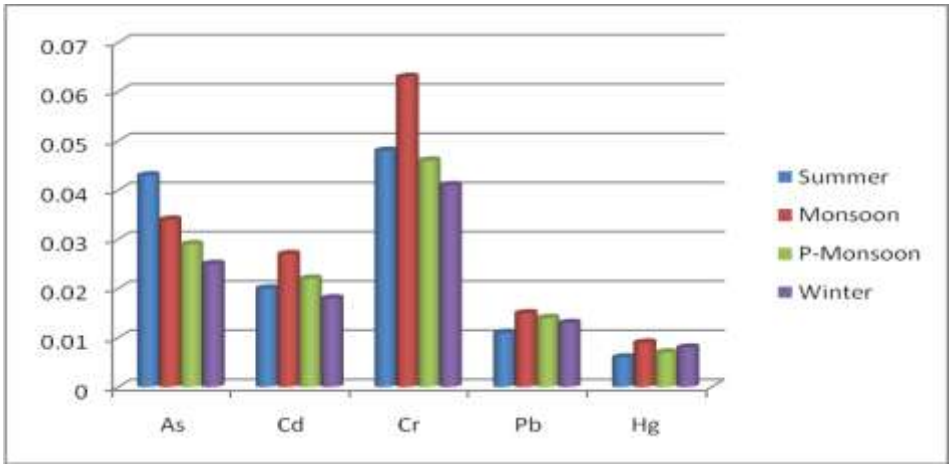

Fig 2. Concentration of H.M. in water collected in different seasons (mg/l)

of heavy metals in sediments collected in 4 seasons are given in Table 3 and the in Figure 3. The maximum concentration of Arsenic (2.518 mg/kg), Cadmium

(1.815 mg/kg) Chromium (3.082 mg/kg) and Mercury (0.483 mg/kg) are observed in post-monsoon. Maximum concentration of Lead (1.481 mg/kg) is observed in monsoon season.

TABLE III. CONCENTRATION OF H.M. IN SEDIMENT COLLECTED IN DIFFERENT SEASONS (MG/KG)

Seasons	As	Cd	Cr	Pb	Hg
Summer	1.526	1.12	1.492	1.034	0.382
Monsoon	1.841	1.374	1.157	1.481	0.394
Post-Monsoon	2.518	1.815	3.082	1.273	0.483
Winter	1.218	1.613	1.494	1.123	0.256

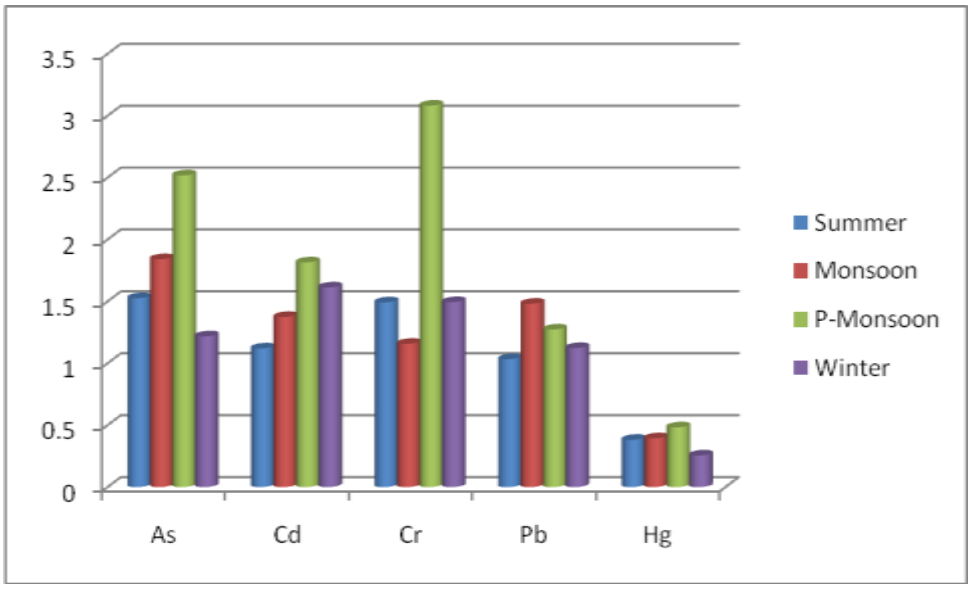

Fig 3. Concentration of H.M. in sediment collected in different seasons (mg/kg)

4. Conclusion

It is observed from this study that there is no much seasonal variation in concentrations of the heavy metals in fish samples, however the concentration of some metals are higher in summer season. The concentrations of most of the heavy metals in water are observed in monsoon season. This may be mainly due to the addition of heavy metals by run off during the monsoon. The concentrations of most of the heavy metals in sediment are observed in post-monsoon season and this may be due to the settlement of H.M. from the water.

5. References

[1] Sabine Martin and Wendy Griswold, Human Health Effects of Heavy Metals. *Environmental Science and Technology Briefs for Citizens* Page 1 Issue 15, March 2009

Sha Ato and P. A. Annune. Bioaccumulation of Heavy Metals in Fish (Tilapia Zilli and *rgans from River Benue, North ñ Central Nigeria*
. Chem. Vol. 12, No. 1 & 2 (2011) 25-31

[3] Padmini, E. and Kavitha, M. 2005a. Contaminant induced stress impact on biochemical changes in brain of estuarine grey mullets. Poll. Res., 24: 647-651.

[4] Jayaprakash,.M., Srinivasalu. S.Jonathan.M.P. and Mohan.V. 2005. A baseline study of physicochemical parameters and trace metals in water of Ennore Creek, Chennai, India. Mar. Poll. Bull., 50: 583-589.

[5] E.Padmini and B.Vijaya Geetha, A comparative seasonal pollution assessment study on Ennore Estuary with respect to metal accumulation in the grey mullet, *Mugil cephalus.* Oceanological and Hydrobiological Studies. Volume 36, Issue 4, Pages 91–103.

[6] Rajkumar, J.S.I., John Milton, M.C and Ambrose, T. Distribution of heavy metal concentrations in surface waters from Ennore Estuary, Tamil Nadu, India, *International Journal of Current Research*, Vol.3, Issue.3, Pages 237-244, March,2011

[7] V.Shanthi1 and N. Gajendran. The impact of water pollution on the socio-economic status of the stakeholders of Ennore Creek,Bay of Bengal (India): Part I. Indian Journal of Science and Technology Vol.2 No 3 (Mar. 2009)

[8] C.Ganga Baheerathi and K.Revathi. Seasonal variation in heavy metal accumulation in edible oysters Crassostrea madrasensis from Royapuram coastal water. Ind J Biol Stud Res Vol. 2 (2), 2013 pp 108-111

[9] Ahmad, M. K., Islam, S. , Rahman, S. , Haque, M. R. and Islam, M. M. Heavy Metals in Water, Sediment and Some Fishes of Buriganga River, Bangladesh Int. J. Environ. Res., 4(2):321-332,Spring 2010

[10] A. Walsh. Atomic absorption spectroscopy and its applications old and new. Pure & Appi. Chern., Vol. 49, pp. 1621 — 1628. Pergamon Press, 1977. Printed in Great Britain.

< Previous article | Next article >

Frequent pattern sub-space clustering optimisation algorithm for data mining from large database

T. Sheik Yousuf ⓘ, M. Indra Devi ⓘ

https://doi.org/10.1504/IJBIDM.2018.088433

Abstract

Data mining environment gives a quick response to the user by fast and correctly pick-out the item from the large database is a very challenging task. Previously, multiple algorithms were proposed to identify the frequent item since they are scanning database at multiple times. To overcome those problems, we proposed Rehashing based Apriori Technique in which hashing technology is used to store the data in horizontal and vertical formats. Rehash Based Apriori uses hashing function to reduce the size of candidate item set and scanning of database, eliminate non-frequent items and avoid hash collision. After finding frequent item sets, perform level wise subspace clustering. We instigate generalised self organised tree based (GSTB) mechanism to adaptively selecting root to construct the path from the cluster head to neighbours when constructing the tree. Our experimental results show that our proposed mechanisms reduce the computational time of overall process.

Keywords: sub-space clustering, generalised self-organised tree-based cluster head selection, GSTB

TRUE COPY ATTESTED

PRINCIPAL
MOHAMED SATHAK ENGINEERING COLLEGE
KILAKARAI-623806.

RCUHP-SM: A RULES GENERATION AND CLUSTERING BASED UNCOVERING HIDDEN PATTERNS IN SOCIAL MEDIA

T.Kumaragurubaran, *Assistant Professor, Department of Computer Science and Engineering, Mohamed Sathak Engineering College, Kilakarai, Ramanathapuram, Tamilnadu – 623 806,* **Dr. M. Indra Devi**, *Professor, Department of Computer Science and Engineering, Kamaraj College of Engineering and Technology, Virudhunagar, Tamilnadu - 626001*

***Abstract*— In recent days, uncovering the hidden patterns from social media is an important and essential task. For this purpose, some of pattern mining techniques are proposed in the traditional works. But, it has some drawbacks include vagueness of termination criteria, lack of interpretability, may extract the meaningless patterns and cannot adapt any constraints within the time interval. In order to overcome these issues, this paper proposed a Rules Generation and Clustering based Uncovering Hidden Patterns in Social Media (RCUHP-SM) technique to uncover the hidden patterns. The main aim of this technique is to analyze, observe and understand the human behavior. At first, the customer review dataset is given as the input and it will be preprocessed by eliminating the irrelevant and unwanted attributes. After that, the descriptive sentences are extracted from the preprocessed data and its score is calculated by counting the tagged words. It is based on the positive, negative and neutral reviews of the user of each product. Then, a set of rules from R1 to R27 is framed to predict the category of review. Consequently, the threshold value is calculated to create the cluster groups into least similar, moderately similar and most similar. Then, it will be labeled as C1 to C6 based on its category. In the analysis phase, the features are extracted from the product description and it's corresponding score is computed. Based on the score, the features are sorted and analyzed for the recommendation. In this work, the novelty is presented in rule generation, similarity computation, threshold based cluster formation and analysis stages. In experiments, the performance of the proposed uncovering hidden pattern system is evaluated and compared in terms of Mean Absolute Precision (MAP), Mean Absolute Error (MAE) and Root Mean Squared Error (RMSE) measures.**

***Index Terms* — Hidden Pattern Mining, Stop Words Removal, Parts of Speech (POS) Tagging, Rule Generation, Threshold based Clustering, Similarity Computation, Filtering and Feature Analysis.**

I. INTRODUCTION

SOCIAL NETWORKING sites include Google+, Facebook, Twitter, LinkedIn and etc., contains an effective channel to be connected with internet subscribers for sharing the views and thoughts with others [1-3]. It has been adopted by many businesses and more companies are using these sites to offer different services. Moreover, recent research works indicate that more people are using social media for iving and entertaining purposes. is support sales, customer care, innovation. These sites [4] of data such as comments, tweets tributed over different sites. This type of data hides the implicit pattern that cannot be determined by the traditional habitual analysis procedures. To identify and analyze the implicit patterns, the data mining techniques are used. Normally, the social media datasets are large in size, complex and not standardized. The main intentions of uncovering hidden patterns from large datasets are as follows:

- Analyze
- Observe
- Understand

A. Problem Description

In recent days, the process of discovering hidden pattern information [5, 6] from the social data has emerged as an interesting field of data mining. The data mining techniques provide an effective procedure to retrieve the information, preprocess the data, and analyze the data and to extract the hidden patterns. The reviewers use the hidden pattern analysis to provide their opinion about various subject matters in the course of discussion. The opinion analysis [7-10] is defined as the recommendations and suggestions of the reviewers that is based on his/her own perspectives. Moreover, the opinions are categorized into positive, negative and neutral polarities. Further the opinions are expresses in their own languages and the contents are not conveniently tagged. Thus, to extract information the content will need some level of text mining, text extraction or possibly full-up natural language processing techniques. Thus the text analysis and pattern mining techniques are the backbone of opinion analysis.

B. Motivation

In this work, a new recommender system, namely, Rules Generation and Clustering based Uncovering Hidden Patterns in Social Media (RCUHP-SM) is developed to generate an interface based on the social data by analyzing, observing and understanding the user views [11]. In addition, an improved association rule is formed to classify the reviews of the user and an exclusive similarity based clustering algorithms are proposed for data generalization. Here, a prediction estimation is generated based on a quality regression function. Then, the data validation is performed with the help of an efficient recommender system.

C. Contribution

The major contributions of this paper are as follows:

- To preprocess the customer review dataset, stop words removal and Parts of Speech (POS) tagging processes are performed in the preprocessing stage.

- To compute the score, the positive, negative and neutral reviews of each product are estimated.
- To compute the similarity between the user reviews of the product, a set of predefined rules from R1 to R27 are generated.
- To form a cluster group, the threshold value is computed based on the similarity between the reviews.

D. Organization

The remaining sections of the paper are organized as follows: Section II reviews some of the existing works related to hidden pattern mining and feature extraction in social media. Section III presents the detailed description of the proposed uncovering hidden pattern mining algorithm. Section IV evaluates the results of both existing and proposed mining techniques. Finally, the paper is concluded and the future work to be carried out is stated in Section V.

II. Related Work

This section reviews some of the existing works related to pattern mining, data preprocessing, stop word removal, clustering and POs tagging. *Liu, et al* [3] developed a temporal skeletonization approach to address the problem of curse of cardinality in sequential data analysis. The main aim of this paper was to identify the temporal patterns by summarizing the temporal correlations in an undirected graph. The challenging tasks faced in this work were as follows:

- Computational Complexity – It identified the frequent sequential patterns for large symbol sets.
- Rareness – The growing cardinality of the specific sequential pattern was decreased.
- Granularity – The useful patterns were diluted due to the large number of symbols in a sequence.
- Noise – The multi-modality of events and useful patterns were not replicated, due to the nature of sequential events.

Lyons, et al [12] introduced a Hidden Markov Model (HMM) fold technique for protein fold recognition. Here, the HMM profiles were extracted by using the profile-profile sequence alignment technique. The temporal clusters are identified in the low-dimensional embedding space of the temporal graph. The cardinality of the sequential data was reduced

To evaluate the performance of the suggested technique, three difference benchmark datasets such as Ding and Dubchak (DD), Extended Ding and Dubchak (EDD) and Taguchi and Gromiha (TG) were utilized in this paper. *Ruiz, et al* [13] suggested a new approach to mine the rules based on the fuzzy rules. Moreover, a new approach was presented to represent and evaluate the fuzzy rules, then the formal model was implemented for feature extraction.

The major advantages of this paper were as follows:

- It expressed some knowledge useful in different domains include fraud detection, chemical processes, ly deviations.
- lerstandable results by using the

confidence and certainty factor number of rules. *Song, et al* [14] introduced a cluster based feature subset selection algorithm to find a subset of features in a high dimensional data. The stages involved in this concept were as follows:

- Irrelevant features removal
- Minimum Spanning Tree (MST) construction
- MST partitioning and representative features selection

In this paper, the redundant and irrelevant features were removed by using the feature subset selection algorithm. The dimensionality of the data was reduced by considering each cluster as a single feature. *Lu, et al* [15] developed a framework to discover various user search goals based on the feedback sessions. The performance of inferring user search goals were evaluated with the help of Classified Average Precision (CAP). This work was categorized into three classes include query classification, search result recognition and session boundary detection. *Hu, et al* [16] recommended a clustering based collaborative filtering approach for big data applications. The main objectives of this technique was to select the similar services in the same cluster for recommending the collaborative services. The advantage of this work was, it reduced the online execution time of collaborative filtering.

Pimpale and Patel [17] conducted an experiment with POS tagging for Indian social media text. In this application, the WEKA tool was utilized to test various machine learning techniques. The features used for training and testing were as follows:

- Language of the word
- Language of the previous and next word
- POS tags
- Position of the word in sentence

Also, the authors utilized an unlabeled data for training to represent the use of distributed vectors. *Pandya, et al* [18] compared the classification and association rule mining techniques to uncover the hidden patterns in an Indian university. The main intention of this paper was to find the fitness of the technique in an education field. *Karami, et al* [19] suggested a new approach, namely, Fuzzy Approach Topic Model (FATM) to uncover the hidden patterns in medical text collections. The document term frequency matrix was evaluated by calculating the value of Global Term Weighting (GTM). To model an unstructured document, a fuzzy set theory and clustering techniques were utilized in this paper. *Bellogin, et al* [20] suggested a coverage metric to uncover and compensate the precision metrics used for social, collaborative and hybrid recommenders. The main intention of this paper was to adjust each recommender's weight based on the user correctness and relevance in a social network. The main drawback of this concept was, it don't have the capability to produce recommendations for users. *Havens, et al* [21] recommended a Fuzzy C-Means (FCM) clustering technique for processing very large data. In this paper, the methods were compared based on the followings:

- Sampling followed by non-iterative extension
- Kernelized version of FCM
- Incremental techniques

From the analysis, it was identified that the kernel clustering required high memory for storing the kernel matrix, which

was the main drawback of this FCM. Moreover, the complexity of these algorithms were also analyzed in this paper. *Thilagavathi, et al* [22] investigated different hierarchical clustering algorithms based on its advantages and disadvantages in data mining. From the survey, it was analyzed that the hierarchical clustering provided more informative structure compared than the unstructured set of clusters. *Wu, et al* [23] recommended a neighborhood based collaborative filtering approach to predict the Quality of Service (QoS). The main considerations of this paper were listed as follows:

- The impact of different QoS scale was improved by calculating the adjusted cosine based similarity.
- It used a similarity fusion based approach to increase the prediction accuracy.
- It handled the data sparsity problem

The major drawbacks of this paper were, not- scalable and it don't learn anything from the user profile. *Li, et al* [24] developed a multidimensional clustering based collaborative filtering approach to improve the recommendation diversity. This work includes the following stages:

- Data preprocessing
- Multidimensional clustering
- Selecting the appropriate clusters for recommendation

The main aim of this paper was to increase the effectiveness and diversity of user recommendation. *Pham, et al* [25] introduced a clustering based collaborative filtering approach for social network analysis. The authors of this paper applied this approach on the following scenarios:

- Academic venue recommendation
- Trust-based recommendation

Here, the social relationship between the users was identified based on the ratings data. Also, a complex network clustering algorithm was applied in this work to group the similar users. *Renaud-Deputter, et al* [26] developed a new approach based on implicit recommender system by integrating both the clustering and matrix factorization. In this paper, a high dimensional, parameter free, and divisive hierarchical technique was implemented. The major advantage of this technique were, easy to implement, very effective and could be applied to any datasets. *Vyas, et al* [27] analyzed the normalization and transliteration problems for multilingual context. From the paper, it was analyzed that the language identification, normalization and POS tagging were considered for improving the results.

Lin, et al [28] introduced a new similarity measure to estimate the similarity between two documents based on a feature. In this paper, the real time datasets were utilized to measure the effectiveness of the text classification and clustering problems. An average score of the features occurring at the least two documents was considered. The algorithms considered in this work were, single linkage, average linkage, complex linkage, k-means, DBSCAN and [29] suggested a collaborative implicit data based on clustering similar interest patterns were ıg a modified preprocessing size of the data and the dimensionality of item space were reduced by employing the clustering technique. *Lee and Yun* [30] provided an efficient approach to mine an uncertain frequent patterns without false positives. The proposed list-based data structures and pruning techniques efficiently mines the frequent patterns without any pattern loss. The efficiency of the method was analyzed in terms of runtime, scalability and runtime.

From the survey, the merits and drawbacks of existing pattern mining techniques are investigated. In order to solve those issues, this paper proposed a new technique for uncovering patterns in social media. The description about the proposed technique is discussed in the next section.

III. PROPOSED METHOD

This section presents the detailed description of the proposed Rules Generation and Clustering based Uncovering Hidden Patterns in Social Media (RCUHP-SM) system. The overall flow of the proposed system is shown in Fig 1, which includes the following stages:

- Preprocessing
- Score computation
- Rule generation
- Thresholding based clustering
- Overall recommendation

At first, the input customer review dataset is given as the input, which is preprocessed to eliminate the irrelevant and unwanted attributes in the dataset. After that, the stop words like *wh* words and conjunction words are removed from the sentence. Then, the Parts of Speech (POS) tagging is applied to extract the adjectives and adverbs from the sentence. Because, it describes the mode such as positive or negative of the sentence. The descriptive sentences are extracted to compute the score value. Here, we generate some rules to find the similarity between the reviews in the social media. Then, the threshold value is computed to create the cluster of reviews based on the similarity values. It is categorized into least similar, moderately similar and most similar. Then, the overall recommendation is displayed for further process. In the analysis phase, the features are extracted and its corresponding score is calculated. Based on this value, the features are analyzed for the recommendation.

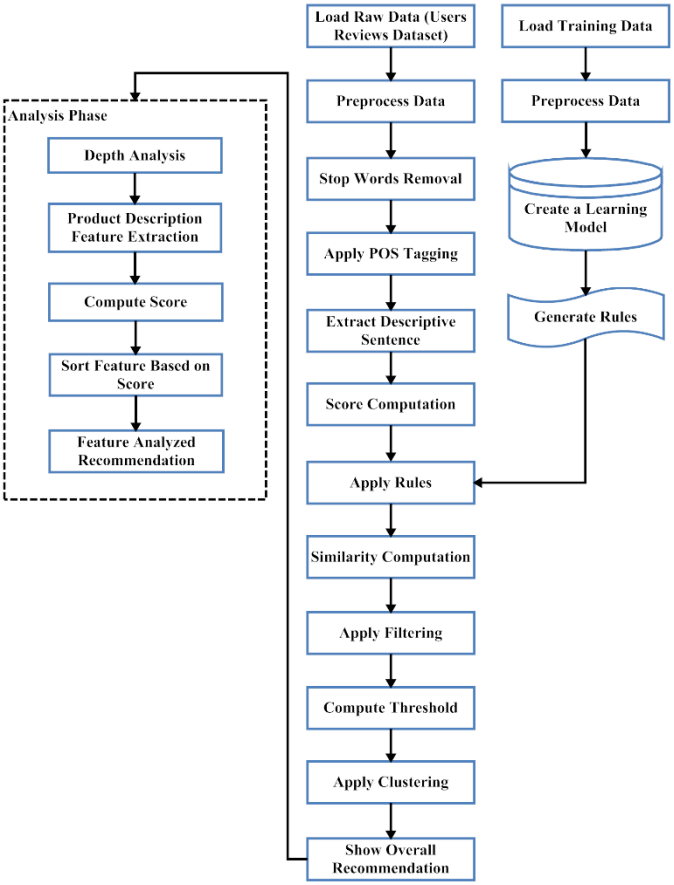

Fig 1. Overall flow of the proposed system

A. *Preprocessing*

Initially, the given Word Net dataset is given as the input, where the sentences are synchronized by finding the positive and negative scores for the user ID. After that, the dataset dictionary is created in which the positive words, negative words and neutral words are extracted. Based on the user ID and number of reviews, the comparative sentences are identified and removed. The main aim of preprocessing the dataset is to reduce the file size and to improve the quality of the data. In this stage, the following processes are performed.

- Special characters removal
- Unwanted spaces removal
- Stemming
- Stop words removal
- POS tagging

The purpose of stemming is to reduce the inflectional forms and different grammatical forms. In order to save memory and time, the stemming is performed, which eliminates the number of words and suffixes by accurately matching the stems. After stemming, the stop words include *wh* words, conjunction words, auxiliary verbs, articles, prepositions, pro-nouns and etc. Removing these words from the dataset can reduce the dimensionality of term space. In text mining applications, the l as keywords. The stop words ocessing step, because which are words and has no information. ls, the POS tagging is applied to ce. Typically, the POS contains information. The main aim of POS tagging is to select a most probable speech sequence of the words in the sentence. Moreover, it separates the sentence into a noun, adjective, adverb, verb and all the parts of speech tag.

B. *Score Computation and Rule Generation*

After preprocessing, the tagged words from the database are compared with the Word Net dictionary to calculate the number of positive, negative and neutral words in each review. Based on this value, the score is computed for each review. To identify each review as positive, negative or neutral based on the calculated score, some predefined rules are generated in this paper. In this process, there are 27 numbers of rules include R1 to R27 are formed to predict whether the review is positive, negative or neutral. If the number of positives, negatives and neutrals are 1, it is set to be rule 1 and its review is considered as neutral. Moreover, the review is categorized based on the greater value, for instance, if the number of positives is greater than the negatives and neutrals, it is considered as a positive review. Likewise, if the number of negatives is greater than the other, it is considered as negative. Similarly, the neutral is also estimated. Based on the category of reviews, the similarity is computed. The rules are tabularized in Table 1.

Table 1. Rule generation

Rules	***No of positive***	***No of negative***	***No of neutral***	***Review***
R1	1	1	1	Neutral
R2	1	1	2	Neutral
R3	1	1	3	Neutral
R4	1	2	1	Negative
R5	1	2	2	Negative
R6	1	2	3	Negative
R7	1	3	1	Negative
R8	1	3	2	Negative
R9	1	3	3	Negative
R10	2	1	1	Positive
R11	2	1	2	Positive
R12	2	1	3	Positive
R13	2	2	1	Neutral
R14	2	2	2	Neutral
R15	2	2	3	Neutral
R16	2	3	1	Negative
R17	2	3	2	Negative
R18	2	3	3	Negative
R19	3	1	1	Positive
R20	3	1	2	Positive
R21	3	1	3	Positive
R22	3	2	1	Positive
R23	3	2	2	Positive
R24	3	2	3	Positive
R25	3	3	1	Neutral
R26	3	3	2	Neutral
R27	3	3	3	Neutral

C. Similarity Computation

After generating the rules, the filtering process is performed for computing the similarity. In this stage, the number of positive, negative and neutral reviews are calculated. The similarity values are calculated by comparing all reviews with the other reviews of the product. Then, the comparative values for the reviews with the same type of reviews are retained, where the other reviews are filtered. For instance, if all the reviews are positive, it is considered as positive; otherwise, it is filtered out.

In this algorithm, the product Id *R* aer id U_n are given as the input. Then, for each product, the number of reviews in the list are listed. For each review of the user, the similarity is computed and the similar words of the reviews are listed. Also, the distinct of the reviews are collected and the size of two lists is calculated. After that, the common words in N_1 and N_2 are computed and the similarity between the total words and distinct words is computed. Then, this process will be repeated until computing the similarity between all the products.

Algorithm I – Similarity Computation

Input: Product Id R = {R1, R2, R3, R4, R5}
User id (U_n), n = 1, 2 … N; // Where, N represents the number of user who reviewed each product;
Output: Similarity and distance values;
Procedure:
For each product R,
Load the list of reviews in the Review List Rlist;
For i =1; // Where, i represents the review of the user with user id U_i;
For j = i+1 is the review of the user with the user id U_j
s P_i = Review of the user U_i;
P_j = Review of the user U_j;
Similarity (P_i, P_j);
N_1 = Words list P_i;
N_2 = Words list P_j;
Retain distinct words in the list N_1 and N_2;
Compute the size of both list (S_1, S_2);
$C_{Tot} = S_1 + S_2$;
C_{Uniq} = Common words in N_1 and N_2;
Similarity value = $2 \times (C_{Uniq} / C_{Tot})$;
Distance = 1 – Similarity;
End for;
End for;
Continue until computing the similarity for all products;
End;

D. Threshold based Clustering

larity, the threshold is computed orithm, the number of products *n* he similarity score is calculated similarity calculation. Then, the ducts are stored in the similarity list (simlist). This list is sorted by arranging the values as minimum to maximum, then the average is calculated. Here, the smallest value of the list is considered and the list is split into three groups. The threshold value is calculated as follows:

Threshold = average – smallest value/3;
C1 = (initial value – (initial + 1)× threshold);
Increment the initial value;
C2 = (initial value – (initial + 1)× threshold);
Increment the initial value;
C3 = (initial value – final value in the list);

It will be sorted in which the minimum and maximum similarity are estimated and the summation is performed. Based on the size of simlist, the mean is calculated and, the range is estimated as low, medium or high from the minimum and maximum values.

Algorithm II – Threshold Computation

N = 5 (number of products);
For N = 1 to 5;
Simlist ← Similarity values of the product
// Where distance ! = 1;
Sort (Simlist);
Minval ← Simlist (l);
Simsum = Sum (Sorted Simlist);
Let S_z be the size of the Simlist;
Maxval = Mean (SimSum);
Let M = 3;
Calculate the range as low, medium or high from Minval and Maxval;
End;

After calculating the threshold value, the reviews are grouped into the clusters based on the similarity values with respective to the type of reviews of all the products. Then, the clusters are comes under the category of least similar, moderately similar and most similar in the cases of positive and negative reviews.
Furthermore, it will be labeled by using the following table:

Table 2. Clustering based on the reviews

Review	***Cluster Name***
Positive and Most Similar	C1
Positive and Moderately Similar	C2
Positive and Least Similar	C3
Negative and Most Similar	C4
Negative and Moderately Similar	C5
Negative and Least Similar	C6

E. Analysis Phase

After clustering, the processes include depth analysis, feature extraction for product description, score computation, feature sorting and recommendation are performed during the analysis phase. Here, the number of positive and negative comments are identified, based on this value, the score is calculated for the descriptive words. In this algorithm, the

number of products *N* that are reviewed, total number of products P_i, number of positive reviews *NOP*, number of negative reviews *NON* and number of neutral reviews *NOU* are considered. If the value of NOP is greater than the NON & NOU or if the NOP is less than the NON & NOU values, it is considered as a positive review. If the value of NON is greater than the NOP & NOU or if the NON is less than the NOP & NOU values, it is considered as a negative review. If the review is positive, the reviews are sorted based on the minimal verge score. Then, the tagging is applied to extract the product features and the relevancy is computed for those features. Then, it will be displayed in the descending order. If the review is negative, the reviews are sorted based on the minimal verge score. Then, the same process mentioned in the positive review is applied for the negative review. Finally, it will be recommended for further analysis.

Algorithm III - Deep Analysis

Let, N - Number of products that are reviewed, P_i - Product, where i = 1 to N, NOP – number of positive reviews, NON – number of negative reviews, NOU – number of neutral reviews;

Begin

If (NOP > (NON && NOU)) || (NOP == NOU) > NOP)

Type (P_i) → Positive;

Identify the overall dimension of the review based on NON, NOP and NOU;

If (NON > (NOP && NOU) || (NON == NOU) > NOP)

Type (P_i) → Negative;

If (Type (P_i) → Positive)

Extract Plist ← sort (Positive reviews based on the minimal verge score);

P_feat ← Apply tagging to extract the features;

Compute relevance (P_feat);

Rank P_feat based on relevancy;

Display feature that are in descending order;

End if;

If (Type (P_i) → Negative)

Extract Plist ← Sort (Negative reviews based Minimal verge vector);

N_feat ← Apply tagging to extract features;

Compute relevancy (N_feat);

Rank N-feat based on relevancy;

Display features that are in descending order;

End if;

End;

The major advantages of this pattern mining system are as

t similarity matching results

e meaningful patterns

alculation

The superiority of the proposed RCUHP-SM technique is proved in the next section.

IV. Performance Analysis

This section evaluates the performance results of both existing and proposed techniques in terms of execution time, accuracy, mean average precision, Root Mean Squared Error (RMSE) and Mean Absolute Error (MAE). The dataset used in this analysis is customer review dataset [31], which contains the details of customer reviews of multiple usage products.

A. Dataset

Fig 2 compares the existing [32] and proposed clustering techniques based on the dataset purity value, where the x-axis represents the algorithms and the y-axis represents the dataset purity value. Dataset purity value is an external evaluation criterion of cluster quality. It is the percent of the total number of objects that were classified correctly, in the unit range. The existing techniques considered in this analysis are, Kl-FCM-GM, IWKM, EKP, OCIL and ACC-FSFDP. *Kl-FCM-GM* is an existing clustering technique that is an extension of Gath-Geva and is mainly designed for the multinomial distributed data clustering. *IWKM* represents the cluster's prototype by integrating the mean value of all distribution centroids. *EKP* is a kind of evolutionary algorithm that is mainly develop to increase the capability of global search. OCIL is an iterative clustering algorithm that finds the cluster similarity based on the objects. *ACC-FSFDP* is a self-adaptive peak density clustering algorithm that is mainly used for mixed attributes. In this technique, three different types of data such as balanced data, categorical data and numeric dominant data are considered.

Here, the purity is calculated for the Apex DVD player, Canon G3 Camera, Zen MP3 Player, Nikon Camera and Nokia Phone products. From the analysis, it is observed that the proposed RCUHP-SM technique provides high dataset purity value, when compared to the other techniques.

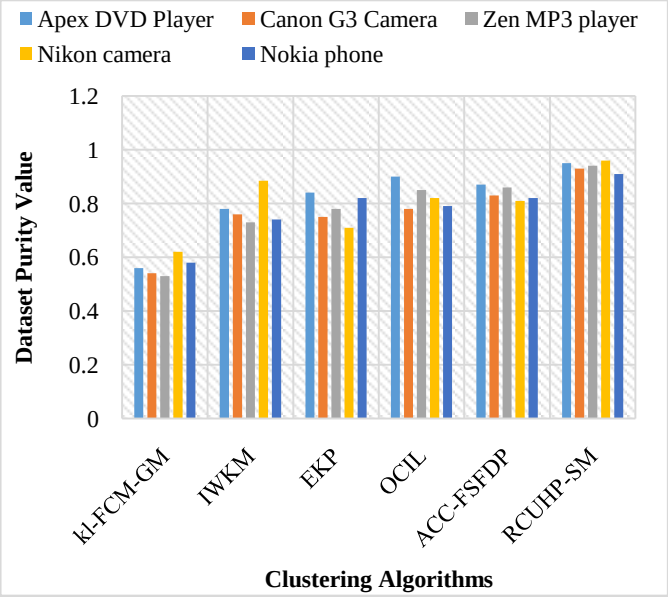

Fig 2. Dataset purity value

B. *Execution Time*

Execution time is defined as the amount of time taken to execute the process. Fig 3 illustrates the execution time of existing and proposed clustering techniques. Here, the products such as an Apex DVD player, Canon G3 camera, Zen MP3 player, Nikon camera and Nokia phones are considered for comparison. When compared to the existing techniques, the proposed RCUHP-SM provides the best results. Also, the execution time with respect to number of user reviews is analyzed in Fig 4, where the x-axis represents the reviews from 100 to 300 and the y-axis represents the execution time. In this analysis, the techniques such as StrAP, StrDenAP, Str-FSFDP and proposed RCUHP-SM are considered. The StrAP is a data streaming technique that is mainly developed to attain high field intensity during the process of clustering. The SteDenAP is based on the StrAP technique that adapts the decay density of micro cluster and guaranteed the better clustering results. The SteFSFDP technique dynamically maintains the mixed data objects and maximum frequency of categorical attributes. From the analysis, it is observed that the proposed technique provides requires minimum execution time, when compared to the other techniques.

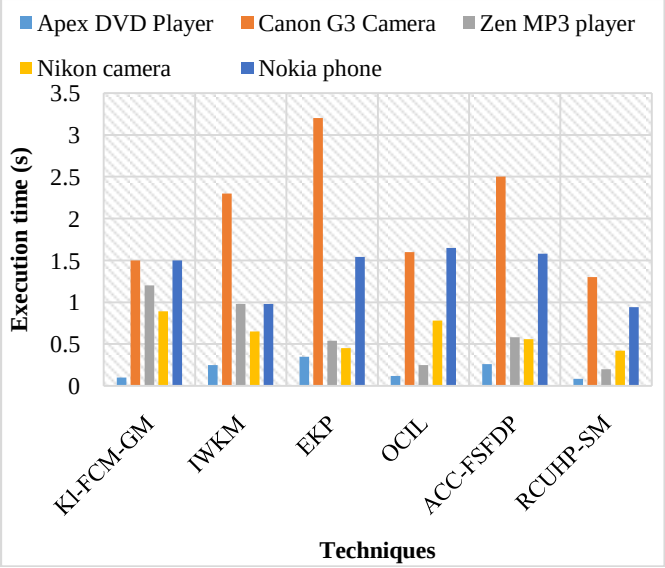

Fig 3. Average execution time of existing and proposed clustering techniques

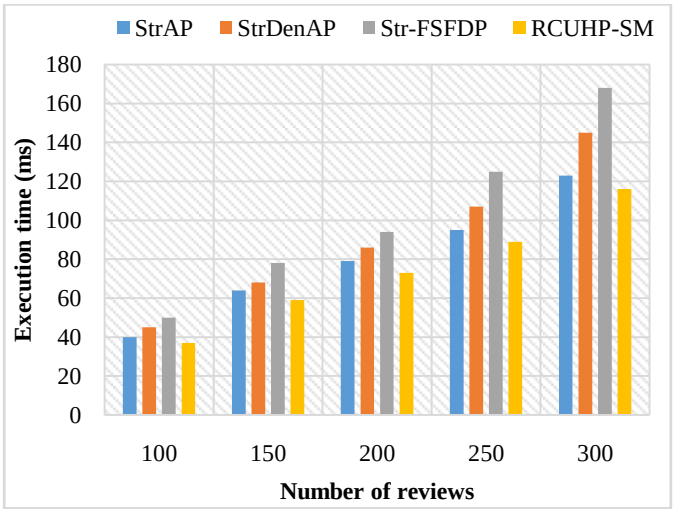

Fig 4. Execution time Vs Number of reviews

C. *Mean Average Precision (MAP)*

The Mean Average Precision (MAP) is a ranked precision metric that provides a larger credit to correctly recommended items in the top ranks. It is calculated for a given top-N recommendation list, which is shown in below:

$$Precision@N = \frac{|U_{N,rec} \cap U_{adopted}|}{N} \quad (1)$$

Where, N represents the number of recommendations received and $C_{adopted}$ indicates the items that a user adopted in the test data. Fig 5 shows the MAP of both existing [33] and proposed techniques, where the x-axis represents the training set and the y-axis represents the MAP. The existing techniques considered in this analysis are, SR2, HSR, LRMVL, PMF, GRMC, and MVUPL. The SR2 is a social recommender approach that uses the pearson correlation coefficient and graph regularization term to constrain the trained model. The HSR uses the rating information by incorporating the items and user preferences. Similarly, the PMF is a type of collaborative filtering technique that utilizes the probabilistic matrix factorization for fully Bayesian treatment. The GRMC regularized the result of matrix completion for improving the basic matrix completion based on the social relations. The LRMVL is defined as the low rank multi-view matrix completion method that learns the representation of low rank for all the views. The MVUPL is a multi-view user preference learning model that utilizes the measures of tagging information, user social relations, item side information and rating information. For this analysis, the canon G3 dataset is used. Also, the MAP is analyzed with respect to the % of dataset as shown in Fig 6, where the Nokia 6610 dataset is used. From these results, it is observed that the proposed RCUHP-SM provides high precision value, when compared to the other techniques.

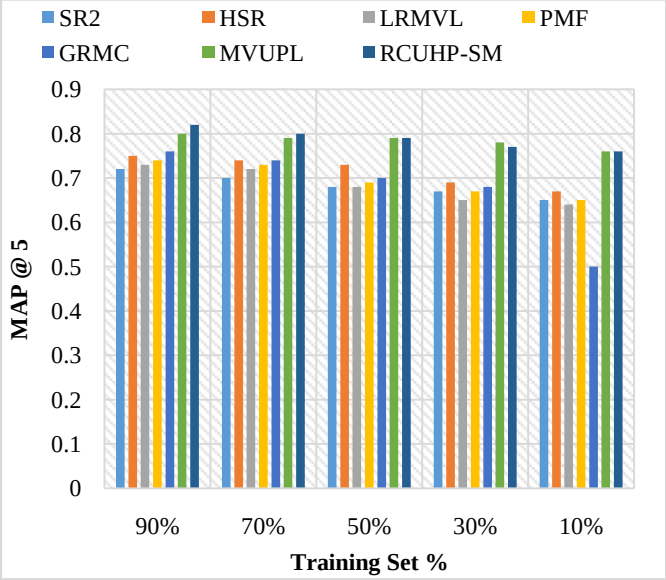

Fig 5. MAP for Canon G3 dataset

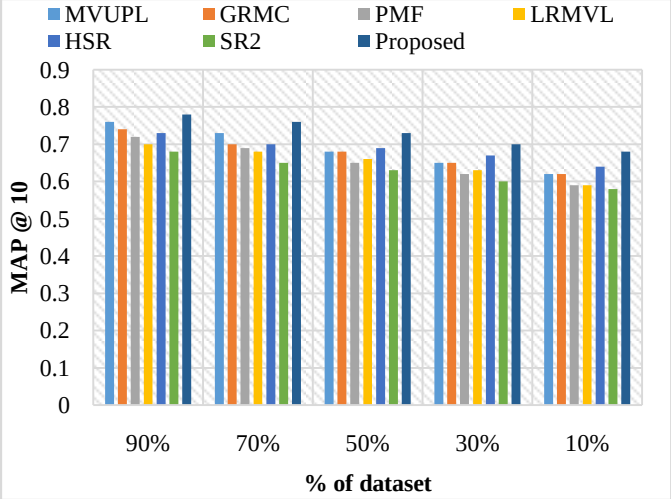

Fig 6. MAP for Nokia 6610 dataset

D. *Root Mean Squared Error (RMSE)*

The RMSE is one of the widely used error measures in data mining applications. In this measure, the sum of the individual squared errors is obtained, where each error indicates the sum of individual errors. Moreover, it can be varied with respect to the error magnitude. The RMSE value is calculated as follows:

$$RMSE = \sqrt{\frac{1}{n}\sum_{i=1}^{n} e_i^2} \qquad (2)$$

Where, the n represents the number of samples of model error e_i. Fig 7 shows the RMSE value of proposed RCUHP-SM technique with respect to different alpha values, where the For this analysis, the hyper e taken to evaluate the sensitivity , the parameter c represents the ions and the value of α can vary r, these parameters are more important for the sensitivity analysis of the proposed system. Here, the RMSE values for the Nokia 6610 dataset is analyzed in Figure 8. From the results, it is analyzed that the proposed technique provides the minimized RMSE value for both datasets.

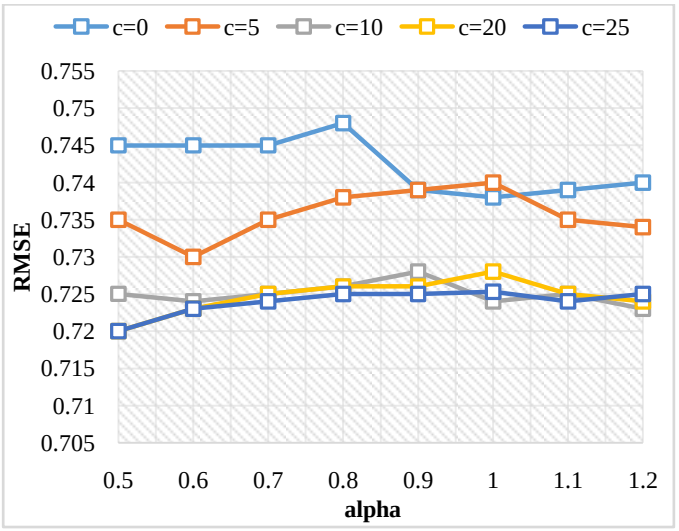

Fig 7. RMSE for canon G3

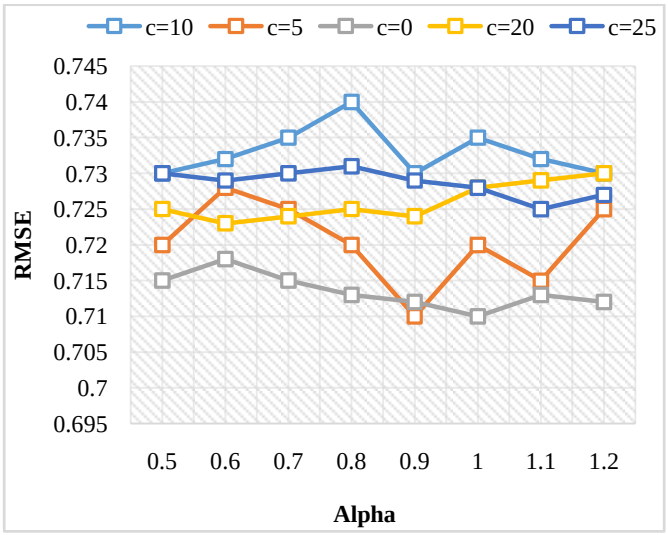

Fig 8. RMSE for Nokia 6610 dataset

E. *Mean Absolute Error (MAE)*

The MAE is also an important measure that is widely used in many model evaluation applications. It obtains the total error by summing the magnitudes of the errors and dividing the total error. The MAE is calculated as follows:

$$MAE = \frac{1}{n}\sum_{i=1}^{n} |e_i| \qquad (3)$$

Where, the n represents the number of samples of model error e_i. Fig 9 shows the MAE of both existing [16] and proposed techniques, where the x-axis represents the k values and the y-axis represents the MAE. In this graph, the value of k represents the size of the matrix. The existing techniques

considered in this analysis are, IbCF and ClubCF. The IbCF is defines the item based collaborative filtering technique that is mainly used for filtering based clustering data. The ClubCF is an extension of IbCF that collaboratively recommends the services by finding the similar services in the same cluster. In this algorithm, the large data is segregated into manageable parts by performing the clustering process. Moreover, each cluster contains some similar services like a club. From the analysis, it is observed that the proposed RCUHP-SM provides the minimized error value, when compared to the other techniques.

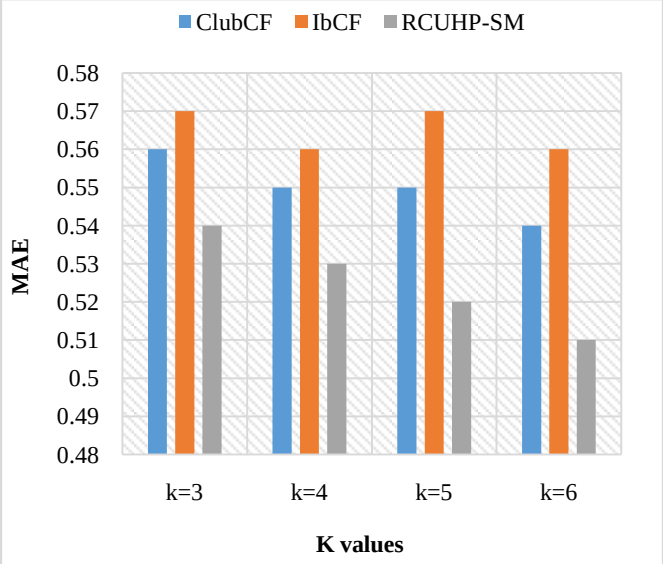

Fig 9. MAE of existing and proposed techniques

V. Conclusion and Future Work

This paper proposed a RCUHP-SM technique for uncovering the hidden patterns from social media. Here, the customer reviewer dataset is used to validate the proposed pattern mining system. The data preprocessing performed on the dataset by eliminating the unwanted attributes. In this stage, the procedures that include special characters removal, unwanted spaces removal, stemming, stop words removal and Parts of Speech (POS) tagging are applied for preprocessing data. The descriptive sentence extraction and its score calculation are performed based on the tagged words. Moreover, a set of rules are formed to categorize the review as positive, negative and neutral. Furthermore, the cluster is formed based on the obtained threshold value. In the analysis module, the feature extraction and score computation processes are performed for the recommendation. The major advantages of this paper are, easy to implement, minimized error value, highly efficient and low cost. In experiments, the performance of the proposed mining technique is evaluated in AP, MAE and RMSE measures. re compared with the existing r proving the superiority of the s analysis, it is analyzed that the es the best results compared than

In future, this work will be enhanced by implementing the proposed technique in observing and understanding phases.

REFERENCES

[1] B. C. Fung, *et al.*, "Anonymizing Social Network Data for Maximal Frequent-Sharing Pattern Mining," in *Recommendation and Search in Social Networks*, ed: Springer, 2015, pp. 77-100.

[2] G. Bello-Orgaz, *et al.*, "Social big data: Recent achievements and new challenges," *Information Fusion*, vol. 28, pp. 45-59, 2016.

[3] C. Liu, *et al.*, "Temporal skeletonization on sequential data: patterns, categorization, and visualization," *IEEE Transactions on Knowledge and Data Engineering*, vol. 28, pp. 211-223, 2016.

[4] M. Injadat, *et al.*, "Data mining techniques in social media: A survey," *Neurocomputing*, vol. 214, pp. 654-670, 2016.

[5] S. Qiao, *et al.*, "A self-adaptive parameter selection trajectory prediction approach via hidden Markov models," *IEEE Transactions on Intelligent Transportation Systems*, vol. 16, pp. 284-296, 2015.

[6] D. J. Peuquet, *et al.*, "A method for discovery and analysis of temporal patterns in complex event data," *International Journal of Geographical Information Science*, vol. 29, pp. 1588-1611, 2015.

[7] L. Zhang and B. Liu, "Aspect and entity extraction for opinion mining," in *Data mining and knowledge discovery for big data*, ed: Springer, 2014, pp. 1-40.

[8] K. Khan, *et al.*, "Mining opinion components from unstructured reviews: A review," *Journal of King Saud University-Computer and Information Sciences*, vol. 26, pp. 258-275, 2014.

[9] M. Anjaria and R. M. R. Guddeti, "Influence factor based opinion mining of Twitter data using supervised learning," in *2014 Sixth International Conference on Communication Systems and Networks (COMSNETS)*, 2014, pp. 1-8.

[10] J. P. Verma, *et al.*, "Big data analysis: recommendation system with Hadoop framework," in *Computational Intelligence & Communication Technology (CICT), 2015 IEEE International Conference on*, 2015, pp. 92-97.

[11] J. Bao, *et al.*, "Recommendations in location-based social networks: a survey," *Geoinformatica*, vol. 19, pp. 525-565, 2015.

[12] J. Lyons, *et al.*, "Advancing the accuracy of protein fold recognition by utilizing profiles from hidden Markov models," *IEEE transactions on nanobioscience*, vol. 14, pp. 761-772, 2015.

[13] M. D. Ruiz, *et al.*, "Discovering Fuzzy Exception and Anomalous Rules," *IEEE Transactions on Fuzzy Systems*, vol. 24, pp. 930-944, 2016.

[14] Q. Song, *et al.*, "A fast clustering-based feature subset selection algorithm for high-dimensional data," *IEEE Transactions on Knowledge and Data Engineering*, vol. 25, pp. 1-14, 2013.

[15] Z. Lu, *et al.*, "A new algorithm for inferring user search goals with feedback sessions," *IEEE Transactions on Knowledge and Data Engineering*, vol. 25, pp. 502-513, 2013.

[16] R. Hu, *et al.*, "ClubCF: A Clustering-Based Collaborative Filtering Approach for Big Data Application," *IEEE Transactions on Emerging Topics in Computing*, vol. 2, pp. 302-313, 2014.

[17] P. B. Pimpale and R. N. Patel, "Experiments with POS Tagging Code-mixed Indian Social Media Text," *arXiv preprint arXiv:1610.09799*, 2016.

[18] S. D. Pandya and P. V. Virparia, "Comparing the application of classification and association rule mining techniques of data mining in an Indian university to uncover hidden patterns," in *Intelligent Systems and Signal Processing (ISSP), 2013 International Conference on*, 2013, pp. 361-364.

[19] A. Karami, *et al.*, "A fuzzy approach model for uncovering hidden latent semantic structure in medical text collections," *iConference 2015 Proceedings*, 2015.

[20] A. Bellogín, *et al.*, "An empirical comparison of social, collaborative filtering, and hybrid recommenders," *ACM Transactions on Intelligent Systems and Technology (TIST)*, vol. 4, p. 14, 2013.

[21] T. C. Havens, *et al.*, "Fuzzy c-means algorithms for very large data," *IEEE Transactions on Fuzzy Systems*, vol. 20, pp. 1130-1146, 2012.

[22] G. Thilagavathi, *et al.*, "A survey on efficient hierarchical algorithm used in clustering," in *International Journal of Engineering Research and Technology*, 2013.

[23] J. Wu, *et al.*, "Predicting quality of service for selection by neighborhood-based collaborative filtering," *IEEE Transactions on Systems, Man, and Cybernetics: Systems*, vol. 43, pp. 428-439, 2013.

[24] X. Li and T. Murata, "Using multidimensional clustering based collaborative filtering approach improving recommendation diversity," in *Web Intelligence and Intelligent Agent Technology (WI-IAT), 2012 IEEE/WIC/ACM International Conferences on*, 2012, pp. 169-174.

[25] M. C. Pham, *et al.*, "A Clustering Approach for Collaborative Filtering Recommendation Using Social Network Analysis," *Journal of Universal Computer Science*, vol. 17, pp. 583-604, 2011.

[26] S. Renaud-Deputter, *et al.*, "Combining collaborative filtering and clustering for implicit recommender system," in *Advanced Information Networking and Applications (AINA), 2013 IEEE 27th International Conference on*, 2013, pp. 748-755.

[27] Y. Vyas, *et al.*, "POS Tagging of English-Hindi Code-Mixed Social Media Content," in *EMNLP*, 2014, pp. 974-979.

[28] 'A similarity measure for text ıstering," *IEEE Transactions on ı Engineering*, vol. 26, pp. 1575-

al., "Improving the accuracy of ing recommendations using

clustering and association rules mining on implicit data," *Computers in Human Behavior*, vol. 67, pp. 113-128, 2017.

[30] G. Lee and U. Yun, "A new efficient approach for mining uncertain frequent patterns using minimum data structure without false positives," *Future Generation Computer Systems*, vol. 68, pp. 89-110, 2017.

[31] (2004). *Opinion Mining, Sentiment Analysis, and Opinion Spam Detection*. Available: https://www.cs.uic.edu/~liub/FBS/sentiment-analysis.html

[32] J.-Y. Chen and H.-H. He, "A fast density-based data stream clustering algorithm with cluster centers self-determined for mixed data," *Information Sciences*, vol. 345, pp. 271-293, 2016.

[33] H. Lu, *et al.*, "Social recommendation via multi-view user preference learning," *Neurocomputing*, vol. 216, pp. 61-71, 2016.

CLUSTER COMPUTING

Submissions with an Editorial Office Decision for Author T Kumarakurubaran

Page: 1 of 1 (1 total completed submissions) Display 10 results per page.

Action	Manuscript Number	Title	Initial Date Submitted	Status Date	Current Status	Date Final Disposition Set	Final Disposition
Action Links	CLUS-D-18-00882	RCUHP-SM: A RULES GENERATION AND CLUSTERING BASED UNCOVERING HIDDEN PATTERNS IN SOCIAL MEDIA	22 Feb 2018	21 Mar 2018	Accept		

Page: 1 of 1 (1 total completed submissions) Display 10 results per page.

<< Author Main Menu

You should use the free Adobe Reader 10 or later for best PDF Viewing results.

Get ADOBE READER

TRUE COPY ATTESTED

PRINCIPAL
MOHAMED SATHAK ENGINEERING COLLEGE
KILAKARAI-623806.

Novel power reduction framework for enhancing cloud computing by integrated GSNN scheduling method

R. Karthikeyan & P. Chitra

Cluster Computing
The Journal of Networks, Software Tools and Applications

ISSN 1386-7857

Cluster Comput
DOI 10.1007/s10586-017-0889-1

Springer

Cluster Comput
DOI 10.1007/s10586-017-0889-1

Novel power reduction framework for enhancing cloud computing by integrated GSNN scheduling method

R. Karthikeyan[1] · **P. Chitra**[2]

Received: 28 February 2017 / Revised: 6 April 2017 / Accepted: 27 April 2017

Abstract Popularity of cloud computing is being increased drastically by the use of people all over the world in their comfort zone. For the purpose of withholding the performance of cloud, it is significant to design an efficient scheduling methodology. Researches have designed methods like directed acyclic graph, MinES, MinCS, ant colony optimization, cross-entropy stochastic scheduling, interlacing peak scheduling method, etc for enhancing cloud and user experience. The major problem existed in these methods was higher execution time, overload issues and higher power consumption. To overwhelm the problems, we design a novel framework that is comprised with queue manager (QM), scheduler (SH), virtual machine manager (VMMA), VM allocator (VMA) and VM power manager (VMP). Firstly, in QM the incoming tasks are split into two queues based on task's deadline, they are represented as urgent queue (UQ) and waiting queue (WQ). Secondly, we perform hybrid scheduling which combines grey system and neural network (GSNN) that considers three significant parameters as task length, CPU intensive and memory intensive. This GSNN scheduling is enabled to withstand effectively even for '*N*' number of tasks and that leads to minimization of execution time. Then thirdly, each task is allocated to corresponding VM with respect to the capacity and workload of VM. Finally VMP keeps updating the VM information for computing the underutilized hosts then it performs VM migration to put up the idle host to OFF state, for reducing the unwanted power consumption. Simulation results of our entire framework shows improvements when compared with state-of-the-art methods.

Keywords Cloud computing · VM scheduling · Power consumption · Neural network · Queue · Execution time

✉ R. Karthikeyan
karthikeyancse77@gmail.com

; College, Ramanathapuram,

ıeering, Madurai, Tamilnadu,

1 Introduction

Cloud computing have become ubiquitous by the use of enormous people all over the world. Cloud is highly preferred due to its accessibility, scalability, availability and high performance. To maintain all these positive aspects in cloud it is significant to concentrate over the challenges existing in it. Scheduling is one of the major challenging function to be performed. Scheduling was performed on the basis of metaheuristic algorithms, energy aware scheduling, QoS based scheduling, multi-objective scheduling, resource based scheduling, etc. [1–10,27]. Metaheuristic scheduling algorithms were more widely used for scheduling the tasks [1,7]. Metaheuristic Scheduling algorithms involves with representation, transition, evaluation and determination. Those algorithms are listed as, genetic algorithm (GA), ant colony optimization (ACO), particle swarm optimization (PSO), firefly algorithm (FFA) and hybrid metaheuristic algorithm. FFA is performed with the computation of attractiveness which is directly proportional to the brightness, and then in turn the brightness is inversely proportional to distance [7].

Metaheuristic algorithms involves with certain representations as visual representation, image representation and word representation [12–14]. Word representation is about vector space models for different languages [13], and then kernel in SVM is also used for representation [14]. Cuckoo search algorithm and simulate Annealing consumes larger time and cost when compared with firefly algorithm which is presented

in their experimental results with some performance metrics. This increases time complexity so the tasks take up time. Scheduling based on energy efficient algorithms was also researched in [2,5]. Each algorithm designed has their own merits also. Authors of paper [2] designed two approximation greedy heuristic algorithms they are minimum energy virtual machine scheduling algorithm (MinES) and minimum communication virtual machine scheduling algorithm (MinCS). Here MinES avoids working of additional servers, by positioning the available VMs. Then total energy consumption is reduced by MinCS. Both MinCS and MinES perform separate computation. MinES deals with the computation of required bandwidth for VM and cost of the VM. This MinES is little complex in computation. In this work the communication takes place only between the VMs present in the same tenant. MinCS scheduling is performed in VM by means of rack by rack manner. This computes the total capacity of the rack and aggregates the requirement. But it requires separate mechanism to manage tenants.

Zhu et al. in their proposal [9], they developed a novel energy aware scheduling scheme which is based on rolling horizon (EARH). This scheme involves with two strategies resource scaling up and scaling down. The scheduler keep on checking system status such as remaining running time, active number of hosts, VMs deployments, start time of task, etc,. Based on the rolling-horizon the tasks are sorted by their deadlines. With the deadline the tasks are allocated to VM if available, if VM is not available then it adds a VM for starting a new task. All the decision of the rolling-horizon is updated by the scheduler. On updating the tasks they are dispatched to VM for processing. Hereby this reduces the energy consumption.

DVFS-enabled energy-efficient workflow task scheduling (DEWTS) algorithm was designed for reducing the power consumption [8]. This scheduling algorithm starts with the construction of DAG for the input tasks. Then the scheduled tasks are thrown into processors and calculate makespan value. DEWTS algorithm involves with processing on three phases such as initial task mapping phase, processor merging phase and task drawing phase. The processors without any jobs are shut downed. In processor merging phase the processors are sorted and arranged in descending order. Based on the task execution time each processor is split into time slots in Time Slacking Phase. But the construction of directed acyclic graph has to be constructed each time and hence it increases the execution time.

Cloud-based workflow scheduling (CWSA) policy was designed for the application of multi-tenant computing environment [3]. As per using multi-tenancy the complexity [illegible] involvements of major compo-
her, service queue, workflow
ol, tenant information and per-
of service (QoS) monitoring
and executor. Here the QoS component helps to monitor the QoS parameters and improves the performance. Energy efficient algorithms are of data center energy-efficient network aware scheduling (DENS), DVFS, e-STAB and adaptive energy-efficient scheduling algorithm [5]. On the basis of the resources the scheduling was performed by modified ant colony optimization [4]. This was designed for reducing the delay in resource allocation for tasks. The input attributes are aggregated for evaluating to obtain the best solution. Based on the procedure of Pheromone the attributes are updated. This is performed for allocation of resources for tasks.

Multi-objective based task scheduling was also concentrated by many authors [3,6,15,16]. In [6] by using QoS based multi-objective task scheduling algorithm the throughput is improved. Multi-Objective task scheduling methods will consider more than a single parameter for retrieving effective scheduling results. Here the value of QoS is assigned for each task and then two objective functions are defined one is based on the size of the task and the other is QoS value of the task. But throughput is not the only constraint that is present in QoS. Multi-objective ACO was presented in [17] which involves with the choice of the behavior. Here multi-objective involves with the task deadline, budget costs and number of resources. Further evaluate fitness values and then update the values of pheromone. Ant colony optimization is combined with cuckoo search algorithm and forms a Hybrid algorithm for reducing the energy consumption in cloud [18].

First ACO algorithm is performed and then cuckoo search algorithm is followed. In cuckoo search algorithm the host's nests are fixed and the probability of the laid bird is found by the cuckoo bird. Here the resources are searched and then allocated to different jobs, hence the resource searching should be performed quicker and so the jobs are allocated in time. But the cuckoo search algorithm consumes more execution time. All these algorithms was popularly used for task scheduling in cloud which was based on energy efficiency, QoS, multi-objective scheduling, and meta-heuristic scheduling algorithms. Scheduling is also involved in global navigation satellite systems [19–21]. Scheduling in [19] was performed in global navigation satellite systems-satellites by taking in account of capabilities of individuals as slewing rates, antenna sensitivity, etc,. Then decomposition and integration based method was proposed for the many-objective ground station problem [20]. In decomposition step the plan horizon is divided into periods and time windows into atomic tasks. Atomic tasks are planned for each period in planning stage then splicing operation is performed in integration stage. This process is simpler and computationally easy.

We handle all the problems existed in previous works and this paper work proves that it diminishes the power consumption by effective allocation of VMs periodically in the hosts. We also majorly concentrate on scheduling the tasks within a

short period of time and hereby we reduce the execution time and successfully improve the resource utilization among the tasks. Let's have a view on all our major proposal of this paper. The major contribution of our proposed work is well-defined as follows,

- Dividing the queue based on deadline of tasks, in which shorter deadline tasks are given higher priority for scheduling
- GSNN scheduling method is used to tolerate with 'N' number of tasks and reduces execution time
- Then VMA assigns each task with VMs, based on the capacity and Workload of the VM
- VMP shuts down the host and VM that are in idle state and if a single VM in host is performing task then that VM is migrated to another host
- Finally we analyze our work with the performance metrics and hence our proposed work reduces execution time and power consumption and performs effective scheduling

This paper is organized into following sections as, Sect. 2 deals with state-of-the art concepts, then Sect. 3 summarizes the problems existed in previous works, in Sect. 4 we illustrate the detailed description of our proposed work, and then Sect. 5 is completely about the experimental analysis and finally in Sect. 6 we consolidate with conclusion of this paper work. This complete paper gives a novel framework design which achieves the entire goal in cloud computing.

2 Literature review

Quality of service was a major concept involved in task scheduling for obtaining better results in the basis of satisfying the user and improving the overall performance of cloud [3,6,15]. Authors of [15] developed a QoS model (i.e.) cross-entropy based stochastic scheduling (CESS) algorithm to optimize the QoS and execution time. The entire system is modeled as M/M/1 system in which the cloud datacenter's Services follows first come first serve (FCFS). This FCFS increases the waiting time of jobs that are present in the queue. QoS model is designed with the QoS requirements like availability, timeliness, security and then reliability. But here the particular QoS parameter is not specified. This model is completely complex in computations and hence it increases the execution time as well.

Power consumption was focused in the constraints as CPU utilization, I/O utilization and memory utilization [22,23].] they proposed a method for g peak scheduling method. In like CPU, I/O and memory usage of resources are collected and updated periodically. In this method tasks are separated into three queues with the CPU intensive, I/O intensive and Memory intensive. Based on these three queues their demands over the resources are defined and scheduled. Here the computation complexity is highly reduced. Interlacing peak scheduling method organizes resource queues from smaller to larger in CPU utilization, I/O usage and Memory Usage. But here it seems that the smaller resources utilization tasks have to be stayed for a longer time in the queue and hence the shorter utilization tasks increases the waiting time.

Resources based scheduling was addressed by Fan et al. [24]. The base layer model, metal layer model, meta-object protocol and other components are built by Petri nets. This entire resource scheduling strategy was proposed to improve the reliability within the deadline. The waiting time and the execution time of tasks increase when using directed acyclic graph [8,25]. Yao et al. proposed directed acyclic graph for task model which involves task critical degree, task reminder, task execution time and average communication time [25]. This task model deigns a DAG with the total number of tasks. Then priority is computed with the above mentioned constraints. It follows FCFS process in processing the tasks. Finally the time taken for the formation of DAG along with the different constraints is larger. Hence reducing the waiting time and execution time remains as a major challenging work.

But in case of most of the multi-objective task scheduling the time consumption is higher. In [16] particle swarm optimization (PSO)-based adaptive multi-objective task scheduling (AMTS) was proposed. This was designed for optimal resource utilization, task completion time, average cost and average energy consumption. Here each task is split into subtasks, due to this the process is performed faster but recombining the tasks divided remains challenging. Real time tasks scheduling in virtualized cloud is designed by different concepts in [9,26]. One is based on the concept of reduction of energy consumption [9] and the other is focused for reducing the execution time [26].

In [26] agent based dynamic scheduling algorithm was proposed (ANGEL). This algorithms works by bidirectional announcement bidding mechanism, which is capable to perform two phases, one is forward announcement-bidding phase and other is backward announcement-bidding phase. This algorithm is performed among three agents, they are VM agent set, task agent set and manager agent set. The forward bidding values are computed by VM agent set and provided to task agent set, then the backward bidding values are computed by task agent set and provide to VM agent set. Both forward and backward bidding announcement is applicable and so this is named as bidirectional announcement bidding mechanism. Here scheduling is performed with little time delay, since based on the agents bidding the bidding values are calculated and again they are intimated, then only

Fig. 1 System architecture

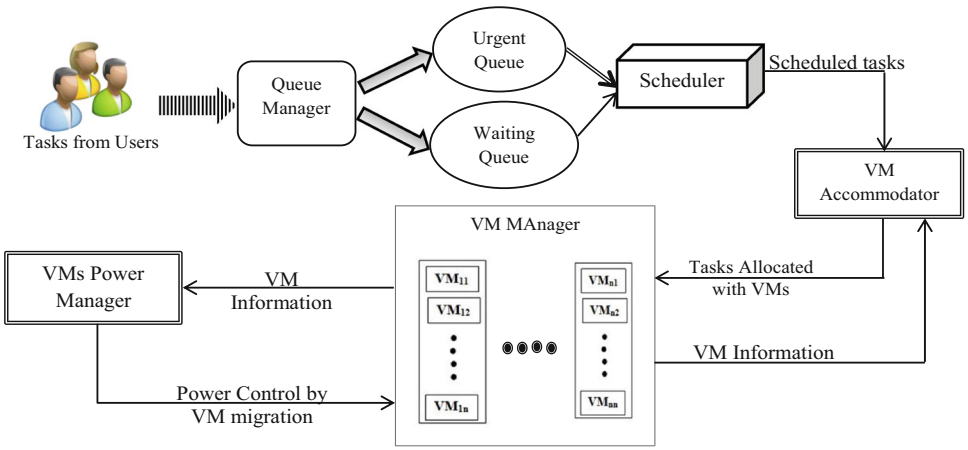

the tasks are processed. Zhu et al. was focused on in cloud scheduling by the design of evolutionary multi-objective (EMO) optimization algorithm [10]. This algorithm includes basic genetic operators as encoding, evaluation function, crossover, mutation and population initialization. Genetic algorithm based chaotic ant swarm (GA-CAS) algorithm was introduced for solving multi-objective optimization problem 27. The main objective of this algorithm was to minimize the makespan and flow time. Here also genetic algorithm's operations are performed, with additional computations of distances, optimal path and storage positions and cost is involved.

On the whole, most of the state-of-the-art methods and algorithms were focused on reducing the energy consumption and execution time. It is little challenging to reduce both the above mentioned constraints. Hereby we propose this paper work with these improvements.

3 Problem formulation

Scheduling tasks in cloud is the most significant process which is to be performed for satisfying the number of users arrived. Scheduling was concentrated by many researchers and they have introduced various mechanisms for task scheduling. Energy consumption was the major constraint which is to be reduced, since the processing of higher number of VMs consumes higher amount of energy. In [2] authors have introduced greedy approximation algorithms MinCS and MinES. MinCS scheduling of VMs is performed one by one, each time a VM is allocated. By executing step by step VM allocation, it consumes higher energy for iteration. Due to this the energy consumption is higher. Then in MinES also the scheduling is performed one by one for reducing the

the tasks have to wait for longer ends to consume higher energy.)AG based scheduling [8] and ısumes more time for construction of DAG each time based on the arrival of tasks. Further in [22] the tasks are scheduled based on the resources by forming three queues as formulated below,

$$
\begin{aligned}
Q_C &= \{U_1, U_2, \ldots, U_{iC}, \ldots, U_N\} \\
Q_O &= \{U_1, U_2, \ldots, U_{iO}, \ldots, U_N\} \\
Q_M &= \{U_1, U_2, \ldots, U_{iM}, \ldots, U_N\}
\end{aligned} \tag{1}
$$

4 System model

The proposed system model is designed for scheduling the tasks effectively by reducing its execution time and energy consumption and thereby we improve the resource utilization. We propose a novel framework in which the process is initiated with queue management where the incoming tasks are split into two queues based on their deadlines. Then the tasks are moved to scheduler, and then the scheduled tasks are allocated with VMs. Grey system with neural network based scheduling is performed by considering three constraints [27]. Further the scheduled tasks are allocated with VMs.

Figure 1 implies the overall architecture of our proposed work which includes the components like scheduler, VM allocator, VM manager and power manager. In our work the VM information is updated to both VMA and VMP. With this VM information VMA allocates VMs for tasks and VMP controls the power consumption. By this we effectively allocate tasks and the power consumption is also reduced. The entire proposed work is elaborated in the following subsections.

4.1 Queue manager

Queue manager (QM) is responsible for maintaining the queues properly. All the incoming tasks at time't'are aggregated by QM and then they are divided into urgent queue and waiting queue with respect to the deadlines. Deadline of

the tasks are defined as $D_i = d_1, d_2, d_3 \ldots$, with these time period for each task the queue is divided into two. Tasks in UQ consist of low deadlines, whereas in WQ the tasks considered are of higher deadlines. With these Queues the tasks are scheduled by GSNN.

Pseudo Code for Queue Management

Input – Users Tasks
Output – UQ and WQ

1. Begin
2. QM⟵Tasks $\boldsymbol{T = T_1, T_2, \ldots T_N}$
3. Tasks$\{\boldsymbol{T_1, T_2, \ldots T_N}\}$ = Deadline $\{\boldsymbol{d_1, d_2, \ldots, d_N}\}$
4. If
   {
   $\boldsymbol{T(D_i) = Min}$
   }
   Put the task in **UQ**
   Else
   Put the task in **WQ**
5. End if
6. End

This pseudo code implies the simple queue management steps. As mentioned in the pseudo code, each task is comprised with unique deadline. The deadline of the tasks is based on the task length that is user defined. If a number of 'N' tasks are arrived at queue manager, it evaluates the deadline of each task and then the task's with minimum deadline enters UQ and other tasks into WQ. UQ tasks are provided higher priority than the tasks in WQ. When the deadline of tasks in WQ reduces then they move into UQ for scheduling process. After dividing the tasks into their corresponding queues they are continued for scheduling process.

4.2 Scheduler

Tasks from the 'UQ', $UQ = \{T_1, T_2, \ldots T_N\}$ are moved towards the scheduler for scheduling the tasks. Each task consists of their corresponding task length; the task length is represented as $T_{len} = S_i, S_j, \ldots S_N$ the task with minimum length is define as,

$$Min\ f\ (T_{len}) = T_{len} | \forall j,\ f\ (S_i) \leq f\ \left(S_j\right) \tag{2}$$

With equation (2) the minimum task length of the incoming tasks in time 't' is determined. Then the each task with lower ure considered.
$2, \ldots T_N\}$, ratios are calculated esources [22]. The ratio is rep-

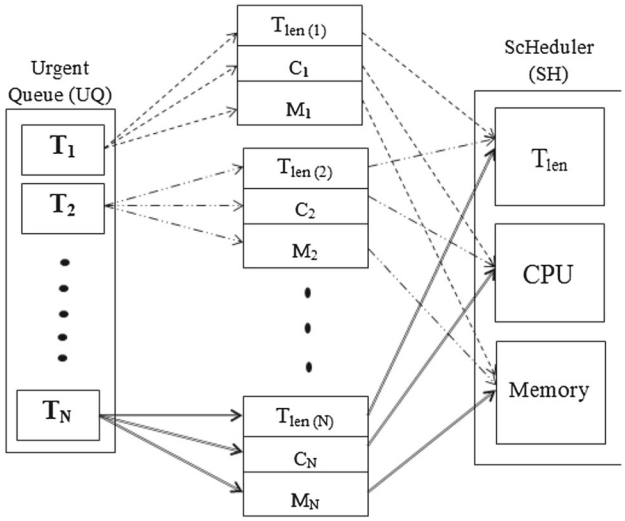

Fig. 2 Scheduling of tasks in UQ

$$UQ = \max\ (C, M) = \max\left(\frac{C_1}{C_S}, \frac{M_1}{M_S}\right) \tag{3}$$

We consider the CPU intensive as 'a', I/O intensive as 'b' and Memory intensive as '$K - a - b$'. Here we have mentioned I/O intensive for the purpose of evaluating Memory Intensive. The task categories of CPU intensive and memory intensive are estimated as follows,

$$CPU_{Ti} = \left\{T_1, T_2, \ldots, T_{UQ(CPU)}, \ldots, T_a\right\} \tag{4}$$

$$MM_{Ti} = \left\{T_{a+b+1}, T_{a+b+2}, \ldots, T_{UQ(MM)}, \ldots T_{K-a-b}\right\} \tag{5}$$

CPU utilization is defined as the usage of processors inside the physical host. This would indicate the processor capacity being used in an operating system. All the three parameters are estimated by using (2), (4) and (5). With these computation of each task is applied to the scheduler. Then the scheduler schedules the tasks and then the tasks are moved to VM Allocator.

Figure 2 illustrates the tasks in UQ are scheduled with respect to the three parameters. A novel method for scheduling is used which combines grey system with neural network (GSNN). This combination is made to perform scheduling for 'N' number of users. In general the grey system is modeled as '$GM\ (n,m)$' . In this representation 'n' implies the order of differential equations and 'm' implies the number of variables. This system is applicable to compute (N+1)th report. We consider three parameters for scheduling the tasks. The parameters taken in account are task length, CPU intensive and memory intensive.

The mathematical computation of our proposed grey system model is as follows. Initially the original array of the input parameters is given as,

$$X_i^{(0)} = \left\{ x_i^{(0)}(1), x_i^{(0)}(2), \ldots\ldots\ldots\ldots x_i^{(0)}(N) \right\} i = 1, 2, 3 \tag{6}$$

It implies that $X_i^{(1)}$ is the first order accumulated generating operation (AGO) of $X_i^{(0)}$, then their corresponding relationship is defined as,

$$x_i^{(1)}(k) = \sum_{j=1}^{k} x_i^{(0)}(j)\ j = 1, 2, \ldots . N \tag{7}$$

Further the value of first order AGO can be estimated with the input parameters as follows,

$$X_i^{(1)} = \left\{ x_i^{(1)}(1), x_i^{(1)}(2), \ldots\ldots\ldots\ldots x_i^{(1)}(N) \right\} i = 1, 2, 3 \tag{8}$$

Then the first order differential equation for set of GM (1, N) is described below,

$$\begin{aligned}
\frac{dX_1^{(1)}}{dt} &= a_{11}X_1^{(1)} + a_{12}X_2^{(1)} + a_{13}X_3^{(1)} + B_1 \\
\frac{dX_2^{(1)}}{dt} &= a_{21}X_1^{(1)} + a_{22}X_2^{(1)} + a_{23}X_3^{(1)} + B_2 \\
&\vdots \qquad\qquad\qquad\quad \vdots \\
&\vdots \qquad\qquad\qquad\quad \vdots \\
\frac{dX_N^{(1)}}{dt} &= a_{N1}X_1^{(1)} + a_{N2}X_2^{(1)} + a_{N3}X_3^{(1)} + B_N
\end{aligned} \tag{9}$$

where $B_i = \{b_i, b_i, \ldots\ldots, b_i\}$ is $1 \times$ N vector
i = 1,2,3.

Now we transform these differential equations set in equation (9) into a matrix form represented as equation (10) below,

$$\frac{dx_i^{(1)}(k)}{dt} = \left(x_i^{(1)}(k) - x_i^{(1)}(k-1) \right) \tag{10}$$

The matrix form is obtained in the equation below which consists of three components,

$$\begin{bmatrix} X_1^{(0)} \\ X_2^{(0)} \\ \vdots \\ X_N^{(0)} \end{bmatrix} = \begin{bmatrix} a_{11}, & a_{12}, & \cdots a_{1N} \\ a_{21}, & a_{22}, & \cdots a_{2N} \\ & \vdots & \\ a_{N1}, & a_{N2}, & \cdots a_{NN} \end{bmatrix} \begin{bmatrix} X_1^{(1)} \\ X_2^{(1)} \\ \vdots \\ X_N^{(1)} \end{bmatrix} + \begin{bmatrix} b_1, & b_1, & \cdots\cdots b_1 \\ b_2, & b_2, & \cdots\cdots b_2 \\ \vdots & \vdots & \vdots \\ b_N, & b_N, & \cdots\cdots b_N \end{bmatrix} \tag{11}$$

Now we expand the matrix from the matric form represented above (11),

$$\begin{bmatrix} x_1^{(0)}(2), x_2^{(0)}(2), x_3^{(0)}(2) \\ x_1^{(0)}(3), x_2^{(0)}(3), x_3^{(0)}(3) \\ \vdots \\ x_1^{(0)}(N), x_2^{(0)}(N), x_3^{(0)}(N) \end{bmatrix} = \begin{bmatrix} x_1^{(1)}(2), x_2^{(1)}(2), x_3^{(1)}(2), 1 \\ x_1^{(1)}(3), x_2^{(1)}(3), x_3^{(1)}(3), 1 \\ \vdots \\ x_1^{(1)}(N), x_2^{(1)}(N), x_3^{(1)}(N) \end{bmatrix} \times \begin{bmatrix} a_{11} & a_{21} & a_{N1} \\ a_{12} & a_{22} & a_{N2} \\ a_{13} & a_{23} & a_{N3} \\ b_1 & b_2 & b_N \end{bmatrix} \tag{12}$$

For accurate prediction we replace $x_i^{(1)}$(k) with the following components,

$$\left(x_i^{(1)}(k-1) + x_i^{(1)}(k) \right)/2$$

Hereby using least square method we find matrix $\hat{A}$ and vector $\hat{B}$ by the following equation,

$$\begin{bmatrix} \hat{A} \\ \hat{B} \end{bmatrix} = \left(U^T U \right)^{-1} U^T Y \tag{13}$$

From equation (13), we determine the parameters '$\hat{A}$' and '$\hat{B}$' for grey model prediction at time 't'. Where the values of each components in equation (13) is given as,

$$J = \begin{bmatrix} \frac{1}{2}\left(x_1^{(1)}(1) + x_1^{(1)}(2) \right), \frac{1}{2}\left(x_2^{(1)}(1) + x_2^{(1)}(2) \right), \ldots, \frac{1}{2}\left(x_N^{(1)}(1) + x_N^{(1)}(2) \right), 1 \\ \frac{1}{2}\left(x_1^{(1)}(2) + x_1^{(1)}(3) \right), \frac{1}{2}\left(x_2^{(1)}(2) + x_2^{(1)}(3) \right), \ldots, \frac{1}{2}\left(x_N^{(1)}(2) + x_N^{(1)}(3) \right), 1 \\ \frac{1}{2}\left(x_1^{(1)}(N-1) + x_1^{(1)}(N) \right), \frac{1}{2}\left(x_2^{(1)}(N-1) + x_2^{(1)}(N) \right), \ldots, \frac{1}{2}\left(x_N^{(1)}(N-1) + x_N^{(1)}(N) \right), 1 \end{bmatrix}$$

$$Y = \begin{bmatrix} x_1^{(0)}(2), x_2^{(0)}(2), x_3^{(0)}(2) \\ x_1^{(0)}(3), x_2^{(0)}(3), x_3^{(0)}(3) \\ \vdots \\ x_1^{(0)}(N), x_2^{(0)}(N), x_3^{(0)}(N) \end{bmatrix}, B^T = \begin{bmatrix} b_1 \\ b_2 \\ \vdots \\ b_N \end{bmatrix}$$

$$A = \begin{bmatrix} a_{11}, a_{21}, \ldots, a_{N1} \\ a_{12}, a_{22}, \ldots, a_{N2} \\ \vdots \\ a_{1N}, a_{2N}, \ldots, a_{NN} \end{bmatrix}$$

The estimated arrays are summarized into,

$$\hat{X}^{(1)}(N+1) = \left[\hat{x}_1^1(N+1), \hat{x}_2^1(N+1), \hat{x}_3^1(N+1)\right]^T \tag{14}$$

Finally with the calculated values in (10) and (11),

$$X^{(1)}(1) = \left[x_1^{(1)}(1), x_2^{(1)}(1), x_3^{(1)}(1)\right]^T \tag{15}$$

$$x_i^{(1)}(1) = x_i^{(0)}(1) \tag{16}$$

Final values are computed as,

$$\hat{X}^{(1)}(N+1) = e^{\hat{A}N} X^{(1)}(1) + \hat{A}^{-1}\left(e^{\hat{A}N} - I\right)\hat{B}^T \tag{17}$$

$$\hat{X}^{(0)}(N+1) = \hat{X}^{(1)}(N+1) - X^{(1)}(N) \tag{18}$$

The incoming $'N'$ numbers of tasks are scheduled and they are organized in an order. The task with minimum task length, CPU intensive and memory intensive is given higher priority for allocation of VM. With this GSNN we schedule the number of incoming tasks.

4.3 VM allocator

VM Allocation is a significant part which assigns the tasks with VM. VM allocation is a challenging task which maps each task to VM with the available resources present in the host machine. VM allocation is focused to improve the effective results of the given tasks within the deadline. In our work we consider 'n' number of hosts with 'N' number of VMs. More than one task can be allocated to a VM. On the whole VMA is in charge for allocating the scheduled tasks in the appropriate VMs. This VMA keeps updating the VM information, which helps the VMA to know about the status of tasks being performed in particular VMs. With this information VMA computes the workload of VM and the capacity to perform a task. With these constraints the tasks [illegible] e capacity of individual VM is

$$\cdot VM_{Bw,x} \tag{19}$$

where 'P_{num}' represents the number of processing elements of VM, 'P_{MIPS}' is the millions Instructions Per Second of the processor and 'VM_{Bw}' is said to be the communication bandwidth ability of VM. VMA calculates capacity of each VM, since with this capacity a task will be allocated to VM. The capacity of each VM varies with respect to the parameters that are involved in equation (20).

Load is the major reason for consuming large amount of power. The load of individual VM is defined by the number of tasks and the service rate of the individual VM.

$$Load_{x,t} = \frac{N(T,t)}{S(VM,t)} \tag{20}$$

With respect to the minimum load and higher capacity of VM, the task with higher priority after scheduling is allocated with VM. In our work the VM with minimum load is assigned for the task with minimum deadline and so the particular task can be completed within the deadline.

Pseudo code for VM Allocator

Input - ST_k
Output – Allocation of each task

1. Begin
2. Scheduled Tasks $\boldsymbol{ST_k} = \{\boldsymbol{T_1}, \boldsymbol{T_2}, \ldots, \boldsymbol{T_N}\}$
3. If
{
$\boldsymbol{T_i(Priority)} > \boldsymbol{T_1}, \boldsymbol{T_2}, \ldots, \boldsymbol{T_N}$
Then
$\boldsymbol{T_i}$ is assigned with VM first
Else
Repeat step 3
}
4. Compute $\boldsymbol{CP_x}$ **and** $\boldsymbol{Load_{VM_x,t}}$
5. If
{
$\boldsymbol{Load_{VM_x,t}} < \boldsymbol{Load_{VM_N,t}}$
$\boldsymbol{CP_x} > \boldsymbol{CP_N}$
}
6. End if
7. Allocate task $\boldsymbol{T_i}$ to VM_j
8. Repeat step 3 – 7 until all tasks are assigned to VMs
9. End

Pseudo code defines the processing steps of VMA by which the scheduled tasks are assigned to VMs. These entire steps are performed one after the other, as we reduce the execution time during scheduling, our VM allocation time is also lesser. In accordance with the load and capacity of VM, we allocate tasks, here the tasks has the possibility to be migrated which means VM Migration.

4.4 VM power manager

Power manager is appointed for the purpose of reducing the amount of power consumption. VMA allocates each task with VMs. We reduced the power by turning off the idle host. If single VM is performing task in a host then that particular VM is migrated to another host. By doing this the host can be put over OFF state until other set of tasks are allocated. The power consumption of a VM is given as,

$$P_{VM_i} = p_{VM_i}^{CPU} + p_{VM_i}^{MM} + p_{VM_i}^{IO} \tag{21}$$

Power utilization of each VM is computed with the utilization of CPU, memory and I/O. For the purpose of scheduling we have considered CPU and memory of the incoming tasks. We reduce power by computing the power of the executing hosts, for identifying the underutilized host presence. The effective value of power is estimated as given below,

$$Pw_j = \frac{p_j}{VM_j} \tag{22}$$

Power exhibited in host 'j' is computed using (22) which include 'p_j' the power consumption at jth host and 'VM_j' that represent the number of VMs running over jth host. With this computation of power consumption the state of the host is predicted. For this prediction we present some of the conditions as follows,

$$S_i(t) = \begin{cases} Switched - Off\ Pw_j(t) = 0 \\ idle\ Pw_j(t) = Pw_{idle}^j \\ underutilized\ Pw_{idle}^j < Pw_j(t) \leq Pw_{min}^j \end{cases} \tag{23}$$

Based on this condition the underutilized host is identified and the VMs in that particular host is migrated to another host and hence the underutilized host is turned off, until the next set of tasks are arrived. Here the power is calculated by VMP, since it updates the VM information from VMMA. VMP Manager plays an important role, which manages the power for the purpose of increasing the effective utilization of cloud computing. If the host is overloaded it may not work properly with the tasks allocated to it. This is the major reason to bring a unique VM power manager which reduces the power consumption by means of VM migration. The reason to turn off the host is to reduce the consumption of unwanted power consumption. We migrate VM performing the tasks only if the host is underutilized. By this the host gets certain amount of time to rest it. This also helps to make host to [illegible] d on.

Pseudo Code for VM migration

Input – VM information
Output – VM migration

1. Begin
2. VMP (VM info) ⟵VMMA
3. Compute PW_j ⟵VMP
   $j=1,2,3,.....,n$
4. If
{
Check condition
$\boldsymbol{Pw_{idle}^j < Pw_j(t) \leq Pw_{min}^j}$
}
Perform VM Migration
Else
Goto step 3
5. End if
6. Repeat step 3 until PW_j is computed for all hosts
7. End

The host to be turned on and off is intimated by VMP to VMMA. Further the VMMA migrates the VM and then turns off that particular host present in the cloud. This is the major reason to migrate VM with VMP manager. By this we achieve our goal in reducing the power consumption. The processing steps of VMP are descripted as pseudo code. Pseudo code illustrates the working of VMP for reducing the power consumption. By this we determine the underutilized host and move the tasks performed by VM to another host and then the particular host if turned off. We perform this computation for the set of tasks arrived at time as T_e={$t,t_1,t_2,t_{3,...}$}. After completely scheduled the UQ then we move on to the tasks present in WQ. By this novel approach our entire work reduces power consumption by identifying the underutilized hosts and GSNN based scheduling reduces the execution time, this is capable to perform with $'N'$ number of tasks.

5 Performance evaluation

This section presents all the outcomes of our experimental results that have been conducted for our proposed framework. Here we evaluate our proposed work with state-of-the-art works. Our main goal is to reduce power consumption and the execution time. This paper proposes a novel GSNN method for scheduling which supports $'N'$ number of tasks. This method reduces the execution time taken for scheduling. In this section we further discuss the parameters used for our simulation and the comparative results which show improvements of our proposed work.

Table 1 Scheduling performed in state-of-the-art and their demerits

State-of-the-art	Demerits
MinCS and MinES algorithms [2]	• Lengthier process • More power consuming
Interlacing peak scheduling method [22]	• Smaller utilization tasks has to wait for longer time
DVFS-enabled energy-efficient workflow task scheduling (DEWTS) algorithm [8]	• Higher execution time • Larger resource utilization
Cross-entropy stochastic scheduling (CESS) algorithm [15]	• Higher execution time

Table 2 Parameters set for our simulation

Entity	Specification	Value/ranges
Data center	Number of data center	10
	Number of host	2–6
Cloudlet (task)	Task length	1000–20,000
	Number of task	50–500
	Average length	50,000
	File size	500
Virtual machine	Memory (RAM)	128–2048
	MIPS	500–2000
	Bandwidth	500–1000
	Number of processing unit	4
	Storage	11 TB

Table 1 list up the previous research works and the demerits that existed. With these demerits we have designed this paper to overcome those demerits. To demonstrate the excellence of our proposed framework, we compare it with the state-of-the-art algorithms as MinCS and MinES algorithm and DVFS-enabled energy-efficient workflow task scheduling (DEWTS) algorithm.

Following Sect. 5.1 illustrates the parameters taken in account for simulation and further in Sect. 5.2 all the comparative results prove the improvements of our proposed work.

5.1 Simulation setup

All the aforementioned working procedures of different components in our framework are evaluated with CloudSim toolkit which is the simulating environment. Our simulation is set with entities as data center, hosts, Virtual Machines and tasks. These entities play major part in improving our entire framework. With all these required entities we perform our proposed framework. All the entities and the specifications shown below.

ired parameters for performing
e numbers of tasks are varied
ated.

5.2 Comparative results

This section demonstrates the superiority performance of our proposed framework. Our framework is majorly designed for reducing the execution time and power consumption. Power Manager is responsible for the reduction of power by identifying the underutilized hosts. We reduce execution time with the novel GSNN scheduling method, which supports '*N*' number of user tasks. As per our framework, execution time, Power consumption and Resource Utilization are considered to be performance metrics. Following sections will show the comparative plots and hereby we prove the superiority of our proposed framework.

5.2.1 Power consumption

Power consumption in cloud consumes power due to the use of CPU, memory, etc. Without these components it is not applicable to run tasks in cloud, which consumes power. The way to use those components in hosts can reduce unnecessary power consumption. Our proposed framework is compared with state-of-the-art work MinCS and MinES [2]. The comparison between MinES and MinCS implies that MinCS consumes higher power than MinES. Power consumption is contrasted based on the time period and the load.

Our framework reduces power by means of using a separate power manager who is capable to reduce unwanted power by shutting down the host. Figure 3 below illustrates the power consumption comparison between the state-of-the-art and our proposed framework.

Figure 3a depicts the comparison between power consumption and time period whereas in Fig. 3b the plot is given between power consumption and load present. Load indicates the number of tasks that are being performed in a host. Our proposed work the energy consumption at medium load and high load is little differing, it means that the energy consumption is greatly reduced.

5.3 Execution time

Here the execution time is defined as the time taken for scheduling the tasks. Based on the designed scheduling methods the tasks are organized into a form. The execution time not only depends on the scheduling method, but also on the number of incoming tasks at the time. In our work the tasks are scheduled and processed within the deadline. In the previous work [8] tasks are constructed into DAG and then they are scheduled, but the construction of DAG at each time '*t*' takes up higher amount of time hence DEWTS algorithm was designed to only save energy even if the tasks increases. Now the comparison of both the DEWTS and our work shows the improvements in execution time.

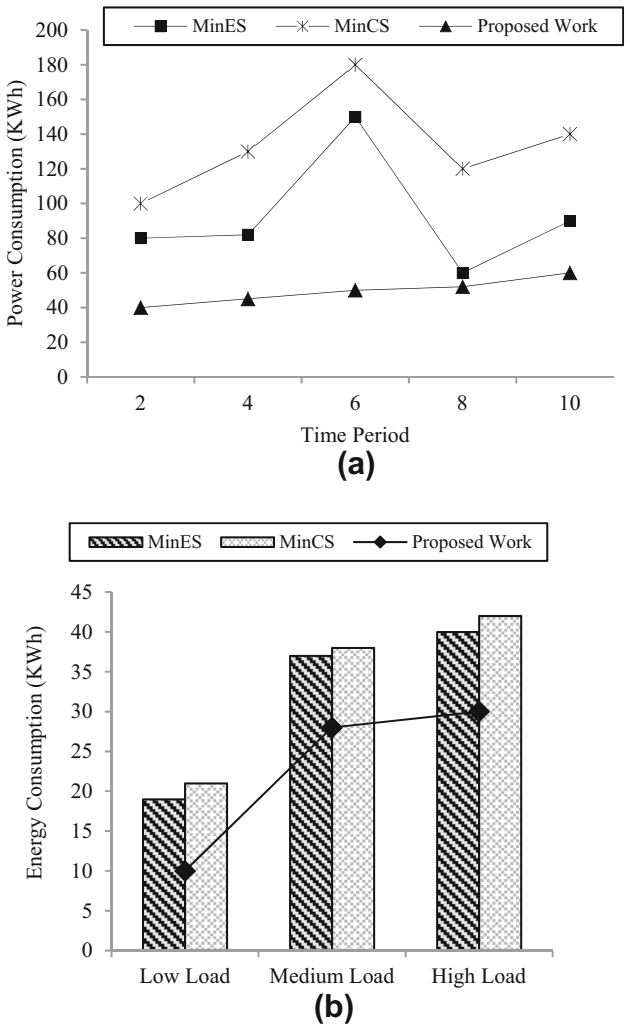

Fig. 3 Comparative results on power consumption

Figure 4 clearly illustrates that scheduling of tasks by the proposed grey system with neural network method which reduces execution time. The average time is estimated by dividing the total execution time with the number of tasks. The number of tasks increases our proposed method does not increases a lot in its execution time. But in the state-of-the-art work the execution time grows linearly as per the increase in the number of tasks. The grey system is combined with neural network for the purpose to withstand with more number of tasks and thereby reduces the execution time when compared with the previous work. On the whole the time complexity measures the amount of time required to execute the methods proposed.

5.3.1 Resource utilization

for each task based on their
ıe task. Resource utilization
› and make use of the required

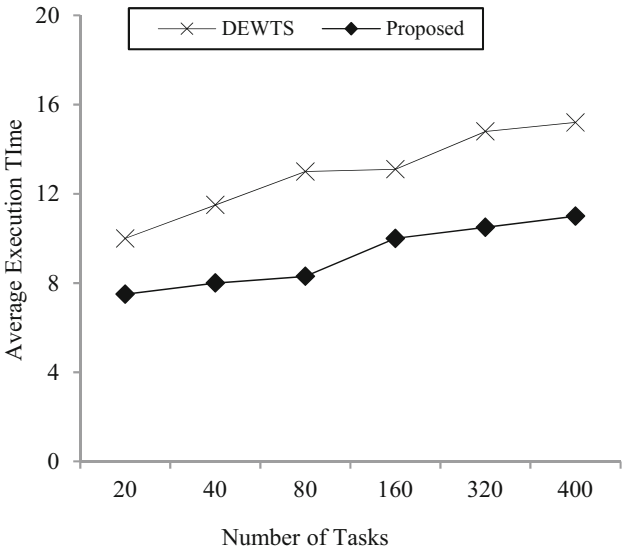

Fig. 4 Evaluating the comparative results for average execution time

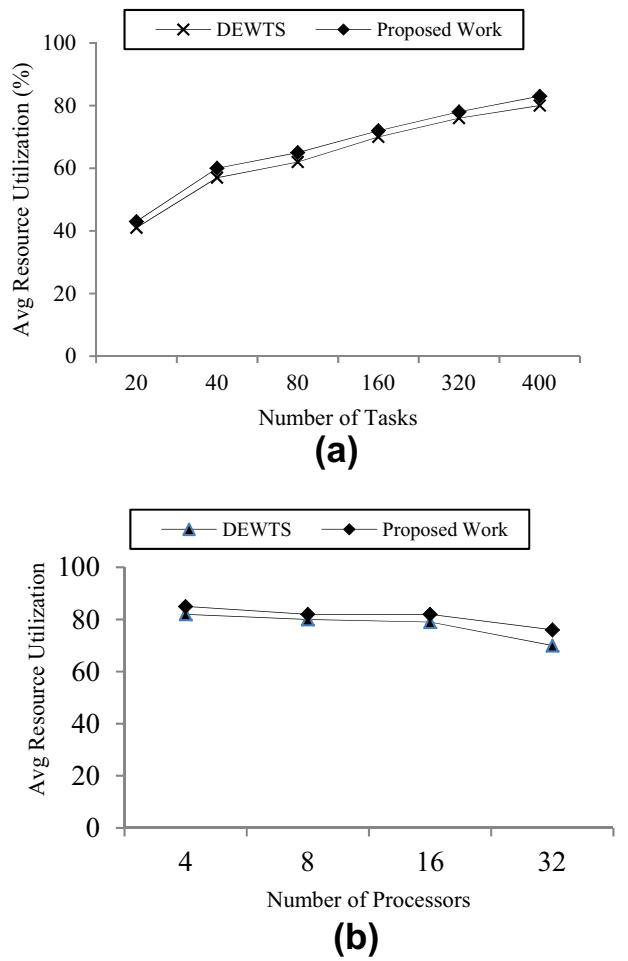

Fig. 5 Experimental evaluation for resource utilization

resources. Resource utilization is compared in two plots with respect to the number of tasks and number of processors used. The resources are said to be the parameters CPU, I/O and memory. Each virtual machine is defined with these parameters, we say$U_i = (CPU_i, IO_i, MM_i)$. Hereby these parameters represent the usage of CPU, I/O waiting time and memory. We illustrate this performance metric in the following plot for resource utilization.

Figure 5 illustrates the comparative experimental results of resource utilization. This plot proves the effective utilization of resources when compared with state-of-the-art. As per this paper work, we have achieved our goal completely with the proposed novel scheduling and power management procedures.

6 Conclusion

Cloud is a well-known worldwide popular environment which involves with the use of huge amount of users for their own purpose. Due to the use of large number of users, scheduling is necessary to be performed for organizing the tasks and to process it in an effective manner. Our proposed framework is designed in such a way to reduce execution time and power consumption hence we have ultimately achieved our goal. Our framework design is initiated with splitting the incoming tasks into two, according to their deadline. Then the proposed novel grey system with neural network scheduling method is capable to schedule 'N' number of tasks, and followed by perfect VM allocation by VMA with the estimated load and capacity. By this scheduling we greatly reduce the execution time and with the help of VMP we perform VM migration for reducing the unwanted power consumption.

In our work the non-working hosts are shut-down and hence when they are switched on again they work actively. This is also a reason to obtain results as early as possible. All the previous works are overcome and our experimental evaluation proves better results with a plot. In future we have planned to consider Resource Utilization as a major constraint for scheduling and improving the utilization of resource.

References

1. Tsai, C.-W., Rodrigues, J.J.P.C.: Metaheuristic scheduling for cloud: a survey. IEEE Syst. J. **8**(1), 1–13 (2013)
2. Dai, X., Wang, J.M., Bensaou, B.: Energy-efficient virtual machines scheduling in multi-tenant data centers. IEEE Trans. Cloud Comput. **4**(2), 1–12 (2015)
3. Bimal, P.P., Major, M.: Workflow scheduling in multi-tenant cloud E Trans. Parallel Distrib. Syst. **28**(1),
4. Benedict, S.: A modified and colony ng cloud resources in manufacturing sector. In: 2nd International Conference on Green High Performance Computing (ICGHPC), IEEE, pp. 1–6 (2016)
5. Atiewi, S., Yussof, S., Ezanee, M., Almiani, M.: A review energy-efficient task scheduling algorithms in cloud computing. In: IEEE Long Island Systems, Applications and Technology Conference (LISAT), pp. 1–6 (2016)
6. Lakra, A.V., Yadav, D.K.: Multi-objective tasks scheduling algorithm for cloud computing throughput optimization. In: International Conference on Intelligent Computing, Communication & Convergence, pp. 107–113. Elsevier (2015)
7. Mandal, T., Acharyya, S.: Optimal task scheduling in cloud computing environments: meta heuristic approaches. In: Proceedings of International Conference on Electrical Information and Communication Technology, pp. 24–28 (2015)
8. Tang, Z., Qi, L., Cheng, Z., Li, K.: An Energy-Efficient Task Scheduling Algorithm in DVFS-enabled Cloud Environment, vol. 14. Springer, New York (2016)
9. Zhu, X., Chen, H., Wang, J., Yin, S., Liu, X.: Real-time tasks oriented energy-aware scheduling in virtualized clouds. IEEE Trans. Cloud Comput. **2**(2), 1–14 (2013)
10. Zhu, Z., Zhang, G., Li, M., Liu, X.: Evolutionary multi-objective workflow scheduling in cloud. IEEE Trans. Parallel Distrib. Syst. **27**(5), 1–14 (2015)
11. Lu, H., Niu, R., Liu, J., Zhu, Z.: A chaotic non-dominated sorting genetic algorithm for the multi-objective automatic test task scheduling problem, Appl. Soft Comput. **13**, 2790–2802 (2013)
12. Luyta, R., Welchb, C., Lobban, R.: Diversity in gender and visual representation: an introduction. J. Gend. Stud. **24**(4), 383–385 (2015)
13. Pennington, J., Socher, R., Manning, C.D.: GloVe: global vectors forword representation. In: Proceedings of the 2014 Conference on Empirical Methods in Natural Language Processing, pp. 1532–1543 (2014)
14. Wang, H., Wang, J.: An effective image representation method using kernel classification. In: IEEE 26th International Conference on Tools with Artificial Intelligence, pp. 383–358 (2014)
15. Chen, Y., Wang, L., Chen, X., Ranjan, R., Zomaya, A.Y., Zhou, Y., Hu, S.: Stochastic workload scheduling for uncoordinated datacenter clouds with multiple QoS constraints. IEEE Trans. Cloud Comput. 1–12 (2016). doi:10.1109/TCC.2016.2586048
16. He, H., Xu, G., Pang, S., Zhao, Z.: AMTS: adaptive multi- objective task scheduling strategy in cloud computing. China Commun. **13**(4), 162–171 (2016)
17. Zuo, L., Shu, L., Zhu, C., Hara, T.: A multi-objective optimization scheduling method based on the ant colony algorithm in cloud computing. IEEE Access **3**, 2687–3699 (2015)
18. Moganarangan, N., Babukarthik, R.G., Bhuvaneswari, S., Saleem Basha, M.S., Dhavachelvan, P.: A novel algorithm for reducing energy-consumption in cloud computing environment: web service computing approach. J. King Saud Univ. Comput. Inf. Sci. **28**(1), 55–67 (2016)
19. Plank, L., Hellerschmied, A., McCallum, J., Böhm, J., Lovell, J.: VLBI Observations of GNSS-Satellites: From Scheduling to Analysis. Springer, Berlin (2017)
20. Zhang, Z., Xing, L., Chen, Y., Wang, P.: Evolutionary algorithms for many-objective ground station scheduling problem. In: Bio-Inspired Computing-Theories and Applications, pp. 256–270. Springer (2016)
21. Meng, X., Xie, Y., Bhatia, P., Sowter, A., Psimoulis, P.: Research and Development of a Pilot Project Using GNSS and Earth Observation (GeoSHM) for Structural Health Monitoring of the Forth Road Bridge in Scotland (2016)
22. Zuo, L., Dong, S., Shu, L., Zhu, C., Han, G.: A multiqueue interlacing peak scheduling method based on tasks' classification in cloud computing. IEEE Syst. J. **PP**(99), 1–13 (2016)

23. Gu, C., Huang, H., Jia, X.: Power metering for virtual machine in cloud computing-challenges and opportunities. IEEE Access **2**, 1106–1116 (2014)
24. Fan, G., Yu, H., Chen, L.: A formal aspect-oriented method for modeling and analyzing adaptive resource scheduling in cloud computing. IEEE Trans. Netw. Serv. Manag. **11**(4), 1–14 (2012)
25. Yao, X., Geng, P., Du, X.: A task scheduling algorithm for multi-core processors. In: International Conference on Parallel and Distributed Computing, Applications and Technologies, IEEE Computer Society, pp. 259–264 (2013)
26. Zhu, X., Chen, C., Yang, L.T., Xiang, Y.: ANGEL: agent-based scheduling for real-time tasks in virtualized clouds. IEEE Trans. Comput. **64**(12), 1–14 (2015)
27. Zhu, C., Luan, Q., Hao, Z., Ju, Q.: Integration of grey with neural network model and its application in data mining. J. Softw. **6**(4), 716–723 (2011)

R. Karthikeyan is an Assistant Professor at Department of Computer Science Engineering, Mohammed Sathak Engineering College, Kilakarai, Ramanathapuram, Tamilnadu. He is currently a research scholar for doing Ph.D. His main research areas include cloud computing, grid computing, etc. He participated in National and International conferences on cloud computing and grid computing. Now, he is researching on cloud based applications at real time.

P. Chitra is an Assistant Professor (Senior Grade) in Department of Computer Science & Engineering, Thiagarajar College of Engineering. She completed her B.E from Madurai Kamaraj University during 1995; subsequently she worked as lecturer and completed her M.E and Ph.D. in CSE during 2004 and 2011, respectively. She is a reviewer for many national and international peer reviewed journals and member of technical program committee for many IEEE national and international conferences. She has under her credits many publications in reputed international conferences and journals in the areas of distributed systems, cloud computing, Multicore architectures.

JKKN ICACT'2015
5th International Conference on "Advanced Computing, Control Systems, Machines and Embedded Technology"
20th & 21st March 2015

Light Weight Hash Function for Scalable Data Sharing in Cloud Storage

Mr V R Sathish Kumar
Assistant professor
Department of Computer Science and Engineering
Mohamed Sathak Engineering College
Ramanathapuram, India sksathish77@gmail.com

Ms Hameema Fathima H PG
Scholar
Department of Computer Science and Engineering
Mohamed Sathak Engineering College,
Ramanathapuram, India fathimahh@gmail.com

Abstract — The data sharing on cloud needs security for the items which are shared to some others in the cloud. The concept of light weight hash function based data sharing in the cloud is used for secure sharing. This work easily maintains the scalability and throughput. The process behind the proposed system is to share the data from sender to receiver in the cloud. First, the users named as senders and receivers are entering into the cloud with the help of registration process. At the time of registration the secret key can be generated with the help of RSA algorithm. The key can be send to the user's mail. After getting the key, enter into the cloud by the way of login. Then the sender can choose a file to be send and it can be encrypted with light weight hash function. This produces public key for encrypting and private key decrypting the files. The results of the experiments can increase accuracy of the network.

Key Words: light weight hash function; Internet secret key; data sharing.

I INTRODUCTION

Cloud storage can provide the benefits of greater accessibility and reliability, rapid deployment, storing protection for backup and disaster recovery purposes, lowers the overall storage costs as a result of not having to purchase. Also known as mobile cloud storage, personal cloud storage is a descendant of public cloud storage that applies to storing an individual data in the cloud and providing the individual with access to the data from anywhere provides data syncing and sharing capabilities across multiple devices.

The key aggregation property is especially useful when we expect the delegation to be highly efficient and flexible Cryptographic key assignment schemes aim to lower the expense in storing and managing secret keys. Using a tree structure, a key for a given branch can be used to derive the keys of its descendant nodes (but not the other way round). Granting the parent key implicitly grants all the keys of its descendant nodes.

A method is used to generate a tree hierarchy of symmetric keys by using unlimited evaluations of pseudo-random function/block-cipher on a fixed secret. The concept can be more specialized from a tree to a graph. More programmed cryptographic key assignment schemes also supports access policy that can be modeled by an acyclic graph or a cyclic graph. Most of these schemes produces keys for symmetric-key modular arithmetic as used in public-key cryptosystems.

II RELATED WORK

It is unrealistic to assume there is a single authority which can monitor every single attribute of all users. Multi-authority attribute-based encryption capsulate a more realistic deployment of attribute-based access control, such that different authorities are responsible for issuing different sets of attributes.[1]

Since key material is the most important concern in unconditionally secure verification, given the message is encrypted with a perfect secret one-time pad cipher, achieve unconditionally secure authentication with almost free key material. Propose a method for unconditionally authenticating arbitrarily long messages with much shorter keys.[2]

Key reduction is achieved by utilizing the special structure of the authenticated encryption. That is, authentication exploits the privacy of the message to reduce the key material required for authentication.[5]

After the detailed description of the method, key material is the most important concern in unconditional secure authentication, given that the message is encrypted with a perfectly secret one-time pad cipher, achieve unconditional secure authentication with almost free key material.[7]

III EXISTING METHOD

A well-known application of KAC is data sharing. The key aggregation property is particularly beneficial when we expect the authorization to be adept and heritable. The schemes enable a content provider to share their data in a centralized and particular way, with a fixed and small cipher-text enlargement, by spreading to each authorized user a single and small aggregate key.

Cryptographic key assignment schemes aim to reduce the expense in storing and conducting secret keys for general cryptographic use. Deploying a tree structure, a key for a given branch can be pre-owned to derive the keys of its descendant nodes. Just consider the parent key implicitly grants all the keys of its descendant nodes.

A method to generate a tree hierarchy of symmetric keys by using iterated evaluations of pseudorandom function/block-cipher on a fixed secret. The concept can be unspecialized from a tree to a graph. Wide innovative cryptographic key assignment schemes support access policy that can be procedure by an acyclic graph or a cyclic graph

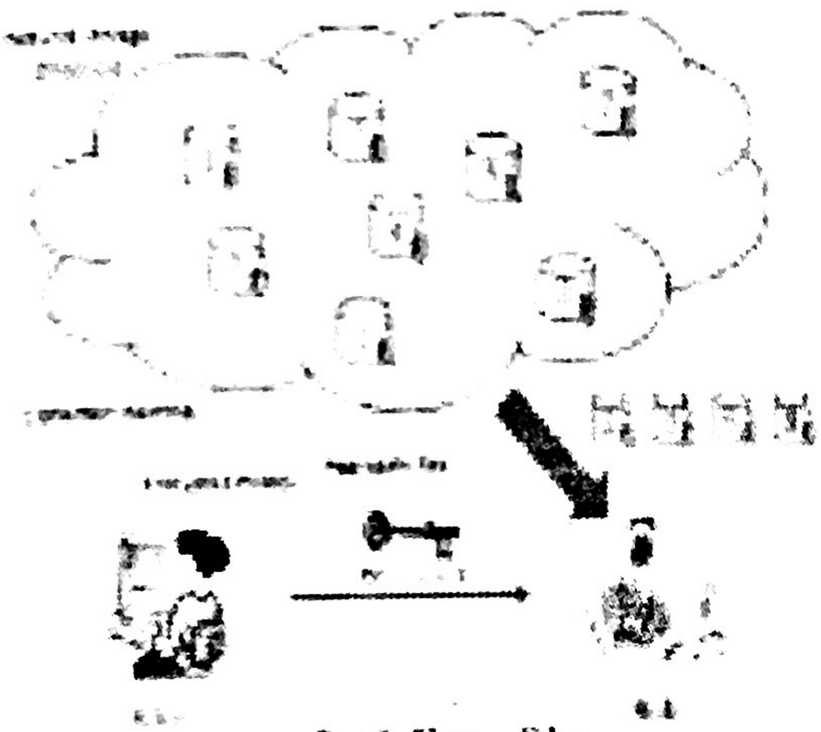

Fig 1 Sharing Files

Most of these schemes produce keys for symmetric-key cryptosystems, against the key Inferences may require commutable arithmetic as used in public-key cryptosystems.

A key-aggregate encryption scheme is composed of five polynomial-time algorithms. The data owner creates the public system parameter by Setup and generates a public/master-secret key pair by KeyGen. Messages can be encrypted by Encrypt by anyone who decides what cipher text class is related with the plaintext message to be encrypted.

The data owner handles the master-secret to generate an aggregate decryption key for a set of cipher text Classes Extract. The generated keys can be passed to representative securely. Any user with an aggregate key can decrypt any cipher text presuming that the cipher text's class is enclosed in the aggregate key via Decrypt

IV PROPOSED METHOD

In proposed system the users must register into the cloud system. At the time of registration they can provide some information related to them particularly unique name and id. After the successful completion of the registration the digital signature can be generated to user's mail. The signature can be accomplished with the help of DSA algorithm. After the registration user can login to the cloud. At that time the user must give their individual signature because according to that signature the validation of the user can be made.

If the user can give any invalid signature means they will not enter into the system. After entering the cloud user need to perform the operations of file sharing. Here, the file can be encrypted with the help of light weight hash function. This generates the public key and also the private key. The sender can send the public key to the receiver side. The receivers decrypt the modification with the private key.

A. Authentication

First the user can enroll their details into cloud. After registration the digital signature key can be send to user's mail. According to the key the user can login to the cloud system and do further process. For digital signature process we have to use DSA algorithm. DSA algorithm is used to generate a secret key for each user in the cloud.

This system maintains the scalability and throughput. The process behind is to share the data's from sender to receiver. Initially the users enters into the cloud with the help of registration. At the time of registration the secret key can be generated with of DSA algorithm.

The key can be send to the user's mail. After getting the key user have to enter into the cloud the way of login. Then the sender can choose a file to be sent and that can be encrypted with key aggregate process. For such purpose, use light weight hash function. This produces the same public key for decrypting the files. The same process will be made at the receiver end of the cloud. The results of the experiments can increase latency of the network.

B. File Transfer

The user can select the images from the system and for sending to another user in the receiver side. The total selected images are to be 10 in the folder. But another user wants only 3 images.

from the folder other images are not known to another user. For that purpose we have to use the encryption technique for the folder of images. Functions with these properties are used as hash functions for a variety of intent. Practical applications include message integrity checks, digital signature, authentication and various information of security applications hash function takes a string of any length as input and produces a fixed length string which acts as a kind of "signature" for the data provided.

In this way, a person knowing the "hash value" is unable to know the authentic message, but only the person who knows the authentic message can prove the "hash value" as created from that message. A cryptographic hash function should behave as much as possible like a random function while still being deterministic and efficient computable. A cryptographic hash function is considered "insecure" from a cryptographic point of view.

Design a new system that contains a limited no of keys to encrypt and decrypt operation. Mobile user can easily send a data to the receiver with a secure key and maintain the confidential. In our designed system must

DSA algorithm. Both the process of encryption and decryption is carried out only with the verification of secret key, that has been generated. Fig (a) shows the process of registration. Fig (b) shows the process of light weight hash encryption where, the images can be encrypted using light weight hash function.

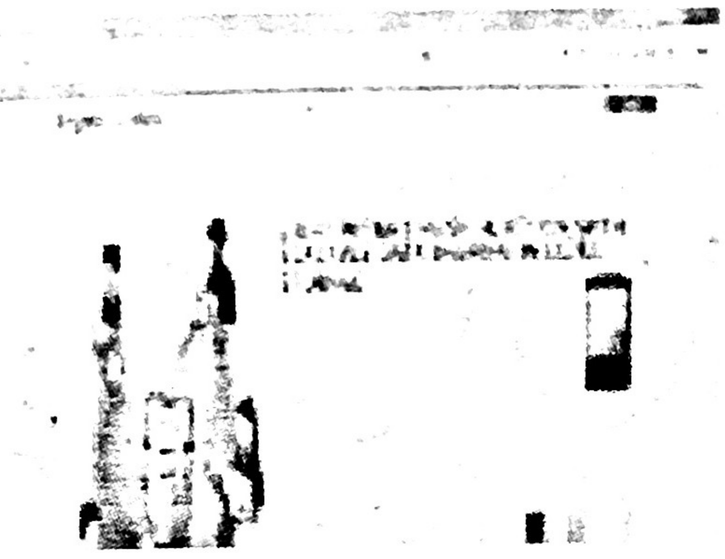

(a)

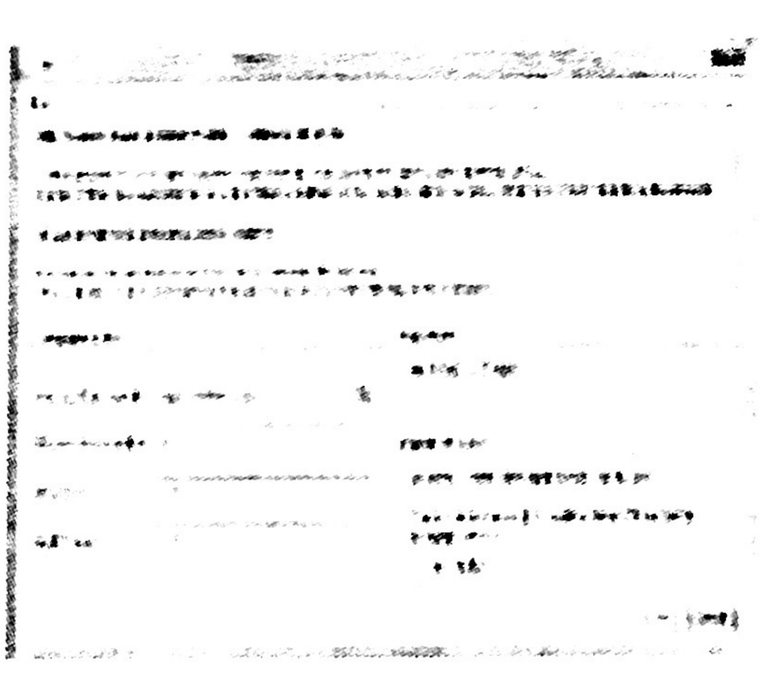

(b)

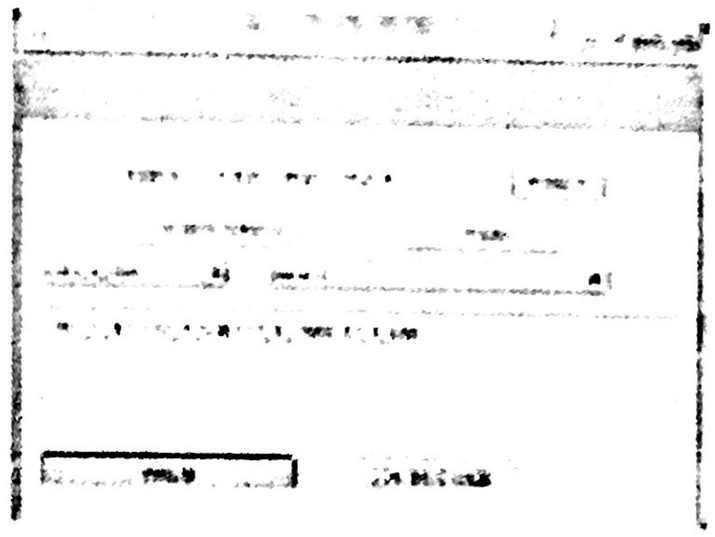

(c)

(d)

Fig. 3. Results of the proposed method (a)Registration process, (b)Light Weight Hash function applied for the purpose of encryption (c) showing the number of images using efficacy propagation method (d) secure way of decrypting the images

VII. CONCLUSION AND FUTURE WORK

A. Conclusion

Overcomes the drawbacks associated with the existing system. In proposed concept, provide a secure sharing of data in cloud environment. Security is achieved through DSA algorithm.

B. Future Work

In future, this can be expanded by enhancing another segment of algorithm for improvising the security. Also enhance to share the videos between the sender and the receiver. Try to develop the algorithm more simplified for the smart phone users.

ACKNOWLEDGEMENT

The author would like to thank the respective Head of the Institution, Head of the Department and Faculty members for giving valuable advices and providing technical support.

REFERENCES

[1] T.H. Yuen, S.S.M. Chow, Y. Zhang, and S.M. Yiu, "Identity-Based Encryption Resilient to Continual Auxiliary Leakage," Proc. Advances in Cryptology Conf. (EUROCRYPT '12), vol. 7237, pp. 117-134, 2012.

[2] D. Boneh, X. Boyen, and E-J. Goh, "Hierarchical Identity Based Encryption with Constant Size Ciphertext," Proc. Advances in Cryptology Conf. (EUROCRYPT '05), vol. 3494, pp. 440-456, 2005.

[3] D. Boneh, R. Canetti, S. Halevi, and J. Katz, "Chosen-Ciphertext Security from Identity-Based Encryption," SIAM J. Computing, vol. 36, no. 5, pp. 1301-1328, 2007.

[4] R. Canetti and S. Hohenberger, "Chosen-Ciphertext Secure Proxy Re-Encryption," Proc. 14th ACM Conf. Computer and Comm. Security (CCS '07), pp. 185-194, 2007.

improve the reliability of cloud system by using simple light weight hash function

The sender searches the requested images of the receiver and compresses all the images in a single folder and a single public key is generated for the compressed folder, and forwarded to the receiver, by mail. When, the receiver tries to decrypt the images, verification of digital signature is carried out

C. Light Weight Hash Function Encryption

The sender can use the light weight hash function for encrypting that files. The function of light weight hash function is to encrypt the files it could generate the public key and also private key. Here, the send can use the public key for sending process. At the end of receiver side the private key can be used to decrypt the files. Data clustering is an effective method for data analysis and pattern recognition which has been applied in many fields such as image segmentation

It is a process of classifying the multidimensional data into several groups or clusters based on some similarity measures. A cluster is usually defined by a cluster center. The information of the features may differ from each other and the contributions to the clustering are different.

Some features play an important role in explaining the differences among the samples, thus should pay a more attention in the clustering process to get a exact grouping. In order to emulate the particular contribution of the feature, this paper proposes a new feature weighted affinity propagation clustering (AP) algorithm. LHash is based on extended sponge functions framework, which allows trade-offs among architectural, speed, energy consumption and implementation cost by adjusting parameters.

The internal permutation is designed using a structure, named as Feistel-PG which is an extended variant of improved generalized Feistel. Feistel-PG has fast diffusion, shorter differential paths and integral distinguishers than similar structures. The S-boxes and MDS linear layer used in the internal permutation are designed to be hardware-friendly. Both have very compact hardware development. The MDS linear layer has an iterated implementation, which is similar to and even more compact than the linear layer used in photon.

We present the LHash achieves remarkably compact implementation in hardware. In our smallest implementation, the area requirements are 817 and 1028 GE with 666 and 882 cycles per block, respectively. Meanwhile, at its efficiency on energy consumption evaluated by the metric of energy per bit proposed as is the smallest class among current lightweight hash functions in literature. Especially, for the competition with similar pre image and collision resistance levels, it also competes well in terms of area and throughput tradeoff.

D. Decryption Process

The decryption process is to be done in the receiver side. For decryption process the user can use the light weight hash function. This will provide the secured decryption in a system. The receiver wants particular images from the folder means they get the private key of those images from sender side with the help of sending requests.

V. SYSTEM FLOW DIAGRAM

The overall system design reviews, that the user can enroll their details into cloud. After registration the digital signature key can be send to user's mail. According to the key the user can login to the cloud system and do further process. For digital signature process we have to use DSA algorithm.

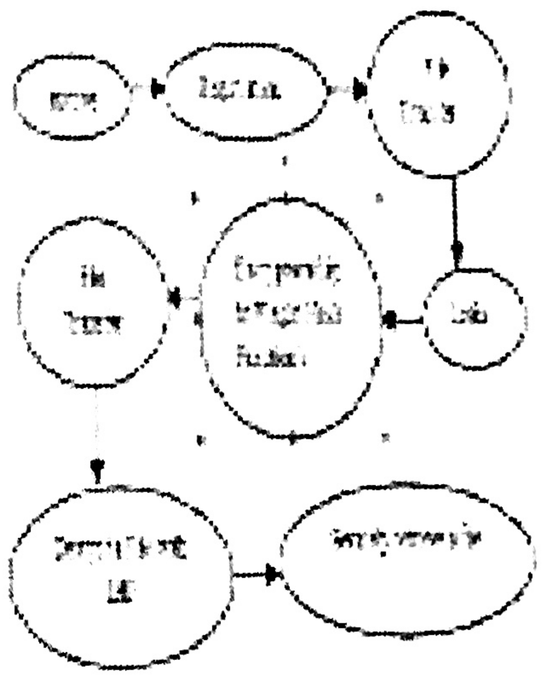

Fig 2. system flow diagram

The user can select the images from the system and for sending to another user in the receiver side. Then encrypt the files which can be sending by the sender. Here the sender can use the light weight hash function for encrypting that files. The function of light weight hash function is to encrypt the files it could generate the public key and also private key. Here, the send can use the public key for sending process. At the end of receiver side the private key can be used to decrypt the files.

VI. EXPERIMENTAL RESULTS

To protect users' data privacy is a central question of cloud storage. We consider how to "compress" secret keys in public-key cryptosystems which support delegation of secret keys for different ciphertext classes in cloud storage. No concern which one among the power set of associated classes the delegate can always get an aggregate key of constant size. Our approach 2thus hierarchical key assignment which can only save spaces of all key-holders share a similar set of privileges. A light weight hash function takes a string of any length as input and produces a fixed length string which acts as a kind of "signature"

Initially registration takes place and once the registration is completed, a secret key is generated by

[6] C.-K. Chu and W.-G. Tzeng, "Identity-Based Proxy Re-encryption without Random Oracles," Proc. Information Security Conf. (ISC '07), vol. 4779, pp. 189-202, 2007.

[7] C.-K. Chu, J. Weng, S.S.M. Chow, J. Zhou, and R.H. Deng, "Conditional Proxy Broadcast Re-Encryption," Proc. 14th Australasian Conf. Information Security and Privacy (ACISP '09), vol. 5594, pp. 327-342, 2009.

[8] S.S.M. Chow, J. Weng, Y. Yang, and R.H. Deng, "Efficient Unidirectional Proxy Re-Encryption," Proc. Progress in Cryptology (AFRICACRYPT '10), vol. 6055, pp. 316-332, 2010.

[9] G. Ateniese, K. Fu, M. Green, and S. Hohenberger, "Improved Proxy Re-Encryption Schemes with Applications to Secure Distributed Storage," ACM Trans. Information and System Security, vol. 9, no. 1, pp. 1-30, 2006.

[5] D. Boneh, C. Gentry, and B. Waters, "Collusion Resistant Broadcast Encryption with Short Ciphertexts and Private Keys," Proc. Advances in Cryptology (CRYPTO '05), vol. 3621, pp. 258-275, 2005.

[10] L.B. Oliveira, D. Aranha, E. Morais, F. Daguano, J. Lopez, and R. Dahab, "TinyTate: Computing the Tate Pairing in Resource-Constrained Sensor Nodes," Proc. IEEE Sixth Int'l Symp. Network Computing and Applications (NCA '07), pp. 318-323, 2007.

[11] T. Okamoto and K. Takashima, "Achieving Short Ciphertexts or Short Secret-Keys for Adaptively Secure General Inner-Product Encryption," Proc. 10th Int'l Conf. Cryptology and Network Security (CANS '11), pp. 138-159, 2011.

[12] Rafail Ostrovsky, Amit Sahai, and Brent Waters, "Attribute-Based Encryption with Non-Monotonic Access Structures," In Computer and Communications Security, pages 195-203, 2007.

[13] W.-G. Tzeng, "A Time-Bound Cryptographic Key Assignment Scheme for Access Control in a Hierarchy," IEEE Trans. Knowledge and Data Eng., vol. 14, no. 1, pp. 182-188, Jan./Feb. 2002.

[14] G. Ateniese, A.D. Santis, A.L. Ferrara, and B. Masucci, "Provably-Secure Time-Bound Hierarchical Key Assignment Schemes," J. Cryptology, vol. 25, no. 2, pp. 243-270, 2012.

[15] M.S. Sandhu, "Cryptographic Implementation of a Tree Hierarchy for Access Control," Information Processing Letters, vol. 27, no. 2, pp. 95-98, 1988.

[16] Y. Sun and K.J.R. Liu, "Scalable Hierarchical Access Control in Secure Group Communications," Proc. IEEE INFOCOM '04, 2004.

[17] Q. Zhang and Y. Wang, "A Centralized Key Management Scheme for Hierarchical Access Control," Proc. IEEE Global Telecomm. Conf. (GLOBECOM '04), pp. 2067-2071, 2004.

[18] J. Benaloh, "Key Compression and Its Application to Digital Fingerprinting," technical report, Microsoft Research, 2009.

[19] R. Alomair and R. Poovendran, "Information Theoretically Secure Encryption with Almost Free Authentication," J. Universal Computer Science, vol. 15, no. 15, pp. 2937-2956, 2009.

[20] D. Boneh and M.K. Franklin, "Identity-Based Encryption from the Weil Pairing," Proc. Advances in Cryptology (CRYPTO '01), vol. 2139, pp. 213-229, 2001.

[21] A. Sahai and B. Waters, "Fuzzy Identity-Based Encryption," Proc. 24th Int'l Conf. Theory and Applications of Cryptographic Techniques (EUROCRYPT '05), vol. 3494, pp. 457-473, 2005.

[22] S.S.M. Chow, Y. Dodis, Y. Rouselakis, and B. Waters, "Practical Leakage-Resilient Identity-Based Encryption from Simple Assumptions," Proc. ACM Conf. Computer and Comm. Security, pp. 152-161, 2010.

[23] P. Chu, Y. Ma, and J. Chen, "Identity Based Encryption How to Decrypt Multiple Ciphertexts Using a Single Decryption Key," Proc. Pairing-Based Cryptography Conf. (Pairing '07), vol. 4575, pp. 392-406, 2007.

[24] M. Chase and S.S.M. Chow, "Improving Privacy and Security in Multi-Authority Attribute-Based Encryption," Proc. ACM Conf. Computer and Comm. Security, pp. 121-130, 2009.

[25] T. Okamoto and K. Takashima, "Achieving Short Ciphertexts or Short Secret-Keys for Adaptively Secure General Inner-Product Encryption," Proc. 10th Int'l Conf. Cryptology and Network Security (CANS '11), pp. 138-159, 2011.

5th INTERNATIONAL CONFERENCE ON "ADVANCED COMPUTING, CONTROL SYSTEMS, MACHINES AND EMBEDDED TECHNOLOGY" (ICACT2015)

Organized By **Department of Computer Science and Engineering**, Information Technology, Electronics and Communication Engineering, Electrical and Electronics Engineering, **Mechanical Engineering and Science & Humanities**

JKKN J.K.K.NATTRAJA COLLEGE OF ENGINEERING AND TECHNOLOGY

(Approved by AICTE, New Delhi and Affiliated to Anna University, Chennai.)

Kumarapalayam - 638 183, Namakkal Tamilnadu, India.

ISBN : 978 - 93 - 80757 - 74 - 2

This is to certify that Dr./Mr/Ms /Mrs. SATHISH KUMAR V.R / AP

MOHAMED SATHAK ENGINEERING COLLEGE has presented

a paper titled LIGHT WEIGHT HASH FUNCTION FOR SCALABLE DATA SHARING IN CLOUD STORAGE

in the International Conference on "ICACT-2015" held on 20th & 21st March 2015 at J. K. K. Nattraja College of Engineering and Technology, TamilNadu, India.

Mrs. N. SENDAMARAAI
Chairperson

Dr. C. SURESHKUMAR
Principal

S.K.MAHALINGAM
Vice Principal

TRUE COPY ATTESTED
PRINCIPAL
MOHAMED SATHAK ENGINEERING COLLEGE
KILAKARAI-623806.

Sponsored by :

ORACLE
IEEE BOMBAY SECTION
Springer
acm

Madras University Post Centenary
Diamond Jubilee

2nd International Conference on Recent Trends in Analytical Chemistry

(ICORTAC-2018)

15 - 17 March, 2018

Abstracts and Souvenir

Organized by

Department of Analytical Chemistry
University of Madras, Chennai - 25

Sponsored by

TRUE COPY ATTESTED

PRINCIPAL
MOHAMED SATHAK ENGINEERING COLLEGE
KILAKARAI-623806.

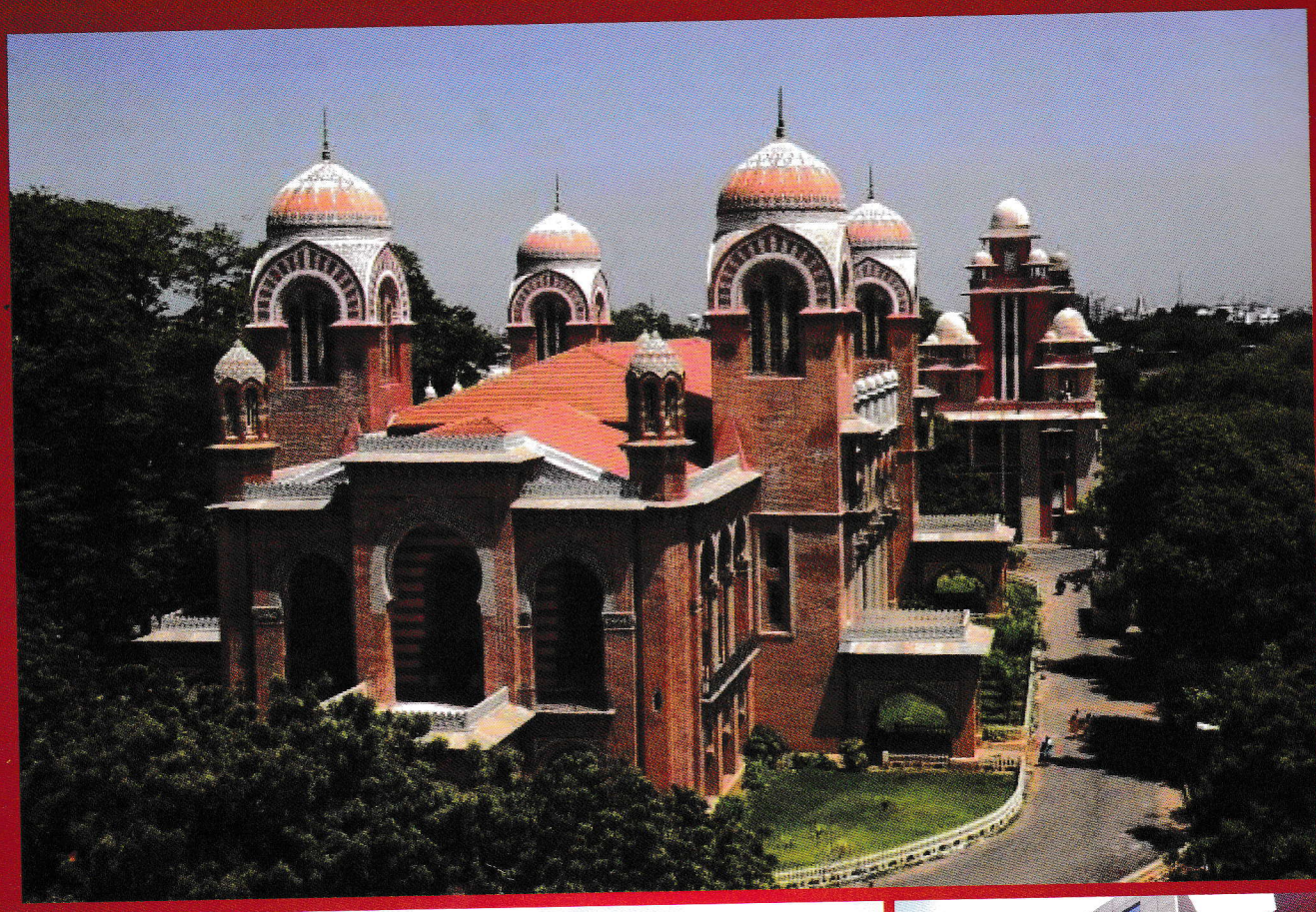

Convenor

Dr. K. Ravichandran

Associate Professor and Head i/c

Dept. of Analytical Chemistry

...tras, Guindy Campus, Chennai-600025

9789385374821

159	**AB259**	Investigation Of Graphene-Based Polymer Composites Of Li(Nca)Electrode Materials For Application Of Lithium-Ion Battery	Poster	95
160	**AB260**	5-(4-(2-(5-ethylpyridin-2-yl) ethoxy) benzyl) thiazolidine-2, 4-dione as potential inhibitor for the corrosion of mild steel in Sulphuric acid medium	Poster	115
161	**AB261**	Effect of structure on the adsorption of basic dyes by activated carbon containing nano Co_3O_4	Poster	189
162	**AB262**	Extraction Of Chitosan From Crustacean Shells And Antimicrobial Activity Of Its Metal Complexes	Poster	176
163	**AB263**	Synthesis, Characterisation And Antimicrobial Activity Of Chitosan-Metal Oxide Nanocomposite	Poster	177
164	**AB264**	Synthesis, Spectroscopic, Thermogravimetric kinetics, Antioxidant, Antimicrobial, DNA/BSA Interaction and Cytotoxicity Studies on Co(II) Ni(II) and Mn(II) Complexes of Bromo Substituted NNO Tridentate Schiff base.	Poster	177
165	**AB265**	Bandgap and nano size modulated doped nano crystalline metal ferrites as efficient solar photocatalyts for remediation of drug polluted waters	Oral	189
166	**AB266**	Selective synthesis of Terephthalic acid over Ce containing 3D microporous catalysts	Poster	215
167	**AB267**	Antibacterial Effects Of Biosynthesized Silver Nanoparticles On Surface Ultra structure And nanomechanical Properties Of Gram-Negative Bacteria Viz. Escherichia Coli And Pseudomonas Aeruginosa	Oral	77
168	**AB268**	A Novel Design And Construction Of Semiconductor Based Pyranometer For Solar Radiation Measurements	Poster	95
169	**AB269**	Surface Functionalized Biosilica Nano Particles For Effective Catalysis Of Oxidative Degradation Of Acidic Theraupeutic Drugs	Oral	78
170	**AB270**	Synthesis, Characterizations And Thermal Stability Of New Polyesters From Schiff Base Monomers	Poster	204
171	**AB271**	Enhanced Visible-Light Active La-Tio_2 Nanotubes For Rhodamine B And Crystal Violet Dye Degradation	Poster	79
172	**AB272**	Studies on the Optoelectronic Properties of npSnO-PVA polymer Composite	Poster	204
173	**AB273**	Evaluation Of Certain Zero-Cost Biomass Derived Carbon Materials For Supercapacitor Electrodes	Poster	96
174	**AB274**	PVK-Tio_2 Hybrid Nanocomposite Coatings: Synthesis, Characterization And Its Corrosion Protection Performance In 3.5 Wt. % NaCl Medium	Oral	116
175	**AB275**	Green synthesis of Zinc oxide nanoparticles using Dolichos lablap	Poster	79
	AB276	Effect of PANI incorporation on the corrosion behavior of titania nanotubes on Cp-titanium	Oral	116
	AB277	DPP based Multistep Heterocyclic π-conjugated Sonogashira polymer Synthesis and Characterization for OBHJ Solar cell- Theoretical and Experimental investigation	Oral	96

Cu^{2+} etc., form an important group of antimicrobial agents, which have different active target from most bacteriostatic polymers. Chitosan is a powerful chelating agent, which is easy to form complexes with transition metals and heavy metals. Most researches of chitosan-metal complexes focused on their applications in the removal of metal ions, dyeing, catalysis, water treatment, and many other industrial processes. In the previous work, we report the synthesis of chitosan from the crustacean shells by chemical method involving deproteination, demineralisation and deacetylation of isolated chitin. The metal complexes of chitosan were prepared and characterised by uv-visible, FTIR and XRD techniques. The antimicrobial activity of the chitosan-metal complexes were investigated in comparison with free chitosan and metal salts.

AB263

Synthesis, Characterisation and Antimicrobial Activity of Chitosan-Metal Oxide Nanocomposite

F.Priyanka and S.Anuja*

Department of Chemistry, Loyola College, Chennai-600034
**E-mail: anujamanikandan@gmail.com*

Chitin is the second most abundant biopolymer found in nature. It is mainly derived from the exoskeletons of crustaceans, insects, molluscs and the cell wall of microorganisms. Chitosan is the deacetylated derivative of chitin, which is chemically defined as a copolymer of a -(1,4) glucosamine $(C_6H_{11}O_4N)_n$, having different number of N-acetyl groups. Chitosan being a non-toxic, biodegradable, and biocompatible polysaccharide polymer has received enormous worldwide attention as one of the promising renewable polymeric materials for their extensive applications in industrial and biomedical domains.Chitosan also has antimicrobial activity, haemostatic activity, anti-tumor activity, accelerates wound healing, can be used tissue-engineering scaffolds and also for drug delivery. Here in, we present the syntheses of chitosan from shrimp shell wastes and chitosan-metal oxide nanocomposites.

The synthesised nanocomposites were characterised by FTIR, XRD and FESEM techniques. Metal oxide nanocomposites are widely used to remove heavy metals, organic dyes and energy storage applications. In the present work, we have studied the antimicrobial activity of synthesised chitosan-metal oxide nanocomposites.

AB264

Synthesis, Spectroscopic, Thermogravimetric kinetics, Antioxidant, Antimicrobial, DNA/BSA Interaction and Cytotoxicity Studies on Co(II) Ni(II) and Mn(II) Complexes of Bromo Substituted NNO Tridentate Schiff base.

Karunganathan Sakthikumar[1] and Jeyaraj Dhaveethu Raja[1]*

[1]Chemistry Research Centre, Mohamed Sathak Engineering College, Kilakarai, Ramanathapuram 623 806, Tamilnadu, India
**Correspondence autor Email: jdrajapriya@gmail.com*

) complexes of the type $[ML(AcO)].nH_2O$ (1–3) { where M = Co (1), Ni (2) and Mn (3), nthesized from bromo substituted NNO tridentate Schiff base ligand (HL) in a 1:1 molar by elemental analysis, Magnetic susceptibility, Molar conductance, FTIR, UV-Vis, ^1H NMR, EPR and LC-MS-Mass Spectral techniques. The spectral data of these complexes suggest a square planar

geometry around the central metal ion and found to possess [ML] stoichiometry. The thermal behaviour of complex (1) was studied by TGA / DTA technique in a static nitrogen atmosphere at a heating of 20 °C/min. the kinetic parameters, such as activation energy (E_a), entropy change (ΔS), free energy (ΔF), enthalpy change (ΔH) and the order of reaction (n) were determined by Freeman-Carroll, Wentworth, Coat Redfern, Friedman and Chang methods and the results were in good agreement with each other.

In vitro antimicrobial activities of all compounds were examined against selected bacterial (Escherichia coli, Salmonella typhi, Chromo bacterim violaceum, Staphylococcus aureus bacteremia and Bacillus cereus) and fungal (Aspergillus flavus, Aspergillus niger and Candida albicans) strains by the disc diffusion method. The results indicates that the complexes (1-3) exhibit higher antimicrobial activity than free ligand (HL). In vitro antioxidant activity results of DPPH assay, hydroxyl radical, super oxide and nitric oxide for complexes (1-3) were compared with ligand (HL). Gel electrophoresis results indicated that, complexes (1) and (2) were exhibited more DNA cleavage efficiency than others. In vitro DNA / BSA binding properties of complexes (1-3) have been carried out by electronic absorption, fluorescence and viscosity titration measurements. The observed results of DNA binding behaviour of the complexes (1-3) were in the order (1) > (2) > (3) and suggest that the complexes bind to DNA via partial intercalation mode. In vitro cytotoxicity of the complexes (1–3) were tested against three cancerous cells, such as MCF-7, Hep-2 and HeLa cell lines. Complex (1) was revealed remarkable cytotoxicity against them.

Keywords: *Square planar, Antimicrobial, Antioxidant, DNA interactions and Cytotoxicity.*

Synthesis, Characterization and Biological Applications of Hydrazone Based Ligand and their Transition Metal Complexes

A.Ashma[1], S.L.Ashok Kumar[2] and S.J. Askar Ali[1*]

[1]PG & Research Department of Chemistry, The New College, Chennai.
[2]Department of Chemistry, GRT Institute of Engineering and Technology, Truthani.
**PG & Research Department of Chemistry, The New College, Chennai.*
Corresponding author: askaralisj@gmail.com, ashmacader@gmail.com

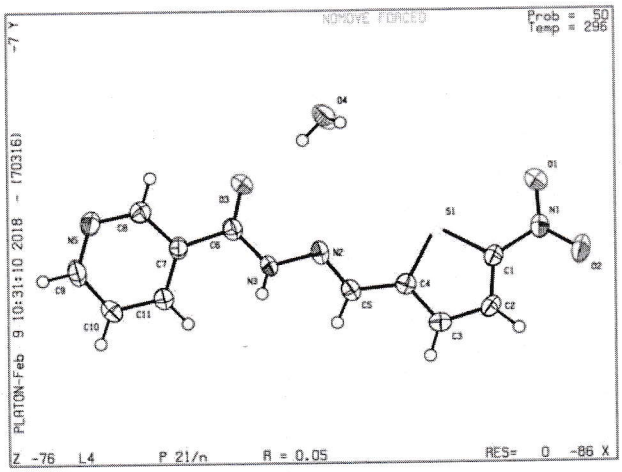

Fig. (1) Crystal structure of Ligand (L)

Certificate

ALAGAPPA UNIVERSITY

(Accredited with A+ Grade by NAAC (CGPA:3.64) in the Third Cycle)

KARAIKUDI -630 003

DEPARTMENT OF PHYSICS

(UGC-SAP and DST-FIST supported)

INTERNATIONAL CONFERENCE ON
MOMENTOUS ROLE OF NANOMATERIALS IN
RENEWABLE ENERGY DEVICES
(IC MNRE-2018)

CERTIFICATE

This is to certify that H. Mohamed Mohaideen

Raja Doraisingam Govt. Arts College, Sivagangai has delivered invited talk / chaired the session/participated/presented (Oral/Poster) paper entitled The AC Impedance Spectroscopy and Antibacterial - - - - - - - - Nio Nanoparticles in **International Conference on Momentous Role of Nanomaterials in Renewable Energy Devices (IC MNRE-2018)** organized by the Department of Physics, Alagappa University, Karaikudi during 1-2 March, 2018.

TRUE COPY ATTESTED

PRINCIPAL
MOHAMED SATHAK ENGINEERING COLLEGE
KILAKARAI-623806.

Prof. G. Ravi
Co-ordinator

Dr. M. Sivakumar
Convener

Dr. R. Subadevi
Convener

IC MNRE-2018

ALAGAPPA UNIVERSITY

(Accredited with A+ Grade by NAAC (CGPA:3.64) in the Third Cycle & Graded as Category I University MHRD - UGC)

KARAIKUDI -630 003

DEPARTMENT OF PHYSICS

(UGC-SAP and DST-FIST supported)

IC MNRE 2018

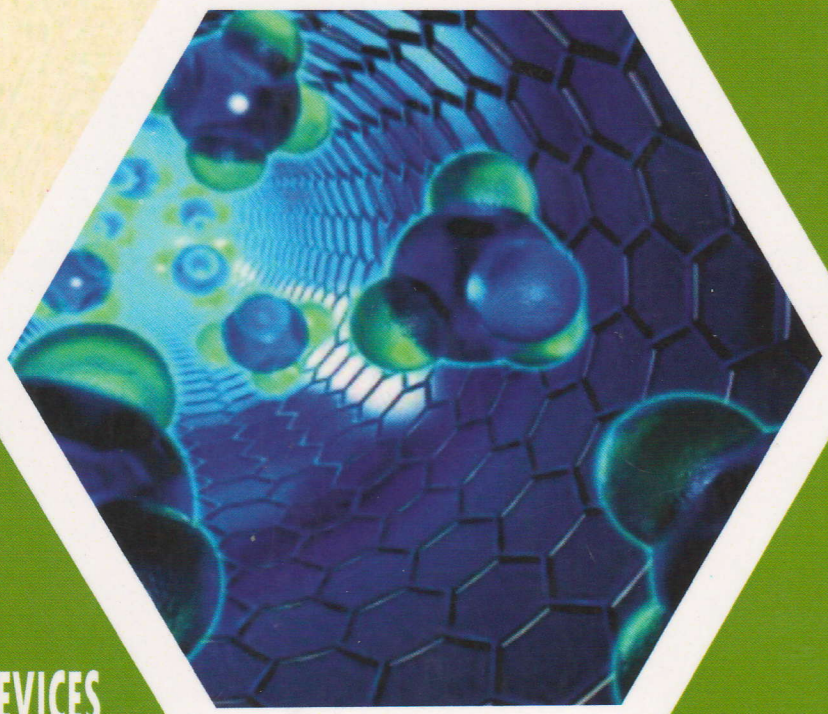

INTERNATIONAL CONFERENCE ON MOMENTOUS ROLE OF NANOMATERIALS IN RENEWABLE ENERGY DEVICES

SOUVENIR

PP - 44

THE AC IMPEDANCE SPECTROSCOPY AND ANTIBACTERIAL STUDIES ON NiO NANOPARTICLES

H. Mohamed Mohaideen[a, b], S. Sheik Fareed[a], B. Natarajan[b]*

[a]Department of Physics, Mohamed Sathak Engineering College, Kilakarai-623 806, Tamilnadu, India.

[b]PG and Research Department of Physics, Raja Doraisingam Govt. Arts College, Sivagangai - 630 561, Tamilnadu, India.

*Email of the corresponding author: b_natraj_b@rediffmail.com

ABSTRACT

The Nickel oxide (NiO) nanoparticles were synthesised by Sol-Gel method without any surface mediated. The prepared NiO nanoparticles was characterized by TGA, FTIR, XRD and AFM. The calcination temperature of as prepared nanoparticles has been confirmed from TGA analysis. The fuctional group present in the nanoparticles was analysed using FTIR spectroscopy. The prepared nanoparticles shows diffraction peak conrresponding to cubic NiO. The electrical and dielectrical properties were characteriazed by complex impedance spectroscopy as a function of frequency at different temperature. The frequency dependent ac conductivity is analysed and the activation energy is calculated.Tangent loss spectrum reveals that loss peak shits to the higher frequency with increase in temperature which is due to long range hopping of charge carriers. The antibactrial efficency of NiO nanoparticles was tested against the growth of bacterial species using disc diffucion method. The NiO nanoparticles exhibited antibacterial activity against the *E. coli*, *P. Vulgaris* and *K. Pneumoniae.*

Keywords: *Nickel oxide nanoparticles, AFM, Impedance spectroscopy and antibacterial activity*

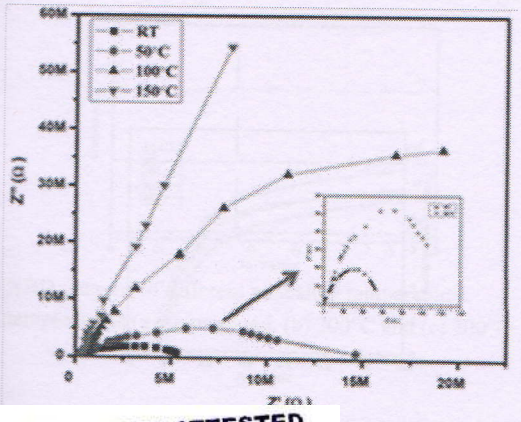

) nanoparticles.

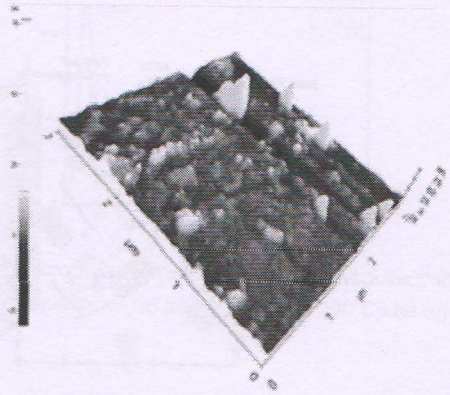

Fig. 3D AFM image of NiO nanoparticles.

ISSN : 2348 - 6600

Proceedings of the
International Conference on

ALEGEBRA AND DISCRETE MATHEMATICS

« ICADM 2018 »

JANUARY 08 - 10, 2018

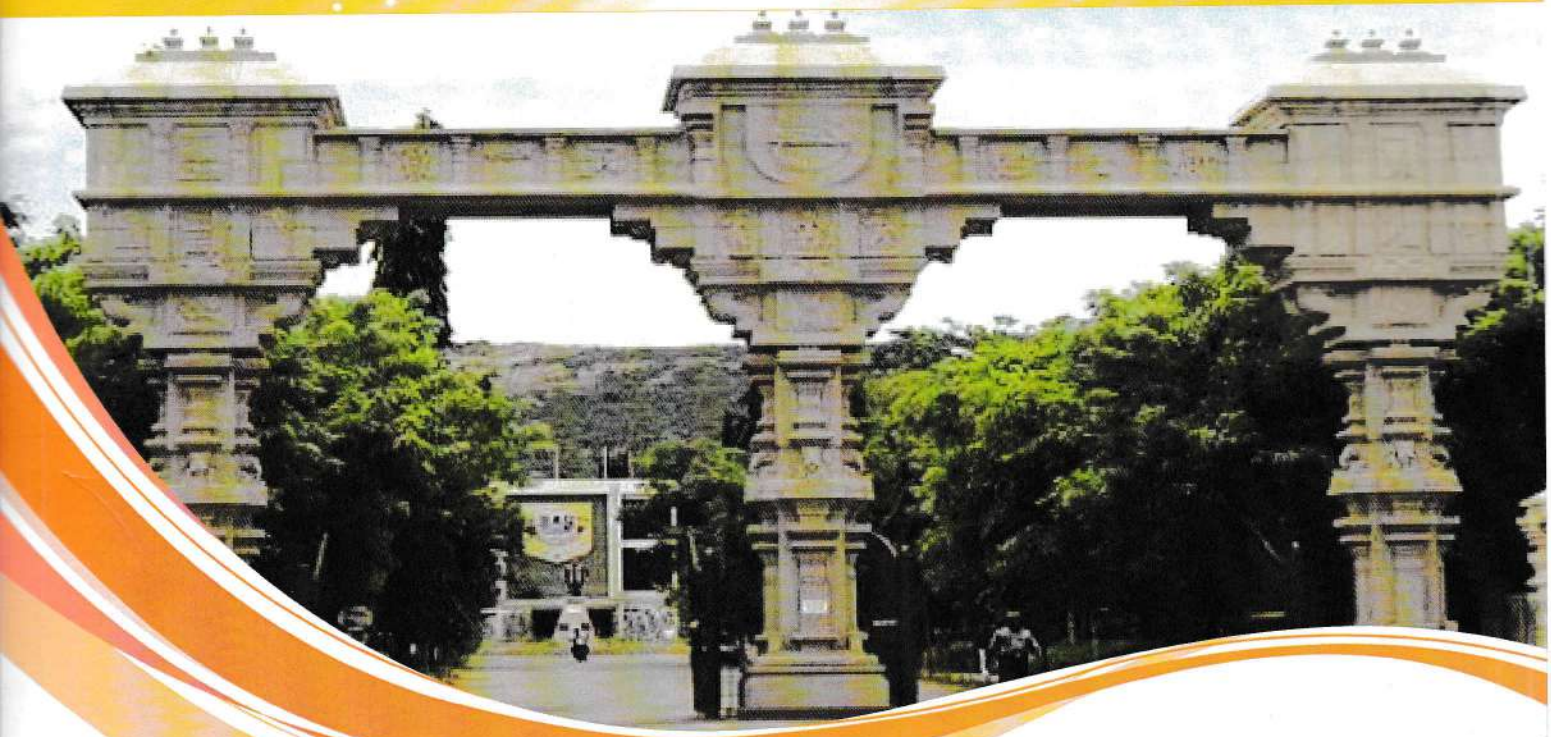

Organized by

Department of Mathematics - DDE

MADURAI KAMARAJ UNIVERSITY

MADURAI - 625 021, Tamil Nadu, India.

Editors :

Dr. T. Asir, Asst. Prof.
Dept. of Mathematics - DDE
MK University, Madurai.

Dr. T. Tamizh Chelvam, Prof.
Dept. of Mathematics
MS University, Tirunelveli.

Sponsored by :

SERB INDIA
nce and Engineering
earch Board (SERB)

CSIR·INDIA

ational Journal of Computer Science

Scholarly Peer Reviewed Research Journal - PRESS - OPEN ACCESS

ISSN : 2348 - 6600

IJCS

SKRGC
Since 2012

LIST OF PAPERS

CONNECTIVITY OF PRODUCT OF S-VALUED GRAPHS

P.Victor [1] and M.Chandramouleeswaran [2]
[1] Department of Mathematics
Mohamed Sathak Engineering College
Kilakarai- 623 806
[2] Department of Mathematics
Saiva Bhanu Kshatriya College, Aruppukottai - 626101.
India.
e-mail: antonyraj96@gmail.com moulee59@gmail.com

ABSTRACT. Motivated by the study of products and connectedness of graphs in crisp graph theory and the notion of S-valued graphs, in this paper, we discuss the connectivity of Categorical product of S-valued graphs and prove some simple results.

Keywords: Product of Graphs, S-Valued Graphs, Semiring, S-Connected.
AMS classifiications: 16Y60, 05C25, 05C76

1. INTRODUCTION

In the year 2015, the notion of semiring valued graphs (Simply called $S-$ valued graphs) have been introduced and studied [4]. In [1] and [2], the authors studied the notion of connectivity on $S-$ valued graphs. Motivated by the theory on product of graphs [5], in our earlier paper [6], we have discussed the Categorical product of two $S-$ valued graphs. In this paper, we connect the two notions: Connectivity in $S-$ valued graphs and the Categorical product of $S-$ valued graphs.

2. PRELIMINARIES

In this section, we recall some basic definitions that are needed for our work.

Definition 2.1. [3] *A semiring $(S,+,\cdot)$ is an algebraic system with a non-empty set S together with two binary operations $+$ and $\cdot$ such that*

(1) *$(S,+)$ is a semigroup.*
(2) *$(S,\cdot)$ is a semigroup.*
(3) *For all $a,b,c \in S, a\cdot(b+c) = a\cdot b + a\cdot c$ and $(a+b)\cdot c = a\cdot c + b\cdot c$*

Definition 2.2. [3] *Let $(S,+,\cdot)$ be a semiring. $\preceq$ is said to be a canonical pre-order if for $a,b \in S, a \preceq b$ if and only if there exists $c \in S$ such that $a+c=b$.*

ion 2.3. [4] *Let $G=(V, E \subset V\times V)$ be a given graph with $V, E \neq \phi$. For any g $(S,+,\cdot)$, a semiring valued graph (or a S-valued graph) G^S is defined to be ph $G^S=(V,E,\sigma,\psi)$ where $\sigma : V \to S$ and $\psi : E \to S$ is defined by: for all $E \subseteq V\times V$.*

$$\psi(x,y) = \begin{cases} min\{\sigma(x),\sigma(y)\} & if\ \sigma(x) \preceq \sigma(y)\ (or)\ \sigma(y) \preceq \sigma(x) \\ 0 & otherwise \end{cases}$$

We call σ, a $S-$ vertex set and ψ an $S-$ edge set of $S-$ valued graph G^S.

Definition 2.4. [1] *Let $G^S = (V, E, \sigma, \psi)$ be a $S-$ valued graph. G^S is said to have a $S-$ path if there is a path in its underlying graph G along with $S-$ values for the vertices and edges of the path.*

Definition 2.5. [1] *Two vertices u and v are said to be $S-$ connected in a $S-$ valued graph G^S, if there is a $S-$ path between them. If every pair of vertices in G^S is $S-$ connected, then the $S-$ valued graph G^S said to be $S-$ connected.*

Definition 2.6. [2] *By a $S-$ path $P^S(uv)$ between $u, v \in V$ in a $S-$ valued graph G^S, we mean the edges that connect the vertices u and v by $P^S(uv)$.*

The Weight of the $S-$ path $P^S(uv)$ is defined as $wt(P^S(uv)) = \sum_{e \in P^S(uv)} \psi(e)$.

Definition 2.7. [2] *Consider the $S-$ valued graph G^S. Let $u, v \in V$. Let $P_i^S(uv)$ be the $i^{th}-$ path that connects u and v. $i = 1, 2, \cdots$ The length of the path $P_i^S(uv)$, denoted by $l(P_i^S(uv)$, is defined to be the number of edges along the path $P_i^S(uv)$.*

Let the set of all paths $P_i^S(uv)$ that connects u and v along with their weights and lengths be denoted by P_{uv}^S. That is

$$P_{uv}^S = \left\{(wt(P_i^S), l(P_i^S)) \mid P_i \text{ is any path connecting } u \text{ and } v,\ i = 1, 2, \cdots, k\right\}$$

Definition 2.8. [7] *Let $G_1^{S_1} = (V_1, E_1, \sigma_1, \psi_1)$ and $G_2^{S_2} = (V_2, E_2, \sigma_2, \psi_2)$ be two given S_1- valued and S_2- valued graphs.*

A homomorphism $f = (\alpha, \beta) : G_1^{S_1} \to G_2^{S_2}$ between two $S-$ valued graphs is a pair of homomorphisms $\alpha : V_1 \to V_2$ which is a graph bijection and $\beta : S_1 \to S_2$, a semiring homomorphism such that $\beta(\sigma_1(v_i)) \preceq \sigma_2(\alpha(v_i))$ and $\beta(\psi_1(v_iv_j)) \preceq \psi_2(\alpha(v_i)\alpha(v_j))\ \forall\ v_i, v_j \in V_1$.

Definition 2.9. [6] *Let $G_1^S = (V_1, E_1, \sigma_1, \psi_1)$ and $G_2^S = (V_2, E_2, \sigma_2, \psi_2)$ be two given $S-$ valued graphs.*

The Categorical product of G_1^S and G_2^S is a $S-$ valued graph defined by

$$G_\times^S = G_1^S \times G_2^S = (V, E, \sigma, \psi)$$

where $V = V_1 \times V_2 = \{w_{ij} = (v_i, u_j) \mid v_i \in V_1$ and $u_j \in V_2\}$

and two vertices $w_{ij} = (v_i, u_j), w_{kl} = (v_k, u_l)$ are adjacent if $v_iv_k \in E_1$ and $u_ju_l \in E_2$

Define $\sigma : V \to S$ by $\sigma(w_{ij}) = \min\{\sigma_1(v_i), \sigma_2(u_j)\}$.

and $\psi : E \to S$ by $\psi(e_{ij}^{kl}) = \psi(w_{ij}, w_{kl}) = \min\left\{\psi_1(e_i^k), \psi_2(e_j^l)\right\}$.

3. Connectivity of Product of $S-$ valued Graphs

In this section, we discuss the connectivity of $S-$ valued graphs under Categorical product and prove some results.

Theorem 3.1. *Homomorphic image of a $S-$path in G_1^S is a $S-$path in G_2^S. That is $S-$valued homomorphism preserves $S-$paths.*

Proof: Let $G_1^S = (V_1, E_1, \sigma_1, \psi_1)$ and $G_2^S = (V_2, E_2, \sigma_2, \psi_2)$ be two given $S-$valued graphs.

Consider a $S-$path

$$P^S(v_1v_n) \text{ in } G_1^S \text{ as } P^S(v_1v_n) = v_1(e_1^2)v_2(e_2^3)v_3\cdots(e_{n-1}^n)v_n$$

with length $l(P^S(v_1v_n)) = n-1$ and weight $wt(P^S(v_1v_n)) = a$ for some $a \in S$.

Consider a $S-$valued homomorphism $f = (\alpha, \beta) : G_1^S \to G_2^S$.

Then $\alpha : V_1 \to V_2$ is graph isomomorphism and $\beta : S \to S$ is semiring homomorphism that satisfies

$$\beta(\sigma_1(v_i)) \preceq \sigma_2(\alpha(v_i)) \text{ and } \beta(\psi_1(e_i^j)) \preceq \psi_2(\alpha(v_i)\alpha(v_j)). \tag{3.1}$$

To prove that $f(P^S(v_1v_n)) = P^S(u_1u_n)$ with $\beta(wt(P^S(v_1v_n)) \preceq wt(\alpha(P^S(v_1v_n))$.

Now $f(P^S(v_1v_n)) = f(v_1(e_1^2)v_2\cdots(e_{n-1}^n)v_n) = (\alpha,\beta)(v_1(e_1^2)v_2\cdots(e_{n-1}^n)v_n)$

$$f(P^S(v_1v_n)) = \Big((\alpha(v_1)\alpha(e_1^2)\alpha(v_2)\cdots\alpha(v_n), \beta(\sigma_1(v_1)\beta(\psi_1(e_1^2))\beta(\sigma_2(v_2))\cdots\beta(\sigma_1(v_n)\Big) \tag{3.2}$$

Since α is graph isomorphism, α preserves edges. That is,

$$\alpha(v_i) = u_j \text{ for some } u_j \in V_2 \text{ and } \alpha(e_i^j) = \alpha(v_i)\alpha(u_j) = (u_iu_j) \in E_2. \tag{3.3}$$

Since β is semiring homomorphism and satifying the condition 3.1, we have

$$\beta(\sigma_1(v_i)) \preceq \sigma_2(\alpha(v_i)) = \sigma_2(u_i) \text{ and } \beta(\psi_1(v_iv_j)) \preceq \psi_2(\alpha(v_i)\alpha(v_j)) = \psi_2(u_iu_j) \tag{3.4}$$

Applying the equations (3.3) and (3.4) in (3.2), we get

$f(P^S(v_1v_n)) = P^S(u_1u_n)$ for some $u_1, u_n \in V_2$.

$$\begin{aligned}
\text{Also } \beta(wt(P^S(v_1v_n)) &= \beta\Big(\sum_{e_i^j \in P^S(v_1v_n)} \psi_1(e_i^j)\Big) = \beta\Big(\sum_{e_i^j \in P^S(v_1v_n)} \psi_1(v_iv_j)\Big) \\
&\preceq \Big(\sum_{\alpha(v_i)\alpha(v_j) \in P^S(u_1u_n)} \psi_2(\alpha(v_i)\alpha(v_j))\Big) \\
&= \Big(\sum_{u_iu_j \in P^S(u_1u_n)} \psi_2(u_iu_j)\Big) \\
&= wt(P^S(u_1u_n))
\end{aligned}$$

Thus $f(P^S(v_1v_n)) = P^S(u_1u_n)$ with $wt(P^S(v_1v_n)) \preceq wt(P^S(u_1u_n))$ and $l(P^S(v_1v_n)) = l(P^S(u_1u_n)) = n-1$.

This implies that, $S-$valued homomorphism preserves $S-$paths between two $S-$valued graphs

cycle is a $S-$path having origin and terminus are same vertex and rem, we obtain the following result easily.

momorphic image of a $S-$cycle in G_1^S is a $S-$cycle in G_2^S.

Definition 3.3. *Let $G_{\times}^{S} = G_1^S \times G_2^S$ be the Categorical product of G_1^S and G_2^S.*
We define the projections $\pi_1 : G_{\times}^{S} \to G_1^S$ by $\pi_1((v_i,u_j),\sigma(v_i,u_j)) = (v_i,\sigma_1(v_i))$
and $\pi_2 : G_{\times}^{S} \to G_2^S$ by $\pi_1((v_i,u_j),\sigma(v_i,u_j)) = (u_j,\sigma_2(u_j))$
Clearly, the projections π_1 and π_2 are $S-$valued homomorphisms.

Theorem 3.4. *Suppose (v,u) and (v',u') are vertices of a Categorical product $G_{\times}^{S} = G_1^S \times G_2^S$, and n is an integer for which G_1^S has a $S-$path $P^S(vv')$ of length n and G_2^S has a $S-$path $P^S(uu')$ of length n. Then $G_{\times}^{S} = G_1^S \times G_2^S$ has a $S-$path of length n from (v,u) to (v',u').*

Proof: Let $G_{\times}^{S} : G_1^S \times G_2^S$ be the Categorical product of $G_1^S = (V_1,E_1,\sigma_1,\psi_1)$ and $G_2^S = (V_2,E_2,\sigma_2,\psi_2)$.

Let $(v,u),(v',u') \in V_1 \times V_2$, where $v,v' \in V_1$ and $u,u' \in V_2$.

Assume that G_1^S has a $S-$path $P^S(vv')$,

$$P^S(vv') = \Big(v = v_0e_1v_1e_2v_2\cdots v_{n-1}e_nv_n = v'\Big)$$

with $l(P^S(vv')) = n$ and $wt(P^S(vv')) = a$ for some $a \in S$.

Also G_2^S has a $S-$path $P^S(uu')$,

$$P^S(uu') = \Big(u = u_0e_1u_1e_2u_2\cdots u_{n-1}e_nu_n = u'\Big)$$

with $l(P^S(uu')) = n$ and $wt(P^S(uu')) = b$ for some $b \in S$.

From the definition of Categorical product,

if $vv_1 \in E_1$ and $uu_1 \in E_2$ then $(v,u)(v_1,u_1) \in E = E_1 \times E_2$.

Then by continuously applying the defintion of categorical product,

we can construct a $S-$path

$$\Big((v,u) = (v_0,u_0)e_{00}^{11}(v_1,u_1)\cdots(v_{n-1},u_{n-1})e_{n-1n-1}^{nn}(v_n,u_n) = (v',u')\Big) \text{ of length } n \text{ in } G_{\times}^{S}$$

That is, $P^S((v,u)(v',u'))$ is a $S-$path with $l(P^S((v,u)(v',u'))) = n$.

$$\begin{aligned}
Now,\ wt\Big(P^S((v,u)(v',u'))\Big) &= \Big(\sum_{e_{ij}^{kl} \in P^S((v,u)(v',u'))} \psi(e_{ij}^{kl})\Big) \\
&= \Big(\sum_{e_{ij}^{kl} \in P^S((v,u)(v',u'))} \psi((v_i,u_j)(v_k,u_l))\Big) \\
&= \Big(\sum_{e_{ij}^{kl} \in P^S((v,u)(v',u'))} min\left\{\psi_1(v_iv_k),\psi_2(u_ju_l)\right\}\Big) \\
&= \begin{cases} \sum\limits_{e_i^k \in P^S(vv')} \psi_1(v_iv_k) & if\ \psi_1(v_iv_k) \preceq \psi_2(u_ju_l) \\ \sum\limits_{e_j^l \in P^S(uu')} \psi_1(u_ju_l) & if\ \psi_2(u_ju_l) \preceq \psi_1(v_iv_k) \end{cases} \\
&= \begin{cases} wt(P^S(vv')) & if\ \psi_1(v_iv_k) \preceq \psi_2(u_ju_l) \\ wt(P^S(uu')) & if\ \psi_2(u_ju_l) \preceq \psi_1(v_iv_k) \end{cases}
\end{aligned}$$

$$= min\left\{wt(P^S(vv')), wt(P^S(uu'))\right\}.$$

Hence, $P^S((v,u)(v',u'))$ is a $S-$path in $G_\times^S = G_1^S \times G_2^S$ if $P^S(vv')$ and $P^S(uu')$ are $S-$paths in G_1^S and G_2^S respectively.

The Converse of the above theorem is proved in the following theorem.

Theorem 3.5. *Suppose there is a $S-$path of length n from (v,u) to (v',u') in $G_\times^S = G_1^S \times G_2^S$. Then each factor G_1^S and G_2^S of $G_\times^S$ has a $S-$path of length n from v to v' and u to u' respectively.*

Proof: Let (v,u) and (v',u') be two vertices in $G_\times^S = G_1^S \times G_2^S$.

Assume that $G_\times^S$ has a $S-$path of length n from (v,u) and (v',u').

Then

$P^S((v,u)(v',u')) = \Big((v,u) = (v_0,u_0)e_{00}^{11}(v_1,u_1)\cdots e_{n-1n-1}^{nn}(v_n,u_n) = (v',u')\Big)$

with length $l(P^S((v,u)(v',u'))) = n$.

Define the projections π_1 and π_2 as follows;

$\pi_1 : G_\times^S \to G_1^S$ by $\pi_1((v_i,u_j),\sigma(v_i,u_j)) = (v_i,\sigma_1(v_i))$

and $\pi_2 : G_\times^S \to G_1^S$ by $\pi_1((v_i,u_j),\sigma(v_i,u_j)) = (u_j,\sigma_2(u_j))$

Clearly, π_1 and π_2 are $S-$valued homomorphisms.

Then by theorem 3.1, we have

$\pi_1(P^S((v,u)(v',u'))) = \Big(v = v_0e_0^1v_1\cdots e_{n-1}^n v_n = v'\Big) = P^S(vv')$ also

$\pi_2(P^S((v,u)(v',u'))) = \Big(u = u_0e_0^1u_1\cdots e_{n-1}^n u_n = u'\Big) = P^S(uu')$

are $S-$paths in G_1^S and G_2^S of length n respectively.

Theorem 3.6. *Consider the Categorical product $G_\times^S = G_1^S \times G_2^S$. If $G_\times^S = G_1^S \times G_2^S$ is $S-$ connected then the factors G_1^S and G_2^S of $G_\times^S$ are $S-$ connected.*

Proof: Let $G_\times^S = G_1^S \times G_2^S$ be a $S-$connected $S-$valued graph.

Then, any two vertices (v,u) and (v',u') in $G_\times^S$ are $S-$connected.

That is , there is a $S-$ path $P^S((v,u)(v',u'))$ between (v,u) and (v',u').

Then by theorem 3.5, there is a $S-$ path between v and v' in G_1^S and

a $S-$path between u and u' in G_2^S for any two vertices $v,v' \in V_1$ and $u,u' \in V_2$.

This implies that, G_1^S and G_2^S are $S-$connected.

The converse of the above theorem need not be true in genral. This is illustrated by the following Example.

Example 3.7. Consider the semiring $S = (\{0,a,b,c\},+,\cdot)$ with the binary operations '+' and' $\cdot$' defined by the following Cayley tables.

+	0	a	b	c
0	0	a	b	c
a	a	b	c	c
b	b	c	c	c
c	c	c	c	c

·	0	a	b	c
0	0	0	0	0
a	0	a	b	c
b	0	b	c	c
c	0	c	c	c

In S we define a canonical pre-order $\preceq$ by

$$0 \preceq 0,\ 0 \preceq a,\ 0 \preceq b,\ 0 \preceq c,\ a \preceq a,\ b \preceq b,\ c \preceq c,\ a \preceq b,\ a \preceq c,\ b \preceq c,$$

Consider the two $S-$ connected bipartite graphs G_1^S and G_2^S :

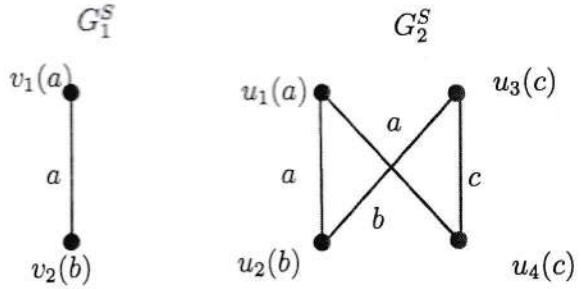

Then the Categorical product $G_1^S \times G_2^S$:

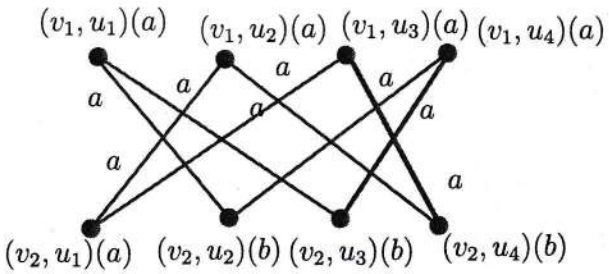

In, $G_\times^S$ the vertices (v_1,u_1) and (v_1,u_2) are not $S-$ Connected.

This implies that, $G_\times^S = G_1^S \times G_2^S$ is not $S-$connected while G_1^S and G_2^S are $S-$connected.

4. Conclusion

In this paper, we have studied the connectivity of Categorical product of $S-$valued graphs. In our future work we will be discussing further results on connectivity of the Categorical product of $S-$valued graphs.

References

[1] **Jeyalakshmi. S and Chandramouleeswaran. M:** *Connected S-Valued Graphs,* Mathematical Sciences International Research Journal, Vol.6(1), (2016).

[2] **Jeyalakshmi. S and Chandramouleeswaran. M:** *Diameter on $S-$valued Graphs,* Mathematical Sciences International Research Journal, Vol.6(1), (2017), pp.121-123.

[3] **Jonathan Golan** *Semirings and Their Applications*, Kluwer Academic Publishers, London.

[4] **Rajkumar. M, Jeyalakshmi. S. and Chandramouleeswaran. M** *Semiring Valued Graphs*, International Journal of Math.Sci. and Engg. Appls., Vol. 9 (3), 2015 pp. 141-152.

[5] **Richard Hammack, Wilfried Imrich and Sandy Klavzar**, *Handbook of Product Graphs,* University of Ljubljana and University of Maribor, Slovenia.

[6] **Victor. P. Chandramouleeswaran. M**, *Categorical Product of Two $S-$valued Graphs.*, thematical Sciences and Engineering Research, Vol. 11(II) (2017), pp.

[7] d **Chandramouleeswaran. M**, *Isomorphism on $S-$ Valued Graphs.*, national Research Journal, Vol. 6 (Spl. Issue)(2017), pp.253-257.

PROCEEDINGS OF THE INTERNATIONAL CONFERENCE ON ADVANCES IN PURE & APPLIED MATHEMATICS 2018

Govt of India Approved International Conference

(MHA Vide F.No 42180123/CC-195, MEA Video No. F.No AA/162/01/2018-903)

Sep 06-08, 2018

ISBN 978-93-86435-53-8

Editors

Dr.M.Lellis Thivagar
Dr. Ratnakar D B

Organized by

thematics, Madurai Kamaraj University, Madurai, India
ional Multidisciplinary Research Foundation, India

CONTENTS

ISBN 978-93-86435-53-8

COST ANALYSIS OF FUZZY QUEUEING MODELS

DR. M.S. ANNIE CHRISTI, R. SINDHUJA

Abstract: In this paper, the performance measures of intuitionistic fuzzy queueing models are analyzed using DSW (Dong, Shah, Wong) algorithm. The priority discipline will have wider applications in the fuzzy queueing models due to its uncertainty. Hence the intuitionistic Hexagonal fuzzy numbers are introduced and the cost of fuzzy -priority queueing models are compared. In many real life situations, Fuzzy queues are more realistic than the commonly used crisp queues.

Keywords: Intuitionistic Hexagonal Fuzzy Number, Priority Discipline Queues, DSW Algorithm.

***

Dr. M.S. Annie Christi
Department of Mathematics, Providence College for Women, Coonoor
R. Sindhuja
Department of Mathematics, Providence College for Women, Coonoor

LEXICOGRAPHIC PRODUCT OF S-VALUED GRAPHS

P. VICTOR, M. CHANDRAMOULEESWARAN

Abstract: In this paper, we study the concept of lexicographic product of two S-valued graphs and prove that the collection of all S-valued graphs forms a right near-semiring under the disjoint union and the lexicographic product.

Keywords: Graph Operations, Lexicographic Product, Semiring, S-Valued Graphs.

***

P. Victor
Assistant Professor, Mohamed Sathak Engineering College,
Kilakarai – 623 806, Tamilnadu, India
M. Chandramouleeswaran
Head, PG Department of Mathematics,
Sri Ramanas College of Arts and Science for Women
Aruppukottai-626134, Tamilnadu, India

LEXICOGRAPHIC PRODUCT OF S-VALUED GRAPHS

P. Victor
Assistant Professor, Mohamed Sathak Engineering College, Kilakarai – 623 806, Tamilnadu, India
M. Chandramouleeswaran
Head, PG Department of Mathematics, Sri Ramanas College of Arts and Science for Women Aruppukottai-626134, Tamilnadu, India

Abstract: In this paper, we study the concept of lexicographic product of two S-valued graphs and prove that the collection of all S-valued graphs forms a right near-semiring under the disjoint union and the lexicographic product.

Keywords: Graph Operations, Lexicographic Product, Semiring, S-Valued Graphs.

1. **Introduction**: The concept of the product of graphs has been defined to generalize the Vizing's theorem. In crisp graph theory there are four types of graph products. Lexicographic product is one such type of product which was introduced as the composition of graphs by Harary [1]. The lexicographic product is also known as graph substitution as, $G \circ H$ can be obtained from G by substituting a copy H_g of H for every vertex g of G and then joining all vertices of H_g with all vertices of $H_{g'}$ if $gg' \in E(G)$.

In [3], the authors introduced the notion of semiring valued graphs by assigning the values for vertices of a given graph from a semiring. The edges are assigned S-values by comparing the S-values for the vertices, using the canonical pre order existing in the semiring. In our earlier paper [7], we have discussed the notion of Categorical product of S-valued graphs and hence proved that the collection of all S-valued graphs forms a semiring under the disjoint union and categorical product. In this paper, we study the concept of lexicographic product of two S-valued graphs and prove that the collection of all S-valued graphs forms a right near-semiring under the disjoint union and the lexicographic product.

2. ***Preliminaries:*** In this section, we recall some basic definitions that are needed in the sequel.
Definition 2.1: [5] The Lexicographic product of the graphs G and H is the graph, $G \circ H$, whose vertex set is $V(G) \times V(H)$, and for which $(g,h)(g',h')$ is an edge of $G \circ H$ if $gg' \in E(G)$ or $g = g'$ and $hh' \in E(H)$.

Definition 2.2: [2] A semiring $(S, +, \cdot)$ is an algebraic system with a non-empty set S together with two binary operations + and · such that
(1) $(S, +)$ is a monoid with identity 0.
(2) $(S, \cdot)$ is a semigroup.
(3) For all $a, b, c \in S, a \cdot (b + c) = a \cdot b + a \cdot c$ and $(a + b).c = a \cdot c + b \cdot c$
(4) $0 \cdot a = a \cdot 0 = 0 \ \forall a \in S$.

Definition 2.3: [2] Let $(S, +, \cdot)$ be a semiring. $\preceq$ is said to be a canonical pre-order if
for a, b ∈ S, a $\preceq$ b if and only if there exists an element c ∈ S such that a + c = b.

Definition 2.4: [3] An algebraic structure $(S, +, \cdot)$ is said to be right near-semiring with a constant 0 if it satisfies the following axioms:

1.
2.
3. $1\ a, b, c \in S$.
4.

Analogously, one can define the left near-semiring.

Definition 2.5: [4] Let $G = (V, E \subset V \times V)$ be a given graph with $V, E \neq \emptyset$. For any semiring $(S, +\ \cdot)$, a semiring valued graph (or a S-valued graph) G^S is defined to be the graph $G^S = (V, E, \sigma, \psi)$ where $\sigma: V \to S$ and $\psi: E \to S$ is defined by: for all $(x, y) \in E \subseteq V \times V$

$$\psi(x,y) = \begin{cases} \min\{\sigma(x), \sigma(y)\} & if\ \sigma(x) \preceq \sigma(y) \text{ or } \sigma(y) \preceq \sigma(x) \\ 0 & otherwise \end{cases}$$

We call σ, a S-vertex set and ψ an S-edge set of the S-valued graph G^S.

Definition 2.6: [5] Let $G_1^S = (V_1, E_1, \sigma_1, \psi_1)$ and $G_2^S = (V_2, E_2, \sigma_2, \psi_2)$ be two given S-valued graphs such that $V_1 \cap V_2 = \phi$. The disjoint union of G_1^S and G_2^S denoted by $G_1^S \cup G_2^S$, is defined by $G_1^S \cup G_2^S = (V, E, \sigma, \psi)$ where $V = V_1 \cup V_2$; $E = E_1 \cup E_2$

1. For $v \in V, \sigma(v) = \begin{cases} \sigma_1(v)\ if\ v \in V_1 \\ \sigma_2(v)\ \ if\ v \in V_2 \end{cases}$

2. For $(v_i, u_j) \in E$, $\psi(v_i, u_j) = \begin{cases} \psi_1(v_i, u_j)\ if\ (v_i, u_j) \in E_1 \\ \psi_2(v_i, u_j)\ if\ (v_i, u_j) \in E_2 \end{cases}$

Definition 2.7: [4] A S-valued graph G^S is said to be

1. Vertex regular if $\sigma(v) = a\ \forall\ v \in V$ and for some $a \in S$
2. Edge regular if $\psi(u, v) = a\ \forall\ (u, v) \in E$ and for some $a \in S$
3. S-regular if it is both vertex as well as edge regular.

Definition 2.8: [6] An S-isomorphism $f = (\alpha, \beta): G_1^{S_1} \to G_2^{S_2}$ is a pair of homomorphisms $\alpha: V_1 \to V_2$, $\beta: S_1 \to S_2$ is such that $\beta(\sigma_1(x)) = \sigma_2(\alpha(x))$ and $\beta(\psi_1(xy)) = \psi_2(\alpha(x)\alpha(y))\ \forall\ xy \in E_1$. If such an isomorphism from $G_1^{S_1}$ to $G_2^{S_2}$ exists and α and β are onto isomorphisms then $G_1^{S_1}$ is said to be S −valued isomorphic to $G_2^{S_2}$ and we write it as $G_1^{S_1} \cong_S G_2^{S_2}$.

3. *Algebraic Structure on Lexicographic Product of S-Valued Graphs:*

In this section, we introduce the notion of lexicographic product of two S-valued graphs and illustrate it with some examples. We prove that the collection of all S-valued graphs forms a right near-semiring under the disjoint union and the lexicographic product.

Definition 3.1: Let $G_1^S = (V_1, E_1, \sigma_1, \psi_1)$ and $G_2^S = (V_2, E_2, \sigma_2, \psi_2)$ be two S-valued graphs with $V_1 = \{\ v_i \mid i = 1, 2, \cdots, n\ \}$ and $V_2 = \{\ u_j \mid j = 1, 2, \cdots, m\ \}$.

Then the lexicographic product of G_1^S and G_2^S is defined as the S-valued graph $G_\circ^S = G_1^S \circ G_2^S = (V, E, \sigma, \psi)$ where $V = V_1 \times V_2 = \{\ w_{ij} = (v_i, u_j) \mid v_i \in V_1, u_j \in V_2\ \}$ and the two vertices w_{ij} and w_{kl} are adjacent if $v_i v_k \in E_1$ or $v_i = v_k$ and $u_j u_l \in E_2$.

Then $E = \{\ e_{ij}^{kl} \mid v_i v_k \in E_1\ or\ v_i = v_k\ and\ u_j u_l \in E_2\ \} \subseteq E_1 \times E_2$. The S-valued function $\sigma: V \to S$ is defined by $\sigma(w_{ij}) = (\sigma_1 \circ \sigma_2)(w_{ij}) = \min\{\ \sigma_1(v_i), \sigma_2(u_j)\}$ and $\psi: E \to S$ is defined by

$$\psi(e_{ij}^{kl}) = (\psi_1 \circ \psi_2)(e_{ij}^{kl}) = \min \begin{cases} \min\{\psi_1(v_i v_k), \min\{\sigma_2(u_j), \sigma_2(u_l)\}\} & if\ v_i v_k \in E_1 \\ \min\{\min\{\ \sigma_1(v_i), \sigma_1(v_k)\}, \psi_2(u_j u_l)\}\ if\ v_i = v_k and\ u_j u_l \in E_2 \end{cases}$$

Example 3.2: Consider the semiring $S = B(5,3) = (\{0,1,2,3,4\},\ \oplus,\ \odot)$ with the binary operations $+$ and $\cdot$ defined by $a \oplus b = \begin{cases} a + b & if\ a + b \leq 4 \\ c & if\ c \equiv a + b\ mod\ 2, 3 \leq c \leq 4 \end{cases}$ and

$a \odot b = \begin{cases} a \cdot b & if\ a \cdot b \leq 4 \\ c, & if\ c \equiv a \cdot b\ mod\ 2, 3 \leq c \leq 4 \end{cases}$

These operations can be represented by the following Cayley Tables:

$\oplus$	0	1	2	3	4
0	0	1	2	3	4
1	1	2	3	4	3
2	2	3	4	3	4
3	3	4	3	4	3
4	4	3	4	3	4

$\odot$	0	1	2	3	4
0	0	0	0	0	0
1	0	1	2	3	4
2	0	2	4	4	4
3	0	3	4	3	4
4	0	4	4	4	4

In S we define a canonical pre-order $\preccurlyeq$ by
$0 \preccurlyeq 0, 0 \preccurlyeq 1, 0 \preccurlyeq 2, 0 \preccurlyeq 3, 0 \preccurlyeq 4, 1 \preccurlyeq 1, 1 \preccurlyeq 2, 1 \preccurlyeq 3, 1 \preccurlyeq 4, 2 \preccurlyeq 2, 2 \preccurlyeq 3,$
$2 \preccurlyeq 4, 3 \preccurlyeq 3,\ 3 \preccurlyeq 4, 4 \preccurlyeq 4, 4 \preccurlyeq 3.$
The lexicographic product of G_1^S and G_2^S is illustrated below:

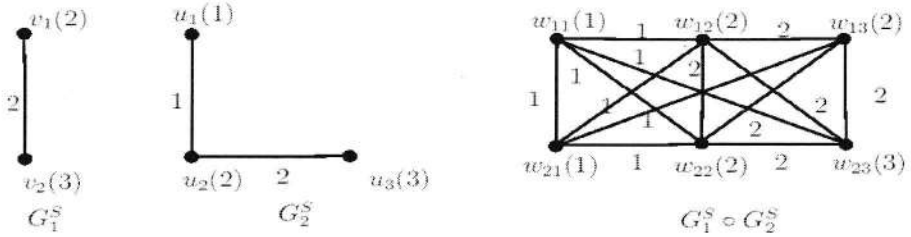

And the lexicographic product of $G_2^S \circ G_1^S$ is given below:

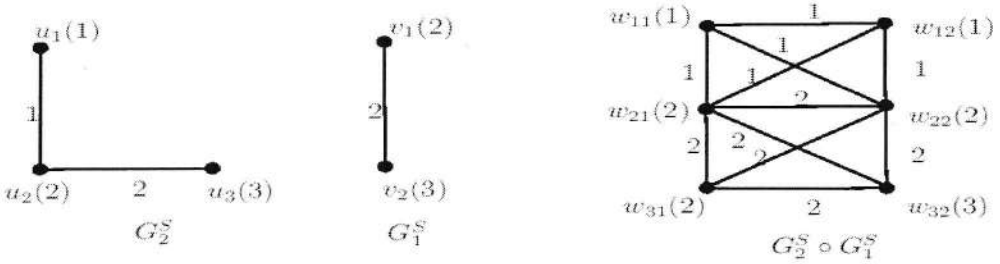

Remark 3.3: From the above example, we observe that the lexicographic product of two S-valued graphs need not be commutative in general.

Theorem 3.4: The lexicographic product of two S-regular graphs is again a S-regular graph.
Proof: Let $G_1^S = (V_1, E_1, \sigma_1, \psi_1)$ and $G_2^S = (V_2, E_2, \sigma_2, \psi_2)$ be two S-regular graphs.
That is, G_1^S and G_2^S is both vertex regular as well as edge regular.

Claim: $G_\circ^S = G_1^S \circ G_2^S = (V, E, \sigma, \psi)$ is S-regular. That is to prove, $\sigma(w_{ij})$ is equal for all $w_{ij} \in V$ and $\psi(e_{ij}^{kl})$ is equal for all $e_{ij}^{kl} \in E$.
Now by definition, for all $i = 1,2,, n$ *and* $j = 1,2,\cdots, m$

$$\sigma(w_{ij}) = \min\left\{\sigma_{1(v_i)}, \sigma_{2(u_j)}\right\} = \begin{cases} \sigma_1(v_i) \ \text{if} \ \sigma_{1(v_i)} \preccurlyeq \sigma_2(u_j) \\ \sigma_2(u_j) \ \text{if} \ \sigma_2(u_j) \preccurlyeq \sigma_1(v_i) \end{cases}$$

Thus in both the cases $\sigma(w_{ij})$ is equal for all $w_{ij} \in V, i = 1,2,\cdots, n$ and $j = 1,2,\cdots, m$.
This implies that $G_\circ^S = G_1^S \circ G_2^S$ is vertex regular. Further,

$$\begin{cases} \min\{\psi_1(v_i v_k), \min\{\sigma_2(u_j), \sigma_2(u_l)\}\} & \text{if } v_i v_k \in E_1 \\ \text{in}\{min\{\sigma_1(v_i), \sigma_1(v_k)\}, \psi_2(u_j u_l)\} & \text{if } v_i = v_k \text{ and } u_j u_l \in E_2 \end{cases}$$

ar, $\sigma_1(v_i) = \psi_1(e_i^k)$ and $\sigma_2(u_j) = \psi_2(e_i^l)$ for all $v_i \in V_1, e_i^k \in E_1$ and $u_j \in$
$_j)$ or $\sigma_2(u_j) \preccurlyeq \sigma_1(v_i)$ in S.

Thus, for all edges $i,k = 1,2,\cdots,n$ *and* $j,l = 1,2,\cdots,m$; $e_{ij}^{kl} \in E$,

$$\psi(e_{ij}^{kl}) = \begin{cases} \sigma_1(v_i) \text{ if } \sigma_1(v_i) \preccurlyeq \sigma_2(u_j) \\ \sigma_2(u_j) \text{ if } \sigma_2(u_j) \preccurlyeq \sigma_1(v_i) \end{cases}$$

This implies that, $\psi(e_{ij}^{kl})$ is equal for all $e_{ij}^{kl} \in E$.
Thus, $G_\circ^S = G_1^S \circ G_2^S$ is S-regular.

Remark 3.5: The lexicographic product of two edge regular S-valued graphs is need not be a edge regular S-valued graph. This is illustrated by the following example.

Example 3.6: Consider the semiring $S = (\{0,a,b,c\},+,\cdot)$ with the binary operations + and · defined by the following Cayley Tables.

+	o	a	b	c
o	o	a	b	c
a	a	b	c	c
b	b	c	c	c
c	c	c	c	c

·	o	a	b	c
o	o	o	o	o
a	o	a	b	c
b	o	b	c	c
c	o	c	c	c

In S, we define a canonical pre-order by $0 \preccurlyeq 0,a,b,c$; $a \preccurlyeq a,b,c$; $b \preccurlyeq b,c$; $c \preccurlyeq c$.

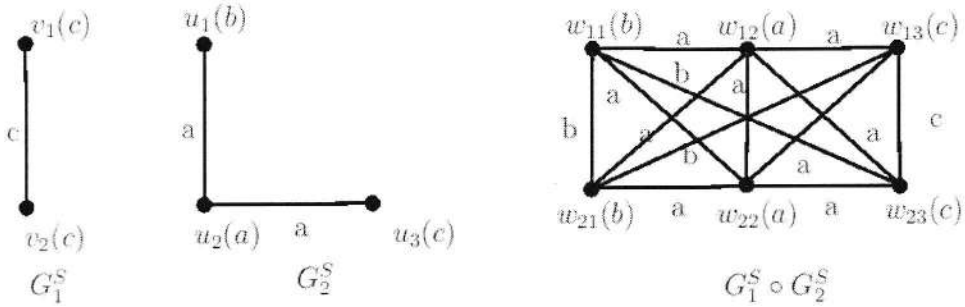

In this example, G_1^S and G_2^S are edge regular S-valued graphs while their lexicographic product $G_\circ^S$ is not a edge regular S-valued graph.

Definition 3.7: Let $G_1^S = (V_1,E_1,\sigma_1,\psi_1), G_2^S = (V_2,E_2,\sigma_2,\psi_2)$ and $G_3^S = (V_3,E_3,\sigma_3,\psi_3)$ be three S-valued graphs.
Then the lexicographic product $G_1^S \circ (G_2^S \circ G_3^S)$ is defined as $G_1^S \circ (G_2^S \circ G_3^S) = G_\circ^S = (V,E,\sigma,\psi)$
where $V = V_1 \times (V_2 \times V_3) = \left\{ z_{i(jk)} = \left(u_i,(v_j,w_k)\right) \mid u_i \in V_1, v_j \in V_2, w_k \in V_3 \right\}$ and two vertices $\left(u_l,(v_j,w_k)\right),(u_l,(v_m,w_n))$ are adjacent if $u_iu_l \in E_1$ or $u_i = u_l$ and $(v_j,w_k)(v_m,w_n) \in E_2 \times E_3$.
Then, $E = \left\{ e_{i(jk)}^{l(mn)} \mid u_iu_l \in E_1 \text{ or } u_i = u_l \text{ and } (v_j,w_k)(v_m,w_n) \in E_2 \times E_3 \right\}$.
The S-valued functions $\sigma = \sigma_1 \circ (\sigma_2 \circ \sigma_3): V \to S$ and $\psi = \psi_1 \circ (\psi_2 \circ \psi_3): E \to S$ is defined by $\sigma\left(u_i,(v_j,w_k)\right) = \min\{\sigma_1(u_i),(\sigma_2 \circ \sigma_3)(v_j,w_k)\}$ and

$$\psi\left(e_{i(jk)}^{l(mn)}\right)$$

$$= \begin{cases} \min\{\psi_{1(u_iu_l)}, \min\{\psi_1(u_iu_l), \min\{(\sigma_2 \circ \sigma_3)(v_j,w_k),(\sigma_2 \circ \sigma_3)(v_m,w_n)\}\} & \text{if } e_i^l \in E_1 \\ \min\left\{\min\{\sigma_1(u_i),\sigma_1(u_l)\},(\psi_2 \circ \psi_3)\left((v_j,w_k)(v_m,w_n)\right)\right\} & \text{if } u_i = u_k, e_{jk}^{mn} \in E_2 \end{cases}$$

$$= \min\left\{\sigma\left(u_i,(v_j,w_k)\right),\sigma\left(u_l,(v_m,w_n)\right)\right\}$$

milarly, we can define $G'^S = (G_1^S \circ G_2^S) \circ G_3^S = (V',E',\sigma',\psi')$ where
$= (V_1 \times V_2) \times V_3 = \left\{ z_{(ij)k} = \left((u_i,v_j),w_k\right) \mid u_i \in V_1, v_j \in V_2, w_k \in V_3 \right\}$ and

$E' = \left\{ e_{(ij)k}^{(lm)n} \mid (u_i, v_j)(u_l, v_m) \in E_1 \times E_2 or\ (u_i, v_j) = (u_l, v_m) and\ w_k w_n \in E_3 \right\}$.

Theorem 3.8: The lexicographic product of S-valued graphs satisfies the associativity upto isomorphism. That is $G_1^S \circ (G_2^S \circ G_3^S) \cong_S (G_1^S \circ G_2^S) \circ G_3^S$.
Proof: Let $G^S = G_1^S \circ (G_2^S \circ G_3^S)$ and $G'^S = (G_1^S \circ G_2^S) \circ G_3^S$.

Claim: $G^S \cong_S G'^S$

For, define a mapping $f = (\alpha, \beta): G^S \to G'^S$ by $f\left(u_i, (v_j, w_k)\right) = \left(\alpha\left(u_i, (v_j, w_k)\right), \beta\left(\sigma\left(u_i, (v_j, w_k)\right)\right)\right)$

where $\alpha: V \to V'$ defined by

$\alpha\left(z_{i(jk)}\right) = z_{(ij)k}$ and $\beta: \sigma(V) \to \sigma'(V')$ defined by $\beta\left(\sigma\left(z_{i(jk)}\right)\right) = \sigma'\left(z_{(ij)k}\right)$.

Claim 1: α is Graph Isomorphism:

From the definition of lexicographic product, $\left(u_i, (v_j, w_k)\right)\left(u_l, (v_m, w_n)\right)$ is an edge of $G_1^S \circ (G_2^S \circ G_3^S)$ if one of the following three conditions holds:
$u_i u_l \in E_1\ or\ u_i = u_l and\ v_{jv_m} \in E_2 or\ u_i = u_l and\ v_j = v_m and\ w_k w_n \in E_3$.
On the other hand, the same conditions are hold for an edge $\left((u_i, v_j), w_k\right)\left((u_l, v_m), w_n\right)) \in E'$.
This implies that α is graph homomorphism.
Moreover, α is bijective mapping.
Hence, α is graph isomorphism.

Claim 2: β is Semiring Homomorphism:

Since $\left(u_i, (v_j, w_k)\right) = \min\{\sigma_1(u_i), (\sigma_2 \circ \sigma_3)(v_j, w_k)\} = \sigma'\left((u_i, v_j), w_k\right)$, $\beta(\sigma\left(u_i, (v_j, w_k)\right) = \sigma'\left((u_i, v_j), w_k\right)$ is an identity map.
This implies that, β is well defined and bijective.
Also β is an additive and multiplicative map.
Thus β is semiring homomorphism.

Claim 3:

To prove, $\beta(\sigma\left(z_{i(jk)}\right) = \sigma'\left(\alpha\left(z_{i(jk)}\right)\right)$ and $\beta\left(\psi\left(e_{i(jk)}^{l(km)}\right)\right) = \psi'\left(\alpha\left(z_{i(jk)}\right)\alpha\left(z_{l(km)}\right)\right)$

For, $\beta\left(\sigma\left(z_{i(jk)}\right)\right) = \beta\left(\sigma\left(u_i, (v_j, w_k)\right)\right) = \sigma'\left(\alpha\left(z_{i(jk)}\right)\right)$

And $\beta\left(\psi\left(e_{i(jk)}^{l(mn)}\right)\right) = \beta\left(\min\left\{\sigma\left(u_i, (v_j, w_k)\right), \sigma(u_l, (v_m, w_n))\right\}\right)$

$$= \begin{cases} \sigma'\left((u_i, v_j), w_k\right) & if\ \sigma\left(u_i, (v_j, w_k)\right) \preccurlyeq \sigma(u_l, (v_m, w_n)) \\ \sigma'\left((u_l, v_m), w_n\right) & if\ \sigma(u_l, (v_m, w_n)) \preccurlyeq \sigma\left(u_i, (v_j, w_k)\right) \end{cases} \cdots\cdots (3.1)$$

Now, $\psi'\left(\alpha\left(z_{i(jk)}\right)\alpha\left(z_{l(mn)}\right)\right) = \psi'\left(z_{(ij)k} z_{(lm)n}\right) = \psi'\left(\left((u_i v_j), w_k\right)\left((u_l, v_m), w_n\right)\right)$

$$= \begin{cases} \sigma'\left((u_i, v_j), w_k\right) & if\ \sigma'\left((u_i, v_j), w_k\right) \preccurlyeq \sigma'\left((u_l, v_m), w_n\right) \\ \sigma'\left((u_l, v_m), w_n\right) & if\ \sigma'\left((u_l, v_m), w_n\right) \preccurlyeq \sigma'\left((u_i, v_j), w_k\right) \end{cases} \cdots\cdots (3.2)$$

From equations 3.1 and 3.2 we get $\beta\left(\psi\left(e_{i(jk)}^{l(mn)}\right)\right) = \psi\left(\alpha\left(z_{i(jk)}\right)\alpha\left(z_{l(mn)}\right)\right)$.

Therefore $f = (\alpha, \beta): G^S \to G'^S$ is an S-isomorphism.
That is $G_1^S \circ (G_2^S \circ G_3^S) \cong_S (G_1^S \circ G_2^S) \circ G_3^S$.
This implies that, lexicographic product of S-valued graphs satisfies the associativity upto isomorphism.

ıphic product of S-valued graphs satisfies the right distributive law over the
aphs. That is, $(G_1^S \cup G_2^S) \circ G_3^S = (G_1^S \circ G_3^S) \cup (G_2^S \circ G_3^S)$.
$_1), G_2^S = (V_2, E_2, \sigma_2, \psi_2)$ and $G_3^S = (V_3, E_3, \sigma_3, \psi_3)$ be three S-valued graphs.

Let $G_1^S \cup G_2^S = (V', E', \sigma', \psi')$ where $V' = V_1 \cup V_2$ and $E' = E_1 \cup E_2$.
The S-valued function $\sigma': V' \to S$ and $\psi': E' \to S$ is defined by

$$\sigma'(u') = \begin{cases} \sigma_1(u_i) \text{ if } u' = u_i \in V_1 \text{ for some } i \\ \sigma_2(v_j) \text{ if } u' = v_j \in V_2 \text{ for some } j \end{cases}$$

$$\text{And } \psi'(u'v') = \begin{cases} \psi_1(u_iu_l) \text{ if } u'v' \in E_1 \\ \psi_2(v_jv_m) \text{ if } vu'v' \in E_2 \end{cases}$$

Now, $(G_1^S \cup G_2^S) \circ G_3^S = \big((V_1 \cup V_2) \times V_3, (E_1 \cup E_2) \times E_3, \sigma = \sigma' \circ \sigma_3, \psi = \psi' \circ \psi_3\big)$

$$\sigma: (V_1 \cup V_2) \times V_3 \to S \text{ by } \sigma(u', w_k) = \begin{cases} \min\{\sigma_1(u_i), \sigma_3(w_k)\} \text{ if } u' \in V_1 \\ \min\{\sigma_2(v_j), \sigma_3(w_k)\} \text{ if } u' \in V_2 \end{cases}$$

and $\psi: (E_1 \cup E_2) \times E_3 \to S$ by

$$\psi\big((u', w_k)(v', w_n)\big) = \begin{cases} \min\{\psi'(u'v'), min\{\sigma_3(w_k), \sigma_3(w_n)\}\} & \text{if } u'v' \in E' \\ \min\{\min\{\sigma'(u'), \sigma'(v')\}, \psi_3(w_kw_n)\} \text{ if } u' = v' \text{ and } w_kw_n \in E_3 \end{cases}$$

$$\psi\big((u', w_k)(v', w_n)\big) = \begin{cases} \min\{\psi_1(u_iu_l), \min\{\sigma_3(w_k), \sigma_3(w_n)\}\} & \text{if } u'v' \in E_1 \\ \min\{\psi_2(v_jv_m), min\{\sigma_3(w_k), \sigma_3(w_n)\}\} & \text{if } u'v' \in E_2 \\ \min[min\{\sigma_1(u_i), \sigma_1(u_i)\}, \psi_3(w_kw_n)\} \text{ if } u' = v' \in V_1; w_kw_n \in E_2 & \\ \min\{min\{\sigma_2(v_j), \sigma_2(v_j)\}, \psi_3(w_kw_n)\} \text{ if } u' = v' \in V_2; w_kw_n \in E_3 & \end{cases} \quad \ldots(3.3)$$

Now, $G_1^S \circ G_3^S = (V_1 \times V_3, E_1 \times E_3, \sigma_1 \circ \sigma_3, \psi_1 \circ \psi_3)$ where $(\sigma_1 \circ \sigma_3)(u_i, w_k) = \min\{\sigma_1(u_i), \sigma_3(w_k)\}$ and

$$(\psi_1 \circ \psi_3)\big((u_i, w_k)(u_l, w_n)\big) = \begin{cases} \min\{\psi_1(u_iu_l), min\{\sigma_3(w_k), \sigma_3(w_n)\}\} & \text{if } u_iu_l \in E_1 \\ \min\{min\{\sigma_1(u_i), \sigma_1(u_l)\}, \psi_3(w_kw_n)\} & \text{if } u_i = u_l; w_kw_n \in E_3 \end{cases}$$

And $G_2^S \circ G_3^S = (V_2 \times V_3, E_2 \times E_3, \sigma_2 \times \sigma_3, \psi_2 \times \psi_3)$ where $(\sigma_2 \times \sigma_3)(v_j, w_k) = \min\{\sigma_2(v_j), \sigma_3(w_k)\}$ and

$$(\psi_2 \circ \psi_3)\big((v_j, w_k)(v_m, w_n)\big) = \begin{cases} \min\{\psi_2(v_jv_m), min\{\sigma_3(w_k), \sigma_3(w_n)\}\} & \text{if } v_jv_m \in E_2 \\ \min\{\min\{\sigma_2(v_j), \sigma_2(v_m)\}, \psi_3(w_kw_n)\} \text{ if } v_j = v_m; w_kw_n \in E_3 & \end{cases}$$

Then, $(G_1^S \circ G_3^S) \cup (G_2^S \circ G_3^S) = (V, E, \sigma, \psi)$ where $V = (V_1 \times V_3) \cup (V_2 \times V_3)$,
$E = (E_1 \times E_3) \cup (E_2 \times E_3)$ and $\sigma: V \to S$ is defined by

$$\sigma(u, v) = \begin{cases} \min\{\sigma_1(u_i), \sigma_3(w_k) \text{ if } (u, v) = (u_i, w_k) \in (V_1 \times V_3) \\ \min\{\sigma_2(v_j), \sigma_3(w_k)\} \text{ if } (u, v) = (v_j, w_k) \in (V_1 \times V_3) \end{cases}$$

and $\psi: E \to S$ is defined by

$$\psi\big((u, v)(u', v')\big) = \begin{cases} (\psi_1 \circ \psi_3)\big((u_i, w_k)(u_l, w_n)\big) & \text{if } (u, v)(u', v') \in E_1 \times E_3 \\ (\psi_2 \circ \psi_3)\big((v_j, w_k)(v_m, w_n)\big) & \text{if } (u, v)(u', v') \in E_2 \times E_3. \end{cases}$$

$$\psi\big((u, v)(u', v')\big) = \begin{cases} \min\{\psi_1(u_iu_l), min\{\sigma_3(w_k), \sigma_3(w_n)\}\} & \text{if } u_iu_l \in E_1 \\ \min\{min\{\sigma_1(u_i), \sigma_1(u_i)\}, \psi_3(w_kw_n)\} \text{ if } u_i = u_l \in V_1 \text{and } w_kw_n \in E_3 & \\ \min\{\psi_2(v_jv_m), min\{\sigma_3(w_k), \sigma_3(w_n)\}\} & \text{if } v_jv_m \in E_2 \\ \min\{\min\{\sigma_2(v_j), \sigma_2(v_j)\}, \psi_3(w_kw_n)\} & \text{if } v_j = v_m \in V_2; w_kw_n \in E_3 \end{cases}$$
$$\ldots\ldots\ldots\ldots\ldots\ldots (3.4)$$

Therefore from the equations (3.3) and (3.4), both $(G_1^S \cup G_2^S) \circ G_3^S$ and
$(G_1^S \circ G_3^S) \cup (G_2^S \circ G_3^S)$ have the same S-vertex set and S-edge set.
Thus, $(G_1^S \cup G_2^S) \circ G_3^S = (G_1^S \circ G_3^S) \cup (G_2^S \circ G_3^S)$.

Remark 3.10: The lexicographic product of S-valued graphs does not satisfy the left distributive law over the union of S-valued graphs as seen in the following example.

Example 3.11: Consider the semiring $S = B(5,3) = (\{0,1,2,3,4\}, +, \cdot)$ as in example 3.2
For the S-valued graphs G_1^S, G_2^S and G_3^S, $G_1^S \circ (G_2^S \cup G_3^S)$ is:

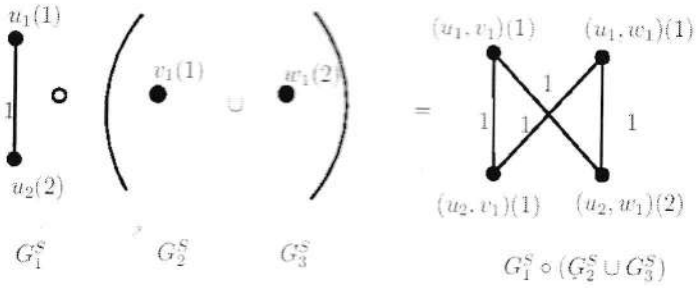

And $(G_1^S \circ G_2^S) \cup (G_1^S \circ G_3^S)$ is

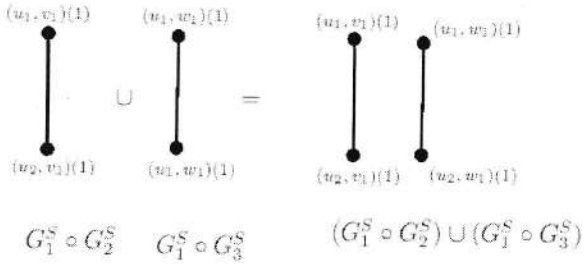

This example illustrates that $G_1^S \circ (G_2^S \cup G_3^S) \neq (G_1^S \circ G_2^S) \cup (G_1^S \circ G_3^S)$.

Theorem 3.12: The set of all S-valued graphs Γ^S forms a right near semiring with respect to the disjoint union and the lexicographic product of S-valued graphs.
That is, $(\Gamma^S, \cup, \circ)$ is a right near semiring.
Proof: Let Γ^S be the set of all S-valued graphs. Trivially $(\Gamma^S, \cup)$ is a semigroup.
Moreover, the empty graph acts as a constant 0 of Γ^S.
Thus, $(\Gamma^S, \cup, 0)$ is a monoid.
From the theorems, 3.8 and 3.9 we have, $(\Gamma^S, \circ)$ is a semigroup and $\circ$ satisfy the right distributive law with respect to disjoint union.
Also, lexicographic product of any S-valued graphs with empty S-valued graph is a empty graph.
Thus, $(\Gamma^S, \cup, \circ)$ is a right near semiring.

References:

1. Harary. F: *On the group of Composition of two Graphs,* Duke.Math.J., Vol.26 (1959), 29-36.
2. Jonathan Golan: *Semirings and their Applications,* Kluwer Academic Publishers, London.
3. Krishna. K.V: *Near-Semirings,* Theory and Application, Ph.D.,thesis, IIT Delhi. India(2005)
4. Rajkumar. M, Jeyalakshmi. S. and Chandramouleeswaran. M: *Semiring Valued Graphs*, International Journal of Math.Sci. and Engg. Appls., Vol. 9 (3), 2015 pp. 141-152.
5. Richard Hammack, Wilfried Imrich and Sandy Klavzar: *Handbook of Product Graphs*, CRC Press, Newyork (2011).
6. Victor. P, Sundar. M. and Chandramouleeswaran. M: *Isomorphism on S-Valued Graphs,* Mathematical Sciences International Research Journal, Vol.6 (2017), pp.253-257.
7. Victor. P, Chandramouleeswaran. M: *Categorical Product of two S-valued Graphs,* International Journal of Math.Sci and Engg.Appls., Vol.11(III),(2017), pp.113-122.

***

Asian Journal of Chemistry; Vol. 28, No. 11 (2016), 2487-2494

ASIAN JOURNAL OF CHEMISTRY

http://dx.doi.org/10.14233/ajchem.2016.20039

Synthesis, Characterization and Biological Activity of Zn(II) Complexes with Dibasic Tridentate ONS-Donor Ligand

B. KARPAGAM[1], S. MATHAN KUMAR[2], J. RAJESH[3], K. DHAHAGANI[4] and G. RAJAGOPAL[5,*]

[1]Department of Chemistry, St. Michael College of Engineering and Technology, Kalayarkoil-630 551, India
[2]Department of Chemistry, K.S. Rangasamy College of Arts and Science (Autonomous), K.S.R. Kalvi Nagar, Tiruchengode-637 215, India
[3]Department of Chemistry, Sethu Institute of Technology, Kariapatti-626 106, India
[4]Department of Chemistry, M.S.S. Wakf Board College, Madurai-625 020, India
[5]PG & Research Department of Chemistry, Chikkanna Government Arts College, Tiruppur-641 602, India

*Corresponding author: E-mail: rajagopal18@yahoo.com

Received: 13 April 2016; *Accepted*: 30 July 2016; *Published online*: 10 August 2016; AJC-18024

A new kind of zinc(II) complexes **1** and **2** with new Schiff base ligand **(L)** have been synthesized and characterized by ^{1}H NMR, X-ray crystallography, IR and UV-visible spectroscopic studies. The trigonality index τ of 0.63 for complex **2** indicates that the coordination geometry around zinc is intermediate between trigonal bipyramidal and square pyramidal geometries and is better described as trigonal bipyramidal distorted square based pyramid (TBDSBP) with zinc displaced above the N(2), N(4), O(1) and S(1) coordination plane and towards the elongated apical N(1) atom. The newly synthesized Schiff base ligand **(L)** and its Zn(II) complexes **1**-**2** were assayed for *in vitro* antibacterial activity against two Gram-positive bacteria strains *(Staphylococcus aureus*, *Pseudomonas aeruginosa)* and Gram-negative bacteria *E. coli.* The cancer cell line studies of the effect of the ligand **(L)** and its Zn(II) complexes **1**-**2** on a MCF-7 cancer cell line by an MTT assay indicates that the ligand **(L)** exhibits higher activity towards the metal complexes **1** and **2** when compared with cyclophosphamide as reference drug.

Keywords: Thiosemicarbazone ligand, Zn(II) complexes, Crystal structure, Cell line studies.

INTRODUCTION

Thiosemicarbazones and their metal complexes exhibit a wide range of applications that extend from their use in analytical chemistry through pharmacology to nuclear medicine [1-4]. Schiff bases are regarded as "privileged ligands" due to their capability to form complexes with a wide range of transition metal ions yielding stable and intensely coloured metal complexes. Some of them have been shown to exhibit interesting physical and chemical properties and potential biological activities [5-10]. Attempts are being made to replace these platinum-based drugs with suitable alternatives and numerous metal complexes are synthesized and screened for their anticancer activities [11,12]. A wide repertoire of Zn(II) complexes have been utilized as radio protective agents [13] tumor photosensitizers [14] antidiabetic insulin-mimetic [15] and antibacterial or antimicrobial agents [16]. It is also eful to reduce the cardio and anticancer drugs [17]. However, city of zinc-based compounds s are as yet available [18].

In continuation of our work in the area of Schiff base complexes [19,20] a new type of Zn(II) complexes have been synthesized and characterized by NMR, IR, UV-visible spectroscopic methods and single crystal X-ray studies for the newly synthesized Zn(II) complexes **1** and **2**. Based on these studies a trigonal bipyramidal distorted square based pyramid (TBDSBP) has been proposed for the Zn(II) complexes. Apart from these studies in order to get a clear cut idea about the pharmacological properties of the Zn(II) complexes, antibacterial, antifungal and cancer cell line studies have been carried out.

EXPERIMENTAL

3-Ethoxysalicylaldehyde (Sigma-Aldrich) and N(4)-phenylthiosemicarbazide (Sigma-Aldrich), $Zn(OAc)_2{\cdot}2H_2O$, 2,2'-bipyridine (bpy) (Sigma-Aldrich), 1,10-phenanthroline (Phen) (E-Merck) were obtained commercially and used without further purification. Double distilled water is used for all the experiments. All the reagents and solvents were analytical, spectroscopic grade and they were used without further purification for the preparation of thiosemicarbazone ligand **(L)** and Zn(II) complexes **1** and **2**.

Physical measurements: Crystal data collection APEX2 (Bruker, 2004); cell refinement: SAINT (Bruker, 2004), ^{1}H NMR spectra are recorded on a Bruker 300 MHz spectrometer. IR spectra are recorded in KBr disks with a Perkin Elmer FT-IR spectrophotometer. UV-visible spectra of solution are recorded on a Shimadzu 1700 series spectrometer.

Antifungal screening: The antifungal activity of the ligand (**L**) and their Zn(II) complexes (**1-2**) are studied by paper disc method [21]. *Candida albicans sp*, *Aspergillus niger sp* and *Macrophonia sp* are used as test organisms. Solution of desired concentration (1 mg/mL) was obtained by dissolving 2, 4, 6 mg of each compound in DMSO and added to potato dextrose agar (PDA) medium in sterile Petri dishes. The sterilized medium with the added sample solution is poured into sterile Petri plates and allowed to solidify. Filter paper discs of 5 mm diameter are prepared prior to the experiment. The filter paper discs are placed on nutrient medium mixed with fungal strains. These Petri dishes are incubated at 35 °C for 48 h. The per cent reduction in the radial growth diameter over the control is calculated. The growth is compared with dimethyl sulfoxide as the control and *Ketokonazole* as a standard drug.

Antibacterial screening: Antibacterial activities are investigated using agar well diffusion method. The activity of the free ligand (**L**) and its Zn(II) complexes **1-2** and standard drug amikacin are studied against the Gram-positive bacteria strains (*Stapholococcus aureus*, *Pseudomonas aeruginosa*) and Gram-negative bacteria *E. coli*. The solution of 2 mg/mL of each compound [free ligand (**L**)] and its Zn(II) complexes (**1-2**) and standard drug (amikacin) in DMSO is prepared for testing against bacteria. Centrifuged pellets of bacteria from a 24 h old culture containing approximately 10^4 to 10^6 CFU (colony forming unit) per mL are spread on the surface of Muller Hinton agar plates. Wells are created in medium with the help of a sterile metallic bores and nutrients agar media (agar 20 g + beef extract 3 g + peptones 5 g) in 1000 mL of distilled water (pH 7.0), autoclaved and cooled down to 45 °C. Then, it is seeded with 10 mL of prepared inocula to have 10^6 CFU/mL. Petri plates are prepared by pouring 75 mL of seeded nutrient agar. The activity is determined by measuring the diameter of the inhibition zone (mm). The growth inhibition is calculated according to Kumar *et al.* [21].

Cell viability test: The viability of cells is assessed by MTT assay using mononuclear cells. The assay is based on the reduction of soluble yellow tetrazolium salt to insoluble purple formazan crystals by metabolically active cells. Only live cells are able to take up the tetrazolium salt. The enzyme (mitochondrial succinate dehydrogenase) present in the mitochondria of the live cells is able to convert internalized tetrazolium salt to formazan crystals, which are purple in colour. Then, the cells are lysed and dissolved in DMSO solution. The colour developed is then determined in an ELISA reader at 570 nm.

The Hepatocellular carcinoma cells (HepG2 cells) are plated separately in 96 well plates at a concentration of 1 × 10^5 cells/well. After 24 h, cells are washed twice with 100 µL [illegible]rved for 0.5 h at 37 °C. After [illegible]ith different concentrations of [illegible]) for 24 h. At the end of the treatment period, the medium is aspirated and serum free medium containing MTT (0.5 mg/mL) is added, then it is incubated for 4 h at 37 °C in a CO_2 incubator.

The MTT containing medium is then discarded and the cells are washed with PBS (200 µL). The crystals are then dissolved by adding 100 µL of DMSO and this is mixed properly by pipetting up and down. Spectrophotometrical absorbance of the purple blue formazan dye is measured in a micro-plate reader at 570 nm [22].

Synthesis of Schiff base ligand (L): 3-Ethoxy salicylaldehyde (0.5 mmol) in methanol (0.83 g) was taken in a round bottomed flask and stirred by a magnetic stirrer followed by dropwise addition of methanolic solution of 4-phenylthiosemicarbazide (3.0 mmol) for 2 to 4 h (**Scheme-I**). The resulting white solid was removed by filtration and washed with cold ethanol and dried *in vacuo* over anhydrous $CaCl_2$ to remove any moisture. m.p.: 210 °C, Yield: 82 %

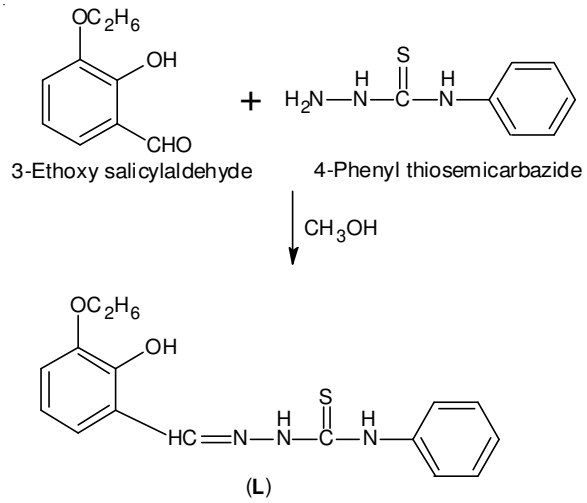

Scheme-I: Synthesis of the new thiosemicarbazone ligand (**L**)

Synthesis of the Zn(II) complexes 1-2: A solution of $Zn(OAc)_2{\cdot}2H_2O$ (0.55 g, 0.25 mmol) in ethanol, was added to a solution of thiosemicarbazone ligand (**L**) (0.79 g, 0.25 mmol) in a round bottomed flask with constant stirring. After 0.5 h, the base (0.25 mmol 2,2'-bipyridine)/(0.25 mmol 1,10-phenanthroline) dissolved in ethanol was added in the round bottomed flask. The stirring was continued for about 1 h and the yellow colour compound formed was filtered, washed with cold ethanol and ether and dried *in vacuo* over anhydrous $CaCl_2$. A single orange colour crystal suitable for the X-ray diffraction was obtained by slow evaporation of a solution of chloroform (**Scheme-II**).

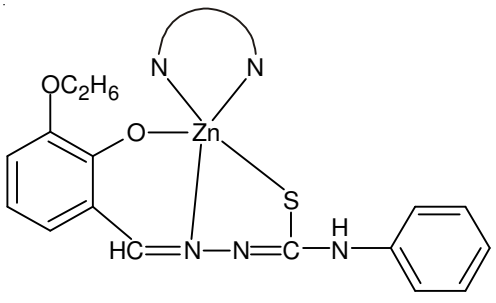

Scheme-II: Proposed structure of the complexes **1** and **2**

TABLE-1
CRYSTAL DATA AND STRUCTURE REFINEMENT FOR COMPLEX [ZnL(phen) (**1**) AND [ZnL(bpy)] (**2**)

Crystal data	Compound **1**	Compound **2**
Empirical formula	$C_{29}H_{24}N_5O_2SZnCl_3$	$C_{55}H_{52}N_{10}O_5S_2Zn_2$
Formula weight	678.31	1127.93
Wavelength	0.71073 Å	0.71073 Å
Crystal system	Monoclinic	Monoclinic
Space group	C2/c	P21/n
a, b, c (Å)	25.6400(6), 14.7350(4), 15.7130(3)	13.6702(4), 14.6101(5), 26.4561(8)
α, β, γ (°)	90, 90.7280(10), 90	90, 93.9540(10), 90
Volume	5936.0 (2) $Å^3$	5271.3 (3) $Å^3$
Z, Calculated density	8, 1.518 Mg/m^3	4, 1.421 Mg/m^3
F(000)	2768	2336
Crystal size	0.35 × 0.35 × 0.30 mm^3	0.30 × 0.20 × 0.20 mm^3
Temperature	293 (2) K	293 (2) K
θ Min-Max	2.05 to 25.00°	1.59 to 25.00°
Completeness to θ	25.00 99.9 %	25.00 99.8 %
Max. and Min. transmission	0.7536 and 0.6536	0.8563 and 0.7236
Final R indices [I >2σ(I)]	R1 = 0.0329, wR2 = 0.0828	R1 = 0.0360, wR2 = 0.0780
R indices (all data)	R1 = 0.0443, wR2 = 0.0916	R1 = 0.0648, wR2 = 0.0935
Largest diff. peak and hole	0.543 and -0.362 e.$Å^{-3}$	0.331 and -0.246 e.$Å^{-3}$

RESULTS AND DISCUSSION

Crystal structure of complex 1: The molecular structure of the complex along with atomic numbering is given in Fig. 1, Crystallographic parameters and selected bond lengths and angles are given in Tables 1 and 2. The compound crystallizes in a monoclinic lattice with space group C2/c. The zinc in the mononuclear complex is five-coordinate and is having approximately trigonal bipyramidal geometry. The basal coordination positions are occupied by the phenolato oxygen, O(1), azomethine nitrogen, N(5) and thiolate sulfur, S(1), of the thiosemicarbazone and the phen nitrogen, N(2). In a five-coordinate system, the angular structural parameter (τ) is used to propose an index of trigonality. In a five-coordinate system, the angular structural parameter (τ) is used to propose an index of trigonality. The trigonality index τ of 0.55 [According to Addison *et al.* [23], τ = (β-α)/60, where β = N(5)-Zn(1)-N(1) = 174.81(8)° and α = O(1)-Zn(1)-S(1) = 141.29(6)°] for perfect square pyramidal and trigonal bipyramidal geometries the values of τ are zero and unity, respectively [23]. This indicates that the coordination geometry around zinc is intermediate between trigonal bipyramidal and square pyramidal geometries and is better described as trigonal bipyramidal distorted square based pyramid (TBDSBP) with zinc displaced above the N(1), N(5), O(1) and S(1) coordination plane and towards the elongated apical N(2) atom [24]. The four base atoms are coplanar showing a significant distortion form a trigonal bipyramidal distorted square based pyramid geometry indicated by O(1)-Cu(1)-S(1) bond angle (141.29°). The central zinc atom is displayed from the basal plane in the direction of the axial nitrogen, which is evident from the bond angles of N(5)-Zn(1)-N(1), (174.81°), O(1)-Zn(1)-N(5), (89.95°). The bond angles O(1)-Zn(1)-N(2), (106.06°), N(2)-Zn(1)-N(1), (76.91°), N(5)-Zn(1)-N(2), (99.20°) indicate the distortion from a trigonal bipyramidal d geometry (τ = 0.55). One of om an ideal stereochemistry is osed by both the ligand and -N(2) bond angle 106.06° and

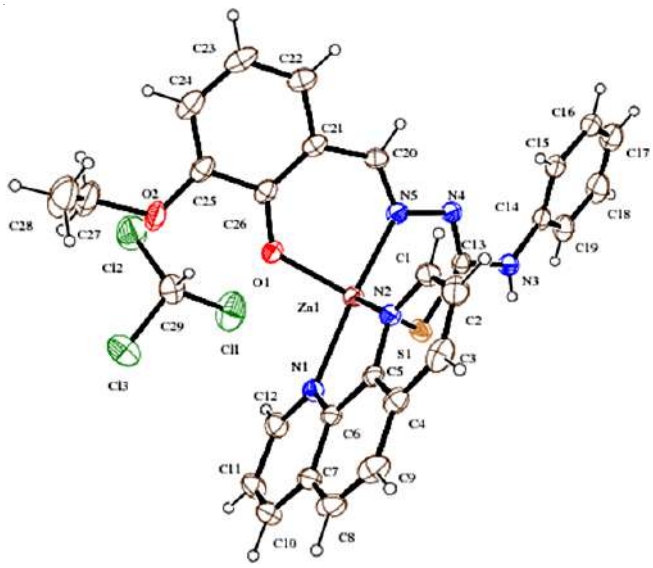

Fig. 1. Structure and labeling diagram of the complex **1**

TABLE-2
SELECTED BOND LENGTHS AND ANGLES FOR COMPLEXES **1-2**

Atoms	Compound **1**	Compound **2**
	Bond lengths	
N(1)-Zn(1)	2.189(2)	2.117(2)
N(2)-Zn(1)	2.132(2)	2.171(2)
O(1)-Zn(1)	1.9625(16)	1.944(2)
S(1)-Zn(1)	2.3737(7)	2.3362(8)
	Bond angles	
O(1)-Zn(1)-N(2)	106.06(8)	76.27(10)
O(1)-Zn(1)-N(1)	94.42(7)	101.59(9)
O(1)-Zn(1)-S(1)	141.29(6)	134.92(7)
N(2)-Zn(1)-S(1)	112.57(5)	96.13(7)
N(1)-Zn(1)-S(1)	96.49(6)	123.46(7)

N(1)-Zn(1)-S(1) bond angle 141.29°, indicate a slight tilting of the axial Zn(1)-N(1) bond in the direction of the O(1)-Zn(1) bond away from the S(1)-Zn(1) bond. The variation in Zn-N bond distances, Zn(1)-N(1) (2.189 Å), Zn(1)-N(2) (2.132 Å)

and Zn(1)-N(5) (2.059 Å) indicate differences in the strength of the bond formed by each of the coordinating nitrogen atoms. The difference in bond lengths can be attributed to the difference in the extent of π back-bonding between the 1,10-phenanthroline and thiosemicarbazone moieties. However, the large bond distance at the axial Zn (1)-N(1) positions supports the lack of significant out of plane π-bonding. Coordination to Zn(II) lengthens the C-S bond substantially to 1.752 Å from 1.680 Å in unsubstitued salicylaldehyde N(4) phenylthiosemicarbazone [25] as would be expected on coordination of thiolate sulfur. Hydrogen bonding interactions for complex **1** is shown in Fig. 2 and unit cell packing diagram of the compound is shown in Fig. 3.

Crystal structure of complex 2: The molecular structure of the compound **2** along with the atom numbering scheme is represented in Fig. 4. Crystallographic parameters and selected bond lengths and angles are given in Table-2. Suitable pale yellow crystals were obtained from a solution of **2** in a solvent of acetone. The compound **2** is monoclinic with a space group P21/n. This complex is mononuclear and five coordinated. In the complex [ZnLbpy], Zn(II) is located in an approximately trigonal bipyramidal geometry in which the equatorial positions are occupied by the S(1), O(1), N(1) and the axial positions by N(2) and N(4) [Zn(1)-N(2), 2.171(2), Zn(1)-N(4), 2.072(2) Å] with the N(4)-Zn(1)-N(2) angle of 173.06(9)° being close to the 'ideal' value of 180° which is usual for such systems [26]. In a five-coordinate system, the angular structural parameter (τ) is used to propose an index of trigonality. The trigonality index τ of 0.63 {According to Addison *et al.* [23], τ = (β-α)/60, where β = N(4)-Zn(1)-N(2) = 173.06(9)° and α

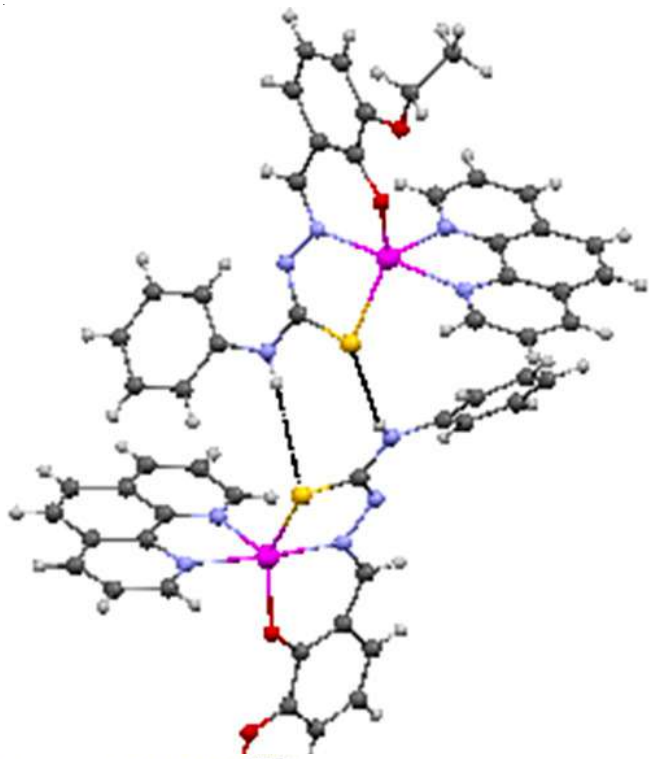

interaction for complex **1**

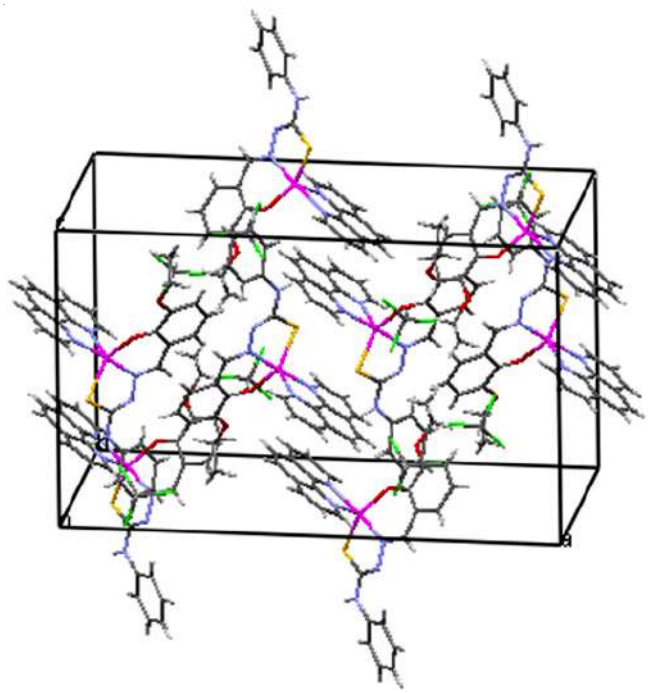

Fig. 3. Unit cell packing diagram of the complex **1**

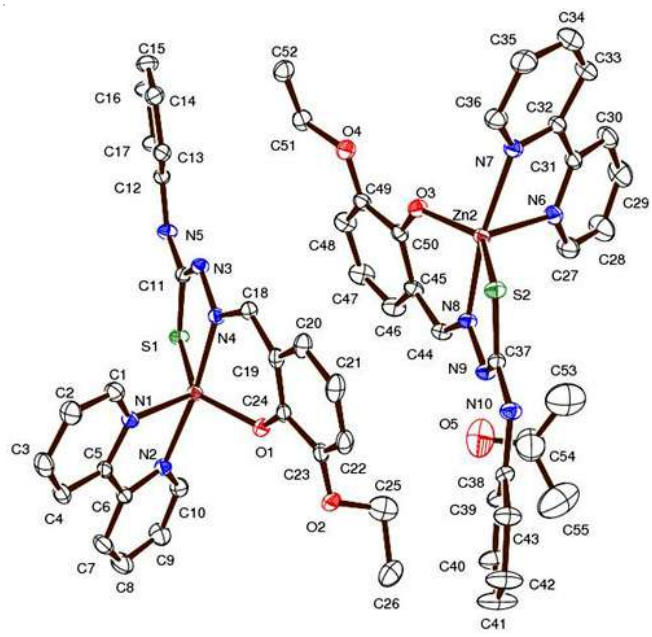

Fig. 4. Structure and labeling diagram of the complex **2**

= O(1)-Zn(1)-S(1) = 134.92(7)°; for perfect square pyramidal and trigonal bipyramidal geometries the values of τ are zero and unity, respectively [27]} indicates that the coordination geometry around zinc is intermediate between trigonal bipyramidal and square pyramidal geometries and is better described as trigonal bipyramidal distorted square based pyramid (TBDSBP) with zinc displaced above the N(2), N(4), O(1) and S(1) coordination plane and towards the elongated apical N(1) atom [28]. One of the reasons for the deviation from an ideal stereochemistry is the restricted bite angle imposed by both the $(L)^{2-}$ and 2,2'-bipyridine ligand. The bite angle around the metal *viz.* N(1)-Zn(1)-N(2) of 76.27(10)° may be considered normal, when compared with an average value of 77°

cited in the literature [35-37]. The variation in Zn-N bond distances, Zn(1)-N(1), 2.117(2), Zn(1)-N(4), 2.072(2) and Zn(1)-N(2), 2.171(2) indicate differences in the strengths of the bonds formed by each of the coordinating nitrogen atoms. The Zn-N bond lengths are shorter than those reported for mononuclear Zn(II) complexes, while there is no significant variation in the Zn-S bond lengths reported [29]. The dihedral angle formed by the least square plane for the compound **2**. The imine bond formation is evidenced from N(4)-C(18) and N(3)-C(11) distances of 1.283(4) Å and 1.296(4) Å. The C-N bond length of 1.396(4) Å and C-S bond length of 1.750(3) is similar to those reported for coordination of thiosemicarbazone in the thiolate form [30,31]. For complex **2**, hydrogen bonding inter-action (Fig. 5) and unit cell packing diagram of the compound is shown in Fig. 6. The molecules in the crystal lattice are stabilized by combination of hydrogen bonding and π-π interactions between aromatic rings.

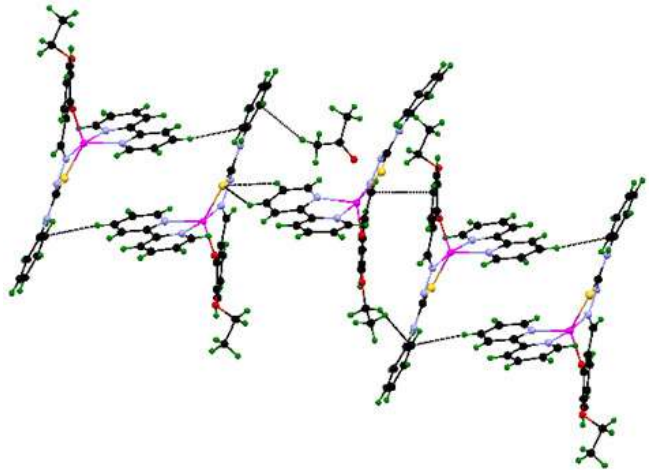

Fig. 5. Hydrogen bonding interaction for complex **2**

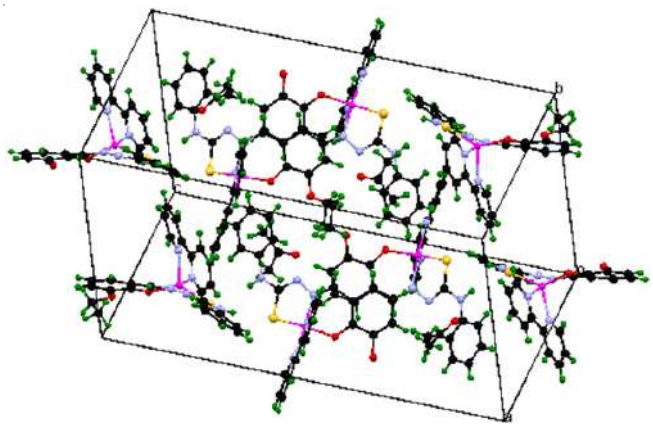

Fig. 6. Unit cell packing diagram of the complex **2**

^{1}H NMR spectra: ^{1}H NMR spectra of ligand **(L)** and its Zn(II) complexes (**1** and **2)** are recorded in DMSO-d_6 and the corresponding spectrum is given in Fig. 7. A singlet observed at δ 11.78 ppm in ligand **(L)** due to phenolic OH proton has disappeared in the complexes **1** and **2** [29]. The azomethine proton attributed to azomethine proton shifted to δ 8.76 ppm in the complex **2**. The ligand (**L**) shows a singlet at

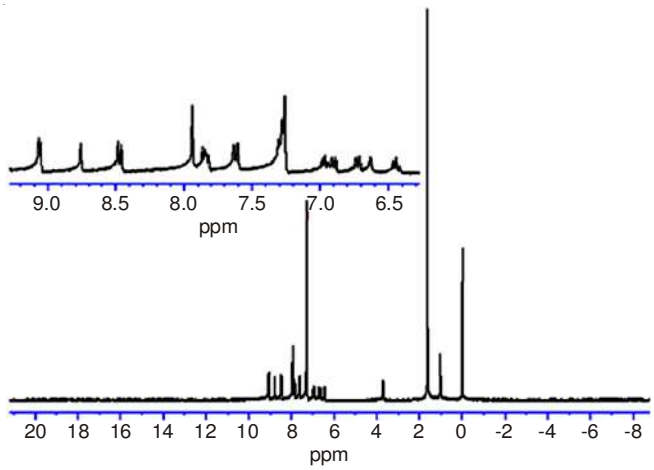

Fig. 7. ^{1}H NMR spectra of complex **2**

δ 10.03 ppm for NH proton and it is absent in the spectra of complex **2**, which clearly indicates the enolization of –NH-C=S group of the ligand (**L**) followed by deprotonation prior to coordination of the thiolate sulfur [32]. The two NH signals of the ligand **(L)** at δ 9.08 ppm and δ 10.04 ppm, respectively, were absent in the complex **2**. (One NH signal of the complex is disappeared, probably exchanged with the solvent) Signals observed in the ^{1}H NMR spectra of ligand at δ 10.03 and δ 8.51 ppm is due to the presence of NH (NH^1) and phenyl NH (NH^2) protons, respectively. The peak due to NH^1 has absent and the peak due to the phenyl NH proton shifted to downfield in the spectrum of complex **2**. The peaks displayed in the region of δ 7.2-7.5 ppm in the complex **2** are due to the aromatic protons of thiosemicarbazone and phenanthroline ligands. The ethoxy protons appeared as a quartet and a triplet at δ 3.00 and δ 1.22 ppm, respectively. Similar observations are observed for complex **1**. From the spectral data, it is clear that the coordination occurs through ONS donor ligand **(L)** for both the complexes **1** and **2**.

IR spectra: IR spectral data of the ligand (**L**) and complexes **1**-**2** are given in Table-3. The intense band in the region 1593 cm^{-1} in the IR spectrum of Schiff base ligand (**L**) is associated with C=N stretching vibration and is shifted to lower frequencies 1539 cm^{-1} in the spectrum of corresponding complex **1** and this change in value indicate the coordination of azomethine nitrogen to the metal ion [20a]. The band due to phenolic OH group disappeared in the IR spectrum of complex **1** in the region 3394-3299 cm^{-1} (Fig. 8) suggesting deprotonation of metal ion. In addition, a band appeared at 1275 cm^{-1} due to phenolic C-O stretching in the Schiff base ligand (**L**) has been shifted to 1308 cm^{-1} in the IR spectrum of the complex **1** indicating the coordination through phenolic oxygen atom. IR spectrum of free ligand (**L**) showed one band at 3468 cm^{-1} due to terminal NH^2 and this bands position altered in the spectrum of the corresponding complex **1**, revealing non participation of NH^2 in coordination [20b]. A band which appeared in the region 3174-2980 cm^{-1} due to N-H in the ligand (**L**) disappeared on complexation. Further, a band due to C=S (781 cm^{-1}) which appeared in the ligand has completely disappeared in the spectrum of the complexes and a new band appeared at 756 (**1**) and 737 (**2**) cm^{-1} (for C-S) due to enolization of -NH-C=S group of the ligand, followed by

TABLE-3
IR SPECTRAL DATA (cm^{-1}) AND UV SPECTRAL DATA (nm) OF FREE LIGAND (**L**) AND ITS Zn(II) COMPLEXES **1-2**

Compound	ν(CH=N)	ν(C-O)	ν(N-H)	ν(C=S)	ν(O-H)	ν(Zn-N)	ν(Zn-O)	λ_{max} (nm)
L	1593	1275	3468	781	3286	–	–	299, 336
1	1581	1308	3476	756	–	435	525	376
2	1583	1309	3482	737	–	483	575	375

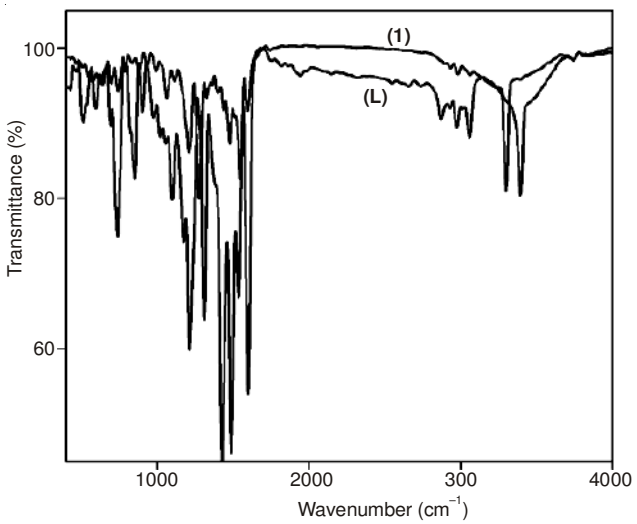

Fig. 8. IR spectra of ligand **(L)** and complex **1**

deprotonation prior to coordination of the thiolate sulfur [33]. The non-ligand bands observed in far IR region for complex **1** are assigned to ν(M-N) (483-435, cm^{-1}) and ν(M-O) (575-525, cm^{-1}) stretching vibrations. Two strong bands at 1580 and 1560 cm^{-1} assigned to ν(-C=C-) and ν(-C=N-) (of 2,2'-bipyridine), are shifted to higher frequencies by 12-29 cm^{-1}. Similarly, the strong bands observed at 1430, 1580 and 1560 cm^{-1} assigned to ν(ring), ν(C=C) and ν(C=N), respectively for 1,10-phenanthroline, are shifted to higher frequencies by 29-58 cm^{-1}. This indicates that the nitrogen atoms in phen and bpy coordinate to the complexes **1-2** [33,34].

Electronic spectra: The electronic spectra of the ligand (**L**) and its Zn(II) complexes **1-2** recorded in DMSO solvent and it shows four bands in the region 247, 297, 334 and 375 nm. The peaks below 300 nm are assigned to intraligand transitions, $n\rightarrow\pi^*$ and $\pi\rightarrow\pi^*$.The bands appeared in the region 377 nm (Table-3) are assigned to MLCT, respectively.

Antifungal activity: Table-4 indicates that the ligand as well as the complexes **1** and **2** has a significant degree of antifungal activity against, *Candida albicans*, *Aspergillus niger* and *Macrophonia* at 2 mg/mL concentration. The effect is susceptible to the concentration of the compound used for inhibition. The complex **2** shows greater activity against *Candida albicans* species. The antifungal activity of the ligand **(L)** and its Zn(II) complexes **1** and **2** varies in the following order of fungal species *Macrophonia* > *Candida albicans* > *Aspergillus niger*. The antifungal experimental results of the compounds were compared with the standard antifungal drugs ketokonazole at the same concentration. The complex **2** exhibit greater antifungal activities against *Candida albicans sp* and *Aspergillus niger sp* and the complex **1** is resistant to the above fungus. They also show low activity against *Macrophonia sp* than complex **1**. From the observed data it shows that the antifungal activity depends upon the type of metal complexes and varies in the following order of the metal complexes **2 > 1**.

Antibacterial activity: The antibacterial activity of the newly synthesized ligand **(L)** and its Zn(II) complexes **1** and **2** were determined by the standard 'disc diffusion' method. The ligand **(L)** it Zn(II) complexes **1** and **2** with the standard drug amikacin were screened separately for their antibacterial activity against the Gram-positive bacteria *Stapholococcus aureus*, *Pseudomonas aeruginosa* and Gram-negative bacteria *E. coli*. The results of the bacterial study of the synthesized compounds are shown in Table-5. The antibacterial activity of the ligand **(L)** and its Zn(II) complexes **1** and **2** varies in the following order of fungal species *Pseudomonas aeruginosa* > *Stapholococcus aureus* > *E. coli*. The antibacterial experimental results of the compounds were compared with the standard antibacterial drug amikacin at the same concentration. The complex **2** exhibit greater antibacterial activities against *Pseudomonas aeruginosa, Stapholococcus aureus* and *E. coli* and the complex **1** is resistant to the bacteria *E. coli*. Complex **1** also shows low activity against *Pseudomonas aeruginosa, Stapholococcus aureus* than complex **2**. From the observed data it shows that the antibacterial activity depends upon the type of Zn(II) complexes and varies in the following order of the metal complexes **2 > 1**. The increased activity of the Zn(II) chelates can be explained on the basis of chelation theory. It is known that chelation tends to make the metal complexes act as more powerful and potent bactericidal agents, thus killing more of the bacteria than the ligand **(L)**. It is observed that, in a complex, the positive charge of the metal is partially shared with the donor atoms present in the ligands and there may be π-electron delocalization over the whole chelating [35]. This increases the lipophilic character of the metal chelate and favours its permeation through the lipoid layer of the bacterial

TABLE-4
MINIMUM INHIBITION CONCENTRATION (MIC) DATA OF THE SYNTHESIZED LIGAND **(L)** AND Zn(II) COMPLEXES **1-2** AGAINST GROWTH OF BACTERIA AND FUNGI

	Microorganism (MIC) values				
	S. aureus	*P. aeruginosa*	*C. albicans*	*A. niger*	*Macrophonia*
	R	6	R	R	R
	7	12	R	R	12
	13	14	12	5	10

TABLE-5
PERCENTAGE OF CELL VIABILITY AND DEATH ANALYSIS IN DUPLICATE STUDY MODEL FOR LIGAND (L) AND Zn(II) COMPLEXES **1-2**

Compound	12.5 µg	25 µg	50 µg	100 µg
L	52.49	51.77	36.56	19.63
1	88.75	79.93	61.60	52.48
2	89.05	70.21	51.87	40.62
Cyclophosphamide	100	100	100	100

membranes. There are other factors which also increase the activity, which are solubility, conductivity and bond length between the metal and the ligand.

Cytotoxicity: The *in vitro* cytotoxic activities of the synthesized Schiff base ligand (**L**) and its Zn(II) complexes **1-2** are studied on human breast cancer cell lines (MCF-7) by applying the MTT colorimetric assay (Table-6). The calculated values, that is, the concentration (µg/mL) of a compound able to cause 50 % of cell death with respect to the control culture, are presented in Fig. 9. Cyclophosphamide is used as a reference compound. The MCF-7 cells are sensitive to the O-N-S Schiff base with the cell viability value of ligand **(L)** and their complexes **1-2** in µg. Taking into the account that thiosemicarbazone molecules exhibit cytotoxicity activity [36]. We have tested the ability of the ligands (**L**) and its Zn(II) complexes **1-2** inhibit the tumor cell growth. On comparison with the ligand and its Zn(II) complexes **1-2**, Ligand **(L)** show a higher value than Zn(II) complexes **1-2** which indicate the presence of bulky groups at position N(4) of the thiosemicarbazone moiety and heterocyclic bases 1,10-phenanthroline, 2,2′-bipyridine enhanced the anti-tumour activity [37-40]. The complexes **1** and **2** are cytotoxic to the breast cancer cell lines. Although the schiff base ligand (**L**) and its Zn(II) complexes

TABLE-6
IC_{50} VALUES FOR THE LIGAND (**L**) AND COMPLEXES **1-2**

Sample	IC_{50} values
Ligand (L)	25.5
[ZnL(phen)]	198.0
[ZnL(bpy)]	103.0

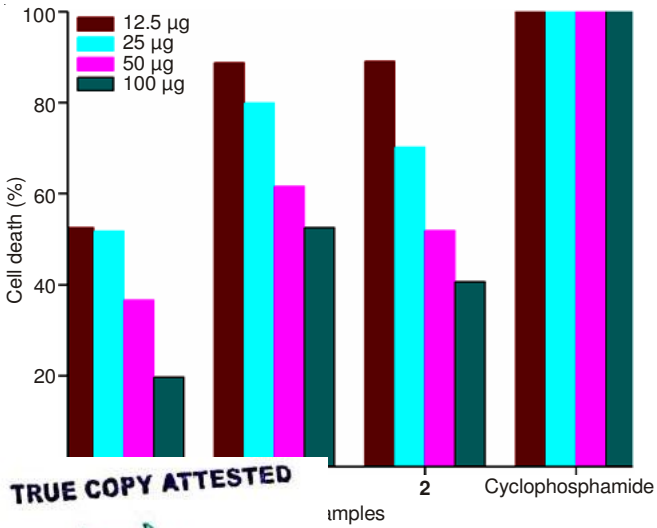

umples

nst cyclophosphamide, ligand (L) and

are less effective than cyclophosphamide, the schiff base ligand (**L**) is more effective than the complexes **1-2**. The different activities are currently being investigated in terms of the mechanism of action of these compounds at the cellular level [41].

IC_{50} values (compound concentration that produces 50 % of cell death) were calculated for the free ligand (**L**) and the title complexes **1-2** against human breast cancer cell lines (MCF-7). The ligand (**L**) and its Zn(II) complexes **1-2** exhibited significant anticancer activity. It is worth nothing that the free ligand (**L**) showed a lower IC_{50} value than the Zn(II) complex **1-2**, indicating that the antitumor activity of the ligand (**L**) is greater than that of the complexes **1-2**. Further, as revealed by the observed IC_{50} values, the potency of the ligand and its Zn(II) complexes to kill the cancer cells follows the order **L > 2 >1**, revealing that it varies with the mode and extent of interaction of the complexes with cyclophosphamide.

Supplementary data

CCDC 964627 and CCDC 964628 contain the supplementary crystallographic data for **1** and **2**. These data can be obtained free of charge viahttp://www.ccdc.cam.ac.uk/conts/retrieving.html, or from the Cambridge Crystallographic Data Centre, 12 Union Road, Cambridge CB2 1EZ, UK; fax: (+44) 1223-336-033; or e-mail: deposit@ccdc.cam.ac.uk.

ACKNOWLEDGEMENTS

Financial assistance received from the Department of Science and Technology, New Delhi, India [Grant No. SR/FTP/CS-40/2007] and University Grants Commission, New Delhi, India [F.No: 38-70/2009 (SR)] are gratefully acknowledged.

REFERENCES

1. D.X. West, J.K. Swearingen, J. Valdes-Martinez, S. Hernandez-Ortega, A.K. El-Sawaf, F. van Meurs, A. Castiñeiras, I. Garcia and E. Bermejo, *Polyhedron*, **18**, 2919 (1999).
2. P. Tarasconi, S. Capacchi, G. Pelosi, M. Cornia, R. Albertini, A. Bonati, P. Dall Aglio, P. Lunghi and S. Pinelli, *Bioorg. Med. Chem.*, **8**, 157 (2000).
3. S.E. Ghazy, M.A. Kabil, A.A. El-Asmy and Y.A. Sherief, *Anal. Lett.*, **29**, 1215 (1996).
4. A.R. Cowley, J.R. Dilworth, P.S. Donnelly, A.D. Gee and J.M. Heslop, *Dalton Trans.*, **31**, 2404 (2004).
5. S. Chandra, P. Shikha and K. Yatender, *Bioinorg. Chem. Appl.*, **Article ID 851316** (2009).
6. R. Kothari and B. Sharma, *J. Chem. Chem. Sci.*, **1**, 158 (2011).
7. U. Kumar and S. Chandra, *J. Saudi Chem. Soc.*, **15**, 19 (2011).
8. S. Chandra, L.K. Gupta and S. Agrawal, *Transition Met. Chem.*, **32**, 558 (2007).
9. S. Chandra and Ruchi, *Spectrochim. Acta A*, **103**, 338 (2013).
10. S. Chandra, S. Bargujar, R. Nirwal and N. Yadav, *Spectrochim. Acta A*, **106**, 91 (2013).
11. (a) S. Ramakrishnan, V. Rajendiran, M. Palaniandavar, V.S. Periasamy, B.S. Srinag, H. Krishnamurthy and M.A. Akbarsha, *Inorg. Chem.*, **48**, 1309 (2009); (b) S. Ramakrishnan, D. Shakthipriya, E. Suresh, V.S. Periasamy, M.A. Akbarsha and M. Palaniandavar, *Inorg. Chem.*, **50**, 6458 (2011).
12. (a) H.H. Thorp, *Chem. Biol.*, **5**, R125 (1998); (b) H. Vahrenkamp, *Dalton Trans.*, **42**, 4751 (2007); (c) A.I. Anzellotti and N.P. Farrell, *Chem. Soc. Rev.*, **37**, 1629 (2008).
13. S. Emami, S.J. Hosseinimehr, S.M. Taghdisi and S. Akhlaghpoor, *Bioorg. Med. Chem. Lett.*, **17**, 45 (2007).
14. Q. Huang, Z. Pan, P. Wang, Z. Chen, X. Zhang and H. Xu, *Bioorg. Med. Chem. Lett.*, **16**, 3030 (2006).
15. (a) A. Nakayama, M. Hiromura, Y. Adachi and H.J. Sakurai, *Biol. Inorg. Chem.*, **13**, 675 (2008); (b) H. Sakurai, Y. Yoshikawa and H. Yasui, *Chem. Soc. Rev.*, **37**, 2383 (2008).

16. M.T. Kaczmarek, R. Jastrzab, E. Holderna-Kedzia and W. Radecka-Paryzek, *Inorg. Chim. Acta*, **362**, 3127 (2009).
17. M.M. Ali, E. Frei, J. Straub, A. Breuer and M. Wiessler, *Toxicology*, **179**, 85 (2002).
18. Q. Jiang, J. Zhu, Y. Zhang, N. Xiao and Z. Guo, *Biometals*, **22**, 297 (2009).
19. (a) S. Mathan Kumar, K. Dhahagani, J. Rajesh, K. Nehru, J. Annaraj, G. Chakkaravarthi and G. Rajagopal, *Polyhedron*, **59**, 58 (2013); (b) K. Dhahagani, S. Mathan Kumar, G. Chakkaravarthi, K. Anitha, J. Rajesh, A. Ramu and G. Rajagopal, *Spectrochim. Acta A*, **117**, 87 (2014); (c) K.K. Raja, D. Easwaramoorthy, S.K. Rani, J. Rajesh, Y. Jorapur, S. Thambidurai, P. Athappan and G. Rajagopal, *J. Mol. Catal. Chem.*, **303**, 52 (2009); (d) G. Puthilibai, S. Vasudhevan, S. Kutti Rani and G. Rajagopal, *Spectrochim. Acta A*, **72**, 796 (2009).
20. (a) J. Rajesh, A. Gubendran, G. Rajagopal and P.R. Athappan, *J. Mol. Struct.*, **1010**, 169 (2012); (b) J. Rajesh, M. Rajasekaran, G. Rajagopal and P.R. Athappan, *Spectrochim. Acta A*, **97**, 223 (2012); (c) A. Gubendran, J. Rajesh, K. Anitha and P.R. Athappan, *J. Mol. Struct.*, **1075**, 419 (2014).
21. G. Kumar, D. Kumar, S. Devi, R. Johari and C.P. Singh, *Eur. J. Med. Chem.*, **45**, 3056 (2010).
22. T. Mosmann, *J. Immunol. Methods*, **65**, 55 (1983).
23. A.W. Addison, T.N. Rao, J. Reedijk, J. van Rijn and G.C. Verschoor, *J. Chem. Soc., Dalton Trans.*, **158**, 1349 (1984).
24. Y. Hayashi, R. Matsuda, K. Ito, W. Nishimura, K. Imai and M. Maeda, *Anal. Sci.*, **21**, 167 (2005).
25. E.B. Seena and M.R.P. Kurup, *Spectrochim. Acta A*, **69**, 726 (2008).
26. C.B. Castellani, G. Gatti and R. Millini, *Inorg. Chem.*, **23**, 4004 (1984).
27. N.J. Ray and B.J. Hathaway, *Acta Crystallogr.*, **34**, 3224 (1978).
28. R.P. John, A. Sreekanth, V. Rajakannan, T.A. Ajith and M.R.P. Kurup, *Polyhedron*, **23**, 2549 (2004).
29. C. Zhang and C. Janiak, *J. Chem. Crystallogr.*, **31**, 29 (2001).
30. E.B. Seena, M.R. Prathapachandra Kurup and E. Suresh, *J. Chem. Crystallogr.*, **38**, 93 (2008).
31. T. Bal-Demirci, *Polyhedron*, **27**, 440 (2008).
32. S. Güveli, N. Özdemir, T. Bal-Demirci, B. Ülküseven, M. Dinçer and Ö. Andaç, *Polyhedron*, **29**, 2393 (2010).
33. R. Prabhakaran, R. Sivasamy, J. Angayarkanni, R. Huang, P. Kalaivani, R. Karvembu, F. Dallemer and K. Natarajan, *Inorg. Chim. Acta*, **374**, 647 (2011).
34. T.A. Gerber, A. Abrahams, P. Mayer and E. Hosten, *J. Coord. Chem.*, **56**, 1397 (2003).
35. J.R. Dilworth, *Coord. Chem. Rev.*, **21**, 29 (1976).
36. S.G. Teoh, S.H. Ang, S.B. Teo, H.K. Fun, K.L. Khew and C.W. Ong, *J. Chem. Soc., Dalton Trans.*, 465 (1997).
37. S.K. Jain, B.S. Garg and Y.K. Bhoon, *Spectrochim. Acta A*, **42**, 959 (1986).
38. M.E. Hossain, M.N. Alam, J. Begum, M. Akbar Ali, M. Nazimuddin, F.E. Smith and R.C. Hynes, *Inorg. Chim. Acta*, **249**, 207 (1996).
39. D. Gambino, *J. Med. Chem.*, **4**, 1 (2004).
40. S. Singh, N. Bharti, F. Naqvi and A. Azam, *Eur. J. Med. Chem.*, **39**, 459 (2004).
41. X.Y. Qiu, S.Z. Li, A.R. Shi, Q. Li and B. Zhai, *Chin. J. Struct. Chem.*, **31**, 555 (2012).

TEQIP–II SPONSORED

AMPC

National Conference on Advanced Materials: Processing and Characterization

2017

Certificate

This is to certify that Dr./Mr./ Ms . Mohamed Mohaideen.H

Raja Doraisingam Govt. Arts college, Sivagangai

has participated / presented a paper (~~oral~~ / poster) in the National Conference on Advanced Materials: Processing and Characterization held at Department of Physics, National Institute of Technology, Tiruchirappalli, during 27th & 28th of February 2017.

TRUE COPY ATTESTED

PRINCIPAL
MOHAMED SATHAK ENGINEERING COLLEGE
KILAKARAI-623806.

D

Dr. M. C. Santhosh Kumar
Convener

Dr. N. Gopalakrishnan
Head , Department of physics

Excel
INDIA PUBLISHERS

Advanced Materials
Processing and Characterization

Editors
J. Hemalatha
M.C. Santhosh Kumar

DEPARTMENT OF PHYSICS
NATIONAL INSTITUTE OF TECHNOLOGY
TIRUCHIRAPPALLI – 620 015
TAMILNADU, INDIA

AMPC
2017

Proceedings of TEQIP-II Sponsored
National Conference on Advanced Materials:
Processing and Characterization (AMPC-2017)

Contents

Studies on the Synthesis and Characterization of Nanostructured NiO for Biomedical Application

H. Mohamed Mohaideen[1], S. Sheik Fareed[2], N. Mythili[3] and B. Natarajan[4]

[1,2,3]Department of Physics, Mohamed Sathak Engineering College, Kilakarai-623806, Tamilnadu, India
[1,4]PG and Research Department of Physics, Raja Doraisingam Govt. Arts College, Sivagangai-630561, Tamilnadu, India
E-mail: [4]b_natraj_b@rediffmail.com

Abstract. Nanostructured NiO particles were prepared by chemical precipitation method. The prepared Nanoparticles were calcined at different temperature and were characterized by X-ray Diffraction (XRD), Fourier Transform Infrared spectroscopy (FTIR), UV-Visible spectroscopy (UV), and Photoluminescence spectroscopy (PL). The XRD result reveals that the crystallite size varies from 12 nm to 45 nm with respect to increase in calcination temperature. FTIR studies shows the presence of NiO group. Optical transmittance and absorption were studied by using UV spectroscopy. Band gap values vareis from 3 to 3.75 eV with calcination. The defect chemistry was analyzed using PL studies. Suitability of synthesis nanoparticles for biomedical application were discused.

Keywords: Metal Oxide Nanoparticles, Nanostructured NiO, Biomedical, Physicochemical

1. Introduction

Metal oxide nanoparticles have interesting strucutural, electrical, magnetic and optical properties. Hence, they are used in various application such as electronics, gas sensor and energy strorage devices[1]. Apart from above said application the metal oxide NPs are used as drug delivery system and Magnetic Resonance Imaging contrasting agent in the biomedical field and as decontaminant in the environment field [2,3]. According to the reports, Various metal oxide nanoparticles have received great interest as antimicrobial agents. Methods of synthesising nanoparticles and their size and morphology are the key factors which influences the effect of antimicrobial agents[4,5].

NiO nanoparticles have drawn lot of interest in recent research, because of high chemical stability, electro catalysis, super conductance characteristics and electron transfer capability. It is an environmentally active material as it finds applications in the adsorption of hazardous dye and inorganic pollutants. Due to their anti- inflammatory properties they are employed in the field of biomedicine. NiO nanoparticle was found to forces poisonous impacts over microscopic organisms and microalgae, because of the capability of prompting oxidative stress and the inclination to discharge nickel particles (Ni^{2+}) inside the cell. NiO have records for their cytotoxic effects, because of their unique properties like surface area, metal ion releasing and adsorbing ability[6].

ANANDA COLLEGE

Accredited with 'B' Grade by NAAC
Affiliated to Alagappa University, Karaikudi
(UGC Recognized 2(f) and 12 (B) Institution)
Devakottai – 630303

Department of English

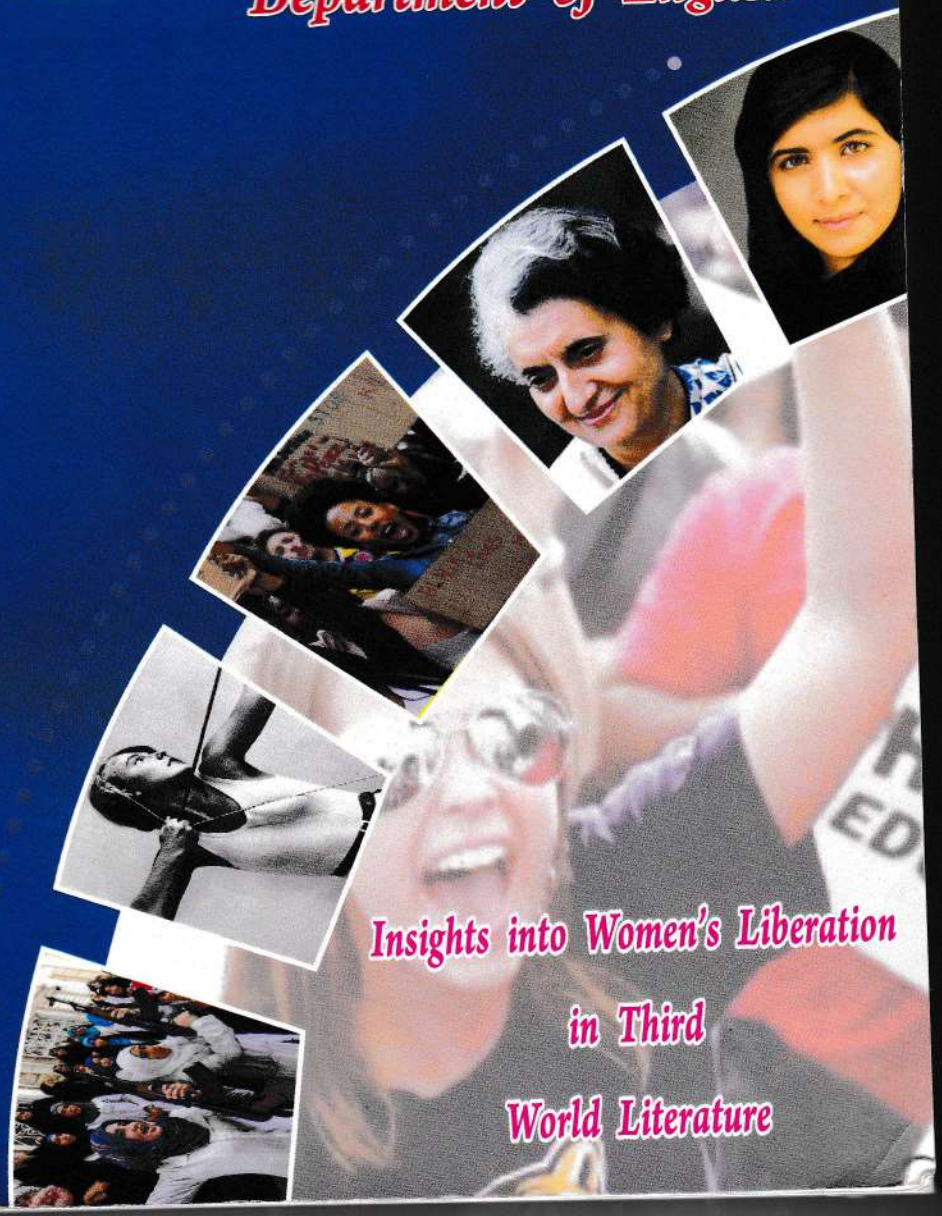

Insights into Women's Liberation in Third World Literature

	Dr.Sheila Royappa. R. C	Alice Walker and Bama
31	**Mageswaran. K**	Feminine Perceptive of Modern society in Shashi Despande's *Dark Holds No Terror*
32	**Dr.Mahalakshmi. B**	Feminine Sensitivity in Anita Desai's Where *Shall We Go this Summer*?
33	**Malarvizhi. S**	Women the Proponent in Anita Desai's *Fire on the Mountain*
34	**Manivannan. K**	Atrocities on Women Through Marriage and Their Survival in Bapsi Sidhwa's Novel *The Pakistani Bride*
35	**Mehala. V**	Marital Sufferings of a Female in Anita Desai's *Cry, the Peacock*
36	**Moorthi. S**	Cultural Representation in Paule Marshall's *The Chosen Place, The Timeless People*
37	**Nissi Karunya E.R** **Dr. Shanthi. K**	Nature –The Sacred Space of Resuscitation and Rejuvenation: A Comparative Study of Eco feministic Insights into Terry Tempest Williams' *Refuge* and Maya Angelou's Select Poems
38	**Nivetha Rak. A**	Survival of Women in Githa Hariharan's *The Thousand Faces of Night*
39	**Pandi Selvi .M** **Stella. A**	Woman's Search for Freedom in Anita Nair's "*Ladies Coupe*"
40	**Praba Vinnarasi. M**	Feminine Consciousness in Anita Nair's *Mistress*
41	**Prabhu .M**	Dawn of Black Angels in Maya Angelou's *Still I Rise*
42	**Priya. A**	Woman's anguish in Shashi Deshpande's *the Dark Holds no Terrors*
43	**Priyanka. R**	Pursuit to Consummate Equal Rights for Woman in Literature
44	**Dr. Priyakant H ved**	Feminism and Marital discord in Shobha De's *Second Thoughts*
45.	**Rajeswari. R**	Feminine Vulnerability in the Select Poems of Kamala Das
46	**Rajalakshmi. A** **Roshini. A**	THE CONCEPTION OF MODERN WOMAN IN BHARATI MUKHERJEE'S WIFE
47	**Rekha. M**	Feminism in Shashi Deshpande's novel *That Long Silence*

	[illegible]	Culture is the Widening of the M[illegible] the Spirit: A Study on the Diaspo[illegible] Anita Rau Badami's *Hero's Walk*
	[illegible]	Women's Spirit of Liberation as [illegible] in Bharati Mukherjee's *Wife*
	[illegible]	Social Injustice with Women: A [illegible] Arundhati Roy's*The God of Small*
	[illegible]	Voiceless Woman in Shashi Desh[illegible] *That Long Silence*
	[illegible]	Revealing the New Women in Ra[illegible] Mehta's *Inside the Haveli*
	[illegible]	Broken Memories in Shashi Desh[illegible] *Matter of Time*
	[illegible]	Rising of Courage in Nikita Sing[illegible] *All This Time*
	[illegible]	Quest for Identity in Bharati Mu[illegible] *Jasmine*
	[illegible]	Exploring Relationship and Repr[illegible] of Women in Sudha Murthy's Se[illegible] Novels
	[illegible]	Portrayal of Persecuted Protagon[illegible] Select Novels of Indian Women
	[illegible]	Freedom ends when Responsibil[illegible] in Manju Kapur's *A Married Wo*
	[illegible]	A Grand Retrieval: The Polemic[illegible] Replenishing Acquity
	[illegible]	The Feminine Depression and su[illegible] Anita Desai' in *Cry, the Peacock*
	[illegible]	Destiny of Personage and Resid[illegible] Colonial and Neo-Colonial Pow[illegible] Structures: A Study of Gita Meh[illegible]
	[illegible]	The Raise of Women Status in L[illegible] Hansberry's *A Raisin in the Sun*
	[illegible]	An Illuminating Portrait of Kay[illegible] Radhika Jha's *My Beautiful Sha*
	[illegible]	Portrayal of Alienation through [illegible] Fate, Time and Chance in Thom[illegible] novel *Tess of the D'Urbervilles*

TRUE COPY ATTESTED

PRINCIPAL
MOHAMED SATHAK ENGINEERING COLLEGE
KILAKARAI-623806.

Feminism in Shashi Deshpande's novel *That Long Silence*

Dr.J.Mary Jeyanthi,
Asst. Professor, Dept of English,
Seetha Lakshmi Aachi College for Women,
Pallathur.

M.Rekha
Asst Professor, Dept. of English,
Msec, Kilakarai.

Feminism is a range of political movements, ideologies, and social movements that share common goal: to define, establish, and achieve political, economic, personal, and social rights for women. This includes seeking to establish equal opportunities for women in education and employment. This paper attempts to discuss the theme of feminism with reference to Shashi Deshpande's novel *That Long Silence.*

The concept of Feminism, in general, has been concerned to an analysis of the trend of male domination in the society; the general attitude of male towards female; the exploitation and discrimination faced by females; the need for and ways of improving the condition of women; and, so on. In concern to literature, this movement has concentrated on the role played by literature to support gender discrimination as well as to oppose it; the reasons for lesser significance of the contribution by female writers in the literary tradition than that of the male writers; the difference in the ways in which works of male writers and female writers respectively, have represented gender discrimination and the ways in which social conditions and literary traditions regarding gender discrimination have affected one another. The concept got proper identification in the literary field during 1960s. Before that, feminism was limited to the authorship of female writers and the representation given to women in

literature with the help of female characters. The condition of women in society, in general, got expression through the situations faced by fictional female characters and their responses to these situations.

The adoption of the concept by literature in a formal manner led to the study of all the aspects of human life; like social, cultural, educational, professional and financial; with an intent to expose the intentional and unintentional efforts of the society to maintain or intensify the effects of patriarchal superiority.

The evolution of feminism as a literary movement could be divided into following stages:

It was concerned mainly to the treatment of women at the hands of male members of the society. The major works that raised the issues of feminism during this phase include- Mary Elman's 'Thinking about Women' (1968), Kate Millet's "Sexual Politics' (1969) and Germaine Greer's 'The Female Eunuch' (1970). A number of prominent works of the past were also analyzed during this stage so as to study the attitude of male members of society, in general, to the female ones.

It is more commonly also known as 'Gynocriticism'. This stage is believed to have begun with Elaine Showalter's 'A Literature of Their Own' published in 1970. This phase introduced, more or less the first time, a direct analysis of the relation between female and literature. It was during this phase that female writers and the significance they got in the society were studied. Female characters were studied with an approach to understand the difference between

the treatment of female characters at the hands or male and female writers, respectively.

The most important aspect of this phase is the efforts to understand the evolution of the female literary tradition. Showalter suggested that female writers have passed through 3 basic phases, namely the 'feminine' phase, the 'feminist' phase, and the 'female' phase. In the first phase, the female writers did not try to oppose the male writers in any sense. They simply wrote trying to imitate the attitude of male writers towards female characters. Some even wrote with pseudonyms resembling male names. The second phase saw female writers writing, mainly, on the themes of the role of women and the oppression faced by her in society. The third phase lacked the anger and dissatisfaction in the works of female writers. The female writers, in this stage, created works which suggested that they had developed an independent identity as writers.

The French concept of feminism even raised the issue of a separate language that belongs exclusively to women. It was believed to be a language lacking expression of the user's ego and to be marked by use of sentences which are comparatively less to the point.

Feminist movement advocates the equal rights and equal opportunities for women. The true spirit of feminism is into look at women and men as human beings. There should not be a gender bias or discrimination in familial and social life. Establishing gender justice and gender equity is the key aspects of feminist movement. In India,

women writers have come forward to voice their feminist approach to life and the patriarchal family set up. They believe that the very concept of gender is not merely biological phenomenon but it has a social construction.

Shashi Deshpande is a renowned novelist of Indian writing in English. She has the credit of writing well known novels namely; *The Dark Holds No Terrors; Roots and Shadows; and That Long Silence*. Her works primarily deals with the problems of women in the present social context. Deshpande's quest for identity and freedom has become dominant themes in literature. She unfolds the problems of women in the patriarchal society in a very positive way. According to her, woman has every right to live her life, to develop her qualities, to take her decisions, to be independent and to take charge of her destiny.

That Long Silence is one of the unique works of Shashi Deshpande which signifies the pathetic condition of Indian woman. It is a reflection of sufferings of an Indian woman in the dogmatic social milieu i.e., family. It also reflects how woman suffers deeply and ends up life silently baring molestations of male. The sacrifice made by women counterpart is hardly noticed by the male dominated society. The writer wants such women who suffer to break their silence in the wake of feminist movement. The novel illustrates the image of women in the middle-class family and the way she is sandwiched between the tradition and modernity.

The title of the novel depicts the intention of the novelist in order to reveal the female psyche during the quest of Jaya, the protagonist,

for self. She is the protagonist of *That Long Silence* who is an intelligent woman with graduation in English, a writer and a columnist had a bright career. Unfortunately, none of these attributes would provide her a respectable position in the eyes of her husband Mohan, who had socialization in a typical traditional environment. He perceived his wife on par with Seeta, Savitri and Draupadi. His mother and sister Vimala were very much submissive to father. The decisions relating to familial and financial matters were taken by the male members of the family. So he wanted his wife to be submissive like them as a homemaker.

In a male-dominated society, a woman has no space to be independent. She is dependent on men either on father, husband or son. They are hardly given freedom and independence. Slavery to man makes them suffer from dual roles of child bearing and domestic chores. She has no freedom regarding the selection of her life partner and marriage. Marriage becomes their destiny as Jaya thinks;

> ....As we grew into young women, we realized it was not love, but marriage that was the destiny waiting for us. (That Long Silence 19)

Jaya's parents and Vanita Mami go on hammering onto her that 'husband is like a sheltering tree'. Women should be dependent on the male member of the family in order to be safe and protected. In other words, a woman is undermined ignoring the fact that she is equal to men in all the spheres of life. Her abilities and strengths are undermined. However, she is inferior to men in patriarchal society.

The author clearly depicts the image of marriage institution and familial relations in India. Husband and wife hardly speak openly about their sexual life. It is treated as sinful and immoral. Jaya had dreamt about her marital life that she would love her husband first and then sex. A mechanical relationship and artificial love were the consequence of her marriage. It was a total failure. She had lost interest and tired of with the acts of sex. Unfortunately, with Mohan she had only sex but not love either before or after marriage. In other words, she hardly enjoyed marital relationship with her husband. She had no freedom to express or share her desires with Mohan. Her feelings of love and sex are suppressed as she says;

> In any case, whatever my feelings had been then, I had never spoken of them to him. In fact, we had never spoken of sex at all. It had been as if the experience was erased each time after it happened, it never existed in words. The only words between us had been his question, 'Did I hurt you?' and my answer, 'No' (That Long Silence 95)

Jaya was introduced to her neighbor Kamat who motivate her to think and act independently about her writing by appreciating and admiring. He inspires and cheers her to get serious, to be real and true to herself. This made her regain her self-confidence which had been lost. He further makes her to speak frankly about sex. What she could not speak with Mohan, was able to speak to Kamat. It makes her realize her 'self'. In this way, Kamat enables her to break 'long silence'. Jaya now resolves to assert her individuality by breaking *That long silence*, putting down on paper that in her entire seventeen years of silence she had suppressed her desires.

Self- Revelation of the Writers in Post-Colonial Literature

DEPARTMENT OF ENGLISH

ANANDA COLLEGE

Accredited with 'B' Grade by NAAC
Affiliated to Alagappa University, Karaikudi
(UGC Recognized 2(f) and 12 (B) Institution)
Devakottai- 630 303
Sivaganga District, Tamil Nadu.

registeri
women.
paper p

Works

Markan
Pri

ıove this novel represented the sufferings of Indian
ad in many ways in their life. Thus in this way, this
of Middle Class women in the Indian society.

tar in a Sieve. New Delhi: Penguin Books, 2009.

Diasporic Experience in Jhumpa Lahiri's Novel *The Namesake*

A.Gowrimanohari
Asst. Professor
Mohamed Sathak Engg. College, Kilakarai

The word 'diaspora' itself, coming, as it does, from Greek 'dia' ('through') and 'speirein' 'to scatter', etymologically means 'dispersal,' and involves, at least two countries, two cultures, which are embedded in the mind of the migrant, side-by-side. Although the past is invoked now and then, the focus is persistently on the 'moment.' The past is invoked to indicate a certain contrast, which must be incorporated, and controlled in the present life in order to negotiate the network of social relations in the immediate world. The past, thus, becomes a part of the present consciousness of the diasporic subject. Literary works, written particularly by second generation diasporic writers, concentrate more on synchronic dimension than on diachronic one. It is quite natural that they approach the narratives from comparative perspectives, both from the points of view of cultures and generations.

The lived experience of the children of first generation migrants to which Jhumpa Lahiri belongs is characterized by their participation in the American mainstream culture available in the larger social space, outside the limited, 'sanctified' family space. This their parents often disapprove. Jhumpa Lahiri stresses not only the immigrants who leave somewhere called home to make a new home in the United States but also the endless process of coming and goings that create familial, cultural, linguistic and economic ties across national borders. Her characters live in between, straddling two worlds, making their identity transnational.

Jhumpa Lahiri's first novel *The Namesake* explores the theme of transnational identity and trauma of cultural dislocation. Being "an Indian by ancestry, British by birth, American by immigration" (Nayak:206:2002) and her parents having the experience of "the perplexing bicultural universe" of Calcutta in India (now Kolkata) and the United States, "Lahiri mines the immigrants experience in a way superior to Bharti Mukherjee and others" observes Aditya Sinha (Sinha:2003). This novel is a story about the assimilation of an Indian Bengali family from Calcutta, the Ganguli, into America, over thirty years (from 1968- 2000); the cultural conflict experienced by them and their American born children in different ways, the spatial,

cul dislocation suffered by them in their effort to settle
"hc

sional Indians" who "in the waves of the early sixty's",
"w States, as part of the brain drain" (*Spivak*:61:1990).
As ves his homeland ,and comes to America in pursuit of
hig search in the field of "fibre optics" with a prospect of
set ecurity and respect" (*The Namesake:*105). After two year's stay in the USA he comes back to India, marries a nineteen years old Bengali girl from Calcutta named Ashima, who has no idea or dream of going to a place called Boston so far off from her parents ,but agrees for the marriage since 'he would be there'. After the legal formalities, she flies alone to be with her husband, with a heavy heart and lots of instructions from her family members and relatives who come to see her off at Dum Dum Airport "not to eat beef or wear skirts or cut off her hair and forget the family the moment she landed in Boston. (*The Namesake*-37)

Ashima often feels upset and homesick and sulks alone in their three room apartment which is too hot in summer and too cold in the winter, far removed from the description of house in the English novels she has read, she feels spatially and emotionally dislocated from the comfortable 'home 'of her father full of so many loving ones and yearns to go back .Home is a 'a mystic place of desire' in the immigrants imagination. (*Brah:*192:1997) Most of the time she remains lost in the memories of her 'home' thinking of the activities going there by calculating 'the Indians time on her hands 'which is 'ten and a half hours ahead in Calcutta '.She spends her time on rereading Bengali Short Stories ,poems and article from the Bengali magazines, she has brought with her. She "keeps her ears trained, between the hours of twelve and two, for the sound of the postman's footsteps on the porch, followed by the soft click of the mail slot in the door" (36), waiting for her parents letters which she keeps collecting in her white bag and re-reads them often. But the most terrifying experience for her is 'mother hood in a foreign land', 'so far from home', unmonitored and unobserved by those she loved, 'without a single grandparent or parent or uncle or aunt at her side' and to 'raise a child in a country where she is related to no one, where she knows so little, where life seems so tentative and spare' (*The Namesake:* 2003). After the birth of her son Gogol, she wants to back to Calcutta and raise her child there in the company of the caring and loving ones but decides to stay back for Ashoke's sake and brings up the baby in the Bengali 'ways' so 'to put him to sleep, she sings him the Bengali songs

her mother had sung to her' (*The Namesake-35*). She keeps all her emotional hazards and disappoints to herself and not intending to worry her parents. She presents in her letter a good picture of the domestic facilities and cleanliness here.

Gradually she learns how to be independent. Takes pride in rearing up the child, moves out alone in the market with her baby in the pram, communicates with the passersby who smile at him and goes to meet her husband on the campus, thus she grows confident. The very feeling of displacement is felt more by her, after their migration from the University Apartments to a University town outside Boston when Ashoke is 'hired as an Assistant Professor of Electrical Engineering at the University'. The shift to this suburban area with no 'streetlights, no public transportation, no stores for miles' makes Ashima feel 'more drastic more distressing than the move from Calcutta to Cambridge had been'. Feeling lonely and displaced in foreign land. Ashima begins to realize that,

> being a foreigner... is a sort of lifelong pregnancy-a perpetual wait, a constant burden, a continuous feeling out of sorts. It is an ongoing responsibility, a parenthesis in what had once been ordinary life, only to discover that previous life has vanished, replaced by something more complicated and demanding. Like pregnancy, being a foreigner, Ashima believes, is something that elicits the same curiosity from strangers, the same combination of pity and respect. (*The Namesake*: 49-50)

Like immigrant of other communication Ashima and Ashoke to make their circle of Bengali acquaintance .They all become friends only for the reason that "they all come from Calcutta" (38). Robert Cohen rightly remarks "a member's adherence to a diasporic community is demonstrated by an acceptance of an inescapable link with their past migration history" (Cohen: ix: 1997). These Bengali families celebrate these different customs and ceremonies like, marriages, death, childbirth, festivals etc together. They celebrate these as per Bengali customs, wearing their best traditional attire, thus trying to preserves their culture in a new land. John McLeod remarks that "their belief, tradition, customs, behaviours and values along with their 'possession and belonging' are carried by migrants with them to 'new places' (*Mc Lead-211*:2000). The immigrants also face political displacement "they argue riotously over the films of Ritwik Ghatak verses those of Satyajit Ray...,

about the politics of America, a country in which none of
te" (*The Namesake*-38).

ovel *The Namesake* also shows how these immigrants are
eserve their 'home culture' in their new homes. The first
ts train their children in Bengali language literature and
through special Bengali Classes and expose them to their
religious custom, rites, beliefs food tastes, habit and
manerisms. They also groom them to cope with the way of life in America.

Lahiri shows that the immigrants in their enthusiasm to stick to their own cultural belief and customs gradually imbibe the cultural ways of the host country to. Ashima teaches Gogol 'to memorize a four line children poem by Tagore, names of deities at the same time when she goes to sleep in the same time when she goes to sleep in the afternoon she switches the television to channel -2 and tells Gogol to watch 'sesame street' and the electronic company "in order to keep up with the English he uses at nursery school" (54). Though initially Ashoke did not like the celebration of Christmas and thanksgiving but as Gogol recalls that "...it was for him, for Sonia (his younger sister) that his parents had gone to the trouble of learning these customs" (286). Their own children groomed to be 'bilingual 'and 'bicultural' face cultural dilemmas and displacement more though forced to sit in pujas and other religious ceremonies along with the children of other Bengali families. Gogol and Sonia, like them, relish American and continental food more than the syrupy Bengali dishes and enjoy the celebration of the Christmas.

Lahiri shows that all migrants carve their own 'routes' in the course of time and it is not necessary that they want to settle in the countries of their origin. Ashima is shown to grow with passage of time during her thirty two years of stay in America, retaining her culture in dress and values as well as assimilating the American culture for her personal growth and for the sake of her children. She after the death of her husband decides to divide her time every year both at Calcutta and in America, she has grown more confident, and enjoys the best of both cultures. Sonia's decision to marry Ben (a half Chinese boy) and Maushumi's attitude of not sticking to any one culture or country shows how the second generations are going Global and are becoming multicultural. They are also exploring new identities through "transnational contingencies of routes" (*Gilroy*- 1993).

So, it is conclude that while portraying the theme of cultural dilemmas and dislocations of the migrants, Lahiri does not remain confined to the dislocations of migrants in foreign lands alone. Lahiri's 'The Namesake' is an example of the Contemporary immigrant narration which doesn't place the idea of an 'American Drama' at the centre of the story, but rather positions the immigrant ethnic family within a community of cosmopolitan travelers. She chronicles dislocation and social unease in a fresh manner. She blends the two cultures and creates inner turmoil for many of her characters who struggle to balance the Western and Indian influence. Though she lives in US, got married with a Spanish American boyfriend, Alberto Vourvoulias in the traditional Bengali fashion but her works are imbued with the ethos of Indian culture and sensibility. Her novels are more about the co-operation of culture than about confrontation. Stereotypes are examined from a number of angles and deconstructed from both sides- Indian and American.

Works Cited

Lahiri, Jhumpa. *The Namesake*. New Delhi: Harper Collins, 2003. Print.

Bhabha Homi.K. *The Location of Culture*. London: Routledge, 1994. Print.

Eagletun, Terry. *The Idea of Culture Oxford*. Blaekwell, 2000. Print.

Hall,Stuart. *Cultural Identity and Diaspora's in Colonial Discourse and Post Colonial Theory*, London: longman, 1993. Print.

Lowe, Lisa, *Immigrant Acts Durham*. Duke up.1996. Print.

Review of the namesake by Adithya sinha *The malady of naming* in Hindustan times, September 28,2003. Print.

Sharma, Kavitha, Desphpal. *Theoring and Critiquing Indian Diaspora, Creative New Literature Series*. New Delhi: Creative Books. 2000. Print.

ANANDA COLLEGE

Accredited with 'B' Grade by NAAC
Affiliated to Alagappa University, Karaikudi
(UGC Recognized 2(f) and 12 (B) Institution)
Devakottai – 630303

Department of English

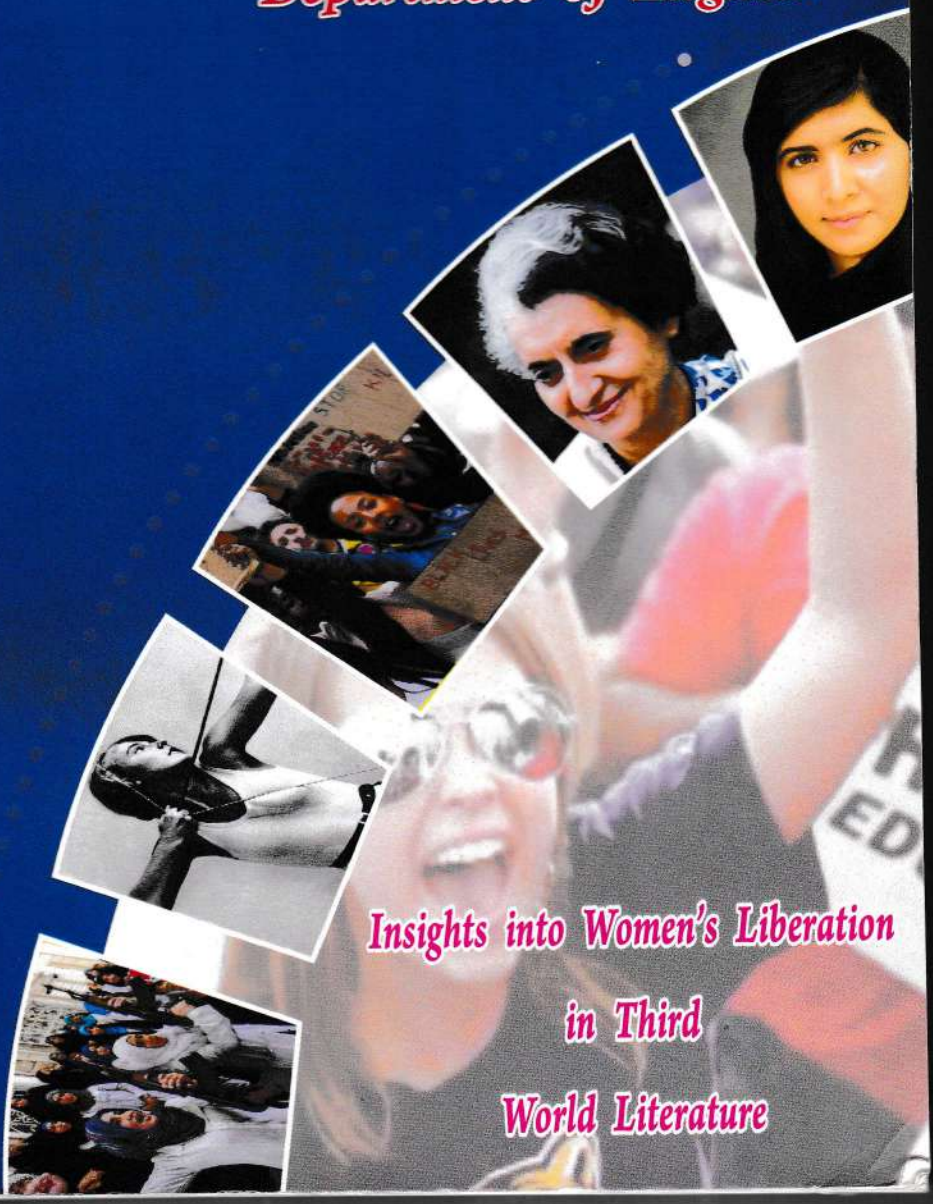

Insights into Women's Liberation in Third World Literature

E PAPER | P N

ected short

ala

by Shalini

turned out
tity in
celet
s

ctive
f an Indian
a Devi's

shpande's

ghts: Gender
ee
usions

's *The*

ove in Nikita
meone Like

anju Kapur's

he darkness

Custody

f Kamala

Irrationality and Injustice in Domestic and Social Life of Women in Arundhati Roy's Novel *The God of Small Things*

Dr. A.Gowrimanoha
Asst. Profess
Dept .of Engli
MSEC, Kilakar

The growth of feminism in India has led to the questioning of th prominent old patriarchal domination. The women of today refuse t be puppets in the hands of men. Hence the image of women ha undergone a radical change. The Indian female writers have made transition from the traditional portrayals of lasting self-sacrificin women to depiction of their inner life and subtle interperson relationships. The conflicting interest of man and woman in th society as a result of self-asserting women, who are engrossed in ke search for their identity, is the hall-mark of modern portrayal female characters.

In the orthodox and conservative society like India, women hav always been undervalued due to patriarchal assumptions. They hav been tutored that their greatness lies in their sufferings and therefor happiness of others is always prioritized to their own. In fact, the perceptions of their aspirations and expectations are within th framework of Indian social and moral commitments.

Arundhati Roy has her own opinion on society and ha successfully made a mark for herself in the literary arena by her nove *The God of Small Things*. The novel reveals her feminist stance an her protagonist represents feminine sensibility. *The God of Sma Things* is not a story or just a telling of a tale but as the novelist ha

herself claimed to tell the readers how things that happened and affected the lives of the people concerned. In the course of writing, she draws into the eddy of her story the teeming and flaming issues of life. The novel assumes the dimension of a protest novel which is keenly alert to the social injustice that goes sanctioned by the prevalent traditional norms. Stepping into the world of *The God of Small Things* we feel that we have entered into a world of males. The major women characters of the novel, Mammachi, Baby Kochamma, Margaret, Ammu and Rahel are repeatedly defeated and derailed either by circumstances or by themselves.

All the characters in the novel speak for themselves and show the hold of patriarchy and power dynamics in the family and the society. It is through the dynamics of relations that we learn how the domination and subjugation work. The focus of this paper is greatly on the character depiction in the novel so as to examine it from a Postcolonial Feminist perspective. It also presents the constant struggle of women against their incessant exploitation, torture and struggle which they undergo because of the male dominated conservative society Ammu, the tragic heroine of the novel, is the most conspicuous representative of the fourth generation who died at a young age of thirty-one which is described as "not old, not young" and "viable die-able age". Her suffering started at a very young age. Her father Pappachi insisted that college education was unnecessary for a girl, so she had to leave Delhi after schooling; she had nothing to do at Ayemenem other than waiting for marriage proposals. But no proposals came her way because her father did not have enough

money to raise a suitable dowry. She dreamed of escaping from Ayemenem, from her ill-tempered father and bitter, long suffering mother. Finally, she was left to spend the summer with a distant aunt who lived in Calcutta. There she met her future husband at someone else's wedding reception there. She had an elaborate Calcutta wedding. But very soon things began to take a very bad shape. Her husband was really a misfit to her. He was an alcoholic and he made her smoke. Twins were born to her and by the time they were two years old, drinking had driven him into an alcoholic stupor. Meanwhile, Mr.Hollick, the bungalow to tell him that he should resign. He referred Ammu as "An extremely attractive wife" (P.41) clearly the manager had an eye on her. He suggested that Ammu be sent to his bungalow to be 'looked after'. The only choice left before her was to return, unwelcomed, to her parents in Ayemenem and she did so.

Greater misery awaited her at Ayemenem on her arrival with her children there. Her world, there, was confined to the front and back verandah of Ayemenem. Somehow the well-built Velutha, the paravan carpenter created ripples in her. Ammu was drawn to Velutha and this was, in fact, the beginning of the end. Very soon this developed into physical relations between them. Vellya Paapen, Velutha's father, was a mute witness to whatever went on near his house and he rushed to Ayemenem house to give a full factual report. Ammu was locked in a room and meanwhile as a coincidence Sophie Mol got drowned. Then we hear about her death in a grimy room in the Bharat Lodge in

Alleppey, where she had gone for a job interview. Ammu went away without anyone there even to bid goodbye to her. The church refused to bury Ammu. So Chacko had to take the body to the electric crematorium. He had her wrapped in a dirty bed sheet and laid out on a stretcher. Finally she became a number; Receipt No. Q 498673. That was the number of the pink receipt the crematorium 'In-Charge' gave them. That entitled Chacko and Rahel to collect Ammu's remains.

Ammu's story is more than a tragedy. She is made to suffer even from a very young age and continues to suffer throughout her life. She would have liked to study in a college if she had got a chance. She did have the dreams of a young girl about marriage and married life. But the hope was believed when she came to know that nobody was there to provide her dowry to get her married off. Her escape to Calcutta invited fresh troubles. What she achieved if at all it was an achievement was only a married life which lasted for less than a couple of years.

Hopes were once again shattered when she returned to Ayemenem to discover that nobody was interested in her. Later as fate would have it, she was drawn to Velutha and that marked the beginning of the ultimate tragedy. She was humiliated at the hands of the police, her near and dear ones and also the public at large. In short Ammu, without her knowledge becomes an instrument in the hands of the patriarchal society.

Most of the male characters in this family chronicle exhibit chauvinistic tendencies which vary in degrees. The subaltern male and

the subordinated female in, become comrades-in-arms in a losing battle against the forces of oppression.

Pappachi, whose double-dealing crushes the lives of the members of his family, there is no escape from his clutches and utter dependence on him makes Mammachi and her daughter bear the brunt of his calculating cruelty which settles like a moth on the family. Seventeen years older than his wife he realized with a shock that he was an old man when his wife was still in her prime. Every night he beat her with a brass flower vase, only the frequency changed. One night Pappachi broke the bow of Mammachi's violin and threw it in the river when her violin master complimented her on her exceptional talent. Back at Ayemenem the Imperial Entomologst, retired, slouched around the compound, jealous of the attention his wife was getting on account of her pickles. He stopped speaking to her until his death, for being reprimanded by his son on beating his mother. When Mammachi cried at Pappachi's funeral, Ammu told her twins that it was 'more because she was used to him than because she loved him' (50). She 'was used to' being beaten from time to time.

It is Chacko, the only son of Pappachi who inherits his father's kingdom, the property and proprietorship of Ayemenem house and the factory. Though Ammu did as much work in the factory as Chacko, he always referred to it as 'my factory, my pineapple, my pickles'. Legally, Ammu as a daughter had no claim to the property. Chacko said, "What's yours is mine and what's mine is also mine" (57). Chacko told Rahel and Estha that 'Ammu had no Locusts Stand I'

(57). Chacko was privileged to transgress all social and moral laws. He missed no opportunity to insult Ammu in her own home.

Women who constitute half of the human population but paradoxically not treated on par with man in all spheres of human activity. They are oppressed, suppressed and marginalized in the matter of sharing the available chance for accomplishment of their lives, despite the fact that every woman slaves for the development of her family, her husband and children. This is the predicament of women all over the world. In Arundhati Roy's novel we can see the compulsion faced by women in the male dominant society.

Thus, Women are treated and considered as soulless beings, sub-human and playthings for men. This imbalance in society explains much of the unhappiness prevailing in our families and the battered lives of children who are exposed to this very partial and unjust view of life. The end result is a paralyzed society unable and unwilling to grow.

Work Cited:

Beavior, Simone de. *The Second Sex,* London: Vintage series, 2011. Print.

Prasad, Amar Nath. *Arundhati Roy's The God of Small Things: a critical appraisal,* New Delhi: Sarup & Sons, 2004. Print.

Rajimwale, Sharad. *Arundhati Roy's The God of Small Things: a critical appraisal* New Delhi:Rama Brothers India Pvt. Ltd., 2006. Print.

Roy, Arundhati. *The God of Small Things*, New Delhi: Penguin Books India Pvt. Ltd, 2002. Print.

Enhancing Learning English through Effective Teaching

Department of English
ANANDA COLLEGE
Accredited with 'B' Grade by NAAC
Affiliated to Alagappa University, Karaikudi
(UGC Recognized 2(f) and 12 (B) Institution)
Devakottai – 630303

The Impact of Today's English Communication for Engineering Students in Tamil Nadu

*C.Saifuddeen,
*Assistant Professor,
P.hD., Part-Time Research Scholar.
Mohamed Sathak Engineering College,
Kilakarai.

**Dr. S. Ravikumar,
**Assistant Professor,
Research Supervisor ,
Sree Sevugan Annamalai College,
Devakottai.

> "Communication is a skill that you can learn. it's like reading a bicycle or typing. if you're willing to work at it, you can rapidly improve the quality of every part of your life."
>
> - Brain Tracy.

The present paper is an attempt to focus on *The Impact of Today's English Communication for Engineering students in Tamil Nadu*. The English Language is the most important medium of acquiring information from various printed, Audio-visual or electronic media and materials. It is also of immense importance for them in publishing the findings of their research, communicating in their office and also for furthering their academic career. It suggests that the English language is indispensable for the people who have adopted engineering as their career. In this particular context, it appears to be perfectly relevant to cite the quotation from:

> ... I am aware, though, of the ambiguity to which English as a study is being subjected in the evolving scheme of our national life. But I believe that as we open up to the ruthlessly competitive modern world politically and culturally, English should continue to serve our leading citizens as a necessary window of intellectual and cultural ventilation.

In his view, English serves as a window of intellectual and cultural ventilation for the people and ıables them to peep out through it into the vast material, scientific and technological perity that our advanced distant neighbor countries have attained in the recent days and ıt their techniques to lead our nation to her ultimate goal.

As mentioned in Collins English Dictionary, 'Communication' refers to 'the art of sharing or exchanging information with someone, for example by speaking, writing or sending radio signals'. Communication is a process of exchanging messages between the source and the audience through spoken or written signals. In the modern age of science and technology, communication is possible through various means. According to,

> "The term communication has been derived from the Greek word 'communicate', which means 'to share'."

It is true that communication is sharing as it involves interchange of ideas, feelings and experiences between the participants of any communicative contexts. Very often communication is a two way process.

Today's Engineering is the biggest field of study in the world. First of all English is a tool that significantly affect engineering students in academic life. While most of the theories in engineering are taught in English, it requires to have good English communication competence. In academic life ,engineering students have to deal with the countless English lectures, tutorials, labs, project reports and papers. Most engineering professors in various universities are also conducting lectures in English. The most convenient source of information i.e. Internet provides most of the information in English. During the job seeking process in interviews, GD's ,it is but of crucial importance to achieve mastery in English proficiency. After securing the job they are required to work in groups since their task seldom be solved by an individual. So, being an engineer requires to co-operate and communicate with different people from different part of the world. English is used as the working language on large extent. In order to co-ordinate with the colleagues, engineers have to speak fluent English. So, English communication competence plays an important role in the academic life and career of engineering students in Tamil Nadu also.

Tamil Nadu cannot remain aloof from the changing scenario in the global context. The impact of globalization in the international arena has also been rather visible in the engineering education in Tamil Nadu. The effect of globalization is now appearing in Tamil Nadu. The ence are the prime issues now. Unless The Tamil engineers prove to be ent in the global market, the situation in going to be much harder for them

Enhancing Learning English through Effective Teaching

Right from the inception, 'Anna University (AU) in Tamil Nadu has incorporated English as one of the compulsory subjects in the curriculum for the students of first year-Communicative English and third year-Communication and Soft Skills lab. Undoubtedly, there have been changes in the English syllabus and significant modifications have taken place in the course. But the most interesting thing is that every change has refined the English syllabus further. Every time the new syllabus has been designed, certain parts of the syllabus have been removed and replaced by some new, and more relevant teaching items have been incorporated.

Teaching of the English language in engineering in Tamil Nadu has remained equally relevant even at this moment as the use of English is widespread. It is taught as one of the compulsory subjects in engineering not because it is taught in other foreign universities but because there are strong evidences that the English language is still a very essential means of communication in both academic life and the future career of the engineers in Tamil Nadu.

In our country ,about 75% students of the engineering are from rural areas and most of them are coming through regional language medium schools. No doubt that as they have entered into the engineering colleges ,they do possess intelligence i.e. necessary qualification for higher education and bright future. But, at every walk of life and career English becomes an obstacle in their way of career. So, let us examine the reasons which make English as a souring grape for rural students even today in this modern era. The rural area students lacks the exposure to the English communication in the family , society as well as in the colleges. As a result of this even the merituous gold medalist fail to achieve success during personal interviews due to lack of communication skills, soft skills, interpersonal skills and personality development. During academics also lack of confidence of being unable to communicate in English leads to feeling of inferiority complex, as a result students keep themselves lonely and isolated.

The other important factor is the traditional education system which affects English language learning and acquisition. Many complaints have been made against the traditional education system which is more inclined towards memorization and long systematic study hours. Basically it requires four skills i.e. Listening, Speaking, Reading and ing.(LSRW).Our students are being trained in reading and writing for long ages and ıing and speaking skills are neglected and ignored which are very important. Learning is the ɔasic skill which makes speaking possible. Learning language is possible only through active

listening. As an illustration we can take an example of language acquisition by a baby. It starts speaking the words which it listens frequently. Our education neglects the importance of listening which results in lack of skill of speaking. Lack of modern and advanced technology in the process of language learning also affects the language acquisition. e.g. use of computers and internet, power point presentation, OHP etc.

The growing problem not only in Tamil Nadu but all over India is that students are more stressed than ever. In fact, India has one of the highest rate of suicides among people aged between 15 and 29. Although the reasons are myriad but failure in Examination and Unemployment.

Knowing the importance and growing demand of English communication competence for engineering students from rural areas, there a need for the teachers as well the students to make integrated efforts.

Faculty is expected to fulfill their assigned responsibilities. But apart from that they should think it as their moral responsibility to take more efforts to provide more exposure to English language for students as to achieve communication competence. The students when forced to learn communication on their own, they find it as a herculean task. So, they expect assistance and warmth understanding from teachers. Now days a comprehensive course which focus on both writing and speaking skills is introduced in most of the universities in Maharashtra. So, during the interactive sessions the students should be encouraged and helped to talk .So, that the students can built an ability to participate in various activities such as paper presentations, GD's, mock interviews, role plays etc. to develop English communication competence. It is necessary that Students Talk Time should be higher than Teacher Talk Time .

Students from the secondary and higher secondary level should be given dictionary of technical words with their meanings in regional language for use. The technical teachers should help students in understanding the technical words in English and their equivalents in regional languages. Again they should help the students to understand the meanings of long and complicated sentences in technical subjects.

Grammar should be taught in the form of application of it in day to day life. When we age ,it requires a lot of time .We get a lot of exposure to it as all our eals takes place in the regional language. So, it is but natural that it does not e grammar of regional language. Unfortunately it does not happen with English

which is a second language. From the experience ,it is essential to learn grammar of Englis second language for getting confidence of speaking and performing the best in all walks of lif

In this modern era, new trends and methods of teaching are emerging in the learnin the English language competence which involves the use of Computer assisted language lear in the Language Labs. Most of the students are tired of the traditional way of teaching and more interested in doing exercises on a computer than by hand. Use of Audio /video c Interlingua method-Listen and see clippings in regional language and English, Langu Learning-vocabulary-synonyms and antonyms, Etymology reading Grammar, Role pl Speaking task, Translation and Fluency Task by this method of learning students are provid lot of practice and exposure to the English language. This method leads to individualizatic learning, where teachers acts as mentor ,trainer and aspirant to facilitate learning. The teac should be aware of the latest technologies ,explore new ideas and have certain amour specialization in the subject and Students on their own should make use of English jour television programs, newspapers, magazines, English language Resource centers to acquir English communication skills.

English communication skills are recognized as the important element in the acad life and career of the engineering students. It requires to make use of integrated metho facilitate advanced communication skills, which is the demand of industry as well as society rural area engineering students should effectively make use of the faculty, education systen the amenities provided to them in combination with the self efforts, to emerge as a comp user of English communication to become successful in life and career.

References

- Freeman D. Techniques and Principles in Language Teaching. New Delhi: O University Press, 2007.Print.
- Reimer MJ. English and Communication Skills for the Global Engineer, Aust *Global Journal of Engineering Education*. 2002.
- Konar N. *Communication Skills for Professionals*. New Delhi. PHI Learning P Limited. 2010.Print.

International Conference on Smart Engineering Materials ICSEM - 2016

RV College Of Engineering, Bengaluru,

An initiative under TECHNICAL EDUCATION QUALITY IMPROVEMENT PROGRAMME TEQIP-II

[Sub-component 1.2.1]

This is to certify that

S SHEIK FAREED

presented (Oral / ~~Poster~~) paper **α-Fe_2O_3 nanoparticles as a by-product from the thin film (SILAR) deposition process: A study on the product** at the International Conference on Smart Engineering Materials **ICSEM - 2016**, organized by R. V. College of Engineering, Bengaluru during 20-22 October 2016.

Dr. Sham Aan General Chair	Dr,. M Krishna *Technical Chair*	Prof K N Raja Rao *TEQIP Coordinator*	Dr. K N Subramanya *Principal RVCE*

TRUE COPY ATTESTED

PRINCIPAL
MOHAMED SATHAK ENGINEERING COLLEGE
KILAKARAI-623806.

Rashtreeya Sikshana Samithi Trust
RV INSTITUTIONS

ICSEM

20 - 22 October, 2016

INTERNATIONAL CONFERENCE ON SMART ENGINEERING MATERIALS

SOUVENIR

ICSEM - 2016

RV College Of Engineering,
Bengaluru – 560 059

TECHNICAL EDUCATION QUALITTY
IMPROVEMENT PROGRAMME
TEQIP –II INITIATIVE
[Sub-component – 1.2.1]

In collaboration with

materials today

ROYAL SOCIETY OF CHEMISTRY

TEQIP SPFU

THEME-4 Functional Materials (FM)

Theme ID	Paper ID	Titile of The Paper	Authors
FM-1	ICSEM-1036	Assessment of porous media combustion with foam porous media for surface/submerged flame	Ayub Ahmed Janvekar et.al
FM-2	ICSEM-1037	Nano-indentation properties and behaviour of machining parameters in dry turning of AISI 304 steel using nc-AlTiN/Si3N4, TiAlN and TiN coated inserts	Aaditya V.B et.al.
FM-3	ICSEM-1049	Hygrothermal Effect on Mechanical properties of Vinylester/Carbon and Isopolyester/Carbon Composites	Kanchiraya S and Shivakum
FM-4	ICSEM-1056	Development of Electrospinning System for Synthesis of PolyVinylPyloridine Thin Films for Sensor Applications	Amith.V et.al.
FM-5	ICSEM-1062	The Study of Tensile and Flexural Strength of Cattle Bone Particulate Reinforced Epoxy Composites	Harish.S et.al.
FM-6	ICSEM-1080	α-Fe2O3 nanoparticles as a byproduct from the thin film (SILAR) deposition process: A study on the product	S.Sheik Fareed et.al.
FM-7	ICSEM-1086	State of the Art on Automotive Lightweight Body-in-WhiteDesign	Kiran Kumar Dama et.al.
FM-8	ICSEM-1087	State of the Art on ConstructionalConcepts ofAutomotive Body Structures	Kiran Kumar Dama et.al.
FM-9	ICSEM-1101	Pzt: The Great Potential of Future Electricity Cohort	K. Viswanath Allamraju
FM-10	ICSEM-1102	Thermo physical properties of Jute, Pineapple leaf and Glass fiber reinforced polyester hybrid composites	M. Indra Reddy et.al.
FM-11	ICSEM-1181	Low temperature synthesis and optical and electrical characterization of ZnO thin films	B.R. Nagabushana and Vishwas
FM-12	ICSEM-1143	A comparative study on the electrocatalytic activity of electrodeposited Ni-W and Ni-P alloy coatings	Liju Elias and A. Chithar Hegde

ICSEM-1076

Effect of Thermal Cycling on Nano Enhanced Myo-Inositol for Sola Thermal Energy Storage

Durgesh Kumar Singh and S Suresh
Department of Mechanical Engineering, National Institute of Technology, Tiruchirappalli- 620015, Tamil India

Abstract:

Present study investigates chemical and thermal stability of myo-inositol (a sugar alc laden with alumina-CuO nanoparticles (size 40-50 nm) with 1.0, 2.0 and 3.0 wt. %as p change materials for solar thermal energy storage in the temperature range of100°C to 26 Thermal and chemical stability were checked by differential scanning calorimetry (DSC) Fourier transform-Infra red (FT-IR) techniques. Surface morphology was investigate scanning electron microscopy technique (SEM). Heat of enthalpies decrease was les myo-inositol after adding alumina-CuO nanoparticles as compared to pure myo-inositol 50 thermal cycles. FT-IR results showed that no new bond formation takes place betwee and alumina-CuO nanoparticles during thermal cycling and only physical interaction t place.

Keywords: Phase change material, Thermal cycling, Nanoparticles, Melting tempera Heat of fusion, Heat of solidification and Solidification temperature

ICSEM-1080

α-Fe2O3 Nanoparticles as a Byproduct from the Thin Film (SILAR) Deposition Process: A Study on the Product

[1]S Sheik Fareed, [2]N Mythili, [3]G Vijayaprasath, [4]R Chandramohan, [5]G Ravi
[1,2]Department of Physics, Mohamed Sathak Engineering College, Kilakarai-623806, Tamil Nadu, India
[3,5]Department of Physics, Alagappa University, Karaikudi- 630003, Tamil Nadu, India
[4]Department of Physics Sree Sevugan Annamalai College, Devakottai-630303, Tamil Nadu, India.

Abstract:

The residual bath obtained from the SILAR deposition of magnetite thin films v processed to have particles. Obtained particles were calcined at 200, 400 and 600°C. particles were characterized using XRD, FTIR, UV-Vis-DRS, PL, HRTEM and VSM. X and FTIR analysis reveals that all the calcined particles were in α-Fe2O3 nanophase. Unif spherical morphological particles formation was observed from HRTEM images. Obta particles exhibit spin canted-ferromagnetic behavior. Results were compared with prev reports, which confirms the applicability of these byproduct (α-Fe2O3) nanoparticles in reported applications.

E.R.K ARTS & SCIENCE COLLEGE

(Affiliated to Periyar University, Salem)
Erumiyampatti, Kokkarapatti (Po.), Pappireddipatti (Tk.), Dharmapuri (Dt.) - 636 905.
Ph: 04346 - 322885, 242777, Website : www.erk.co.in, E-mail: erkasc@gmail.com

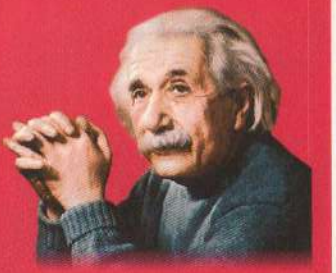

ALBERT EINSTEIN ASSOCIATION

DEPARTMENT OF PHYSICS

Organizes

National Conference on

"GRAVITATE APPLICATIONS IN NANOTECHNOLOGY"

(GAIN'16)

Certificate

This is to certify that ~~Dr.~~ / Mr. / ~~Ms.~~ / ~~Mrs.~~ S. SHEIK FAREED *of* Mohamed Sathak Engg. College , Kilakarai *has attended the Conference and Presented a Paper entitled* Influence of PVA Addition on the structure & optical Properties of SILAR Deposited Fe_3O_4 Thin Films *in the one Day National Conference on the topic "GRAVITATE APPLICATIONS IN NANOTECHNOLOGY" Organized by Albert Einstein Association, Department of Physics, E.R.K. Arts & Science College held on 21st July 2016*

TRUE COPY ATTESTED

PRINCIPAL
MOHAMED SATHAK ENGINEERING COLLEGE
KILAKARAI-623806.

Organizing Secretary

Mr. D. SAKTHI
Convener

Dr. A. PALVANNAN
Patron

NATIONAL CONFERENCE
ON
"GRAVITATE APPLICATIONS IN NANOTECHNOLOGY"

GAIN '16

On 21st July 2016

SOUVENIR

ORGANIZED BY

ALBERT EINSTEIN ASSOCIATION
...HYSICS
...IENCE COLLEGE
... University)
...apatti PO, Pappireddipatti TK,
...6905,
Ph.No: 04346 322885, 242777
Website: www.erk.co.in
E-Mail: erknhysics@gmail.com

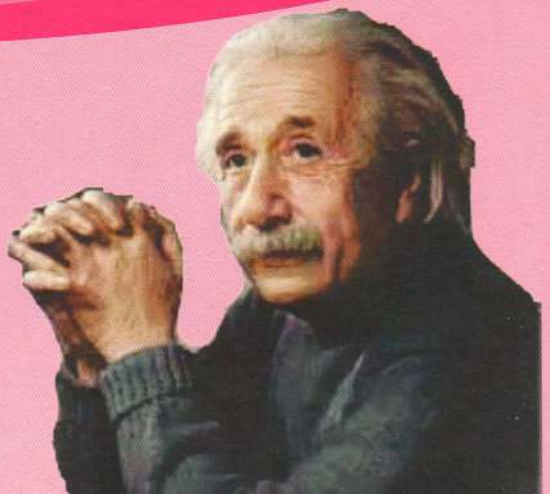

CP - 32

INFLUENCE OF PVA ADDITION ON THE STRUCTURE AND OPTICAL PROPERTIES OF SILAR DEPOSITED Fe_3O_4 THIN FILMS

*S.Sheik Fareed[1] and G.Ravi[2]**

[1] *Department of Physics, Mohamed Sathak Engineering College, Kilakarai-623806*

[2] *Department of Physics, Alagappa University, Karaikudi -603001*

Capping agent plays a key role in stabilizing the size and morphology of metal oxides. Poly vinyl alcohol (PVA) acts as a binder with the functional O-H group at the end of the polymer chain. Fe_3O_4 (magnetite) thin films were prepared by simplified SILAR deposition process with PVA as capping agent. The required precursor solution was prepared by adding 0.1 M of Iron (II) Sulfate heptahydrate ($FeSO_4.7H_2O$) and 0.5 M of NH_4OH, 0.001 M of PVA in 100 ml of water with effective stirring. The cleaned glass slides were immersed in precursor solution maintained at 85°C and water for 15 s alternatively for 30 cycles to have well adherent film of thickness around 1.5 µm. The prepared films were annealed at 100 and 300°C. Structural studies show the peak broadening and increase in intensity for PVA capped Fe_3O_4 films annealed at 300°C. The crystallite size decreases with the increase in annealing temperature of PVA capped Fe_3O_4 films. UV-Vis studies reveal that the band gap of the films increases from 2.45 to 2.57 eV with annealing which were calculated from Tauc's plot. The results exhibits that the PVA influences the size and property of Fe_3O_4 thin films.

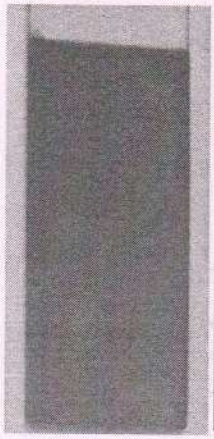

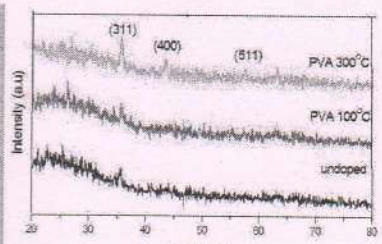

S.No	Sample	Crystallite size (D) nm	Energy gap (E_g) eV
1.	Undoped	61	2.45
2.	PVA capped Fe_3O_4 films annealed at 100°C	29	2.49
3.	PVA capped Fe_3O_4 films annealed at 300°C	18	2.57

: SILAR deposition, magnetite, Tauc's plot, PVA

NATIONAL CONFERENCE
ON
"GRAVITATE APPLICATIONS IN NANOTECHNOLOGY"

GAIN '16

On 21st July 2016

SOUVENIR

ORGANIZED BY

ALBERT EINSTEIN ASSOCIATION
...HYSICS
...IENCE COLLEGE
... University)
...apatti PO, Pappireddipatti TK,
...6905,
Ph.No: 04346 322885, 242777
Website: www.erk.co.in
E-Mail: erknhysics@gmail.com

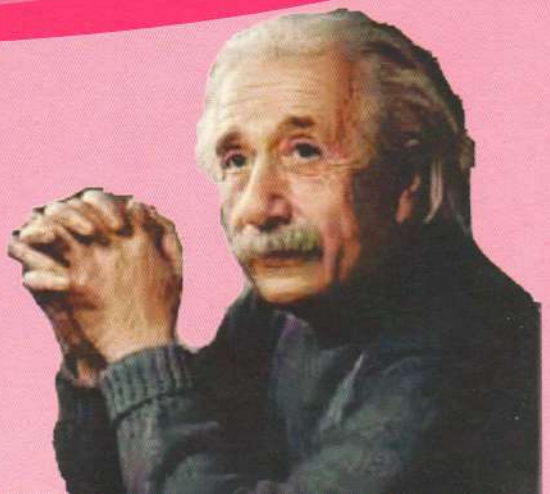

CP - 26

A STUDY ON THE STRUCTURAL AND MORPHOLOGICAL PROPERTIES OF BOEHMITE NANOFLAKES PREPARED BY SOL-GEL METHOD

N.Mythili[1], C.L.Aiswarya[2], S.Sheik Fareed[1], S.Sabeena Begum[1] and M.Mohamed Yaseen[1]*

[1]Assistant Professor, Department of Physics, Mohamed Sathak Engineering College, Kilakarai-623806

[2]Student, Department of Aeronautical Engineering, Mohamed Sathak Engineering College, Kilakarai

Email*: *mythuwinmile@gmail.com*

ABSTRACT

Boehmite (alumina) is a crystalline form of aluminum oxides and hydroxides used as functional binder in refinery, hydro treatments and biomedical industries. Boehmite was synthesized by sol-gel method using the precursors Aluminium nitrate non hydrate $Al(NO)_3 .9H_2O$ and Sodium Hydroxide (NaOH) and urea ($NH_2.Co.NH_2$) as complexing agents. The sol was stirred, sonicated and it was converted to gel by ageing-drying and finally calcined at 300 °C. The prepared sample was characterized using XRD, UV-Vis, PL, FTIR and TEM. Structural studies (XRD) reveal the Boehmite phases of aluminum with the crystallite size of 5 nm. Optical band gap and defects related analysis were carried out from UV-Vis and PL studies. Vibrational studies reveal the presence of Al-O stretching modes. TEM images show the formation of nanoflakes Boehmite with some agglomeration. The prepared Boehmite can be used in nanocomposite for mechanical applications.

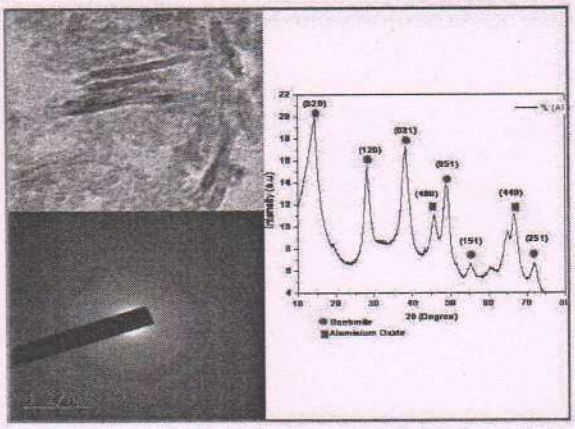

s: Boehmite, sol-gel method, nanocomposite, TEM

NATIONAL CONFERENCE
ON
"GRAVITATE APPLICATIONS IN NANOTECHNOLOGY"

GAIN '16
On 21st July 2016

SOUVENIR

ORGANIZED BY

ALBERT EINSTEIN ASSOCIATION
HYSICS
IENCE COLLEGE
r University)
apatti PO,Pappireddipatti TK,
36905,
Ph.No: 04346 322885, 242777
Website: www.erk.co.in

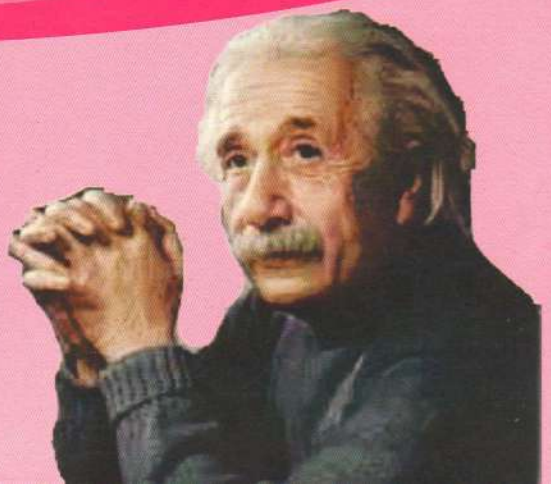

CP - 85

EFFECT OF COMPLEXING AGENTS ON THE SYNTHESIS OF IRON OXIDE NANOPARTICLES BY CHEMICAL METHOD

M. Mohamed Yaseen, N. Meera Mohideen, N.Mythili, S.Sheik Fareed, S.Sabeena Begum and H. Mohamed Mohaideen

Department of Physics, Mohamed Sathak Engineering College, Kilakarai-623806

Email: useen2005@gmail.com

Iron oxides of nanostructures have promising applications in magnetic recording, magneto-optical, catalysis and biomedical domains. Various polymorphs of iron oxide have widened the possibilities of research based on its structural, magnetic and optical aspects. Fe_3O_4 and α-Fe_2O_3 nanoparticles were synthesized by chemical precipitation method by using the same precursor of $FeSO_4.7H_2O$. Polymorphs of Iron oxide were achieved by varying the complexing agents like NaOH and NH_4OH for Fe_3O_4 and α-Fe_2O_3 synthesis. Structural, vibrational and optical studies of the samples were analyzed using XRD, FTIR and UV-Vis spectroscopy. Structural studies show the cubic and rhombohedra crystal systems of Fe_3O_4 and α-Fe_2O_3. FTIR analysis shows (a) sharp doublet peak in the fingerprint region confirms the presence of α-Fe_2O_3 (b) suppressed single broad peak around the same region explains the formation of Fe_3O_4. A UV-Vis spectrum shows the characteristic absorption maximum of iron oxide with slight variation in energy gap values. Thus the results validates that by varying the complexing agents, phases of Iron oxide can be modified.

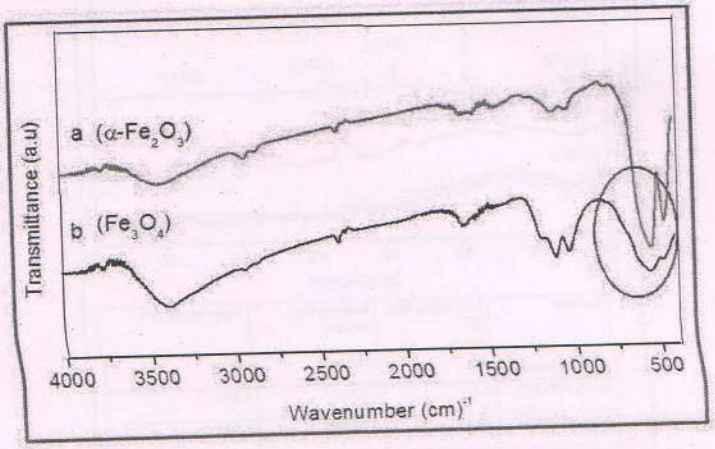

Keywords: nanostructures, magneto-optical, biomedical domains, Polymorphs

NATIONAL CONFERENCE
ON
"GRAVITATE APPLICATIONS IN NANOTECHNOLOGY"

ORGANIZED BY

ASSOCIATION
HYSICS
CIENCE COLLEGE
ar University)
arapatti PO,Pappireddipatti TK,
Dharmapuri DT, PIN-636905,
Ph.No: 04346 322885, 242777
Website: www.erk.co.in

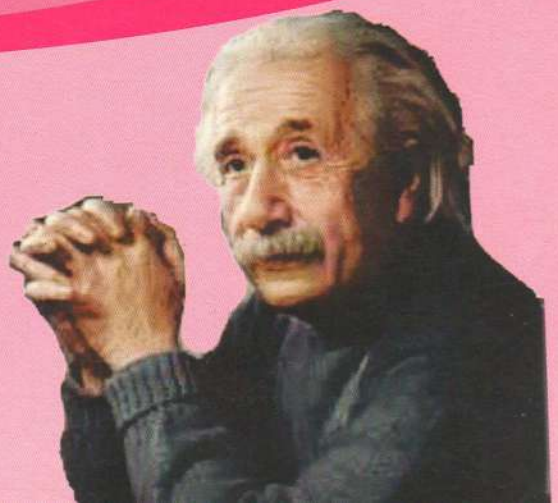

CP-

STRUCTURAL ANALYSIS OF Al_2O_3 NANOPARTICLES ON THE EFFECT OF TEMPERATURE BY CHEMICAL METHOD

S.Sabeena Begum[1], N.Mythili[1], C.L.Aiswarya[2], S.Sheik Fareed[1] and M.Mohamed Yaseen[1]

[1] Department of Physics, Mohamed Sathak Engineering College, Kilakarai-623806

[2]Student, Department of Aeronautical Engineering, Mohamed Sathak Engineering College, Kilakarai

Email: sabeenabatcha@gmail.com

High hardness and strength, excellent resistance to heat and corrosion with less weight makes aluminium a suitable material for composities, absorbents, propellants and explosives. The aim of the present work is to study the effect of temperature on the crystallographic modification on aluminium oxide nanoparticles. Aluminium nitrate non hydrate $Al(NO)_3 .9H_2O$ and Sodium Hydroxide (NaOH) was used to prepare Al_2O_3 nanoparticles by chemical precipitation method. The prepared samples were calcined in air at 200, 400 and 600°C. XRD analysis was carried out to study the crystallinity and the crystallographic parameters such as crystallite size (D), dislocation density (δ), microstrain (ε). The diffraction peaks matches with Al_2O_3 phase of 42-1468 of the JCPDS card. Crystallinity increases with temperature and at 700°C the peaks shows well defined peaks crystallinity. Crystallite size, dislocation density and microstrain increases with temperature. Thus by varying the calcinations temperature crystallographic parameters of aluminium nanoparticles can be tuned.

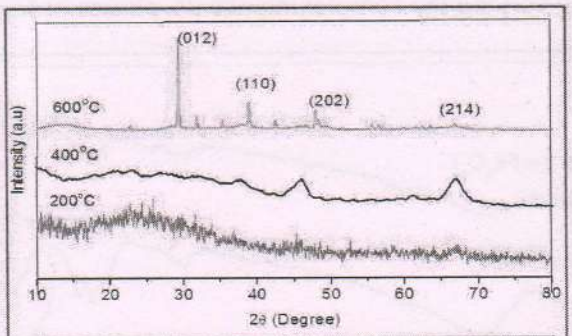

Sample	Crystallite size (D) (nm)	Dislocation density	Microstrain 10^{-3}
Al_2O_3 at 200°C	6.1	6.2510^{14}	0.876
Al_2O_3 at 400°C	9.3	1.2310^{15}	4.893
Al_2O_3 at 600°C	40.2	2.7710^{15}	5.587

posites, chemical precipitation, crystallinity, microstrain

SREE SEVUGAN ANNAMALAI COLLEGE

Devakottai

National Seminar

11th October, 2014

The Literature of the Marginalized

Critical Essays

Organized by

Department of English

University Grants Commission

54. Sufferings of Downtrodden in Mulk Raj Anand's *Untouchable*

*C.Alagesan **S.Sundaram
*Assistant Professor,Department of English,Mohamad Sathak Engineer college,Kilakarai.
**Guest Lecturer in English,Bharathidasan University Model College,Vedaranyam.

A colossus in the Indian English literature, Mulk Raj Anand occupies a pride of place among the Indian novelists by occupying himself historically the two worlds: one the colonial decades and the other post-colonial generations. A committed humanist he believes in the amelioration of society on the socialist principles with which he thinks that heaven on earth is possible. As a writer he sees the relation of the concrete with the universal.

The novel *Untouchable* covers the events of a single day in the life of a low caste boy Bakha, in the town of Bulashah. The eighteen-year-old boy is one of the sons of Lakha, the jemedar of the sweepers of the town. Bakha is the child of the 20th century. He comes under the influences of the modern world which causes ripples within him. From Tommy he has secured a pair of old breeches and from a sepoy a pair of old boots. At the dawn of every day he begins his work of latrine cleaning and he thinks that he is an efficient worker. His sister Sohini faces the onslaught of the upper class people in the area when she approaches the well to get water. She tells her father "they think we are dirt because we clean their dirt" (105). Similarly her brother faces the wrath of the upper class people when Bakha lifts the boy who is injured in a hockey game. The boy's mother yells at him saying that he has polluted her son by touching him and lifting him from the ground. Now Bakha understands twin problems of caste and poverty squalor and backwardness.

As suggested by Mahatma Gandhi, Anand had made certain changes in the novel *Untouchable*. Anand's life and experience in Sabarmati Ashram proved in realizing the characters in the novel. The periods of meditation in the Ashram helped Anand to recollect the social structure of India where the downtrodden were made to suffer because of their birth and station in life. His recollection and Gandhiji's preachings to show devotion to the poor was a strong source of conversion for Anand. He began to realize in his mind to create an oppressed character caught in the villainy of the Indian social structure subjecting them to untold suffering and humiliation. The result was the creatin Bakha in *Untouchable*. The intense and passionate feelings of Anand for the oppressed comes to the fore in the novel. It is sensitive subject which Anand has taken up to deal with in the novel. Though it has been more than half a century hence a social evil has not died down nor has it been completely wiped out in India. Anand is the harbinger to focus on the social onslaught in absolute realistic terms in his novel *Untouchable*.

Anand is committed writer to the social causes. His penetrating thought and humane attitude in understanding the grim social realities in India found their expression in his novel. *Untouchable* is a revolutionary novel of protest against the pervading social evil in India. Anand's social awareness and objectives impelled him to create the novel to focus the social evil and to rally for the removal of the social evil by inculcating in the minds of the Indian intellectuals to put their mite to end the social reformers in India were engaged in an earnest way to remove casteism and untouchability.

ommitment to remove the deep-rooted social malice in the Indian society made him create
. He had wanted to show the youth's "unique sensitiveness as against the people of the
thought merely touching him is a degradation" (107). He further narrated that " I meant
how that such small tenderness among people in private life or the catharsis of human

Bakha arrests our attention in the entire novel. As E.M. Forster observes that

Bakha is a real individual, lovable, thwarted, sometimes grand, sometimes weak, and thoroughly

Anand concludes the novel *Untouchable* with a note of faith and idealism. As Bakha returns home his mind is raised with the hope that soon the flush system would come then the sweepers " can be free from the stigma of untouchability and assume the dignity of status that is their right as useful members of a casteless and classless society" (109). The manifest plea in the novel is for the total abolition of untouchability. Bakha fervently hopes for the drawn to his nature of his work and his relevance in the society without the label of 'Untouchable'.

The novel *Untouchable* acquires human significance and social relevance when Anand meticulously brings out the inner life of Bakha. It was a growing concern for metaphoric untouchables in all cultures and walks of life. Anand also brings to focus Bakha's smouldering rage. His feelings are compared to "spurts of smoke from a self smothered fire" (109). His unspoken words are described as the soundless speech of cells receiving and transmitting the emotions, which one day would spit fire that is what Anand felt probably when he wrote the novel. The novelist wants humane gestures towards the underprivileged like Bakha. The novels 'cleanness' of structure celebrates un-cleanness not so much of Bakha's work as of the minds and sensibilities of those among whom he lives. The cheap minded temple priest and the cruel townsmen and the malicious gossiping women with their assumed superior upper casteness are in striking contrast to Bakha. It is not Bakha who pollutes them so much as it is their own fear of being polluted, a fear that destroys to see the realities. The fear also dehumanizes them.

Anand's down-to-earth portrayal of the naked realities of our social evils which are dismal and harrowing makes *Untouchable* a social document besides being a novel first of its kind in the colonial Indian social context. Despite the legal protection offered to the Untouchables in the Indian society, even now when such inhuman incidents are reported in the Indian dailies we are compelled to think past social maladies still continue in some parts of our nation. Hence Anand's *Untouchable* is relevant even today and if social evils are not eradicated completely in India, probably this novel all the more would become significant to the present and posterity, as a pathetic social document.

The central theme of *Untouchable* is the age-old injustice perpetrated by traditional Hindu society upon a whole class of people within its fold. The very choice of the theme was a bold stroke of genius. To make a sweeper the hero of his novel was a revolutionary departure for an Indian writer of nineteen-thirties. First, Indian fiction in most of the Indian languages was then a fiction about middle and higher classes for the middle-class writers. Secondly, even when low class life did enter it, it could not descend so low as to write about sweepers messing about with excrement. Furthermore, even if the average middle class Indian writer wanted to write about so ugly a subject, he would hardly have know the life of his protagonist in intimate detail. In contrast with this, Anand was well-equipped to embark upon this revolutionary departure. As a child, he had played with the children of the sweepers attached to the regiment in which his father was employed. In fact, Bakha, the hero of Untouchables, appears in both the autobiographical novels of Anandviz- *ning Face.* There was little about his hero and his life that Anand did not know. and his life has thus a clear ring of authenticity about it. As E.M. Forster remarks, ave been written by an Indian, and by anindian who observed from the outside. No athetic, could have created the character of Bakha, because he would not have roubles. And no Untouchablecould have written the book, because he would have been involved in indignation and self-pity (25).

References:

SREE SEVUGAN ANNAMALAI COLLEGE

(Accredited with 'B' Grade by NAAC)

DEVAKOTTAI,

Sivagangai District, Tamilnadu, South India

DEPARTMENT OF ENGLISH

UGC SPONSORED NATIONAL SEMINAR ON THE LITERATURE OF THE MARGINALIZED

(NALAMA'2014)

CERTIFICATE

This is to certify that ~~Dr/Prof~~/Mr/~~Ms~~ C. Alagesan, Asst. Prof. of English, of Mohammed Sathak Engg. College, Kilakarai ~~participated~~ / presented a paper / ~~chaired a session~~ under the title Sufferings of Downtrodden in Mulk Raj Anand's 'Untouchable' in the UGC Sponsored National Seminar on The Literature of the Marginalized organized by the Department of English, Sree Sevugan Annamalai College, Devakottai, Sivagangai District, Tamilnadu, South India In collaboration with Tamilnadu English Language Teachers Association (TELTA) on 11.10.2014.

Organizing Secretary

Principal

TRUE COPY ATTESTED

PRINCIPAL
MOHAMED SATHAK ENGINEERING COLLEGE
KILAKARAI-623806.

Journal of Chemical and Pharmaceutical Sciences www.jchps.com ISSN: 0974-2115

DEVELOPMENT AND CORROSION PERFORMANCE OF 3-AMINOPROPYLTRIETHOXYSILANE GRAFTED EPOXIDIZED ETHYLENE-PROPYLENE-DIENE TERPOLYMER RUBBER COATINGS

M. Vadivel[a]*, M. Suresh Chandra Kumar[b], C. Vedhi[c],V. Selvam[d], J. Dhaveethu Raja[a]

[a]Department of Chemistry, Mohamed Sathak Engineering College, Kilakarai - 623 806, Ramanathapuram (Dist), Tamilnadu, India.

[b] Polymer Nanocomposite Centre, Department of Chemistry, Scott Christian College, Nagercoil 629 003, India

[c] Department of Chemistry, V.O. Chidambaram College,Tuticorin 628 008, India

[d]Department of Chemistry, K. Ramakrishnan Engineering College, Tiruchirapalli - 621 112, Tamilnadu, India.

***Corresponding author:E.Mail:vadivelche@gmail.com**

ABSTRACT

A novel copolymer of 3-aminopropyltriethoxysilane (APTES) grafted epoxidized ethylene-propylene-diene terpolymer (eEPDM-g-APTES) was synthesized in toluene, 25% red iron oxide as additive. The chemical structure of eEPDM-g-APTES was confirmed by FT-IR spectroscopy. The corrosion resistant behaviors of EPDM, eEPDM, eEPDM-g-APTES with or without red iron oxide were investigated by potentiodynamic polarization and electrochemical impedance spectroscopic methods and also studied salt-spray tests in 3.5% NaCl solution. The experimental results reveal that the eEPDM-g-APTES with 25% red iron oxide offers the maximum corrosion protection to the steel surface. The better protective action offered by the reaction of APTES amine with oxirane groups of the eEPDM, which gives coating films with a high cross-link density.

Keywords: eEPDM, eEPDM-g-APTES, potentiodynamic polarization, electrochemical impedance spectroscopy.

INTRODUCTION

Rubber based coatings have, for a long time, found use in industrial maintenance, marine and concrete and masonry walls. Rubber is a polymer with good barrier properties for water and oxygen. Ethylene-propylene-diene terpolymer (EPDM) is widely used as adhesive materials, due to its excellent physical and durability properties. Cross linked ethylene-propylene-diene terpolymer (EPDM) is one of the majority commonly used industrial polymer because of its marvelous resistance to heat, light, oxygen and ozone. Due to simple reaction condition (low temperature and low pressure), the silanization of MWNTs has attracted increasing attention for preparing MWNT/polymer composites. Silane coupling agent can be chemically described as R[BOND]Si[BOND]inline image. The R′ group is generally alkoxy group that reacts readily with the hydroxyls on nanotube surface; The R group is usually ethylene, amine, epoxy, thiohydroxy, etc., and chosen to be reactive with different polymeric resins. Ma et al., however, due to the incompatibility of EPDM with inorganic pigment, the corrosion-resistant property of EPDM coating is very poor, which strongly limits their practical applications. However, noticeable improvements of above properties of EPDM can be obtained through grafting by other functional compounds. Silanes are also used as coupling agents that improves the adhesion of different nature of surfaces. Coupling agents are having both organic and inorganic groups; they bridge the interface between polymeric matrix resin and reinforcement through covalent bonding. The inorganic group is compatible with filler and the organic group is compatible with polymer matrix resins. In the present study, the EPDM was first epoxidized with in situ formed per formic acid, which induced functional epoxy groups into the EPDM macromolecular backbone. A novel and new graft copolymer of 3-aminopropyltriethoxysilane onto epoxidized ethylene-propylene-diene terpolymer (eEPDM-g- APTES) has been synthesized in toluene. The corrosion resistant behaviors of EPDM, eEPDM, eEPDM-g-APTES with or without red iron oxide were investigated by potentiodynamic polarization and electrochemical impedance spectroscopic methods and also studied salt-spray tests in 3.5% NaCl solution.

EXPERIMENTAL

Materials: The EPDM (ENB) elastomer used in this study was a commercial grade Nordel IP 4770P (ethylene/propylene/ 5-ethylidene-2-norbornene = 70/25/5 by wt.% , Mooney viscosity, ML $_{(1+4)}$ at 125°C is 70 and Pont Dow elastomers, USA. Hydroxyl-terminated polydimethylsiloxane (HTPDMS) as thoxysilane (APTES), (M_w = 221.3, boiling point = 217°C, density = 0.946 g.cm^{-3},) was emicals, USA. Dibutyltindilaurate (DBTDL) was purchased from Merck, Germany. l (88%), hydrogen peroxide (30%), toluene,n-hexane were used as received.

Journal of Chemical and Pharmaceutical Sciences www.jchps.com ISSN: 0974-2115

In situ epoxidation of ethylene–propylene– diene terpolymer: The EPDM was first dissolved in toluene in a three necked flask equipped with a mechanical stirrer and thermometer, and maintained at 50°C in a water bath. Under continuous stirring, the EPDM solution was acidified stepwise with 88% formic acid to pH 2–3. The epoxidation was performed by dropping the required amount of H_2O_2 (30%) for 30 min. A rapid introduction of this reagent is not recommended, because it causes excessive development of oxygen due to the decomposition of hydrogen peroxide at high temperature. The reaction was continued for 7 h at 50°C. After epoxidation, the rubber was coagulated in acetone, thoroughly washed with distilled water, soaked in 1% w/v Na_2CO_3 solution for 24 h, and finally rinsed with distilled water. The rubber prepared was dried in a vacuum oven at 40°C to a constant weight.

Preparation of eEPDM-g-APTES: The reactions were carried out in 500 ml three necked, round bottom flask equipped with a reflux condenser, a Teflon-coated mechanical stirring and a nitrogen inlet. 10gm of eEPDM was dissolved in 200 ml toluene and refluxed until complete dissolution of eEPDM. Further, 0.25 wt.% APTES dissolved in 50 ml of toluene were added to eEPDM, using dibutyl tindilaurate catalyst, with continuous stirring for 2 h at 50°C. After the completion of reaction, the products were precipitated with methanol, filtered and dried in vacuum.

RESULTS AND DISCUSSION

Fourier-transform infrared spectroscopy: Fig. 1 shows the FTIR spectra of EPDM, eEPDM and Siliconized epoxidized EPDM. The IR spectra of EPDM (Fig. 1(a)) shows the C–H stretching vibration (aliphatic) at 2911 cm^{-1}, $–CH_2$ rocking vibration at 1451 cm^{-1}, CH_3 symmetric bending vibration at 1367 cm^{-1} due to the presence of propylene group, $–(CH_2)_n–$ wagging vibration at 721 cm^{-1} due to the presence of polyethylene chain, C–C stretching vibration at 2851 cm^{-1}, and the unsaturation band (>C=CH–) at 811 cm^{-1} due to the presence of ENB content. The FTIR spectrum of eEPDM (Fig. 1(b)) was characterized by the presence of an epoxide band at 870 cm^{-1} due to asymmetric epoxide ring stretching. Furthermore, the intensity of the >C=CH– band at 811 cm^{-1} decreases because of the epoxidation of EPDM, which demonstrates that the C=C double bond in EPDM was converted to the epoxy functional group in eEPDM. The conversion of double bonds to epoxide was obtained as 50% (ca.2.4 mol %). To take advantage of relative change of absorbance at 811 and 870 cm^{-1}, a quantitative analysis was performed by area measurement of methyl deformation band at 1369 cm^{-1} as internal standard Fig. 1(c) illustrates the IR spectra of Siliconized epoxidized EPDM which reveals: Absorption peak appeared at 2900 cm^{-1} and between 1140 cm^{-1} to 960 cm^{-1} confirms the presence of $–Si-(CH_2)_3-$ and residual –Si-OH respectively.Absence of peak at 2850 cm^{-1} of $–Si-OCH_2CH_3$ and formation of Si-O-Si at 1143 cm^{-1} confirms the completion of reaction between HTPDMS and APTES coupled epoxidized EPDM.

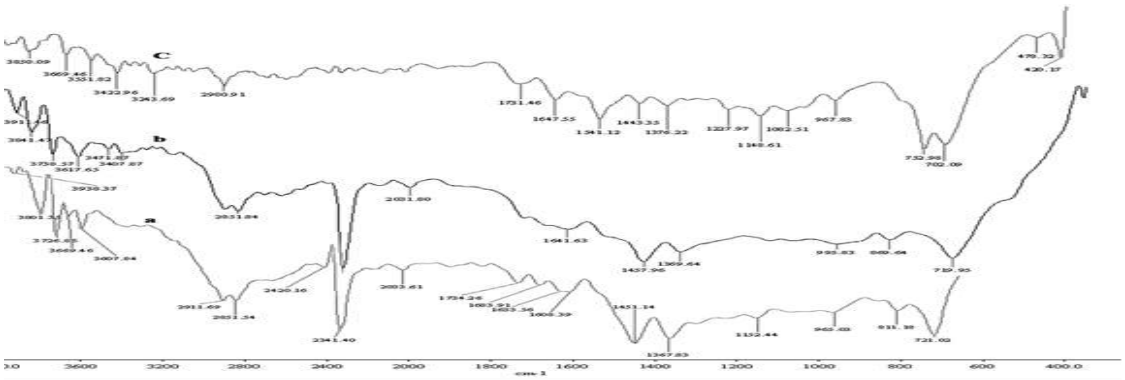

Fig. 1 FTIR spectra of (a) EPDM (b) eEPDM and (c) Siliconized epoxidized EPDM

Corrosion protection performance of the EPDM, eEPDM and eEPDM-g-APTES: The EPDM, eEPDM and eEPDM-g-APTES films coated mild steel was studied by potentiodynamic polarization and electrochemical impedance spectroscopy [10, 11]. In a typical polarization curve, the lower the polarization current is, the better the corrosion resistance is. The potentiodynamic polarization curves of bare mild steel, EPDM, eEPDM and eEPDM-g-APTES with or without red iron oxide coating in 3.5% NaCl solution are shown in Fig. 2a. The values of the E_{corr} Tafel polarization curves are given in. It is clearly observed that the corrosion current M to eEPDM-g-APTES, and the corrosion potential (E_{corr}) increases from EPDM to The positive shift increases red iron oxide coating system which implies that the

eEPDM-g-APTES film provides effective protection for mild steel coating against corrosion in aqueous 3.5% NaCl in comparison with EPDM and eEPDM.

EIS plays an important role to monitor and predict degradation of organic coatings. The Nyquist plot obtained from EIS measurements for all coating mild steel specimen after 30 min immersion in 3.5% NaCl solution is shown in Fig. 2 b. The plot is characterized by a depressed semicircle from high to medium frequencies and an inductive loop at low frequencies. The appearance of the inductive loop in the Nyquist plot is attributed to the adsorption of an intermediate product in the corrosion reaction. Six different coatings, with or without red iron oxide coatings, were examined in chloride electrolyte. Nyquist plots are displayed. It can be seen that, with the exception of coating system eEPDM-g-APTES with or without red iron oxide coating, the other coating system EPDM, eEPDM with or without red iron oxide coating exhibits an incomplete semicircle in the high frequency region, followed by a low-frequency diffusion tail commonly called a Warburg diffusion tail The formation of an incomplete semicircle suggests that the sodium chloride solution has started permeating through the coating in the case of coating system EPDM,eEPDM with or without red iron oxide .

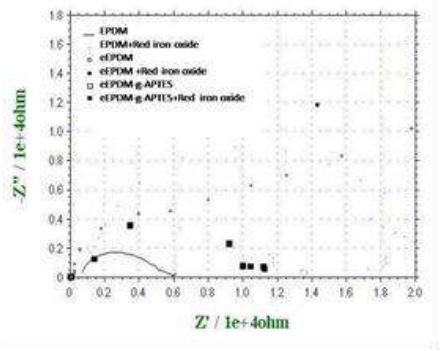

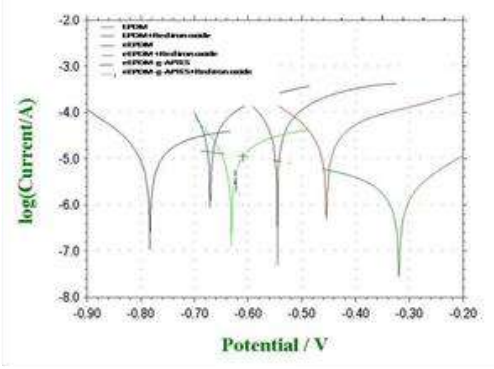

CONCLUSIONS

In this study, the chemical structure of eEPDM-g-APTES was confirmed by FT-IR spectroscopy. eEPDM-g-APTES with or without red iron oxide coatings were used to protect mild steel against corrosion in 3.5% NaCl medium, and potentiodynamic polarization measurements and electrochemical impedance spectroscopy were applied to assess the ability of corrosion resistance.

REFERENCES

Beving, D.E., McDonnell, A.M.P., Yang, W.S., Yan, Y.S., J. Electrochem. Soc. 2006, 153, 325.
C. L. Meredith, R.E. Barret, W. H. Bishop, US Patent 3 **538** (1970) 190
C. Velasco-Santos, A.L. Martinez-Hernandez, M. Lozada-Cassou, A. Alvarez-Castillo, and V.M. Castano, Nanotechnology, 13, 495 (2002).
H. F. Mark, N. M. Bikales, C. G. Overberger, G. Menges, Encyclopedia of polymer science and engineering, Wiley, New York, USA, (1985) 720
Hu, J., Gan, M., Ma, L., Zhang, J., Xie, S., Xu, F., Shen, J.Y.Z.X., Yin, H., Applied Surface Science 2014, http://dx.doi.org/10.1016/j.apsusc.2014.12.042
Li, P.Y., Yin, L.L., Song, G.J., Sun, J., Wang, L., Wang, H.L., Appl. Clay Sci. 2008,40, 38.
Mitra, A., Wang, Z.B., Cao, T.G., Wang, H.T., Huang, L.M., Yan, Y.S. J.electrochem Soc. 2002, 149, 447.
P.C. Ma, J.K. Kim, and B.Z. Tang, Carbon, **44**, 3232 (2006).
Plueddemann E.P., Silane coupling agents, 2 nd Ed., Plenum Press: New York. 1991.
Shen C., Zhou Y., Dou R., Wang W., Yin B., Yang M-b., Polymer 2014, doi: 10.1016/j.polymer.2014.11.027.
Thomas, N.L., J. Prot. Coat. Linings, 1989, 6, 63.

ज्ञान - विज्ञानं विमुक्तये

PG & Research Department of Physics

AVVM SRI PUSHPAM COLLEGE (Autonomous)

Poondi, Thanjavur (Dt), Tamil Nadu.

UGC Sponsored National Conference on

RECENT TRENDS IN NANO MATERIALS AND THIN FILMS RESEARCH (RTNMTR-2015)

Certificate

This is to certify that Dr./Mr./Ms. H. Mohamed Mohaideen Asst. Prof., Mohamed sathak Engg. College has participated / presented a research paper in the UGC Sponsored National Conference on **"RECENT TRENDS IN NANO MATERIALS AND THIN FILMS RESEARCH"-(RTNMTR-2015)** organized by PG & Research Department of Physics, AVVM Sri Pushpam College (Autonomous), Poondi, Thanjavur (Dt), Tamil Nadu in collaboration with Periyar Maniammai University, Vallam, Thanjavur, during 3rd & 4th March, 2015.

Mode of Presentation : Oral / Poster

Title : Effect of Sulfur Concentration on the Physical Properties of Zinc Sulphide Thin Film Deposited by SILAR Method.

Research Department of Physi RTNMTR-2015 3rd & 4th

TRUE COPY ATTESTED

PRINCIPAL
MOHAMED SATHAK ENGINEERING COLLEGE
KILAKARAI-623806.

Dr. K. Ravichandran
Organizing Secretary

Dr. V.S. Nagarethinam
Co-ordinator

Dr. G. Ravikumar
Dean of Sciences

Dr. U. Balasubramanian
Principal

UGC Sponsored National Conference on

RECENT TRENDS IN NANO MATERIALS AND THIN FILMS RESEARCH (RTNMTR-2015)

MARCH 3 -4, 2015

Organized by

PG & Research Department of Physics
A.V.V.M. Sri Pushpam College (Autonomous)
Poondi - 613 503, Thanjavur (Dt)

Book of Abstracts

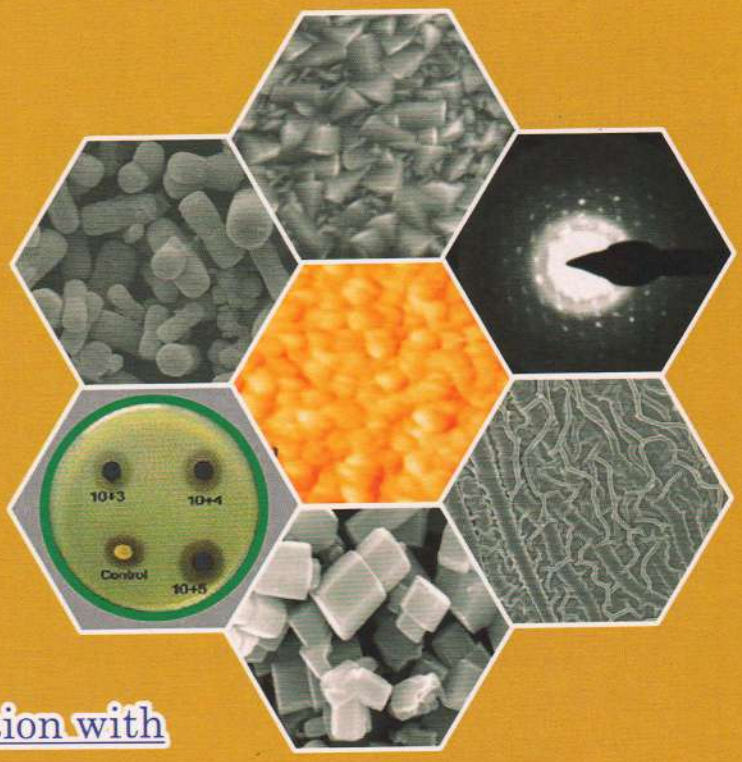

collaboration with

eriyar
aniammai
University,
Vallam, Thanjavur

Editor
Dr.K.Ravichandran

Effect of Sulphur Concentration on the Physical Properties of Zinc Sulphide Thin Films Deposited by SILAR Method

H. Mohamed Mohaideen[1], K. Saravanakumar[1*], S. Sheik Fareed[1], M. Mohamed Gani Kalvathee[2], J. Dhaveethu Raja[2].

[1]Department of Physics, Mohamed Sathak Engineering College, Kilakarai-623 806, India.
[2]Department of Chemistry, Mohamed Sathak Engineering College, Kilakarai-623 806, India.

Email: saravanan.phy@gmail.com

Abstract

Chalcopyrite-based thin film devices (CIGS) contain a so-called buffer layer, made of cadmium sulphide (CdS). Cadmium is highly toxic and therefore, alternative materials are being sought that can replace CdS without losses in its performance. The zinc sulphide (ZnS) is one of the best alternative, to CdS. In the present work, semiconducting ZnS thin films were deposited on glass substrates using successive ionic layer adsorption and reaction (SILAR) technique with different sulfur concentrations (0.2 M to 1 M). The preparative parameters such as concentration, temperature, deposition time, pH of solution have been optimized. The thin films were characterized by using X-ray diffraction (XRD), UV-Vis spectra, photoluminescence (PL) and scanning electron microscope (SEM). The XRD analysis indicates that all the films show an obvious peak corresponding to (111) plane of cubic form ZnS. The average optical transmittance in the visible range is ≥85%. The band gap varies from 3.45 to 4.2 eV. Photoluminescence spectra showed blue emission band (488 nm) and green emission band (521 nm) at an excitation wavelength of 365 nm. The surface morphology of the ZnS thin film is found that the smoothness of the surface varies with the concentration of sulphur. The above discussed results are very much suitable for modern thin film photovoltaic applications.

Acknowledgement:

The authors gratefully acknowledge the financial support from the Department of Science and Technology (DST)-Science and Engineering Research Board (SERB-Ref. No. SR/FT/CS-117/2011 dated 29.06.2012), Government of India.

Self- Revelation of the Writers in Post-Colonial Literature

DEPARTMENT OF ENGLISH

ANANDA COLLEGE

Accredited with 'B' Grade by NAAC
Affiliated to Alagappa University, Karaikudi
(UGC Recognized 2(f) and 12 (B) Institution)
Devakottai- 630 303
Sivaganga District, Tamil Nadu.

From the detailed study of this work, the theme alienation shows a specification. It shows how a man could separate from his own family and society an how painful it should be faced by him. Though a man feel alienation he could try to overcome it and find a solution for it as in A House for Mr. Biswas. Then he will identify who you really are. This is the most important to know themselves in an alienatic nation. This is done by Mr. Biswas at last and find his solution to had a house of his own.

Works Cited

Naipaul, V.S. *A House for Mr Biswas.* London: Penguin Books, 1982. Print.

Fischer-Tiné. *Harald Postcolonial Studies. European History Online.* 2011. Print.

Revie, Linda L. *The Niagara Companion: Explorers, Artists and Writers at the Falls, from Discovery through the Twentieth Century.* Wilfrid Laurier University Press. 2003. Print.

Diasporic Elements and Identity Crisis in Bharati Mukherjee's Novel *Jasmine*

M.Rekha
Asst. Professor
Mohamed Sathak Engg. College, Kilakarai

Jasmine (1989), a novel by Bharati Mukherjee is a story of a woman who crosses the border of her country to end her life as a "sati", but discovers an interesting fluidity in her identity. She realizes that she can adapt in order to survive and to adjust herself in different surroundings. Instead of being a victim she becomes a warrior. Jasmine shifts to different places and takes a new identity every time. She is Jyoti by birth, Jasmine by her husband Prakash, Jazzy by Lillian Gordon, Jase by Taylor Hayes, Jane by Bud Ripplemeyer. This paper deals with how the protagonist lost her identity and shift over to diasporic life.

The story of Jasmine, protagonist of Bharati Mukherjee's novel of the same name begins as Joyti, in a small village of Hasnapur in Punjab. She is renamed Jasmine after her marriage to Prakash Vijh. Prakash wants her to become a modern city woman and as he aids her in her transformation from 'Jyoti' to 'Jasmine' she both perceives herself as, and eventually becomes the figure that Prakash desires to create. Here Mukherjee is depicting identity formation as a complex process that is dependent not solely upon the agency of the individual, but also upon the surrounding environment. Her renaming is a sign of her initial migration away from traditional India. Jyoti and Jasmine are two separate selves, yet Jasmine finds herself occupying both identities.

Jasmine's changes of identity are very much depended on her diasporic changes. Diaspora, etymologically derived from the Greek term "diasperien" where "dia" means "across" and "sperien" means "to sow or scatter seeds", diaspora suggests a displacement from the hom[illegible] circumstances or environmental location of origin and transfer in o[illegible] states, territories or foreign countries Diaspora refers to dis[illegible] which have been dislocated from their homeland through m[illegible] ion or exile. A Diaspora is the movement, migration, or [illegible] away from their root.

Jasmine goes through the flow of her multiple[illegible] to see different faces and phases of Jasmine, Mukherjee's[illegible] have more to do with cultural identity as Jasmine kee[illegible] new

identity, Just like the music genre Jazz, Jazzy is restless. Here the two very important ideas is how jasmine goes trough different identity as if she is going through a flow. The novel focuses on jasmine's changes of cultural identity and her Diasporic experience as an immigrant.

Her Diasporic experiences start when she is married of and moves to a city with her husband. Her husband inspires her to become a modern woman who calls her husband by first name, and dreams about living in America with their own shop. This is where she first face the conflict between her two identity, one is the identity of an "Indian woman" another one is what husband wanted her to be. Then after she enters America she enters a flux of changes, she gets raped by half faced and she takes revenge like Kali the goddess. It is also noticeable that she cuts her tongue before killing half face. After this event she meets Lillian Gordon who makes herself conscious about her dress and sandals, Lillian Gordon also teaches her how to look like a true American, she is thrilled when Gordon calls her Jazzy. The culture of the United States begins to influence her.

Then Jasmine becomes settled in with Taylor and Wylie, she receives a new name, Jase, which is given to her by Taylor. Now more than ever Jasmine is beginning to see herself as an American, she is amazed and fascinated by the ideologies of the family and how they perceive reality. Jase enjoys her new found financial independence and starts to learn more about American culture.

Then she moves to Iowa and finds her "American lover" Bud who gives her the name Jane. Iowa shows her a different picture of United States, a traditional hub for immigrants, and brings her deeper into the United States. Here the only person to whom she connects the most is Du, her adopted son, who is also an immigrant from Vietnam.

Even though she becomes very powerful in the household of Bud and Bud wants to marry her, she chooses Taylor over Bud. She rejects the life of Jane Eyre; her resistance towards the stereotypes is remarkable because she is not afraid to face the unknown. There is always a conflict in Jasmine before she makes any choice, here we see that she breaks the shell of traditional Indian woman and choose to walk away because she wants to. "I am not choosing between men. I am caught between the promise of America and old-world dutifulness" (240). At the beginning she expresses how she is in love with the personality of Taylor, and as finally she goes with Taylor there is a suggestion that she wants to be a true American, not a temporary immigrant.

Bharati Mukherjee through the experiences of jasmine sho interesting panorama of human strength to adopt when she moves throu uncertainty of living in a foreign land like America. Stuart Hall say "identity" should not be thought of as an accomplished fact, but should b as a production which is never complete. Cultural identity is a mat becoming as well as of "being". Cultural identities have history and i through constant transformations.

The concept of 'self' is fluid throughout an individual's lifetime, w person's experiences shape who they are. Throughout the novel we s effects immigration and culture have on the 'self' of Jasmine. Jasmine with the idea of cultural identity, her mode of identity changes every ti is going to a new place, not only she assimilates but her whole being t different shift. Jasmine's identity has multiple folds and layers; she also the roles of a daughter, wife, widow, friend, goddess, and mother. "I ha a husband for each of the women I have been, Prakash for Jasmine, Tay Jaze, Bud for Jane, Half-Face for Kali (197)."

Her idea of "self" is decorated with different pattern and multi facade, but in the core of her being Jasmine never allow changes, we looking at a dead dog flowing in the river and its body is broken the m she touches it, "A stench leaked out of the broken body, and then both quickly sank" . That's the moment she realizes "I know what I don't become" (5). Her identity is also depended on the myths about her history even though that's what she is trying to get rid of. She still tall Indian accent and her "priceless face" makes interesting photographs b she is exotic and foreign. Throughout the novel Jasmine never chooses her name, but when she is called by Jazzy, Jane or Jase assimilates to person. Jasmine is after all an immigrant, no matter how she tries to ge the boundaries she is always manipulated by patriarchy, family and values. But Jasmine's exploration of self helps her to create a space own. She learns quickly and adopts new though she is always becoming internally she stay survival she lets her outer "self" mold by new ex Iukherjee that Jasmine's relation with the state and not dime rather dialectical. Jasmine, the assimila own wa changes America as she floats through difi

Hence Bharati Mukherjee's *Jasmine* is the movement of Jasmine's life towards achieving true identity. Her journey to America is a process of her quest of true self. Even when the protagonist goes through the worst experiences of her life, she is able to come through the obstacles and attains self-awareness and a new identity and overthrows her past life. The protagonist Jasmine repositions her stars in the adopted country by deciding to remain as a care-giver to Duff in which she gets her peace of mind. At every step of her life, Jasmine is a winner, she does not allow her troubles and struggles to obstruct her progress in life and she is finding a place for herself in the society. In other words, she is a true feminist who fights every challenge in life to establish herself in the society. Jasmine realizes that the true identity of a person does not lie in being an Indian or an American but it lies in the inner spirit of the person to be at peace with her. Bharati Mukherjee has employed metamorphosis transformations in the life of Jasmine in the process of her search of her true identity. In this regard, the remark of Sumita Roy is significant: "Consequently, to read Bharati Mukherjee's *Jasmine* as an ambitious endeavor to outline the life of a woman engaged in a serious quest for values is rewarding." (1996:187).

Work Cited

Bhabha, Homi. The Location of Culture, London: Routledge, 1994.

Ghosh, Amitav. "The Diaspora in Indian Culture" in The Imam and the

Indian: Prose Pieces, Delhi: Ravi Dayal Publ. &Permanent Black, 2002. 243-250.

Mukherjee, Bharati. The Holder of the World, New York: Viking, 1993.

— Jasmine. NewYork: Viking, 1989.

— Leave it to me. New York: Viking, 1997.

— Wife. New York: Viking, 1975.

The Conflict of Two Colours in Ruskin Bond's *The Cherry Tree*

Research Scholar: M. Richard Enrico
Ph.D English (Part-Time)
Alagappa Govt. Arts College, Karaikudi.
Research Supervisor: Dr.V. Nagarajan

In this fiction *The Cherry Tree*, Ruskin Bond substantiated the ecological problems by referring green and red colours. Green colour referred to happiness, rejoice and pleasantness. Red colour referred to danger, threat and indirectly he said that people are in the risk of our life by destroying the natural resources for constructing houses, establishing corporate companies, and most of the agricultural lands have turned into deserted lands.

The author purposely chose the cherry tree because he wanted to show the dangerous end of human life if it is going to be continued. From this story, he strengthened his notion through the character Rakesh.

Rakesh, a six years old boy, planted a cherry tree in his grandfather's garden. He raised a question to his grandfather that "Are cherry seeds lucky, Dada?"(TCT–07). His grandfather replied him,

> "Nothing is lucky if you put it away.
> If you want luck, you must put the
> seed to work" (TCT-08).

The writer beautifully described the growing of a tree stage by stage with magical simple words. Likewise, he enunciated the growth of a man and his maturity to change a modern world by destroying dense forests and its natural wealth. Through words of the fiction, Ruskin Bond insisted the echoed voice of nature to the human world that they should be lovers of nature and not against them.

Bond exclaimed the beauty of Himalayas and is in this work. In mid-August, the monsoon rains wer lants sprouted everywhere even from cracks in the walls s no need to look after the seeds and seedlings. When it wind blew down from the snows of the mountain. In spri aped formation of ducks flew towards Siberia.

Rakesh found that the Cherry tree had grown a ather for assurance. Grandfather ensured that it was the tre kesh

47

PCR AMPLIFICATION AND CLONING OF PPE41 GENE OF MYCOBACTERIUM TUBERCULOSIS IN E. COLI

N. LEEBANON POONKUIL, Research Scholar, Manonmaniam Sundaranar University, Tirunelveli.
Dr. J. DHAVEETHU RAJA, Head & Asso. Prof in Chemistry, Mohamed Sathak Engineering College, Kilakarai.

Abstract

Tuberculosis (TB) is an infection, primarily in the lung, caused by bacteria called Mycobacterium Tuberculosis, is one of the most successful human pathogens infecting nearly one- third of the world's population. Among the various factors that contribute, certainly the bacterium's ability to multiply and persist within professional phagocytic cells. The current vaccine for TB is an attenuated strain of Mycobacterium bovis called Bacillus Calmette Guerin (BCG). People have been vaccinated with BCG than any other vaccine, TB continue to kill some 3milion people annually and approximately 2 billion people worldwide are infected with M. Tuberculosis. Thus the protective efficacy of the BCG vaccine remains doubtful. Failure of BCG in several recent field trials indicated that a large number of mutations have taken place during the long in vitro propagation of this strain. PPE41 is secreted by pathogenic mycobacteria.180 amino acid residues in the N- terminal regions of PPE proteins are conserved.

Several genes encoding PPE proteins are deleted in the genome of the vaccine strain Mycobacterium bovis BCG and by the demonstration that certain PPE proteins induce strong immune responses in animals and humans infected with M. Tuberculosis. The PPE41 gene from Mycobacterium. Tuberculosis has been PCR amplified. A 601 bp amplicon was obtained. The PPE41 gene of M. Tuberculosis has been cloned into an E. coli expression vector pRSET-A. Recombinant PPE41 plasmid has been obtained. Immunogenic protein PPE41 is currently being used as an adjuvant to improve the efficacy of vaccines against tuberculosis. Further studies can be done in the field to evaluated various vaccine to treat tuberculosis by the expression of the gene of PPE41.

Key words: Mycobacterium Tuberculosis H37Rv, PPE41 gene, pRSET -A vectors, PCR, Transformation.

Introduction

Tuberculosis is an air borne disease and has plagued human kind since ancient times. It remains a massive global health problem today. It is the world's second commonest cause of death from [illegible]DS. One and half billion people have [illegible] 1998). The causative agents of [illegible] of the genus Mycobacterium, with [illegible] causing the vast majority of cases. [illegible]us Mycobacterium are very thin, rod shaped, non motile and stain acid fast (Volkman 2004). Waxes and long-chain mycolic acid in mycobacterium cell wall makes mycobacterium difficult to Gram stain. Mycobacterium is highly resistant to drying and can remain viable for 6-8 months in dried sputum (Mc donough et al., 1993). The current vaccine for tuberculosis is an attenuated strain of Mycobacterium bovis called Bacillus Calmette Guenn (BCG).

These resistant strains can infect others in community and are increasingly responsible for new infections. The problem of drug resistant M. Tuberculosis strains has reached alarming proportions in some areas and has motivated the search for new vaccines against the diseases. The complete genome of Mycobacterium Tuberculosis H37Rv comprises a nucleotide sequence of 4,411,529 bp containing around 4000 genes, and has high GC content (65.6%) (Brennan et al., 2001). Sequencing of genome of mycobacterium tuberculosis, the causative agent of tuberculosis (TB) has revealed that approximately 10% of the genome encodes two families of glycine-rich proteins termed PE and PPE on the basis of their characteristic Pro-Glu (PE) and Pro-Pro-Glu (PPE) families of proteins. PPE proteins act as an immunogenic and stimulate both T cells and B cells. This protective cellular immune response to M. Tuberculosis is initiated in the lung and consists primarily of alveolar macrophages and activated T cells (Okkels 2003).

The pRSET-A vectors are pUC derived expression vectors designed for high level protein expression and purification from cloned genes in E. coli are made possible by the presence of T7 promoters. Molecular cloning allows DNA fragments to be isolated and amplified, the basis of the technology is an in vitro joining of autonomously replicating vector DNA molecules with DNA insert fragments from the desired source organism performed by DNA Ligation (Sambrook et al., 1999).

Methodology Gene Cloning - Plasmid DNA Isolation

It involves the insertion of DNA fragment into a cloning vector. The recombinant vector is subsequently transformed into a suitable host to generate the desired clones. E. coli with pRSET was grown in LB broth with ampicillin by overnight incubation at 370C, 250 rpm in a shaker incubator. M. Tuberculosis was cultured in LJ medium. After 16 hours incubation, 5 mL of Bacteral Culture containing the plasmid was Centrifuged at 10,000 rpm for 1 minute and discarded the supernatant and centrifuged at 10,000 rpm for 30 seconds.

To the Pellet added 250 ?L of suspension buffer Mixed by vortexing and Inverted 5 times then incubated at 370C for 5 minutes. Added 350 ?L of solution binding buffer and centrifuged at 10,000 rpm for 10 minutes. Spin the Column, transferred the clear lysate to the column and centrifuged at 10,000 rpm for 15 minutes. Added 500 ?L of wash buffer then Centrifuged at 10,000 rpm for 15 minutes. Transferred the column into a fresh eppendrof tube. Added 60 ?L of Elution buffer to the centre of the column. Incubated at 370C for 1 minute again centrifuged at 10,000 rpm for 10 minutes. Dissolved the pellet in 50 ?L of double distilled water and the samples were loaded in 0.7% agarose gel checked (Sambrook et al., 1999).

Isolation Of M.tuberculosis H37rv Strain

During the late log phase of the liquid culture glycine (1.5%) was added and incubated for 48-72 hours. Cells were harvested by centrifugation at 10,000 rpm for 20 minutes and resuspended in 10mL of Lysis buffer, to which 5 ?L of Lysozymes were added. Incubated at 370C for 3 hours. Added 10 ?L of Proteinase K and incubated at 370C for 2 hour. Added 20 ?L of 20% SDS solution then incubated at 370C for one hour, Heated at 700C for 5 minutes. Added 10 ?L of 5 M Sodium acetate and incubated at 40C for 12-18 hours. Centrifuged at 12,000 rpm for 30 minutes. Added once with P: C: I (25:24:1), added twice with C : I (24:1) Precipitated the pellet. And then incubated at 200C for overnight, centrifuged at 12,000 rpm for 30 minutes. Washed with 70% ethanol and dissolved in 20 ?L of TE buffer (Cole and Barrell 1998).

Agarose Gel Electrophoresis

To the 0.7% agarose with 70 mL of 1xTBE buffer , added 3.4 ?L of ethidium bromide and heated the agarose for 20 minutes Gel placed into the Electrophoresis tank.1xTBE buffer was filled in tank. Loaded the samples and run the gel (reached 3/4 th of gel) at the voltage 50 V, switched on the power supply and observed under UV transilluminator.

PCR Amplification Of PPE 41 & PCR Program

The PPE41 gene from Mycobacterium Tuberculosis H37Rv strain genomic DNA was amplified using ppe41 primers. PCR was performed in a programmable thermal cycler. The reaction mixture contained the mixture of sterile double distilled water - 39µL, 10 x Buffer with 2 mM MgCl2 - 5µL, dNTP mix (2.5 mM each) - 1µL, Forward primer (125 ng/µL) - 1.5?L, Reverse primer (125ng/µL) -1.5µl, M. Tuberculosis DNA template - 1µL, Taq polymerase (5U/µL) - 1µL This mixture was amplified for 29 cycles with an Initial Denaturation at 930C ed at 930C for 30 seconds. Annealing at on at 720C for 40 seconds. Repeated 29 20C for 2 minutes. The PCR product was ambrook et al., 1999).

Purification

Sample of PCR and digestion product was added 1/10th volume of 3M sodium acetate. Added 2.5 ?L of absolute Ethanol and incubated at 200C for 1 hour. Centrifuged at 12,000 rpm at 40C for 15 minutes. Added 70% ethanol and centrifuged at 12,000 rpm at 40C for 15 minutes. Dissolved the pellet in 40 ?L of double distilled water and checked the Agarose Gel Electrophoresis.

Double Digestion & Ligation

Purified PCR product - 13 ?L, pRSET-A -10?L, 10x Y+ Tango buffer -7µL, Sterile double distilled water - 39µL, Bam HI enzyme - 1µL, Eco RI enzyme-1µL were taken and incubated the reaction mixture for 2 hour at 370C in a water bath then dissolved in 17?L of sterile double distilled water. T4 DNA ligase - 1µL, 10 x ligation buffer - 2µL, Sterile Double distilled water - 2µL , Digested PPE 41 PCR product & pRSET-A DNA - 15µL were taken and incubated the reaction mixture for 2 hours at 250C in a water bath.

Transformation & Release Of The Ppe41 Insert

To the XL10 GOLD Strain, added XL10 Gold without Ampicillin and XL10 Gold with Ampicillin. Incubated Overnight and seen the Growth. 100 ?L of overnight culture (Sub culture) was taken and incubated at 370C for 21 hour. Incubated at 25 minutes in ice bath then centrifuged at 6000 rpm for 6 minutes. Added 10mL of CaCl2 and centrifuged at 6000 rpm for 6 minutes. Added 1 mL of CaCl2 then incubated at 1 hour in ice bath. 500 ?L of component cell was transferred to the ligated mixture. Alternated Cold & heat stock were given. Incubated repeatly for 25 minutes in ice bath, water bath again in ice bath and added 500 ?L of LB broth, incubated for 1 hour at 370C. Centrifuged 6,000 rpm for 6 minutes. The Pellet was transferred to the agar plate with ampicillin then incubated at 370C for over night. Colonies were picked with wooden tooth pick. Subculture in each colonies and incubated at 370C for overnight. Isolated the recombinant plasmids (3?L) Digested with 1 ?L of Bam HI & Eco RI, 10x Y+ Tango buffer in 1.4 ?L of sterile double distilled water for 2 hours at 370C in a water bath and was electrophoresed in 1 % agarose Gel (Cole and Barrell 1998).

Result

The plasmid DNA was isolated from E.coli culture containing pRSET-A. This methodology resulted in high yield of C DNA. This plasmid DNA preparation was used for cloning of PPE 41 PCR amplicon. The isolated plasmid DNA was then electrophoresed in 0.7% agarose gel. M. Tuberculosis genomic DNA was isolated and used as a template for amplification of ppe 41 gene by using the PPE specific primers. The amplicons were subjected to electrophoresis in 0.7% agarose gel along with the control (100 bp ladder). The 601 bp PCR product of M. Tuberculosis was compared with control (Figure

1). The isolated plasmid DNA pRSET-A and M. Tuberculosis PPE 41 PCR product were digested with restriction enzymes BamHI and EcoRI sequentially. These digested plasmid and PPE41 PCR product were ligated with T4 DNA ligase. The ligated product was transformed into E. coli XL10 Gold employing calcium chloride method. The transformed cells were spread on LB agar plates containing ampicillin (100µg/mL). The plates were incubated at 370C overnight. A total of 15 colonies were obtained from 2 plates (Figure 2). 15 transformed colonies were randomly selected and were patched on LB ampicillin agar plates. Furthermore, each of these colonies were inoculated in 10 mL LB broth. Both the plates and tubes were incubated at 370C in an incubator and a shaking incubator respectively for16 hours. Plasmid DNA from transformants were isolated and electrophoresed in 0.7% agarose gel with appropriate control, isolates 1,2,5,7,8,11,12,14 and 15 showed recombinant plasmids (Figure 3).

Figure : 1

AGAROSE (0.7%) ELECTROPHOREGRAM OF PCR AMPLIFICATION

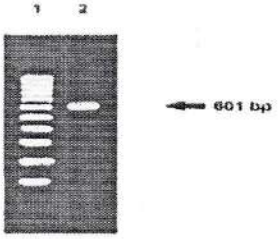

LANE 1 100 Kb DNA Ladder
LANE 2 PPE 41 PCR Product

Figure: 2

AGAROSE (0.7%) ELECTROPHOREGRAM OF MOBILITY SHIFT

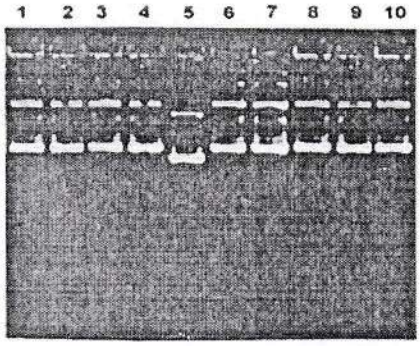

LANE 1 to 4 Mobility Shift (Sample number 1,2,5,7)
-A
(Sample number 8,10,11,12,13)

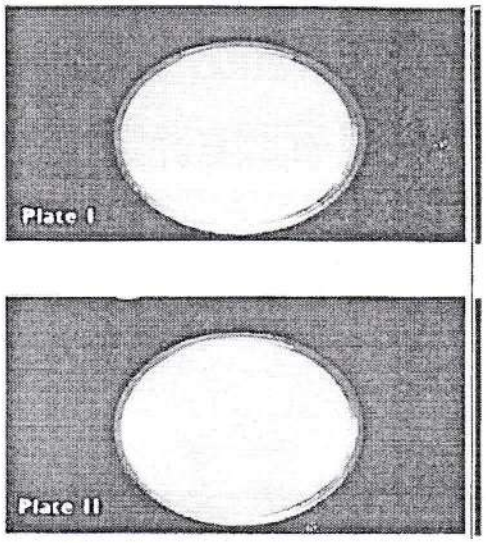

Figure : 3

AGAROSE (1%) ELECTROPHOREGRAM OF RELEASE OF INSERTS

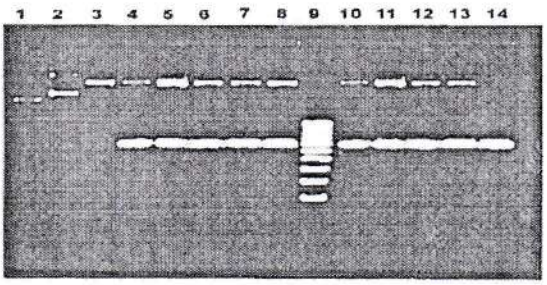

LANE 1 Control pRSPT-A
LANE 2 Recombinant DNA
LANE 3 Digestion Control
LANE 4 to 8 Insert released (Sample number 1,2,5,7,8)
LANE 9 100 kb DNA Ladder
LANE 10 to 13 Insert released (Sample number 10,11,12,13)
LANE 14 PPE 41 PCR Product

Figure : 4

Plasmid DNA from the transformants No. 1,2,5,7,8,11,12,14 and 15 were subjected to BamHI and EcoRI digestion. The digests were electrophoresed in a 1% agarose gel along with the PPE 41 PCR product of M. Tuberculosis. Transformants No. 1,2,5,7,8,11,12,14 and 15 release a 601 bp insert which co-migrated along with the PPE 41 PCR product (Figure 4). This confirms successful cloning of ppe41 sequence of M. Tuberculosis H37Rv in pRSET-A vector.

Discussion

Interestingly, mycobacterial ppe genes act as immunogenic agents (Andersen et al., 2000). PPE families act as protein folding nano-machines which when conjugated to weakly immunogenic

antigens could present the latter for greater immunogenic response from the host. Hence, mycobacterial ppe genes will form excellent hybrid protein partners to weakly immunogenic antigens (Krishna et al., 2005).

Keeping this in view, in the present study, as a first step towards achieving this goal. M. Tuberculosis H37Rv PPE41 gene segment comprising nucleotide which has been shown to be sufficient to elicit immune response has been PCR amplified and cloned in expression vector pRSET-A and transformed into E. coli XL10 Gold. This recombinant plasmid would form the basis for future research programs in this laboratory which envisage cloning of various human pathogenic viral protein coding genes to enable us to produce M. Tuberculosis PPE41 - viral antigen hybrid vaccines.

Conclusion

The ppe41 gene from Mycobacterium Tuberculosis has been PCR amplified. A 601 bp amplicon was obtained. The ppe41 gene of M. Tuberculosis has been cloned into an E.coli expression vector pRSET-A. Recombinant PPE41 plasmid has been obtained. Immunogenic protein PPE41 is currently being used as an adjuvant to improve the efficacy of vaccines against tuberculosis. Currently, over expression of M. Tuberculosis PPE41 peptide in E. coli XL10 Gold by IPTG induction is under way. Further studies can be done in the field to evaluated various vaccine to treat tuberculosis by the expression of the gene of PPE41.

Acknowledgment

We greatly acknowledge the help of Management and Principal from Mohamed Sathak Engineering College, Kilakarai who provided constant encouragement and research facilities. We express our sincere thanks to the Science and Engineering Research Board (SERB)-Department of Science and technology (DST), New Delhi for financial assistance.

References

Anderson, P., Munk, M.E., Pollock, J.M., Doherty, T.M. 2000. Specific immune based diagnosis of tuberculosis. Lancet 356: 1099-1104.

Brennan, M.J., Delogu, G., Chen, Y., Bardarov, S., Kriakov, J., Alavi, M., Jacobs, W.R. 2001. Evidence that mycobacterial PE_PGRS proteins are cell surface constituents that influence interactions with other cells. Infect. Immun 69: 452-458.

Cole, S.T., Barrell, B.G. 1998. Analysis of the genome of Mycobacterium Tuberculosis H37Rv. Novartis Found Symp 217: 160-172.

Krishna, K., Singh, N., Arora, K. 2005. Immunogenecity of the Mycobacterium Tuberculosis PPe(RV 3347c) protein during incipient and clinical Tuberculosis. Exp. Med 60: 5004-5014.

Mc donough, K.A., Kress, Y., Bloom, B.R. 1993. Pathogenesis of Tuberculosis: interaction of Mycobacterium Tuberculosis with macrophages. Infect. Immun 61: 2763-2773.

Okkels, L.M. 2003. PPE protein(Rv3873) from DNA segment RDI of Mycobacterium Tuberculosis: strong recognition of both specific T-cell epitopes and epitopes conserved within the PPE family. Infect. Immun 71: 6116-6123.

Sambrook, J., Fritsch, E.F., Maniatis, T. 1999. Molecular cloning: a laboratory manual. 2 nd ed. Cold spring Harbor laboratory press, Cold spring Harbor, New yark. pp. 450-457.

Volkman, H.E 2004. Tuberculosis granuloma formations enhanced by a Mycobacterium virulence determinutesant. Plos Biol 2: 367.

ISBN : 978-93-81521-49-6

Conference Proceeding

International Conference on Chemistry and Materials (ICCM'2014)

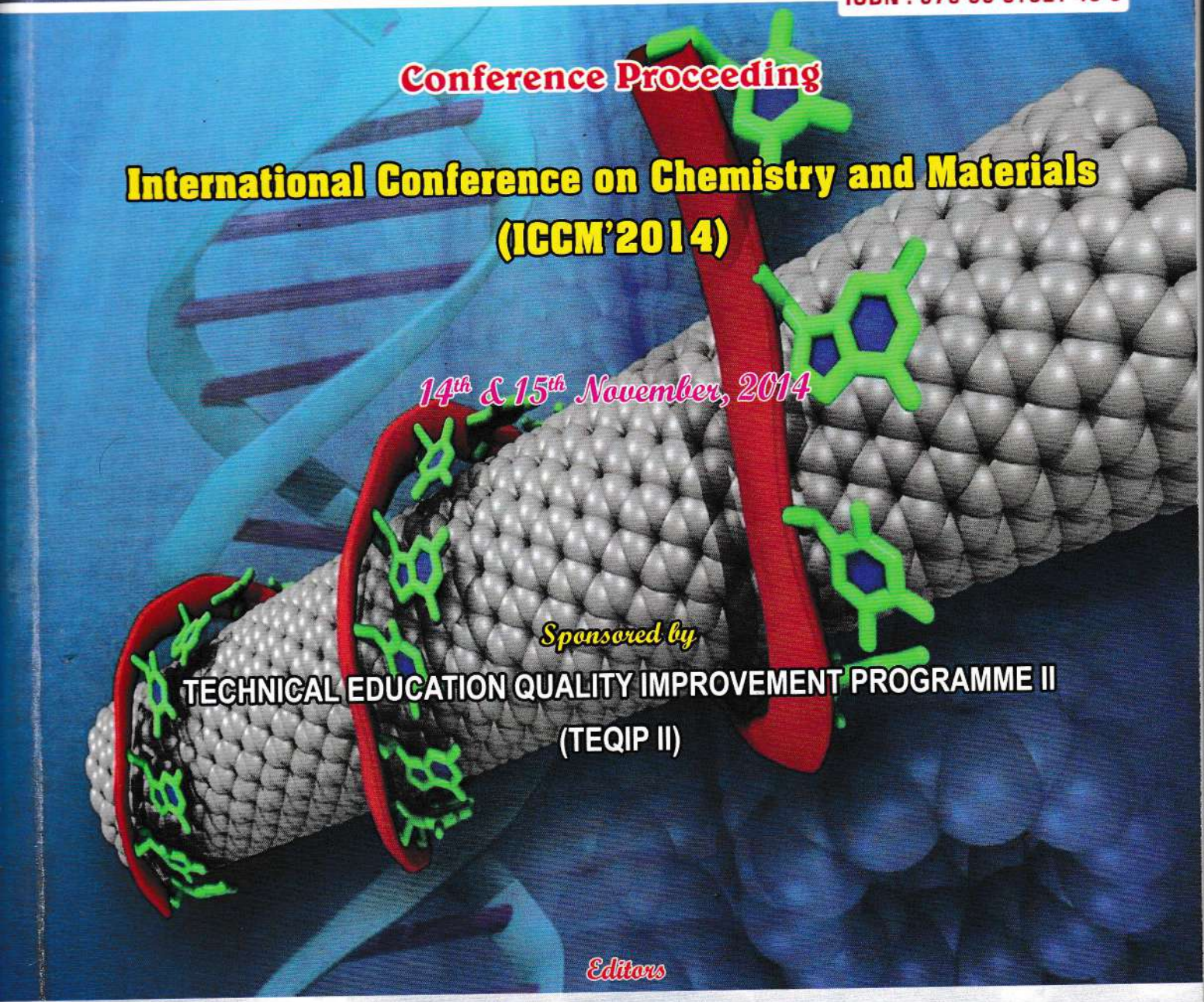

14th & 15th November, 2014

Sponsored by

TECHNICAL EDUCATION QUALITY IMPROVEMENT PROGRAMME II

(TEQIP II)

Editors

Dr. R. Thiruneelakandan
Dr. K. Jothivenkatachalam

Organized by

DEPARTMENT OF CHEMISTRY
ATHIDASAN INSTITUTE OF TECHNOLOGY (BIT) CAMPUS
ANNA UNIVERSITY
TIRUCHIRAPPALLI – 620 024

 ISBN : 978-93-81521-49-6

DNA BINDING, OXIDATIVE CLEAVAGE STUDIES OF PYRIMIDINE WITH MORPHOLINE DERIVATIVE LIGANDS AND ITS GOLD, COPPER, PLATINUM AND ZINC COMPLEXES

M. SANKARGANESH & J.DHAVEETHU RAJA*

DST-SERB sponsored Research Lab, Department of Chemistry, Mohamed Sathak Engineering College, Kilakarai- 623 806, Ramanathapuram, Tamilnadu, India.

E-mail: jdrajapriya@gmail.com

The Novel Schiff base has been synthesized from Pyrimidine with Morpholine derivatives. Metal complexes of Schiff base have been prepared from perchlorate salts of Cu(II), Zn(II) and chloride salts of Au(III), Pt(IV). The structures of the Schiff base ligand and its metal complexes were elucidated by elemental analyses, conductivity measurements, IR, ^{1}H-NMR, UV-Visible, ESR and Mass Spectroscopy. The redox behavior of Au & Cu metal complexes were studied by cyclic voltammetry. The UV-Visible spectral data suggest that square-planar geometry. The oxidative cleavage studies of the complexes with Calf Thymus (CT) DNA have been investigated by using gel electrophoresis method. Pt(II) complex showed that more pronounced activity than ligands and other complexes in the presence of oxidant (H_2O_2). The binding strength and binding mode of the Cu-complex with herring sperm (HS-DNA) have been investigated by electronic absorption spectroscopy measurements results hyperchromism with blue shift and hypochromism with red shift should be observed.

Key words: Square planar geometry, DNA Binding & Cleavage Study.

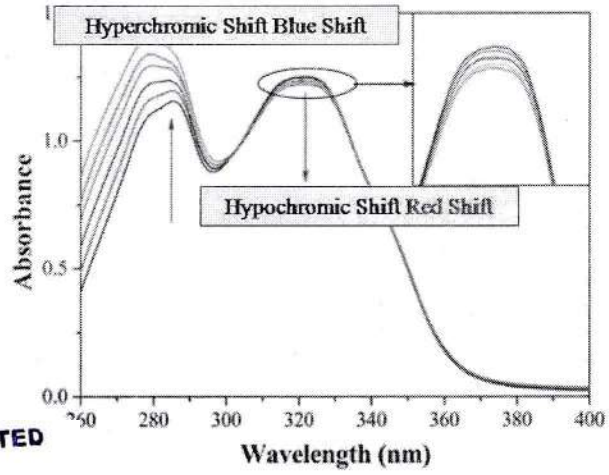

Department of Inorganic Chemistry
University of Madras

International Conference on Advances in New materials [ICAN 2014]

20th & 21st June 2014

electron-releasing substituent on Carboxylate bridge. The phenoxyl radical complexes of 1-3 were generated at 25°C by CAN and the radical complexes stability follows the order of 1 > 3 > 2. The superoxide ($O_2^{\cdot-}$) dismutation activity of the ligand and complexes were investigated by the riboflavin–methionine–nitro blue tetrazolium assay. Furthermore, the antioxidant activity of the ligand and its complexes was also determined by hydroxyl radical scavenging, DPPH, NO, reducing power methods *in vitro*.

BOC-17 Synthesis And Characterisation Of 1-(3-Hydrazinyl-2-Oxoindolin-3-Yl) Pyrrolidine-2,5-Dione

MuthusamyVijayachandrasekar and S. Rajeswari *
SRM University, Department of Chemistry, Faculty of Engineering and Technology, Kattankulathur-603203.
Email : raji.802000@gmail.com

The present study deals with the synthesis and characterization of a mannich base derived from simple isatin, secondary amine and hydrazine compound derivatives. The reaction was carried out by mixing the constituents in equimolar ratio in ethanol and refluxing for 5 hours. The solid product obtained was then purified by washing with water and then recrystallised from ethanol. The recrystallised product obtained was 1-(3-hydrazinyl-2-oxoindolin-3-yl) pyrrolidine-2,5-dione. The melting point was found to be in range 194-198°C. This organic compound was characterized by elemental analysis, ultraviolet, infrared, ^{1}H NMR, ^{13}C NMR, mass spectra and cryoscopic molecular weight determination. The molecular mass of the compound was found at m/z 338. The result of single crystal x-ray diffraction study is awaited.

BOC-18 Synthesis And Characterization Of 1-((Dicyclohexylamino)(Phenyl)Methyl)Pyrrolidine-2,5-Dione

S. Rajeswari *[1] , MuthusamyVijayachandrasekar[1] and G.Venkatesa Prabhu[2]
[1]*SRM University, Department of Chemistry, Faculty of Engineering and Technology, Kattankulathur-603203.*
[2]*Department of Chemistry, National Institute of Technology, Tiruchirappalli-620 015;*
Email : raji.802000@gmail.com

The chemistry of Mannich bases first studied by Mannich, has been the subject of investigations by an ever increasing number of researchers. The present study deals with the synthesis and characterization of a mannich base derived from succinimide, dicyclohexylamine and benzaldehyde. The reactants were mixed in 1:1:1 ratio in ethanol and refluxed for 3 h. The solid product was purified by washing with water and acetone. The melting point was found to be in range 132-134°C. The organic compound was characterized by various spectroscopic tools. The molecular mass of this compound at m/z 368 confirms the formation of the product.

BOC-19 Study On Synthesis, Structural Elucidation Of Biologically Active Schiff Base Transition Metal Complexes

S.Angeline and J.Dhaveethu Raja*
Department of Chemistry, Mohamed Sathak Engineering College, Kilakarai-623 806, India.
**Email: jdrajapriya@gmail.com*

The synthesis and spectral characterization of new series of transition metal complexes of Cu(II), Ni(II), Co(II) and Zn(II) have been done from a Schiff base ligand (L), 2((4,6-dimethoxypyrimidin-2-ylimino)methyl)phenol. Structural study has been carried out from their elemental analysis, molar conductance, mass, IR, UV-Vis, ^{1}H-NMR and ESR spectral studies. The structural data reveal that the formed complexes have ML type composition and the complexes have square-planar geometry. The redox behaviour of metal complexes has been studied by cyclic voltammetry studies. Antibacterial study shows Cu(II) and Co(II) have significant activity compared to other complexes. The DNA cleavage and binding studies have also been investigated using calf thymus DNA (CT-DNA) by Gel electrophoresis and absorption spectral studies.

BOC-20 Synthesis, Structural Characterization, Antibacterial Activity, Dna Cleavage And Binding Study Of Pyrimidine Derivative Schiff Base Metal Complexes

N.Revathi[1] and J.Dhaveethu Raja*[2]
[1] *Department of Chemistry, Renganayagi Varatharaj College of Engineering, Sivakasi- 626 128;*[2] *Department of Che* *neering College, Kilakarai-623 806; *Email: jdrajapriya@gmail.com*

e Schiff base has been synthesized from 2-amino-4, 6-dimethylpyrimidine and 5-ni exes of Schiff base have been prepared from acetate salts of Cu (II), Co (II), Ni (II) the Schiff base ligand and its metal complexes were elucidated by elemental anal s, IR, ^{1}H-NMR, UV-Visible, ESR and Mass Spectroscopy. The redox behaviour

of metal complexes was studied by cyclic voltammetry. The structural data reveal that the formed complexes have ML type composition and the complexes have octahedral geometry. The Schiff base and metal complexes have been screened for the antibacterial activity against some bacteria's. The results indicated mild antibacterial activity of some of the complexes. The interaction of the complexes with calf thymus DNA (CT-DNA) has been investigated by UV absorption method and the mode of binding to the complex has been investigated. UV studies of the interaction of the complexes with DNA have shown that they can bind to CT DNA.

BOC-21 Scrambling in Porphyrins: Synthesis, Characterization and Quantitative Crystal Structure Analysis

Fasalu Rahman Kooriyaden, Subramaniam Sujatha and Chellaiah Arunkumar*
*Bio-inorganic Materials Laboratory, Department of Chemistry, School of Natural Sciences, National Institute of Technology Calicut, Kozhikode, Kerala, 673 601, India; *Email: arunkumarc@nitc.ac.in*

Condensation of a dipyrromethane with an aldehyde in a McDonald type synthesis has been accepted for the synthesis of a wide variety of trans-A_2B_2 type meso-substituted porphyrins. In addition to trans-porphyrins, scrambling leads to form cis-isomer owing to the exchange process in polypyrrane condensation. The acid catalyzed fragmentation of polypyrrane breaks into pyrrolic and azafulvene. Recombination of these components leads to new cis-porphyrin. Here, we report, the cis- and trans-bis(pentaflorophenyl)-bis(4-cyanophenyl) porphyrins and their copper derivatives which were synthesized by the condensation of 5-benzonitrile dipyrromethane and pentafluorobenzaldehyde followed by metal insertion reaction using copper acetate. All the synthesised porphyrins were characterized by UV-Visible, ^{1}H NMR and mass spectroscopic techniques as well as by single crystal X-ray diffraction analysis. In order to quantify the various intermolecular interactions present in the porphyrins, the quantitative crystal structure analysis were done by Hirshfeld surface analysis using Crystal Explorer 3.1. Crystal structure of these porphyrins exhibit interesting weak intermolecular interactions referred as F···F, F···H (β-pyr) , F···H (Ph) , N···H (β-pyr) , N···H (Ph) , C (β-pyr) ···H (Ph) , C (β-pyr) ···C (Ph) which controls the packing motif.

BOC-22 Growth and characterization of semi organic urea phosphoric acid single crystals.

K. Rajeswari, P. Vinothkumar, G. Rajsekar, and A.Bhaskaran*
Department of Physics, Presidency College (Autonomous), Chennai-600 005, Tamilnadu, India
Email: newtonphysics329@gmail.com

Second harmonic generation semi organic material, urea phosphoric acid, has been synthesized and grown as quality single crystals by the slow evaporation technique. As-grown crystals were characterized by high resolution X-ray diffraction (HRXRD) and Fourier transforms infrared spectroscopy. The UV-Vis transmittance spectrum shows that the material has wide optical transparency in the entire visible region. The optical band gap was estimated for UP crystal using UV–vis study. Measuring transmittance of UP permitted the calculation of the refractive index n. The mechanical anisotropy property of the grown crystals was studied using Vickers microhardness tester at different planes. The growth features were analyzed by wet chemical etching studies. Density functional theory has been used to calculate the first-order hyperpolarizability of UP single crystal.The second harmonic conversion efficiency of UP single crystal was determined using Kurtz powder technique.

BOC-23 Growth, Optical, Electrical and Mechanical Properties of Mono Methyl Urea Maleic Acid Single Crystals.

P.Vinothkumar, K.Rajeswari, G.Rajsekar, A.Bhaskaran*
Department of Physics, Presidency College (Autonomous), Chennai-600 005, Tamilnadu, India.
Email: vinothphysicist@gmail.com

A mono methyl urea maleic acid single crystal, an organic nonlinear optical material, has been synthesized and single crystals were grown from aqueous solution. Single crystals of NMUM have been grown by slow evaporation of solvent at room temperature. Single-crystal X-ray diffraction study on grown crystals shows that they belong to monoclinic system. The structural perfection of the grown crystals has been analysed by high-resolution X-ray diffraction (HRXRD) rocking curve measurements. Fourier transform infrared (FTIR) spectroscopic study was performed for the identification of different modes of functional groups present in the compound. The UV–Vis transmission spectrum has been recorded in the range 200–1200 nm. The dielectric studies were performed. From rements, Vicker's hardness number (Hv), Stiffness constant (C_{11}), fracture toughness (k_c), ld strength (σ_y) have been calculated. The SHG relative efficiency of NMUM crystal was

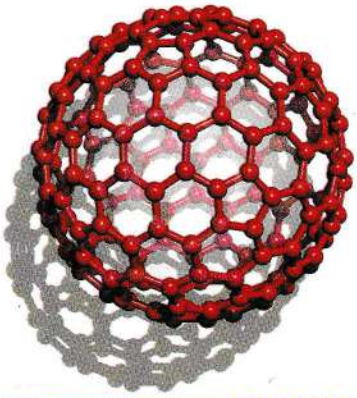

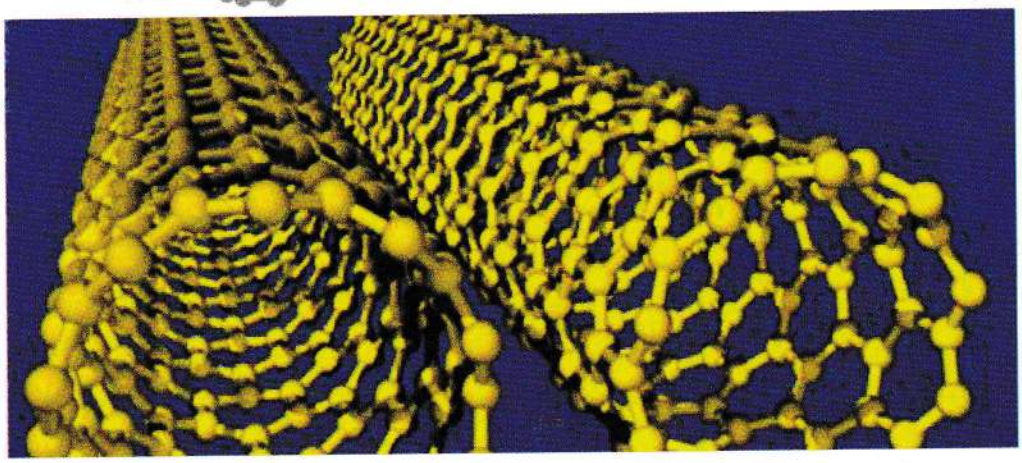

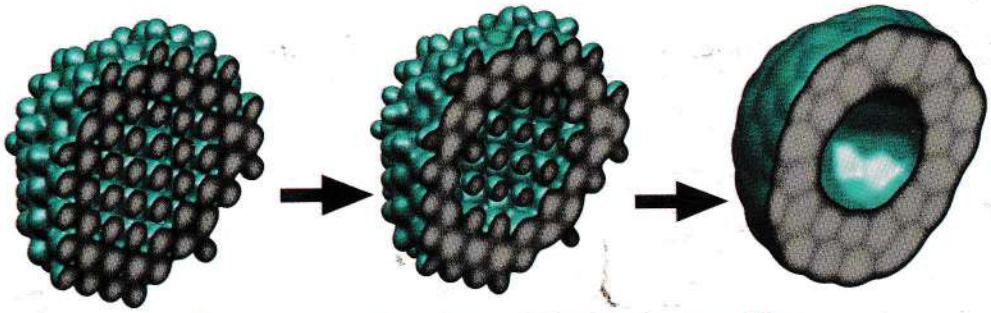

Porous to Hollow Transformation

Convener

Dr. V. Narayanan

Department of Inorganic Chemistry

Tel: +91-9444299226

il: vnnara@yahoo.co.in

v.ican2014@gmail.com

ISBN 978-81-89843-57-1

9 788189 843571

A Study on Cation Exchange Capacity using Resorcinol-Formaldehyde Resin Blended with Low-Cost Plant Material

A. Girija and R.K. Seenivasan

Keywords--- *Resin, Cation Exchange*

I. INTRODUCTION

THE effluents from many industries contain heavy metals along with other pollutants. As heavy metals are not biodegradable, pose a serious problem to the environment. Hence these metals must be removed before discharging in to the environment [1]. Among many techniques, ion-exchange process is useful under field condition than other processes [2-9]. The present work represent a simple method for preparing and characterizing of low cost ion-exchanger of sulphonated carbon prepared from orange peel as a source of cheap plant material blended with resorcinol-formaldehyde as a cross linking agent.

II. OBJECTIVES

1. To prepare sulphonated carbon from orange peel as cheap material.
2. To prepare resorcinol-formaldehyde resin and composite resin obtained by blending with various % w/w of sulphonated carbon obtained from plant materials.
3. To estimate the cation-exchange capacity for various heavy metal ions and to study effect of initial concentaration of heavy metal ions, particle size, chemical and thermal treatment of cation exchange resin and regeneration level using NaCl solution.

III. MATERIALS AND METHODS

Orange peel was carbononised (SOPC) [10-12] and pure resorcinol-formaldehyde resin (RFR) was prepared [10-13].The composites/blends of RFR with various % (w/w) of SOPC were obtained as per reports in the literature [10-13]. Various physicochemical properties such as absolute density in g/ml under wet and dry conditions, gravimetric swelling of the composites were determined. Column experiments were carried out in order to measure the extent of cation exchange capacity.

IV. RESULTS AND DISCUSSION

The experimental and theoretical compositions of composites (OP1-OP5) are in good agreement with each other.

The absolute density values in hydrated (in water) and in dehydrated (toluene) states decreases steadily from RFR (100% pure resin) to 50% (w/w).SOPC (100% pure SC) showing the RFR and composites (OP1-OP5) are closely packed [10-17].

The percentage of gravimetric swelling decreases from RFR to SOPC. It indicated that the values for RFR and composites are not as high as compared to conventional gel type IERs, indicating rigidity in the matrix and therefore the pores of composites are of non-gel type and macromolecular [18].

acity values indicated that the CEC values decreases when the content of SOPC (%w/w) in at the composites up to 20% (w/w) of SOPC retains 75-90% of CEC of RFR.

ing College, Kilakarai, Tamil Nadu. E-mail:girijabalaji@ymail.com
lelur, Tamil Nadu.

ISBN 978-93-82338-36-9

REFERENCES

[1] B.A. Bolto and L. Pawlowsk,eds. , Waste Water Treatment by Ion-Exchange, Oxford and IBH, New Delhi, 1987.
[2] J.L. Cortina, N. Miralles, M. Aguilar and A.M. Saster, Hydrometallurgy, 40(1999)195
[3] M. Yu, W. Tian, D. Sun, W. Shen, G. Wang and N. Xu, Chim. Acta, 428 (2001) 209.
[4] B. Yu, Y. Zhang, A. Shukla, S.S. Shukla and K.L, Dorris, J. Hazard. Mater.B, 80 (2000)33.
[5] A. Seco, C. Gabaldon, P. Marzal and A. Aucejo, J. Chem.Technol, Biotechnol., 74 (1999) 911.
[6] P.A. Brown, S.A. Gill and S.J. Allen, Water Res., 34 (16) (2000) 3907.
[7] M. Soylak and L. Elc, Int. J. Environ. Anal. Chem., 66 (1) (1997) 51.
[8] N.A. Badawy, A.A. Bayaa, A. Abdel-Y. Abdel-AAI, S.E. Garamon, J. Hazard Materials, 166(2-3) (2009) 1266.
[9] K. Seenivasan, E. Sathiya, E-Journal of Chemistry, 6(4) (2009)1167.
[10] T. Dheiveesan and S. Krishnamoorthy, J. Indian Chem. Soc., 65(1988)731.
[11] D. Kathiresapandian and S. Krishnamoorthy, Indian. J. Technol., 29 (1991) 487.
[12] A. Mariamichel and S. Krishnamoorthy, Asian J. Chem., 9 (1) (1997) 136.
[13] P. Vasudevan and N.L.N. Sharma, J. Appl. Poly. Sci., 23 (1979) 1443.
[14] N. Kanna , R.K. Seenivasan and R. Mayilmurugan, Indian J. Chem. Technol., 10 (20030623.
[15] M.S. Metwally, N.E. Metwally and T.M. Samy J, Aool. Poly. Sci., 52 (1994) 61.
[16] G.J. Mohan rao and S.C. Pillai, J. Indian Inst.Sci.,36 A (1954) 70.
[17] S. Shahha and S.L.Batna, J. Appl. Chem. Lon.,8 (1953) 335.
[18] M. Natarajan and S.Krishnamoorthy, Res.Ind., 38 (1993) 278.

ISBN 978-93-82338-36-9

International J. of Math. Sci. & Engg. Appls. (IJMSEA)
ISSN 0973-9424, Vol. 11 No. I (April, 2017), pp. 195-204

PUBLICKEY CRYPTOGRAPHY - KEY SHARING WITH SEMIRING ACTION

M. SUNDAR[1], P. VICTOR[2] AND M. CHANDRAMOULEESWARAN[3]
[1] Sree Sowdambika College of Engineering, Aruppukottai, India.
[2] Mohamed Sathak Engineering College, Killakarai, India.
[3] Saiva Bhanu Kshatriya College, Aruppukottai, India.

Abstract

In this paper we present a generalised procedure for Diffie-Hellman key exchange problem to share secret key in a publickey cryptosystem using action of a semiring over a semimodule.

Key Words and Phrases : Public key, Private key, Semiring, Semimodule and Semiring action

2000 AMS Subject Classification : 11T71,14G50,94A60,16Y60.

1 Introduction

The brilliant and important cryptographic system is the RSA system which has the strange but extremely useful asymmetric property: There are two keys involved - Publickey and Private key. Each recipient of messages could have both the keys. The recipient announces his publickey to everyone but keeps the private key secret. Anyone can encode messages for a particular recipient using the publickey. However only someone with the knowledge of the private key can decode them.

Asymmetric cryptographic system used the notion of a (one way)trapdoor functions - functions whose outputs can be computed in a reasonable amount of time but whose inverses are inordinately difficult and time consuming to compute. Cryptographic systems based on trapdoor functions are now used in real world communications by governments, businesses and individuals, notably for secured transactions over internet.

The first step in a cryptosystem is to label all possible plaintext message units and all possible cyphertext message units by means of mathematical objects from which enciphering transformation and deciphering transformation can easily be constructed. There are several techniques available in the literature to construct these structural informations. In practice one can have an equipment for enciphering and deciphering which is constructed to implement only one type of crptosystem. Over a peroid of time the information about the type of system they are using be leakout. To increase the security, they need to change frequently the choice of parameters used with the system. The parameter is called a key(secret key).

The origin of using the discrete logarithmic problem in cryptographic schemes goes back to the seminal paper of Diffie and Helllman [1]. The discrete logarithm problem is the basic incredient of many cryptographic protocols. Given a finite group G and elements $g, h \in G$,find a positive integer $n \in \mathbb{N}$ such that $g^n = h$. The above problem has a solution if and only if $h \in < g >$,the cyclic group generated by g.If $h \in < g >$ then there is a unique integer n satisfying $1 \leq n \leq ord(g)$such that $g^n = h$. We call this unique integer the discrete logarithm of h with base g and we denote it by $log_g\ h$. Diffie

and Hellman proposed the DLP as a good source for a (one way)trapdoor function. In Diffie and Hellman method, using the DLP, two users agree on a secret cryptographic key using only an insecure channel of communication. Before the discovery of publickey systems the two parties wishing to communicate will meet beforehand to agree upon a secter key. This severly limits the spontaneity of secure communication and may require a courier. The Diffie-Hellman key selection protocol eliminates this problem. It is desccribed as follows: The key construction between two parties A and B proceeds as follows. Let M be a large integer (say $> 10^{40}$).

1. A chooses a random integer x with $0 < x < M$,computes g^x and sends the result to B, keeping x secret.

2. B chooses a random integer y with $0 < y < M$,computes g^y and sends the result to A, keeping y secret.

3. Both A and B construct the key from g^{xy}, which A computes from $(g^y)^x$ and B computes from $(g^x)^y$.

If this scheme is to be secure then the problem of computing g^{xy} from knowledge of $g, g^x$and g^yshould be interactable. We shall refer this problem as the Diffie-Hellman problem. It is clear that solving the underlying discrete logarithm problem is sufficient for breaking the Diffie-Hellman protocol. For this reason researchers have been searching for groups where the discrete logarithm problem is considered a computationally difficult problem. In the literature many groups have been proposed as candidates for studying the discrete logarithm problem.The discrete logarithm problem over a group can be seen as a special instance of an action by a semigroup. The interesting thing is that every semigroup action by an abelian group gives rise to a Diffie-Hellman key exchange. The generalisation of the original Diffie-Hellman key exchange in $(\mathbb{Z}/p\mathbb{Z})^*$found a new depth when Koblitz [4] suggested that such a protocol could be used with the group over an elliptic curve.

The idea of using semigroup actions for the purpose of buiding one-way trapdoor function is not a new one and it appeared in one way or the other in several

papers[5],[6],[7]. In this paper, we present a generalisation of the Diffie-Hellman key exchange protocol. Crucial for this generalisation is the semigroup actions on finite sets. Our main aim will be the semigroup actions built from multiplicative structure on semirings, acting on finite semimodules over semirings. In particular, we construct semiring action on a finite left-semimodule over a semiring. The setup is general enough that it includes the Diffie-Hellman protocol over a general finite left semimodule.

2 Preliminaries

In this section we recall some basic definitions from cryptosystem and semirings that are needed for our work. [2] Let A denote a finite set called alphabet of definition and M denote the set called the message space which consists of strings of symbols from alphabet of definition. An element of M is called a plain text message.
Let C denote a set called ciphertext space. It consisits of strings of symbols from the alphabet of definition which may differ from the alphabet of definition of M. An element of C is called a ciphertext.

[2] A one-to-one function f from a set M to a set C is called one-way if it is easy to compute $f(m)$ for all $m \in M$,but for a randomly selected $c \in C$,finding an $m \in M$such that $c = f(m)$is computationally infeasible. In otherwords, we can easily compute f,but it is computationally infeasible to compute f^{-1}. [2] A key is a piece of information or a parameter that determines the functional output of a cryptographic algorithm. A key specifies the transformation of plaintext into ciphertext, and vice versa. Let K denote the key space which consists of a set of keys. We can classify the key into two types- one is a publickey and the other is a private key.
Public key is made available to everyone through publicly accessible directory and the private key must remain confidential to its respective owner. [2] An Encryption function e_k is a mapping from M to C and a Decryption function d_k is a mapping from C to M such that $d_k(e_k(x)) = x$, for every $x \in M$. Let E denote the set of all encryption functions from M to C and D, the set of all decryption functions from C to M.

[2] A cryptosystem is defined as a five-tuple (M, C, K, E, D) where M, C, K, E, D are mentioned above. There are two types of cryptosystems based on the manner in which encryption-decryption is carried out in the system.
(i)Symmetric key cryptosystem

(ii) Asymmetric or Publickey cryptosystem
The former one is the encryption process where same keys are used for encryption and decryption. But in the Publickey cryptosystem different keys are used for encryption and decryption

[3] A semiring is a non-empty set S together with two binary operations $+$ and $\cdot$ such that

1. $(S, +)$ is a commutative monoid with identity element 0.
2. $(S, \cdot)$ is a moniod with 1.
3. Multiplication distributes over addition from either sides.
4. $0r = 0 = r0, \forall r \in S$.

[3] A left-ideal I of S is a non-empty subset of S satisfying the following conditions:

1. $1 \notin I$.
2. If $a, b \in I$,then $a + b \in I$,
3. If $a \in I, r \in S$ then $ra \in S$,

Analogously we can define right-ideal of a semiring. [3] Let S be a semiring. A left S-semimodule is a commutative monoid $(M, +)$ with additive identity 0_M for which we have a function $S \times M \to M$, denoted by $(r, m) \mapsto rm$ and called the scalar multiplication, which satisfies the following conditions :

1. $(rr^{'})m = r(r^{'}m)$;
2. $r(m + m^{'}) = rm + rm^{'}$;
3. $(r + r^{'})m = rm + r^{'}m$;
4. $r0_M = 0_M = 0_R m$.

If the semiring S consists of an unity 1 in S then the semimodule M over S satisfies $1 \cdot m = m \ \forall \ m \in M$.

Analogously we can define right semimodules over S. **(Group Action)**[5] Let $A = (S, \cdot)$ be a semigroup and A a semimodule over S. Then a left semigroup action of A on M is a map from $A \times M \to M$ such that

1. $ex = x$
2. $(ab)x = a(bx), \ \forall \ a, b \in A, x \in M$

(Semiroup Action Problem)[5] Given a semigroup G acting on a set $S$and elements $x \in S$and $y \in Gx$,find $g \in G$such that $gx = y$.

3 Key Sharing with semiring Actions

In this section we describe a procedure to share the secret key in a publickey cryptosystem using semiring action on a semimodule. We start with the following definitions. Let S be a semiring and M be a semimodule over S.The mapping $S \times M \to M$is said to be an action of S on Mif the following conditions are satisfied:

1. $s_1(s_2m) = (s_1s_2)m$;
2. $(s_1 + s_2)m = s_1m + s_2m$;
3. $s_1(m + n) = s_1m + s_1n$, for all $s_1, s_2 \in S$ and $m, n \in M$.

A semigroup M is said to be bicyclic if for any $x \in M$,there exists two elements a, b such that $x = a^m b^n$ for some $m, n \in \mathbb{N}$. We consider two commutative semirings S_1 and S_2 and M_1 is a S_1-left semimodule and M_2 is a S_2-left semimodule.
Then $A = S_1 \times S_2$ is a commutative semiring and $M = M_1 \times M_2$ is a left semimodule of A. Define $\phi : A \times M \to M$ by

$$\phi[(f, g), (m_1, m_2)] \mapsto (fm_1, gm_2), \forall f \in S_1, g \in S_2, m_1 \in M_1, m_2 \in M_2.$$

Then ϕ is a semiring action on M. Now define

$$\phi_{S_1} : A \times M \to M \ by \ \phi_{S_1}[(f, g), (m_1, m_2)] \mapsto (fm_1, m_2)$$

$$\phi_{S_2} : A \times M \to M \text{ by } \phi_{S_2}[(f,g),(m_1,m_2)] \mapsto (m_1, gm_2.)$$

Protocol:

Let $A = S_1 \times S_2$ be a commutative semiring, $M = M_1 \times M_2$ be a left semimodule of A, and ϕ_{S_1}, ϕ_{S_2} are semiring actions on M. Then the key exchange in $(A, M, \phi_{S_1}, \phi_{S_2})$ is the following protocol.

1. Alice and Bob publicly agree on an element $m = (m_1, m_2) \in M$
2. Alice chooses $(s_1, s_2) \in A$ and computes $\phi_{S_1}[(s_1, s_2)(m_1, m_2)]$. Alice's private key is (s_1, s_2), her public key is $\phi_{S_1}[(s_1, s_2)(m_1, m_2)]$.
3. Bob chooses $(t_1, t_2) \in A$ and computes $\phi_{S_2}[(t_1, t_2)(m_1, m_2)]$. Bob's private key is (t_1, t_2), his public key is $\phi_{S_2}[(t_1, t_2)(m_1, m_2)]$.
4. Their common secret key is then

$$\phi_{S_1}[(s_1, s_2)\phi_{S_2}(t_1, t_2)(m_1, m_2)] = \phi_{S_1}[(s_1, s_2)(m_1, t_2 m_2)] = (s_1 m_1, t_2 m_2)$$

$$\phi_{S_2}[(t_1, t_2)\phi_{S_1}(s_1, s_2)(m_1, m_2)] = \phi_{S_2}[(t_1, t_2)(s_1 m_1, m_2)] = (s_1 m_1, t_2 m_2)$$

This protocol is illustrated by the following example: Let $S_1 = B(5,3) = (\{0,1,2,3,4\}, \oplus, \odot)$ be a semiring with the following Cayley tables.

$\oplus$	0	1	2	3	4
0	0	1	2	3	4
1	1	2	3	4	3
2	2	3	4	3	4
3	3	4	3	4	3
4	4	3	4	3	4

$\odot$	0	1	2	3	4
0	0	0	0	0	0
1	0	1	2	3	4
2	0	2	4	4	4
3	0	3	4	3	4
4	0	4	4	4	4

Let $M_1 = \{e_1, x, y\}$ be an S_1-semimodule under addition and scalar multiplication defined by the following cayley table:

$+$	e_1	x	y
e_1	e_1	x	y
x	x	x	e_1
y	y	e_1	y

$*$	e_1	x	y
0	e_1	e_1	e_1
1	e_1	x	e_1
2	e_1	x	e_1
3	e_1	x	e_1
4	e_1	x	e_1

Let $S_2 = B(4,2) = (\{0,1,2,3\}, \oplus, \odot)$ be a semiring with the following Cayley tables.

$\oplus$	0	1	2	3
0	0	1	2	3
1	1	2	3	2
2	2	3	2	3
3	3	2	3	2

$\odot$	0	1	2	3
0	0	0	0	0
1	0	1	2	3
2	0	2	2	2
3	0	3	2	3

Let $M_2 = \{e_2, a, b, c\}$be an S_2-semimodule under addition and scalar multiplication defined by the following cayley table:

$+$	e_2	a	b	c
e_2	e_2	a	b	c
a	a	a	b	b
b	b	b	b	a
c	c	b	a	c

$*$	e_2	a	b	c
0	e_2	e_2	e_2	e_2
1	e_2	e_2	e_2	e_2
2	e_2	b	b	e_2
3	e_2	b	b	e_2

Let $A = S_1 \times S_2$ be the semiring with the operations $\oplus$ and $\odot$ defined componentwise. Let $M = M_1 \times M_2$ be the semimodule over A. Let $(x, b) \in M$ be the public key.

Alice chooses $(2,3) \in A$ as her private key and calculates

$$\phi_{S_1}[(2,3),(x,b)] = (2x,b) = (x,b)$$

and sends it to Bob. Bob chooses $(3,1) \in A$ as his private key and calculates

$$\phi_{S_2}[(3,1),(x,b)] = (x,1b) = (x,e_2)$$

and sends it to Alice. Now Alice calculates

$\phi_{S_1}((2,3),(x,e_2)) = (2x,e_2) = (x,e_2)$Bob calculate

$\phi_{S_2}((3,1),(x,b)) = (x,1.b) = (x,e_2)$Since 3 and 3 are equal Allice and Bob have exchanged the secret key.

Let S_1 and S_2 and $A = S_1 \times S_2$ be the semirings as in the previous example. Let $M_1 = \{0,3,4\}$ be a left ideal of $S_1$and let $M_2 = \{0,2,3\}$ be a left ideal of S_2. Then $M = M_1 \times M_2$ is a left semi-module over A.

Let $(3,2) \in M$ be the public key. Alice chooses $(1,3) \in A$ as her private key and calculates $\phi_{S_1}[(1,3),(3,2)] = (1.3,2) = (3,2)$ and sends it to Bob. Bob chooses

$(1,0) \in A$ as his private key and calculates $\phi_{S_2}[(1,0),(3,2)] = (3,0.2) = (3,0)$ and sends it to Alice.

Now Alice calculates

$\phi_{S_1}((1,3),(3,0)) = (1.3,0) = (3,0)$Bob calculates

$\phi_{S_2}((1,0),(3,2)) = (3,0.2) = (3,0)$Since 3 and 3 are equal both Allice and Bob have exchanged the secret key.

Problem (Semiring Action Problem (SAP)): Given a semiring $A = S_1 \times S_2$ acting on a left semimodule $M = M_1 \times M_2$ and elements $n = (n_1, n_2) \in M$ and $r = (r_1, r_2) \in \phi_{S_1}(An)$ (or) $\phi_{S_2}(An)$, find $q = (q_1, q_2) \in A$ such that $\phi_{S_1}(qn) = r$ (or) $\phi_{S_2}(qn) = r$.

Generic Attacks of SAP: If an attacker, Eve, can find an $\alpha = (\alpha_1, \alpha_2) \in A$ such that $(\alpha_1, \alpha_2)(m_1, m_2) = (s_1, s_2)(m_1, m_2)$, then Eve may find the shared secret by computing

$$\begin{aligned}
\phi_{S_1}[(\alpha_1,\alpha_2)\phi_{S_2}[(t_1,t_2)(m_1,m_2)]] &= (\phi_{S_1}[(\alpha_1,\alpha_2)]\phi_{S_2}[(t_1,t_2)])\,(m_1,m_2) \\
&= \phi_{S_2}[(t_1,t_2)]\,(\phi_{S_1}[(\alpha_1,\alpha_2)(m_1,m_2)]) \\
&= \phi_{S_2}[(t_1,t_2)]\,(\phi_{S_1}[(s_1,s_2)(m_1,m_2)]) \\
&= \phi_{S_2}[(t_1,t_2)]\,(s_1m_1,m_2) \\
&= (s_1m_1,t_2m_2)
\end{aligned}$$

Eve computes $\phi_{S_1}(rm)$ for all possible $r = (r_1, r_2) \in A$ intil she finds some $\alpha = (\alpha_1, \alpha_2)$ with $\phi_{S_1}[(\alpha_1, \alpha_2)(m_1, m_2)] = \phi_{S_1}[(s_1, s_2)(m_1, m_2)]$
Then she is able to break the system as explained above. To avoid this attack, Bob and Alice must choose A and M sufficiently large and select a good candidate for $m = (m_1, m_2)$,such that the size of the set

$$A_{Eve} = \{\alpha \in A \mid \phi_{S_1}[(\alpha_1, \alpha_2)(m_1, m_2)] = \phi_{S_1}[(s_1, s_2)(m_1, m_2)]\}$$

is small with respect to the size of A.
Define $Stab(m) = \{q \in A \mid qm = m\}$,the subsemiring of A. One can observe thet $A_{Eve}$is simply a left coset of $Stab(m)$. Now A_{Eve} will be small in size if $A/Stab(m)$ is large or in other words $Stab(m)$ is small in size with respect to the size of A. This is true since

every element $\alpha \in Stab(m)$ has the property that $\alpha \in A_{Eve}$, that is $r\ Stab(m) \subset A_{Eve}$. Consider S_1, S_2 and M_1, M_2 as in the previous example. Let $(3,2) \in M$ be the public key. Alice chooses $(1,3) \in A$ as her private key and calculates $\phi_{S_1}((1,3),(3,2)) = (3,2)$. Now Eve chooses $(3,3) \in A$ and calculates $\phi_{S_1}((3,3),(3,2)) = (3,2)$. Then Eve may find the shared secret by computing $\phi_{S_1}[(3,3)\phi_{S_2}[(4,2)(3,2)]] = (3,4)$ and break the cryptosystem.

Here $A_{Eve} = \{(1,3),(3,3)\}$ and $Stab(3,2) = \{(1,3),(3,3)\}$. To avoid the attack by Eve, Alice and Bob choose A and M sufficiently large and select $m \in M$ such that the size of A_{Eve} is small with respect to the size of A. If one has the ability to compute efficiently the canonical representatives for the right coset $a\ Stab(m)$ this computed value could potentially be used to an attacker's advantage. However, we use the linear action of commutative semirings on semi modules, so that the above task become difficult.

References

[1] **Diffie W. and Hellman M.:**New directions in cryptography, IEEE Transactions, Inform.theory 22(1976),472-492.

[2] **Douglas R. Stinson:** Cryptography Theory and Practice, CRC Press.

[3] **Jonathan S. Golan:** The Semirings and their Applications, Kluwer Academic Publishers-Londan.

[4] **Koblitz N.:** Elliptic curve cryptosystems, Math. Comp., 48 (1987), 203209.

[5] **Maze G., Monico C. and Rosenthal J.:** Public key Cryptography Based On Semigroup Actions, Advances in Mathematics of Communications, Vol.1, No.4 (2007), 489-507.

[6] **Shpilrain V. and Ushakov A.:** Thompsons group and public key cryptography, in Third International Conference, ACNS 2005, 3531, Lecture Notes in Comput. Sci., Springer, Berlin, 2005, 151163.

[7] **Yamamura A.** Public-key cryptosystems using the modular group in Public Key Cryptography, Lecture Notes in Computer Science, 1431, Springer, Berlin, 1998, 203216.

International J. of Math. Sci. & Engg. Appls. (IJMSEA)
ISSN 0973-9424, Vol. 11 No. III (December, 2017), pp. 113-122

CATEGORICAL PRODUCT OF TWO S-VALUED GRAPHS

P. VICTOR[1] AND M. CHANDRAMOULEESWARAN[2]
[1] Mohamed Sathak Engineering College,
Kilakarai - 623 806, Tamilandu, India
[2] Saiva Bhanu Kshatriya College,
Aruppukottai - 626101, Tamilnadu, India

Abstract

Motivated by the study of products in crisp graph theory and the notion of S-valued graphs, in this paper, we study the concept of categorical product of two S-valued graphs.

1. Introduction

Graphs are, of course, basic combinatorial structures. Products of structures are a fundamental construction in mathematics, for which theorems abound in set theory, category theory, and universal algebra. One can expect many of the nice properties of products to be a result of a role played in some Category-theoretic construct. However, the graph product such as, [6] Cartesian product, Categorical product, Strong product and the lexicographic product do not arrive in that way. Thus, it is not surprising that good things happen when we take products of graphs; many unique and new ideas emerge.

Key Words : *Graph operations, Product of Graphs, Semiring, S-valued graphs.*

2000 AMS Subject Classification : 16Y60, 05C25, 05C76.

 University approved journal (Sl No. 48305)

Algebraic graph theory can be viewed as an extension of graph theory in which algebraic methods are applied to problems about graphs [1]. Recently in [4], Chandramouleeswaran et.al. introduced the concept of semiring valued graphs, called S-valued graphs. In [2] the authors have studied the regularity of S-valued graphs. In [5], the authors have discussed the concept of degree regular S-valued graphs. This motivated us to study, the notion of categorical product of two S-valued graphs and their regularity properties.

2. Preliminaries

In this section, we recall the basic definitions that are needed in the sequel.

Definition 2.1. [6] : The Categorical product of two graphs $G = (V(G); E(G))$ and $H = (V(H), E(H))$ is the graph denoted as $G \times H$, whose vertex set is $V(G) \times V(H)$, and for which vertices (g, h) and (g', h') are adjacent precisely if $gg' \in E(G)$ and $hh' \in E(H)$. Thus $V(G \times H) = \{(g, h) | g \in V(G) \text{ and } h \in V(H)\}$, $E(G \times H) = \{(g, h)(g', h') | gg' \in E(G) \text{ and } hh' \in E(H)\}$.

Definition 2.2 [3] : A semiring $(S, +, \cdot)$ is an algebraic system with a non-empty set S together with two binary operations $+$ and $\cdot$ such that

(1) $(S, +, \cdot)$ is a monoid.

(2) $(S, \cdot)$ is a semigroup.

(3) For all $a, b, c \in S$, $a \cdot (b + c) = a \cdot b + a \cdot c$ and $(a + b) \cdot c = a \cdot c + b \cdot c$.

(4) $0 \cdot x = x \cdot 0 = 0 \ \forall x \in S$.

The element 0 in S is called the additive identity of the Semiring S.

Definition 2.3 [3] : Let $(S, +, \cdot)$ be a semiring. $\preceq$ is said to be a canonical pre- order if for $a, b \in S$, $a \preceq b$ if and only if there exists $c \in S$ such that $a + c = b$.

Definition 2.4 [4] : Let $G = (V, E \subset V \times V)$ be a given graph with $V, E \neq \phi$. For any semiring $(S, +, \cdot)$, a semiring valued graph (or a S-valued graph) G^S is defined to be the graph $G^S = (V, E, \sigma, \psi)$ where $\sigma : V \to S$ and $\psi : E \to S$ is defined to be

$$\psi(x, y) = \begin{cases} \min\{\sigma(x), \sigma(y)\} & \text{if} \quad \sigma(x) \preceq \sigma(y) \quad (\text{or}) \quad \sigma(y) \preceq \sigma(x) \\ 0 & \text{otherwise} \end{cases}$$

for every unordered pair (x, y) of $E \subset V \times V$. we call σ, a S-vertex set and ψ an S-edge set of S-valued graph G^S.

Definition 2.5 [4] : Let $G^S = (V, E, \sigma, \psi)$ be the S-valued graph corresponding to a given crisp graph $G = (V, E)$. A S-valued graph $H^S = (P.L, \tau, \gamma)$ is called a S-subgraph of G^S if $H = (P, L)$ is a subgraph of G with $P \subset V, L \subset E$, $\tau \subset \sigma$ and $\gamma \subset \psi$. That is $\tau \subset \sigma \Rightarrow \tau(x) \preceq \sigma(x), x \in P$ and $\gamma \subset \psi \Rightarrow \gamma(x, y) \preceq \psi(x, y)$, $(x, y) \in L \subset P \times P$.

Definition 2.6 [4] : Let $G^S = (V, E, \sigma, \psi)$ be a S-valued graph and $H^S = (P, L, \tau, \gamma)$ be its S-subgraph. H^S is called a S-subgraph of G^S induced by P if $P \subset V$, $L \subset E$, $\tau(x) = \sigma(x)$, for every $x \in P$ and $\gamma(x, y) = \psi(x, y)$ for every $(x, y) \in L$.

Definition 2.7 [4] : The open neighbourhood of v_i in G^S is defined as

$$N_S(v_i) = \{(v_j, \sigma(v_j))|(v_i, v_j) \in E \ \psi(v_i, v_j) \in S\}.$$

The closed neighbourhood of v_i in G^S is defined as $N_S[v_i] = N_S(v_i) \cup \{(v_i, \sigma(v_i))\}$,.

Definition 2.8 [5] : The degree of a vertex v_i of the S-valued graph G^S is defined as $deg_S(v_i) = \left(\sum_{v_j \in N_S(v_i)} \psi(v_i, v_j), l \right)$ where l is the number of edges incident with v_i.

Definition 2.9 [4] : A S-valued graph G^S is said to be

(1) vertex regular if $\sigma(v) = a \ \forall \ \ v \in V$ and for some $a \in S$

(2) Edge regular if $\psi(u, v) = a \ \forall \ (u, v) \in E$ and for some $a \in S$.

(3) S-regular if it is both vertex as well as edge regular.

Definition 2.10 [5] : A S-valued graph G^S is said to be degree regular S-valued graph (d_S-regular graph) if $deg_S(v) = (a, n) \ \forall \ v \in V$ and some $a \in S$ and $n \in Z_+$.

Definition 2.11 [2] : A graph G^S is said to be (a, k) regular if the underlying crisp graph G is k-regular and $\sigma(v) = a, \ \forall \ v \in V$.

3. Categorical Product of Two S-valued Graphs

In this section, we introduce the notion of categorical product of two S-valued graphs, illustrate with some examples, and prove simple properties.

Definition 3.1 : Let $G_1^S = (V_1, E_1, \sigma_1, \psi_1)$ where $V_1 = \{v_i|1 \leq i \leq p_1\}$, $E_1 \subseteq V_1 \times V_1$ and $G_2^S = (V_1, E_2, \sigma_2, \psi_2)$ where $V_2 = \{u_j|1 \leq j \leq p_2\}$, $E_2 \subseteq V_2 \times V_2$ be two given S-valued graphs.

The Categorical product of two S-valued graphs G_1^S and G_2^S is defined by

$$G_\times^S = G_1^S \times G_2^S = (V, E, \sigma, \psi),$$

where $V = V_1 \times V_2 = \{w_{ij} = (v_i, u_j) | v_i \in V_1, u_j \in V_2\}$; $1 \leq i \leq p_1$; $1 \leq j \leq p_2$ the two vertices $w_{ij} = (v_i, u_j)$, $w_{kl} = (v_k, u_l)$ are adjacent if $v_i v_k \in E_1$ and $u_j u_l \in E_2$. Then $E = \{e_{ij}^{kl} = (w_{ij}, w_{kl}) | e_i^k = v_i v_k \in E_1 \text{ and } e_j^l = u_j u_l \in E_2\}$.

Define the S-valued functions, $\sigma : V \to S$ by $\sigma(v_i, u_j) = \min\{\sigma_1(v_i), \sigma_2(u_j)\}$ and $\psi : E \to S$ by $\psi(w_{ij}) = \min\{\psi_1(e_i^k), \psi_2(e_j^l)\}$.

Example 3.2 : Consider the semiring $S = (\{0, a, b, c\}, +, \cdot)$ with the binary operations '$+$' and '$\cdot$ defined by the following Cayley tables.

$+$	0	a	b	c
0	0	a	b	c
a	a	b	c	c
b	b	c	c	c
c	c	c	c	c

$\cdot$	0	a	b	c
0	0	0	0	0
a	0	a	b	c
b	0	b	c	c
c	0	c	c	c

In S we define a canonical pre-order $\preceq$ by

$$0 \preceq 0,\ 0 \preceq a, 0 \preceq b, 0 \preceq c, a \preceq a, b \preceq b, c \preceq c, a \preceq b, a \preceq c, b \preceq c.$$

Consider the two S-valued graphs G_1^S and G_2^S:

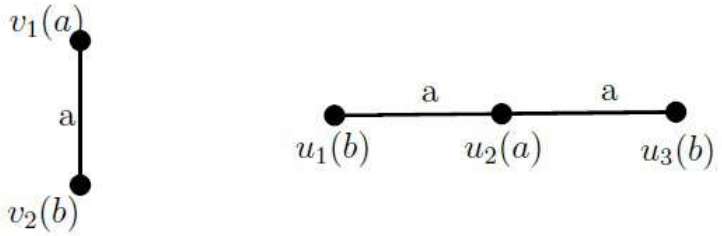

Then the categorical product $G_\times^S = G_1^S \times G_2^S = (V, E, \sigma, \psi)$ is

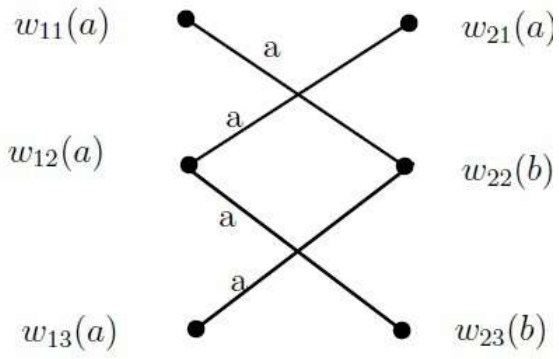

Here, $V = \{w_{11}, w_{12}, w_{13}, w_{21}, w_{22}, w_{23}\}$ and $E = \{e_{11}^{22}, e_{12}^{21}, e_{12}^{23}, e_{13}^{22}\}$.

The S-vertex set of $G_1^S \times G_2^S = \{a, b\}$ and the S-edge set of $G_1^S \times G_2^S = \{a\}$.

Theorem 3.3 : The Categorical product of two S-regular graph is again a S-regular graph.

Proof : Let $G_1^S = (V_1, E_1, \sigma_1, \psi_1)$ and $G_2^S = (V_2, E_2, \sigma_2, \psi_2)$ be two S-regular graphs. That is, G_1^S and G_2^S is both vertex regular as well as edge regular.

Claim : $G_\times^S = (V, E, \sigma, \psi)$ is S-regular. That is to prove that, $\sigma(w_{ij})$ is equal for all $w_{ij} \in V$ and $\psi(e_{ij}^{kl})$ is equal for all $e_{ij}^{kl} \in E$.

Now by definition

$$\sigma(w_{ij}) = \min\{\sigma_1(v_i), \sigma(u_j)\} = \begin{cases} \sigma_1(v_i) & \text{if} \quad \sigma_1(v_i) \preceq \sigma_2(u_j) \\ \\ \sigma_2(u_j) & \text{if} \quad \sigma_2(u_j) \preceq \sigma_1(v_i) \end{cases}$$

Then in both the cases $\sigma(w_{ij})$ is equal for all $w_{ij} \in V, 1 \leq i \leq p_1, 1 \leq j \leq p_2$.

This implies that $G_x^S = G_1^S \times G_2^S$ is vertex regular. Further,

$$\begin{aligned} \psi(e_{ij}^{kl}) &= \min\{\psi_1(e_i^k), \psi_2(e_j^l)\} \\ &= \min\{\sigma_1(v_i), \sigma_2(u_j)\} \quad (\because \ G_1^S \ \textit{and} \ G_2^S \ \textit{are} \ S-\textit{regular}) \\ &= \begin{cases} \sigma_1(v_i) & \text{if} \quad \sigma_1(v_i) \preceq \sigma_2(u_j) \\ \\ \sigma_2(u_j) & \text{if} \quad \sigma_2(u_j) \preceq \sigma_1 v_i) \end{cases} \end{aligned}$$

Thus $\psi(e_{ij}^{kl}) = \sigma_1(v_i)$ or $\psi(e_{ij}^{kl}) = \sigma_2(u_j)$ for all eges $e_{ij}^{kl} \in E$.

This implies that, $G_\times^S = G_1^S \times G_2^S$ is edge regular.

Thus the Categorical product, $G_\times^S = G_1^S \times G_2^S$ is a S-regular graph.

The converse of the above theorem need not be true in general, as seen from the following example.

Example 3.4 : Consider the semiring $(S = \{0, a, b, c\}, +, \cdot)$ as in the example 3.2. Consider the S-valued graphs G_1^S and G_2^S and its categorical product $G_\times^S$:

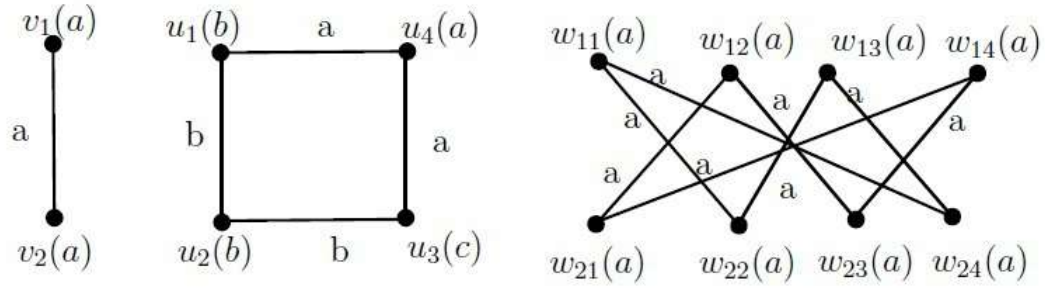

Clearly $G_\times^S = G_1^S \times G_2^S$ and G_1^S are S-regular while G_2^S is not.

However, the following example gives that the product G_x^S is not S-regular eventhough one of the factors G_1^S or G_2^S is S-regular.

Example 3.5 : Consider the semiring $S = \{a, b, c\}, +, \cdot$ as in the example 3.2. Consider the S-valued graphs G_1^S and G_2^S and its categorical product $G_\times^S$:

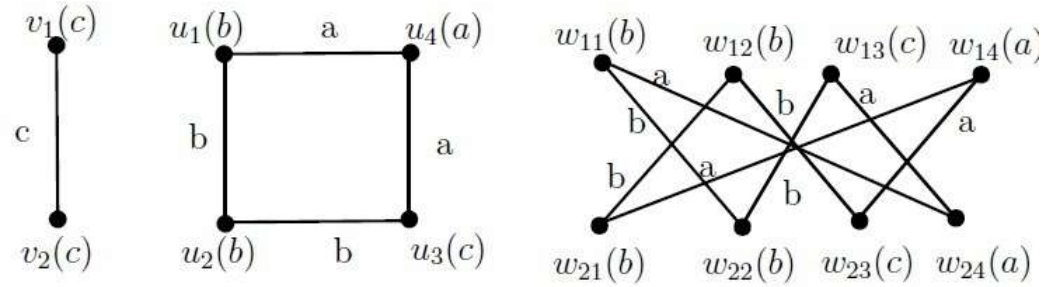

$G_\times^S = G_1^S \times G_2^S$ is not Sregular, eventhough G_1^S is S-regular while G_2^S is not for $b \preceq c$ in S.

The above example leads to the following theorem.

Theorem 3.6 : The Categorical product of two S-valued graphs is S-regular if the S-value corresponding to the S-regular graph is minimum among the S-values.

Proof : Let G_1^S and G_2^S be two S-valued graphs such that G_1^S is S-regular with the S-value is minimum among the S-values.

That is,$\sigma_1(v_i) = a$ for all $v_i \in V_1$ and for some $a \in S$, which is minimum in the semiring S.

Claim : $G_\times^S = G_1^S \times G_2^S$ is S-regular with the S-value $a \in S$.

Now, For any $w_{ij} \in V$,

$$\begin{aligned} \sigma(w_{ij}) &= \min\{\sigma_1(v_i), \sigma_2(u_j)\} = \min\{a, \sigma_2(u_j)\} \\ &= a \quad (\because \quad a \preceq \sigma_2(u_j) \ \ \forall \ \ u_j \in V_2). \end{aligned}$$

Thus $G_\times^S = G_1^S \times G_2^S$ is a vertex regular.

Since every vertex regular S-valued graph is edge regular, $G_\times^S$ is edge regular.

Then, $G_\times^S$ is S-regular with the S-value a, which is minimum among the S-values. This proves that $G_\times^S$ is S-regular with S-value $\min\{\sigma_1(v_i), \sigma_2(u_j), 1 \le i \le p_1, 1 \le j \le p_2\}$.

Theorem 3.7 : The Categorical product of two edge regular S-valued graphs is an edge regular S-valued graph.

Proof : Let$G_1^S = (V_1, E_1, \sigma_1, \psi_1)$ and $G_2^S = (V_2, E_2, \sigma_2, \psi_2)$ be two edge regular S-valued graphs.

Then $\forall \ \ e_i^k \in E_1$ and $\forall \ \ e_j^l \in E_2$, the values $\psi_1(e_i^k)$ and $\psi_2(e_j^l)$ are all equal.

Claim : $G_\times^S = G_1^S \times G_2^S$ is an edge regular S-valued graph.

That is to prove that $\psi(e_{ij}^{kl})$ is equal for every $e_{ij}^{kl} \in E$. By definition

$$\psi(e_{ij}^{kl}) = \min\{\psi_1(e_i^k), \psi_2(e_j^l)\} = \begin{cases} \psi_1(e_i^k) & if \quad \psi_1(e_i^k) \preceq \psi_2(e_j^l) \\ \psi_2(e_j^l) & if \quad \psi_2(e_j^l) \preceq \psi_1(e_i^k) \end{cases}$$

This implies that, $\psi(e_{ij}^{kl})$ is equal for every edges $e_{ij}^{kl} \in E$.

Thus the categorical product of G_1^S and G_2^S, $G_\times^S = G_1^S \times G_2^S$ is again an edge regular S-valued graph.

Theorem 3.8 : The Categorical product of two degree regular S-valued graphs (d_S-regular) is again a degree regular S-valued graph.

Proof : Let G_1^S and G_2^S be two degree regular S-valued graphs.

Then $deg_S(v_i) = \left(\sum_{v_k \in N_S(v_i)} \psi_1(v_i v_k), m \right) = (a, m)$ for some $a \in S$ and $\forall \ \ v_i \in V_1$.

$deg_S(u_j) = \left(\sum_{u_l \in N_S(u_j)} \psi_2(u_j u_l), n \right) = (b, n)$ for some $b \in S$ and $\forall \ \ u_j \in E_2$.

Claim : $G_{\times}^{S} = G_1^S \times G_2^S$ is degree regular S-valued graph. That is to prove that for all vertices $w_{ij} \in V, deg_S(w_{ij}) = \left(\sum_{w_{kl} \in N_S(w_{ij})} \psi(w_{ij}w_{kl}), r \right)$ is equal where r is the number of incident edges of $w_{ij} = (v_i, u_j)$ in $G_{\times}^{S}$.

In crisp graph, the number of incident edges of $w_{ij} = (v_i, u_j)$ is equal to the product of number of incident edges of v_i and the number of incident edges of u_j.

That is, The no. of incident edges of $w_{ij} =$

The no. of incident edges of $v_i \times$ The no. of incident edges of u_j.

This implies that, $r = m \times n = mn$.

Then, for any vertices $w_{ij} \in V,\ 1 \leq i \leq p_1; 1 \leq j \leq p_2$.

$$\begin{aligned} deg_S(w_{ij}) &= \left(\sum_{w_{kl} \in N_S(w_{ij})} \psi(e_{ij}^{kl}), mn \right) \\ &= \left(\sum_{w_{kl} \in N_S(w_{ij})} \min\{\psi_1(e_i^k), \psi_2(e_j^l)\}, mn \right) \\ &= \left(\sum_{1}^{mn} \min \left\{ \sum_{k=1}^{m} \psi_1(e_i^k), \sum_{l=1}^{n} \psi_2(e_j^l) \right\}, mn \right). \end{aligned}$$

Since G_1^S is d_S-regular, $\sum_{k=1}^{m} \psi_1(e_1^k)$ is eqaul for all edges $e_i^k \in E_1$ and G_2^S is d_S-regular, $\sum_{l=1}^{n} \psi_2(e_j^l)$ is equal for all edges $e_j^l \in E_2$.

Thus for all vertices $w_{ij} \in V$ of $G_{\times}^{S}$,

$$deg_S(w_{ij}) = \left(\sum_{1}^{mn} \min \left\{ \sum_{k=1}^{m} \psi_1(e_i^k)\psi_2(e_j^l) \right\}, \min \right)$$

is equal.

Hence, every vertices of $G_{\times}^{S} = G_1^S \times G_2^S$ have the same degree.

This implies that, the Categorical product $G_{\times}^{S} = G_1^S \times G_2^S$ is a degree regular S-valued graph.

Proposition 3.9 : Let $(S, +, \cdot)$ be a semiring and $a, b \in S$. If G_1^S is (a, m)-regular graph and G_2^S is (b, n)-regular graph then the Categorical product $G_{\times}^{S} = G_1^S \times G_2^S$ is either (a, mn)-regular or (b, mn)-regular graph, depending on $a \preceq b$ or $b \preceq a$ respectively.

Proof : Let $G_1^S = (V_1, E_1, \sigma_1, \psi_1)$ be a (a, m)-regular graph for some $a \in S$ and $m \in Z_+$.

Then $\sigma_1(v_i) = a$ for all $v_i \in V_1$ and no. of incident edges of v_i is m. (1)

Let $G_2^S = (V_2, E_2, \sigma_2, \psi_2)$ be a (b, n)-regular graph for some $b \in S$ and $n \in Z_+$.
Then $\sigma_2(u_j) = b$ for all $u_j \in V_2$ and no. of incident edges of u_j is n. (2)
Claim : $G_x^S = G_1^S \times G_2^S$ is either (a, mn)-regular or (b, mn)-regular graph.
Then we have to prove that $\sigma(w_{ij}) = a$ or $\sigma(w_{ij}) = b$ for some $a, b \in S$ and the number of incident edges of w_{ij} is $k \in Z_+$ for all vertices $w_{ij} \in V, 1 \leq i \leq p_1; 1 \leq j \leq p_2$.
By Definition

$$\begin{aligned} \sigma(w_{ij}) &= \min\{\sigma_1(v_i), \sigma_2(_j)\} \\ &= \min\{a, b\} \text{ (By (1) and (2))} \\ &= \begin{cases} a & if \quad a \preceq b \\ \\ b & if \quad b \preceq a \end{cases} \end{aligned}$$

Thus for all vertices $w_{ij} \in V$, $\sigma(w_{ij}) = b$, $1 \leq i \leq p_1$; $1 \leq j \leq p_2$.
This implies that, in both the cases, $G_\times^S = G_1^S \times G_2^S$ is vertex regular.
In $G_\times^S = G_1^S \times G_2^S$, the number of incident edges of any vertices w_{ij} is equal to the product of number of incident edges of v_i and the number of incident edges of u_j.
Then from equation (1) and (2), we have
The no. of $\cdot$ incident edges of $w_{ij} = m \times n = mn = k$ (say).
Thus the categorical product $G_\times^S = G_1^S \times G_2^S$ is vertex regular as well as all the vertices have the same number of incident edges.
Hence, $G_\times^S = G_1^S \times G_2^S$ is either (a, k)-regular or (b, k)-regular graph.

4. Conclusion

Motivated by the study of S-valued graphs in [4], [3] and [5], we studied the regularity and degree regularity conditions on the categorical product of two S-valued graphs. In future, we have proposed to study the notions of minimal and maximal degree and their properties on $G_\times^S$.

References

[1] Chris Godsil and Gordon Royle. Algebraic Graph Theory, Springer, (2001).
[2] Jeyalakshmi S., Rajkumar M. and Chandramouleeswaran M., Regularity on S-valued graphs, Global J. of Pure and Applied Maths., 2(5) (2015), 2971-2978.

[3] Jonathan Golan, Semirings and Their Applications, Kluwer Academic Publishers, London.

[4] Rajkumar M., Jeyalakshmi S. and Chandramouleeswaran M., Semiring valued graphs, International Journal of Math. Sci. and Engg. Appls., 9(3) (2015), 141-152.

[5] Rajkumar M. and Chandramouleeswaran M., Degree regular S-valued graphs, Mathematical Sciences International Journal of Math. Sci. and Engg. Appls., 4(2) (2015).

[6] Richard Hammack, Wilfried Imrich and Sandy Klavzar, Handbook of Product Graphs, University of Ljubljana and University of Maribor, Slovenia.

Available online www.jocpr.com

Journal of Chemical and Pharmaceutical Research, 2015, 7(10S):1-14

Research Article

ISSN : 0975-7384
CODEN(USA) : JCPRC5

Synthesis, structural characterization, electrochemical, biological, antioxidant and nuclease activities of 3-morpholinopropyl amine mixed ligand complexes

Jeyaraj Dhaveethu Raja*[a], Gurusamy Sankararaj Senthilkumar[b,d], Chinnapiyan Vedhi[c] and Manokaran Vadivel[a]

[a]*Chemistry Research Centre, Mohamed Sathak Engineering College, Kilakarai, Ramanathapuram (Dist), Tamilnadu, India*
[b]*Department of Chemistry, Sri Vidya College of Engineering & Technology, Virudhunagar, Tamilnadu, India*
[c]*PG & Research Department of Chemistry, V. O. Chidambaram College, Thoothukudi, Tamilnadu, India*
[d]*Manonmaniam Sundaranar University, Tirunelveli, Tamilnadu, India*

ABSTRACT

A new series of water-soluble transition mixed ligand complexes of Co (II) and Ni (II) have been synthesized from the Schiff base ligand (HL) derived from morpholine derivatives as a primary ligand with 1,10-phenonthroline (X) and 2,2'-bipyridine (Y) as co-ligands. Structural features were obtained from their elemental analyses, magnetic susceptibility, molar conductance, mass, FT-IR, UV–Vis., spectral studies. The data show that all the mixed ligand complexes have composition of [MLX]4H_2O and [MLY]4H_2O. The spectral data showed octahedral geometry around the central metal ion. The redox behavior of metal complexes was studied by cyclic voltammetry. The binding strength and binding mode of complexes with HS DNA (Herring Sperm) have been investigated by absorption titration and viscosity measurement studies. The results show a considerable interaction between complexes and HS-DNA. The nuclease activities of the complexes have shown that they cleave calf thymus DNA under aerobic condition and in the presence of H_2O_2 through redox chemistry. The in vitro biological and antioxidant activities have shown that the mixed ligand complexes have higher potent activities than the free ligand.

Keywords: Morpholine, Schiff base, Antioxidant, DNA binding, DNA cleavage.

INTRODUCTION

Schiff base complexes are used as ligand because of the combination of molecular nitrogen with central metal ions and also it has been reported to possess antimicrobial properties [1-4]. Morpholine derivatives were reported to possess antimicrobial [5-6] anti-inflammatory [7-9] and central nervous system activities [10-11]. The heterocyclic compounds exhibit biological activities due to the presence of multifunctional groups. Most of them have N, O and S containing groups which form strain-free five or six-membered ring and give 1:1 (M-L) chelate with metal ions such as Ni (II) and Co (II). Metal complexes exhibit interactions with DNA have been studied with the aims of developing both probes for nucleic acid structures and chemotherapy agents [12]. Bidentate ligand, such as 2,2'-bipyridine, 1,10-phenanthroline readily form complexes with most of the transition metal ions. These have been extensively used in both biological and preparative coordination chemistry [13-15]. Transition metal complexes have been adopted for their spectral, electrochemical properties and ability to change the ligand environment while binding and cleaving with DNA. These studies are also important in determining the pathway of metal ion toxicity [16-17]. The aromatic rings of the ligands were used to stack the bases of DNA. The existence of oxygen and create hydrogen bonds with the DNA, and the metal complexes show a positive charge so as ally with phosphate groups of DNA. Generally, metal complexes capable of abstracting xpected to oxidize guanine or other nucleobases. Current efforts are carried out to design s as chemical nucleases suitable for direct strand scission. The interaction studies between

complexes and DNA is one of the most important aspects in biological research aimed at discovering and developing new type of anti- proliferative agents [18] because DNA is one of the main molecular targets in the design of anticancer compounds [19]. The practical use of transition metal complexes as chemical nuclease is also documented [20-21]. Hence, we have explored the synthesis, characterization, biological, electrochemical, radical scavenging, DNA binding and cleavage studies of mixed ligand complexes containing tridentate schiff base.

EXPERIMENTAL SECTION

All reagents 3-morpholinopropylamine, salicylaldehyde, metal(II) salts and DPPH used were extra pure AR grade (Sigma/Aldrich) and used without further purification. Solvents were used for physical measurements are of AR grade and purified by standard methods [22]. Triply distilled water (specific conductance = 1.81± 0.1 Λ^{-1} cm^{-1}) was stored in a CO_2 free atmosphere and was used for solution preparations. Melting points of all the mixed ligand complexes were determined on Gallen kamp apparatus in open glass capillaries and were uncorrected. The elemental analysis of carbon, hydrogen and nitrogen were recorded in an Elementar Vario EL III, CHNS analyser at STIC, CUSAT, India. Molar conductance of the complexes was measured in EtOH solvent using 305 systronic conductivity bridge by using 0.01 M KCl solutions as calibrant. The mass spectra were analyzed by FAB & ESI-MS spectrum in a 3-nitro-benzylalcohol matrix. Magnetic susceptibility measurement on power samples was carried out by the Gouy method using $Hg[Co(SCN)_4]$ as calibrant and the diamagnetic corrections were applied in compliance with Pascal's constant. Electronic absorption spectra of the complexes in ethanol medium were recorded on a Shimadzu UV1800 spectrometer (path length, 1 cm) 100-1000nm range. IR spectra were recorded using KBr pellet on a Shimadzu FT-IR affinity spectrometer in 4000 – 400 cm^{-1} range and Electrochemical studies were carried out using electrochemical analyser model CHI620C. Cyclic voltammetric measurements were performed using a glassy carbon working electrode (3 mm dia), Pt wire auxiliary electrode and an Ag/AgCl reference electrode. All solutions were purged with N_2 for 30 min prior to each set of experiments. Tetrabutylammonium perchlorate TBAP was used as the supporting electrolyte. The magnetic susceptibility data of the complexes were obtained with a Gouy balance at room temperature using copper sulphate as a calibrant. Calf thymus DNA was purchased from Gene (India). Viscosity experiments were carried on an Ubbelodhe viscometer, immersed in a thermostated water-bath maintained at 30 ± 0.1°C. The CT-DNA Cleavage, HS-DNA binding and antioxidant studies were recorded in EtOH solution using UV-Transilluminator, and 1800 UV-Visible spectrophotometer in DST-SERB sponsored Research lab, Chemistry Research Centre, MSEC, Kilakarai, Ramanathapuram, Tamilnadu, India.

2.2 *Synthesis of Schiff base [HL]*

An ethanolic solution (20 ml) of 3-morpholinopropylamine (1.44 g, 10 mmol) and salicylaldehyde (1.22 g, 10 mmol) were reflux for 3h. The resulting solution was evaporated slowly to separate solvent completely from reaction mixture. On cooling, the yellow orange liquid of 2-(3-morpholinopropylimino) methyl phenol (Figure 1) was formed then purified by column chromatography with petroleum ether and methanol solvent mixture.

[HL]: [Yield: 2.1 g, 79 %] Analysis: calculated for $C_{14}H_{20}N_2O_2$: C, 67.7; H, 8.1; N, 11.3 %. Found: C, 67.1; H, 8.9; N, 11.7 %; FAB-MS (relative abundance, %): m/z 248; IR (KBr, cm^{-1}): 3210 ν(O-H phenolic), 1630 ν(-CH=N), 1200 ν(C-O Phenolic), 1143 ν(C-O aliphatic), 1338 ν(C-N aliphatic), 3056 ν(C-H aromatic), 2949 ν(C-H aliphatic), 2852 ν(C-H iminic); UV-Vis in EtOH (λ_{max}/nm):399, 315, 254.

2.3 *Synthesis of metal complexes with 1,10-phenonthroline [MLX]4H$_2$O*

A solution of the LH (0.124 g, 0.5 mmol) in ethanol (20 ml) was added to a solution of metal salts like $[Co(Ac)_2]4H_2O$ and $[Ni(Ac)_2]4H_2O$ (0.5 mmol) in 20 ml ethanol and the mixture was refluxed for ca. 4 h. An ethanolic solution of 1,10-phenonthroline (X) (0.090 g, 0.5 mmol) was mixed and refluxed for 2 h. The resulting solution then concentrated to one third and kept at room temperature for 48 h. The solid complexes were formed washed thoroughly with ethanol and dried in vacuum desiccator. All the complexes were recrystallized from ethanol.

[CoLX]4H$_2$O: [Yield: 0.20 g, 60 %] Analysis: calculated for $CoC_{28}H_{38}N_4O_8$: C, 54.5; H, 6.2; N, 9.1 %. Found: C, 54.4; H, 6.1; N, 9.1 %; FAB-MS (relative abundance, %): m/z 617; IR (KBr, cm^{-1}): 1620 ν(-CH=N); 1401 ν(acetate), 1223 ν(C-O Phenolic), 1143 ν(C-O aliphatic), 1338 ν(C-N aliphatic), 3067 ν(C-H aromatic), 2955 ν(C-H aliphatic), 2850 ν(C-H iminic), 1570 ν(C-N phenonthroline), 860 ν(H_2O), 653 ν(M-O), 492 ν(M-N); UV-Vis in EtOH (λ_{max}/nm): 980, 612, 399; Conductance in EtOH (Λ_M): 21.2 $ohm^{-1}cm^2 mol^{-1}$; Magnetic moment, μ_{eff} (BM): 4.8.

[illegible]).13 g, 59 %] Analysis: calculated for $NiC_{28}H_{38}N_4O_8$: C, 54.5; H, 6.2; N, 9.1 %. Found: C, [illegible] %; FAB-MS (relative abundance, %): m/z 617; IR (KBr, cm^{-1}): 1622 ν(-CH=N); 1404 Phenolic), 1139 ν(C-O aliphatic), 1349 ν(C-N aliphatic), 3050 ν(C-H aromatic), 2956 ν(C-H

aliphatic), 2856 ν(C-H iminic), 1558 ν(C-N phenonthroline), 845 ν(H_2O), 659 ν(M-O), 483 ν(M-N); UV-Vis in EtOH (λ_{max}/nm): 942, 548, 418; Conductance in EtOH (Λ_M): 19.6 $ohm^{-1}cm^2 mol^{-1}$; Magnetic moment, μ_{eff} (BM): 3.1.

2.4 *Synthesis of metal complexes with 2,2'-bipyridine [MLY]4H_2O*

A solution of the LH (0.124 g, 0.5 mmol) in ethanol (20 ml) was added to a solution of metal salts like $[Co(Ac)_2]4H_2O$ and $[Ni(Ac)_2]4H_2O$ (0.5mmol) in 20 ml ethanol and the mixture was refluxed for ca. 4 h. An ethanolic solution of 2,2'-bipyridine (Y) (0.0781 g, 0.5 mmol) was mixed and refluxed for 2 h. The resulting solution then concentrated to one third and kept at room temperature for 48 h. The solid complexes were formed washed thoroughly with ethanol and dried in vacuum desiccators. All the complexes were recrystallized from ethanol.

[CoLY]4H_2O: [Yield: 0.18 g, 59 %] Analysis: calculated for $CoC_{26}H_{38}N_4O_8$: C, 52.6; H, 6.4; N, 9.4 %. Found: C, 52.5; H, 6.6; N, 9.5 %; FAB-MS (relative abundance, %): m/z 593; IR (KBr, cm^{-1}): 1598 ν(-CH=N); 1399 ν(acetate), 1232 ν(C-O Phenolic), 1140 ν(C-O aliphatic), 1340 ν(C-N aliphatic), 3065 ν(C-H aromatic), 2943 ν(C-H aliphatic), 2848 ν(C-H iminic), 1569 ν(C-N bipyridine), 855 ν(H_2O), 617 ν(M-O), 497 ν(M-N); UV-Vis in EtOH (λ_{max}/nm): 987, 617, 410; Conductance in EtOH (Λ_M): 19.4 $ohm^{-1}cm^2 mol^{-1}$; Magnetic moment, μ_{eff} (BM): 4.7.

[NiLY]4H_2O: [Yield: 0.17 g, 57 %] Analysis: calculated for $NiC_{26}H_{38}N_4O_8$: C, 52.6; H, 6.4; N, 9.4 %. Found: C, 52.7; H, 6.3; N, 9.7 %; FAB-MS (relative abundance, %): m/z 593; IR (KBr, cm^{-1}): 1616 ν(-CH=N); 1400 ν(acetate), 1229 ν(C-O Phenolic), 1139 ν(C-O aliphatic), 1344 ν(C-N aliphatic), 3069 ν(C-H aromatic), 2941 ν(C-H aliphatic), 2849 ν(C-H iminic), 1565 ν(C-N bipyridine), 840 ν(H_2O), 657 ν(M-O), 487 ν(M-N); UV-Vis in EtOH (λ_{max}/nm): 975, 607, 380; Conductance in EtOH (Λ_M): 21.2 $ohm^{-1}cm^2 mol^{-1}$; Magnetic moment, μ_{eff} (BM): 3.3.

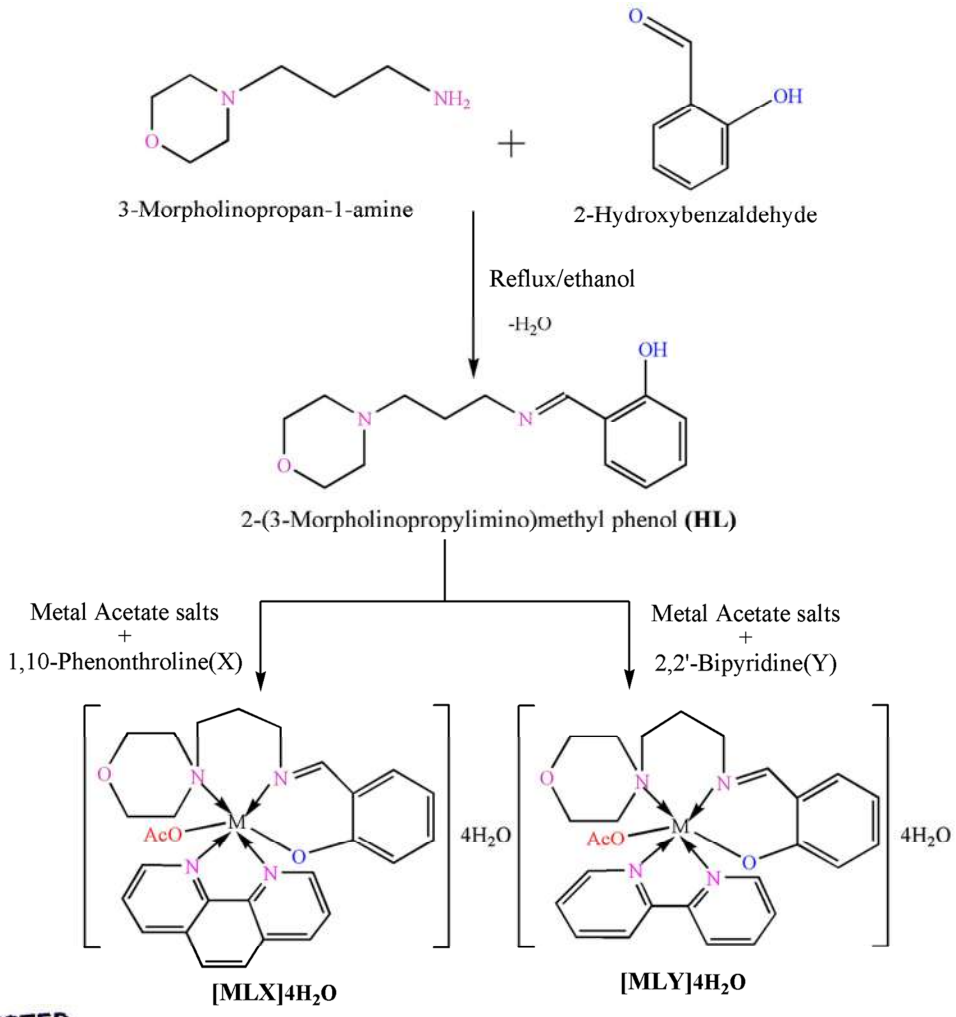

Figure 1 Synthesis of schiff base ligand and its mixed ligand complexes

2.5 *DNA binding Studies*

2.5.1 Absorption method

All the experiments involving the interaction of the complexes with herring sperm (HS) DNA were carried out in Tris-HCl buffer (50 mM NaCl/5 mM Tris-HCl, pH 7.1) at room temperature. A solution of HS DNA in the buffer gave a ratio of UV absorbance at 260 and 280 nm of about 1.8-1.9, indicating that DNA was sufficiently free from protein [23]. The HS-DNA concentration per nucleotide was determined by absorption spectroscopy using the molar absorption coefficient of 6600 M^{-1} cm^{-1} at 260 nm [24]. The compounds were dissolved in a mixed solvent of 5% methanol and 95% Tris-HCl buffer for all the experiments. Stock solutions were stored at 4 °C and used within 4 days. Absorption titration experiments were performed with fixed concentration of the compounds (30 µM) with varying concentration of DNA (0–60 µM). The absorption spectra have measured by an equal amount of DNA was added to all the test solutions and the reference solution to eliminate the absorbance of DNA itself [25].

2.5.2 Viscosity measurements

Cannon-Ubbelodhe viscometer maintained at a constant temperature of 27.0 ± 0.1°C in a thermostatic jacket was used to measure the relative viscosity of DNA solutions. A 3.0 mM stock solution of each ethidium bromide was prepared. A 0.4 mM solution of HS DNA was used. The [Complex]/[DNA] ratio was maintained in the range 0-0.2. Flow time was measured with a digital stopwatch with an accuracy of 0.01 s. The flow time of each sample was measured three times and an average flow time was calculated. Data were represented graphically as $(\eta/\eta_0)^{1/3}$ versus concentration ratio ([Complex]/[DNA]), where η is viscosity of DNA in the presence of complex and η_0 is viscosity of DNA alone [26]. Viscosity values were calculated from the observed flow time of DNA-containing solutions (t > 100 s) corrected for the flow time of buffer alone (t_o) i.e. $\eta \alpha t - t_o$.

2.6 *DNA cleavage Studies*

The DNA cleavage experiment was conducted using CT-DNA by gel electrophoresis with the corresponding metal complex in the presence of H_2O_2 as an oxidant. The reaction mixture was incubated before electrophoresis experiment at 35 °C for 2 h as follows: CT DNA 30 µM, 50 µM each complex, 50 µM H_2O_2 in 50 mM Tris-HCl buffer (pH = 7.2). The samples were electrophoresed for 2 h at 50 V on 1% agarose gel using Tris-acetic acid-EDTA buffer (pH = 7.2). After electrophoresis, the gel was stained using 1 µg/cm^3 ethidium bromide and photographed under UV light.

2.7 In vitro Antioxidant activity

All the mixed ligand complexes were tested for *in vitro* antioxidant activities at 37 ˚C by DPPH free radical scavenging assay method as prepared by Blois [27]. Solutions of mixed ligand complexes at different concentrations (10, 20, 30, 40 and 50 µM) were prepared in EtOH solvent. 1 mL of each sample solution having different concentrations and 4 mL of 0.1 mM DPPH solution were taken in different test tubes and the mixture was shook vigorously for about 2-3 min. Then test tubes were incubated in dark room for 20-30 min at 37 ˚C. A blank DPPH solution without the sample was used for the baseline correction and it gives a strong absorption maximum at 517 nm (purple color with $\varepsilon = 8.32 \times 10^3$ M^{-1} cm^{-1}). After incubation, the absorbance value for each sample 510-520 nm was measured using a UV-visible spectrometer. The observed decrease in the absorbance values indicate that the mixed ligand complexes show scavenging activity. Free radical scavenging effects in percentage was calculated using the formula:

$$\text{Scavenging effects (\%)} = \left[\frac{(A_{control} - A_{sample})}{A_{control}}\right] x\ 100$$

Where $A_{control}$ is the absorbance of the control (blank) and A_{sample} is the absorbance of the complex. All the analyses were made in three replicate for each and this results were compared with each other.

2.8 In vitro biological study

2.8.1 *Antibacterial activity*

NCCLS approved standard nutrient agar was used as medium for testing the activity of microorganisms as antibacterial agents. For preparing the agar media, 3 g of beef extract, 5 g of peptone, 5 g of yeast extract and 5 g of sodium chloride were dissolved in 1000 ml of distilled water in a clean conical flask. The pH of the solution was maintained at 7.0. The solution was boiled to dissolve the medium completely and sterilized by autoclaving at 15 lbs pressure (120 ^oC) for 30 min. After sterilization, 20 ml of media was poured into the sterilized petri plates. These petri plates were kept at room temperature for some time. After few minutes the medium got solidified in the plates. [illegible] with microorganisms using sterile swabs. The stock solutions were prepared by dissolving [illegible]ol at $1x10^{-2}$ M to find the inhibition zone values. In a typical procedure, a well was made on [illegible]ulated with microorganisms [28]. The well was filled with the test solutions using a

micropipette and the plates were incubated at 37 ^{o}C for 24 h. During this period, the test solution diffused and affected the growth of the inoculated bacteria. The inhibition zone was developed and it was noted in mm.

2.8.2 *Antifungal activity*

NCCLS approved standard potato dextrose agar was used as medium for antifungal activity by well diffusion method. For preparing the agar media, 200 g of potato extract, 20 g of agar and 20 g of dextrose were dissolved in 1000 ml of distilled water in a clean conical flask. The solution was boiled to dissolve the medium completely and sterilized by autoclaving at 15 lbs. pressure (120 °C) for 30 min. After sterilization, 20 ml of media was poured into the sterilized Petri plates. These Petri plates were kept at room temperature for some time. After few minutes the medium got solidified in the plates. Then, it was inoculated with microorganisms using sterile swabs. The stock solutions were prepared by dissolving the compounds in ethanol at 10^{-2} M to find the inhibition zone values. In a characteristic procedure, a well was made on the agar medium inoculated with microorganisms [29]. The well was filled with the test solutions using a micropipette and the plates were incubated at 37°C for 72 h. During this period, the test solution diffused and affected the growth of the inoculated fungi. The inhibition zone was developed and it was noted in mm.

RESULTS AND DISCUSSION

All the mixed ligand complexes are hygroscopic in nature. They are soluble in water, ethanol, methanol, cholorform and insoluble in petroleum ether and hexane. The micro-analytical data for the synthesized complexes show that the metal to primary ligand and co-ligand ratio is 1:1:1. The observed molar conductance of the complexes in EtOH (10^{-3} M) at room temperature is constituent with the non-electrolytic nature of the complexes and in the absence of counter ions in the proposed structure of the metal complexes [30]. Figure 1 shows the structure of ligand and synthesized mixed ligand complexes. The physical properties of the complexes are summarized in Table 1. The analytical data correspond well with the general formula of complexes like [MLX]4H_2O and [MLY]4H_2O.

3.1 *Mass spectroscopy*

The observed molecular ion peak confirms the proposed formulae and is in good agreement with their theoretical molecular weight as calculated from micro-analytical data. The Schiff base ligand [HL] showed a molecular ion peak at m/z 248 which was also supported by the 'nitrogen rule', since the compound possesses two nitrogen atoms. The molecular ion peaks for the [CoLX]4H_2O and [CoLY]4H_2O complexes have observed at m/z 617 and 593 confirms the stoichiometry of metal chelates as [MLX]4H_2O type.

Table 1 Physical characterization, analytical, molar conductance and magnetic susceptibility data of the ligand and the complexes

Compound	Molecular formula	Colour	Yield (%)	Found (Cacld.) (%)				Molar Conductance $\wedge_m$ (ohm^{-1} cm^2 mol^{-1})	μ_{eff} (BM)
				M	C	H	N		
[HL]	$C_{14}H_{20}N_2O_2$	Orange	79	----	67.1 (67.7)	8.9 (8.1)	11.7 (11.3)	----	----
[CoLX]4H_2O	$CoC_{28}H_{38}N_4O_8$	Dark Pink	60	9.8 (9.6)	54.4 (54.5)	6.1 (6.2)	9.1 (9.1)	21.2	4.8
[NiLX]4H_2O	$NiC_{28}H_{38}N_4O_8$	Pale Green	59	9.4 (9.6)	54.2 (54.2)	6.2 (6.2)	9.0 (9.1)	19.6	3.1
[CoLY]4H_2O	$CoC_{26}H_{38}N_4O_8$	Dark Pink	59	9.9 (10.0)	52.5 (52.6)	6.6 (6.4)	9.5 (9.4)	19.4	4.7
[NiLY]4H_2O	$NiC_{26}H_{38}N_4O_8$	Pale Green	57	10.2 (10.0)	52.7 (52.6)	6.3 (6.4)	9.7 (9.4)	21.2	3.3

3.2 *Electronic absorption spectroscopy*

The electronic absorption spectra of the ligand, and its mixed ligand complexes were recorded in ethanol at 300 K. Ligand is showed two intra ligand charge transfer (INCT) transition bands for phenyl ring and the azomethine chromophore (-CH=N). In the metal complexes this bands are shifted to a longer wavelength which is attributed to the donation of lone pair electron of nitrogen atom of the ligand to the metal (N⟶M). The electronic spectrum (Figure 2) of [CoLX]4H_2O complex is showed three d–d bands which are assigned as $^4T_{1g}(F) \longrightarrow {}^4T_{2g}(F)$ ν_1 (10204 cm^{-1}), $^4T_{1g}(F)\longrightarrow {}^4A_{2g}(F)$ ν_2 (16340 cm^{-1}) and $^4T_{1g}(F)\longrightarrow {}^4T_{1g}(P)$ ν_3 (25062 cm^{-1}) d-d transitions respectively, which are strongly favoured for the octahedral geometry [31-37] and also the observed magnetic moment value of Co (II) complex is 4.7-5.2 BM (paramagnetic), which is confirmed the octahedral geometry. Similarly, the spectrum of is showed three d–d bands which are assigned as $^3A_{2g}(F)\longrightarrow {}^3T_{2g}(F)$ ν_1 (10615 cm^{-1}), 8248 cm^{-1}) and $^3A_{2g}(F)\longrightarrow {}^3T_{1g}(P)$ ν_3 (23923 cm^{-1}) d-d transitions respectively, which are ıe octahedral geometry and also the observed magnetic moment value of Ni (II) complex is

2.9-3.4 BM, which is confirmed the octahedral geometry. The d–d transition favours octahedral geometry around the metal ion and the data were summarized in Table 2. The calculated Dq values of Ni (II) and Co (II) complexes are in the range of 608-1062 cm^{-1} which is suggested as a weak field ligand. The values of Racah inter electronic repulsion parameter (B) for the complexes are always less than the corresponding free ion B_0 value. The observed B (complex) values are less B_0 (free ion) which is indicated that the ligand is coordinated to the metal ion and Dq values for the Ni (II) and Co (II) complexes were also calculated from the equation Dq = $[\nu_1/10]$ and $[\nu_2-\nu_1/10]$ respectively. If the value of Nephelauxetic parameter (β) is equal to unity or greater than unity (β > 1), it is indicated the greater ionic character of M-L bond. The observed β values of the complexes were less than unity (β < 1), was suggested the greater covalency of the M-L bond. The observed value of β_0 value of (ν_2/ν_1) ratio is in the range of 1.60 – 1.72 which is considered as an identification of octahedral geometry in the Ni (II) and Co (II) mixed ligand complexes. The LFSE values were calculated from the equations LFSE = 12 Dq for Ni (II) and 6 Dq for Co (II) complexes. The ligand field parameters and magnetic values have been proposed that an octahedral geometry [38].

Table 2 Electronic absorption spectral data of the complexes

Complex	Abs. Region cm^{-1} (λ_{max})	Band assignment	Ligand Field parameter							Suggested Geometry
			Dq cm^{-1}	B cm^{-1}	β cm^{-1}	β_0 (%)	ν_2/ν_1 cm^{-1}	LFSE K Cal	Dq/B	
[HL]	25062 (399) 31746 (315) 39370 (254)	INCT INCT	-	-	-	-	-	-	-	---
[CoLX] $4H_2O$	10204 (980) 16340 (612) 25062 (399)	$^4T_{1g}(F)\rightarrow{}^4T_{2g}(F)\ \nu_1$ $^4T_{1g}(F)\rightarrow{}^4A_{2g}(F)\ \nu_2$ $^4T_{1g}(F)\rightarrow{}^4T_{1g}(P)\ \nu_3$	614	719	0.70	30	1.60	36.8	0.85	Octahedral
[NiLX] $4H_2O$	10615 (942) 18248 (548) 23923 (418)	$^3A_{2g}(F)\rightarrow{}^3T_{2g}(F)\ \nu_1$ $^3A_{2g}(F)\rightarrow{}^3T_{1g}(F)\ \nu_2$ $^3A_{2g}(F)\rightarrow{}^3T_{1g}(P)\ \nu_3$	1062	688	0.71	29	1.72	12.7	1.54	Octahedral
[CoLY] $4H_2O$	10132 (987) 16207 (617) 24390 (410)	$^4T_{1g}(F)\rightarrow{}^4T_{2g}(F)\ \nu_1$ $^4T_{1g}(F)\rightarrow{}^4A_{2g}(F)\ \nu_3$ $^4T_{1g}(F)\rightarrow{}^4T_{1g}(P)\ \nu_3$	608	680	0.66	34	1.60	36.5	0.89	Octahedral
[NiLY] $4H_2O$	10256 (975) 16474 (607) 26316 (380)	$^3A_{2g}(F)\rightarrow{}^3T_{2g}(F)\ \nu_1$ $^3A_{2g}(F)\rightarrow{}^3T_{1g}(F)\ \nu_2$ $^3A_{2g}(F)\rightarrow{}^3T_{1g}(P)\ \nu_3$	1026	801	0.82	18	1.61	12.31	1.28	Octahedral

Where INCT = intra ligand charge transfer band

**Racah inter electronic repulsion parameter (B_0) for free ions = 1030 and 971 cm^{-1} for Co^{2+} and Ni^{2+}.*

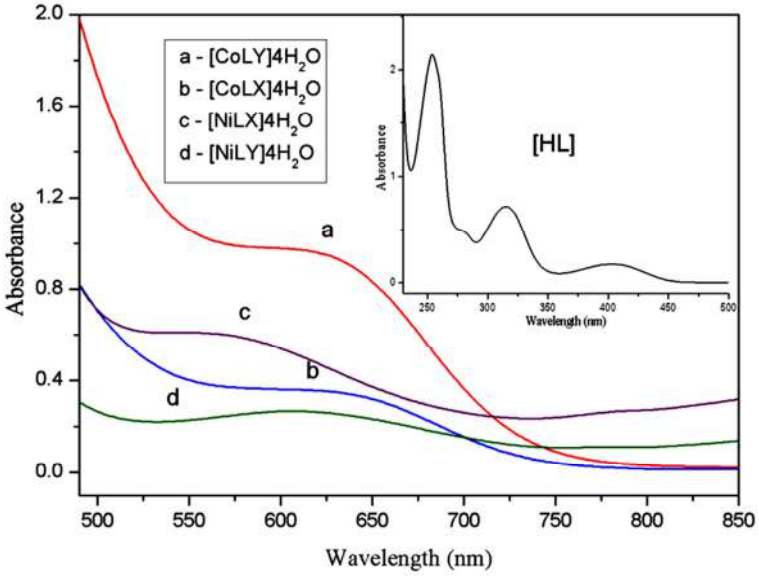

ure 2 Electronic absorption spectra of mixed ligand complexes and ligand peak (inset)

3.3 *IR Spectroscopy*

The IR spectrum of the ligand is showed the characteristic ν(-CH=N) bands in the region 1630 cm^{-1}, which is shifted to lower frequencies in the spectra of all the complexes (1620-1598 cm^{-1}) indicating the involvement of -CH=N nitrogen in coordination to the metal ion [39-40]. The ligand is showed a broad band in the region 3210 cm^{-1}, assignable to phenolic –OH groups, which is absent in the spectra of the all metal complexes suggest confirming the disappearance of phenolic proton and oxygen atom involved in the formation of M-O bond. Morpholine *υ*(C-N-C) band is appeared in the region 1375 cm^{-1}, which is shifted to lower frequencies in the spectra of all the complexes (1355-1338 cm^{-1}) indicating the involvement of C-N-C nitrogen in coordination to the metal ion. The IR spectra are evident that the ligand acts as tridentate chelating agent. In all complexes, carboxylate of the acetate group is strongly absorbed (ν_{asy}) in the range of 1667-1662 cm^{-1} and (ν_{sym}) more weakly at 1404-1399 cm^{-1} (Table 3). It is suggested that they are consisting of unidentate co-ordination site due to the value of differences between asymmetry and symmetry is greater than 200 cm^{-1} ($\Delta\nu_{a-s} \geq 200$ cm^{-1}). The spectra of the metal chelates is also showed new bands in the region 659-617 cm^{-1} and 497-483 cm^{-1}, which are indicated the formation of ν(M-O) and ν(M-N) bonds.

Table 3 IR spectral data of the synthesized compounds

Complex	*υ*(C=N)	*υ*(C-O)	Ali-ν(C-O-C)	Ali-ν(C-N-C)	Ph-OH *υ*(O-H)	*υ* (Acetate)	*υ* (H_20)	Co-ligand (X/Y) *υ*(C=N)	*υ*(M-O)	*υ*(M-N)
[HL]	1630	1200	1146	1375	3210	-	-	-	-	-
[CoLX] $4H_2O$	1620	1223	1143	1338	-	1662(a) 1401(s)	860	1570	653	492
[NiLX] $4H_2O$	1622	1229	1139	1349	-	1665(a) 1404(s)	845	1558	659	483
[CoLY] $4H_2O$	1598	1232	1140	1340	-	1664(a) 1399(s)	855	1569	617	497
[NiLY] $4H_2O$	1616	1229	1134	1355	-	1667(a) 1400(s)	840	1565	657	487

Where a-asymmetry and s-symmetry

3.4 *Redox studies*

Cyclic voltammogram of the cobalt and nickel complexes were recorded in ethanol solution (potential range 1.0 to -1.0 V) show a well-defined redox process (Figure 3 (a) and (b)) corresponding to the formation of Co(II)/Co(I) couple and Ni(II)/Ni(I) couple. The $[CuLX]4H_2O$ and $[NiLX]4H_2O$ complexes display a reversible voltametric cathodic peak at 0.11 and 0.14 V and reversible anodic peak at -0.25 and -0.29 V. The quasi-reversible peak is obtained for the copper complexes of 0.14 and 0.15 V respectively at a scan rate of 100 mVs^{-1}. In addition, the ratio of anodic and cathodic peak current ($Ip_c/Ip_a \approx 1$) is being corresponded to one electron transfer process (Table 4).

Table 4 Cyclic voltammogram data of the mixed ligand complexes (0.001M) in ethanol at 300 K in ethanol containing 0.1M (TBAP). Scan rate 100 mVs^{-1}

Complex	Couple	Ep_c (V)	Ep_a (V)	ΔEp (V)	Ip_a (μA)	Ip_c (μA)	Ip_a/Ip_c
$[CoLX]4H_2O$	Co(II)/Co(I)	0.11	-0.25	0.14	-2.89	2.92	0.99
$[NiLX]4H_2O$	Ni(II)/Ni(I)	0.14	-0.29	0.15	-2.74	2.90	0.95

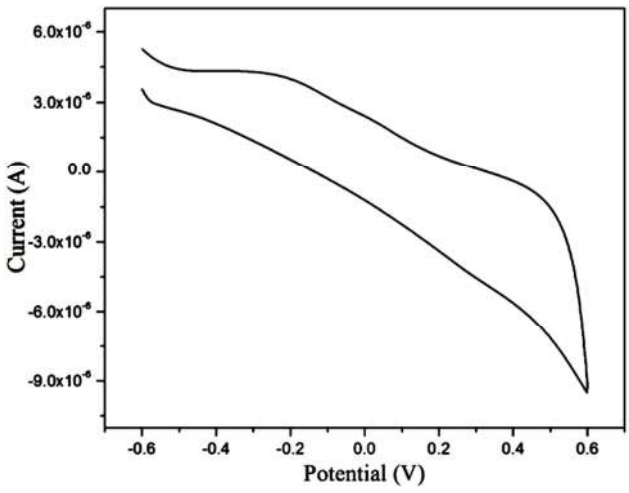

gure 3 (a) The cyclic voltammogram of the $[NiLX]4H_2O$ complex in ethanol at 300 K

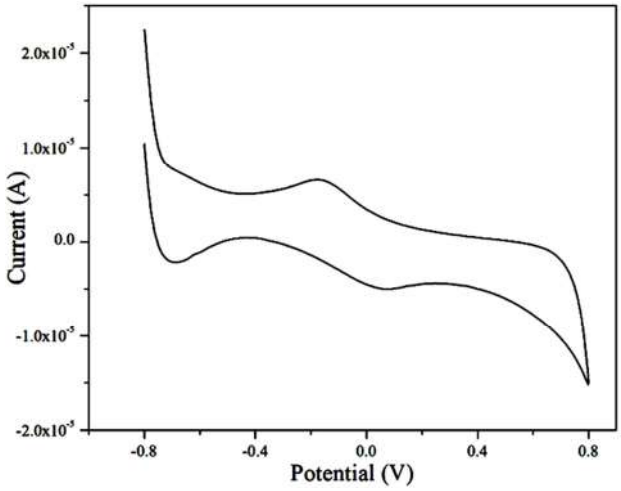

Figure 3 (b) The cyclic voltammogram of the [CoLX]4H$_2$O complex in EtOH at 300 K

3.5 *DNA binding studies*

3.5.1 Electronic Absorption method

Absorption titration is employed to determine the binding mode and binding strength of the complexes with DNA. Transition metal complexes can be bound to DNA via covalent and/or non-covalent interactions (intercalative, electrostatic and groove binding). Complex bind to DNA through intercalation usually results in hypochromism (decrease in absorbance) and bathochromism (red shift), because intercalative mode involves a strong stacking interaction between aromatic chromophore and the base pairs of DNA [41]. Electrostatic interaction of complex with DNA is showed the lower hypochromicity with no bathochromic shift [42]. Complex binds to DNA through covalent binding generally results in hyperchromism resulting from breakage of secondary structure of DNA due to the fact that phosphate group can be provided the suitable anchors for coordination with complexes. The extent of hyperchromism is also revealed the nature of binding affinity. The absorption spectrum of Co(II) and Ni(II) complexes with increasing concentration of HS-DNA is shown in Figure 4 (a), (b), (c) & (d). As the concentration of DNA increases, hypochromism is observed in the charge transfer band of each complex along with the red shift of about 2-5 nm which is suggested to the covalent binding of metal complexes with DNA. The K_b values were calculated from the perturbation observed in charge transfer band of the complexes. The absorption data was analyzed to evaluate the intrinsic binding constant (K_b), which can be determined from a plot of [DNA]/(ε_a-ε_f) versus [DNA] using the following equation [43].

$$\frac{[\mathrm{DNA}]}{(\varepsilon_a - \varepsilon_f)} = \frac{[\mathrm{DNA}]}{(\varepsilon_b - \varepsilon_f)} + \frac{1}{\mathrm{K_b}(\varepsilon_b - \varepsilon_f)}$$

Where [DNA] is the concentration of HS-DNA in base pairs. The apparent absorption coefficients ε_a, ε_f and ε_b correspond to A_{obsd}/[M], the extinction coefficient for the metal(II) complex in fully bound form respectively. K_b is given by the ratio of slope to the intercept. The lower K_b values can be accredited to non–planarity of substituent which might be caused the severe steric constraints near the metal core when the complex approaches the DNA base pairs. The values of K_b in Table 5 clearly show that the [CoLX]4H$_2$O have more DNA-binding activity compared to [CoLY]4H$_2$O, [NiLX]4H$_2$O and [NiLY]4H$_2$O complexes. The calculated intrinsic binding constant (K_b) and free energy change ($\Delta G_b^{\neq}$) of mixed ligand complexes are presented in Table 5. The negative free energy changes observed in all cases indicate that the complexes interact with DNA in a spontaneous manner [44-46].

Table 5 Intrinsic binding constant (K_b) and free energy change ($\Delta G_b^{\neq}$) of mixed ligand complexes

Complex	λ_{max}(nm)		$\Delta\lambda$ (nm)	Chromism (H%)	Binding constant K_b x10^3 (M^{-1})	Type of Chromism & shift	$\Delta G_b^{\neq}$ (kJ M^{-1})
	Free	Bound					
[CoLX]4H$_2$O	394	399	5	84.91	8.04	Hypo & red	-53.73
[NiLX]4H$_2$O	306	309	3	23.13	7.10	Hypo & red	-50.53
[CoLY]4H$_2$O	388	391	3	11.17	4.17	Hypo & red	-36.81
[NiLY]4H$_2$O	306	308	2	41.88	6.79	Hypo & red	-49.38

H% = [(A … A …) / A …] 100%

…t determined from the UV-Vis. absorption spectral titration.

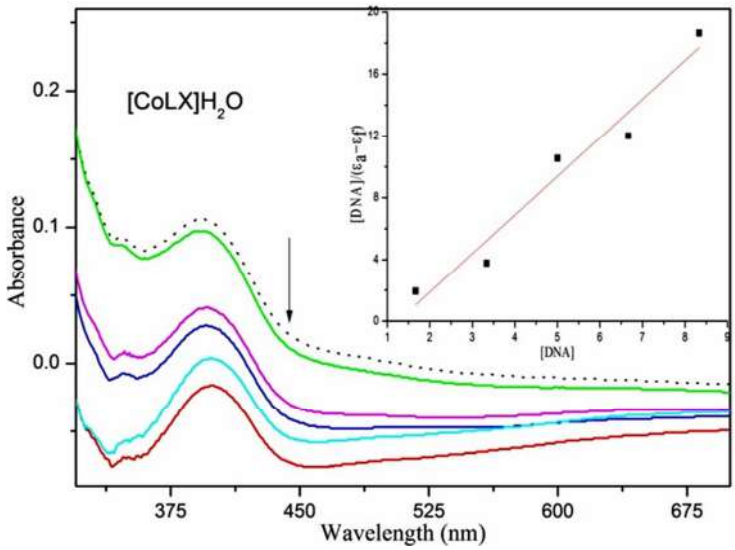

Figure 4 (a) Electronic spectra of [CoLX]4H_2O in Tris–HCl buffer upon addition of HS-DNA. [Complex] = 30 µM, [DNA] = 0–50 µM. Dotted line shows free complex and thick line shows complex upon addition of [DNA]

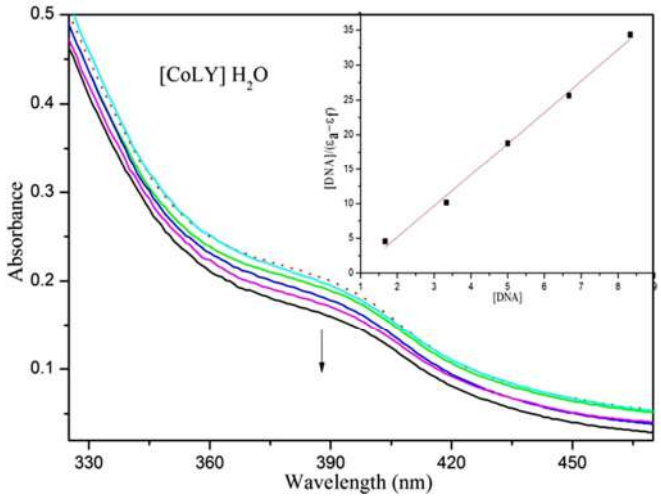

Figure 4 (b) Electronic spectra of [CoLY]4H_2O in Tris–HCl buffer upon addition of HS-DNA. [Complex] = 30 µM, [DNA] = 0–50 µM. Dotted line shows free complex and thick line shows complex upon addition of [DNA]

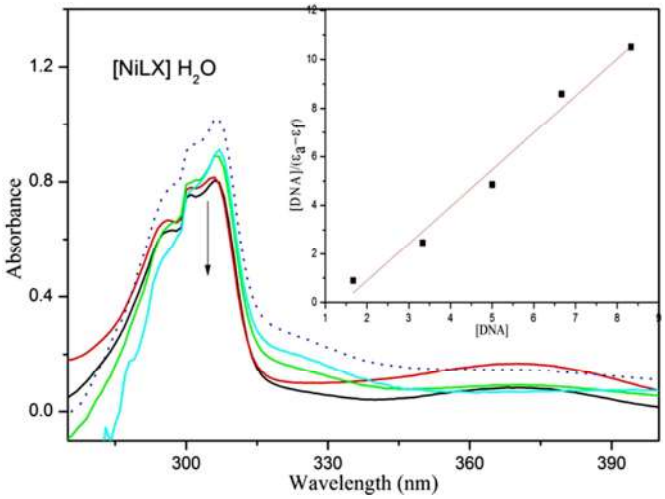

ectra of [NiLX]4H_2O in Tris–HCl buffer upon addition of HS-DNA. [Complex] = 30 µM, [DNA] = 0–50 µM. otted line shows free complex and thick line shows complex upon addition of [DNA]

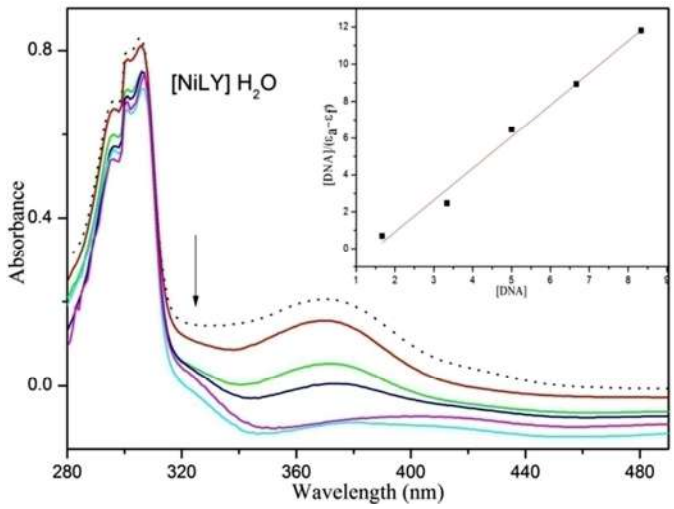

Figure 4 (d) Electronic spectra of [NiLY]4H$_2$O in Tris–HCl buffer upon addition of HS-DNA. [Complex] = 30 µM, [DNA] = 0–50 µM. Dotted line shows free complex and thick line shows complex upon addition of [DNA]

3.5.2 Viscosity titration measurement

As a means for further clarifying the binding of the Co and Ni complexes, viscosity measurements were carried out on HS DNA by varying the concentration of the added complexes. Hydrodynamic measurements which are sensitive to length increase are regarded as the least ambiguous and the most critical tests of binding in solution in the absence of crystallographic structure data [47]. A classical intercalative mode causes a significant increase in separation of base pairs at intercalation sites and hence an increase in overall DNA length. By contrast, complexes that binds exclusively in the DNA grooves by partial and/or non-classical intercalation, under the same conditions, typically cause less pronounced or no charge in DNA solution viscosity [48]. The values of $(\eta/\eta_0)^{1/3}$ were plotted against [complex]/[DNA] (Figure 5). The results reveal that all the complexes exhibit increase in relative viscosity of DNA, which suggest all the complexes bind to DNA by intercalation [49].

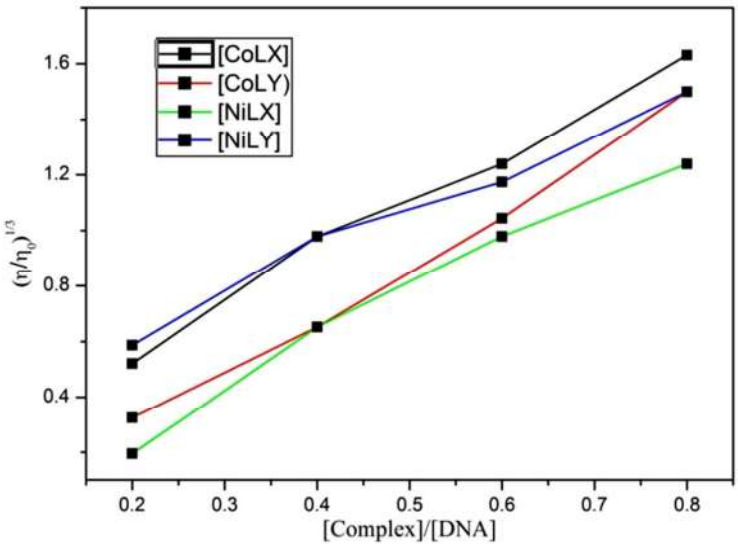

Figure 5 Effect of increasing amounts of complexes on the relative viscosities of HS DNA

3.7 *DNA Cleavage activity*

The CT-DNA cleavage study by gel electrophoresis method was performed with mixed ligand complexes at 37 ˚C. The cleavage properties were studied in a medium of 50 mM Tris-HCl/NaCl buffer (pH = 7.2) in the presence of H_2O_2. Bromophenol blue was used as a photosensitizer. The DNA cleavage efficiency of the complex depends on its different attaching capacity to DNA. The observed elecrophoretic results (Figure 6) conclude that [NiLX]4H$_2$O (lane 4) and [CoLY]4H$_2$O (lane 5) complexes cleave the DNA appreciably as compared to the control DNA while [NiLY]4H$_2$O (lane 6) and ligand (lane 2) fail to include any significant cleavage on DNA time. It is also observed that free radical scavengers inhibited the DNA cleavage which nt of free radical. On the basis, a general radical oxidative mechanism is proposed for DNA

cleavage. It is believed that the DNA cleavage by metal complexes arises as a result of attack of diffusible hydroxyl radical ($OH^{\cdot}$) on DNA through Fenton type mechanism as reported earlier. The hydroxyl free radical is formed a result of reaction between the complex and the oxidising agent, H_2O_2 via Fenton or Haber-Weiss mechanism [50]. According to the Fenton mechanism, the complex acts as a catalyst for hydroxyl radical generation from H_2O_2 [51].

$$M^{II}AB + e^- \rightarrow M^{I}AB$$
$$M^{I}AB + H_2O_2 \rightarrow M^{II}AB + OH^- + OH^{\cdot}$$

The hydroxyl free radical abstracts a hydrogen atom from sugar moiety of DNA to form sugar radical. These sugar radicals then undergo hydrolytic cleavage at sugar-phosphate backbone to release specific residues depending on the position from which the hydrogen atom is being removed. Further, it was reported that when DNA is run through agarose gel during elecrophoresis, the fastest migration was observed for the open cicular form. The considerable activity fo DNA cleavage found with mixed ligand complexes containing Co(II) and Ni(II) compared with that of the control may also be partially due to the ability of these complexes to convert open circular DNA into its linear form.

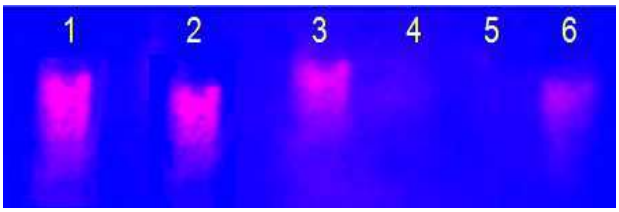

Figure 6 The nuclease activity of present complexes, investigated on CT DNA by agarose gel electrophoresis in the presence of oxidant (H_2O_2)

Lanes right to left → Lane 1, CT DNA alone; Lane 2, DNA + [HL]; Lane 3, DNA + [CoLX]$4H_2O$ +H_2O_2; Lane 4, DNA + [NiLX]$4H_2O$ +H_2O_2; Lane 5, DNA + [CoLY]$4H_2O$ +H_2O_2; Lane 6, DNA + [NiLY]$4H_2O$ +H_2O_2.

3.8 DPPH Radical Scavenging studies

Antioxidant activities of mixed ligand complexes were ascertained by DPPH free radical scavenging assay. This method depends on the ability of the antioxidant to donate its electron to DPPH which in turn depends on the ability of 1,1-diphenyl-2-picryl-hydrazyl (DPPH) to change color from purple to yellow. From the results, it is shown that the mixed ligand complexes have higher activities than ligand (Table 6) which may due to the presence of the M(II) ion moiety in the complex [52]. In additon, the antioxidant activities of these complexes are given in Figure 7 and 8.

$$\text{Scavenging effects (\%)} = \left[\frac{(A_{control} - A_{sample})}{A_{control}}\right] \text{x } 100$$

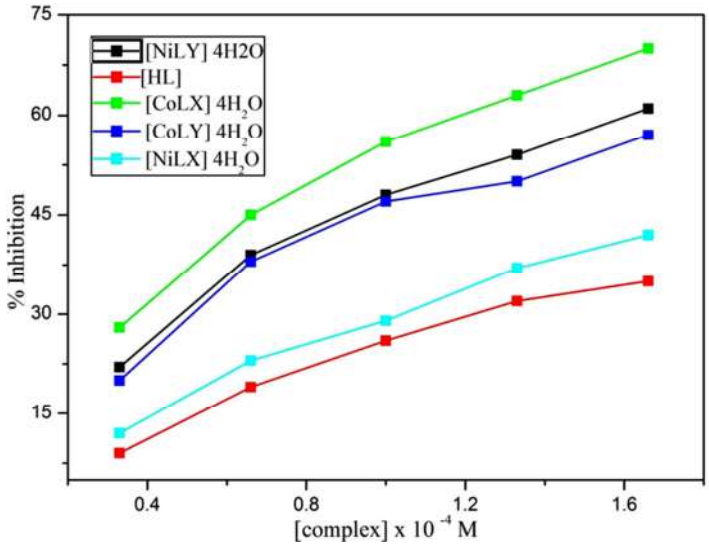

ronic absorption spectrum of DPPH free radical scavenging activityfor mixed ligand complexes

Table 6 *In vitro* antioxidant of activities of ligand and its mixed ligand complexes at different concentraion by DPPH free radical scavenging assay method

Complex	Scavenging activity (%)				
	10 µM	20 µM	30 µM	40 µM	50 µM
[HL]	9	19	26	32	35
[CoLX]4H_2O	28	45	59	68	78
[CoLY]4H_2O	20	38	47	50	57
[NiLX]4H_2O	12	23	29	37	42
[NiLY]4H_2O	22	39	48	54	61

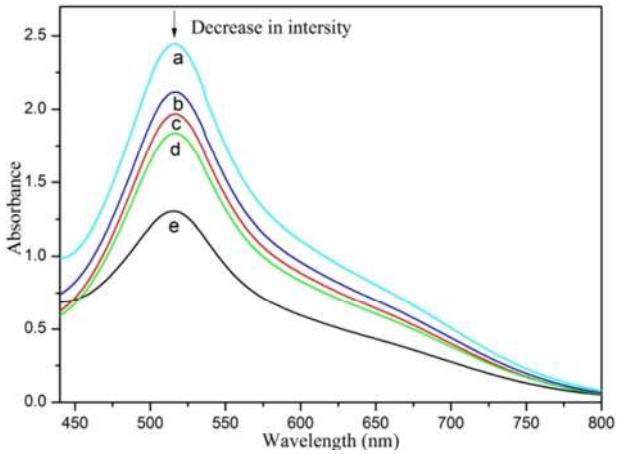

Figure 8 Electronic absorption spectra of a= [HL], b= [NiLX]4H_2O, c= [CoLY]4H_2O, d= [NiLY]4H_2O and e= [CoLX]4H_2O by DPPH free radical scavenging method at a concentration of 100 µM

3.9 *Antimicrobial activity*

The in vitro antimicrobial activity of the investigated compounds were tested against the bacteria *Salmonella typhi, Escherichia coli, Bacillus subtilis, Staphylococcus aureus, Streptococcus faecalis, Salmonella typhimurim, Klebsiella pneumonia and fungi Shigella boydii, Candida albicans, Aspergillus niger* by well diffusion method. The sensitivity of microorganisms to antimicrobial complex was measured as inhibition zone (mm) are summarized in Table 7. A comparative study of the ligand and its mixed ligand complexes (inhibition zone values) indicates that complexes exhibit higher antimicrobial activity than the free ligand is given in Figure 9. From the inhibition zone values, it was found that the mixed ligand complexes were more potent than ligand. Further studies are required to explore these complexes as drugs. Such increased activity of the complexes can be explained on the basis of Overtone's concept [53] and Tweedy's Chelation theory [54]. According to Overtone's concept of cell permeability, the lipid membrane that surrounds the cell favors the passage of only the lipid-soluble materials due to which liposolubility is an important factor, which controls the antifungal activity. On chelation, the polarity of the metal ion will be reduced to a greater extent due to the overlap of the ligand orbital and partial sharing of the positive charge of the metal ion with donor groups. Furthermore, the mode of action of the compound may be involved the formation of a hydrogen bond through the azomethine group with the active centre of cell constituents, resulting in interference with the normal cell process.

Table 7 Antibacterial activity of the Schiff base ligand and its mixed metal complexes

Complex	Gram positive bacteria			Gram negative bacteria				Fungi	
	B	C	D	*E*	F	G	H	I	J
[HL]	7.7	8.4	10.2	11.5	7.2	15.7	10.6	11.3	10.2
[CoL]4H_2O	18.6	16.6	17.4	21.4	12.3	18.8	19.3	15.8	17.4
[NiL]4H_2O	20.3	22.2	18.6	22.9	18.6	20.5	20.3	19.7	18.6
[CoLX]4H_2O	15.7	21.4	20.3	17.3	15.1	22.7	20.2	19.2	24.3
[NiLX]4H_2O	19.3	20.2	20.4	21.3	18.5	20.6	19.8	21.3	22.4
[CoLY]4H_2O	17.7	19.4	20.4	17.5	19.1	20.6	20.2	19.3	22.5
[NiLY]4H_2O	20.3	20.2	20.7	21.5	18.5	22.6	18.8	20.3	21.4
Streptomycin	28.7	27.2	28.7	26.1	27.4	25.5	27.3	28.7	28.6

s, D = S. faecalis, E = E. coli, F = S. typhimurim, G = K. pneumonia, H = S. boydii, I = C. albican and J = A. niger

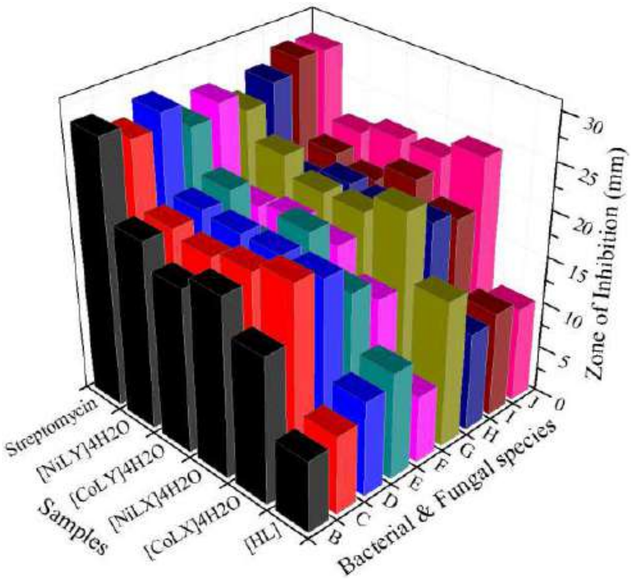

Figure 9 Antibacterial and antifungal activities of complexes at a concentration of 10^{-2} M determined by well diffusion method

CONCLUSION

A new tridentate schiff base ligand N_2 type was derived from the condensation of 3-morpholinopropyl amine and salicyladehyde. Four mixed ligand complexes containing Co(II) and Ni(II) and ligand were synthesized and characterized by spectral and analytical techniques. From the study it has been concluded that the ligand bind to the M(II) ions through two N (imine & morpholine ring) and phenolic C-O atoms. The data is showed that the mixed ligand complexes have the composition of type [MLX]4H_2O and [MLY]4H_2O. The UV-Vis spectral data suggest that these complexes exhibit octahedral geometry. They have showed low electrical conductance which reveals that the chelates are non-electrolytes. Their magnetic susceptibility values are provided evidence for the monomeric nature. The measurement of DNA binding affinity of mixed ligand complexes towards HS-DNA using absorption spectral analysis is suggested the highest K_b value for complex [CoLX]4H_2O. The binding of M(II) complexes with DNA has been confirmed from a red shift along with a decrease in intensity of the charge transfer band (hypochromicity).The spontaneous nature of binding between complex and DNA was inferred from the negative free energy value calculated from K_b value. The results from absorption spectral and viscosity studies revealed that all the complexes can bind to DNA by intercalation through the covalent binding mode of interaction. Further, the interaction of the complexes with CT-DNA was investigated by gel electrophoresis. The presence of a smear in the gel diagram indicates the presence of radical cleavage. The DNA cleavage activity of [CoLX]4H_2O and [NiLY]4H_2O complexes with CT-DNA demonstrated remarkable activity, while [CoLY]4H_2O, [NiLX]4H_2O complexes and ligand (HL) showed no activity under aerobic condition and in the presence of H_2O_2. The *in vitro* biological and antioxidant studies have shown that the mixed ligand complexes have higher potent activities than the free ligand. The higher activity of complexes exhibited against bacterial and fungal strains have been interpreted on the basis of the presence of both electron withdrawing and electron donating moieties in the chelate ring.

Acknowledgements
The authors express their sincere and heartfelt thanks to the Department of Science and Technology (DST) – Science and Engineering Research Board (SERB-Ref. SR/FT/CS-117/2011 dated 29.06.2012), Government of India, New Delhi for their funding assistance, the Managing Board, Principal and Chemistry Research Centre of Mohamed Sathak Engineering College, Kilakarai. The authors thank the Managing Board and Principal of Sri Vidya College of Engineering & Technology, Virudhunagar and V.O.C College of Arts & Science, Tuticorin for providing all the research and instrumental facilities. The authors also thank the SAIF, IIT Bombay, STIC CUSAT, Cochin.

REFERENCES

[1] K Siddappa; SB Mane; D Manikprabhu. *Spectrochim. Acta* A, **2014**, 130, 634.
[2] ML Sundararajan; T Jeyakumar; J Anandakumaran;BK Selvan. *Spectrochim. Acta* A, **2014**, 131, 82.
[3] ... Abu Al-Nasr; FH Noureldeen. *Spectrochim. Acta* A, **2014,** 132, 417.
... vanan; A Ramesh. *Eur. J. Med. Chem.* **2001,** 36, 615-625.
... r. *Spectrochim. Acta* A, **2008**, 69, 1.

[6] K Dhahagani; SM Kumar; G Chakkaravarthi; K Anitha; J Rajesh; A Ramu; G Rajagopal. *Spectrochim. Acta* A **2014**, 117, 87.
[7] P Majumdar; AK Ghosh; LR Falvello; SM Peng; Goswami. *Inorg. Chem.* **1998**, 37, 1651.
[8] MG Verma; VR Sharma; AK Saxena; TN Bhalla; JN Sinha; KP Bhargava et al., *Pharmacol. Res. Commun.* 16, 9.
[9] S Chandra; LK Gupta; S Agrawal. *Trans. Met. Chem.* **2007**, 32, 558.
[10] Kathrin Wahlar; Anja Ludewig; Patrick Szabo; Klaus Harms; Eric Meggers. *Eur. J. Inorg. Chem.* **2014**, 5, 807.
[11] SK Padhi; R Sahu; V Manivannan. *Polyhedron*, **2008**, 27, 805.
[12] Y Liu; N Wang; W Mei; F Chen; H Li-Xin; L Jian; R Wang. *Trans. Met. Chem.* **2007**, 32, 332.
[13] BO West. *Chemistry of Coordination Compounds of Schiff bases in New pathways in Inorganic chemistry*, Eds. Ebsworth EAV, Sharpe AG, Cambridge University Press, **1968**, *p.* 303.
[14] P Mukherjee; MGB Drew; V Tangoulis; M Estrader; C Diaz; A Ghosh. *Polyhedron*, **2009**, 28, 2989.
[15] PJ Steel. *Coord. Chem. Rev.* **1990**, 106, 227.
[16] R Vijayalakshmi; M Kanthimathi; V Subramanian; BU Nair. *Biochem. Biophys. Acta*, **2000**, 1475, 157.
[17] KS Ksaprzak. *Chem. Res. Toxicol.* **1991**, 4, 604.
[18] A Kamal; R Ramu; V Tekumalla; GBR Khanna; MS Barkume; AS Juvekarb; SM Zingde. *Bioorg. Med. Chem.* **2007**, 15, 6868.
[19] SA Bourne; J Lu; A Mondal; B Moulton; MJ Zaworotko. *Angrew. Chem. Int.* **2001**, Ed. 40, 2111.
[20] C Sissi; F Mancin; M Gatos; M Palumbo; P Tecilla; U Tonellato. *Inorg. Chem.***1999**, 44, 2310.
[21] ST Frey; HHJ Sun; NN Murthy; KD Karlin. *Inorg. Chim. Acta*, **1996**, 242, 329.
[22] DD Perrin; WLF Armarego; DR Perrin; *Purification of Laboratory Chemicals, Pergamo Press, Oxford*, **1980**.
[23] J Marmur. *J. Mol. Biol.***1961**, 3, 208.
[24] ME Reichmann; SA Rice; CA Thomas; P Doty. *J. Am. Chem. Soc.* **1954**, 76, 3047.
[25] A Wolfe; GH Shimer; T Meehan. *Biochemistry*, **1987**, 26, 6392.
[26] S Satyanarayana; JC Daborusak; JB Chaires. *Biochemistry*, **1993**, 32, 2573–2584.
[27] MS Blois. *Nature*, **1958**, 4617 (181), 1199-1200.
[28] MJ Pelczar; ECS Chan; NR Krieg. *Microbiology*, 5th Edn. **1998**, New York.
[29] N Kannan. *Laboratory Manual in Microbiology 1st Edn. Paramount Publication*, **1996**, Palani.
[30] WJ Geary. *Coord. Chem. Rev.***1971**, 7, 81-122.
[31] BJ Hathaway; DE Billing; P Nicholls; IM Procter. *J. Chem. Soc.* (A), **1969**, 319.
[32] BJ Hathaway; IM Procter; RC Slade; AAG Tomlinson. *J. Chem. Soc.* (A), **1969**, 2219.
[33] H Okawa; DH Busch. *Inorg. Chem.* **1979**, 18**,** 1555.
[34] ABP Lever; E Mantovani. *Inorg. Chem.* **1971**, 10, 817.
[35] M Calligaris; G Nardin; L Randaccio; A Ripaamonti. *J. Chem. Soc.* (A), **1970**, 1069.
[36] Y Nishida; S Kida. *Bull Chem. Soc. Jpn.* **1978**, 51, 143.
[37] AL Crumbliss; F Basolo. *J. Am. Chem. Soc.* **1970**, 92, 55.
[38] ABP Lever. *Inorganic electronic spectroscopy*, 2nd edition, **1968**, New York.
[39] JL Lamboy; A Pasquale; AL Rheingold; E Meléndez. *Inorg. Chim. Acta*, **2007**, 360, 2115.
[40] AG de A Fernandes; PI de S Maia; J de Souza; SS Lemos; AA Batista; U Abram; J Ellena; EE Castellano; VM Deflon. *Polyhedron*, **2008**, 27, 2983.
[41] Nahid Shahabadi; Soheila Kashanian; Mehdi Purfoulad. *Spectrochim. Acta. Part A*, **2009**, 72, 757.
[42] R Indumathy; M Kanthimathi; T Weyhermuller; BU Nair. *Polyhedron*, **2008**, 27, 3443.
[43] CS Allardyce; PJ Dyson; DJ Ellis; SL Heath. *Chem. Commun.* **2001**, 1396.
[44] J Dharmaraja; T Esakkidurai; P Subbaraj; Sutha Shobana. *Spectrochim. Acta*, **2013**, 114A, 607-621.
[45] Shobana; P Subramaniam; J Dharmaraja; S Arvindnarayan. *Spectrochim. Acta*, **2014**, 126A, 242-253.
[46] S Zang; J Zhou. *J. Coord. Chem.* **2008**, 61(15), 2488-2498.
[47] BC Beguley; M LeBret. *Biochemistry*, **1984**, 23, 937.
[48] TM Kelly; AB Tossi; DJ McConnell; TC Strekas. *Nucleic acids Res.* **1985**, 13, 6017.
[49] F Liu; KA Meadows; DR McMillan. *J. Am. Chem. Soc.* **1993**, 115, 6699.
[50] A Charles; III Detmer; V Filomena; Pamatong, R Jaffery, Bocarcly. *Inorg. Chem.* **1996**, 35, 6292-6298.
[51] TD Tullus. (Ed.), *Metal-DNA Chemistry, ACS Symposium Series 402, American Chemical Society*, Washington, DC, **1989**.
[52] MS Blois. *Nature*, **1958**, 181, 4617, 1199-1200.
[53] Y Ding; XX Hu; XL Sun; ZL Zuo. *J. Natural Science*, **2010**, 15, 165.
[54] N Dharamaraj; P Viswanathamurthi; K Natarajan. *Trans. Met. Chem.* **2001**, 26, 105.

Available online www.jocpr.com

Journal of Chemical and Pharmaceutical Research, 2015, 7(10S):15-22

Research Article

ISSN : 0975-7384
CODEN(USA) : JCPRC5

Novel schiff base metal complexes from morpholine derivatives as potent antioxidant and DNA interacting agents

Jeyaraj Dhaveethu Raja[1]*, Subbiah Jeyaveeramadhavi[2,4], Chinnapiyan Vedhi[3], Murugesan Sankarganesh[5] and Manokaran Vadivel[1]

[1]Chemistry Research Centre, Mohamed Sathak Engineering College, Kilakarai, Tamilnadu, India
[2]Department of Chemistry, Sri Vidya College of Engineering & Technology, Virudhunagar, Tamilnadu, India
[3]PG & Research Department of Chemistry, V.O. Chidambaram College, Thoothukudi, Tamilnadu, India
[4]Manonmaniam Sundaranar University, Tirunelveli, Tamilnadu, India
[5]Department of Chemistry, Sethu Institute of Technology, Pulloor, Kariapatti, Virudhunagar (Dist), Tamil Nadu, India

---

ABSTRACT

*We report the synthesis of a series of mixed ligand transition metal complexes from novel Schiff base (**HL**) of morpholine derivative, 2,2'-bipyridine and acetate salts of Cu(II), Zn(II), Ni(II) and Co(II). The ligand and its metal were characterized by molar conductance, elemental analysis, UV-Vis., FTIR, ^{1}H NMR, ESR and mass spectrometric techniques. The spectral data revealed that the complexes have [ML(bpy)] type composition and square planar geometry. The redox behaviour of copper complexes was studied by cyclic voltammetry. Antimicrobial and antifungal screening tests gave good results in the presence of metal ion in the ligand system. The nuclease activity of the above metal complexes shows that the complexes cleave DNA through redox chemistry. Further the interaction of complexes with HS-DNA by absorption and viscometric measurements suggested that the complexes bind via intercalation mode.*

Key words: Schiff base, Nuclease activity, Antimicrobial activity, Square planar geometry

---

INTRODUCTION

In the past few decades, considerable attention has been paid to the chemistry of the complexes of the Schiff bases with transition metal ions because of their stability, biological activity and potential applications in many fields [1]. Morpholine derivative plays an important role in the treatment of several diseases. Morpholine derivatives were reported to posses anti inflammatory, analgesic, local anesthetic, anti HIV, anti cancer, appetite suppressant, anti depressant, antimicrobial activity [2-5] etc. So we have chosen, 4-(2-aminoethyl)morpholine as one of the reagent to synthesis Schiff base ligand.

Many drugs possess modified pharmacological and toxicological properties when administered in the form of metallic complexes. Transition metal complexes those are suitable for binding and cleaving double-stranded DNA are of considerable current interest due to their various applications in nucleic acid chemistry like foot printing and sequence-specific binding agents, for modeling the restriction enzymes in genomic research, and as structural probes for therapeutic applications in cancer treatment [6]. This inspires synthetic chemists to search for new metal complexes for bioactive compounds have attracted the researchers. Hence this review concentrates on the synthesis ities of Schiff base and its mixed ligand metal complexes derived from oline and 2-hydroxy-5-nitro benzaldehyde.

EXPERIMENTAL SECTION

4-(2-aminoethyl) morpholine, 2-hydroxy-5-nitrobenzaldehyde and various metal salts were Merck products and used as received. Microanalytical data of the compounds were recorded at STIC, SUSAT, Cochin. The molar conductance of the complexes was measured using a Systronic conductivity bridge. The UV-Vis. Spectra were recorded on a Shimadzu UV-1800 spectrometer. The IR spectra were recorded on Perkin Elmer 783 spectrophotometer in 4000-400 cm^{-1} range using KBr pellet. The ^1H NMR spectra (300MHz) of the ligand and its zinc complexes were recorded on a Bruker Advance DRX 300 FT-NMR spectrometer using $CDCl_3$ with trimethylsilane as internal standard. The ESI mass spectra were recorded at SAIF, IIT, Mumbai. The X-band ESR spectra were recorded at 300K and 77K at IIT Bombay, Mumbai using TCNE (tetracyanoethylene) as the g-marker. Cyclic voltammetric measurements were performed using a glassy carbon working electrode (3mm dia), Pt wire auxillary electrode and Ag/AgCl reference electrode. Solutions of calf thymus DNA (CT-DNA) in 50mM NaCl/50mM tris-HCl (pH 7.2) gave a ratio of UV absorbance at 260 and 280 nm, A260/A280 of Ca 1.8 – 1.9, indicating that the DNA was sufficiently free of protein contamination. The DNA concentration was determined by the UV absorbance at 260 nm after 1:100 dilutions. The molar absorption coefficient was taken as $6600M^{-1}cm^{-1}$. Stock solutions were kept at 4^oC and used after not more than 4 days. Doubly distilled water was used to prepare the buffer. Viscometric experiments were carried out using an Oswald-type viscometer of 2mL capacity.

Synthesis of Schiff base

An ethanolic solution of 4-(2-aminoethyl morpholine (1.3mL ,10mM) was refluxed with an ethanolic solution of 2-hydroxy-5-nitrobenzaldehyde (1.67g, 10mM) for 12h. The resultant solution was evaporated until the mixture was almost dry. The product obtained was washed and recrystallized in ethanol and dried in *vacuo*. Anal. Calcd for $\mathbf{C_{13}H_{17}O_4N_3}$ (%): C, 55.9; H, 6.1; N, 15.1. Found (%): C, 55.7; H, 5.9; N, 15.0. Yield: 74%. FT-IR (KBr disc): 3300-3550 (-OH), 1649 (-HC=N), 1319 ($-NO_2$), 1438 (C-C), 2960 (C-H) cm^{-1}. ^1H NMR ($CDCl_3$): phenyl multiplet at 7.1-7.5 δ (m); (-N=CH-) at 8.4 δ (s); ($-O-CH_2$) at 3.5 δ (t); ($-N-CH_2$) in morpholine ring at 2.5 δ (t); ($=N-CH_2$) at 3.7 δ (t); ($-CH_2-N-$)in ethylenic moiety at 2.8 δ (t) and –OH at 13.7 δ. λmax in EtOH, 38,759 and 28818 cm^{-1} (258 and 347nm), m/z, 279. The outline of the synthesis of ligand is given in figure 1.

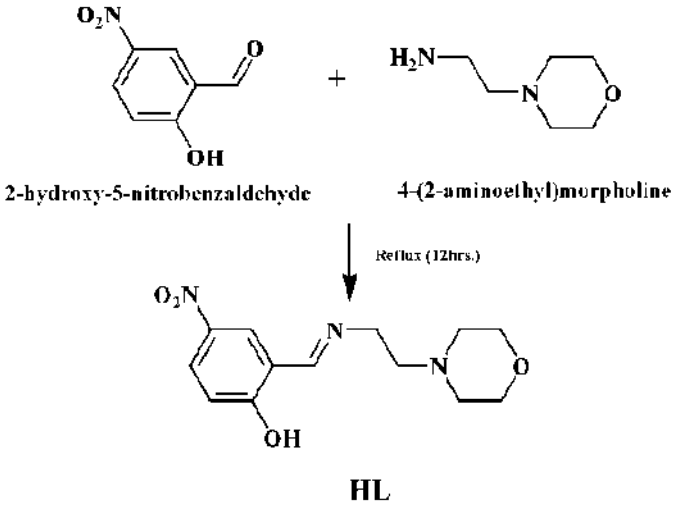

Figure 1. The outline of synthesis of ligand (HL)

Synthesis of metal complexes of [ML(bpy)] type

A solution of Schiff base ligand (0.279g, 1 mM) in ethanol (20 mL) was added to a solution of metal acetate (1 mM) in ethanol (20 mL) and the mixture was refluxed for *ca* 4 h. An ethanolic solution of 2,2'-bipyridine (Y) (0.156g, 1 mM) was added to the reaction mixture. (For the synthesis of the nickel complex, an ethanolic solution of 2,2'-bipyridine was added to the ethanolic solution of ligand at first and the mixture was refluxed and then an ethanolic solution of nickel acetate was added to the reaction mixture.) The mixture was refluxed for *ca* 3 h. The resulting solution then concentrated to one third and kept at room temperature. The solid complex so formed was washed thoroughly with ethanol and dried in *vacuo*.

$_4\mathbf{O_4N_5Cu}$ (%): C, 55.4; H, 4.8; N, 14.1, Cu, 12.8. Found (%): C, 55.2; H, 4.7; N, 14.0, FT-IR (KBr disc): 1624 (-HC=N), 1314 ($-NO_2$), 1436 (C-C), 2957 (C-H), 440 (M-N), 480 ıho $cm^2\ mol^{-1}$), 14. λmax in DMSO, 35,461, 24,272 and 15,314cm^{-1} (282, 412 and 653nm).

Anal. Calcd for **$C_{23}H_{24}O_4N_5Zn$** (%): C, 55.2; H, 4.8; N, 14.0, Zn, 13.1. Found (%): C, 55.0; H, 4.5; N, 13.8, Zn, 13.0. Yield: 59%. FT-IR (KBr disc): 1631 (-HC=N), 1315 (-NO_2), 1435 (C-C), 2954 (C-H), 401 (M-N), 475 (M-O) cm^{-1}. ^1H NMR ($CDCl_3$): phenyl multiplet at 7.1-8.6 δ (m); (-HC=N-) at 8.6 δ (s); (-O-CH_2) at 3.5 δ (t); (-N-CH_2) in morpholine ring at 2.5 δ (t); (=N-CH_2) at 3.7 δ (t); (-CH_2-N-) in ethylenic moiety at 2.8 δ (t) and (CH-N) in bipyridine moiety 9.3 δ (s). $\Lambda_M 10^{-3}$ (mho cm^2 mol^{-1}), 16. m/z, 501.

Anal. Calcd for **$C_{23}H_{24}O_4N_5Ni$** (%): C, 56.0; H, 4.9; N, 14.2, Ni, 11.9. Found (%): C, 55.8; H, 4.7; N, 14.0, Ni, 11.7. Yield: 63%. FT-IR (KBr disc): 1600 (-HC=N), 1364 (-NO_2), 1436 (C-C), 2952 (C-H), 410 (M-N), 507 (M-O) cm^{-1}. $\Lambda_M 10^{-3}$ (mhocm^{2}mol^{-1}), 17. λmax in EtOH, 40,161, 21,598 and 13,175cm^{-1} (249, 463 and 759nm). m/z, 493.

Anal. Calcd for **$C_{23}H_{24}O_4N_5Co$** (%): C, 55.9; H, 4.9; N, 14.2, Co, 11.9. Found (%): C, 55.6; H, 4.8; N, 14.1, Co, 11.6. Yield: 69%. FT-IR (KBr disc): 1641 (-HC=N), 1316 (-NO_2), 1437 (C-C), 2954 (C-H), 411 (M-N), 502 (M-O) cm^{-1}. $\Lambda_M 10^{-3}$ (mhocm^{2}mol^{-1}), 18. λmax in EtOH, 33,003 and 15,082 cm^{-1} (303 and 663nm), m/z, 493.

Antibacterial activity

The *in vitro* biological screening effects of the investigated compounds were tested against four gram positive bacteria, *Staphylococcus aureus, Streptococcus pneumoniae, Staphylococcus pneumoniae, Bascillus subtilis* and four gram negative bacteria, *Shigella flexneri, Salmonella typhi, Klebsiella pneumoniae, Haemophilus influenzae* by the well diffusion method [7] using agar nutrient as the medium and Sparfloxacin as the standard. The stock solution (10^{-2}M) was prepared by dissolving the compounds in DMSO and the solutions were serially diluted. In a typical procedure, a well was made on the agar medium inoculated with microorganisms. The well was filled with the test solution using a micropipette and the plate was incubated for 24h at 35^0C. During this period, the test solution diffused and the growth of the inoculated microorganisms was affected. After 24 h of incubation at 35^oC the diameter of the inhibition zone was measured.

DNA Cleavage activity

The gel electrophoresis experiments were performed by incubation at 35^0c for 2 h as follows: CT DNA 30µM, 50µM each complex and 50µM H_2O_2 in 50mM tris-HCl buffer (pH 7.2) were electrophoresized for 2 h at 50V on 1% agarose gel using tris-acetic acid-EDTA buffer pH=8.3. After electrophoresis, the gel was stained using 1µg/cm3 EB (Ethidiumbromide) and photographed under UV light.

DNA Binding studies

Absorption titration

Binding of DNA via intercalation mode usually results in hypochromism and bathochromism [8, 9] because intercalation mode involves a strong stacking interaction between an aromatic chromophore and the DNA base pair [10] with a selection of an appropriate absorbance peak by performing spectrophotometric wavelength scans of complexes. The DNA binding experiments were performed in Tris-HCl buffer (50mM Tris-HCl, pH 7.5) using DMSO solution of the complex. Absorption titrations were performed by keeping the concentration of the complexes constant (10^{-5}M) and by varying [HS-DNA] from 0 to 400µM. The intrinsic binding constant, K_b was determined by making it a subject in following equation [11]

$[DNA] / (\varepsilon_a-\varepsilon_f) = [DNA] / (\varepsilon_b-\varepsilon_f) + 1/ K_b (\varepsilon_b-\varepsilon_f)$

where [DNA] is the concentration of DNA in base pairs, ε_a the apparent extinction coefficient is obtained by calculating A_{obs} / [Complex], ε_f corresponds to the extinction coefficient of the complex in its free form and ε_b refers to the extinction coefficient of the complex in the fully bound form when each set of data filled to the above equation, gave a straight line with a slope of $1/(\varepsilon_b-\varepsilon_f)$ and y-intercept of $1/ K_b(\varepsilon_b-\varepsilon_f)$. The K_b value was determined from the ratio of the slope to intercept.

2.6.2. Viscosity measurements

Viscosity experiments were carried out on an Ostwald viscometer, immersed in a thermostated water-bath maintained at 30.0^0C±0.1^0C. Flow time was measured with a digital stopwatch three times for the sample and an average flow time was calculated. Data are presented as $(\eta/\eta^o)^{1/3}$ versus [Complex]/[DNA], where η is the viscosity of DNA solution in the presence of complex and η^o is the viscosity of DNA solution in the absence of complex. Viscosity values were calculated after correcting the flow time of buffer alone (t_0), $\eta = (t-t_0)/t_0$ [12].

2.7. Antioxidant activity

The free radical scavenging activities of the complex were measured by the 1,1-diphenyl-2-picrylhydrazil ($DPPH^·$) ution of the $DPPH^·$ radical in DMSO was prepared and 150µL of this solution was added to ıe complex in DMSO at different concentrations (0.33, 0.67, 1.00, 1.33, 1.67 X 10^{-4}M). The gorously and allowed to stand at room temperature for 20 min. Then the absorbance at

524nm was measured by a spectrometer. Lowering of the absorbance of the reaction mixture indicated the higher of the free radical scavenging activity. The capacity to scavenge the DPPH radical was calculated using the following equation:

DPPH· Scavenging effect (%) = $[\frac{Ao-A1}{Ao}]\ X100$

Where, A_0 is the absorbance of the control solution and $A_1$is the absorbance in the presence of sample solutions or standards for positive control.

RESULTS AND DISCUSSION

The Schiff base and its mixed ligand complexes of Cu(II), Zn(II), Ni(II) and Co(II) have been synthesized and characterized by usual spectral and analytical studies. Physical characterization, microanalytical and molar conductance data of the synthesized compounds are given in section 2. The analytical data of the complexes correspond well with the general formula [ML(bpy)]. The low conductance of the chelates supports their non electrolytic nature.

Mass spectra

The ESI-MS spectrum of the ligand shows the molecular ion peak at *m/z* 279 corresponding to $C_{13}H_{17}O_4N_3$. The mass spectrum of the copper complex shows a molecular ion peak at m/z 499 which confirms the stoichiometry of metal chelates as [ML(bpy)]. The mass spectra of the other complexes support the above stoichiometry. The stoichiometry is further supported by the micro analytical data of the complexes.

IR spectra

The preliminary identification of the macrocyclic complexes was done from their IR spectra. The free ligand gave broad band in the region of 3300-3550 cm^{-1} indicating the presence of –OH group. This band disappeared on complexation due to involvement of –OH group on chelation [13]. The IR spectrum of the ligand shows characteristic –HC=N band at 1649 cm^{-1}[14], which is shifted to lower frequencies in all of the complexes indicating the coordination of –HC=N nitrogen to metal ion [14]. Hence from the IR spectra it is evident that ligand acts as a bidentate chelating agent, bonded to metal via azomethine nitrogen and phenolic oxygen atom of lignad. In all of the metal complexes, new bands seen in the region 460-510 cm^{-1} and 405-460 cm^{-1} are probably due to the formation of M-N bond and M-O bond respectively [15].

^{1}H NMR spectra

The ^{1}H NMR spectra of ligand and zinc complex were recorded in CDCl3. Ligand shows phenyl multiplet at 7.1-7.5 δ (m); (-N=CH-) at 8.4 δ (s); (-O-CH_2) at 3.5 δ (t); (-N-CH_2) in morpholine ring at 2.5 δ (t); (=N-CH_2) at 3.7 δ (t); (-CH_2-N-)in ethylenic moiety at 2.8 δ (t) and phenolic –OH peak at 13.7 δ. In zinc complex the azomethine proton signal shifts downfield due to coordination with metal, -OH proton signal disappears due to deprotonation on chelation and -CH=N proton signal appeared at 9.3 δ (s). There is no appreciable change in all of the other signals of zinc complex.

Electronic absorption spectra

The UV-Vis. spectral data of Schiff base ligand and its metal complexes are specified in Table 1 which includes the solvent, absorption regions, band assignments and the proposed geometry of the complexes. These values are comparable with other reported complexes [16-20].

Table 1. Electronic absorption spectral data of the complexes

Compound	Solvent	Absorption region	Band assignment	Geometry
HL	EtOH	38759	INCT	--------
		28218	INCT	
[CuL(bpy)]	DMSO	35461	INCT	
		24272	INCT	Square planar
		15314	$^2B_{1g}\rightarrow{}^2A_{1g}$	
[NiL(bpy)]	EtOH	40161	INCT	
		21598	$^1A_{1g}\rightarrow{}^1A_{2g}$	Square planar
		13175	$^1A_{1g}\rightarrow{}^1B_{1g}$	
[CoL(bpy)]	EtOH	15082	INCT	
		33003	$^1A_{1g}\rightarrow{}^1B_{1g}$	Square planar

ESR spectra

The X-band powder ESR spectrum of the copper complex shows good resolved nitrogen superfine structure at 77K in perpendicular region due to interaction of odd electron with nitrogen atoms. The magnetic moment calculated from the spectrum was 1.88 BM which corresponds to one unpaired electron, indicating the copper complex is mononuclear. The observed g-values are $g_{\perp} > g_{\parallel} > 2$, indicating that Cu(II) metal has a $d_{x^2-y^2}$ ground state. The $A_{\parallel}$ value was 150G. The observed value for the exchange interaction parameter (G) for copper complex was 5.21 i.e. (G >4) suggests that local tetragonal axes are aligned parallel and the unpaired electron is present in the $d_{x^2-y^2}$ orbital and the exchange coupling effects are not operative in the present complex [21].

Based on the above spectral and analytical data, the structure of Schiff base complexes are given the figure 2.

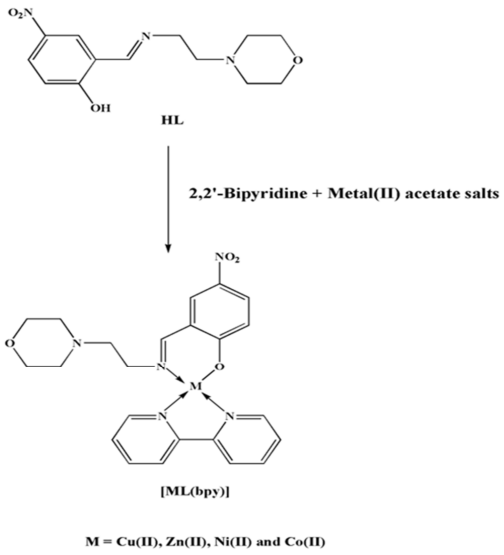

Figure 2. Structure of metal complexes

Redox studies

The cyclic voltammogram of copper complex was recorded in DMSO solution which shows a quasireversible peak for the couple Cu(II)/Cu(III) at Ep_a = -0.84 V with direct cathodic peak at Ep_c = -0.57 V and the ratio, anodic to cathodic peak currents ($Ip_a/Ip_c \approx 1$), is corresponding to simple one electron transfer.

Antimicrobial activity

For *in vitro* antimicrobial activity, the investigated compounds were tested against four gram positive and four gram negative bacteria (*Staphylococcus aureus, Streptococcus pneumoniae, Staphylococcus pneumoniae, Bascillus subtilis, Shigella flexneri, Salmonella typhi, Klebsiella pneumonia* and *Haemophilus influenzae*). The zone of inhibition values of synthesized compounds are given in Table 2. Antibacterial activity of the metal chelates can be explained on the basis of chelation theory [22]. On chelation, the polarity of the metal ion is reduced to a greater extent due to the overlap of the ligand orbital and partial sharing of the positive charge of the metal ion with donor groups. Further, it increases the delocalization of π-electrons over the whole chelate ring and enhances the penetration of the complexes into lipid membranes and blocking of the metal binding sites in the enzymes of microorganisms. These complexes also disturb the respiration process of the cell and thus block the synthesis of proteins, which restricts further growth of the organisms.

Table 2. Antibactirial activity of the Schiff base ligand and its metal complexes (10^{-2}M) (Calculated value of Zone of inhibition)

	Zone of inhibition (mm)							
Compound	*S.aureus*	*Strep.pneumoniae*	*Stap.pneumoniae*	*B.subtilis*	*S.flexneri*	*S.typhi*	*K.pneumoniae*	*H.influenzae*
Sparfloxacin	32	35	32	34	33	32	31	32
HL	9	6	7	6	8	6	8	9
[CuL(bpy)]	16	18	15	14	19	19	15	17
[ZnL(bpy)]	14	17	16	18	22	20	16	21
[NiL(bpy)]	15	14	16	19	14	19	15	19
[CoL(bpy)]	16	18	15	19	14	17	15	16

DNA cleavage studies

In the present study, the gel electrophoresis experiment was conducted at 35^{o}C using our synthesized complexes in the presence of H_2O_2 as an oxidant. As can be seen from the results (figure 3), at very low concentration, copper complex exhibits nuclease activity in the presence of H_2O_2. Control experiment using DNA alone does not show any significant cleavage of CT-DNA even on longer exposure. From the results, it is observed that in the presence of H_2O_2 the copper complex (lane 5) cleaves DNA more efficiently than the other complexes and the control DNA. Further, the presence of a smear in the gel diagram indicates the presence of radical cleavage.

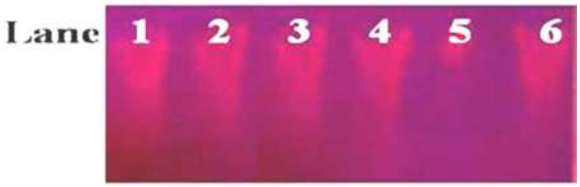

Figure 3. Gel electrophoretic separation of CT-DNA induced by the synthesized complexes in the presence of H_2O_2

*Lane 1, DNA alone; Lane 2, DNA+**HL**; Lane 3, DNA+**[CoL(bpy)]**+ H_2O_2; Lane 4, DNA+**[NiL(bpy)]**+ H_2O_2; Lane 5, DNA+**[CuL(bpy)]**+ H_2O_2; Lane 6, DNA+**[ZnL(bpy)]**+ H_2O_2*

DNA Binding studies

Absorption titration

The potential binding ability of the copper complexes with HS-DNA was studied by UV spectroscopy. The typical titration curve for the copper complex is shown in Figure 4. Absorption titration experiments were performed by varying the concentration of the HS-DNA (0-400µM) keeping the complex concentration (10^{-5}M) as constant. With increasing concentration of DNA, the copper complex showed hypochromicity and red-shifted charge transfer peak. The results showed that the copper complex has binding ability with HS-DNA. In order to find the binding strength of the complex with HS-DNA, the intrinsic binding constant, K_b was obtained by monitoring the changes in the absorbance of the complex with increasing concentration of DNA. The K_b value obtained for the complex was 8.47 x 10^3 M^{-1}. Our results are consistent with earlier reports on preferential binding to DNA in the metal complexes [23].

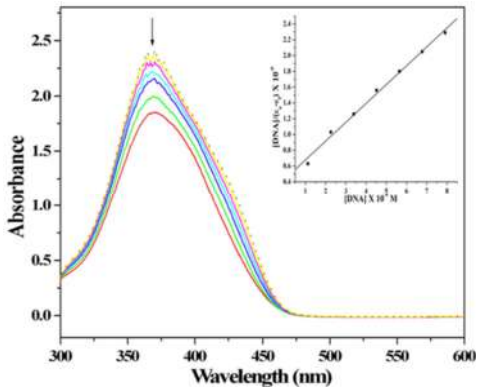

Figure 4. Absorption spectra of the copper complex in the absence and presence of increasing amounts of DNA

Viscosity measurements

Mode of binding of complexes to HS-DNA was investigated by using viscosity measurements also. Complex that interact in the DNA grooves by partial and or non classical intercalation leads no change in relative viscosity of DNA solution when an increasing the concentration of complex. A classical intercalative mode causes a significant increase in viscosity of DNA solution due to increase in separation of base pairs at intercalation sites and hence an increase in overall DNA length [24]. To explore the interaction between the complexes to HS-DNA, viscosity measurements were carried out by keeping the DNA concentration as constant and varying the concentration of complexes. The results (figure 5) lead us to support the above spectral studies which suggest that the copper complex interact with DNA via intercalation between DNA base pairs.

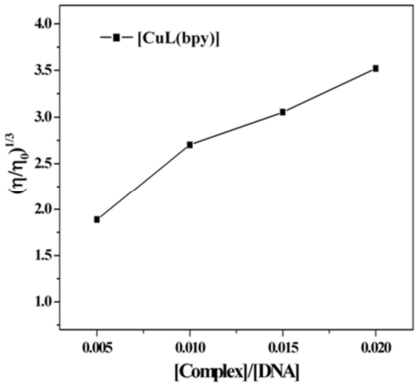

Figure 5. Effect of increasing amount of the copper complex on the relative viscosity of HS-DNA in Tris-HCl buffer

Radical scavenging activity

The scavenging activity of the complexes on the DPPH radical as a fast and reliable parameter to measure the *in vitro* antioxidant activity of such sample have been used by diverse researchers. This assay is based on the measurement of the decrease in molar absorptivity of DPPH at 524nm after reaction with the complex. The effect of antioxidants on DPPH radical scavenging is due to the hydrogen donating ability or radical scavenging activity of the samples [25]. Figure 6 shows the DPPH radical scavenging activity of the copper complex.

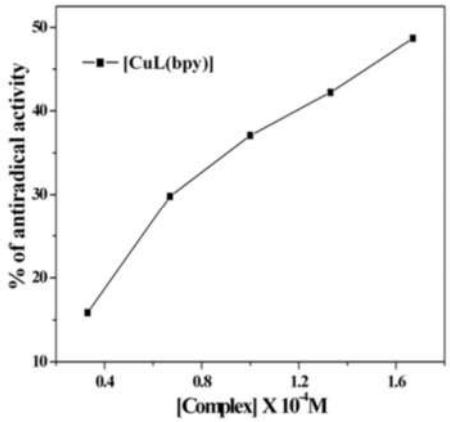

Figure 6. The DPPH radical scavenging activity at various concentrations of the complexes

CONCLUSION

A new bidentate schiff base from 4-(2-aminoethyl) morpholine and 2-hydroxy-5-nitrobenzaldehyde and its mixed ligand transition metal complexes of Cu(II), Zn(II), Ni(II) & Co(II) were synthesized and characterized by UV-Vis., IR, ^{1}H NMR, Mass, ESR and elemental analysis. The spectral data suggest that the ligand acts as bidentate site and coordinates through N and O donor atoms. The UV-Vis. and ESR spectral data suggest that the complexes have spuare planar geometry. Changes occur in spectroscopic studies and viscosity studies confirm that the copper complex had strong interaction with DNA. The copper complex exhibits better antioxidant activity.

Acknowledgements

The authors express their sincere thanks to Managing Board, Principal and Chemistry research centre of Mohamed Sathak Engineering College, Kilakarai for their constant encouragement and providing research facilities. The authors are grateful to the Department of Science and Technology (DST)-Science and Engineering Research Board (SERB-Ref.No. SR/FT/CS-117/2011 dated 29.06.2012), Government of India, New Delhi for financial support. The authors also thank the SAIF, IIT Bombay, STIC CUSAT, Cochin. The authors also thank the Principal and Management of Sri Vidya college of Engineering & Technology, Virudhunagar.

REFERENCES

rnational Journal of Organic Chemistry, **2013**, 3,73-95.
l. *Indian Journal of Advances in Chemical Science*, **2013,** 1(3), 157-163.

[3] Merck Index, *An Encyclopedia of chemicals Drug and Biologicals*, **1983**, 10th Edn., 6138.
[4] R. George; Brpwm; J. Alan. *J. Chem. Soc., Perkin Trans 1*, **1987**.
[5] H. Afaf; EI-masry; H.H. Fahmy; S.H. Ali Abdelwahed. *Molecules*, **2000**, 1426.
[6] K. Szacilowski; W. Macyk; A. Drazewiecka-Matuszek; M. Brindell; G. Stochel. *Chem. Rev*., **2005**, 105, 2647.
[7] N. Raman; S. Syed Ali Fathima; J Dhaveethu Raja. *J. Serb. Chem. Soc*., **2008**, 73, 1063.
[8] Q. L. Zhang; J. G. Liu; H. Chao; G. Q. Xue; L. N. Ji. *J. Inorg. Biochem*., **2001**, 83**,** 49-55.
[9] S. Shi; J. Liu; J. Li; K. Zheng; X. Huang; C. Tan; L. Chen; L. J. Ji. *Inorg. Biochem*., **2006**, 100, 385-395.
[10] A. Wolfe; G. H. Shimer Jr; T. Meehan. *Biochemistry*, **1987**, 26, 6392-6396.
[11] H. Ihmels; D. Otto. *Top. Curr. Chem*., **2005**, 258, 161-204.
[12] S. Satyanarayana; J.C. Daborusak; J.B. Caries. *Biochemistry*, **1983**, 32, 2573.
[13] K. Nakamoto, *Infrared and Raman Spectra of Inorganic and Coordination Compounds*, **1997**, 5th Edn, J. Wiley, New York.
[14] M.C.R. Arhuelles; P.T. Touceda; R. Cao; A.M.G. Deibe; P. Pelagatti; C. Pelizzi; F. Zani. *J. Inorg. Biochem*., **2009**, 103, 35.
[15] D.C. Goodman; R.M. Buonomo; P.J. Farmer; J.H. Reibenspie; M. Y. Darensbourg. *Inorg. Chem*., **1996** , 35, 4029.
[16] R.K. Lonibala; T.R. Rao; R.K. Babitadevi. *J. Chem. Sci*., **2006**, 118, 327.
[17] N. Raman; A. Sakthivel; K. Rajasekaran. *J. Coord. Chem*., **2009**, 62, 1661-1676.
[18] Y.Dong; L.F. Lindoy; P. Turner; G. Wei. *J. Chem. Soc., Dalton Trans*., **2004**, 1264.
[19] A.P. Mishra; I.R. Pandy. *Indian J. Chem*., **2006**, 45A, 2035.
[20] A.B.P. Lever. *Inorganic Electronic Spectroscopy*, 2nd Edn, Elsvier, New York.
[21] A.M.F. Benial; V. Ramalingam; R. Murugesan. *Spectrochim. Acta A*, **2005**, 56, 2775.
[22] N. Dharmaraj; P. Viswanathamurthi; K. Natarajan. *Transition Met. Chem*., **2001**, 26, 105.
[23] D.D. Li; J.L. Tian; W. Gu; X. Liu; S.P. Yan. *J. Inorg. Biochem*, **2010**, 104, 171-179.
[24] Q.F. Guo; S.H. Liu; Q.H. Liu; H.H. Xu; J.H. Zhao; H.F. Wu; X.Y. Li; J.W. Wang. *J. Coord. Chem*., **2012**, 65, 1781.
[25] J.R. Soares; T.C.P. Dins; A.P. Cunha; L.M. Ameida. *Free Radical Res.*, **1997**, 26, 469.

Available online www.jocpr.com

Journal of Chemical and Pharmaceutical Research, 2015, 7(10S):23-34

Research Article

ISSN : 0975-7384
CODEN(USA) : JCPRC5

Synthesis of water soluble transition metal(II) complexes from morpholine condensed tridentate schiff base: Structural elucidation, antimicrobial, antioxidant and DNA interaction studies

Jeyaraj Dhaveethu Raja* and Karunganathan Sakthikumar

Chemistry Research Centre, Mohamed Sathak Engineering College, Kilakarai, Tamilnadu, India

---

ABSTRACT

A new series of water soluble transition metal Cu(II), Co(II), Ni(II), Mn(II) and Zn(II) complexes have been synthesized from 2-(2-Morpholinoethylimino)methyl)phenol Schiff base ligand (LH) in a 1:2 molar ratio. The resulting compounds were characterized by elemental analysis, Magnetic susceptibility, Molar conductance, IR, UV-Vis, ^1H NMR, EPR and ESI-Mass Spectral techniques. The spectral data of these complexes suggest an octahedral geometry around the central metal ion and found to possess [ML_2] stoichiometry. In vitro antimicrobial activities of all compounds were examined against selected bacterial and fungal strains by the disc diffusion method which indicates that the complexes exhibit higher antimicrobial activity than free ligand. The DNA cleavage activity of all compounds was monitored by the agarose gel electrophoresis method using Calf – Thymus DNA. In this result Cu(II), Co(II) and Ni(II) complexes showed a significant cleavage property than others. In vitro antioxidant and DNA-binding properties of these complexes have been investigated by electronic absorption technique. The intrinsic binding constant (K_b) values of Cu(II), Co(II) and Ni(II) complexes are found as 1.1461 X 10^5, 5.1063 X 10^4 and 2.4324 X 10^4 M^{-1} respectively. The binding affinity to DNA has been investigated by viscosity titration measurements, The binding affinity values of these complexes were slightly lower than those observed for classical intercalator (Ethidium bromide-DNA) and observed in the order of EB > Cu(II) > Co(II) > Ni(II)>Zn(II)>Mn(II). The experimental results suggest that the complexes bind to DNA via intercalation.

Key words: Schiff base, Octahedral, Antioxidant, Antimicrobial, DNA interaction.

INTRODUCTION

Schiff bases derived from an amino and carbonyl compound are an important class of ligands that coordinate to metal ions via azomethine nitrogen. In azomethine derivatives, the C=N linkage is essential for remarkable biological activity [1]. It is well-known that Morpholine is a synthetically versatile substrate used as a substitution in many heterocyclic moieties and as a raw material for drug synthesis because it plays a significant role in medicinal chemistry [2]. Morpholine substituted Schiff bases and its Metal complexes exhibits numerous biological activities such as antimicrobial, anticancer, antitumor, anticonvulsant, antiproliferative, antinflammatory and antidiabetic etc**.,** **[**3-9**].** Large number of biological experiments has confirmed that DNA is the primary intracellular target of anticancer drugs; interaction between small molecules and DNA can cause damage in cancer cells, inhibiting the division and resulting in cell demise [10]. DNA-binding metal complexes, especially those with small molecular weight, have been extensively studied as DNA structural and conformational probes, DNA-dependent electron transfer and sequence-specific cleaving agents and potential anticancer drugs [11–14]. Besides, Platinum(II) complexes are used as anticancer drugs since long and among them cis-platin have proven to be a highly effective for treating various types of cancers like ovarian, testicular, head and neck cancer [15-17]. en limited because of many the serious side effects such as hair follicle, neurotoxicity, bone d the lining of gastro-intestinal tract due to strong covalently binding to DNA. To overcome mited activity of cis-platin, great efforts have been made to synthesize other alternatives such

as transition metal complexes which act as better antitumor drugs due to non-covalently binding to DNA [18-21]. Antioxidants are compounds which possess the ability to protect cells from the damage caused by unstable molecules known as free radicals. Free radicals have been implicated as mediators of many diseases, including cancer, atherosclerosis and heart diseases [22-23]. Antioxidants have the capacity in preventing or slowing the oxidation reactions and have been recognized for their potential in promoting health and lowering the risk for cancer, hypertension and heart disease [24-25]. Since synthetic antioxidants like butylated hydroxytoluene (BHT) and butylated hydroxyanisole (BHA), tertiary butyl hydroquinone (TBHQ) and propyl galate (PG) are suspected to be toxic and have carcinogenic effects, naturally occurring antioxidants has considerably increased for use in food, cosmetic and pharmaceutical products [26-28]. Our present work report regarding the synthesis, structural elucidation, antimicrobial, antioxidant, DNA binding and cleavage studies of Transition Metal(II) complexes.

EXPERIMENTAL SECTION

Materials and Methods

The starting materials 4-(2-aminoethyl)-morpholine, salicylaldehyde, $Cu(OAc)_2.H_2O$, $Zn(OAc)_2.2H_2O$, $Mn(OAc)_2.4H_2O$, $Co(OAc)_2.4H_2O$ and $Ni(OAc)_2.4H_2O$ were procured from Sigma Aldrich chemical company (USA) and other reagents and solvents were of analytical grade.

Instrumentation

Melting points of all the compounds were noted on Cintex apparatus (Guna-BMQR) in open glass capillaries. The C, H, and N contents of the synthesized ligand and the complexes were performed by Elementar Vario EL III CHNS. Molar Conductivity of complexes in methanolic solution (10^{-3}M) were recorded at room temperature by systronics model 304 digital conductivity bridge using a dip type conductivity cell fitted with a platinum electrode. Magnetic susceptibility for powder sample of the complexes was recorded by Guoy balance at room temperature. IR spectra of Schiff base and their complexes were recorded on a Shimadzu FT-IR spectrophotometer in the range of 4000 to 400 cm^{-1}. Electronic absorption spectra of all compounds were recorded in methanolic solution (10^{-3}M) by Shimadzu UV-Vis 1800 spectrophotometer in the range of 200 to 1100 nm. Antioxidant and DNA binding studies were examined by Shimadzu UV-Vis 1800 spectrophotometer. DNA Cleavage studies of all compounds were carried out by agarose gel electrophoresis technique in the presence of H_2O_2. The ^1H NMR spectra of the ligand and its zinc complex were recorded on a Bruker 300 MHz NMR spectrometer using $CDCl_3$. EPR spectra of powder sample of the copper (II) Complex were recorded on a Varian E112 EPR spectrometer at RT and LNT using TCNE as the field marker (g_e= 2.00277). Mass spectra of Schiff base and their complexes were recorded on ESI MS 3000 Bruker Daltonics instrument.

Synthesis of Schiff base ligand (LH)

The Schiff bases were synthesized by stirring an equal molar quantities (0.01 mol) of 4-(2-amino ethyl)-Morpholine and Salicylaldehyde in methanol (30 ml) were refluxed for two hours. The reaction was completed after TLC confirmation test. Yellow solution was obtained at the end of the reaction and the volume of the solution was reduced to one-third on water bath and cooled at room temperature. The ligand was purified by column chromatography using ethanol and chloroform mixture. The collected pure yellow liquid ligand was dried slowly at room temperature in vacuum desiccators over anhydrous $CaCl_2$. The yield of the isolated ligand was found to be 87% (Scheme 1).

Synthesis of metal complexes [$M(L)_2$]

A solution of 2-(2-Morpholinoethylimino)methyl)phenol Schiff base (LH) (0.004M) in methanol (40 mL) was added slowly to a solution of Metal(II) acetate(0.002M) [$Cu(OAc)_2.H_2O$, $Zn(OAc)_2.2H_2O$, $Mn(OAc)_2.4H_2O$, $Co(OAc)_2.4H_2O$ and $Ni(OAc)_2.4H_2O$] in 30 ml of absolute methanol and stirred for 30 minutes. The resulting mixture was refluxed for 3 hrs. The solid product so formed was separated by filtration and purified by recrystallization using methanol and petroleum ether. Trace of water and solvents were recovered by keeping in vacuum desiccators over anhydrous $CaCl_2$. The preparation of all complexes was followed by the similar method and the yield was found to be 74–80% (Scheme 1).

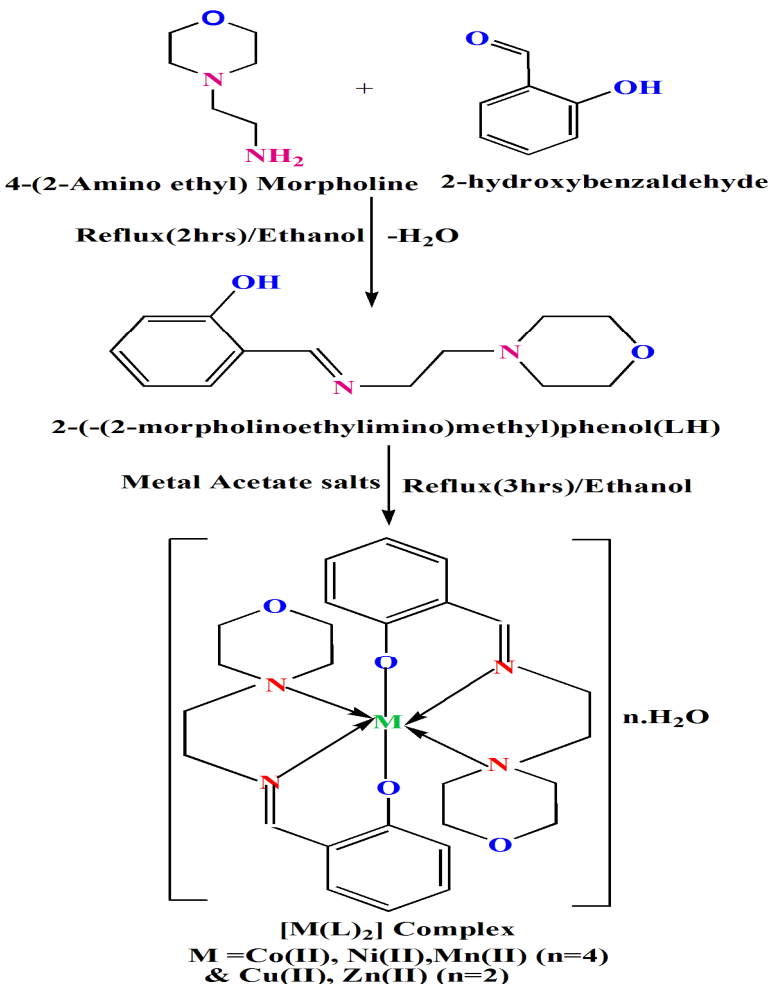

Scheme 1. Schematic representation of synthesis of Ligand & the coordinated complexes

DNA interaction studies

DNA cleavage study by Gel electrophoresis

DNA cleavage activities of Schiff base ligand and their metal complexes with CT-DNA were monitored by agarose gel electrophoresis method[29-30]. The gel electrophoresis experiments were performed under aerobic conditions with H_2O_2 by incubation at 35^0C for 2 hours. The samples (Cocktail mixture) containing CT-DNA 15 µL (30 µM), synthesized compounds 5 µL (50 µM), buffer solution (pH = 7.2) 29 µL (50 mM TrisHCl & 18 mM NaCl) and H_2O_2 1µL (500 µM). The Cocktail mixture was shaked well and maintained incubation at room temperature for 2 hours. After incubation, 1 µL Bromophenol blue (photosensitizer) dye solution (0.25% bromo phenol blue and 40% sucrose in H_2O) was added with Cocktail mixture, the resulting mixture was injected into 1% agarose gel chamber wells. The gel was stained by immersing it in tank buffer solution containing ethidium bromide (EB) (0.5 µg/ml).When power supply (50 V) was introduced into the tank buffer solution, the DNA migration was occurred towards to positive pole. After completion of DNA migration, the electric current was turned off, the gel layer was taken out from the solution tank and was snapped under a UV Transilluminator and the bands were observed the extent of DNA cleavage by comparing with standard DNA marker.

DNA binding study by UV-Visible spectroscopy

The Concentrated herring sperm DNA stock solution was prepared in 5 Mm Tris–HCl/50 mM NaCl in deionized water at pH 7.2. The purity of DNA was verified by monitoring the ratio of absorbance at 260 nm to that at 280 nm, A_{260}/A_{280} which was in the range 1.8–1.9 indicating that the DNA is sufficiently free from protein and the initial concentration of the DNA was confirmed from its absorption intensity at 260 nm with a molar extinction coefficient (ε) of 6600 M^{-1} cm^{-1}[31]. The Electronic Absorption titrations were performed by keeping a fixed complex concentration (10^{-5}M) to which increments of the DNA stock solutions were added from 1.1308 X 10^{-5} to 12.0464 X

inding constant (K_b) of Metal(II) complexes with DNA was calculated from the Wolfe–

$$\frac{[DNA]}{(\varepsilon_a-\varepsilon_f)} = \frac{[DNA]}{(\varepsilon_b-\varepsilon_f)} + \frac{1}{K_b(\varepsilon_b-\varepsilon_f)} \quad (1)$$

Where, [DNA] is the concentration of HS-DNA in base pairs. The apparent extinction coefficient (ε_a) observed for the MLCT absorption band at the given DNA concentration was obtained by calculating Abs / [complex], ε_f and ε_b correspond to the extinction coefficient of the complex free (unbound) and fully bound to DNA. The K_b values can be obtained from the ratio of the slope to the intercept of the plots of [DNA] / (ε_a-ε_f) Vs [DNA]. The standard Gibb's free energy change (ΔG_b^0) for DNA binding can be calculated using van't Hoff equation (2).

$$\Delta G_b^0 = -RT \ln K_b \quad (2)$$

DNA binding study by Viscometry titration

The experiments were carried out by an Oswald viscometer, immersed in a thermo stated water-bath maintained at $25^oC \pm 0.1^oC$ which helps to further clarify the nature of the interaction between the complexes and DNA. They are sensitive to length change of DNA and they are observed as the least ambiguous and the most critical test of binding mode in solution[32]. The titrations were performed for Cu(II), Co(II), Ni(II) complexes and control-Ethidium bromide(EB) (0.2, 0.4, 0.6, 0.8, 1.0 X 10^{-5}M) and each compound was introduced into the HS-DNA solution (10^{-4}M) present in the viscometer. Each sample was measured three times and an average flow time was calculated [33]. The viscosity of DNA increased with rising ratio of complexes to DNA, further suggesting a binding of the complexes with DNA. Relative specific viscosity for DNA either in the presence or absence of complexes were calculated from the equation (3).

$$\left(\frac{\eta}{\eta_0}\right)^{1/3} = \frac{\left\{\frac{(t_{complex}-t_0)}{t_0}\right\}}{\left\{\frac{(t_{DNA}-t_0)}{t_0}\right\}} \quad (3)$$

Data were analyzed as $(\eta/\eta_o)^{1/3}$ versus binding ratio R=[complex]/[DNA], where η is the specific viscosity of DNA in the presence of the complex and η_0 is the specific viscosity of DNA alone; $t_{complex}$, t_{DNA} and t_o are the average flow time for the DNA in the presence of the complex, DNA alone and Tris-HCl buffer respectively [34].

DPPH radical scavenging studies

Antioxidant activities were determined in vitro by 2,2-diphenyl-1-(2,4,6-trinirophenyl)hydrazyl (DPPH) free radical scavenging assay. 3.9037 mg of DPPH was dissolved in 3.3 mL methanol. 0.3 mL of the stock solution (3 mM) was added to 3.5 mL methanol (2.5714 X10^{-4} M) and absorbance was noted immediately at 517 nm for the control. Various concentration solutions (2.9411, 6.0606, 9.3750, 12.9032 and 16.6666 X10^{-5} M) were prepared in methanol using 1mM test samples and 3 mM DPPH stock solution. The resulting mixture was incubated in dark at room temperature for 1 hour. It was protected from light by covering the test tubes with aluminium foil. While DPPH reacts with an antioxidant compounds, it is reduced by the typical H-absorption and the colour changes from deep violet to light yellow to form a stable macromolecular radical. The absorbance of the resulting solution was measured by UV-visible spectrophotometer at 517 nm. The control was measured from the values of absorbance of the DPPH radical without antioxidant and Special care was taken to minimize the loss of free radical activity of the DPPH radical stock solution [35].

Pharmacological studies

In vitro antimicrobial assay

Antimicrobial activities of the ligand and their complexes (10^{-4}M) were screened in vitro against the selected pathogenic bacterial strains and fungi species by the disc diffusion method. Amikacin and Ketokonazole were used as standard drugs for antibacterial and antifungal studies respectively. The test organisms were grown on nutrient agar medium in sterile Petri plates. The paper discs were saturated with 10 µL of the ligand and its complexes solution. The saturated paper discs were placed aseptically in the Petri dishes containing Mueller Hinton nutrient agar with 2% of glucose media inoculated with the above mentioned pathogenic bacteria and fungi separately. The inoculated culture plates were incubated at 37°C for 24 hrs for the bacteria and at 30°C for 48 hrs for the fungi. After incubation, the antimicrobial activity was evaluated by measuring the diameter (in mm) of the inhibition zone formed around the discs [36].

RESULTS AND DISCUSSION

erization

and complexes were found to be intensely coloured and they were slightly hygroscopic ature. The synthesized complexes were soluble in Water, Methanol, Ethanol, $CHCl_3$ and data and physical properties of the ligand and its complexes are listed in Table 1.

Table 1 Analytical and Physical data of the Schiff base ligand and its complexes.

Compounds (Formula Weight & Empirical Formula)	Colour	Yield (%)	M.P (^{0}C)	Found (Calcd) (%)				($\wedge_m$) Molar Conductance $Ohm^{-1}cm^2 mol^{-1}$
				C	H	N	M	
[LH] (234.31) ($C_{13}H_{18}N_2O_2$)	Yellow liquid	87.48	--	66.90 (66.64)	07.60 (07.74)	11.39 (11.95)	----	----
$[Cu(L)_2]$ (566.16) ($C_{26}H_{38}N_4O_6$)Cu	Green	80.10	120	55.10 (54.45)	06.71 (06.22)	09.89 (09.43)	11.22 (11.56)	61.07
$[Co(L)_2]$ (597.55) ($C_{26}H_{42}N_4O_8$)Co	Dark Brown	76.32	>280	52.21 (51.88)	07.02 (06.91)	09.37 (08.66)	09.86 (9.35)	46.35
$[Mn(L)_2]$ (593.56) ($C_{26}H_{42}N_4O_8$)Mn	Black	78.65	110	52.56 (52.08)	07.07 (06.59)	09.43 (09.78)	09.25 (09.66)	56.65
$[Ni(L)_2]$ (597.32) ($C_{26}H_{42}N_4O_8$)Ni	Dark green	74.50	294	52.23 (51.85)	07.03 (06.83)	09.37 (08.65)	09.82 (09.24)	41.20
$[Zn(L)_2]$ (567.99) ($C_{26}H_{38}N_4O_6$)Zn	Yellow	76.34	112	54.93 (53.86)	06.69 (06.02)	09.85 (09.04)	11.50 (11.83)	48.52

Elemental analysis

The composition and purity of the coordinative compounds were determined by the elemental analysis (C, H, N and metal contents) and the result shows they are in good agreement with the proposed formula (Table 1)

Conductivity studies

The molar conductivity of all complexes was in the range of 41.20-61.07 ohm^{-1} cm^2 mol^{-1}(Table 1). The low value shows that they are non electrolytic nature due to lack of dissociation.

Mass spectra

ESI-MS Mass spectrometry is used to confirm the stoichiometry composition of compounds. The mass spectrum of ligand shows the molecular ion peak at m/z 235 corresponding to $C_{13}H_{18}N_2O_2$ and the CuL_2 complex molecular ion peak at m/z 565 corresponding to ($C_{26}H_{38}N_4O_6$)Cu (Fig 1) which confirms the formation of $[ML_2]$ stoichiometry (Scheme 1). The molecular ion peaks of other complexes Co(II), Mn(II), Ni(II) and Zn(II) complexes were observed at m/z with relative abundance 598, 592, 596 and 568 respectively and are in good agreement with the formula weight (Table 1).

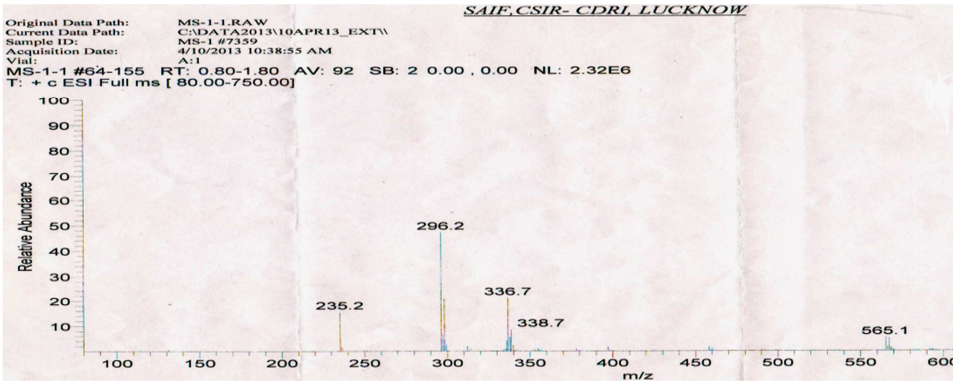

Fig. 1 ESI-MS Mass spectrum of $[Cu(L)_2]$ complex

^{1}H NMR spectra

The ^{1}H NMR spectra of the Schiff base ligand [L] and Zinc complex show the following signals: δ values of Schiff base ligand [L] : Aromatic Protons (m,4H) at 6.84-7.32 ppm; Azomethine proton(-HC=N-) (s,1H) at 7.9 ppm; Morpholino-OCH_2 (t,4H) at 3.6 ppm; Morpholino-N-CH_2 (t,4H) at 2.50 ppm; Phenolic-OH proton (s,1H) at 8.5 ppm[37]. $[Zn(L)_2]$ Complex: Aromatic Protons (m,8H) at 6.7 -7.5 ppm; Azomethine proton(-HC=N-) (s,1H) at 8.16 ppm; morpholino-OCH_2 (t,8H) at 3.6 ppm; Morpholino-N-CH_2 (t,8H) at 3.12 ppm; The low intensity singlet peak at water proton (s,1H)[38].The above ^{1}H NMR spectra data assigned that the azomethine proton proton signals in the spectrum of the zinc complex are shifted down field compared to the leshielding due to nitrogen atom is taking part in complexation. The absence of singlet peak

at the rage of 8.5 ppm, noted in the zinc complexes, indicates the loss of the –OH proton due to complexation[39] and there is no appreciable change in all other signals in these complexes.

IR spectra

Table 2. Infrared spectral data of the ligand and its metal complexes (cm^{-1})

Com pounds	C=N	Phenolic C-O	Morpholino C-N-C	Morpholino C-O-C	Aromatic C-H	Aliphatic C-H	Iminic C-H	(H_2O)	M-N	M-O
Ligand [LH]	1635	1278	1342	1197(as) 1114 (s)	3056	2974	2854	---	---	---
$[Cu(L)_2]$	1600	1284	1320	1195(as) 1112 (s)	3195	2970	2866	3413 813(b)	468	495
$[Co(L)_2]$	1595	1302	1332	1190(as) 1110 (s)	3180	2976	2874	3425 848(b)	462	502
$[Mn(L)_2]$	1598	1294	1335	1196(as) 1114 (s)	3160	2972	2885	3339 846(b)	475	510
$[Ni(L)_2]$	1585	1300	1335	1194(as) 1119 (s)	3060	2965	2875	3339 845(b)	470	502
$[Zn(L)_2]$	1627	1286	1340	1193(as) 1112 (s)	3152	2972	2870	3340 846(b)	462	520

The IR spectra of the complexes were compared with the free ligand for the frequency change during the complexation and are summarized in Table 2. IR Spectrum of Schiff base ligand showed a strong sharp band observed at 1635 cm^{-1} region is assigned to the -HC=N-mode of the azomethine group which was shifted to lower frequencies in the spectra of all the complexes indicating the involvement of imino nitrogen(-HC=N-) in coordination to the central metal ion [40] and morpholino-C-N-C bands at 1342 cm^{-1} found in the ligand is shifted lower frequencies in the spectra of all the complexes indicating the involvement of C-N-C nitrogen in coordination to the metal ion. The peak due to the presence of phenolic C-O at 1278 cm^{-1} in ligand is shifted to higher frequencies in the spectra of all the complexes indicating confirming deprotonation of the phenolic–OH on chelation[41]. In the spectra of all metal complexes a broad diffuse band was identified (stretching) in the range of 3413–3340 cm^{-1} and week band in-plane bending (rocking) at 813–848 cm^{-1}. It suggests that the presence of water molecules in the metal complexes [42]. The far IR spectra of the complexes show medium bands in the region 462–475 cm^{-1} and 495–520 cm^{-1} corresponding to M-N and M-O vibrations respectively and other absorption bands are no appreciable change in the ligand and metal complexes (Table 2).

Electronic Spectra and Magnetic susceptibility

The electronic absorption spectral data of the ligand and its metal complexes were recorded in methanol. The absorption maxima and magnetic moment values are depicted in Table 3. The electronic spectra of the free ligand displayed two bands at 38700 cm^{-1} and 31300 cm^{-1} are intra ligand charge transfer assigned to $\pi\rightarrow\pi^*$ and $n\rightarrow\pi^*$ transitions for phenyl ring and the azomethine chromophore (–CH=N–)[43]. In the metal complexes this band is shifted to a longer wavelength which may be attributed to the donation of lone pair electron in a sp^2-hybridized orbital of the imino nitrogen atom of the ligand to the metal (N→M). $[Cu(L)_2]$ complex exhibited only one low intensity broad band d-d transition at 649 nm (15,408 cm^{-1}) due to dynamic Jahn–Teller distortion[44-45] which are assigned to the $^2E_g\rightarrow{}^2T_{2g}$ transition and showed magnetic moment value is slightly higher than the spin-only value(1.73) for one unpaired electron which suggests possibility of a distorted octahedral geometry[46]. $[Co(L)_2]$ and $[Ni(L)_2]$ complexes exhibited three bands for each(Table 3) and magnetic moment values, which is further supported to an octahedral geometry.

Table 3 Electronic spectral data and magnetic Susceptibility values of the synthesized compounds (10^{-3} M in Methanol).

Com pounds	Band Position λ_{max} nm (γ-cm^{-1})	Assignment	μ_{eff} B.M	Suggested geometry
[LH]	258 (38,760)	$\pi\rightarrow\pi^*$	--	--
	319 (31,348)	$n\rightarrow\pi^*$		
$[Cu(L)_2]$	649(15,408)	$^2E_g\rightarrow{}^2T_{2g}$	1.82	Distorted Octahedral
	847(11,806)	$^4T_1g(F)\rightarrow{}^4T_2g(F)$		
$[Co(L)_2]$	528(18,939)	$^4T_1g(F)\rightarrow{}^4A_2g(F)$	4.83	Octahedral
	402(24,875)	$^4T_1g(F)\rightarrow{}^4T_1g(P)$		
	892 (11,210)	$^3A_2g(F)\rightarrow{}^3T_2g(F)$		
$[Ni(L)_2]$	747 (13,386)	$^3A_2g(F)\rightarrow{}^3T_1g(F)$	3.18	Octahedral
	407 (24,570)	$^3A_2g(F)\rightarrow{}^3T_1g(P)$		

:a of the $[Cu(L)_2]$ complex in powder state was recorded at 300 K and 77 K under 9.10 GHz lation using tetracyanoethylene (g_e = 2.00277). The copper complex at 300 K gave one in the high field region and was isotropic because of the tumbling motion of the molecules

and the complex in the frozen state exhibited anisotropic pattern with well-resolved hyperfine lines. The results are summarized in Table 4**.** The spin Hamiltonian parameters have been calculated by Kivelson's method. The observed g-values are in the order $g_{||}$ (2.1248) > $g_{\perp}$(2.0211) > g_e (2.00277) indicating that the unpaired electron lies predominantly in the $d_{x^2-y^2}$ orbital of Cu(II)[47] and the observed $g_{||}$ values for copper complex is less than 2.3 in agreement with the covalent environment character of the M-L bond[48]. The covalent nature of the M–L bond in the complex is further supported by the $g_{eff} = [(g_{||} + g_{\perp}) / 3]$ value less than 2.00277[49]. The observed value of g_{eff} = 1.3819 was less than 2.00277. The observed hyperfine constant parameters are very clear that in the order $A_{||}$ =124G >A_{av}(96G) > $A_{\perp}$= 82G. The values were obtained from the following equations (4-8).

$$g_{\perp} = \frac{(3g_{av} - g_{||})}{2} \quad (4)$$

$$K_{\perp} = \frac{(3A_{av} - A_{||})}{2} \quad (5)$$

$$g_{av} = \frac{g_{||} + 2g_{\perp}}{3} \quad (6)$$

$$A_{av} = \frac{(A_{||} + 2A_{\perp})}{3} \quad (7)$$

$$G = \frac{(g_{||} - 2.00277)}{(g_{\perp} - 2.00277)} \quad (8)$$

The observed value of interaction coupling constant G = 6.657 is in the present complex suggesting that there is no interaction between Cu-Cu centers in the solid state complex and the absence of half field signal at 1600G corresponding to the ΔMs = ± 2 transition rules out a Cu-Cu interaction[50]. EPR and optical spectra have been further used to determine covalent bonding for the Cu(II) ion in a variety of environments. The values of molecular orbital coefficient parameters (α^2, β^2, γ^2) were calculated by Kivelson and Neimann formulae (9-11).

$$\alpha^2 = \frac{A_{||}}{P} + (g_{||} - 2.00277) + \frac{3}{7}(g_{\perp} - 2.00277) + 0.04 \quad (9)$$

$$\beta^2 = (g_{||} - 2.00277)\left(\frac{E_{d-d}}{-8\lambda_0 a^2}\right) \quad (10)$$

$$\gamma^2 = (g_{\perp} - 2.00277)\left(\frac{E_{d-d}}{-2\lambda_0 a^2}\right) \quad (11)$$

In-plane σ-bonding parameter α^2 = 1.0 indicates the pure ionic character whereas, α^2 = 0.344 indicates the pure covalent bonding. The observed α^2 value indicates that the complex has covalent character. The observed β^2 (in-plane π-bonding) and γ^2 (out-plane π-bonding) values which indicate π-bonding is completely covalent character due to the value is less than 1.0 (Table 4). Hathaway has pointed out that for the pure σ-bonding in case of orbital reduction factors are equal ($K_{||} = K_{\perp}$)[51]. In case of $K_{||} < K_{\perp}$ denotes considerable in-plane π-bonding and if the value is to be $K_{||} > K_{\perp}$ which leads to out-of-plane π–bonding. The observed orbital reduction factor values for the present $[Cu(L)_2]$ complex are $K_{\parallel} > K_{\perp}$ which indicates the presence of out-plane π-bonding in metal ligand π-bonding. The values are calculated from the equation(12,13).

$$K_{||}^2 = (g_{||} - 2.00277)\left(\frac{E_{d-d}}{-8\lambda_0}\right) \approx \alpha^2\beta^2 \quad (12)$$

$$K_{\perp}^2 = (g_{\perp} - 2.00277)\left(\frac{E_{d-d}}{-2\lambda_0}\right) \approx \alpha^2\gamma^2 \quad (13)$$

The Co-factors of degree of geometrical distortion $f_{||}$ = 171.35 cm^{-1} indicating an octahedral geometry around the Cu(II) ion. Spectral data and magnetic measurements of the Cu(II) complex has been proposed as a distorted octahedral geometry (Scheme 1).

Table 4 The EPR spectral data for polycrystalline sample of the $[Cu(L)_2]$complex at 77K

Complex	g tensor			Hyperfine constant X 10^{-4} cm^{-1}		Bonding parameters					
	g_{av}	$A_{||}$	$A_{\perp}$	A_{av}	G	$f_{||}(cm^{-1})$	α^2	β^2	γ^2	$K_{||}$	$K_{\perp}$
	2.05	124	82	96	6.657	171.35	0.344	0.825	0.495	0.283	0.170

') = 9.114 X10^9cycle/sec, 1G = 10^{-4} cm^{-1}, E_{d-d} = 15,408 cm^{-1}, one-electron spin orbit coupling constant of free Cu(II) ion λ_0 - 828 cm^{-1}, μ_{eff} = 1.82 B.M (exp), Free ion dipolar term(P) = 0.036 cm^{-1}, $f_{||} = g_{||} / A_{||}$.

DNA nuclease activity by gel electrophoresis

Lane:1 DNA alone,
Lane:2 ligand +DNA+H_2O_2,
Lane:3 $[Cu(L)_2]$+DNA+H_2O_2,
Lane:4 $[Co\ (L)_2]$+DNA+H_2O_2,
Lane:5 $[Mn(L)_2]$+DNA+H_2O_2,
Lane:6 $[Ni(L)_2]$+DNA+H_2O_2,
Lane:7 $[Zn(L)_2]$+DNA+H_2O_2,

Fig. 2 Gel electrophoresis showing the chemical nuclease activity of CT DNA by the synthesized compounds in the presence of oxidant, lane (1-7)

The gel electrophoresis clearly revealed that there was difference in migration of the lanes 2–7 by comparing with CT-DNA control (Lane-1) (Fig 2). The DNA cleavage efficiency of the complex was observed due to the different binding affinity of complexes respect to rate of the conversion of open circular into linear. In oxidative DNA cleavage mechanism, metal ions of the complexes react with H_2O_2 to generate the hydroxyl radical ($OH^{\bullet}$) or reactive oxygen species (O_2) which attacks the C_4' position of the sugar moiety which finally cleave the DNA and inhibit the replication ability of the cancer gene is thereby destroyed. The DNA cleavage activities of the complexes are shown in the fig 2 Lane 1 is for the control (DNA + H_2O_2) which does not exhibit significant cleavage even on longer exposure time and lane 2 is for the ligand alone is inactive in the presence and absence of external agents. Lane: 3 $[Cu(L)_2]$, Lane: 4 $[Co(L)_2]$ and Lane: 6 $[Ni(L)_2]$ Complexes cleave DNA more efficiently in the presence of an oxidant than the ligand and other complexes. This may be attributed to the formation of hydroxyl free radicals, which can be produced by metal ions reacting with H_2O_2 to produce the diffusible hydroxyl radical or molecular oxygen, which may damage DNA through Fenton type chemistry [52]. This hydroxyl radical participates in the oxidation of the deoxyribose moiety, followed by hydrolytic cleavage of sugar–phosphate backbone [53]. Further, the presence of a smear in the gel diagram indicates the presence of radical cleavage.

Evaluation of binding constants by Electronic absorption titration

Electronic absorption spectroscopy is one of the most powerful techniques to examine the binding mode of DNA with metal complexes. In this studies, K_b and ΔG_b^0 values for Cu(II), Co(II) and Ni(II) complexes have been evaluated by absorption titration(Table 5). These complexes were exhibited greater DNA cleavage efficiency than others while observing the gel electrophoresis. The binding of the complexes to DNA helixes were characterized by monitoring the changes in the absorbance of π–π* bands and shift in wavelength on each addition of DNA solution to the complex. While the concentration of CT-DNA increases from 1 X 10^{-5} to 12 X 10^{-5} M, a significant hypochromic shift of the intra ligand bands were observed accompanied by a moderate red shift (Figs 3a & 3b). The π* orbital of the intercalated ligand can couple with the π orbital of the base pairs thus decreasing the π–π* transition energy and resulting in bathochromism (red shift). On the other hand, the coupling π orbital is partially filled by electrons thus decreasing the transition probabilities and concomitantly resulting in hypochromism [54]. The intrinsic binding constant K_b values are calculated from the ratio of the slope to the intercept of the plot of [DNA] / (ε_a - ε_f) X 10^{-7} Vs [DNA] X 10^{-5} M by Wolfe–Shimmer equation (1) and ΔG_b^0 values for these complexes were calculated by Van't Hoff equation (2) which indicate that the complexes can interact with DNA in a spontaneous manner and also the percentage of hypochromicity for the complexes were determined from the equation (14).

$$\% H = \frac{(\varepsilon_b - \varepsilon_f)}{\varepsilon_f} X\ 100 \qquad (14)$$

Hypochromism results indicated that the contraction of DNA helix axes as well as the conformational changes on molecule of DNA. The observed results of hypochromism effect with a red shift is attributive an intercalative binding mode due to strong stacking interactions between aromatic chromophore of molecule and DNA base pairs. To compare quantitatively the affinity of the synthesized complexes towards DNA, the intrinsic binding constants K_b of the synthesized complexes to CT DNA are shown in table 5. From this table, it is clear that $[CuL_2]$ complex acy than other complexes.

Table 5 Spectral parameters for DNA interaction with the synthesized complexes

Complexes	λ_{max} free (nm)	λ_{max} bound(nm)	$\Delta\lambda$ (nm)	Types of Chromism	Chromism (%)	Binding constant (K_b) M^{-1}	$\Delta G_b^{\neq}$ $KJmol^{-1}$
$[CuL_2]$	362	368	06	Hypo & Red shift	18.32	1.1461 X 10^5	-28.8671
$[CoL_2]$	354	362	08	Hypo & Red shift	32.56	5.1063 X 10^4	-26.8637
$[NiL_2]$	364	372	08	Hypo & Red shift	28.73	2.4324 X 10^4	-25.0260

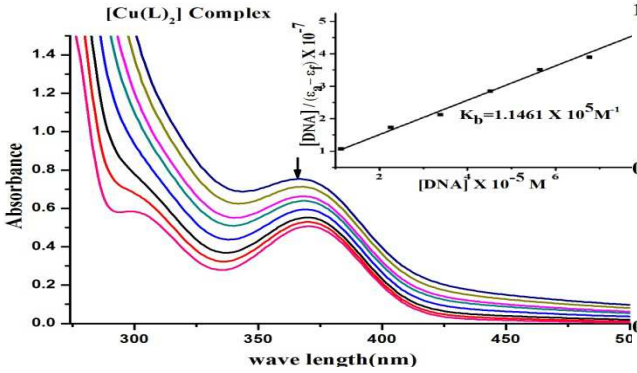

Fig. 3a. Electronic Absorption spectrum of $[Cu(L)_2]$ Complex through titration with DNA in Tris-HCl buffer; [Complex] =1 X 10^{-5} M; [DNA]: 0.0–12 X 10^{-5} Mol L^{-1}. The increase of DNA concentration is indicated by an arrow. Plot of [DNA] / (ε_a - ε_f) Vs [DNA]. Binding constant K_b= 1.1461 X 10^5

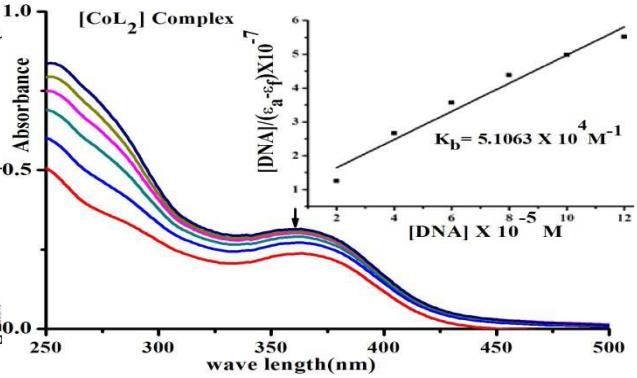

Fig. 3b. Electronic Absorption spectrum of $[Co(L)_2]$ Complex through titration with DNA in Tris-HCl buffer; [Complex] =1 X 10^{-5} M; [DNA]: .0–12 X 10^{-5} Mol L^{-1}. The increase of DNA concentration is indicated by an arrow. Plot of [DNA] / (ε_a - ε_f) Vs [DNA]. Binding constant K_b= 5.1063 X 10^4

Viscosity titration measurements

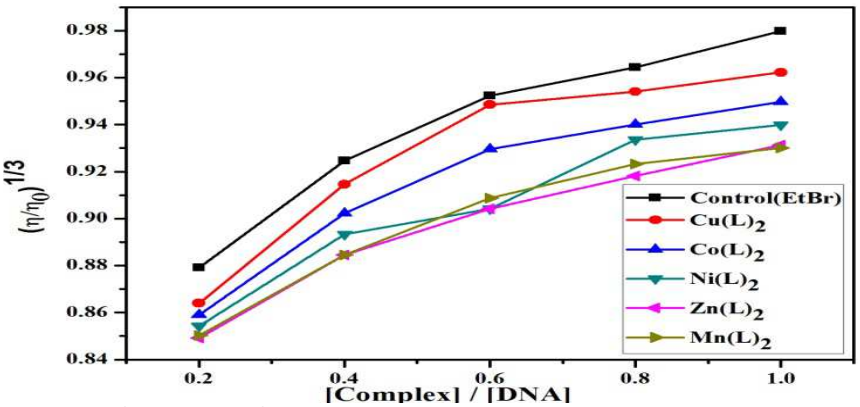

Fig. 4. Plot of Relative specific viscosity (η/η_0) versus R = [Complex] / [DNA]

The Interaction between the complexes and DNA was investigated by viscosity measurements. Ethidium bromide (EB) a well known DNA classical intercalator increases the viscosity strongly by lengthening the DNA double helix through intercalation. While increasing the concentration of the complexes, the relative viscosity of complexes also increases steadily similar to the performance of ethidium bromide. The rised degree of viscosity may depend on the binding affinity to DNA which was observed in the following order EB > Cu(II) > Co(II) > Ni(II) (Fig 4). The significant increase in viscosity of the complexes is obviously due to the partial insertion of the ligand between the DNA base pairs leading to an increase in the separation of base pairs at intercalation locations, hence an increase in overall DNA contour length[55].

DPPH radical scavenging studies

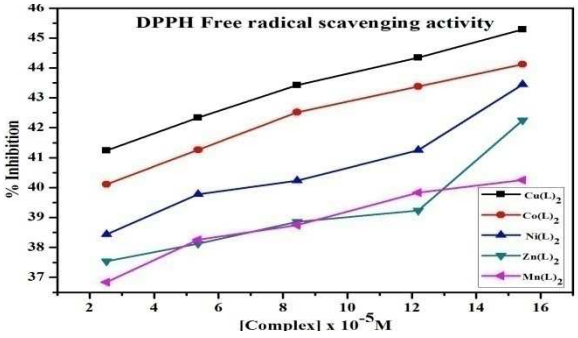

Table 6 DPPH Free radical scavenging activity

Final Concentration of Complex X 10^{-5} M	% Inhibition				
	$Cu(L)_2$	$Co(L)_2$	$Ni(L)_2$	$Zn(L)_2$	$Mn(L)_2$
2.5231	41.24	40.11	38.44	37.54	36.84
5.3674	42.34	41.26	39.78	38.12	38.26
8.4331	43.42	42.52	40.23	38.86	38.75
12.2014	44.34	43.38	41.25	39.23	39.83
15.4364	45.28	44.12	43.44	42.25	40.25

Fig. 5. DPPH Free radical scavenging activity (% Inhibition) of each complex (DPPH-FRSA)

Antioxidants are chemical substances that donate an electron to the free radical and convert into a harmless molecule. They may decrease the energy of the free radical or suppress radical formation or break chain propagation or repair damage and reconstitute membranes. DPPH free radical method is an antioxidant assay based on electron-transfer that produces a violet solution in methanol [56]. This free radical stable at room temperature is reduced in the presence of an antioxidant molecule, giving rise to colourless alcoholic solution. The DPPH assay provides an simple and rapid approach to evaluate antioxidants by electronic spectrophotometer and it can be useful to assess various products at a time. The percentage of antioxidant activity of each substance was assessed by DPPH free radical assay (Fig 5, Table 6). The measurement of the DPPH free radical scavenging activity was performed according to methodology described by Brand-Williams et al. Radical scavenging activity (RSA) was calculated as percentage of DPPH discoloration by the following equation (15)[57]. A_{DPPH} is absorbance of DPPH (control) and A_S is absorbance of sample.

$$\% \text{ RSA} = \frac{A_{DPPH} - A_S}{A_{DPPH}} \text{ X } 100 \qquad (15)$$

Antimicrobial assay

On the basis of observed zones of inhibition, it was found that most of the complexes exhibit good antimicrobial activity than the free ligand [58]. The observed higher activity of the metal complexes could be explained on the basis of Overtone's concept and Tweedy's chelation theory[59]. The Chelation tends to make the ligand a more powerful agent and the cell permeability, the lipid membrane surrounded the cell, favors the passage of only lipid soluble material (liposolubility) which is an important factor that controls antimicrobial activity. A possible explanation for this increase in the activity upon chelation is that, the polarity of the metal ion in a chelated complex is reduced to a greater extent due to the overlap of the ligand orbital and partial sharing of the positive charge of the metal ion. It increases the delocalization of π- and d-electrons over the whole chelated ring and enhances the lipophilicity of the metal complexes. The increased lipophilicity of complexes enhances the cell permeability into lipid membranes which leads to breakdown of the barrier of the cell and thus retards the normal cell processes [60]. The observed inhibition diameter zone values (in mm) of all the complexes exhibited better antimicrobial activities than the free ligand. The Cu(II), Co(II) and Zn(II) complexes showed significant antimicrobial activity compared to others (Table 7) and (Fig 6a). However, they are less active than the standard drugs (Amikacin and Ketokonazole). In addition, the activities of the complexes were confirmed by calculating the activity index (Fig 6b) according to the following relation (16).

$$\text{Activity index(A)} \% = \frac{\text{Inhibion zone of compound(mm)}}{\text{Inhibion zone of standard drug(mm)}} \times 100 \qquad (16)$$

Table 7 Evaluation of Antimicrobial activities (Diameter of zone of inhibition in mm) and Activity intex (A) % of the investigated compounds (10^{-4} M) by Agar disc diffusion method

Compounds	Antibacterial activity (% of A)					Antifungal activity (% of A)		
	E. coli (-)	*Salmonellatyphi(-)*	*Chromo bacterim (-)*	*Staph Aureus (+)*	*Bacillus Cereus (+)*	*Aspergillus Flavus*	*Aspergillus niger*	*Candida albicans*
Ligand [LH]	10 (62)	09 (47)	07 (39)	09 (47)	10 (55)	08 (47)	09 (60)	11 (69)
$[Cu(L)_2]$	15 (94)	16 (84)	14 (78)	17 (94)	16 (94)	13 (76)	14 (93)	15 (94)
$[Co(L)_2]$	14 (88)	14 (74)	15 (83)	14 (78)	14 (82)	14 (82)	13 (87)	13 (81)
[Mn(L)$_2$]	12 (75)	13 (68)	12 (67)	13 (72)	12 (71)	12 (71)	11 (73)	12 (75)
		15 (79)	14 (78)	13 (72)	11 (65)	12 (71)	13 (87)	14 (88)
		14 (74)	15 (83)	16 (89)	15 (88)	14 (82)	13 (87)	14 (88)
		19(100)	18(100)	18(100)	17(100)	---	---	---
		---	---	---	---	17(100)	15(100)	16(100)

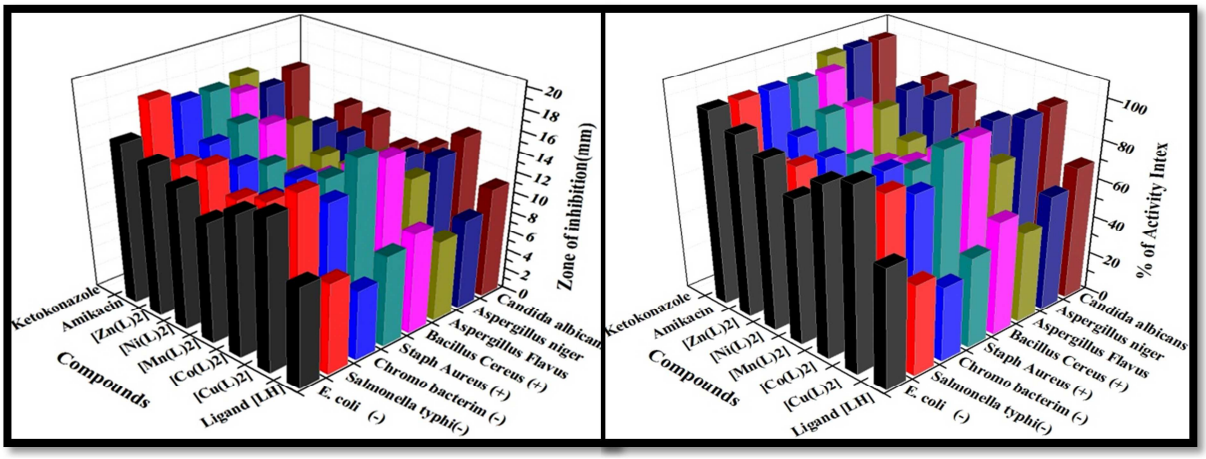

Fig. 6a. Antimicrobial activities (Diameter of zone of inhibition in mm) of the investigated compounds (10^{-4} M) by Agar disc diffusion method

Fig. 6b. Percentage of Activity intex of the investigated compounds (10^{-4} M) by Agar disc diffusion method

CONCLUSION

The work described in this report involves synthesis and characterization of Schiff base ligand and its Mn(II), Co(II), Ni(II), Cu(II) and Zn(II) complexes. The spectral data of the complexes suggest an octahedral geometry and $[ML_2]$ stoichiometry. The lower electrical conductivity values reveal that they are non electrolytes. The interaction of these complexes with DNA was investigated by gel electrophoresis. The results disclose that Cu(II), Co(II) and Ni(II) complexes have been revealed a significant DNA cleavage property than others in the presence of H_2O_2. The Binding experiment results obtained from Electronic absorption and Viscosity titration measurements indicate that the complexes are bound to DNA via intercalation and has also been observed a significant radical scavenging activity by DPPH. The most of the complexes were exposed good antimicrobial activity than the ligand.

Acknowledgements

We thank the Department of Science and Technology (DST) – Science and Engineering Research Board (SERB), Government of India, New Delhi for financial support (SERB-Ref.No.SR/FT/CS-117/2011dated 29.06.2012) and express deepest gratitude to the Managing Board, Principal and Chemistry research centre MSEC, Kilakarai for providing research facilities.

REFERENCES

[1] CT Barboiu; M Luca; C Pop; E Brewster; EM Dinculescu. *Eur. J. Med. Chem.*, **1996**, 31(7-8), 597-606.
[2] P Panneerselvam; M Gnanarupa Priya; N Ramesh Kumar; G Saravanan. *Indian. J. Pharm Sci.*, **2009,** 71(4), 428–432.
[3] P Pannerselvam; RV Pradeep Chandran; SK Sridhar. *Indian. J. Pharm Sci.*, **2003**, 65, 268–273.
[4] P Panneerselvam; RN Rajasree; G Vijayalakshmi; EH Subramanian; SK Sridhar. *Eur. J. Med Chem*. **2005**, 40, 225–229.
[5] S Liu; W Cao; L Yu; W Zheng; L Li; C Fan; T Chen. *Dalton Trans.*, **2013,** 42(16), 5932–5940.
[6] J Benítez; L Becco; I Correia; SM Leal; H Guiset; JC Pessoa; S Tanco; P Escobar; V Moreno; B Garat; D Gambino. *J. Inorg. Biochem.*, **2011**, 105, 303–312.
[7] MS Karthikeyan; DJ Prasad; B Poojary; KS Bhat, BS Holla; NS Kumari. *Bioorganic. Med.* **2006**, 14, 7482-7489.
[8] Kucukguzel; SG Kucukguzel; S Rollas; M Kiraz. *Bioorg. Med. Chem. Lett*., **2001**, 11, 1703-1707.
[9] L Zahajska; V Klimesova; J Koci; K Waisser; J Kaustova. *Arch. Pharm. Med. Chem*., **2004**, 337, 549-555.
[10] C Hemmert; M Piti´e; M Renz; H Gornitzka; S Soulet; B Meunier. *J. Bio. Inorg. Chem.*, **2001,** 6(1), 14-22.
[11] L Leelavathy; S Anbu; M Kandaswamy; N Karthikeyan; N Mohan. *Polyhedron.*, **2009**, 28, 903–910.
[12] N Shahabadi; S Kashanian; M Purfoulad. *Spectrochim. Acta A.*, **2009**, 72, 757–761.
[13] A Bishayee; A Waghray; MA Patel. *Cancer Lett*., **2010**, 294, 1–12.
[14] EK Efthimiadou; N Katsaros; A Karaliota. *Bioorg. Med. Chem. Lett.*, **2007**, 17, 1238–1242.
es-Boza; M Patricia Bradley; KL Patty Fu; E Sara Wicke; John Bacsa; R Kim Dunbar; . *chem.*, **2004,** 43, 8510-8519.
lith Burstyn. *J. Inorg. Chem*., **1996,** 26, 7474-7481.

[17] M Patricia Bradley; M Alfredo Angeles-Boza; R Kim Dunbar; Claudia Turro. *J. Inorg. Chem*., **2004,** 43, 2450-2452.
[18] C Joel1; S Theodore David; R Biju Bennie; S Daniel Abraham; S Iyyam Pillai. J. Chem. Pharm Res., **2015**, 7(5), 1159-1176.
[19] S Patitungkho; S Adsule; P Dandawate; S Padhye; A Ahmad; FH Sarkar. *Bioorg., Med. Chem. Lett*., **2011,** 21, 1802-1806.
[20] M Skander; P Retailleau; B Bourri; L Schio; P Mailliet; A Marinetti. *J. Med. Chem.*, **2010,** 53, 2146–2154.
[21] Z Wu; Q Liu; X Liang; X Yang; N Wang; X Wang; H Sun; Y Lu; Z Guo. *J. Biol. Inorg. Chem.*, **2009**, 14, 1313–1323.
[22] G Tirzitis; G Bartosz. *Acta Biochimica Polonica*., **2010**, 57(1), 139-142.
[23] E Hayet; M Maha; A Samia; M Mata; P Gros; H Raida; MM Ali; AS Mohamed; L Gutmann; Z Mighri; A Mahjoub. *World J. Microbiol. Biotechnol.*, **2008**, 24, 2933-2940.
[24] E Souri; G Amin; H Farsam; H Jalalizadeh; S Barezi. *Iran. J. Pharm. Res*., **2008**, 7, 149-154.
[25] I Fidrianny; A Rizkiya; Komar Ruslan. *Journal of Chemical and Pharmaceutical Research.*, **2015**, 7(5), 666-672.
[26] P Li; L Huo; W Su; R Lu; C Deng; L Liu; Y Deng; N Guo; C Lu; C He, *J. Serb. Chem. Soc.*, **2011**, 76(5), 709-717.
[27] T Kulisica; A Radonicb; V Katalinicc; M Milosa. *Food Chemistry*., **2004**, 85, 633–640.
[28] AA Hamid; OO Aiyelaagbe; LA Usman; OM Ameen; A Lawal. *Afr. J. of Pure and App. Chem.*, **2010**, 4(8), 142-151.
[29] RS Joseyphus; MS Nair. *Arab. J. Chem.*, **2010**, 3(4), 195-204.
[30] L Ana; Di Virgilio; Miguel Reigosa; MF Lorenzo de Mele. *J. Biomed Mater. Res B. Appl Biomater.*, **2011,** 99B(1), 111-119.
[31] J Marmur. *J. Mol. Biol.*, **1961**, 3(5), 585-594.
[32] N Raman; R Jeyamurugan; A Sakthivel; L Mitu. *Spectrochim. Acta A.*, **2010,** 75**,** 88.
[33] J B Charies; N Dattagupta; DM Crothers. *Biochemistry*., **1982**, 21(17), 3933-3940.
[34] C P Tan; J Liu; LM Chen; S Shi; LN Ji. *J. Inorg. Biochem.*, **2008,** 102(8), 1644-1653.
[35] M Sirajuddin; Nooruddin; Saqib Ali; V McKee; S Zeb Khan; K Malook. *Spectrochim. Acta A.*, **2015,** 134, 244-250.
[36] S Chandra; LK Gupta. *Spectrochim. Acta A.*, **2004**, 60(7), 1563-1571.
[37] M Silverstein; X Webster. Spectrometric Identification of Organic Compounds, 6th Edition, **1996**, 150**.**
[38] AK Singh; OP Pandey. *Spectrachim. Acta A.*, **2012**, 85, 1.
[39] Tas E; M Aslanoglu; K Kilic; OH Kaplan; Temel. *J. Chem. Res.*, **2006,** 4, 242-245.
[40] ES Aazam; AF El Husseiny; HM Al-Amri. *Arab. J. Chem.*, **2012**, 5(1), 45-53
[41] Y Li; ZY Yang; ZC Liao, ZC Han; ZC Liu. *Inorg. Chem. Commun.*, **2010**, 13, 1213-1216.
[42] MS Masoud; MF Amira; AM Ramadan; GM El-Ashry. *Spectrochim. Acta A.*, **2008**, 69**,** 230-238.
[43] M Shakir; A Abbasi; M Azam; Asad; U Khan. *Spectrochim. Acta A.*, **2011**, 79(5), 1866-1875.
[44] B Kumar Das; S Jyoti Bora; M Deepa Chakrabortty; L Kalita; R Chakrabarty; R Barman. *J. Chem. Sci.*, **2006**,118**(**6), 487–494.
[45] ABP Lever. *Inorganic Electronic Spectroscopy.*, **1968**, 2nd Ed New York.
[46] DP Singh; R Kumar; V Malik; P Tyagi. *Trans. Met. Chem*., **2007**, 32, 1051-1055.
[47] RL Dutta; A Syamal. *Elemens of magnetochemistry*., **1993**, 97, 106 (2nd Ed East-West press pvt, ISBN: 81-85336-92-X).
[48] D Kivelson; R Neeman. *J. Chem. Phys.*, **1961**, 35 (1) 149.
[49] A Syamal. *Chem. Edu*., **1985**, 62 (2), 143.
[50] AL Sharma; IO Singh; HR Singh; RM Kadam; MK Bhide; MD Sastry. *Transition Met. Chem.*, **2001,** 26, 532-537.
[51] BJ Hathaway; G Wilkinson; RD Gillard; JA McCleverty. *Comprehensive Coordination Chemistry.*, **1987**, 5 (Pergamon. Oxford press).
[52] HJHJ Fenton. *J. Chem. Soc.*, **1894,** 65, 899. doi:10.1039/ct8946500899.
[53] MSS Babu; KH Reddy; GK Pitchika. *Polyhedron.*, **2007**, 26(3), 572–580.
[54] V Uma; M Kanthimathi; T Weyhermuller; B Unni Nair. *J. Inorg. Biochem*., **2005**, 99, 2299-2307.
[55] S Parveen; F Arjmand. *Spectrochim. Acta A*., **2012**, 85(1), 53-60.
[56] W Brand-Williams; ME Cuvelier; C Berset. *LWT-Food science and Technology.*, **1995**, 28(1), 25-30.
[57] S Albayrak; A Aksoy; OM Sagdic; Hamzaoglu. *Food Chemistry*., **2010**,119 (1),114-122.
[58] P Perumal; R Rajasree. *Eur. J. Med. Chem*., **2005**, 40 (2), 225-229.
[59] KN Thimmaiah; WD Lloyd; GT Chandrappa. *Inorg. Chim. Acta*., **1985,** 106 (2), 81-83.
[60] Ji; J Dhaveethu Raja. *J. Serb. Chem. Soc*., **2008**, 73(11), 1063-1071.doi:10.2298/jsc0811063r.

Available online www.jocpr.com

Journal of Chemical and Pharmaceutical Research, 2015, 7(10S):56-66

Research Article

ISSN : 0975-7384
CODEN(USA) : JCPRC5

A study on *invitro* antioxidants, antimicrobial, antileukemia activities of *Cocos nucifera* (coconut) female flowers

Jeyaraj Dhaveethu Raja[1]* and N. Leebanon Poonkuil[2,3]

[1]Chemistry Research Centre, Mohamed Sathak Engineering College, Kilakarai, Tamilnadu, India
[2]Department of Biochemistry, New prince Shri Bhavani Arts and Science College, Medavakkam, Chennai
[3]Manonmaniam Sundaranar University, Tirunelveli, Tamil Nadu, India

---

ABSTRACT

The present study was conducted to document the knowledge of better health benefits of Coconut (Cocos nucifera) Female flowers. The waste fallen flowers can be used in ayurvedic preparations in the place of inflorescence. This studies showed that , the fallen female flowers of Cocos nucifera can be used as antimicrobial agents, to a slight extend as antitumorals and has high antioxidant activity too. On comparing with both the fresh and dried sample, the acetone : water extract of fresh has high phenolic content and was less in the case of dried sample . And it is seen that the combination of organic solvents with that of water gives better extractives than organic solvents alone in the case of fresh sample. But in the case of dried sample the single organic solvents are better than combinations in the case of yield of the extractives as well as the activity. On comparing both the fresh and dried sample, the acetone :water extract of fresh sample possess a high DPPH (2,2-diphenyl-1-picryl-hydrazyl-hydrate) scavenging activity , may take place rapidly with lower amounts of the fresh sample than that of dried sample. ABTS (2,2'-azino-bis (3-ethyl benz thiazoline-6-sulphonic acid) cation decolorisation capacity was found to be high in acetone : water extract. The other extracts like ethyl acetate : water, ethanol : water, water shows a low decolourisation capacity. In the case of dried sample, methanol extract possess a maximum decolourisation capacity while other extracts shows low decolourisation capacity. On comparing both the samples, the ABTS decolourisation capacity was more promising to fresh sample than the dried sample. Antimicrobial activity of ethyl acetate : water (fresh) and ethyl acetate (dried sample) extract of Cocos nucifera female flowers were tested in three bacteria namely Staphylococcos aureus, Escherichia coli, Bacillus subtilis. Among these three bacteria, the extracts showed antibacterial activity against Staphylococcos aureus, and was found to be inactive for other organisms. The extract exhibits a potent anti-staphylococcal activity. Probable compounds responsible for the bioactivity were identified by means of HPTLC analysis. Their structures were deduced as 5-O-caffeoylquinic acid (chlorogenic acid), dicaffeoylquinic acid and three tentative isomers of caffeoyl shikimic acid. the ethyl acetate : water extract is showing better % cytotoxicity, out of the dried sample extract of the female flowers, when different concentration of the same are subjected for % cytotoxicity against K-562, the Human Leukemia cell lines. And it is clear from the data that the antitumor activity of the dried sample extract namely ethyl acetate extract is less than that of the fresh female flower extract. There is a concentration dependent increase in the percentage of cyto toxicity of the fractions. The Purified fraction may be found to be more effective. This study concluded that fresh sample of Cocos nucifera has high antioxidant potential than the dried sample. In the case of anti tumour screening there is a concentration dependent increase in the percentage of cytotoxicity of the fractions against K562,the leukemic cell lines. Thus the waste products, the fallen fertilized female flowers have also a better position in the place of medicinal plants .

Key words: Coconut female flowers, DPPH & ABTS antioxidant, antimicrobial, anti leukemia activity.

INTRODUCTION

ces of phenolic compounds. A great number of aromatic, spicy, medicinal and other plants ound exhibiting antioxidant properties. Many of these antioxidant compound possess anti-

inflammatory, anti tumour, anti mutagenic, antibacterial or antiviral activities to a greater or lesser extent [1] . Medicinal plants play a key role in the emergence of several compounds. The ability of plants (herbal medicine) to affect the body system depends on their chemical constituent. The inflorescence sap, traditionally called "neera" is produced from the unopened spathe . It has varied commercial application for production of palm sugar, wine, jaggery and arrack in many countries. Besides, the inflorescence is used to make ayurvedic medicine. Coconut oil may boost ampicillins effectiveness because it contains lauric acid, which is known to have antimicrobial properties. Coconut palm is one of the multipurpose perennial crops of the humid tropics. *Cocos nucifera L.* was first grown as a plantation crop in the 1840's [2]. The Coconut Palm (*Cocos nucifera*) is a member of the Family Arecaceae (palm family)[3]. Coconut is a monoecious palm producing both male and female flowers on the same inflorescence. The central axis of the inflorescence has up to 40 lateral branches, each of which bears 200-300 male flowers and one or a few female flowers [4] The female flowers are usually few in number and occasionally completely absent [5]. The development of the female flowers has been studied. This fallen flowers can be used for many ayurvedic preparation. *Cocos nucifera* female flowers may possess antioxidant, antimicrobial, antitumour activity because of its phenolic contents. Because of its low toxicity it may not produce any side effects. Thus the waste products, the fallen fertilized female flowers have also a better position in the place of medicinal plants.

EXPERIMENTAL SECTION

2.1 Extraction Procedure:

Cocos nucifera female flowers were collected from Chennai during January 2015.The female flowers of *Cocos nucifera* were dried overnight in two separate tray in RRL-NC dryer at 40°C.The sample so obtained was processed in two ways. 10 g of the sample was then ground in a blender. The acetone, ethyl acetate, ethanol, water,(mixed with water in 1:1 ratio) were used to prepare the extracts. The dried powder of *Cocos nucifera* female flowers was extracted with hexane, ethyl acetate and methanol sequentially in a soxhlet apparatus. The extracts were filtered through a filter paper and concentrated in a rotary evaporator at below 50°C under reduced pressure. Each of the extracts was made up to a definite volume, keeping it as stock solution and stored below 4°C in a refrigerator.

2.2 Estimation of Total Phenolic content of Cocos nucifera Female flowers

$$\% \text{ TPC} = (\text{Observed concentration} / \text{Actual concentration}) \times 100$$

The Total Phenolic Content was determined using Folin- Ciocalteu reagent. Appropriately diluted extracts and standard gallic acid were made up to 3.5 mL using distilled water in a series of test tubes. Various extracts and standard were treated with 0.5 mL 2N Folin- Ciocalteu's reagent and incubated for 3 minutes in room temperature. The reaction was then neutralized with the addition of 1mL 20% Na_2CO_3. The reaction mixture was incubated at room temperature for 90 minutes and the absorbance of the blue color developed was read at 760nm using a Spectrophotometer (Shimadzu UV Vis - Spectrophotometer, model 2450) [6]. The Total Phenolic Contents was expressed as:

2.3 Determination of DPPH radical Scavenging Capacity

The assay contained 1mL of 0.1mM DPPH in ethanol and various concentrations of extracts and the standards in methanol were made up to 3.5 mL with methanol. The contents were mixed well immediately and then incubated for 30 minutes at room temperature (24-30ºC). The degree of reduction of absorbance was recorded in the UV-visible spectrophotometer at 517 nm (Shimadzu UV-2450)The percentage of scavenging activity was calculated as:

$$(AC-AS) / AC \times 100$$

Where AC is the absorbance of control (without extract) and AS is the absorbance of the sample.

Percentage of radical scavenging activity was plotted against the corresponding concentration of the extract to obtain IC_{50} value. IC_{50} is defined as the amount of the antioxidant material required to scavenge 50% of the free radical in the assay system. The IC_{50} values are inversely proportional to the antioxidant activity [7]

2.4 Determination of ABTS Cation Decolorisation Capacity

The ABTS radical cation ($ABTS^+$) was produced by reacting 7mM stock solution ABTS with 2.45mM potassium persulphate (final concentration) and allow the mixture to stand in the dark for at least 6 hours at room temperature solution diluted to an absorbance 0.7 ± 0.05 at 736nm. Absorbance was measured 7 minutes of different concentrations of the extracts. The $ABTS^+$ decolorisation capacity of the extracts he standard Trolox. A standard curve was prepared by measuring the reduction in the

absorbance of $ABTS^+$ solution at different concentration of Trolox over a period of 7 minutes. The percentage of scavenging activity was calculated as:

$(AC-AS)/AC \times 100$

where, Ac is the absorbance of control (without extract) and as is the absorbance of sample [8].

2.5 Estimation of Anti leukemia activities

Cells harvested in the log phase of growth were counted and seeded (5×10^3 cells/well in 100 µL) in 96 well titer plates. PBS was added to the outer wells (200µL/well). To allow cell attachment (in the case of adherent cells), cultures were treated with varying concentrations of the extract in medium and were incubated at 37°C in 5% CO_2 for 24 hours .Each treatment was carried out in triplicates. Untreated cells served as negative control. The plates were incubated for 48 and /or 72 hours. On completion of incubation, the media were removed from wells without disturbing the cells. To each well 100µL of 1mg/mL solution of MTT were added and plates were incubated for 2 hours in dark at 37ºC in a CO_2 incubator. 100 µL of lysis buffer was added to each well and the plates were further incubated for 4 hours in dark in a CO_2 incubator. After the incubation period, absorbance was read at 570 nm using a multi well plate reader [9] and % of cyto toxicity was calculated as,

$$\% \text{ of Cytotoxicity} = 100 - \frac{\text{OD of the treated cells}}{\text{OD of control cells}} \times 100$$

2.6 Determination of Antibacterial activity

Organisms used : *Staphylococcos aureus, Escherichia coli, Bacillus subtilis.* Antibiotics used: Ampicillin

Broth dilution technique:

The tubes with nutrient broth were sterilized. The tubes were removed from the autoclave and mixed well. The flask was then cooled and cultures were inoculated. And kept in a rotary shaker for 2 hour at 37ºC at 120 rpm. The organisms were selected for the experiment once the OD reaches 0.3 at 650 nm. 10 mg of *Cocos nucifera* flower extract was dissolved in 1mL DMSO. Plated 100 µL of cells into all the wells in a 96 well plate. Added 100 µL of different concentrations of the serially diluted extracts. Positive (with Ampicillin) and negative control cells were treated with 10% DMSO diluted in Nutrient broth and added in respective wells. The plate was incubated at 37ºC for 48 hours. Absorbance was taken at 620 nm in an ELISA reader and the % inhibition was calculated as follows:

$\%\ \text{inhibition} = 100 - (T/C) \times 100$

Where T = absorbance of the test sample
C =absorbance of control [10]

2.7 Isolation of chemical constituents from the active extracts by HPTLC :

As the chemical constituents of hexane and ethyl acetate extracts behave similarly on TLC ,mixed and a column chromatography was performed over silica gel(100-120 mesh) size of 1:30(w/w). and the column was eluted with hexane, ethyl acetate and methanol in increasing polarity. Readymade HPTLC plates (kieselgel 60 F_{254}, 20cm x 20cm, 0.2mm thickness, Merck, Darmstadt Germany) was kept at 60°C for 5minutes. The samples were spotted in the form of bands of width 6mm with a Hamilton micro liter syringe using a Camag Linomat V (switzer land). A constant application rate of 0.1mL/s was employed and the space between two bands was maintained as 5 mm. The plates were developed in an ascending manner with a solvent system consisting of 5:4:1 acetic acid: ethylacetate : water in a developing chamber pre saturated with the mobile phase. The developed plates were dried and scanned at 290nm (TLC scanner 3, Camag, Switzerland). Data processing was performed using the software 'WinCATS planar chromatography manager [11-12].

RESULTS AND DISCUSSION

Table 1 revealed that among the fresh extract, 1:1 acetone :water possess a total phenolic content of 37.450 mg/g of the extract and also it shows the high antioxidant effects. The total phenolic content was less in other extracts like ethanol :water (1:1)and ethyl acetate :water 1:1.The water extract has comparable total phenolic content that of 1:1 acetone extract in the case of fresh extract of the female flowers. The values are tabulated in Table1. In the dried extract methanol possess a high total phenolic content and it was found to be 24.381mg/g extract and the phenolic d in other extracts like ethyl acetate and hexane (21.864, 20.935). On comparing with both uple, the acetone :water (1:1) extract of fresh has high phenolic content and was less in the Thus it is clear from the studies that total phenolic content extraction has to be monitored

using different combinations of solvents. And it is seen that the combination of organic solvents with that of water gives better extractives than organic solvents alone in the case of fresh sample. But in the case of dried sample the single organic solvents are better than combinations in the case of yield of the extractives as well as the activity [13-14].

The Table 2 revealed the concentration of various extracts required for the 50% inhibition (IC_{50}) of DPPH . It was seen that as in the case of Total phenolics, the radical scavenging activity was also higher in acetone :water (1:1) extract and it was found to be 21.68 µg/ µL of the extract. The following extracts like water, ethanol :water, ethyl acetate :water, shows low scavenging activity due to the less phenolic content and the values are found to be (25.32,32.19 41.54). In case of dried sample, methanol extract shows a better scavenging activity and it was found to be 75.75 µg/ µL**.** Other extracts like hexane and ethyl acetate shows a less scavenging activity and the values are found to be (180.633, 274.23 µg/ µL). On comparing both the fresh and dried sample**,** the acetone :water extract of fresh sample possess a high scavenging activity. The mechanism of action of DPPH Scavenging may take place rapidly with lower amounts of the fresh sample than that of dried sample. The exact mechanism could be identified by isolating the active principle and its structure. Here also the activity is more predominant for the fresh sample extract. This may be due the difference in the chemical components present in the different extracts. That may be due to some chemical changes take place during drying .Graph 1,2,3. Shows the graphical representation DPPH Scavenging Activity. Topic treatment of rabbits with the *Cocos nucifera* extract indicated that it does not induce any significant dermic or ocular irritation. In vitro experiments using the 2,2-diphenyl-1-picryl-hydrazyl-hydrate (DPPH) photometric assay demonstrated that this plant extract also possesses free radical scavenging properties [15].

The Table 3 revealed ABTS cation decolorisation capacity was found to be high in acetone :water extract (1:1) and the value was found to be 6.27 (µg/ µL). The other extracts like ethyl acetate :water, ethanol :water, water , shows a low decolourisation capacity and it was found to be (11.98, 11.98,18.27) .In the case of dried sample, methanol extract possess a maximum decolourisation capacity of 20.11(µg/µL), while other extracts shows low decolourisation capacity. On comparing both the samples, the ABTS decolourisation capacity was more promising to fresh sample than the dried sample. The inhibitory concentrations for 50% activity was compared with the standard trolax and listed in Table 3. It is found from the results that the acetone water extract is some what comparable to the standard Trolax. By fractionating this extract the activity can be increased and can be made even better than the standard Trolax [14].

In all the antioxidant methods performed, the fresh female flowers of *Cocos nucifera* possess a high antioxidant activity when compared with dried sample. And also the acetone : water (1:1) is the most active extract of the fresh sample and the methanol extract of the dried flowers showed better activity out of the three extract of the dried sample tested. Graph 4,5,6 Shows the graphical representation ABTS Cation Decolorisation Capacity [15].

K-562, the Human Leukemia cell lines were used for the antitumor studies. Table 4 shows that the active extracts namely ethyl acetate :water(1:1) and ethyl acetate at concentration like 200 µg/mL, 400 µg/mL , 800 µg/mL were used for the study. The result showed that the % cyto toxicity is increasing in accordance with the increase in concentration i.e dose dependent manner. In the case of fresh female flowers (ethylacetate :water) extract the activity is 29% at 800 µg/mL, while 21% at 400 µg/mL and 5% for 200 µg/mL. As the ethyl acetate :water (1:1) extract is showing better % cyto toxicity, out of the dried sample extract of the female flowers, when different concentration of the same are subjected for % cyto toxicity. And it is clear from the data that the antitumor activity of the dried sample extract namely ethyl acetate extract is less than that of the fresh female flower extract. There is a concentration dependent increase in the percentage of cyto toxicity of the fractions. The low activity may be due to the crude nature of the sample. Purified fraction may be found to be more effective. After studying the acute toxicity levels of the extracts higher concentration can be employed for antitumor studies invitro as well as invivo. This is well evident from the Graph 7. *C. nucifera* extracts were also active against Lucena 1, a multidrug-resistant leukemia cell line. Their cyto toxicity against this cell line was about 50% (51.9 ± 3.2 and 56.3 ± 2.9 for varieties typical A and common, respectively). Since the common *C. nucifera* variety is extensively cultured in Brazil and the husk fiber is its industrial by-product, the results obtained in the present study suggest that it might be a very inexpensive source of new anti neo plastic and anti-multidrug resistant drugs that warrants further investigation [9].

Out of the different extracts on antimicrobial activity studies at higher concentration, two of the extracts namely Ethylacetate :water (1:1) extract of the fresh *Cocos nucifera* female flowers and the ethyl acetate extract of the dried sample gave some inhibitory effects. And thus a detailed study of these two extracts were performed on three er different concentrations. Higher antimicrobial activities were obtained in the crude extract en compared with fresh sample. Antimicrobial activity of ethyl acetate :water (1:1) (fresh) d sample) extract of *Cocos nucifera* female flowers were tested in three bacteria namely

Staphylococcos aureus, *Escherichia coli*, *Bacillus subtilis*. Among these three bacteria, the extracts showed antibacterial activity against *Staphylococcos aureus*, and was found to be inactive for other organisms. The IC_{50} values were calculated and the value was found to be 1.02mg/mL for the crude ethyl acetate extract of the dried sample and 2.75 mg/mL for the fresh ethyl acetate: water (1:1) extract. Comparing the IC_{50} values, the crude extract shows more cyto toxicity towards the bacteria and there is a dose dependent increase in the inhibition of the microbes. As the concentration of the drug increases, the % cytotoxicity also increases. The results are tabulated in Table 5 and this is well evident from the Graph 8. In the case of *Bacillus subtilis* , table 6 shows the % cyto toxicity varies from 16.25 mg/mL to 0.313 mg/mL at various concentration ranging from 5mg /mL to 0.3125 mg/ mL for ethyl acetate extract (dried) and for the ethyl acetate : water (fresh) extract, the % cyto toxicity varies from 17.187 to 5.93% at concentration ranging from 5 mg to 0.3125 mg. Since the % cyto toxicity is less than 50%, we cannot found out the IC_{50} values. This is well evident from the Graph 9. In the case of *E coli* table 7 the % cyto toxicity varies from 19.70 to 6.470 % at various concentration ranging from 5mg to .3125 mg for ethylacetate extract and for the ethylacetate : water extract the % cyto toxicity varies from 18.23 to 8.23 % at concentration ranging from 5 mg to .3125 mg. Since the % cyto toxicity is less than 50%, we cannot found out the IC_{50} values. This is well evident from the Graph 10 .Antimicrobial activity of the crude mesocarp extract was tested against *Staphylococcus aureus* ATCC 25923, *Bacillus subtilis* ATCC 441, *Escherichia coli* ATCC 25922 and *Pseudomonas aeruginosa* MTCC 7925. The extract exhibits a potent anti-staphylococcal activity. Probable compounds responsible for the bioactivity were identified by means of HPTLC analyses. Their structures were deduced as 5-*O*-caffeoylquinic acid (chlorogenic acid), dicaffeoylquinic acid and three tentative isomers of caffeoyl shikimic acid. This is well evident from the Graph 11.

Table 1 Determination of Total phenolic content of extracts of *Cocos nucifera* female flowers

Sl. No.	Name of the parts	Name of the Extract	TPC (mg/g. of extract)
1	Fresh	Acetone : Water Extract(1:1)	37.450
		Ethyl acetate:water extract (1:1)	31.471
		Ethanol:water extract (1:1)	32.645
		Water extract	35.662
2	Dried	Hexane extract	20.935
		Ethyl acetate extract	21.864
		Methanol extract	24.381

Table 2 Determination of DPPH radical Scavenging Capacity of *Cocos nucifera* female flowers

Sl.No	Name of the parts	Name of the standard/ Extract	IC_{50} (µg/µL)
1	-	Gallic acid	1.57
2	Fresh	Acetone :water extract (1:1)	21.68
		Ethyl acetate :water extract (1:1)	41.54
		Ethanol :water extract (1:1)	32.19
		Water extract	25.32
3	Dried	Hexane extract	180.633
		Ethyl acetate extract	274.23
		Methanol extract	75.75

Table 3 Determination of ABTS Cation Decolorisation Capacity of *Cocos nucifera* female flowers.

Sl. No.	Name of the parts	Name of the Extract	IC_{50} (µg/µ L)
1	-	Trolax	2.066
2	Fresh	Acetone:water Extract (1:1)	6.27
		Ethyl acetate:water Extract (1:1)	18.27
		Ethanol :water (1:1)	11.947
		Water extract	11.98
3	Dried	Hexane Extract	66.131
		Ethyl acetate Extract	122.35
		Methanol Extract	20.11

Table 4 Determination of Anti leukemia activity of *Cocos nucifera* female flowers

Sl.No	Name of the extract	Cells used	Concentration of the extract(µg/m L)	% of Cyto toxicity
1	Ethylacetate:water(1:1) (fresh)	K-562(Human leukemia cells)	200	5
			400	21
			800	29
2	Ethyl acetate	K-562(Human leukemia cells)	200	8
			400	9
			800	14

Table 5 Determination of Antibacterial activity of *Cocos nucifera* female flower against *Staphylococcos aureus*,

Sl.No	Name of the extract	Name of the organism	Concentration of the extract (mg/m L)	% of Cyto toxicity	IC_{50} (mg/mL)
1	Ethylacetate (dried)	*Staphylococcos aureus*	5 2.5 1.25 0.625 0.3125	60 55.8 51.3 47.2 43	1.0228
2.	Ethylacetate:water(1:1) (Fresh)	*Staphylococcos aureus*	5 2.5 1.25 0.625 0.3125	58 49.07 47.85 42.15 37.85	2.75

Table 6 Determination of Antibacterial activity of *Cocos nucifera* female flower against *Bacillus subtilis*

Sl.No	Name of the extract	Name of the organism	Concentration of the extract (mg/m L)	% of Cyto toxicity
1	Ethylacetate (dried)	*Bacillus subtilis*	5 2.5 1.25 0.625 0.3125	16.25 9.687 8.4375 3.75 3.125
2.	Ethylacetate:water(1:1) (Fresh)	*Bacillus subtilis*	5 2.5 1.25 0.625 0.3125	17.187 15 12.18 7.187 5.93

Table 7 Determination of Antibacterial activity of *Cocos nucifera* female flower against *Escherichia coli*

Sl.No	Name of the extract	Name of the organism	Concentration of the extract (mg/m L)	% of Cytotoxicity
1	Ethylacetate (dried**)**	*Escherichia coli*	5 2.5 1.25 0.625 0.3125	19.70 14.41 12.64 12.05 6.470
2.	Ethylacetate:water(1:1) (Fresh)	*Escherichia coli*	5 2.5 1.25 0.625 0.3125	18.23 15.29 14.11 12.05 8.23

Graph 1 Determination of DPPH scavenging activity of standard gallic acid

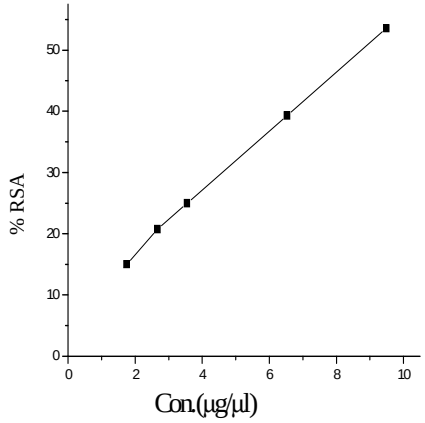

Graph 2 Determination of DPPH scavenging activity for dried female *C.nucifera* flowers

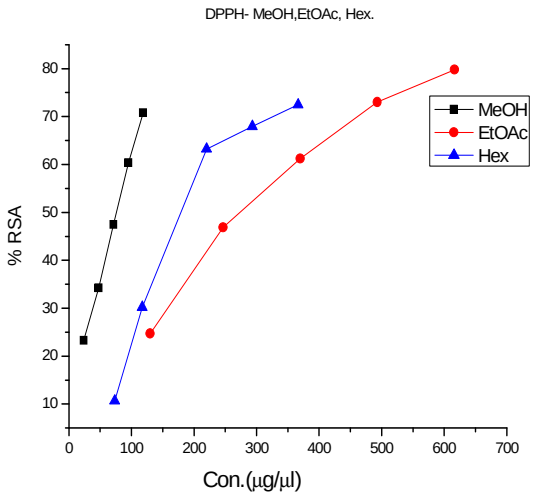

- radical scavenging activity, MeOH – methanol extract, EtOAc – ethyl acetate extract, Hex – hexane extract

Graph 3 Determination of DPPH scavenging activity for fresh female *C.nucifera* flowers

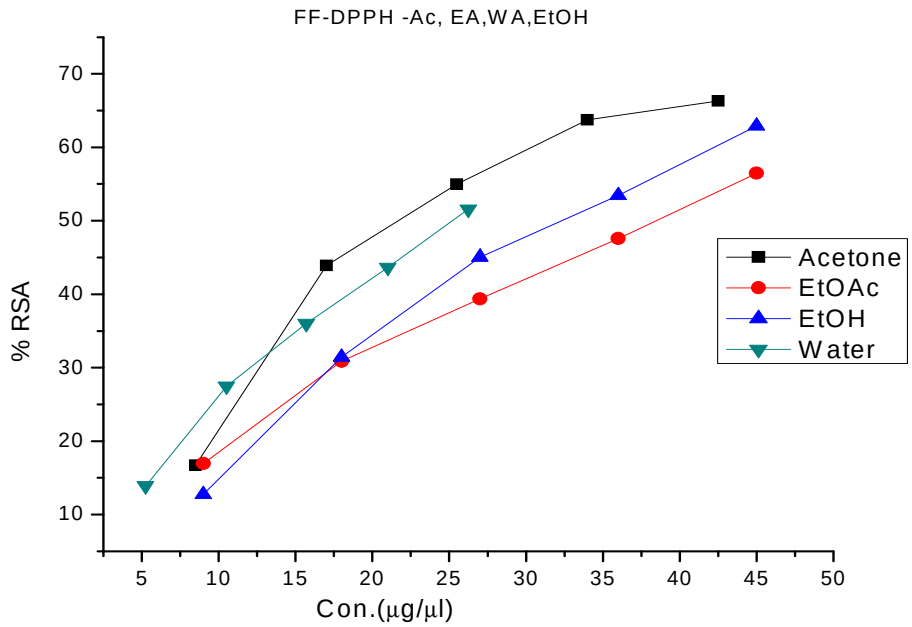

Con - concentration ,% RSA - radical Scavenging Activity, EtOAc – ethyl acetate : Water (1:1) extract, Acetone - acetone : water (1:1) extract, EtOH - ethanol : water (1:1) extract, Water – water extract

Graph 4 Determination of ABTS Cation Decolorisation Capacity Of Standard Trolox

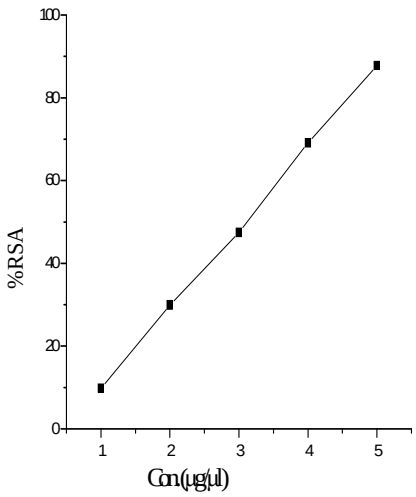

Graph 5 Determination of ABTS Cation Decolorisation Capacity for fresh *C.nucifera*

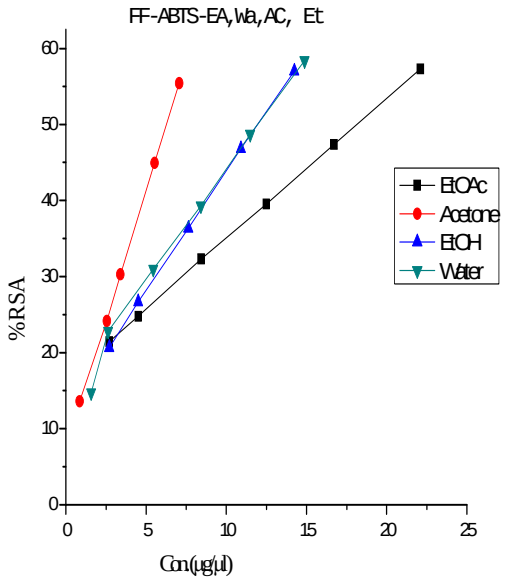

Con - concentration ,% RSA - radical scavenging activity, EtOAc – ethyl acetate : Water (1:1) extract, Acetone - acetone : water (1:1) extract, EtOH - ethanol : water (1:1) extract, Water – water extract

Graph 6 Determination of ABTS Cation Decolorisation Capacity for dried female *Cocos nucifera* flowers

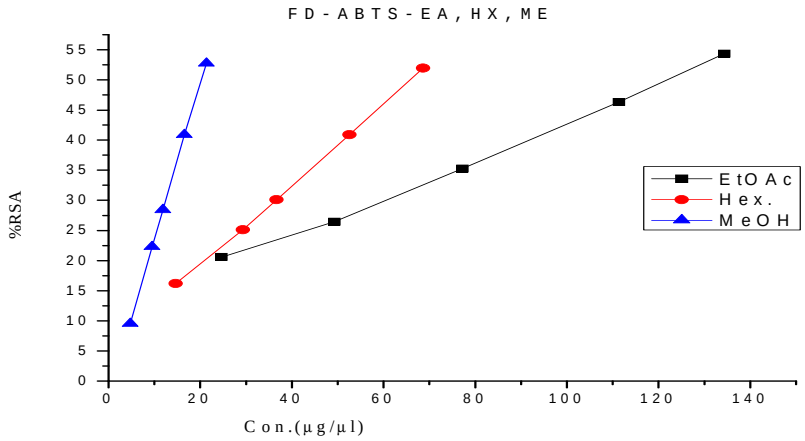

Con - concentration ,% RSA - radical scavenging activity, MeOH – methanol extract, EtOAc – ethyl acetate extract, Hex – hexane extract

Graph 7 Determination of Anti leukemia activity of fresh and dried *C.nucifera* female flowers

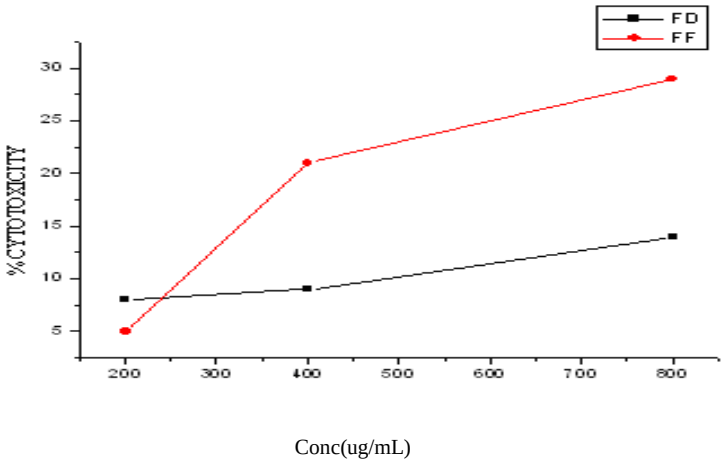

Graph 8 Determination of Antibacterial activity of *Cocos nucifera* female flowers against *Staphylococcos aureus*

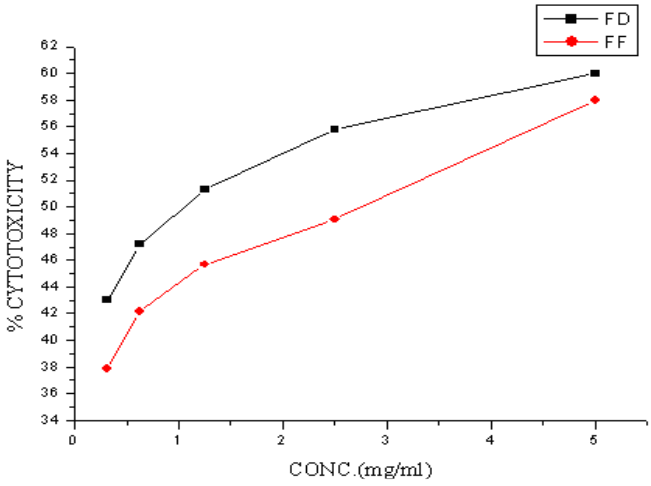

Graph 9 Determination of Antibacterial activity of *Cocos nucifera* female flowers against *Bacillus subtilis*

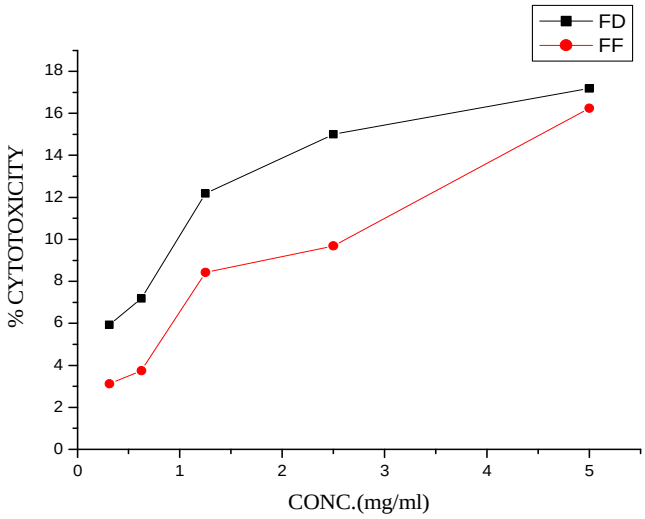

Graph 10 Determination of Antibacterial activity of *Cocos nucifera* female flowers against *Escherichia coli*

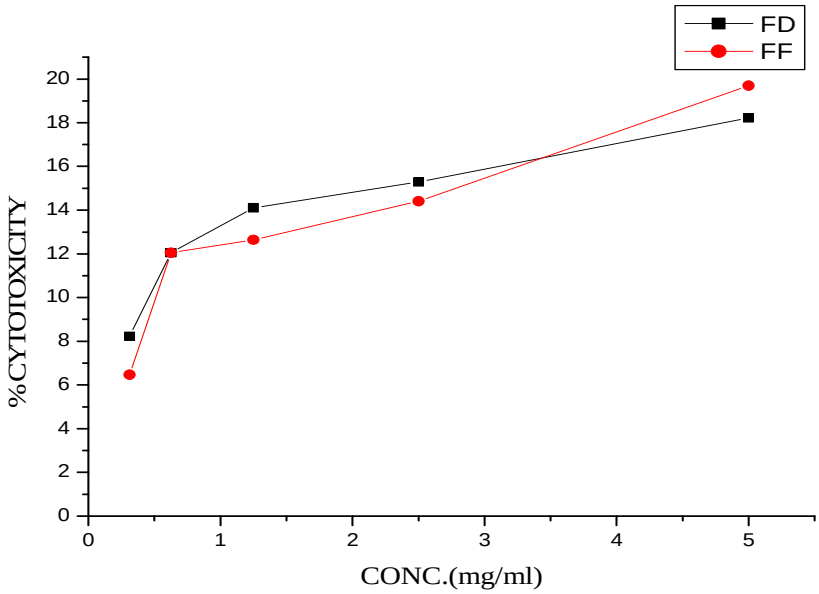

Conc – concentration,FD – female dried extract,FF – female fresh extract

Graph 11 HPTLC chromatogram of *Cocos nucifera* female flowers sample

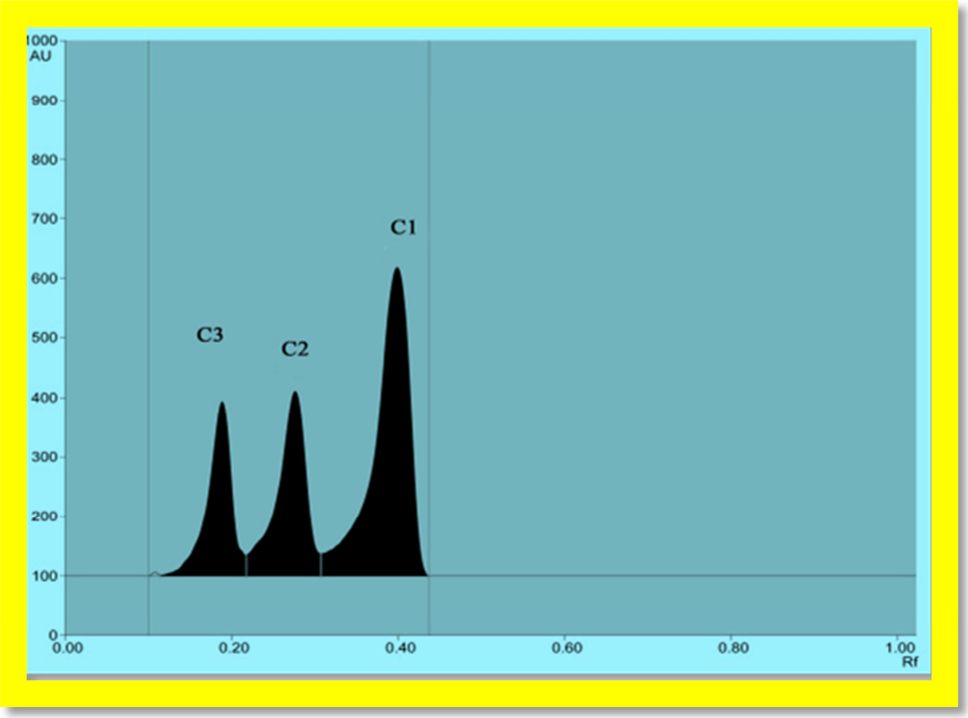

C1-5-Ocaffeoylquinic acid (chlorogenic acid); C2- dicaffeoylquinic acid ;C3- caffeoyl shikimic acid

CONCLUSION

Antioxidant activities of the extracts of different increasing polarity namely hexane, ethyl acetate, methanol of *Cocos nucifera* dried female flowers , a waste from coconut tree were compared in three different assays ,total phenolic content, DPPH radical scavenging activity and ABTS cation decolorisation capacity. It was shown that acetone :water (1:1) extract of fresh sample were having high antioxidant activity compared to other extracts. In comparison of different extracts of dried sample, methanol extract has the highest antioxidant activity of all the tested extracts and in all the assays. The study, concluded that fresh sample of *Cocos nucifera* has high antioxidant potential than the dried sample. In the case of anti tumour screening there is a concentration dependent increase in the percentage of cyto toxicity of the fractions against K562,the leukemic cell lines. The low activity may be due to the crude nature of the sample. Purified fraction may be found to be more effective. And also the activity can be increased by increasing the concentration of the extract as these extracts are non toxic in nature.

Among three bacteria namely, *Staphylococcos aureus* , *Bacillus subtilis*, *Escherichia coli* the crude extracts showed antibacterial activity against *Staphylococcos aureus* , and was found to be less active for other organisms. The Table 5,6,7 clearly indicated the antimicrobial effects against the pathogens listed above. The IC_{50} values were calculated and the value was found to be 1.02mg/mL for the crude ethyl acetate extract of the dried sample and 2.75mg/mL for the fresh ethyl acetate :water (1:1) fresh extract for *Staphylococcos aureus* . The antibacterial activities , by comparing the IC_{50} values, the crude extract shows more cyto toxicity towards the bacteria *Staphylococcos aureu*s and there is a dose dependent increase in the inhibition of the microbes in total. The Table 4 indicated that as the concentration of the drug increases, the % cyto toxicity also increases and the antimicrobial activity .

Because of the better health benefits , *Cocos nucifera* inflorescence has been used as functional food during pregnancy and child birth period. *Cocos nucifera* was known as tree of life because of its valuable uses. Each and every part of coconut tree is used in different preparation of ayurveda and all it's parts are edible, this can be considered as the Tree of Life . This studies showed that , the fallen female flowers of *Cocos nucifera* can be used as antimicrobial agents, to a slight extend as antitumorals and has high antioxidant activity too.

This fallen flowers can also be used for better ayurveda preparation for good health of mankind without plucking the
Thus the waste products, the fallen fertilized female flowers have also a better position in the
ts. Now a days ayurvedic preparations were made out of the whole inflorescence and thereby
uction of the coconut and hence the lowering of income to the country. As the economy of
much dependent on the production of coconut and its products, the waste, the fallen flowers

can be used in ayurvedic preparations in the place of inflorescence. The isolation of the active compounds from the extracts were completed and its structural elucidation of the particular compounds are under progress.

Acknowledgements
The authors greatly acknowledge the help of Management and Director, Principal from New prince Shri Bhavani Arts and Science College, Medavakkam, Chennai and Mohamed Sathak Engineering College, Kilakarai who provided constant encouragement and research facilities. The authors express sincere thanks to the Science and Engineering Research Board (SERB)-Department of Science and technology (DST), New Delhi for financial assistance.

REFERENCES

[1] PIP Perera; V Hocher; JL Verdeil; S Doulbeau; DM Yakandawala; LK DWerrakoon. *Plant cell reports*, **2007** ,20(1), 21-28.
[2] PR Koschek; DS Alviano; CK Gattass. *Brazilian Journal of Medicinal and Biological research*, **2007**, 40(10):1339-1343.
[3] CY Lim-Sylianco; AY Guevarra; E Serrame; N De Guzman; MP Casino; L Sylianco-Wu. *Philippines Journal of Science*, **1991**, 120(4): 339.
[4] K Arzani; F Zare-Mahandi; ME Amiri. *Indian Journal Agricultural Sciences*, **2005**,75(II): 731-734.
[5]V Melendez-Ramirez; V Parra-Tabla; PG Keran; I Ramirez-Morillo; H Harries; M Fernandez-Barrera; D Izumbo Villarear. *Agricultural and Forest Entamology*, **2004**, 6(2):155-163.
[6] D Gargi; C Moumita; M Adinpunya. *Journal of Plant Physiology*, **2005**,162(4):375-381.
[7] M Dizdaroglu; P Jaruga; M Birincioglu; H Rodriguez. *Free Radical Biological Chemistry*, **2002**,3(2): 1102-1115.
[8] JP Kehrer; ME Murhy. Free radicals in muscular dystrophy: In Free radical Mechanisms of Tissue Injury, CRC Press BacaRaton, Florida, **1992**;189-202.
[9] PIP Perera; IP Wickremasinghe; WMV Fernando. *Journal of National Science Foundation of Sri Lanka*, **2008**,36(1):103-108.
[10] HG Preuss; B Echard; M Enig; I Brook; TB Elliott. *Molecular cell Biochemistry*, **2005** , 2(72): 29-34.
[11] GE Liya; et al. *Journal of Chromatography B: Analytical technologies in the Biomedical and Life Sciences*, **2005**, 829(12): 26-34.
[12] Ma-Zhen;et al. *Analitica Chimica Acta*, **2008**, 610(2): 274-281.
[13] M Moumita Chakraborty; M Adinpunya Mitra. *Food Chemistry*, **2008**, 107(3): 994-999.
[14] CA Rice Evans; NT Miller; G Paganga. *Free Radical Biology Med*, **1996** , 20(1): 933-956.
[15] H Bayir. *Crit. Care Med*, **2005**, 33(12): 498-501.

Available online www.jocpr.com

Journal of Chemical and Pharmaceutical Research, 2015, 7(10S):67-76

Research Article

ISSN : 0975-7384
CODEN(USA) : JCPRC5

Synthesis of transition metal(II) complexes from piperonal condensed schiff base: Structural elucidation, antimicrobial, antioxidant, DNA-binding and oxidative cleavage studies

Jeyaraj Dhaveethu Raja[1]*, Shahulhameed Sukkur Saleem[1], Karunganathan Sakthikumar[1], Murugesan Sankarganesh[2] and Manokaran Vadivel[1]

[1]Chemistry Research centre, Mohamed Sathak Engineering College, Kilakarai, Tamilnadu, India
[2]Department of Chemistry, Sethu Institute of Technology, Pulloor, Kariapatti, Virudhunagar (Dist), Tamil Nadu, India

---

ABSTRACT

A new series of transition metal Mn(II), Co(II), Ni(II), Cu(II) and Zn(II) complexes have been synthesized from N,N'-bis[1,3-benzodioxol-5-ylmethylene]ethane-1,2-diamine(L) Schiff base ligand in 1:2 molar ratio. The resulting complexes were characterized by elemental analysis, Magnetic susceptibility, Molar conductance, IR, UV-Vis, ^{1}HNMR, EPR and ESI-Mass Spectral techniques. The UV Visible, Magnetic Susceptibility and EPR spectral data of these complexes suggest an octahedral geometry around the central metal ion and found to possess [ML_2] stoichiometry. All compounds were screened for their in vitro antimicrobial activity against selected bacterial strains and fungi by the disc diffusion method. A comparative study of zone inhibition values (mm) of the ligand and its metal complexes indicates that metal complexes exhibit higher antimicrobial activity than free ligand. The DNA cleavage activity of all compounds was monitored by the agarose gel electrophoresis method. In this result Co(II), Ni(II) and Cu(II) complexes showed a completely cleavage property than others. Invitro antioxidant and DNA-binding properties of these complexes have been investigated by electronic absorption technique. The intrinsic binding constants (K_b) for Co(II), Ni(II) and Cu(II) complexes are found as 3.02 x 10^5, 2.93 X 10^5 and 4.84 X 10^5 M^{-1} respectively. The binding affinity to DNA has also been investigated by viscosity titration measurements which was observed in the order of EB > Cu(II) > Co(II) > Ni(II).The experimental results suggest that the complexes bind to DNA via intercalation.

Key words: Schiff base, Octahedral, DPPH, DNA binding, Oxidative Cleavage

---

INTRODUCTION

In recent years, the development in the field of bioinorganic chemistry has increased the interest in Schiff base metal complexes because of O, N and S play a key role in the coordination of metals at the active sites of numerous metallo bio molecules [1]. The metal ions bonded to biologically dynamic compounds may enhance their activities [2-4]. Piperonal condensed Schiff bases and their metal complexes have variety of applications in biological, clinical, analytical and pharmacological fields [5-6]. Large number of biological experiments has confirmed that DNA is the primary intracellular target of anticancer drugs; interaction between small molecules and DNA can cause damage in cancer cells, inhibiting the division and resulting in cell demise [7-8]. Besides, due to the ability of Copper(II) complexes to cleave DNA, many find possible medical uses in the treatment of diseases including cancer [9]. The synthetic anti-oxidant 2, 2-diphenyl-1-picrylhyrazyl (DPPH) was used as preservatives in foods. It can be ioration of food flavours and odours and increase the shelf life of many foods. Free-radical ants which can provide protection to living organisms from damage caused by uncontrolled oxygen species and subsequent lipid peroxidation, protein damaging and DNA strand wn that the antioxidant activity is reasonably related to the electrochemical behaviour where

low oxidation potential meant high antioxidant power [10]. Our present work report regarding the synthesis, structural elucidation, antimicrobial, antioxidant, DNA binding and cleavage studies of Transition Metal(II) complexes.

EXPERIMENTAL SECTION

Materials and Methods

The starting materials piperonal, Ethylene diamine, $Cu(CH_3COO)_2.H_2O$, $Zn(CH_3COO)_2.2H_2O$, $Mn(CH_3COO)_2.4H_2O$, $Co(CH_3COO)_2.4H_2O$ and $Ni(CH_3COO)_2.4H_2O$ were purchased from Sigma Aldrich and other reagents and solvents were of analytical grade.

Instrumentation

Melting points of all the compounds were noted on Cintex apparatus (Guna-BMQR) in open glass capillaries. The C, H, and N contents of the synthesized ligand and the complexes were performed by Elementar Vario EL III CHNS Molar Conductivity of complexes in methanolic solution (10^{-3}M) were recorded at room temperature by systronics model 304 digital conductivity bridge using a dip type conductivity cell fitted with a platinum electrode. Magnetic susceptibility for powder sample of the complexes was recorded by Guoy balance at room temperature. IR spectra of Schiff base and their complexes were recorded on a Shimadzu FT-IR spectrophotometer in the range of 4000 to 400 cm^{-1}. Electronic absorption spectra of all compounds were recorded in methanolic solution (10^{-3}M) by Shimadzu UV Vis 1800 spectrophotometer in the range of 200 to 1100 nm. Antioxidant and DNA binding studies were examined by Shimadzu UV Vis 1800 spectrophotometer. DNA Cleavage studies of all compounds were carried out by agarose gel electrophoresis technique in the presence of H_2O_2. The ^1H NMR spectra of the ligand and its zinc complex were recorded on a Bruker 300 MHz NMR spectrometer using $CDCl_3$. EPR spectra of powder sample of the copper (II) Complex were recorded on a Varian E112 EPR spectrometer at RT and LNT using TCNE as the field marker (g_e= 2.00277). Mass spectra of Schiff base and their complexes were recorded on ESI-MS 3000 Bruker Daltonics instrument.

Synthesis of Schiff base ligand (L)

Piperonal (0.02 M) in 40 ml of ethanol was stirred with ethylene diamine (0.01 M) and the resulting mixture was stirred and refluxed for 1 hr. The white precipitate formed was filtered and recrystallised from chloroform. The pure solid was dried at room temperature in vacuum desiccators over anhydrous Calcium Chloride. The yield was found to be 78.9 %.

Synthesis of metal complexes (ML_2)

A solution of Schiff base ligand (0.004M) in chloroform (40 mL) was added slowly to a solution of Metal(II) acetate (0.002M) in 30 ml of absolute methanol. The resulting mixture was vigorously stirred and refluxed for 2 hrs. The solution was then reduced to one-third on water bath; the solid complex precipitated was filtered, washed carefully with ethanol and dried at room temperature in vacuum desiccators over anhydrous $CaCl_2$. Similarly, all complexes were obtained and the yield was found to be 62–84 %. (Scheme 1)

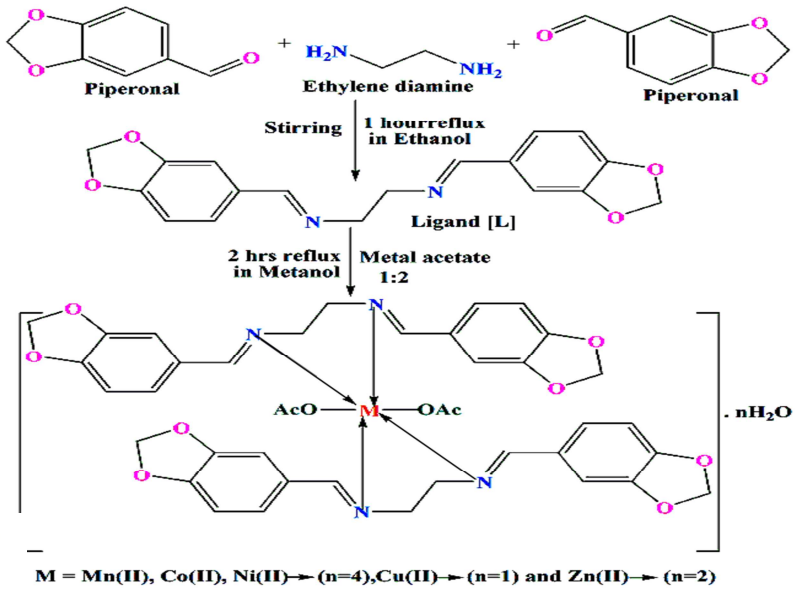

ıeme 1. Schematic representation of synthesis of ligand & the coordinated complexes

DNA interaction studies

Gel electrophoresis for DNA cleavage

DNA cleavage activities of the ligand and its metal complexes with CT DNA were monitored by agarose gel electrophoresis [11-12]. The experiments were performed under aerobic conditions with H_2O_2 by incubation at 35^0C for 2 hours. When 50 V of power supply was being passed into the tank buffer solution, the DNA migration was occurred towards to positive pole. At the end of electrophoresis, the electric current was turned off, the gel layer was taken out from the tank solution and was snapped under a UV-Trans illuminator and the bands were observed the extent of DNA cleavage by comparing with standard DNA marker.

Absorption spectroscopic studies

Electronic absorption spectroscopy is one of the most powerful techniques to examine the binding mode of DNA with metal complexes. The Concentrated CT-DNA stock solution was prepared in 5 Mm Tris–HCl/50 mM NaCl in deionized water at pH 7.5. The purity of DNA was verified by monitoring the ratio of absorbance at nearly 260 nm to that at 280 nm, A_{260}/A_{280} there was in the range 1.8–1.9 indicating that the DNA is sufficiently free from protein and the initial concentration of the CT DNA was confirmed from its absorption intensity (A) at 260 nm with a molar extinction coefficient (ε) of 6600 M^{-1} cm^{-1} [13].

In vitro antimicrobial assay

Antimicrobial activities of the ligand and its metal complexes (10^{-4}M) were screened *in vitro* against the selected pathogenic bacterial strains and fungi species by the disc diffusion method. Sparfloxacin and Ketokonazole were used as standard drugs for antibacterial and antifungal studies respectively. The saturated paper discs were placed aseptically in the Petri dishes containing Mueller Hinton nutrient agar with 2% of glucose media inoculated with pathogenic bacteria and fungi separately. The inoculated culture plates were incubated at 37°C for 24 hrs for the bacteria and at 30°C for 48 hrs for the fungi. After incubation, the antimicrobial activity was evaluated by measuring the diameter (in mm) of the inhibition zone formed around the discs [14].

DPPH radical scavenging studies

3.9037 mg of DPPH was dissolved in 3.3 mL methanol. 0.3 mL of the stock solution (3 mM) was added to 3.5 mL methanol (2.5714 $X10^{-4}$ M) and absorbance was noted immediately at 517 nm for the control. Various concentration solutions (2.9411, 6.0606, 9.3750, 12.9032 and 16.6666 $X10^{-5}$ M) were prepared in methanol using 1mM test samples and 3 mM DPPH stock solution. The resulting mixture was incubated in dark at room temperature for 1 hour. It was protected from light by covering the test tubes with aluminium foil. While DPPH reacts with an antioxidant compounds which can donate hydrogen, it is reduced. The changes in colour from deep violet to light yellow and absorbance of the resulting solution was measured by UV-visible spectrophotometer at 517 nm. The control was measured from the values of absorbance of the DPPH radical without antioxidant and Special care was taken to minimize the loss of free radical activity of the DPPH radical stock solution [15].

RESULTS AND DISCUSSION

Synthesis and characterization

The synthesized ligand and its metal complexes were found to be intensely coloured and they were slightly hygroscopic nature at room temperature. The analytical data and physical properties of the ligand and its metal complexes are listed in Table 1.

Elemental analysis

The purity of the compounds was determined by the elemental analysis (C, H, N and metal contents) and the result shows they are in good agreement with the proposed formula (Table 1).

Conductivity studies

The molar conductivity of the compounds is in the range of 14.55-21.45 ohm^{-1} cm^2 mol^{-1} (Table1). The low value shows that they are non electrolytic due to lack of dissociation.

Mass spectra

Mass spectra of the ligand (L) and its copper complex $[Cu(L)_2(AcO)_2]$ recorded at room temperature were used to compare their composition. The ligand showed a molecular ion peak at m/z 324 corresponding to their composition (Table1). The molecular ion peak for the zinc complex observed at m/z 867 confirms the stoichiometry of metal chelates as ML$_2$ type. It is also supported by the mass spectra of other complexes. The molecular ion peaks of nd Cu(II) complexes were observed at m/z with relative abundance 893, 897, 897 and 848 good agreement with the formula weight (Table 1).

Table 1. Analytical and Physical data of the Schiff base ligand (L) and its metal complexes

Compounds (Empirical Formula & Formula Weight)	Colour	Yield (%)	M.P (^{0}C)	Found (Cacld) (%)				Molar Conductance ($\wedge_m$) Ohm^{-1} cm^2 mol^{-1}
				C	H	N	M	
[L] $C_{18}H_{16}N_2O_4$ (324.26)	White	79	160	65.7 (66.6)	4.6 (4.9)	8.8 (8.6)	----	----
$[MnL_2(AcO)_2]4H_2O$ $MnC_{40}H_{46}N_4O_{16}$(893.46)	Brown	82	120	58.3 (53.7)	4.5 (5.1)	6.9 (6.3)	6.5 (6.1)	20.12
$[CoL_2(AcO)_2]4H_2O$ $CoC_{40}H_{46}N_4O_{12}$(897.45)	Pink	84	102	58.6 (53.5)	4.4 (5.1)	6.9 (6.2)	7.3 (6.6)	16.23
$[NiL2(AcO)_2]4H_2O$ $NiC_{40}H_{46}N_4O_{12}$(897.22)	Pale green	67	210	58.1 (53.5)	4.3 (5.1)	6.2 (6.2)	7.4 (6.5)	14.55
$[CuL_2(AcO)_2]$ H_2O $CuC_{40}H_{40}N_4O_{12}$(848.06)	Green	78	190	57.9 (56.6)	4.2 (4.7)	6.3 (6.6)	7.9 (7.5)	18.83
$[ZnL_2(AcO)_2]$ $2H_2O$ $ZnC_{40}H_{42}N_4O_{12}$(867.89)	Brown	62	210	57.4 (55.3)	4.5 (4.8)	6.8 (6.5)	7.6 (7.5)	21.45

^{1}H NMR spectra

The ^{1}H NMR spectra of the Schiff base ligand and its zinc complex shows the following signals: δ values of Schiff base ligand [L] : Aromatic Protons at 6.00-7.33 ppm; Azomethine proton(-HC=N-) at 8.16 ppm; -OCH_2 at 3.91 ppm. $[ZnL_2(AcO)_2]$ Complex: Aromatic Protons at 6.00-7.31 ppm; Azomethine proton(-HC=N-) at 8.34 ppm; -OCH_2 at 3.89 ppm; Acetate protons (CH_3COO-) at 2.05 ppm; The singlet peak at 5.8 ppm attributable water proton [16]. The above ^{1}H NMR spectra data assigned that the azomethine proton signal in the spectrum of the zinc complex is shifted down field compared to the free ligand suggesting deshielding due to azomethine nitrogen involving in complexation and there is no appreciable change in all other signals in the complex.

IR spectra

IR Spectrum of Schiff base ligand showed a strong sharp band observed at 1637 cm^{-1} region is assigned to the -HC=N-mode of the azomethine group which was shifted to lower frequencies in the spectra of all complexes indicating the involvement of -HC=N- nitrogen in coordination to the central metal ion [17]. In the spectra of the all metal complexes a broad diffuse band was identified (stretching) in the range of 3326–3425 cm^{-1} and week band in-plane bending (rocking) in the range of 813–858 cm^{-1}. It suggests that the presence of water molecules in the metal complexes [18].

Table 2. Infrared spectral data of the ligand and its metal complexes (cm^{-1})

Compounds	C=N	Aliphatic C-O-C	Aromatic C-H	Aliphatic C-H	iminic C-H	Acetate COO-	(H_2O)	M-N	M-O
[L]	1637	1039(s) 1097 (as)	3072	2924	2837	-	-	-	-
$[MnL_2(AcO)_2]$	1627	1031(s) 1098(as)	3019	2926	2855	1411(s) 1654(as)	3421 858(b)	410	518
$[CoL_2(AcO)_2]$	1628	1037(s) 1100(as)	3018	2924	2853	1419(s) 1640(as)	3425 848(b)	422	512
$[NiL2(AcO)_2]$	1634	1022(s) 1099(as)	3009	2924	2839	1402(s) 1664(as)	3339 846(b)	447	498
$[CuL_2(AcO)_2]$	1600	1041(s) 1099(as)	2956	2926	2837	1421(s) 1639(as)	3421 813(b)	428	511
$[ZnL_2(AcO)_2]$	1626	1040(s) 1107(as)	3020	2925	2838	1406(s) 1668(as)	3326 828(b)	434	510

s → symmetry, as → asymmetry, b →in-plane bending (rocking).

In all complexes, carboxylate of the acetate group (CH_3COO) strongly absorbs in the range of 1639–1668 cm^{-1} ($\gamma_{asymmetry}$) and more weakly at 1402–1421 cm^{-1}($\gamma_{symmetry}$). It suggests that they are consisting of unidentate co-ordination site due to the value of differences between asymmetry and symmetry is greater than 200 $cm^{-1}$and other absorption bands are no appreciable change in the ligand and metal complexes[19]. The results are summarized in

Electronic Spectra and Magnetic susceptibility

The electronic spectra of the free ligand display two bands at 37,313 cm^{-1} and 33,333 cm^{-1} are intra ligand charge transfer assigned to $\pi\rightarrow\pi^*$ and $n\rightarrow\pi^*$ transitions for phenyl ring and the azomethine chromophore (–CH=N) [20]. In the metal complexes this band is shifted to a longer wavelength which may be attributed to the donation of lone pair electron of N-atom of the ligand to the metal (N→M). Copper complexes exhibited only one low intensity broad band at 645 nm (15,504 cm^{-1}) due to dynamic Jahn–Teller distortion and showed magnetic moment value (μ_{eff} =1.82 B.M) is slightly higher than the spin-only value expected for one unpaired electron, which indicates possibility of a distorted octahedral geometry [21] and the remaining complexes were also assigned to be an octahedral geometry (Table 3).

Table 3. Electronic spectral data and magnetic Susceptibility values of the synthesized compounds (10^{-3} M in Methanol)

Com pounds	Band Position λ_{max} nm (γ-cm^{-1})	Assignment	μ_{eff} B.M	Suggested geometry
[L]	268(37,313) 300 (33,333)	$\pi\rightarrow\pi^*$ $n\rightarrow\pi^*$	--	--
$[CoL_2(AcO)_2]$	846(11,820) 673(14,859) 462(21,645)	$^4T_1g(F)\rightarrow{}^4T_2g(F)$ ($V_{1,}$) $^4T_1g(F)\rightarrow{}^4A_2g(F)$ (V_2) $^4T_1g(F)\rightarrow{}^4T_1g(P)$ (V_3)	3.94	Octahedral
$[NiL_2(AcO)_2]$	887(11,274) 748(13,369) 350 (28,571)	$^3A_2g(F)\rightarrow{}^3T_2g(F)$ ($V_{1,}$) $^3A_2g(F)\rightarrow{}^3T_1g(F)$ (V_2) $^3A_2g(F)\rightarrow{}^3T_1g(P)$ (V_3)	3.24	Octahedral
$[CuL_2(AcO)_2]$	645(15,504)	$^2E_g\rightarrow{}^2T_{2g}$	1.82	Distorted Octahedral

EPR spectra

The X-band EPR spectra of the $[CuL_2(AcO)_2]$ complex was recorded in DMSO at RT and LNT (Fig 1a & 1b)under 9.10 GHz Microwave field modulation using TCNE (g_e = 2.00277). The frozen solution spectrum shows well resolved four line spectrum lines. The results are summarized in Table 4**.** The spin Hamiltonian parameters have been calculated by Kivelson's method. The observed g-values are in the order $g_{\|}$ (2.24) > $g_{\perp}$(2.05) > g_e (2.00277) indicating that the unpaired electron lies predominantly in the $d_{x^2-y^2}$ orbital of Cu(II) [22] and the observed $g_{\|}$ values for Copper complex is less than 2.3 in agreement with the covalent environment character of the M-L bond [23]. The covalent nature of the M–L bond in the complex is further supported by g_{eff} value less than 2.00277 [24]. The obtained hyperfine constant parameters are very clear that in the order $A_{\|}$ (140G) > A_{av}(109.33G) > $A_{\perp}$= 94G. The value of interaction coupling constant obtained from the equation (1).

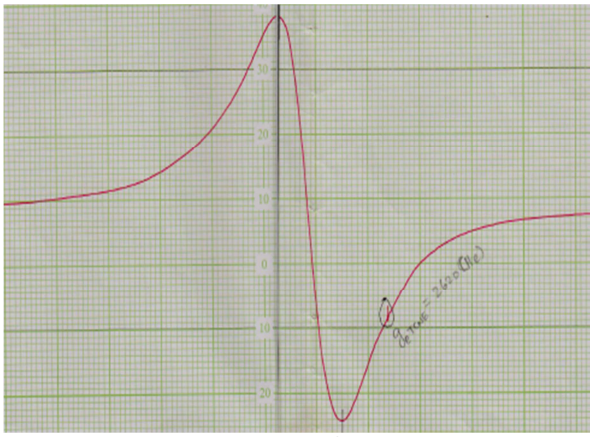

Fig. 1a. The EPR spectrum of Cu complex at 300K.

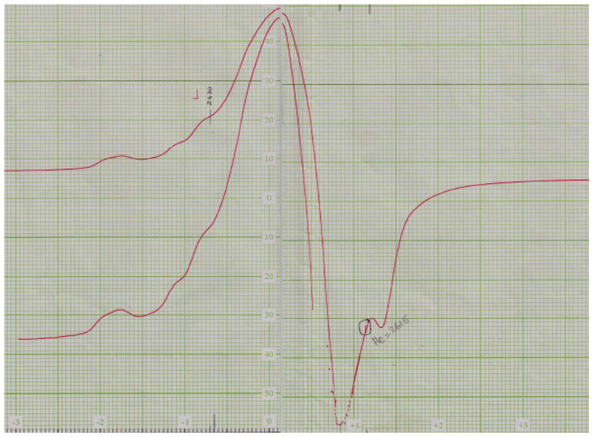

Fig. 1b. The EPR spectrum of Cu complex at 77 K.

$$G = \frac{(g_{||} - 2.00277)}{(g_{\perp} - 2.00277)} \quad (1)$$

If it is greater than 4, the exchange interaction is negligible [25]. The observed value of G =5.02 is in the present complex suggesting that there is no interaction between Cu-Cu centres in the solid state complex. EPR spectra have been further used to determine covalent bonding for the Cu(II) ion in a variety of environments. The values of molecular orbital coefficient parameters (α^2, β^2, γ^2) were determined by Kivelson and Neimann formulae.

$$)277) + \frac{3}{7}(g_{\perp} - 2.00277) + 0.04 \quad (2)$$

$$\beta^2 = (g_{||} - 2.00277)(\frac{E_{d-d}}{-8\lambda_0 a^2}) \quad (3)$$

$$\gamma^2 = (g_{\perp} - 2.00277)(\frac{E_{d-d}}{-2\lambda_0 a^2}) \quad (4)$$

The observed values of α^2 (In-plane σ-bonding), β^2 (in-plane π-bonding) and γ^2 (out-plane π-bonding) parameters have less than 1.0 which indicates that they are completely covalent characters. Hathaway has pointed out that for the pure σ-bonding in case of orbital reduction factors are equal ($K_{||} \approx K_{\perp}$). In case of $K_{||} < K_{\perp}$ denotes considerable in-plane π-bonding and if the value is to be $K_{||} > K_{\perp}$ which leads to out-of-plane π–bonding. The observed orbital reduction factor values for the present copper complex are $K_{\|} > K_{\perp}$ which indicates the presence of out-plane π-bonding in metal ligand π-bonding. The values are calculated from the equation [26].

$$K_{||}^2 = (g_{||} - 2.00277)(\frac{E_{d-d}}{-8\lambda_0}) \approx \alpha^2\beta^2 \quad (5)$$

$$K_{\perp}^2 = (g_{\perp} - 2.00277)(\frac{E_{d-d}}{-2\lambda_0}) \approx \alpha^2\gamma^2 \quad (6)$$

Table 4. The EPR spectral data of the $[CuL_2(AcO)_2]$complex at 77K

g tensor			Hyperfine constant x 10^{-4} cm^{-1}			Bonding parameters								
$g_{\|}$	$g_{\perp}$	g_{av}	$A_{\|}$	$A_{\perp}$	A_{av}	G	$f_{\|}$ (cm^{-1})	α^2	β^2	γ^2	$K_{\|}$	$K_{\perp}$	g_{eff}	μ_{eff} (B.M)
2.24	2.05	2.11	140	94	109.33	5.02	160	0.68	0.82	0.65	0.55	0.44	1.43	1.83

1G = 10^{-4} cm^{-1}, E_{d-d} = 15,455.95 cm^{-1}, one-electron spin orbit coupling constant of free Cu(II) ion(λ_0) = - 828 cm^{-1}, Free ion dipolar term(P) = 0.036 cm^{-1}, $f_{||} = g_{||}/A_{||}$, $\mu_{eff} = g_{av}[S(S+1)]^{1/2}$. $g_{eff} = \frac{g_{||} + g_{\perp}}{3}$

The Co-factors of degree of geometrical distortion $f_{||}$ = 167.14 cm^{-1} representing an octahedral geometry around the Cu(II) ion. Spectral data and magnetic measurements of the Cu(II) complex has been proposed as a distorted octahedral geometry.

DNA nuclease activity (Gel electrophoresis)

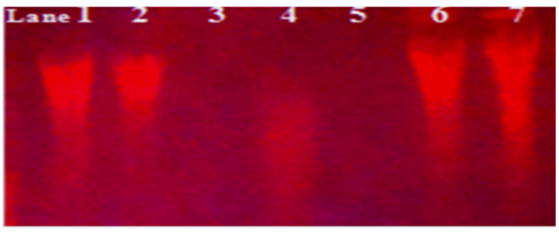

Lane:1 DNA alone,
Lane:2 ligand +DNA+H_2O_2,
Lane:3 $[Co(L)_2(AcO)_2]$+DNA+H_2O_2,
Lane:4 $[Ni\ (L)_2\ (AcO)_2]$+DNA+H_2O_2,
Lane:5 $[Cu(L)_2(AcO)_2]$+DNA+H_2O_2,
Lane:6 $[Zn\ (L)_2(AcO)_2]$+DNA+H_2O_2,
Lane:7 $[Mn\ (L)_2(AcO)_2$+DNA+H_2O_2,

Fig. 2. Gel electrophoresis showing the chemical nuclease activity of CT DNA by all compounds in the presence of oxidant (lane 1-7)

The gel electrophoresis clearly revealed that there was difference in migration of the lanes 1–7 by comparing with CT DNA controller (Lane-1) (Fig 2).When the concentration of metal complexes slightly increases over the optimal value led to extensive degradations, resulting in the disappearance of bands on agarose gel [27- 28]. The proposed general oxidative mechanism of DNA cleavage by hydroxyl radicals occurs via abstraction of a hydrogen atom [29]. Metal ions in the complexes react with hydrogen peroxide to generate the diffusible hydroxyl radical ($OH^{\bullet}$) or reactive oxygen species (O_2) which attacks the C_4' position of the sugar moiety which finally cleave the DNA and inhibit the replication ability of the cancer gene is destroyed. They are shown in the Fig 2. Lane 1 is for the control (DNA + H_2O_2) which does not exhibit significant cleavage even on longer exposure time and lane 2 is for the ligand alone is inactive in the presence and absence of external agents. At very low concentration, Cobalt (Lane:3), Nickel (Lane:4) and Copper(Lane:5) complexes exhibit significant nuclease activity than others. It is clearly noted that the formation of three activated oxygen intermediates (hydroxyl radical, singlet oxygen and superoxide) the formation of diffusible hydroxyl free radical scavenger ($OH^{\bullet}$) which involves in the oxidation of the deoxy ribose moiety through Fenton type mechanism [30].

constants by Electronic absorption titration

s of Co(II), Cu(II) and Ni(II) complexes have been observed by absorption titration due to DNA cleavage efficiency during the gel electrophoresis. The binding of these complexes to acterized by monitoring the changes in the absorbance of π–π* bands and shift in wavelength

on each addition of DNA solution to the complex. A significant "hyperchromic" shift of the intra ligand bands were observed accompanied by a moderate red shift (Fig 3a & 3b). The intrinsic binding constant (K_b) values are calculated from the ratio of the slope to the intercept of the plot of [DNA] / (ε_a - ε_f) versus [DNA] by Wolfe–Shimmer equation (7). These values are slightly lower than those observed for classical intercalator (Ethidium bromide-DNA, 1.4 x10^6 M^{-1}) [31]. The binding results indicate that the complexes are bound to DNA via intercalation and The standard Gibb's free energy change (ΔG_b^0) values for these complexes were calculated by Van't Hoff equation (8) which indicates that the complexes can interact with DNA in a spontaneous manner and also the percentage of hyperchromicity for these complexes were determined from the equation (9)

$$\frac{[DNA]}{(\varepsilon_a-\varepsilon_f)} = \frac{[DNA]}{(\varepsilon_b-\varepsilon_f)} + \frac{1}{K_b(\varepsilon_b-\varepsilon_f)} \quad (7)$$

$$\Delta G_b^0 = -RT \ln K_b \quad (8)$$

$$\% H = \frac{(\varepsilon_b-\varepsilon_f)}{\varepsilon_f} X\ 100 \quad (9)$$

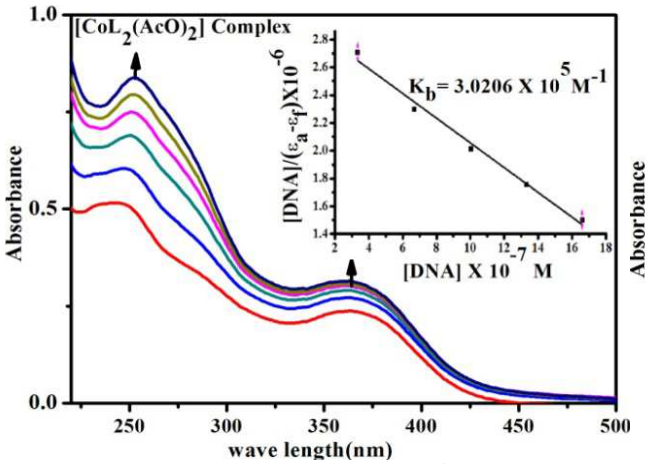

Fig. 3a. Electronic Absorption spectrum of $[CoL_2(AcO)_2]$ Complex through titration with DNA in Tris-HCl buffer; [Complex] =1 X 10^{-5} M; [DNA]: 0.0–12 X 10^{-7} mol L^{-1} . The increase of DNA concentration is indicated by an arrow. Plot of [DNA] / (ε_a - ε_f) Vs [DNA]. Binding constant K_b= 3.0206 X 10^5

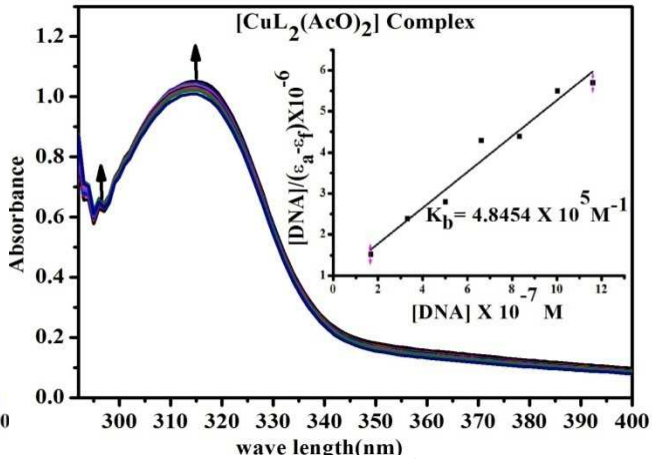

Fig. 3b. Electronic Absorption spectrum of $[CuL_2(AcO)_2]$ Complex through titration with DNA in Tris-HCl buffer; [Complex] =1 X 10^{-5} M; [DNA]: 0.0–12 X 10^{-7} mol L^{-1} . The increase of DNA concentration is indicated by an arrow. Plot of [DNA] / (ε_a - ε_f) Vs [DNA]. Binding constant K_b= 4.8454 X 10^5

The results are summarized in Table 5. The experimental results propose that the complexes bind to DNA via intercalation [32].

Table 5. Electronic Absorption Spectral parameters for DNA binding with the synthesized complexes

Complexes	λ_{max} free (nm)	λ_{max} bound (nm)	$\Delta\lambda$ (nm)	Types of Chromism	Chromism (%)	Binding constant (K_b) M^{-1}	$\Delta G_b^{\neq}$ $KJmol^{-1}$
$[CoL_2(AcO)_2]$	356	365	09	Hyper & Red shift	33.20	3.0206 X 10^5	-31.2677
$[NiL_2(AcO)_2]$	268	275	07	Hyper & Red shift	24.32	2.930 X 10^5	-31.1928
$[CuL_2(AcO)_2]$	311	316	05	Hyper & Red shift	12.99	4.8454 X 10^5	-32.4393

Uv-Spectral data of Complexes through titration with DNA in Tris-HCl buffer; [Complex] =1 X 10^{-5} M; [DNA]: (a) 0.0, (b) 2.0 X 10^{-7}, (c) 4.0 X 10^{-7}, (d) 6.0 X 10^{-7}, (e) 8.0 X 10^{-7}, (f) 1.0 X 10^{-6}, 1.2 X 10^{-6} mol L^{-1}. Plot of [DNA] / (ε_a - ε_f) Vs [DNA].

Viscosity titration measurements

The Interaction between the complexes and DNA was investigated by viscosity titration measurements. The experiments were carried out by an Oswald viscometer, immersed in a thermo stated water-bath maintained at 25°C ± 0.1°C. Titrations were performed for Cu(II),Co(II),Ni(II) complexes and control-EB (0.2, 0.4, 0.6, 0.8, 1.0 X 10^{-5}M) and each compound was introduced into the CT-DNA solution (10^{-4}M) present in the viscometer. Each sample was measured three times and an average flow time was calculated (Table 6). The viscosity of CT-DNA increased with rising ratio of complexes to CT-DNA, further suggesting an intercalative binding of the complexes with CT-DNA. Relative specific viscosity for DNA either in the presence or absence of complexes were calculated from the

$$\{(t_{DNA} - t_o)/t_o\}/\{(t_{DNA} - t_o)/ t_o\} \quad (10)$$

Data were analyzed as $(\eta/\eta_o)^{1/3}$ versus binding ratio R= [complex] / [DNA] (Table 6), where η is the specific viscosity of DNA in the presence of the complex and η_0 is the specific viscosity of DNA alone; $t_{complex}$, t_{DNA} and t_o are the average flow time for the DNA in the presence of the complex, DNA alone and Tris-HCl buffer respectively [33]. Ethidium bromide a well known DNA classical intercalator increases the viscosity strongly by lengthening the DNA double helix through intercalation. Upon increasing the concentration of complexes Cu(II), Co(II) and Ni(II) the relative specific viscosity of complexes increases steadily similar to the performance of Ethidium Bromide. The increased degree of viscosity may depend on the binding affinity to DNA which was observed in the following order EB > Cu(II) > Co(II) > Ni(II) (Fig 4). The increase in viscosity suggests that the complexes could bind to DNA by the intercalation binding mode which is consistent with electronic spectral data.

Table 6. Relative specific viscosity versus [Complex] / [DNA]

[Complex] / [DNA] = R	$(\eta/\eta_0)^{1/3}$ for control [EtBr]	$(\eta/\eta_0)^{1/3}$ for $[Cu(L)_2(AcO)_2]$	$(\eta/\eta_0)^{1/3}$ for $[Co(L)_2(AcO)_2]$	$(\eta/\eta_0)^{1/3}$ for $[Ni(L)_2(AcO)_2]$
0.2	0.8791	0.8042	0.7459	0.8759
0.4	0.9247	0.9137	0.9024	0.9024
0.6	0.9523	0.9488	0.9301	0.9201
0.8	0.9743	0.9622	0.9406	0.9406
1	0.9798	0.9676	0.9502	0.9502

DPPH radical scavenging studies

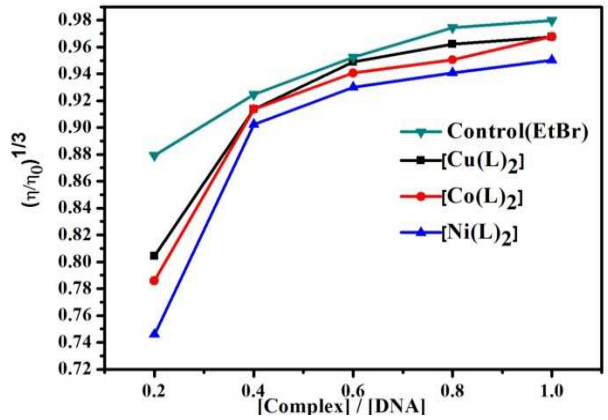

Fig. 4. Plot of Relative specific viscosity (η/η_0) versus R = [Complex] / [DNA]

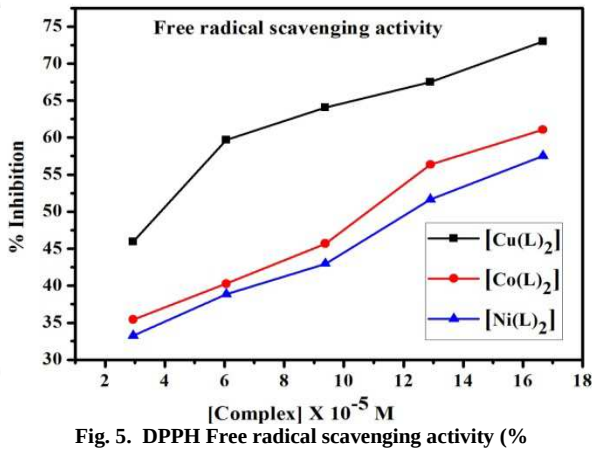

Fig. 5. DPPH Free radical scavenging activity (% Inhibition) of each complex (DPPH-FRSA)

Antioxidants are chemical substances that donate an electron to the free radical and convert into a harmless molecule. They may reduce the energy of the free radical or suppress radical formation or break chain propagation or repair damage and reconstitute membranes. DPPH free radical method is an antioxidant assay based on electron-transfer that produces a violet solution in methanol [34]. This free radical stable at room temperature is reduced in the presence of an antioxidant molecule, giving rise to colourless ethanol solution. The use of the DPPH assay provides an easy and rapid way to evaluate antioxidants by spectrophotometer and it can be useful to assess various products at a time. The percentage of antioxidant activity of each substance was assessed by DPPH free radical assay (Fig 5). The measurement of the DPPH radical scavenging activity was performed according to methodology described by Brand-Williams et al. Radical scavenging activity was expressed as percentage inhibition of DPPH radical and was calculated by following equation(11) [35] (Table 7)

$$\% \text{ Inhibition} = \frac{(\text{Absorbance of control} - \text{Absorbance of sample})}{\text{Absorbance of control}} \text{ X } 100 \qquad (11)$$

Table 7. DPPH Free radical scavenging activity of each complex

Final Concentration of Complex X 10^{-5} M	% Inhibition		
	$[Cu(L)_2(AcO)_2]$	$[Co(L)_2(AcO)_2]$	$[Ni(L)_2(AcO)_2]$
2.9411	45.94	35.43	33.24
6.0606	59.68	40.26	38.83
9.3750	64.05	45.68	42.98
12.9032	67.5	56.35	51.65
16.6666	72.98	61.08	57.54

Antimicrobial assay

On the basis of observed zones of inhibition (mm), it was found that most of the complexes exhibit good antimicrobial activity than the free ligand (Table 8) and (Fig 6a & 6b). But, they are less active than the standard drugs (Sparfloxacin and Ketokonazole) and activity intex was calculated from the equation (12).

$$\text{Activity index(A)\%} = \frac{\text{Inhibion zone of compound(mm)}}{\text{Inhibion zone of standard drug(mm)}} \times 100 \qquad (12)$$

Table 8. Evaluation of Antimicrobial activities (Diameter of zone of inhibition in mm) and Activity intex (A) % of the investigated compounds (10^{-4} M) by Agar disc diffusion method

Compounds	Antibacterial activity (% of A)				Antifungal activity (% of A)	
	Stap. Aureus(G+)	Stap. Pneumonia(G+)	Salmonella Typhi(G-)	Haemophilus Influenzae (G-)	Aspergillus Flavus	Aspergillus niger
Ligand [L]	06 (19)	06 (18)	10 (38)	06 (19)	07 (28)	08 (29)
[$Mn(L)_2$]	10 (32)	13 (39)	10 (38)	08 (26)	10 (40)	11 (39)
[Co $(L)_2$]	06 (19)	10 (30)	10 (38)	06 (19)	09 (36)	10 (36)
[$Ni(L)_2$]	17 (55)	20 (61)	14 (54)	12 (39)	11 (44)	14 (50)
[$Cu(L)_2$]	10 (32)	08 (24)	12 (46)	13 (42)	08 (32)	13 (46)
[$Zn(L)_2$]	09 (29)	08 (24)	12 (46)	08 (26)	10 (40)	11 (39)
Sparfloxacin	31(100)	33(100)	26(100)	31(100)	---	---
Ketokonazole	---	---	---	---	25(100)	28(100)

The observed higher activity of the metal complexes could be explained on the basis of Overtone's concept and Tweedy's chelation theory **[**36]. On chelation, lipophilicity is an important factor that controls antimicrobial activity [37]. The polarity of the metal ion in a chelated complex is reduced to a greater extent due to the overlap of the ligand orbital and partial sharing of the positive charge of the metal ion with donor groups. It increases the delocalization of π and d-electrons over the whole chelated ring and enhances the penetration of the complexes into lipid membranes due to lipophilicity which leads to breakdown of the barrier of the cell and disturbs the respiration process of the cell and also blocks the synthesis of proteins, which restricts further growth of the organism [38].

CONCLUSION

The novel Schiff's base ligand and its complexes [Mn(II), Co(II), Ni(II), Cu(II) and Zn(II)] have been synthesized and characterized by electronic absorption spectra, IR, ^{1}H NMR, and mass spectral analysis. All the metal ions are six-coordinate and the geometry can be described as octahedral and [ML_2] stoichiometry. The lower electrical conductivity values reveal that they are non electrolytes. The metal complexes have exhibited higher antimicrobial activity than the ligand. The interaction of these complexes with CT–DNA was investigated by gel electrophoresis. The results disclose that Co(II), Ni(II) and Cu(II) complexes have been completely cleaved DNA than others in the presence of H_2O_2. The Binding experiment results indicate that the complexes are bound to DNA via intercalation and has been observed a significant radical scavenging activity by DPPH.

Acknowledgements

The authors would like to thank the Department of Science and Technology (DST) – Science and Engineering Research Board (SERB), Government of India, New Delhi for financial support (SERB-Ref.No.SR/FT/CS-117/2011dated 29.06.2012) and express deepest gratitude to the Managing Board, Principal and Chemistry research centre MSEC, Kilakarai for providing research facilities.

REFERENCES

[1] H Laila; A Rahman; M Rafat; El-Khatib; AE Lobna; Nassr; M Ahmed; A Dief; M Ismael; AA Seleem. *Spectrochim. Acta A.*, **2014**, 117, 366-378.
[2] TD Thangadurai; M Gowri; K Natarajan. *Synth. React. J. Inorg. Met.-Org. Chem.*, **2002**, 32(2), 329-343.
[3] K Singh; MS Barwa; P Tagi. *Eur. J. Med. Chem.*, **2007**, 42(3), 394-402.
[4] MB Ferrari; S Capacchi; G Pelosi; G Reffo; P Tarasconi; R Albertini; S Pinelli; P Lunghi. *Inorg. Chim. Acta.*, **1999,** 286(2), 134-141.
[5] E Canpolat; M Kaya. *J. Coord. Chem.*, **2004,** 57(4), 1217-1223.
[6] T Hitoshit; N Tamao; A Hideyuki; F Manabu; M Takayuki. *Polyhedron.*, **1997,** 16(21), 3787-3794.
[7] S Liu; W Cao; L Yu; W Zheng; L Li; C Fan; T Chen. *Dalton Trans.*, **2013,** 42(16), 5932–5940.
[8] C Hammert; M Pitié; M Renz; H Gornitzka; S Soulet; B Meunier. *J. Bio. Inorg. Chem.*, **2001,** 6(1), 14-22.
[9] i; F Tisato. *Anti-Cancer Agents Med. Chem.*, **2009**, 9(2), 185-211.
[10] nzalez; A Escarpa. *Anal. Chim. Acta.*, **2004**, 511(1), 71-81.
[11] Nair. *Arab. J. Chem.*, **2010**, 3(4), 195-204.

[12] L Ana; Di Virgilio; Miguel Reigosa; MF Lorenzo de Mele. *J. Biomed Mater. Res B: Appl Biomater.*, **2011,** 99B(1), 111-119.
[13] J Marmur. *J. Mol. Biol.*, **1961**, 3(5), 585-594.
[14] S Chandra; LK Gupta. *Spectrochim. Acta A.*, **2004**, 60(7), 1563-1571.
[15] DJ Huang; BX Ou; RL Prior. *J. Agric Food Chem.*, **2005,** 53(6), 1841-1856.
[16] M Silverstein; X Webster. Spectrometric Identification of Organic Compounds, 6th Edition, **1996**; 150.
[17] ES Aazam; AFEL Husseiny; HM Al-Amri. *Arab. J. Chem.*, **2012**, 5(1), 45-53.
[18] MS Masoud; MF Amira; AM Ramadan; GM El-Ashry. *Spectrochim. Acta A.*, **2008,** 69(1), 230-238.
[19] BN Figgis; J Lewis. *Prog. Inorg chem.*, **1964**, 157, 37-239.
[20]M Shakir; Ambreen Abbasi; Mohammad Azam; Asad U Khan. *Spectrochim. Acta A.*, **2011**, 79(5), 1866-185.
[21] ABP Lever. Inorganic Electronic Spectroscopy, 2nd Edition, New York, **1968.**
[22] RL Dutta; A Syamal. Elemens of magnetochemistry, 2nd Edition, **1993,**106. ISBN: 81-85336-92-X.
[23] D Kivelson; R Neeman. *J. Chem. Phys.*, **1961,** 35(1), 149. doi.org/10.1063/1.1731880.
[24] A Syamal. *Chem. Edu*., **1985,** 62(2), 143. doi.org/10.1021/ed062p143.
[25] BJ Hathaway; DE Billing. *Coord. Chem. Rev.*, **1970,** 5(2), 143-207.
[26] PU Maheswari; M Palaniandavar. *Inorg. Chim. Acta.*, **2004,** 357(4), 901-912.
[27] MSS Babu; KH Reddy; GK Pitchika. *Polyhedron.*, **2007**, 26(3), 572-580.
[28] NP Singh; MT McCoy; RR Tice; EL Schneider. *Exp Cell Res.*, **1988,** 175(1), 184-191.
[29] G Prativel; M Pitie; J Bernadou; B Meunier. *Angew. Chem. Int. Ed. Eng.*, **1991,** 30(6), 702-704
[30] HJH Fenton. *J. Chem. Soc.*, **1894,** 65, 899. doi.org/10.1039/ct8946500899.
[31] JB Le Pecq; C Paoletti . *J. Mol. Biol.*, **1967,** 27(1), 87-106.
[32] AY Louie; TJ Meade. *Chem. Rev.*, **1999,** 99(9), 2711-2734.
[33] CP Tan; J Liu; LM Chen; S Shi; LN Ji. *J. Inorg. Biochem.*, **2008**, 102(8), 1644-1653.
[34] W Brand-Williams; ME Cuvelier; C Berset. *LWT-Food science and Technology.*, **1995**, 28(1), 25-30.
[35] S Albayrak, A Aksoy; OM Sagdic; Hamzaoglu. *Food Chemistry.*, **2010**, 119(1), 114-122.
[36] KN Thimmaiah; WDLloyd; GT Chandrappa. *Inorg. Chim. Acta.*, **1985**, 106(2), 81-83.
[37] A Peramo; CL Marcelo, *Ann Biomed Eng.*, **2010**, 38(6), 2013-2031.
[38] G G Mohamed; ZHA DEl-Wahab. *Spectrachim. Acta A.*, **2005**, 61(6), 1059-1068.

The studies on optical and structural properties of zinc sulfide thin films deposited by SILAR method

Article · January 2015

CITATION
1

READS
27

5 authors, including:

H. Mohamed Mohaideen
Mohamed sathak engineering college, kilakarai
5 PUBLICATIONS **6** CITATIONS
SEE PROFILE

K. Saravanakumar
AVVM Sri Pushpam College
16 PUBLICATIONS **338** CITATIONS
SEE PROFILE

Sheik Fareed
Mohamed Sathak Engineering College, KILAKARAI
8 PUBLICATIONS **10** CITATIONS
SEE PROFILE

Dhaveethu Raja
Mohamed Sathak Engineering College, Kilakarai, Ramanathapuram ...
41 PUBLICATIONS **294** CITATIONS
SEE PROFILE

TRUE COPY ATTESTED

PRINCIPAL
MOHAMED SATHAK ENGINEERING COLLEGE
KILAKARAI-623806.

Available online www.jocpr.com

Journal of Chemical and Pharmaceutical Research, 2015, 7(10S):141-145

Research Article

ISSN : 0975-7384
CODEN(USA) : JCPRC5

The studies on optical and structural properties of zinc sulfide thin films deposited by SILAR method

Haneefa Mohamed Mohaideen[1], Kandasamy Saravanakumar[1*], Suldanmohideen Sheik Fareed[1], Mohideen Mohamed Gani Kalvathee[2] and Jeyaraj Dhaveethu Raja[2]

[1]Department of Physics, Mohamed Sathak Engineering College, Kilakarai, India
[2]Chemistry Research Center, Mohamed Sathak Engineering College, Kilakarai, India

---

ABSTRACT

In the present work, the compound semiconducting zinc sulfide (ZnS) thin films were deposited on glass substrate using successive ionic layer adsorption and reaction technique by the various sulfur concentration(0.2 M to 1 M). The preparative parameters such as concentration, temperature, deposition time, pH of solution have been optimized. The characterization of thin films was carried out for the structural and optical properties. The thin films were characterized by using X-ray diffraction (XRD), UV-VIS Spectra and photoluminescence (PL). The X-ray diffraction pattern (XRD) revealed that the ZnS film has hexagonal and cubic crystal structure. All deposited films exhibit a relatively high transparency in the range of 300 to 800 nm. The band gap varies from 3 to 3.75 eV. Photoluminescence spectra showed blue emission band (480 nm) and green emission band (524 nm).

Key words: zinc sulfide, absorption coefficient and photoluminescence (PL).

INTRODUCTION

ZnS is one of the earliest semiconductors discovered and has novel fundamental property in order to suit diverged application. It is non toxic to human body and abundant. ZnS in its nano structures form attracted researches attention due to its special structure (Zinc blend and wurtzite) related to chemical and physical properties and for potential application in optoelectronic and nano electronic devices which includes blue LED's, electroluminescence, photoluminescence, cathodoluminescence, sensors, solar cells etc.[1]. In addition, Chalcopyrite-based thin film devices (CIGS) contain a so-called buffer layer, made of cadmium sulfide (CdS). Cadmium is highly toxic and therefore, alternative materials are being sought that can replace CdS without losses in its performance. The ZnS is an alternative to CdS [2-5]. Several techniques on growing ZnS thin film have been reported, which include sputtering[6], spray pyrolysis[7], chemical bath deposition[8,9], molecular beam epitaxy (MBE) [10], pulsed-laser deposition (PLD) [11], chemical vapour deposition (CVD) [12], metalorganic chemical vapour deposition (MOCVD) [13], metalorganic vapour-phase epitaxy (MOVPE) [13], atomic layer epitaxy (ALE) [14] and successive ionic layer adsorption and reaction (SILAR) [15]. Among these methods, the SILAR is relatively cost effect, simple and convenient for large area deposition which suit for doping different element in an easy way and which require any sophistication. In the present work, ZnS thin films were grown by SILAR technique through a different set of precursor. Different ZnS thin films were deposited by varying five different anion source concentrations and were characterized for their optical and structural properties.

EXPERIMENTAL SECTION

›strate cleaning of ZnS thin films

›own on glass substrates by the SILAR technique. To deposit ZnS one SILAR growth cycle four steps: a well-cleaned glass substrate is immersed in the first reaction vessel containing

aqueous cation precursor 0.2M Zinc acetate dehydrate solution at pH 10. After the cation immersion, the substrate is moved to the rinsing vessel where it is washed with purified water. The sulphide ions were adsorbed from an aqueous 0.2 M Thiourea solution with pH 12 which acts as anion source. After anion immersion the substrate was washed as described above; thus the first SILAR growth cycle is finished. Repeating these cycles a thin film with desired thickness can be grown. The cation and anion immersion times were 15 s. The temperature of the solutions was maintained at 65 °C (± 5°C). The ammonium hydroxide was used as complexing agent. The different thin films were prepared by varying the zinc to sulphide source ratio as 1:1, 2, 3, 4 and 5 respectively. The preparative parameters used for the deposition of ZnS thin films are summarized as below (Table 1). The glass slides of dimensions 26mm×76mm×2mm were used. Before deposition, they were etched by using chromic acid bath kept at 70^0c for 2h. After the etching process, they were cleaned with deionized water and acetone. The substrate cleaning plays an important role in the deposition of thin film. The cleaned substrate surface provides nucleation sites, which results in uniform film growth [16].

Table 1. ZnS thin film synthesis parameter.

S.NO.	PARAMETER	CATION SOULTION	ANION SOLUTION
1.	Materials	Zinc acetate dehydrate	Thiourea
2.	Concentration of solution	0.2 M	0.2, 0.4, 0.6, 0.8 and 1 M
3.	pH value	10	12
4.	Solution temperature	65°C	65°C
5.	Immersion time	15 s	15 s
6.	Total number of deposition cycles	100	100

The overall chemical reaction is summarized as

$$\mathbf{Zn(CH_3COO)_2 2H_2O + 4NH_3 \rightleftharpoons 2(CH_3COO)^- + Zn(NH_3)_4^{2+} + 2H_2O} \quad (\mathbf{1a})$$

$$\mathbf{Zn(NH_3)_4^{2+} \rightleftharpoons Zn^{2+} + 4NH_3} \quad (\mathbf{1b})$$

$$\mathbf{SC(NH_2)_2 + 2OH^- \longrightarrow S^{2-} + CH_2N_2 + 2H_2O} \quad (\mathbf{2})$$

$$\mathbf{Zn^{2+} + S^{2-} \longrightarrow ZnS} \quad (\mathbf{3})$$

2.2 Characterization of thin films

The thickness of the sample was determined by the gravimetric method. The optical properties of ZnS thin films were calculated as a function of concentration of sulphide solution. The UltraViolet-Visible (UV-Vis) spectrophotograph was recorded using the PERKIN ELMER Lambda 35 spectrometer. As the films were examined along with the substrates on which they were formed, it was necessary to take into account the absorbance in the glass substrate even though it was small. Hence, the absorbance spectra of the glass substrates were taken and used for the elimination of the optical absorbance in the glass substrate from the total absorbance in the film–substrate combination to obtain the optical absorbance of the film. The band gap energy change was investigated as function of concentration of sulphide solution. Room temperature photoluminescence (PL) study was performed by using Varian Cary Eclipse fluorescence spectrophotometer. The samples were excited using the 385 nm line. The structure of the film was identified by X-ray diffraction (XRD) with XPERT-PRO (PW-3071) equipped with a Cu Kα (λ=0.154060 nm) radiation source. Data were collected by step scanning from 20^0 to 80^0 with step size of 0.05^0 (2θ).

RESULTS AND DISCUSSION

3.1 Optical characterization

The optical transmittance of as deposited ZnS thin film which deposited varies with respect to the sulphur concentration is shown below (Fig 1). The wavelength of the incident light is 220-1000nm. It reveals that nearly 85% transmittance in the visible wavelength range. In addition, the transmittance decreases at the Zn:S ratio of 1:5. It can be seen that the Zn:S ratio of 1:5 thin film has lower transparency, because it has thicker than the others. Moreover, this film was densely covered by particles and the space of the particle was less so the light cannot transmit easily. So the concentration of sulphur is very important to obtain the high quality ZnS thin film. The optical absorption spectrum of as deposited ZnS thin film varies with respect to the sulphur concentration is shown below (Fig 2). It is clearly seen from the spectra that the film has sharp absorption and the absorption edge slightly shifting towards the lower wavelength indicates the increase of optical band gap. The energy band gap of these thin om absorption spectra using Tauc's relation, [17]

$$\alpha = \frac{K}{h\nu}\left(h\nu - E_g\right)^n \quad (4)$$

Where K is a constant, hν is the photon energy, α is a absorption coefficient and n assumes values of 1/2, 2, 3/2 and 3 for allowed direct, allowed indirect and forbidden indirect transitions respectively. The value of the absorption coefficient 'α' has calculated using the relation, [18]

$$\alpha = \frac{2.3026\ A}{t} \quad (5)$$

Where A is the absorbance and t is the film thickness.

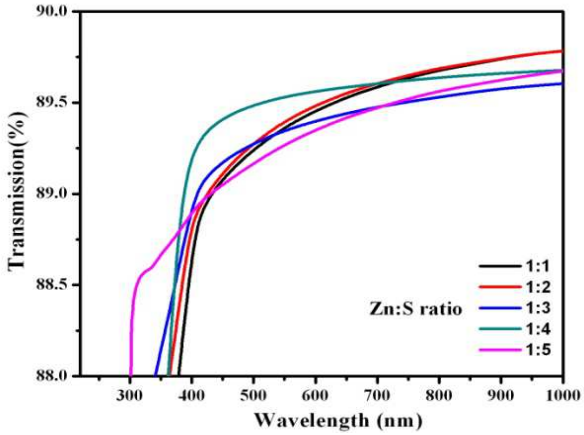

Fig. (1). Transmittance spectra of ZnS films

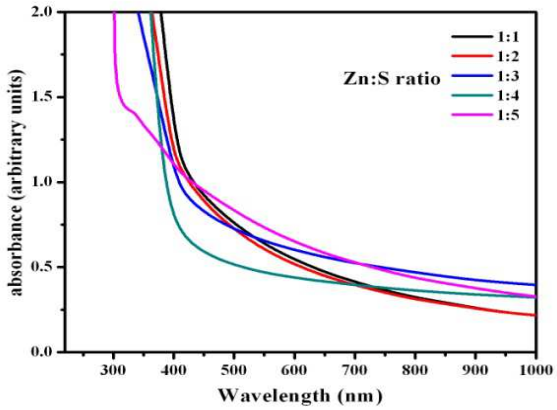

Fig. (2). Absorbance spectra of ZnS thin film

Thus a plot of α^2 vs. hν is a straight line whose intercept on the energy axis gives the energy gap, E_g. The variation of α^2 vs. hν for different sulphur concentration is as shown below (Fig 3). The band gap energies of thin film have been determined by the extrapolation of the linear region on the energy axis. The band gap energy in ZnS thin film is increasing with increasing sulphur concentration. The band gap energy varies from 3 eV to 3.75 eV. The extinction coefficient K_f value decreases with increase in wavelength and becomes constant at higher wavelength (Fig 4). The Extinction coefficients are calculated using the following equation (Equ 6). The extinction coefficient (K_f) is directly related to the absorption of light. In the case of polycrystalline films, extra absorption of light occurs at the grain boundaries [19-20]. This leads to non-zero value of (K) for photon energies smaller than the fundamental absorption edge [21-23].

$$K_f = \frac{\alpha\lambda}{4\pi} \quad (6)$$

3.2 Photoluminescence (PL) study

The room temperature Photoluminescence spectrum of ZnS thin films for various Zn:S ratios are shown in below (Fig 5). It can be seen that the emission is quite symmetric and sharp. There are mainly three luminescence bands present in the all the films, two blue emission band around 413 nm and 480 nm and one green emission band around 525 nm. The luminescence peaks located around 413 nm is associated with the zinc vacancies and that at 480 nm is probably due to sulphur vacancies [24-28]. The green luminescence peaks located around 524 nm is associated with oxide vacancies. It can be seen that as the concentration of sulphur increases the intensity of the emission decreases. The PL signal obtained is quite sensitive to the impurities of defect present within the sample. The decrease in intensity explains that the defect present in the sample also decreases. The emission might be arising from vacancy of sulphur which gets reduced with an increase in concentration of sulphur.

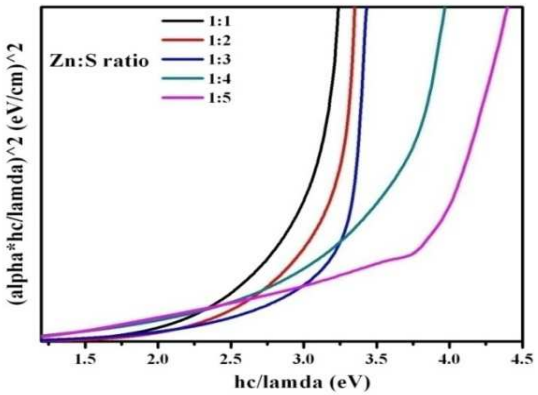

Fig. (3). The plot of $(\alpha hv)^2$ vs. photon energy

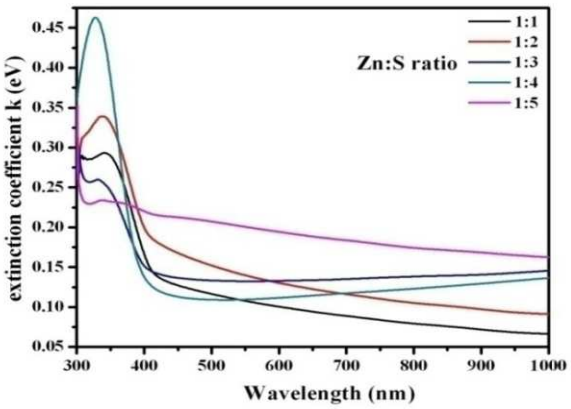

Fig. (4). The plot of Extinction coefficient K_f vs wavelength of ZnS film

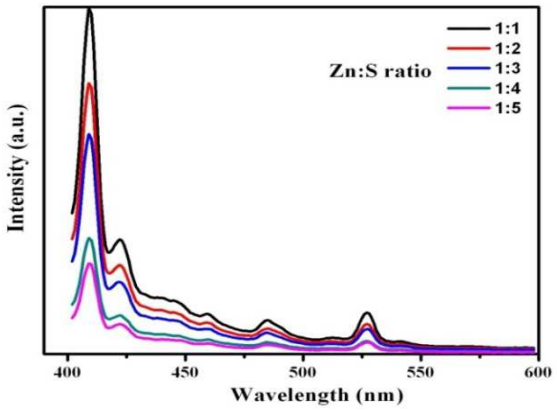

Fig. (5). Photoluminescence spectra of ZnS thin film

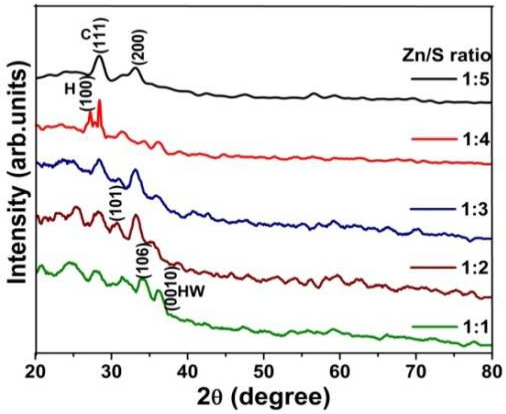

Fig. (6). XRD pattern of ZnS thin film

3.3 Structural studies

The XRD pattern of ZnS thin film is shown as above (Fig 6). It is clearly seen that all the diffraction peaks are well indexed to the standard diffraction pattern of hexagonal and cubic ZnS phases (JCPDS card NO. 89-2344 and JCPDS card NO. 05-0566). A polycrystalline nature is observed for all the deposited films. There is a modification in crystal structure from hexagonal to cubic with increase in sulphur concentration. The crystallite size of the deposited films was decreased from 42 nm to 8 nm by varying the Zn:S ratio. The grain size (D) was calculated from the full width at half maximum (FWHM) (β) by using the Scherer's formula,

$$D = \frac{0.94\lambda}{\beta \cos\theta} \qquad (7)$$

Where λ is the wavelength of X-ray (1.5405Å) and θ is the Bragg's angle.

CONCLUSION

The ZnS thin films exhibit an average transmittance of 85% along the range, confirming the suitability of the films to be used as a buffer layer in photovoltaic applications. The band gap varies from 3 to 3.75 eV. The presence of intrinsic and extrinsic defects is confirmed through PL spectra. The XRD patterns show the standard diffraction pattern of hexagonal and cubic ZnS phases. From these studies, we conclude that the results are very much suitable for optoelectronics and nano electronics devices.

Acknowledgements

The authors express their sincere and heartfelt thanks to Managing Board, Principal, Mohamed Sathak Engineering their constant encouragement and providing research facilities. The authors gratefully ial support from the Department of Science and Technology (DST)-Science and Engineering -Ref.No. SR/FT/CS-117/2011 dated 29.06.2012), Government of India.

REFERENCES

[1] A Ates; MA Yıldırım; M Kundakcı; A Astam. *Mater. Sci. Semicond. Process.,* **2007,** 10(6), 281-286.
[2] L Zhou; N Tang; S Wu; X Hu; Y Xue. *Physics Procedia,* **2011,** 22, 354-359.
[3] M Oikkonen; M Blomberg; T Tuomi; M Tammenmaa. *Thin Solid Films,* **1985,** 124(3-4), 317-321.
[4] T Nakada; M Hongo; E Hayashi. *Thin Solid Films,* **2003,** 431-432, 242-248.
[5] J Vidal; OD Melo; O Vigil; N López; GC Puente; OZ Angel. *Thin Solid Films,* **2002,** 419(1-2), 118-123.
[6] H Murray; A Tosser. *Thin Solid Films,* **1974,** 24(1), 165-180.
[7] H L Kwok. *J. Phys. D, Appl. Phys.,* **1983,** 16(12), 2367-2377.
[8] JM Doña. *J. ElectrocheM. Soc.,* **1994,** 141(1), 205.
[9] MS Akhtar; MA Malik; S Riaz; S Naseem; PO Brien. *Mater. Sci. Semicond. Process.,* **2015,** 30, 292-297.
[10] K Ichino; T Onishi; Y Kawakami; S Fujita; S Fujita. *J. Cryst. Growth,* **1994,** 138(1-4), 28-34.
[11] Z Xin; RJ Peaty; HN Rutt; RW Eason. *Semicond. Sci. Technol.,* **1999,** 14(8), 695-698.
[12] TL Chu; SS Chu; J Britt; C Ferekides; CQ Wu. *J. Appl. Phys.,* **1991,** 70(5), 2688.
[13] KA Dhese; JE Nicholls; WE Hagston; PJ Wright; B Cockayne; JJ Davies. *J. Cryst. Growth,* **1994,** 138(1-4), 140-144.
[14] J Ihanus; M Ritala; M Leskelä; T Prohaska; R Resch; G Friedbacher; M Grasserbauer. *Appl.Surf.Sci.,* **1997,** 120(1-2), 43-50.
[15] A Ates; MA Yıldırım; M Kundakcı; A Astam. *Mater. Sci. Semicond. Process.,* **2007,** 10(6), 281-286.
[16] M Ashokkumar; S Muthukumaran. *J. Lumin.,* **2014,** 145, 167-174.
[17] V Kumar; KLA Khan; G Singh; TP Sharma; M Hussain. *Appl.Surf.Sci.,* **2007,** 253(7), 3543-3546.
[18] V Cottrell. An Introduction to Metallurgy, **1975,** P-173.
[19] VD Damodara; KS Bhat. *J. Mater. Sci.-Mater. Electron.,* **1990,** 1(4), 169-174.
[20] AN Molin; AI Dikusar. *Thin Solid Films,* **1995,** 265(1-2), 3-9.
[21] H Metin; R Esen. *Semicond. Sci. Technol.,* **2003,** 18(7), 647-654.
[22] S Mathew; PS Mukerjee; KP Vijayakumar. *Thin Solid Films,* **1995,** 254(1-2), 278-284.
[23] GC Morris; R Vanderveen. *Sol. Energy Mater. Sol. Cells.,* **1992,** 27(4), 305-319.
[24] X Zhang; H Song; L Yu; T Wang; X Ren; X Kong; Y Xie; X Wang. *J. Lumin.,* **2006,** 118(2), 251-256.
[25] MS Niasari; F Davar; MRL Estarki. *J. Alloys Compd.,* **2010,** 494(1-2), 199-204.
[26] K Sooklal; BS Cullum; SM Angel; CJ Murphy. *J. Phys. Chem.,* **1996,** 100(11), 4551-4555.
[27] WG Becker; AJ Bard. *J. Phys. Chem.,* **1983,** 87(24), 4888-4893.
[28] MS Niasari; F Davar; MRL Estarki. *J. Alloys Compd.,* **2009,** 475(1-2), 782-788.

Journal of Chemical and Pharmaceutical Sciences www.jchps.com ISSN: 0974-2115

DEVELOPMENT AND CORROSION PERFORMANCE OF 3-AMINOPROPYLTRIETHOXYSILANE GRAFTED EPOXIDIZED ETHYLENE-PROPYLENE-DIENE TERPOLYMER RUBBER COATINGS

M. Vadivel[a]*, M. Suresh Chandra Kumar[b], C. Vedhi[c],V. Selvam[d], J. Dhaveethu Raja[a]

[a]Department of Chemistry, Mohamed Sathak Engineering College, Kilakarai - 623 806, Ramanathapuram (Dist), Tamilnadu, India.

[b] Polymer Nanocomposite Centre, Department of Chemistry, Scott Christian College, Nagercoil 629 003, India

[c] Department of Chemistry, V.O. Chidambaram College,Tuticorin 628 008, India

[d]Department of Chemistry, K. Ramakrishnan Engineering College, Tiruchirapalli - 621 112, Tamilnadu, India.

***Corresponding author:E.Mail:vadivelche@gmail.com**

ABSTRACT

A novel copolymer of 3-aminopropyltriethoxysilane (APTES) grafted epoxidized ethylene-propylene-diene terpolymer (eEPDM-g-APTES) was synthesized in toluene, 25% red iron oxide as additive. The chemical structure of eEPDM-g-APTES was confirmed by FT-IR spectroscopy. The corrosion resistant behaviors of EPDM, eEPDM, eEPDM-g-APTES with or without red iron oxide were investigated by potentiodynamic polarization and electrochemical impedance spectroscopic methods and also studied salt-spray tests in 3.5% NaCl solution. The experimental results reveal that the eEPDM-g-APTES with 25% red iron oxide offers the maximum corrosion protection to the steel surface. The better protective action offered by the reaction of APTES amine with oxirane groups of the eEPDM, which gives coating films with a high cross-link density.

Keywords: eEPDM, eEPDM-g-APTES, potentiodynamic polarization, electrochemical impedance spectroscopy.

INTRODUCTION

Rubber based coatings have, for a long time, found use in industrial maintenance, marine and concrete and masonry walls. Rubber is a polymer with good barrier properties for water and oxygen. Ethylene-propylene-diene terpolymer (EPDM) is widely used as adhesive materials, due to its excellent physical and durability properties. Cross linked ethylene-propylene-diene terpolymer (EPDM) is one of the majority commonly used industrial polymer because of its marvelous resistance to heat, light, oxygen and ozone. Due to simple reaction condition (low temperature and low pressure), the silanization of MWNTs has attracted increasing attention for preparing MWNT/polymer composites. Silane coupling agent can be chemically described as R[BOND]Si[BOND]inline image. The R′ group is generally alkoxy group that reacts readily with the hydroxyls on nanotube surface; The R group is usually ethylene, amine, epoxy, thiohydroxy, etc., and chosen to be reactive with different polymeric resins. Ma et al., however, due to the incompatibility of EPDM with inorganic pigment, the corrosion-resistant property of EPDM coating is very poor, which strongly limits their practical applications. However, noticeable improvements of above properties of EPDM can be obtained through grafting by other functional compounds. Silanes are also used as coupling agents that improves the adhesion of different nature of surfaces. Coupling agents are having both organic and inorganic groups; they bridge the interface between polymeric matrix resin and reinforcement through covalent bonding. The inorganic group is compatible with filler and the organic group is compatible with polymer matrix resins. In the present study, the EPDM was first epoxidized with in situ formed per formic acid, which induced functional epoxy groups into the EPDM macromolecular backbone. A novel and new graft copolymer of 3-aminopropyltriethoxysilane onto epoxidized ethylene-propylene-diene terpolymer (eEPDM-g- APTES) has been synthesized in toluene. The corrosion resistant behaviors of EPDM, eEPDM, eEPDM-g-APTES with or without red iron oxide were investigated by potentiodynamic polarization and electrochemical impedance spectroscopic methods and also studied salt-spray tests in 3.5% NaCl solution.

EXPERIMENTAL

Materials: The EPDM (ENB) elastomer used in this study was a commercial grade Nordel IP 4770P (ethylene/propylene/ 5-ethylidene-2-norbornene = 70/25/5 by wt.% , Mooney viscosity, ML $_{(1+4)}$ at 125°C is 70 and Pont Dow elastomers, USA. Hydroxyl-terminated polydimethylsiloxane (HTPDMS) as thoxysilane (APTES), (M_w = 221.3, boiling point = 217°C, density = 0.946 g.cm^{-3},) was emicals, USA. Dibutyltindilaurate (DBTDL) was purchased from Merck, Germany. l (88%), hydrogen peroxide (30%), toluene,n-hexane were used as received.

Journal of Chemical and Pharmaceutical Sciences www.jchps.com ISSN: 0974-2115

In situ epoxidation of ethylene–propylene– diene terpolymer: The EPDM was first dissolved in toluene in a three necked flask equipped with a mechanical stirrer and thermometer, and maintained at 50°C in a water bath. Under continuous stirring, the EPDM solution was acidified stepwise with 88% formic acid to pH 2–3. The epoxidation was performed by dropping the required amount of H_2O_2 (30%) for 30 min. A rapid introduction of this reagent is not recommended, because it causes excessive development of oxygen due to the decomposition of hydrogen peroxide at high temperature. The reaction was continued for 7 h at 50°C. After epoxidation, the rubber was coagulated in acetone, thoroughly washed with distilled water, soaked in 1% w/v Na_2CO_3 solution for 24 h, and finally rinsed with distilled water. The rubber prepared was dried in a vacuum oven at 40°C to a constant weight.

Preparation of eEPDM-g-APTES: The reactions were carried out in 500 ml three necked, round bottom flask equipped with a reflux condenser, a Teflon-coated mechanical stirring and a nitrogen inlet. 10gm of eEPDM was dissolved in 200 ml toluene and refluxed until complete dissolution of eEPDM. Further, 0.25 wt.% APTES dissolved in 50 ml of toluene were added to eEPDM, using dibutyl tindilaurate catalyst, with continuous stirring for 2 h at 50°C. After the completion of reaction, the products were precipitated with methanol, filtered and dried in vacuum.

RESULTS AND DISCUSSION

Fourier-transform infrared spectroscopy: Fig. 1 shows the FTIR spectra of EPDM, eEPDM and Siliconized epoxidized EPDM. The IR spectra of EPDM (Fig. 1(a)) shows the C–H stretching vibration (aliphatic) at 2911 cm^{-1}, $–CH_2$ rocking vibration at 1451 cm^{-1}, CH_3 symmetric bending vibration at 1367 cm^{-1} due to the presence of propylene group, $–(CH_2)_n–$ wagging vibration at 721 cm^{-1} due to the presence of polyethylene chain, C–C stretching vibration at 2851 cm^{-1}, and the unsaturation band (>C=CH–) at 811 cm^{-1} due to the presence of ENB content. The FTIR spectrum of eEPDM (Fig. 1(b)) was characterized by the presence of an epoxide band at 870 cm^{-1} due to asymmetric epoxide ring stretching. Furthermore, the intensity of the >C=CH– band at 811 cm^{-1} decreases because of the epoxidation of EPDM, which demonstrates that the C=C double bond in EPDM was converted to the epoxy functional group in eEPDM. The conversion of double bonds to epoxide was obtained as 50% (ca.2.4 mol %). To take advantage of relative change of absorbance at 811 and 870 cm^{-1}, a quantitative analysis was performed by area measurement of methyl deformation band at 1369 cm^{-1} as internal standard Fig. 1(c) illustrates the IR spectra of Siliconized epoxidized EPDM which reveals: Absorption peak appeared at 2900 cm^{-1} and between 1140 cm^{-1} to 960 cm^{-1} confirms the presence of $–Si-(CH_2)_3-$ and residual –Si-OH respectively.Absence of peak at 2850 cm^{-1} of $–Si-OCH_2CH_3$ and formation of Si-O-Si at 1143 cm^{-1} confirms the completion of reaction between HTPDMS and APTES coupled epoxidized EPDM.

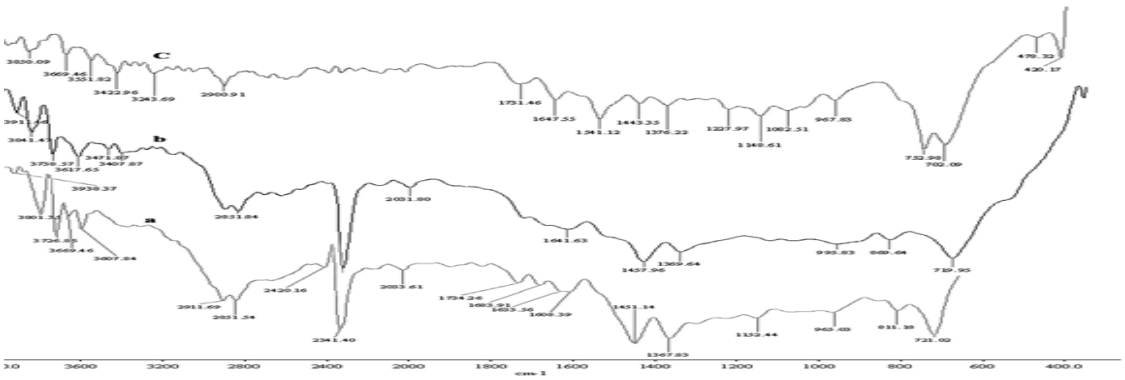

Fig. 1 FTIR spectra of (a) EPDM (b) eEPDM and (c) Siliconized epoxidized EPDM

Corrosion protection performance of the EPDM, eEPDM and eEPDM-g-APTES: The EPDM, eEPDM and eEPDM-g-APTES films coated mild steel was studied by potentiodynamic polarization and electrochemical impedance spectroscopy [10, 11]. In a typical polarization curve, the lower the polarization current is, the better the corrosion resistance is. The potentiodynamic polarization curves of bare mild steel, EPDM, eEPDM and eEPDM-g-APTES with or without red iron oxide coating in 3.5% NaCl solution are shown in Fig. 2a. The values of the E_{corr} Tafel polarization curves are given in. It is clearly observed that the corrosion current M to eEPDM-g-APTES, and the corrosion potential (E_{corr}) increases from EPDM to The positive shift increases red iron oxide coating system which implies that the

eEPDM-g-APTES film provides effective protection for mild steel coating against corrosion in aqueous 3.5% NaCl in comparison with EPDM and eEPDM.

EIS plays an important role to monitor and predict degradation of organic coatings. The Nyquist plot obtained from EIS measurements for all coating mild steel specimen after 30 min immersion in 3.5% NaCl solution is shown in Fig. 2 b. The plot is characterized by a depressed semicircle from high to medium frequencies and an inductive loop at low frequencies. The appearance of the inductive loop in the Nyquist plot is attributed to the adsorption of an intermediate product in the corrosion reaction. Six different coatings, with or without red iron oxide coatings, were examined in chloride electrolyte. Nyquist plots are displayed. It can be seen that, with the exception of coating system eEPDM-g-APTES with or without red iron oxide coating, the other coating system EPDM, eEPDM with or without red iron oxide coating exhibits an incomplete semicircle in the high frequency region, followed by a low-frequency diffusion tail commonly called a Warburg diffusion tail The formation of an incomplete semicircle suggests that the sodium chloride solution has started permeating through the coating in the case of coating system EPDM,eEPDM with or without red iron oxide .

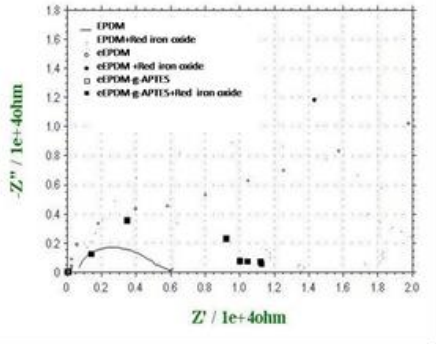

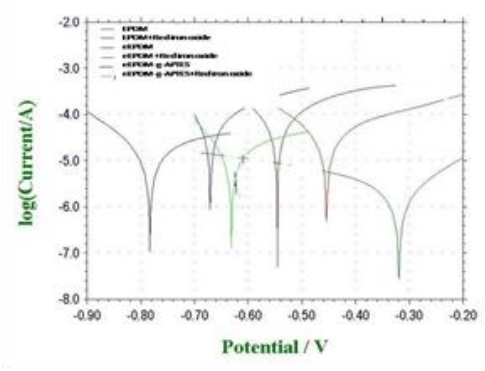

CONCLUSIONS

In this study, the chemical structure of eEPDM-g-APTES was confirmed by FT-IR spectroscopy. eEPDM-g-APTES with or without red iron oxide coatings were used to protect mild steel against corrosion in 3.5% NaCl medium, and potentiodynamic polarization measurements and electrochemical impedance spectroscopy were applied to assess the ability of corrosion resistance.

REFERENCES

Beving, D.E., McDonnell, A.M.P., Yang, W.S., Yan, Y.S., J. Electrochem. Soc. 2006, 153, 325.
C. L. Meredith, R.E. Barret, W. H. Bishop, US Patent 3 **538** (1970) 190
C. Velasco-Santos, A.L. Martinez-Hernandez, M. Lozada-Cassou, A. Alvarez-Castillo, and V.M. Castano, Nanotechnology, 13, 495 (2002).
H. F. Mark, N. M. Bikales, C. G. Overberger, G. Menges, Encyclopedia of polymer science and engineering, Wiley, New York, USA, (1985) 720
Hu, J., Gan, M., Ma, L., Zhang, J., Xie, S., Xu, F., Shen, J.Y.Z.X., Yin, H., Applied Surface Science 2014, http://dx.doi.org/10.1016/j.apsusc.2014.12.042
Li, P.Y., Yin, L.L., Song, G.J., Sun, J., Wang, L., Wang, H.L., Appl. Clay Sci. 2008,40, 38.
Mitra, A., Wang, Z.B., Cao, T.G., Wang, H.T., Huang, L.M., Yan, Y.S. J.electrochem Soc. 2002, 149, 447.
P.C. Ma, J.K. Kim, and B.Z. Tang, Carbon, **44**, 3232 (2006).
Plueddemann E.P., Silane coupling agents, 2 nd Ed., Plenum Press: New York. 1991.
Shen C., Zhou Y., Dou R., Wang W., Yin B., Yang M-b., Polymer 2014, doi: 10.1016/j.polymer.2014.11.027.
Thomas, N.L., J. Prot. Coat. Linings, 1989, 6, 63.

Int. J. Chem. Sci.: 13(2), 2015, 737-746
ISSN 0972-768X
www.sadgurupublications.com

THERMAL AND MORPHOLOGY STUDIES OF SILICONIZED EPOXIDIZED ETHYLENE-PROPYLENE-DIENE TERPOLYMER

M. VADIVEL[a], M. SURESH CHANDRA KUMAR[*], J. DHAVEETHU RAJA[a], M. SANKAR GANESH[a] and S. ARVIND NARAYAN[b]

Polymer Nanocomposite Centre, Department of Chemistry & Research Centre, Scott Chrisitian College, NAGERCOIL – 629 003 (T.N.) INDIA
[a]Department of Chemistry, Mohamed Sathak Engineering College, KILAKARAI – 623 806, Dist.: Ramanathapuram (T.N.) INDIA
[b]Faculty of Science and Humanities K. N. S. K. College of Engineering, Therekalputhoor, NAGERCOIL – 629901, Dist.: Kanyakumari (T.N.) INDIA

ABSTRACT

Siliconized epoxidized ethylene-propylene-diene terpolymer was developed by ethylene-propylene-diene terpolymer (EPDM) was epoxidized with an *in situ* formed per formic acd to prepare epoxidized EPDM (eEPDM) with hydroxyl terminated polydimethysiloxane (silicone) modifier using 3-aminopropyltriethoxysilane (APTES) crosslinker and dibutyltindilaurate (DBTDL) as catalyst. The chemical structure of Siliconized epoxidized ethylene-propylene-diene terpolymer was confirmed by FT-IR spectroscopy. The thermal properties and morpholiges of the EPDM, eEPDM and Siliconized epoxidized ethylene-propylene-diene terpolymer were investigated. Siliconized epoxidized ethylene-propylene-diene terpolymer is observed that the improves their thermal stability due to the partial ionic nature, high bond energy and thermal stability of –Si-O-Si- linkage. Siliconized epoxidized ethylene-propylene-diene terpolymer systems show heterogeneous morphology.

Key words: eEPDM, Dibutyltindilaurate, Thermal properties, Morphology.

INTRODUCTION

It has been reported that ethylene-propylene-diene terpolymer (EPDM) has superior resistances to light, heat, ozone and oxygen because it has little contents of the nonconjugated diene component[1-4]. Epoxidation is the easy and efficient method for

[*]Author for correspondence; E-mail: vadivelche@gmail.com; +91 94422 58686; Fax: +91 443330 3334

introducing a novel reactive group into polyolefins, leading to innovative and useful properties and broad use in an assortment of applications[5-8]. Epoxidation of olefinic compounds using organic peracids has been widely studied since oxiranes were prepared by reacting ethylenic compounds with perbenzoic acid. Oxiranes are generally prepared using perbenzoic acid[9], chlorperbenzoic acid[10] and monoperphalic acid[11]. Performic acid is an extremely active organic peracid[12-16] used for the epoxidation, but, owing to its instability[17], it has to be prepared in situ. In recent years, silicone compounds are considered to be among the finest modifies owing to their better thermal and thermo-oxidative stability, outstanding moisture resistance, partial ionic nature, low surface energy, superior flame retardancy and the probable free rotation of chains about the Si-O bonds contribution unique flexibility, as well as the excellent hydrophobicity and compressivity[18]. Silicone rubbers, particularly poly(dimetylsiloxane) (PDMS), exhibited a number of good-looking properties including soaring chain flexibility, elevated thermal and oxidative stability, low temperature flexiblility and excellent hydrophobic behavior[19,20]. This combination of excellent features provided the essential conditions for the application of PDMS as an elastomeric modifier to build the modified epoxy resin with enhanced properties[21-23]. However, pure PDMS had extremely little use as a toughening agent because of the deprived compatibility between soft segments of PDMS and polar hard segments in epoxy, which principally resulted from the lack of hydrogen bonding. These materials, which typically exhibited separate T_g values due to thermodynamic inaptness, were either macroscopically immiscible or exuded from the cross-liked matrix during curing procedure in the conservative introduction of siloxane into polymers during blending methods[24,25], ensuing in deprived thermo-mechanical properties and compositional heterogeneity ensuing from poor segmental compatability, this partial the use of larger silicone concentrations[26,27]. To conquer this limitation and improve the interface between PDMS and epoxy matrices with enhanced thermo-mechanical properties and toughness, numerous techniques were reported in the literature, counting using silane coupling agents[28,29].

In our study, the EPDM was first epoxidized with *in situ* formed per formic acid, which induced functional epoxy groups into the EPDM macromolecular backbone. Further, 3-aminopropyltriethoxysilane and poly dimethlsiloxane on epoxidized ethylene-propylene-diene terpolymer has been synthesized in toluene. The structural, thermal and morphological properties were investigated using FTIR, TGA and SEM.

EXPERIMENTAL

Materials

The EPDM (ENB) elastomer used in this study was a commercial grade Nordel IP

4770P (ethylene/propylene/5-ethylidene-2-norborane = 70/25/5 by wt. %, Mooney viscosity, $MIL_{(1+4)}$ at 125°C is 70 and density of 0.87 g/cc) of DuPont Dow elastomer, USA. Hydroxl-terminated polydimethylsiloxane (HTPDMS) as modifier, 3-aminopropyltriethoxysilane (APTES), was procured from Aldrich Chemicals, USA. Dibutyltindilauarate (DBTDL) was purchased from Merck, Germany. Analytical grade formic acid (88%), hydrogen peroxide (30%), toluene-hexane were used as received.

In situ epoxidation of ethylene-propylene-diene terpolymer

The EPDM was first dissolved in toluene in a three necked flask equipped with a mechanical stirrer and thermometer and maintained at 50°C in water bath. Under continuous stirring, the EPDM solution was acidified stepwise with 88% formic acid to pH 2-3. The epoxidation was performed by dropping the required amount of H_2O_2 (30%) for 30 min. A rapid introduction of this reagent is not recommended, because it causes excessive development of oxygen due to the decomposition of hydrogen peroxide at high temperature. The reaction was continued for 7 hr at 50°C. After epoxidation, the rubber was coagulated in acetone, thoroughly washed with distilled water, soaked in 1% w/v Na_2CO_3 solution for 24 hr and finally rinsed with distilled water. The rubber prepared was dried in a vacuum oven at 40°C to a constant weight.

Preparation of Siliconized epoxidized EPDM

The reactions are carried out in 500 mL three necked, round bottom flask equipped with a reflux condenser, a Teflon-coated mechanical stirring and a nitrogen inlet. 10 g of eEPDM was dissolved in 2900 mL toluene and refluxed untill complete dissolution of eEPDM. Further, 0.25 wt.% APTES and 0.75 wt.% dissolved in 50 mL of toluene were added to eEPDM, using dibutyl tindilaurate catalyst, with continuous stirring for 2 hr at 50°C. After the completion of reaction, the products were precipitated with methanol, filtered and dried in vacuum.

Measurments

EPDM, eEPDM and Siliconized epoxidized EPDM were characterized with the help of IR spectra obtained from Shimadzu-1800S, using solvent casted thin films. Thermo gravimetric analysis (TGA) were carried using a NETZSCA TG 209 instrument under nitrogen atmosphere at a heating rate of 10°C/min. Scanning electron micrographs were performed on a Quanta-200, FEG (SEM, Netherland) at accelerating voltages of 20.00 kV. The surface of samples was sputtered with a thin layer of gold.

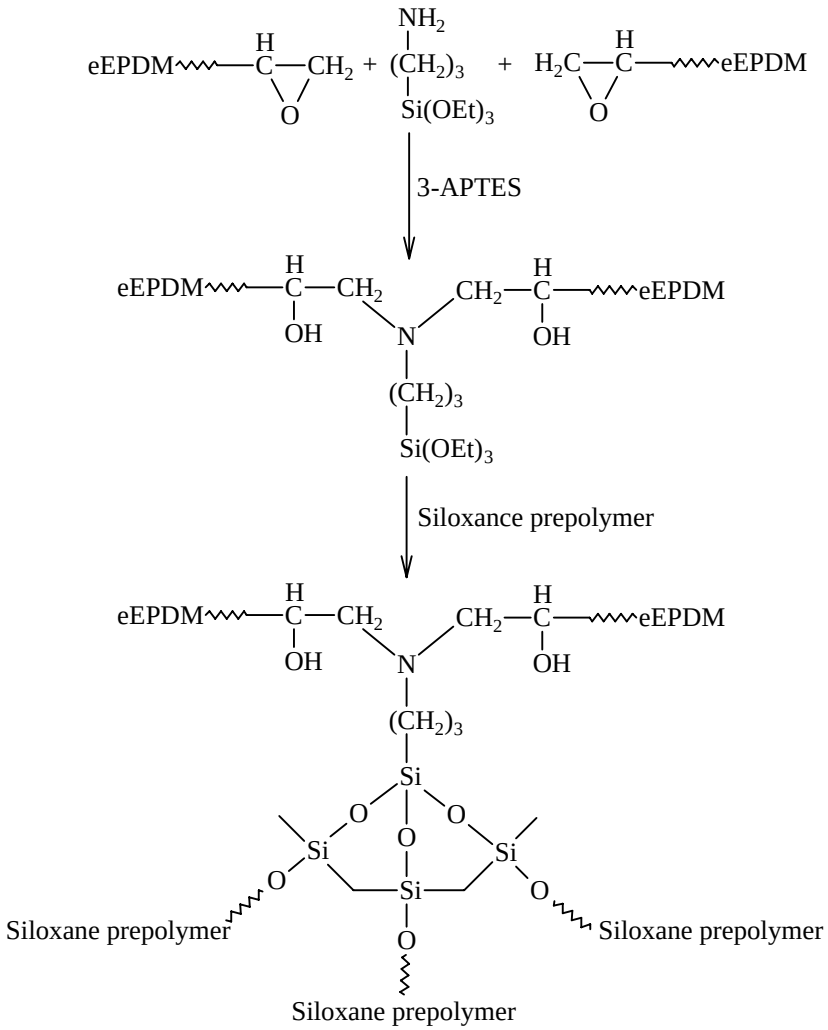

Scheme 1: Schematic representation of Siliconized epoxidized EPDM

RESULTS AND DISCUSSION

Fourier-transform infrared spectroscopy

Fig. 1 shows the FTIR spectra of EPDM, eEPDM and Siliconized epoxidized EPDM. The IR spectra of EPDM (Fig. 1(a)) shows the C-H stretching vibration (aliphatic) at 2911 cm^{-1}, -CH_2 rocking vibration at 1451 cm^{-1}, CH_3 symmetric bending vibration at 1367 cm^{-1} due to the presence of propylene group, -$(CH2)_n$- wagging vibration at 721 cm^{-1} due to the presence of polyethylene chain, C-C stretching vibration at 2851 cm^{-1} and the

unsaturation band (>C=CH-) at 811 cm^{-1} due to the presence of ENB content. The FTIR spectrum of EPDM (Fig. 1 (b)) was characterized by the presence of an epoxides band at 870 cm^{-1} due to asymmetric epoxides ring stretching. Furthermore, the intensity of the >C=CH- band at 811 cm^{-1} decreases because o the expoxidation of EPDM, which demonstrates that the C=C double bond in EPDM was converted to the epoxy functional group in eEPDM. The conversion of double bond to epoxides was obtained as 50% (ca.2.4 mol %). To take advantage of relative change of absorbance at 811 and 870 cm^{-1}, a quantitative analysis was performed by area measurement of methyl deformation band at 1369 cm^{-1} as internal standard[30].

Fig. 1 (c) illustrates the IR spectra of Siliconized epoxidized EPDM, which reveals; absorption peak appeared at 2900 cm^{-1} and between 1140 cm^{-1} to 960 cm^{-1} confirms the presence of –Si-$(CH_2)_3$- and residual –Si-OH, respectively. Absence of peak at 2850 cm^{-1} of –Si-OCH_2CH_3 and formation of Si-O-Si at 1143 cm^{-1} confirms the completion of reaction between HTPDMS and APTES coupled epoxidized EPDM.

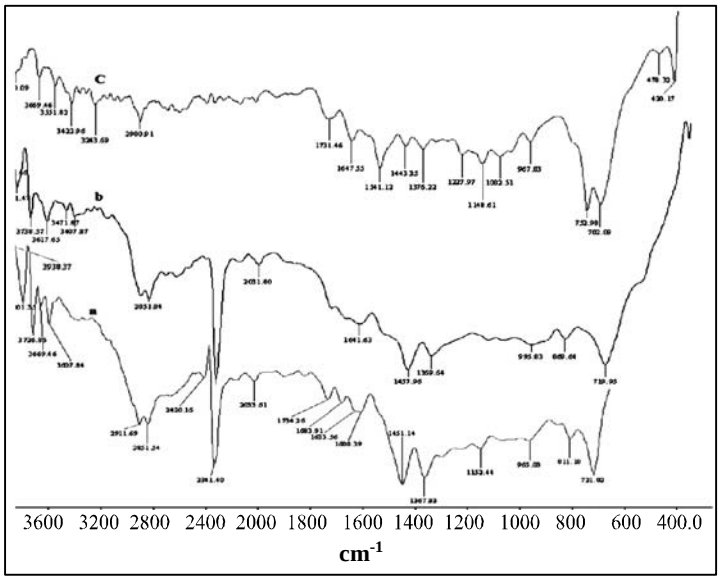

Fig. 1: FTIR spectra of (a) EPDM (b) eEPDM and (c) Siliconized epoxidized EPDM

Thermal properties

Thermogravimetric analysis

Thermograms of EPDM, eEPDM and siliconized epoxidized EPDM are given in Fig. 2. The inception decomposition temperature of EPDM, eEPDM and siliconized

epoxidized EPDM are 440, 444 and 453°C, respectively. Similarly the final decomposition temperatures of EPDM, eEPDM and Siliconized epoxidized EPDM are 482, 486 and 494°C, respectively. The higher thermal stability of eEPDM compared to EPDM can be explained by the substitution of the double bond on the EPDM side chain with the epoxy rings[31]. Siliconized epoxidized EPDM also increases both inception and final decomposition temperatures because of the delay in degradation caused by silicone moiety may be attributed to its, high bond energy and thermal partial ionic nature and thermal stability of -Si-O-Si- linkage.

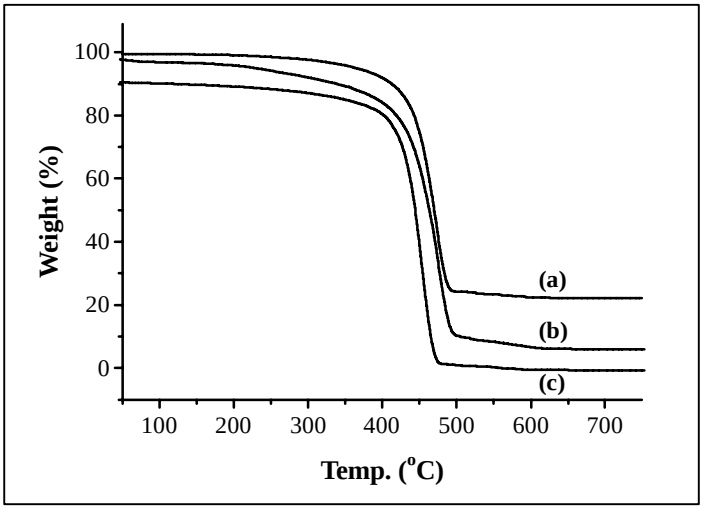

Fig. 2: TGA curves of (a) EPDM (b) eEPDM (c) Siliconized epoxidized EPDM

Differential scanning calorimetry

The glass transition behavior of the hybrid material is associated with cooperative motion of large chain segment. The DSC results of EPDM, eEPDM and Siliconized epoxided EPDM are shown in Fig. 3. The midpoints of the transition temperature curve in the DSC curve are recorded as T_g values. The T_g values EPDM, eEPDM and Siliconized epoxided EPDM are 43, -40 and -36°C. The glass transition temperatures T_g, increased due epoxidation. The increase in T_g as a result of epoxidation may be caused by the presence o the polar epoxides group, which gives more backbone than the unsaturated group[32,33]. The results also indicate that the T_g value for Siliconized EPDM is higher than eEPDM and EPDM, due to the silane content. Similar behavior was obtained for PMMA-MSMA hybrid system[34].

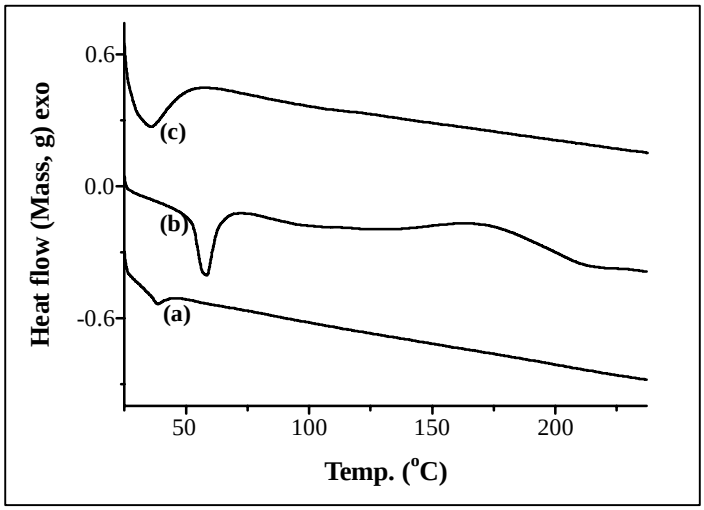

Fig. 3: DSC curves of (a) EPDM (b) eEPDM (c) Siliconized epoxidized EPDM

SEM Analysis

The morphological characterization of the films was carried out through SEM analysis. Fig. 4, 5 show the SEM photographs of EPDM and eEPDM, which indicates a plane and smooth surface with some bigger particles. However, the surface of Siliconized epoxidized EPDM is some orientations as seen in Fig. 6. The optimal network structure appears on the surface of Siliconized epoxidized EPDM can be probably due to –Si-O-Si- linkage.

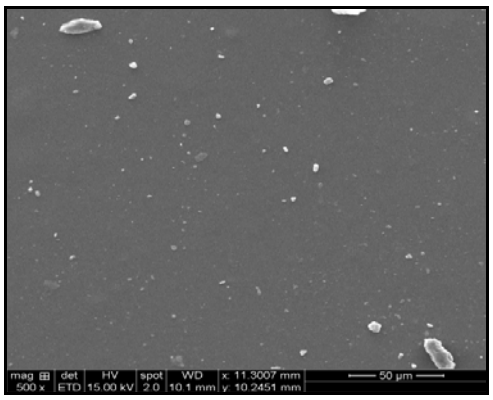

Fig. 4: SEM photograph of EPDM

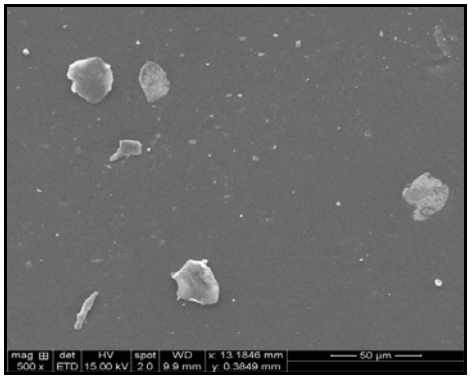

Fig. 5: SEM photograph of eEPDM

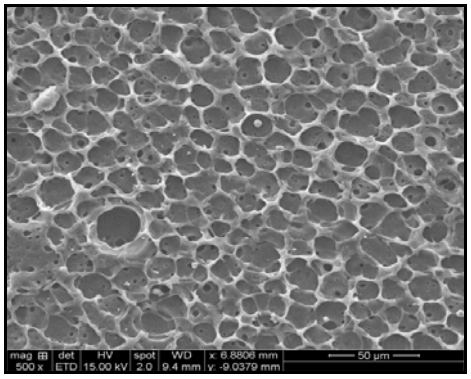

Fig. 6: SEM photograph of Siliconized epoxidized EPDM

CONCLUSION

Siliconized epoxidized EPDM was synthesized in toluene. The following conclusions were made based on the data resulted from different experimental studies. The completion of reaction between HTPDMS and APTES coupled, which has been confirmed from FTIR spectra. Siliconized epoxidized EPDM also increaseas both inception and final decomposition temperatures because of the delay in degradation due to their inherent flexibility and free rotation about bond. The SEM micrograph of the Siliconized epoxidized EPDM system reveals that the optimal network structure appears on the surface can be probably due to –Si-O-Si- linkage.

REFERENCES

1. S. Ahmad, S. M. Ashraf, S. N. Nusrat and A. Hsanat, J. Appl. Polym. Sci., **95**, 494-501 (2005).

2. S. Ahamd, A. P. Gupta, E. Sharmin, M. Alam and S. K. Pandey, Prog. Org. Coat., **54**, 248-255 (2005).

3. M. Alagar, A. A. Kumar, A. A. Prabu and A. Rajendran, Int. J. Polym. Meter., **53**, 45-58 (2004).

4. M. Alagar, T. V. Thanikaivelan and A. Ashokkumar, J. Polym. Comp., **21**, 739-744 (2000).

5. A. Anand and P. M. Alagar, J. Macromol. Sci. Part A, **42**, 175-188 (2005).

6. P. V. A. Kumar, S. A. Kumar, K. T. Varughese and S. Thomas, J. Mater. Sci., **47**, 3293-3304 (2012).

7. H. Azizi, M. Morshedian, M. Barrikani and M. H. Wagner, Advances in Polymer Technology, **30**, 286-300 (2011).

8. M. Biley and M. Kontoulou, Polymer, **50**, 2472-2480 (2011).

9. R. Bera and S. Koner, Inorganica. Chemica. Acta, **384**, 233-238 (2012).

10. S. Bhattacharjee and J. A. Anderson, J. Mol. Catal. A. Chem., **249**, 103-110 (2006).

11. J. Chojnoswski, M. Cypryk, W. Fortuniak, K. Rozga-Wiijas and M. Scibiorek, Polymer, **43**, 1993-2001 (2002).

12. D. E. Leyden, Silanes, Surfaces and Interfaces, Gordon and Breach, New York (1986).

13. F. Deflorian, S. Rossi, M. Fedal and C. Motte, Progress in Organic Coating, **69**, 158-166 (2010).

14. K. A. Dubey, Y. K. Bhardwaj, K. R. Kumar, L. Panicker, C. V. Chaudhari, S. K. Chakraborty and S. J. Sabharwal, Polym. Res., **19**, 9876-9885 (2012).

15. G. Grigoropolulou, J. H. Clark and J. A. Elings, Green Chem., **5**, 1-7 (2003).

16. N. Hiyoshi, Applied. Catalysis. A, **420**, 164-169 (2012).

17. S. S. Hou and Y. P. Chaung and P. L. Kuo, Polymer, **41**, 3263-3272 (2000).

18. G. H. Hsiue, W. J. Wang and F. C. Chang, J. Appl. Polym. Sci., **73**, 1231-1238 (1999).

19. K. J. Kim, J. Appl. Polym. Sci., **116** 237-244 (2010).

20. L. Konczol, W. Doll, U. Buchholz and R Mulhaupt, J. Appl. Polym. Sci., **54**, 815-826 (1994).

21. S. P. Mahapatra, D. K. Tripathy and J. Lee, Polym. Bull., **68**, 1965-1976.

22. K. Matuska, K. Hagesawa, H. Inoue, A. Fukuda and Y. Arita, J. Polym. Sci. Part. A., **30**, 2045-2048 (1992).

23. L. Rey, J. Mater. Sci., **34**, 1775-1781 (1999).

24. S. K. Samantaray, Pure. Appl. Chem., **72**, 1289-1304 (2000)

25. X. Shen, W. Fan, Y. He, P. Wu, J. Wang and T. Tatsumi, Applied. Catalysis A., **401**, 37-45 (2011)

26. W. Noll. Chemistry and Technology of Silicones, Academic Press, New York (1969).

27. C. S. Wu and Y. S. Chiu, Polymer, **43**, 4277-4284 (2002).

28. C. Yuken, X. Chuanhui, C. Liming, W. Yanpeng and C. Xiaodong, Polymer. Testiong., **31**, 728-736 (2012).

29. F. Zafar, E. Sharmin, S. M. Ashraf and S. Ahamad, J. Appl. Polym. Sci., **97**, 1818-24 (2005).

30. W. Zhenhua, L. Yonglai, L. Jun, D. Zeimen, Z. Liqun and W. Weimin, J. Appl. Polym. Sci., **119**, 1145-1155 (2011).

31. M. Ziolek, Catal. Today **90**, 145-156 (2004).

32. C. M. Rolan, Macromolecules **25**, 7031-7036 (1992).

33. C. M. Roland, K. J. Kallitisis and K. G. Gravalos, Macromolecules, **26**, 6474-6476 (1993).

34. Z. H. Hung and Y. Qiu, Polymer, **38**, 521-526 (1997).

Accepted : 31.01.2015

Available online www.jocpr.com

Journal of Chemical and Pharmaceutical Research, 2015, 7(10S):94-98

Research Article

ISSN : 0975-7384
CODEN(USA) : JCPRC5

Studies on low-cost Ion-Exchangers

A. Girija[1], R. K. Seenivasan[2] and M. Thenmozhi[3]

[1]*Department of Chemistry, Mohamed Sathak Engineering College Kilakarai*
[2]*Department of Chemistry, Government Arts College, Melur*
[3]*Department of Chemistry, Government Arts College (Women) Pudukkottai*

ABSTRACT

Phenol – formaldehyde resin (PFR) was prepared and blended with sulphonated charcoals (SCs) prepared from Curry Leaf Carbon. Composite ion exchange resins (IERs) were prepared by varying the amount of SCs (10-30%w/w) in the blends. All the important physico - chemical properties have been analysed. Composites up to 20% (w/w) blending retain almost all the essential characteristics and Cation Exchange Capacity (CEC) of the original PFR. It is concluded that blending of PFR by SCs will reduce the cost of IERs.

Key words: Phenol formaldehyde resin, sulphonated carbon, Cation exchange capacity

---

INTRODUCTION

Industrialised nations of the world are taking active measures to control the environmental pollution caused by the hazardous chemicals especially toxic metal ions. In the wastewater treatment, usually a decreasing level of pollutants is achieved, rather than the selective removal and recovery. Ion exchange is an appropriate technique for removal and recovery, as it is employed in the separation and concentration of ionic materials from liquids [1].

Many ion exchangers owe their origin to petroleum products and there is a continual increase in their cost. Further more the difficulty also exists in its procurement due to the scarcity of petroleum resources. Hence, there is an urgent need to find out the new low - cost ion exchange resin (IERs) and reduce the cost of IERs by blending it with sulphonated carbons (SCs) prepared from plant materials containing phenolic groups. Earlier studies show that the cheaper composite ion-exchangers could be prepared by partially blending the macro porous / macro reticular phenol-formaldehyde sulphonic acid resin (PFSAR) matrix by SCs prepared from coal [2], saw dust [3], spent coffee [4], cashew nut husk [5], wheat husk [6], turmeric plant [7], spent tea, gum tree bark [8], *Accacia nilotica* [9] and Egyptian bagasse pith [10].

Attempts have been does made to prepare cheaper cationic resins (CRs) from natural products. Ion-exchange process finds a valuable place in the treatment of waters and waste water discharged from plating and other industrial processes containing metal ions.

The aims and objectives of the present work are to synthesise, characterise the new composite ion exchangers of PhOH – HCHO type/cationic matrices blended with sulphonated Curry Leaf Carbon (CLC) and to estimate the column exchange capacity (CEC) for some selective metal ions.

EXPERIMENTAL SECTION

2.1 Materials

The raw/plant material used was Curry Leaf Carbon (CLC). This is a plant material freely available in Tamil Nadu, India. Phenol and formaldehyde used were of Fischer reagents (India). LR grade of con. sulphuric acid (Sp.gr.= 1.82) was used. The plant material was locally collected, cleaned, dried and cut into small pieces of about 0.5cm length. The other chemicals / reagents used were of chemically pure grade(AnalaR) procured from SD fine chemicals, India.

2.2 Methods

Curry Leaf Carbon (500g) was carbonised and sulphonated by con. sulphuric acid, washed to remove excess free acid and dried at 70^0C for 12 h [6-10]. It was labeled as CLC. Pure phenol – formaldehyde resin (PFR) was prepared according to the literature method [3, 6 – 8]. It was then ground, washed with distilled water and finally with double distilled (DD) water to remove free acid, dried, sieved (210 – 300 μm) using Jayant sieves (India) and preserved for characterisation [3,6-8,11]. It was labeled as PFR. The composites were obtained as per the method reported in literature[3,6– 8]. The products with 10, 20 and 30%(w/w) of CLC in the blend / composites, respectively were labeled as R1,R2 and R3. A separate sample o (Commercial Resin) and CLC were also subjected to the characterisation studies.

2.3 Characterisation of samples

Samples were ground and sieved into a size of 210 – 300μm using Jayant sieves (India). This was used for further characterisation by using standard procedures [3,7,8,] to find out the values of absolute density (Wet and dry in water and toluene, respectively), percentage of gravimetric swelling and percentage of attritional breaking.

The solubility of these samples was tested by using various organic solvents and inorganic reagents.

The values of cation exchange capacity (CEC) were determined by using standard titration techniques [12], as per the literature method [13].

RESULTS AND DISCUSSION

3.1 Synthesis

The experimental and theoretical compositions of CLC in the composites (R1 – R3) are in good agreement with each other (Table 1). The results are similar to those obtained by Sharma *et al* [2] . This indicates that the preparative methods adopted for the synthesis of PFR and its composites (R1 – R3) are more reliable and reproducible. The optimum value of formaldehyde and phenol are found to be 10mL and 11.5 mL, respectively.

3.2 Characterisation studies

3.2.1 Physico – chemical properties

The data given in Table 2 show that the values are absolute density (wet and dry in water and toluene respectively) are decreased from CR to PFR to composite with highest %(*w/w*) of CLC and finally to pure CLC. The values of absolute density of composite in dry and wet forms depend upon the structure of the resins and its degree of cross linking and ionic form [14]. Generally the absolute density decreased with increase in CLC content in the composite.

The high value of absolute density indicates a high degree of cross linking, and hence suitable for making columns for treating polar and non - polar effluent liquids of high density. The values of absolute densities for the different composites in the dehydrated states are higher than the hydrated states. Moreover, the values of wet and dry density are close to each other indicates that the pores of the sample may be macro porous in nature.

The data given in Table 2 indicate that the % of gravimetric swelling decreases from CR (73.08%), PFR (68.96%) to CLC (27.29%). The value of average % of gravimetric swelling decreased with increasing CLC content in the composite. The values of % gravimetric swelling are found to be 52.80%, 41.70% and 36.76% respectively, for 10, 20 and 30% (*w/w*) of mixing of CLC with PFR compared to that of pure PFR. This indicates that up to 20% (*w/w*) CLC could be mixed with the PFR. The rigidity of the resin matrix was thus concluded from the % of gravimetric swelling measurements. Therefore, these composite resins with increasing amount of CLC content in the composites showed lower % of gravimetric swelling which revealed much lower rigid shape, and the rigidity of composites (from R1 to R3). It indicates that, pure resin and composites are rigid with non - gel macro porous structure [11].

ttritional breaking (Table 2) increase with increase in % (w/w) of CLC content in the ; the stability of the resin, which decreases from PFR to CLC. Therefore, the mechanical

stability is good upto 20 - 30% *(w/w)* substitution of CLC in pure resin. This observation also shows that, the capillaries of the IER may be occupied by the sulphonated carbon(CLC) particles[6-8].

3.2.2. Solubility of Ion Exchangers

The chemical stability of ion exchange resins under the present study are established by testing their solubility in a few selected organic solvents and reagents the results are presented in Table 3.

The samples tested viz., CR, PFR, SC, R1, R2, and R3, are all practically insoluble in almost all the reagents and polar and organic solvents. It was noted that the resins and condensates (except CLC) are partially soluble (5 - 10%) in 20% NaOH solution. This is because these samples have phenolic groups in them and hence could not be used in strongly basic medium owing to its solubility. This indicates a high degree of cross-linking in all the samples (*i.e.*) the basic polymer unit is mostly of higher molecular weight fractions or atleast the absence of very low molecular weight fractions in the resins. Hence, the samples could be used to make cations exchanger column, which could be used acidic neutral and light alkaline medium and treat non-aqueous industrial effluents.

3.2.2 Cation exchange capacity (CEC)

CEC data shown in Table 4 indicate that, the CEC values (for 0.1M solution of metal ions) decrease when the % (*w/w*) of CLC content *(w/w)* in the composite increases.

The relative value of CEC of individual metal ions depends upon the atomic radius or atomic number [15]. At the same time the CEC also depends upon the anionic part of the metal salt. *i.e.*, inter ionic forces of attraction between anions and cations, which plays a vital role in cation exchange capacity of particular metal salt solution [16,17].

From the CEC data given in Table 4, the cation exchange capacity of the samples was found to decrease in the following order.

$$\mathbf{Cu^{2+} > Mg^{2+} > Ca^{2+} > Zn^{2+} > Na^{+}}$$

The selectivity order of metal ions *i.e.*, orders of CEC values also depends upon the ionic potential and the hydrated atomic radius of the metal ions in solution [17]. The order of exchange affinities of various metal ions is not unique to ion exchange system. Only under dilute conditions Hofmeister or lyotropic series [14] is obeyed. But, under high concentration it is different [14]. It is equally important to note that the relative behaviour of these ions for other ionic phenomena deviates the affinity order under the same conditions [18]. The observed order in the present study is different from that of the Hofmeister or lyotropic series [14]. This may be due to the concentration of the influent metal ion solutions, which is relatively high and also due to the selectivity of the metal ions. Also, the CEC data given in the Fig.1, conclude that, upto 20% *(w/w)* blending of CLC with PFR retains 77.12 - 95.7% of CEC for all metal ions. Hence, 20% (*w/w*) blending of CLC with PFR to an extent of 20 %(*w/w*) will reduce the cost of the IER.

It is observed that there is a continuous decrease in cation exchange capacity (CEC), as the percentage of CLC content in the blend increases. Hence, any chemical methods requiring ion exchangers of small ion exchange capacity, 20% (*w/w*) blended CLC –PFR resin could be used. CLC can be inexpensively prepared from the plant materials, Curry Leaf., which is freely available in plenty, in India, especially in Tamil Nadu.

TABLE :1 Amount of regents used and yield of condensates

Sample	Percentage of SC* (w/w)	Amount of reagents taken				% of SC (w/w) in yield (experimental)
		Phenol (ml)	HCHO (ml)	SC (g)	Yield (g)	
PFR	0	10	11.5	0.00	21.4	0
R1	10	10	11.5	2.37	22.08	10.73
R2	20	10	11.5	5.35	26.91	19.88
R3	30	10	11.5	9.17	44.38	20.66
SKC	100	-	-	-	-	-

- *SC – Sulphonated Carbon derived from a **Curry Leaf Carbon** (CLC)*

Table.2. Physico–chemical properties of Resins

Properties		CR	PFR	R1	R2	R3	SC
Absolute Density ($g\ mL^{-1}$)	Dry	1.49	1.34	1.26	1.23	1.20	1.00
	Wet	1.69	1.54	1.43	1.30	1.19	0.92
% of Gravimetric swelling		73.08	68.96	52.80	41.70	36.76	27.29
% of Attritional breaking		13.26	7.61	12.6	13.9	16.10	21.5
pH		6.6	6.8	6.5	6.9	6.4	6.7
Conductivity$x10^{-3}$ (ohm/cm)		0.43	1.43	0.06	0.1	0.72	0.83
% of Moisture		0.46	0.43	0.51	0.54	0.67	0.56

Table.3 Solubility of pure resin and condensates

Solvent	CR	PFR	R1	R2	R3	SC
Con.H_2SO_4	X	X	X	X	X	X
Con.HCl	X	X	X	X	X	X
Con.HNO_3	X	X	X	X	X	X
NaOH(20%)	PS	PS	PS	PS	PS	X
Benzene	X	X	X	X	X	X
Toluene	X	X	X	X	X	X
Ethanol	X	X	X	X	X	X
Methanol	X	X	X	X	X	X
Acetaldehyde	X	X	X	X	X	X
Chloroform	X	X	X	X	X	X
Diethyl ether	X	X	X	X	X	X
CCL_4	X	X	X	X	X	X
CS_2	X	X	X	X	X	X

Where x – Insoluble and PS – Partially soluble (up to 5 – 10%)
SC – Insoluble in all the solvents and reagent

Table : 4 CEC in meq g^{-1} for various metal ions (for 0.1m solution)

Sample	% of SC in resin (*w/w*)	Na^+	Ca^{2+}	Mg^{2+}	Zn^{2+}	Cu^{2+}
CR	-	1.51	1.68	1.52	1.32	1.76
PFR	-	0.64	1.42	1.41	1.29	1.55
R1	10	0.48	1.28	1.38	1.21	1.49
R2	20	0.32	1.20	1.28	1.19	1.46
R3	30	0.21	1.10	1.20	1.12	1.42
SC	100	0.10	0.91	1.08	1.14	1.32

Fig 1 Cation Exchange Capacities of H^+ form of IERs, for Various Metal Ions Relative to PFR

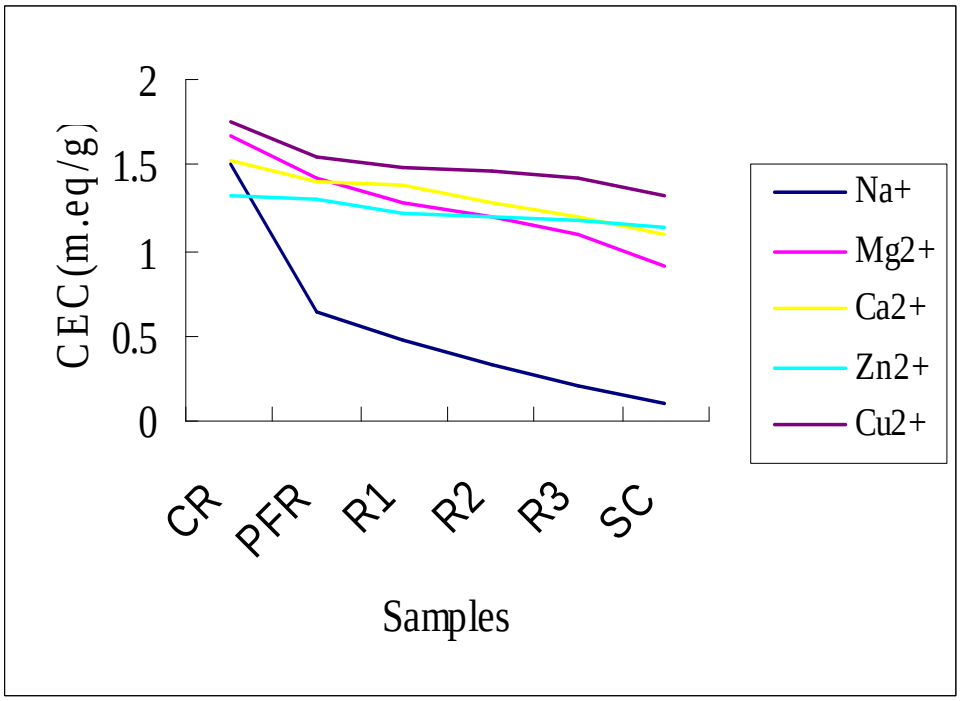

CONCLUSION

It is concluded from the result of the present study that PFR sample could be blended with 20% (*w/w*) of CLC, without affecting its physico-chemical and ion exchange properties. Hence, blending of PFR with 20% (*w/w*) of CLC will definitely lower the cost of IER for the treatment of industrial effluent for the removal of metal ions.

REFERENCES

[1] B.A. Bolto and L. Pawlowsk, *Waste Water Treatment by Ion-exchange*, Oxford & IBH Publ. Co., New Delhi, (**1987**).
[2] N.L.N. Sharma, Joseph Mary and Padma Vasudevan, *Res.Ind*., **21** 173 (**1976**)
[3] Padma Vasudevan and N.L.N. Sharma, *J.Appl. Poly.Sci*., **23,** 1443 (**1979**)
[4] G.J. Mohan Rao and S.C. Pillai, *J. Indian Inst .Sci*., **36A,** 70 (**1954**)
[5] Shahha and S.L. Batna , *J. Appl. Chem. Lond*., **8,** 335 (**1953**)
[6] T. Dheiveesan and S. Krishnamoorthy, *J. Indian Chem.Soc*.,**65,** 731 (**1988**)
[7] D. Kathiresapandian and S. Krishnamoorthy, Indian. *J. Technol*.,**29,** 487 (**1991**)
[8] A. Mariamichel and S. Krishnamoorthy, *Asian J. Chem*., **9(1),** 136 (**1997**)
[9] N. Kannan, R.K. Seenivasan and R. Mayilmurugan, *Indian J. Chem. Technol*., **10,** 623 (**2003**)
[10] M.S. Metwally, N.E. Metwally and T.M. Samy, *J. Appl. Poly. Sci*., **52**, 61 (**1994**)
[11] M. Natarajan and S. Krishnamoorthy, *Res. Ind*., **38,** 278 (**1993**)
[12] G.H. Bassett, J. Jeffery, J. Mendham and R.C. Denney, *Vogel's Text Book of Quantitative Chemical Analysis*, 5th Edn. Longman Group Ltd., London, (**1989**)
[13] S. Ramachandran and S. Krishnamoorthy, *Indian J. Technol***., 22,** 355 (**1984**)
[14] R. Kunin, *Ion Exchange Resin*, Wiley, Newyork and London, 2nd Edition, (**1958**)
[15] S. Mattson, *Ann. Agric. Coll., Sweden*, **10,** 56 (**1942**)
[17] W.K. Son, S.H. Kim and S.G. Park, *Bull.Korean Chem.Soc*., **22 (1) ,** 53 (**2001**)
[16] D.K. Dimov, E.B. Petrova, I.M. Panayotov and Ch.B.Tsvetanov,
[17] *Macromolecules*, **21**, 2733 (**1990**)
[18] O. Bonner, G. Easterling, D. Weit and V. Holland, *J.Am.Chem.Soc*., **77**, 242 (**1955**).

Available online www.jocpr.com

Journal of Chemical and Pharmaceutical Research, 2015, 7(10S):141-145

Research Article

ISSN : 0975-7384
CODEN(USA) : JCPRC5

The studies on optical and structural properties of zinc sulfide thin films deposited by SILAR method

Haneefa Mohamed Mohaideen[1], Kandasamy Saravanakumar[1*], Suldanmohideen Sheik Fareed[1], Mohideen Mohamed Gani Kalvathee[2] and Jeyaraj Dhaveethu Raja[2]

[1]Department of Physics, Mohamed Sathak Engineering College, Kilakarai, India
[2]Chemistry Research Center, Mohamed Sathak Engineering College, Kilakarai, India

---

ABSTRACT

In the present work, the compound semiconducting zinc sulfide (ZnS) thin films were deposited on glass substrate using successive ionic layer adsorption and reaction technique by the various sulfur concentration(0.2 M to 1 M). The preparative parameters such as concentration, temperature, deposition time, pH of solution have been optimized. The characterization of thin films was carried out for the structural and optical properties. The thin films were characterized by using X-ray diffraction (XRD), UV-VIS Spectra and photoluminescence (PL). The X-ray diffraction pattern (XRD) revealed that the ZnS film has hexagonal and cubic crystal structure. All deposited films exhibit a relatively high transparency in the range of 300 to 800 nm. The band gap varies from 3 to 3.75 eV. Photoluminescence spectra showed blue emission band (480 nm) and green emission band (524 nm).

Key words: zinc sulfide, absorption coefficient and photoluminescence (PL).

INTRODUCTION

ZnS is one of the earliest semiconductors discovered and has novel fundamental property in order to suit diverged application. It is non toxic to human body and abundant. ZnS in its nano structures form attracted researches attention due to its special structure (Zinc blend and wurtzite) related to chemical and physical properties and for potential application in optoelectronic and nano electronic devices which includes blue LED's, electroluminescence, photoluminescence, cathodoluminescence, sensors, solar cells etc.[1]. In addition, Chalcopyrite-based thin film devices (CIGS) contain a so-called buffer layer, made of cadmium sulfide (CdS). Cadmium is highly toxic and therefore, alternative materials are being sought that can replace CdS without losses in its performance. The ZnS is an alternative to CdS [2-5]. Several techniques on growing ZnS thin film have been reported, which include sputtering[6], spray pyrolysis[7], chemical bath deposition[8,9], molecular beam epitaxy (MBE) [10], pulsed-laser deposition (PLD) [11], chemical vapour deposition (CVD) [12], metalorganic chemical vapour deposition (MOCVD) [13], metalorganic vapour-phase epitaxy (MOVPE) [13], atomic layer epitaxy (ALE) [14] and successive ionic layer adsorption and reaction (SILAR) [15]. Among these methods, the SILAR is relatively cost effect, simple and convenient for large area deposition which suit for doping different element in an easy way and which require any sophistication. In the present work, ZnS thin films were grown by SILAR technique through a different set of precursor. Different ZnS thin films were deposited by varying five different anion source concentrations and were characterized for their optical and structural properties.

EXPERIMENTAL SECTION

›strate cleaning of ZnS thin films

›own on glass substrates by the SILAR technique. To deposit ZnS one SILAR growth cycle four steps: a well-cleaned glass substrate is immersed in the first reaction vessel containing

aqueous cation precursor 0.2M Zinc acetate dehydrate solution at pH 10. After the cation immersion, the substrate is moved to the rinsing vessel where it is washed with purified water. The sulphide ions were adsorbed from an aqueous 0.2 M Thiourea solution with pH 12 which acts as anion source. After anion immersion the substrate was washed as described above; thus the first SILAR growth cycle is finished. Repeating these cycles a thin film with desired thickness can be grown. The cation and anion immersion times were 15 s. The temperature of the solutions was maintained at 65 °C (± 5°C). The ammonium hydroxide was used as complexing agent. The different thin films were prepared by varying the zinc to sulphide source ratio as 1:1, 2, 3, 4 and 5 respectively. The preparative parameters used for the deposition of ZnS thin films are summarized as below (Table 1). The glass slides of dimensions 26mm×76mm×2mm were used. Before deposition, they were etched by using chromic acid bath kept at 70^0c for 2h. After the etching process, they were cleaned with deionized water and acetone. The substrate cleaning plays an important role in the deposition of thin film. The cleaned substrate surface provides nucleation sites, which results in uniform film growth [16].

Table 1. ZnS thin film synthesis parameter.

S.NO.	PARAMETER	CATION SOULTION	ANION SOLUTION
1.	Materials	Zinc acetate dehydrate	Thiourea
2.	Concentration of solution	0.2 M	0.2, 0.4, 0.6, 0.8 and 1 M
3.	pH value	10	12
4.	Solution temperature	65°C	65°C
5.	Immersion time	15 s	15 s
6.	Total number of deposition cycles	100	100

The overall chemical reaction is summarized as

$$\mathbf{Zn(CH_3COO)_2 2H_2O + 4NH_3 \rightleftharpoons 2(CH_3COO)^- + Zn(NH_3)_4^{2+} + 2H_2O} \quad (\mathbf{1a})$$

$$\mathbf{Zn(NH_3)_4^{2+} \rightleftharpoons Zn^{2+} + 4NH_3} \quad (\mathbf{1b})$$

$$\mathbf{SC(NH_2)_2 + 2OH^- \longrightarrow S^{2-} + CH_2N_2 + 2H_2O} \quad (\mathbf{2})$$

$$\mathbf{Zn^{2+} + S^{2-} \longrightarrow ZnS} \quad (\mathbf{3})$$

2.2 Characterization of thin films

The thickness of the sample was determined by the gravimetric method. The optical properties of ZnS thin films were calculated as a function of concentration of sulphide solution. The UltraViolet-Visible (UV-Vis) spectrophotograph was recorded using the PERKIN ELMER Lambda 35 spectrometer. As the films were examined along with the substrates on which they were formed, it was necessary to take into account the absorbance in the glass substrate even though it was small. Hence, the absorbance spectra of the glass substrates were taken and used for the elimination of the optical absorbance in the glass substrate from the total absorbance in the film–substrate combination to obtain the optical absorbance of the film. The band gap energy change was investigated as function of concentration of sulphide solution. Room temperature photoluminescence (PL) study was performed by using Varian Cary Eclipse fluorescence spectrophotometer. The samples were excited using the 385 nm line. The structure of the film was identified by X-ray diffraction (XRD) with XPERT-PRO (PW-3071) equipped with a Cu Kα (λ=0.154060 nm) radiation source. Data were collected by step scanning from 20^0 to 80^0 with step size of 0.05^0 (2θ).

RESULTS AND DISCUSSION

3.1 Optical characterization

The optical transmittance of as deposited ZnS thin film which deposited varies with respect to the sulphur concentration is shown below (Fig 1). The wavelength of the incident light is 220-1000nm. It reveals that nearly 85% transmittance in the visible wavelength range. In addition, the transmittance decreases at the Zn:S ratio of 1:5. It can be seen that the Zn:S ratio of 1:5 thin film has lower transparency, because it has thicker than the others. Moreover, this film was densely covered by particles and the space of the particle was less so the light cannot transmit easily. So the concentration of sulphur is very important to obtain the high quality ZnS thin film. The optical absorption spectrum of as deposited ZnS thin film varies with respect to the sulphur concentration is shown below (Fig 2). It is clearly seen from the spectra that the film has sharp absorption and the absorption edge slightly shifting towards the lower wavelength indicates the increase of optical band gap. The energy band gap of these thin om absorption spectra using Tauc's relation, [17]

$$\alpha = \frac{K}{h\nu}\left(h\nu - E_g\right)^n \quad (4)$$

Where K is a constant, hν is the photon energy, α is a absorption coefficient and n assumes values of 1/2, 2, 3/2 and 3 for allowed direct, allowed indirect and forbidden indirect transitions respectively. The value of the absorption coefficient 'α' has calculated using the relation, [18]

$$\alpha = \frac{2.3026\ A}{t} \quad (5)$$

Where A is the absorbance and t is the film thickness.

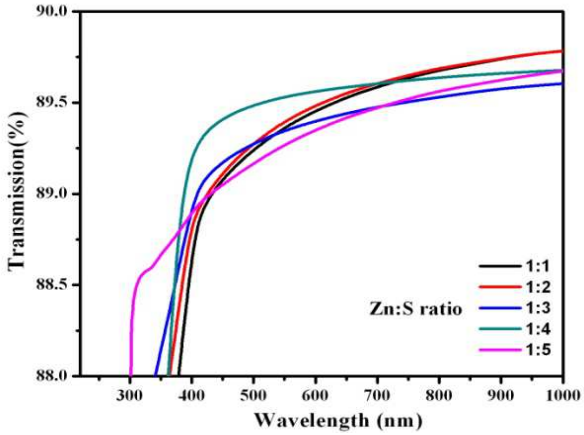

Fig. (1). Transmittance spectra of ZnS films

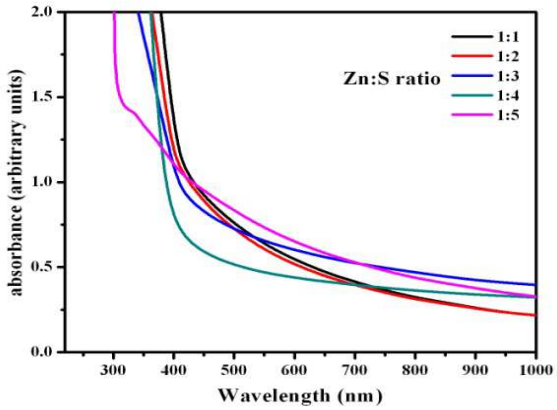

Fig. (2). Absorbance spectra of ZnS thin film

Thus a plot of α^2 vs. hν is a straight line whose intercept on the energy axis gives the energy gap, E_g. The variation of α^2 vs. hν for different sulphur concentration is as shown below (Fig 3). The band gap energies of thin film have been determined by the extrapolation of the linear region on the energy axis. The band gap energy in ZnS thin film is increasing with increasing sulphur concentration. The band gap energy varies from 3 eV to 3.75 eV. The extinction coefficient K_f value decreases with increase in wavelength and becomes constant at higher wavelength (Fig 4). The Extinction coefficients are calculated using the following equation (Equ 6). The extinction coefficient (K_f) is directly related to the absorption of light. In the case of polycrystalline films, extra absorption of light occurs at the grain boundaries [19-20]. This leads to non-zero value of (K) for photon energies smaller than the fundamental absorption edge [21-23].

$$K_f = \frac{\alpha\lambda}{4\pi} \quad (6)$$

3.2 Photoluminescence (PL) study

The room temperature Photoluminescence spectrum of ZnS thin films for various Zn:S ratios are shown in below (Fig 5). It can be seen that the emission is quite symmetric and sharp. There are mainly three luminescence bands present in the all the films, two blue emission band around 413 nm and 480 nm and one green emission band around 525 nm. The luminescence peaks located around 413 nm is associated with the zinc vacancies and that at 480 nm is probably due to sulphur vacancies [24-28]. The green luminescence peaks located around 524 nm is associated with oxide vacancies. It can be seen that as the concentration of sulphur increases the intensity of the emission decreases. The PL signal obtained is quite sensitive to the impurities of defect present within the sample. The decrease in intensity explains that the defect present in the sample also decreases. The emission might be arising from vacancy of sulphur which gets reduced with an increase in concentration of sulphur.

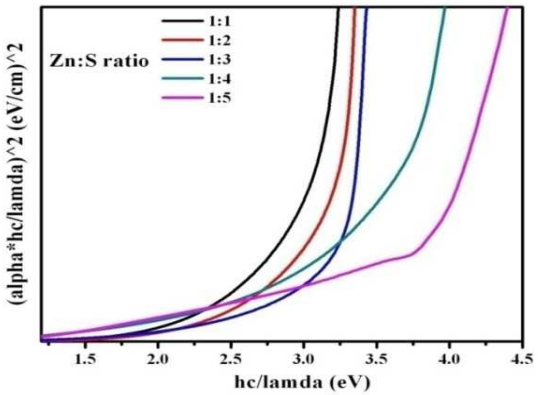

Fig. (3). The plot of $(\alpha hv)^2$ vs. photon energy

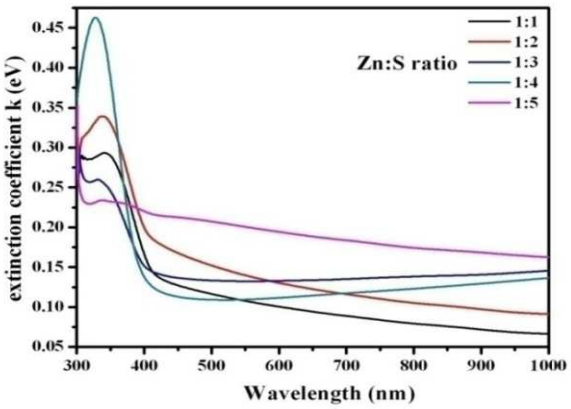

Fig. (4). The plot of Extinction coefficient K_f vs wavelength of ZnS film

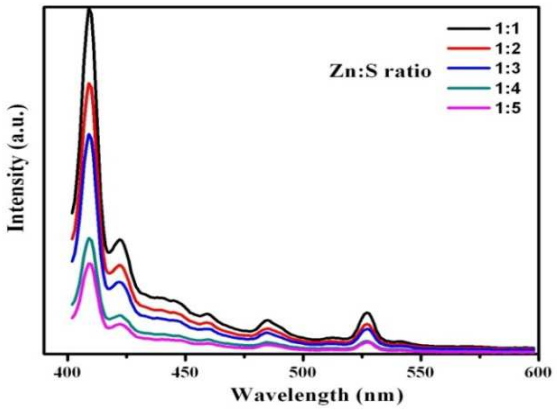

Fig. (5). Photoluminescence spectra of ZnS thin film

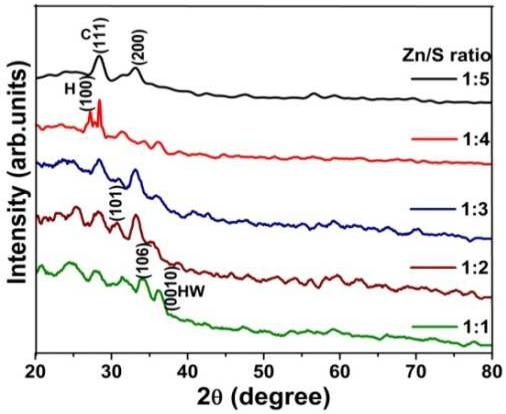

Fig. (6). XRD pattern of ZnS thin film

3.3 Structural studies

The XRD pattern of ZnS thin film is shown as above (Fig 6). It is clearly seen that all the diffraction peaks are well indexed to the standard diffraction pattern of hexagonal and cubic ZnS phases (JCPDS card NO. 89-2344 and JCPDS card NO. 05-0566). A polycrystalline nature is observed for all the deposited films. There is a modification in crystal structure from hexagonal to cubic with increase in sulphur concentration. The crystallite size of the deposited films was decreased from 42 nm to 8 nm by varying the Zn:S ratio. The grain size (D) was calculated from the full width at half maximum (FWHM) (β) by using the Scherer's formula,

$$D = \frac{0.94\lambda}{\beta \cos\theta} \qquad (7)$$

Where λ is the wavelength of X-ray (1.5405Å) and θ is the Bragg's angle.

CONCLUSION

The ZnS thin films exhibit an average transmittance of 85% along the range, confirming the suitability of the films to be used as a buffer layer in photovoltaic applications. The band gap varies from 3 to 3.75 eV. The presence of intrinsic and extrinsic defects is confirmed through PL spectra. The XRD patterns show the standard diffraction pattern of hexagonal and cubic ZnS phases. From these studies, we conclude that the results are very much suitable for optoelectronics and nano electronics devices.

Acknowledgements

The authors express their sincere and heartfelt thanks to Managing Board, Principal, Mohamed Sathak Engineering their constant encouragement and providing research facilities. The authors gratefully ial support from the Department of Science and Technology (DST)-Science and Engineering -Ref.No. SR/FT/CS-117/2011 dated 29.06.2012), Government of India.

REFERENCES

[1] A Ates; MA Yıldırım; M Kundakcı; A Astam. *Mater. Sci. Semicond. Process.,* **2007,** 10(6), 281-286.
[2] L Zhou; N Tang; S Wu; X Hu; Y Xue. *Physics Procedia,* **2011,** 22, 354-359.
[3] M Oikkonen; M Blomberg; T Tuomi; M Tammenmaa. *Thin Solid Films,* **1985,** 124(3-4), 317-321.
[4] T Nakada; M Hongo; E Hayashi. *Thin Solid Films,* **2003,** 431-432, 242-248.
[5] J Vidal; OD Melo; O Vigil; N López; GC Puente; OZ Angel. *Thin Solid Films,* **2002,** 419(1-2), 118-123.
[6] H Murray; A Tosser. *Thin Solid Films,* **1974,** 24(1), 165-180.
[7] H L Kwok. *J. Phys. D, Appl. Phys.,* **1983,** 16(12), 2367-2377.
[8] JM Doña. *J. ElectrocheM. Soc.,* **1994,** 141(1), 205.
[9] MS Akhtar; MA Malik; S Riaz; S Naseem; PO Brien. *Mater. Sci. Semicond. Process.,* **2015,** 30, 292-297.
[10] K Ichino; T Onishi; Y Kawakami; S Fujita; S Fujita. *J. Cryst. Growth,* **1994,** 138(1-4), 28-34.
[11] Z Xin; RJ Peaty; HN Rutt; RW Eason. *Semicond. Sci. Technol.,* **1999,** 14(8), 695-698.
[12] TL Chu; SS Chu; J Britt; C Ferekides; CQ Wu. *J. Appl. Phys.,* **1991,** 70(5), 2688.
[13] KA Dhese; JE Nicholls; WE Hagston; PJ Wright; B Cockayne; JJ Davies. *J. Cryst. Growth,* **1994,** 138(1-4), 140-144.
[14] J Ihanus; M Ritala; M Leskelä; T Prohaska; R Resch; G Friedbacher; M Grasserbauer. *Appl.Surf.Sci.,* **1997,** 120(1-2), 43-50.
[15] A Ates; MA Yıldırım; M Kundakcı; A Astam. *Mater. Sci. Semicond. Process.,* **2007,** 10(6), 281-286.
[16] M Ashokkumar; S Muthukumaran. *J. Lumin.,* **2014,** 145, 167-174.
[17] V Kumar; KLA Khan; G Singh; TP Sharma; M Hussain. *Appl.Surf.Sci.,* **2007,** 253(7), 3543-3546.
[18] V Cottrell. An Introduction to Metallurgy, **1975,** P-173.
[19] VD Damodara; KS Bhat. *J. Mater. Sci.-Mater. Electron.,* **1990,** 1(4), 169-174.
[20] AN Molin; AI Dikusar. *Thin Solid Films,* **1995,** 265(1-2), 3-9.
[21] H Metin; R Esen. *Semicond. Sci. Technol.,* **2003,** 18(7), 647-654.
[22] S Mathew; PS Mukerjee; KP Vijayakumar. *Thin Solid Films,* **1995,** 254(1-2), 278-284.
[23] GC Morris; R Vanderveen. *Sol. Energy Mater. Sol. Cells.,* **1992,** 27(4), 305-319.
[24] X Zhang; H Song; L Yu; T Wang; X Ren; X Kong; Y Xie; X Wang. *J. Lumin.,* **2006,** 118(2), 251-256.
[25] MS Niasari; F Davar; MRL Estarki. *J. Alloys Compd.,* **2010,** 494(1-2), 199-204.
[26] K Sooklal; BS Cullum; SM Angel; CJ Murphy. *J. Phys. Chem.,* **1996,** 100(11), 4551-4555.
[27] WG Becker; AJ Bard. *J. Phys. Chem.,* **1983,** 87(24), 4888-4893.
[28] MS Niasari; F Davar; MRL Estarki. *J. Alloys Compd.,* **2009,** 475(1-2), 782-788.

International Mathematical Forum, Vol. 10, 2015, no. 8, 395 - 403
HIKARI Ltd, www. m-hikari.com
http://dx.doi.org/10.12988/imf.2015.5641

L-Fuzzy β-Ideals of β-Algebras

K. Rajam

Department of Mathematics
Mohamed Sathak Engineering College
Kilakarai-623806, India

M. Chandramouleeswaran

Department of Mathematics
Saiva Bhanu Kshatriya College
Aruppukottai - 626101, India

Abstract

In this paper, we introduce the notion of $L-$ fuzzy $\beta-$ideals of $\beta-$algebras and investigate some of their properties.

Mathematics Subject Classification: 03E72, 06F35, 03G25

Keywords: BCK/BCI -algebras, $\beta-$algebras, $L-$ Fuzzy $\beta-$subalgebra, $L-$ Fuzzy $\beta-$ideals

1 Introduction

An important point in the evaluation of the modern concept of uncertainity was the notion of fuzzy sets introduced by Lofti A. Zadeh[8]. L. Goguen [4] generalized the notion of fuzzy sets into the notion of $L-$fuzzy sets. O.G. Xi [7] applied the concept of fuzzy sets to BCK algebras and got some results. Since then many researchers worked on fuzzifying various algebras that arise from ... calculi - BCI-algebra, BCH-algebra, BF-algebra, BH-algebra, K-... In 2001,Dudek W.A. and Jun Y.B., [3] fuzzified the ideals in ... s.

J. Neggers and H.S. Kim introduced the notion of $\beta-$algebras [5]. For the general study of structures of $\beta-$ algebras, the ideal theory and fuzzy ideal theory play an important role. In [1] the authors have introduced the notion of fuzzy $\beta-$ subalgebras of $\beta-$algebras. In [2] they have introduced the notion of fuzzy $\beta-$ideals of $\beta-$algebras. In [6], we introduced the notion of $L-$ fuzzy $\beta-$ subalgebras of $\beta-$algebras and investigated their properties. In this paper, we introduce the notion of $L-$ fuzzy $\beta-$ideals of a $\beta-$algebra, and investigate some of their properties.

2 Preliminaries

In this section we recall some basic definitions that are required in the sequel.

Definition 2.1 *[5] A $\beta-$algebra is a non-empty set X with a constant 0 and two binary operations $+$ and $-$ satisfying the following axioms:*

1. $x - 0 = x$.
2. $(0 - x) + x = 0$.
3. $(x - y) - z = x - (z + y)\ \forall\ x, y, z\ \in\ X$.

Example 2.2 Let $X = \{0, 1, 2, 3\}$ be a set with constant 0 and two binary operations + and - are defined on X with the Cayley's table

+	0	1	2	3
0	0	1	2	3
1	1	0	3	2
2	2	3	1	0
3	3	2	0	1

−	0	1	2	3
0	0	1	3	2
1	1	0	2	3
2	2	3	0	1
3	3	2	1	0

Then $(X, +, -, 0)$ is a β-algebra.

Definition 2.3 *Let X be a set of universal discourse. A fuzzy set μ in X is defined as a function $\mu : X \to [0, 1]$. For each element x in X, $\mu(x)$ is called the membership value of x in X.*

Definition 2.4 *Let X be any non-empty set. A $L-$fuzzy set μ on X is defined as a function $\mu : X \to L$, where L is a complete lattice with glb 0 and lub 1.*

Definition 2.5 *Let μ be an $L-$ fuzzy set in a $\beta-$algebra X. Then μ is called a $L-$fuzzy $\beta-$subalgebra of X if*

$\prime) \geq \mu(x) \wedge \mu(y) \quad \forall x, y \in X.$

$\prime) \geq \mu(x) \wedge \mu(y) \quad \forall x, y \in X.$

3 $L-$ Fuzzy $\beta-$ ideals of $\beta-$algebras

In this section we introduce the notion of $L-$fuzzy $\beta-$ideals of $\beta-$algebras and prove some simple theorems.

Definition 3.1 *A non -empty subset I of a $\beta-$algebra of $(X,+,-,0)$ is called $\beta-$ ideal of X if*

1. $0 \in I$
2. $x+y \in I, \forall x,y \in I$ *and*
3. $x-y$ *and* $y \in I$ *then* $x \in I, \quad \forall x,y \in X.$

Definition 3.2 *Let μ be an L- fuzzy set in a $\beta-$algebra X. Then μ is called an $L-$fuzzy $\beta-$ ideal of X if*

1. $\mu(0) \geq \mu(x) \quad \forall x \in X.$
2. $\mu(x+y) \geq \mu(x) \wedge \mu(y) \quad \forall x,y \in X$*and*
3. $\mu(x) \geq \mu(x-y) \wedge \mu(y) \quad \forall x,y \in X.$

Example 3.3 In example2.2 of $\beta-$algebra X, define the fuzzy set $\mu_1 : X \to [0,1]$ such that

$$\mu_1(x) = \begin{cases} t_3 & if x = 0 \\ t_2 & if x = 1 \\ t_1 & if x = 2,3 \end{cases}$$

where $0 \leq t_1 < t_2 < t_3 \leq 1, t_1, t_2, t_3 \in L$. Then μ_1 is an $L-$fuzzy $\beta-$ideal of X.
The fuzzy set $\mu_2 : X \to [0,1]$ such that

$$\mu_2(x) = \begin{cases} t_3 & if x = 0 \\ t_1 & if x = 1,3 \\ t_2 & if x = 2 \end{cases}$$

where $0 \leq t_1 < t_2 < t_3 \leq 1.t_1, t_2, t_3 \in L$, is also an $L-$fuzzy $\beta-$ideal of X.

Lemma 3.4 *Intersection of two L-fuzzy $\beta-$ideals of a $\beta-$algebra is again a L-fuzzy $\beta-$ideal.*

Proof: Let μ_1 and μ_2 be two L-fuzzy $\beta-$ideals of a $\beta-$algebra X.

1. *Now* $\forall x \in X,$

$$\begin{aligned} (\mu_1 \cap \mu_2)(0) &= \mu_1(0) \wedge \mu_2(0) \\ &\geq (\mu_1(x) \wedge \mu_2(x)) \\ &= (\mu_1 \cap \mu_2)(x) \end{aligned}$$

2.

$$\begin{aligned}(\mu_1 \cap \mu_2)(x+y) &= \mu_1(x+y) \wedge \mu_2(x+y) \\ &\geq (\mu_1(x) \wedge \mu_1(y)) \wedge (\mu_2(x) \wedge \mu_2(y)) \\ &\geq (\mu_1(x) \wedge \mu_2(x)) \wedge (\mu_1(y) \wedge \mu_2(y)) \\ &= (\mu_1 \cap \mu_2)(x) \wedge (\mu_1 \cap \mu_2)(y)\end{aligned}$$

3.

$$\begin{aligned}(\mu_1 \cap \mu_2)(x) &= \mu_1(x) \wedge \mu_2(x) \\ &\geq (\mu_1(x-y) \wedge \mu_1(y)) \wedge (\mu_2(x-y) \wedge \mu_2(y)) \\ &= (\mu_1(x-y) \wedge \mu_2(x-y)) \wedge (\mu_1(y) \wedge \mu_2(y)) \\ &= (\mu_1 \cap \mu_2)(x-y) \wedge (\mu_1 \cap \mu_2)(y)\end{aligned}$$

Hence $\mu_1 \cap \mu_2$ is a L-fuzzy $\beta-$ideal of X.
The above result can be generalized as

Corollary 3.5 *The intersection of any collection of L-fuzzy $\beta-$ideals of a $\beta-$algebra is again a L-fuzzy $\beta-$ideal.*

Remark: Union of two L-fuzzy $\beta-$ideals of X need not be a L-fuzzy $\beta-$ideal of X. In example3.3 the fuzzy sets μ_1 and μ_2 are L- fuzzy $\beta-$ ideals of X. But $\mu_1 \cup \mu_2$ with $(\mu_1 \cup \mu_2)(0) = t_3, (\mu_1 \cup \mu_2)(1) = (\mu_1 \cup \mu_2)(2) = t_2, (\mu_1 \cup \mu_2)(3) = t_1$, is not an L- fuzzy $\beta-$ ideals of X.

Theorem 3.6 *Let μ be an $L-$fuzzy $\beta-$ ideal of a $\beta-$algebra X. If $x \leq z + y$ then $\mu(x) \geq \mu(z) \wedge \mu(y)$.*

Proof: $\forall x, y, z \in X$

$$\begin{aligned}\mu(x) &\geq \mu(x-y) \wedge \mu(y) \\ &\geq ((\mu(x-y)-z)) \wedge \mu(z)) \wedge \mu(y) \\ &= (\mu(x-(z+y)) \wedge \mu(z)) \wedge \mu(y) \\ &= (\mu(0) \wedge \mu(z)) \wedge \mu(y) \\ &= \mu(z) \wedge \mu(y)\end{aligned}$$

Let μ be an $L-$fuzzy $\beta-$ ideal of a $\beta-$algebra X. If $x \leq y$ then

Proof: For $x, y \in X$, $x \leq y \Rightarrow x - y = 0$ then $\mu(x) \geq \mu(x-y) \wedge \mu(y) = \mu(0) \wedge \mu(y)$. Hence the theorem.

Theorem 3.8 *Let A is a subset of X. Define an $L-$ fuzzy set $\mu : X \to [0,1]$ such that*

$$\mu(x) = \begin{cases} t_0 & if x \in A \\ t_1 & if x \notin A \end{cases}$$

where $t_0, t_1 \in [0,1]$ with $t_0 > t_1$. Then μ is an $L-$fuzzy $\beta-$ ideal of a $\beta-$algebra X if and only if A is a $\beta-$ ideal of X.

Proof: Assume that μ is an $L-$fuzzy $\beta-$ ideal of X.

1. If $x \in A$, $\mu(0) \geq t_0$ and if $x \notin A$, $\mu(0) \geq t_1$
   Since $t_0 > t_1$, $\mu(0) \geq t_0 > t_1$
   $\Rightarrow \mu(0) = t_0$
   $\Rightarrow 0 \in A$.

2. For $x, y \in A \Rightarrow \mu(x) = t_0 = \mu(y)$.
   Now $\mu(x+y) \geq \mu(x) \wedge \mu(y) = t_0 \wedge t_0 = t_0$.
   Therefore $\mu(x+y) = t_0 \Rightarrow x + y \in A$.

3. For any $x, y \in X, if x - y \in A$ and $y \in A \Rightarrow \mu(x-y) = t_0 = \mu(y)$.
   Now $\mu(x) \geq \mu(x-y) \wedge \mu(y) = t_0 \wedge t_0 = t_0$
   $\Rightarrow \mu(x) = t_0$
   $\Rightarrow x \in A$.

Hence A is a $\beta-$ ideal of X.
Conversely, Suppose A is a $\beta-$ ideal of X.

1. Now $0 \in A \Rightarrow \mu(0) = t_0$.
   Also $\forall x \in X, Im(\mu) = t_0, t_1$ and $t_0 > t_1$
   $\Rightarrow \mu(0) \geq \mu(x)$.

2. For $x, y \in A \Rightarrow x + y \in A$
   $\Rightarrow \mu(x) = \mu(y) = \mu(x+y) = t_0 = t_0 \wedge t_0 = \mu(x) \wedge \mu(y)$.
   Hence $\mu(x+y) \geq \mu(x) \wedge \mu(y)$.

3. For $x, y \in X$, if $x - y \in A$ and $y \in A \Rightarrow x \in A$
   $\Rightarrow \mu(x) = t_0 = t_0 \wedge t_0 = \mu(x-y) \wedge \mu(y)$.
   And for some $x \in X$ if $x - y \notin A$ and $y \notin A$
   $\Rightarrow x \in A$ or $x \notin A$
   $\Rightarrow \mu(x) = t_0$ or t_1
   $= t_1 \geq t_1 \wedge t_1 = \mu(x-y) \wedge \mu(y)$.
   $\mu(x+y) \geq \mu(x) \wedge \mu(y)$.
   μ is an $L-$fuzzy $\beta-$ ideal of X.

Corollary 3.9 *For any non-empty subset A in a $\beta-$ algebra X, the characteristic function χ_A of A is an $L-$fuzzy $\beta-$ideal of X.*

Theorem 3.10 *An L- fuzzy set μ is a $\beta-$ ideal of X if and only if the non empty level subset μ_t is a $\beta-$ ideal of X, $\forall t \in [0,1]$.*

Proof: Assume that μ is a $\beta-$ ideal of X.

(a) Now $\mu(0) \geq \mu(x) \ \ \forall x \in X$
$\Rightarrow \mu(0) \geq t$ for any t $\in [0,1]$
$\Rightarrow 0 \in \mu_t$, $\forall t \in [0,1]$.

(b) For any $t \in [0,1]$, $\mu_t \neq \emptyset$.
For any $x, y \in \mu_t$, we have $\mu(x) \geq t$ and $\mu(y) \geq t$.
Now $\mu(x+y) \geq \mu(x) \wedge \mu(y) \geq t$, hence $\ x+y \in \mu_t$.

(c) Let $x, y \in X$ be such that $x-y, y \in \mu_t$. Then we have $\mu(x-y) \geq t$ and $\mu(y) \geq t$.
Now $\mu(x) \geq \mu(x-y) \wedge \mu(y) \geq t \wedge t = t$.
Hence μ_t is a $\beta-$ ideal of X.

Conversely assume that each non empty level subset μ_t is a $\beta-$ ideal of X for some L-fuzzy subset μ of X.Then we claim that μ is an $L-$ fuzzy $\beta-$ ideal of X.

(a) For any $x \in X$, let $\mu(x) = t$. Then μ_t is a $\beta-$ ideal of $X \Rightarrow 0 \in \mu_t$.
$\Rightarrow 0 \in \mu_t \Rightarrow \mu(0) \geq \mu(x) \ \ \forall x \in X$.

(b) Choose $x, y \in X$, such that $\mu(x) = t_1$ and $\mu(y) = t_2$, where $t_1, t_2 \in [0,1]$.
Then $x \in \mu_{t_1}$ and $y \in \mu_{t_2}$
Assume $t_1 \leq \ t_2$. Then $\mu_{t_2} \subseteq \mu_{t_1}$, hence $y \in \mu_{t_1}$
Since μ_t is a $\beta-$ ideal of X, we have $x+y \in \mu_{t_1}$.
Thus $\mu(x+y) \geq t_1 = \mu(x) \wedge \mu(y)$.

(c) Suppose that there exists $x, y \in X$ such that $\mu(x) \leq \mu(x-y) \wedge \mu(y)$.
Let $t' = \frac{\{\mu(x-y)+(\mu(x)\wedge\mu(y))\}}{2}$
Clearly $t' \in [0,1]$.
Then $\mu(x-y) \geq t'$ and $\mu(y) \geq t' \Rightarrow x-y \in \mu_{t'}$ and $y \in \mu_{t'}$.
However, $\mu(x) \leq t' \wedge t' = t' \Rightarrow x \notin \mu_{t'}$ which contradicts the facts that $\mu_{t'}$ is a $\beta-$ ideal of X.

Hence for $x, y \in X, \mu(x) \geq \mu(x-y) \wedge \mu(y)$.
Therefore μ is a fuzzy $\beta-$ ideal of X.

Corollary 3.11 *If μ is an $L-$ fuzzy $\beta-$ ideal of X, then the set $X_{\mu(x')} = \{x \in X/\mu(x) = \mu(x')\}$ is a $\beta-$ ideal of X for any $x' \in X$.*

Corollary 3.12 *If μ is an $L-$ fuzzy $\beta-$ ideal of X, then the set $X_{\mu} = \{x \in X/\mu(x) = \mu(0)\}$ is a $\beta-$ ideal of X.*

Theorem 3.13 *If every $L-$fuzzy $\beta-$ ideal μ of a $\beta-$algebra X is such that $|Im(\mu)| < \infty$, then every descending chain of $\beta-$ ideals of X terminates after a finite stage.*

Proof: Let μ be any $L-$ fuzzy $\beta-$ ideal of X such that $|Im(\mu)| < \infty$.Suppose a strictly descending chain $X = A_1 \supset A_2 \supset .....A_n \supset ...$ of $\beta-$ideals X does not terminate after a finite stage.Then define a fuzzy set μ of X by

$$\mu(x) = \begin{cases} \frac{n}{n+1} & if x \in A_n - A_{n-1} \\ 1 & if x \in \cap A_n \end{cases}$$

(a) Every $\beta-$ ideal A_n contains $0 \Rightarrow 0 \in \cap A_n \Rightarrow \mu(0) \geq \mu(x) \ \ \forall x \in X$.

(b) Let $x, y \in X$.
If $x + y \in \cap A_n$, then $\mu(x+y) = 1 \geq \mu(x) \wedge \mu(y)$.
If $x + y \notin \cap A_n$ Assume that $x + y \in A_t - A_{t+1}$ for some $t \geq 1$. Then atleast one of the x or y does not lie in $\cap A_n$. (Since if both x and y lies in $\cap A_n$, then $x + y \in \cap A_n$ which implies $x + y \in A_n$,$\forall n$). Let A_m be a maximal $\beta-$ ideal of X such that x or $y \in A_m - A_{m+1}$. Hence both x and $y \in A_m$
If $t \geq m$ then $A_m \subseteq A_{t+1} \subset A_t$ implies $x + y \in A_{t+1}$ which contradicts to our assumption.Hence $m \geq t$
Now $\mu(x+y) = \frac{t}{t+1} \geq \frac{m}{m+1} = \mu(x) \wedge \mu(y)$.

(c) Let $x, y \in X$.

i. If $x - y \in A_t - A_{t+1}$ and $y \in A_k - A_{k+1}$ for some $t, k \in N \cup \{0\}$. Let $t \geq k$. Then $x - y$ and $y \in A_t \Rightarrow x \in A_t$. (Since A_t is a closed $\beta-$ ideal in X).
Hence $\mu(x) \geq \frac{t}{t+1} = \mu(x) \wedge \mu(y)$.

ii. If $x - y \in \cap A_n$ and $y \in \cap A_n$ then $x \in \cap A_n$ $\mu(x) \geq 1 = \mu(x-y) \wedge \mu(y)$.

iii. If $x - y \notin \cap A_n$ and $y \in \cap A_n$ then $x - y \in A_k - A_{k+1}$ for some $k \in N \cup \{0\}$. Then $x \in \cap A_n$.Hence $\mu(x) \geq \frac{k}{k+1} = \mu(x-y) \wedge \mu(y)$.

iv. If $x - y \in \cap A_n$ and $y \notin \cap A_n$ then $y \in A_k - A_{k+1}$ for some $k \in N \cup \{0\}$. Then $x \in \cap A_k$.Hence $\mu(x) \geq \frac{k}{k+1} = \mu(x-y) \wedge \mu(y)$.

Therefore μ is an $L-$ fuzzy $\beta-$ ideal μ of a X. Clearly $|Im(\mu)| = \infty$ which is a contradiction to our assumption.
Therefore every descending chain of $\beta-$ ideal X terminates after a finite stage.This completes the proof.

Theorem 3.14 *Let $X = A_1 \subset A_2 \subset .....A_n \subset ...$ be a strictly ascending sequence of $\beta-$ ideals of X and (t_n) be a strictly descending sequence in (0,1). Let μ be a fuzzy set defined by*

$$\mu(x) = \begin{cases} 0 & if x \notin A_n \ \ \forall n \in N \\ t_n & if x \in A_n - A_{n-1} \ \ \forall n \in N \end{cases}$$

where $A_0 = \emptyset$. Then μ is a $L-$ fuzzy $\beta-$ ideal of X.

Proof:

(a) Let $A = \cup A_n$ Then by above lemma, A is a $\beta-$ ideal of X.
Clearly $\mu(0) = t_1 \geq \mu(x), \forall x \in X$.

(b) **Case(i):** If $x, y \in A_n - A_{n-1} \Rightarrow x, y \in A_n \Rightarrow x + y \in A_n$, Since A_n is a $\beta-$ ideal of X.
Also $x, y \in A_n - A_{n-1} \Rightarrow \mu(x) = t_n = \mu(y) \Rightarrow \mu(x) \wedge \mu(y) = t_n$
Now $x + y \in A_n \Rightarrow x + y \in A_n - A_{n-1}$ or $x + y \in A_{n-1}$
$\Rightarrow \mu(x + y) = t_n$.
Hence $\mu(x + y) \geq t_n$.
Therefore $\mu(x + y) \geq t_n = \mu(x) \wedge \mu(y)$.
Case(ii): For $i > j \Rightarrow t_j > t_i \Rightarrow A_j \subset A_i$.
If $x \in A_i - A_{i-1} \Rightarrow \mu(x) = t_i$ and $y \in A_j - A_{j-1}$
$\Rightarrow \mu(y) = t_j > t_i \Rightarrow \mu(x) \wedge \mu(y) = t_i \wedge t_j = t_i$.
And $x \in A_i - A_{i-1} \Rightarrow x \in A_i$ and $y \in A_j - A_{j-1}$
$y \in A_j \subset A_i \Rightarrow x, y \in A_i$ then $x + y \in A_i$, since it is a $\beta-$ ideal X. Therefore $\mu(x + y) \geq t_i = \mu(x) \wedge \mu(y)$.

(c) Let $x, y \in X$.
Case(i): If $x \notin A \Rightarrow x - y \notin A$ or $y \notin A \Rightarrow \mu(x) = 0 = \mu(x - y) \wedge \mu(y)$
Case(ii): If $x \in A \Rightarrow x \in A_n - A_{n-1}$ for some n $\Rightarrow x \in A_n$ and $x \notin A_{n-1} \Rightarrow x - y \notin A_{n-1}$ or $y \notin A_{n-1}$
Hence $\mu(x - y) \leq t_n$ or $\mu(y) \leq t_n$.
Therefore $\mu(x) = t_n \geq \mu(x - y) \wedge \mu(y)$
Hence μ is a $L-$ fuzzy $\beta-$ ideal of X.

References

[1] M. Abu Ayub Ansari and M. Chandramouleeswaran, Fuzzy $\beta-$ subalgebras of $\beta-$algebras., *International J. of Maths. Sci. and Engg. Appls.*, **7**, no.V (2013), 239 - 249.

[2] M. Abu Ayub Ansari and M. Chandramouleeswaran, Fuzzy $\beta-$ideals of $\beta-$algebras., *International J. of Maths. Sci. and Engg. Appls.*, **8**, no.1 (2014), 1 - 10.

[3] W.A. Dudek and Y.B. Jun, Fuzzification of ideals in BCC-algebras, *Glasnik Mathematicki*, **36** (2001), 127 - 138.

[4] J. A. Goguen, L-fuzzy sets, *J. Maths. Analysis and Appls.*, **18** (1967), 145 - 174. http://dx.doi.org/10.1016/0022-247x(67)90189-8

[5] J. Neggers and H.S. Kim, On $\beta-$algebras, *Math. Slovaca*, **52**(5) (2002), 517 - 530. http://dml.cz/dmlcz/131570

[6] K. Rajam and M. Chandramouleeswaran, $L-$ Fuzzy $\beta-$ subalgebras of $\beta-$algebras, *Applied Mathematical Sciences*, **8** (2014), 4241 - 4248. http://dx.doi.org/10.12988/ams.2014.45322

[7] O.G. Xi, Fuzzy BCK-algebras, *Math. Japan*, **36**(5) (1991), 935 - 942.

[8] L.A. Zadeh, Fuzzy sets, *Inform. Control*, **8** (1965), 338 - 353. http://dx.doi.org/10.1016/s0019-9958(65)90241-x

Received: June 17, 2015; Published: July 29, 2015

Applied Mathematical Sciences, Vol. 9, 2015, no. 145, 7221 - 7228
HIKARI Ltd, www.m-hikari.com
http://dx.doi.org/10.12988/ams.2015.59581

$L-$Fuzzy $T-$Ideals of $\beta-$Algebras

K. Rajam

Department of Mathematics
Mohamed Sathak Engineering College
Kilakarai-623806, India

M. Chandramouleeswaran

Department of Mathematics
Saiva Bhanu Kshatriya College
Aruppukottai - 626101, India

Abstract

In this paper, we introduce the notion of $L-$ fuzzy $T-$ideals of $\beta-$algebras and investigate some of their properties.

Mathematics Subject Classification: 03E72, 06F35, 03G25

Keywords: $\beta-$algebras, $L-$ Fuzzy $\beta-$subalgebra, $L-$ Fuzzy $T-$ideals

1 Introduction

J.Neggers and H.S. Kim introduced the notion of $\beta-$algebras [4]. An important point in the evaluation of the modern concept of uncertainity was the notion of fuzzy sets introduced by Lofti A. Zadeh[7]. L.Goguen [3] generalized the notion of fuzzy sets into the notion of $L-$fuzzy sets. For the general study of structures of $\beta-$ algebras, the ideal theory and fuzzy ideal theory play an important role.

In [1] the authors have introduced the notion of fuzzy $\beta-$ subalgebras ...s. In [2] they have introduced the notion of fuzzy $\beta-$ideals of ... In [5], we introduced the notion of $L-$ fuzzy $\beta-$ subalgebras of

$\beta-$algebras and investigated their properties. In [6], we introduced the notion of $L-$ fuzzy $\beta-$ ideals of $\beta-$algebras and investigated their properties. In this paper, we introduce the notion of $L-$ fuzzy T-ideals of a $\beta-$algebra, and investigate some of their properties.

2 Preliminaries

In this section we recall some basic definitions that are required in the sequel.

Definition 2.1 *[4] A $\beta-$algebra is a non-empty set X with a constant 0 and two binary operations $+$ and $-$ satisfying the following axioms:*

1. $x - 0 = x$.
2. $(0 - x) + x = 0$.
3. $(x - y) - z = x - (z + y)\ \forall\ x, y, z\ \in\ X$.

Example 2.2 Let $X = \{0, 1, 2, 3, 4, 5\}$ be a set with constant 0 and two binary operations + and - defined by the Cayley tables:

+	0	1	2	3	4	5
0	0	1	2	3	4	5
1	1	0	4	5	2	3
2	2	5	0	4	3	1
3	3	4	5	0	1	2
4	4	3	1	2	5	0
5	5	2	3	1	0	4

−	0	1	2	3	4	5
0	0	1	2	3	4	5
1	1	0	4	5	3	2
2	2	5	0	4	1	3
3	3	4	5	0	2	1
4	4	3	1	2	0	5
5	5	2	3	1	4	0

Then $(X, +, -, 0)$ is a β-algebra.

Definition 2.3 *Let X be any non-empty set. A $L-$fuzzy set μ on X is defined as a function $\mu : X \to L$, where L is a complete lattice with glb 0 and lub 1.*

Definition 2.4 *Let μ be a fuzzy set in a set X. For $t \in [0, 1]$, then the set $\mu_t = \{x \in X/\mu(x) \geq t\}$ is called a level subset of μ.*

Definition 2.5 *[1] Let μ be a fuzzy set in a $\beta-$algebra X. Then μ is called a $L-$fuzzy $\beta-$subalgebra of X if*

$\iota) \geq \mu(x) \wedge \mu(y)\ \ \forall x, y \in X.$

$\iota) \geq \mu(x) \wedge \mu(y)\ \ \forall x, y \in X.$

3 $L-$ Fuzzy T- ideals of $\beta-$algebras

In this section we introduce the notion of $L-$fuzzy $T-$ideals of $\beta-$algebras and prove some simple theorems.

Definition 3.1 *A non-empty subset I of a $\beta-$algebra of $(X,+,-,0)$ is called $T-$ ideal of X if the following conditions are satisfied.*

1. $0 \in I$
2. $(x+y)+z \in I$ *and* $y \in I \Rightarrow (x+z) \in I$ *and*
3. $(x-y)-z \in I$ *and* $y \in I \Rightarrow (x-z) \in I \quad \forall x,y,z \in I.$

Example 3.2 In example 2.2 of the $\beta-$algebra of X, $I_1 = \{0,2\}$ is a T-ideal of X while $I_2 = \{0,4\}$ is not a T-ideal of X - for, (0+4)+4 =4+4 = 5$\notin I_2$.

Definition 3.3 *Let μ be an L- fuzzy set in a $\beta-$algebra of X. Then μ is called an $L-$fuzzy $T-$ ideal of X if*

1. $\mu(0) \geq \mu(x)$.
2. $\mu(x+z) \geq \mu((x+y)+z) \wedge \mu(y)$ *and*
3. $\mu(x-z) \geq \mu((x-y)-z) \wedge \mu(y) \quad \forall x,y,z \in X.$

Example 3.4 In the $\beta-$algebra X of example 2.2, the fuzzy set $\mu_1 : X \to [0,1]$ defined by

$$\mu_1(x) = \begin{cases} t_5 & if \quad x = 0 \\ t_4 & if \quad x = 1 \\ t_3 & if \quad x = 2 \\ t_2 & if \quad x = 3 \\ t_1 & if \quad x = 4,5 \end{cases}$$

where $0 \leq t_1 < t_2 < t_3 < t_4 < t_5 \leq 1, t_1, t_2, t_3, t_4, t_5 \in L$ is an $L-$fuzzy $T-$ideal of X.

Lemma 3.5 *Let μ be an $L-$fuzzy $T-$ ideal of a $\beta-$algebra X. If $x \leq y$ then $\mu(x) \geq \mu(y)$.*

Proof: For $x, y \in$X, $x \leq y \Rightarrow x - y = 0$. Then

$0) \geq \mu((x-y)-0) \wedge \mu(y) = \mu(0-0) \wedge \mu(y) = \mu(0) \wedge \mu(y) = \mu(y).$

$\geq \mu(y).$

Theorem 3.6 *Let A be a subset of X. Define an $L-$ fuzzy set $\mu : X \to [0,1]$ such that*

$$\mu(x) = \begin{cases} t_0 & if \quad x \in A \\ t_1 & if \quad x \notin A \end{cases}$$

where $t_0, t_1 \in [0,1]$ with $t_0 > t_1$. Then μ is an $L-$fuzzy $T-$ ideal of a $\beta-$algebra X if and only if A is a $T-$ ideal of X .

Proof: Assume that μ is an $L-$fuzzy $T-$ ideal of X.
If $x \in A$, $\mu(0) \geq t_0$.
and if $x \notin A$, $\mu(0) \geq t_1$ *since* $t_0 > t_1$.
$\Rightarrow \mu(0) \geq t_0 > t_1$
$\Rightarrow \mu(0) = t_0$
$\Rightarrow 0 \in A$.
For $x, y, z \in A \Rightarrow \mu(x) = t_0, \mu(y) = t_0$ and $\mu(z) = t_0$.

$$\begin{aligned} \mu(x+z) &\geq \mu((x+y)+z) \wedge \mu(y) \\ &\geq (\mu(x+y) \wedge \mu(z)) \wedge \mu(y) \\ &= (((\mu(x) \wedge \mu(y)) \wedge \mu(z))) \wedge \mu(y) \\ &= t_0 \wedge t_0 \wedge t_0 \\ &= t_0 \end{aligned}$$

Therefore $\mu(x+z) \geq t_0 \Rightarrow x + z \in A$.
For $x, y, z \in A \Rightarrow \mu((x-y)-z) = t_0$ and $\mu(y) = t_0$.
Now $\mu(x-z) \geq \mu((x-y)-z) \wedge \mu(y) = t_0 \wedge t_0 = t_0$
$\Rightarrow \mu(x-z) = t_0 \Rightarrow x - z \in A$.
Hence A is a $T-$ ideal of X.
Conversely, Suppose A is a $T-$ ideal of X.
Now $0 \in A \Rightarrow \mu(0) = t_0$.
Also $\forall x \in X, Im(\mu) = \{t_0, t_1\}$ and $t_0 > t_1$
$\Rightarrow \mu(0) \geq \mu(x)$.
Since A is a $T-$ideal of X,
$\forall\ x, y, z \in S,\ (x+y)+z \in A$ and $y \in A \Rightarrow x+z, x-z \in A$.
Then $\mu(x+z) = t_0 \geq \mu((x+y)+z) \wedge \mu(y)$.
Similarly we can prove that $\mu(x-z) \geq \mu((x-y)-z) \wedge \mu(y)$.
Hence μ is an $L-$fuzzy $T-$ ideal of X.

Theorem 3.7 *An L- fuzzy set μ is a $T-$ ideal of X if and only if the non empty level subset μ_t is a $T-$ ideal of X, $\forall t \in [0,1]$.*

Proof: Assume that μ is an L-fuzzy $T-$ ideal of X.
$u(x)\ \ \forall x \in X$
or any t $\in [0,1] \Rightarrow 0 \in \mu_t, \forall t \in [0,1]$.
$0,1]$, $\mu_t \neq \emptyset$.

For any $x, y, z \in \mu_t$, we have $\mu((x+y)+z) \geq t$ and $\mu(y) \geq t$.
Now $\mu(x+z) \geq \mu((x+y)+z) \wedge \mu(y) \geq t \Rightarrow\ x+z \in \mu_t$.
Also we have $\mu((x-y)-z) \geq t$ and $\mu(y) \geq t$.
Hence $\mu((x-y)-z) \geq \mu((x-y)-z) \wedge \mu(y) \geq t \wedge t = t \Rightarrow\ x-z \in \mu_t$.
Hence μ_t is a $T-$ ideal of X.
Conversely assume that each non empty level subset μ_t of a fuzzy subset μ of X is a $T-$ ideal of X.
Then we claim that μ is an $L-$ fuzzy $T-$ ideal of X.
For any $x \in X$, let $\mu(x) = t$. Since μ_t is a $T-$ ideal of $X,\ 0 \in \mu_t$.
$\Rightarrow \mu(0) \geq \mu(x),\ \ \forall x \in X$.
Choose $x, y, z \in X$, such that $\mu((x+y)+z) = t_1$ and $\mu(y) = t_2$, where $t_1, t_2 \in [0,1]$.Then $x+z \in \mu_{t_1}$ and $y \in \mu_{t_2}$.
Assume $t_1 \leq\ t_2$.Then $\mu_{t_2} \subseteq \mu_{t_1}$, hence $y \in \mu_{t_1}$.
Since μ_t is a $T-$ ideal of X, we have $x+z \in \mu_{t_1}$.
Thus $\mu(x+z) \geq t_1 = \mu((x+y)+z) \wedge \mu(y)$.
Similiarly we can prove that $\mu((x-y)-z) \geq \mu((x-y)-z) \wedge \mu(y)$.
Therefore μ is an L- fuzzy $T-$ ideal of X.

Theorem 3.8 *Let μ_1 and μ_2 be two $L-$ fuzzy T- ideals in a $\beta-$ algebra X. Then the direct product $\mu_1 \times \mu_2$ is an $L-$ fuzzy T-ideals in $X_1 \times X_2$.*

Proof For any $(x, y) \in X_1 \times X_2$ we have

$$\begin{aligned}(\mu_1 \times \mu_2)(0,0) &= \mu_1(0) \wedge \mu_2(0)\\ &\geq \mu_1(x) \wedge \mu_2(y)\\ &= (\mu_1 \times \mu_2)(x,y)\end{aligned}$$

Let $(x_1, x_2), (y_1, y_2)$ and $(z_1, z_2) \in X_1 \times X_2$. Then
$(\mu_1 \times \mu_2)((x_1, x_2) + (z_1, z_2))$

$$\begin{aligned}&= (\mu_1 \times \mu_2)((x_1+z_1), (x_2+z_2))\\ &= \mu_1(x_1+z_1) \wedge \mu_2(x_2+z_2)\\ &\geq (\mu_1((x_1+y_1)+z_1) \wedge \mu_1(y_1)) \wedge (\mu_2((x_2+y_2)+z_2) \wedge \mu_2(y_2))\\ &= (\mu_1((x_1+y_1)+z_1) \wedge \mu_2((x_2+y_2)+z_2)) \wedge (\mu_1(y_1) \wedge \mu_2(y_2))\\ &= (\mu_1 \times \mu_2)((x_1+y_1)+z_1, (x_2+y_2)+z_2)) \wedge (\mu_1 \times \mu_2)(y_1, y_2)\\ &= (\mu_1 \times \mu_2)(((x_1+y_1), (x_2+y_2)) + (z_1, z_2)) \wedge (\mu_1 \times \mu_2)(y_1, y_2)\\ &= (\mu_1 \times \mu_2)(((x_1, x_2), (y_1, y_2))) + (z_1, z_2)) \wedge (\mu_1 \times \mu_2)(y_1, y_2)\end{aligned}$$

Similarly we can prove that

$x_2) - (z_1, z_2)) \geq (\mu_1 \times \mu_2)(((x_1, x_2), (y_1, y_2))) + (z_1, z_2)) \wedge (\mu_1 \times \mu_2)(y_1, y_2)$

ι_2 is an $L-$fuzzy T- ideal of a β-algebra in $X_1 \times X_2$.

Theorem 3.9 *Let μ_1 and μ_2 be two fuzzy sets in a $\beta-$ algebra X such that $\mu_1 \times \mu_2$ is an $L-$ fuzzy T-ideal of $X_1 \times X_2$. Then*

1. *Either $\mu_1(0) \geq \mu_1(x)$ or $\mu_2(0) \geq \mu_2(x)$ $\forall x \in X$.*
2. *If $\mu_1(0) \geq \mu_1(x)$, $\forall x \in X$ then either $\mu_2(0) \geq \mu_1(x)$ or $\mu_2(0) \geq \mu_2(x)$.*
3. *If $\mu_2(0) \geq \mu_2(x)$, $\forall x \in X$ then either $\mu_1(0) \geq \mu_1(x)$ or $\mu_1(0) \geq \mu_2(x)$.*
4. *Either μ_1 or μ_2 is a $L-$ fuzzy T-ideal of X.*

Proof: Let $\mu_1 \times \mu_2$ is an $L-$ fuzzy T-ideal of $X_1 \times X_2$.
Suppose that $\mu_1(0) < \mu_1(x)$ and $\mu_2(0) < \mu_2(y)$ for some $x, y \in X$. Then

$$(\mu_1 \times \mu_2)(x, y) = \mu_1(x) \wedge \mu_2(y) \geq \mu_1(0) \wedge \mu_2(0) = (\mu_1 \times \mu_2)(0, 0)$$

This contradication yields that either $\mu_1(0) \geq \mu_1(x)$ or $\mu_2(0) \geq \mu_2(x)$ $\forall x \in X$.
Given $\mu_1(0) \geq \mu_1(x)$, $\forall x \in X$ and assume that there exist $x, y \in X$ such that $\mu_2(0) < \mu_1(x)$ and $\mu_2(0) < \mu_2(y)$ $\forall x, y \in X$.
Now $\mu_2(0) < \mu_1(x) \leq \mu_1(0) \Rightarrow \mu_2(0) < \mu_1(0)$.
Then $(\mu_1 \times \mu_2)(0, 0) = \mu_1(0) \wedge \mu_2(0) = \mu_2(0)$.
$(\mu_1 \times \mu_2)(x, y) = \mu_1(x) \wedge \mu_2(y) > \mu_2(0) \wedge \mu_2(0) = \mu_2(0) = (\mu_1 \times \mu_2)(0, 0)$
Thus $(\mu_1 \times \mu_2)(x, y) \geq (\mu_1 \times \mu_2)(0, 0)$ which is a contradication.
Hence if $\mu_1(0) \geq \mu_1(x)$, $\forall x \in X$ then either $\mu_2(0) \geq \mu_1(x)$ or $\mu_2(0) \geq \mu_2(x)$.
Similarly we can prove that if $\mu_2(0) \geq \mu_2(x)$, $\forall x \in X$ then either $\mu_1(0) \geq \mu_1(x)$ or $\mu_1(0) \geq \mu_2(x)$.
First we prove that μ_2 is a $L-$ fuzzy T-ideal of X.
Assume that $\mu_2(0) \geq \mu_2(x)$ $\forall x \in X$.
Then it follows that either $\mu_1(0) \geq \mu_1(x)$ or $\mu_1(0) \geq \mu_2(x)$.
If $\mu_1(0) \geq \mu_2(x)$ for any $x \in X$. Then

$$\begin{aligned}
\mu_2(x) &\geq \mu_1(0) \wedge \mu_2(x) \\
&= (\mu_1 \times \mu_2)(0, x) \\
\mu_2(x + z) &\geq \mu_1(0) \wedge \mu_2(x + z) \\
&= (\mu_1 \times \mu_2)(0, x + z) \\
&= (\mu_1 \times \mu_2)(0 + 0, x + z) \\
&= (\mu_1 \times \mu_2)((0, x) + (0, z)) \\
&\geq (\mu_1 \times \mu_2)(((0, x) + (0, y)) + (0, z)) \wedge (\mu_1 \times \mu_2)(0, y) \\
&= (\mu_1 \times \mu_2)(((0 + 0), (x + y)) + (0, z)) \wedge (\mu_1 \times \mu_2)(0, y) \\
&= (\mu_1 \times \mu_2)(((0 + 0) + 0, (x + y) + z)) \wedge (\mu_1 \times \mu_2)(0, y) \\
&= (\mu_1 \times \mu_2)((0, (x + y) + z)) \wedge (\mu_1 \times \mu_2)(0, y) \\
&= \mu_2((x + y) + z)) \wedge \mu_2(y)
\end{aligned}$$

Similarly we can prove that $\mu_2(x-z) \geq \mu_2((x-y)-z)) \wedge \mu_2(y)$.
Hence μ_2 is a $L-$ fuzzy T-ideal of X.
Similarly we can prove that μ_1 is a $L-$ fuzzy T-ideal of X.

Theorem 3.10 *Let $f : X \to X$ be an endomorphism on a $\beta-$algebra . Let μ be an $L-$fuzzy $T-$ideal of X. Define a fuzzy set $\mu_f : X \to [0,1]$ defined by $\mu_f(x) = \mu(f(x)), \forall x \in X$. Then μ_f is an $L-$fuzzy $T-$ideal of X.*

Proof: Let $x \in X$. Then $\mu_f(x) = \mu(f(x)) \leq \mu(0) = \mu(f(0)) = \mu_f(0)$.
Let $x, y \in X$.

$$\begin{aligned}
\mu_f(x+z) &= \mu(f(x+z)) = \mu(f(x)+f(z)) \\
&\geq \mu((f(x)+f(y))+f(z)) \wedge \mu(f(y)) \\
&= \mu((f(x+y))+f(z)) \wedge \mu(f(y)) \\
&= \mu(f((x+y)+z)) \wedge \mu(f(y)) \\
&= \mu_f((x+y)+z)) \wedge \mu_f(y)
\end{aligned}$$

Similarly we can prove that $\mu_f(x-z) \geq \mu_f((x-y)-z)) \wedge \mu_f(y)$.
Hence μ_f is an $L-$ fuzzy $T-$ ideal of X .

References

[1] M. Abu Ayub Ansari and M. Chandramouleeswaran, Fuzzy $\beta-$ subalgebras of $\beta-$algebras, *International J. of Maths. Sci. and Engg. Appls.*, **7** (2013), no. V, 239-249.

[2] M. Abu Ayub Ansari and M. Chandramouleeswaran, Fuzzy $\beta-$ideals of $\beta-$algebras, *International J. of Maths. Sci. and Engg. Appls.*, **8** (2014), no. 1, 1-10.

[3] J. A. Goguen, L-fuzzy sets, *J. Maths. Analysis, Appls.*, **18** (1967), 145-174. http://dx.doi.org/10.1016/0022-247x(67)90189-8

[4] J. Neggers and H.S. Kim, On $\beta-$algebras, *Math. Slovaca*, **52** (2002), no. 5, 517-530.

[5] K. Rajam and M. Chandramouleeswaran, $L-$ Fuzzy $\beta-$ subalgebras of $\beta-$algebras, *Applied Mathematical Sciences*, **8** (2014), no. 85, 4241-4248. http://dx.doi.org/10.12988/ams.2014.45322

[6] K. Rajam and M. Chandramouleeswaran, $L-$ Fuzzy $\beta-$ ideals of $\beta-$algebras., *International Mathematical Forum*, **10** (2015), no. 8, 395-tp://dx.doi.org/10.12988/imf.2015.5641

[7] L.A. Zadeh, Fuzzy sets, *Inform. and Control*, **8** (1965), 338-353. http://dx.doi.org/10.1016/s0019-9958(65)90241-x

Received: September 24, 2015; Published: December 12, 2015

International Journal of Mathematics And its Applications
Volume 3, Issue 2 (2015), 115–120.
ISSN: 2347-1557
Available Online: http://ijmaa.in/

International Journal of Mathematics And its Applications

Soft Expert Generalized Closed Sets with Respect to Soft Expert Ideals

Research Article

S.Tharmar[1]*

1 Department of Mathematics, Mohamed Sathak Engineering College, Kilakarai, Ramanathapuram, Tamilnadu, India.

Abstract: The soft expert models are richer than soft set models since the soft set models are created with the help of one expert whereas but the soft expert models are made with the opinions of all experts. In this paper, we introduce soft expert generalized closed sets and soft expert generalized open sets with respect to soft expert ideals in soft expert topological spaces and study their basic properties.

MSC: 06D72.

Keywords: Soft expert sets, Soft expert topological space, Soft expert g-closed sets, Soft expert $\mathcal{I}_g$-closed sets and Soft expert $\mathcal{I}_g$-open sets.

1. Introduction

Several set theories such as theory of vague sets, theory of interval mathematics [5, 10], theory of fuzzy sets [29], theory of intuitionistic fuzzy sets [6] and theory of rough sets [27] can be used as tools for dealing with uncertainties, but all these theories have their own difficulties. According to Molodtsov in [23], in-adequacy of the parametrization tool of the theory is the main reason for these difficulties. To overcome this, he initiated the concept of soft set theory as a new mathematical tool which is free from the problems mentioned above and presented the fundamental results of the new theory. In [23, 24], Molodtsov successfully applied it to several directions such as smoothness of functions, game theory, operations research, Riemann-integration, Perron integration, probability, theory of measurement, and so on.

After presentation of the operations of soft sets [21], the properties and applications of soft set theory have been studied increasingly [3, 18, 24]. In recent years, many interesting applications of soft set theory have been expanded by embedding the ideas of fuzzy sets [1, 2, 8, 19–22, 24, 25]. To develop soft set theory, the operations of the soft sets are redefined and a uni-int decision making method was constructed by using these new operations [9].

d Naz [28] initiated the study of soft topological spaces. They defined soft topology on the X. Consequently, they defined basic notions of soft topological spaces such as soft open and

*ail.com

soft closed sets, soft subspace, soft interior, soft closure, soft neighborhood of a point, soft separation axioms, soft regular spaces and soft normal spaces and established their several properties. Hussain and Ahmad [11] investigated the properties of soft open, soft closed, soft interior, soft closure and soft neighborhood of a point. They also defined and discussed the properties of soft interior, soft exterior and soft boundary which are fundamental for further research on soft topology and will strengthen the foundations of the theory of soft topological spaces.

Kandil et al.[13] introduced a unification of some types of different kinds of subsets of soft topological spaces using the notions of γ-operation. The notion of soft ideal is initiated for the first time by Kandil et al.[15]. They also introduced the concept of soft local function. These concepts are discussed with a view to find new soft topologies from the original one, called soft topological spaces with soft ideal (X, τ, E, $\mathcal{I}$). Applications to various fields were further investigated by Kandil et al. [14, 15].

Shawkat Alkhazaleh and Abdul Razak Salleh [4] defined soft expert sets and created the model in which user can know the opinion of all experts in one model. Sabir Hussain [12] introduced soft expert topological spaces which are defined over an initial universe with a fixed set of parameters and with the opinion of all expert instead of only one expert. The notions of soft expert open sets, soft expert closed sets, soft expert closure, soft expert interior, soft expert exterior and soft expert boundary are introduced and their basic properties are investigated. Finally, these notions have been applied to the problem of decision-making.

In this paper we introduce and study the notion of soft expert generalized closed sets in soft expert topological spaces with soft expert ideals and give basic definitions and theorems about it.

2. Preliminaries

Definition 2.1 ([4]). *Let U be an initial universe, E be a set of parameters, X be a set of expets(agents) and O={1=agree, 0=disagree} be a set of opinions, Z=E × X × O and A⊂Z. Let ℘(U) denote the power set of U and A be a non-empty subset of Z. A pair (F, A) is called a soft expert set over U, where F is a mapping given by F : A → ℘(U).*

Definition 2.2 ([4]). *For two soft sets (F, A) and (G, B) over a common universe U, we say that (F, A) is a soft expert subset of (G, B) if (1) A⊂B and (2) for all e∈B, G(e)⊂F(e). We write (F, A)⊂(G, B).*

Definition 2.3 ([4]). *Let E be a set of parameters and X be a set of experts. The NOT set of Z=E × X × O denoted by ⌉Z, is defined by ⌉Z={(⌈e_i, x_j, o_k), ∀i, j, k} where ⌉e_i is not e_i.*

Definition 2.4 ([4]). *The complement of a soft expert set (F, A) is denoted by (F, A)^c and is defined by (F, A)^c=(F^c, ⌉A) where F^c : ⌉A→℘(U) is a mapping given by F^c(e)=U−F(⌈e) for all e∈⌉A.*

Definition 2.5 ([4]). *An agree-soft expert set (F, A)_1 over U is a soft expert subset of (F, A) defined as follows: (F, A) = {F(e) : e∈E × X × {1}}*

agree-soft expert set (F, A)_0 over U is a soft expert subset of (F, A) defined as follows: (F, A) = {F(e) : e∈E × X × {0}}

nion of two soft expert sets of (F, A) and (G, B) over the common universe U is the soft expert

set (H, C), where C = A∪B and for each e∈C,

$$H(e) = \begin{cases} F(e) \ if \ e \in A\text{-}B, \\ G(e) \ if \ e \in B\text{-}A \\ F(e) \cup G(e) \ if \ e \in A \cap B \end{cases}$$

We write (F, A)∪(G, B)=(H, C).

Definition 2.8 ([17]). *The intersection of two soft expert sets of (F, A) and (G, B) over the common universe U, denoted (F, A)∩(G, B), is defined as C=A∩B, and H(e)=F(e)∩G(e) for all e∈C.*

Definition 2.9 ([17]). *A soft expert set (F, A) over U is said to be a NULL soft expert set denoted by ∅ if for all e∈A, F(e)=∅.*

Definition 2.10 ([17]). *A soft expert set (F, A) over U is called an absolute soft expert set, denoted by $\tilde{U}$, if e∈A, F(e)=U.*

Definition 2.11 ([17]). *Let x∈U, then (x, A) denotes the soft expert set over U for which x(e)={x}, for all e∈A.*

Definition 2.12 ([17]). *A soft expert topology τ is a family of soft expert sets over U satisfying the following properties.*

(1) ∅, $\tilde{U}$ belong to τ.

(2) The union of any number of soft expert sets in τ belongs to τ.

(3) The intersection of any two soft expert sets in τ belongs to τ.

The triplet (U, τ, A) is called a soft expert topological space.

Definition 2.13 ([17]). *Let (U, τ, A) be a soft expert topological space. Then*

(1) The members of τ are called soft expert open sets in U.

(2) A soft expert set (F, A) over U is said to be a soft expert closed set in U if $(F, A)^c \in \tau$.

(3) The soft expert interior of a soft expert set (F, A) is the union of all soft expert open subsets of (F, A). The soft expert interior of (F, A) is denoted by $(F, A)^0$.

(4) The soft expert closure of (F, A) is the intersection of all soft expert closed super sets of (F, A). The soft expert closure of (F, A) is denoted by $\overline{(F, A)}$.

Definition 2.14 ([17]). *A soft expert set (F, A) in a soft expert topological space (U, τ, A) is called soft expert generalized closed (briefly soft expert g-closed) if $\overline{(F, A)} \subset (G, A)$ whenever (F, A)⊂(G, A) and (G, A) is soft expert open in U.*

ry soft expert closed set is soft expert g-closed.

3. Soft Expert Generalized Closed Sets with Respect to Soft Expert Ideal

Definition 3.1. *A non-empty collections $\mathcal{I}$ of soft expert subsets over U is called a soft expert ideal on U if the following holds*

(1) If (F, A)$\in\mathcal{I}$ and (G, A)$\subset$(F, A) implies (G, A)$\in\mathcal{I}$ (heredity).

(2) If (F, A)$\in\mathcal{I}$ and (G, A)$\in\mathcal{I}$, then (F, A)$\cup$(G, A)$\in\mathcal{I}$ (additivity).

Definition 3.2. *A soft expert set (F, A) in a soft expert topological space (U, τ, A) is called soft expert generalized closed set with respect to soft expert ideal (briefly soft expert $\mathcal{I}_g$-closed) if $\overline{(F,\ A)}\backslash$(G, A)$\in\mathcal{I}$ whenever (F, A)$\subset$(G, A) and (G, A) is soft expert open in U.*

Example 3.1. *Let U=$\{u_1, u_2\}$, X=$\{a\}$, E=$\{e\}$ and (F, A) be a soft expert set where (F, A)=$\{((e, a, 1), \{u_1\}), ((e, a, 0), U)\}$. Then τ=$\{\emptyset, \tilde{U}, (F, A)\}$ is a soft expert topology and $\mathcal{I}$=$\{\emptyset, (G, A), (H, A), (K, A)\}$ is a soft expert ideal on U, where* $(G, A) = \{((e, a, 1), \{u_2\}), ((e, a, 0), \emptyset)\}$

$$(H, A) = \{((e, a, 1), \emptyset), ((e, a, 0), \{u_1\})\}$$
$$(K, A) = \{((e, a, 1), \{u_2\}), ((e, a, 0), \{u_1\})\}$$

Clearly (F, A) is soft expert $\mathcal{I}_g$-closed.

Proposition 3.1. *Every soft expert g-closed set is soft expert $\mathcal{I}_g$-closed but not conversely*

Proof. Let (F, A) be a soft expert g-closed set and (F, A)$\subset$(G, A) and (G, A)$\in\tau$. Since (F, A) is soft expert g-closed, then $\overline{(F,\ A)}\subset$(G, A) and hence $\overline{(F,\ A)}\backslash$(G, A)=$\emptyset\in\mathcal{I}$. Therefore (F, A) is soft expert $\mathcal{I}_g$-closed. □

Example 3.2. *In example 3.1, (F, A) is soft expert $\mathcal{I}_g$-closed but not soft expert g-closed.*

Theorem 3.1. *Let $\mathcal{I}$ be a soft expert ideal on a soft expert topological space (U, τ, A). Then, the concepts of soft expert g-closed set and soft expert $\mathcal{I}_g$-closed set are the same if $\mathcal{I}$=$\{\emptyset\}$.*

Proof. Suppose that $\mathcal{I}$=$\{\emptyset\}$. If (F, A) is soft expert $\mathcal{I}_g$-closed, then $\overline{(F,\ A)}\backslash$(G, A)$\in\mathcal{I}$ whenever (F, A)$\subset$(G, A) and (G, A)$\in\tau$ and so $\overline{(F,\ A)}\subset$(G, A), proving that (F, A) is soft expert g-closed. □

Remark 3.1. *soft expert closed $\Rightarrow$ soft expert g-closed $\Rightarrow$ soft expert $\mathcal{I}_g$-closed*

Theorem 3.2. *A soft expert set (F, A) is soft expert $\mathcal{I}_g$-closed in a soft expert topological space (U, τ, A) iff (G, A)$\subset\overline{(F,\ A)}\backslash$(F, A) and (G, A) is soft expert closed implies (G, A)$\in\mathcal{I}$.*

Proof. Assume that (F, A) is soft expert $\mathcal{I}_g$-closed. Let (G, A)$\subset\overline{(F,\ A)}\backslash$(F, A) and (G, A) be soft expert closed. Then is soft expert open. By our assumption, $\overline{(F,\ A)}\backslash$(G, A)$^c\in\mathcal{I}$. But (G, A)$\subset\overline{(F,\ A)}\backslash$(G, A)^c, then

A)$\subset\overline{(F,\ A)}\backslash$(F, A) and (G, A) is soft expert closed implies that (G, A)$\in\mathcal{I}$. Suppose that (F, hen $\overline{(F,\ A)}\backslash$(H, A)=$\overline{(F,\ A)}\cap$(H, A)^c is a soft expert closed set and $\overline{(F,\ A)}\backslash$(H, A)$\subset\overline{(F,\ A)}\backslash$(F, A). By assumption $(F,\ A)\backslash$(H, A)$\in\mathcal{I}$. This implies that (F, A) is soft expert $\mathcal{I}_g$-closed. □

Theorem 3.3. *If (F, A) and (G, A) are soft expert $\mathcal{I}_g$-closed sets in a soft expert topological space (U, τ, A), then their union (F, A)$\cup$(G, A) is also soft expert $\mathcal{I}_g$-closed.*

Proof. Suppose (F, A) and (G, A) are soft expert $\mathcal{I}_g$-closed sets. If (F, A)$\cup$(G, A)$\subset$(H, A) and (H, A)$\in\tau$, then (F, A)$\subset$(H, A) and (G, A)$\subset$(H, A). By assumption, $\overline{(F,\ A)}\backslash$(H, A)$\in\mathcal{I}$ and $\overline{(G,\ A)}\backslash$(H, A)$\in\mathcal{I}$ and hence $\overline{((F,\ A)\cup(G,\ A))}\backslash$(H, A)=($\overline{(F,\ A)}\backslash$(H, A))$\cup$($\overline{(G,\ A)}\backslash$(H, A))$\in\mathcal{I}$. That is (F, A)$\cup$(G, A) is soft expert $\mathcal{I}_g$-closed. □

Proposition 3.2. *$\emptyset$ and $\tilde{U}$ are always soft expert $\mathcal{I}_g$-closed.*

Remark 3.2. *The intersection of two soft expert $\mathcal{I}_g$-closed sets need not be a soft expert $\mathcal{I}_g$-closed as shown by the following example.*

Example 3.3. *Let U={u_1, u_2, u_3}, X={a}, E={e} and (F, A) be a soft expert set where (F, A)={((e, a, 1), {u_2}), ((e, a, 0), {u_1})}. Then τ={$\emptyset$, $\tilde{U}$, (F, A)} is a soft expert topology and $\mathcal{I}$={$\emptyset$} is a soft expert ideal on U. Let (G, A) and (H, A) be soft expert sets such that (G, A)={((e, a, 1), {u_1, u_2}), ((e, a, 0), $\emptyset$)} and (H, A)={((e, a, 1), {u_2, u_3}), ((e, a, o), $\emptyset$)}. Thus (G, A) and (H, A) are soft expert $\mathcal{I}_g$-closed but their intersection (G, A)$\cap$(H, A)={((e, a, 1), {u_2}), ((e, a, 0), $\emptyset$)} is not soft expert $\mathcal{I}_g$-closed.*

Theorem 3.4. *If (F, A) is soft expert $\mathcal{I}_g$-closed in a soft expert topological space (U, τ, A) and (F, A)$\subset$(G, A)$\subset\overline{(F,\ A)}$, then (G, A) is soft expert $\mathcal{I}_g$-closed.*

Proof. If (F, A) is soft expert $\mathcal{I}_g$-closed and (F, A)$\subset$(G, A)$\subset\overline{(F,\ A)}$. Suppose that (G, A)$\subset$(H, A) and (H, A)$\in\tau$. Then (F, A)$\subset$(H, A). Since (F, A) is soft expert $\mathcal{I}_g$-closed, then $\overline{(F,\ A)}\backslash$(H, A)$\in\mathcal{I}$. Now (G, A)$\subset\overline{(F,\ A)}$ implies that $\overline{(G,\ A)}\subset\overline{(F,\ A)}$. So $\overline{(G,\ A)}\backslash$(H, A)$\subset\overline{(F,\ A)}\backslash$(H, A) and thus $\overline{(G,\ A)}\backslash$(H, A)$\in\mathcal{I}$. Therefore (G, A) is soft expert $\mathcal{I}_g$-closed. □

Theorem 3.5. *If (F, A) is soft expert $\mathcal{I}_g$-closed and (G, A) is soft expert closed in a soft expert topological space (U, τ, A). Then (F, A)$\cap$(G, A) is soft expert $\mathcal{I}_g$-closed.*

Proof. Assume that (F, A)$\cap$(G, A)$\subset$(H, A) and (H, A)$\in\tau$. Then (F, A)$\subset$(H, A)$\cup$(G, A)^c and (H, A)$\cup$(G, A)^c is soft expert open in U. Since (F, A) is soft expert $\mathcal{I}_g$-closed, we have $\overline{(F,\ A)}\backslash$((H, A)$\cup$(G, A)^c)$\in\mathcal{I}$. Now, $\overline{(F,\ A)\cap(G,\ A)}\subset\overline{(F,\ A)}\cap$(G, A)=($\overline{(F,\ A)}\cap$(G, A))$\backslash$(G, A)^c. Therefore ($\overline{(F,\ A)\cap(G,\ A)}$)$\backslash$(H, A)$\subset$($\overline{(F,\ A)}\cap$(G, A))$\backslash$((H, A)$\cap$(G, A)^c)$\subset\overline{(F,\ A)}\backslash$((H, A)$\cup$(G, A)^c)$\in\mathcal{I}$. Hence (F, A)$\cap$(G, A) is soft expert $\mathcal{I}_g$-closed. □

Definition 3.3. *A soft expert set (F, A) in a soft expert topological space (U, τ, A) is called soft expert generalized open set with respect to soft expert ideal (briefly soft expert $\mathcal{I}_g$-open) iff the relative complement (F, A)^c is soft expert $\mathcal{I}_g$-closed.*

Theorem 3.6. *A soft expert set (F, A) is soft expert $\mathcal{I}_g$-open in (U, τ, A) iff (G, A)$\backslash$(H, A)$\subset$(F, A)^0 for some (H, A)$\in\mathcal{I}$, whenever (G, A)$\subset$(F, A) and (G, A) is soft expert closed.*

) is soft expert $\mathcal{I}_g$-open. Suppose (G, A)$\subset$(F, A) and (G, A) is soft expert closed. We have oft expert $\mathcal{I}_g$-closed and (G, A)$^c\in\tau$. By assumption, $\overline{(F,\ A)^c}\backslash$(G, A)$^c\in\mathcal{I}$. Hence $\overline{(F,\ A)^c}\subset$(G, $\in\mathcal{I}$. So $((G,A)^c\cup(H,A))^c\subset(\overline{(F,\ A)^c})^c$=(F, A)^0 and therefore (G, A)$\backslash$(H, A)$\subset$(F, A)^0.

A)$\subset$(F, A) and (G, A) is soft expert closed imply (G, A)$\backslash$(H, A)$\subset$(F, A)^0, for some (H, A)$\in\mathcal{I}$. et (V, A) such that (F, A)$^c\subset$(V, A). Then (V, A)$^c\subset$(F, A). By assumption (V, A)$^c\backslash$(H, A)$\subset$(F,

$A)^0$ for some (H, A)$\in\mathcal{I}$. This give that $((V, A)\cup(H, A))^c\subset(\overline{(F, A)^c})^c$. Then $\overline{(F, A)^c}\subset(V, A)\cup(H, A)$ for some (H, A)$\in\mathcal{I}$. This shows that $\overline{(F, A)^c}\backslash(V, A)\in\mathcal{I}$. Hence $(F, A)^c$ is soft expert $\mathcal{I}_g$-closed and therefore (F, A) is soft expert $\mathcal{I}_g$-open. □

Theorem 3.7. *If $(F, A)^0\subset(G, A)\subset(F, A)$ and (F, A) is soft expert $\mathcal{I}_g$-open in a soft expert topological space (U, τ, A), then (G, A) is soft expert $\mathcal{I}_g$-open.*

Proof. Suppose that $(F, A)^0\subset(G, A)\subset(F, A)$ and (F, A) is soft expert $\mathcal{I}_g$-open. Then $(F, A)^c\subset(G, A)^c\subset\overline{(F, A)^c}$ and $(F, A)^c$ is soft expert $\mathcal{I}_g$-closed. By Theorem 3.4, $(G, A)^c$ is soft expert $\mathcal{I}_g$-closed and hence (G, A) is soft expert $\mathcal{I}_g$-open. □

Proposition 3.3. *Let $\mathcal{I}$ and $\mathcal{I}'$ be two soft expert ideals on a soft expert topological space (U, τ, A).*

(1) $\mathcal{I}\subset\mathcal{I}'$, then every soft expert $\mathcal{I}_g$-open set (F, A) is soft expert $\mathcal{I}'_g$-open.

(2) If (F, A) is soft expert $(\mathcal{I}\cap\mathcal{I}')_g$-open, then it is simultaneously soft expert $\mathcal{I}_g$-open and soft expert $\mathcal{I}'$-open.

4. Conclusion

In the present work, we have continued to study the properties of soft expert topological spaces. We introduce the notions of soft expert $\mathcal{I}_g$-closed sets and soft expert $\mathcal{I}_g$-open sets and have established several interesting properties. Hence, generalized closed set concepts are possible in soft expert topological spaces. We hope the findings in this paper will help the researchers to enhance and promote the further study on soft expert topology to carry out a general framework for their applications in practical life.

References

[1] B.Ahmad and A.Kharal, *On fuzzy soft sets*, Advances in Fuzzy Systems, (2009), 1-6.

[2] H.Aktas and N.Cagman, *Soft sets and soft groups*, Information Sciences, 77(1)(2007), 2726-2735.

[3] M.I.Ali, F.Feng, X.Liu, W.K.Min and M.Shabir, *On some new operations in soft set theory*, Computers and Mathematics with Applications, 57(2009), 1547-1553.

[4] S.Alkhazaleh and A.R.Salleh, *Soft Expert Sets*, Advances in Decision Sciences, 2011(2011).

[5] K.Atanassov, *Operators over interval valued intuitionistic fuzzy sets*, Fuzzy Sets and Systems, 64(1994), 159-174.

[6] K.Atanassov, *Intuitionistic fuzzy sets*, Fuzzy Sets and Systems, 20(1986), 87-96.

[7] A.Aygüoğlu, H.Aygün, *Some notes on soft topological spaces*, Neural Computing and Applications, 21(2012), 113-119.

[8] N.Cagman, F.Citak and S.Enginoglu, *Fuzzy parameterized fuzzy soft set theory and its applications*, Turkish Journal of Fuzzy Systems, 1(1)(2010), 21-35.

[9] N.Cagman and S.Enginoglu, *Soft set theory and uni-int decision making*, European Journal of Operational Research,

iod of inference in approximate reasoning based on interval-valued fuzzy sets, Fuzzy Sets and

, *Some properties of soft topological spaces*, Comput. Math. Appl., 62(2011), 4058-4067.

t topological spaces, SpringerPlus, 42(1)(2012), 1-42.

[13] A.Kandil, O.A.E.Tantawy, S.A.El-Sheikh and A.M.Abd El-latif, *γ-operation and decompositions of some forms of soft continuity in soft topological spaces*, Annals of Fuzzy Mathematics and Informatics, 7(2014), 181-196.

[14] A.Kandil, O.A.E.Tantawy, S.A.El-Sheikh and A.M.Abd El-latif, *Semi-soft compactness via soft ideals*, Appl. Math. Inf. Sci., 8(5)(2014), 1-10.

[15] A.Kandil, O.A.E.Tantawy, S.A.El-Sheikh and A.M.Abd El-latif, *Soft ideal theory, Soft local function and generated soft topological spaces*, Appl. Math. Inf. Sci., 8(4)(2014), 1-9.

[16] K.Kannan, *Soft generalized closed sets in soft topological spaces*, Journal of theoretical and applied information technology, 37(1)(2012), 17-21.

[17] K.Kannan and D.Narasimhan, *Soft expert generalized closed sets*, International Journal of Pure and Applied Mathematics, 93(2)(2014), 233-242.

[18] D.V.Kovkov, V.M.Kolbanov and D.A.Molodtsov, *Soft sets theory-based optimization*, Journal of Computer and Systems Sciences International, 46(6)(2007), 872-880.

[19] P.K.Maji, R.Biswas and A.R.Roy, *Fuzzy soft sets*, Journal of Fuzzy Mathematics, 9(3)(2001), 589-602.

[20] P.K.Maji, R.Biswas and A.R.Roy, *Intuitionistic fuzzy soft sets*, Journal of Fuzzy Mathematics, 9(3)(2001), 677-691.

[21] P.K.Maji, R.Biswas and A.R.Roy, *Soft set theory*, Computers and Mathematics with Applications, 45(2003), 555-562.

[22] P.Majumdar and S.K.Samanta, *Generalised fuzzy soft sets*, Computers and Mathematics with Applications, 59(2010), 1425-1432.

[23] D.A.Molodtsov, *Soft set theory-first results*, Computers and Mathematics with Applications, 37(1999), 19-31.

[24] D.Molodtsov, V.Y.Leonov and D.V.Kovkov, *Soft sets technique and its application*, Nechetkie Sistemy i Myagkie Vychisleniya, 1(1)(2006), 8-39.

[25] A.Mukherjee and S.B.Chakraborty, *On intuitionistic fuzzy soft relations*, Bulletin of Kerala Mathematics Association, 5(1)(2008), 35-42.

[26] H.I.Mustafa and F.M.Sleim, *Soft generalized closed sets with respect to an ideal in soft topological spaces*, Appl. Math. Inf. Sci., 2(8)(2014), 665-671.

[27] Z.Pawlak, *Rough sets*, Int. J. Comput. Sci., 11(1982), 341-356.

[28] M.Shabir and M.Naz, *On soft topological spaces*, Comp. Math. Appl., 61(2011), 1786-1799.

[29] L.A.Zadeh, *Fuzzy sets*, Information and Control, 8(1965), 338-353.

[30] I.Zorlutuna, M.Akdag, W.K.Min and S.Atmaca, *Remarks on soft topological spaces*, Annals of fuzzy Mathematics and Informatics, 3(2012), 171-185.

STM JOURNALS

Journal of Geotechnical Engineering
ISSN: 2394-1987(online)
Volume 1, Issue 3
www.stmjournals.com

Comparative Study on Stabilization of Expansive Soil using Cement Kiln Dust and Ceramic Dust

G. Muthumari**, R. Nasar Ali, J. Dhaveethu Raja*
Department of Civil Engineering & Department of Chemistry, Mohamed Sathak Engineering College, Kilakarai, Ramanathapuram, Tamilnadu, India

Abstract

In India, expansive soils cover about 20% of total land area, these soils increase in volume (swell) during winter season and decrease in volume (shrink) during summer season. Due to this contradiction behaviour many civil engineering structures constructed on expansive soils get damaged severely, out of which pavement is the most because they are lightweight and extend over large areas. Stabilization of Expansive soil is of most importance, since to increase the strength of soil and to reduce the construction cost by making best use of locally available materials. The effects of Cement Kiln Dust (CKD) and Ceramic Dust (CD) on expansive soil by conducting the laboratory tests like Atterberg's limit, Compaction characteristics, Unconfined Compressive Strength, California Bearing Ratio, and Free Swell Index etc were studied. Locally collected Black Cotton (BC) soil was mixed with addition of industrial waste materials such as; CKD and CD from 0 to 6% with an increment of 2%. From the analysis of test results, it was found that Liquid Limit (LL), Plasticity Index (PI), Optimum Moisture Content (OMC) and Free Swell Index (FSI) were decreased with an increment of CKD and CD percentage. Plastic Limit (PL), Maximum dry density (MDD), Unconfined Compressive Strength (UCS) and California Bearing Ratio (CBR) were increased with an increment of CKD and CD percentage. From this study we have concluded that CKD has very high lime (CaO) content up to 60% and CD has very high Silicon dioxide (SiO_2) because of these characteristics, they can be used as effective utilization in roads, embankment and soil treatment for foundation.

***Keywords**: Expansive Soil, BC soil, soil stabilization, CKD, CD*

****Author for Correspondence*** E-mail: g.muthumari@gmail.com

INTRODUCTION

Road construction in India faces the big challenge to complete huge projects in the shortest possible construction time. In the booming economy, thousands of new road kilometers are needed and will be built over the short years to expand the network of traffic arteries in the country. Now a day, the major roads are damaged within a short interval of time because of limitation and faster construction. We are focusing on the same problem arising in Sakkarakottai village, Ramanathapuram town, Tamilnadu, India there is a lot of damages occur in the road within a very short interval of time, since the l the road without grade. And also the main nount of Expansive soils ea. When load is applied to Expansive soil, it causes serious problem on civil engineering structures, pavements and canal linings due to its tendency of swelling when they absorbs water and shrinks when they dry out. Therefore, it is necessary to stabilize these BC soils before constructing the roads in order to achieve useful and long lasting life [1, 2]. There are numerous innovative foundation techniques have been available in the field to overcome the problem of expansive soils, but they are not suggested in the field, since they are uneconomical [2]. In economical and strengthening point of view, Soil stabilization with various additives is the best method for improving the strength of in-situ soil by means of mechanical or chemical [3–5]. Out of these, chemical stabilization is the vital role for many of the geotechnical engineering applications to avoid

the damage due to swelling action of the expansive soils [6, 1, 2]. Since it is a time saving and efficient method that enables the sub grade to formulate good strength as compared to costly excavation and replacement with borrow material.

According to earlier studies they mainly focused on the utilization of chemical additives such as cement, lime, fly ash etc., but they have kept the cost of construction of stabilized road financially high [7, 3, 4]. In order to make the problematic soils useful and meet geotechnical engineering design requirements, we are focusing more on the use of potentially cost effective materials that are locally available (industrial waste). On the other hand, there are many problems arise from the growth of industries in the country. One of them is the proper and effective disposal of its waste in the land, since they causes many serious environment problems [8, 3, 6, 7]. Using industrial waste in construction industry, it is beneficial in many ways such as disposal of waste and also it helps to improve the engineering properties of the soil. In this study, the local expansive soil was mixed with addition of industrial waste materials such as CKD and CD from 0 to 6% with an increment of every 2%. The choice and effectiveness of an additive depends on the type of soil and its field conditions [3, 7]. The main aim of the present work is, to develop an optimum mix composition which can be economically used for stabilization of expansive soil [9].

PROBLEM DESCRIPTION

Clay soil is the major soil naturally occurring near Sakkarakottai village, Ramanathapuram town, Tamilnadu, India. Clay soils are generally classified as expansive one. This means that there is a contradiction, (i.e., shrink and swell) behavior because of seasonal moisture content variation this will create major changes in civil engineering structures all over the world. All civil engineering structural components may crack and heave as the underlying expansive soils become wet and swell. In sometimes the cracking and heaving appear temporarily as the soils dry and shrink as sown in Figure 1. To solve this take preventive measures excess water, by mixing different soil which has the same characteristics as that of BC soil and soil stabilization. Purpose of this study is to find the suitable additives for soil stabilization which will give good results and as well as economical one.

Fig. 1: *Cracks in Expansive Soil when Soil is Dry.*

STUDY METHODOLOGY

Selection of Site

In Ramanathapuram city, near Sakkarakottai there is a lot of damages occurs in the road within a short interval of time. Since, a huge volume of BC soils is present in that area; the cracks are induced in the road because of its variation of seasonal moisture content in the soil. To overcome this situation, we are planned to stabilize the soil with different additives such as CKD and CD. The soil sample has been collected from that location at a depth of 1m from the ground level to study the various properties of soil as per IS 2720 code of practice and it was shown in Table.1.BC soil used for this study was classified as well graded soil as per IS Soil Classification system based on the grain size (Figure 2).

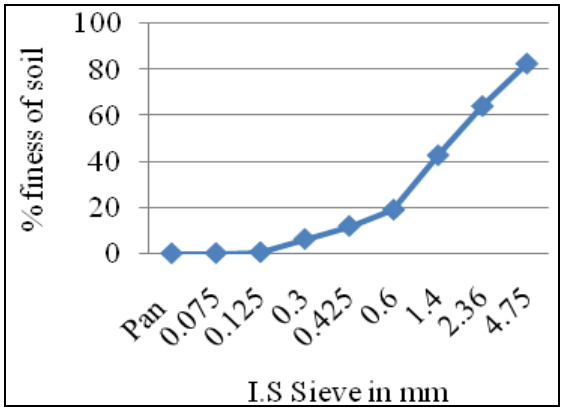

Fig. 2: *Grain Size Distribution Curve for Expansive Soil.*

Table 1: *Properties of Expansive Soil.*

S.No	Characteristics	Description
1.	Grain size Analysis • Sand content (%) • Silt content (%) • Clay content (%)	 99.5 0.4 0.1
2.	Specific Gravity	2.8
3.	Atterberg's Limit • Liquid Limit (%) • Plastic Limit (%) • Plasticity Index (%)	 50 26.71 23.29
4.	Compaction Characteristics • Maximum Dry Density (MDD) in kN/m^3 • Optimum Moisture Content (OMC) in %	 14.13 18
5.	Unconfined Compressive Strength (UCS) in kN/m^2	74
6.	California Bearing Ratio (CBR)	1.60
7.	Free Swell Index (%)	31.80
8.	Color	Black

Selection of Materials as Soil Stabilizers

After studying the literatures on soil stabilization using various additives and visiting various industries, it has been decided to choose the CKD and CD as best suitable additive with expansive soil for stabilization. The main reasons for choosing these materials are they are economical, they have disposal problem since they are waste products and also they are locally available materials [10, 11, 4].

MATERIALS

Cement Kiln Dust (CKD)

Globally growing demand of cement; results in huge emission of kiln dust from cement plants. It is important to dispose this waste material in an economic and safe manner. To overcome this problem, research is being carried out in different parts of world for utilization of CKD in various applications like soil stabilization, cement production, pavements, agriculture and cement products etc. [12, 13, 6, 7].

Production of CKD

CKD is a by- product of Portland cement manufacturing process. Generally, for each one ton of clinker, a typical kiln generates around 0.06 to 0.07 ton of CKD. More than six crore fifty thousand lakhs tons of CKD, unsuitable for recycling in the cement ess were disposed of st of the wastes are lls, creating a disposal problem and gradual loss of landfill space. And about more than 1 crore tons of CKD, that are not suitable for recycling, are disposed-off annually by cement manufacturing companies in India. In parts of the country CKD is being used increasingly for soil stabilization.

Characteristics of CKD

CKD consists primarily of calcium oxide and silicon dioxide which is similar to the cement kiln raw feed, but the amount of alkalis, chloride and sulphate is usually considerably higher in the dust [6, 8, 13]. However, the alkali by-pass process contains the highest amount by weight of calcium oxide and lowest Loss on Ignition (LOI), both of which are key components in many beneficial applications of CKD [14, 7]. The CKD collected from Ramco cement production plant located in Ariyalur. Because of the high calcium content present in CKD, the hydration process will occur quickly it will induce good bonding characteristics. With this characteristic, we are using this material as additive for soil stabilization.

Chemical Properties of CKD

CKD have different physical and chemical properties and it depends upon the source, type of raw materials used, type of plant operation, fuel type used and disposal practices [15,12]. Table 2 shows the chemical properties of CKD and CD. Generally CKD is grayish in color.

Table 2: *Chemical Properties of CKD and CD.*

CONTENT	CKD (%)	CD (%)
Silicon dioxide (SiO_2)	17.62	68.58
Aluminum Oxide (Al_2O_3)	4.90	27.45
Iron Oxide (Fe_2O_3)	2.58	0.47
Calcium Oxide (CaO)	62.09	0.17
Magnesium Oxide (MgO)	1.93	0.16
Potassium Oxide (K_2O)	3.76	1.84
Sodium Oxide (Na_2O)	0.56	0.32
Sulphur Oxide (SO_3)	5.79	0.13
Titanium oxide (TiO_2)	-	0.75

Ceramic Dust (CD)

In the world a lot of CD is produced during production, transportation and placing of ceramic tiles. This wastage or scrap material is inorganic material and hazardous. Hence its disposal is a problem which can be removed with the idea of utilizing it as an admixture to

stabilize BC soil, so that the mix prove to be very economical and can be used as sub grade in low traffic roads or village roads.

Production of CD

It has been estimated that about 30% of daily production in the ceramic industry goes to be CD. The disposal of which creates environmental and economical problem. To overcome this situation this industrial waste can be used in different application, one of prime is soil stabilization.

Characteristics of CD

CD consists of high SiO_2, Al_2O_3 and Fe_2O_3 contents reaching up to 96%, but the amount of Fe_2O_3 and Tio_2 is 1.22% [16]. The CD collected from Government Ceramic Institute (ceramic plant), Vridhachalam, Tamilnadu, India. Because of high silica content present in CD, the binding capacity of soil is increased.

EXPERIMENTAL STUDY

Preparation of sample

BC soil has been tested to find the various properties using additives such as CKD and CD with partial replacement of weight of soil. CKD and CD is added to natural soil for preparation of sample from 0 to 6% with every increment of 2%. Total of seven different specimens were prepared to study the properties of stabilized soil. For the preparation of each specimen all the materials were mixed thoroughly by hand so that homogenous sample can be prepared.

Testing Procedure

Different soil laboratory tests carried out on the above samples as per IS-2720 such as Particle size distribution, Specific gravity, Atterberg's limit, Compaction Characteristics, UCS, CBR and FSI etc. From these test results, Geotechnical and Engineering properties of the soil were determined. For UCS test, the sample is prepared at OMC and MDD.

RESULTS AND DISCUSSIONS

Soil has been tested with the additive at different proportion to find the basic index properties like Liquid Limit (LL), Plastic y Index (PI), Maximum D), Optimum Moisture e Swell Index (FSI) and Engineering properties such as Unconfined Compressive Strength (UCS) and California Bearing Ratio (CBR). The result analysis is carried out for both admixtures and the results are as shown in the following figures.

Effect of Additives on Atterberg's Limits

The results of Liquid Limit (LL) tests on expansive soil treated with different percentage of CKD and CD are shown in Figure 3. From the figure, it can be seen that the LL of soil goes on decreasing with increase in percentage of CKD and CD [17, 18]. The effect of CKD on LL shows better performance than CD.

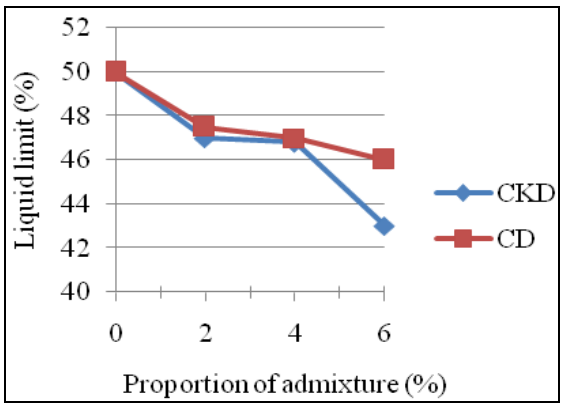

Fig. 3: *Comparison of LL for CKD and CD.*

The results of Plastic Limit (PL) tests on expansive soil treated with different percentage of CKD and CD are shown in Figure 4. From the figure, it can be seen that the PL of soil goes on increasing when the soil is treated with different percentages of CKD and the PL of soil goes on decreasing when the soil is treated with CD up to 4%, after that it was increasing [19, 18].

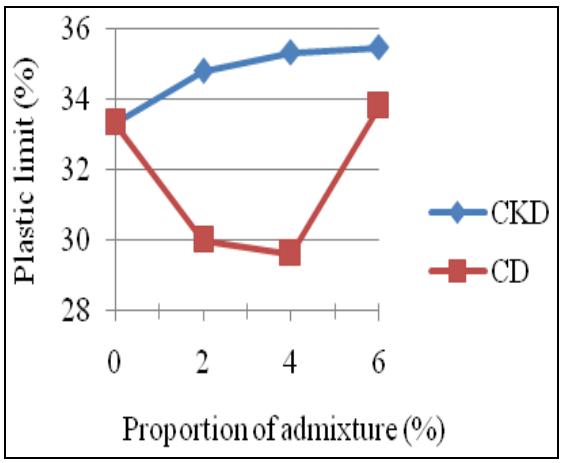

Fig. 4: *Comparison of PL for CKD and CD.*

The results of Plasticity Index (PI) on expansive soil treated with different percentage of CKD and CD are shown in Figure 5. From the figure, it can be seen that the PI of soil goes on decreasing with increase in percentage of CKD and CD [18, 19]. If lesser the PI, the strength will be high and also the workability of soil will increase having less affinity for water [20].

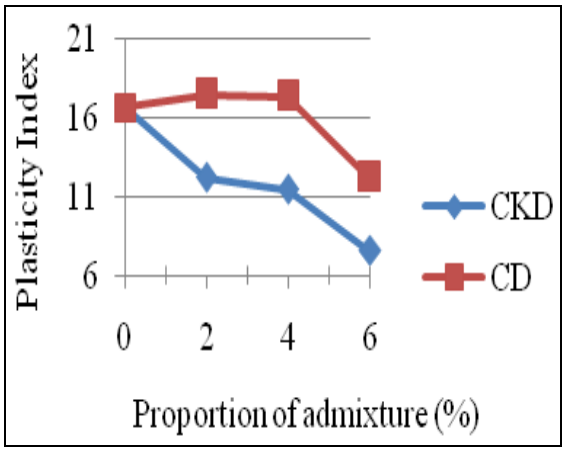

Fig. 5: *Comparison of PI for CKD & CD.*

Effect of Additives on MDD and OMC

The results of standard Proctor tests on expansive soil treated with different percentage of CKD and CD are shown in Figure 6 and 7. From the figure, with increase in percentage of CKD up to 4, the MDD of soil goes on increased and after that it was decreased in 6% but OMC was increasing [19]. With increase in percentage of CD, MDD of soil goes on increasing but OMC was decreasing [18]. Reason of such behavior is due to replacement of additive particles having high specific gravity with soil particles having low specific gravity.

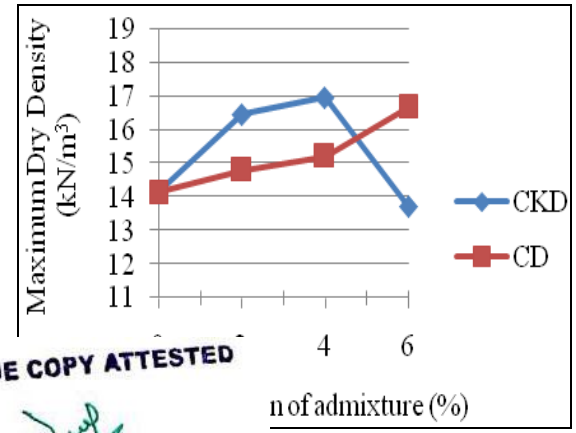

of MDD for CKD & CD.

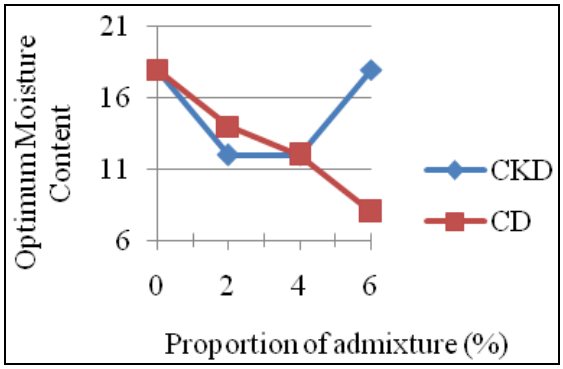

Fig. 7: *Comparison of OMC for CKD &CD.*

Effect of Additives on CBR

The results of CBR on expansive soil treated with different percentage of CKD and CD are shown in Figure 8. From figure it has been concluded that the value of CBR constantly increases with the increase in proportion of CKD. With increase in percentage of CD up to 4%, the CBR of soil goes on increased and after that it was decreased in 6% [18]. CKD has more effective than CD in soil while doing the CBR test.

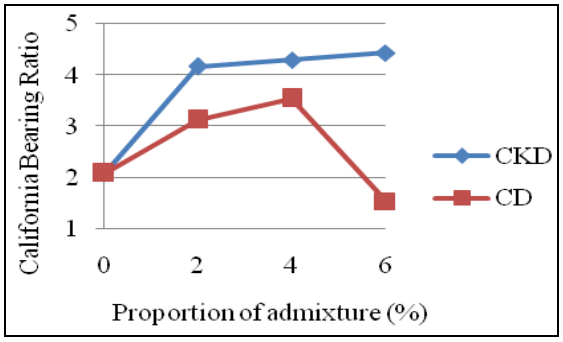

Fig. 8: *Comparison of CBR for CKD and CD.*

Effect of Additives on UCS

Figure 9 shows the UCS tests results for both admixtures used in soil. With increase in CKD and CD content leads to an increment of the strength [18, 19].

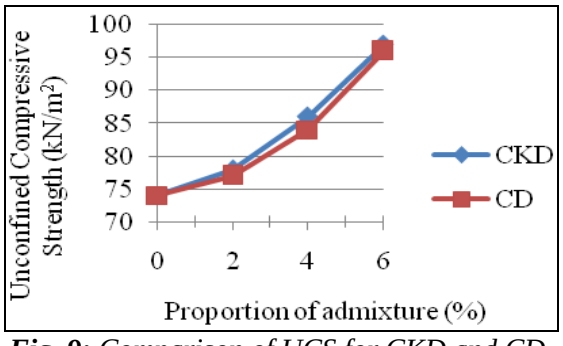

Fig. 9: *Comparison of UCS for CKD and CD.*

Effect of Additives on FSI

Table 3 shows the FSI value for expansive soil before and after the treatment. The results showed that the FSI value decreases with increase in percentage of CKD and there is no swelling in the soil, after treating the soil with CD.

Table 3: *Comparison of FSI for CKD and CD.*

Proportion of admixture (%)	FSI for CKD	FSI for CD
0	31.08	31.08
2	22	Nil
4	18.18	Nil
6	18.18	Nil

CONCLUSION

LL, PI and FSI properties was decreased but PL and CBR value was increased when CKD was added with BC soil. MDD value was increased with 4% addition of CKD and it was decreased while 6% addition with BC soil. But OMC value decreased with 4% usage of CKD and with 6% usage of CKD, the OMC value was same as untreated expansive soil. With addition of CD to BC soil, LL, PI and OMC value was decreased but MDD was increased, there is no free swell occurs in the soil. While using CD up to 4%, the PL and CBR value was increased and after that it was decreased with 6% addition with BC soil. With these test results, in economic and strengthening point of view we have suggested that up to 4% both the additives, (i.e., CKD and CD) are effective for stabilizing the expansive soil in road works. But, CKD is more effective than CD for stabilization of soil.

ACKNOWLEDGEMENT

The authors express their sincere and heartfelt thanks to the Managing Board, Principal, Department of Civil engineering and Department of Chemistry, Mohamed Sathak Engineering College, Kilakarai for providing all research and instrumental facilities. Also the author expresses sincere thanks to Department of Science and Technology (DST) –Science and Engineering Research Board (SERB), New Delhi.

REFERENCES

1. A... ...ukesh Kumar. Study Of ...our Of Black Cotton Soil ... Sand Column. *IJAET*. ...010p.
2. Gandhi KS. Stabilization of Expansive Soil of Surat Region using Rice Husk Ash & Marble Dust. *IJCET*. 2013; 3(4): 1516–21p.
3. Kumar B, Puri N. Stabilization of weak pavement sub grades using Cement kiln dust. *IJCIET*. 2013; 4(1): 26–37p.
4. Roy A. Soil Stabilization using Rice Husk Ash and Cement. *IJCER*. 2014; 5(1): 49-54p.
5. Ameta NK, Wayal AS, Hiranandani P. Stabilization of Dune Sand with Ceramic Tile Waste as Admixture. *AJER*. 2013; 2(9): 133–39p.
6. Ismaiel H. Cement Kiln Dust Chemical Stabilization of Expansive Soil Exposed at El-Kawther Quarter, Sohag Region, Egypt. *IJG*. 2013; 4: 1416–24p.
7. Keerthi Y, Divya Kanthi P, Tejaswi N, *et al*. Stabilization of Clayey Soil using Cement Kiln Waste. *IJASGE*. 2013; 7(1): 77–82p.
8. Rahman MK, Rehman S, Al-Amoudi OSB. Literature Review on Cement Kiln Dust Usage in Soil and Waste Stabilization and Experimental Investigation. *IJRRS*. 2011; 7(1): 77–87p.
9. Singh B, Sharma RK. Evaluation of Geotechnical Properties of Local Clayey Soil Blended with Waste Materials. *JJCE*. 2014; 8(2): 135–51p.
10. Abdel Aziz M, Altohamy AK, Towfeek AR. Physical and Chemical Properties for Stabilized Sand using Cement Kiln Dust. *JES*. 2010; 38(3): 655–69p.
11. El- Dakroury A, Sayed MS, EL- Sherif E. Mechanism and Modelling for Sorption of Toxic Ion on Cement Kiln Dust. *Nat. Sci.* 2011; 9(5): 100–08p.
12. Albusoda BS, Salem AK. Stabilization of Dune Sand by Using Cement Kiln Dust (CKD). *JESGE*. 2012; 2(1): 131–43p.
13. Koteswara Rao PV, Satish Kumar K, Blessingstone T. Performance of Recron-3s Fiber with Cement Kiln Dust in Expansive soils. *IJEST*. 2012; 4(4): 1361–66p.
14. Salahudeen AB, Akiije I. Stabilization of Highway Expansive Soils with High Loss on Ignition Content Kiln Dust. *NIJOTECH*. 2014; 33(2): 141–48p.
15. Marku J, Dumi I, Lico E, *et al*. The characterization and the utilization of

Cement Kiln Dust (CKD) as partial Replacement of Portland Cement in Mortar and Concrete Production. *Zaštita Materijala* 2012; 53: Proj 4: 334–44p. *UDC:666.971.3.4.052*

16. Rajamannan B, Ramesh M, Viruthagiri G. Mechanical Properties of Ceramic White ware Samples with Different Amount of Quartz Addition. *IJPMR*, 2012; 1(1): 001–04p.
17. Baghdadi ZA. Utilization of Kiln Dust in Clay Stabilization. *JKAU: Eng. Sci*. 1990; 2: 153–63p.
18. Sabat AK. Stabilization of Expansive Soil Using Waste Ceramic Dust. *EJGE*, 2012; 17-Bundle Z: 3915–26p.
19. Moses GK, Saminu A. Cement Kiln Dust Stabilization of Compacted Black Cotton Soil. *EJGE*, 2012; 17-Bundle F: 825–833p.
20. Al Karagooly HJ. Effect of Cement Kiln Dust on Some Properties of Soil. *JBU: Eng. Sci.* 2012; 20(4): 1100–07p.

Study on Synthesis, Structural Elucidation of Biologically Active Schiff Base Transition Metal Complexes

J.Dhaveethu Raja[a*] and S.Angeline[b]
[a]Department of Chemistry, Mohamed Sathak Engineering College, Kilakarai-623 806, India.
[b]Bharathiyar University, Coimbatore, India
e-mail: jdrajapriya@gmail.com

Abstract— **The synthesis and spectral characterization of new series of transition metal complexes of Cu(II), Ni(II), Co(II) and Zn(II) have been carried out from a Schiff base ligand (L), 2((4,6-dimethoxypyrimidin-2-ylimino)methyl)phenol. Structural study has been carried out from their elemental analysis, molar conductance, mass, IR, UV-Vis, ^{1}H-NMR and ESR spectral studies. The structural data reveal that the formed complexes have ML type composition and the complexes have square-planar geometry. The redox behaviour of metal complexes has been studied by cyclic voltammetry studies. The DNA cleavage and binding studies have also been investigated using calf thymus DNA (CT-DNA) by gel electrophoresis and absorption spectral studies.**

Keywords- Schiff Base; Square planar geometry; DNA cleavage and DNA binding.

I. INTRODUCTION

The condensation reaction between an aromatic aldehyde and a primary amine leads to the formation of an imine known an as Schiff base. The wide variety of possible structures for the ligand has made the field of Schiff base complexes fast developing [1]. Compounds containing pyrimidine ring systems play an important role in many biological systems. These provide potential binding sites for metal ions, and any information on their coordinating properties is important as a means of understanding the role of metal ions in biological systems. The flexibility of disposition of different donor sites is the secret behind their successful performance in mimicking peculiar geometries around the metal centers [2]. Many compounds of therapeutic importance are known to contain pyrimidine ring system. Pyrimidine compounds are also used as hypnotic drugs for nervous system [3]. In view of this context we have undertaken this present study.

II. EXPERIMENTAL

A. Materials and methods

All reagents 2-amino-4, 6-dimethoxypyrimidine and salicylaldehyde used for the preparation of ligand and complexes were sigma products. Spectroscopic grade solvents were used for spectral and cyclic voltammetric measurements. The carbon, hydrogen and nitrogen microanalysis content of each sample was determined at the STIC, CUSAT, Cochin. I.R. Spectra using KBr pellets were recorded on a FTIR Shimadzu spectrophotometer in 4000-400 cm^{-1} range. Electronic absorption spectra of the complexes in DMSO were recorded on a Shimadzu UV-1800 spectrometer at the MSEC, Kilakarai. The X-band ESR spectra of the samples in methanol were obtained at 300K and 77K using a Varian $E_{1/2}$ spectrometer, the field being calibrated with TCNE (Tetracyanoethylene) as the g-marker at the SAIF, IIT, Bombay. Electrochemical studies were carried out using EG & E Princeton Applied Research Potentiostat/galvanostat model 273 A, controlled by M270 software. Cyclic voltammetric measurements were performed using a glassy carbon working electrode (3mm dia), Pt wire auxiliary electrode and an Ag/AgCl reference electrode. All solutions were purged with N_2 for 30 min prior to each set of experiments. TBAP was used as the supporting electrolyte. The molar conductance values of the complexes in DMSO solution were measured using a type 305 systronic conductivity bridge. Solutions of CT DNA in 50 mM NaCl /5 mM tris-HCl (pH 7.2) gave a ratio of UV absorbance at 260 and 280 nm, A_{260}/A_{280} of around 1.8 – 1.9, indicating that the DNA was sufficiently free of protein contamination. The DNA rmined by the UV absorbance at 260 nm after 1:100 dilutions. The Molar absorption s 6600 M^{-1} cm^{-1}. Stock solutions were kept at 4^0C and used after no more than 4 days. was used to prepare the buffer.

B. Synthesis of Schiff base Ligand ,2-((4,6-dimethoxypyrimidin-2-ylimino)methyl)phenol

A methanolic solution (20 ml) of 2-amino-4,6-dimethoxypyrimidin (1.55g, 10 mmol) and salicylaldehyde (1.065 ml, 10 mmol) Were mixed and refluxed for 5h, the course of reaction was followed by TLC. After the completion of the reaction the resulting yellow colored solution was allowed to evaporate slowly. Yellow solid separates out after complete solvent evaporation. The formed Ligand 2-((4,6-dimethoxypyrimidin-2-ylimino)methyl)phenol was washed with ether to remove excess methanol. The resulting powder was again purified by column chromatography.

C. Synthesis of complexes

A solution of Schiff base ligand (L), (0.2592g, 1mmol) and a solution of metal salts like $Cu(Ac)_2$, $Co(Ac)_2$, $Ni(Ac)_2$ and $Zn(Ac)_2$ (1mmol), was refluxed for 6h, the course of the reaction was followed by TLC. After the completion of reaction the resulting reaction mixture was reduced to one third of its volume and the solute on was cooled to room temperature. The resulting solid was washed in ether. The solid was recrystallized from chloroform.

D. Scheme of the Reaction

a) Synthesis of Schiff base ligand

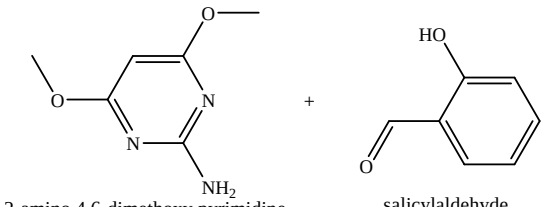

2-amino 4,6-dimethoxy pyrimidine salicylaldehyde

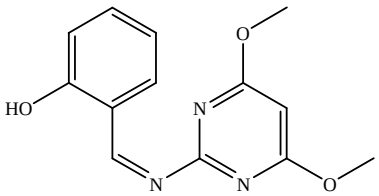

2-((4,6-dimethoxypyrimidin-2-ylimino)methyl)phenol

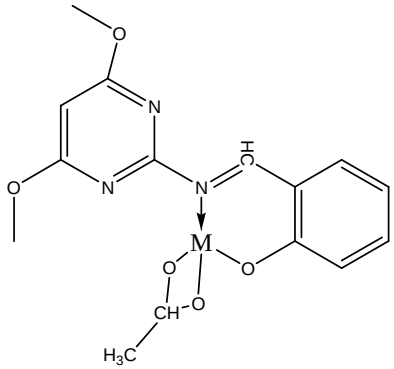

c) Proposed Structure of the complex

Where M = Cu(II), Co(II), Ni(II) and Zn(II)

III. RESULTS AND DISCUSSION

The Ligand and the prepared metal complexes were analyzed using various spectroscopic techniques.

A. Physical Characterization

Physical characterization, analytical and molar conductance studies were carried out (Table I). The complexes show low electrical conductance which reveals that these are non-electrolytes. The elemental analysis confirms the predicted structure of complexes.

B. Infrared Spectra of the Ligand and its Complexes

The free ligand gave broad band in the region of 3200cm^{-1}-3600 cm^{-1} indicating the presence of intramolecular hydrogen bonded –OH groups. This band disappeared on complexation due to involvement of –OH group on chelation. The IR spectrum of the ligand shows characteristic –C=N bands in the region of 1566cm^{-1}, which is shifted to lower frequencies in all of the complexes, indicating the involvement of –C=N nitrogen in coordination to metal ion. Hence from the IR spectra it is evident that ligand acts as a bidentate chelating agent, bonded to metal via azomethine nitrogen and phenolic oxygen atom of Schiff base ligand (L). The presence of new bands in all the complexes at 440 $cm^{-1}$to 750 cm^{-1} is probably due to formation of $\upsilon_{(M\text{-}O \text{ and } M\text{-}N)}$ bonds (4) (Table II).

C. Electronic Absorption Spectra

The spectrum displayed high-energy bands at 274nm and 323 nm assignable to π-π^* transitions corresponding to intraligand charge transfer. The spectrum of the complexes shows bands at 623nm-681nm which is in the region of d-d transitions. The Copper complex shows bands at 677nm assignable to $^2B_1g \rightarrow {}^2A_1g$ corresponding to square planar geometry (5) (Table II).

D. ^1H NMR Spectra

The spectra showed –CH=N signals at 8.1 ppm (s, 1H), phenyl multiplet at 6.66-7.26 ppm (m, 4H), -OCH_3 signal at 3.71ppm (m, 6H) and free –OH peak at 5.0ppm (s, H), assigned to the Ligand (L). The azomethine proton of Zn(II) complex is obtained at (8.3ppm) suggesting deshielding of azomethine group due to coordination with metal ion. Also acetate peak appears at 1.8ppm (Table II).

E. Electron Spin resonance Spectra

The X-band powder EPR spectrum of Cu(II) complexes show good resolved nitrogen superfine structure at 77 K in perpendicular region due to interaction of odd electron with nitrogen atoms. The magnetic moment calculated from the spectrum was 1.88 BM for Cu(II) complexes, which corresponds to one unpaired electron, indicating the complex is mononuclear. The observed g-values are $g_{II} > g_{\perp} > 2.0023$, indicating that Cu(II) metal has a d_{x2-y2} ground state. The $A_{\parallel}$ value was 150G. The observed value for the exchange interaction parameter (G) for copper complex was 6.27 i.e (G>4) suggests that local tetragonal axes are aligned parallel and the unpaired electron is present in the $d_{x^2-y^2}$ orbital and the exchange coupling effects are not operative in the present copper complex (6).

F. Cyclic Voltammetry

The cyclic voltammograms of Cu complex were examined in DMSO and found to be well behaved. The $E_{½}$ potentials were estimated from anionic and cathodic peak potentials. The ratio of cathodic to anodic current values indicates that the reaction is quasi-reversible. The data also confirms the redox process is corresponding to the formation of Cu (II)/Cu (I) couple.

G. Mass Spectra

The EI mass spectrum of the ligand and its copper complex were measured in room temperature and the data was used to compare their stoichiometric composition. The Schiff base ligand showed a molecular ion peak at m/z 259, which confirms the existence of odd number of nitrogen atoms in the ligand. The m/z peak of the complex were found to be 383, which is in accordance with the proposed structures.

H. DNA Cleavage Studies.

ɔn was monitored by gel electrophoresis. The electrophoresis revealed that the Schiff base complexes have acted on DNA as there was difference in bands of these lanes compared ı in fig (I). The metal complexes were able to convert supercoiled DNA to open circular

DNA (7). The presence of smear in the gel diagram indicates a radical cleavage. The copper complex have higher cleavage efficiency compared with the other complexes. The DNA cleavage reaction of the complexes probably proceeds through oxidative hydroxyl radical pathway in a similar way proposed by Sigman and co-workers.

I. DNA Binding Studies

DNA binding studies are important for the rational design and construction of new and more efficient drugs targeted to DNA. A variety of small molecules interact reversibly with double stranded DNA, primarily through three modes: (i) electrostatic interactions with negatively charged nucleic sugar –phosphate structure, which are along the external DNA double helix and do not posses selectivity; (ii) binding interaction with two grooves of DNA double helix and (iii) intercalation between the stacked base pairs of native DNA. Upon addition of CT-DNA, notable hyperchromic shift was observed, as seen in fig (II). The hyperchromic effect, characteristic of intercalation has been attributed to the interaction between electronic states of the compound chromophores and those of DNA bases. Thus the spectroscopic changes suggested that the complexes had strong interaction with DNA (8).

IV. CONCLUSION

A new pyrimidine based Schiff base ligand (L) was derived from the condensation of Salicylaldehyde and 2-amino 4,6-dimethoxy pyrimidine. This ligand was characterized using various spectrochemical techniques like IR, UV-Vis, NMR, ESR, Mass and elemental analysis. The spectral data suggest that the ligand coordinates through N and O donor atoms and hence acts as bidentate site. The complexes were predicted to be square planar in structure. The spectroscopic changes that occur in the binding studies confirm that the complex had strong interaction with DNA.

Figures and Tables

TABLE I

Compounds	**Physical Characterization**							
	Color	***Molecular Formula***	***Mol. Wt***	***Mt.Pt*** ℃	***Found (Cal)%***			***MOLAR CONDUCTANCE***
					M	***C***	***H***	***N***	
HL	Yellow	$C_{13}H_{13}N_3O_3$	259.2	228	--	63.6 (63.4)	5.5 (5.3)	20.5 (19.0)	--
Cu(OAc)L	Green	$C_{15}H_{15}N_3O_5Cu$	381.5	178	16.6 (16.4)	36.4 (36.5)	2.1 (2.3)	9.5 (9.2)	14.9
Co(OAc)L	Brown	$C_{15}H_{15}N_3O_5Co$	376.2	173	15.6 (15.5)	47.8 (47.7)	4.0 (3.8)	11.1 (11.0)	12.9
Ni(OAc)L	Green	$C_{15}H_{15}N_3O_5Ni$	375.9	180	15.5 (15.6)	47.9 (47.8)	4.2 (4.0)	11.1 (11.0)	11.0
Zn (OAc)L	Yellow	$C_{15}H_{15}N_3O_5Zn$	382.6	220	17.0 (16.9)	47.0 (47.1)	3.9 (4.0)	10.9 (11.0)	32.0

TABLE II

Compounds	**Spectral characterization**								
	UV-Vis (cm^{-1})			***IR (cm^{-1})***				***^{1}H NMR (ppm)***	
	Absorption (cm^{-1})	***Band Assignment***	***Geometry***	***-OH***	***-C=N***	***M-N***	***M-O***	***C=N***	***-OH***
HL	30959	INCT	--	3200-3500	1566	--	--	8.1	5.0
Cu(OAc)L	14598	$^2B_1g \rightarrow {}^2A_1g$	Square-planar	--	1547	756	462	--	--
Co(OAc)L	14880	$^1A_1g \rightarrow {}^1B_1g$	Square-planar	--	1549	756	518	--	--
Ni(OAc)L	20040 14771	$^1A_1g \rightarrow {}^1A_2g$ $^1A_1g \rightarrow {}^1B_1g$	Square-planar	--	1554	759	441	--	--
Zn(OAc)L	---			--	1543	758	447	8.3	--

LANE 1 2 3 4 5 6

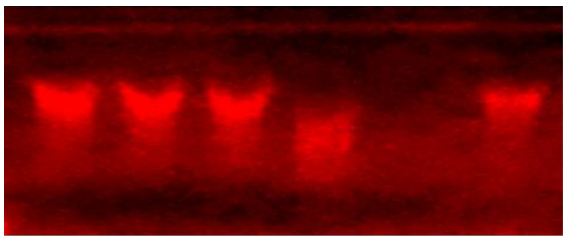

FIGURE 1
DNA CLEAVAGE

LANE 1: DNA alone, LANE 2: DNA + Ligand, LANE 3: DNA+ [CoL] +H_2O_2, LANE 4: DNA + [NiL] + H_2O_2, LANE 5:DNA + [CuL] + H_2O_2, LANE 6 : DNA +[ZnL] + H_2O_2

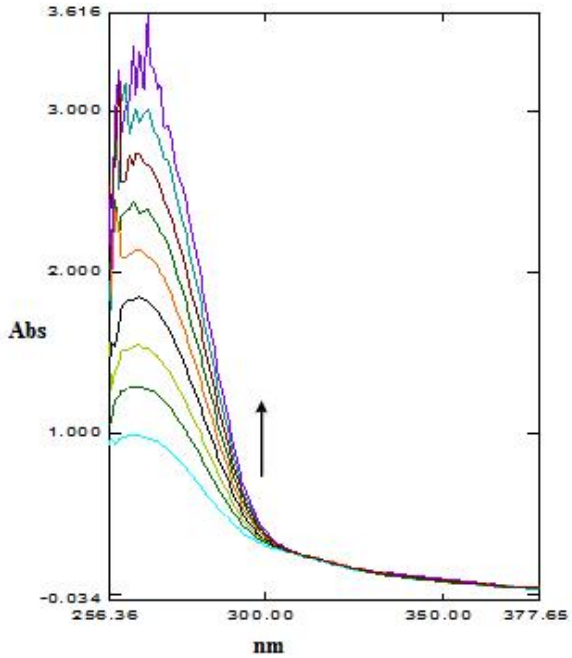

Figure *2:* UV spectrum for [Cu(OAc)L] in the presence of CT-DNA

ACKNOWLEDGMENT

The authors express their sincere and heartfelt thanks to the Managing Board, Principal, Mohammed Sathak Engineering College, Kilakarai for their constant encouragement and providing research facilities. The author also thanks the Department of Science and Technology (DST) - Science and Engineering Research Board (SERB), Government of India, New Delhi for financial support.

REFERENCES

[1] L. Ronconi, and P.J. Sadler, Coord. Chem. Rev., vol. 251, pp.1633–1648, 2007.
[2] N. Raman, R. Jeyamurugan, R. Senthilkumar, B. Rajkapoor, and S.G. Franzblau, Eur. J. Med. Chem., vol. 45, pp.5438–5451, 2010.
[3] M.H. Habibi, E. Shojaee, M. Ranjbar, H.R. Memarian, A. Kanayama, and T. Suzuki, Spectrochim. Acta A, vol.105, pp.563–568, 2013.
[4] R. Sharma, K.A. Banasal, and M. Nagar, Iindian.J.Chem. vol.44 A, p.2256, 2005.
[5] A.B.J. Lever, and E. Mantovani, Inorg. Chem., 10, 1971.
[6] A.M.F. Benial, V. Ramalingam and R. Murugesan, Spectrochim. Acta A, vol.56, pp.2775, 2005.
[7] H.L. Seng, H.K.A. Ong, R.N.Z.R.A. Rahman, B.M. Yamin, E.R.T. Tiekink, K.W. Tan, M.J. Maah, I. Caracelli, and C.H. Ng, J. Inorg. Biochem., vol.102, pp.1997–2011, 2008.
[8] V. Galasso, F. Asaro, F. Berti, B. Pergolese, B. Kovac, and F. Pichierri, Chem. Phys. , vol.330, pp. 457–468, 2006.

Synthesis, Structural Characterization, Antibacterial Activity, DNA Cleavage and Binding Study of Pyrimidine Derivative Schiff Base Metal Complexes

N.Revathi[a,b] and J.Dhaveethu Raja[*c]
[a] Department of Chemistry, Renganayagi Varatharaj College of Engineering, Sivakasi – 626 128, India.
[b]Department of Chemistry, Manonmanium Sundaranar University, Tirunelveli – 627 012, India
[*c] Department of Chemistry, Mohammed Sathak Engineering College, Kilakarai - 623 806, India.
E-mail: jdrajapriya@gmail.com

Abstract—**A new pyrimidine derivative Schiff base has been synthesized from 2-amino-4, 6-dimethylpyrimidine and 5-nitrosalicylaldehyde. Metal complexes of Schiff base have been prepared from acetate salts of Cu (II), Co (II), Ni (II) and Zn (II) and Sciff bases. The structures of the Schiff base ligand and its metal complexes were elucidated by elemental analyses, conductivity measurements, IR, ^{1}H-NMR, UV-Visible, ESR and Mass Spectroscopy. The redox behaviour of metal complexes was studied by cyclic voltammetry. The structural data reveal that the formed complexes have ML(OAc) type composition and the complexes have square planar geometry. The Schiff base and metal complexes have been screened for the antibacterial activity against some bacteria's. The results indicated mild antibacterial activity of some of the complexes. The interaction of the complexes with calf thymus DNA (CT-DNA) has been investigated by UV absorption method and the mode of binding to the complex has been investigated. UV studies of the interaction of the complexes with DNA have shown that they can bind to CT DNA.**

Key words: Pyrimidine derivative, Schiff base, Antibacterial activity

I. INTRODUCTION

Medicinal chemistry concerns with the discovery, development, identification and interpretation of the mode of action of biologically active compounds at molecular level. Synthetic drugs have resulted by simple changes in the structural alignment of a few novel heterocyclic compounds. Pyrimidine was first isolated by Gabriel and Colman in 1899(1). Pyrimidine represents one of the most active class of compounds possessing wide spectrum of biological activity viz. significant in vitro activity against unrelated DNA and RNA, viruses including polio herpes viruses, diuretic, antitumor, anti HIV, cardiovascular(2). The biodynamic property of the pyrimidine ring system prompted us to account for their pharmacological properties as antimicrobials acting against micro organisms (3). 2-amino-4,6-dimethylpyrimidine is the key to understand one step of enzyme reaction activity in the mechanism of the Vitamin B1 and mutation of DNA. The interactions of transition metal complexes with DNA have attracted considerable interest during recent decades. Metal complexes that exhibit interactions with DNA have been studied with the goals of developing both probes for nucleic acid structures and chemotherapy agents (4). Literature survey reveals that Schiff base using 2-amino-4 6-dimethyl pyrimidine and 5-nitrosalicylaldehyde have not yet been synthesised. We report here the synthesis, spectroscopic, antibacterial activity, DNA cleavage and binding studies of Schiff's base and its copper (II), cobalt (II), nickel (II) and Zinc (II) complexes.

II. EXPERIMENTAL

A. Materials and methods

All reagents 2-amino-4, 6-dimethylpyrimidine and 5-nitrosalicylaldehyde used for the preparation of ligand and complexes were sigma products. Spectroscopic grade solvents were used for spectral and cyclic voltammetric measurements. The carbon, hydrogen and nitrogen microanalysis content of each sample was determined at the STIC, CUSAT, Cochin. I.R. Spectra using KBr pellets were recorded on a FTIR Shimadzu spectrophotometer in 4000-400 cm^{-1} range. Electronic absorption spectra of the complexes in DMSO were recorded on a Shimadzu UV-1800 spectrometer at the MSEC, Kilakarai. The X-band ESR spectra of the samples in methanol were obtained at [illegible] Varian $E_{1/2}$ spectrometer, the field being calibrated with TCNE (Tetracyanoethylene) as the [illegible] IIT, Bombay. Electrochemical studies were carried out using EG & E Princeton Applied [illegible]alvanostat model 273 A, controlled by M270 software. Cyclic voltammetric measurements [illegible]a glassy carbon working electrode (3mm dia), Pt wire auxiliary electrode and an Ag/AgCl

reference electrode. All solutions were purged with N_2 for 30 min prior to each set of experiments. TBAP was used as the supporting electrolyte. The molar conductance values of the complexes in DMSO solution were measured using a type 305 systronic conductivity bridge. Solutions of CT DNA in 50 mM NaCl /5 mM tris-HCl (pH 7.2) gave a ratio of UV absorbance at 260 and 280 nm, A_{260}/A_{280} of around 1.8 – 1.9, indicating that the DNA was sufficiently free of protein contamination. The DNA concentration was determined by the UV absorbance at 260 nm after 1:100 dilutions. The Molar absorption coefficient was taken as 6600 M^{-1} cm^{-1}. Stock solutions were kept at 4°C and used after no more than 4 days. Doubly distilled water was used to prepare the buffer.

B. Synthesis of Schiff base (L) 2-(4,6-dimethylpyrimidin-2-ylimino)methyl)-4-nitrophenol

An equimolar amount of the methanolic solution (30 mL) solution of 2-amino-4, 6-dimethylpyrimidine and 5-nitrosalicylaldehyde was boiled under reflux for 10-11 h in presence of few drops of acetic acid as catalyst. At the end of the reaction, determined by thin layer chromatography, the reaction mixture was cooled to an ambient temperature. On slow evaporation of the mixture, yellow solid was isolated and washed with distilled water. Then the product was recrystallized with ethanol.

C. Synthesis of metal complexes

An equimolar amount of the methanolic solution (30 mL) of the acetate salts of metal and ligand was boiled under reflux for 7-8 h. The reaction mixture was cooled to room temperature. On slow evaporation of the mixture, the product was isolated and recrystallized with ethanol.

D. Antibacterial Activity

The in vitro biological screening effects of the investigated compounds were tested against the gram positive bacteria like as *Staphylococcus aureus, streptococcus pneumonia, staphylococcus pneumonia, bascillus subtilis* and gram negative bacteria like as *shigella flexneri, salmonella typi, klebsiella pneumonia, haemophyllus influenza* by the well diffusion method, using agar nutrient as the medium. The stock solutions (0.001 M) were prepared by the dissolving the compounds in DMSO. In a typical procedure, a well was made on the agar medium inoculated with microorganisms. The well was filled with the test solution using a micropipette and the plate was incubated for 24 h in the case of bacteria. During the period, the test solution diffused and the growth of the inoculated microorganisms was affected. The inhibition zone developed and the diameter of inhibition zone was measured.

E. DNA Cleavage Experiment

The nuclease activity of present complexes, investigated on CT DNA by agarose gel electrophoresis in the presence of H_2O_2 as oxidant. The gel electrophoresis experiments were performed by incubation at 35°C for 2h as follows: CT DNA each complex and H_2O_2 in tris-HCl buffer (pH=7.2) were eletrophoresed for 2h at 50 V on 1% agarose gel using tris-acetic acid-EDTA buffer, pH=8.3. After electrophoresis, the gel was stained using 1µg/cm^3 EB (ethidiumbromide) and photographed under UV light.

F. DNA BindingExperiment

All the experiments involving the interaction of the complexes with calf thymus (CT) DNA were carried out in Tris – HCl buffer at room temperature. Absorption titration experiments were performed by maintaining the metal complex concentration as constant, while measuring the absorption spectra, equal quantity of CT DNA and Tris-HCl buffer was added to both the complex solution and the reference solution to eliminate the absorbance of CT DNA itself. From the absorption data, the intrinsic binding constant K_b was determined from a plot of [DNA]/($\varepsilon_a - \varepsilon_f$) versus [DNA] using the following equation

$$\frac{[DNA]}{\varepsilon_a - \varepsilon_f} = \frac{[DNA]}{\varepsilon_b - \varepsilon_f} + [K_b(\varepsilon_b - \varepsilon_f)]^{-1}$$

Where, [DNA] is the concentration of CT DNA in base pairs. The apparent absorption coefficients ε_a, ε_f and ε_b correspond to $A_{obs.}/[M]$, the extinction coefficient for the free metal (II) complex and extinction coefficient for the metal (II) complex in the fully bound form respectively. K_b is given by the ratio of slope to the intercept.

III. RESULTS AND DISCUSSION

The Schiff base ligand and its Cu(II), Co(II), Ni(II) and Zn(II) complexes have been synthesized and characterized by spectral and elemental analytical data given in Table I. They are found to be air stable and pure in nature. The analytical data of the complexes correspond well with the general formula ML where M=Cu(II), Co(II), Ni(II) and Zn(II) and L=ligand. The molar conductance values clearly indicated non-electrolytic nature of the metal complexes.

A. Electronic Absorption Spectroscopy

The electronic absorption spectra of ligand (L) and its metal complexes, Cu(II), Co(II), Ni(II) and Zn(II) were recorded in DMSO at room temperature. The spectrum displayed high-energy bands at 298nm and 362 nm assignable to π -π^* transitions corresponding to intra ligand charge transfer. The spectrum of the complexes shows bands at 618nm-670nm which is in the region of d-d transitions. The Copper complex shows band at 19685 cm^{-1} assignable to $^2B_1g \rightarrow {}^2A_1g$ corresponding to square planar geometry (5). The absorption data are given in Table II.

B. IR Spectroscopy

The free ligand shows broad $\upsilon_{(OH)}$ band in the region of 3200cm^{-1}-3500 cm^{-1} indicating the presence of intramolecular hydrogen bonded –OH groups. This band disappeared on complexation due to involvement of –OH group on chelation. The IR spectrum of the ligand shows characteristic –CH=N band in the region of 1658cm^{-1}, which is shifted to lower frequencies in all of the complexes (1600-1651 cm^{-1}), indicating the involvement of –CH=N nitrogen in coordination to metal ion. Hence, from the IR spectra it is evident that ligand acts as a bidentate chelating agent, bonded to metal via azomethine nitrogen and phenolic oxygen atom of Schiff base ligand (L). The presence of new bands in all the complexes at 460 $cm^{-1}$to 680cm^{-1} is probably due to formation of υ (M-O and M-N) bonds(6). The important IR bands of the ligand (L) and its complexes are given in Table II.

TABLE I. Physical characterization, analytical and molar conductance data of the ligand and its complexes

S.No	Compound	Formula	Colour	Molecular Weight (g)	Yield (%)	Melting Point (°C)	C Calculated (Found)	H Calculated (Found)	N Calculated (Found)	M Calculated (Found)	Λ_m (mho,c m^2mol^{-1})
1	HL	$C_{13}H_{12}N_4O_3$	Yellow	272	84	170-172°C	57.34 (57.32)	4.44 (4.40)	20.58 (20.51)	-	-
2	Cu(OAc)L	$C_{15}H_{14}N_4O_5Cu$	Deep Brown	393	93	168-170°C	45.80 (45.78)	3.56 (3.58)	14.25 (14.31)	16.03 (15.98)	17.5
3	Co(OAc)L	$C_{15}H_{14}N_4O_5Co$	Pale Brown	358	83	182-184°C	50.28 (50.30)	3.94 (3.92)	15.64 (15.58)	7.82 (7.85)	31.6
4	Ni(OAc)L	$C_{15}H_{14}N_4O_5Ni$	Pale Green	389	83	166-168°C	46.33 (46.40)	3.60 (3.63)	14.40 (14.37)	15.09 (15.1)	32.6
5	Zn(OAc)L	$C_{15}H_{14}N_4O_5Zn$	Orange	396	75	180-182°C	45.53 (45.50)	3.57 (3.58)	14.16 (14.13)	16.52 (16.43)	21.0

TABLE II. UV-Visible IR and ^{1}H-NMR Spectral Data

S.NO	Compound	UV		IR			^{1}H-NMR		Geometry
		Λ_{max} (cm^{-1})	Band Assignment	$\upsilon_{(C=N)}cm^{-1}$	$\upsilon_{(M-N)}cm^{-1}$	$\upsilon_{(M-O)}cm^{-1}$	-CH=N-	-OH	
1	Ligand	33112 23201	INCT	1658	-	-	8.4	5.7	-
2	Cu(OAc)L	19685	$^2B_1g \rightarrow {}^2A_1g$	1651	671	498	-	-	Square Planar
3	Co(OAc)L	20202	$^1A_{1g} \rightarrow {}^1B_{1g}$	1647	678	462	-	-	Square Planar
4	Ni(OAc)L	20080 14925	$^1A_1g \rightarrow {}^1A_2g$ $^1A_1g \rightarrow {}^1B_1g$	1643	669	518	-	-	Square Planar
5	Zn(OAc)L	-	-	1600	648	503	9.8	-	Square Planar

C. ^{1}H NMR Spectroscopy

The ^{1}H NMR spectra of the ligand and complexes were recorded in DMSO-d_6. The spectra showed –CH=N signals at 8.4ppm (s, 1H), phenyl multiplet at 6.2-8.2ppm (m, 4H), -CH_3 signal at 2.1ppm (m, 6H) and peak obtained at 5.7ppm (s, 1H) is assigned to free –OH group of the Ligand (L). The absence of phenolic peak at 5.7 ppm in es that –OH proton of the ligand is involved in chelation with the metal. The azomethine ex is shifted to lower frequency (9.8ppm) suggesting deshielding of azomethine group due to l ion. Also acetate peak appears at 1.8ppm (s, 3H). There is no appreciable change in all the plex.

D. Mass Spectroscopy

The EI mass spectrum of the ligand and its copper complex was measured in room temperature and the data was used to compare their stoichiometric composition. The Schiff base ligand showed a molecular ion peak at m/z 272, which confirmed the existence of odd number of nitrogen atoms in the ligand. And the copper complex showed a molecular ion peak at m/z at 393, which confirmed the molecular formula of the complex, ML(OAc).

E. EPR Spectroscopy

The X-band EPR spectra of copper complex in methanol recorded at 300K and 77K. The spectrum of the complex at 300K shows one intense absorption band in the high field region and is isotropic due to dumpling motion of the molecules. The magnetic moment (1.89 BM) calculated from the equation $\mu_{eff} = g[s(s+1)]^{1/2}$ using the experimental g_{iso} values (2.18) indicating that the solid structure is retained in methanol solution. The EPR spectrum of the copper complex at 77 K indicates a poorly resolved nitrogen super hyperfine structure in the perpendicular region due to the interaction of the Cu (II) odd electron with nitrogen atoms. The copper complex has a magnetic moment 1.89 BM, corresponding to the one unpaired electron, indicating that the complex is mononuclear. The frozen methanol solution is axial with $g_{||} > g_{\perp} > 2.0023$, indicating a $d_{x^2-y^2}$ ground state (7) which is in agreement with the electronic absorption spectroscopic assignments. From the observed values, it is clear that $A_{||}$ (135) $> A_{\perp}$ (26); $g_{||}$ (2.38) $> g_{\perp}$ (2.09) > 2.0023 and the EPR parameters of the complex coincide well with related systems which suggest that the complex has square planar geometry and the system is axially symmetric. This is also supported by the fact the unpaired electron lies predominately in the $d_{x^2-y^2}$ orbital. In the axial spectra the g-values are related with exchange interaction coupling constant (G) by the expression, $G = (g_{||} - 2.0023) / (g_{\perp} - 2.0023)$. According to Hathaway (8), if the G value is larger than four, the exchange interaction is negligible because the local tetragonal axes are aligned parallel or are slightly misaligned. If the G value is less than four, the exchange interaction is considerable and the local tetragonal axes are misaligned. The observed value for the exchange interaction parameter for the copper complex (G=4.3) suggests that the ligand forming complex is regarded as a weak field, and the local tetragonal axes are aligned parallel or slightly misaligned, and the unpaired electron is present in the $d_{x^2-y^2}$ orbital and the exchange coupling effects are not operative in the present copper complex.

F. Cyclic Voltammetry

The cyclic voltammograms of Cu complex (Fig.2) in DMSO exhibit two cathodic waves at -0.2V (E_{pc1}) and at -0.048 (E_{pc2}) followed by two anodic waves at -0.02 (E_{pa1}) and at 0.36 ($_{Epa2}$) found to be well behaved. The data shows well defined redox process (9) corresponding to the formation of Cu (III) → Cu (II) and Cu (II) → Cu (I) couple. Based on the spectral data the following structure given in Fig.1.have been proposed for the ligand and its complexes.

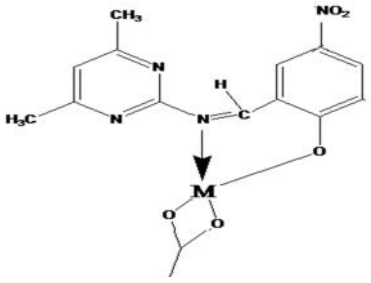

Figure 1: Structure of complexes where M = Cu(II),Co(II),Zn(II) and Ni(II)

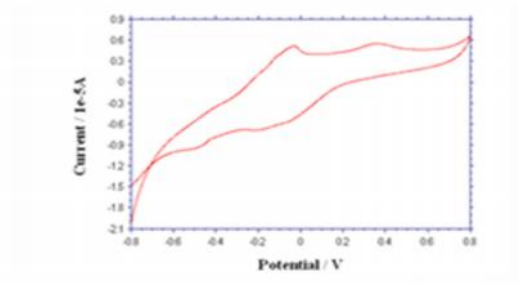

Figure 2. Cyclic Voltammatogram for [CuL(OAc)]

G. Antibacterial Activity

The newly synthesized pyrimidine derivatives were screened for antibacterial activity using Kirby Bauer method acteria like as *staphylococcus aureus, streptococcus pneumonia, staphylococcus pneumonia,* gram negative bactria like as *shigella flexneri, salmonella typhi, klebsiella pneumonia,* . Sparfloxacin was used as the standard. The results indicated mild antibacterial activity of

cobalt complex against *Bascillus subtilis* only. And also there was no antibacterial activity of other complexes in all other bacterium (10).

H. DNA Cleavage Study

The cleavage reaction was monitored by gel electrophoresis. The gel diagram is shown in the figure 3.The results indicated that there was no cleavage in the complexes (11).

I. DNA Binding study

DNA binding studies are important for the rational design and construction of new and more efficient drugs targeted to DNA. A variety of small molecules interact reversibly with double stranded DNA, primarily through three modes: (i) electrostatic interactions with negatively charged nucleic sugar–phosphate structure, which are along the external DNA double helix and do not posses selectivity; (ii) binding interaction with two grooves of DNA double helix and (iii) intercalation between the stacked base pairs of native DNA (12). Upon addition of CT-DNA, notable hypo chromic shift and hyper chromic shift were observed which is shown in Fig.4. The hypo chromic effect and hyper chromic effect, characteristic of intercalation has been attributed to the interaction between electronic states of the compound chromophores and those of DNA bases. Thus the spectroscopic changes suggested that the complexes had strong interaction with DNA.

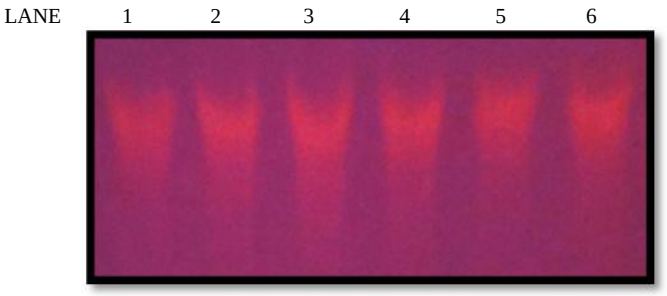

Figure 3.DNA Cleavage activity. LANE 1: DNA alone, LANE 2: DNA + Ligand, LANE 3: DNA+ [Cu(OAc)L] +H_2O_2, LANE 4: DNA + [Zn(OAc)L] + H_2O_2, LANE 5:DNA + [Co(OAc)L] + H_2O_2, LANE 6 : DNA +[Ni(OAc)L] + H_2O_2

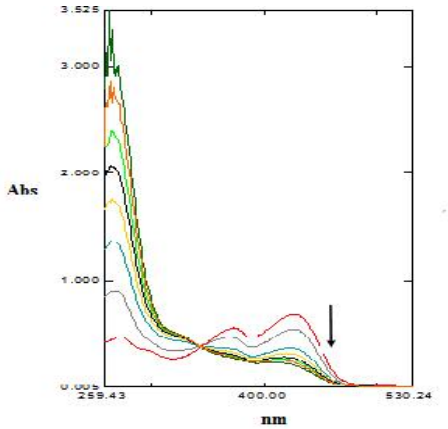

Figure 4 UV spectrum for [Cu(OAc)L] in the presence of CT-DNA

IV. CONCLUSION

A new pyrimidine based Schiff base ligand (L) was derived from the condensation of 5-nitrosalicylaldehyde and 2-amino 4, 6-dimethyl pyrimidine. The spectral data suggest that the ligand coordinates through N and O donor atoms and hence acts as bidentate site. The complexes were predicted to be square planar in structure. The spectroscopic changes that occur in the binding studies confirm that the complex had strong interaction with DNA.

ACKNOWLEDGMENT

The authors express their sincere and heartfelt thanks to the Managing Board, Principal, Mohammed Sathak Engineering College, Kilakarai for their constant encouragement and providing research facilities. The author also thanks the Department of Science and Technology (DST) - Science and Engineering Research Board (SERB), Government of India, New Delhi for financial support.

REFERENCES

[1] S.Gabriel, and Colman. J, Ber. Dtsch. Chem. Ges.,vol.32, pp.1536, 1899.
[2] C.O.Kappe, Tetrahedron, vol.49,pp. 6937-6963, 1993.
[3] M.Kidwai,S.Saxena,S.Rastogi, and R.Venkataramanan, Curr. Med.Chem.-Anti- Infect Agents,vol. 24,pp. 269-286, 2003.
[4] Y.Liu,Na.Wang,W.Mei,F.Chen,H.Li-Xin,L.Jian, and R.Wang,Transit.Met.Chem.,vol.32,pp.332-337,2007.
[5] A.B.J. Lever, and E. Mantovani, Inorg. Chem., 10, 1971.
[6] I. Georgieva, N. Tredafilova, and G. Bauer, Spectrochim. Acta A., Vol. 63 pp. 403–414, 2006.
[7] R.N.Patel,N.Singh,K.K.Shukla,U.K.Chauhan,J.Nicols Gutierrez, and A.Castineiras,Inorg.Chim.Acta.,vol.357pp. 2469-2476,2004.
[8] B.J.Hathaway, and A.A.G.Tomlinson, Coord.Chem.Rev.,vol.5pp.1-43,1970.
. Tangoulis, I. Turel, D.P. Kessissoglou, and G. Psomas, J. Inorg. Biochem., vol.105, pp. 476–489, 2011
vol.69,issue.12,pp.1555–623,2009.
etmer, J.R. Bocarsly, J. Am. Chem. Soc., Vol. 118, pp. 5339–5345, 1996.
3. Wu, C.X. Yin, P. Yang, J. Inorg. Biochem., vol. 101, pp. 10–18, 2007.

INTERNATIONAL JOURNAL OF INNOVATIVE RESEARCH & DEVELOPMENT

ISSN 2278 – 0211 (Online)

Synthesis, Characterisation and Application of Phenol-Formaldehyde Resin Blended with Sulphonated *Terminalia Bellerica,* Roxb. Charcoal

D. Ragavan
Department of Chemistry, Raja Durai Singam Government Atrs College, Sivagangai, India
A. Girija
Department of Chemistry, Mohamed Sathak Engineering College Kilakarai, India
B. Kathereen
Department of Chemistry, Government Arts College, Melur, Madurai, India
R. K. Seenivasan
Department of Chemistry, Government Arts College, Melur, Madurai, India

Abstract:
Phenol – Formaldehyde Resin (PFR) is the prepared base for cross linking agent for blending of Sulphonated Terminalia bellerica, Roxb., Charcoal (STBC). A few composite cation-exchangers were prepared by varying the amount of STBC (sulphonated carbon prepared from a source of cheap and renevable plant material) in the blends from 0 to 100% (w/w). Optimum principal reaction conditions for the preparation of blends were determined. All the important physico-chemical, thermal and spectral properties of the composites resins have been determined and analysed. The composites are insoluble in various organic solvents and reagents. The composites are thermally stable and stable towards various reagents. It was found that the ion-exchange capacity (IEC) of the composite resins, decreased with the increasing percentage of STBC in the blend. The thermodynamic equilibrium constants (ln K) are calculated for H^+ - Zn^{2+} ion exchanges on the resins having a various amount of STBC. Thermodynamic parameters are also computed and suitable explanations are given. The composites up to 30% (w/w) blending retains the essential properties of the original PFR, since the Terminalia bellerica, Roxb., is the low cost, freely available plant material. Therefore, the composites could be used as low cost ion-exchangers, when STBC partly replaces the original PFR up to 30% (w/w) blending without affecting the properties of PFR.

Key words*: Phenol – formaldehyde Resin – Sulphonated Terminalia bellerica. Roxb.Charcoal – Cation Exchange Capacity – Composite resins – Ion Exchangers –Equilibrium constants – Thermodynamic properties*

1. Introduction

Industrialised nations of the world are taking active measures to control the environmental pollution caused by chemicals. In the wastewater treatment, usually a decreasing level of pollutants is achieved rather than the selective removal and recovery. Ion exchange is an appropriate technique for removal and recovery, as it is employed in the separation and concentration of ionic materials from liquids [1].

Many ion exchangers owe their origin to petroleum products and there is a continual increase in their cost. Hence, there is an urgent need to find out the new low cost ion exchange resin (IERs) and reduce the cost of IERs by blending it with sulphonated carbons prepared from plant materials. Earlier studies show that the cheaper composite ion-exchangers could be prepared by partially blending the macro porous phenol-formaldehyde sulphonic acid resin matrix by sulphonated charcoals prepared from coal[2], Saw dust[3], Spent Coffee[4], Cashew nut husk[5], Wheat husk[6], Turmeric plant[7], Spent tea, Gum tree bark[8], *Accacia nilotica* [9] and *Egyptian bagasse pith* [10]. activated carbons obtained from agricultural wastes[11], *Terminalia chebula* Retz., Carbon[12] *Ashwagandha* ...on[13], *Eugenia jambolana*, Lam, Carbon[14], Heavy metals are also removed by bamboo activated ...ate nanoflowers and poly(Hydroxy ethyal methacrylate/Malemic acid) hydro gel[15-18]

...pare cheaper cationic resins from natural products. Ion-exchange process finds a valuable place in the ...lating and other industrial processes.

...resent work are to synthesise, characterise the new composite ion exchangers of PhOH – HCHO type ***...minalia bellerica***, Roxb**.,** charcoal (STBC) and estimate the column exchange capacity for some

selective metal ions, to study the selectively coefficients of H^+ - Zn^{2+} ion exchanges and to find out the optimum conditions for using cationic resins for the separation of Zn^{2+} from aqueous solution.

2. Materials and methods

2.1. Chemicals

The raw/plant material used was *Terminalia bellerica*, Roxb. This is a plant material freely available in Tamil Nadu, India. Phenol and formaldehyde used were of Fischer reagents (India). LR grade of con. sulphuric acid (Sp.gr.= 1.82) was used. The plant material was locally collected, cleaned, dried and cut into small pieces of about 0.5cm length. The other chemicals / reagents used were of chemically pure grade (AnalaR) procured from SD fine chemicals, India.

2.2. Methods

Terminalia bellerica, Roxb., (500g) was carbonised and sulphonated by con. sulphuric acid, washed to remove excess free acid and dried at 70^0C for 12 h. It was labeled as STBC.

Pure phenol – formaldehyde resin was prepared according to the literature method [3, 6 – 8]. It was then ground, washed with distilled water and finally with double distilled (DD) water to remove free acid, dried, sieved (210 – 300 μm) using Jayant sieves (India) and preserved for characterisation [3,6-8,19]. It was labeled as PFR.

The composites were obtained as per the method reported in literature [3, 6– 8].The products with 10, 20, 30, 40 and 50% (*w/w*) of STBC in the blend / composites, respectively were labeled as TB1, TB2, TB3, TB4 and TB5. A separate sample of STBC was also subjected to the characterisation studies.

2.3. Characterisation of samples

Samples were ground and sieved into a size of 210 – 300μm using Jayant sieves (India). This was used for further characterisation by using standard procedures [3, 7, 8,] to find out the values of absolute density, percentage of gravimetric swelling and percentage of attritional breaking. The solubility of these samples was tested by using various organic solvents and inorganic reagents.

The values of cation exchange capacity (CEC) were determined by using standard titration techniques [20] as per the literature method [21]. The effect of initial concentration of metal ions, particle size, chemical and thermal stability of the resins on CEC was determined [22].

After the exchange of H^+ ion by the metal ions, the regeneration level of the composites loaded with a metal ions were determined by using NaCl (brine) solution.

The equilibrium constants (K_{eq}) of ion exchange reaction between metal ions (Zn^{2+}) and the PFR and its composites were obtained as per the literature method [23,24].

The FT-IR spectral data of pure resin (PFR), 10% *(w/w)* composite and pure sulphonated *Terminalia bellerica*, Roxb., charcoal (STBC) were recorded with a JASCO FT-IR 460 plus FT-IR spectrometer by using KBr pellets. To establish the thermal degradation of the samples, TGA and DTA traces were obtained for phenol – formaldehyde resin (PFR) and 20% *(w/w)* composite resin by using TZSCH- Geratebau GmbH Thermal analysis.

3. Results and Discussion

The experimental and theoretical compositions of STBC in the composites

(TB1 – TB5) are in good agreement with each other. The results are similar to those obtained by Sharma *et al* [2]. This indicates that the preparative methods adopted for the synthesis of PFR and its composites (TB1 – TB5) are more reliable and reproducible.

The relationship between the various amounts of para-formaldehyde in the resin and the CEC reveal that the higher values of CEC are shown by the resins prepared with 15 – 25% (*w/w*) para-formaldehyde. However, these percentages are less chemically stable than the resins that contain 35% (*w/w*) para - formaldehyde. The CEC values decreased with the increased para-formaldehyde content in the matrix. The optimum value of para-formaldehyde and phenol are found to be 10ml and 11.5 ml, respectively.

The data given in Table 1 show that the values are absolute density are decreased from pure resin to highest percentage of composite resin and then finally to pure STBC.

The values of absolute density of composite resin in dry and wet forms depend upon the structure of resins and its degree of cross linking and ionic form [25]. Generally the absolute density decreased with increase in STBC content in the resin. The high value of absolute density indicates high degree of cross linking, and hence suitable for making columns for treating polar and non - polar effluent liquids of high density. The values of absolute densities for the different resins in the dehydrated states are higher than the hydrated states. Moreover, the values of wet and dry density are close to each other indicates that the pores of the sample may be macro porous in nature.

The data given in Table 1 indicate that the swelling percentage decreases from PFR (85.56%) to STBC (45.06%). The value of l with increasing STBC content. The values of swelling percentage are found to be 89.03%, 75.07% , 20 and 30% (*w/w*) of mixing of STBC compare with the parent resin, *viz*., PFR. This indicates that be mixed with the PFR. The rigidity of the resin matrix was thus concluded from the swelling e cationic resins with increasing STBC content showed lower swelling which revealed much lower

rigid shape, and the rigidity decreased with the increase in % of STBC. It indicates that, pure resin and composites are rigid with non - gel macro porous structure [19].

The values of attritional breaking (Table 1) increase with increase in STBC content (w/w) in the resins, representing the stability of the resin, which decreases from pure resin to STBC. Therefore, the mechanical stability is good upto 20 - 30% *(w/w)* substitution of STBC in pure resin. This observation also shows that, the capillaries of the resin may be occupied by the sulphonated carbon (STBC) particles [6-8].

The chemical stability of the samples in terms of its solubility in various solvents was determined. It reveals that PFR, composites and STBC are practically insoluble in almost all the solvents. Hence, they can be used as ion exchangers for treating non-aqueous effluents. At the same time, the samples were found to be partially soluble in 20% NaOH solution which indicate the presence of phenolic groups. Hence, these ion exchange materials cannot be used for the treatment of industrial effluents having high alkalinity (pH > 7). The insolubility of the samples even in the trichloroacetic acid expresses the rigidity *i.e.*, having high degree of cross-linking in them.

CEC data shown in Table 2 indicate that, the CEC values (for 0.1M solution of metal ions) decrease when the STBC % content *(w/w)* in PFR increases.The relative value of CEC of individual metal ions depends upon the atomic radius or atomic number [26]. At the same time the CEC also depends upon the anionic part of the metal salt. *i.e.,* inter ionic forces of attraction between anions and cations, which plays a vital role in cation exchange capacity of particular metal salt solution [23,24].

From the CEC data given in Table 2, the cation exchange capacity of the samples was found to decrease in the following order.

- **$Pb^{2+} > Zn^{2+} > Mg^{2+} > Ca^{2+} > Cu^{2+} > Fe^{2+} > Na^{+}$**

The selectivity order of metal ions *i.e.,* orders of CEC values also depends upon the ionic potential and the hydrated atomic radius of the metal ions in solution [24]. The order of exchange affinities of various metal ions is not unique to ion exchange system. Only under dilute conditions Hofmeister or lyotropic series [25] is obeyed. But, under high concentration it is different [25]. It is equally important to note that the relative behaviour of these ions for other ionic phenomena deviates the affinity order under the same conditions [27]. The observed order in the present study is different from that of the Hofmeister or lyotropic series [25]. This may be due to the concentration of the influent metal ion solutions, which is relatively high and also due to the selectivity of the metal ions.

Also, the CEC data given in the Fig.1 conclude that, upto 30% *(w/w)* blending of STBC with PFR retains 75.43 – 94.66% of CEC for all metal ions, except Cu^{2+} ion. Hence, 30% (*w/w*) blending of STBC in PFR reduces the cost of original resin. It is observed that there is a continuous decrease in cation exchange capacity (CEC), as the percentage of STBC content in the blend increases. Hence, any chemical methods requiring ion exchangers of small ion exchange capacity, 30% (*w/w*) blended STBC –PFR resin could be used. STBC can be inexpensively prepared from the plant materials, *Terminalia bellerica,* Roxb., which is freely available in plenty, in India.

The percentage values of CEC of the blends for exchange of H^{+} ions with Na^{+}, Fe^{2+}, Cu^{2+}, Ca^{2+}, Mg^{2+}, Zn^{2+} and Pb^{2+} ions in 0.1M solution are about 60-65% for TB1 – TB5 and nearly 60% as compared to that of the pure commercial resin (SD's; CEC = 100%). This indicates that the composites can partially replace commercial IERs in making the ion exchangers for industrial applications.

The values of cation exchange capacity (CEC) increase with increase in the concentration of Ca^{2+} ions. The equilibrium load of Ca^{2+} ions in unit mass of resin linearly increases with increasing the initial concentration of Ca^{2+} ions in solution from 0.025M to 0.15M [28]. Linear plots were obtained (not shown). The values of slope, intercept and correlation coefficient are given in Table 3. Beyond 0.15M there is a leveling effect of the value of CEC (*i.e.*, a constant CEC value) is noticed for all the metal ions at high concentrations above 0.15M of $CaCl_2$.

The effects of different reagents on the values of CEC of various cationic resins are shown in Table 4. On treatment with 0.2M NaOH 1.0 – 4.8% reduction in CEC value was noted. A higher decrease was observed for resin containing 50% of STBC. Upon treatment of resins with various organic solvents, the loss in CEC value was 1.4 - 3.5%.

The decrease in CEC value with boiling water was 0.9 – 4.4% according to the decreasing amount of STBC in the resin. Heating the resins for 10h at 100^{0} C caused a loss in the CEC between 8.0 – 19.1%. All these observations reveal that the composites have high thermal and chemical stability.

CEC data given in Table 5, described that the particle size of <200 μm are fine and > 500μm are coarse compared to a particle size of 300 - 500μm to cause very low ion exchange capacity. Hence, for the effective CEC, the bed size and particle size are be maintained and the recommended particle size is 300 – 500μm (mesh size is 0.2mm to 1.4mm)

The regeneration data with forty ml of 0.2M brine solution (NaCl) reveal that it effectively regenerates all composite resin and STBC (Fig.2). Most of the commercial IERs are in Na^{+} form and hence 40ml of 0.2M NaCl was used as a regenerant for every 2g of the resin.

The thermodynamic equilibrium constants (lnK) are given in Table 6 for the removal of Zn^{2+} ions using PFR and composites ($R\text{-}SO_3^{-}H^{+}$). It has been found that the equilibrium constant (K_{eq}) for the ion exchange reaction increased with the increase in temperature and decreased with the increase in the content of STBC (% *w/w*) in the resin. The standard values of thermodynamic parameters (ΔG^{0}, Δ nd also listed in Table 6. ΔG^{0} values range from – 403 to -1033 $J.mol^{-1}$ which indicate that the ion eous which is attributed due to the negative values of Gibbs free energy. The stability of system l with IERs. The ΔH^{0} values range from 2366 - 9462 $J.mol^{-1}$, which implied that the ion exchange queous solution of Zn^{2+} was endothermic. Similarly, it was found that the ΔS^{0} values range from 9.14 tes the increased randomness or disorderliness from STBC to PFR. This may be due to higher amount resin and therefore causing much more amount of H^{+} ions released into the solution. Hence, the

increased amount of H^+ ions in solution reflects the randomness (or) disorderliness *i.e.*, ΔS^0 values increases from PFR to STBC. Hence, PFR has higher CEC values and therefore has higher positive ΔS^0 value. The results are consistent with the earlier reports [10].
FT-IR studies are used to confirm the various stretching frequencies and to identify the ion exchangeable groups [29]. Fig.3a and b indicate the appearance of absorption band at 1039 – 1055 cm^{-1} (S = 0 str.) 1163 – 1193 cm^{-1} (SO_2 sym str) and 575 – 602 cm^{-1} (C – S str.) in pure resin (PFR), 10% composite resin and pure STBC confirm the presence of sulphonic acid group .
The appearance of broad absorption band at 3169 – 3409 cm^{-1} (bonded –OH str.) indicate the presence of phenolic and sulphonic – OH group in the samples. The appearance of absorption band at 1611 – 1624 cm^{-1} (C-C str.) confirms the presence of aromatic ring in PFR, 10% blending of STBC in PFR and pure STBC. The absorption band at 1447 – 1471 cm^{-1} (-CH_2.def.) confirms the presence of – CH_2 group in the samples. The weak absorption band at 888 – 902 cm^{-1} (-C-H def.) in the samples indicate that the phenols are tetra substituted.
Thermal gravimetric analysis (TGA) is used for rapidly assessing the thermal stability of various substances [30]. TGA curves shown in Figs.4a and b reveal that there is a very small (6%) loss in weight for both PFR and resin blended with 20% (*w/w*) STBC up to 80^0C. This is due to the loss of moisture absorbed by the pure resin and resin blended with 20% (*w/w*) STBC. Between 50 - 190^0C there, is 20% weight loss in PFR and 16% loss in weight in resin blended with 20% (*w/w*) STBC. Up to 450^0C, approximately 57% loss in weight in PFR and up to 530^0C, approximately 52% weight loss in resin blended with 20% (*w/w*) STBC was observed.
Two exothermic peaks were obtained in PFR, approximately at 80^0C and at 466^0C, respectively (Fig.4a). At 80^0C, the presence of broad peak was observed, due to the dehydration process of resin (PFR). A peak at 466^0C, indicates, the chemical changes of pure resin, which reflect approximately 57% weight loss in PFR.
DTA curves of 20% (*w/w*) STBC (Fig.4b) show that, the same two exothermic peaks were obtained at 80^0C and at 530^0C, respectively. Again the first broad peak indicates the dehydration of 20% (*w/w*) STBC and second moderate sharp peak indicates the chemical changes of 20% (*w/w*) STBC.
From Figs. 4a and b it is concluded that, the limiting temperature for the safer use of PFR, and resin blended with 20% (*w/w*) STBC as ion exchangers was 80^0C, since the resin degrade thermally after 80^0C.

4. Conclusion

It is concluded from the present study that PFR sample could be blended with 30% (*w/w*) of STBC, without affecting its physico-chemical, thermal properties. Also the effect of particle size and the concentration effect of Ca^{2+} ions on CEC, its regeneration level by using NaCl, spectral properties and the CEC values of various metal ions of resins blended with 30% (*w/w*) STBC were very close to the original PFR resin. Equilibrium constant for the removal of Zn^{2+} ion and thermodynamic parameters reveal that the process is spontaneous, endothermic and occur within randomness. Hence, blending of PFR with STBC will definitely lower the cost of IER.

Sample	% of STBC in PFR	Density (g mL^{-1})		% of Gravimetric swelling	% of attritional breaking
		Wet	Dry		
PFR	0	2.011	2.066	85.56	8.00
TB1	10	1.926	1.929	76.17	10.89
TB2	20	1.901	1.854	64.23	11.00
TB3	30	1.768	1.783	59.50	11.89
TB4	40	1.506	1.663	52.15	15.00
TB5	50	1.371	1.556	46.01	17.65
STBC	100	1.235	1.322	45.06	22.77

Table 1: Physico chemical properties of PFR and its composites prepared from Sulphonated Terminalia bellerica, Roxb., Charcoal

Sample	% of STBC in PFR	Cation exchange capacity (m.mol g^{-1})						
		Na^+	Fe^{2+}	Cu^{2+}	Ca^{2+}	Mg^{2+}	Zn^{2+}	Pb^{2+}
PFR	0	0.822	1.624	1.835	1.644	1.816	1.779	1.840
TB1	10	0.798	1.350	1.555	1.565	1.732	1.714	1.726
TB2	20	0.754	1.300	1.415	1.505	1.636	1.702	1.678
TB3	30	0.726	1.225	1.305	1.446	1.535	1.684	1.600
TB4	40	0.711	1.150	1.160	1.351	1.369	1.428	1.488
TB5	50	0.594	0.950	1.005	1.131	1.256	1.208	1.422
STBC	100	0.038	0.675	0.770	0.512	0.559	0.643	0.655

Table 2: Cation exchange capacities of H^+ form of the IERs

Sample	Correlation Co-efficient	Slope	Intercept
PFR	0.988	0.700	0.0125
TB1	0.903	0.362	0.0248
TB2	0.902	0.347	0.0245
TB3	0.919	0.352	0.0216
TB4	0.961	0.301	0.0204
TB5	0.949	0.310	0.0154
STBC	0.937	0.178	0.0069

Table 3: Correlation analysis on the concentration of Ca^{2+} ion by PFR, Composites and STBC

Reagents	Cation Exchange Capacity (m.mol. g^{-1})					
	PFR	TB1	TB2	TB3	TB4	TB5
Original Capacity	1.816	1.732	1.636	1.535	1.369	1.256
0.2M NaOH boiled for 1 h	1.798	1.700	1.599	1.509	1.313	1.196
Benzene boiled for 1h	1.762	1.708	1.609	1.514	1.309	1.212
Boiling water for 1h	1.800	1.720	1.618	1.516	1.333	1.201
Thermal treatment in hot air oven at 100^0C for 12h.	1.671	1.472	1.374	1.259	1.123	1.017

Table 4: Chemical and Thermal effect on CEC of PFR and its composites (by blending with STBC) Exchange with 0.1M Mg^{2+} ions at 303K

Sample	Particle Size μm	Cation exchange Capacity (m.mol g^{-1})			
		Na^+	Mg^{2+}	Ca^{2+}	Zn^{2+}
PFR	< 200	0.785	1.409	1.047	1.325
	200 – 300	0.822	1.816	1.644	1.779
	300 – 500	0.793	1.475	1.562	1.680
	> 500	0.780	1.350	1.432	1.651
TB2	< 200	0.689	1.033	1.257	1.513
	200 – 300	0.754	1.636	1.505	1.702
	300 – 500	0.737	1.183	1.483	1.542
	> 500	0.681	0.964	1.405	1.420

Table 5: Effect of particle size on cation exchange capacity of PFR and 20% (w/w) of STBC

Sample	ln K		$-\Delta G^0$ ($J.mol^{-1}$)	ΔH^0 ($J.mol^{-1}$)	ΔS^0 ($J.mol^{-1}K^{-1}$)
	303K	313K			
PFR	0.41	0.53	1033	9462	34.64
TB1	0.40	0.50	1008	7855	29.35
TB2	0.36	0.44	907	6308	23.81
TB3	0.30	0.37	756	5520	20.71
TB4	0.28	0.34	705	4731	17.94
TB5	0.24	0.29	605	3943	15.01
STBC	0.16	0.19	403	2366	9.14

Table 6: Thermodynamic equilibrium constant (in terms of lnK), at 303K, 313K and Standard Gibbs Free energy, Enthalpy and Entropy of H^+ / Zn^{2+} ion exchanges on various IERs at 303K

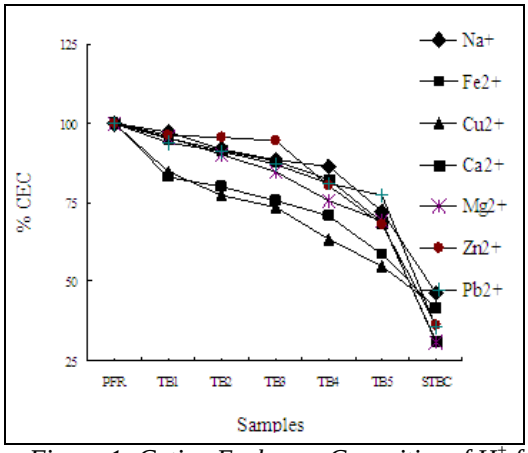

Figure 1: Cation Exchange Capacities of H^+ form of IERs, for Various Metal Ions Relative to PFR

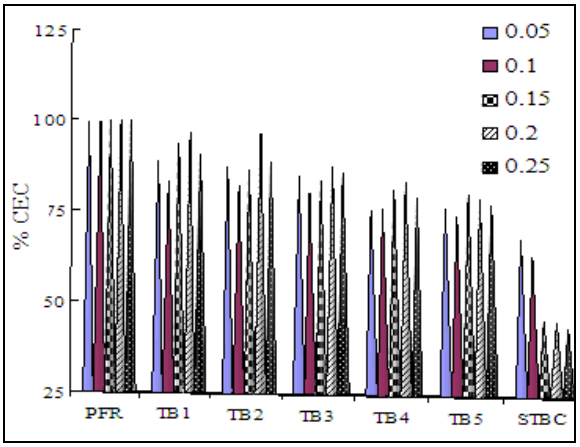

Figure 2: Regeneration level for PFR, its Composites and STBC by using NaCl after exchange with Mg^{2+} ions

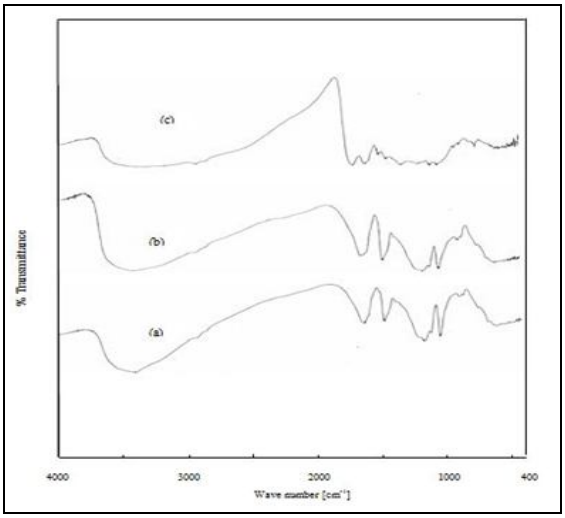

Figure 3: FT-IR Spectra of (a) PFR, (b) 10 % (W/W) STBC in composite and (c) Pure STBC

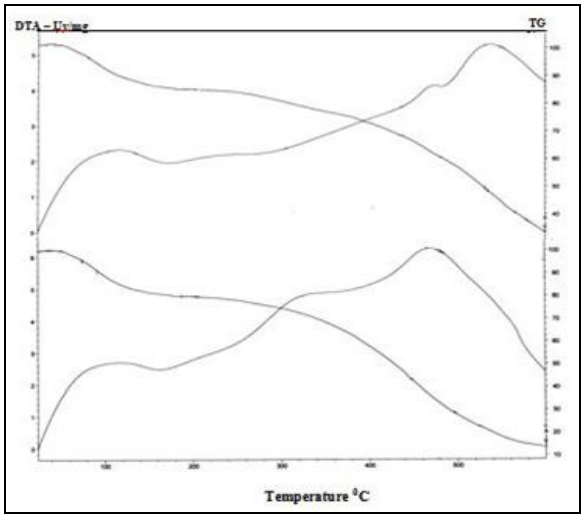

Figure 4: Thermal Studies of (a) PFR, (b) 20% (W/W) STBC in Composite

4. References

1. Bolto. B.A and Pawlowsk L., Waste Water Treatment by Ion-exchange, Oxford & IBH Publ. Co., New Delhi, 1987.
2. Sharma N.L.N., Joseph Mary and Padma Vasudevan. Res.Ind., 21, (1976) 173
3. Padma Vasudevan and Sarma. N.L.N. J.Appl. Poly.Sci., 23, (1979) 1443
4. Mohan Rao. G.J. and Pillai, S.C. J. Indian Inst .Sci., 36A, (1954) 70
5. Shahha and Batna. S.L. J. Appl. Chem. Lond., 8, (1953) 335
6. Dheiveesan. T., and Krishnamoorthy. S. J. Indian Chem.Soc.,65, (1988) 731
7. Kathiresapandian. D. and Krishnamoorthy. S. Indian. J. Technol.,29, (1991) 487
8. Mariamichel. A. and Krishnamoorthy. S. Asian J. Chem., 9(1), (1997) 136
9. Kannan .N. Seenivasan R.K., and Mayilmurugan. R. Indian J. Chem. Technol., 10,(2003) 623
10. Metwally M.S., Metwally. N.E and Samy. T.M. J. Appl. Poly. Sci., 52, (1994) 61
11. Kannan. N. Murugavel. S., Seenivasan R.K., and Rengasamy. G. Indian J. Env. Prot., 23 (12), (2003), pp. 1367 – 1376
12. Kannan. N.and Seenivasan. R.K. J. Appl. Poly. Sci. 101,4104
13. Kannan. N.and Seenivasan .R.K. J. Ion Exch.,16, 164 (2005)
14. Kannan.N.and Seenivasan .R.K. Desalivation.,216, 77 (2006)
15. Fong Lo. S, Wang. S.Y, Tsai. M.J and.Lin. L.D, Chemical Engg. Res. and Design, 90(9), 1397, (2012).
16. Jovanovic. M, Rajic. N and Obradovic. B. J. Haz.Mat., 233, 57, (2012).
17. Huang J., Cao Y., Liu Z. and.Deng Z, Chem.Engg. J., 80(15), 75, (2012).
18. Wu. N and Zale, Chem.Engg. J. 215, 894, (2013).
19. Natarajan. M and Krishnamoorthy. S. Res. Ind., 38, (1993) 278
20. Bassett. G.H, Jeffery.J, Mendham. J and Denney. R.C, Vogel's Text Book of Quantitative Chemical Analysis, 5th Edn. Longman Group Ltd., London, 1989.
21. Ramachandran. S and. Krishnamoorthy.S, Indian J. Technol., 22, (1984) 355
22. Chandrasekaran. M.B and Krishnamoorthy. S, J. Indian Chem. Soc., 64, (1987)134
23. Son.W.K, Kim. S.H and Park. S.G, Bull.Korean Chem...Soc., 22 (1), (2001) 53
24. Dimov. D.K, Petrova.E.B, Panayotov. I.M and Tsvetanov. Ch.B, Macromolecules, 21, (1990) 2733
25. Kunin.R, Ion Exchange Resin, Wiley, Newyork and London, 2nd Edition, (1958)
26. Mattson.S, Ann. Agric. Coll., Sweden, 10, (1942) 56
27. Bonner.O,. Easterling.G, Weit.D and Holland.V, J.Am.Chem.Soc., 77,(1955)
28. Kim.Y.K and Lee.K.J, J.Nucl. Sci. Tech., 38 (9), (2001) 785
29. Zagorodni.A.A, Kotova.D.L and. Selemenev.V.F, Reac. Func. Poly. 53, (2002)
30. Anderson.H.C, SPETrans., 1, (1962) 202

RJC

RASĀYAN *J. Chem.*
Vol. 6 | No.3 | 212-222| July- September | 2013
ISSN: 0974-1496 | e-ISSN: 0976-0083 | CODEN: RJCABP
http://www.rasayanjournal.com
http://www.rasayanjournal.co.in

SYNERGISM MODIFIED ION-EXCHANGE PROCESS OF SELECTIVE METAL IONS AND ITS BINARY MIXTURES BY USING LOW COST ION EXCHANGE RESIN AND ITS BINARY MIXTURE

A.Girija[1] and R.K.Seenivasan[2,*]
[1]Department of Chemistry, Mohamed Sathak Engineering College, Kilakarai-623517 (TN), India
[2]Department of Chemistry, Government Arts College, Melur-625106 (TN), India
*E mail: rksvasan@rediffmail.com

ABSTRACT

A few composite ion exchangers were prepared by blending sulphonated carbons (SCs) prepared from plant materials, such as *Phyllanthus emblica,* Linn.(PE), *Eugenia jambolana*, Lam.(EJ), *Terminalia chebula*, Retz. (TC) *Terminalia bellarica*, Roxb. (TB) and *Achyranthes aspere*, Linn.(AA),blended with phenol-formaldehyde resin (PFR) in different weight ratios (from 0 to 50% *w/w*). These, SCs were partially blended into the polymeric matrix of Phenol-Formaldehyde sulphonic acid, which could be used as new cheap/low cost ion exchangers (IERs) for the removal of some selective metal ions.. CEC of selective single metal ions (Cu^{2+}, Zn^{2+}, Pb^{2+} and Ca^{2+}) and binary mixture metal ions such as (Zn^{2+} + Cu^{2+} and Pb^{2+}+ Ca^{2+}) and were determined for using PFR, composite resin with different *%(w/w)* of SCs and 100% SC. Binary mixture of resins(R_1 and R_2) were prepared by mixing of two low cost IERs obtained by blending PFR with 20% SC(prepared from plant materials PE,TB, and AA) which possess high and low CEC value. CEC of selective single and binary metal ions for the binary mixture of resins (R_1 and R_2) was determined. It shows that composites/low cost IERs up to blending PFR with 20% (*w/w*) SC, retains the CEC of the original PFR. CEC values were theoretically calculated using linear or additive (ideal) behaviour and found to be less than that of the observed values of CEC for all the ion exchange systems. This may be due to synergism modified ion exchange process.

Keywords: Cation Exchange Capacity – Composites – Single and Binary mixture of metal ions - Low cost Ion Exchangers – phenol – formaldehyde resin- Binary mixture of resins.

INTRODUCTION

The discovery of ion exchange dates from the middle of the nineteenth century when Thomson and Way noticed that ammonium sulphate was transformed into calcium sulphate after percolation through a tube filled with soil[1, 2]. In 1935, Liebknecht and Smith discovered that certain types of coal could be sulphonated to give a chemically and mechanically stable cation exchanger[3,4]. In addition Adams and Holmes produced the first synthetic cation exchangers by poly condensation of phenol with formaldehyde[5].

Since, the modern commercial ion exchangers owe their origin to the products of petroleum; there is a phenomenal increase in the cost of these ion exchangers. Hence, there is an urgent need of the hour either to find out entirely new resins which are cheaper than the existing ones or to prepare composite ion exchangers by partly replacing the polymeric content of the current ion exchangers to a considerable extent by blending it with the sulphonated carbons (SCs) prepared from plant materials while the important characteristics of the parent resins are being retained. The composite could be very efficient, if the substitute it-self could act as an ion exchange. Earlier studies showed that the cheaper composite ion-exchangers (IERs) could be used to remove heavy metal ions from solutions and prepared by partially blending the macro porous phenol-formaldehyde sulphonic acid resin (PFR) matrix by blending it with carbons obtained from coal, saw dust, spent Coffee, cashew nut husk, wheat husk, turmeric plant, spent *ccacia nilotica* and Egyptian bagasse pith[6-14]. Heavy metals are also removed by

bamboo activated carbon, natural clinptitolite, titanate nanoflowers and poly(Hydroxy ethyal methacrylate/Malemic acid) hydro gel[15-18]

The present work deals with the synthesis, characterization and CEC values of single metal ions (Cu^{2+}, Zn^{2+}, Pb^{2+} and Ca^{2+}) and binary mixture of metal ions (Cu^{2+}+ $Zn^{2+}$and Pb^{2+}+Ca^{2+}) of new low cost IERs obtained by blending PFR with various % by weight of SCs prepared from plant materials such as *Phyllanthus emblica,* Linn.(PE), *Eugenia jambolana*, Lam.(EJ), *Terminalia chebula*, Retz. (TC),*Terminalia bellarica*, Roxb. (TB) and *Achyranthes aspere*, Linn.(AA). Also binary mixture of resins were prepared by mixing two low cost IERs obtained by blending PFR with 20% SC (prepared from the plant materials PE,TB and AA) which possess high and low CEC values. CEC values of these binary mixtures of resin for single and binary mixture of metal ions were also obtained. Synergism modified ion exchange process is reported in this paper for the low cost IERs and binary mixture of these IERs.

EXPERIMENTAL

Materials

Phenol and formaldehyde used were of Fischer reagents (India). LR grade of con. Sulphuric acid (Sp.gr. = 1.82) was used. Sulphonated carbon (SC) obtained from plant materials *viz*., *Phyllanthus emblica,* Linn.,(PE), *Eugenia jambolana*, Lam.,(EJ), *Terminalia chebula*, Retz.,(TC), *Terminalia bellarica*, Roxb.,(TB) and *Achyranthes aspere*, Linn.,(AA), which were the locally available plants in southern part of India, especially in Tamil Nadu. These plant materials were cleaned, dried and cut into small pieces of about 0.5cm length.

Preparation of Sulphonated Carbons (SC)

About 500g plant materials were carbonized and sulphonated by con. Sulphuric acid (500mL) and kept at room temperature (30 ± 1^0C) for 24 h and heated at 90^0C in a hot air-oven for 6 hours. It was then cooled, washed with distilled water several times and finally with double distilled (DD) water in order to remove excess free acid and dried at 70^0C for 12 h. They were labeled as SPEC,(Sulphonated *Phyllanthus emblica* Linn., Carbon) SEJC (Sulphonated *Eugenia jambolana* Lam.,Carbon), STCC *(*Sulphonated *Terminalia chebula* Retz.,Carbon), STBC(Sulphonated *Terminalia bellarica* Roxb.,Carbon) and SAAC (Sulphonated *Achyranthes aspere* Linn.,Carbon*)*, respectively for the SCs prepared from the plant materials PE, EJ, TC, TB and AA.

Preparation of Pure Phenol- Formaldehyde Resin (PFR)

Con. Sulphuric acid (12.5mL) was slowly added to phenol (10mL) in drop wise with constant stirring by placing it in an ice-bath at 0 – 5^0C. The mixture was heated at 70^0C for 3 h in a hot air -oven, then cooled immediately in an ice bath and kept over-night. It was then polymerized with formaldehyde solution (11.5mL) at 80^0C and the product was cured in a hot air-oven for 3 h. A brown colored chunky solid mass was obtained. It was then ground, washed with distilled water and finally with double distilled (DD) water to remove excess free acid, dried, sieved (210µm – 300µm size) using Jayant Sieves (India) and preserved for characterisation[19-22]. It was labeled as PFR.

Preparation of Low- Cost Ion-Exchange Resins (IERs)

A known amount of phenol (10 mL) was sulphonated with con. sulphuric acid (12.5 mL) to produce phenol sulphonic acid. Then, it was blended with various percentage by weight *(w/w)* of sulphonated carbons (SCs) obtained from various plant material (PE, EJ, TC, TB and AA) in the blend as 10, 20, 30, 40 and 50,%(*w/w*) respectively. In order to fix the composition of SC as 10, 20, 30, 40 and 50 % (*w/w*) in the composites the following formula was used [7, 10-12, 19]-

$$\text{Required percentage} = b / (a + b) \quad (1)$$

Where, a = mass of PFR (in g); b = mass of the SC required (in g)

Each mixture was polymerized with formaldehyde solution (11.5mL) at 80^0C and the product was cured in a hot air –oven for 3 h. A brown chunky solid mass was obtained which was ground, washed, dried and preserved for characterization. The product with 10, 20, 30, 40 and 50% (*w/w*) of SCs (obtained from various plant materials) in the blend / composite, respectively were labeled as A, B, C, D and E for each composite, Physico –chemical parameters of PFR, composites and (100%) SC were determined as per the literature methods[23-26]**.** The percentage of SC in the resin calculated in terms of weight of materials used and their actual percentage in the yields are given in Table-1.

Cation Exchange Capacity of Low-cost IERs

A known weight (2g) of the low cost composite/ IER samples were converted into H^+ form by washing it with 2M HCl acid, and washed with distilled water and finally rinsed with DD water in order to remove excess free acid (tested with $AgNO_3$). The test column was prepared by using graduated burette, glass – wool plug and the slurry of treated resin sample. Forty ml of 0.1M solutions of single metal ions (Cu^{2+} , Zn^{2+} , Pb^{2+} and Ca^{2+}) and binary mixture of metal ions (Cu^{2+} + Zn^{2+} and Pb^{2+} + Ca^{2+}) were used as influents. The rate of flow of effluent was adjusted to 1mL min^{-1}. The low-cost IER samples exchanged its H^+ ion to the corresponding metal ions. The total amount of cation exchanged was determined by using the standard titration techniques[24]. The values of cation exchange capacity (CEC) were determined as per the literature method[25-27]. The CEC value of single metal ions and binary mixture of metal ions for various low-cost IERs / composites resins were shown in Figs. 1-5. The theoretical total cation exchange capacity (CEC) for various low -cost IERs for the binary mixture of metal ions from the CEC value of individual metal ions is calculated as follows:

$$\text{Theoretical total CEC of binary Mixture of metal ions} = \frac{1}{2}\left\{\text{Sum of CEC of individual metal ions}\right] \quad (2)$$

Preparation of Binary Mixture of Resin

Based on the results obtained from Figs. 1-5, the CEC value of single metal ion and binary mixture of metal ions by using low-cost IERs was found to be unaffected up to 20% (w/w) blending of SCs obtained from various plant materials with PFR. Therefore in the present study the binary mixture of resins (R_1) were obtained by mixing of the composite resin/IER prepared by blending PFR with 20% (*w/w*) SPEC (X) having high CEC value with the IER obtained by blending PFR with 20% (*w/w*) SAAC (Y) having least CEC value in five different weight proportion ratio (% *w/w*) 100, 75, 50 , 25 and 0 %.These resins were labeled as X, XY1, XY2, XY3 and Y, respectively (Table 2). Similarly, another binary mixture of resins (R_2) were obtained by mixing the composite resin/IER prepared by blending PFR with 20% (*w/w*) STBC (Z) having highest CEC value with the composite resin/IER prepared by blending PFR with 20% (*w/w*) SAAC (Y) having least CEC value in five different weight proportion ratio (% *w/w*) 100, 75, 50 , 25 and 0 % and were labeled as Z, ZY1, ZY2, ZY3 and Y, respectively (Table-2).

CEC of Binary Mixture of Resin

CEC values of various selected single metal ions and binary mixture of metal ions were determined by using these two binary mixture of resins (R_1 andR_2) prepared as given in Table 2.The theoretical CEC value of binary mixture of resins for both single and binary mixture of metal ions is calculated from CEC value of the 100 % pure resin (*i.e.*, Y and Z) as follows:

$$\text{CEC value of binary mixture of Resin} = 1/100\ (C_1 P_1 + C_2 P_2) \quad (3)$$

Where,

C_1 = CEC of (100%) pure low cost IER 'X' or 'Z'

C_2 = CEC of(100%) pure low cost IER 'Y'

P_1 = weight of low cost IER 'X' or 'Z' in the binary mixture of resin

P_2 = Percentage by weight of low cost IER 'Y' in the binary mixture of resin

RESULTS AND DISCUSSION

The data given in Table-1 show that, the experimental and theoretical compositions of SC in the composites (A - E) are in good agreement with each other. The results are similar to those obtained by Sharma *et al* [6]. This indicates that the experimental methods adopted for the synthesis of PFR and its composites (A - E) are more reliable and reproducible.

Table-1: Amount of reagents used and yields of the PFR and IERs prepared by blending PFR with SCs obtained from various plant materials[+]

Low cost IERs	% of SC in PFR Theoretical	Amount of Reagents used				Yield* (g)	% of SC in PFR Experimental*
		Phenol (mL)	HCHO (mL)	Con.H_2SO_4 (mL)	SC (g)		
PFR	0	10.0	11.5	12.5	0.00	17.00	0.00
A	10	10.0	11.5	12.5	1.89	18.64 - 18.93	9.98 – 10.13
B	20	10.0	11.5	12.5	4.25	20.68 – 21.63	19.65 – 20.55
C	30	10.0	11.5	12.5	7.29	23.83 – 24.63	29.58 – 30.57
D	40	10.0	11.5	12.5	11.33	27.85 – 28.40	39.91 – 40.69
E	50	10.0	11.5	12.5	17.00	33.64 – 34.28	45.59 – 50.54
SC	100	--	--	--	--	--	100

* Range for various plant materials ([+]PE, EJ, TC, TB and AA)

Physico – Chemical Characteristics

The absolute density (Table-3) values in both hydrated (wet) and dehydrated (dry) states decrease steadily from pure resin to 50% (*w/w*) SC in composite resins and then finally to pure SC(100%). This indicates that PFR and the composites/low cost IERs (A – E) are more closely packed[7 - 14]. It is found that the values of absolute density of 100% SCs prepared from various plants are 41.77 – 61.16% and 47.92 – 63.89% compared to that of density of PFR in hydrated (wet) and dehydrated (dry) states, respectively. This indicates that SCs also have closely packed structure[19, 23].

The value of density of composite resins in dry and wet form depends upon the structure of the resin, its degree of cross linking and ionic form[28-30]. Hence, the high density values are obtained for the low cost IERs /composite resins. Moreover, the wet and dry density values are close to each other, which indicate that the samples may be macro porous in nature[31]. From the data given in Table-3, it is clear that there is no considerable decrease or change in absolute density in both in hydrated (wet) and dehydrated (dry) states up to 20% (*w/w*) blending of PFR with SC in the low-cost IERs compared to that of PFR. This indicates that they also have similar closely packed structures with high degree of cross-linking and hence could become suitable for making ion exchange columns for effluents of high density[23-27].

It is observed that, the % of gravimetric swelling of pure resin (PFR) is higher than that of the other samples (Table-3). Therefore, it indicates that the porosity and polarity are greater in the PFR. The composite resin, in which 50% *(w/w)* blends with SC (sample E) has a gravimetric swelling capacity of 36.35 – 45.06% as compared to that of PFR. This extremely low value of % gravimetric swelling may be due to certain rigidity in their matrix and therefore the pores of the composites are of non-gel type and macro reticular[19]. The decrease in % gravimetric swelling value with % of SC in the blend is attributed due to the loss of polarity and porosity in the composites. Thus, the composites may prove to be highly useful where they are required to withstand a large osmotic shock[23].

The values of % attritional breaking presented in Table 3 also represent the stability of the resin, which decrease from PFR to SC (100%). Therefore, the mechanical stability is good up to 20% *(w/w)* blending of SC with PFR. This observation also shows the possibility of formation of resin in the capillaries of the sulphonated carbon (SC) particles[10-12].

CEC of Single Low-Cost Ion Exchange Resin

The values of Cation exchange capacity (CEC) of 0.1 M solution of single metal ions (Cu^{2+}, Zn^{2+}, Pb^{2+} and Ca^{2+} ions) and binary metal ions (Cu^{2+}+ $Zn^{2+}$and Pb^{2+} + Ca^{2+} ions) were determined by using single low cost IERs are shown in Figs. 1-5. The data indicate that, the CEC value decreases, when the percentage of SC *(w/w)* in PFR increases (*i.e.* from A to E) for various low-cost IERs. CEC of individual metal ions depends upon the atomic radius or atomic number[30-33]. At the same time the CEC value also depends upon the inter ionic forces of attraction between anions and cations of the metal salt solutions, valance of the metal ion and concentration of influent[31,33]. From figures 1 –5, it is observed that the CEC value of Cu^{2+} is higher than Zn^{2+} ions in the binary mixture of solutions of 0.1M metal ions (Copper + Zinc ions) used as influent. Similarly, the CEC value of Pb^{2+} ion is higher than Ca^{2+} ions in the binary mixture of solution of 0.1M metal ions (Lead + Calcium) used as influents. The relative affinities of these cations depend upon their size, mobility, ability to diffuse inside the resin matrix and resin selectivity[34]. Kunnin has found that the CEC value decreases as the ionic size of the cations increases. Kressman, Kitchener and Gregor *et al*. have found that the rate of diffusion of large size ions into and through ion exchange resin precede very slowly[25, 26]. Figs.1–5 also indicate that Cu^{2+} and Pb^{2+} ions are preferentially removed by ion exchange to a greater extent compared to Zn^{2+} and Ca^{2+}ions, respectively from aqueous solution of binary mixture of metal ions.

Table-2: Weight proportion of Single low-cost IERs (PFR blended with 20 %(*w/w*) SCs) of Binary mixture of resins (R_1 and R_2)

Binary Mixture of Resin R_1	% Weight Ratio		Binary Mixture of Resin R_2	% Weight Ratio	
	X	Y		Z	Y
X	100	0	Z	100	0
XY1	75	25	ZY1	75	25
XY2	50	50	ZY2	50	50
XY3	25	75	ZY3	25	75
Y	0	100	Y	0	100

* SC obtained from plant materials PE (X), AA(Y) and TB (Z)

Table-3: Physico-chemical properties of PFR and IERs prepared by blending PFR with SCs obtained from various plant materials[+]

Low cost IERs	% of SC in PFR	Density (g mL^{-1})*		% of Gravimetric swelling*	% of attritional breaking*
		Wet	Dry		
PFR	0	2.01	2.066	85.56	8.00
A	10	1.62 – 1.93	1.35 – 1.94	72.16 – 78.11	8.91 – 20.00
B	20	1.21 – 1.90	1.29 – 1.92	63.00 – 72.66	9.00 – 23.53
C	30	1.05 – 1.77	1.20 – 1.83	56.15 – 68.23	11.58 – 27.45
D	40	1.00 – 1.51	1.17 – 1.71	50.24 – 57.45	13.63 – 28.43
E	50	0.98 – 1.37	0.99 – 1.56	40.48 – 52.99	16.83 – 29.00
SC	100	0.84 – 1.23	0.99 – 1.32	36.35 – 45.06	21.78 – 51.49

* Range for various plant materials ([+]PE, EJ, TC, TB and AA)

Table-4: Observed and Theoretical total cation exchange capacity of Copper and Zinc metal ions for various single low-cost IERs prepared from various SCs

SCs	Total CEC of Binary Mixture of 0.1M metal (Cu^{2+} +Zn^{2+}) ions (m.mol.g^{-1})						
	PFR	A	B	C	D	E	SC
SPEC	1.923 (1.807)*	1.720 (1.611)	1.531 (1.478)	1.462 (1.433)	1.371 (1.355)	1.293 (1.272)	0.768 (0.761)
	)23	1.632	1.521	1.398	1.323	1.284	0.721

	(1.807)	(1.550)	(1.486)	(1.369)	(1.304)	(1.257)	(0.600)
STCC	1.923 (1.807)	1.636 (1.570)	1.514 (1.444)	1.412 (1.350)	1.333 (1.277)	1.189 (1.095)	0.779 (0.759)
STBC	1.923 (1.807)	1.712 (1.635)	1.629 (1.559)	1.531 (1.495)	1.318 (1.294)	1.210 (1.107)	0.815 (0.707)
SAAC	1.923 (1.807)	1.532 (1.457)	1.418 (1.343)	1.296 (0.231)	1.185 (1.170)	1.125 (1.116)	0.731 (0.628)

* Values in parentheses are theoretical total CEC obtained by using eqn. 2.

Also the CEC values of single and binary mixture of metal ion solutions (Figs.1-5) by using single low-cost IERs vary by varying the SC prepared from different plant materials. For binary mixture of metal ions, CEC value is high for the low IER prepared from blending of PFR with 20% SC obtained from the plant material *Phyllanthus emblica*, Linn.,(PE) and *Terminalia bellerica.* Roxb.,(TB) compared to other plant materials and CEC value is low for the low-cost IER prepared by blending of PFR with 20% SC obtained from the plant material AA.
Figs.1–5, also indicate that CEC value of the single IER samples (A – E) obtained from various SCs, for single metal ions was found to decrease in the following order-

STBC > SPEC > SEJC > STCC > SAAC

Similarly, for CEC value of binary mixture of metal ions containing Copper and Zinc ions by using single low cost IERs obtained from various SCs, was found to decrease the following order:

SEJC > SPEC > STBC > STCC > SAAC.

CEC value of samples for binary mixture of metal ion containing Lead and Calcium ions by using single IERs obtained from various SCs was found to be decrease in the following order:

STBC > SPEC > SEJC > STCC > SAAC

Many attempts have been made to explain the difference in the ion exchange behavior of the various cations[36, 37]. The order of ion exchange affinities for the various cations is not unique in ion exchange systems [29].

Synergistic Effect in Single Low-Cost IER

Table-4 and 5 show that, the observed total cation exchange capacity (total CEC) of both binary mixture of metal ions (Cu^{2+}+ $Zn^{2+}$and Pb^{2+} + Ca^{2+}) in a single low cost IER are always, greater than that of the theoretically calculated values (using equation 2). The total CEC for all the IERs prepared from blending of PFR with various SCs such as SPEC, SEJC, STCC, STBC and SAAC.
The predicted / theoretical value (by using eqn.2)of the CEC of the single and binary mixture of metal ions by single low-cost IERs by varying the percentage by weight of SC in the composite are also given in parenthesis (Tables 4 and 5).The actually observed total values of CEC for both single and binary mixture of metal ions for the single low-cost IERs (PFR, A,B,C,D,E and SC) for various percentage by weight of SC in the composite are found to be greater than that of the CEC values predicted/theoretical value by the linear equation (eqn.2). This indicate that this may be due to the synergistic effect[38,-40]. Since $CEC_{obs} > CEC_{cal}$ the process of metal ions exchange may be due to Synergism modified ion exchange.

CEC of Binary Mixtures of Resin

Table-6 show that the CEC values of binary mixture of resins for all the metal ions in single and binary mixture decrease from the pure resin sample X[PFR blended with 20% (*w/w*) SPEC] to pure Y [PFR blended with 20% *(w/w)* SAAC]. It is observed that by mixing of these two single low-cost IERs - X and

Y (resin R_1) in equal proportions (sample XY2) retains approximately 95.8 – 99.2% of CEC values for the metal ions *viz.*, Cu^{2+}, Zn^{2+}, Pb^{2+} and Ca^{2+} ions and approximately 94.9 – 97.7% of CEC value for the binary mixture of metal ions Cu^{2+} +$Zn^{2+}$and Pb^{2+} + Ca^{2+} compared to that of the pure resin X (100%). Hence, for the removal of metal ions from the single and binary mixture of metal ions in aqueous solution, binary mixture of resin X and Y in equal weight proportion (50:50%)– sample: XY2 could be used as a low- cost ion exchange material.

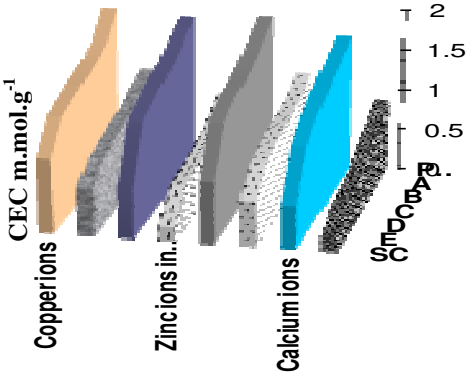

Fig.-1: CEC values of various IERs obtained from *Phyllanthus emblica*, Linn. Carbon for single and binary mixture of metal ions.

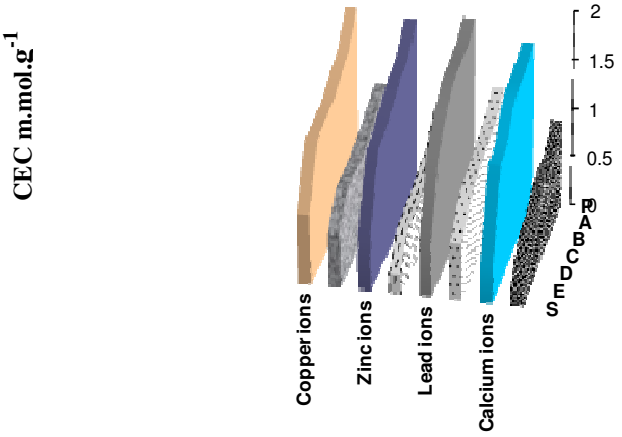

Fig.-2: CEC values of various IERs obtained from *Eugenia jambolana,* Lam. Carbon for single metal ions and its binary mixture of metal ions.

Table-5: Observed and Theoretical total cation exchange capacity of Lead and Calcium metal ions for various single low-cost IERs prepared from various SCs

SCs	Total CEC of Binary Mixture of 0.1M metal (Pb^{2+} +Ca^{2+}) ions (m.mol.g^{-1})						
	PFR	A	B	C	D	E	SC
SPEC	2.024 (1.742)*	1.759 (1.642)	1.446 (1.435)	1.446 (1.435)	1.352 (1.344)	1.267 (1.207)	0.773 (0.652)
SEJC	2.024 (1.742)	1.678 (1.657)	1.642 (1.632)	1.600 (1.592)	1.432 (1.385)	1.314 (1.235)	0.714 (0.464)
STCC	2.024 (1.742	1.703 (1.625)	1.619 (1.574)	1.512 (1.411)	1.428 (1.339)	1.366 (1.312)	0.929 (0.681)

STBC	2.024 (1.742	1.844 (1.646)	1.785 (1.592)	1.595 (1.523)	1.547 (1.420)	1.404 (1.277)	0.868 (0.584)
SAAC	2.024 (1.742)	1.547 (1.512)	1.495 (1.352)	1.321 (1.280)	1.202 (1.116)	1.077 (0.993)	0.762 (0.623)

* Values in parentheses are theoretical total CEC obtained by using eqn. 2.

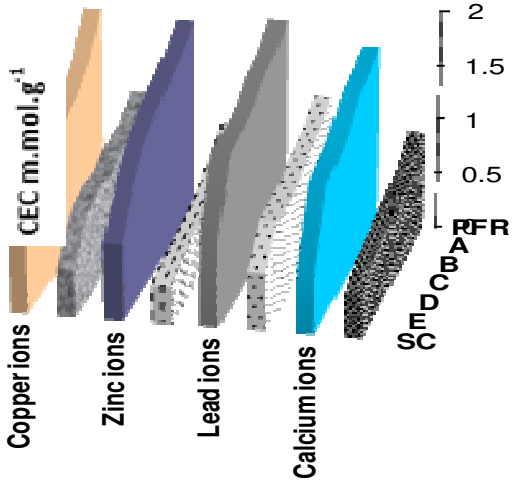

Fig.-3: CEC values of various IERs obtained from *Terminalia chebula*, Retz. Carbon for single and binary mixture of metal ions

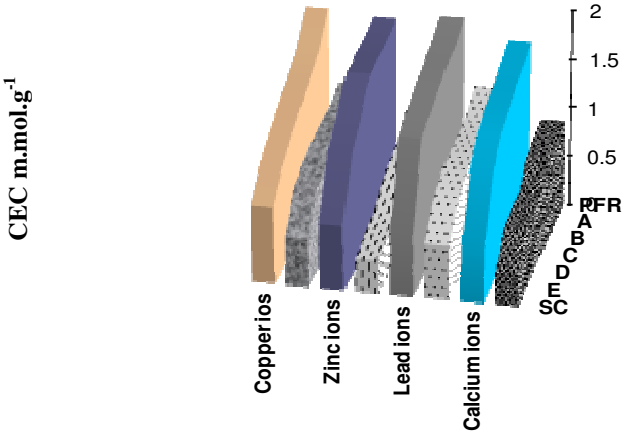

Fig.-4: CEC values of various IERs obtained from *Terminalia bellerica*, Roxb. Carbon for single and binary mixture of metal ions

Table-6: CEC of single and binary mixture of metal ions for binary mixture of resin, R_1

R_1	Cation Exchange Capacity (m.mol g^{-1})							
	Single Metal Ions				Binary Metal Ions Solution			
					0.1M [Cu^{2+} + Zn^{2+}]		0.1M [Pb^{2+} + Ca^{2+}]	
	Cu^{2+}	Zn^{2+}	Pb^{2+}	Ca^{2+}	Cu^{2+}	Zn^{2+}	Pb^{2+}	Ca^{2+}

X	1.445	1.511	1.583	1.458	0.832	0.691	0.993	0.623
XY1	1.441 (1.429)*	1.483 (1.459)	1.551 (1.539)	1.442 (1.418)	0.826 (0.818)	0.678 (0.673)	0.965 (0.956)	0.615 (0.608)
XY2	1.434 (1.413)	1.447 (1.408)	1.536 (1.494)	1.405 (1.378)	0.813 (0.804)	0.667 (0.654)	0.942 (0.919)	0.608 (0.594)
XY3	1.401 (1.397)	1.414 (1.356)	1.491 (1.450)	1.366 (1.338)	0.802 (0.79)	0.644 (0.636)	0.922 (0.881)	0.595 (0.579)
Y	1.382	1.304	1.405	1.298	0.776	0.617	0.843	0.564

* Values in parentheses are theoretical total CEC obtained by using eqn. 3.

Table-7 show that the CEC values of binary mixture of resins for all the metal ions in single and binary mixture decrease from the pure resin sample Z [PFR blended with 20% (*w/w*) STBC] to pure Y [PFR blended with 20% (*w/w)* SAAC]. It is observed that by mixing of these two single low-cost IERs - Z and Y (resin R_2) in equal proportions (sample : ZY2) retains approximately 93.0–99.65% of CEC values for the metal ions *viz.*, Cu^{2+}, Zn^{2+}, Pb^{2+} and Ca^{2+} ions and approximately 90.8 – 96.1% of CEC value for the binary mixture of metal ions Cu^{2+} +$Zn^{2+}$and Pb^{2+} + Ca^{2+} compared to that of the pure resin Z (100%).Therefore, for the removal of metal ions from the single and binary mixture of metal ions in aqueous solution, mixture of resin Z and resin Y in equal weight proportion (50:50%) – sample : ZY2 could be used as a low-cost ion exchange material.

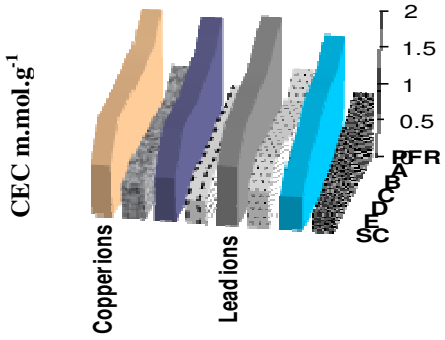

Fig.-5: CEC values of various IERs obtained from *Achyranthes aspera*, Linn. Carbon for single and binary mixture of metal ions

Synergim modified ion exchange process

The experimentally observed values of CEC are also given in Tables 6 and 7 along with the theoretically calculated values of CEC (using eqn.3). The predicted/ theoretical values of CEC of binary mixture resins (R_1 and R_2)for both single metal ions (Cu^{2+} , Zn^{2+}, Pb^{2+} and Ca^{2+} ions) and binary mixture of metal ions (Cu^{2+} + Zn^{2+}; and Pb^{2+} + Ca^{2+} ions) were calculated by using the linear equation (eqn.3). The observed values of CEC (Table. 6) of the single and binary mixture of metal ions by using the binary mixture of resins are found to be greater than that of the theoretically calculated values obtained by using eqn.3. If calculated and observed CEC values are equal, then it indicates that the linear or additive (ideal) behaviour of ion exchange process exists. The observation.$CEC_{obs.} > CEC_{cal}$ indicate that the linear or additive(ideal) behaviour(eqn.3) of ion exchange process is not applicable for mixed resin (binary mixture of resin *viz.,* R_1 and R_2).A similar behaviour on adsorption capacity of mixed adsorbents was noticed and reported earlier in literature[38,41]. The high observed value of CEC, than that of the theoretical value, may be due to the non-ideal (non – linear) and non – additive cation exchange process of the mixed resins (binary mixture of resins R_1 and R_2). This may be probably due to synergistic effect of the mixture of (mixed) resins. The phenomenon may be termed as 'synergism – modified ion exchange processes.

CONCLUSION

From the present study, it is concluded that, the single low-cost IERs prepared by blending PFR with d from various plant materials(PE, EJ,TC,TB,and AA) almost retain the CEC value

of PFR. Also, these single low-cost IERs are found to be suitable for the removal of metal ions, particularly Copper, Zinc, Lead and Calcium ions for single and binary mixtures from water and wastewater. Hence, these IERs could be used as low-cost IERs, compared to the available commercial IER. It is also concluded that, the mixing of these low-cost IERs to form binary mixture of resins($R_1$and R_2) shows greater CEC value compared to that of the theoretically calculated value based on the linear or additive (ideal) property. This may be due to synergism modified ion – exchange process.

Table-7: CEC of single and binary mixture of metal ions for binary mixture of resin R_2

R_2	Cation Exchange Capacity (m.mol g^{-1})							
	Single Metal Ions				Binary Metal Ions Solution			
					0.1M [Cu^{2+} + Zn^{2+}]		0.1M [Pb^{2+} + Ca^{2+}]	
	Cu^{2+}	Zn^{2+}	Pb^{2+}	Ca^{2+}	Cu^{2+}	Zn^{2+}	Pb^{2+}	Ca^{2+}
Z	1.415	1.702	1.678	1.505	0.900	0.703	0.946	0.682
ZY1	1.412 (1.407)*	1.684 (1.603)	1.638 (1.610)	1.475 (1.453)	0.893 (0.866)	0.694 (0.676)	0.926 (0.919)	0.666 (0.645)
ZY2	1.410 (1.399)	1.583 (1.503)	1.587 (1.542)	1.439 (1.402)	0.846 (0.833)	0.668 (0.650)	0.909 (0.892)	0.619 (0.609)
ZY3	1.406 (1.390)	1.463 (1.404)	1.501 (1.473)	1.410 (1.350)	0.808 (0.797)	0.654 (0.623)	0.891 (0.865)	0.593 (0.572)
Y	1.382	1.304	1.405	1.298	0.765	0.596	0.838	0.535

* Values in parentheses are theoretical total CEC obtained by using eqn. 3.

ACKNOWLEDGEMENTS

The authors thank the management and principal of their colleges for providing research facilities and encouragement, respectively.

REFERENCES

1. H.S.Thomson and J.Roy, *Agr.Soc.Engl.*, **11,** 68(1850).
2. J.T. Way and J.Roy, *Agr.Soc.Engl.*, **13**, 123(1852**).**
3. O.Liebknecht, US. Patent 2,206,007, (June 23, 1940**).**
4. P.Smit, US. Patent 2,191,063 (Feb. 20, 1940**).**
5. B.A.Adams and E.L. Holmes., *J.Soc.Chem.Ind.London*, **54**, 1(1935).
6. N.L.N.Sharma, Joseph Mary and Padma Vasudevan, *Res. Ind.*, **21,** 173(1976).
7. Padma Vasudevan and N.L.N. Sarma, *J.Appl. Poly.Sci.*, **23,** 1443(1979**)**.
8. G.J.Mohan Rao and S.C. Pillai, *J. Indian Inst.Sci.* , **36A,** 70(1954**).**
9. Shahha and S.L.Batna, *J.Appl. Chem. Lond.,* **8,** 335(1953**).**
10. T.Dheiveesan and S.Krishnamoorthy, *J. Indian Chem.Soc.,***65**, 731(1988).
11. D.Kathiresapandian and S.Krishnamoorthy, *Indian. J. Technol.*, **29,** 487(1991).
12. A.Mariamichel and S.Krishnamoorthy, *Asian J. Chem.,* **9(1),** 136(1997).
13. N.Kannan, R.K.Seenivasan and R.Mayilmurugan, *Indian J. Chem. Technol.*, **10, 623**(2003**).**
14. M.S.Metwally, N.E.Metwally and T.M. Samy, *J. Appl. Poly. Sci.,* **52**, 61(1994).
15. S.Fong Lo, S.Y.Wang, M.J.Tsai and L.D.Lin, *Chemical Engg. Res. and Design*, **90(9)**,1397(2012).
16. M.Jovanovic, N.Rajic and B.Obradovic, *J. Haz.Mat.*, **233**,57(2012).
17. J.Huang, Y.Cao, Z. Liu and Z.Deng, *Chem.Engg. J.,* **80(15)**,75(2012).
18. N.Wu and Zale, *Chem.Engg. J.,* **215**,894(2013).
19. M.Natarajan and S.Krishnamoorthy, *Res. Ind.,* **38**, 278(1993).
20. N. Kannan, R.K. Seenivasan, *Desalination,* 216, 77(2006).
21. N.Kannan, R.K. Seenivasan, *J. Appl. Poly. Sci.,* **101**, 4104(2006).
22. N. Kannan, R.K. Seenivasan, *J. Ion Exch.,* **16**, 164(2005).
23. Padma Vasudevan, M.Sing, S.Nanda, and N.L.N. Sharma, *J. Poly. Sci.*, **16**, 2545(1978).

24. A.I. Vogel, Text Book of Quantitative Chemical Analysis, 5th Edn. Longman Group Ltd., London, pp 186 -192,(1989).
25. T.R.E.Kressman and J.A. J. Kitchener, *Chem. Soc.*, 1190(1949).
26. H.P.Gregor, M.J.Hamilton, J.Becher and F.Bernstein, *J. Phys. Chem.*, **59**, 374(1955).
27. S.Ramachandran and S.Krishnamoorthy, *Indian J. Technol***., 22**, 355(1984).
28. C.E. Harland, Ion Exchange Theory and Practice, Royal Society of Chemistry, UK, pp 84-90,(1994).
29. R.Kunin, Ion Exchange Resin, Wiley, Newyork and London, 2nd Edition, pp.320 – 325(1958).
30. J.G.Grantham, Ion Exchange Resin Testing, Duolite International Ltd, Section, **14**, pp.60 – 68(1982).
31. A. Maria Michel and S Krishna moorthy, *J. Sci. Ind. Res.*, **56,** 680(1997).
32. W.K Son, S.H Kim and S.G Park, *Bull. Korean Chem.Soc.,* **22 (1)**, 53, (2001).
33. D.K. Dimov, E.B.Petrova, I.M. Panayotov and Ch.B.Tsvetanov, *Macromolecules*, **21**, 2733(1990).
34. H.M. Fahmy and Z. El-Sayed, *Poly. Plastic Technol. Eng.,* **41(4),** 751(2002).
35. R. Kunnin, *Ind. Eng. Chem.,* **40**, 41(1948).
36. D. Ongaro, *Chimica e Industria (Sao Paulo)*, **32**, 264(1950**).**
37. D. Ongaro., *Riv. Viticolt.e Enol. (Crneglcano),* **3,** 277(1950).
38. A. Bandyopadhyay and M.M. Biswas, *Indian J.Env.Prot.***, 8(9),** 662(1998).
39. C.J.Borman, PV. Bonnesen and BA. Moyer, *Anal. Chem.*, **84(19),** 8214(2012).
40. D.Chen, J.Chen, X.Luen, H.Ji and Z.Xia, *Chem.Engg. J.*, **171,** 1150(2011).
41. N. Kannan and A Xavier, *Indian J. Env.Prot.,* **20 (7)**, 508(2000)**.**

[RJC-1062/2013]

Available online www.jocpr.com

Journal of Chemical and Pharmaceutical Research, 2015, 7(10S):23-34

Research Article

ISSN : 0975-7384
CODEN(USA) : JCPRC5

Synthesis of water soluble transition metal(II) complexes from morpholine condensed tridentate schiff base: Structural elucidation, antimicrobial, antioxidant and DNA interaction studies

Jeyaraj Dhaveethu Raja* and Karunganathan Sakthikumar

Chemistry Research Centre, Mohamed Sathak Engineering College, Kilakarai, Tamilnadu, India

---

ABSTRACT

A new series of water soluble transition metal Cu(II), Co(II), Ni(II), Mn(II) and Zn(II) complexes have been synthesized from 2-(2-Morpholinoethylimino)methyl)phenol Schiff base ligand (LH) in a 1:2 molar ratio. The resulting compounds were characterized by elemental analysis, Magnetic susceptibility, Molar conductance, IR, UV-Vis, ^1H NMR, EPR and ESI-Mass Spectral techniques. The spectral data of these complexes suggest an octahedral geometry around the central metal ion and found to possess [ML_2] stoichiometry. In vitro antimicrobial activities of all compounds were examined against selected bacterial and fungal strains by the disc diffusion method which indicates that the complexes exhibit higher antimicrobial activity than free ligand. The DNA cleavage activity of all compounds was monitored by the agarose gel electrophoresis method using Calf – Thymus DNA. In this result Cu(II), Co(II) and Ni(II) complexes showed a significant cleavage property than others. In vitro antioxidant and DNA-binding properties of these complexes have been investigated by electronic absorption technique. The intrinsic binding constant (K_b) values of Cu(II), Co(II) and Ni(II) complexes are found as 1.1461 X 10^5, 5.1063 X 10^4 and 2.4324 X 10^4 M^{-1} respectively. The binding affinity to DNA has been investigated by viscosity titration measurements, The binding affinity values of these complexes were slightly lower than those observed for classical intercalator (Ethidium bromide-DNA) and observed in the order of EB > Cu(II) > Co(II) > Ni(II)>Zn(II)>Mn(II). The experimental results suggest that the complexes bind to DNA via intercalation.

Key words: Schiff base, Octahedral, Antioxidant, Antimicrobial, DNA interaction.

INTRODUCTION

Schiff bases derived from an amino and carbonyl compound are an important class of ligands that coordinate to metal ions via azomethine nitrogen. In azomethine derivatives, the C=N linkage is essential for remarkable biological activity [1]. It is well-known that Morpholine is a synthetically versatile substrate used as a substitution in many heterocyclic moieties and as a raw material for drug synthesis because it plays a significant role in medicinal chemistry [2]. Morpholine substituted Schiff bases and its Metal complexes exhibits numerous biological activities such as antimicrobial, anticancer, antitumor, anticonvulsant, antiproliferative, antinflammatory and antidiabetic etc**.,** **[**3-9**].** Large number of biological experiments has confirmed that DNA is the primary intracellular target of anticancer drugs; interaction between small molecules and DNA can cause damage in cancer cells, inhibiting the division and resulting in cell demise [10]. DNA-binding metal complexes, especially those with small molecular weight, have been extensively studied as DNA structural and conformational probes, DNA-dependent electron transfer and sequence-specific cleaving agents and potential anticancer drugs [11–14]. Besides, Platinum(II) complexes are used as anticancer drugs since long and among them cis-platin have proven to be a highly effective for treating various types of cancers like ovarian, testicular, head and neck cancer [15-17]. en limited because of many the serious side effects such as hair follicle, neurotoxicity, bone d the lining of gastro-intestinal tract due to strong covalently binding to DNA. To overcome mited activity of cis-platin, great efforts have been made to synthesize other alternatives such

as transition metal complexes which act as better antitumor drugs due to non-covalently binding to DNA [18-21]. Antioxidants are compounds which possess the ability to protect cells from the damage caused by unstable molecules known as free radicals. Free radicals have been implicated as mediators of many diseases, including cancer, atherosclerosis and heart diseases [22-23]. Antioxidants have the capacity in preventing or slowing the oxidation reactions and have been recognized for their potential in promoting health and lowering the risk for cancer, hypertension and heart disease [24-25]. Since synthetic antioxidants like butylated hydroxytoluene (BHT) and butylated hydroxyanisole (BHA), tertiary butyl hydroquinone (TBHQ) and propyl galate (PG) are suspected to be toxic and have carcinogenic effects, naturally occurring antioxidants has considerably increased for use in food, cosmetic and pharmaceutical products [26-28]. Our present work report regarding the synthesis, structural elucidation, antimicrobial, antioxidant, DNA binding and cleavage studies of Transition Metal(II) complexes.

EXPERIMENTAL SECTION

Materials and Methods

The starting materials 4-(2-aminoethyl)-morpholine, salicylaldehyde, $Cu(OAc)_2.H_2O$, $Zn(OAc)_2.2H_2O$, $Mn(OAc)_2.4H_2O$, $Co(OAc)_2.4H_2O$ and $Ni(OAc)_2.4H_2O$ were procured from Sigma Aldrich chemical company (USA) and other reagents and solvents were of analytical grade.

Instrumentation

Melting points of all the compounds were noted on Cintex apparatus (Guna-BMQR) in open glass capillaries. The C, H, and N contents of the synthesized ligand and the complexes were performed by Elementar Vario EL III CHNS. Molar Conductivity of complexes in methanolic solution (10^{-3}M) were recorded at room temperature by systronics model 304 digital conductivity bridge using a dip type conductivity cell fitted with a platinum electrode. Magnetic susceptibility for powder sample of the complexes was recorded by Guoy balance at room temperature. IR spectra of Schiff base and their complexes were recorded on a Shimadzu FT-IR spectrophotometer in the range of 4000 to 400 cm^{-1}. Electronic absorption spectra of all compounds were recorded in methanolic solution (10^{-3}M) by Shimadzu UV-Vis 1800 spectrophotometer in the range of 200 to 1100 nm. Antioxidant and DNA binding studies were examined by Shimadzu UV-Vis 1800 spectrophotometer. DNA Cleavage studies of all compounds were carried out by agarose gel electrophoresis technique in the presence of H_2O_2. The ^1H NMR spectra of the ligand and its zinc complex were recorded on a Bruker 300 MHz NMR spectrometer using $CDCl_3$. EPR spectra of powder sample of the copper (II) Complex were recorded on a Varian E112 EPR spectrometer at RT and LNT using TCNE as the field marker (g_e= 2.00277). Mass spectra of Schiff base and their complexes were recorded on ESI MS 3000 Bruker Daltonics instrument.

Synthesis of Schiff base ligand (LH)

The Schiff bases were synthesized by stirring an equal molar quantities (0.01 mol) of 4-(2-amino ethyl)-Morpholine and Salicylaldehyde in methanol (30 ml) were refluxed for two hours. The reaction was completed after TLC confirmation test. Yellow solution was obtained at the end of the reaction and the volume of the solution was reduced to one-third on water bath and cooled at room temperature. The ligand was purified by column chromatography using ethanol and chloroform mixture. The collected pure yellow liquid ligand was dried slowly at room temperature in vacuum desiccators over anhydrous $CaCl_2$. The yield of the isolated ligand was found to be 87% (Scheme 1).

Synthesis of metal complexes [$M(L)_2$]

A solution of 2-(2-Morpholinoethylimino)methyl)phenol Schiff base (LH) (0.004M) in methanol (40 mL) was added slowly to a solution of Metal(II) acetate(0.002M) [$Cu(OAc)_2.H_2O$, $Zn(OAc)_2.2H_2O$, $Mn(OAc)_2.4H_2O$, $Co(OAc)_2.4H_2O$ and $Ni(OAc)_2.4H_2O$] in 30 ml of absolute methanol and stirred for 30 minutes. The resulting mixture was refluxed for 3 hrs. The solid product so formed was separated by filtration and purified by recrystallization using methanol and petroleum ether. Trace of water and solvents were recovered by keeping in vacuum desiccators over anhydrous $CaCl_2$. The preparation of all complexes was followed by the similar method and the yield was found to be 74–80% (Scheme 1).

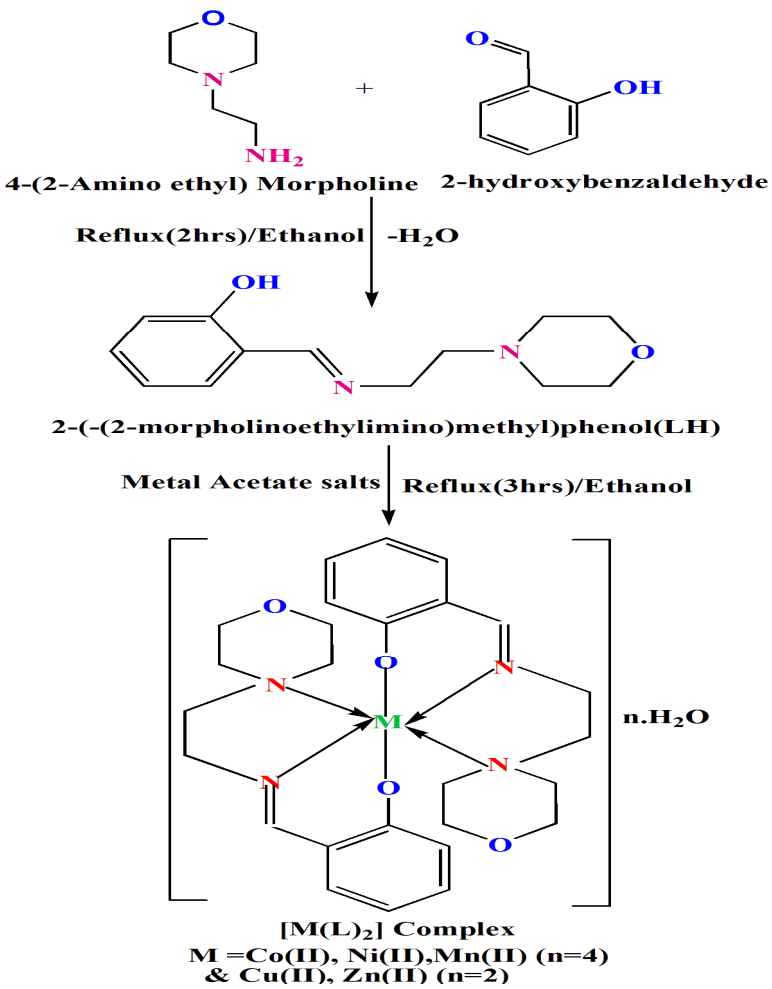

Scheme 1. Schematic representation of synthesis of Ligand & the coordinated complexes

DNA interaction studies

DNA cleavage study by Gel electrophoresis

DNA cleavage activities of Schiff base ligand and their metal complexes with CT-DNA were monitored by agarose gel electrophoresis method[29-30]. The gel electrophoresis experiments were performed under aerobic conditions with H_2O_2 by incubation at 35^0C for 2 hours. The samples (Cocktail mixture) containing CT-DNA 15 µL (30 µM), synthesized compounds 5 µL (50 µM), buffer solution (pH = 7.2) 29 µL (50 mM TrisHCl & 18 mM NaCl) and H_2O_2 1µL (500 µM). The Cocktail mixture was shaked well and maintained incubation at room temperature for 2 hours. After incubation, 1 µL Bromophenol blue (photosensitizer) dye solution (0.25% bromo phenol blue and 40% sucrose in H_2O) was added with Cocktail mixture, the resulting mixture was injected into 1% agarose gel chamber wells. The gel was stained by immersing it in tank buffer solution containing ethidium bromide (EB) (0.5 µg/ml).When power supply (50 V) was introduced into the tank buffer solution, the DNA migration was occurred towards to positive pole. After completion of DNA migration, the electric current was turned off, the gel layer was taken out from the solution tank and was snapped under a UV Transilluminator and the bands were observed the extent of DNA cleavage by comparing with standard DNA marker.

DNA binding study by UV-Visible spectroscopy

The Concentrated herring sperm DNA stock solution was prepared in 5 Mm Tris–HCl/50 mM NaCl in deionized water at pH 7.2. The purity of DNA was verified by monitoring the ratio of absorbance at 260 nm to that at 280 nm, A_{260}/A_{280} which was in the range 1.8–1.9 indicating that the DNA is sufficiently free from protein and the initial concentration of the DNA was confirmed from its absorption intensity at 260 nm with a molar extinction coefficient (ε) of 6600 M^{-1} cm^{-1}[31]. The Electronic Absorption titrations were performed by keeping a fixed complex concentration (10^{-5}M) to which increments of the DNA stock solutions were added from 1.1308 X 10^{-5} to 12.0464 X

inding constant (K_b) of Metal(II) complexes with DNA was calculated from the Wolfe–

$$\frac{[DNA]}{(\varepsilon_a-\varepsilon_f)} = \frac{[DNA]}{(\varepsilon_b-\varepsilon_f)} + \frac{1}{K_b(\varepsilon_b-\varepsilon_f)} \quad (1)$$

Where, [DNA] is the concentration of HS-DNA in base pairs. The apparent extinction coefficient (ε_a) observed for the MLCT absorption band at the given DNA concentration was obtained by calculating Abs / [complex], ε_f and ε_b correspond to the extinction coefficient of the complex free (unbound) and fully bound to DNA. The K_b values can be obtained from the ratio of the slope to the intercept of the plots of [DNA] / (ε_a-ε_f) Vs [DNA]. The standard Gibb's free energy change (ΔG_b^0) for DNA binding can be calculated using van't Hoff equation (2).

$$\Delta G_b^0 = -RT \ln K_b \quad (2)$$

DNA binding study by Viscometry titration

The experiments were carried out by an Oswald viscometer, immersed in a thermo stated water-bath maintained at $25^oC \pm 0.1^oC$ which helps to further clarify the nature of the interaction between the complexes and DNA. They are sensitive to length change of DNA and they are observed as the least ambiguous and the most critical test of binding mode in solution[32]. The titrations were performed for Cu(II), Co(II), Ni(II) complexes and control-Ethidium bromide(EB) (0.2, 0.4, 0.6, 0.8, 1.0 X 10^{-5}M) and each compound was introduced into the HS-DNA solution (10^{-4}M) present in the viscometer. Each sample was measured three times and an average flow time was calculated [33]. The viscosity of DNA increased with rising ratio of complexes to DNA, further suggesting a binding of the complexes with DNA. Relative specific viscosity for DNA either in the presence or absence of complexes were calculated from the equation (3).

$$\left(\frac{\eta}{\eta_0}\right)^{1/3} = \frac{\left\{\frac{(t_{complex}-t_0)}{t_0}\right\}}{\left\{\frac{(t_{DNA}-t_0)}{t_0}\right\}} \quad (3)$$

Data were analyzed as $(\eta/\eta_o)^{1/3}$ versus binding ratio R=[complex]/[DNA], where η is the specific viscosity of DNA in the presence of the complex and η_0 is the specific viscosity of DNA alone; $t_{complex}$, t_{DNA} and t_o are the average flow time for the DNA in the presence of the complex, DNA alone and Tris-HCl buffer respectively [34].

DPPH radical scavenging studies

Antioxidant activities were determined in vitro by 2,2-diphenyl-1-(2,4,6-trinirophenyl)hydrazyl (DPPH) free radical scavenging assay. 3.9037 mg of DPPH was dissolved in 3.3 mL methanol. 0.3 mL of the stock solution (3 mM) was added to 3.5 mL methanol (2.5714 X10^{-4} M) and absorbance was noted immediately at 517 nm for the control. Various concentration solutions (2.9411, 6.0606, 9.3750, 12.9032 and 16.6666 X10^{-5} M) were prepared in methanol using 1mM test samples and 3 mM DPPH stock solution. The resulting mixture was incubated in dark at room temperature for 1 hour. It was protected from light by covering the test tubes with aluminium foil. While DPPH reacts with an antioxidant compounds, it is reduced by the typical H-absorption and the colour changes from deep violet to light yellow to form a stable macromolecular radical. The absorbance of the resulting solution was measured by UV-visible spectrophotometer at 517 nm. The control was measured from the values of absorbance of the DPPH radical without antioxidant and Special care was taken to minimize the loss of free radical activity of the DPPH radical stock solution [35].

Pharmacological studies

In vitro antimicrobial assay

Antimicrobial activities of the ligand and their complexes (10^{-4}M) were screened in vitro against the selected pathogenic bacterial strains and fungi species by the disc diffusion method. Amikacin and Ketokonazole were used as standard drugs for antibacterial and antifungal studies respectively. The test organisms were grown on nutrient agar medium in sterile Petri plates. The paper discs were saturated with 10 µL of the ligand and its complexes solution. The saturated paper discs were placed aseptically in the Petri dishes containing Mueller Hinton nutrient agar with 2% of glucose media inoculated with the above mentioned pathogenic bacteria and fungi separately. The inoculated culture plates were incubated at 37°C for 24 hrs for the bacteria and at 30°C for 48 hrs for the fungi. After incubation, the antimicrobial activity was evaluated by measuring the diameter (in mm) of the inhibition zone formed around the discs [36].

RESULTS AND DISCUSSION

erization

and complexes were found to be intensely coloured and they were slightly hygroscopic ature. The synthesized complexes were soluble in Water, Methanol, Ethanol, $CHCl_3$ and data and physical properties of the ligand and its complexes are listed in Table 1.

Table 1 Analytical and Physical data of the Schiff base ligand and its complexes.

Compounds (Formula Weight & Empirical Formula)	Colour	Yield (%)	M.P (^{0}C)	Found (Calcd) (%)				($\wedge_m$) Molar Conductance $Ohm^{-1}cm^2 mol^{-1}$
				C	H	N	M	
[LH] (234.31) ($C_{13}H_{18}N_2O_2$)	Yellow liquid	87.48	--	66.90 (66.64)	07.60 (07.74)	11.39 (11.95)	----	----
$[Cu(L)_2]$ (566.16) ($C_{26}H_{38}N_4O_6$)Cu	Green	80.10	120	55.10 (54.45)	06.71 (06.22)	09.89 (09.43)	11.22 (11.56)	61.07
$[Co(L)_2]$ (597.55) ($C_{26}H_{42}N_4O_8$)Co	Dark Brown	76.32	>280	52.21 (51.88)	07.02 (06.91)	09.37 (08.66)	09.86 (9.35)	46.35
$[Mn(L)_2]$ (593.56) ($C_{26}H_{42}N_4O_8$)Mn	Black	78.65	110	52.56 (52.08)	07.07 (06.59)	09.43 (09.78)	09.25 (09.66)	56.65
$[Ni(L)_2]$ (597.32) ($C_{26}H_{42}N_4O_8$)Ni	Dark green	74.50	294	52.23 (51.85)	07.03 (06.83)	09.37 (08.65)	09.82 (09.24)	41.20
$[Zn(L)_2]$ (567.99) ($C_{26}H_{38}N_4O_6$)Zn	Yellow	76.34	112	54.93 (53.86)	06.69 (06.02)	09.85 (09.04)	11.50 (11.83)	48.52

Elemental analysis

The composition and purity of the coordinative compounds were determined by the elemental analysis (C, H, N and metal contents) and the result shows they are in good agreement with the proposed formula (Table 1)

Conductivity studies

The molar conductivity of all complexes was in the range of 41.20-61.07 ohm^{-1} cm^2 mol^{-1}(Table 1). The low value shows that they are non electrolytic nature due to lack of dissociation.

Mass spectra

ESI-MS Mass spectrometry is used to confirm the stoichiometry composition of compounds. The mass spectrum of ligand shows the molecular ion peak at m/z 235 corresponding to $C_{13}H_{18}N_2O_2$ and the CuL_2 complex molecular ion peak at m/z 565 corresponding to ($C_{26}H_{38}N_4O_6$)Cu (Fig 1) which confirms the formation of $[ML_2]$ stoichiometry (Scheme 1). The molecular ion peaks of other complexes Co(II), Mn(II), Ni(II) and Zn(II) complexes were observed at m/z with relative abundance 598, 592, 596 and 568 respectively and are in good agreement with the formula weight (Table 1).

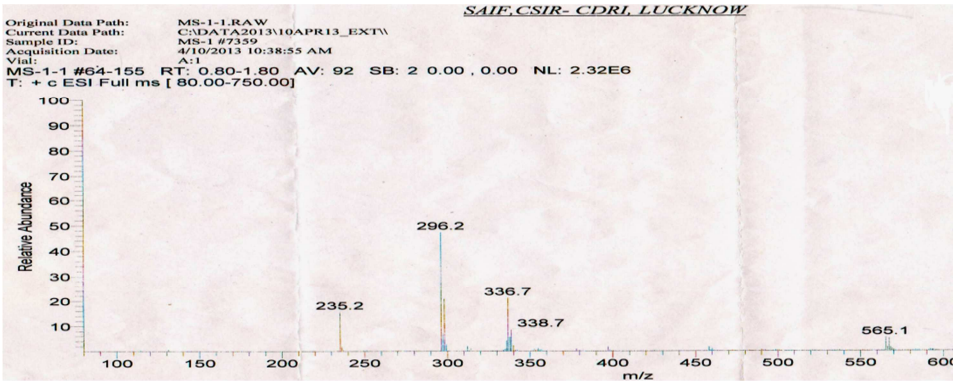

Fig. 1 ESI-MS Mass spectrum of $[Cu(L)_2]$ complex

^{1}H NMR spectra

The ^{1}H NMR spectra of the Schiff base ligand [L] and Zinc complex show the following signals: δ values of Schiff base ligand [L] : Aromatic Protons (m,4H) at 6.84-7.32 ppm; Azomethine proton(-HC=N-) (s,1H) at 7.9 ppm; Morpholino-OCH_2 (t,4H) at 3.6 ppm; Morpholino-N-CH_2 (t,4H) at 2.50 ppm; Phenolic-OH proton (s,1H) at 8.5 ppm[37]. $[Zn(L)_2]$ Complex: Aromatic Protons (m,8H) at 6.7 -7.5 ppm; Azomethine proton(-HC=N-) (s,1H) at 8.16 ppm; morpholino-OCH_2 (t,8H) at 3.6 ppm; Morpholino-N-CH_2 (t,8H) at 3.12 ppm; The low intensity singlet peak at water proton (s,1H)[38].The above ^{1}H NMR spectra data assigned that the azomethine proton proton signals in the spectrum of the zinc complex are shifted down field compared to the leshielding due to nitrogen atom is taking part in complexation. The absence of singlet peak

at the rage of 8.5 ppm, noted in the zinc complexes, indicates the loss of the –OH proton due to complexation[39] and there is no appreciable change in all other signals in these complexes.

IR spectra

Table 2. Infrared spectral data of the ligand and its metal complexes (cm^{-1})

Com pounds	C=N	Phenolic C-O	Morpholino C-N-C	Morpholino C-O-C	Aromatic C-H	Aliphatic C-H	Iminic C-H	(H_2O)	M-N	M-O
Ligand [LH]	1635	1278	1342	1197(as) 1114 (s)	3056	2974	2854	---	---	---
$[Cu(L)_2]$	1600	1284	1320	1195(as) 1112 (s)	3195	2970	2866	3413 813(b)	468	495
$[Co(L)_2]$	1595	1302	1332	1190(as) 1110 (s)	3180	2976	2874	3425 848(b)	462	502
$[Mn(L)_2]$	1598	1294	1335	1196(as) 1114 (s)	3160	2972	2885	3339 846(b)	475	510
$[Ni(L)_2]$	1585	1300	1335	1194(as) 1119 (s)	3060	2965	2875	3339 845(b)	470	502
$[Zn(L)_2]$	1627	1286	1340	1193(as) 1112 (s)	3152	2972	2870	3340 846(b)	462	520

The IR spectra of the complexes were compared with the free ligand for the frequency change during the complexation and are summarized in Table 2. IR Spectrum of Schiff base ligand showed a strong sharp band observed at 1635 cm^{-1} region is assigned to the -HC=N-mode of the azomethine group which was shifted to lower frequencies in the spectra of all the complexes indicating the involvement of imino nitrogen(-HC=N-) in coordination to the central metal ion [40] and morpholino-C-N-C bands at 1342 cm^{-1} found in the ligand is shifted lower frequencies in the spectra of all the complexes indicating the involvement of C-N-C nitrogen in coordination to the metal ion. The peak due to the presence of phenolic C-O at 1278 cm^{-1} in ligand is shifted to higher frequencies in the spectra of all the complexes indicating confirming deprotonation of the phenolic–OH on chelation[41]. In the spectra of all metal complexes a broad diffuse band was identified (stretching) in the range of 3413–3340 cm^{-1} and week band in-plane bending (rocking) at 813–848 cm^{-1}. It suggests that the presence of water molecules in the metal complexes [42]. The far IR spectra of the complexes show medium bands in the region 462–475 cm^{-1} and 495–520 cm^{-1} corresponding to M-N and M-O vibrations respectively and other absorption bands are no appreciable change in the ligand and metal complexes (Table 2).

Electronic Spectra and Magnetic susceptibility

The electronic absorption spectral data of the ligand and its metal complexes were recorded in methanol. The absorption maxima and magnetic moment values are depicted in Table 3. The electronic spectra of the free ligand displayed two bands at 38700 cm^{-1} and 31300 cm^{-1} are intra ligand charge transfer assigned to $\pi\rightarrow\pi^*$ and $n\rightarrow\pi^*$ transitions for phenyl ring and the azomethine chromophore (–CH=N–)[43]. In the metal complexes this band is shifted to a longer wavelength which may be attributed to the donation of lone pair electron in a sp^2-hybridized orbital of the imino nitrogen atom of the ligand to the metal (N→M). $[Cu(L)_2]$ complex exhibited only one low intensity broad band d-d transition at 649 nm (15,408 cm^{-1}) due to dynamic Jahn–Teller distortion[44-45] which are assigned to the $^2E_g\rightarrow{}^2T_{2g}$ transition and showed magnetic moment value is slightly higher than the spin-only value(1.73) for one unpaired electron which suggests possibility of a distorted octahedral geometry[46]. $[Co(L)_2]$ and $[Ni(L)_2]$ complexes exhibited three bands for each(Table 3) and magnetic moment values, which is further supported to an octahedral geometry.

Table 3 Electronic spectral data and magnetic Susceptibility values of the synthesized compounds (10^{-3} M in Methanol).

Com pounds	Band Position λ_{max} nm (γ-cm^{-1})	Assignment	μ_{eff} B.M	Suggested geometry
[LH]	258 (38,760)	$\pi\rightarrow\pi^*$	--	--
	319 (31,348)	$n\rightarrow\pi^*$		
$[Cu(L)_2]$	649(15,408)	$^2E_g\rightarrow{}^2T_{2g}$	1.82	Distorted Octahedral
	847(11,806)	$^4T_1g(F)\rightarrow{}^4T_2g(F)$		
$[Co(L)_2]$	528(18,939)	$^4T_1g(F)\rightarrow{}^4A_2g(F)$	4.83	Octahedral
	402(24,875)	$^4T_1g(F)\rightarrow{}^4T_1g(P)$		
	892 (11,210)	$^3A_2g(F)\rightarrow{}^3T_2g(F)$		
$[Ni(L)_2]$	747 (13,386)	$^3A_2g(F)\rightarrow{}^3T_1g(F)$	3.18	Octahedral
	407 (24,570)	$^3A_2g(F)\rightarrow{}^3T_1g(P)$		

:a of the $[Cu(L)_2]$ complex in powder state was recorded at 300 K and 77 K under 9.10 GHz lation using tetracyanoethylene (g_e = 2.00277). The copper complex at 300 K gave one in the high field region and was isotropic because of the tumbling motion of the molecules

and the complex in the frozen state exhibited anisotropic pattern with well-resolved hyperfine lines. The results are summarized in Table 4**.** The spin Hamiltonian parameters have been calculated by Kivelson's method. The observed g-values are in the order $g_{||}$ (2.1248) > $g_{\perp}$(2.0211) > g_e (2.00277) indicating that the unpaired electron lies predominantly in the $d_{x^2-y^2}$ orbital of Cu(II)[47] and the observed $g_{||}$ values for copper complex is less than 2.3 in agreement with the covalent environment character of the M-L bond[48]. The covalent nature of the M–L bond in the complex is further supported by the $g_{eff} = [(g_{||} + g_{\perp}) / 3]$ value less than 2.00277[49]. The observed value of g_{eff} = 1.3819 was less than 2.00277. The observed hyperfine constant parameters are very clear that in the order $A_{||}$ =124G >A_{av}(96G) > $A_{\perp}$= 82G. The values were obtained from the following equations (4-8).

$$g_{\perp} = \frac{(3g_{av} - g_{||})}{2} \quad (4)$$

$$K_{\perp} = \frac{(3A_{av} - A_{||})}{2} \quad (5)$$

$$g_{av} = \frac{g_{||} + 2g_{\perp}}{3} \quad (6)$$

$$A_{av} = \frac{(A_{||} + 2A_{\perp})}{3} \quad (7)$$

$$G = \frac{(g_{||} - 2.00277)}{(g_{\perp} - 2.00277)} \quad (8)$$

The observed value of interaction coupling constant G = 6.657 is in the present complex suggesting that there is no interaction between Cu-Cu centers in the solid state complex and the absence of half field signal at 1600G corresponding to the ΔMs = ± 2 transition rules out a Cu-Cu interaction[50]. EPR and optical spectra have been further used to determine covalent bonding for the Cu(II) ion in a variety of environments. The values of molecular orbital coefficient parameters (α^2, β^2, γ^2) were calculated by Kivelson and Neimann formulae (9-11).

$$\alpha^2 = \frac{A_{||}}{P} + (g_{||} - 2.00277) + \frac{3}{7}(g_{\perp} - 2.00277) + 0.04 \quad (9)$$

$$\beta^2 = (g_{||} - 2.00277)\left(\frac{E_{d-d}}{-8\lambda_0 a^2}\right) \quad (10)$$

$$\gamma^2 = (g_{\perp} - 2.00277)\left(\frac{E_{d-d}}{-2\lambda_0 a^2}\right) \quad (11)$$

In-plane σ-bonding parameter α^2 = 1.0 indicates the pure ionic character whereas, α^2 = 0.344 indicates the pure covalent bonding. The observed α^2 value indicates that the complex has covalent character. The observed β^2 (in-plane π-bonding) and γ^2 (out-plane π-bonding) values which indicate π-bonding is completely covalent character due to the value is less than 1.0 (Table 4). Hathaway has pointed out that for the pure σ-bonding in case of orbital reduction factors are equal ($K_{||} = K_{\perp}$)[51]. In case of $K_{||} < K_{\perp}$ denotes considerable in-plane π-bonding and if the value is to be $K_{||} > K_{\perp}$ which leads to out-of-plane π–bonding. The observed orbital reduction factor values for the present $[Cu(L)_2]$ complex are $K_{\parallel} > K_{\perp}$ which indicates the presence of out-plane π-bonding in metal ligand π-bonding. The values are calculated from the equation(12,13).

$$K_{||}^2 = (g_{||} - 2.00277)\left(\frac{E_{d-d}}{-8\lambda_0}\right) \approx \alpha^2\beta^2 \quad (12)$$

$$K_{\perp}^2 = (g_{\perp} - 2.00277)\left(\frac{E_{d-d}}{-2\lambda_0}\right) \approx \alpha^2\gamma^2 \quad (13)$$

The Co-factors of degree of geometrical distortion $f_{||}$ = 171.35 cm^{-1} indicating an octahedral geometry around the Cu(II) ion. Spectral data and magnetic measurements of the Cu(II) complex has been proposed as a distorted octahedral geometry (Scheme 1).

Table 4 The EPR spectral data for polycrystalline sample of the $[Cu(L)_2]$complex at 77K

Complex	g tensor			Hyperfine constant X 10^{-4} cm^{-1}		Bonding parameters					
	g_{av}	$A_{||}$	$A_{\perp}$	A_{av}	G	$f_{||}(cm^{-1})$	α^2	β^2	γ^2	$K_{||}$	$K_{\perp}$
	2.05	124	82	96	6.657	171.35	0.344	0.825	0.495	0.283	0.170

') = 9.114 X10^9cycle/sec, 1G = 10^{-4} cm^{-1}, E_{d-d} = 15,408 cm^{-1}, one-electron spin orbit coupling constant of free Cu(II) ion λ_0 - 828 cm^{-1}, μ_{eff} = 1.82 B.M (exp), Free ion dipolar term(P) = 0.036 cm^{-1}, $f_{||} = g_{||} / A_{||}$.

DNA nuclease activity by gel electrophoresis

Lane:1 DNA alone,
Lane:2 ligand +DNA+H_2O_2,
Lane:3 $[Cu(L)_2]$+DNA+H_2O_2,
Lane:4 $[Co\ (L)_2]$+DNA+H_2O_2,
Lane:5 $[Mn(L)_2]$+DNA+H_2O_2,
Lane:6 $[Ni(L)_2]$+DNA+H_2O_2,
Lane:7 $[Zn(L)_2]$+DNA+H_2O_2,

Fig. 2 Gel electrophoresis showing the chemical nuclease activity of CT DNA by the synthesized compounds in the presence of oxidant, lane (1-7)

The gel electrophoresis clearly revealed that there was difference in migration of the lanes 2–7 by comparing with CT-DNA control (Lane-1) (Fig 2). The DNA cleavage efficiency of the complex was observed due to the different binding affinity of complexes respect to rate of the conversion of open circular into linear. In oxidative DNA cleavage mechanism, metal ions of the complexes react with H_2O_2 to generate the hydroxyl radical ($OH^{\bullet}$) or reactive oxygen species (O_2) which attacks the C_4' position of the sugar moiety which finally cleave the DNA and inhibit the replication ability of the cancer gene is thereby destroyed. The DNA cleavage activities of the complexes are shown in the fig 2 Lane 1 is for the control (DNA + H_2O_2) which does not exhibit significant cleavage even on longer exposure time and lane 2 is for the ligand alone is inactive in the presence and absence of external agents. Lane: 3 $[Cu(L)_2]$, Lane: 4 $[Co(L)_2]$ and Lane: 6 $[Ni(L)_2]$ Complexes cleave DNA more efficiently in the presence of an oxidant than the ligand and other complexes. This may be attributed to the formation of hydroxyl free radicals, which can be produced by metal ions reacting with H_2O_2 to produce the diffusible hydroxyl radical or molecular oxygen, which may damage DNA through Fenton type chemistry [52]. This hydroxyl radical participates in the oxidation of the deoxyribose moiety, followed by hydrolytic cleavage of sugar–phosphate backbone [53]. Further, the presence of a smear in the gel diagram indicates the presence of radical cleavage.

Evaluation of binding constants by Electronic absorption titration

Electronic absorption spectroscopy is one of the most powerful techniques to examine the binding mode of DNA with metal complexes. In this studies, K_b and ΔG_b^0 values for Cu(II), Co(II) and Ni(II) complexes have been evaluated by absorption titration(Table 5). These complexes were exhibited greater DNA cleavage efficiency than others while observing the gel electrophoresis. The binding of the complexes to DNA helixes were characterized by monitoring the changes in the absorbance of π–π* bands and shift in wavelength on each addition of DNA solution to the complex. While the concentration of CT-DNA increases from 1 X 10^{-5} to 12 X 10^{-5} M, a significant hypochromic shift of the intra ligand bands were observed accompanied by a moderate red shift (Figs 3a & 3b). The π* orbital of the intercalated ligand can couple with the π orbital of the base pairs thus decreasing the π–π* transition energy and resulting in bathochromism (red shift). On the other hand, the coupling π orbital is partially filled by electrons thus decreasing the transition probabilities and concomitantly resulting in hypochromism [54]. The intrinsic binding constant K_b values are calculated from the ratio of the slope to the intercept of the plot of [DNA] / (ε_a - ε_f) X 10^{-7} Vs [DNA] X 10^{-5} M by Wolfe–Shimmer equation (1) and ΔG_b^0 values for these complexes were calculated by Van't Hoff equation (2) which indicate that the complexes can interact with DNA in a spontaneous manner and also the percentage of hypochromicity for the complexes were determined from the equation (14).

$$\% H = \frac{(\varepsilon_b - \varepsilon_f)}{\varepsilon_f} X\ 100 \qquad (14)$$

Hypochromism results indicated that the contraction of DNA helix axes as well as the conformational changes on molecule of DNA. The observed results of hypochromism effect with a red shift is attributive an intercalative binding mode due to strong stacking interactions between aromatic chromophore of molecule and DNA base pairs. To compare quantitatively the affinity of the synthesized complexes towards DNA, the intrinsic binding constants K_b of the synthesized complexes to CT DNA are shown in table 5. From this table, it is clear that $[CuL_2]$ complex acy than other complexes.

Table 5 Spectral parameters for DNA interaction with the synthesized complexes

Complexes	λ_{max} free (nm)	λ_{max} bound(nm)	$\Delta\lambda$ (nm)	Types of Chromism	Chromism (%)	Binding constant (K_b) M^{-1}	$\Delta G_b^{\neq}$ $KJmol^{-1}$
$[CuL_2]$	362	368	06	Hypo & Red shift	18.32	1.1461 X 10^5	-28.8671
$[CoL_2]$	354	362	08	Hypo & Red shift	32.56	5.1063 X 10^4	-26.8637
$[NiL_2]$	364	372	08	Hypo & Red shift	28.73	2.4324 X 10^4	-25.0260

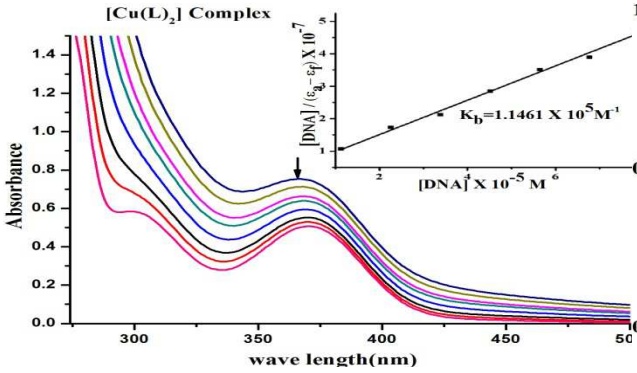

Fig. 3a. Electronic Absorption spectrum of $[Cu(L)_2]$ Complex through titration with DNA in Tris-HCl buffer; [Complex] =1 X 10^{-5} M; [DNA]: 0.0–12 X 10^{-5} Mol L^{-1}. The increase of DNA concentration is indicated by an arrow. Plot of [DNA] / (ε_a - ε_f) Vs [DNA]. Binding constant K_b= 1.1461 X 10^5

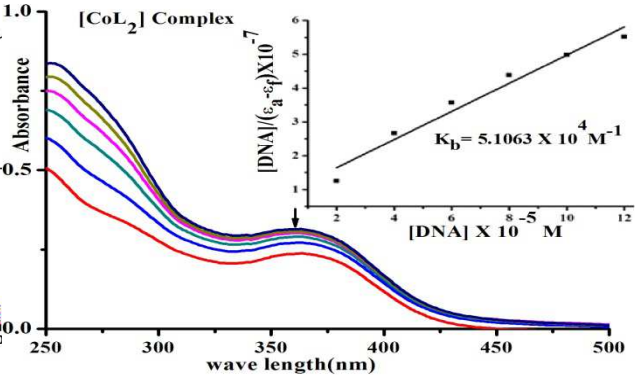

Fig. 3b. Electronic Absorption spectrum of $[Co(L)_2]$ Complex through titration with DNA in Tris-HCl buffer; [Complex] =1 X 10^{-5} M; [DNA]: .0–12 X 10^{-5} Mol L^{-1}. The increase of DNA concentration is indicated by an arrow. Plot of [DNA] / (ε_a - ε_f) Vs [DNA]. Binding constant K_b= 5.1063 X 10^4

Viscosity titration measurements

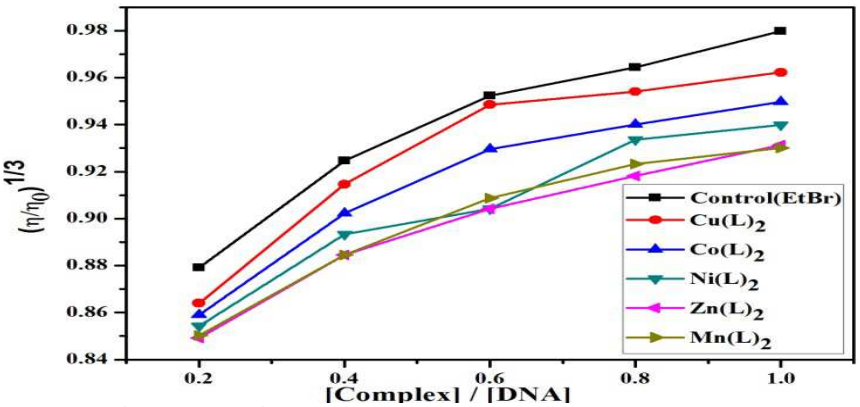

Fig. 4. Plot of Relative specific viscosity (η/η_0) versus R = [Complex] / [DNA]

The Interaction between the complexes and DNA was investigated by viscosity measurements. Ethidium bromide (EB) a well known DNA classical intercalator increases the viscosity strongly by lengthening the DNA double helix through intercalation. While increasing the concentration of the complexes, the relative viscosity of complexes also increases steadily similar to the performance of ethidium bromide. The rised degree of viscosity may depend on the binding affinity to DNA which was observed in the following order EB > Cu(II) > Co(II) > Ni(II) (Fig 4). The significant increase in viscosity of the complexes is obviously due to the partial insertion of the ligand between the DNA base pairs leading to an increase in the separation of base pairs at intercalation locations, hence an increase in overall DNA contour length[55].

DPPH radical scavenging studies

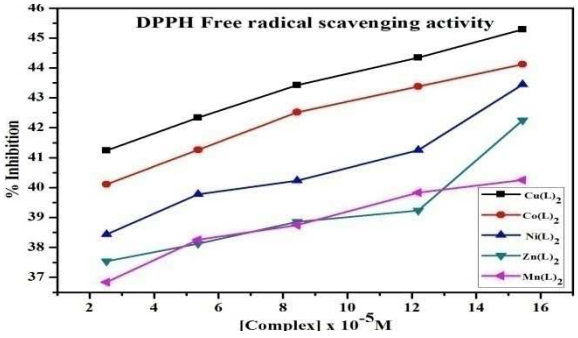

Table 6 DPPH Free radical scavenging activity

Final Concentration of Complex X 10^{-5} M	% Inhibition				
	$Cu(L)_2$	$Co(L)_2$	$Ni(L)_2$	$Zn(L)_2$	$Mn(L)_2$
2.5231	41.24	40.11	38.44	37.54	36.84
5.3674	42.34	41.26	39.78	38.12	38.26
8.4331	43.42	42.52	40.23	38.86	38.75
12.2014	44.34	43.38	41.25	39.23	39.83
15.4364	45.28	44.12	43.44	42.25	40.25

Fig. 5. DPPH Free radical scavenging activity (% Inhibition) of each complex (DPPH-FRSA)

Antioxidants are chemical substances that donate an electron to the free radical and convert into a harmless molecule. They may decrease the energy of the free radical or suppress radical formation or break chain propagation or repair damage and reconstitute membranes. DPPH free radical method is an antioxidant assay based on electron-transfer that produces a violet solution in methanol [56]. This free radical stable at room temperature is reduced in the presence of an antioxidant molecule, giving rise to colourless alcoholic solution. The DPPH assay provides an simple and rapid approach to evaluate antioxidants by electronic spectrophotometer and it can be useful to assess various products at a time. The percentage of antioxidant activity of each substance was assessed by DPPH free radical assay (Fig 5, Table 6). The measurement of the DPPH free radical scavenging activity was performed according to methodology described by Brand-Williams et al. Radical scavenging activity (RSA) was calculated as percentage of DPPH discoloration by the following equation (15)[57]. A_{DPPH} is absorbance of DPPH (control) and A_S is absorbance of sample.

$$\% \text{ RSA} = \frac{A_{DPPH} - A_S}{A_{DPPH}} \text{ X } 100 \qquad (15)$$

Antimicrobial assay

On the basis of observed zones of inhibition, it was found that most of the complexes exhibit good antimicrobial activity than the free ligand [58]. The observed higher activity of the metal complexes could be explained on the basis of Overtone's concept and Tweedy's chelation theory[59]. The Chelation tends to make the ligand a more powerful agent and the cell permeability, the lipid membrane surrounded the cell, favors the passage of only lipid soluble material (liposolubility) which is an important factor that controls antimicrobial activity. A possible explanation for this increase in the activity upon chelation is that, the polarity of the metal ion in a chelated complex is reduced to a greater extent due to the overlap of the ligand orbital and partial sharing of the positive charge of the metal ion. It increases the delocalization of π- and d-electrons over the whole chelated ring and enhances the lipophilicity of the metal complexes. The increased lipophilicity of complexes enhances the cell permeability into lipid membranes which leads to breakdown of the barrier of the cell and thus retards the normal cell processes [60]. The observed inhibition diameter zone values (in mm) of all the complexes exhibited better antimicrobial activities than the free ligand. The Cu(II), Co(II) and Zn(II) complexes showed significant antimicrobial activity compared to others (Table 7) and (Fig 6a). However, they are less active than the standard drugs (Amikacin and Ketokonazole). In addition, the activities of the complexes were confirmed by calculating the activity index (Fig 6b) according to the following relation (16).

$$\text{Activity index(A)} \% = \frac{\text{Inhibion zone of compound(mm)}}{\text{Inhibion zone of standard drug(mm)}} \times 100 \qquad (16)$$

Table 7 Evaluation of Antimicrobial activities (Diameter of zone of inhibition in mm) and Activity intex (A) % of the investigated compounds (10^{-4} M) by Agar disc diffusion method

Compounds	Antibacterial activity (% of A)					Antifungal activity (% of A)		
	E. coli (-)	*Salmonellatyphi(-)*	*Chromo bacterim (-)*	*Staph Aureus (+)*	*Bacillus Cereus (+)*	*Aspergillus Flavus*	*Aspergillus niger*	*Candida albicans*
Ligand [LH]	10 (62)	09 (47)	07 (39)	09 (47)	10 (55)	08 (47)	09 (60)	11 (69)
$[Cu(L)_2]$	15 (94)	16 (84)	14 (78)	17 (94)	16 (94)	13 (76)	14 (93)	15 (94)
$[Co(L)_2]$	14 (88)	14 (74)	15 (83)	14 (78)	14 (82)	14 (82)	13 (87)	13 (81)
[Mn(L)$_2$]	12 (75)	13 (68)	12 (67)	13 (72)	12 (71)	12 (71)	11 (73)	12 (75)
		15 (79)	14 (78)	13 (72)	11 (65)	12 (71)	13 (87)	14 (88)
		14 (74)	15 (83)	16 (89)	15 (88)	14 (82)	13 (87)	14 (88)
		19(100)	18(100)	18(100)	17(100)	---	---	---
		---	---	---	---	17(100)	15(100)	16(100)

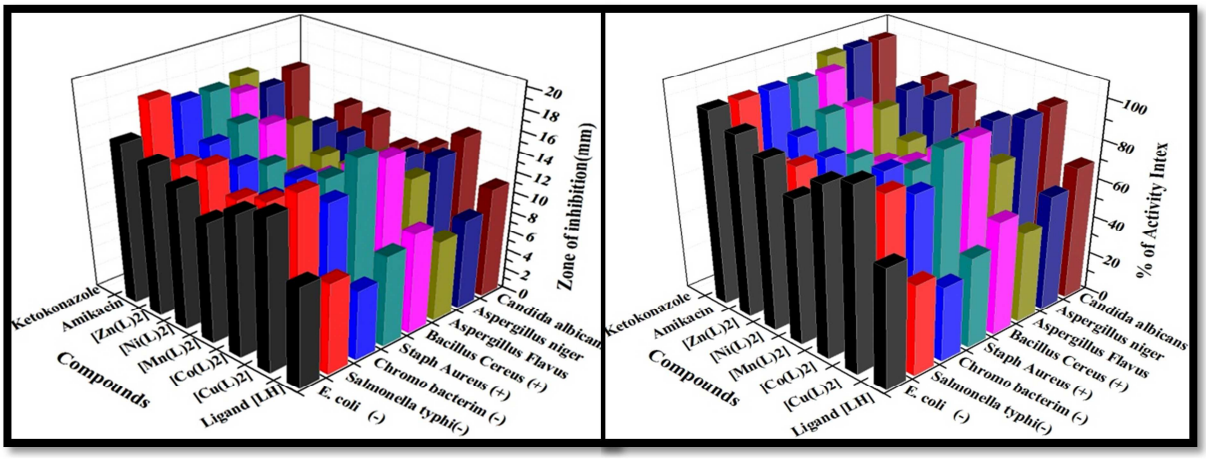

Fig. 6a. Antimicrobial activities (Diameter of zone of inhibition in mm) of the investigated compounds (10^{-4} M) by Agar disc diffusion method

Fig. 6b. Percentage of Activity intex of the investigated compounds (10^{-4} M) by Agar disc diffusion method

CONCLUSION

The work described in this report involves synthesis and characterization of Schiff base ligand and its Mn(II), Co(II), Ni(II), Cu(II) and Zn(II) complexes. The spectral data of the complexes suggest an octahedral geometry and $[ML_2]$ stoichiometry. The lower electrical conductivity values reveal that they are non electrolytes. The interaction of these complexes with DNA was investigated by gel electrophoresis. The results disclose that Cu(II), Co(II) and Ni(II) complexes have been revealed a significant DNA cleavage property than others in the presence of H_2O_2. The Binding experiment results obtained from Electronic absorption and Viscosity titration measurements indicate that the complexes are bound to DNA via intercalation and has also been observed a significant radical scavenging activity by DPPH. The most of the complexes were exposed good antimicrobial activity than the ligand.

Acknowledgements

We thank the Department of Science and Technology (DST) – Science and Engineering Research Board (SERB), Government of India, New Delhi for financial support (SERB-Ref.No.SR/FT/CS-117/2011dated 29.06.2012) and express deepest gratitude to the Managing Board, Principal and Chemistry research centre MSEC, Kilakarai for providing research facilities.

REFERENCES

[1] CT Barboiu; M Luca; C Pop; E Brewster; EM Dinculescu. *Eur. J. Med. Chem.*, **1996**, 31(7-8), 597-606.
[2] P Panneerselvam; M Gnanarupa Priya; N Ramesh Kumar; G Saravanan. *Indian. J. Pharm Sci.*, **2009,** 71(4), 428–432.
[3] P Pannerselvam; RV Pradeep Chandran; SK Sridhar. *Indian. J. Pharm Sci.*, **2003**, 65, 268–273.
[4] P Panneerselvam; RN Rajasree; G Vijayalakshmi; EH Subramanian; SK Sridhar. *Eur. J. Med Chem*. **2005**, 40, 225–229.
[5] S Liu; W Cao; L Yu; W Zheng; L Li; C Fan; T Chen. *Dalton Trans.*, **2013,** 42(16), 5932–5940.
[6] J Benítez; L Becco; I Correia; SM Leal; H Guiset; JC Pessoa; S Tanco; P Escobar; V Moreno; B Garat; D Gambino. *J. Inorg. Biochem.*, **2011**, 105, 303–312.
[7] MS Karthikeyan; DJ Prasad; B Poojary; KS Bhat, BS Holla; NS Kumari. *Bioorganic. Med.* **2006**, 14, 7482-7489.
[8] Kucukguzel; SG Kucukguzel; S Rollas; M Kiraz. *Bioorg. Med. Chem. Lett*., **2001**, 11, 1703-1707.
[9] L Zahajska; V Klimesova; J Koci; K Waisser; J Kaustova. *Arch. Pharm. Med. Chem*., **2004**, 337, 549-555.
[10] C Hemmert; M Piti´e; M Renz; H Gornitzka; S Soulet; B Meunier. *J. Bio. Inorg. Chem.*, **2001,** 6(1), 14-22.
[11] L Leelavathy; S Anbu; M Kandaswamy; N Karthikeyan; N Mohan. *Polyhedron.*, **2009**, 28, 903–910.
[12] N Shahabadi; S Kashanian; M Purfoulad. *Spectrochim. Acta A.*, **2009**, 72, 757–761.
[13] A Bishayee; A Waghray; MA Patel. *Cancer Lett*., **2010**, 294, 1–12.
[14] EK Efthimiadou; N Katsaros; A Karaliota. *Bioorg. Med. Chem. Lett.*, **2007**, 17, 1238–1242.
es-Boza; M Patricia Bradley; KL Patty Fu; E Sara Wicke; John Bacsa; R Kim Dunbar; . *chem.*, **2004,** 43, 8510-8519.
lith Burstyn. *J. Inorg. Chem*., **1996,** 26, 7474-7481.

[17] M Patricia Bradley; M Alfredo Angeles-Boza; R Kim Dunbar; Claudia Turro. *J. Inorg. Chem*., **2004,** 43, 2450-2452.
[18] C Joel1; S Theodore David; R Biju Bennie; S Daniel Abraham; S Iyyam Pillai. J. Chem. Pharm Res., **2015**, 7(5), 1159-1176.
[19] S Patitungkho; S Adsule; P Dandawate; S Padhye; A Ahmad; FH Sarkar. *Bioorg., Med. Chem. Lett*., **2011,** 21, 1802-1806.
[20] M Skander; P Retailleau; B Bourri; L Schio; P Mailliet; A Marinetti. *J. Med. Chem.*, **2010,** 53, 2146–2154.
[21] Z Wu; Q Liu; X Liang; X Yang; N Wang; X Wang; H Sun; Y Lu; Z Guo. *J. Biol. Inorg. Chem.*, **2009**, 14, 1313–1323.
[22] G Tirzitis; G Bartosz. *Acta Biochimica Polonica*., **2010**, 57(1), 139-142.
[23] E Hayet; M Maha; A Samia; M Mata; P Gros; H Raida; MM Ali; AS Mohamed; L Gutmann; Z Mighri; A Mahjoub. *World J. Microbiol. Biotechnol.*, **2008**, 24, 2933-2940.
[24] E Souri; G Amin; H Farsam; H Jalalizadeh; S Barezi. *Iran. J. Pharm. Res*., **2008**, 7, 149-154.
[25] I Fidrianny; A Rizkiya; Komar Ruslan. *Journal of Chemical and Pharmaceutical Research.*, **2015**, 7(5), 666-672.
[26] P Li; L Huo; W Su; R Lu; C Deng; L Liu; Y Deng; N Guo; C Lu; C He, *J. Serb. Chem. Soc.*, **2011**, 76(5), 709-717.
[27] T Kulisica; A Radonicb; V Katalinicc; M Milosa. *Food Chemistry*., **2004**, 85, 633–640.
[28] AA Hamid; OO Aiyelaagbe; LA Usman; OM Ameen; A Lawal. *Afr. J. of Pure and App. Chem.*, **2010**, 4(8), 142-151.
[29] RS Joseyphus; MS Nair. *Arab. J. Chem.*, **2010**, 3(4), 195-204.
[30] L Ana; Di Virgilio; Miguel Reigosa; MF Lorenzo de Mele. *J. Biomed Mater. Res B. Appl Biomater.*, **2011,** 99B(1), 111-119.
[31] J Marmur. *J. Mol. Biol.*, **1961**, 3(5), 585-594.
[32] N Raman; R Jeyamurugan; A Sakthivel; L Mitu. *Spectrochim. Acta A.*, **2010,** 75**,** 88.
[33] J B Charies; N Dattagupta; DM Crothers. *Biochemistry*., **1982**, 21(17), 3933-3940.
[34] C P Tan; J Liu; LM Chen; S Shi; LN Ji. *J. Inorg. Biochem.*, **2008,** 102(8), 1644-1653.
[35] M Sirajuddin; Nooruddin; Saqib Ali; V McKee; S Zeb Khan; K Malook. *Spectrochim. Acta A.*, **2015,** 134, 244-250.
[36] S Chandra; LK Gupta. *Spectrochim. Acta A.*, **2004**, 60(7), 1563-1571.
[37] M Silverstein; X Webster. Spectrometric Identification of Organic Compounds, 6th Edition, **1996**, 150**.**
[38] AK Singh; OP Pandey. *Spectrachim. Acta A.*, **2012**, 85, 1.
[39] Tas E; M Aslanoglu; K Kilic; OH Kaplan; Temel. *J. Chem. Res.*, **2006,** 4, 242-245.
[40] ES Aazam; AF El Husseiny; HM Al-Amri. *Arab. J. Chem.*, **2012**, 5(1), 45-53
[41] Y Li; ZY Yang; ZC Liao, ZC Han; ZC Liu. *Inorg. Chem. Commun.*, **2010**, 13, 1213-1216.
[42] MS Masoud; MF Amira; AM Ramadan; GM El-Ashry. *Spectrochim. Acta A.*, **2008**, 69**,** 230-238.
[43] M Shakir; A Abbasi; M Azam; Asad; U Khan. *Spectrochim. Acta A.*, **2011**, 79(5), 1866-1875.
[44] B Kumar Das; S Jyoti Bora; M Deepa Chakrabortty; L Kalita; R Chakrabarty; R Barman. *J. Chem. Sci.*, **2006**,118**(**6), 487–494.
[45] ABP Lever. *Inorganic Electronic Spectroscopy.*, **1968**, 2nd Ed New York.
[46] DP Singh; R Kumar; V Malik; P Tyagi. *Trans. Met. Chem*., **2007**, 32, 1051-1055.
[47] RL Dutta; A Syamal. *Elemens of magnetochemistry*., **1993**, 97, 106 (2nd Ed East-West press pvt, ISBN: 81-85336-92-X).
[48] D Kivelson; R Neeman. *J. Chem. Phys.*, **1961**, 35 (1) 149.
[49] A Syamal. *Chem. Edu*., **1985**, 62 (2), 143.
[50] AL Sharma; IO Singh; HR Singh; RM Kadam; MK Bhide; MD Sastry. *Transition Met. Chem.*, **2001,** 26, 532-537.
[51] BJ Hathaway; G Wilkinson; RD Gillard; JA McCleverty. *Comprehensive Coordination Chemistry.*, **1987**, 5 (Pergamon. Oxford press).
[52] HJHJ Fenton. *J. Chem. Soc.*, **1894,** 65, 899. doi:10.1039/ct8946500899.
[53] MSS Babu; KH Reddy; GK Pitchika. *Polyhedron.*, **2007**, 26(3), 572–580.
[54] V Uma; M Kanthimathi; T Weyhermuller; B Unni Nair. *J. Inorg. Biochem*., **2005**, 99, 2299-2307.
[55] S Parveen; F Arjmand. *Spectrochim. Acta A*., **2012**, 85(1), 53-60.
[56] W Brand-Williams; ME Cuvelier; C Berset. *LWT-Food science and Technology.*, **1995**, 28(1), 25-30.
[57] S Albayrak; A Aksoy; OM Sagdic; Hamzaoglu. *Food Chemistry*., **2010**,119 (1),114-122.
[58] P Perumal; R Rajasree. *Eur. J. Med. Chem*., **2005**, 40 (2), 225-229.
[59] KN Thimmaiah; WD Lloyd; GT Chandrappa. *Inorg. Chim. Acta*., **1985,** 106 (2), 81-83.
[60] Ji; J Dhaveethu Raja. *J. Serb. Chem. Soc*., **2008**, 73(11), 1063-1071.doi:10.2298/jsc0811063r.

www.literaryendeavour.com

ISSN 0976-299X

LITERARY ENDEAVOUR

A Quarterly International Refereed Journal of
English Language, Literature and Criticism

VOL. VII NO. 4 OCTOBER 2016

Chief Editors

- Dr. Ramesh Chougule
- Dr. S. Subbiah

www.literaryendeavour.com ISSN 0976-299X

LITERARY ENDEAVOUR

A Quarterly International Refereed Journal of English
Language, Literature and Criticism
VOL. VII NO. 4 OCTOBER 2016

CONTENTS

04

HUMAN PREDICAMENT IN ARUN JOSHI'S *THE APPRENTICE*

Dr. A. Gowrimanohari, Asst. Prof in English, MSEC, Kilakarai, TN

Arun Joshi is one of the most prominent writers among the younger Indian English novelists. His place in the field of Indian English literature during the post-independence era is undeniable. Joshi came into the limelight with his very first novel *TheForeigner* which appeared in 1968. He instantly grabbed the attention of readers as well as critics by his new thematic concerns in the genre of novel. Unlike his predecessors he neither writes fiction for entertainment nor for any social or political propaganda. He experiments with the medium of novel writing, for studying the modern man's predicament, particularly the motives responsible for his actions, and the effect of these actions on his psyche.

Arun Joshi himself explains that, "My novels are essentially attempts towards a better understanding of the world and of myself" (Dhawan, 18). Joshi probes deep into the psyche of the protagonist and posterizes their mental toil and anxiety. Trapped between the Indian upbringing and Western influences, his protagonist suffers from evils of materialism which leads to up-rootedness, suspicion, loss of faith, and an identity crisis. Joshi's protagonists are modern men of this world who are lost in a society of mixed ideals. His heroes, who rather turn anti-heroes due to this confused idealism, are running a fruitless expedition. They are struggling to sustain their faith in a world which stands in opposition to them. They are unable to hold on their identity in such a world of moral confusion. So either they revolt with the society or completely yield to it. In both cases there comes alienation. If the character revolts he is alienated from the society, and if he yields, he in turn gets alienated from his own 'real' self. The result initially is restlessness, and finally a self-exploration and self-introspection.

Ratan Rathor, the protagonist, who narrates the story of his life to a N.C.C. cadet who came to New Delhi to participate in the Republic Day parade. Ratan narrates his own story an episode after another episode ranging from his childhood to his apprenticeship and as a shoe shiner on the steps of a temple as a sort of compensation for his sins. The novel, 'The Apprentice' deals with Ratan Rathor's adolescent innocence, his manly experience and his saintly expiation.

Ratan Rathor presents before us a background of his childhood life both before and after the death of his father. Ratan has been an eye-witness to the sight of his father lying dead, who was brutally killed by a British Sergeant while he was leading a procession protesting against British Rule in India. Ratan Rathor, with the background of his middle class family, is torn between the world of his father's idealism and his mother's pragmatism. On one hand his father, an ardent patriot, gives up his lucrative practice as a lawyer to politics at Gandhi's call. Up holding moral values, he donates everything to the national cause without thinking of his family's difficulties. On other hand his mother, who was disappointed about the sacrifices made by the patriots during the freedom struggle. A woman suffering all the time physically, mentally, and economically may become almost cynical about money as it is the only means needed to make a man's life happy in this world.

As a student Ratan Rathor also had ideals like his father and hoped that free India will bring new light to the citizens of the Republic. But, after the achievement of Independence all his hopes for better

He thought that the politicians of free India are worse substitutes for the alien

lem becomes so nagging that Ratan Rathor compelled to think that it has simply

ıthor comes to Delhi, after his graduation in search of a job for his livelihood, he is

disillusioned with stark realities of the present system. In his search for employment he realizes that the posts advertised are already filled in some manner. Even his father's friends could not come to his aid for finding job for him. During his stay in Delhi he gets shelter in an inn beside a masque where several others also occupy the same room with him. A stenographer living at the same inn manages a temporary job for him in a Government office, dealing with war purchases.

Ratan Rathor begins his life as an apprentice clerk. Ratan Rathor keeps his eye upon his career despised by his father as bourgeois filth. He leaves the inn as soon as he gets the job to settle somewhere and tries to keep himself away even from the stenographer who had been instrumental in securing a job for him. He works hard to please his superintendent. In very short time of six months, on the recommendation of the superintendent, he gets confirmation in the service on his assurance that he would marry the superintendent's niece. Henceforth he never looks back and on the superintendent's retirement he gets this most coveted post which brings him every comfort in his life. With the accumulation of riches, Ratan rather gets overwhelmed in the vices associated with wealth such as taste for wine and woman. In Bombay he once gets engaged in 'fantasies of pleasure.'

There is nothing unethical about the fact that the son of the freedom fighter runs after a bureaucratic career. But it is highly illegal, unethical and unscrupulous that he should get corrupt and act against the national interest. During the time of the nation's adversity, he is not only one to gain prosperity by clearing sub-standard war materials supplied by the Sheikh Himmat Singh, being used in Indo-China war without caring for the lives of innocent people.

The self-destructive confusion and moral ambivalence of Ratan Rathor, which finally make him succumb to the mounting temptation of accepting tainted money by sacrificing his patriotism and honour, result from the spineless structure of bourgeois morality. By accepting the bribe from Himmat Singh, he has risked the lives of thousands of patriotic soldiers who fought with the enemy with inferior weapons. Ironically, when it comes to rationalization, one of the last resorts of a criminal like our hero, Ratan Rathor is frantically obsessed more by his honour than by the severity and magnitude of his crime.

Ratan Rathor is guilty of accepting a bribe would characterize as compound fraud, the sin against community. His bribery and fraud threatened his honour for which he determined to take revenge from Himmat Singh, and then from the Secretary who hatched a conspiracy of supplying defective weapons to the army and also responsible for the committing suicide of his childhood friend Brigadier. Ratan Rathor did not opt for death like his Brigadier friend for his guilt of accepting bribe but expiate his guilt in more Gandhian way than Vedantic way:

> Each morning, before I go to work, I come here. I sit on the steps of the temple and while they pray I wipe the shoes of the congregation. Then, when they are gone, I stand in the doorway. I never enter the temple. I am not concerned with what goes on in there. I stand at the doorstep and I fold my hands, my hands smelling of leather and I say things. Be good, I tell myself. Be good. Be decent. Be of use. Then, I beg forgiveness. Of a large host: my father, my mother, the brigadier, the unknown dead of the war, of those whom I harmed, with deliberation and with cunning, of all those who have been the victims of my cleverness, those whom I could have helped and did not(115).
>
> After this I get into my car and go to office. And during the day whenever I find myself getting to be clever, lazy, vain, indifferent, I put up my hands to my face and there is the smell of hundred feet that must at that moment be toiling somewhere and I am put in my place .

The gravity of the offence committed by Ratan Rathor is surely more intense than the solution of polishing the shoes in front of the temple. Ratan rather forms a view that a successful career cannot be ;ence and sincerity, but be realized through flattery and cunning. So he deceives his giving a false statement without admitting his crime. Ultimately, the Brigadier ilarly, Ratan plays havoc with many who are sacrificing their lives for the nation's

cause. Ratan deceives Himmat Singh, a contractor holding him responsible for the supply of defective materials, but the words of Himmat Singh exposing the character of Ratan Rathor are soul-searching when he comments: "You are bogus, Ratan Rathor.... from to bottom. Your work, your religion, your friendship, your honour nothing but a pile of dung" (97).

Thus Ratan Rathor's search for spiritual identity includes his concern for humanity. Ratan Rathor is freed from the fear of a possible judgment of society, but he remains bound to his own moral conscience in a voluntary attempt to redeem himself from the sin he had committed. However in the process of discovery of self, there are magical moments when the individual sees congruence between social morality and individual consciousness.

References:

1. Dhawan, R.K. *The Fictional World of Arun Joshi*. New Delhi: Classical Publishing Company, 1986.
2. Ghosh, Tapan Kumar. *Arun Joshi's Fiction: The Labyrinth of Life*. New Delhi: Prestige Books, 1996.
3. Joshi, Arun. *The Apprentice*. New Delhi: Orient Paperbacks, 1993.
4. Kumar, Lokesh. *Arun Joshi's Novels: His Vision of Life*. New Delhi: Sarup & Sons, 2004.
5. Sharma, Siddhartha. *Arun Joshi's Novels: A Critical Study*. New Delhi: Atlantic Publishers and Distributors, 2004.

www.literaryendeavour.com

ISSN 0976-299X

LITERARY ENDEAVOUR

A Quarterly International Refereed Journal of
English Language, Literature and Criticism

VOL. VII NO. 4 OCTOBER 2016

Chief Editors

■ Dr. Ramesh Chougule ■ Dr. S. Subbiah

www.literaryendeavour.com ISSN 0976-299X

LITERARY ENDEAVOUR

A Quarterly International Refereed Journal of English
Language, Literature and Criticism
VOL. VII NO. 4 OCTOBER 2016

CONTENTS

05

ALIENATION IN ARUN JOSHI'S *THE FOREIGNER*

M. Rekha, Asst. Prof in English, MSEC, Kilakarai, TN, India

Arun Joshi is the most outstanding sensitive and thought-provoking novelist. He is quite an exceptional novelist who stands apart from the rest of the novelists, who has taken up the themes of human behaviour. The central characters of Joshi's novels are mentally disturbed and filled with despair, self-hatred and self-pity and regard themselves as strangers in this lonely planet. The concept of alienation is not quite new in the modern world it has been in use in the theological, philosophical, sociological and psychological writings for an extensive while. The present study will also centre around the theme of alienation in Joshi's first novel *The Foreigner* which is identified as theme of anguish, alienation and existentialism.

The most besetting problems that man faces today are the problems of alienation and emptiness. To established norms and values, man's psyche generates a contemptuous attitude, which makes him fumble for the meaning of life. Having nothing to fall back upon in moments of crisis, modern man finds himself alienated not only from his fellow men, but also from himself. The depression of the modern man has been greatly annoyed by the spiritual stress, which is the characteristic of the current era. The alienation primarily arises in all the novels of Joshi because of social maladjustment and emotional insecurity.

Sindi Oberoi in *The Foreigner* has been always lonely and effortlessness in the world of alienation to find a meaning in existence. His dilemma is socio-psychological, deprived of familial nourishment, cultural roots and affection in his very roots; he grows with a built-in gap in his personality and becomes a wandering alien. Whatsoever encounters him notices this foreignness in him. He felt as an alien belonging to no place and his words and behaviour created the same impression. He is a man without roots and remains a foreigner, whether he is in London, in Boston and in New Delhi. After his parents were killed in Cairo in a flight accident, his uncle in Kenya brought him up, and consequently, he could not consider himself belonging to any country in particular. Sindi's origin and early life made him an ideal foreigner, the man who did not belong anywhere. He narrates:

> I wondered in what way, if any, I belonged to the world that roared beneath my apartment window. Somebody had begotten me without a purpose and so far I had lived without a purpose, unless you could call the search for peace a purpose. Perhaps I felt like that because I was a foreigner in America. But then, what difference would it have made if I had lived in Kenya or India or any other place for that matter! It seemed to me that I would still be a foreigner. My foreignness lay within me and I couldn't leave myself behind wherever I went (1).

Like other foreign students in the United States, Sindi could not consider himself an ambassador of his country because he considers it as a perfectly comical and even the bartenders never consider him as an

here he more poignantly experienced the feeling of alienation. *Sindi Oberoi* is alien

ysically as well as metaphorically, but this alienation is that of his soul which made him

very different track. When Mr. Khemka, a businessman in India asks about his family, he

narks that he had mentioned for the hundredth time the story of the strangers whose only

uple of wrinkled and cracked photographs.

vel explores the unique consciousness of Sindi in being an outsider in the scope of society

and his frustration of failure in finding a meaning of existence. Therefore, he was a man who did not have

his roots anywhere in the globe. The Foreigner relates how Sindi, an immigrant Indian, blinded by his own detachment in the course of his search for meaning and purpose of his life wherever he lives. He was bound to become cynical, misogynistic and detached with alienation and rootlessness.

As a study in alienation, The Foreigner explains Sindi's embarrassment projection of himself as a permanent foreigner, an existentialist exile and a stranger to himself, engrossed with the enigmatic nature of life. He acquires mental equanimity and redeems himself of his detachment and alienation with disinterested involvement. His alienation from the world is similar to many existing heroes in the west suffer from. His rootlessness is rooted within his soul like an ancient curse and drives him from crisis to crisis. Trapped in his loneliness, Sindi is accelerated by his withdrawal from the society around him and feels like a miserable alien that left him pale and exhausted. Sindi is lonely, anxious, depressed and dependent person who is painfully aware of the mess and is oppressed with the sadness of living. In this struggle for survival, he finds himself in a wilderness.

As a student of Engineering at Boston Sindi meets an American girl June at a foreign students' gathering.June is a woman craving to be of help to someone. His sense of detachment and rootlessness is evident when June asks Sindi where he was from. This reaction provides a clue to his alienation: Everybody always asked me the same silly question. "Where are you from?" as if it really mattered a great deal where I was from?" (2). Sindi looked uncomfortable at the very beginning of the encounter with June, when she says- "There is something strange about you, you know. Something distant. I'd guess that when people are with you they don't feel like they're with a human being. May be it's an Indian characteristic, but I have a feeling you'd be a foreigner anywhere" (3).

The painful experiences weighed heavily on his heart in the primary stage an abruptly becomes detached from everything, except himself. Sindi shows a positive attitude to various situations and problems in life. His search for the meaning of life ends and engages himself in the battle of survival that the workers of the factory could not have won without his help and guidance. He decides to infuse new life into the ruined business of Mr. Khemka and thus uplifts the employees who earn the daily bread of their families. He is lucky enough not to find absurdity and estrangement as the ultimate condition of life, and shows a tremendous capacity for transcendence. Such an enlightened attitude of Sindi not only minimizes psychic conflict arising out of the feelings of loneliness and worthlessness, but also creates one of the deepest forms of human happiness and shared enjoyment. There are other characters too, who are quite alienated in *TheForeigner*, Babu Khemka feels alienated from June and commits suicide. His father, an awful bully, is alienated from his son who is taken only as a pawn rather than a human being with individual traits. He can be considered as the first among Joshi's alienated foreigners who turn inwards to overcome the sense of futility and discern a world of meaningful relatedness within themselves, however limited it may be. The reason for his failure is not difficult to get. As he himself suggests: "Life is not a business account... once your soul goes bankrupt, no amount of plundering can enrich it again" (10). Towards the end, he becomes oriented towards duty without selfish desires. He takes up a line of reasoning that led to the inevitable conclusion that detachment consisted in getting involved with the world.

Arun Joshi gives the impression of a rebel who fights against the greed, violence, shams, and hypocrisy of the people and in the process alienates himself and his art from his fellow creatures. Joshi also gives the impression that his art is not social minded as he does not give any suggestions for the individual's integration with society. To counter this change one can say that the very fact that Joshi portrays such a society is an example of his concern with the evils of society and hence an unmistakable evidence of his social consciousness. The inner conflict of an individual is really his inner relations to the outward conflicts. An artist is not at all a preacher and it is not his task, like a physician to prescribe remedies. The

ıised by Arun Joshi, as a myth and the protagonists act as alien either to the
elves. The central characters are alien because they are exposed by their either
ıtification with the world.

The principal concern is to study the sense of alienation in the novels of Arun Joshi that intimidates to crush every sphere of human life. In discussing the theme of alienation in the Joshi's novels, it is mainly concerned, with man's alienation from society, which is the most prevalent kind of alienation, and his alienation from his own self.

References:

1. Joshi. Arun. *The Foreigner.* New Delhi: Orient, 1968. Print.
2. Bhatnagar, M.K. *The Novels of Arun Joshi: A Critical Study*. New Delhi: Atlantic, 2001.
3. Dhawan, R.K. *The Fictional World of Arun Joshi*. New Delhi: Prestige, 1986.
4. _____. *The Novels of Arun Joshi*. New Delhi: Prestige, 1992. Print.
5. Kumar, Lokesh. *Arun Joshi's Novels: His Vision of Life*. New Delhi: Sarup, 2004. Print.

Asian Journal of Chemistry; Vol. 28, No. 11 (2016), 2487-2494

ASIAN JOURNAL OF CHEMISTRY

http://dx.doi.org/10.14233/ajchem.2016.20039

Synthesis, Characterization and Biological Activity of Zn(II) Complexes with Dibasic Tridentate ONS-Donor Ligand

B. KARPAGAM[1], S. MATHAN KUMAR[2], J. RAJESH[3], K. DHAHAGANI[4] and G. RAJAGOPAL[5,*]

[1]Department of Chemistry, St. Michael College of Engineering and Technology, Kalayarkoil-630 551, India
[2]Department of Chemistry, K.S. Rangasamy College of Arts and Science (Autonomous), K.S.R. Kalvi Nagar, Tiruchengode-637 215, India
[3]Department of Chemistry, Sethu Institute of Technology, Kariapatti-626 106, India
[4]Department of Chemistry, M.S.S. Wakf Board College, Madurai-625 020, India
[5]PG & Research Department of Chemistry, Chikkanna Government Arts College, Tiruppur-641 602, India

*Corresponding author: E-mail: rajagopal18@yahoo.com

Received: 13 April 2016; *Accepted*: 30 July 2016; *Published online*: 10 August 2016; AJC-18024

A new kind of zinc(II) complexes **1** and **2** with new Schiff base ligand **(L)** have been synthesized and characterized by ^{1}H NMR, X-ray crystallography, IR and UV-visible spectroscopic studies. The trigonality index τ of 0.63 for complex **2** indicates that the coordination geometry around zinc is intermediate between trigonal bipyramidal and square pyramidal geometries and is better described as trigonal bipyramidal distorted square based pyramid (TBDSBP) with zinc displaced above the N(2), N(4), O(1) and S(1) coordination plane and towards the elongated apical N(1) atom. The newly synthesized Schiff base ligand **(L)** and its Zn(II) complexes **1**-**2** were assayed for *in vitro* antibacterial activity against two Gram-positive bacteria strains *(Staphylococcus aureus*, *Pseudomonas aeruginosa)* and Gram-negative bacteria *E. coli.* The cancer cell line studies of the effect of the ligand **(L)** and its Zn(II) complexes **1**-**2** on a MCF-7 cancer cell line by an MTT assay indicates that the ligand **(L)** exhibits higher activity towards the metal complexes **1** and **2** when compared with cyclophosphamide as reference drug.

Keywords: Thiosemicarbazone ligand, Zn(II) complexes, Crystal structure, Cell line studies.

INTRODUCTION

Thiosemicarbazones and their metal complexes exhibit a wide range of applications that extend from their use in analytical chemistry through pharmacology to nuclear medicine [1-4]. Schiff bases are regarded as "privileged ligands" due to their capability to form complexes with a wide range of transition metal ions yielding stable and intensely coloured metal complexes. Some of them have been shown to exhibit interesting physical and chemical properties and potential biological activities [5-10]. Attempts are being made to replace these platinum-based drugs with suitable alternatives and numerous metal complexes are synthesized and screened for their anticancer activities [11,12]. A wide repertoire of Zn(II) complexes have been utilized as radio protective agents [13] tumor photosensitizers [14] antidiabetic insulin-mimetic [15] and antibacterial or antimicrobial agents [16]. It is also eful to reduce the cardio and anticancer drugs [17]. However, city of zinc-based compounds s are as yet available [18].

In continuation of our work in the area of Schiff base complexes [19,20] a new type of Zn(II) complexes have been synthesized and characterized by NMR, IR, UV-visible spectroscopic methods and single crystal X-ray studies for the newly synthesized Zn(II) complexes **1** and **2**. Based on these studies a trigonal bipyramidal distorted square based pyramid (TBDSBP) has been proposed for the Zn(II) complexes. Apart from these studies in order to get a clear cut idea about the pharmacological properties of the Zn(II) complexes, antibacterial, antifungal and cancer cell line studies have been carried out.

EXPERIMENTAL

3-Ethoxysalicylaldehyde (Sigma-Aldrich) and N(4)-phenylthiosemicarbazide (Sigma-Aldrich), $Zn(OAc)_2{\cdot}2H_2O$, 2,2'-bipyridine (bpy) (Sigma-Aldrich), 1,10-phenanthroline (Phen) (E-Merck) were obtained commercially and used without further purification. Double distilled water is used for all the experiments. All the reagents and solvents were analytical, spectroscopic grade and they were used without further purification for the preparation of thiosemicarbazone ligand **(L)** and Zn(II) complexes **1** and **2**.

Physical measurements: Crystal data collection APEX2 (Bruker, 2004); cell refinement: SAINT (Bruker, 2004), ^{1}H NMR spectra are recorded on a Bruker 300 MHz spectrometer. IR spectra are recorded in KBr disks with a Perkin Elmer FT-IR spectrophotometer. UV-visible spectra of solution are recorded on a Shimadzu 1700 series spectrometer.

Antifungal screening: The antifungal activity of the ligand (**L**) and their Zn(II) complexes (**1-2**) are studied by paper disc method [21]. *Candida albicans sp*, *Aspergillus niger sp* and *Macrophonia sp* are used as test organisms. Solution of desired concentration (1 mg/mL) was obtained by dissolving 2, 4, 6 mg of each compound in DMSO and added to potato dextrose agar (PDA) medium in sterile Petri dishes. The sterilized medium with the added sample solution is poured into sterile Petri plates and allowed to solidify. Filter paper discs of 5 mm diameter are prepared prior to the experiment. The filter paper discs are placed on nutrient medium mixed with fungal strains. These Petri dishes are incubated at 35 °C for 48 h. The per cent reduction in the radial growth diameter over the control is calculated. The growth is compared with dimethyl sulfoxide as the control and *Ketokonazole* as a standard drug.

Antibacterial screening: Antibacterial activities are investigated using agar well diffusion method. The activity of the free ligand (**L**) and its Zn(II) complexes **1-2** and standard drug amikacin are studied against the Gram-positive bacteria strains (*Stapholococcus aureus*, *Pseudomonas aeruginosa*) and Gram-negative bacteria *E. coli*. The solution of 2 mg/mL of each compound [free ligand (**L**)] and its Zn(II) complexes (**1-2**) and standard drug (amikacin) in DMSO is prepared for testing against bacteria. Centrifuged pellets of bacteria from a 24 h old culture containing approximately 10^4 to 10^6 CFU (colony forming unit) per mL are spread on the surface of Muller Hinton agar plates. Wells are created in medium with the help of a sterile metallic bores and nutrients agar media (agar 20 g + beef extract 3 g + peptones 5 g) in 1000 mL of distilled water (pH 7.0), autoclaved and cooled down to 45 °C. Then, it is seeded with 10 mL of prepared inocula to have 10^6 CFU/mL. Petri plates are prepared by pouring 75 mL of seeded nutrient agar. The activity is determined by measuring the diameter of the inhibition zone (mm). The growth inhibition is calculated according to Kumar *et al.* [21].

Cell viability test: The viability of cells is assessed by MTT assay using mononuclear cells. The assay is based on the reduction of soluble yellow tetrazolium salt to insoluble purple formazan crystals by metabolically active cells. Only live cells are able to take up the tetrazolium salt. The enzyme (mitochondrial succinate dehydrogenase) present in the mitochondria of the live cells is able to convert internalized tetrazolium salt to formazan crystals, which are purple in colour. Then, the cells are lysed and dissolved in DMSO solution. The colour developed is then determined in an ELISA reader at 570 nm.

The Hepatocellular carcinoma cells (HepG2 cells) are plated separately in 96 well plates at a concentration of 1 × 10^5 cells/well. After 24 h, cells are washed twice with 100 µL [illegible]rved for 0.5 h at 37 °C. After [illegible]ith different concentrations of [illegible]) for 24 h. At the end of the treatment period, the medium is aspirated and serum free medium containing MTT (0.5 mg/mL) is added, then it is incubated for 4 h at 37 °C in a CO_2 incubator.

The MTT containing medium is then discarded and the cells are washed with PBS (200 µL). The crystals are then dissolved by adding 100 µL of DMSO and this is mixed properly by pipetting up and down. Spectrophotometrical absorbance of the purple blue formazan dye is measured in a micro-plate reader at 570 nm [22].

Synthesis of Schiff base ligand (L): 3-Ethoxy salicylaldehyde (0.5 mmol) in methanol (0.83 g) was taken in a round bottomed flask and stirred by a magnetic stirrer followed by dropwise addition of methanolic solution of 4-phenylthiosemicarbazide (3.0 mmol) for 2 to 4 h (**Scheme-I**). The resulting white solid was removed by filtration and washed with cold ethanol and dried *in vacuo* over anhydrous $CaCl_2$ to remove any moisture. m.p.: 210 °C, Yield: 82 %

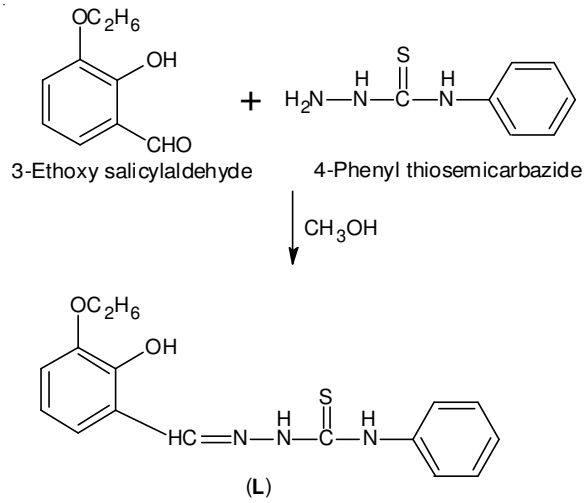

Scheme-I: Synthesis of the new thiosemicarbazone ligand (**L**)

Synthesis of the Zn(II) complexes 1-2: A solution of $Zn(OAc)_2{\cdot}2H_2O$ (0.55 g, 0.25 mmol) in ethanol, was added to a solution of thiosemicarbazone ligand (**L**) (0.79 g, 0.25 mmol) in a round bottomed flask with constant stirring. After 0.5 h, the base (0.25 mmol 2,2'-bipyridine)/(0.25 mmol 1,10-phenanthroline) dissolved in ethanol was added in the round bottomed flask. The stirring was continued for about 1 h and the yellow colour compound formed was filtered, washed with cold ethanol and ether and dried *in vacuo* over anhydrous $CaCl_2$. A single orange colour crystal suitable for the X-ray diffraction was obtained by slow evaporation of a solution of chloroform (**Scheme-II**).

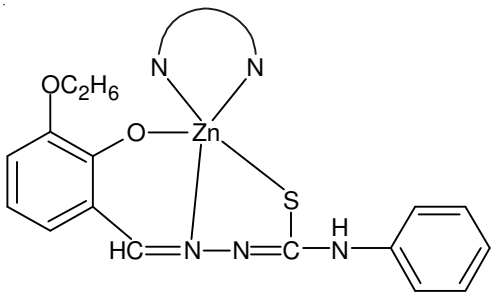

Scheme-II: Proposed structure of the complexes **1** and **2**

TABLE-1
CRYSTAL DATA AND STRUCTURE REFINEMENT FOR COMPLEX [ZnL(phen) (**1**) AND [ZnL(bpy)] (**2**)

Crystal data	Compound **1**	Compound **2**
Empirical formula	$C_{29}H_{24}N_5O_2SZnCl_3$	$C_{55}H_{52}N_{10}O_5S_2Zn_2$
Formula weight	678.31	1127.93
Wavelength	0.71073 Å	0.71073 Å
Crystal system	Monoclinic	Monoclinic
Space group	C2/c	P21/n
a, b, c (Å)	25.6400(6), 14.7350(4), 15.7130(3)	13.6702(4), 14.6101(5), 26.4561(8)
α, β, γ (°)	90, 90.7280(10), 90	90, 93.9540(10), 90
Volume	5936.0 (2) $Å^3$	5271.3 (3) $Å^3$
Z, Calculated density	8, 1.518 Mg/m^3	4, 1.421 Mg/m^3
F(000)	2768	2336
Crystal size	0.35 × 0.35 × 0.30 mm^3	0.30 × 0.20 × 0.20 mm^3
Temperature	293 (2) K	293 (2) K
θ Min-Max	2.05 to 25.00°	1.59 to 25.00°
Completeness to θ	25.00 99.9 %	25.00 99.8 %
Max. and Min. transmission	0.7536 and 0.6536	0.8563 and 0.7236
Final R indices [I >2σ(I)]	R1 = 0.0329, wR2 = 0.0828	R1 = 0.0360, wR2 = 0.0780
R indices (all data)	R1 = 0.0443, wR2 = 0.0916	R1 = 0.0648, wR2 = 0.0935
Largest diff. peak and hole	0.543 and -0.362 e.$Å^{-3}$	0.331 and -0.246 e.$Å^{-3}$

RESULTS AND DISCUSSION

Crystal structure of complex 1: The molecular structure of the complex along with atomic numbering is given in Fig. 1, Crystallographic parameters and selected bond lengths and angles are given in Tables 1 and 2. The compound crystallizes in a monoclinic lattice with space group C2/c. The zinc in the mononuclear complex is five-coordinate and is having approximately trigonal bipyramidal geometry. The basal coordination positions are occupied by the phenolato oxygen, O(1), azomethine nitrogen, N(5) and thiolate sulfur, S(1), of the thiosemicarbazone and the phen nitrogen, N(2). In a five-coordinate system, the angular structural parameter (τ) is used to propose an index of trigonality. In a five-coordinate system, the angular structural parameter (τ) is used to propose an index of trigonality. The trigonality index τ of 0.55 [According to Addison *et al.* [23], τ = (β-α)/60, where β = N(5)-Zn(1)-N(1) = 174.81(8)° and α = O(1)-Zn(1)-S(1) = 141.29(6)°] for perfect square pyramidal and trigonal bipyramidal geometries the values of τ are zero and unity, respectively [23]. This indicates that the coordination geometry around zinc is intermediate between trigonal bipyramidal and square pyramidal geometries and is better described as trigonal bipyramidal distorted square based pyramid (TBDSBP) with zinc displaced above the N(1), N(5), O(1) and S(1) coordination plane and towards the elongated apical N(2) atom [24]. The four base atoms are coplanar showing a significant distortion form a trigonal bipyramidal distorted square based pyramid geometry indicated by O(1)-Cu(1)-S(1) bond angle (141.29°). The central zinc atom is displayed from the basal plane in the direction of the axial nitrogen, which is evident from the bond angles of N(5)-Zn(1)-N(1), (174.81°), O(1)-Zn(1)-N(5), (89.95°). The bond angles O(1)-Zn(1)-N(2), (106.06°), N(2)-Zn(1)-N(1), (76.91°), N(5)-Zn(1)-N(2), (99.20°) indicate the distortion from a trigonal bipyramidal d geometry (τ = 0.55). One of om an ideal stereochemistry is osed by both the ligand and -N(2) bond angle 106.06° and

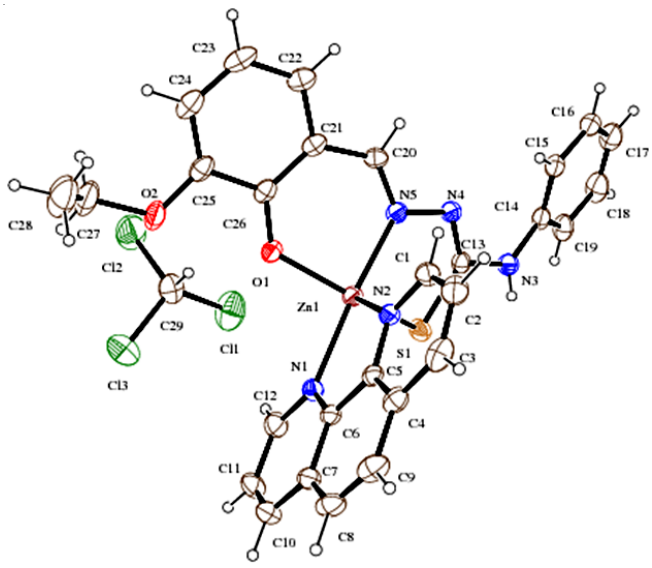

Fig. 1. Structure and labeling diagram of the complex **1**

TABLE-2
SELECTED BOND LENGTHS AND ANGLES FOR COMPLEXES **1-2**

Atoms	Compound **1**	Compound **2**
	Bond lengths	
N(1)-Zn(1)	2.189(2)	2.117(2)
N(2)-Zn(1)	2.132(2)	2.171(2)
O(1)-Zn(1)	1.9625(16)	1.944(2)
S(1)-Zn(1)	2.3737(7)	2.3362(8)
	Bond angles	
O(1)-Zn(1)-N(2)	106.06(8)	76.27(10)
O(1)-Zn(1)-N(1)	94.42(7)	101.59(9)
O(1)-Zn(1)-S(1)	141.29(6)	134.92(7)
N(2)-Zn(1)-S(1)	112.57(5)	96.13(7)
N(1)-Zn(1)-S(1)	96.49(6)	123.46(7)

N(1)-Zn(1)-S(1) bond angle 141.29°, indicate a slight tilting of the axial Zn(1)-N(1) bond in the direction of the O(1)-Zn(1) bond away from the S(1)-Zn(1) bond. The variation in Zn-N bond distances, Zn(1)-N(1) (2.189 Å), Zn(1)-N(2) (2.132 Å)

and Zn(1)-N(5) (2.059 Å) indicate differences in the strength of the bond formed by each of the coordinating nitrogen atoms. The difference in bond lengths can be attributed to the difference in the extent of π back-bonding between the 1,10-phenanthroline and thiosemicarbazone moieties. However, the large bond distance at the axial Zn (1)-N(1) positions supports the lack of significant out of plane π-bonding. Coordination to Zn(II) lengthens the C-S bond substantially to 1.752 Å from 1.680 Å in unsubstitued salicylaldehyde N(4) phenylthiosemicarbazone [25] as would be expected on coordination of thiolate sulfur. Hydrogen bonding interactions for complex **1** is shown in Fig. 2 and unit cell packing diagram of the compound is shown in Fig. 3.

Crystal structure of complex 2: The molecular structure of the compound **2** along with the atom numbering scheme is represented in Fig. 4. Crystallographic parameters and selected bond lengths and angles are given in Table-2. Suitable pale yellow crystals were obtained from a solution of **2** in a solvent of acetone. The compound **2** is monoclinic with a space group P21/n. This complex is mononuclear and five coordinated. In the complex [ZnLbpy], Zn(II) is located in an approximately trigonal bipyramidal geometry in which the equatorial positions are occupied by the S(1), O(1), N(1) and the axial positions by N(2) and N(4) [Zn(1)-N(2), 2.171(2), Zn(1)-N(4), 2.072(2) Å] with the N(4)-Zn(1)-N(2) angle of 173.06(9)° being close to the 'ideal' value of 180° which is usual for such systems [26]. In a five-coordinate system, the angular structural parameter (τ) is used to propose an index of trigonality. The trigonality index τ of 0.63 {According to Addison *et al.* [23], τ = (β-α)/60, where β = N(4)-Zn(1)-N(2) = 173.06(9)° and α

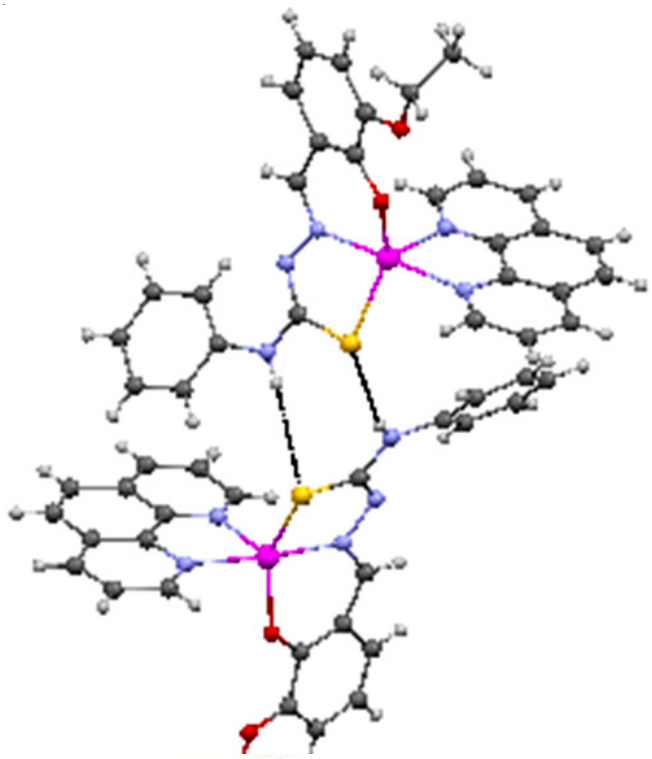

interaction for complex **1**

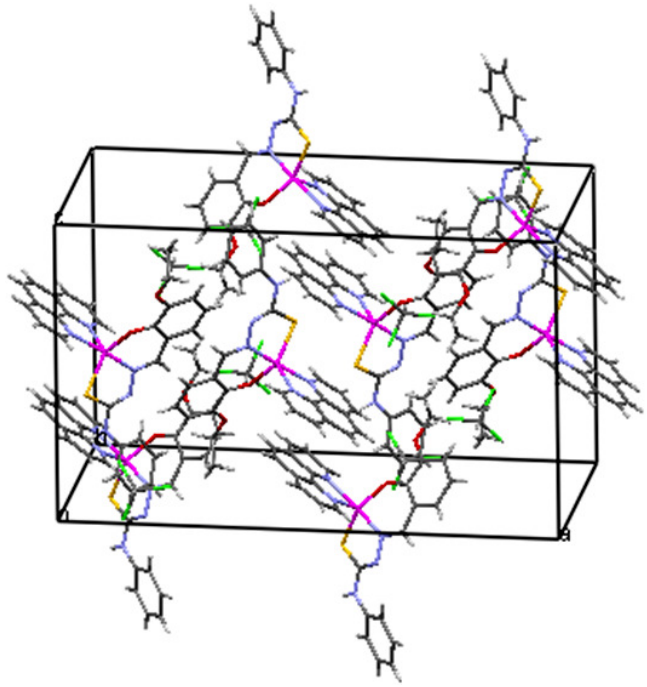

Fig. 3. Unit cell packing diagram of the complex **1**

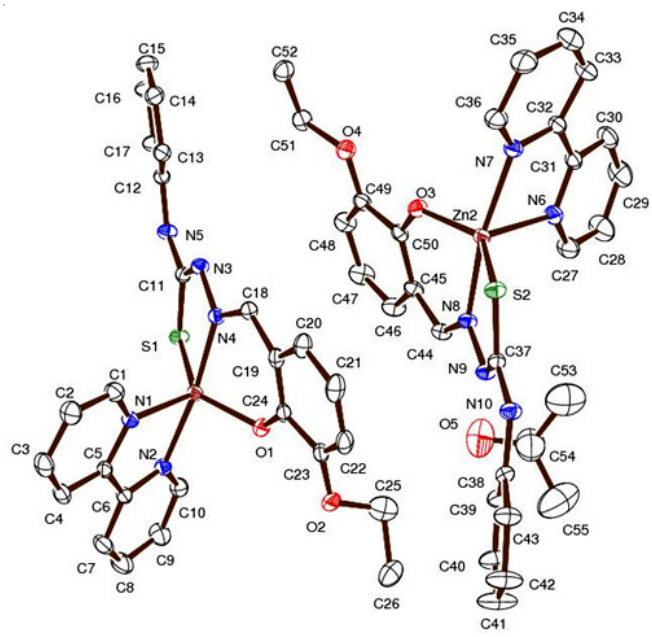

Fig. 4. Structure and labeling diagram of the complex **2**

= O(1)-Zn(1)-S(1) = 134.92(7)°; for perfect square pyramidal and trigonal bipyramidal geometries the values of τ are zero and unity, respectively [27]} indicates that the coordination geometry around zinc is intermediate between trigonal bipyramidal and square pyramidal geometries and is better described as trigonal bipyramidal distorted square based pyramid (TBDSBP) with zinc displaced above the N(2), N(4), O(1) and S(1) coordination plane and towards the elongated apical N(1) atom [28]. One of the reasons for the deviation from an ideal stereochemistry is the restricted bite angle imposed by both the $(L)^{2-}$ and 2,2'-bipyridine ligand. The bite angle around the metal *viz.* N(1)-Zn(1)-N(2) of 76.27(10)° may be considered normal, when compared with an average value of 77°

cited in the literature [35-37]. The variation in Zn-N bond distances, Zn(1)-N(1), 2.117(2), Zn(1)-N(4), 2.072(2) and Zn(1)-N(2), 2.171(2) indicate differences in the strengths of the bonds formed by each of the coordinating nitrogen atoms. The Zn-N bond lengths are shorter than those reported for mononuclear Zn(II) complexes, while there is no significant variation in the Zn-S bond lengths reported [29]. The dihedral angle formed by the least square plane for the compound **2**. The imine bond formation is evidenced from N(4)-C(18) and N(3)-C(11) distances of 1.283(4) Å and 1.296(4) Å. The C-N bond length of 1.396(4) Å and C-S bond length of 1.750(3) is similar to those reported for coordination of thiosemicarbazone in the thiolate form [30,31]. For complex **2**, hydrogen bonding inter-action (Fig. 5) and unit cell packing diagram of the compound is shown in Fig. 6. The molecules in the crystal lattice are stabilized by combination of hydrogen bonding and π-π interactions between aromatic rings.

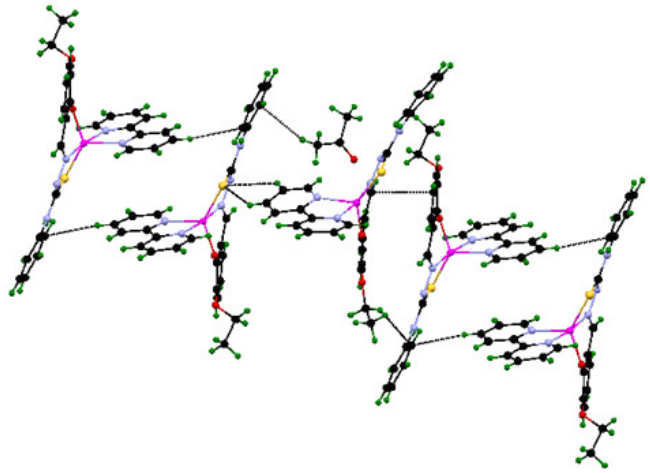

Fig. 5. Hydrogen bonding interaction for complex **2**

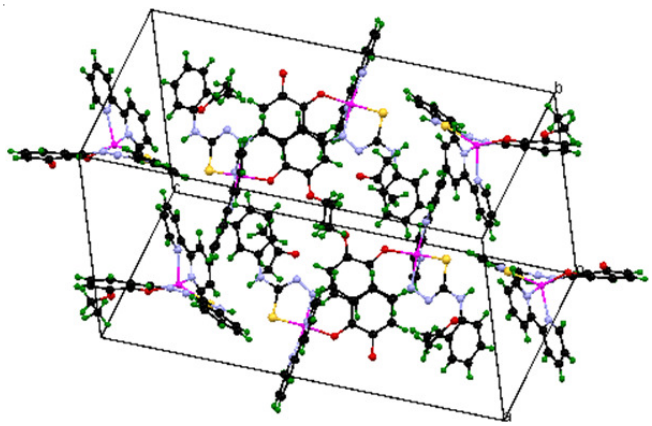

Fig. 6. Unit cell packing diagram of the complex **2**

^{1}H NMR spectra: ^{1}H NMR spectra of ligand **(L)** and its Zn(II) complexes (**1** and **2)** are recorded in DMSO-d_6 and the corresponding spectrum is given in Fig. 7. A singlet observed at δ 11.78 ppm in ligand **(L)** due to phenolic OH proton has disappeared in the complexes **1** and **2** [29]. The multiplet attributed to azomethine proton observed at δ 8.51 ppm is shifted to δ 8.76 ppm in the complex **2**. The ligand (**L**) shows a singlet at

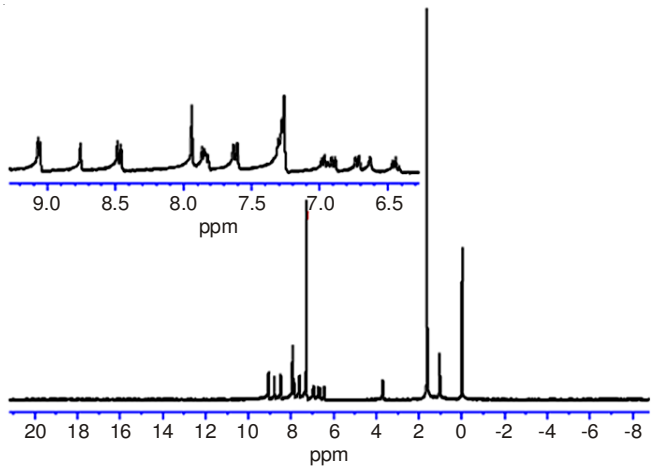

Fig. 7. ^{1}H NMR spectra of complex **2**

δ 10.03 ppm for NH proton and it is absent in the spectra of complex **2**, which clearly indicates the enolization of –NH-C=S group of the ligand (**L**) followed by deprotonation prior to coordination of the thiolate sulfur [32]. The two NH signals of the ligand **(L)** at δ 9.08 ppm and δ 10.04 ppm, respectively, were absent in the complex **2**. (One NH signal of the complex is disappeared, probably exchanged with the solvent) Signals observed in the ^{1}H NMR spectra of ligand at δ 10.03 and δ 8.51 ppm is due to the presence of NH (NH^1) and phenyl NH (NH^2) protons, respectively. The peak due to NH^1 has absent and the peak due to the phenyl NH proton shifted to downfield in the spectrum of complex **2**. The peaks displayed in the region of δ 7.2-7.5 ppm in the complex **2** are due to the aromatic protons of thiosemicarbazone and phenanthroline ligands. The ethoxy protons appeared as a quartet and a triplet at δ 3.00 and δ 1.22 ppm, respectively. Similar observations are observed for complex **1**. From the spectral data, it is clear that the coordination occurs through ONS donor ligand **(L)** for both the complexes **1** and **2**.

IR spectra: IR spectral data of the ligand (**L**) and complexes **1**-**2** are given in Table-3. The intense band in the region 1593 cm^{-1} in the IR spectrum of Schiff base ligand (**L**) is associated with C=N stretching vibration and is shifted to lower frequencies 1539 cm^{-1} in the spectrum of corresponding complex **1** and this change in value indicate the coordination of azomethine nitrogen to the metal ion [20a]. The band due to phenolic OH group disappeared in the IR spectrum of complex **1** in the region 3394-3299 cm^{-1} (Fig. 8) suggesting deprotonation of metal ion. In addition, a band appeared at 1275 cm^{-1} due to phenolic C-O stretching in the Schiff base ligand (**L**) has been shifted to 1308 cm^{-1} in the IR spectrum of the complex **1** indicating the coordination through phenolic oxygen atom. IR spectrum of free ligand (**L**) showed one band at 3468 cm^{-1} due to terminal NH^2 and this bands position altered in the spectrum of the corresponding complex **1**, revealing non participation of NH^2 in coordination [20b]. A band which appeared in the region 3174-2980 cm^{-1} due to N-H in the ligand (**L**) disappeared on complexation. Further, a band due to C=S (781 cm^{-1}) which appeared in the ligand has completely disappeared in the spectrum of the complexes and a new band appeared at 756 (**1**) and 737 (**2**) cm^{-1} (for C-S) due to enolization of -NH-C=S group of the ligand, followed by

TABLE-3
IR SPECTRAL DATA (cm^{-1}) AND UV SPECTRAL DATA (nm) OF FREE LIGAND (**L**) AND ITS Zn(II) COMPLEXES **1-2**

Compound	ν(CH=N)	ν(C-O)	ν(N-H)	ν(C=S)	ν(O-H)	ν(Zn-N)	ν(Zn-O)	λ_{max} (nm)
L	1593	1275	3468	781	3286	–	–	299, 336
1	1581	1308	3476	756	–	435	525	376
2	1583	1309	3482	737	–	483	575	375

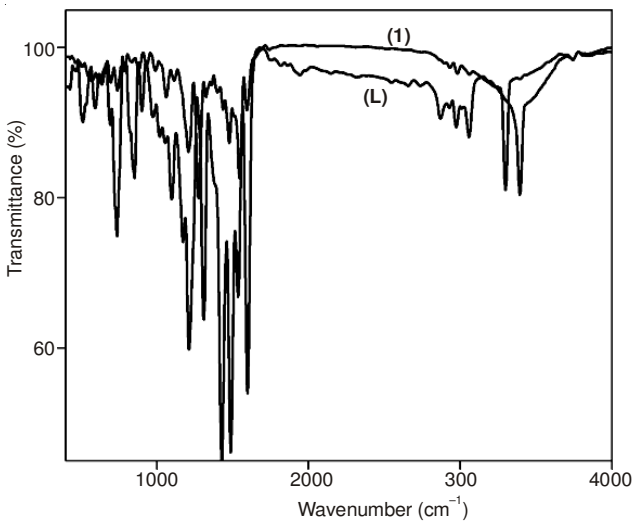

Fig. 8. IR spectra of ligand **(L)** and complex **1**

deprotonation prior to coordination of the thiolate sulfur [33]. The non-ligand bands observed in far IR region for complex **1** are assigned to ν(M-N) (483-435, cm^{-1}) and ν(M-O) (575-525, cm^{-1}) stretching vibrations. Two strong bands at 1580 and 1560 cm^{-1} assigned to ν(-C=C-) and ν(-C=N-) (of 2,2'-bipyridine), are shifted to higher frequencies by 12-29 cm^{-1}. Similarly, the strong bands observed at 1430, 1580 and 1560 cm^{-1} assigned to ν(ring), ν(C=C) and ν(C=N), respectively for 1,10-phenanthroline, are shifted to higher frequencies by 29-58 cm^{-1}. This indicates that the nitrogen atoms in phen and bpy coordinate to the complexes **1-2** [33,34].

Electronic spectra: The electronic spectra of the ligand (**L**) and its Zn(II) complexes **1-2** recorded in DMSO solvent and it shows four bands in the region 247, 297, 334 and 375 nm. The peaks below 300 nm are assigned to intraligand transitions, $n\rightarrow\pi^*$ and $\pi\rightarrow\pi^*$.The bands appeared in the region 377 nm (Table-3) are assigned to MLCT, respectively.

Antifungal activity: Table-4 indicates that the ligand as well as the complexes **1** and **2** has a significant degree of antifungal activity against, *Candida albicans*, *Aspergillus niger* and *Macrophonia* at 2 mg/mL concentration. The effect is susceptible to the concentration of the compound used for inhibition. The complex **2** shows greater activity against *Candida albicans* species. The antifungal activity of the ligand **(L)** and its Zn(II) complexes **1** and **2** varies in the following order of fungal species *Macrophonia* > *Candida albicans* > *Aspergillus niger*. The antifungal experimental results of the compounds were compared with the standard antifungal drugs ketokonazole at the same concentration. The complex **2** exhibit greater antifungal activities against *Candida albicans sp* and *Aspergillus niger sp* and the complex **1** is resistant to the above fungus. They also show low activity against *Macrophonia sp* than complex **1**. From the observed data it shows that the antifungal activity depends upon the type of metal complexes and varies in the following order of the metal complexes **2 > 1**.

Antibacterial activity: The antibacterial activity of the newly synthesized ligand **(L)** and its Zn(II) complexes **1** and **2** were determined by the standard 'disc diffusion' method. The ligand **(L)** it Zn(II) complexes **1** and **2** with the standard drug amikacin were screened separately for their antibacterial activity against the Gram-positive bacteria *Stapholococcus aureus*, *Pseudomonas aeruginosa* and Gram-negative bacteria *E. coli*. The results of the bacterial study of the synthesized compounds are shown in Table-5. The antibacterial activity of the ligand **(L)** and its Zn(II) complexes **1** and **2** varies in the following order of fungal species *Pseudomonas aeruginosa* > *Stapholococcus aureus* > *E. coli*. The antibacterial experimental results of the compounds were compared with the standard antibacterial drug amikacin at the same concentration. The complex **2** exhibit greater antibacterial activities against *Pseudomonas aeruginosa, Stapholococcus aureus* and *E. coli* and the complex **1** is resistant to the bacteria *E. coli*. Complex **1** also shows low activity against *Pseudomonas aeruginosa, Stapholococcus aureus* than complex **2**. From the observed data it shows that the antibacterial activity depends upon the type of Zn(II) complexes and varies in the following order of the metal complexes **2 > 1**. The increased activity of the Zn(II) chelates can be explained on the basis of chelation theory. It is known that chelation tends to make the metal complexes act as more powerful and potent bactericidal agents, thus killing more of the bacteria than the ligand **(L)**. It is observed that, in a complex, the positive charge of the metal is partially shared with the donor atoms present in the ligands and there may be π-electron delocalization over the whole chelating [35]. This increases the lipophilic character of the metal chelate and favours its permeation through the lipoid layer of the bacterial

TABLE-4
MINIMUM INHIBITION CONCENTRATION (MIC) DATA OF THE SYNTHESIZED LIGAND **(L)** AND Zn(II) COMPLEXES **1-2** AGAINST GROWTH OF BACTERIA AND FUNGI

	Microorganism (MIC) values				
	S. aureus	*P. aeruginosa*	*C. albicans*	*A. niger*	*Macrophonia*
	R	6	R	R	R
	7	12	R	R	12
	13	14	12	5	10

TABLE-5
PERCENTAGE OF CELL VIABILITY AND DEATH ANALYSIS IN DUPLICATE STUDY MODEL FOR LIGAND (L) AND Zn(II) COMPLEXES **1-2**

Compound	12.5 µg	25 µg	50 µg	100 µg
L	52.49	51.77	36.56	19.63
1	88.75	79.93	61.60	52.48
2	89.05	70.21	51.87	40.62
Cyclophosphamide	100	100	100	100

membranes. There are other factors which also increase the activity, which are solubility, conductivity and bond length between the metal and the ligand.

Cytotoxicity: The *in vitro* cytotoxic activities of the synthesized Schiff base ligand (**L**) and its Zn(II) complexes **1-2** are studied on human breast cancer cell lines (MCF-7) by applying the MTT colorimetric assay (Table-6). The calculated values, that is, the concentration (µg/mL) of a compound able to cause 50 % of cell death with respect to the control culture, are presented in Fig. 9. Cyclophosphamide is used as a reference compound. The MCF-7 cells are sensitive to the O-N-S Schiff base with the cell viability value of ligand **(L)** and their complexes **1-2** in µg. Taking into the account that thiosemicarbazone molecules exhibit cytotoxicity activity [36]. We have tested the ability of the ligands (**L**) and its Zn(II) complexes **1-2** inhibit the tumor cell growth. On comparison with the ligand and its Zn(II) complexes **1-2**, Ligand (**L**) show a higher value than Zn(II) complexes **1-2** which indicate the presence of bulky groups at position N(4) of the thiosemicarbazone moiety and heterocyclic bases 1,10-phenanthroline, 2,2′-bipyridine enhanced the anti-tumour activity [37-40]. The complexes **1** and **2** are cytotoxic to the breast cancer cell lines. Although the schiff base ligand (**L**) and its Zn(II) complexes

TABLE-6
IC_{50} VALUES FOR THE LIGAND (**L**) AND COMPLEXES **1-2**

Sample	IC_{50} values
Ligand (L)	25.5
[ZnL(phen)]	198.0
[ZnL(bpy)]	103.0

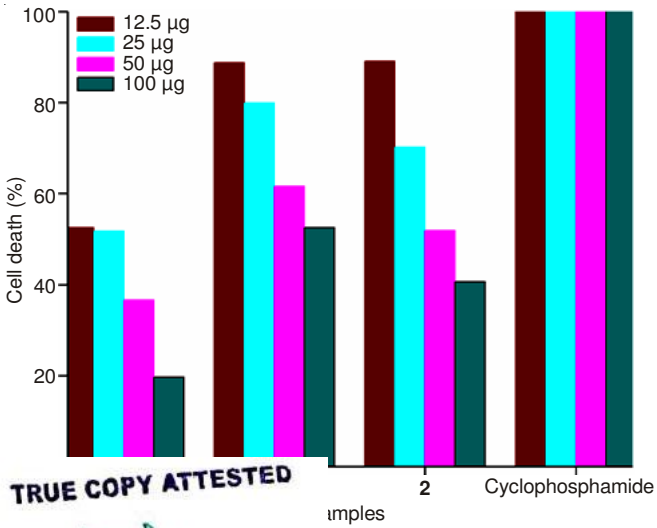

umples

nst cyclophosphamide, ligand (L) and

are less effective than cyclophosphamide, the schiff base ligand (**L**) is more effective than the complexes **1-2**. The different activities are currently being investigated in terms of the mechanism of action of these compounds at the cellular level [41].

IC_{50} values (compound concentration that produces 50 % of cell death) were calculated for the free ligand (**L**) and the title complexes **1-2** against human breast cancer cell lines (MCF-7). The ligand (**L**) and its Zn(II) complexes **1-2** exhibited significant anticancer activity. It is worth nothing that the free ligand (**L**) showed a lower IC_{50} value than the Zn(II) complex **1-2**, indicating that the antitumor activity of the ligand (**L**) is greater than that of the complexes **1-2**. Further, as revealed by the observed IC_{50} values, the potency of the ligand and its Zn(II) complexes to kill the cancer cells follows the order **L > 2 >1**, revealing that it varies with the mode and extent of interaction of the complexes with cyclophosphamide.

Supplementary data

CCDC 964627 and CCDC 964628 contain the supplementary crystallographic data for **1** and **2**. These data can be obtained free of charge viahttp://www.ccdc.cam.ac.uk/conts/retrieving.html, or from the Cambridge Crystallographic Data Centre, 12 Union Road, Cambridge CB2 1EZ, UK; fax: (+44) 1223-336-033; or e-mail: deposit@ccdc.cam.ac.uk.

ACKNOWLEDGEMENTS

Financial assistance received from the Department of Science and Technology, New Delhi, India [Grant No. SR/FTP/CS-40/2007] and University Grants Commission, New Delhi, India [F.No: 38-70/2009 (SR)] are gratefully acknowledged.

REFERENCES

1. D.X. West, J.K. Swearingen, J. Valdes-Martinez, S. Hernandez-Ortega, A.K. El-Sawaf, F. van Meurs, A. Castiñeiras, I. Garcia and E. Bermejo, *Polyhedron*, **18**, 2919 (1999).
2. P. Tarasconi, S. Capacchi, G. Pelosi, M. Cornia, R. Albertini, A. Bonati, P. Dall Aglio, P. Lunghi and S. Pinelli, *Bioorg. Med. Chem.*, **8**, 157 (2000).
3. S.E. Ghazy, M.A. Kabil, A.A. El-Asmy and Y.A. Sherief, *Anal. Lett.*, **29**, 1215 (1996).
4. A.R. Cowley, J.R. Dilworth, P.S. Donnelly, A.D. Gee and J.M. Heslop, *Dalton Trans.*, **31**, 2404 (2004).
5. S. Chandra, P. Shikha and K. Yatender, *Bioinorg. Chem. Appl.*, **Article ID 851316** (2009).
6. R. Kothari and B. Sharma, *J. Chem. Chem. Sci.*, **1**, 158 (2011).
7. U. Kumar and S. Chandra, *J. Saudi Chem. Soc.*, **15**, 19 (2011).
8. S. Chandra, L.K. Gupta and S. Agrawal, *Transition Met. Chem.*, **32**, 558 (2007).
9. S. Chandra and Ruchi, *Spectrochim. Acta A*, **103**, 338 (2013).
10. S. Chandra, S. Bargujar, R. Nirwal and N. Yadav, *Spectrochim. Acta A*, **106**, 91 (2013).
11. (a) S. Ramakrishnan, V. Rajendiran, M. Palaniandavar, V.S. Periasamy, B.S. Srinag, H. Krishnamurthy and M.A. Akbarsha, *Inorg. Chem.*, **48**, 1309 (2009); (b) S. Ramakrishnan, D. Shakthipriya, E. Suresh, V.S. Periasamy, M.A. Akbarsha and M. Palaniandavar, *Inorg. Chem.*, **50**, 6458 (2011).
12. (a) H.H. Thorp, *Chem. Biol.*, **5**, R125 (1998); (b) H. Vahrenkamp, *Dalton Trans.*, **42**, 4751 (2007); (c) A.I. Anzellotti and N.P. Farrell, *Chem. Soc. Rev.*, **37**, 1629 (2008).
13. S. Emami, S.J. Hosseinimehr, S.M. Taghdisi and S. Akhlaghpoor, *Bioorg. Med. Chem. Lett.*, **17**, 45 (2007).
14. Q. Huang, Z. Pan, P. Wang, Z. Chen, X. Zhang and H. Xu, *Bioorg. Med. Chem. Lett.*, **16**, 3030 (2006).
15. (a) A. Nakayama, M. Hiromura, Y. Adachi and H.J. Sakurai, *Biol. Inorg. Chem.*, **13**, 675 (2008); (b) H. Sakurai, Y. Yoshikawa and H. Yasui, *Chem. Soc. Rev.*, **37**, 2383 (2008).

16. M.T. Kaczmarek, R. Jastrzab, E. Holderna-Kedzia and W. Radecka-Paryzek, *Inorg. Chim. Acta*, **362**, 3127 (2009).
17. M.M. Ali, E. Frei, J. Straub, A. Breuer and M. Wiessler, *Toxicology*, **179**, 85 (2002).
18. Q. Jiang, J. Zhu, Y. Zhang, N. Xiao and Z. Guo, *Biometals*, **22**, 297 (2009).
19. (a) S. Mathan Kumar, K. Dhahagani, J. Rajesh, K. Nehru, J. Annaraj, G. Chakkaravarthi and G. Rajagopal, *Polyhedron*, **59**, 58 (2013); (b) K. Dhahagani, S. Mathan Kumar, G. Chakkaravarthi, K. Anitha, J. Rajesh, A. Ramu and G. Rajagopal, *Spectrochim. Acta A*, **117**, 87 (2014); (c) K.K. Raja, D. Easwaramoorthy, S.K. Rani, J. Rajesh, Y. Jorapur, S. Thambidurai, P. Athappan and G. Rajagopal, *J. Mol. Catal. Chem.*, **303**, 52 (2009); (d) G. Puthilibai, S. Vasudhevan, S. Kutti Rani and G. Rajagopal, *Spectrochim. Acta A*, **72**, 796 (2009).
20. (a) J. Rajesh, A. Gubendran, G. Rajagopal and P.R. Athappan, *J. Mol. Struct.*, **1010**, 169 (2012); (b) J. Rajesh, M. Rajasekaran, G. Rajagopal and P.R. Athappan, *Spectrochim. Acta A*, **97**, 223 (2012); (c) A. Gubendran, J. Rajesh, K. Anitha and P.R. Athappan, *J. Mol. Struct.*, **1075**, 419 (2014).
21. G. Kumar, D. Kumar, S. Devi, R. Johari and C.P. Singh, *Eur. J. Med. Chem.*, **45**, 3056 (2010).
22. T. Mosmann, *J. Immunol. Methods*, **65**, 55 (1983).
23. A.W. Addison, T.N. Rao, J. Reedijk, J. van Rijn and G.C. Verschoor, *J. Chem. Soc., Dalton Trans.*, **158**, 1349 (1984).
24. Y. Hayashi, R. Matsuda, K. Ito, W. Nishimura, K. Imai and M. Maeda, *Anal. Sci.*, **21**, 167 (2005).
25. E.B. Seena and M.R.P. Kurup, *Spectrochim. Acta A*, **69**, 726 (2008).
26. C.B. Castellani, G. Gatti and R. Millini, *Inorg. Chem.*, **23**, 4004 (1984).
27. N.J. Ray and B.J. Hathaway, *Acta Crystallogr.*, **34**, 3224 (1978).
28. R.P. John, A. Sreekanth, V. Rajakannan, T.A. Ajith and M.R.P. Kurup, *Polyhedron*, **23**, 2549 (2004).
29. C. Zhang and C. Janiak, *J. Chem. Crystallogr.*, **31**, 29 (2001).
30. E.B. Seena, M.R. Prathapachandra Kurup and E. Suresh, *J. Chem. Crystallogr.*, **38**, 93 (2008).
31. T. Bal-Demirci, *Polyhedron*, **27**, 440 (2008).
32. S. Güveli, N. Özdemir, T. Bal-Demirci, B. Ülküseven, M. Dinçer and Ö. Andaç, *Polyhedron*, **29**, 2393 (2010).
33. R. Prabhakaran, R. Sivasamy, J. Angayarkanni, R. Huang, P. Kalaivani, R. Karvembu, F. Dallemer and K. Natarajan, *Inorg. Chim. Acta*, **374**, 647 (2011).
34. T.A. Gerber, A. Abrahams, P. Mayer and E. Hosten, *J. Coord. Chem.*, **56**, 1397 (2003).
35. J.R. Dilworth, *Coord. Chem. Rev.*, **21**, 29 (1976).
36. S.G. Teoh, S.H. Ang, S.B. Teo, H.K. Fun, K.L. Khew and C.W. Ong, *J. Chem. Soc., Dalton Trans.*, 465 (1997).
37. S.K. Jain, B.S. Garg and Y.K. Bhoon, *Spectrochim. Acta A*, **42**, 959 (1986).
38. M.E. Hossain, M.N. Alam, J. Begum, M. Akbar Ali, M. Nazimuddin, F.E. Smith and R.C. Hynes, *Inorg. Chim. Acta*, **249**, 207 (1996).
39. D. Gambino, *J. Med. Chem.*, **4**, 1 (2004).
40. S. Singh, N. Bharti, F. Naqvi and A. Azam, *Eur. J. Med. Chem.*, **39**, 459 (2004).
41. X.Y. Qiu, S.Z. Li, A.R. Shi, Q. Li and B. Zhai, *Chin. J. Struct. Chem.*, **31**, 555 (2012).

Certain Investigation on Gabor Filter Based Facial Expression Recognition Viewed Automatically

H. Peer Oli and Dr.S. Senthamarai Kannan

Abstract--- *Today facial expression recognition and gender detection are great impact in various applications. Even though various level of papers are recognizing individual impact in both above mention needs. In this paper it resolve the drawbacks by combine both two applications. Computer vision toolbox is used for fast and accurate extraction of feature points such as pupils, nostrils and mouth edges. It has a wide scope of applications in different fields like pattern recognition and commercial market. In various extraction methods proposed in the past, steady extraction was difficult due to influences such as individual differences, expression variations, face direction or illumination variations and so forth. These methods are better than the previous PCA technique in terms of extraction accuracy and processing speed. This proposed method achieves high position accuracy at a low computing cost by combining shape extraction with pattern matching. Results of testing facial images under various conditions show for 35 static images the feature point extraction rate was 96%. In the case of dynamic images the extraction rate for 22 was 91% at a speed of 11trials/s, without using hardware. Finally Gabor filter is used to extract noise present in the image and facial expression should detect from input image.*

Keywords--- *Face Recognition, Gender Detection, Resolution Computer Vision Toolbox, Image Processing Toolbox, PCA.*

I. INTRODUCTION

Already lot of paper are described about either face expression detection or filter techniques. Even though some paper initiate about the both concept their filtering image are not clear. In this paper described about Gabor filter technique. The Gabor filter also like also like a band pass filter. So it allow only rest of high and low frequently that mean it is intermediate between high and low pass filter. Then we get the filtered image as output act as input to face detection. Computer vision tools box is a predefined tool used to recognize the expression of the human, PCA technique supports for the gender detection.

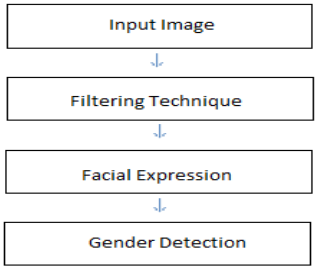

Figure 1: General Flow

Professor, Department of Electronics and Communication Engineering, Mohamed Sathak Engineering College, Tamilnadu, India. E-mail:peer@rediffmail.com
ıan, Professor, Department of Computer Science Engineering, Pannai College of Engineering and Technology, ımilnadu, India.

Power Efficient Probabilistic Multiplier for Digital Image Processing Subsystems

VenkateshBabu.S [#1], Ravichandran.C.G [*2]

[#] Information and Communication Engineering, Anna University
Mohamed Sathak Engineering College, Kilakarai, Tamilnadu, India
[1] ecebabu06@gmail.com

[*] Information and Communication Engineering, Anna University
Excel Engineering College, Namakkal, Tamilnadu, India
[2] cg_ravi@yahoo.com

***Abstract*—Power efficient is an important availability for various image processing subsystems and portable devices applications. The design of proposed probabilistic multiplier is to trade a lesser amount of accuracy with reduced power consumption. In this paper, the probabilistic multiplier is eliminating the some part of the partial product generating path in least significant bit to reduce the power consumption and transistor count. The power consumption and probabilistic error behaviour of the proposed multiplier is verified and compared with other multipliers.**

Keyword-Acceptable Accuracy, Partial Product Generation Path, Probabilistic Approach, Minimum Absolute Mean Error, Image processing Subsystem

I. INTRODUCTION

Multipliers are the basic blocks in different digital image processing applications such as image compression, image filtering and so on. In most of the image processing applications; human being can obtained valuable information from a little incorrect yield. The design of multiplier having low power consumption and low propagation delay results of great interest for the implementation of modern digital systems. The optimization of multipliers in terms of power, delay and transistor count have been presented in the literature [1], [2]. Braun multiplier consists of group of AND gates and adders [3]. It does not require any logic registers. This multiplier is inefficient for larger input bit widths. The Braun multiplier has produced more switching problem due to carry ripple adder in final stage.

The design of Baugh Woolley multiplier is based on carry save logic [4]. The power consumption of this multiplier depends on the number of bit sizes and the layout. It requires larger transistor counts. The booth multiplier accepts the bits in 2's complement logic based on radix-2 calculation [5], [6]. It reduces the partial product generation of the multiplier. The booth multiplier is suitable for larger input bit pattern. The design complexity of booth multiplier is due to the storage capability of secondary circuits for signed operands. Wallace tree multiplier is to minimize the partial product by the use of carry save adder trees [7]. This tree multiplier is efficient for the input bit widths of less than 32 bits. It has complex inter connection path in the layout design. The design time of this tree multiplier is very large and it consumes a lot of area.

Many research efforts have been reviewed for designing power efficient multiplier [8], [9]. The truncated multipliers are not producing all the LSB part of the partial product with reduced area and delay. It has more error for larger input bit width multiplication process. The truncation error produced from the fixed width truncated multiplier is to reduce in booth and array multiplier. Post truncated booth multiplier has lesser amount of truncation error, but it consumes larger area [10]. The process gain of these multipliers is adjusted by the different hardware logic elements.

The idea of an error tolerance and the PCMOS (Probabilistic CMOS) are important in digital image processing subsystems [11], [18] - [20]. The circuit is error tolerant if it contains faults that may cause both internal and external errors. The ways of improving chip yield by using imperfect chips in application where degradation of output quality is acceptable. The generation of acceptable results is more important than totally accurate results in digital application [12]. The n-bit ETM (Error Tolerant Multiplier) is splitting into two blocks. This multiplier contains an equal bit of two separate parts such as accurate and inaccurate multiplier part. The chance of receiving an exact product becomes possible with longer delay path [13]. The design complexity is high for these multipliers with reasonable power consumption and accuracy. The upper part of LSB values are suffered by accuracy problem for smaller as well as larger input bit width.

multipliers [14], [15] are designed by using the speculative adders to calculate the final ucts. It is to reduce the critical path of summing the partial products. The LSB parts in neglected by the use of error compensation techniques for high speed operation. The is multiplier is high for larger input bit pattern. The imprecise multiplier architecture is

A ULTRA-LOW POWER ROUTER DESIGN FOR NETWORK ON CHIP

Alaaudeen K.M, Vengatesh Kumar S

Department of Electronics & Communication Engineering,
Mohammed Sathak Engineering College, Ramnad, TN, India

ABSTRACT

The design of more complex systems becomes an increasingly difficult task because of different issues related to latency, design reuse, throughput and cost that has to be considered while designing. In Real-time applications there are different communication needs among the cores. When NoCs (Networks on chip) are the means to interconnect the cores, use of some techniques to optimize the communication are indispensable. From the performance point of view, large buffer sizes ensure performance during different applications execution. But unfortunately, these same buffers are the main responsible for the router total power dissipation. Another aspect is that by sizing buffers for the worst case latency incurs in extra dissipation for the mean case, which is much more frequent. Reconfigurable router architecture for NOC is designed for processing elements communicate over a second communication level using direct-links between another node elements. Several possibilities to use the router as additional resources to enhance complexity of modules are presented. The reconfigurable router is evaluated in terms of area, speed and latencies. The proposed router was described in VHDL and used the ModelSim tool to simulate the code. Analyses the average power consumption, area, and frequency results to a standard cell library using the Design Compiler tool. With the reconfigurable router it was possible to reduce the congestion in the network, while at the same time reducing power dissipation and improving energy.

KEYWORDS

Buffer, Latency, Network on chip, reconfigurable router, Throughput

1. INTRODUCTION

For Future MPSoC, a new communication design paradigm is needed. This communication medium should aim to provide high throughput, scalability, low power, reduced packet loss, utilize link efficiently, reduce contention and occupy less area on silicon. Chip density is increasing, allowing even larger systems to be implemented on a single chip.With increasing demands on flexibility and performance, these systems, known as Systems-on-Chips (SoCs), combine several types of processor cores, memories and custom modules of widely different sizes to form Multi-Processor Systems-on-Chips (MPSoCs). The bottleneck in such systems is shifting from computation to communication. The traditional way of using bus-based mechanisms for inter-module communication has two main limitations. Firstly, it does not scale well with complexity. Secondly, it couples computation and communication of the longer design times. Networks-on- Chip (NoCs) have been proposed as an

efficient and scalable alternative to shared buses which allow systems to be designed modularly. From the above MPSoC examples one can see that, as it happens in the microprocessor market, each NoC used in an MPSoC can have different communication performance and costs, depending on the target application. Designing the same NoC router to cover the whole spectra of applications would mean an oversized and expensive router, in terms of area and power. At the same time, designing specific routers for different markets would mean that many important decisions would have to be taken at design time, hence precluding scalability and online optimizations targeting different behaviours with different application demands. This paper is organized as follows. Section II presents an analysis of the problem and identifies low efficiency in homogenous routers. The reconfigurable router is proposed in Section IV, where we describe the differences between the original and the new router architecture. In Section V, we present results of latency, buffer utilization, frequency, and power consumption. In Section VI, show some related works and a specific comparison of our proposal with the conclusions.

2. SYSTEM OVERVIEW

Communication between the hardware resources will occupy a very important place in future System-on-Chip designs. From the communication point of view it is convenient to use the OSI model to describe our platform. As Fig. 1 shows, at the highest-level the application designer uses the services offered by the layer beneath, the OS. For out platform the OS that manages the underlying communication infrastructure is called the operating system for reconfigurable systems .It is based on real-time Linux on top of which specific capabilities have been added. Part of the OS is implemented in hardware. The hardware part provides a standard interface to the IPs and the means to manage the data network. The transport level is also implemented by the interfaces. Router is the main building block of the Network. It serves two main functions, First it acts as the interface between the PEs and network. To provide re-configurability, wrappers are used to provide interface for non -compatible PEs. And secondly, it routes the data packets to the right path.

3. SOC ARCHITECTURE

System-on-Chip consists of a heterogeneous set of processors connected via a Network-on-Chip as depicted in Fig.2. The net work consists of a set of interconnected by links. In this paper a regular two dimensional mesh topology of the routers. Ever y router is connected with its four neighbouring routers via bidirectional point-to-point links and with a single processor tile via the tile interface The SoC system is organized as a centralized system: one node, called Central Coordination Node (CCN), performs system coordination functions. The main task of the CCN is to manage the system resources. It performs run -time mapping of the newly arrived applications to suitable processing tiles and inter-processing communications to a concatenation of net work links. It also tries to satisfy Quality of Service (QoS) requirements, to optimize the resources usage and to minimize the energy consumption.

A. RECONFIGURABLE ROUTER ARCHITECTURE

The router architecture used in a Network on chip is a routing switch with up to five bi-directional ports (Local, North, South, West, and East), each port with two unidirectional router connected to four neighboring routers (North, South, West, and East).

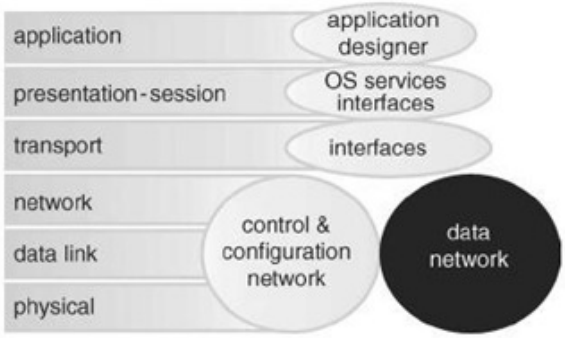

Fig 1. The Structure of our Platform from the Communication Point of View

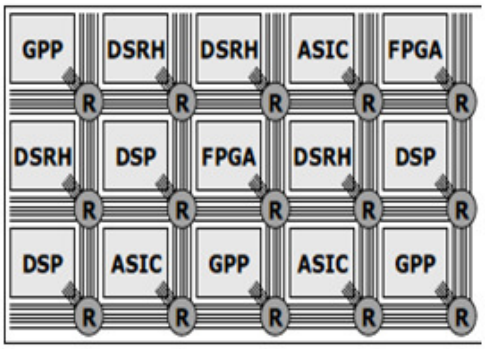

Fig 2. An Example of a Heterogeneous System-on-Chip (SoC) with a Network-on-Chip (NoC)

This router is a VHDL soft core, parameterized in three dimensions: communication width, input buffers depth, and routing information width. The architecture use the wormhole switching approach and a deterministic source based routing algorithm. The routing algorithm used is XY routing, capable of supporting dead-lock-free data transmission and the flow control is based on the handshake protocol.

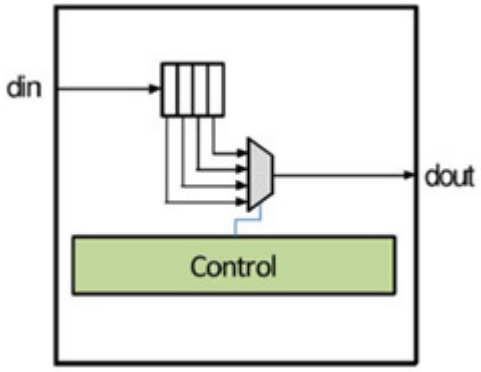

Fig 3. Input FIFO for Original Router

The wormhole strategy breaks a packet into multiple flow control units called flits, and they are sized as an integral multiple of the channel width. The first flit is a header with destination address followed by a set of payload flits and a tail flit. To indicate this information (header, payload, and tail flits) two bits of each flit are used. There is a round-robin arbiter at each output channel. The buffering is present only at the input channel. Each flit is stored in a FIFO buffer unit. The input channel is instantiated to all channels of the NoC, and thus all channels have the same buffer depth defined at design time.

B. RECONFIGURABLE ROUTER ARCHITECTURE

The proposed architecture is able to sustain performance due to the fact that, statistically, not all buffers are used all the time. In our architecture it is possible to dynamically reconfigure different buffer depths for each channel. A channel can lend part or the whole of its buffer slots h the requirements of the neighbouring buffers. To reduce connection costs, only use the available buffer slots of its right and left neighbour channels.

This way each channel may have up to three times more buffer slots than its original buffer with the size defined at design time.

Figure 4 present the reconfigurable channel as an example. In this architecture it is possible to dynamically configure different buffer depths for the channels. In accordance with this figure, each channel has five multiplexers, and two of these multiplexers are responsible to control the input and output of data. These multiplexers present a fixed size, being independent of the buffer size. Other three multiplexers are necessary to control the read and write process of the FIFO. The size of the multiplexers that control the buffer slots increases according to the depth of the buffer. These multiplexers are controlled by the FSM of the FIFO.

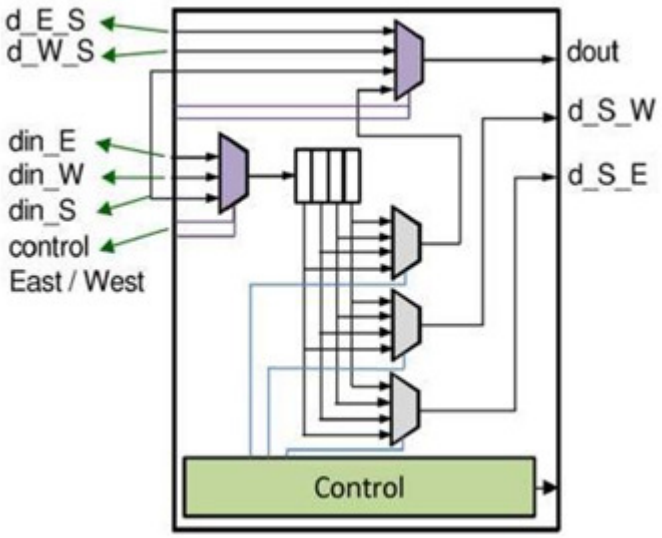

Fig.4. Input FIFO for Reconfigurable Router

In order to reduce routing and extra multiplexers, it adopted the strategy of changing the control part of each channel. Some rules were defined in order to enable the use of buffers from one channel by other adjacent channels. When a channel fills all its FIFO it can borrow more buffer words from its neighbours. First the channel asks for buffer words to the right neighbour, and if it still needs more buffers, it tries to borrow from the left neighbor FIFO. In this manner, some signals of each channel must be sent for the neighboring channels in order to control its stored flits.

Each channel needs to know how many buffer words it uses of its own channel and of the neighboring channels, and also how much the neighbor channels occupy of its own buffer set. A control block informs this number. Then, based on this information, each channel controls the storage of its flits. These flits can be stored on its buffer slots or in the neighbor channel buffer slots. Each input port has a control to store the flits and this control is based in pointers. Each input channel needs six pointers to control the read and writing process: two pointers to control its own buffer slots, two pointers to control the left neighbor buffer slots, and two more pointers to control the right neighbor buffer slots. In this design, it's not considering the possibility of the Local Channel using neighboring buffers, only the South, North, West, and East Channel of a e use of their adjacent neighbours.

C. RELIABLE ROUTER ARCHITECTURES

On-chip networks have a tight area and power budget, necessitating simple router structures. Architectural approaches to reliable router architectures include triple modular redundancy (TMR) based approaches, such as the Bullet Proof router. However, in general, N modular redundancy approaches are expensive, as they require at least N times the silicon area. Another strategy explores the trade-offs of various levels of redundancy. Other working vest gates the reliability of single components, for example a reliability-enhanced crossbar. Reconfiguration is approached by for pipelines, by for link failures, and by with modular design. Protection against transient errors has been explored.

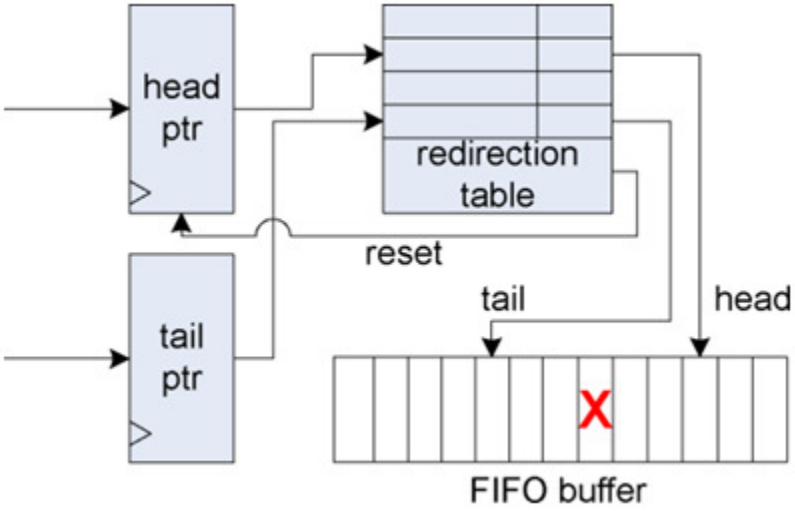

Fig.5. Flexible FIFO buffer logic

The reconfiguration process begins when one router broadcasts an error status bit through the network, although not necessarily its location, via an extra wire in each link. The initialized BIST unit then performs a distributed synchronization algorithm with other routers BIST units, ensuring that each BIST in the network runs all remaining routines in lock-step. After synchronization, each component of each router is diagnosed for faults. The diagnosis step does not rely on information from previous diagnostic phases, or from the detection mechanism, thus all permanent faults are diagnosed (or re-diagnosed), regardless of whether they are responsible for triggering this reconfiguration event, or not. Once all components and routers have been tested, faulty components are disabled and normal operation resumes. Since the BIST units are operational only during reconfiguration, they are power-gated off during normal operation for wear out protection.

D. INPUT PORT SWAPPING

During the initial evaluation often a few faults would disable multiple network links or disconnect important processor nodes. To prevent this, we developed input port swapping to consolidate several faults into a single link failure, and to provide additional priority for maintaining connected processors. In order to safely route through the network, the routing algorithm requires ional links. Each link is comprised of two input ports and two output ports, all st be fully functional for the link to be operational. If one of these ports fails,

port swapping may be used to maximize functional bidirectional links. Each input port is comprised of a FIFO buffer and a decode unit, identical for each direction of traffic input port swapper is used to modify which physical links are connected to each input port. For instance, Fig. 6 illustrates an example where a fault on the South port and a second fault in the adapter FIFO are consolidated, allowing the adapter link to use the former South FIFO. While it would be possible to include an additional output port swapper at the output ports, their small area and consequent low probability of faults did not warrant the area overhead of an additional swapper. On the other hand, the input ports constitute the majority of the total router area and therefore are most susceptible to faults. Thus, adding input port swappers provides with the ability to consolidate the impact of several faults into one, or a few, links.

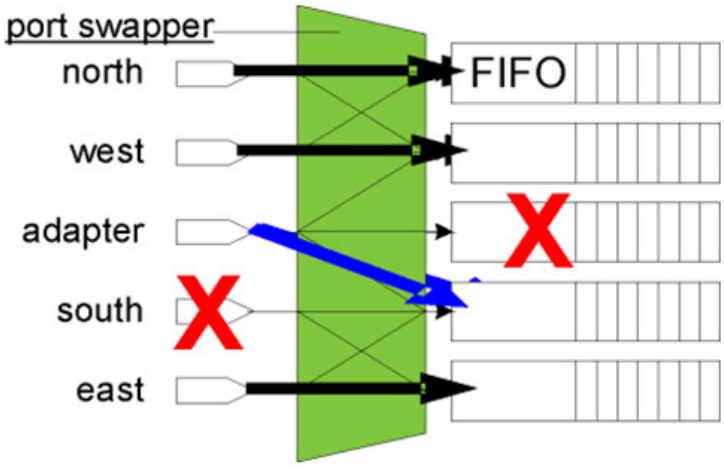

Fig.6. Port swapping unit

4. NETWORK SIMULATION

Figure 7 shows the channel of figure 4 organized to constitute the reconfigurable router. Each channel can receive three data inputs. Let us consider the south channel as an example, having the following inputs: the own input (din_s), the right neighbor input (din_e), and the left neighbor input (din_w). For illustration purposes, let us assume we are using a router with buffer depth equal to 4, and there is a router that needs to be configured as follows: south channel with buffer depth equal to 9, east channel with buffer depth equal to 2, west channel with buffer depth equal to 1, and north channel with buffer depth equal to 4. In such case, the south channel needs to borrow buffer slots from its neighbors. As the east channel occupies two of its four slots, this channel can lend two slots to its neighbor, but even then, the south channel still needs more three buffer slots. As the west channel occupies only one slot, the three missing slots can be lent to the south channel. When the south channel has a flit stored in the east channel, and this flit must be sent to the output, it is passed from the east channel to the south channel (d_e_s), and so the flit is directly sent to the output of the south channel (dout_s) by a multiplexer. The south channel has the following outputs: the own output (dout_s) and two more outputs (d_s_e and d_s_w) to send the flits stored in its channel but belonging to neighbor channels. The choice to resend the flits stored in a neighbor channels to its own channel before sending them to the output was preferred in order to avoid changes in others mechanisms of the architecture.

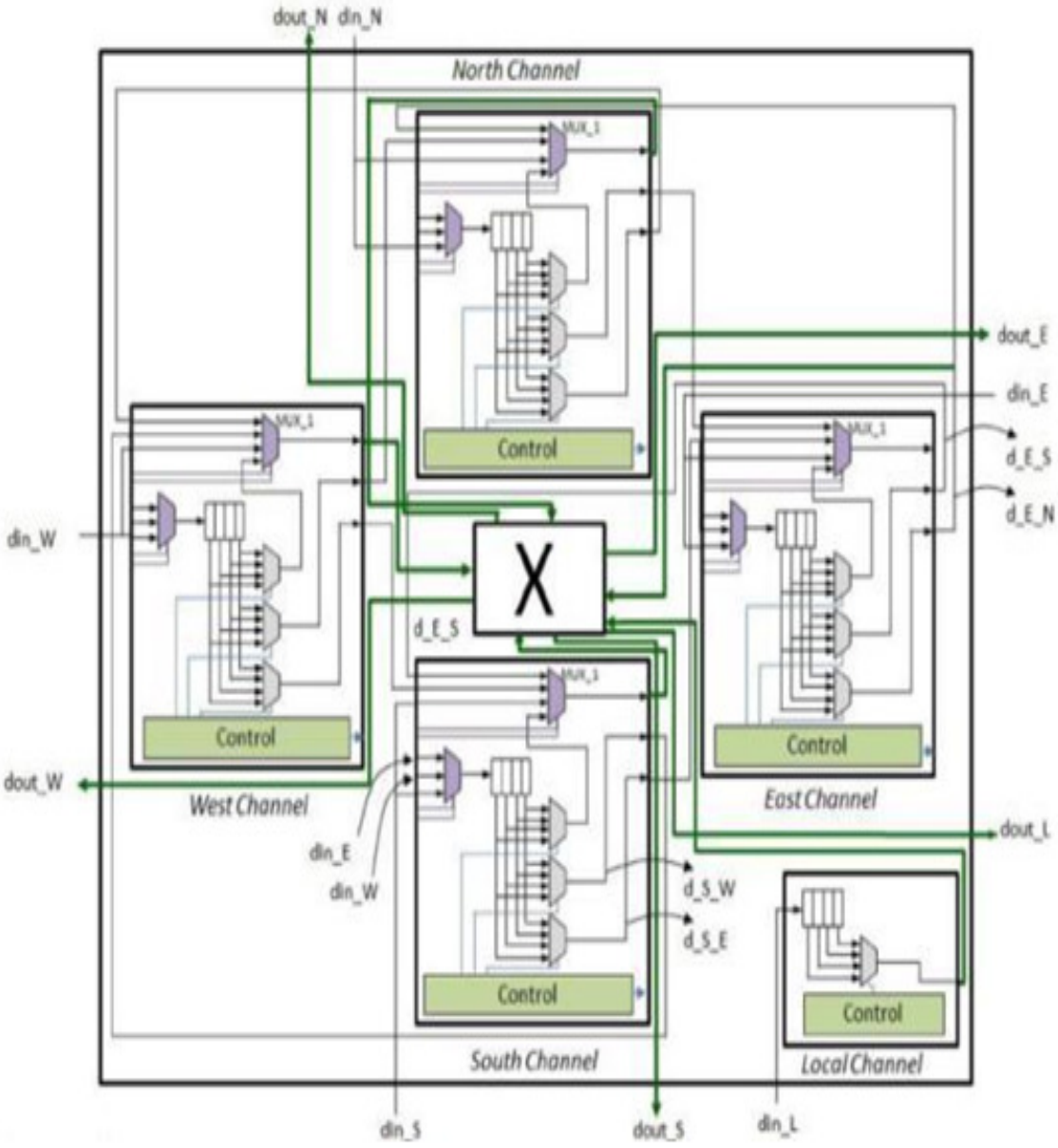

Fig.7. Proposed Router Architecture

Figure 7 shows an example of the reconfiguration in a router according to a needed bandwidth in each channel. First, a buffer depth for all channels is decided at design time in this case, it defined the buffer size equal to 4, as illustrated in Figure 7. After this, the traffic in each channel is verified and a control defines the buffer depth needed in each link to attend to this flow, as shown in Figure 7.The distribution of the buffer words among the neighbor channels is realized as shown in Figure 7.Meanwhile, the buffer physical disposition in each channel correspondent the FIFO depth initially defined, as shown in Figure 7. But the allocation of buffer slots among the channels can be changed at run time, as exemplified in Figure 7.

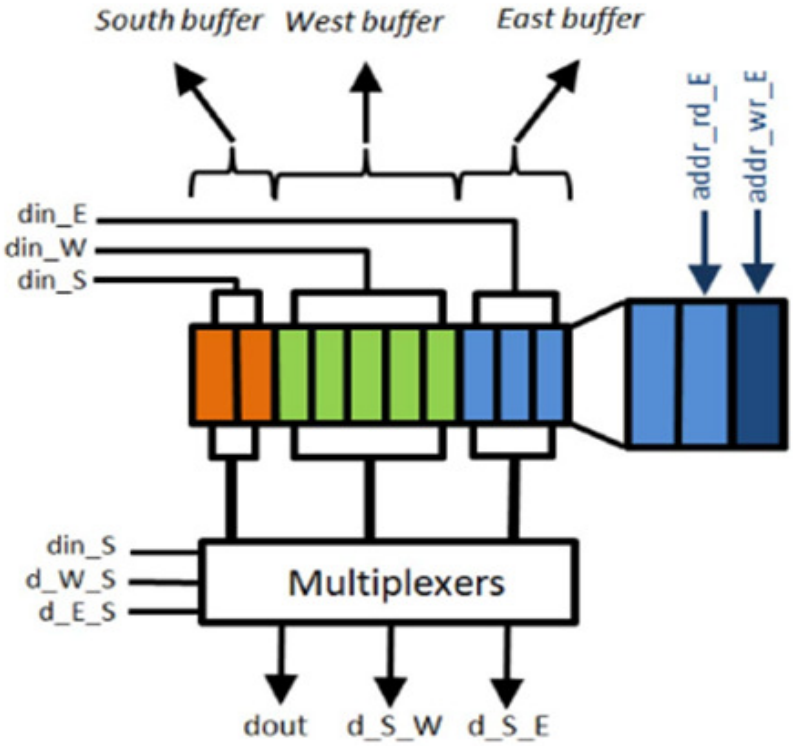

Fig 8 South Input Channel with the Buffers Partitioned for Three Channels

In this example considering again the South channel. Let us assume that the South channel divides part of its buffer with the neighboring channels (West and East channels). In this case, South channel uses only two buffer slots, five buffer slots are used by West channel, and three buffer slots are used by East channel. The number of buffers of a channel is partitioned according to the need for loans among the channels. In this way, each buffer slot is allocated in a mutually independent way. Pointers to each buffer partition are used in order to control the flit storage Figure.8 South input channel with the buffers partitioned for three channels: South, West, and East. Process (read and writes). Each slice of partitioned buffer in a channel has two pointers, one to control the read and another to control the write in the buffer (for example, addr_rd_E and addr_wr_E in Figure 8). Besides the pointers, there are other control signals that are needed, as the signal that indicates when the partitioned buffers are empty and full. With these signals, each channel allows neighbour channels to allocate buffer slots of this port and to guarantee that the flits are not mixed among the channels.

The information about how many slots of buffers are used for each channel can been used to dynamically adjust their usage, consequently improving the efficiency. With this, one can monitor the NoC traffic flow and analyze how the resources are being used. This information can be used to increase the efficiency of the NoC design. In this proposal consists of reconfiguring the channel according to the availability of buffers in the channels. If a new channel depth is required, the buffer depth is updated slot by slot, and this change is made whenever a buffer slot is free.

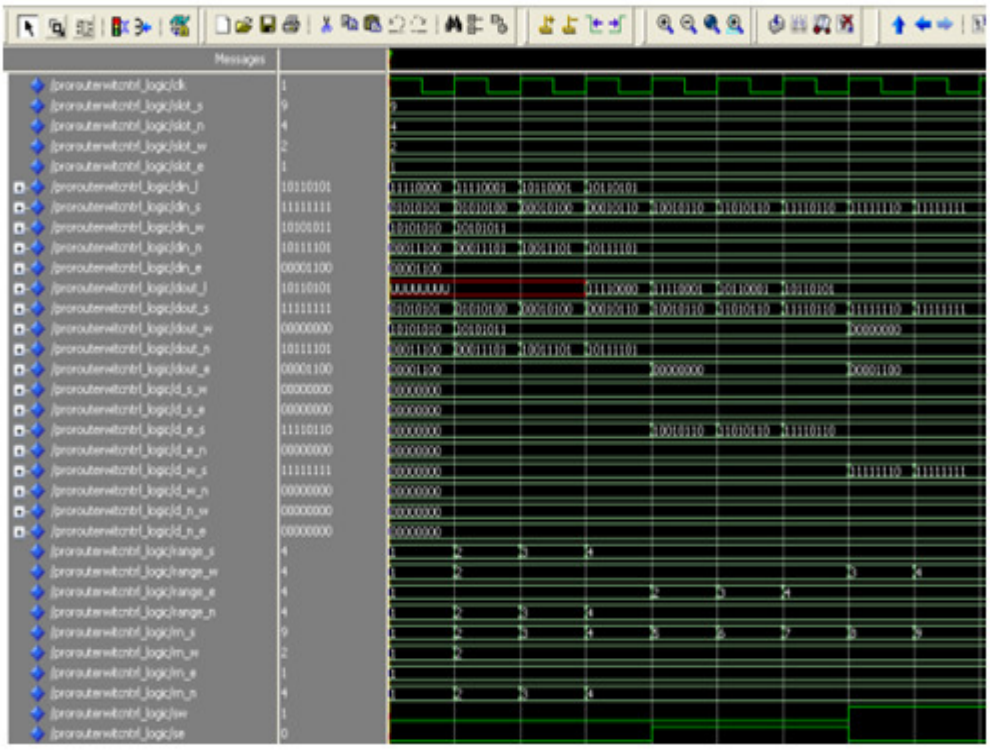

Fig.9 Output Waveform of Reconfigurable Router

5. RESULT ANALYSIS

The proposed router was described in VHDL and used the ModelSim tool to simulate the code. Analyses the average power consumption, area, and frequency results to a standard cell library using the Design Compiler tool. The design operates at a supply voltage of 1.8 V, and the power results were obtained with a 200 MHz clock frequency in both architectures. The performance comparison of Routers is shown in Table 6.1. With the proposed router it is possible to have one single NoC connecting different applications that might change their communicating patterns at run time. In the same way, this architecture allows application updates without compromising the performance of the system. Meanwhile, if a homogeneous router had been used in these situations, design modifications at design time would have had to be made to achieve the optimum case. In such case, one would need to redesign the homogeneous NoC to set buffer sizes and position of the cores in the network. The technique here proposed avoids costly redesigns and new manufacturing.

Table 1. Comparison of Routers and PAR Ameters

Parameters	Area (um^2)	Delay (ns)	Function Block Inputs Used
Original Router	233.815	46.4	59%
Reliable Router	260.5	45.4	95%
Reconfigurable Router	340.861	40.4	89%

6. CONCLUSIONS

This paper has described the architecture of a new dynamically reconfigurable NoC with intelligent nodes that changes the communication parameters for high data throughput and less timing delays. Our simulation results have demonstrated the effective use of network resources, making it a suitable alternative to traditional NoC. The downside of this network in the form of complexity of its node is compensated by the increased data throughput and low silicon cost. This kind of NoC can be ideal for reconfigurable MPSoCs with multimedia capabilities or for safety critical systems where the timing constraints are tight. Future work is to include reconfiguration with fault tolerance for the same modified system. A built-in self-test at each router diagnoses the number and locations of hard faults. Architecture features, including crossbar bypass bus and port swapping, are then to be deployed to work around the faults for better performance.

REFERENCES

[1] Ahmad and T.Arslan,"Dynamically reconfigurable NOC with bus based interface for ease of integration and reduced designed time,"2008.

[2] Ahonen and J.Nurmi, "Hierarchically heterogeneous network - onchip,"2007.

[3] Mahdi Imani and Ulisses M. Braga-Neto" Maximum-Likelihood Adaptive Filter for Partially Observed Boolean Dynamical Systems"2017

[4] S. F. Ghoreishi* and D. L. Allaire "Adaptive Uncertainty Propagation for Coupled Multidisciplinary Systems"2017

[5] Mahdi Imani and Ulisses M. Braga-Neto "Control of Gene Regulatory Networks with Noisy Measurements and Uncertain Inputs

[6] Al Faruque and J. Henk el, "Configurable links for runtime adaptive on-chip communication,"2009.

[7] Azimi, N.Cherukuri, "Integration challenges and tradeoff fortera - scale architectures," Aug 2007.

[8] Benini and De Micheli, "Analysis of power consumption on switch fabrics in network routers,"2002.

[9] Bertozzi, A.Jalabert, "NoC synthesis flow for customized domain specific multiprocessor systems-on-chip," Feb 2005.

[10] Bouhraoua and E.Elrabaa, "Addressing heterogeneous bandwidth requirements in modified fat-tree network-on-chip," 2008.

[11] Jingcao R.Marculescu, "System-level buffer allocation for application-specific networks-on-chip router design," Dec 2006.

[12] Lanand J. Chen, "BiNoC: A bidirectional NoC architecture with dynamic self-reconfigurable channel," 2009.

[13] Lee and N.Bagherzadeh, "Increasing the throughput of an adaptive router in network-on-chip (NoC),"2006.

[14] Leeand H.Yoo, "Low-power network -on-chip for high performance SoC design," Feb 2006.

[15] C.Crall, "challenges and opportunities in many-core computing," May 2008.

CiiT bringing the world locally
Digital Image Processing

Open Access Subscription or Fee Access

Real Time HD Video Segmentation using WavGMM with Shadow Elimination

S.A. Fatima Nuvairah, K. Monisha

Abstract

This paper proposes a high performance foreground detection from HD video frames by incorporating wavelet features in the conventional Gaussian Mixture model namely 'WavGMM'(wavelet based GMM). Compared to other existing background subtraction algorithms, GMM is widely used owing to its better performance in the case of multimodal background. However, GMM degrades from its behavior in the situation such as noisy and non-stationary background, slow foregrounds, and illumination variation. In order to increase the performance of GMM, wavelet subbands are introduced in the mixture of Gaussians. Finally the accuracy of conventional GMM is compared with the proposed GMM.

Keywords

Foreground, HD Video, Wavelet, GMM, Background Subtraction, WavGMM

Full Text:

herjee, Q. M. Jonathan Wu, and Thanh Minh Nguyen,' Multi- resolution based Gaussian Mixture
ground suppression' IEEE Transactions On Image Processing, Vol. 22, No December 2013

M.Genovese, E.Napoli, and N. Petra, "OpenCV compatible real time processor for background foreground identification," in Proceedings of the International Conference on Microelectronics (ICM '10), pp. 467–470, December 2010.

Chiu, M. Y. Ku, and L.W. Liang, "A robust object segmentation system using a probability-based background extraction algorithm," IEEE Transactions on Circuits and Systems for Video Technology, vol. 20, no. 4, pp. 518–528, 2010

H. Jiang, H. Ard¨o, and V. ¨Owall, "A hardware architecture for real-time video segmentation utilizing memory reduction techniques," IEEE Transactions on Circuits and Systems for Video Technology, vol. 19, no. 2, pp. 226–236, 2009

F. Kristensen, H. Hedberg, H. Jiang, P. Nilsson, and V. ¨ Owall, "An embedded real-time surveillance system: implementation and evaluation," Journal of Signal Processing Systems, vol. 52, no. 1, pp. 75–94, 2008

H. Jiang, H. Ardo, and V. ¨ Owall, "Hardware accelerator design for video segmentation with multi-modal background modelling" in Proceedings of the IEEE International Symposium on Circuits and Systems (ISCAS '05), vol. 2, pp. 1142–1145, 2005

J.C.S. Jacques, C. R. Jung, and S. R. Musse,Background subtraction and shadow detection in grayscale video sequences," in Proceedings of the 18th Brazilian Symposium on Computer Graphics and Image Processing (SIBGRAPI '05), pp. 189–196, October 2005

Stauffer and W. E. L. Grimson, "Adaptive background mixture models for real-time tracking," in Proceedings of the IEEE Computer Society Conference on Computer Vision and Pattern Recognition (CVPR '99), pp. 246–252, Fort Collins, USA, June 1999.

K. Toyama, J. Krumm, B. Brumitt, and B. Meyers, "Wallflower: principles and practice of background maintenance," in Proceedings of the 1999 7th IEEE International Conference on Computer Vision (ICCV '99), pp. 255–261, September 1999

Ridder, O.Munkelt, and H. Kirchner, "Adaptive background estimation and foreground Detection using Kalman filtering," in Proceedings of the 10th International Congress for Applied Mineralogy (ICAM '95), pp. 193–199, 1995

Refbacks

There are currently no refbacks.

Influence of Temperature in Scattered SiNW MOSFET

I. Sheik Arafat, N. B. Balamurugan & S. Bismillah Khan

Proceedings of the National Academy of Sciences, India Section A: Physical Sciences

ISSN 0369-8203

Proc. Natl. Acad. Sci., India, Sect. A Phys. Sci.
DOI 10.1007/s40010-017-0385-2

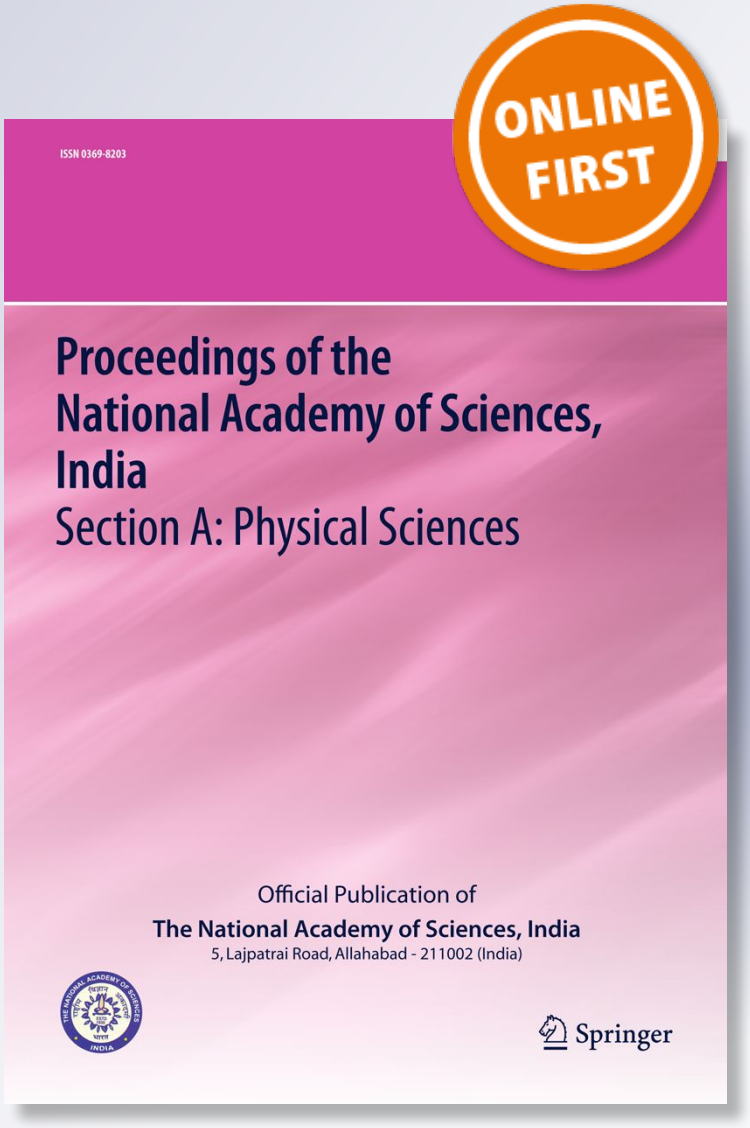

Springer

JÖKULL JOURNAL
JOKULL ISSN: 0449-0576
Vol 64, No. 3;Mar 2014

Role of Discrete Dopants in Carrier Transport of Near Ballistic Silicon NanoWire MOSFET

I.Sheik arafat
Assistant Professor, Mohamed sathak Engineering College, Kilakarai, India,
sheik.arafat@gmail.com
N.B.Balamurugan
Associate Professor, Thiagarajar College of Engineering, Madurai, India.
nbbalamurugan@tce.edu

Abstract – In this paper, we have investigated the Scattering effects in Carrier Transport of Near-ballistic SiNW MOSFET, which incorporates elastic scattering, optical phonon emission and its combination with random discrete dopants. Current–voltage (I–V) characteristics with impurity limited mobility is compared with Natori's Ballistic and Quasi-Ballistic Transport model. We study the impact of random discrete dopants in the device leads on the current variability of a Gate-All-Around (GAA) SiNW MOSFET, which shows a remarkable decrease in electric current, mobility variation and transconductance because of limited dopant mobility. Analog parameters like the transconductance (g_m), the transconductance generation factor (g_m/I_d), the early voltage (V_A) have also been investigated. Effectiveness of the proposed model has been confirmed by comparing the analytical results with the TCAD simulation results.

Keywords: Silicon NanoWire(SiNW) MOSFET, Random Discrete dopants, Elastic scattering, Optical phonon emission, TCAD.

1. Introduction

Integrated Circuit (IC) technology has been regarded as one of the most important inventions in engineering history. The remarkable progresses in IC technology in the past four decades have become the driving force of the Information Technology revolution, which has marvelously changed our lives

orld.

f the miracle in IC ctually simple: scaling sion of each transistor, the basic element of integrated circuits, and also in increasing the total number of transistors in a single IC chip. The device scaling has been successfully predicted by Moore's law.

The advancements in nanofabrication have made it possible to drastically shrink the channel length of electron devices and also to approach ballistic transport. The continued success in device scaling is necessary for maintaining the successive improvements in IC technology.

As the MOSFET gate length enters the nanometer regime, however, short

Applied Mechanics and Materials Vol. 573 (2014) pp 201-208
Online available since 2014/Jun/18 at www.scientific.net

doi:10.4028/www.scientific.net/AMM.573.201

Effects of Roughness Scattering in Carrier Transport of Near Ballistic Silicon NanoWire MOSFET

I.Sheik arafat[1,a *] , N.B.Balamurugan[2,b] ,C.Priya[3,c]

[1] Assistant Professor, Mohamed sathak Engineering College, Kilakarai, India.
[2]Associate Professor,Thiagarajar College of Engineering, Madurai, India.
[3] Assistant Professor, Syed Ammal Engineering College, Ramanathapuram, India.
[a]sheik.arafat@gmail.com,[b]nbbalamurugan@tce.edu,[c] harinikpriya@gmail.com

Keywords: Silicon NanoWire (SiNW) MOSFET, Surface Roughness, Elastic scattering, Optical phonon emission, TCAD.

Abstract – In this paper, we have investigated the Scattering effects in Carrier Transport of Near-ballistic SiNW MOSFET, which incorporates elastic scattering, optical phonon emission and its combination with Roughness Scattering. Current–voltage (I–V) characteristics of Proposed model is compared with Natori's Ballistic and Quasi-Ballistic Transport model. We study the impact of Surface Roughness in the device leads on the current variability of a Gate-All-Around (GAA) SiNW MOSFET, which shows a remarkable decrease in electric current, mobility variation and transconductance because of scattered mobility. Analog parameters like the transconductance (g_m), the transconductance generation factor (g_m/I_d), the early voltage (V_A) have also been investigated. Effectiveness of the proposed model has been confirmed by comparing the analytical results with the TCAD simulation results.

Introduction

Integrated Circuit (IC) technology has been regarded as one of the most important inventions in engineering history. The remarkable progresses in IC technology in the past four decades have become the driving force of the Information Technology revolution, which has marvelously changed our lives and the whole world. The secret of the miracle in IC technology is actually simple: scaling down the dimension of each transistor, the basic element of integrated circuits, and also in increasing the total number of transistors in a single IC chip. The device scaling has been successfully predicted by Moore's law.

The advancements in nanofabrication have made it possible to drastically shrink the channel length of electron devices and also to approach ballistic transport. The continued success in device scaling is necessary for maintaining the successive improvements in IC technology. As the MOSFET gate length enters the nanometer regime, however, short channel effects (SCEs)[14], such as threshold voltage (V_T) rolloff and drain-induced-barrier-lowering (DIBL), become increase significantly, that limits the scaling capability of planar bulk or silicon-on-insulator (SOI) MOSFETs. At the same time, the relatively low carrier mobility in silicon (comparing with other semiconductors) may also degrade the MOSFET device performance (e.g., ON-current and intrinsic device delay). The reason behind on various novel device structures and materials such ras silicon nanowire transistors[15], carbon nanotube FETs , new channel materials (e.g., strained silicon, pure germanium) and molecular transistors has been realized.

Among all most promising post-CMOS structures, the Silicon NanoWire Transistor (SiNWT) has its unique merits. SiNWT is based on silicon, a material that the semiconductor industry has been working on over thirty years, it would be really more attractive to stay on silicon and also achieve good device metrics which nanoelectronics being provided. As a result, the SiNW MOSFET are now
ı from both the semiconductor industry and academia [16] and it is also a
vice structure for future high-density LSI application.
s, to study the impact of Surface Roughness on device current(I_d), mobility
nalog parameters like the transconductance (g_m), the transconductance
$_m/I_d$) and the early voltage (V_A) investigated in SiNW MOSFET.The

International Journal on Applications in Information and Communication Engineering
Volume 1: Issue 7: July 2015, pp 28-30. www.aetsjournal.com ISSN (Online) : 2394-6237

Modelling Of Future Nano Transistor

T.Serlin Mariya , I.Sheik Arafat

Abstract— The study is to focus on different scattering effects in Silicon NanoWire (SiNW) MOSFET. The proposed system shows the impact on Gate All Around (GAA) Silicon NanoWire (SiNW) MOSFET with precisely positioned dopants. I-V characteristics of my proposed model are compared with various other Si nanowire transistor scattering models using the MATLAB simulation tool. The result of this analysis gives the study on the current variability of the device, which shows decrease in electric current. From this it provides the guidance for future development of Si nanowire transistor.

Keywords: Silicon NanoWire MOSFET, Gate All Around, MATLAB

I. INTRODUCTION

Great deal of improvement in performance and the density have been achieved since the invention of integrated circuit(IC) technology. For more than four decades, Dennard's rules of scaling have dominated the evolution of complementary metal oxide semiconductor design, fulfilling the notation of Moore's law. The development in nanofabrication has made it possible to considerably shrink the channel length of the devices and also move towards ballistic transport. However, the last technology do have some additional problems for scaling, which in turn relates to several issues like Short Channel Effects (SCE), Drain Induced Barrier Lowering (DIBL), large static power consumption, increased access resistance and also more pronounced variability and reliability.

Today's solid state research tries to counterbalance these effects by means of such multi-gate configurations with silicon nanowire technology, since it has low carrier mobility in silicon when compared with other semiconductors. The Silicon NanoWire Transistor (SiNWT) has its unique merits like low noise intensity, low cost and are compatible with current. Small size of silicon nanowire makes their electronic and electrical properties strongly dependent on the growth of direction, size, surface and reconstruction.

The aim of this paper is to study the impact of various scattering models by comparing the I-V characteristics using the MATLAB simulation tool.

SiNW MOSFET STRUCTURE

Silicon NanoWire transistors with various types of cross-sections are being extensively explored by a number of experimental groups. The various cross sections are the cylindrical wire (CW), triangular wire (TW) and rectangular wire (RW) nanowire FET. Here we consider the n-channel cylindrical SiNW MOSFET of 2 nm thick SiO_2 gate oxide. Current flow along the direction of source to drain. Continuously the random discrete dopants are added in the 4nm region of Source and Drain leads.

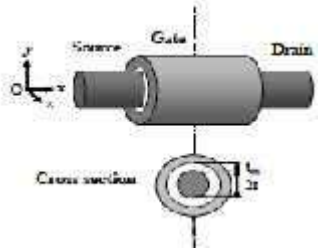

Fig.1.SiNW MOSFET Structure

II. BLOCK DIAGRAM

The above block diagram show the overall work of the project. The first block shows the landauer formalism which yields an expression of electric current I_D from the urce to drain under drain bias V_D.

Second block is the ballistic which means there is no scattering effect. Here the transmission coefficient $T_i(\varepsilon)$ is always one.

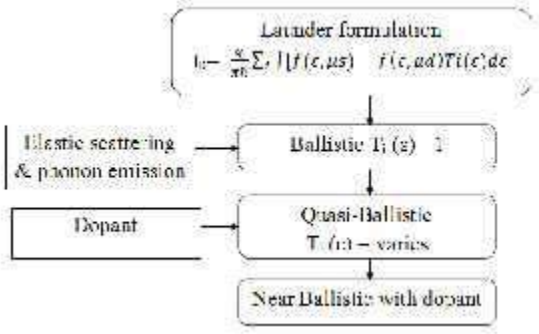

Fig.2.Block Diagram

When the elastic and phonon emission scattering combine with the ballistic which form the quasi-ballistic, and here the transmission coefficient $T_i(\varepsilon)$ varies based on the condition of sub band.

When dopants effect added with the quasi ballistic transport then it is the near ballistic, which means the impurity scattering. By impurities we mean foreign atoms in the solid which are efficient scattering centres especially when they have a net charge. Ionized donors and acceptors in a semiconductor are a common example of such impurities. The amount of scattering due to electrostatic forces between the carrier and the ionized impurity depends on the interaction

Applied Electronics, Mohamed Sathak
il: serlin.thason@gmail.com,)
essor), Department of Electronics &
hamed Sathak Engineering College-
l.com)

Modelling and Analysis of Three Phase Common H-Bridge Asymmetric Cascaded Multilevel Inverter

[1]S.Boobalan, [2]Dr.R.Dhanasekaran
[1]Research scholar, Department of EEE, St.Peter's University Chennai, TN, India. 600 054.
[2]Professor & Director – Research, Syed Ammal Engineering College, Ramanathapuram, TN, India. 623 502.
[1]csbhupalan@gmail.com, [2]rdhanashekar@yahoo.com.

Abstract
This paper presents a binary topology of common H-Bridge cascaded Multi-module level inverter generate three phase staircase output voltage from renewable energy sources. The cascaded MLI (Multi Level Inverter) Requires many number of semiconductor switches involving for generate staircase sine waveform, large no of thyristor is making more switching loss & produce large harmonic distortions. The MLI may be classified as symmetric and asymmetric converters. In symmetrical multilevel inverter may apply desire magnitude voltage level to all cascaded MLI circuit, in asymmetric multilevel inverters may vary input source voltage at each cascaded H-bridge. In this paper, a discrete binary topology is introduced digital gate trigger pulse width modulation (DGTPWM) for common cascaded H-Bridge MLI. It is proposed cascaded sub-multilevel Cells. This sub-multilevel converter may produce thirty one levels of voltage from four discrete DC voltage source. The Total Harmonic Distortions (THD) is minimized by discrete binary topology. The three phase common H-Bridge cascaded MLI working operation and performance of the proposed multilevel inverter studies has been verified by simulation of using SIMULINK / MATLAB results.

Keywords: Asymmetric Three Phase Common H-Bridge Cascaded Multilevel Inverter; Reduction Of Thyristor Switches & Switching loss; Variable switching frequency; Minimized Total Harmonic Distortions; High Output Gain; Discrete Binary Topology.

1. Introduction

Cascade Multilevel Inverter can be convert from Fixed DC voltage to Variable AC output voltage with constant frequency and variable frequency, in which the desire output voltage is generate from many discrete DC source voltage levels. Here switching Trigger of level is generating by Compared with the two discreet nominal levels of voltages, the merits of the multilevel inverter are having smaller output voltage step, minimized switching losses of operating period, minimized THD. Multilevel converters have many effective technologies for medium to high voltage range, which includes induction motor drives, FACTS control, STATCOM, power stability, power quality improvements, and power distribution applications.

Classification of MLI in Structures View:

- Diode Clamped Multilevel Inverter (DCMLI)
- Flying Capacitor Multilevel Inverter (FCMLI)
- Multi-Module Cascaded Inverter (MMCI)

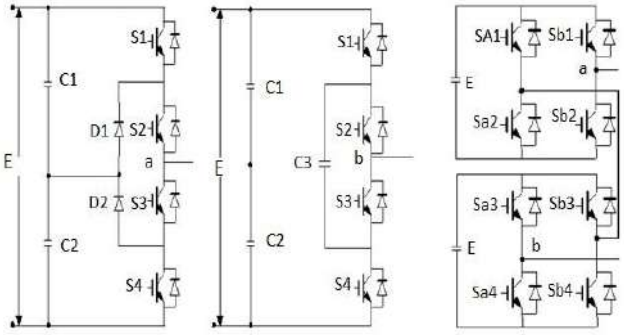

Fig 1 Structure of 3-level Multilevel Inverter topology for (a) DCMLI, (b) FCMLI, (c) MMCI

The Total Harmonic Distortion (THD) for voltage and current was calculated by following equation (1)-(3).

$$THD = \frac{\sqrt{\sum_{n=2}^{\infty} H^{2}{}_{(n)}}}{H_2} \qquad (1)$$

$$h_n = \frac{4E}{n\pi}\sum_{k=1}^{s}\cos(n\alpha_x) \qquad (2)$$

$$let\ H_{(n)} = h_n \quad and \quad H_1 = h_1$$

$$THD = \frac{\sqrt{\sum_{n=2}^{\infty}\left(\frac{1}{n}\sum_{k=1}^{s}\cos(n\alpha_x)\right)^{2}}}{\sum_{k=1}^{s}\cos(n\alpha_k)} \qquad (3)$$

Now a day, many kind of topologies has been introduced to multilevel inverter with a less no of thyristor components and gate triggering circuits, but in our proposed hybrid topology has reduced no of switches other than topology in symmetric or asymmetric, due to binary switching algorithm of digital gate trigger pulse width modulation methods. The switching frequency of multilevel inverters can be classified according to operating frequency.

This paper presents basic cascaded multilevel topologies and selected a few controllable degrees of freedom in the

general hybrid topology. If any changes occur in trigger circuit, they can be resulted in change and combination of the degrees of freedom, which expand the topology collection of unified through introduction of the degrees of freedom in the general cascaded multilevel hybrid topology. Based on research hybrid topologies and multi-carrier SPWM applied to multilevel inverter. Among the topologies, the 2^n levels binary logic switching techniques has been used to increase the no of levels at the output with reduced no of switches.

This paper has main achievement is to get the output voltage based on the input reference voltage by using H-Bridge technique, Binary logic switching technique, Multi-Carrier sub-harmonic pulse width modulation (MCSPWM) technique with variable frequency. It is implementing at the field of medium and high power applications.

2. Cascaded Multilevel Inverter

The General block diagram of single - phase cascade multilevel inverter construction is shown in Fig 1. an output phase voltage waveform of a cascade multilevel inverter with different discreet DC voltage sources is gathered by summing of different H-Bridge output voltages. Similarly Three phase cascaded multilevel inverter produce three phase output voltage. Those are briefly seeing our proposed method. The single phase output voltage of a cascade inverter is obtained by the following sequence order:

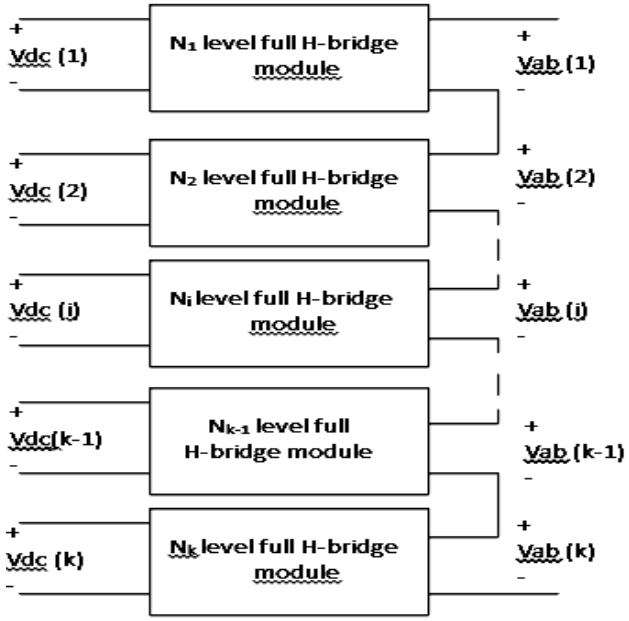

Fig 2 General Block Diagram Of Cascaded MLI

$$V_{out} = V_a+V_b+\ldots\ldots+V_n \qquad (4)$$

Where V_a, V_b… V_n are each H-Bridge output voltage of cascaded multilevel inverter. The maximum number of phase output levels obtained by following:

(5)

of level, n is no of DC sources
ge source is same level at each

H-bridge means that is called symmetrical multilevel inverter. The maximum output voltage equation is as follows:

$$V_{out}(Max)= V_a+V_b+\ldots\ldots+V_n - 2nV_D \qquad (6)$$

Where V_D is on-state voltage drop of single thyristor switch. Another method is asymmetrical multilevel inverter, here we can improve voltage level easily without increasing any additional DC voltage source. Our proposed system taken from geometrical progression of binary topology. The comparison of different cascaded multilevel inverter as shown in Table I. where m represent no of levels. There are many technique used to generate the pulses for triggering purposed like Sine-PWM, 3rd Harmonic PWM, space vector PWM(SVPWM), Selective Harmonic elimination (SHE), Current Controlled PWM(CCPWM). But in our proposed system we are implementing binary topology of sinusoidal pulse width modulation.

3. The Proposed Multilevel Converter Topology

A. Regulator:

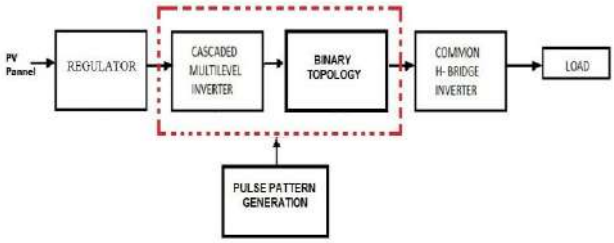

Fig 3 Block Diagram of Proposed Multilevel Inverter

This proposed inverter contains FOUR no of regulator circuit used for generate constant DC output voltage and apply cascaded multilevel inverter circuit, which each input DC voltage values is obtain at different level of 15V, 30V, 60V, 120V respectively.

B. Triggering Pulse Generation Techniques

This proposed inverter control circuit determines the desired output frequency based on the given reference frequency. The output frequencies depend on reference frequency, so the output frequency can be increased at maximum value. In this control circuit the input voltage level is divided into 16 levels and its each adjacent level is compared with reference frequency through relational operator on positive half cycle. In the progress the average voltage level has been obtained. The calculated average voltage values and current stage reference frequency signal is subjected to AND logic operation. The combination of circumstance of AND operation determines present stage whether it belongs to rising level or falling level. Similarly the negative levels were carried out by the same procedure. Each existing stage positive and negative levels are applied to OR operations. This results, determines the present stage whether it belongs to positive half cycle or negative half cycle. This process based on existing stage reference signal value.

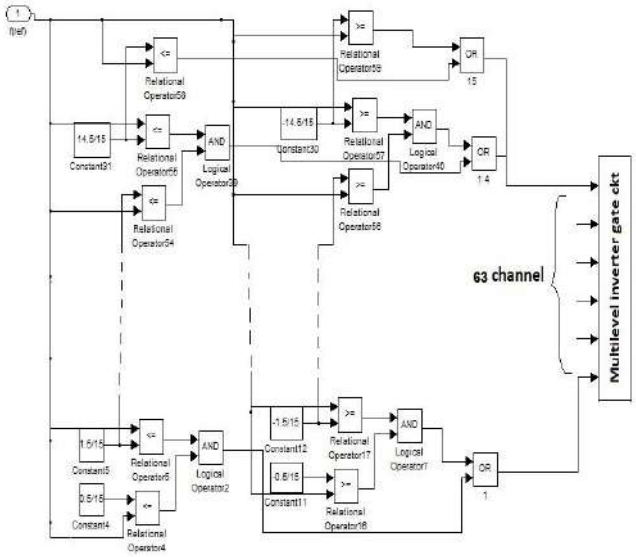

Fig 4 Trigger Pulse Generation Techniques by Logic Gates

Thus, the 32 control signals are achieved and it goes to corresponding switching of gate circuit based on binary logic technique for performed commutation sequence based on truth Table II. In which each switches S1,S2,S3,S4 respectively, the 8 input signals are subjected to the OR operations.

C. Common H-Bridge Inverter and Triggering Circuit

The term of H-bridge current flow diagram is graphical representation in the fig 4 of line draw circuit. The main H-bridge is combination of four thyristor switches. In general H-Bridge, opposite direction of switches making closed path to the load. When the common H-Bridge thyristor switches of H1 and H3 are turn on in the circuit, the positive voltage- current will be flow through the respective load, at the time H3 and H4 are Turn Off. Similarly when the switches H2 and H4 are turn on in the circuit (H1 and H3 are Turn Off) a negative voltage - current will be flow through the respective load. This function is known as shoot-through method. Whichever, the cascaded inverter switches are triggered and its corresponding DC-DC choppers output voltages are combined through H –bridge inverters and supplied the same to the load, based on the binary logic technique and reference signal frequency. The fig 6 indicates the direction of supplied voltage across the given load

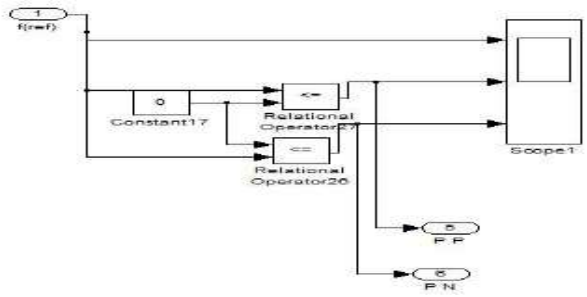

quency with ON-OFF State of Positive ve Cycle

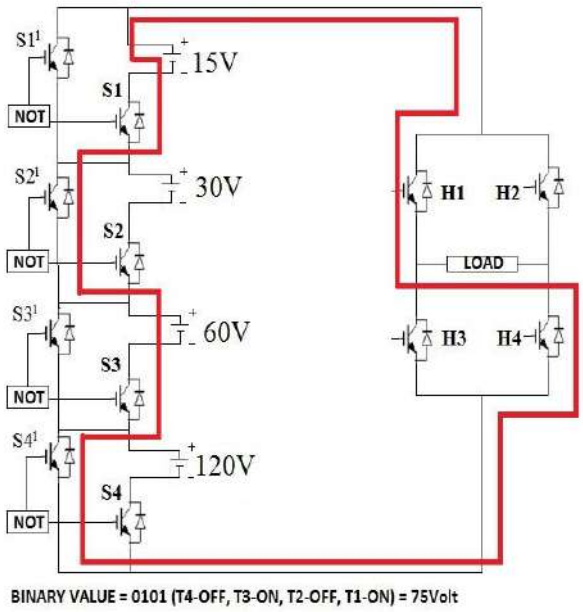

Fig 6 Single Phase Current Flow Diagram for Binary Value of "0101"

This process is achieved with the help of designed control circuit of H-bridge, as per the condition, The pair of thyristor switches H1,H4 and H2,H3 should be turn on, while the reference signal is being positive and negative cycle respectively. For that purpose, both reference frequency signal and constant value zero, has been logically OR operated as shown in Fig 5. The positive and negative stages are selected by combinational logic circuit. The Logic Diagram of Reference Frequency with ON State of Positive & Negative Cycle for single phase as shown in Fig 5.

4. Comparison studies

In General, multilevel inverters was classified into three basic structures: Diode Clamped Multilevel Inverter (DCMLI), Flying Capacitor Multilevel Inverter (FCMLI), Multi-Module Cascaded Inverter (MMCI) and Common H-Bridge Cascaded Multilevel Inverter (CHCMLI). The comparison of components required classical inverters and proposed inverter showed in TABLE I.

The common H-Bridge ON & OFF positions compared with sinusoidal reference signal. Then the switching pulse patron of CHCMLI technique output voltage and gate triggering systems (G1,G2,G3,G4,) wave forms as shown in Fig 7. The main common H-Bridge Gate triggering pulse Position of Positive and Negative Sine Switching Techniques is shown in Fig 8. In comparison studies we have check the following parameters like no of level in MLI circuit, no of capacitor to be used, no of thyristor switches, clamping diodes, no of auxiliary capacitors, no of DC sources. Those are measured referred formulas in existing techniques. The Logical sequence of switching technique for single phase cascade MLI gates (G1,G2,G3,G4) by binary logic topology is shown in Table II. Similarly we are updating three phase cascaded MLI with 120 degree phase shift.

TABLE I COMPARISON OF COMPONENTS REQUIRED CLASSICAL INVERTERS AND PROPOSED INVERTER

Types	Classical systems			Proposed system
	DCMLI	FCMLI	MMCI	CHCMLI
No of Levels	m	m	m=Ns+1	$m=2^n+1$
capacitor	m-1	m-1	m-1	Nil
Switches	2(m-1)	2(m-1)	Ns x 4	(2n+4)
Clamping Diode	(m-1) x (m-2)	Nil	Nil	Nil
Auxiliary capacitor	Nil	(m-1) x ((m-2)/2) + (m-1)	Nil	Nil
No of DC Source	Ns=m	Ns=m	Ns=m/2	Ns=n

TABLE II LOGICAL SEQUENCE OF SWITCHING TECHNIQUE FOR CASCADE MLI GATES (G1,G2,G3,G4)BY BINARY LOGIC TOPOLOGY

Level	Binary Techniques				Switching Techniques								Combined Chopper	Sum of Output Voltage	Wave Form
					Main Switch				Complementary Switch						
	T4	T3	T2	T1	S4	S3	S2	S1	$S4^1$	$S3^1$	$S2^1$	$S1^1$			
1	0	0	0	0	Off	Off	Off	Off	On	On	On	On	Closed path	0V	POSITIVE HALF CYCLE
2	0	0	0	1	Off	Off	Off	On	On	On	On	Off	1	15V	
3	0	0	1	0	Off	Off	On	Off	On	On	Off	On	2	30V	
4	0	0	1	1	Off	Off	On	On	On	On	Off	Off	1&2	45V	
5	0	1	0	0	Off	On	Off	Off	On	Off	On	On	3	60V	
6	0	1	0	1	Off	On	Off	On	On	Off	On	Off	3&1	75V	
7	0	1	1	0	Off	On	On	Off	On	Off	Off	On	3&2	90V	
8	0	1	1	1	Off	On	On	On	On	Off	Off	Off	3,2&1	105V	
9	1	0	0	0	On	Off	Off	Off	Off	On	On	On	4	120V	
10	1	0	0	1	On	Off	Off	On	Off	On	On	Off	4&1	135V	
11	1	0	1	0	On	Off	On	Off	Off	On	Off	On	4&2	150V	
12	1	0	1	1	On	Off	On	On	Off	On	Off	Off	4,2&1	165V	
13	1	1	0	0	On	On	Off	Off	Off	Off	On	On	4&3	180V	
14	1	1	0	1	On	On	Off	On	Off	Off	On	Off	4,3&1	195V	
15	1	1	1	0	On	On	On	Off	Off	Off	Off	On	4,3&2	210V	
16	1	1	1	1	On	On	On	On	Off	Off	Off	Off	4,3,2&1	225V	

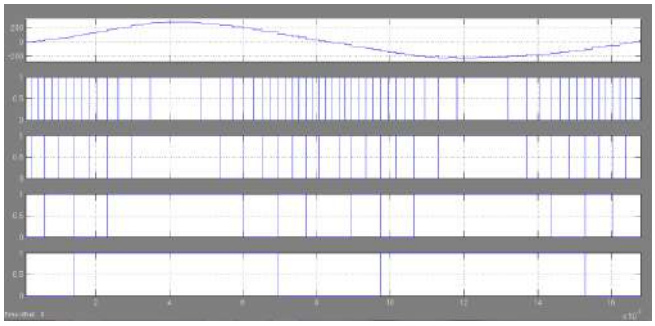

Fig 7 Switching Techniques, Output Voltage and Gate Triggering System (G1,G2,G3,G4) Wave Form of Cascaded Multilevel Inverter.

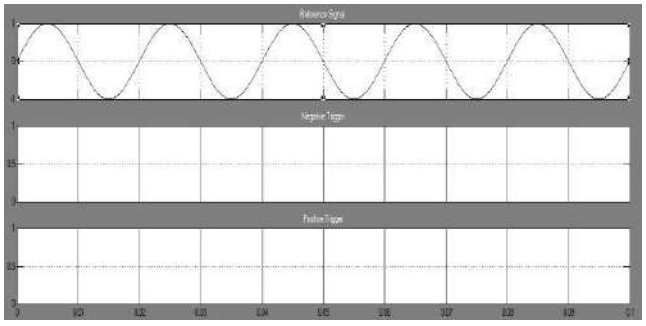

Fig 8 Thyristor Pair ON State Position of Positive and Negative Sine Switching Techniques

5. Simulation Results

The above explanations are single phase MLI circuits and similarly we are applying three phase MLI circuit designs with 120 degree phase shift for each phase (RYB). Then the design of Circuit Diagram of Proposed three phase Common H-Bridge Cascaded 31-Level Asymmetrical Multilevel Inverter as shown in Fig 9. The FFT analyses of Total Harmonic Reduction of three phase Common H-Bridge Cascaded Multilevel Inverter as shown in Fig 10. Here we are reducing THD 1.72% in our proposed system.

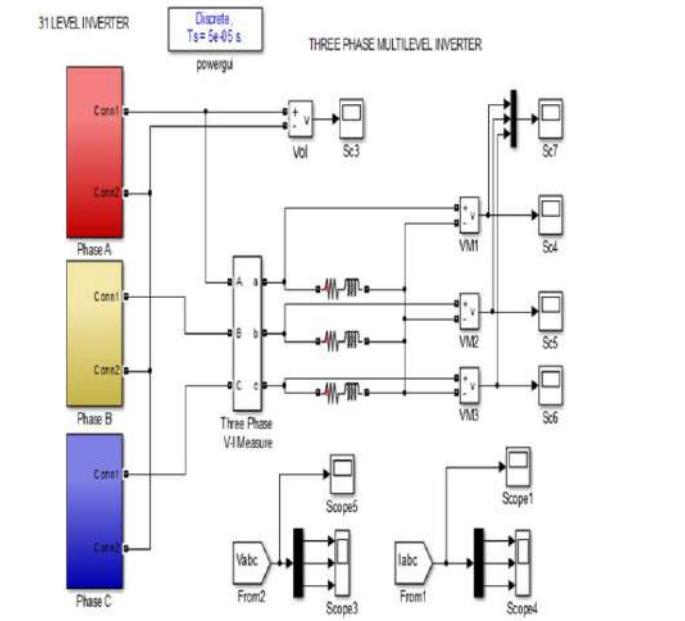

Fig 9 Circuit Diagram of Proposed three phase Common H-Bridge Cascaded 31-Level Asymmetrical Multilevel Inverter

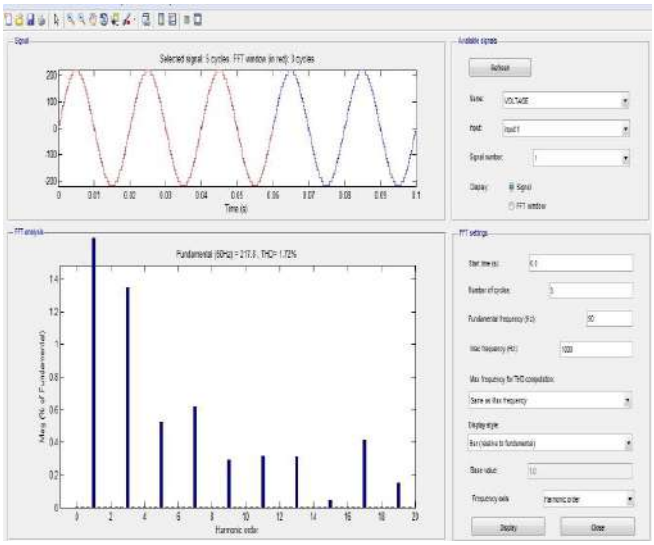

Fig 10 FFT analysis of Total Harmonic Reduction of Common H-Bridge Cascaded Multilevel Inverter

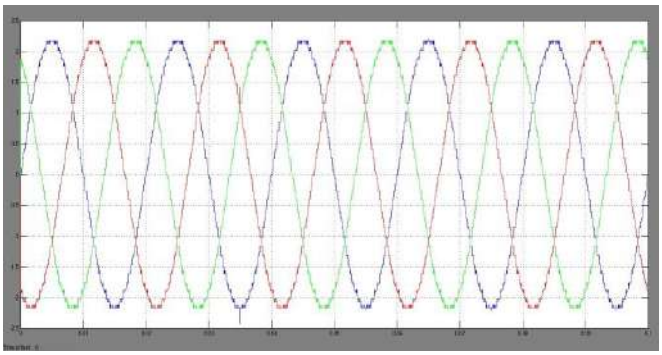

Fig 11 Three Phase Current wave form for Common H-Bridge Cascaded 31-Level Asymmetrical Multilevel Inverter

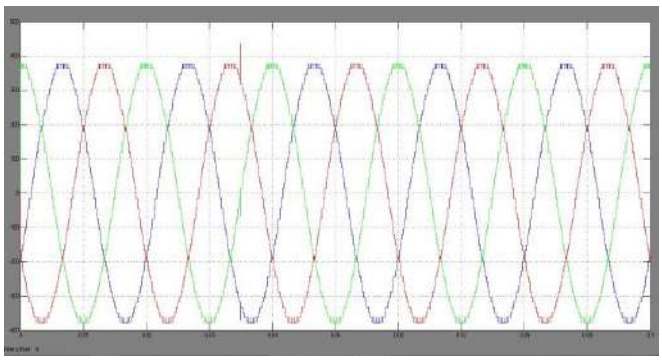

Fig 12 Three Phase Voltage wave form for Common H-Bridge Cascaded 31-Level Asymmetrical Multilevel Inverter

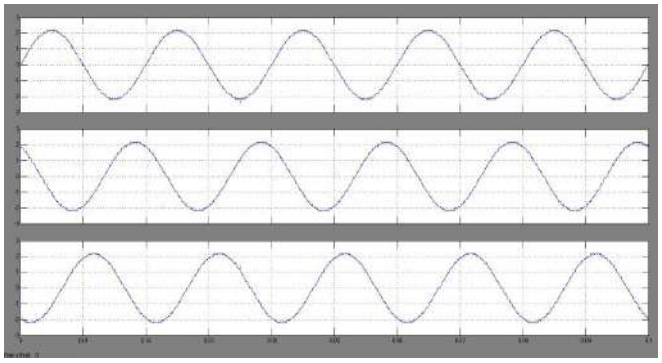

Fig 13 R-Y-B Phase Current wave form for Common H-Bridge Cascaded 31-Level Asymmetrical Multilevel Inverter

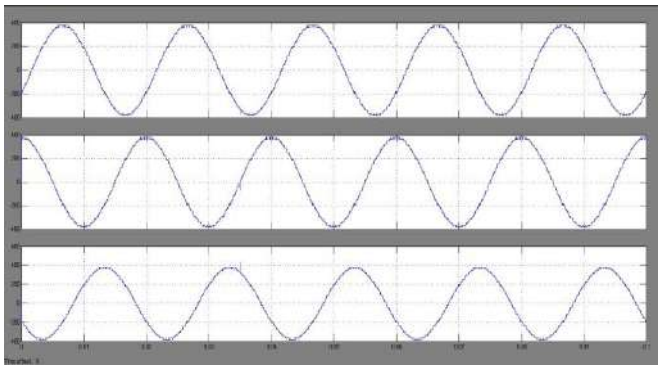

Fig 14 R-Y-B Phase Voltage wave form for Common H-Bridge Cascaded 31-Level Asymmetrical Multilevel Inverter

Three Phase Current wave form for Common H-Bridge Cascaded 31-Level Asymmetrical Multilevel Inverter is as shown in Fig 11.Three Phase Voltage wave form for Common H-Bridge Cascaded 31-Level Asymmetrical Multilevel Inverter is as shown in Fig 12. R-Y-B Phase Current wave form for Common H-Bridge Cascaded 31-Level Asymmetrical Multilevel Inverter is as shown in Fig 13. R-Y-B Phase Voltage wave form for Common H-Bridge Cascaded 31-Level Asymmetrical Multilevel Inverter is as shown in Fig 14.

6. Conclusion

In this paper, The hybrid topology of common H-bridge three phase cascaded multilevel inverter is proposed for variable output AC voltages and frequencies as per given input source. A discrete gate triggering binary topology pulse width modulation was presented for three phase common H-Bridge cascaded multilevel Inverter, which has reduced number of semiconductor switches. The suggested discrete binary topology pulse width modulation requires limited switches for synthesized three phase output voltage levels. So our proposed system may minimize cost level. As a result, the output voltage waveform presents very low total harmonic distortion profile the percentage of THD is 1.72 and provides better efficient for various range of RL loads. If we add one more pair of thyristor, we can get 61 levels & it's improve better waveform performance & does not affect the THD. Then we can easily change to frequency (50Hz or 60Hz). The application of this project is variable speed drives which result in high dynamic response for speed.

7. Reference

[1] Analysis and Control of Three Phase Multi level Inverters with Sinusoidal PWM Feeding Balanced Loads Using MATLAB, International Journal of Engineering Research and General Science Volume 2, Issue 4. (2014)
[2] Fundamental studies of a three phase cascaded H-Bridge and diode clamped multilevel inverter using matlab/simulink, International review of Automatic control (I.RE.A.CO) Vol 6, N.5 (September2013)
[3] A Hybrid Multilevel Inverter System Based on Dodecagonal Space Vectors for Medium Voltage IM Drives, IEEE Transactions On Power Electronics, Vol. 28, No. 8, (August 2013)
[4] Cascaded H-Bridge Multilevel Inverter Using Inverted Sine Wave PWM Technique, International Journal of Emerging Trends in Electrical and Electronics (IJETEE – ISSN: 2320-9569) Vol. 6, Issue. 1,(Aug-2013)
[5] Optimal Design of a Multilevel Modular Capacitor-Clamped DC–DC Converter, IEEE Transactions On Power Electronics, Vol. 28, No. 8, (August 2013)
[6] Digital Control of Three Phase Three-Stage Hybrid Multilevel Inverter, IEEE Transactions On Industrial Informatics, Vol. 9, No. 2, (May 2013)
[7] Design Of Renewable Energy Based Shunt Active Filter With Multilevel Inverter Using Genetic Algorithm, International Journal of Engineering Science and Technology (IJEST) Vol. 5 No.05 (May 2013)
[8] A Five-Level Inverter Topology with Single-DC Supply by Cascading a Flying Capacitor Inverter and an H-Bridge, IEEE Transactions On Power Electronics, Vol. 27, No. 8, (August 2012)
[9] Three-Phase Hybrid Multilevel Inverter Based on Half-Bridge Modules, IEEE Transactions On Industrial Electronics, Vol. 59, No. 2, (February 2012)
[10] Multiloop Control Method for High-Performance Microgrid Inverter Through Load Voltage and Current Decoupling With Only Output Voltage Feedback, IEEE Transactions On Power Electronics, Vol. 26, No. 3, (March 2011)
[11] Verification of New Family for Cascade Multilevel Inverters with Reduction of Components, Journal of Electrical Engineering & Technology Vol. 6, No. 2 (2011)
[12] Voltage-Source PWM Rectifier–Inverter Based on Direct Power Control and Its Operation Characteristics, IEEE Transactions On Power Electronics, Vol. 26, No. 5, (May 2011)
[13] Single-Phase Seven-Level Grid-Connected Inverter for Photovoltaic System, IEEE Transactions On Industrial Electronics, Vol. 58, No. 6, (June 2011)
[14] A New High-Efficiency Single-Phase Transformerless PV Inverter Topology, IEEE Transactions On Industrial Electronics, Vol. 58, No. 1, (January 2011)
[15] Low-Speed Control Improvements for a Two-Level Five-Phase Inverter-Fed Induction Machine Using Classic Direct Torque Control, IEEE Transactions On Industrial Electronics, Vol. 58, No. 7, (July 2011)
[16] A Seven-Level Inverter Topology for Induction Motor Drive Using Two-Level Inverters and Floating Capacitor Fed H-Bridges, IEEE Transactions On Power Electronics, Vol. 26, No. 6, (June 2011)
[17] Three-Phase Cascaded Multilevel Inverter Using Power Cells With Two Inverter Legs in Series, IEEE Transactions On Industrial Electronics, Vol. 57, No. 8, (August 2010)

International Journal of ChemTech Research
CODEN (USA): IJCRGG, ISSN: 0974-4290, ISSN(Online):2455-9555
Vol.11 No.04, pp 127-135, 2018

Investigation of Dual Bridge Multilevel DC Link Inverter for PV Application

R.Niraimathi[1]*, R.Seyezhai[2]

[1]Department of Electrical and Electronics Engineering, Mohamed Sathak Engineering College East Coast Road, Kilakarai-623 806, Tamil Nadu, India.
[2]Department of Electrical and Electronics Engineering, SSN College of Engineering Rajiv Gandhi Sallai, Kalavakkam-603 110, Tamil Nadu, India.

Abstract : The main objectiveof the proposed topology is to synthesize a high quality sinusoidal output voltage with considerably reduced switch count than the conventional MLI. The proposed topology consist of series connected H-bridge and diodes. The number of levels dependson dc source arrangement. Heredc sources can be replaced by PV.The proposed PV based dual bridge MLDCLI (DBMLDCLI) is evaluated using phase disposition (PD) multi-carrier pulse width modulation (MC-PWM) strategy.The performance of a dual bridge dc-link inverter topology is simulated through MATLAB/SIMULINK and the THD of the output voltage is analyzed. The results are validated.
Keywords : Dual Bridge Multilevel Dc Link Inverter (DBMLDCLI), Phase Disposition (PD), THD

Introduction

MLIs are preferred for high power medium voltage applicationsdue to their donation of reduced harmonic content in the output side, lower blocking voltage in the switching devices[1,2].but it requires large number of semiconductor switches, each switch requires a related gate driver circuits which are more expensive and complex[3-6],these demerits are eliminated by the topology called multilevel dc link inverter which gives improved performance. These inverter reduce the number of switches and gate drive as the number of voltage levels increases. However it shows inconveniences in their operation with balancing capacitor voltage[7-9]. Therefore proposed topology PV based Dual Bridge Multilevel DC link Inverter (DBMLDCLI) which requires a less number of power switches with nearly sinusoidal output voltage. It uses lower number of sources, power switches and eliminates the necessity of capacitors. This paper presents dual bridge 15 level inverter with phase disposition(PD) multi-carrier pulse width modulation(MC-PWM) technique which is used forcontrol the switches of inverter and it is carried out in MATLAB/SIMULINK.

PV Modelling

PV module is used for power conversion. The output characteristics of a PV module depend on the solar irradiance, the cell temperature and the output voltage of the PV module. Equivalent circuit of a PV cell is

shown in Fig. 1. The simplified equivalent circuit of solar cell consists of diode and current source which are connected in parallel. The current source I_{ph} representthe cell photo current. R_p and $R_s$are the parallel and series resistances of the cell respectively. The output current and voltage from the PV cells are represented by I and V.

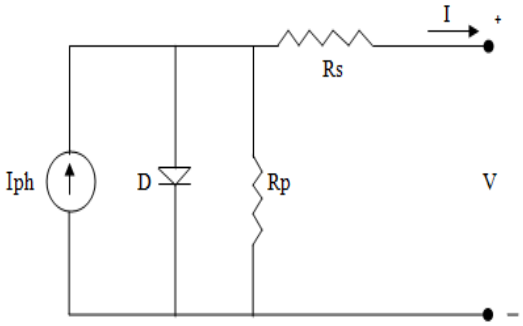

Fig.1 Equivalent circuit of PV

The output currentof PV is given by,

The output current of PV is given by,

$$I = I_{ph} - I_s\left(e^{\frac{q(V+IR_S)}{nkT}} - 1\right) - \frac{V+IR_S}{R_p} \qquad (1)$$

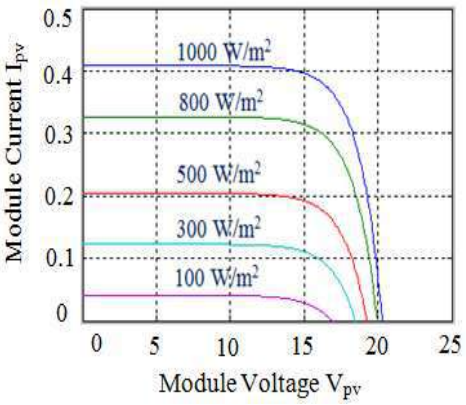

Fig.2 I-V Characteristics of PV module

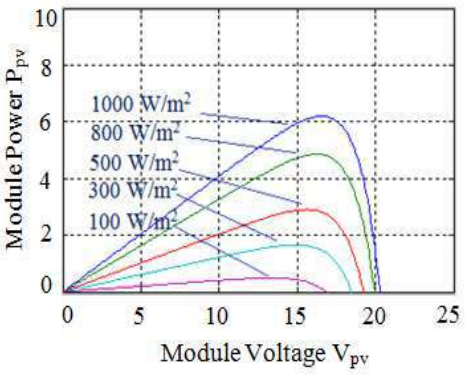

s of PV module

cs of PV module for different irradiation are shown in Fig.2 and the P-V characteristics ent irradiance at 25℃ are shown in Fig.3. Photocurrent depends on the irradiation. The e greater the current[10].

Proposed Topology

Fig.4 shows the generalized structure of dual bridge multilevel dc link inverter which is used to realize as many desired levels. It constituted of two H-bridges, PV sources and a number of distinct modules depending on the output voltage level requirements. The first bridge is connected in series with as several modules for every six level increase with each module inter-twined with a switch in series with the source, the combination shunted through an anti paralleldiode. The first H-bridge serve to increase the level of the dc-link voltage, the second H-bridge provides bi-directional power flow through the load[11,12].

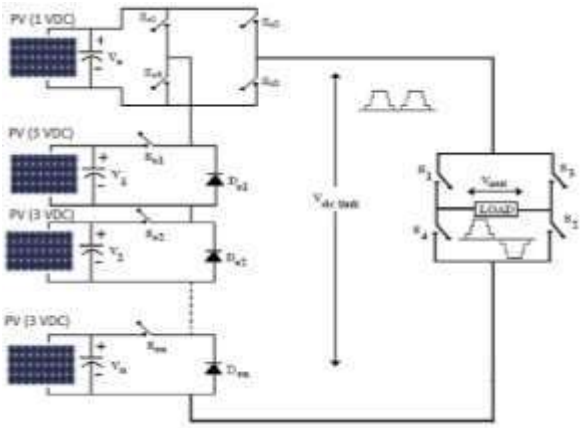

Fig.4 Generalized structure of DBMLDCLI

The defined number of output voltage levels that an new dual bridge dc-link multilevel inverter can synthesize is expressed using a relation (2(3S+1) +1) where S is the number of voltage sources excluding V_0, if arranged in the ratio V_0:V_n = 1:3.

Switching operation: To explain the switching operation for variouslevels, the dc link structure is represented by fixed source. The operation for each level of a fifteen level inverterwith V_0:V_1:V_2 = (4:12:12) V along with positive and negativehalf cycles is explained through switchingtable. It is seenfrom table I that the devices S_{03}, S_{04}, D_{e1} and D_{e2} in the dc-link circuitand either the pair S_1–S_2 or pair S_3–S_4in the H-bridge alternately arerequired to conduct to extract the first level of the output voltageand the second level S_{01},S_{02},D_{e1} and D_{e2} in the dc link circuit and either the pair S_1-S_2 or S_3-S_4 in the H-bridge alternately are required to conduct to extract the second level and so on. Table I. shows switching pattern for proposed dual bridge multilevel dc link inverter.

Table-I switching operation

S_{01}	S_{02}	S_{03}	S_{04}	S_{e1}	S_{e2}	S_1	S_2	S_3	S_4	V_0
0	0	1	1	1	1	1	1	0	0	+7
0	1	0	1	1	1	1	1	0	0	+6
1	1	0	0	1	0	1	1	0	0	+5
0	0	1	1	0	1	1	1	0	0	+4
0	1	0	1	0	1	1	1	0	0	+3
1	1	0	0	0	1	1	1	0	0	+2
0	0	1	1	0	0	1	1	0	0	+1
0	0	0	0	0	0	1	1	0	0	0
0	0	1	1	0	0	0	0	1	1	-1
1	1	0	0	0	1	0	0	1	1	-2
0	1	0	1	0	1	0	0	1	1	-3
					1	0	0	1	1	-4
					0	0	0	1	1	-5
					1	0	0	1	1	-6
					1	0	0	1	1	-7

Control Strategy

In this topology, Phase Disposition (PD) pulse width modulation [13]scheme is used. It is based on a comparison of a sinusoidal reference waveform with vertically shifted carrier waveform generates PWM signals. All the carrier signals have the same amplitude, same frequency and are in phase[14]. The generated seven PWM signals are applied to the switches of H-bridge along with modules to produce dc-link voltage. Common H-bridge used to produce ac output voltage by using reverse voltage technique. ThisPWM method gives rise to the lowest harmonic distortion when compared to other methods [15]. The Fig.12 shows that carrier and reference sinusoidal signals of phase disposition modulation.

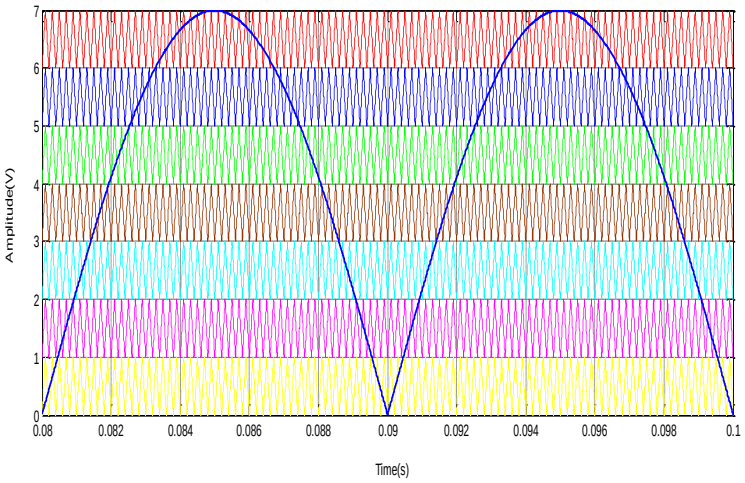

Fig.12The reference and carrier signals of PD PWM technique

Simulation Results

Simulation of the circuit is carried out inMATLAB/SIMULINK. Fig.13 shows the simulation diagram of fifteen level DBMLDCLI. The PV sources are chosen in the ratio 1:3 (V_1 = 4 V, V_2 = V_3 = 12 V) withR load of 100Ω. It uses a PD-MC-PWM technique with a carrier frequency of 5 kHz. Gating pulses for the switches are shown in fig.14. The multilevel dc-link voltage obtained through first H-bridge with distinctive module is shown in Fig.15. Fig.16. shows the output voltage waveform of fifteen level dual bridge multilevel dc link inverter which is obtained through second H-bridge and the FFT analysis of voltage total harmonic distortion is depicted in Fig.17.

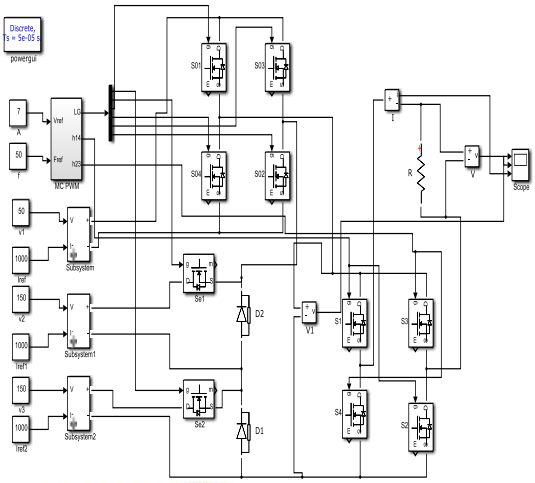

'am of 15-level DBMLDCLI.

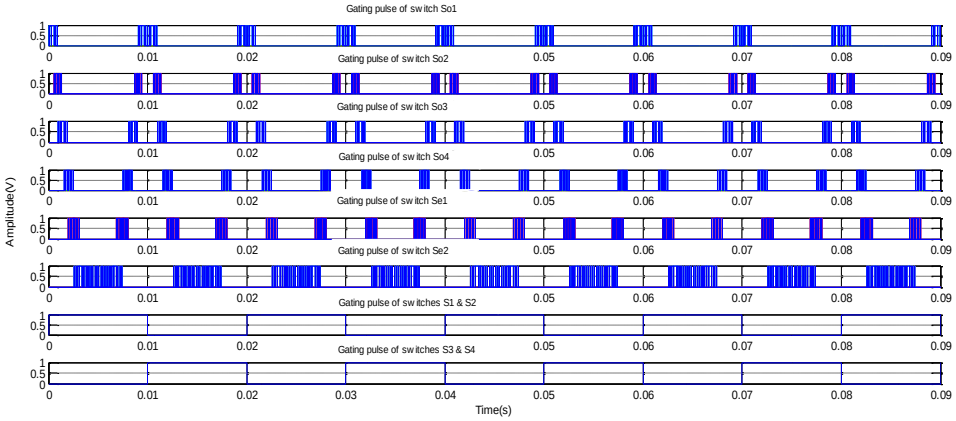

Fig.14 Pulse pattern

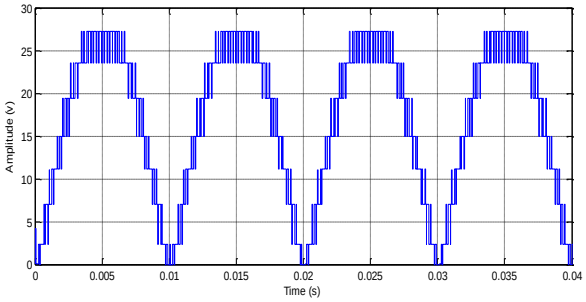

Fig.15 DC Link Voltage Waveform

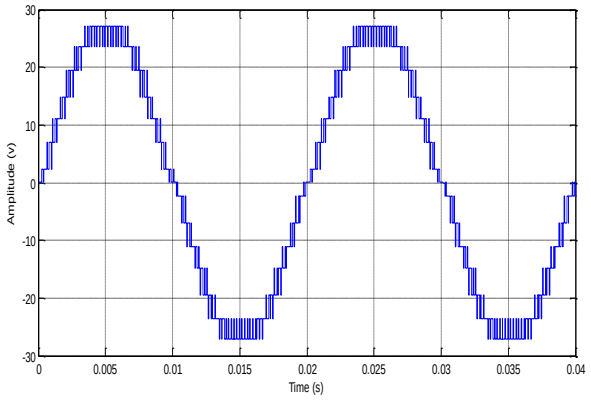

Fig.16Output Voltage Waveform of 15-level DBMLDCLI

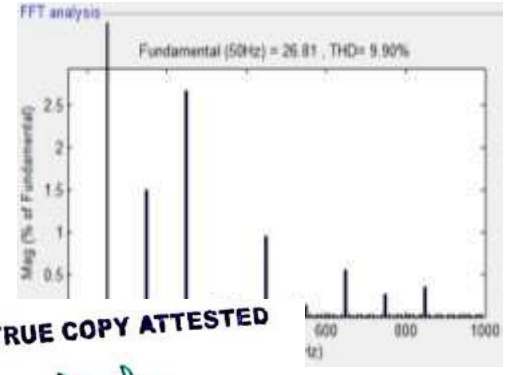

rum of Output Voltage

A detailed comparison of the switch and source requirements is tabulated in Table II to bring out the reduction in the switch count of the proposed DBMLDCLI over the existing MLI topologies for a typical case of fifteen level output. From table II it is observed that conventional topologies switch count increased by 55% than proposed topology.

Table II Comparison between topologies for fifteen level.

Multilevel inverter structure	**Multilevel DC link Inverter**			**Proposed topology**
	Cascaded half bridge	**Diode clamped**	**Flying capacitor**	
Main switches	18	18	18	10
Bypass diodes	-	-	-	2
Clamping diodes	-	12	-	-
DC split capacitors	-	6	6	-
Clamping capacitors	-	-	6	-
Dc sources	7	1	1	3
Total	25	37	31	15

Hardware Implementation

The hardware layout of the system is shown in fig.18. The inverter was constructed using IRF640 MOSFET switches. The inverter is also interfaced with the PV system. The voltage generated from the solar panel given to the inverter are V_1=4V,V_2=12V and V_3=12V.

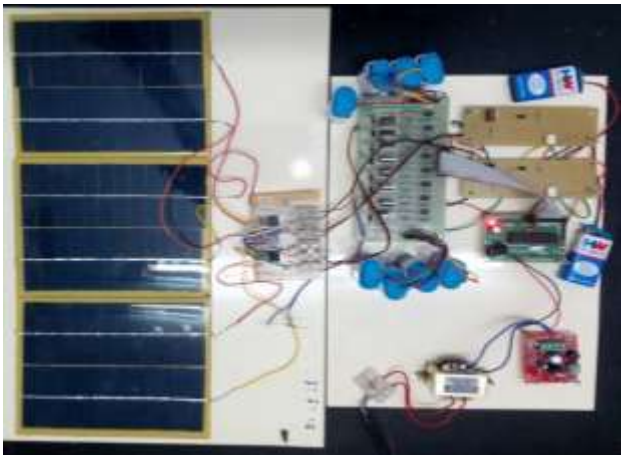

Fig.18 Hardware Circuit

The gating signals for the multilevel inverter are implemented using microcontroller ATMEGA8. Fig.19(i)- 19(x) shows the switching pulses generated for each MOSFET switch where they are given to the gate terminal of the MOSFET switch in the inverter.

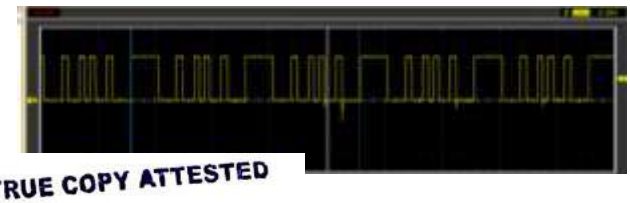

of switch S_1

Fig.19 (ii) Gating pulse of switch S_2

Fig.19 (iii) Gating pulse of switch S_3

Fig.19 (iv) Gating pulse of switch S_4

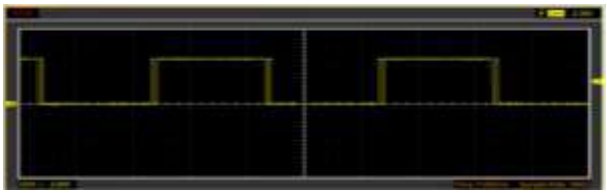

Fig.19 (v) Gating pulse of switch S_5

Fig.19 (vi) Gating pulse of switch S_6

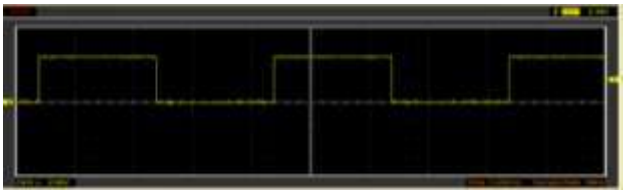

Fig.19 (vii) Gating pulse of switch S_7

se of switch S_8

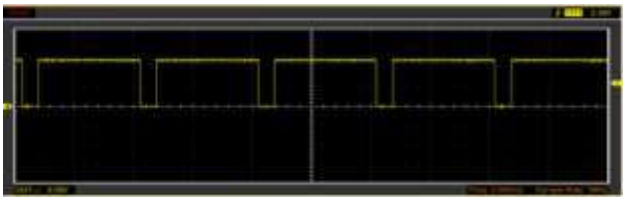

Fig.19 (ix) Gating pulse of switch S_9

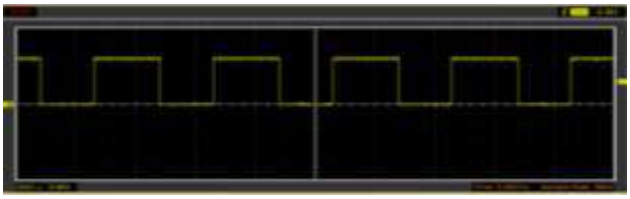

Fig.19(x) Gating pulse of switch S_{10}

Fig.19 Switching Pulse pattern

Fig.20,21 shows dc link voltage and load voltage of DBMLI for dc input voltage (V_1=4V,V_2=12V,V_3=12V) and ac RMSoutput obtained from R load is 26.81V.

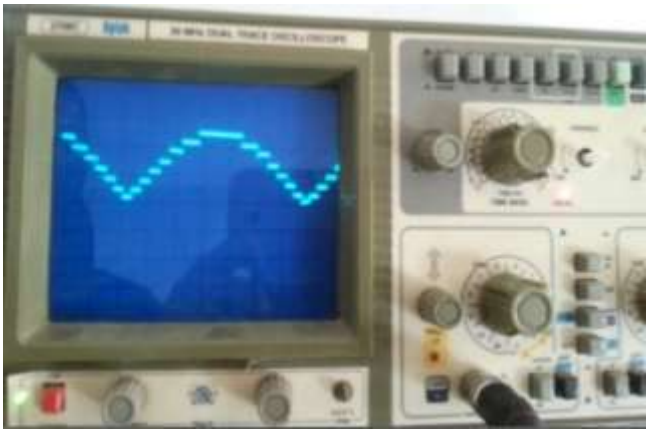

Fig.20 DC Link Voltage Waveform

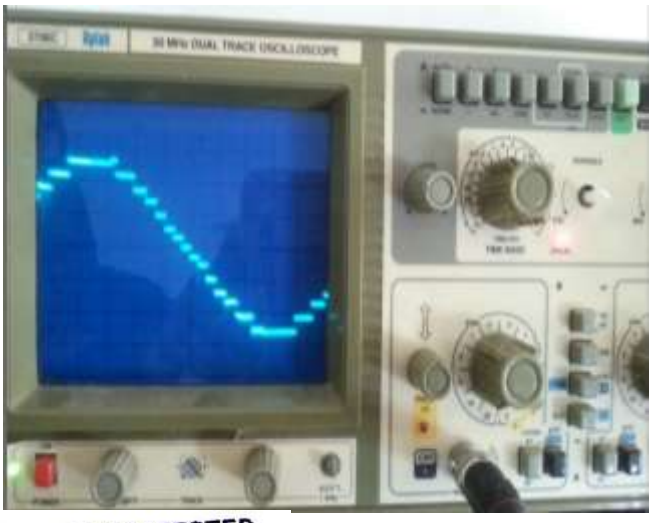

waveform of 15-level DBMLDCLI

VI. Conclusion

In this paper, fifteen level PV based dual bridge DC-link inverter topology is proposed with PD PWM technique and it is simulated with MATLAB/SIMULINK.The complete hardware of fifteen level dual bridge dc link inverter is implemented. The obtained result gives reduced voltage THD of 9.9% .Compared to conventional MLI, proposed topology gives better sinusoidal 15-levels of output voltage with lowest switch count.

References

1. Lai Jih-Sheng and Peng Fang Zheng.Multilevel converters - a new breed of power converters.IEEE Trans IndAppl 1996;32:509-17.
2. Rodriguez J, LaJih-Sheng, Peng Fang Zheng.Multilevel inverters: a survey of topologies, controls, and applications IEEE Trans IndElectron2002;49:724–38.
3. Marchesoni M, TencaP.Diode- clamped multilevel converters: a practicable way to balance dc-link voltages.IEEE Trans Ind Electron 2002;49:752–65.
4. Escalante MF, Vannier JC, Arzande.A flying capacitor multilevel inverters and DTC motor drive applications.IEEE Trans Ind Electron 2002;49:809–15.
5. Kouro S, et al. Recent advances and industrial applications of multilevel converters.IEEE Trans Ind Electron 2010;57:2553–80.
6. FangZhengPeng, Jih-Sheng Lai, et al. A multilevel voltage - source converter system with balanced Dc voltages. In: Proceedings of IEEEinternational conference, vol. 2; 1995. p. 1144 –50.
7. Ramkumar S, Kamaraj V, Thamizharasan S, JeevananthanS.A new series parallel switched multilevel dc-link inverter topology.Int Electric Power Energy Syst 2012;36:93–9.
8. Gui-JiaSu.Multilevel dc-link inverter. IEEE Trans IndAppl 2005; 41: 848–54.
9. Vivek Kumar Singh, Praveen Bansal .Asymmetrical 9-level Dual Bridge DC-Link Inverter Topology.International Journal of Electronics, Electrical and Computational System (IJEECS) Volume 4, Special Issue May 2015.
10. RamosHermanz JA, Campayo Martin JJ, et al. Modeling of photovoltaic module.International Conference on Renewable Energiesand Power Quality (ICREPQ'10), Granada (Spain).
11. Manjunatha YR, AnandBA.MultilevelDC Link Inverter with Reduced Switches and Batteries. International Journal of Power Electronics and Drive System (IJPEDS) Vol. 4, No. 3, September 2014, pp. 299-307.
12. MadhuSagarbabu G, Durga Prasad G and JagathesanV. Multilevel DC-link Inverter Topology with Less Number of Switches. Advance inElectronic and Electric Engineering, Vol 4, No.1 (2014), pp. 67-72.
13. Gomathi C, et al. Comparison of PWM methods for Multilevel inverter.International Journal of Advanced Research in Electrical, Electronics and instrumentation Engineering. vol.2, issue 12, Dec 2013.
14. Mohan D, SreejithB.Kurub.A comparative analysis of multi carrier SPWM control strategies using fifteen level cascaded H-bridge multilevel inverter. International Journal of computer applications. Vol.41-No.21,March 2012.
15. Sangeetha R Gupta, Anitha GS.PD-PWM based cascaded H-bridge multilevel inverter for photovoltaic systems. International Journal of Advanced Research in Electrical, Electronics and instrumentation Engineering. vol.4, issue 7, july 2015.

*****

Middle-East Journal of Scientific Research 23 (5): 761-769, 2015
ISSN 1990-9233

DOI: 10.5829/idosi.mejsr.2015.23.05.22136

Investigation of Multilevel DC Link Inverter to Solve the PV Partial Shading

[1]R. Niraimathi and [2]R. Seyezhai

[1]Department of Electrical and Electronics Engineering,
Mohamed Sathak Engineering College East Coast Road,
Kilakarai-623 806, Tamil Nadu, India
[2]Department of Electrical and Electronics Engineering,
SSN College of Engineering Rajiv Gandhi Sallai,
Kalavakkam-603 110, Tamil Nadu, India

Abstract: The effect of partial shading of individual photovoltaic (PV) sources which are connected in series is solved by the proposed multilevel DC link inverter with a novel control algorithm. The algorithm is based on arrangement of multicarrier pulse width modulation and direct pulse width modulation technique to control the multilevel dc-link inverter. The proposed algorithm is applied effectively to a single-phase seven-level inverter with separate maximum power point tracking algorithm for each PV source under non uniform irradiance (partial shading). Various multicarrier PWM techniques such as Phase Disposition (PD) PWM, Phase Opposition and Disposition (POD) PWM and Phase Shift (PS) PWM have been investigated for the proposed inverter which provides a solution to the partial shading enabling each shaded PV source to be recovered to its maximum power without affecting other PV sources. Simulation studies have been carried out using MATLAB/SIMULINK and the spectral quality of the inverter output is observed under various conditions of partial shading. The results are verified.

Key words: PV · MCPWM · PD · POD · PSP · THD · Switching frequency · MLDCLI

INTRODUCTION

The increasing energy demands and environmental pollution are motivating research and technological investments related to renewable energy sources. Among several types of renewable energy sources, the photovoltaic (PV) energy source has benefits such as high efficiency, reliability and a long life. But the performance of a photovoltaic (PV) array is affected by temperature, solar insolation, shading and array configuration. Often, the PV arrays get shadowed, completely or partially, by the passing clouds, neighboring buildings and towers, trees and telephone poles. The problem of partial shading can be resolved by the following techniques as follows:

The simplest method to reduce the effects of the PV partial shading problem is connecting a bypass diode n the series string. However, more n appear and it is difficult to find the MPP among multiple peaks. Therefore, the power delivered to the load is significantly reduced. When the power sources are connected in series through dc/dc converters [1], the fine-adjustment of duty cycle compensates the reduction of the irradiation of the shaded source which does not then operate at the MPP. Such a topology cannot maintain all series-connected PV sources operating at their MPP under partial shading. Next technique is based on bypassing the power through converters is called "Generation Control Circuit" (GCC) scheme [2], using multistage buck-boost converter. In this topology switches cannot be independently controlled. So, finding the MPP of one PV source does not represent that other series-connected PV sources operate at their MPP.For this purpose, the most favorable duty ratio has to be set by tracking algorithm in order to deliver the maximum power to the load. Concise of a multilevel inverter, PV source to be controlled individually. Among all variety of multilevel inverters, the "cascaded H-bridge

R. Niraimathi, Department of Electrical and Electronics Engineering,
Mohamed Sathak Engineering College East Coast Road, Kilakarai-623 806, Tamil Nadu, India.
E-mail: seyezhair@ssn.edu.

inverter" is most often used due to its same bridge structure. For each PV source, the maximum power can be obtained by using MPPT algorithm. This method has been applied in only in an experimental model [3] where each PV source was emulated by a series connection of dc source and resistance. Another approach, PV multilevel dc-link inverter system with PV permutation algorithm to solve the partial shading problem. In this method all PV sources which form the output PWM voltage are sequentially permutated per each consecutive PWM switching cycle according to the number of PV sources [4].

In this paper, the PV multilevel dc-link inverter with maximum power point tracking (MPPT) algorithm and Novel control algorithm are used to overcome the problem of uneven irradiance. Here, the maximum power point tracking (MPPT) algorithm for tracking the MPP of the PV sources and novel control algorithm to control the inverter switches to form the multilevel output voltage waveform. Beginning with a brief operation of Multilevel DC link inverter power circuit is outlined in section-II, next PV modelling is explained in section-III,novel control algorithm provides the solution to partial shading is described in section-IV and various PWM techniques are discussed in Section-V.finally simulation results are carried out using MATLAB/SIMULINK [5].

Multilevel Dc Link Inverter Topology: A power circuit of multilevel dc link inverter as shown in Fig. 1. Each PV unit consists of a PV source, switch and diode. The units can be switched in or out of the chain by means of the switch-diode pair. The switches of each unit (S1, S2, S3) activate at high PWM frequency (5KHz) to form the multilevel positive dc-link waveform Vlink. The switches S4-S7 in the H-bridge operate at low frequency (50Hz) to form the desired ac output. Table 1. shows switching pattern for proposed multilevel dc link inverter [6].

PV Modelling: PV module is used for power conversion. The output characteristics of a PV module depend on the solar irradiance, the cell temperature and the output voltage of the PV module. Since PV module has non-linear characteristics, it is necessary to model it for the design and simulation of Maximum Power Point Tracking (MPPT) for PV system applications [5-6].Equivalent circuit of a PV cell is shown in Fig. 2.The current source I_{ph} represent the and R_s are the shunt and series spectively.

/ module is

Table 1: Switching Pattern for Proposed Multilevel Dc Link Inverter

S1	S2	S3	S4	S5	S6	S6	Vo
0	0	0	1	1	0	0	0
1	0	0	1	0	0	1	1
1	1	0	1	0	0	1	2
1	1	1	1	0	0	1	3
0	0	0	0	0	1	1	0
1	0	0	0	1	1	0	-1
1	1	0	0	1	1	0	-2
1	1	1	0	1	1	0	-3

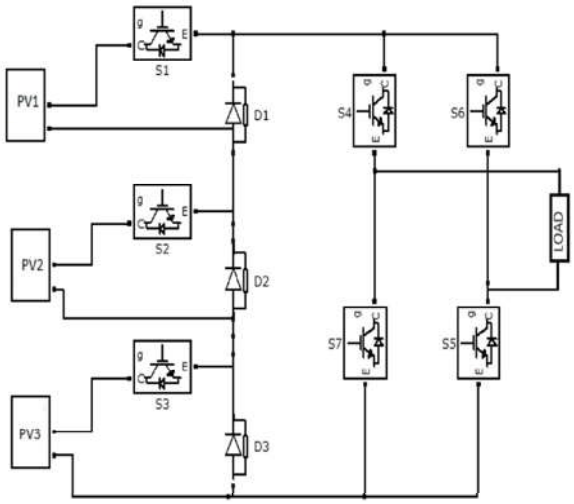

Fig. 1: Power circuit of multilevel dc link inverter

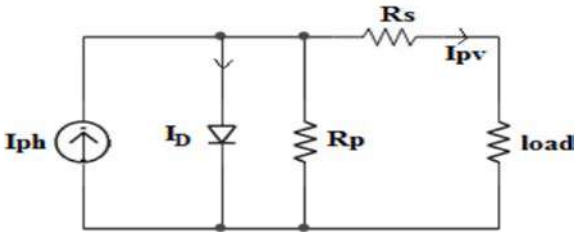

Fig. 2: Equivalent circuit of PV cell

$$I_{pv} = I_{ph} - I_s*(e^{((V+I*R_s)/(N*V_t))}-1) - I_{s2}*(e^{((V+I*R_s)/(N_2*V_t))}-1) - (V+I*R_s)/R_p \quad (1)$$

In equation (1)

- I_s and I_{s2} are the diode saturation currents,
- V_t is the thermal voltage,
- N and N_2 are the quality factors (diode emission coefficients) and
- I_{ph} is the solar-generated current.

The simulink model of PV module is shown in Fig. 3.

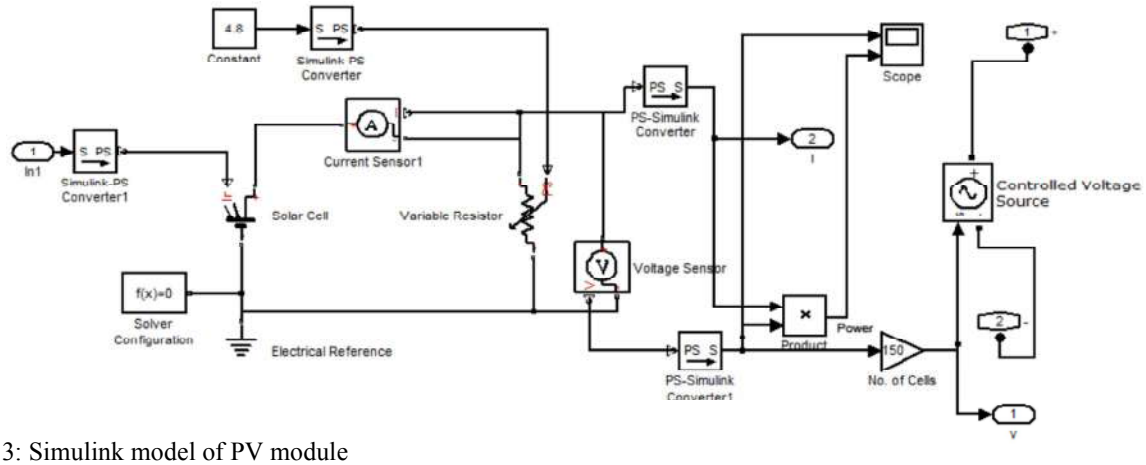

Fig. 3: Simulink model of PV module

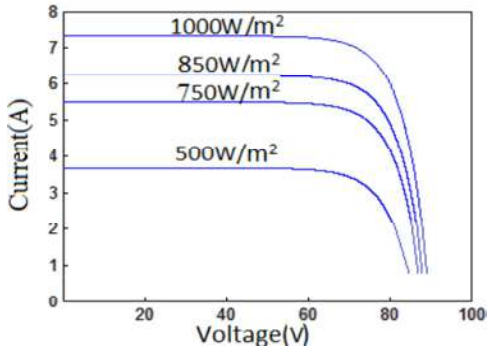

Fig. 4: I-V Characteristics of PV module

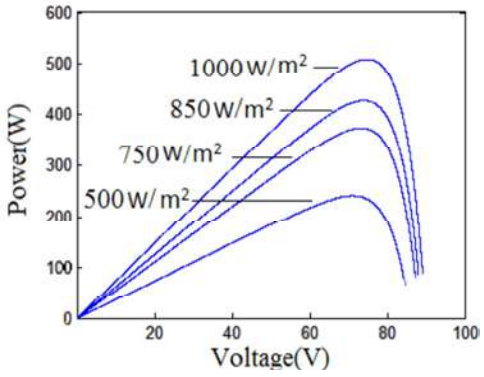

Fig. 5: P-V Characteristics of PV module

The I-V output characteristics of PV module for different irradiation are shown in Fig.4 and the P-V characteristics of PV module for different irradiance at 25° C are shown in Fig. 5.

vel is in accordant throughout the
ctric power generated by the PV
ging with atmospheric conditions.
oblem, Maximum Power Point Tracking (MPPT) algorithm is used [7]. It tracks the operating point of the I-V curve to its maximum value. Therefore, the MPPT algorithm will ensure maximum power is delivered from the PV modules at any particular atmospheric conditions. In this proposed multilevel dc link inverter, Perturb & Observe (P & O) algorithm is used to extract maximum power from the modules [8] and it implemented with M-file coding.

Novel Control Algorithm: The proposed PV multilevel dc-link inverter as shown in Fig. 6 can be separated into two parts; the power circuit and the controller part. Power circuit part explained in section-II. The controller part is consists of a MPPT tracking algorithm and novel control algorithm. Here Maximum Power Point Tracking algorithm uses a method called perturbation and observation (P&O) tracking for each PV source. The output signals of these P&O blocks are called reference signals V_{ref1}, V_{ref2}, V_{ref3}. Next, Novel control algorithm includes multicarrier PWM and output generation. The gating signals for the switches associated with PV employing the multicarrier PWM technique is generated using a digital logic. Here reference signals V_{ref1}, V_{ref2}, V_{ref3} compared with one triangular signal. The comparator output is given to a three 2-input AND gate. The second input to the each AND gate is derived from three triangular carrier signals $V_{carrier1}$, $V_{carrier2}$ and $V_{carrier3}$ compared with unipolar sine wave signal that generates the gating pulses to the corresponding switches which gives required multilevel positive dc-link waveform Vlink. Output generation uses direct PWM technique using sinusoidal signal which produces two inverted pulses. These pulses are used to control H-Bridge switches to form the desired ac output. This novel control algorithm provides a solution to the

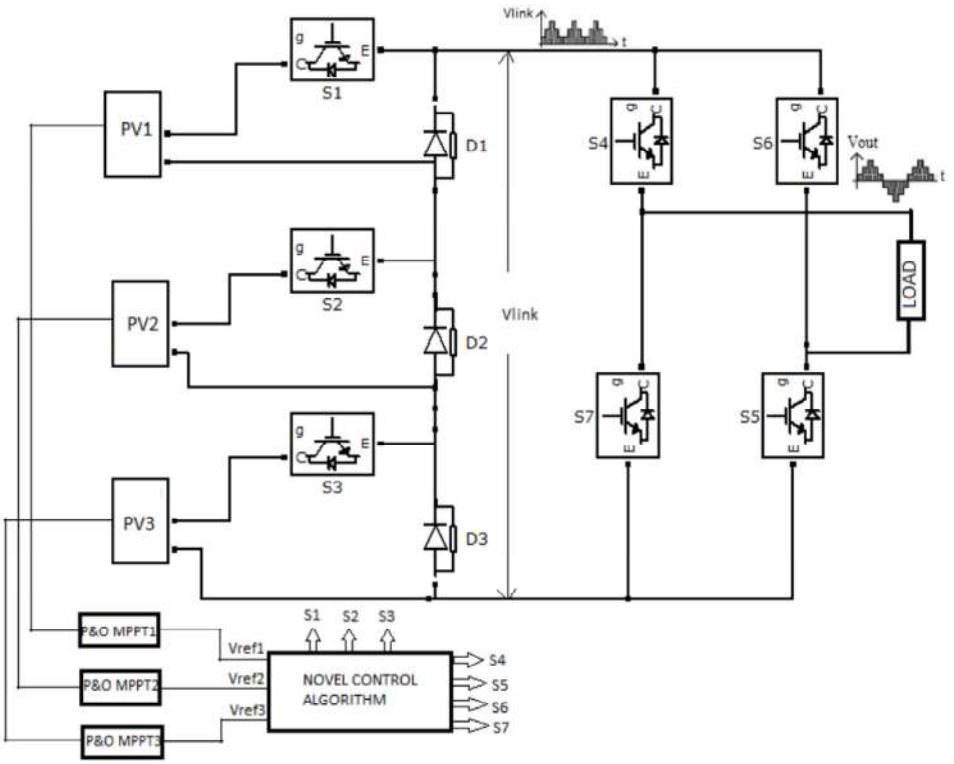

Fig. 6: PV multilevel dc-link inverter

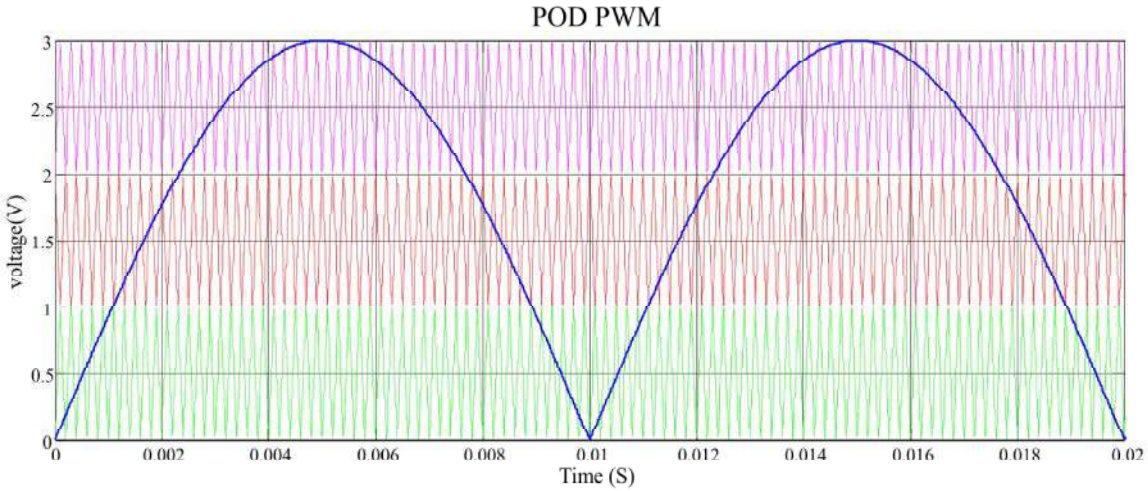

Fig. 7: Phase Opposition Disposition (POD) PWM

partial shading which enables each shaded PV source to be recovered to its MPP without affecting other PV sources. The advantages of such a technique are as follows: 1) all PV sources of the system are used equally, e of PV sources, they yield equal the switching losses of switches source are equal 2) It permits to sitive and negative half-cycles of the output voltage waveform under partial shading, i.e. when non uniform irradiance occurred on PV panel, so PV voltages are different [8].

Types of Multi Carrier Pwm Techniques: In this section various multicarrier PWM techniques are analyzed for seven-level PV dc-link inverter system [9, 10]. Sinusoidal PWM can be classified according to carrier and

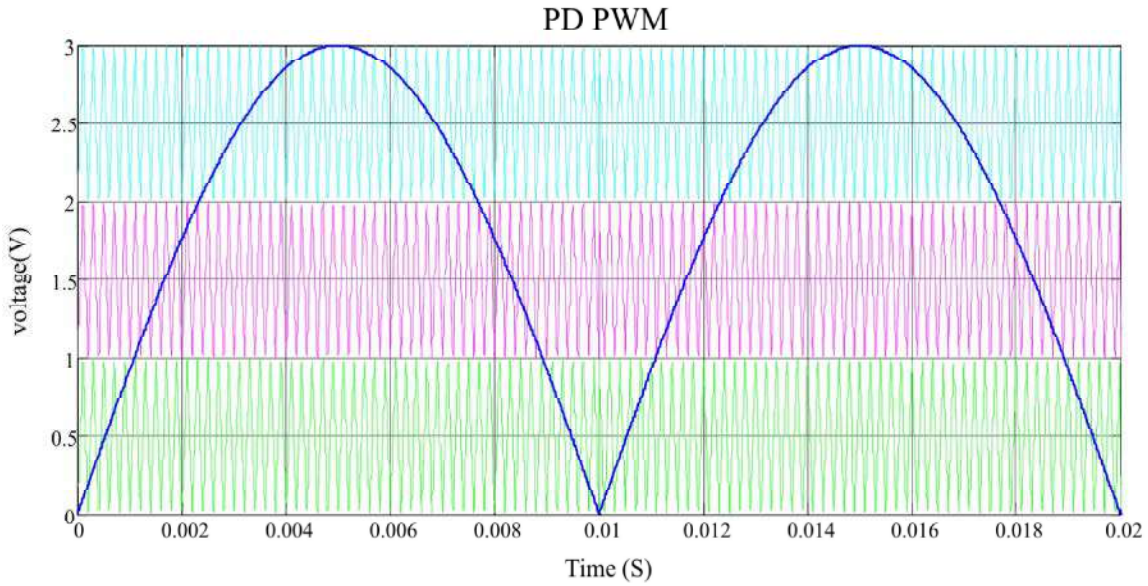

Fig. 8: Phase Disposition (PD) PWM

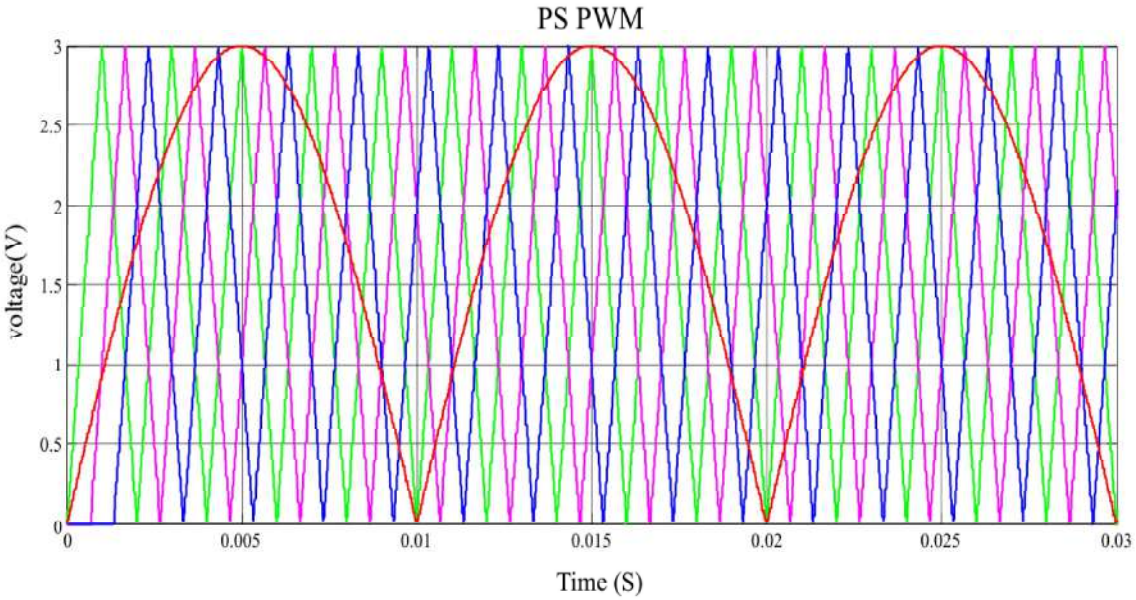

Fig. 9: Phase Shift PWM (PS) PWM

modulating signals. This work used the intersection of a unipolar sine wave reference with a triangular carrier wave to generate firing pulses. There are many alternative strategies to implement this. They are as given below.

Disposition (POD) PWM: arriers above the zero reference fted by 180° from those carriers below the zero reference POD PWM where the alternate carriers are arranged in 180° phase shift and are compared with reference as shown in Fig. 7.

Phase Disposition (PD) PWM: This technique where alternate carriers are in phase with each other and compared with reference as shown in Fig. 8.

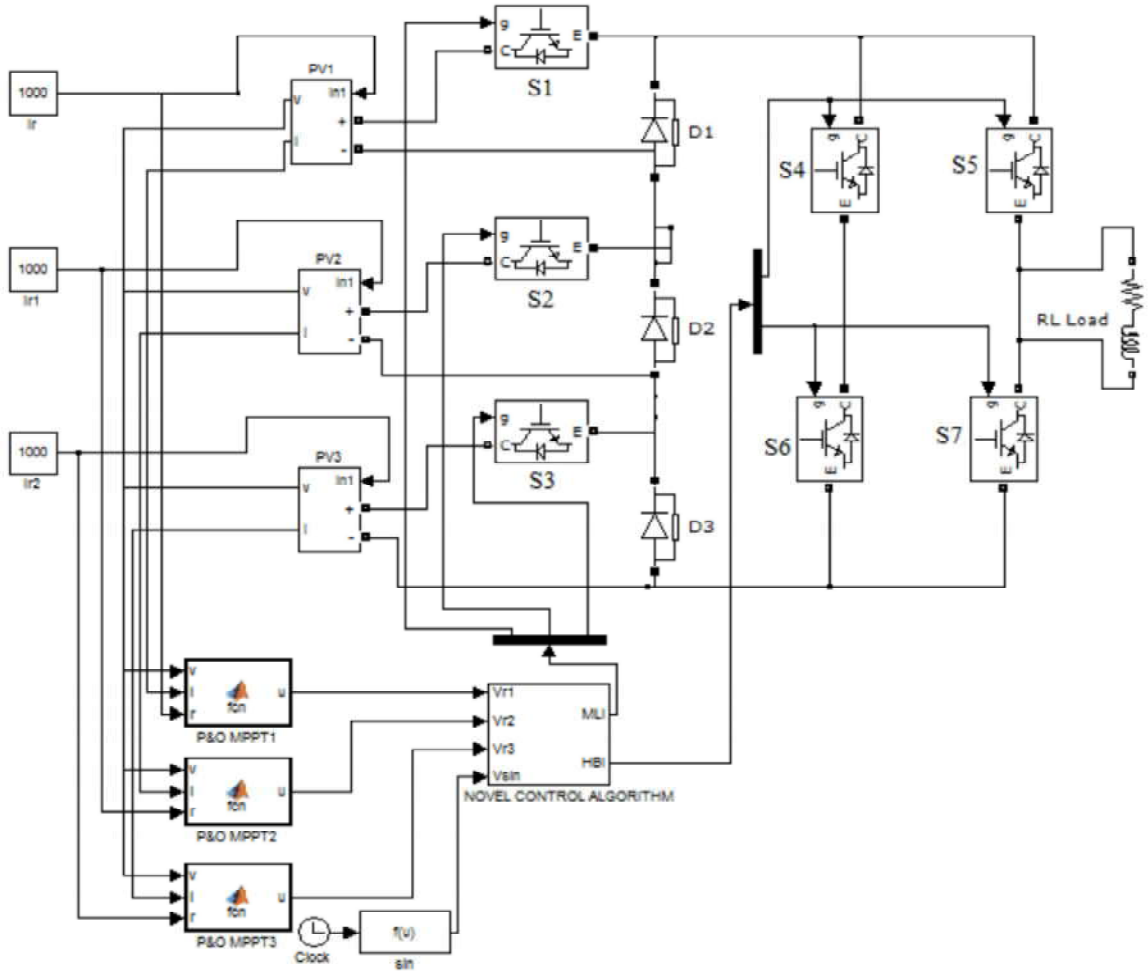

Fig. 10: Simulation diagram of seven level dc link Inverter

Phase Shift PWM (PSPWM): All carrier signals have the same amplitude and frequency but they are phase shifted by 90 degrees to each other. Numbers of carrier all of which are appropriately phase shifted are shown in Fig. 9.

RESULTS

Simulation results are carried out using MATLAB/SIMULINK. Fig. 10 shows the simulation diagram of seven-level PV dc-link inverter system.PV system formed of three PV sources, each rated at 90V, GBT-based inverter. The resulting veforms are shown in Fig. 11 at ls for sources PV1, PV2 and PV3

The comparison between POD PWM, PD PWM and PS PWM is shown in Fig. 12 which clearly shows POD PWM strategy provides the low voltage THD for different modulation indices than PS PWM technique [15-17].

The comparison between POD PWM, PD PWM and PS PWM is shown in Fig. 13 which clearly shows POD PWM strategy provides the low current THD for different modulation indices than PS PWM technique.

The comparison between POD PWM, PD PWM and PS PWM is shown in Fig. 14 which clearly shows POD PWM strategy provides the low voltage THD for different switching frequency than PS PWM technique.

The comparison between POD PWM, PD PWM and PS PWM is shown in Fig. 15 which clearly shows POD PWM strategy provides the low current THD for different switching frequency than PS PWM technique.

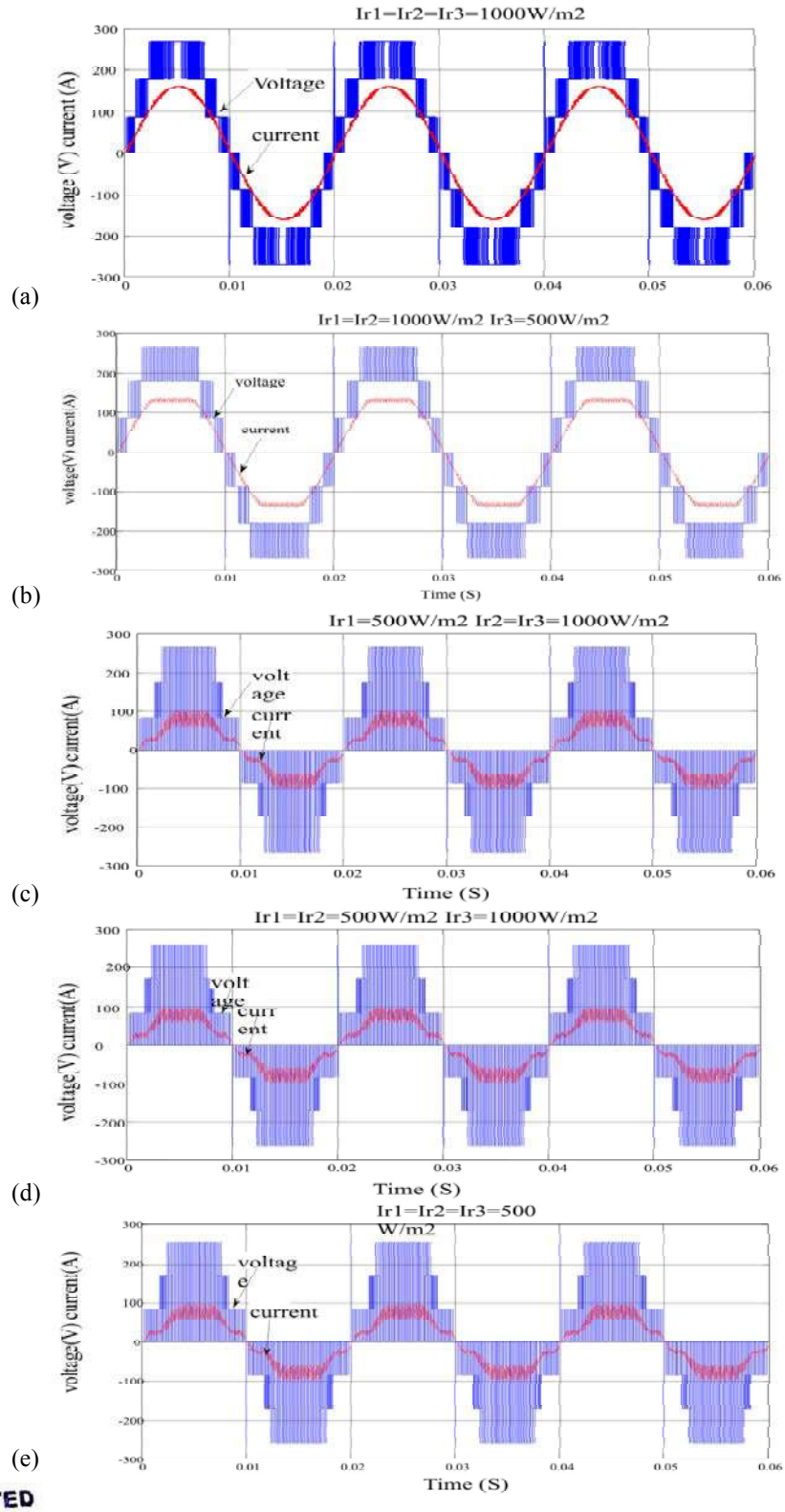

erter output voltage and current waveforms at irradiance levels for sources PV1, PV2, and PV3, 1000W/m2 for all; (b) 1000, 1000, 500W/m2 ; (c) 500, 1000, 1000W/m2 ; (d) 500, 500,1000W/m2; or all . The surface temperatures are 25°C for all irradiance levels.

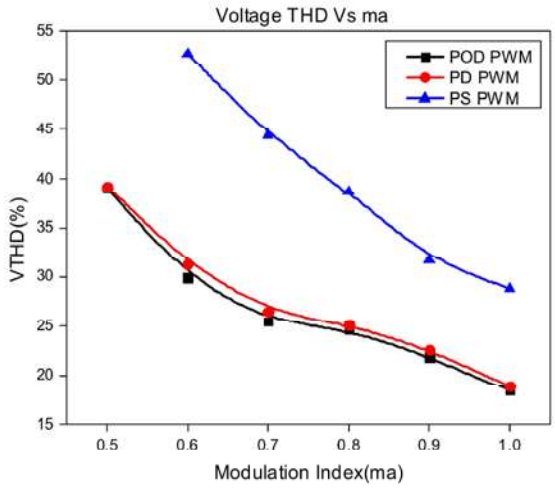

Fig. 12: Voltages THD versus various modulation Index

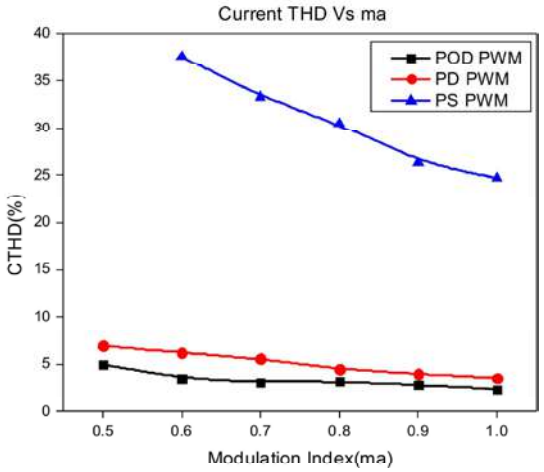

Fig. 13: Current THD versus various modulation index

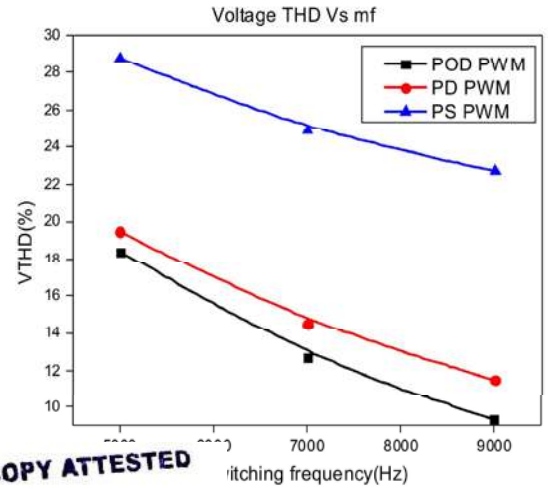

) versus various switching

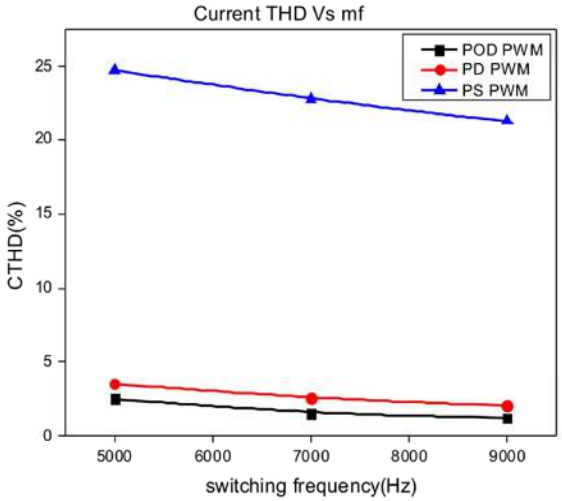

Fig. 15:Current THD versus various switching frequency

CONCLUSION

The presented multilevel dc link inverter system incorporates a novel method of extracting the maximum power from each PV source to the load while maintaining the operation of all PV sources at their MPPs under partial shading.The output voltage waveforms under various partial shading levels were analyzed by Fast Fourier Transform and the results show low THD and also different multicarrier PWM techniques were analyzed. It is found from graph shows that PODPWM technique provides output with relatively low distortion than PSP PWM technique. Appropriate PWM may be employed depending on the performance index required in a chosen application of MLDCI.

ACKNOWLEDGMENT

The authors thank the Management, Principal & Electrical and Electronics Engineering Department of Mohamed Sathak Engineering College and SSN College of Engineering for giving the necessary facilities to carry out this work

REFERENCES

1. Walker, G.R. and P.C. Sernia, 2004. Cascaded DC-DC converter connection of photovoltaic modules, IEEE Trans. Power Electron. 19(4): 1130-1139.

2. Shimizu, T., O. Hashimoto and G. Kimura, 2003. A novel high-performance utility-interactive photovoltaic inverter system, IEEE Transaction on Power Electronics., 18(2): 704-711.
3. Lee, S.J., H.S. Bae and B.H. Cho, 2009. Modeling and control of the singlephase photovoltaic grid-connected cascaded H-bridge multilevel inverter, in Proc. IEEE Energy Convers. Congr. Expo. Conf. Sep., pp: 43-47.
4. Abdulla, I., J. Corda and L. Zhang, 2013. Multilevel DC-Link Inverter and Control Algorithm to Overcome the PV Partial Shading, IEEE Transactions on Power Electronics, 28(1).
5. Atlas, H. and A.M. Sharaf, 2007. A Photovoltaic Array Simulation Model for Matlab-Simulink GUI Environment, IEEE, Clean Electric Power, Internationl Conference on clean Electrical Power (ICCEP'07), Ischia, Italy, pp: 14-16.
6. Cameron, Christopher, P., Boyson E. William and M. Riley Daniel, 2008. Comparison of PV system performance model predictions with measured PV system performance,IEEE Photovoltaic Specialists Conference, pp: 1-6.
7. Chee Wei Tan, Green and T.C. Hernandez-Aramburo, 2008. Analysis of perturb and observe maximum power point tracking algorithm for photovoltaic applications," C.A.Power and Energy Conference, PECon, pp: 237-242.
8. Seyezhai, R., 2011. cascaded hybrid five-level inverter with dual carrier PWM control scheme for PV syste, International Journal of Advances in Engineering & Technology, 1(5): 375-386.
9. Ning-Yi, D., W. Man-Chung, C. Yuan-Hua and H. Ying-Duo, 2005. A 3-D generalized direct PWM algorithm for multilevel converters, IEEE Power Electron. Lett., 3(3): 85-88.
10. Natarajan, S.P., 2012. Performance Evaluation of Multi Carrier Based PWM Techniques for Single Phase Five Level H-Bridge Type FCMLI, IOSR Journal of Engineering (IOSRJEN) ISSN: 2250-3021, 2(7): 82-90.
11. Calais, M., V.G. Agelidis and M.S. Dymond, 2001. A cascaded inverter for transformerless single-phase grid-connected photovoltaic systems, Renew. Energy, 22(1-3): 255-262.
12. Schmid, J. and R. Schatzle, 1982. Simple transformer-less inverter with automatic grid tracking and negligible harmonic content for utility interactive photovoltaic systems,in Proc. EC Photovoltaic Sol. Energy Conf., pp: 316-319.
13. Gui-Jia, S., 2005. Multilevel DC-link inverter, IEEE Trans. Ind. Appl., 41(3): 848-854.
13. Abdalla, I., L.Zhang and J.Corda, 2011. Generalized integration duty cycle conversion pulse-width modulation (IPWM) algorithm for multilevel PV DC-link inverter, in Proc. 14th Power Electron. Appl. Conf., pp: 1-10.
14. Seyezhai, R., 2011. Investigation of performance parameters for asymmetric multilevel inverter using hybrid modulation technique,International Journal of Engineering Science and Technology (IJEST), 3 : 12.
15. Liu, H., L.M. Tolbert, S. Khomfoi, B. Ozpineci and Z. Du, 2008. Hybrid cascaded multilevel inverter with PWM control method, in Proc, IEEE Power Electron, Spec. Conf., pp: 162-166.
16. Sun Ho-Dong, Honnyong Cha, Heung-Geun Kim, Tae-Won Chun and Eui-Cheol Nho, 2012. Multi-level Inverter Capable of Power Factor Control with DC Link Switches,IEEE Transaction, pp: 1639-1643.
17. agarbabu G. Madhu, 2014. Multilevel DC-link Inverter Topology with Less Number of Switches, Advance in Electronic and Electrical Engineering, 4(1): 67-72.

Feasibility Sensitivity Analysis in Potential Area for Standalone Hybrid Renewable Energy in Tamil Nadu, India

Article *in* Applied Mechanics and Materials · June 2014

DOI: 10.4028/www.scientific.net/AMM.573.757

3 authors:

Suresh Kumar
Sethu Institute of Technology
13 PUBLICATIONS **63** CITATIONS

SEE PROFILE

Manoharan P.S.
Thiagarajar College of Engineering
61 PUBLICATIONS **604** CITATIONS

SEE PROFILE

M.Valan Rajkumar
SSM Institute of Engineering and Technology, Dindigul, Tamil Nadu, India
21 PUBLICATIONS **175** CITATIONS

SEE PROFILE

Applied Mechanics and Materials Vol. 573 (2014) pp 757-766

doi:10.4028/www.scientific.net/AMM.573.757

Feasibility Sensitivity Analysis in Potential Area for Standalone Hybrid Renewable Energy in Tamil nadu,India

U. Suresh Kumar[1a*] P.S.Manoharan[2b] M.Valan Rajkumar[3c]

[1]Department of Electrical and Electronics Engineering, Mohamed Sathak Engineering College, Kilakkarai, India
* Corresponding Author: Tel: +91-8098180196, Fax: +91-0452-242327, Email: uskrk@sify.com
[2]Department of Electrical and Electronics Engineering, Thiagarajar College of Engineering, Madurai, India
[3]Department of Electrical and Electronics Engineering, SSM Institute of Engineering and Technology, Dindigul,
[a]uskr@sify.com [b]psmeee@tce.edu [c]valanrajkumar@gmail.com

Keywords: Solar and Wind Energy, HOMER, Potential Analysis, Ranking Status

Abstract

This paper attempts an investigation of the potential area of the standalone hybrid (solar and wind) renewable energy source. The investigation are based on the optimization result and ranking status. The various coastal areas identified for this are Kilakarai, Mandapam, Thirupullani, Kadaladi and Rameswaram in Ramanathapuram District of Tamilnadu State, India. The sensitivity analysis is also conducted. The consumer demand data are collected through the local distribution agency for the identified coastal areas. The wind and solar resources data are collected from NASA's surface meteorology and solar energy resource. HOMER has been used in this paper for optimization result and for sensitivity analysis. The preliminary investigation indicates that Thirupullani area is the potential area for standalone hybrid renewable energy system among the five coastal areas identified. By the sensitivity analysis, it is proved that the cost of energy, net present cost and operating cost was reduced to half of the actual cost, except the capacity shortage in Thirupullani area.

INTRODUCTION

Presently there is an increased awareness on the environmental problem resulting from coal based power sources. Also there are isolated areas in the costal belt of Tamil nadu (state) where people living find it difficult to get electricity. Integrating renewable energy with grid sources introduces the enormous technical difficulties which need to be overcome to obtain a sustainable, climate friendly power system in the near future particularly isolated area. Currently the Government utilities and research communities are collectively trying to increase the use of solar and wind resources as the most promising sources of energy among the renewable energy sources. Tamilnadu Government has currently focused on wind and solar energy generation and introduced a large number of projects in this area to achieve their mission to integrate 20 to 25% renewable energy into the grid by 2020. This paper has identified the potential area for renewable energy sources in the remote costal area of Tamil nadu, because of non- uniformity of resources in that area.The first step of the potential area investigation is based on the following previous works. The concept about integrating renewable energy systems (IRES), which was introduced by [1],[2],[3],[4] and also evaluated the techno economic aspects of small-scale decentralized IRES for existing renewable energy sources in the rural areas of developing countries. These
t on the basis of the divisible energy demands like cooking, irrigation, small-
ıg the cascaded and Tandem approaches. A knowledge-based approach was
nize the capital cost using the concept of loss of power supply probability
ncept [6] explained the off/risk method was to compute the optimal sizes of
V) array and the battery to minimize the capital investment as well as the

minimum loss of load probability (LOLP) requirement. By using an integrated goal programming [7] it is explained that seven energy sources are providing the power in households. HOMER software has been used for simulation of the electricity production of remote places [8], [9]. The major functions of the optimization techniques were being minimized in the total annual cost per year subject to the availability of the energy constraints. An optimum renewable energy model (OREM) was proposed [9],[10] for the effective utilization of renewable energy sources for lighting, cooking, pumping, heating, cooling and transportation in India for the period 2020–2021. Mathematical models have developed [11] for renewable energy system between the distribution system models and power flow calculations. It was found that introduction of diesel generator might improve the system voltage profile and reduce the losses in electrical transmission. This paper [12] discusses the optimization of the renewable energy hybrid system based on the sizing and operational strategy of generating system by the HOMER optimization tool. The operational scheme [13] was dealt by measuring cost efficiency and renewable fraction of different inputs of solar irradiation, water flow and load profile by using the software of the HOMER. In this paper, according to preliminary investigation results, Thirupullani was identified as the potential area for standalone hybrid renewable energy by HOMER tool based upon performance metrics and ranking status.

METHODOLOGY

HOMER models of the physical behavior of a power system evaluates the design options both for off-grid and grid-connected power systems for remote, stand-alone and distributed generation applications. But, this paper deals with potential area and the application of the sensitivity analysis in potential area of power generation from renewable energy source which is available in selected areas inputs to HOMER [16] contain electric load data, renewable source data such as photovoltaic, wind turbines, system component specifications and costs, and information for optimization of the model. It simulates thousands of system configurations, optimizes for life cycle cost and generates results of sensitivity analysis on most of the inputs. It repeats the optimization process for each value of the input, so it is possible to examine the effects of changes in the value on the results. This analysis is useful to support decision making or in the development of recommendations of the model [14]. HOMER is widely used to analyze the technical and financial viability of off-grid and grid-connected hybrid renewable energy system. Necessary data have been collected from NASA's Surface meteorology and Solar Energy [15]. NASA's SSE data is formulated as monthly average data from 24 years of data. To synthesize data using HOMER twelve average monthly values need to be entered, and then build a set of 8760 solar irradiation or wind speed value. The consecutive section discusses the input of HOMER tool.

INPUT OF HOMER

Electric load

A typical daily load profile for the coastal area is illustrated in Fig.1. The least power consumption is from 3:00 am to 4:00 am and the maximum power consumption is from 18:00 to 19:00. The electric load has a seasonal variation from December, to May as the peak months during summer, while June to October has lower loads during the winter.

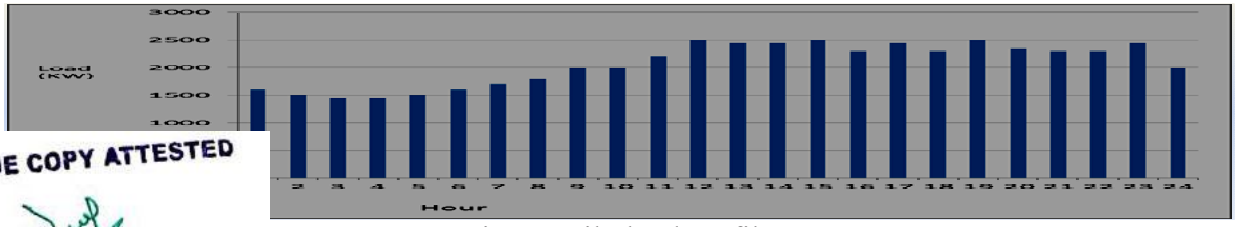

Fig.1. Daily load profile

Solar energy resource

The geographic allocation in terms of latitude and longitude of every area of Kilakarai (9.27, 79.123), Mandapam (8.0, 79.3), Thirupullani (9.55, 78.9), Kadaladi (15.23, 120.49) and Rameswaram (9.23, 78.78) located in Ramanathapuram District, Tamil Nadu State, India.The latitude and longitude value being mentioned within bracket against the each area for getting the solar irradiation during the whole year from the above website. In Fig.2 shows the solar resource data for these coastal areas. It can be seen from Fig. 2 that kilakarai, kadaladi area, possess least annual average solar resources (5.0kWh/m2) in the month of November because of the monsoon season. The other three areas get highest monthly average solar resource of nearly (7.0kWh/m2) during summer season. One of the advantages of solar resources is almost nine months is absorbed the huge amount of solar energy in all (more than 5 kWh/m2) selected areas.The Annual wind speed average is collected from [17,18] for five costal area of Ramanathapuram (Dt) is shown in Fig.3. It illustrates that the maximum annual average belongs to Thirupullani costal area (6m/s). The minimum annual average (4m/s) is observed from Kilakarai costal area. The wind energy resource is observed from all costal area by the wind speed of 4 m/s to 6 m/s.The adequate amount of wind resource is available in coastal areas, but the place was one among the potential area of standalone hybrid renewable power generation through the analysis.

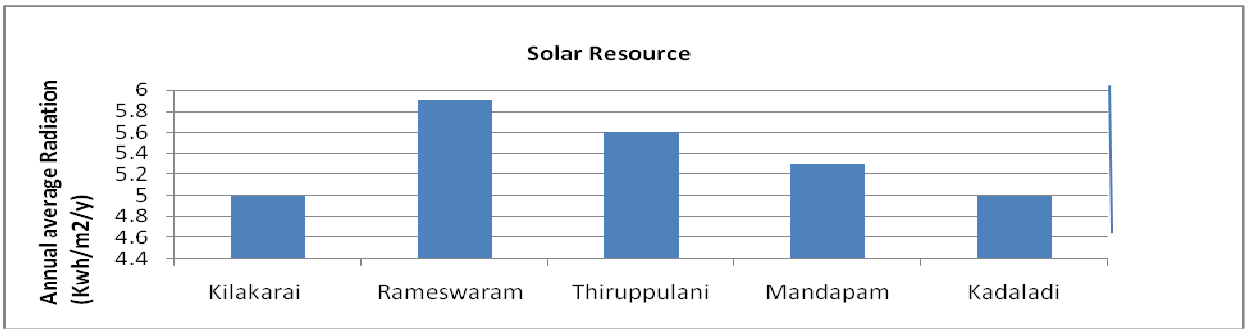

Fig.2.Annual average solar radiation

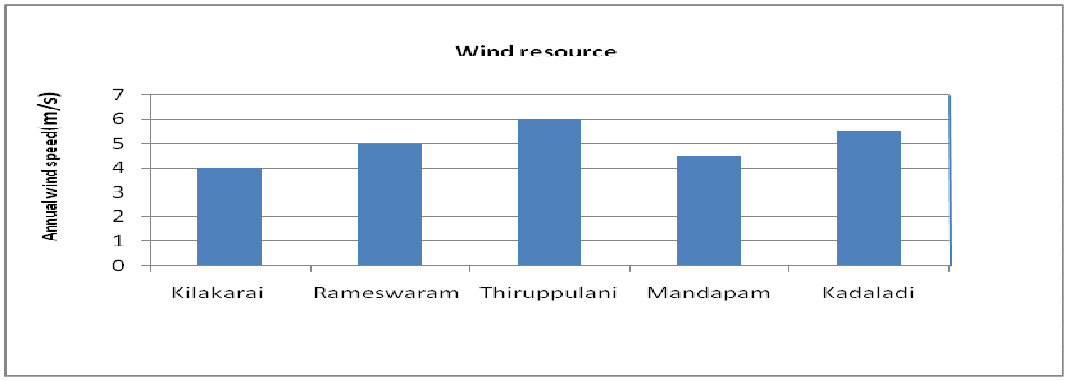

Fig.3. Annual average wind speed

STANDALONE HYBRID SYSTEM COMPONENTS SPECIFICATIONS

In this paper, Vesta wind turbine (1,650 kW) has been used. The installation, replacement and O&M [19] costs of this turbine area respectively $1350/kW, $1346/kW,$500. Its lifetime is estimated at 15 years. The number of units considered for this simulation is 6, 10, 20, 30.The size of ried from 20 to 1000 kW with life time of 20 years. A 1 kW solar energy ıd replacement costs are taken as $2000 and $2000, respectively. The name s Surette 4ks25P (4V, 1900Ah) is considered. The quantities of batteries to 100, 200, 250, 300, 350, 400, 600, 5000,10000.The cost of one battery is ıance cost of $11.The rating of converter is 1 kW, for the purpose of

installation and replacement costs is considered as $800 and $800, respectively. Seven different sizes of converter (1, 10, 50, 10000 kW) are taken in the model. The lifetime of a unit is considered to be 15 years with an efficiency of 90%. The project lifetime is estimated at 25 and 30 years. The annual interest rate is fixed at 6%.

SIMULATION RESULTS

Optimization result

In optimization result [20], the number of optimal combination is based upon the operating cost, net present cost, cost of energy, and capacity shortage. The net present cost is the present value of all the costs that it incurs over its lifetime, minus the present value of all the revenue that it earns over its lifetime. Costs include capital costs, replacement costs, operational and maintenance costs, fuel costs, emissions penalties, etc., on the other hand, the cost of energy is the average cost per kWh of electricity. To calculate the cost of energy, HOMER divides the annualized cost of producing electricity [21] (the total annualized cost minus the cost of serving the thermal load) by the total useful electric energy production. The capacity shortage fraction is equal to the total capacity shortage divided by the total electrical demand. HOMER considers a system feasible only if the capacity shortage fraction is less than or equal to the maximum annual capacity shortage. The optimization result of Thirupullani area is illustrated in Fig.4 According to the optimization results, the optimal combination of standalone hybrid renewable system components consists of a. 200 (kWpeak) PV, b.30 (kW) wind turbine c.battery bank (5000) and d.10 (kW) converter. The total NPC, Capital cost and COE for such a hybrid renewable system(25year) are Rs9,41,629,Rs25,785, Rs4.24 respectively. For the 30 year of system the total NPC, Capital cost and COE are Rs10,08,113, Rs28,776, Rs4.24 respectively. As per the results obtained, the COE remains the same with increasing life span but, there is increase in the total NPC, Capital cost for increase in the life span of the standalone hybrid renewable system. This result is identical for other coastal area selected for analysis although optimal result of these other areas are not displayed in this paper and a consolidated result is displayed in table 1.

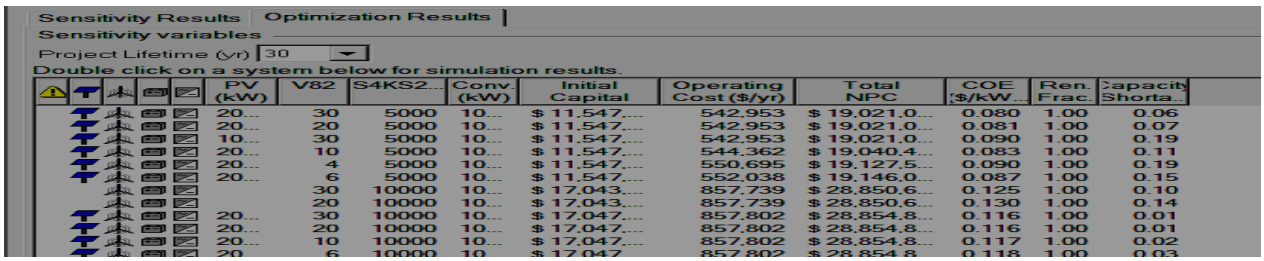

a)Lifetime: 25 years

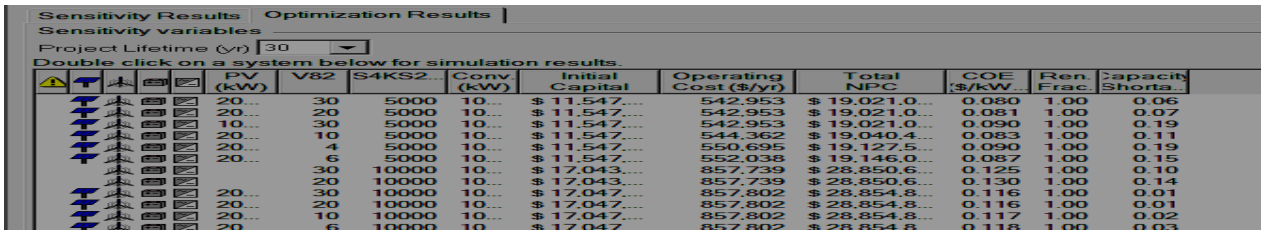

b) Lifetime: 30

Fig. 4.Optimization result for Thirupullani area

Potential Analysis

In this paper potential analysis is based upon the cost of energy, the net present cost, the operating cost and the capacity shortage.

Based upon cost of energy

The COE i.e., The average cost per kWh is observed for 25 and 30 years project life time as shown in table 1. Based upon observation, the least cost of energy for power generation from the renewable energy sources are available in Thiruppullani i.e., Rs 4.24/kWh with a life time of the project for 25 years and also the same cost is retained for same area at a cost of Rs 4.24 /kWh belongs to 30 years of the life of project. The reason is that huge amount renewable energy (wind resource (6m/s), solar resource (5.6 kWh/sqm)) is available in that area. The Kilakarai area is having high cost of energy per kWh at Rs5.67 kWh for 25 years and cost of energy for 30 years at Rs 5.67 /kWh.The main cause for highest cost of energy is that kilakarai area is having a very low amount of renewable energy resources(wind resource (4m/s),solar resource (5 kWh/sqm)).Thus for all the coastal area indentified the COE remain the same for both life time of the project namely 25 years and 30 years. Therefore this paper has recommended that the Thirupullani costal area is the potential area of power generation from renewable energy resources amongst the five areas based upon cost of energy for both
span of lifetime of the project.

Table 1 Potential analysis (Areas Vs COE)

Name of area	Resources		Lifetime(Year)	Cost of energy (Rs)
	Wind (m/s)	Solar(KWh/sqm)		
Kilakarai	4.0	5.0	25	5.67
			30	5.67
Mandapam	4.5	5.3	25	4.45
			30	4.45
Thirupullani	6.0	5.6	25	4.24
			30	4.24
Rameswaram	5.0	5.9	25	4.39
			30	4.34
Kadaladi	5.5	5.0	25	4.39
			30	4.34

Based upon net present cost

The net present cost of a system is the present value of all the costs that it incurs over its lifetime, minus the present value of all the revenue that it earns over its lifetime. Costs include capital costs, replacement costs, operational and maintenance costs, fuel costs, emissions penalties, etc. This analysis starts with the optimization result in Kadaladi area as shown in table 2 for 25years and 30 years respectively. According to the results of the optimization process the consumer demand of 50 MW/day, and peak demand of 4.7MW for Kadaladi area has to satisfy the stand alone hybrid renewable system, which comprises 200 kW PV array, 30 wind turbines at rating of 1650 kW generators each, a 10 kW converter and 5000 batteries at nominal voltage of 4 volts each. The proposed system for Kadaladi gives rise to total net present cost for the 25 year project at Rs 9,46,703 against the higher value of Rs10,12,970 for 30 years project. The remaining costal area's net present cost is shown in table 2. The net present cost of Thirupullani area is Rs 9, 41,629 for 25 ıcreased to Rs10,08,113 for 30 years project life time. By comparing the net s, it is seen that Thirupullani area possess the least net present cost, because ınt of renewable energy sources.One of the most important conclusion is f project increases, the net present cost also increases.

Table 2 Potential analysis (Areas Vs NPC)

Name of area	Resources		Lifetime(Year)	Net present Cost(Rs)
	Wind (m/s)	Solar(KWh/sqm)		
Kilakarai	4.0	5.0	25	11,25,355
			30	12,13,532
Mandapam	4.5	5.3	25	9,56,394
			30	10,22,242
Thirupullani	6.0	5.6	25	9,41,629
			30	10,08,113
Rameswaram	5.0	5.9	25	9,55,836
			30	10,21,709
Kadaladi	5.5	5.0	25	9,46,703
			30	10,12,970

Based upon operating cost

The operating cost depends upon the component cost and it includes wind turbine, solar panel, battery and converter. The Kadaladi area possess low amount of renewable energy sources, which leads to an increase in operating cost. If the increase in operating cost is to be avoided then the number of components will not be able to satisfy the consumer demand. The size of the components considered in Kadaladi area include wind turbine (30), solar panel (200), battery (5000), converter (10) and it satisfies the consumer demand with the operating cost of Rs26,182 for the 25 year lifetime of the project. The operating cost is Rs 29,129 for the 30 year lifetime of the project as shown in Table 3. The least operating cost belongs to Thirupullani area having the highest amount of renewable energy sources when compared with other areas which automatically leads to utilization of fewer components for generating the electricity from renewable energy source. The operating costs of the remaining areas are also shown in the Table 3.

Table 3 Potential analysis (Areas Vs Op cost)

Name of area	Resources		Lifetime(Year)	Operating Cost (Rs)
	Wind (m/s)	Solar(KWh/sqm)		
Kilakarai	4.0	5.0	25	33,173
			30	37,214
Mandapam	4.5	5.3	25	26,940
			30	29,802
Thirupullani	6.0	5.6	25	25,785
			30	28,776
Rameswaram	5.0	5.9	25	26,896
			30	29,764
Kadaladi	5.5	5.0	25	26,182
			30	29,129

Capacity Shortage

The capacity shortage is shown in Table 4 means unmet load or shortage of power generation ces.In HOMER, higher value of the capacity shortage fraction is considered ptable in any system configuration. The capacity shortage fraction value of 0.06 for the project lifetime of 25 years and the same fraction value is of project lifetime, because the availability of renewable energy in particular

area is same for all years. The second and the third least value of the capacity shortage fraction is 0.08 and 0.09 for both the years of life time of project i.e., 25 and 30 years respectively for Rameswaram and Kadaladi areas.The difference between these two areas capacity shortage fraction is very small, because the availability of the solar resource for both Rameshwaram and Kadaladi are slightly different, but in wind resource is remains the same i.e. the wind energy of 5.0 m/s and 5.5 m/s respectively for both areas. The capacity shortage of Mandapam and Kilakarai are 0.10 and 0.17 for both the years of life time project respectively having the next higher value of capacity shortage fraction i.e., the fourth and the fifth position based upon the ranking status is shown in table 5. The least value of the capacity shortage fraction depends upon the availability of the renewable resources from the particular areas, it can be concluded that if the renewable energy resources are available in plenty in area leading to generation of more electricity and thereby minimizing the unmet load .This will give least value of the capacity shortage fraction.

Table 4 Potential analysis (Areas Vs Capacity shortage)

Name of area	Resources		Lifetime(Year)	Capacity shortage(%)
	Wind (m/s)	Solar(KWh/sqm)		
Kilakarai	4.0	5.0	25	0.17
			30	0.17
Mandapam	4.5	5.3	25	0.10
			30	0.10
Thirupullani	6.0	5.6	25	0.06
			30	0.06
Rameswaram	5.0	5.9	25	0.08
			30	0.08
Kadaladi	5.5	5.0	25	0.09
			30	0.09

RANKING STATUS

The Table 5 is shown the ranking status of coastal areas for generation of electricity from the renewable energy sources. The ranking status is assigned by 1 to 5 based upon the minimum value of the cost of energy, the net present cost, the operating cost and the capacity shortage of individual costal area .The minimum value of cost is ranked by 1 and the maximum value of cost is ranked by 5. The location having the maximum no, of 1's could be recommended as a highly potential area for standalone hybrid renewable energy sources. According to the ranking status, Thirupullani area is the highly potential area of power generation from renewable energy sources.

Table.5.Ranking status

Name of area	Wind (m/s)	Solar (kWh/sqm)	Cost of Energy		Net Present Cost		Operating cost		Capacity shortage	
			25Yrs	30Yrs	25Yrs	30Yrs	25Yrs	30Yrs	25Yrs	30Yrs
Kadaladi	5.5	5.0	2	1	2	2	2	2	3	3
Rameswaram	5.0	5.9	4	2	4	4	3	3	2	2
		5.6	1	2	1	1	1	1	1	1
		5.3	3	2	3	3	4	4	4	4
		5.0	5	3	5	5	5	5	5	5

SENSITIVITY ANALYSIS

The sensitivity analysis is a measure that checks the sensitivity of a model when changing the value of the parameters of the model and also changing the structure of the model. In this paper sensitivity analysis has been undertaken to study the effects of variation in the solar radiation and wind speed, and to make appropriate recommendations on developing a hybrid renewable energy system. The simulation software simulates the long-term implementation of the hybrid system based upon the respective search sizes for the predefined sensitivity values of the components. The sensitivity variable has set for the solar resource and wind resource is (G=7.00), wind speed (v=6.5). This sensitivity variable is common for all selected coastal areas. Based and sensitivity analysis, it has been observed that Thirupullani area suitable for potential area of power generation from renewable energy sources, and plays a key role in developing a sustainable society for the future. Table.6 shows the sensitivity analysis for Thirupullani area and also the table 7 shows the sensitivity analysis for all isolated areas.The COE for the Thirupullani area has come down to Rs 2.33/kWh is shown in table from Rs 4.24/kWh (without sensitivity variable) for 25 years of project and also same for 30 years of project, i.e the cost of energy is reduced to Rs 2.27/ kWh from Rs 4.24/kWh (without sensitivity variable). From sensitivity analysis, it is seen that the Kilakarai area only is possed the different amount of NPC for the both year of life time (25 and 30 years respectively) is shown in Table.6. Due to contribution of wind speed and solar irradiation are not promising, then, it leads to need the more no; of components.So this two factors is contributed the different amount of NPC for the Kilakarai area.Figs.5 & 6 represents the before and after the sensitivity results from Thirupullani area.It has seen that the PV/Wind/battery is covered more area than without sensitivity analysis. Application of sensitivity analysis brings about changes in operating cost, Total NPC, COE but no change in capacity shortage.

Table.6 Sensitivity Analysis for Thirupullani area

Solar (kWh/m^2/ daily)	Wind (m/s)	life time(yr)	PV (KW)	V82 (wind)	S4ks25 (bat)	Conv (kW)	Initial Capital (Rs)	Operating Cost (Rs/yr)	Total NPC (Rs)	COE (Rs/kWh)	Capacity Shortage (%)
5.6	6.0	30	200	30	5000	10	6,12,009	28776	10,08,113	4.24	0.06
5.6	6.0	25	200	30	5000	10	6,12,009	25785	9,41,629	4.24	0.06
5.6	6.5	30	200	30	0	10	3,20,509	12089	4,86,919	2.27	0.20
5.6	6.5	25	200	30	0	10	3,20,509	10897	459,810	2.33	0.20
7.0	6.0	30	200	30	5000	10	6,12,009	28776	10,08,113	4.18	0.05
7.0	6.0	25	200	30	5000	10	6,12,009	25785	9,41,629	4.24	0.05
7.0	6.5	30	200	30	0	10	3,20,509	12089	4,86,919	2.27	0.20
7.0	6.5	25	200	30	0	10	3,20,509	10897	4,59,810	2.33	0.20

Table 7. Sensitivity Analysis for all coastal areas

Name of area	Resources		Life Time (Years)	Cost of energy (INR)	Net present cost (INR)	Operating cost (INR)	Capacity shortage (%)
	Wind (m/s) Annually	Solar (kWh/sqm) Annually					
Kilakarai	6.5	7	25	4.87	9,63,907	29,779	0.18
			30	4.92	10,42,676	33,378	0.18
Mandapam	6.5	7	25	2.33	4,59,810	10,897	0.20
			30	2.27	4,89,919	12,089	0.20
Thirupullani	6.5	7	25	2.33	4,59,810	10,897	0.20
			30	2.27	4,89,919	12,089	0.20
		7	25	2.33	4,59,810	10,897	0.19
			30	2.27	4,89,919	12,089	0.19
		7	25	2.33	4,59,810	10,897	0.20
			30	2.27	4,89,919	12,089	0.20

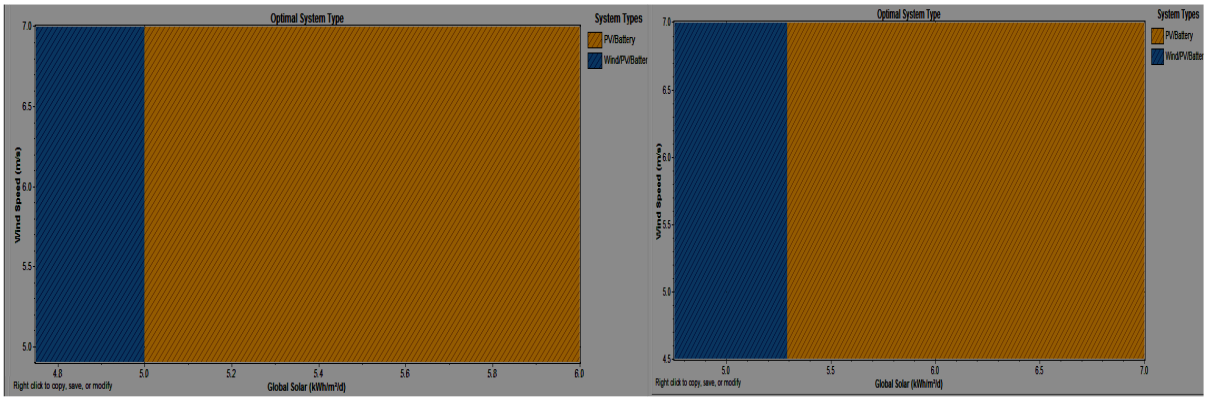

Fig.5 Before sensitivity result for Thirupullani area Fig.6 After sensitivity result for Thirupullani area

8. CONCLUSION

This paper investigates the potential area for renewable energy particularly wind and solar energy available in Ramanathapuram (District), Tamilnadu (State), India. The potential area analysis and sensitivity analysis are conducted to select the most suitable area to deploy the solar and wind plants to generate electricity from renewable sources through by performance analysis and ranking status. Final results show that renewable energy sources not only reduce the cost of energy generation but also reduce GHG emission significantly which plays a key role in developing a sustainable climate and eco friendly environment. It is observed that Thirupullani area of Ramanathapuram is the most potential area to install hybrid (wind and solar) plants. The cost of energy, net present cost, operating cost and capacity shortage of aforesaid area was found 4.24 Rs/kWh,9,41,629 Rs, 25,785 and 0.06 (%) respectively for the project lifetime of 25 years, but for the project lifetime of 30years the net present cost and operating cost were increased to Rs10,08,113 and Rs 28,776 respectively. There is no change in the cost of energy and capacity shortage for the 30years life time. Another major advantage is that Thirupullani area is reduces CO2 emission significantly which helps to develop a climate friendly environment for the future.

REFERENCES

[1]Abdu-Khader, M. M., and Speight. J. G. J.G.2004.The concepts of energy, environment, and cost for process design. Int. J. of Green Energy 1:137–151.

[2]Davetoke, and Kenichioshima, 2007, Comparing market-based renewable energy regimes:the cases of the UK and Japan, International Journal of Green Energy 4:409-415

[3].Ramakumar,2004. Role of renewable energy in the development and electrification of remote and rural areas IEEE Power Engg Soc Gen Meeting 2: 2103-2105.

[4]R.Ramakumar,1996 Energizing rural areas of developing countries using IRES IEEE Conference on Energy&Engg 3: 1536–1541.

[5]Ramakumar,R., and Hughes,W.L, 1981.Renewable energy sources and rural development in developing countries .IEEE Trans on Energy, 24: 242–251.

[6]Ramakumar,R., Butler, N.G., and Rodriguez,A.P,1993 Economic aspects of advanced energy technologies,"in Proceedings of IEEE., 81: 318-332.

[7]Ramakumar,R.,Abouzahr,I.,and Ashenayi,K 1992.A knowledge-based approach to the design of integrated renewable energy systems., IEEE Trans on Energy Converters., 7:648-659. 1992.

l Bakirtzis,A.G ,1992.Design of a standalone system with renewable energy methods. IEEE Trans on Energy Conv.,7: 42-48.

d, Ganesh,L.S, 1995 Energy alternatives for lighting in households: an ıtegrated goal programming," Energy, . 20, 63–72.

[10]Weis, T.M., and Ilinca Adrian., 2008.The utility of energy storage to improve the economics of wind–diesel power plants in Canada. Renewable Energy. 33:1544-1557.

[11] Himri,Y., Boudghene Stambouli, A., and Draoui,B.,2008 Techno-economical study of hybrid power system for a remote village in Algeria. Solar energy 33, 1128–1136.

[10]Iniyan,S.,Suganthi,I.,and T.R.Jagdeesan.,1998. Renewable energy planning for India in the 21st century Renewable Energy.14,453–457.

[12]Ramakumar.,R.and ,P.Chiradeja,2002 Distributed generation and renewable energy systems,37th Intersociety engineering conference (IECEC), IEEE 716–724.

[13]Nurul Arina., Abdull Razak, and Muhammad Murtadha in Othman,2010.,Optimal Sizing and Operational Strategy of Hybrid RenewableEnergy System Using HOMER.Conf. (PEOCO2010), Malaysia..

[14]ShakawatHossan.M.,MarufHossain,M and ReazulHaque A.R.N.M., 2011, Optimization and Modeling of a Hybrid Energy System for Off-grid Electrification 10th International Conference on Environment and Electrical Engineerin (EEEIC 2011) Rome, Italy, 8-11.

[15] T.Lambert, P. Lilienthal, HOMER, "The micro-power optimization model Software Produced by NREL," Available from: <www.nrel/Gov/HOMER>; 2004.

[16]NASA Surface meteorology and Solar Energy, "[Online Availability]: http://eosweb.larc.nasa.gov/ SSE/RET Screen/, "as at 19th December'2012

[17] HOMER," Analysis of micro power system options," [Online Available]: https:/ analysis.nrel.gov/homer/.

[18] "Solar radiation and climate experiment (SORCE), Fact Sheet, Tech. Report, NASA, Earth Observatory," [Online available]: http: //earth observatory. NASA. Gov/Features/SORCE/print all.php.

[19]. D.B.Nelson, M.H. Nehrir, and C.Wang, Renewable Energy, 31, 1641 (2006).

[20] K. Akella, M. P. Sharma, R. P. Saini, Renewable and Sustainable Energy Reviews, 11, 894, 2007.

[21] D.P.Kaundinya, P.Balachandra,N.H. Ravindranath, Renewable and Sustainable Energy Reviews, 13, 2041(2009)..

Research Journal of Applied Sciences, Engineering and Technology 8(19): 2048-2056, 2014
DOI:10.19026/rjaset.8.1197
ISSN: 2040-7459; e-ISSN: 2040-7467

Submitted: April 29, 2014 Accepted: June 02, 2014 Published: November 20, 2014

Research Article

Optimization and Cost of Energy of Renewable Energy System in Health Clinic Building for a Coastal Area in Tamil Nadu, India Using Homer

[1]U. Suresh Kumar and [2]P.S. Manoharan
[1]Department of Electrical and Electronics Engineering, Mohamed Sathak Engineering College, Kilakkarai, India
[2]Department of Electrical and Electronics Engineering, Thiagarajar College of Engineering, Madurai, India

Abstract: The renewable energy potential of coastal areas of Tamil Nadu, India ranks along with the utmost in the world. This study proposes optimization and cost of energy of different hybrid renewable energy system to power a health clinic in that building. The National Renewable Energy Laboratory (NREL) optimization computer model for distributed power, "HOMER," is used to estimate the optimization and its cost of energy. The implementation of RE systems to supply Rural Health Clinics will contribute to reduce both electricity generation cost and to reduce the consumption of fuel while improving health care and quality of life in these isolated coastal regions. We conclude that using the PV+Wind+Diesel+Battery system for these types of applications in justified on technical and economic grounds. The experimental results show that the least cost of energy at Rs 5.00/KWh, is obtained from above said system and also experiment result shows that the COE decreases with 0% of interest. It is noted, that the PV+Wind+Diesel+Battery hybrid system shows the lowest COE and high amount of Renewable energy.

Keywords: Diesel generator, hybrid system, PV, renewable energy systems, rural health, wind energy

INTRODUCTION

Most of the coastal areas in Tamil Nadu are still under developed and in a chaotic state after the demand of development activities and there is a need to provide these areas with electricity. Small standalone hybrid renewable energy systems can play a strategic role in the region's balanced and sustainable development. The region enjoys a huge amount of renewable energy sources during the entire year. Although capable of providing plentiful and reliable electricity, this resource is presently remaining untapped. The renewable energy sources (NASA, 2012) can satisfy the electrical needs of clinics, schools and other social places in a way that can positively affect healthcare and education, ensuring adequate services for the population. An excellent application of these systems is in health clinics. The relation between health and energy is compounding and as interdependent factors, they largely determine the progress of rural development. Reliable electricity generation on site is capable of delivering high-quality electricity for vaccine refrigeration, lighting, communication, medical appliances, clean water supply and sanitation (Lambert, 2012). The latitude and area, is 9°14' N, 78° 50' E. The very hot, with temperatures reaching 49°C in the hot season, from March to September. This study reports the optimization and computes the COE for the different hybrid renewable system. NASA meteorological data has been used for acquiring data of the ambient conditions to measure: hourly (global horizontal irradiance) global irradiance, relative humidity, ambient temperature, direction wind and speed. This recorded data for 2012 have been used to assess renewable energy potential in considered area as shown in Table 1 and 2. The NASA meteorological data found that the yearly solar energy received is 5.0

Table 1: Monthly average solar radiation

Month	Month clearness index	Avg. radiation (kW h/m^2/day)
January	0.61	5.50
Feb.	0.64	6.20
Mar.	0.63	6.50
Apr.	0.58	6.10
May	0.49	5.10
Jun	0.53	5.50
July	0.50	5.20
Aug.	0.55	5.80
Sep.	0.48	5.00
Oct.	0.47	4.60
Nov.	0.41	3.80
Dec.	0.52	4.60
Average		5.32

Avg.: Average

U. Suresh Kumar, Department of Electrical and Electronics Engineering, Mohamed Sathak Engineering College, Kilakkarai, India, Tel.: +91-8098180196; Fax: +91-0452-242327

kWh/m^2 and the wind energy received is at a moderate speed (4 to 6 m/sec).

MATERIALS AND METHODS

Feasibility of the proposed system: The design of the proposed system to power the health clinic is done according to http://www.mem-algeria.org/ medical equipments installed in the clinic. The total load capacity is found to be 34.9 kWh/day. The system consists of wind turbine, PV modules, diesel generator, batteries, charge controller, inverter and the necessary wiring and safety devices. The system feasibility analysis was performed using the HOMER software developed by the National Renewable Energy Laboratory (NREL) to evolve the design of micro power systems. HOMER is a computer model that simplifies the task of evaluating design options for both off-grid (Jennings and Green, 2000) and grid-connected (Bakos *et al*., 2003) power systems for remote, stand-alone and distributed-generation (Cetin *et al*., 2009) applications. HOMER's optimization and sensitivity analysis algorithms allow one to evaluate the economic and technical feasibility of a large number of technology options and to account for variation in technology costs and energy resource availability. HOMER models (Ramakumar *et al*., 1992) both conventional and renewable-energy technologies. HOMER models a power system's physical behavior and its life-cycle (Kabouris and Contaxis, 1992) cost, which is the total cost of installing and operating the system over its life span. HOMER allows the modeler to compare many different design option based on their technical and economic criteria (Antony Day *et al*., 2011). It also assists in understanding and quantifying the effects of uncertainty or changes in the inputs.

Assumptions and homer model inputs:

Clinic load analysis: The typical clinic building (http://www.rsvp.nrel.gov) comprises the following rooms: administration room, doctor room, nurses' room, waiting room, two treatment rooms, small pharmacy and two restrooms. The medical equipment, lighting and other devices used in this clinic are the following: refrigerator (80 W), freezer (80 W), vaporizer (50 W), oxygen concentrator (300 W), electric sterilizer (1500 W), water pump (100 W), color TV set (130 W), 15 florescent lamps (20 W each), seven ceiling fans (60 W each) and three evaporative coolers (500 W each). The estimated daily working hours of the medical equipment and other devices are as follows: fluorescent lamps (exteriors and interiors), 12 h/day; TV set, 6 h/day; refrigerator and freezers, 14 h/day; ceiling fans, 12 h/day; vaporizer, 3 h/day; oxygen concentrator, 2 h/day; electric sterilizer, 3 h/day; and water pump, 6 h/day. The system is assumed to work for 6 days a week. Our analysis found that the total connected wattage is 4460 W and the total average daily load is 31.6 kW h. The load analysis calculation is listed in Table 3. A small base load of 0.18 kW occurs from 5 pm until 7 am. This load is for outside lighting and some inside lighting, whereas the majority of the load occurs during the day time (8 am to 5 pm) (Fig. 1).

Table 2: Monthly average wind energy

Month	Avg. wind source (m/sec)
January	3.5
Feb.	3.9
Mar.	4.0
Apr.	4.8
May	4.8
Jun	5.2
July	4.9
	4.5
	4.2
	3.9
	3.1
	3.7
	4.2

Table 3: Electric load worksheet (abbreviated)

Individual load	Qty	Qty/ watts	Total watts	Total h/day	Watts h
Lamps	13	20	260	12	3120
Lamps (out)	2	20	40	2	80
Refrigerator	1	80	80	14	1120
Freezer	1	80	80	14	1120
Vaporizer	1	50	50	3	150
Oxygen conc.	1	300	300	2	600
Elec. steril.	1	1500	1500	3	4500
Water pump	1	100	100	6	600
TV set	1	150	150	12	1800
Ceiling fan	7	60	320	12	3840
Evap. cooler	3	500	1500	12	18000

AC total connected watts: 4380; AC average daily load: 34930 Wh

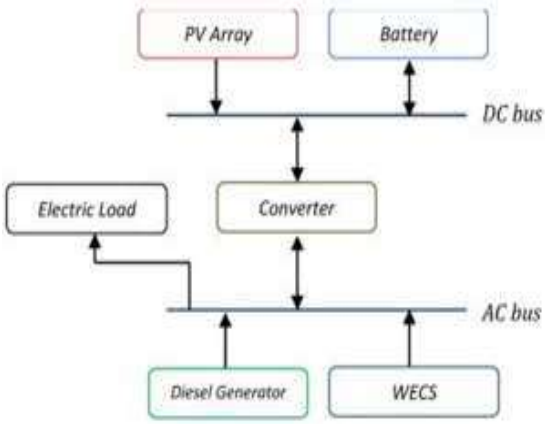

Fig. 1: Block diagram of renewable energy system

The sample clinic to locate in remote costal area called Kilakarai in Tamil Nadu (State) India, (9.27 N, 79.123 E). The wind data and solar radiation data for this region were obtained from the NREL (2011). Table 1 and 2 shows the monthly average solar radiation and wind for this area. The annual average solar radiation is 5.32 kWh/m^2/day and annual average wind energy is 4.2 m/sec.

SYSTEM COMPONENTS AND ESTIMATED PRICES

The proposed system consists of PV modules (http://eosweb.larc.nasa.gov/) batteries, charge controller, inverter, auxiliary diesel generator (Saheb-Koussa *et al*., 2009) and the rest of the balance-of-systems (McGowan *et al*., 1996) which includes modules structure, wiring, fuses and other system safety devices.

PV array: The PV array (without MPPT technique) is an interconnection of PV modules or panels that produces Direct-Current (DC) electricity in direct proportion to the solar radiation incident upon it, independent of its temperature and voltage to which it is exposed. The suggested PV panels to be used in the system simulation are 500 W (Kaldellis and Ninou, 2011) and 24 V and have estimated capital and replacement cost of Rs. 81,000 and 75,600. This cost includes shipping, tariffs, mounting hard-ware, control system, wiring, installation and labor cost. The lifetime is assumed to be 25 years. A de-rating factor of 90% was (Dalton *et al*., 2009; Lockington *et al*., 2008) applied to the electricity generated from each panel. The panels were modeled as fixed and tilted south at an angle equal to the latitude of the site. Capacities of different PV panels (0, 1, 2, 5, 10 and 20 kW, respectively) were considered in the analysis.

Batteries: The battery is capable of storing a certain amount of DC electricity at fixed round-trip energy efficiency, García-Valverde *et al*. (2009) with limits as to how quickly it can be charged or discharged without causing damage and how much energy can cycle through it before it needs to be replaced. HOMER assumes that the properties of the battery remain constant throughout its lifetime and are not affected by external factors such as temperature. The chosen battery has a 24-V, 250-Ah capacity and also SOC is 80%. The cost of one battery is Rs 12,000 with a maintenance cost of Rs 250/year. Different numbers of batteries (0, 1, 5 and 10, respectively) were considered in this analysis.

Inverter: An inverter converts electric power from DC to Alternating Current (AC). Its efficiency is assumed to be 90% (Ibrahim *et al*., 2008) for all sizes considered. The estimated life time is 15 years and various size are s (0, 1, 5 and 10 kW, respectively) considered in this study.

Generator: A generator consumes fuel to produce electricity and possibly heat as a by-product. A vast range of generators are available (diesel, gasoline, propane and bio-fuel) (Ibrahim *et al*., 2008). This analysis, considers a generator producing electricity that operates on diesel fuel, because it is more efficient than the others and its lifetime is longer. The estimated price of the generator is Rs 81/W and various capacities sizes are considered (0, 1 and 2 kW, respectively) in the analysis.

System analysis:

Optimization results: In the optimization process, HOMER simulates every system configuration in the search space and displays the feasible ones in a table, sorted by total net present cost. Figure 2, 4, 6 and 8 shows the results of the sample wind-diesel standalone hybrid renewable energy sources. Each row in the table represents a feasible system configuration. The first four columns contain icons indicating the presence of the different components, the next four columns indicate the number or size of each component and the next five columns contain the key simulation results: namely, the total capital cost of the system, the total net present cost, the levelized cost of energy (cost per kilowatt hour), the annual fuel consumption and the number of hours the generator operates per year. The complete simulation results, for different stand alone hybrid renewable system (PV-Wind-battery, Wind-diesel-battery, PV-diesel-battery, PV-wind-diesel-battery) is shown in Fig. 2, 4, 6 and 8.

Sensitivity Results | Optimization Results

Double click on a system below for simulation results.

PV (kW)	XLS	Label (kW)	H1500	Conv. (kW)	Initial Capital	Operating Cost ($/yr)	Total NPC	COE '$/kW...	Ren. Frac.	Capacity Shorta..	Diesel (L)	Label (hrs)
2	1	1.0	1	1	$ 20,700	1,875	$ 44,675	0.323	0.69	0.25	1,221	4,632
2	1	1.0	5	1	$ 22,700	1,858	$ 46,454	0.323	0.69	0.20	1,219	4,335
1	1	1.0	5	1	$ 19,700	2,206	$ 47,905	0.334	0.60	0.20	1,543	5,274
2	1	1.0	10	1	$ 25,200	1,826	$ 48,536	0.337	0.70	0.20	1,165	4,127
1	1	1.0	10	1	$ 22,200	2,105	$ 49,113	0.341	0.62	0.20	1,467	5,057
	1	1.0	5	1	$ 16,700	2,554	$ 49,354	0.354	0.50	0.23	1,863	6,198
	1	1.0	10	1	$ 19,200	2,561	$ 51,936	0.363	0.50	0.21	1,896	6,334

V-wind-diesel-battery

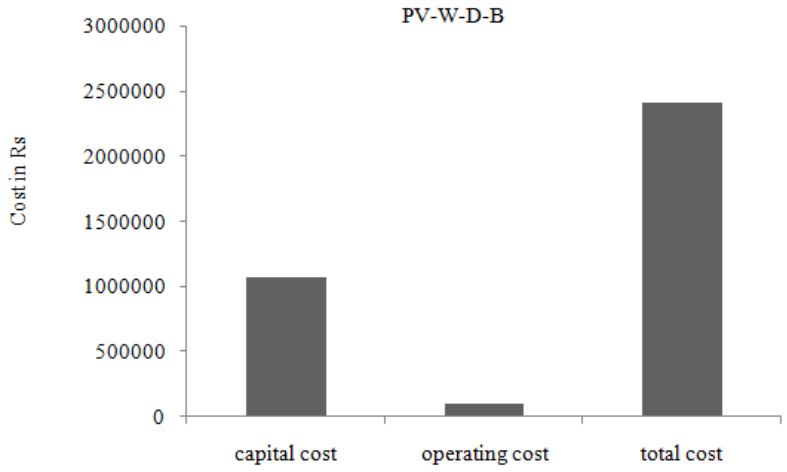

Fig. 3: Cost for PV-wind-diesel-battery

Sensitivity Results | Optimization Results

Double click on a system below for simulation results.

XLS	Label (kW)	H1500	Conv. (kW)	Initial Capital	Operating Cost ($/yr)	Total NPC	COE ($/kW...	Ren. Frac.	Capacity Shorta...	Diesel (L)	Label (hrs)
1	1.0	5	1	$ 16,700	2,554	$ 49,354	0.354	0.50	0.23	1,863	6,198
1	1.0	10	1	$ 19,200	2,561	$ 51,936	0.363	0.50	0.21	1,896	6,334
1	5.0	1	1	$ 16,300	4,331	$ 71,666	0.452	0.34	0.00	3,516	3,699
	5.0	5	1	$ 6,300	5,203	$ 72,813	0.459	0.00	0.00	4,833	4,015
1	5.0	5	1	$ 18,300	4,312	$ 73,419	0.463	0.35	0.00	3,479	3,629
	5.0	10	1	$ 8,800	5,253	$ 75,946	0.479	0.00	0.00	4,833	4,015
1	5.0	10	1	$ 20,800	4,361	$ 76,551	0.483	0.35	0.00	3,479	3,629

Fig. 4: Optimization for wind-diesel-battery

PV-wind-diesel-battery: The Fig. 2 shows that optimization result for PV-wind-diesel-battery hybrid system. This system consists of one 2 kW PV array, one BWC Excel-S wind turbine, one 1 kW diesel generator, 1 battery and a 1kW power converter, with lower COE at Rs 17. This COE remain constant even with changing of PV, wind turbine, generator and converter but, increases when the battery bank increases. The maximum COE is observed for higher rating of battery bank at Rs 19. The important conclusion is that COE is mainly dependant on battery bank. The Fig. 2 show that this hybrid system can supply the power to isolated clinic with minimum fuel consumption 1221/year, the reason being that contribution of power from renewable energy sources are 69%.

The Fig. 3 shows relationship between costs of different components which are associated with PV-wind-Diesel-battery system. As can be seen from Fig. 3, the operating cost is very low for this system.

The Fig. 4 reveals, the second standalone hybrid wind-diesel-consists of one XLS-turbine, one1 5 batteries and a 1 kW power converter, with COE of Rs 19.11/kWh. The COE of this system increases with increase in diesel generator and battery bank.

The Fig. 5 shows relationship between costs of different components which are associated with wind-Diesel-battery system. As can be seen from the Fig. 5, the operating cost is low for this type system, but there is a reduction in capital cost and an increase in operating cost as compared to PV-wind-diesel-battery system.

PV-diesel-battery: The Fig. 6 reveals data on PV-diesel-battery system. In this system Renewable energy share is 58% of the total energy production; the generator will be running about 5472 h/year consuming 1621 L of fuel. The system configuration incorporates 5 KW of PV along with a 1 kw generator, 1 batteries and an inverter capacity of 5 KW for an initial cost of Rs 13,33,800. The NPC over the lifetime of the system is Rs 28,06,488. As can be seen from Fig. 6 COE increases with decrease in PV module. This is due to the fact that as the PV module decrease, the contribution from renewable energy source decreases with corresponding increase in fuel consumption.

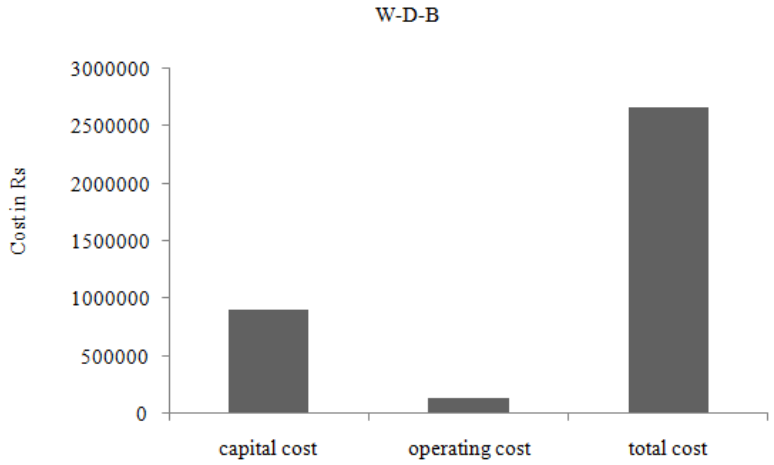

Fig. 5: Cost for wind-diesel-battery

Sensitivity Results | Optimization Results

Double click on a system below for simulation results.

PV (kW)	Label (kW)	H1500	Conv. (kW)	Initial Capital	Operating Cost ($/yr)	Total NPC	COE ($/kW...	Ren. Frac.	Capacity Shorta..	Diesel (L)	Label (hrs)
5	1	1	5	$ 24,700	2,133	$ 51,972	0.364	0.58	0.17	1,621	5,472
5	1	5	5	$ 26,700	2,337	$ 56,575	0.373	0.54	0.07	1,785	5,423
5	1	10	5	$ 29,200	2,393	$ 59,792	0.386	0.53	0.03	1,882	5,704
2	1	5	5	$ 17,700	3,323	$ 60,184	0.453	0.16	0.22	2,888	8,750
2	1	10	5	$ 20,200	3,265	$ 61,940	0.466	0.16	0.21	2,886	8,746
5	1	1	10	$ 33,700	2,433	$ 64,798	0.453	0.58	0.17	1,621	5,472
5	1	5	10	$ 35,700	2,636	$ 69,401	0.458	0.54	0.07	1,785	5,423
5	1	10	10	$ 38,200	2,692	$ 72,617	0.469	0.53	0.03	1,882	5,704
2	1	5	10	$ 26,700	3,623	$ 73,009	0.549	0.16	0.22	2,888	8,750

Fig. 6: Optimization for PV-diesel-battery system

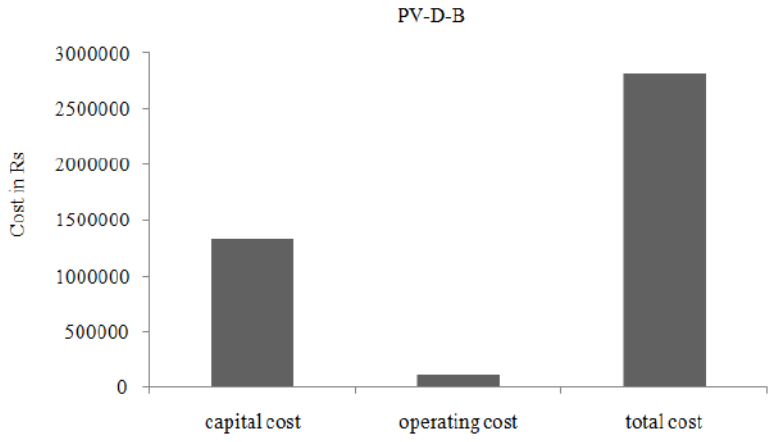

Fig. 7: Cost for PV-diesel-battery

The optimal hybrid power system proposed by HOMER includes PV, diesel generator, battery and omponents needed to satisfy the ay are 5 KW of PV panel, 1 kw or, 1 batteries and 5 kw inverter. system is Rs 13,33,800 and the The RE fraction represents 58% of the energy production. The generator will be running 5,472 h and will consume 1621 L/year of diesel fuel. The least cost system is wind turbine with diesel generator consisting of 1 KW of wind turbine, 1 KW diesel generator, 5 batteries and 1 KW inverter capacity for an initial capital cost of Rs 13,33800 and a NPC of Rs 28,06,488 and COE of Rs 19/KWh.

Sensitivity Results | Optimization Results

Double click on a system below for simulation results.

PV (kW)	XLS	H1500	Conv. (kW)	Initial Capital	Operating Cost ($/yr)	Total NPC	COE ($/kW...	Ren. Frac.	Capacity Shorta..
2		10	3	$ 19,000	228	$ 21,912	0.877	1.00	0.00
2		20	3	$ 26,000	331	$ 30,236	1.207	1.00	0.00
1	1	1	3	$ 21,200	970	$ 33,603	1.359	1.00	0.02
	1	10	3	$ 22,500	1,021	$ 35,552	1.419	1.00	0.00
2	1	1	3	$ 26,200	1,001	$ 38,997	1.568	1.00	0.01
1	1	10	3	$ 27,500	1,053	$ 40,963	1.635	1.00	0.00
	1	20	3	$ 29,500	1,125	$ 43,877	1.751	1.00	0.00
2	1	10	3	$ 32,500	1,085	$ 46,375	1.851	1.00	0.00
1	1	20	3	$ 34,500	1,157	$ 49,288	1.967	1.00	0.00
2	1	20	3	$ 39,500	1,189	$ 54,699	2.183	1.00	0.00
10		10	3	$ 59,000	485	$ 65,201	2.602	1.00	0.00
10		20	3	$ 66,000	589	$ 73,526	2.934	1.00	0.00
10	1	1	3	$ 66,200	1,257	$ 82,268	3.289	1.00	0.00
10	1	10	3	$ 72,500	1,343	$ 89,664	3.579	1.00	0.00

Fig. 8: Optimization for PV-wind-battery

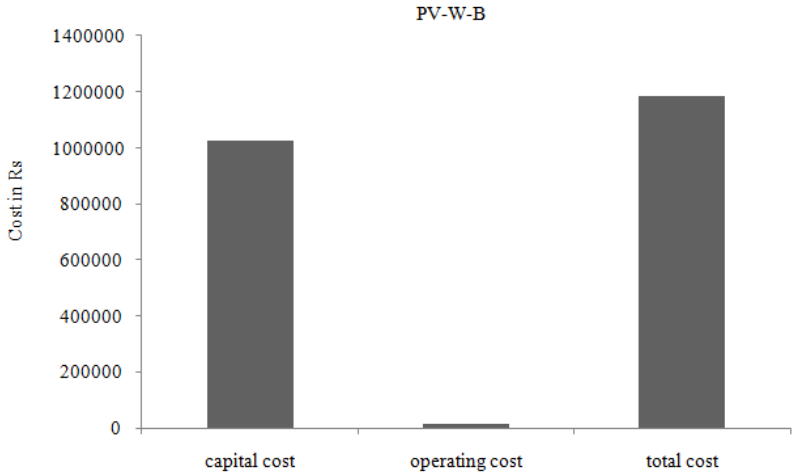

Fig. 9: Cost for PV-wind-battery

PV-wind-battery only: The Fig. 8 details the optimization of PV-wind-battery system. As can be seen, this is the most expensive system of all the hybrid system considered. This is due to the fact that this system being totally renewable energy sources require large number of battery banks.

The Fig. 9 gives the cost structure of PV-wind-battery system. As can be seen from Fig. 9, the operating cost is almost negligible but capital cost and total cost are very high.

Effect of interest and diesel on electricity cost: These types of projects in developing countries are usually government and hence the erest rate when analyzing the ifferent interest rates on the cost l for all types of systessm are figure showed that at 6% interest ctricity produced is almost 75% of actual cost of energy. Similarly the effect of price of fuel has a large impact on the cost of electricity produced (Fig. 4). The simulation showed that varying the price from Rs 50/L to 55/L increases the cost of electricity produced from Rs 5.00/KWh to Rs 7.00 KW/h for the PV+Wind+Diesel+Battery system. The effect of fuel price and interest rate on the COE for other system can be seen in Table 4.

Comparison of COE: A summary of the COE and RF of the different types of hybrid system are listed in Table 5. It is interesting to note, that the PV+Wind+Diesel+Battery hybrid system shows the lowest COE and high amount of RF (the portion of power generated by the renewable energy source compared to that of the total power drawn from the system). The second lowest COE of Rs 7.00/KWh is for Wind+Diesel+Battery hybrid system. The reason for the increase in COE for the other system is that

contribution of RF is reduced and automatically increasing the consumption of fuel. The highest COE and also high amount of RF (100%) belongs to PV+Wind+Battery. The conclusion from the study of Table 5 is that any one renewable energy sources with diesel to produce the power for isolated clinic, leads to decrease in COE.

EXPERIMENTAL RESULTS

The simulation results are verified by experimentally using as different types of hybrid PV/wind system model for power generation to isolated clinic shown in Fig. 1 which is located at Ramanathapuram (District) Tamilnadu (State) in India.

Table 4: Effect of interest rate and diesel price on electricity cost

	Effect of interest rate in COE (Rs/KWh)		Effect of diesel price in COE (Rs/KWh)	
Types of hybrid system	0%	6%	Rs 50	Rs 55
PV+wind+diesel+battery	5.00	17.00	5.00	7.00
Wind+diesel+battery	7.00	19.00	7.00	9.00
PV+diesel+battery	7.00	19.00	7.00	9.00
PV+wind+battery	10.00	43.00	10.00	15.00

Table 5: Comparison of COE

Types of hybrid systems	COE (Rs/KWh)	RF (%)	Consumption of fuel (L)
PV+wind+diesel+battery	5.00	70	1221
Wind+diesel+battery	7.00	55	1863
PV+diesel+battery	7.00	60	1621
PV+wind+battery	10.00	100	Nil

(a)

(b)

(c)

Fig. 10: (a) The photograph of the experimental setup for solar panel, (b) the photograph of the experimental setup for battery bank, (c) the photograph of the experimental setup for generator

The above said system is tested by PV module, wind turbine, battery bank and converter and also the system specification is discussed above. The simulation result of effect of interest and diesel on electricity cost and also comparison of COE for different type's hybrid system is tested by experimental set up as shown in Fig. 10. The experimental results show that the least cost of energy at Rs 5.00/KWh, is obtained from PV+Wind+Diesel+Battery and also experiment result shows that the COE decreases with 0% of interest.

CONCLUSION

From the analysis and the experimental verification the following conclusion are drawn:

- The Health clinic at remote coastal areas of Tamil Nadu in India can render satisfactory service to the community around if they are given hybrid-standalone power system.
- The optimized and least expensive model of such stand alone hybrid system is fund to be PV-diesel-Wind power-battery-converter system.
- As the capital cost is high, the government should provide such system through a subsidized project.

REFERENCES

ıvanni, D. Gurjeet and L. David, ɔn the installation costs of technologies in building: A ıg approach. Energ. Buildings,

Bakos, G.C., M. Soursos and N.F. Tsagas, 2003. Techno economic assessment of a building integrated PV system for electrical energy saving in residential sector. Energ. Buildings, 35(8): 757-762.

Cetin, E., A. Yilanci, Y. Oner, M. Colak, I. Kasikci and H.K. Ozturk, 2009. Electrical analysis of a hybrid photovoltaic-hydrogen/fuel cell energy system in Denizli, Turkey. Energ. Buildings, 41(9): 975-981.

Dalton, G.J., D.A. Lockington and T.E. Baldock, 2009. Case study feasibility analysis of renewable energy supply options for small to medium-sized tourist accommodations. Renew. Energ., 34(4): 1134-1144.

García-Valverde, R., C. Miguel, R. Martínez-Béjar and A. Urbina, 2009. Life cycle assessment study of a 4.2 kWp stand-alone photovoltaic system. Sol. Energ., 83(9): 1434-1445.

Ibrahim, H., A. Ilinca and J. Perron, 2008. Energy storage systems: Characteristics and comparisons. Renew. Sustain. Energ. Rev., 12(5): 1221-1250.

Jennings, W. and J. Green, 2000. Optimization of electric power systems for off-grid domestic applications: An argument for wind/photovoltaic hybrids. J. Undergrad. Res., 12(2000): 1.

Kabouris, J. And G.C. Contaxis, 1992. Autonomous system expansion planning considering renewable energy sources: A computer package. IEEE T. Energ. Convers., 7(3): 374-380.

Kaldellis, J.K. and I. Ninou, 2011. Energy balance analysis of combined photovoltaic-diesel powered telecommunication stations. Int. J. Electr. Pow. Energ. Syst., 33(10): 1739-1749.

Lambert, T., 2012. HOMER: The Hybrid Optimization Model for Electric Renewable. Retrieved from: http://www.nrel.gov/internationa/tools/homer/homer.html.

Lockington, D.A., G.J. Dalton and T.E. Baldock, 2008. Feasibility analysis of stand-alone renewable energy supply options for a large hotel. Renew. Energ., 33(7): 1475-1490.

McGowan, J.G., J.F. Manwell, C. Avelar and C.L. Warner, 1996. Hybrid wind/ PV/diesel hybrid power systems modeling and South American applications. Renew. Energ., 9(1/4): 836-847.

NASA, 2012. NASA Surface Meteorology and Solar Energy. Retrieved from: http://eosweb.larc. nasa.gov/SSE/RET Screen/.

NREL, 2011. HOMER Computer Software. Version 2.68 Beta. National Renewable Energy Laboratory, Retrieved from: https://analysis.nrel.gov/homer/S.

Ramakumar, R., I. Abouzahr and K. Ashenayi, 1992. A knowledge-based approach to the design of integrated renewable energy system. IEEE T. Energ. Convers., 79(4): 648-655.

Saheb-Koussa, D., M. Haddadi and M. Belhamel, 2009. Economic and technical study of a hybrid system (wind-photovoltaic-diesel) for rural electrification in Algeria. Appl. Energ., 86(7/8): 1024-1030.

MATLAB SIMULATION OF PV BASED ASYMMETRIC MULTILEVEL INVERTER

[1]R.NIRAIMATHI, [2]R. SEYEZHAI

[1]Assistant Professor, Department of EEE, Mohamed Sathak Engineering College, Kilakarai.
[2]Associate Professor, Department of EEE, SSN College of Engineering, Kalavakkam.
E-mail id:rniraimathi27@gmail.com

Abstract: This paper deals with simulation of PV based seven level asymmetric multilevel inverter with boost converter using maximum power point tracking algorithm. Maximum power point tracking (MPPT) techniques are used in photovoltaic (PV) systems to maximize the PV array output power by tracking continuously the maximum power point (MPP).In this paper perturb and observe (P&O) is employed. The carrier based PWM is employed for the proposed multilevel Inverter. A detailed study of proposed PV based inverter is carried out in MATLAB /SIMULINK and the results are verified.

Index terms: THD, PWM, maximum power point tracking (MPPT), perturb and observe (P&O), photovol taic (PV).

I. INTRODUCTION

A photovoltaic array converts sunlight in to electricity. The voltage and current available at the terminals of the PV array may directly feed small loads such as lighting systems and DC motors. More sophisticated applications require electronic converters to process the electricity from the array. These converters may be used to regulate the voltage and current at the load, to control the power in gridconnected systems and mainly to track the maximum power point (MPP) of the array. Converters with the maximum power point tracking (MPPT) feature use an algorithm to continuously detect the maximum instantaneous power of the PV array. Because the operating condition of the array may change randomly during the operation of the system an MPPT algorithm is necessary so that the maximum instantaneous power can be extracted and delivered to the ac load through multilevel inverter. One of the advantages of multilevel Inverter is that it enable the interface of renewable sources such as photo voltaic, wind and fuel cells in the dc input portion of the multilevel inverter.

Multilevel inverter is to synthesize a near sinusoidal voltage from several levels of dc voltages typically obtained from capacitor voltages. As the number of level increases, a synthesized output waveform has more steps, which produce staircase wave that approaches a desired waveform. The topology considered for this work is the cascaded H-bridge inverter which requires several independent dc sources. Normally, each phase of a cascaded multilevel inverter requires “n” dc sources for 2n+1 level. An aim to reduce the number of dc sources required for the cascaded multilevel inverter, this paper focuses PV fed asymmetric cascade MLI with MPPT algorithm using fixed frequency carrier based ıl dc sources in each phase to equal step multilevel output. ı power from PV array using P&O. This structure is favourable for high power applications which gives low THD for increased modulation Index.

System Composition

The system explained in this paper is categorized into three individual systems:-

1. Generating a dc signal using photovoltaic system
2. Tracking maximum power from PV using MPPT.
3. Step up of generated DC signal using boost converter.
4. Pulse pattern generation.
5. Conversion of DC signal to AC signal using single phase asymmetric MLI.

II. PV MODELLING

Modeling of a solar cell is done by connecting a current source in parallel with an inverted diode along with a series and a parallel resistance as shown in Fig.3. The series resistance is due to hindrance in the path of flow of electrons from n to p junction and parallel resistance is due to the leakage current. The output characteristic of a PV module depends on the solar insulation, the cell temperature and the output voltage of the PV module. Since PV module has non-linear characteristics, it is necessary to model it for the design and simulation of Maximum Power Point Tracking (MPPT) for PV system applications. The equivalent circuit of single diode model shown in Fig.1.The current source ILrepresent the cell photo current. Rsh and Rs are the shunt and series resistances of the cell respectively.

The simulink model of PV module is shown in Fig.2

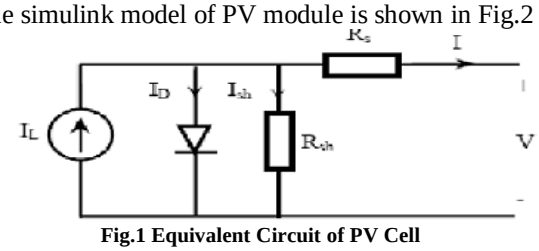

Fig.1 Equivalent Circuit of PV Cell

The equation (1) is the current output of photovoltaic
I=IL-I0 (e(v+IRs)/VT.a)-1-V+RsI/Rsh ----------(1)

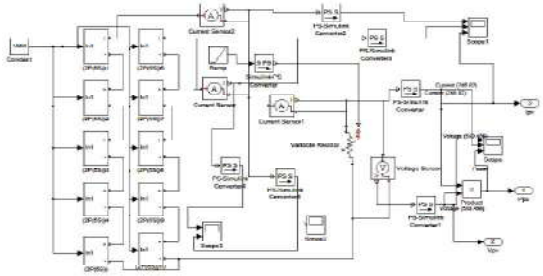

Fig.2.Simulink model of PV module

The I-V and P-V output a characteristic of PV module at 1000W/m2 and 500W/m2 irradiation is shown in Fig.6
a t 25 o C is shown in Fig.7.

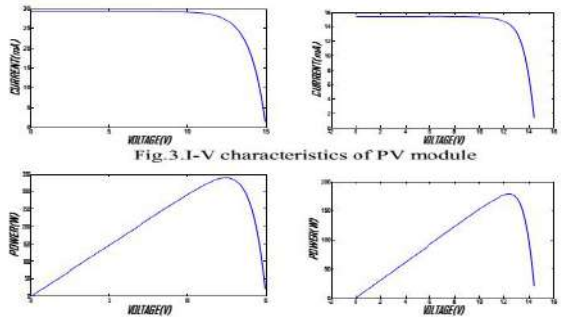

Fig.3.I-V characteristics of PV module

Fig.4.P-V characteristics of PV module

As the irradiance level is inconsistent throughout the day, the amount of electric power generated by the solar module is always changing with weather conditions. To overcome this problem, Maximum Power Point Tracking (MPPT) algorithm is used. It tracks the operating point of the I-V curve to its maximum value. Therefore, the MPPT algorithm will ensure maximum power is delivered from the solar modules at any particular weather conditions. In this proposed inverter, Perturb & Observe (P & O) algorithm is used to extract maximum power from the modules . The flowchart for MPPT is shown in Fig.5and the simulink model for P&O algorithm is shown in Fig.6.

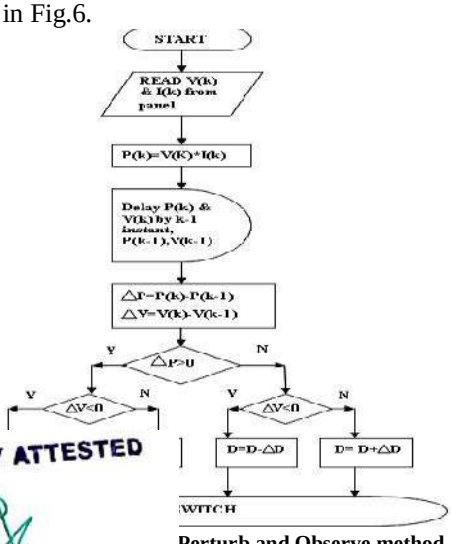

Perturb and Observe method

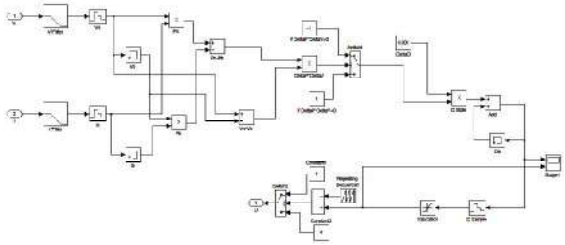

Fig.6. Simulation Diagram of P&O algorithm

III. B O O S T CONVERTER

In boost converter the output voltage is greater than input voltage . In this model a power IGBT is considered in boost converter as shown in Fig. 7.output of the boost
converter as shown in fig.8.

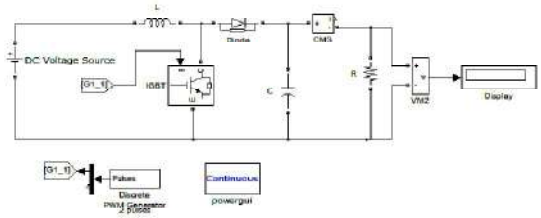

Fig.7. Simulink model for boost converter

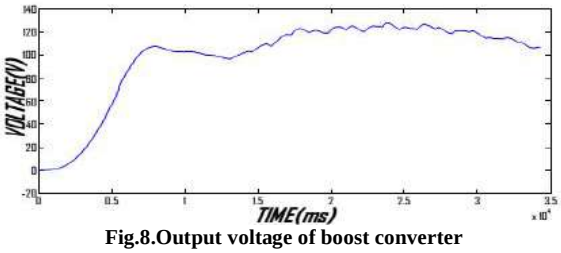

Fig.8.Output voltage of boost converter

IV. SYMMETRIC CASCADED H-BRIDGE MULTILEVEL INVERTER

This paper focuses on an asymmetric topology which uses only two DC sources i.e. the first bridge voltage value is V/2 and the second bridge voltage value is V then the output will be a seven- level voltage waveform.
The proposed topology consists of two H-bridges as shown in Fig.9. By appropriately opening and closing the switches of H1, the output voltage V1 can be made equal to - Vdc , 0, + Vdc. Similarly the output voltage V2 of the second bridge H2 can be made equal to - 0.5Vdc, 0 , 0.5Vdc .Therefore, the output voltage of the MLI have the values of -1.5 Vdc, -Vdc, -0.5Vdc,

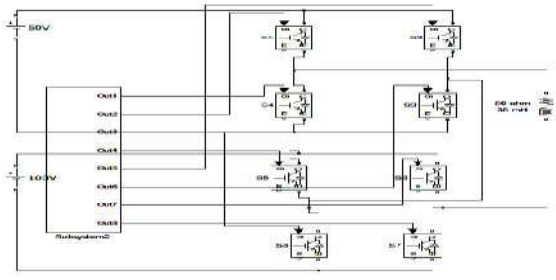

Fig.9. Asymmetric (7- level) cascaded multilevel inverter

V. PHASE DISPOSITION PWM TECHNIQUE FOR CASCADED MULTILEVEL INVERTER

It is generally accepted that the performance of any inverter, with any switching strategy can be related to the harmonic contents of its output voltage. There are many control techniques reported in literature for cascaded multilevel inverter. But the popularly used modulation method is the multicarrier PWM technique. Phase Disposition (PD) PWM technique is the generally used method in cascaded multilevel inverter as it gives a reduced THD.In this paper, fixed frequency carrier based PWM is proposed which uses the conventional sinusoidal reference signal and the carrier signals with same frequency[13]-[14]. To implement a m-level inverter, (m-1) carriers are used. There are six distinct carriers with same frequency and with the same magnitudes; the difference between the carriers is that they are all displaced by a set of DC offset. From the six carrier signals each will have same frequency. The carrier signals C1 to C6 have same frequency. The pulses are generated when the amplitude of the modulating signal is greater than that of the carrier signal as shown in fig.10. generated pulse pattern of asymmetric MLI with same frequency as shown in fig.11.

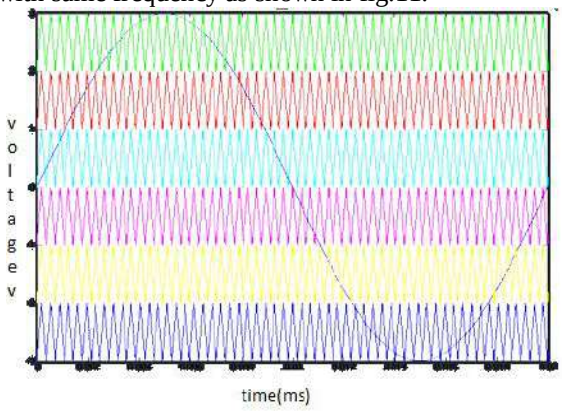

Fig.10. Carrier and reference sine waveform for fixed frequency carrier b a s ed modulation technique

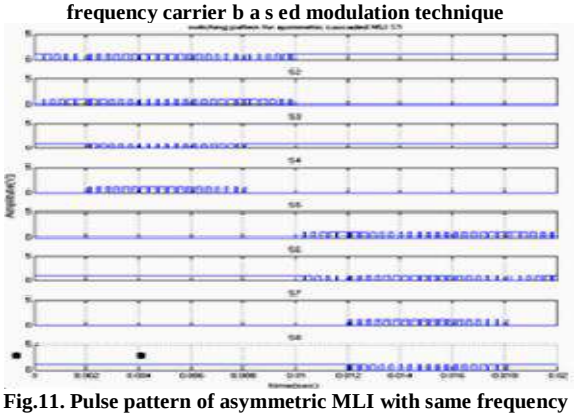

Fig.11. Pulse pattern of asymmetric MLI with same frequency

VI. SIMULATION RESULTS

vs the MATLAB/SIMULINK veform of the proposed single n-level asymmetric cascaded multilevel inverter. The FFT spectrum of the load voltage and current is found using the FFT analysis tool is shown in Fig.14 and fig.15 respectively and the THD of voltage and current are 19.27%,7.33% respectively.fig.16. and fig.17. shows current THD, voltage THD vs modulation Index graph.

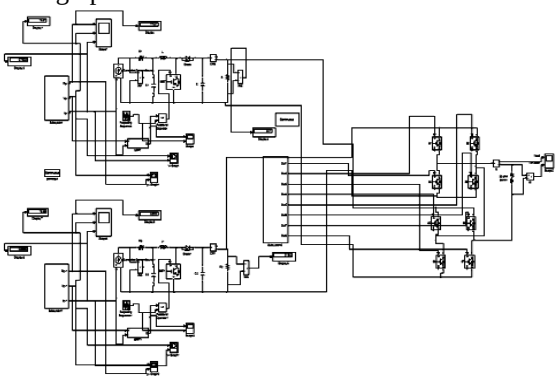

Fig.12. Simulation Diagram of 7-level asymmetric multilevel inverter interfaced with PV

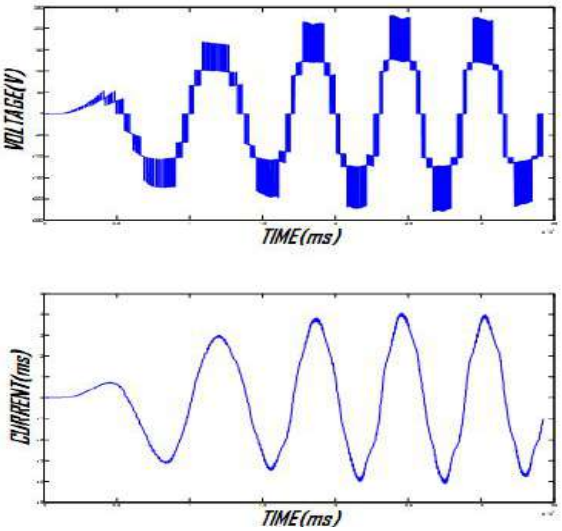

Fig.13.Seven level output voltage and current of PV inverter under open-loop condition

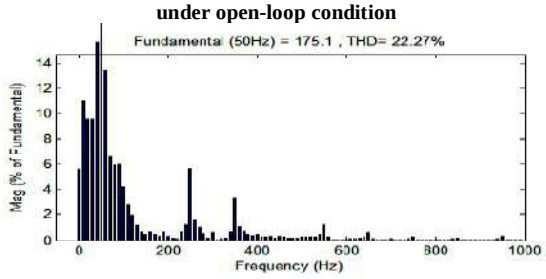

Fig.14. FFT Analysis of load voltage of seven level Inverter

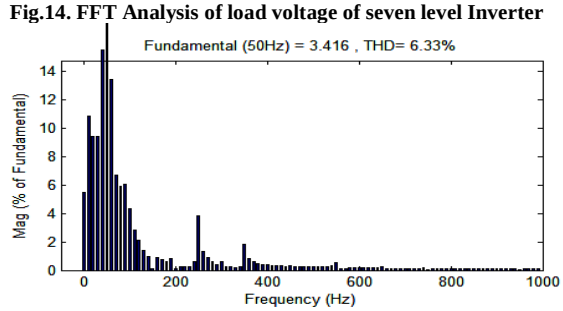

Fig.15. FFT Analysis of load current of seven level Inverter

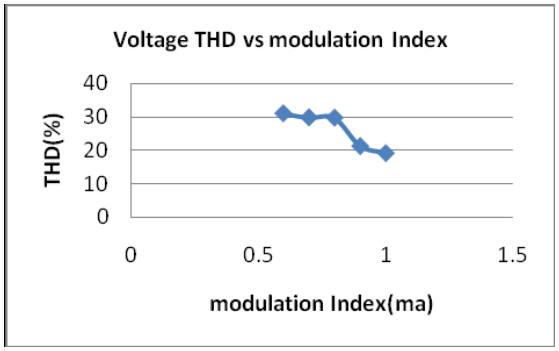

Fig.16.Voltage THD vs ma Graph for fixed frequency carrier based PWM

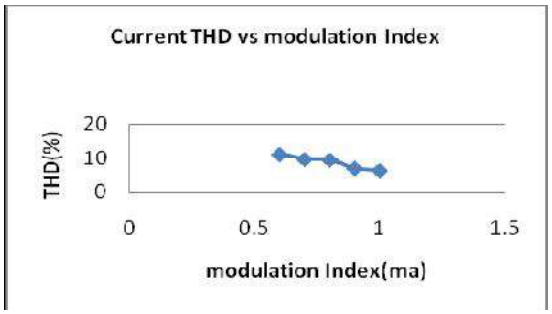

Fig.17.Current THD vs ma Graph for fixed frequency carrier based PWM

CONCLUSION

This paper discussed about the simulation of PV based seven-level asymmetric cascaded multilevel inverter
with intermediate boost converter. The PV array output power delivered to the load can be maximized using P and O control algorithm. The boost converter is allowed to work in continuous mode and the switching sequence of multilevel inverter is decided by a PWM generator which uses a PDPWM technique. Total Harmonic Distortion analysis was performed with different modulation indices for inverter output voltage with open loop configuration. From the FFT analysis, it is observed that THD is less for the proposed PDPWM technique and therefore, asymmetric multilevel inverter is a suitable topology for photovoltaic applications.

REFERENCES

[1] C. Cecati, F. Ciancetta, and P. Siano,(2010) "A Multilevel inverter for photovoltaic systems with fuzzy logic control," IEEE Trans. Ind. Electron.,vol. 57, no. 12, pp. 4115–4125, Dec

[2] Rodriguez, J., Lai, J. S. and Peng, F. Z. (2000) "Multilevel Inverter: A Survey of Topologies, Controls and Applications", IEE E Trans. On Industrial Electronics, Vol. 49, No. 4 pp. 724-738

[3] Peng F.Z., Lai J.S., (1996)"Multilevel Converters - A New Breed of Power Converters ",IEEE Transactions on Industry Applications, Vol. 32, No. 3, pp.509- 517

[4] J. Selvaraj, N. A. Rahim(2011),"Multilevel Inverter for Grid- Connected PV System Employing Digital PI Controller,"IEEE Trans. on Industrial Electronics, vol.56,issue.1,pp.149-158.

[5] U. Boke, (2007) "A simple model of photovoltaic module electric characteristics," European Conference on Power Electronics and Applications, pp.1-8,Sept.

[6] Cameron, Christopher P.; Boyson, William E.; Riley Daniel M.;(2008)" Comparison of PV system performance model predictions with measured PV system performance" IEEE Photovoltaic Specialists Conference,pp. 1-6

[7] H. Altas and A.M. Sharaf,(2007) "A Photovoltaic Array Simulation Model for Matlab-Simulink GUI Environment," IEEE, Clean Electrical Power, International Conference on Clean Electrical Power (ICCEP„07), Ischia,Italy

[8] Marcelo G, Gazoli J. and Filho E., "Comprehensive Approach to Modeling and Simulation of Photovoltaic Arrays", IEEE Transactions On Power Electronics, vol. 24, no. 5, May 2009, p.p.1198-1208.

[9] Bo Yang, Wuhua Li, Yi Zao, and Xiangning He, "Design and analy-sis of grid connected photovoltaic system," IEEE transaction on power electronics, vol. 25, no.4, pp. 992-1000, April 2010.

[10] Dezso Sera, Remus Teodorescu, and Tamas Kerekes, (2009) "Maximum Power Point Trackers Using a Photovoltaic Array Model with Graphical User Interface," Institute of energy technology.

[11] A. Yafaoui., B. Wu, and R. Cheung,(2007) "implementation of maximum power point tracking algo-rithm for residential photovoltaic systems," 2nd Canadian Solar Buildings Conference Calgary, June 10 – 14.

[12] Prashant. V. Thakre, V. M. Deshmkh, and Saroj Rangnekar(2012)" Performance Analysis of Photovoltaic PWM Inverter with Boost Converter for Different Carrier Frequencies Using MATLAB" IACSIT International Journal of Engineering and Technology, Vol. 4, No. 3.

[13] Seyezhai, R.(2012) "A Comparative Study of Asymmetric and Symmetric Cascaded Multilevel Inverter employing Variable Frequency Carrier based PWM", International Journal of Emerging Technology and Advanced Engineering Vol 2, Issue 3, ISSN 2250-2459.

[14] Seyezhai, R. and Mathur, B. L.(2010) "Implementation and control of Variable Frequency ISPWM Method for an Asymmetric Multilevel Inverter", European Journal of Scientific Research, Vol. 39, Issue 4, pp. 558-568.

[15] Calais M., Borle L. G. and Agelidis V. G., (2001). Analysis of Multicarrier PWM Methods for a Single-Phase Five-Level Inverter, IEEE power Electronics Specialists Conference,Vol.3, pp. 1173-1178.

[16] Seyezhai.R(2011) Cascaded Hybrid Five-level Inverter with Dual Carrier PWM Control Scheme for PV System International Journal of Advances in Engineering & Technology, Vol. 1, Issue 5, pp. 375-386.

★★★

ISSN No.- 2231-5063

Golden Research Thoughts

www.aygrt.net

Published By
Laxmi Book Publication
258/34. Raviwar Peth Solapur-413005, Maharashtra
Contact- +91-9595-359-435
mail-ayisrj@yahoo.in / ayisrj2011@gmail.com
Website-www.isrj.net

Chief
yan Shinde

Publisher
Dr.Ashok Yakkaldevi

GOLDEN RESEARCH THOUGHTS

Content

ISSN NO:-2231-5063 VOL.III, ISSUE.XI/May - 2014

Golden Research Thoughts
ISSN 2231-5063
Impact Factor : 2.2052(UIF)
Volume-3 | Issue-11 | May-2014
Available online at www.aygrt.isrj.net

GRT

COMPETENCY ANALYSIS OF TAMILNADU NEWSPRINTS AND PAPERS LIMITED (TNPL) – AN EMERGING SUCCESS AMONG PUBLIC SECTOR

N. Shankar

Assistant Professor, Department of Management Studies, Mohamed Satak Engineering College, Kilakarai , Ramanathapuram District.

Abstract:-Strategy is a process of choosing the best alternative based on environmental conditions. TNPL is an organization and choosing the best business options and withstands in the market among various Public Sector companies. A core competency is generally defined in terms of special technical or product expertise. Acquiring core competencies helps the organization to compete against the new entrants. As far as TNPL is concerned the core competencies are Skilled human resources, Variety of products to the need of customers, Strong brand name, Innovative and updated technologies, Eco-friendly production, Affordable cost of products, manufacturing cost control and the ability to adapt changes.

Keywords: Strategy, core competency, brand name .

INTRODUCTION :-

An organization performs different activities or performs similar activities in different ways in order to face the competition against the competitors. Then there are different definitions for the term strategy. One such definition is that it is a course of action through which an organization relates itself with the environment to achieve its objectives. The strategy specifies selection and ranking of business opportunities and points out the preferred means of achieving the desired objectives. With the above definitions, the steps in formulating corporate strategy are,

1. Setting of corporate objectives with mission, vision and goals describing the main purpose of the business.
2. Finding alternative business opportunities and options of disposal of undesired alternatives.
3. Selection of best business option.
4. Implementation of the chosen line to capitalize the selected business opportunity.

Thus corporate strategy in terms of market is based on self- analysis and analysis of current environment in the market relating to the customers, employees, competitors, community and forecast of future environment conditions. In this paper, corporate strategy of TNPL is being analyzed with an intention of finding the competency of TNPL as to how and why it has achieved a miraculous success among other counterparts.

REASON FOR CHOOSING TNPLAS A CASE STUDY

1.Large newsprint mills manufacture news print, but only small number of paper mills keeps on changing their product mix as per market condition.
2.The strategy of TNPL shows that it is an emerging leader in Indian paper mill even in the high cost of raw material and many Indian paper industries are at great loss and finding difficult to compete in the global market.
3.In India manufacturing industry accounts for 25% of the national GDP and the consumption of paper is estimated to touch 13.95 million tons by 2015 -16' with the steep economic growth. In such situation, it is needed to analyze its strategy.

A Peer-reviewed- Refereed/Scholarly Quarterly Journal with Impact Factor

ISSN : 2321-4643

INTERNATIONAL STANDARD SERIAL NUMBER INTERNATIONAL CENTRE

Shanlax International Journal of Management

VOL : 4 SPECIAL ISSUE : 1 OCTOBER 2016

NATIONAL CONFERENCE ON EMERGING TRENDS ON ENTREPRENEURIAL OPPORTUNITIES AND CHALLENGES

NCEOC - 2016

Organized by

Department of Business Administration
Department of Commerce
Department of Commerce with CA

Caussanel College of Arts and Science

(Affiliated to Alagappa University)

(Run by the Congregation of the Brothers of the Sacred Heart, Palayamkottai)

Muthupettai - 623523

CONTENTS

Volume 4 Special Issue 1 October 2016 ISSN: 2321 – 4643

FACTORS INFLUENCING CONSUMER BUYING BEHAVIOR

A. Abdul Brosekhan
Assistant Professor, Department of Management Studies,
Mohamed Sathak Engineering College, Kilakarai, Ramanathapuram - 623 806

Abstract

Consumer behaviour is the study of individuals, groups, or organizations and the processes they use to select, secure, use, and dispose of products, services, experiences, or ideas to satisfy needs and the impacts that these processes have on the consumer and society. Consumer Buying Behaviour refers to the buying behaviour of the ultimate consumer. Many factors, specificities and characteristics influence the individual in what he is and the consumer in his decision making process, shopping habits, purchasing behavior, the brands he buys or the retailers he goes. A purchase decision is the result of each and every one of these factors. An individual and a consumer is led by his culture, his subculture, his social class, his membership groups, his family, his personality, his psychological factors, etc.. and is influenced by cultural trends as well as his social and societal environment.By identifying and understanding the factors that influence their customers, brands have the opportunity to develop a strategy, a marketing message (Unique Value Proposition) and advertising campaigns more efficient and more in line with the needs and ways of thinking of their target consumers, a real asset to better meet the needs of its customers and increase sales.
Keywords: *- Consumer, Behavior, Culture, Buyer Culture, Sub-culture, and Social Class.*

Introduction

A purchase decision is the result of each and every one of these factors. An individual and a consumer is led by his culture, his subculture, his social class, his membership groups, his family, his personality, his psychological factors, etc.. and is influenced by cultural trends as well as his social and societal environment. By identifying and understanding the factors that influence their customers, brands have the opportunity to develop a strategy, a marketing message (Unique Value Proposition) and advertising campaigns more efficient and more in line with the needs and ways of thinking of their target consumers, a real asset to better meet the needs of its customers and increase sales. Consumer behavior refers to the selection, purchase and consumption of goods and services for the satisfaction of their wants. There are different processes involved in the consumer behavior. Initially the consumer tries to find what commodities he would like to consume, then he selects only those commodities that promise greater utility. After selecting the commodities, the consumer makes an estimate of the available money which he can spend. Lastly, the consumer analyzes the prevailing prices of commodities and takes the decision about the commodities he should consume. DJMcCortandNaresh & KMalhotra have defined culture as the complex whole that includes knowledge, belief art, laws, morals, customs and any other capabilities and habits acquired by humans as members of society. Culture operates primarily by setting somewhat loose boundaries for individual behavior within a society and by influencing the functioning of different institutions such as family and mass media etc. The boundaries set by culture on behaviors are referred to norms derived from cultural values and are the rules permitting or prohibiting certain types of behaviors in specific situations. Culture not only influences consumer behavior but also reflects it. D K Tse and R W Belk believes that cultures are not static but evolve and change slowly over time. Marketing strategies are unlikely to change cultural values but marketing does influence culture.

The Review of Literature

Dennis W Rook (1985) has written about the various dimension of consumer behaviour. The ...the relative importance of various factors of consumer behaviour. Lise ...urch (1992) have justified the behaviour changing of consumer on the ...niversary and gift giving rituals. David M Potter (1954) presented the ...ith diverse nature and ambitions. Cyndee Miller(1995) has described the 80 ...men as a purchaser in different capacities. Kate Fitzerald(1994) has

A Peer-reviewed- Refereed/Scholarly Quarterly Journal with Impact Factor

ISSN : 2321-4643

INTERNATIONAL STANDARD SERIAL NUMBER INTERNATIONAL CENTRE

Shanlax International Journal of Management

VOL : 4 SPECIAL ISSUE : 1 OCTOBER 2016

NATIONAL CONFERENCE ON EMERGING TRENDS ON ENTREPRENEURIAL OPPORTUNITIES AND CHALLENGES

NCEOC - 2016

Organized by

Department of Business Administration

Department of Commerce

Department of Commerce with CA

Caussanel College of Arts and Science

(Affiliated to Alagappa University)

(Run by the Congregation of the Brothers of the Sacred Heart, Palayamkottai)

Muthupettai - 623523

CONTENTS

Volume 4 Special Issue 1 October 2016 ISSN: 2321 – 464

CHALLENGES FACING BY WOMEN ENTREPRENEURS

Dr. M. Abbas Malik
Professor and Head, Department of Management Studies,
Mohamed Sathak Engineering College, Kilakarai

Ms. S. Santhana Jeyalakshmi
Assistant Professor, Department of Management Studies,
Mohamed Sathak Engineering College, Kilakarai

Abstract

Challenges facing women entrepreneurs classified women into "better -off and low-income women". According to them, better-off women face the following challenges; Lack of socialization to entrepreneurship in the home, school and society, Exclusion from traditional business networks, Lack of access to capital and information, Discriminatory attitude of leaders, Gender stereotypes and expectation: Such as the attitude that women entrepreneurs are dabblers or hobbyists, Socialized ambivalence about competition and profit, Lack of self-confidence., Inability to globalize the business: Men are leading in the global market.

Introduction

Women entrepreneurs face many challenges, including government rules and regulations, gaining access to finance, and building an ICT infrastructure that enables efficiency and growth (United Nations, 2006). Women entrepreneurs require confidence, leadership and management skills and must find ways to access new markets. Kantor (1999) rightly argued that women often experience greater constraints on their economic actions relative to men. Mayoux (2001) also noted that "there are certain factors that limit the ability of women entrepreneurs to take advantage of the opportunities available to them in their environment and these factors have been identified as the reasons why women businesses fail". These include poor financial management, liquidity problems, management inexperience and incompetence, problems in coping with inflation and other external economic conditions, poor or non-existent books and records, sales and marketing problems, staffing, difficulties with unions, the failure to seek expert advice, limited social and business networks, a low level of demand in the local economy, the value and system of tenure for housing, constraints in access to finance, lack of work experience and skill, and lack of role models (United Nations, 2006). Other barriers to women entrepreneurship development are cultural obstacles, lack of motivation, high crime rates, government regulation and problems during the transition from reliance on government benefits and employment. More extensively, Mayoux (2001) identified these factors to include:

- **Lack of Access to and Control over Income:** Another constraint that faces women entrepreneurs is lack of access to and control over income. Low income, low investment and low profit may limit women's ability to save. More than 65% of the poor and rural settlers in Tamil Nadu are women. Women usually face discrimination in the labour market (both in their remuneration and the nature of job they are offered). This affects their income, investment, and savings. Inability to save, can affect their start-up capital there by discouraging them from owing businesses. Mayoux (2001) also noted that Women have limited control over the incomes they earn. Gendered rights and responsibilities between man and women within households invariably operate to constrain women's ability to control their own income and access to male income. Even when women have opportunity to earn high income, by virtue of culture and tradition, they are subjected under their husbands who have control over them and their money. This can hinder their participation in business.

- **Lack of access to Information Technology:** The number of women in the technology is very low unlike in other sectors such as health care, hotel, education, restaurant etc.
- **Lack of Information on Women Entrepreneurship:** There is little information available on women entrepreneurship or women owned business in Tamil Nadu in particularly and in the world generally.
- **Age Limit:** Unlike men, there are certain periods in a woman age/time that she cannot do business -for instance, during pregnancy, labour period, child nursing and such other times that are peculiar to woman. Due to this, entrepreneurship therefore tends to be a midlife choice for women. Hence, majority of women start up business after the age of 35 (Dane, 1984).
- **Family Dependence:** Most of the family members depend on women for care and hospitality, thereby limiting their full involvement and participation in business.
- **Restriction to Family Business:** Most women entrepreneurs are some how restricted to family business because of their family commitment. This affects their level of ingenuity, creativity, innovativeness and competitiveness.
- **Inaccessibility to Required Funds:** Women also may not have equal opportunity to access finance from external sources such as banks, and other finance institutions as a result of this, they tend to prefer using personal credit/saving in financing their business. This discourages a lot of women from going into entrepreneurship.
- **Religious Predicament:** Some religion prohibits women from coming out of their homes and environments thereby restricting them from getting involved in business.
- **Non Involvement of Women in Decision Making:** Women all over the world and in all sectors are usually marginalized, especially in the planning stage of development. The decision for the execution of projects done in Tamil Nadu such as construction of roads, building of markets, building of civic centers etc are done without consultation of the women by their men counterparts (Okunade, 2007).
- **The Offensive of the Economic Planner:** The women are totally neglected in the economic planning process. The opinion of the men assumed to be the same with that of women. Even the work they do in most cases, is not giving economic value. Dane (1984) was right when she asserted, "all the work by women in the family enterprises and on the land is given no economic value, and women are being exploited in the employment field".
- **Much Emphasis on Domestic Role:** No matter the role of a woman in the society, she is mainly remembered for the domestic role. A woman, whether a director of a company, an educationalist, an entrepreneur, or a professional, must go back to the kitchen. The popular saying that a *"woman education ends in the kitchen"*- tends to prohibit women from going into business. "The kitchen" role dominates every other role of a woman (Kpohazounde, 1994).
- **Limited Leadership Role:** Women especially in world have always been assumed not to be matured for leadership position. They are usually given the seconding position in company's meetings and as government functionaries. Gould and Perzen (1990) listed the barriers that women entrepreneurs face which are not usually encountered by their men counterpart. He classified the constraints that face women into two groups; "constraints for better- off women and for low-income women". Gould and Perzen (1990) commenting on the challenges facing women entrepreneurs classified women into "better -off and low-income women". According to them, better-off women face the following challenges;
  - Lack of socialization to entrepreneurship in the home, school and society
  - Exclusion from traditional business networks
  - Lack of access to capital and information
  - Discriminatory attitude of leaders
  - Gender stereotypes and expectation: Such as the attitude that women entrepreneurs are dabblers or hobbyists
  - Socialized ambivalence about competition and profit
  - Lack of self-confidence

lize the business: Men are leading in the global market.
women according to Gould and Perzen face the following challenges: i)poor
urs to work, iii) health care and other assistance, iv) illiteracy, v) regulation

that do not distinguish between personal business assets make it extremely difficult to start a business or to invest the time it takes to make it profitable, vi) Lack of managerial skill, vii) cultural bias both within cultural group and in the larger society (viii) high level of poverty.

Motivations of women entrepreneurs empirically, are associated with different factors. The classification of these factors varies from author to author. For instances, Bartol and Martin (1998) classified these factors into (i) Personal characteristics, (ii) Life-path circumstances and (iii) Environmental factors. The results of their findings revealed that most women under their study cited push factors as their major motivation into business. These factors include; factors of frustration and boredom in their pervious jobs, followed by interest in the business, while pull factors include; independence, autonomy and family security.

References

1. Ando, F. and Associates. (1988). "Minorities, Women, Veterans and The 1982 Characteristics of Business Owners Survey". Haverford, PA: Faith Ando and Associates.
2. Anyanwu, C.M. (2004) Microfinance Institutions in Nigeria: Policy, Practice and Potentials, Paper Presented at the G24 Workshop on " Constraints to Growth in Sub Saharan Africa," Pretoria, South Africa, Nov. 29-30
3. Bartol, K. M. and Martin, D. (1998) Management. Int. Edition, Irwin, New York. McGraw-Hill.
4. Bird, B. (1988). "Implementing Entrepreneurial Ideas: The Case for Intention". Academy of Management Review, Vol. No. 3.
5. Birley, S. (1989). "Female Entrepreneurs: Are They Really Any Different?" Journal of Small Business Management 27(1), p. 32-37.
6. Birley, S. and Westhead, P. (1994). "A Taxonomy of Business Start-up Reasons and Their Impact on Firm Growth and Size," Journal of Business Venturing, Vol. 9,7-31.
7. Boyd, N. and G. Vozikis (1994). "The Influence of Self-Efficacy on the Development of Entrepreneurial Intentions and Actions". Entrepreneurship Theory and Practice, Summer, Vol. 18.
8. Brockhaus, R. H. (1986). "Risk Taking Propensity of Entrepreneurship". Academy of Management Journal, Vol. 23, No. 3.
9. Burlingham, B.(1990,)."This Woman Has Changed Business Forever" INC.
10. Buttner, E. H. and Moore, D. P. (1997). "Women's Organizational Exodus to Entrepreneurship: Self- Reported Motivations and Correlates with Success". Journal of Small Business Management, January.
11. Buttner, E.H., Rosen, B. (1989), "Funding New Business Ventures: Are Decision Makers Biased Against Women?", Journal of Business Venturing, Vol. 4 pp.249-61.

A Peer-reviewed- Refereed Scholarly Quarterly Journal with Impact Factor

ISSN : 2321-4643

Shanlax International Journal of Management

VOL : 4 SPECIAL ISSUE : 1 OCTOBER 2016

NATIONAL CONFERENCE ON EMERGING TRENDS ON ENTREPRENEURIAL OPPORTUNITIES AND CHALLENGES

NCEOC - 2016

Organized by

Department of Business Administration

Department of Commerce

Department of Commerce with CA

Caussanel College of Arts and Science

(Affiliated to Alagappa University)

(A Congregation of the Brothers of the Sacred Heart, Palayamkottai)

Muthupettai - 623523

ENTRPRENEURIAL SUCCESS OF Mc DONALD - A CRITICAL STRATEGIC ANALYTICAL APPROACH

Dr. N. Shankar
Associate Professor, Mohamed Sathak Engineering College, Kilakarai, Ramanathapuram District

C. Shalini
Assistant Professor, Mohamed Sathak Engineering College, Kilakarai, Ramanathapuram District

Abstract

In the world of entrepreneurship major changes are witnessed always. Many entrepreneurs appear and disappear in the arena. But successful entrepreneurs only thrive and withstand over a longer period of time as they have perseverance, like to taste and smell the odour of success, love challenges and creative. These attributes really suit Raymond Kroc of Mc Donald. With profound turbulence from the inception of the concern, the founder and progenies established and developed it as multinational. The paper discusses the strategic orientation of McDonald and the ways and means by which it attained success.

Key words: *Business Model, Marketing mix, Promotion, Life cycle.*

Introduction: McDonald's Story - Genesis

The story of McDonald's started in 1954, when its founder Raymond Kroc saw a hamburger stand in San Bernardino, California and envisioned a nationwide fast food chain. Kroc proved himself as a pioneer who revolutionized the American restaurant industry. Today McDonald's is the world's largest fast food chain serving 47 million customers daily. McDonald's is now one of the most valuable brands globally, worth more than $25 billion. The Golden Arches and its mascot Ronald McDonald have gained universal recognition. Though the company has roots in the US, McDonald's today has become an accepted citizen of the world. In 1955, Ray Kroc opens his first restaurant. McDonald's Corporation was created. In the year 1968, Big Maca was introduced. Happy Meal was launched in 1974. McDonald's opened in India, the 95th country in the year 1996.

Business Model

Franchise Model - Only 15% of the total number of restaurants are owned by the Company. The remaining 85% is operated by franchises. The company follows a comprehensive framework of training and monitoring of its franchises to ensure that they adhere to the **Quality, Service, Cleanliness and Value propositions** offered by the company to its customers.

Product Consistency - By developing a sophisticated supplier networked operation and distribution system, the company has been able to achieve consistent product taste and quality across geographies.

Act like a retailer and think like a brand - McDonald's focuses not only on delivering sales for the immediate present, but also protecting its long term brand reputation.

McDonald's in India

McDonald's entered India in 1996. McDonald's India has a joint venture with Connaught Plaza Restaurants and Hard Castle Restaurants. Connaught Plaza Restaurants manages operations in North India whereas Hard Castle Restaurants operates restaurants in Western India. Apart from opening outlets in the major metros, the company is now expanding to Tier two cities like Pune and Jaipur and Chennai.

Challenges in Entering Indian Markets: Regiocentricism: Re-engineering the menu - McDonald's has continually adapted to the customer's tastes, value systems, lifestyle, language and perception. Globally McDonald's was known for its hamburgers, beef and pork burgers. Most Indians are barred by religion not to consume beef or pork. To survive, the company had to be ...ian sensitivities. So McDonald's came up with chicken, lamb and fish burgers ...late.

SHANLAX INTERNATIONAL JOURNALS

BETTER SOUND THROUGH COMPENDIUM

A Peer-reviewed- Refereed/Scholarly Quarterly Journal

Certificate

OF PUBLICATION

We hereby certify that

Dr. N. SHANKAR

Associate Professor, Mohamed Sathak Engineering College, Kilakarai, Ramanathapuram District

C. SHALINI

Assistant Professor, Mohamed Sathak Engineering College, Kilakarai, Ramanathapuram District

In recognition of the Publication of the Paper Entitled

Entrpreneurial Success of Mc Donald - A Critical Strategic Analytical Approach

Published in

Shanlax International Journal of Management

ISSN: 2321- 4643 - Vol. 4, Special Issue. 1, October 2016

Dr. S. Raja Gopalan
Chief

Er. S. Lakshmanan
The Publisher

TRUE COPY ATTESTED

PRINCIPAL
MOHAMED SATHAK ENGINEERING COLLEGE
KILAKARAI-623806.

CONTENTS

IMPACT OF SELF-HELP GROUP IN ENTREPRENEURIAL DEVELOPMENT

Mr. M. Shahul Hameed
Associate Professor, Dept of Management Studies,
Mohamed Sathak Eengineering College, Kilakarai.

Mr. A. Kumar
Assistant Professor, Dept of Management Studies, Mohamed Sathak Engineering College, Kilakarai

Abstract

The SHG method is used by the government, NGOs and others worldwide. Thousands of the poor and the marginalized population in India are building their lives, their families and their society through Self help groups. The main aim of this paper is to examine the impact of Self-help Group in Entrepreneurial development of India. Self-help Groups have been playing considerable role in training of Swarozgaris, infrastructure development, marketing and technology support, communication level of members, self confidence among members, change in family violence, frequency of interaction with outsiders, change in the saving pattern of SHG members, change in the cumulative saving pattern of SHG members per month, involvement in politics, achieving social harmony, achieving social justice, involvement in community action, sustainable quality and accountability, equity within SHGs, defaults and recoveries, and sustainability - financial value of the SHGs.

Keywords: *Poor, Self-Help Group, achieving Social Justice, Sustainable quality, Equity, Empowerment*

Introduction

A Self-Help Group may be registered or unregistered. It typically comprises a group of micro-entrepreneurs having homogenous social and economic backgrounds; all voluntarily coming together to save regular small sums of money, mutually agreeing to contribute to a common fund and to meet their emergency needs on the basis of mutual help. They pool their resources to become financially stable, taking loans from the group members use collective wisdom and peer pressure to ensure proper end-use of credit and timely repayment. This system eliminates the need for collateral and is closely related to that of solidarity lending, widely used by micro-finance institutions. To make the bookkeeping simple enough to be handled by the members, flat interest rates are used for most loan calculations money collected by that group and by making everybody in that group self- employed. Members make small regular savings contributions over a few months until there is enough capital in the group to begin lending. Funds may then be lent back to the members or to others in the village for any purpose

Self-Help Group

Self-help group is a method of organizing the poor people and the marginalized to come together to solve their individual problem. The SHG method is used by the government, NGOs and others worldwide. The poor collect their savings and save it in banks. In return they receive easy access to loans with a small rate of interest to start their micro unit enterprise. Thousands of the poor and the marginalized population in India are building their lives, their families and their society through Self-help groups. Self Help Group (SHGs)-Bank Linkage Programme is emerging as a cost effective mechanism for providing financial services to the "Unreached Poor" which has been successful not only in meeting financial needs of the rural poor women but also strengthen collective self help capacities of the poor ,leading to their empowerment. The main aim of this [illegible] the impact of Self-help Group in Entrepreneurial development. It analyses the [illegible]ts significance and the present status of Self-Help Group, impact of Self-Help [illegible]of Self-Help Group, and the Suggestions to enhance the Entrepreneurial skills [illegible]Gs.

A Peer-reviewed- Refereed/Scholarly Quarterly Journal with Impact Factor

ISSN : 2321-4643

Shanlax International Journal of Management

VOL : 4 SPECIAL ISSUE : 1 OCTOBER 2016

NATIONAL CONFERENCE ON EMERGING TRENDS ON ENTREPRENEURIAL OPPORTUNITIES AND CHALLENGES

NCEOC - 2016

Organized by

Department of Business Administration
Department of Commerce
Department of Commerce with CA

Caussanel College of Arts and Science

(Affiliated to Alagappa University)

(Run by the Congregation of the Brothers of the Sacred Heart, Palayamkottai)

Muthupettai - 623523

CHALLENGES IN REINVENTING THE BUSINESS PROCESS

EDITED BY

MANIAN, PH.D

MARI, PH.D

N

HUMAN RESOURCE ISSUES

GAP ANALYSIS – DISTANCE EDUCATION SERVICES

S. Santhana Jeyalakshmi, Assistant Professor, Department of Management Studies, Mohamed Sathak Engineering College, Kilakarai &
Dr. S. Meenakumari, Assistant Professor, Management Studies, Easwari Engineering College, Chennai

Introduction

Service industries are playing an increasingly important role in the economy of many nations. In today's world of global competition, rendering quality service is a key for success and many experts concur that the most powerful competitive trend currently shaping marketing and business strategy is service quality. Service quality has since emerged as a pervasive strategic force and a key strategic issue on management's agenda. It is no surprise that practitioners and academics alike are keen on accurately measuring service quality in order to better understand its essential antecedents and consequences and ultimately establish methods for improving quality to achieve competitive advantage and build customer loyalty.

In this paper, service quality can be defined as the difference between customers' expectations for service performance prior to the service encounter and their perceptions of the service received. Service quality theory predicts that clients will judge that quality is low if performance does not meet their expectations and quality increases as performance exceeds expectations. Hence, customers' expectations serve as the foundation on which service quality will be evaluated by customers.

Distance Education

Distance education or distance learning is a mode of delivering education and instruction, often on an individual basis, to students who are not physically present in a traditional setting such as a classroom. Distance learning provides "access to learning when the source of information and the learners are separated by time and distance, or both." Distance education courses that require a physical on-site presence for any reason (including taking examinations) have been referred to as hybrid or blended courses of study.

Distance education dates back to at least as early as 1728 when an advertisement in the Boston Gazette promoted "Caleb Phillips, Teacher of the new method of Short Hand," who sought students who wanted to learn through weekly mailed lessons.

Similarly, Isaac Pitman taught shorthand in Great Britain via correspondence in the 1840s. Distance education has a long history, but its popularity and use has grown exponentially as more advanced technology has become available.

Coldeway (1982) identified the following reasons for the limitation of research activities in distance education.

1. Educational researchers are rarely present during the design of distance learning systems.
2. There is no clear paradigm for research in distance learning, and it is difficult to attract funds to develop one.
3. Some institutions are averse to defining boundaries and variables clearly.
4. Educational researchers often ask questions of no practical or even theoretical relevance.
5. Researchers in the distance learning test variables that are really classes of variables (such as comparisons of distance and classroom learning).

Services Definition

The American Marketing Association defines services as - "Activities, benefits and satisfactions which are offered for sale or are provided in connection with the sale of goods." Or "A form of product that consists of activities, benefits, or satisfactions offered for sale that are essentially intangible and do not result in the ownership of anything."

Characteristics of services

The defining characteristics of a service are:

Intangibility: Services are intangible and do not have a physical existence. Hence services cannot be touched, held, tasted or smelt. This is most defining feature of a service and that which primarily differentiates it from a product.

Heterogeneity/Variability: Given the very nature of services, each service offering is unique and cannot be exactly repeated even by the same service provider. While products can be mass produced and be homogenous the same is not true of services.

Definition of Quality in Distance Education

The quality of education is even difficult to define. Some researchers' belief that quality cannot be defined in any simple ways. Due to this reason, researchers agree that there is no one best way to define and measure service quality. However, there have been some early attempts made to define quality in distance education

Service Quality Dimensions in Distance Education

- Reliability - The degree to which education is correct, accurate and up to date. How well an institution keeps its promises? The degree of consistency in educational process
- Responsiveness - Willingness and readiness of staff to help students
- Understanding customers - Understanding students and their needs
- Access - The extent to which staff are available for guidance and advice
- Competence - The theoretical and practical knowledge of staff as well as other presentation skills
- Communication - How well lecturers and students communicate in the classroom?
- Credibility - The degree of trustworthiness of the institution
- Security - Confidentiality of information
- Tangible - State, sufficiency and availability of equipment and facilities
- Performance - Primary knowledge/skills required for students
- Completeness - Supplementary knowledge/skills learned is applicable to other fields
- Flexibility - The degree to which knowledge/skills learned is applicable to other fields
- Redress - How well an institution handles customers' complaints and solves problems?

Brady and Cronin (2001) identified that the foundation of service quality theory has some connection with the product quality and customer satisfaction literature based on the disconfirmation paradigm identified in physical goods literature. The discrepancy between customers' expectations or desires and their perceptions of the actual service performance was elaborated in the Disconfirmation of Expectations Paradigm **(Patterson, 1993)** which related satisfaction to customer's pre-purchase expectations and perceptions of service performance and identified any differences as Disconfirmation. The comparisons which form the basis of the model are as follows:

Comparison Process Results

1. Perceived Performance > Expectation High Satisfaction (Delight)
2. Perceived Performance = Expectation Merely Satisfied
3. Perceived Performance < Expectation Dissatisfaction

The concept of measuring the difference between expectations and perceptions in the form of the SERVQUAL gap score proved very useful for assessing levels of service quality.

Gap analysis

Provider Gap 1: Educational institutions do not know the expectations of the students.

Provider Gap 2: Institutions are not having the desired service designs and standards to meet the requirements of the students.

Provider Gap 3: Educational institutions are not delivering service standards as required to deliver.

Provider Gap 4: They are not matching performance they are supposed to show and promises communicated to the students.

Gap 5: There are lot of differences between expectations of the students and their Perceptions, which is known as Customer Gap

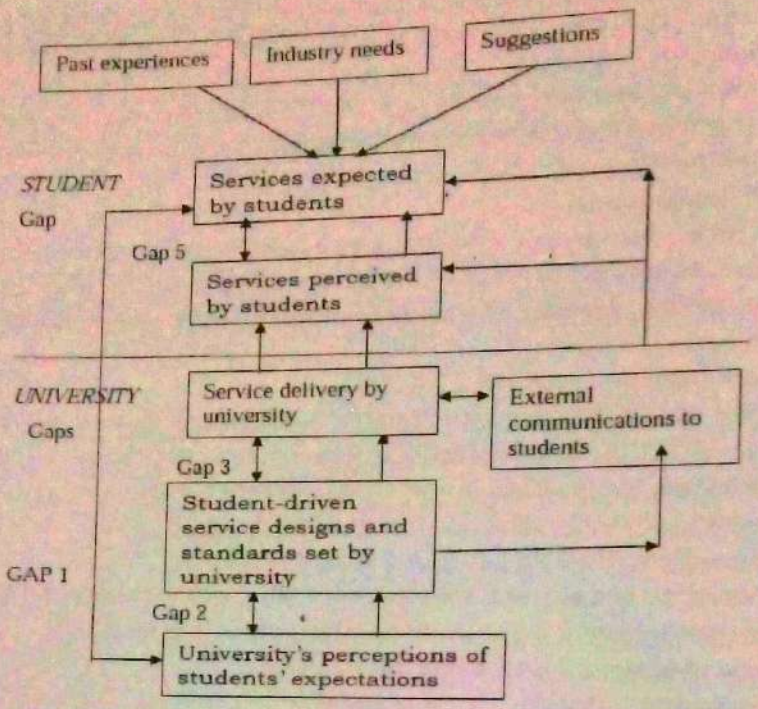

What should be the right approaches to minimize the gap?

Once gaps are identified, the educational institute should take some corrective measures to minimize those gaps. First, they should realize the expectations of the students and try to meet the same accordingly, if meet, customized services are to be rendered. Secondly, the institute should design the services which are market and student oriented. Thirdly, service quality and appropriate delivery process need to maintain properly. Fourthly, institute ought to keep the promises communicated by them. Fifthly, they must not allow creating any expectation and perception gap in the mind of their students. Marketing strategy should be adopted which are exclusive for student / customer satisfaction. The Consumer-Centric Business approach should be the appropriate path for them.

Conclusion

The quality of distance education services must be viewed as a strategic issue for social and technological development and economic growth. It is clear that service quality has significant positive relationship with student satisfaction. Thus, it confirms what other literature try to suggest here, which is by improving service quality, it may potentially improve the students' satisfaction as well and that is the priority of the distance education institutions. It is recommended in this study that the changing nature of the higher education marketplace encourage college administrators to apply the customer-oriented principles that are used in profit making institutions. We also hope that we have raised enough attention to increase the research efforts in this area.

References

1. Gronroos, C. (1984) A Service Quality Model and its Marketing Implications. European Journal of Marketing, 18, 139-150.
2. Joseph, M. (1998) Determinants of Service Quality in Education: a New Zealand perspective. Journal of Professional Services Marketing, 16, 43-71.
3. Parasuraman, V. A. Zeithaml, and L. L. Berry, "A conceptual model of service quality and its implications for future research," Journal of Marketing, vol. 49, 41–50, 1985.
4. Baker, J., & Lamb, C. J. (1993). A gap Analysis of Professional Service Quality. Journal of Professional Services Marketing, 31(7), 528-540.

Shanlax International Journal of Commerce

A Quarterly Journal

Vol. 3 No. 3 July 2015 ISSN :2320 - 4168

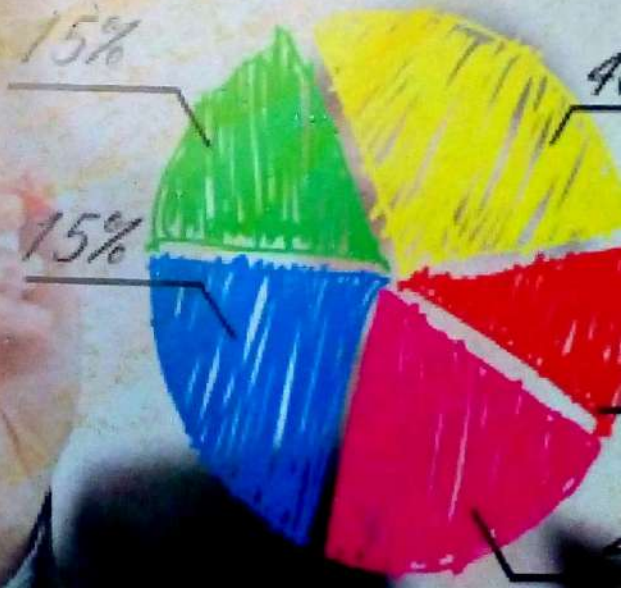

Vol.3 No.3 July 2015 ISSN: 2320-4168

MARKETING OF HOSPITAL SERVICES IN RAMANATHAPURAM DISTRICT

M. Abbas Malik
Associate Professor & Head, Department of Management Studies,
Mohamed Sathak Engineering College, Kilakarai - 623 806

Abstract

Buddha has said that of all the gains of health are the highest and the best. Health is not only basic to leading a happy life for an individual but it is also necessary for all productive activities in the society. Who would deny that a soldier who is not keeping good health cannot be expected to defend the frontiers of his country even when he is provided with the latest sophisticated weapons?

Service marketing by hospital deserves analysis because of its importance in treating its patients which is a service to the community. Analysis of hospital services special significance since it deals with the life of the patients. An inefficient management of hospital service will be disastrous to the patient and will affect the reputation of the hospital.

The study has the following objectives:

1. *To study the origin and growth of the case unit.*
2. *To examine the services provided by the hospitals to the patients.*
3. *To study the attitude and satisfaction of the patients and*
4. *To study the marketing of paramedical services by the hospitals.*

Major Findings of the Study

- *More than one-third of the patients who have visited the hospital feel that they get best treatment in the hospitals*
- *All the patients opine that the nurses in the hospital are prompt in discharging their duties.*
- *According to 92% of the patients the room rent charged in the hospital is reasonable.*
- *More than 96% the patients opine that they are discharged after the complete cure.*
- *There is no significant relationship between the sex of the patients and the attitude towards the hospital services*
- *There is no significant relationship between age of the patients and the attitude towards the hospital services.*
- *The type of treatment such as paying section or free section) does not influence the level of attitude towards the hospital services.*
- *The monthly income of the patients influences the level of attitude towards the hospital services.*
- *The major limitations are:*
- *This study is confined to Ramanathapuram District only.*
- *Convenience sampling method used in this study has its own limitations.*

Key Words: *Attitude of consumer, Satisfaction level, Services, health care, Inpatient, Outpatient, Paramedical, Treatment*

A Peer-reviewed- Refereed/Scholarly Quarterly Journal with Impact Factor

ISSN : 2321-4643

INTERNATIONAL STANDARD SERIAL NUMBER INTERNATIONAL CENTRE

Shanlax International Journal of Management

VOL : 4 SPECIAL ISSUE : 1 OCTOBER 2016

NATIONAL CONFERENCE ON EMERGING TRENDS ON ENTREPRENEURIAL OPPORTUNITIES AND CHALLENGES

NCEOC - 2016

Organized by

Department of Business Administration

Department of Commerce

Department of Commerce with CA

Caussanel College of Arts and Science

(Affiliated to Alagappa University)

(Run by the Congregation of the Brothers of the Sacred Heart, Palayamkottai)

Muthupettai - 623523

CONTENTS

Volume 4 Special Issue 1 October 2016 ISSN: 2321 – 464

CHALLENGES FACING BY WOMEN ENTREPRENEURS

Dr. M. Abbas Malik
Professor and Head, Department of Management Studies,
Mohamed Sathak Engineering College, Kilakarai

Ms. S. Santhana Jeyalakshmi
Assistant Professor, Department of Management Studies,
Mohamed Sathak Engineering College, Kilakarai

Abstract

Challenges facing women entrepreneurs classified women into "better -off and low-income women". According to them, better-off women face the following challenges; Lack of socialization to entrepreneurship in the home, school and society, Exclusion from traditional business networks, Lack of access to capital and information, Discriminatory attitude of leaders, Gender stereotypes and expectation: Such as the attitude that women entrepreneurs are dabblers or hobbyists, Socialized ambivalence about competition and profit, Lack of self-confidence., Inability to globalize the business: Men are leading in the global market.

Introduction

Women entrepreneurs face many challenges, including government rules and regulations, gaining access to finance, and building an ICT infrastructure that enables efficiency and growth (United Nations, 2006). Women entrepreneurs require confidence, leadership and management skills and must find ways to access new markets. Kantor (1999) rightly argued that women often experience greater constraints on their economic actions relative to men. Mayoux (2001) also noted that "there are certain factors that limit the ability of women entrepreneurs to take advantage of the opportunities available to them in their environment and these factors have been identified as the reasons why women businesses fail". These include poor financial management, liquidity problems, management inexperience and incompetence, problems in coping with inflation and other external economic conditions, poor or non-existent books and records, sales and marketing problems, staffing, difficulties with unions, the failure to seek expert advice, limited social and business networks, a low level of demand in the local economy, the value and system of tenure for housing, constraints in access to finance, lack of work experience and skill, and lack of role models (United Nations, 2006). Other barriers to women entrepreneurship development are cultural obstacles, lack of motivation, high crime rates, government regulation and problems during the transition from reliance on government benefits and employment. More extensively, Mayoux (2001) identified these factors to include:

- **Lack of Access to and Control over Income:** Another constraint that faces women entrepreneurs is lack of access to and control over income. Low income, low investment and low profit may limit women's ability to save. More than 65% of the poor and rural settlers in Tamil Nadu are women. Women usually face discrimination in the labour market (both in their remuneration and the nature of job they are offered). This affects their income, investment, and savings. Inability to save, can affect their start-up capital there by discouraging them from owing businesses. Mayoux (2001) also noted that Women have limited control over the incomes they earn. Gendered rights and responsibilities between man and women within households invariably operate to constrain women's ability to control their own income and access to male income. Even when women have opportunity to earn high income, by virtue of culture and tradition, they are subjected under their husbands who have control over them and their money. This can hinder their participation in business.

- **Lack of access to Information Technology:** The number of women in the technology is very low unlike in other sectors such as health care, hotel, education, restaurant etc.
- **Lack of Information on Women Entrepreneurship:** There is little information available on women entrepreneurship or women owned business in Tamil Nadu in particularly and in the world generally.
- **Age Limit:** Unlike men, there are certain periods in a woman age/time that she cannot do business -for instance, during pregnancy, labour period, child nursing and such other times that are peculiar to woman. Due to this, entrepreneurship therefore tends to be a midlife choice for women. Hence, majority of women start up business after the age of 35 (Dane, 1984).
- **Family Dependence:** Most of the family members depend on women for care and hospitality, thereby limiting their full involvement and participation in business.
- **Restriction to Family Business:** Most women entrepreneurs are some how restricted to family business because of their family commitment. This affects their level of ingenuity, creativity, innovativeness and competitiveness.
- **Inaccessibility to Required Funds:** Women also may not have equal opportunity to access finance from external sources such as banks, and other finance institutions as a result of this, they tend to prefer using personal credit/saving in financing their business. This discourages a lot of women from going into entrepreneurship.
- **Religious Predicament:** Some religion prohibits women from coming out of their homes and environments thereby restricting them from getting involved in business.
- **Non Involvement of Women in Decision Making:** Women all over the world and in all sectors are usually marginalized, especially in the planning stage of development. The decision for the execution of projects done in Tamil Nadu such as construction of roads, building of markets, building of civic centers etc are done without consultation of the women by their men counterparts (Okunade, 2007).
- **The Offensive of the Economic Planner:** The women are totally neglected in the economic planning process. The opinion of the men assumed to be the same with that of women. Even the work they do in most cases, is not giving economic value. Dane (1984) was right when she asserted, "all the work by women in the family enterprises and on the land is given no economic value, and women are being exploited in the employment field".
- **Much Emphasis on Domestic Role:** No matter the role of a woman in the society, she is mainly remembered for the domestic role. A woman, whether a director of a company, an educationalist, an entrepreneur, or a professional, must go back to the kitchen. The popular saying that a *"woman education ends in the kitchen"*- tends to prohibit women from going into business. "The kitchen" role dominates every other role of a woman (Kpohazounde, 1994).
- **Limited Leadership Role:** Women especially in world have always been assumed not to be matured for leadership position. They are usually given the seconding position in company's meetings and as government functionaries. Gould and Perzen (1990) listed the barriers that women entrepreneurs face which are not usually encountered by their men counterpart. He classified the constraints that face women into two groups; "constraints for better- off women and for low-income women". Gould and Perzen (1990) commenting on the challenges facing women entrepreneurs classified women into "better -off and low-income women". According to them, better-off women face the following challenges;
  - Lack of socialization to entrepreneurship in the home, school and society
  - Exclusion from traditional business networks
  - Lack of access to capital and information
  - Discriminatory attitude of leaders
  - Gender stereotypes and expectation: Such as the attitude that women entrepreneurs are dabblers or hobbyists
  - Socialized ambivalence about competition and profit
  - Lack of self-confidence

lize the business: Men are leading in the global market.
women according to Gould and Perzen face the following challenges: i)poor
urs to work, iii) health care and other assistance, iv) illiteracy, v) regulation

that do not distinguish between personal business assets make it extremely difficult to start a business or to invest the time it takes to make it profitable, vi) Lack of managerial skill, vii) cultural bias both within cultural group and in the larger society (viii) high level of poverty.

Motivations of women entrepreneurs empirically, are associated with different factors. The classification of these factors varies from author to author. For instances, Bartol and Martin (1998) classified these factors into (i) Personal characteristics, (ii) Life-path circumstances and (iii) Environmental factors. The results of their findings revealed that most women under their study cited push factors as their major motivation into business. These factors include; factors of frustration and boredom in their pervious jobs, followed by interest in the business, while pull factors include; independence, autonomy and family security.

References

1. Ando, F. and Associates. (1988). "Minorities, Women, Veterans and The 1982 Characteristics of Business Owners Survey". Haverford, PA: Faith Ando and Associates.
2. Anyanwu, C.M. (2004) Microfinance Institutions in Nigeria: Policy, Practice and Potentials, Paper Presented at the G24 Workshop on " Constraints to Growth in Sub Saharan Africa," Pretoria, South Africa, Nov. 29-30
3. Bartol, K. M. and Martin, D. (1998) Management. Int. Edition, Irwin, New York. McGraw-Hill.
4. Bird, B. (1988). "Implementing Entrepreneurial Ideas: The Case for Intention". Academy of Management Review, Vol. No. 3.
5. Birley, S. (1989). "Female Entrepreneurs: Are They Really Any Different?" Journal of Small Business Management 27(1), p. 32-37.
6. Birley, S. and Westhead, P. (1994). "A Taxonomy of Business Start-up Reasons and Their Impact on Firm Growth and Size," Journal of Business Venturing, Vol. 9,7-31.
7. Boyd, N. and G. Vozikis (1994). "The Influence of Self-Efficacy on the Development of Entrepreneurial Intentions and Actions". Entrepreneurship Theory and Practice, Summer, Vol. 18.
8. Brockhaus, R. H. (1986). "Risk Taking Propensity of Entrepreneurship". Academy of Management Journal, Vol. 23, No. 3.
9. Burlingham, B.(1990,)."This Woman Has Changed Business Forever" INC.
10. Buttner, E. H. and Moore, D. P. (1997). "Women's Organizational Exodus to Entrepreneurship: Self- Reported Motivations and Correlates with Success". Journal of Small Business Management, January.
11. Buttner, E.H., Rosen, B. (1989), "Funding New Business Ventures: Are Decision Makers Biased Against Women?", Journal of Business Venturing, Vol. 4 pp.249-61.

Shanlax International Journal of Management

A Quarterly Journal

Vol.3 ~ No.1 ~ July 2015 ~ ISSN : 2321 – 4643

CONTENTS

Vol. 3 No. 1 July 2015 ISSN: 2321 - 4848

ROLE OF HIGHER EDUCATION IN PROMOTING ENTREPRENEURSHIP

S.Santhana Jeyalakshmi
Assistant Professor, Department of Management Studies,
Mohamed Sathak Engineering College, Kilakarai, Ramanathapuram - 623 806

Dr.S.Meenakumari
Assistant Professor, Department of Management Studies, Anna University, Chennai - 600 025

Abstract

Entrepreneurship continues to assume a vital role in the Indian economy as well as the economies of many developing nations across the globe. The creation of new business activities has become a major driver in the economy and these greatly affect economic growth, job creation and general prosperity and, to an extent, enhance the national competitiveness of the nation in the global business arena. Although our country is trying to intensify the amount of entrepreneurial activity there are still a wide variety of challenges. According to the Global Entrepreneurship Monitor (GEM) research shows that a low level of overall education and training is still the biggest challenge facing the nation. Consequently a critical performance area must be to improve the level of overall education and training whilst promoting the notion of entrepreneurship as a viable option.

The main purpose of this paper is to configure the importance of Higher Education in promoting Entrepreneurship. The paper would explore the concept of Higher Education and Entrepreneurship. It would also explain the characteristics of both Higher Education and entrepreneurship. Thus the paper provides a clear insight on the role of Higher Education in promoting Entrepreneurship.

Key Words: *Higher Education, Entrepreneurship, Role of Higher Education*

Introduction

New trends of globalization, global competition, social development, corporate downsizing, and the emergence of knowledge based economy have forced attention towards the entrepreneurship. Entrepreneurship is a process of action where an individual searches for a business opportunity, takes the calculated risks and finally launches a new venture. It is known as the engine of individual and society which influences positively the general growth of economies (Gorman et al., 1997; Navarro et al., 2009). Over the past decade, entrepreneurship has been considered as a driver of innovation and wealth creation for individuals and societies, profit and non-profit sectors, and small and large enterprises (Greene and Rice, 2007). The impact of entrepreneurial activity for economic growth, creating career opportunities and developing employability has been well revealed in the literature (Deakins and Freel, 2009). A strong belief emerges that it can develop through systematic development and planned efforts (Vesper, 1994; Gorman et al., 1997; Sethi, 2006). Thus the education for entrepreneurship place importance in their development and increase and foster mindset and skills of an individual to embrace entrepreneurship (Formica, 2002; Hannon, 2005; Li, 2006). Literature support that

appropriate entrepreneur education and training programs are expected to increase the attitudes and intention of people becoming entrepreneurs (Gorman et al., 1997; Alsos and Kolvereid, 1998; Reynolds et al., 1999; Henry et al., 2003; Souitaris et al., 2007). This research investigates the effect of entrepreneurship education for entrepreneurship programmes on entrepreneurial attitudes and intentions. Researcher attempts to investigate the role of higher educational institution in entrepreneurship education and development as an integral part of an enterprise system.

Entrepreneurship

It has been almost a century since Joseph Schumpeter identified the principles of entrepreneurship as qualities of individual willingness that go beyond everyday routines, which should support in overcoming inner-personal resistance as well as resistance of the social environment (Ebner, 2003). Since then entrepreneurship has gone a long way and it is widely accepted that entrepreneurs today increasingly need to take the initiative in designing a new approach for their business. This approach concerns everyday acts of work that contribute to the betterment of people□s life affected by the business□s action (Kuratko and Hodgetts, 2007).

Characteristics

Available literature suggests that entrepreneurs share some common features. In support of this opinion, Ntekop and Umoren (2010) agree that those who possess the entrepreneurial mindset also possess certain recognizable characteristics even though these same characteristics may also be found in some managers, or some successful career-minded individuals. These characteristics according to Mccleuand (1961) are:

- Desire for responsibility;
- Preference for moderate risk;
- Confidence in their ability to succeed
- Desire for immediate feedback
- High level of energy;
- Future orientation;
- Skill at organizing, and
- Value of achievement over money

Literature Review

The vital role of entrepreneurship as an indicator of economic growth, there is an intense interest from policy makers and academics in stimulating economic growth through entrepreneurship, including entrepreneurship education (Gorman et al., 1997). Indeed, ...rship deals with business opportunity identification, risk taking and launching ...r, 2004).

Shanlax International Journal of Management

Peer Review Journal A Quarterly Journal

Vol. 2 No. 2 October 2014 ISSN : 2321 – 4643

RECENT TRENDS IN INSURANCE SERVICES IN TAMIL NADU

M. Abbas Malik
Associate Professor & Head, Department of Management Studies,
Mohamed Sathak Engg.College, Kilakarai-623806

Dr. U. Surya Rao
Senior Professor & Head (Rttd.), Department of Management Studies,
Madurai Kamaraj University, Madurai- 625021

Abstract

Life insurance products assure financial support even in absence. In addition to serving as a protective cover, it creates a flexible money-saving scheme, which empowers one to accumulate wealth to buy a new car, get one's children educational solutions, and even retire comfortably. Buying Life insurance is a way to make unique investment that helps you to meet your dual needs-saving for life's important goals and protecting your assets. From an investor's point of view, an investment can play two roles-asset appreciation or asset protection. While most financial instruments have the underlying benefit of asset appreciation, buying life insurance gets you the unique reassurance of asset protection, along with a stringer element of asset appreciation. When one buys life Insurance, the main benefit is that the financial interests of one's family remain protected from the loss of income due to critical illness or death of the policyholder. The customer therefore benefits on two counts.

Life Insurance Corporation of India Limited is the giant corporation engaged in the business of insurance. The corporation has introduced a number of products in view of the facility of various customers. This paper gives recent trends in insurance services in Tamil Nadu.

Key Words: *Coverage, Death benefit, Investment, Income, Premium, Protection, Risk, Return.*

Introduction

Life insurance is an appropriate financial tool for managing and mitigating the financial risk associated with untimely death. However life insurance decisions are often complex. The choice of a life insurance product for Tamil Nadu Consumer is now a problem of plenty, even when confined to only traditional life insurance products-term insurance and cash value policies (i.e., whole life and endowment insurance). For any given product, we can choose from amongst several competing insurance companies. Depending only on a policy illustration provided by an insurance company can be a big mistake.

While comparing life insurance decisions, the concern of many financial planners is the quantitative assessment of the cost of protection against untimely death and the return on the savings component of the premium paid. Such an analysis can give a rational basis
…t Insurance Policies.
…o find a policy which best suits his needs. Some of the important
…ask himself are:

INTERNATIONAL JOURNAL OF MANAGEMENT RESEARCH AND REVIEW

EFFECT OF SOCIAL FACTORS, ENTREPRENEURIAL BEHAVIOR TOWARDS ENTREPRENEURIAL INTENTION AMONG LAW GRADUATES

Dr. N. Shankar*[1]

[1]Assistant Professor, Department of Management Studies, Mohamed Sathak Engineering College, Kilakarai, Ramanathapuram, Tamilnadu, India.

ABSTRACT

Student entrepreneurship has witnessed significant attention all over the world as it not only encourages venture creation, it also enhances the revenue to the government and distributes dispersal of economic benefits. Among student entrepreneurship, entrepreneurship by professional course pursuing students plays a great significance. The present study has been undertaken on the final year students of Law to find out the determinants of entrepreneurial behavior and to create a conceptual model integrating social factors, entrepreneurial behavior and entrepreneurial intention.

Keywords: Professional courses, entrepreneurial behavior, entrepreneurial intention, Social factor.

INTRODUCTION

Lawyers are considered as Professionals. The term professionals defines that those who are capable of working individually after completion of the study. Hence Law graduates are the one pursuing professional course. Similar to other professional courses, Law graduates also finds difficulties in getting suitable positions. Very few Law graduates after completing their course choose self–employment. But the opportunities are plenty. There are opportunities such as starting Law firms, Legal Process outsourcing, Web Paging, online dispute resolution and the like. The effect of globalization also shows the abundance towards self-employment. The paper constructs a conceptual model integrating social factors, entrepreneurial behavior and entrepreneurial intention of Law graduates. Ajzen‘s theory of planned behavior analyses the factors related to entrepreneurial intention of an individual. Azjen Model says that entrepreneurial intention depends on three independent attitudes. They are attitude towards behavior, Subjective norms and Perceived behavioral control. The behavioral belief is the beliefs about the likely consequence of the behavior. That means to what extent an individual has favorable or unfavorable attitude towards behavior. To align with this, the present paper evaluates the reason for the hindrances for the Law graduates for not choosing self-employment mode.

REVIEW OF LITERATURE

Sasi Misra et al have stated that the background and psychological factors of the entrepreneur g influence on behavior through the attitude and intention of the individual. trepreneurial environment and entrepreneurial resourcefulness also influence

on entrepreneurial behavior. A new model termed as entrepreneurial resourcefulness model was developed which envisages three entrepreneurial competencies – cognitive, affective and action oriented. These competencies explain the behavior pattern of entrepreneur.

Erich J. Schwaz et al. did their study on students from seven universities in Austria of medicine, law, technical, natural, social and business science. They tried to find out significant factors influencing intention start a new venture.. It developed a model of entrepreneurial intention and incorporating human and environmental factors. The model focuses on three components. They are attitude towards entrepreneurship, perception of university environment and regional start-up infrastructure

A study by Pradeep Brijlal investigated the perceptions and knowledge of final year students towards on entrepreneurship. It was identified that economics and management Science students scored the highest in the knowledge on entrepreneurship. The study stressed the need for entrepreneurship education at tertiary institutions across the different faculties.

METHODOLOGY

a) Statement of the Problem

Many studies have been undertaken on a variety of category of entrepreneurs. But the entrepreneurship among Law graduates has not been taken much. In order to fill the gap this work is carried out. Hence the title was chosen as "Effect of Social Factors, Entrepreneurial Behavior towards Entrepreneurial Intention among Law Graduates"

b) Objectives of the Study

The present study has the following objectives.

1. To develop a model for social factors creating entrepreneurship.
2. To frame a model for the behaviors creating entrepreneurs.
3. To frame model for entrepreneurial intention.
4. To create a conceptual model for integrating social factors and entrepreneurial behavior and entrepreneurial intention among Law graduates.

c) Sampling Techniques

Undergraduate students studying final year of Bachelor of Law in Madurai District is the targeted population. The researcher has used random sampling method. Three Hundred questionnaires were distributed to the respondents and 66.6 percent responses were successfully obtained from each professional course. Hence the sample size for the study is 200.

d) Statistical Tools Applied

The present study applies multiple regression and Structural Equation Modeling techniques (SEM) to accomplish its objectives.

ANALYSIS AND INTERPRETATION

1. To develop a model for social factors creating entrepreneurship.

In constructing the model for social factors three dimensions namely perceived educational support, Perceived structural support and Perceived Relational Support are shown. Structural support refers to the support from government and institutions like banks and others in creating entrepreneurs. The relational support refers to the support from societies like family members and friends. Similarly educational support means to support from educational institution from where students pursuing education. Its effort in introducing entrepreneurship related courses, organizing seminars and the related support. The estimate of regression weight for each dimensions are calculated. It has been inferred from the dimensions that law graduate students suffer more with improper and inadequate structural support than relational support and educational support.

Table No 1

Hypothesis Statement			Estimate	S.E.	C.R	P
Perceived Educational Support	<---	Social Factors	1.000			
Perceived Structural Support	<---	Social Factors	-.412	.410	-1.005	.315
Perceived Relational Support	<---	Social Factors	1.934	.856	2.260	.024

2. To develop a model for entrepreneurial behavior creating entrepreneurship.

As indicated in the table for constructing entrepreneurial behavior, ten different relevant dimensions are depicted. They are clearly summarized as initiative, information seeking, Problem solving, Self-confidence, commitment to work contrast, systematic planning, sees and act on opportunity, Assertiveness, Persuasion and efficiency orientation. The estimate of regression weight for each dimensions are identified. It showed that Problem solving accounts for highest value of estimate than the rest of dimensions. As such it indicates that for transformation of law graduates into entrepreneurs, problem solving is playing a significant role.

Table No 2

Hypothesis Statement			Estimate	S.E.	C.R	P
Initiative	<---	Entrepreneurial Behavior	1.000			
Information Seeking	<---	Entrepreneurial Behavior	1.043	.057	18.280	***
Problem Solving	<---	Entrepreneurial Behavior	1.385	.092	15.084	***
Self Confidence	<---	Entrepreneurial Behavior	1.020	.063	16.286	***
Commitment to work contrast	<---	Entrepreneurial Behavior	1.099	.058	18.890	***
Systematic Planning	<---	Entrepreneurial Behavior	.968	.074	13.053	***
Sees and acts on Opportunity	<---	Entrepreneurial Behavior	1.200	.069	17.388	***
Assertiveness	<---	Entrepreneurial Behavior	.474	.081	5.862	***
Persuasion	<---	Entrepreneurial Behavior	.947	.068	13.933	***
ıtation	<---	Entrepreneurial Behavior	.717	.109	6.546	***

5. Creating a Model for Entrepreneurial Intention

The Entrepreneurial Intention Model shows three dimensions namely EI - 1, EI - 2 and EI - 3. The dimension EI - 1 indicates the seriousness towards starting a firm and EI - 2 refers to intention to start a firm within Five years and EI - 3 is the wish and feelings of toughness to become an entrepreneur. The entrepreneurial intention model shows that regression weight of seriousness towards starting a firm (EI - 1) is greater than other dimensions of entrepreneurial intention.

Table No 3

Hypothesis Statement			Estimate	S.E.	C.R	P
EI -3	<---	Entrepreneurial Intention	1.000			
EI-2	<---	Entrepreneurial Intention	.877	.135	6.500	***
EI-1	<---	Entrepreneurial Intention	1.031	.127	8.131	***

5. Creating a conceptual Model integrating Social factor, Entrepreneurial Behavior and Entrepreneurial Intention

The conceptual model integrating Social factor, entrepreneurial behavior and entrepreneurial intention finds that social factor is influencing more on entrepreneurial behavior directly than on entrepreneurial intention. The social factor is influencing the entrepreneurial intention not directly but through entrepreneurial behavior. The Figure No- 1 also shows the same as indicated in the table. It confirms that Social Factor is the one more influencing for the law graduates to become lawpreneur.

Table No 4

Hypothesis Statement			Estimate	S.E.	C.R	P
Entrepreneurial Behavior	<---	Social Factors	4.695	1.936	2.426	.015
Entrepreneurial Intention	<---	Entrepren--eurial Behavior	2.308	1.003	2.302	.021
Entrepreneurial Intention	<---	Social Factors	-5.421	4.799	1.130	.259

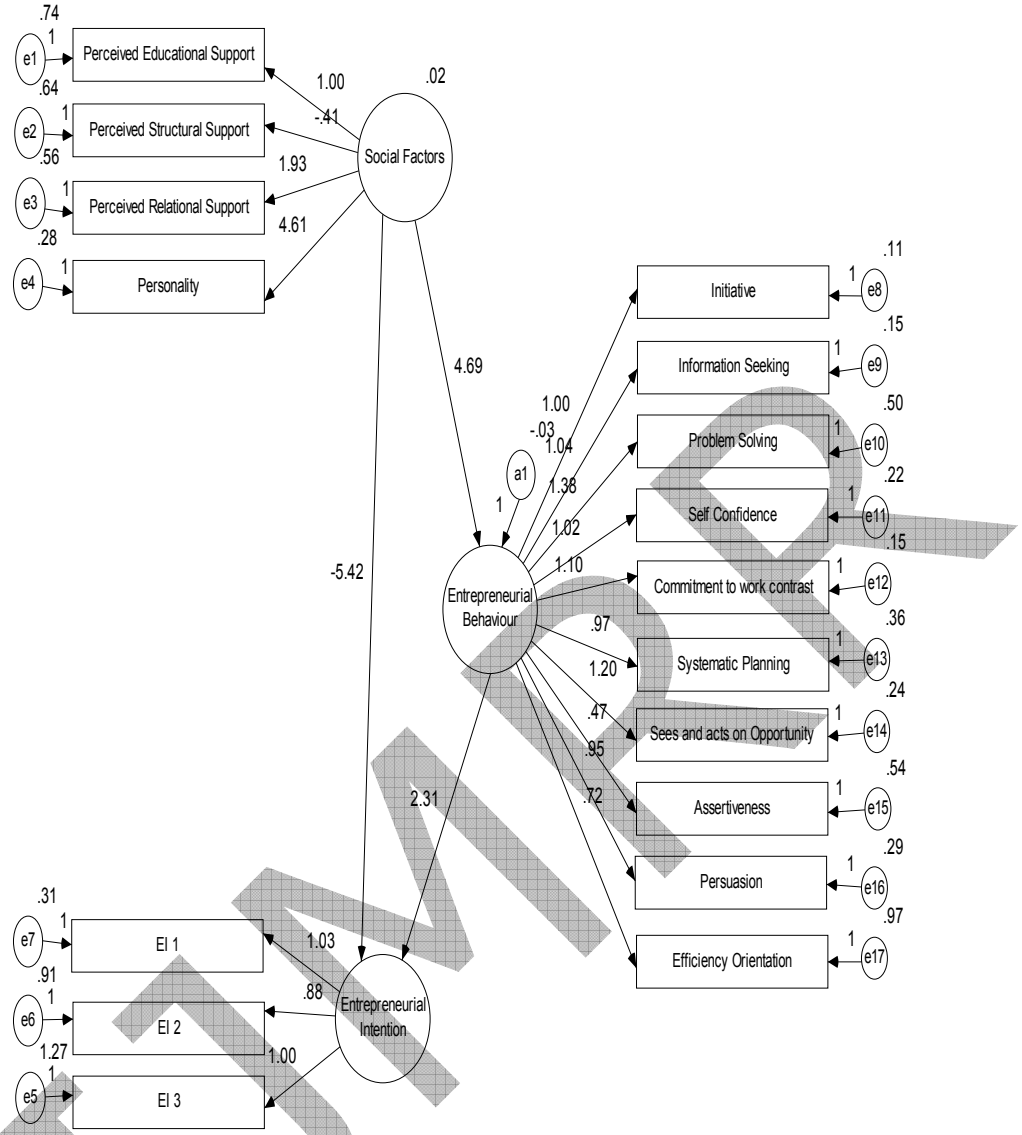

Fig 1: The conceptual model integrating Social Factor, Entrepreneurial Behavior and Entrepreneurial Intention

CONCLUSION AND DISCUSSION

Entrepreneurship is an outstanding phenomenon in the world. In India it is believed that there is tremendous latent entrepreneurial talents, which if properly harnessed could help solve many serious problems the country is facing. Among different entrepreneurship, Student entrepreneurship shall contribute effectively for the prosperity of the nation. This paper is trying to find the probable factors which induce the entrepreneurial intention among law students. The findings of the paper show the relationship between the social factor, entrepreneurial behavior and entrepreneurial intention. The model finds that social factor is the basic and fundamental one which influences the entrepreneurial behavior and intention. Among different social factors, perceived relational support is ng factor than any other factor for the law graduates to transform as n order to strengthen the law graduates entrepreneurship the structural support

from the institutions and banking sectors is really immediate need. The next wave of entrepreneurship can be generated if the structural support would be made properly available to them. In general in many of the law schools there is no concept of entrepreneurial cell and incubators. Hence the structural support of this kind should be created in order to enhance lawpreneurship.

REFERENCES

[1] Misra S, Sendil Kumar E. Resourcefulness: A Proximal Conceptualization Entrepreneurial Behaviour. The Journal of Entrepreneurship 2000; 9(2): 135–151.

[2] Schwarz EJ, Wodowwiak MA, Almer DA, Breitenecker RJ. The Effects and Attitudes and Perceived Environment Conditions on Students' Entrepreneurial Intent – An Australian Perspective. Education+ Training 2009; 51(4): 272–291.

[3] Brijlal P. Entrepreneurial Perceptions and Knowledge of Final Year University Students. African Journal of Business Management 2011; 5(3): 818–825.

[4] Shankar N, Subburajan M. Lawpreneurship and Opportunities, Shanlax International Journal of Arts, Science & Humanities 2013; 1(1).

[5] Azjen I. The Theory of Planned Behavior. Organizational Behavior and Human Decision Processes 1991; 50: 179-211.

[6] Powell J. The University role in the innovative leadership of small to medium sized enterprises: Towards "Universities for a modern renaissance" (UMR). International Journal for Entrepreneurial Behaviour and Research 2012; 18(4).

A Peer-reviewed- Refereed/Scholarly Quarterly Journal

ISSN : 2321-4643

INTERNATIONAL STANDARD SERIAL NUMBER INTERNATIONAL CENTRE

Shanlax International Journal of Management

VOL : 3 NO. : 4 APRIL 2016

Impact Factor

ISRAJIF: 1.117

Contents

CONTENTS

SERVICE QUALITY MANAGEMENT: A LITERATURE REVIEW

S. Santhana Jeyalakshmi[1] and Dr. S. Meenakumari[2]
[1]Assistant Professor, Department of Management Studies,
Mohamed Sathak Engineering College, Kilakarai, Ramanathapuram - 623 806
[2]Assistant Professor, Department of Management Studies, Anna University, Chennai - 600 025

Abstract

Service quality becomes the crucial issue for the education industry and the theory of service quality has evolved over long period of time through testing and trials in service sector. The demanding customers and increased sense of customer satisfaction led to the use of the new service parameters making education institutions to implement quality management as an effective aid. During the last few decades there is phenomenal change experienced in the education industry and the reason being is Service Quality. Knowing that both service quality and value is difficult to measure, education institutions heavily rely on student's quality perception and expectations. It could be achieved by asking students questions related to expectations and their perceptions of the service quality through carefully designed surveys. Various studies have been carried out to consolidate the dimensions of service quality and servqual has been accepted as well constructed instrument to measure service quality. The empirical research in development of service quality theory suggests that improved service quality plays important role in overall customer satisfaction. Study would focus on various studies on Service Quality conducted by earlier researchers in an array of industries. Thus, present study is unique in the sense that it is new to Education industry. The paper explores the development of service quality theory and alternate scales of measuring service quality, its role in customer satisfaction and importance of servqual instrument.

Key Words: *Service Quality, Dimensions of service quality, Servqual, customer satisfaction.*

Introduction

Academic institutions offering higher education in general and those offering professional education in particular are undergoing a process of change similar to what business organizations have undergone a few decades ago when they were confronted by competition. The speed of change is driven by multiple factors. Demands from industry, information-age mind set of the students, increased competition and the renewed quest among academic community are some of the factors driving this change. To ensure that higher education, particularly professional education, is able to deal with market and technological changes coupled with global requirements, it is important for institutions offering higher education to use appropriate curricula, course materials and teaching methodologies that are not only up-to-date, but also effective from learner's point of view. The exponential growth of knowledge, exploding instructional technologies, enhanced access to practices of premier institutions, accessibility to knowledge, globalization of education etc require educators and faculty members to continuously evaluate themselves and improve upon their effectiveness

Vol. 2 No. 2 July - Dec 2013 ISSN : 2321 - 4643

MANAGERIAL HERALD

Bi- Annual Journal of Thoughts

SMCET

DEPARTMENT OF BUSINESS ADMINISTRATION
St.Michael College of Engg. & Tech
Kalayarkoil - 630 551
Sivagangai District
Email : mbasmcet2012@gmail.com

SHANLAX PUBLICATIONS

CONTENTS

RAPID CHANGE IN CONSUMER BUYING BEHAVIOUR - A BIG CHALLENGE FOR SUSTAINABLE GROWTH OF TODAY'S BUSINESS

*A. Abdul Brosekhan & *Dr. C. Muthu Velayutham

1. Introduction

All of us are consumers. We consume things daily and buy these products according to our needs, preferences and purchasing power. These can be consumable goods, durable goods, specialty goods or, industrial goods. What we buy, how we buy, where and when we buy, in how much quantity we buy depends on our perception, self concept, social and cultural background and our age and family cycle, our attitudes, beliefs values, motivation, personality, social class and many other factors that are both internal and external to us. While buying, we also consider whether to buy or not to buy and, from which source or seller to buy. The marketer therefore tries to understand the needs of different consumers and having understood his different behaviors which require an in-depth study of their internal and external environment, they formulate their plans for marketing.

The article discusses the factors influencing pro-environmental consumer behaviors and the policy implications of knowledge about these influences. It presents a conceptual framework that emphasizes the determining roles of both personal and contextual factors and especially of their interactions. The practical usefulness of the framework is illustrated by evidence of the interactive effects of information and material incentives - typical interventions in the personal and contextual domains, respectively.

Objectives of the Study

The main objectives of the study are:

1. To discuss the various factors responsible for consumer buying behavior.
2. To discuss the various methods of measuring consumer behavior.
3. To discuss the rapid changes in customer taste and preferences.
4. To study the impact of changing consumer behavior on sustainable growth of business.

Factors Responsible for Consumer Buying Behavior

Consumer behavior refers to the selection, purchase and consumption of goods and services for the satisfaction of their wants. Initially the consumer tries to find what commodities he would like to consume, then he selects only those commodities that promise greater utility. After selecting the commodities, the consumer makes an estimate of the available money which he can spend. Lastly, the consumer analyzes the prevailing prices of commodities and takes the decision about the commodities he should consume. Meanwhile, there are various other factors influencing the purchases of consumer such as social, cultural, personal and psychological.

Shanlax
International Journal of
Arts, Science & Humanities

A Quarterly Journal

VOL. 1 SPECIAL ISSUE NO. 1 JULY 2013 ISSN : 2321-788X

CONTENTS

Edited by:
Dr.S.Balakrishnan

Vol. 1 Special Issue 1 December 2013 ISSN: 2321 – 788X

LAWPRENEURSHIP AND OPPORTUNITIES

Dr. N. Shankar

M. Subburajan
Research Scholar of Madurai Kamaraj University, Madurai

Abstract

Entrepreneurship is visualized as the process of setting up an enterprises and operating it optimally by seeking economic opportunities and exploiting resources in a coordinated, systematic, innovative and risk bearing manner to achieve the goals. In a broad perspective of entrepreneurial development is an overall development of developing entrepreneurial capabilities, characteristics and potential in individuals having the apparent or latent need for achievement enabling them to tap resources in and around.

India is now a hub for Professional education. Several institutions have been set up and all under the control of concerned affiliation body and universities. Education especially higher education is the most important resource to improve the human resources of any country. It has multiple effects in the development of a society. Among higher education, the professional course is giving unique opportunity to youths. In a broad sense the term Professional course is considered as a course which helps a person becomes a professional immediately after the successful completion of the course. But the basic prerequisite requires be good interaction between educational institution and industry. The entrepreneurship among the professional course students is a dynamic process of vision, change and creation.

The professional courses includes Engineering, Medical, Law, Agriculture, Law, Management education, catering, Tourism and the like. These professional graduates have viable opportunity to transform themselves as entrepreneurs. The engineering entrepreneurs shall become technopreneurs, the agriculture graduates as agropreneurs, the law graduates as nd the like. Though the rse youths are well of talents, their potentiality are not properly utilized and they are kept isolated from the main stream of economy of the nation. So the calamity of the problem of unemployment could be wiped out thoroughly only if there is linkage between the channel of economy and professional youths.

Key Word:

Lawpreneurship,technopreneur, agropreneur, Entrepreneur, Legal

Introduction

Behavior or conduct is the outcome of what one thinks and assumes. Entrepreneurial behavior is the study of human behavior in identifying and exploiting opportunities through creating and developing new ventures. Entrepreneurs react to the environment and it reveals their behavior towards the society. The sociological environment, economic development, government policies help the entrepreneur to acquire specific characteristic feature in developing an entrepreneurial outlook. The major goals of entrepreneurial behavioral research are to explain, predict and control behavior at the individual and team level.

The assumption of Ajzen's theory of planned behavior is that much human behavior is planned and it is preceded by intention towards behavior. Human beings are rational and make systematic use of information available when taking decisions. Intention predicts planned behavior. The theory of planned behavior (TPB) explains on how intention predicts actual behavior.

Lawpreneurhip

Lawpreneurs are law graduates involving in entrepreneurship. There are so many opportunities for law graduates. In India only few law schools train the

Vol. 1 Special Issue 1 December 2013 ISSN: 2321 – 788X

WOMEN AS CONSUMERS AND DECISION MAKER – A CONCEPTUAL FRAMEWORK

A. Abdul Brosekhan
Assistant Professor, Department of Management Studies, Mohamed Sathak Engineering College, Kilakarai, Ramanathapuram - 623 806.

Dr. C. Muthu Velayutham
Associate Professor, Director DODE, Anna University Coimbatore, Coimbatore - 641 047.

Ms. S. Santhana Jeyalakshmi
Assistant Professor, Department of Management Studies, Mohamed Sathak Engineering College, Kilakarai, Ramanathapuram - 623 806.

Abstract

Understanding the buying behaviour of the target market is the essential task of marketing managers in marketing concept. The term consumer behaviour refers to the behaviour that consumers display in searching for, purchasing, using evaluating and disposing of products and services that they expect will satisfy their needs. Consumer behaviour is the most complex aspect of marketing, as it is the most dynamic of all the marketing activities. The consumer preference change rapidly and are affected by multiplicity of factors at a given point of time which are difficult to analyse. To understand the consumer behaviour into consumer motivations, believes, attitudes, learnings, perceptions, emotions and opinion are essential.

Knowledge about buyer behaviour is necessary for the development of effective marketing strategies. The members of a family influence the decision-making process in the purchase of different products, therefore the real target for the marketer is not an individual member but the family as a whole. While there have been several studies on family dynamics in decision-making, very few pertain particularly to the Indian context, where the traditional family is different from its Western counterpart in ge of the family life . A large number of e three generations keter has to compete nds in his product different product categories. This becomes even more significant when the family is considered a unit where the needs of several members have to be met from the limited funds. It is then important for the marketer to understand the intra-family dynamics and inter-personal relationships at play in the purchase of a consumer durable product in order to decide the optimal marketing-mix.

Keywords:

Women Consumer Buying Behavior, Factors Influences, Marketing Strategies

Introduction

Over the years, Indian economy is undergoing through certain changes. Competition has ushered in an altogether new marketing environment in the country. Marketing has become a necessity for survival of business firms. Price, competitiveness, quality assurance and customer service has become vital components of marketing and most business firms are realizing that if they do not have competitive strength, they cannot survive. A business can not succeed by supplying products and services that are not properly designed to serve the needs of the customers. The entire business has to be seen from the point of view of the customer. A company's business therefore, depends on its ability to create and retain its customers. Thus, a company, which wants to enhance it's market share has to think of customers and act customer. Understanding consumer decision making is vital for companies in

CONTENTS

Shanlax
International Journal of
Arts, Science & Humanities

A Quarterly Journal

VOL. 1 SPECIAL ISSUE NO. 1 JULY 2013 ISSN : 2321-788X

CONTENTS

Edited by:
Dr.S.Balakrishnan

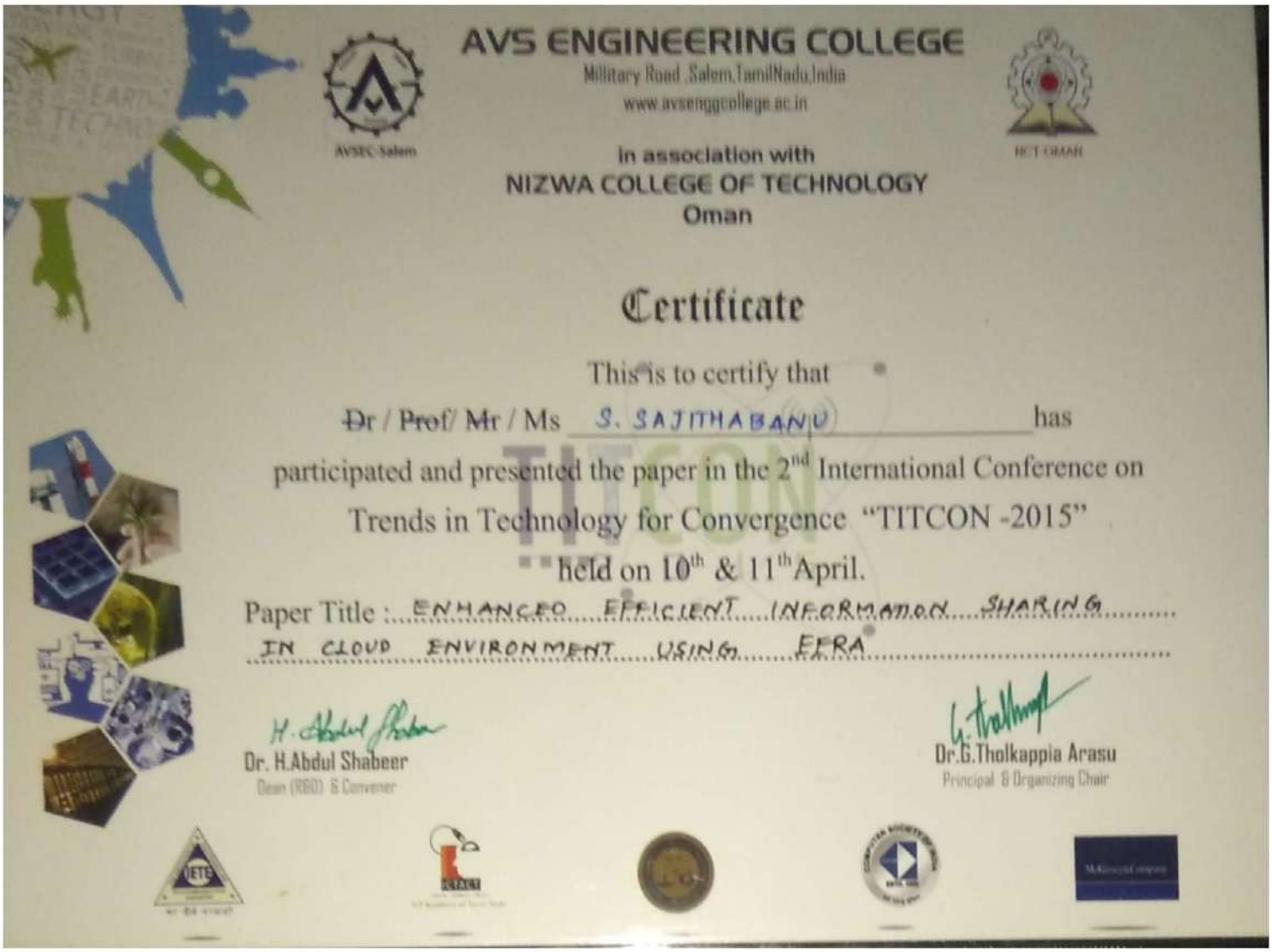

AVS ENGINEERING COLLEGE

Military Road ,Salem,TamilNadu,India

www.avsenggcollege.ac.in

AVSEC-Salem

in association with

NIZWA COLLEGE OF TECHNOLOGY

Oman

NCT-OMAN

Certificate

This is to certify that

~~Dr / Prof/ Mr~~ / Ms S. SAJITHABANU has

participated and presented the paper in the 2nd International Conference on Trends in Technology for Convergence "TITCON -2015"

held on 10th & 11th April.

Paper Title : ENHANCED EFFICIENT INFORMATION SHARING IN CLOUD ENVIRONMENT USING EFRA

Dr. H.Abdul Shabeer

Dean (R&D) & Convener

Dr.G.Tholkappia Arasu

Principal & Organizing Chair

TRUE COPY ATTESTED

PRINCIPAL

MOHAMED SATHAK ENGINEERING COLLEGE

KILAKARAI-623806.

INTERNATIONAL JOURNAL FOR ADVANCE RESEARCH IN ENGINEERING AND TECHNOLOGY

WINGS TO YOUR THOUGHTS…..

MOBILE COMMERCE EXPLORER FOR PERSONAL MOBILE COMMERCE PATTERN MINING AND PREDICTION

Sabari Ramachandran.M[1], B.Rasina Begum[2], Balasubramanian N,[3] Deeba.B[4]

[1]M.E/ CSE Mohamed Sathak Engg. College,
Kilakarai.
sabari_msec@rediffmail.com,sabari_msec@yahoo.co.in
[2] Assistant Professor in Dept. of CSE ,
Mohamed Sathak Engg. College,
Kilakarai.
rasinayousuf@gmail.com
[3] Associate professor in Dept. of MCA,
Mohamed Sathak Engg. Colleg,
Kilakarai.
mugavaibala@gmail.com
[4]Assistant professor in Dept. of MCA,
Mohamed Sathak Engg. Colleg,
Kilakarai.
deebasaravanan@yahoo.in

Abstract *: Mobile Commerce, also known as M-Commerce is the ability to conduct commerce using a mobile device. Research is done by Mining and Prediction of Mobile Users' Commerce Behaviors such as their movements and purchase transactions. The problem of PMCP-Mine algorithm has been overcome by the Collaborative Filtering Algorithm. The main objective is to analyses the Mobile users' movements to the new locations instead of considering only the frequent moving locations. In the existing approach, a Mobile Commerce Explorer Framework has been implemented to make recommendations for stores and items by analyzing the Mobile users'. The drawbacks are the recommendations that made are only for frequently moving locations and stores. The proposed work is to recommend stores and items in new locations by considering the rating of items given by the other users in new locations.*

Keywords– *Mining, Prediction, Mobile Commerce.*

1. INTRODUCTION

With the rapid advance of wireless communication technology and the increasing popularity of powerful portable devices, mobile users not only can access worldwide information from anywhere at any time but also use their mobile devices to make business transactions easily, e.g., via digital wallet [1]. Meanwhile, the availability of location acquisition technology, e.g., Global Positioning System (GPS), facilitates easy acquisition of a moving trajectory, which records a user movement history. At developing pattern mining [1] and prediction techniques [11] [12]that explore the correlation between the moving behaviors and purchasing transactions of mobile users l-Commerce features. Owing to of the web 2.0 technology, le their store information, e.g., on and travel sequence, And features available online .Collecting and analyzing user trajectories with store location information, a users' moving sequence among stores in some shop areas can be Extracted.

The mobile transaction sequence generated by the user is{(A,{i1}), (B,Ø), (C,{i3}), (D,{i2}), (E,Ø), (F,{i3,i4}), (I,Ø), (K,{i5}.

There is an entangling relation between moving patterns and purchase patterns since mobile users are moving between stores to shop for desired items. The moving and purchase patterns of a user can be captured together as mobile commerce patterns for mobile users. To provide this mobile ad hoc advertisement, mining mobile commerce patterns of users and accurately predicts their potential mobile commerce behaviors obviously are essential Operations that require more research. To capture and obtain a better understanding of mobile users' mobile

INTERNATIONAL JOURNAL FOR ADVANCE RESEARCH IN ENGINEERING AND TECHNOLOGY

WINGS TO YOUR THOUGHTS.....

commerce behaviors, data mining has been widely used for discovering valuable information from complex data sets. They do not reflect the personal behaviors of individual users to support M-Commerce services at a personalized level. Mobile Commerce or M-Commerce is about the explosion of applications and services that are becoming accessible from Internet-enabled mobile devices. It involves new technologies, services and business models. It is quite different from traditional ecommerce. Mobile phones impose very different constraints than desktop computers

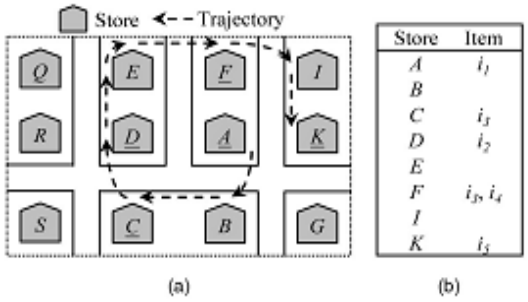

Store	Item
A	i_1
B	
C	i_3
D	i_2
E	
F	i_3, i_4
I	
K	i_3

Figure 1.1: Mobile Transaction Sequence

Figure 1.1(a) shows the transaction sequence for the stores and Figure 1.1(b) shows the mobile transaction sequence for the stores A to K with the items i1, i2, i3, i4.

2. PROBLEM DEFINITION

In the MCE framework, frequently moving locations and frequently purchased items [10] are considered for analyzing mobile users' commerce behavior. The Personal Mobile Commerce Pattern-Mine (PMCP-Mine) algorithm was used to find only frequent datasets, by deleting in-frequent data in the Mobile Commerce Explorer Database. Also, recommendations were done only for the frequent datasets. The similarity values that were found in the Similarity Inference Model (SIM) were not accurate.

Box" approaches. To close the semantic gap, it applies a technique called 'guest view casting' and non-intrusively reconstructs the high level internal VM semantic views from outside. However, it VM watch only focuses on the malware detection in VMs and cannot monitor or detect the security status in the virtual network.

3. LITERATURE SURVEY

. Tseng developed the Mobile Framework for mining and obile users' movements and al and Swami presented an efficient algorithm [2] that generates all significant association rules [2] [9] between items in the database.

Han, Pei and Yin proposed a novel frequent-pattern tree (FP-tree) structure, which is an extended prefix-tree [3] structure for storing compressed, crucial information about frequent patterns [3], and develop an efficient FP-tree, based mining method, FP-growth, for mining the complete set of frequent patterns by pattern fragment growth.

Herlocker, Konstan, Brochers and Riedl developed an Automated Collaborative Filtering[8] is quickly becoming a popular technique for reducing information overload, often as a technique to complement content-based information filtering systems [8]. In this paper, present an algorithmic framework for performing Collaborative Filtering [8]and new algorithmic elements that increase the accuracy of Collaborative Prediction algorithms[11] [12]. Then present a set of recommendations on selection of the right Collaborative Filtering [8] algorithmic components.

4. EXISTING SYSTEM

A novel framework for the mobile users' commerce behaviors has been implemented for mining and prediction [5] of mobile users'. MCE framework has been implemented with three components: 1) Similarity Inference Model (SIM) for measuring the similarities among stores and items, 2) Personal Mobile Commerce Pattern Mine (PMCP-Mine) algorithm for efficient discovery of mobile users' Personal Mobile Commerce Patterns (PMCPs), 3) Mobile Commerce Behavior Predictor (MCBP) for prediction of possible mobile user behaviors [4]. In the MCE framework, only frequently moved locations and frequently purchased items [10] are considered. The modules proposed in framework are:

A. Mobile Network Database

The mobile network database maintains detailed store information which includes locations.

B. Mobile User Data Base

The Mobile User database maintains detailed mobile user information which include network provider.

C. Applying Data Mining Mechanism

System has an "offline" mechanism for Similarity inference and PMCPs mining, and an "online" engine for mobile commerce behavior prediction. When mobile users move between the stores, the mobile information which includes user identification, stores, and item purchased are stored in the mobile transaction database. In the offline data mining mechanism, develop the SIM model and the PMCP Mine algorithm to discover the store/item similarities and the PMCPs, respectively. Similarity Inference Model for measuring the

INTERNATIONAL JOURNAL FOR ADVANCE RESEARCH IN ENGINEERING AND TECHNOLOGY

WINGS TO YOUR THOUGHTS.....

similarities among stores and items. Personal Mobile Commerce Pattern-Mine (PMCP-Mine) algorithm is used for efficient discovery of mobile users' Personal Mobile Commerce Patterns.

D. Behavior prediction engine

In the online prediction engine, implemented a MCBP (Mobile Commerce Behavior Predictor) based on the store and item similarities as well as the mined PMCPs. When a mobile user moves and purchases items among the stores, the next steps will be predicted according to the mobile user's identification and recent mobile transactions. The framework is to support the prediction of next movement and transaction. Mobile Commerce Behavior Predictor for prediction of possible mobile user behaviors.

E. Similarity Inference Model

A parameter-less data mining model, named Similarity Inference Model, to tackle this task of computing store and item similarities. Before computing the SIM, derive two databases, namely, SID and ISD, from the mobile transaction database. An entry SIDpq in database SID represents that a user has purchased item q in store p, while an entry ISDxy in database ISD represents that a user has purchased item x in store y. Deriving the SIM to capture the similarity score between stores/items. For every pair of stores or items, SIM assigns them a similarity score. In SIM, used two different inference heuristics for the similarity of stores and items because some stores, such as supermarkets, may provide various types of items.

By applying the same similarity clustering [6] inference heuristics to both of stores and items, various types of items may be seen as similar since different supermarkets are seen as similar. Based on our heuristics, if two stores provide many similar items, the stores are likely to be similar; if two items are sold by many dissimilar stores, the stores are unlikely to be similar. Since the store similarity and item similarity are interdependent, computing those values iteratively. For the store similarity, consider that two stores are more similar if their provided items are more similar. Given two stores sp and sq, compute their similarity SIM (sp; sq) by calculating the average similarity of item sets provided by sp and sq. For every item sold in sp (and, respectively, sq), first find the most similar item sold in sq (and, Respectively, sp). Then, the store similarity can be obtained by averaging all similar item pairs. Therefore, SIM (sp; sq) is defined as

$$sim(s_p, s_q) = \frac{\sum_{\varphi \in \Gamma_{s_p}} MaxSim(\varphi, \Gamma_{s_q}) + \sum_{\gamma \in \Gamma_{s_q}} MaxSim(\gamma, \Gamma_{s_p})}{|\Gamma_{s_p}| + |\Gamma_{s_q}|},$$

Equation No: 4.1

where $MaxSim(e, E) = Max_{e' \in E} sim(e, e')$ represents maximal similarity between e and the element in E. Γ_{sp} and Γ_{sq} are the sets of items sold in sp and sq, respectively. On the other hand, for the item

similarity, consider that two items are less similar if the items are sold by many dissimilar stores. Given two items i_x and i_y, compute the similarity $sim(i_x,i_y)$ by calculating the average dissimilarity of store sets that provide i_x and i_y. For every store providing i_x (and, respectively, i_y), first find similarity by averaging all dissimilar store pairs.

F. Personal Mobile Commerce Pattern-Mine Algorithm

The PMCP-Mine algorithm is divided into three main phases: 1) Frequent-Transaction Mining: A Frequent-Transaction is a pair of store and items indicating frequently made purchasing transactions. In this phase, first discover all Frequent-Transactions for each user. 2) Mobile Transaction Database Transformation: Based on the all Frequent-Transactions, the original mobile transaction database can be reduced by deleting infrequent items. The main purpose is to increase the database scan efficiency for pattern support counting. 3) PMCP Mining: This phase is mining all sequential patterns [7] of length k from patterns of length k-1 in a bottom-up fashion.

G. Mobile Commerce Behavior Predictor

MCBP measures the similarity score of every PMCP with a user's recent mobile commerce behavior by taking store and item similarities into account. In MCBP, three ideas are considered: 1) the premises of PMCPs with high similarity to the user's recent mobile commerce behavior are considered as prediction knowledge; 2) more recent mobile commerce behaviors potentially have a greater effect on next mobile commerce behavior predictions and 3) PMCPs with higher support provide greater confidence for predicting users' next mobile commerce behavior. Based on the above ideas, propose a weighted scoring function to evaluate the scores of PMCPs. For all PMCPs, calculate their pattern score by the weighted scoring function. The consequence of PMCP with the highest score is used to predict the next mobile commerce behavior.

H. Performance Comparison

Conduct a series of experiments to evaluate the performance of the proposed framework MCE and its three components, i.e., SIM, PMCP-Mine, and MCBP under various system conditions. The experimental results show that the framework MCE achieves a very high precision in mobile commerce behavior predictions. Besides, the prediction [10] technique MCBP in our MCE framework integrates the mined PMCPs and the similarity information from SIM to achieve superior performs in terms of precision, recall, and F-measure. The experimental results show that the

INTERNATIONAL JOURNAL FOR ADVANCE RESEARCH IN ENGINEERING AND TECHNOLOGY

WINGS TO YOUR THOUGHTS.....

proposed framework and three components are highly accurate under various conditions.

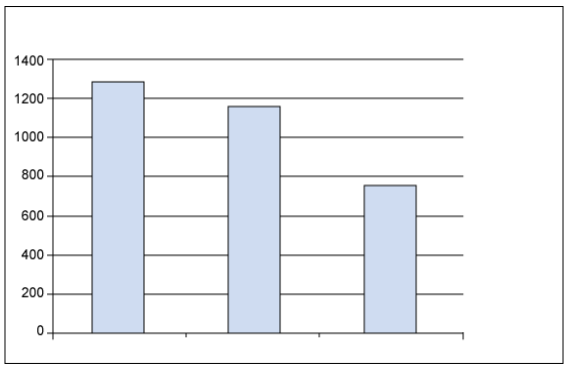

Figure 2: Performance Comparison

Figure 2 describe the performance comparison depends upon the various attributes that are handled between the stores.

5. PROPOSED SYSTEM

5.1 Similarity Inference Model

Propose a parameter-less data mining model, named Similarity Inference Model, to tackle this task of computing store and item similarities. Before computing the SIM, derive two databases, namely, SID and ISD, from the mobile transaction database. An entry SIDpq in database SID represents that a user has purchased item q in store p, while an entry ISDxy in database ISD represents that a user has purchased item x in store y. Deriving the SIM to capture the similarity score between stores/items. For every pair of stores or items, SIM assigns them a similarity score. In SIM, used two different inference heuristics for the similarity of stores and items because some stores, such as supermarkets, may provide various types By applying the same similarity inference heuristics to both of stores and items, various types of items may be seen as similar since different supermarkets are seen as similar. Based on our heuristics, if two stores provide many similar items, the stores are likely to be similar; if two items are sold by many dissimilar stores, the stores are unlikely to be similar. Since the store similarity and item similarity are interdependent, computing those values iteratively. For the store similarity, consider that two stores are more similar if their provided items are more similar. Given two stores sp and sq, compute their similarity SIM (sp; sq) by calculating the average similarity of item sets provided by sp and sq. For every item sold in sp (and respectively sq), first find the most similar item [illegible]pectively, sp). Then, the store [illegible]ed by averaging all similar item

5.2. Collaborative Personal Mobile Commerce Pattern Algorithm

The proposed system is developed by implementing CPCMP - Collaborative PCMP Algorithm which takes into account the newly updated locations and predicts behavior[4],[5][11] [12] of the user based on the Collaborative Filtering[8]. Although collaborative filtering [8] methods have been extensively studied recently, most of these methods require the user-item rating matrix. However, on MCE Database, in most of the cases, other user preferences and transactions are not always available. Hence, collaborative filtering [8] algorithms cannot be directly applied to most of the recommendation tasks on the database, like query suggestion etc.

Combine the Collaborative filtering [8]aspects of predicting the unknown entities along with the proposed PCMP which mining the sequential patterns[7] of the user transactions behavior. This hybrid algorithm facilitates dynamic predictions and hence recommendation to the users for better customer service and experience. For better similarity inference modeling in cases of users visiting unknown locations, a new hybrid similarity inference model is proposed to take into account the items transacted and stores visited by a similar user in the same location who have similar Personal mobile commerce pattern – i.e the frequent mining patterns of the unknown user matches with respect to the user under consideration. So, the proposed work improves the quality of predictions of the preferred items and stores of the customer or user thereby bring about better sales and customer support experience and feedback.

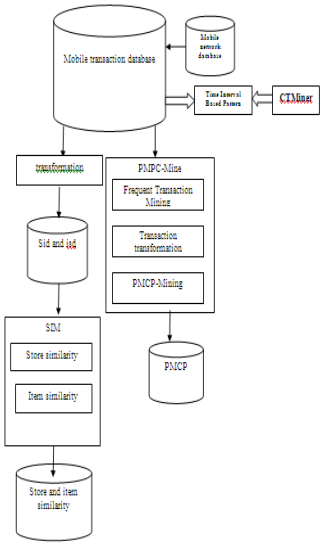

Figure 3: Proposed System architecture

INTERNATIONAL JOURNAL FOR ADVANCE RESEARCH IN ENGINEERING AND TECHNOLOGY

WINGS TO YOUR THOUGHTS.....

Figure no: 3 represents the proposed System architecture for Mobile commerce Prediction and mining with additional future CTMiner to predict the time interval between the customers buying behavior

5.3. Mobile Commerce Behavior Predictor

Propose MCBP, which measures the similarity score of every PMCP with a user's recent mobile commerce behavior by taking store and item similarities into account. In MCBP, three ideas are considered: 1) the premises of PMCPs with high similarity to the user's recent mobile commerce behavior are considered as prediction knowledge; 2) more recent mobile commerce behaviors potentially have a greater effect on next mobile commerce behavior predictions and 3) PMCPs with higher support provide greater confidence for predicting users' next mobile commerce behavior. Based on the above ideas, propose a weighted scoring function to evaluate the scores of PMCPs.

6. CONCLUSION

A novel framework namely MCE was proposed for mining and prediction of mobile users' movements and transactions in mobile commerce environments. In the MCE framework were designed with three major techniques: 1) SIM for measuring the similarities among stores and items; 2) PMCP-Mine algorithm for efficiently discovering mobile users' PMCPs; and 3) MCBP for predicting possible mobile user behaviors. To best knowledge, it is the first work that facilitates mining and prediction [5] of personal mobile commerce behaviors that may recommend stores and items previously unknown to a user. To evaluate the performance of the proposed framework and three proposed techniques, conducted a series of experiments.

The experimental results show that the framework MCE achieves a very high precision in mobile commerce behavior predictions. Besides, the prediction technique MCBP in MCE framework integrates the mined PMCPs and the similarity information from SIM to achieve superior performs in terms of precision, recall, and F-measure. The experimental results show that the proposed framework and three components are highly accurate under various conditions.

To overcome the problems of user moving to new locality, Collaborative Filtering [8] algorithm was implemented to recommend the users about the stores and items instead of considering only frequent data.

NHANCEMENT

e plan to explore more efficient rn mining [1]Identify the hidden process.

Algorithm, design more efficient similarity inference models, and develop profound prediction strategies to further enhance the MCE framework.

In addition, we plan to apply the MCE framework to other applications, such as object tracking sensor networks and location based services, aiming to achieve high precision in predicting object behaviors.

REFERENCES

[1] **Eric Hsueh-Chan Lu, Wang-Chien Lee, and Vincent S. Tseng, "A Framework for Personal Mobile Commerce Pattern Mining and Prediction" IEEE transactions on knowledge and data engineering year 2012.**

[2] **R. Agrawal, T. Imielinski, and A. Swami, "Mining Association Rule between Sets of Items in Large Databases," Proc. ACM SIGMOD Conf. Management of Data, pp. 207–216, May 1993.**

[3] **J. Han, J. Pei and Y. Yin, "Mining Frequent Patterns without Candidate Generation," Proc. ACM SIGMOD Conf. Management of Data, pp. 1-12, May 2000.**

[4] **S.C. Lee, J. Paik, J. Ok, I. Song, and U.M. Kim, "Efficient Mining of User Behaviors by Temporal Mobile Access Patterns," Int'l J. Computer Science Security, vol. 7, no. 2, pp. 285-291, Feb. 2007.**

[5] **V.S. Tseng and K.W. Lin, "Efficient Mining and Prediction of User Behavior Patterns in Mobile Web Systems", Information and Software Technology, vol. 48, no. 6, pp. 357-369, June 2006.**

[6] **X. Yin, J. Han, P.S. Yu, "LinkClus: Efficient Clustering via Heterogeneous Semantic Links," Proc. Int'l Conf. Very Large Data Bases, pp. 427-438, Aug. 2006.**

[7] **C.H. Yun and M.S. Chen, "Mining Mobile Sequential Patterns in a Mobile Commerce Environment," IEEE Trans. Systems, Man, and Cybernetics, Part C, vol. 37, no. 2, pp. 278-295, Mar. 2007.**

[8] **J.L. Herlocker, J.A. Konstan, A. Brochers, and J. Riedl, "An Algorithm Framework for Performing Collaborative Filtering," Proc. Int'l ACM SIGIR Conf. Research and Development in Information Retrieval, pp. 230-237, Aug 1999.**

[9] **J. Han and Y. Fu, "Discovery of Multiple-Level Association Rules in Large Database," Proc. Int'l Conf. Very Large Data Bases, pp. 420-431, Sept. 1995.**

INTERNATIONAL JOURNAL FOR ADVANCE RESEARCH IN ENGINEERING AND TECHNOLOGY

WINGS TO YOUR THOUGHTS…..

[10] Y. Zheng, L. Zhang, X. Xie, and W.Y. Ma, "Mining Interesting Location and Travel Sequences from GPS Trajectories," Proc. Int'l World Wide Web Conf., pp. 791-800, Apr. 2009.

[11] Y. Tao, C. Faloutsos, D. Papadias, and B. Liu, "Prediction and Indexing of Moving Objects with Unknown Motion Patterns," Patterns in Mobile Web Systems", Information and Software Technology, vol. 48, no. 6, pp. 357-369, June 2006.

[12] Y. Tao, C. Faloutsos, D. Papadias, and B. Liu, "Prediction and Indexing of Moving Objects with Unknown Motion Patterns,"

ABOUT THE AUTHOR:

MR. M.Sabari Ramachandran pursuing M.E (CSE) in Mohamed Sathak. Engineering College. He has received MCA from Mohamed Sathak Engineering College. His area of interest includes Data mining, Mobile Computing and Network Security.

中國機械工程學刊第二十八卷第六期第 450~ 469 頁(民國九十六年)
Journal of the Chinese Society of Mechanical Engineers, Vol.39, No.5, pp.450 ~ 469 (2018)

NUMERICAL AND EXPERIMENTAL INVESTIGATION OF LATENT HEAT THERMAL ENERGY STORAGE SYSTEM USING ERYTHRITOL AS A PCM

[1]V. Mayilvelnathan, [2]A. Valan arasu

[1] Department of Mechanical Engineering, Mohamed Sathak Engineering College, Kilakarai – 623 806, Tamil Nadu, India.

[2] Department of Mechanical Engineering, Thiagarajar College of Engineering, Madurai-623015, Tamil Nadu, India.

Keyword : PCM, Latent heat storage , Waste heat recovery , Analysis

ABSTRACT

Thermal energy storage improves the thermal efficiency and reduces the mismatch between the energy supply and energy demand of industrial and solar energy applications. From the different types of thermal energy storage, a phase change material (PCM) thermal energy storage exhibits greater efficiency due to its high storage capacity and constant thermal energy. In this work, the experimental and numerical analysis has been designed to study thermal behavior and heat transfer characteristics of erythritol as PCM during the charging and discharging processes in a shell and tube heat exchanger. The experiments are conducted to investigate the effects of mass flow rates of the heat transfer fluid (HTF) on the melting and solidification processes at constant inlet temperature. The numerical calculations are based on finite-volume mathematical modeling procedure that incorporates a single-domain enthalpy formulation for simulation of the phase change concept. The molten front at various times of process with temperature has been analyzed using numerical simulation. The experimental results show that by increasing the mass flow rate of heat transfer fluid from 30 kg/hr to 90 kg/hr, the experimental efficiency in charging and discharging processes rises from 21.22% to 35.45 % and numerical from 23.01% to 34.59% respectively.

1. INTRODUCTION :

The major challenges in the near future will be to find renewable resources to replace of conventional because of fast depletion of conventional energy, and to meet environmental

pollution concerning CO2 emission reduction. Solar thermal power plants are one of the most promising solution providers for electricity and creates pollution free environment, but a thermal energy storage system is necessary to match the variable supply of solar energy throughout the day. The implementation of proper thermal energy storage is one of the most important solutions for effective utilization renewable energy conversion systems. The latent heat thermal energy storage in phase change materials is accepted as one of the effective methods for solar power plants and industrial waste-heat recovery. The main advantage of the latent heat thermal energy storage systems seems to be the ability of storing a large amount of energy in small volumes at an isothermal condition. Normally the PCM thermal energy storage having melting and solidification processes. Atul Sharma et al. [1] summarizes the investigation of the solar water heating system incorporating with Phase Change Materials. This paper is focused on the past and current research of energy storage through PCMs for solar water heating systems. The paper will also help to find the suitable PCM and provide the various designs for solar water heating systems to store the solar thermal energy. Abhay et al. [2] experimentally investigated on the thermal energy storage using

olications and it stores 5-14

r unit volume than sensible storage materials such as water, masonry or rock. Lavinia Gabrela et al. [3] discussed about the thermal energy storage systems provide several alternatives for efficient energy use and conservation. Ujjwala Sharma et al. [4] discussed about to improve the performance of the parabolic solar collector with a phase change material having a higher heat capacity and melting point can be used. Bruno Cardenas et al. [5] deal with a high density, small volume changes between solid and liquid phases and low vapor pressure at the operating temperature. Anica Trp et al. [6] investigated about transient heat transfer phenomenon during charging and discharging of shell and tube latent thermal energy storage system has been analyzed based on the enthalpy formulation. Mehmet Esen et al. [7] said about the performance cylindrical latent heat storage tank with the two different models are observed, the first is suited to tanks where the phase change material (PCM) is packed in and the HTF flows parallel to it. The second is suited PCM in tube and HTF are embedded in the tank with an enthalpy based method. The value of for second mode is much shorter than that of first one. This is because the thicker the PCM mass, the longer the melting time of the PCM mass. Conti et al. [8] discussed about the thermodynamics of heat storage in a PCM shell and tube heat exchanger and the high variation behavior of the heat source with parallel scheme having maximum thermodynamic efficiency.

Robynne Murray et al. [9] provided the numerical and experimental studies on phase change and thermal behavior of the selected PCM. Anish et al [10] investigates the effects of various design and operating factors on the optimal controls of using the cold storage system to minimize the operating cost while maintaining adequate occupant comfort conditions. Mohammed Farid et al. [11] investigated previous work on latent heat storage and provide an insight to recent efforts to develop new classes of phase change materials for use in energy storage. Belen Zalba et al. [12] reviewed on thermal energy storage with solid-liquid phase change is carried and focuses on the organic and inorganic materials. M. Medrano et al. [13] analyzed the melting and solidification of PCM were experimentally using five different heat exchangers as heat storage systems. Jinjia WEI et al. [14] analyzed the thermal energy storage system employing PCM for rapid heat discharge was studied numerically and experimentally with four different capsules. Prabhu et al. [15] describes the high storage density of salt hydrate materials is difficult to maintain and usually decreases with cycling. Mithat Akgun et al. [16] in this study LHTESS of shell and tube type is analyzed experimentally with effects of the Reynolds number and the Stefan number on the

ification behaviors. Zhenyu

numerical model is used to predict the phase change material melting process in porous media and the inlet conditions of HTF on the thermal characteristics. Jegadheeswaran et al. [18] deals with numerical study with investigate Exergy based performance evaluation of the shell and tube configuration due to the dispersion of high conductivity particles in the PCM during charging processes. Andreozzi et al. [19] deals with Increasing the porosity value means steady state conditions are reached at lower time both in charging and discharging phases. Mehmet Esan et al. [20] studied the cylindrical phase change storage in solar powered heat pump system is investigate experimentally and theoretically. Laing et al. [21] deals with a two phase heat transfer fluid require isothermal energy storage. R. Meenakshi Reddy et al. [22] explained the experimental investigation results of a combined sensible and latent heat TES system integrated with solar heat source is presented for different phase change materials by varying HTF flow rates. Petrone et al. [23] this study deals with numerical investigation of the melting process of a PCM enthalpy equation for both the solid and liquid state. Arthur et.al [24] deals with two major areas to enhance the heat transfer by surface area and forced convection concept .Francesco et al. [25] describes the application of computational fluid dynamics (CFD) to the design and characterization of several different discharging

scenarios characterized by variable Re and St Numbers. Abduljalil et al. [26] investigated the double pipe and shell and tube heat exchanger configurations have high efficiency. Mittal et al. [27] deals with fundamental knowledge on absorption systems used in waste heat energy or water heated through solar collectors. Valan Arasu et al. [28] deal with the latent heat energy storage systems during melting/freezing processes. From the previous work, there are some scopes for latent heat thermal energy storage system using erythritol as a PCM. So in this paper we conducted experimental and numerical studies on charging and discharging process with different mass flow rates at constant temperature conditions.

2. EXPERIMENTAL AND NUMERICAL APPROACHES

2.1 Experimental analysis

2.1.1 Analysis of thermo-physical properties of pcm:

In this study, commercial erythritol with melting point 118°C is used as a PCM. Erythritol is chemically stable, non-poisonous, less cost and non- corrosive over a long storage period which displays a long stable performance through the phase change cycles. The thermo physical properties pure erythritol are shows in table 1.Because of the high melting point of [illegible] used in adsorption chillers, [illegible]nd solar cookers. Fig 1 and Fig 2 shows the FESEM image (JEOL, JSM 6701F) and FTIR image (Shimadzu FTIR spectrometer) of Erythritol.

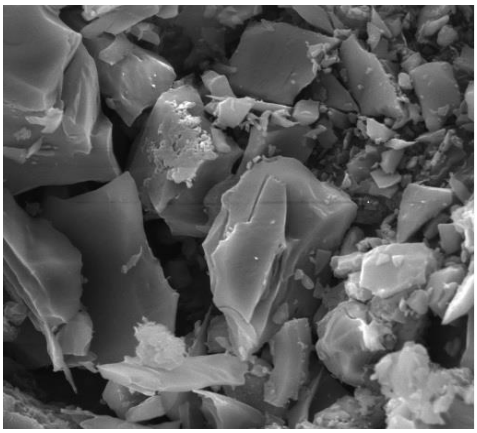

Figure 1. FESEM image of erythritol

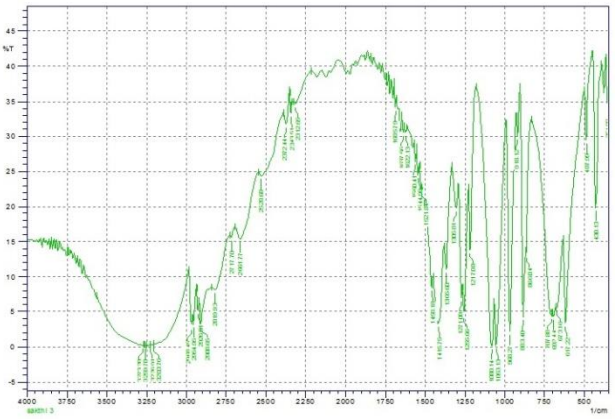

Figure 2 . FTIR image of erythritol

A differential scanning calorimeter (DSC 214, NETZSCH) was used to measure the melting enthalpy and heat capacity of erythritol. The heating rate was 5 C/min. Fig. 3 shows the heat capacity and melting enthalpy curve of erythritol. The melting point of erythritol is about 118.18° C, and its melting enthalpy is about 339.02 kJ/kg.

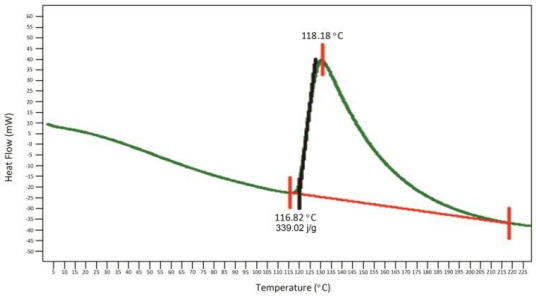

Figure 3 DSC image of pure erythritol for melting process

Table: 1 Thermophysical properties of Erythritol

Property	Value
Melting point	118.18 ^{o}C
Latent heat – L	339.02 kJ/kg
Density – ρ	1480 kg/m^3 (389K) – 1300 (413K)
Specific heat - C_p	1350 J/kg K (389K) – 2740 (413K)
Thermal conductivity – k	0.733 W/mK(389K) – 0.326 (413K)

2.1.2. Experimental setup and procedure:

In this work, a shell and tube LHTES unit is designed and fabricated in order to investigate the thermal storage capabilities of a energy storage system for olidification processes. Fig. 4 illustrates a picture and Fig. 5 a schematic diagram of the experimental set-up, which consists of a flow measurement system, the shell and tube heat exchanger section and the temperature measurement system. The shell and tube heat exchanger section is composed of a 350mm long horizontal cylinder with inner diameter of 270 mm and 2.5 mm thickness. Also a copper tube which is 1500 mm has been located in the cylinder filled with the liquid state PCM. This copper tube is the heat transfer tube which is used release or recovers heat from PCM. The external surface of the heat exchanger is well insulated by glass wool of 60 mm thickness in order to maintain the perfect insulation. Shell is filled with 8.5 kg of erythritol being used as latent heat storage media.The system is having two fluid flow loops; one is charging loop, which transfer the heat from the hot fluid to the PCM and a another one is discharging loop, which transfer the heat from the PCM to HTF. The data acquisition system is consisted of an array of 32 K-type thermocouples, a rota meter with a maximum measuring capacity of 20Lir/min, a data logger and a personal computer system to access and record the different temperature values and the mass flow rate of the HTF.

Figure 4. A picture of experimental setup

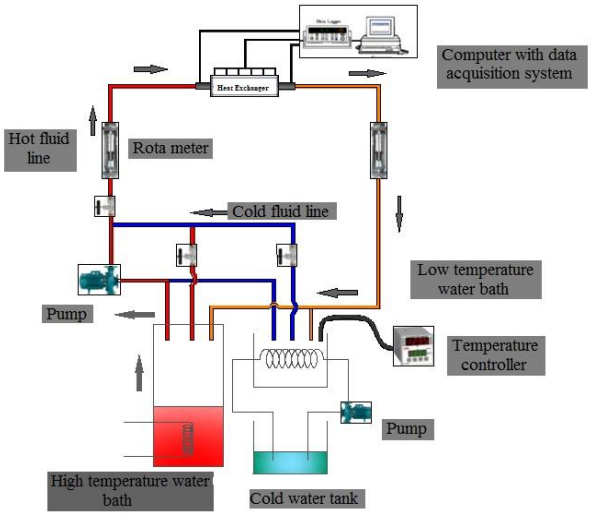

Figure 5. A schematic diagram for charging and discharging loops

The location of the thermocouples in the PCM along the axis, annotated by 1, 2, and 3 are indicated in Fig. 6, detailing the radial and angular distances of the individual thermocouples from the outer wall of the heat measure the temperature at the heat transfer fluid by using two thermocouples are also placed at the inlet and outlet positions of the HTF tube. Heater is also provided in the therminol tanks for the constant inlet HTF temperature during charging. The ambient temperature, flow rate of therminol coming out from the system, PCM temperatures at 3 axial locations were also measured simultaneously at a regular interval. The thermocouple placed at a depth of 41.75mm, 83.50mm and 125.25mm at a distance of 50mm, 150mm and 250mm. The experiment is repeated for different mass flow rates and result was tabulated.

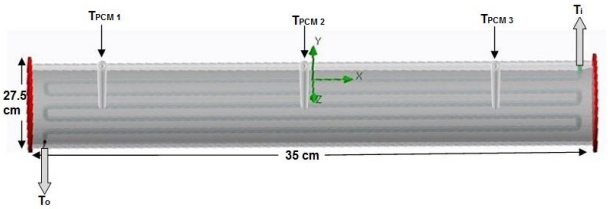

Figure 6. Shell and Tube heat exchanger with thermocouple locations

In charging process heat is absorbed by phase change material from high temperature working fluid. Here, Erythritol is used as PCM and therminol as a working fluid (HTF). When heat is absorbed by the erythritol it undergoes melting process, and melted. This process is called charging. The temperature of the therminol increases and then it remains nearly constant during which erythritol undergoes phase change. After that the HTF temperature increases. The charging process is terminated

when the PCM temperature in all the segments reaches above its melting temperature. The charging process was done for different flow rates like 30 kg/hr, 60 kg/hr and 90 kg/hr. are shows in fig.7 .The temperature readings from the thermocouples are noted and tabulated in the regular time interval.

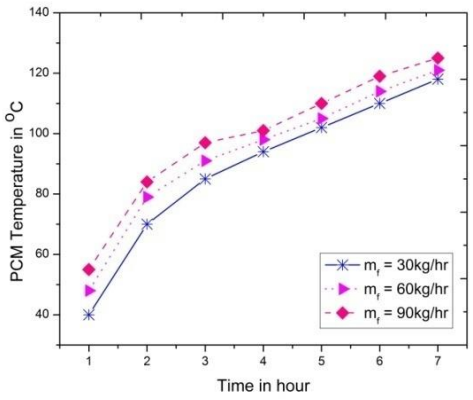

Figure 7 Temperature profile for melting process.

In discharging process the heat is released by the Phase Change Material. Therefore, PCM undergo from liquid state to solid state. When heat is released by the erythritol it undergoes freezing process and solidifies. The solidification of PCM depends upon the flow rate of working fluid, temperature difference between the inlet of working fluid ıre and specific heat capacity ıred latent heat energy in Erythritol was transferred to therminol (HTF). The change of phase from liquid to solid occurs at constant temperature. The discharging process was done for different flow rates like 30 kg/hr, 60 kg/hr and 90 kg/hr are shows in fig.8. The temperature readings from the thermocouples are noted and tabulated in the regular time interval.

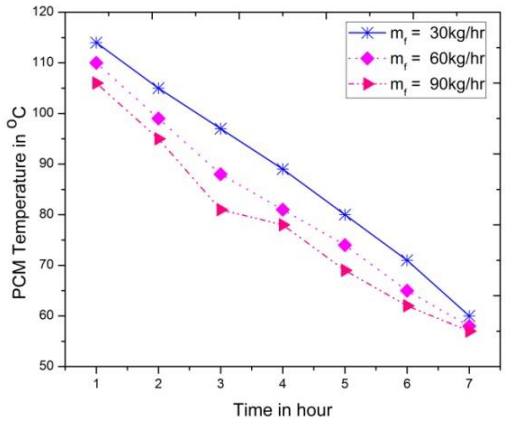

Figure 8 Temperature profile for solidification process

2.1.3. Performance calculations:

The charging efficiency of the process can be calculated as follows

Heat stored

$$Q_s = M_{HTF} * C_{P,HTF} * (T_i - T_o) * t$$

Heat available

$$Q_A = M_{HTF} * C_{p,HTF} * (T_i - T_{PCM}) * t$$

Charging Efficiency $\eta = \left({}^{Q_s}/_{Q_A}\right) * 100$

M_{HTF} is the mass flow rate, $c_{p,HTF}$ is the specific heat capacity, T_i and T_o are the inlet temperature and outlet temperatures of the heat transfer fluid respectively and T_{PCM} is average temperature of PCM. Q_S is heat supplied by the HTF. The t is time taken in seconds.

The discharging efficiency of the process can be calculated as follows

Heat Released

$$Q_R = M_{HTF} \times C_{p,HTF} \times (T_o - T_i) \times t$$

Heat available

$$Q_A = m_{PCM} \times C_{p,PCM} \times (T_{PCM} - T_i) + (m_{PCM} \times L_{PCM})$$

Charging Efficiency $\eta = \left({}^{Q_R}/_{Q_A}\right) * 100$

M_{HTF} is the mass flow rate, $c_{p,HTF}$ is the specific heat capacity, T_i and T_o are the inlet temperature and outlet temperatures of the heat transfer fluid respectively and T_{PCM} is average temperature of PCM. Q_R is the heat rejected by the PCM. The t is time taken in seconds.

The overall efficiency of the latent heat thermal

be calculated by

$$\dot{m}c_p (T_i - T_o)$$

$$q_{dis} = \dot{m}c_p (T_o - T_i)$$

$$Q_{ch\&dis} = \sum q_{ch\&dis}\, \Delta t$$

Where m is the mass flow rate, c_p is the specific heat capacity, T_i and T_o are the inlet temperature and outlet temperatures of the heat transfer fluid respectively. In a transient process, cumulative energy given or gained by HTF ($Q_{char,HTF}$ & $Q_{dischar,HTF}$) and PCM ($Q_{char,PCM}$ & $Q_{dischar,PCM}$) are not equal, because of heat is exchanged by the materials of the heat exchanger.

$$Q_{H.E,ch} = M_{exchanger}\, C_{p,exchanger}\, (T_f - T_i)$$

$$Q_{H.E,dis} = M_{exchanger}\, C_{p,exchanger}\, (T_i - T_f)$$

$M_{exchanger}$ is the mass of empty heat exchanger, $C_{p,\,exchanger}$ is the specific heat for heat exchanger and T_i and T_f are the PCM temperatures at the initial and the final of the process, respectively. The total energy charged and discharged with PCM can be calculated by the following equation:

$$Q_{PCM,ch\&\,dis} = Q_{ch\,\&\,dis} - Q_{H.E,ch\,\&\,dis}$$

In order to analyze the effects of flow rates on the thermal performance of the latent heat storage units, exchanger efficiency ($\eta_{exchanger}$,) and overall efficiency ($\eta_{overall}$) are mentioned as below:

$$\eta_{exchanger} = \frac{Q_{PCM,ch\,\&\,dis}}{Q_{max,ch\,\&\,dis}}$$

$$\eta_{overall} = \frac{Q_{PCM,dis}}{Q_{PCM,ch}}$$

The theoretical maximum amount of energy $Q_{max,ch}$ & $Q_{max,dis}$ during charging and discharging processes as the total energy supplied to or recovered from the PCM can be calculated as:

$$Q_{max,ch} = M_{PCM}\left[C_{p,PCM}\left(T_i - T_{solidus}\right) + L + C_{p,PCM}\left(T_f - T_{liquidus}\right)\right]$$

$$Q_{max,dis} = M_{PCM}\left[C_{p,PCM}\left(T_i - T_{liquidus}\right) + L + C_{p,PCM}\left(T_{liquidus} - T_{solidus}\right)\right]$$

M_{PCM} is the mass of the PCM, $Cp_{,PCM}$ is the PCM specific heat, $T_{solidus}$ and $T_{liquidus}$ are the lower and upper values of the PCM phase change interval and L is the PCM phase change enthalpy.

2.2. Numerical Method analyses:

In the present work, erythritol is used as PCM. The inner wall of the PCM pipe is maintained at constant temperature of T_{max} = 400 K during the melting or charging period and at constant temperature of T_{min} = 300 K during the solidification or discharging period with the outer wall assumed to be adiabatic. Fig.9 show the working model of shell and tube heat exchanger was also drawn by FloEFD software

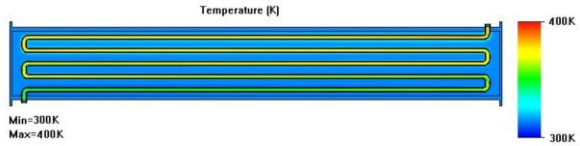

model for Shell and Tube

th boundary conditions

For a mathematical description of the thermal process the following assumptions are made.

- The inner wall is at a constant temperature,
- Thermal losses through the outer wall of the PCM pipe are negligible,
- Thermal resistance of the inner pipe wall is negligible,
- heat transfer in the PCM is both conduction and convection controlled,
- Thermophysical properties of PCM are temperature dependent, and Volume variation resulting from the phase change is neglected and the PCM solid is fixed to the walls at all times.

An enthalpy-porosity technique is used in FloEFD for modeling the solidification/melting process. In this technique, the liquid melt fraction in each cell is computed every iteration, based on enthalpy balance. The mushy zone is the region where the porosity increases from 0 to 1 as the PCM melts. When the region is complete solid, the porosity and the flow velocity values are zero.

The governing conservation equations are:

– Continuity equation

$$\frac{\partial \rho}{\partial t} + \nabla\left(\rho\vec{U}\right) = 0$$

– Momentum equation

$$\frac{\partial}{\partial t}(\rho\vec{U}) + \nabla(\rho\vec{U}\vec{U}) = -\nabla P + \rho\vec{g} + \nabla\tau + \vec{F}$$

Where P is the static pressure, τ – the stress tensor, and $\rho\vec{g}$ and $\vec{F}$ are the gravitational body force and external body forces, respectively,

– Energy equation

$$\frac{\partial(\rho H)}{\partial t} + \nabla(\rho\vec{U}H) = \nabla(K\nabla T) + S$$

Where, H is the enthalpy of the PCM, T – the temperature, ρ – the density of the PCM, K – the thermal conductivity of PCM, $\vec{U}$ – the velocity, and S – the volumetric heat source term and is equal to zero in the present study. The total enthalpy H of the material is computed as the sum of the sensible enthalpy, h and the latent heat:

$$H = h + \nabla H$$

Where,

$$H = h_{ref} + \int_{T_{ref}}^{T} C_p \, dT$$

and h_{ref} is the reference enthalpy, T_{ref} – the reference temperature, and c_p – the specific heat at constant pressure.

The latent heat content, in terms of the latent is:

$$\nabla H = \beta L$$

Where β is the liquid fraction and is defined as:

$$\beta = 0 \text{ if } T < T_{Solidus}$$

$$\beta = 1 \text{ if } T > T_{liquidus}$$

$$\beta = \frac{T - T_{solidus}}{T_{liquidus} - T_{solidus}} \text{ if } T_{solidus} < T < T_{liquidus}$$

The solution for temperature is essentially iteration between the energy, and the liquid fraction. The enthalpy-porosity technique treats the mushy region (partially solidified region) as a porous medium. The porosity in each cell is set equal to the liquid fraction in that cell. The porosity value is zero in fully solidified region. The momentum sinks due to the porosity in the mushy zone in following form:

$$= \frac{(1-\beta)^2}{\beta^3 + 0.001} A_{mesh} \vec{U}$$

The value of mushy zone constant (A_{mush}) varies from 10^2 to 10^7. Generally, 10^5 is used for FloEFD computations. Boundary conditions for PCM pipe inner wall while charging: $T = T_{max}$, while discharging: $T = T_{min}$; for PCM pipe outer wall K_{pcm} $\Delta T = 0$. Initial condition for cyclic process $Ti = T_{min}$, for complete melting and solidification processes

for charging Ti = T_{min}, when discharging: Ti = T_{max}

The computation model for the numerical study was created using software CREO 2 and shown in Figure 9. Meshing of the numerical model was generated and the boundaries were applied at appropriate surfaces. After mesh independence study, the computational domain was resolved with 1900 elements: a fine structured mesh near the inner wall to resolve the boundary layer and an increasingly coarser mesh in the rest of the domain in order to reduce the computational time.

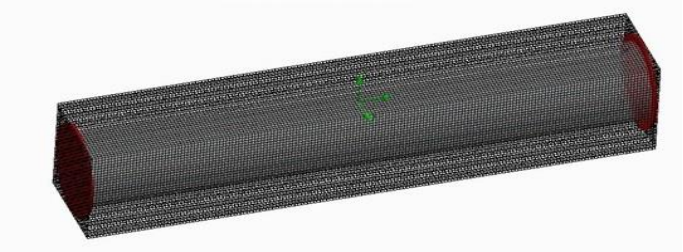

Figure 10 Meshing of the numerical model

As an indication of the computational time, it is observed that on an average, for 3000 iterations, 120-180 minutes are needed for convergence criteria for all relative residuals with a time step of 0.01s using a personal computer with a Intel Core i7 processor and 4 GB random access memory (RAM). The CREO model is then exported to FloEFD for problem solving. The ED method within version mercial code FloEFD was utilized for solving the governing equations. The time step for integrating the temporal derivatives was set to 0.01 s. The FIRST ORDER UPWIND differencing scheme was used for solving the momentum and energy equations, whereas the PRESTO scheme was adopted for the pressure correction equation. The convergence criteria are set as 10^{-3} for continuity and momentum, and 10^{-6} for thermal energy. The model is meshed using the FloEFD software like Fig 10. P-type mesh is followed by the software. During meshing it will ask for coarser or finer, we have to select according to our necessity and the rest is taken care of by the software.

3. RESULTS AND DISCUSSIONS:

3.1 Experimental Method

The thermal conductivity of the tube material has an effect on size of the LHSS. The size of the LHSS increases if the thermal resistance increases. The thermal resistance of conduction of the tube wall heat exchanger does not affect heat transfer, if the tube material has a high value of thermal conductivity. The thermal properties of the tube material have effect on sizing of LHSS and heat transfer process. The maximum amount of solidified Erythritol was obtained when discharge period was reached. Heat transfer rate during the solidification depends on the mass flow rate, the specific heat

of HTF and the temperature difference between outlet and inlet of HTF. In the charging process, mean temperature of erythritol increases and HTF outlet temperature decreases with time. This is reverse in the case of discharging process. The system efficiency of LHSS increases in charging process and decrease in discharging process.

The graph Fig: 11 shows increase in efficiency with increase in time. This is because the thermal energy is stored in the PCM increase with time during charging. The overall charging efficiency of LHSS increases with increase in mass flow rate.

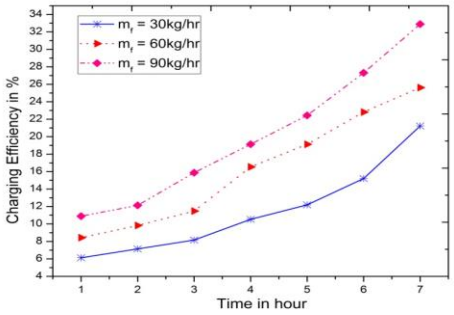

Figure 11 Charging efficiency for different flow rate

The graph Fig: 12 shows decrease in efficiency with increase in time. This is because the thermal energy stored in the PCM decreases with time due to the energy released in the PCM during discharging period. The efficiency of the

to 32.89% during charging

ı discharging cycle.

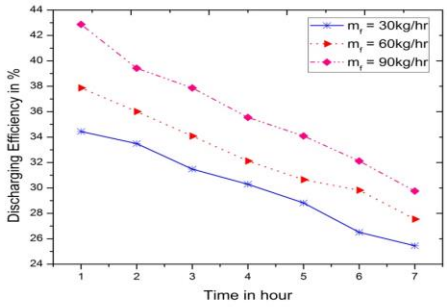

Figure 12 Discharging efficiency for different flow rate

3.2 Validation of the numerical method:

In the numerical method the experiment is done with the help of FloEFD software and solved numerically. In the charging process mean temperature of PCM increases and HTF outlet temperature decreases with time.

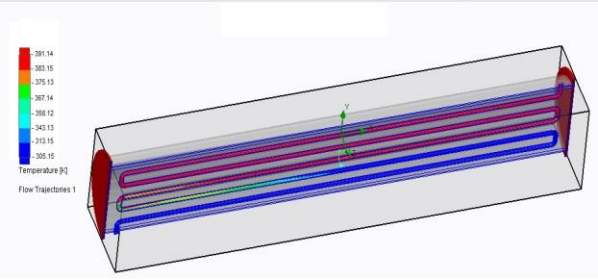

Figure 13 Temperature distribution image for the mass flow rate 30 kg/hr in charging process.

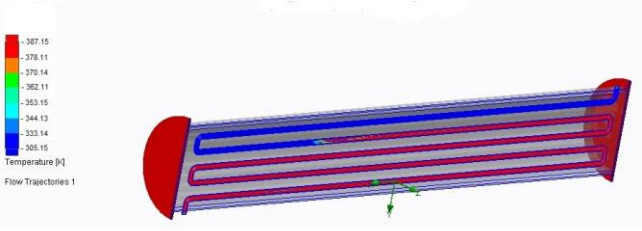

Figure 14 Temperature distribution image for the mass flow rate 30 kg/hr in discharging process.

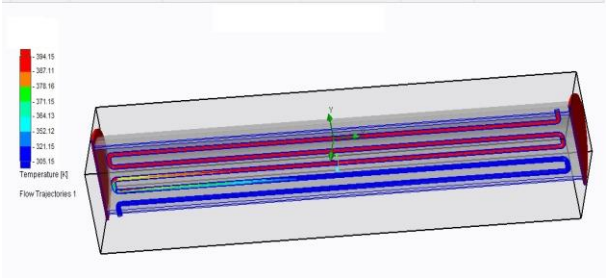

Figure 15 Temperature distribution image for the mass flow rate 60 kg/hr in charging process.

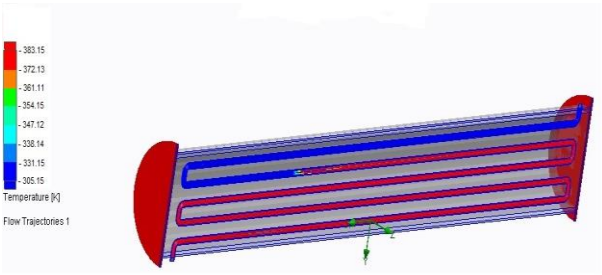

Figure 16 Temperature distribution image for the mass flow rate 60 kg/hr in discharging process.

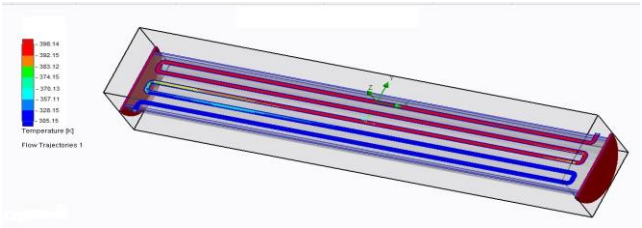

Figure 17 Temperature distribution Image for the mass flow rate 90 kg/hr in charging process.

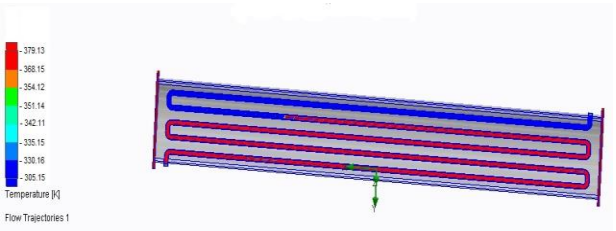

Figure 18 Temperature distribution image for the mass flow rate 90 kg/hr in discharging process.

This is reverse in the case of discharging process. The system efficiency of LHSS increases in charging process and decrease in discharging process. The efficiency of LHSS increases with increase in mass flow rate. The overall charging efficiency of the system reached up to 35.18% during charging cycle and 45.34% in discharging cycle.

The figures 13 and 14 were shows the computational model images of charging and discharging flow rate of 30 kg/hr. The figures 15 and 16 were shows the computational model images of charging and discharging flow rate of 60 kg/hr. The figures 17 and 18 were shows that the computational model images of charging and discharging the flow rate of 90 kg/hr. The figures 19 and 20 were shows the comparison of overall efficiency of the system during charging and discharging processes for different mass flow rates (30 kg/hr. 60 kg/hr and 90 kg/hr.) at a constant inlet temperature T = 130°C. To explain the effect of mass flow rate on the latent heat transfer process of the studied heat storage

system, some results for mass flow rate 30 kg/hr are presented whereas similar trends have been detected for the other mass flow rate. A good repeatability is observed in three repetitions of a charging and discharging processes.

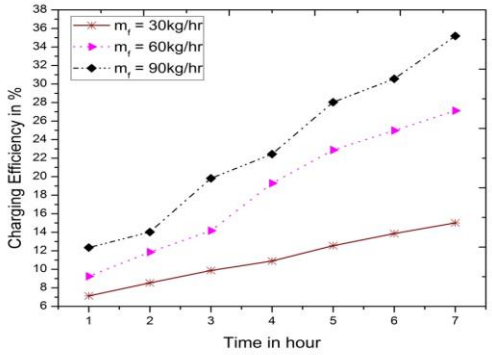

Figure 19 Charging efficiency for different flow rate

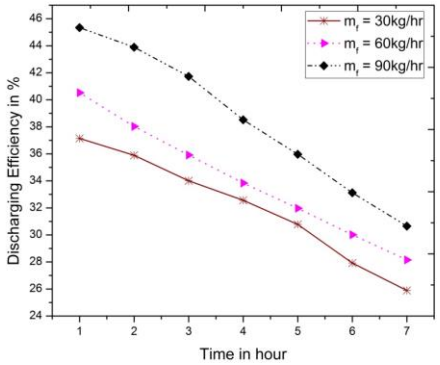

Figure 20 Discharging efficiency for different flow rate

3.3 Comparison between experimental and numerical results:

The experimentally and numerically nperature gradient with time) kg/hr,60 kg/hr and 90 kg/hr during the charging process are in figure 21 (a-c) and during the discharging process plotted in figure 22 (a-c). The dashed lines represent the experimental results, while the continuous lines represent the numerical results.

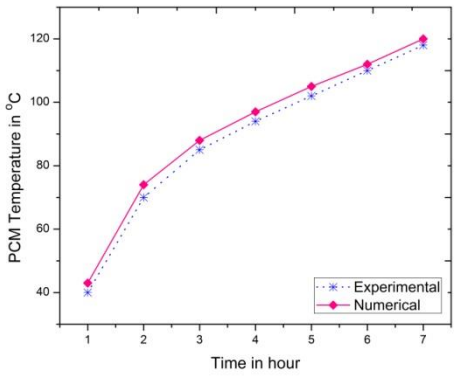

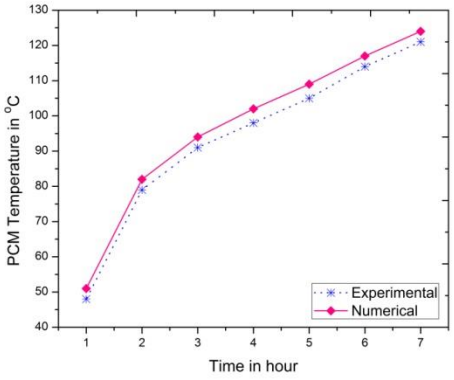

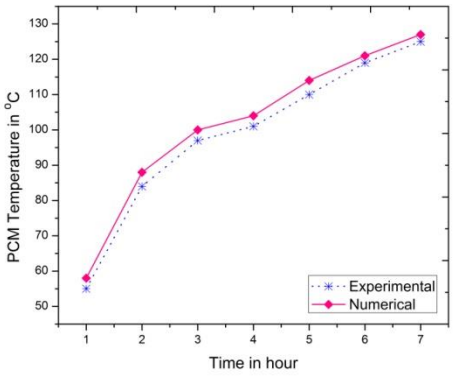

Figure 21 Comparison of average temperature profile for complete melting in the PCM for the flow rates (a) 30 kg/hr (b) 60 kg/hr (c) 90kg/hr between numerical study and experimental study.

From figure 23 and 24 comparing experimental and numerical overall efficiency curves for the charging process and discharging process, it is seems that the results are very similar. The result shows that the experimental and numerical curves shapes are exactly similar, which clearly

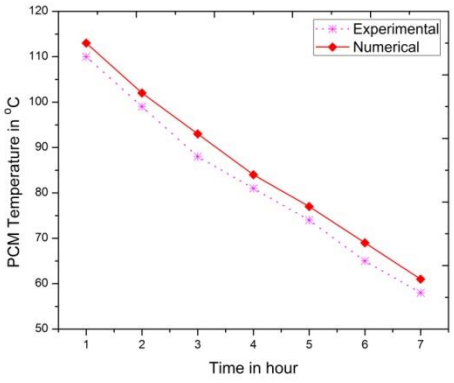

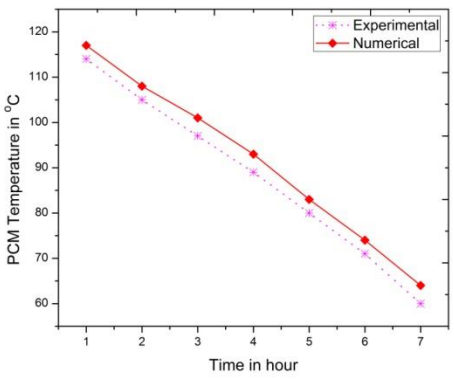

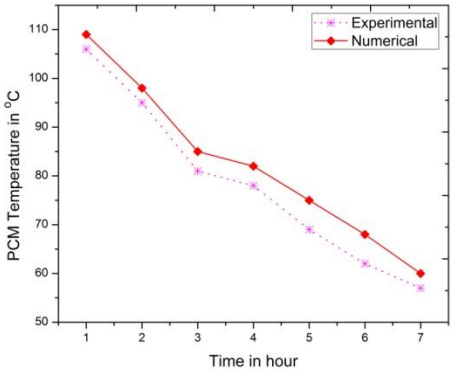

Figure 22 Comparison of average temperature profile for complete solidification in the PCM for the flow rates (a) 30 kg/hr (b) 60 kg/hr (c) 90kg/hr between numerical study and experimental study

indicate that the phenomena are numerically well represented. Concerning the discharging process data, the numerical results are still consistent with the experimental ones.

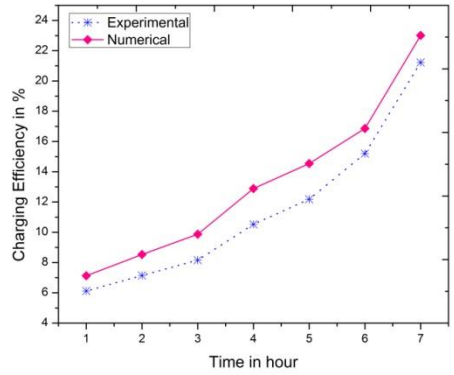

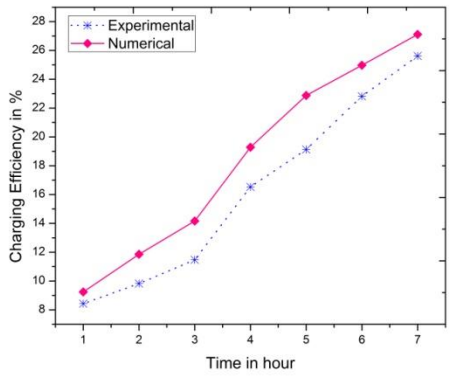

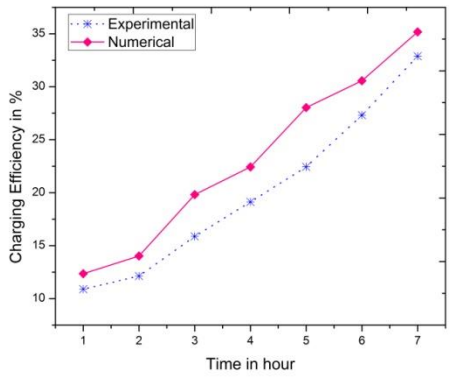

Figure 23 Comparison of overall efficincy for complete melting in the PCM for the flow rates (a) 30 kg/hr (b) 60 kg/hr (c) 90kg/hr between numerical study and experimental study.

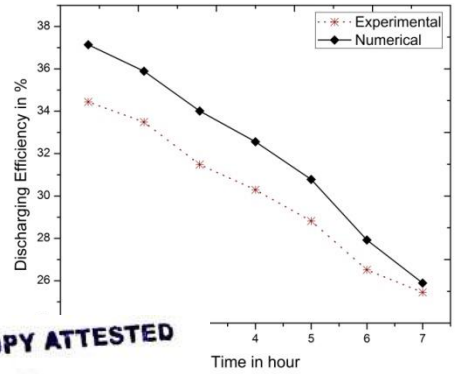

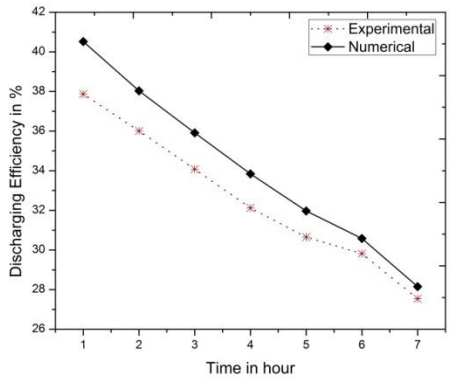

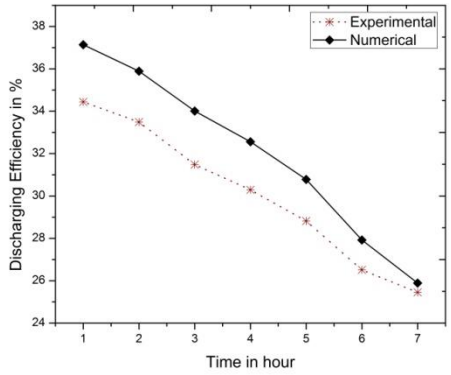

Figure 24 Comparison of overall efficiency for complete solidification in the PCM for the flow rates (a) 30 kg/hr (b) 60 kg/hr (c) 90kg/hr between numerical study and experimental study

4.CONCLUSION:

Based on the findings of the present experimental and computational study of the melting and solidification inside a shell and tube heat exchanger, the following observations are made:

The heat transfer concept in latent heat

storage system is a combination of convection and conduction, but in the charging process, first, conduction dominated heat transfer by and after, convection dominates in charging and discharging process

It is observed that in experimental results by increasing the mass flow rate = 30 kg/hr to 90 kg/hr, overall efficiency of the heat exchanger in charging and discharging processes rise from 21.22% to 32.89% and 34.44% to 42.87% respectively. And numerical results by increasing the mass flow rate = 30 kg/hr to 90 kg/hr, overall efficiency of the heat exchanger in charging and discharging processes rise from 23.01% to 35.18% and 37.14% to 45.34% respectively. From the charging and discharging process data, the numerical results are still consistent with the experimental ones.

REFERENCES

1. Atul Sharma, C. R. Chen. “Solar Water Heating System with Phase Change Materials”. International Review of Chemical Engineering (I.R.E.C.H.E), Vol.1, N.4 July 2009.

2. Lingayat, Yogesh R. Suple. 2013. “Review On Phase Change Material as Thermal Energy Storage Medium”. International Journal of Engineering Research and Applications (Ijera) Vol.3.

3. Lavinia Gabriela. “Thermal Energy Storage With phase Change Material”. Leonardo Electronic Journal of Practices and Technologies, ISSN 1583-1078.

4. Ujjwala Sharma, Vaibhav Dixit and Prof. D. V. Mahindru. “Latent Heat Storage System: A Panacea to Address Energy Needs”. Global Journal of Science Frontier Research. Vol.13 Issue 5-2013.

5. Bruno Cardenas, Noel Leom. “High Temperature Latent Heat Thermal Energy Storage: Phase Change Materials, Design Considerations and Performance Enhancement Techniques”. 14 Jul 2013. Renewable and Sustainable Energy Reviews Volume 27, November 2013, Pages 724-737

6. Anica Trp, Kristian Lenic, Bernard Frankovic. “Analysis of the Influence of Operating Conditions and Geometric Parameters on Heat Transfer in Water-Paraffin Shell and Tube Latent Thermal Energy Storage Unit”. 5 Feb 2006. Applied Thermal Engineering Volume 26, Issue 16, November 2006, Pages 1830-1839

7. Mehmet Esen. “Thermal Performance of a Solar Aided Latent Heat Store Used for Space

Heating by Heat Pump". 30 Nov 1999. Solar Energy Volume 69, Issue 1, 2000, Pages 15-25

8. M. Conti and Ch. Charach. "Thermodynamics of Heat Storage in a PCM Shell and Tube Heat Exchanger in Parallel or in Series With a Heat Engine". Elsevier Science, Solar Energy Vol.57.

9. Robynne Murray, Louis Desgrosseilliers, Jeremy Stewart, Nick Osbourne, Gina Marin, Alex Safatli, Domynic Grouix, Mary Anne White. "Design Of Latent Heat Energy Storage System Coupled With A Domestic Hot Water Solar Thermal System". World Renewable Energy Congress 2011 Sweden 8-13 May 2011.

10. Anish R, S. R. Karale. Vol.1, Issue 8 Oct 2012. "Energy Storage System for Passive Cooling, a Review". PP: 81-83.

11. Mohammed M. Farid, Amar M. Khudhair, Siddique Ali K. Razack B, Said Al Hallaj B. 12 Sep 2003. "A Review on Phase Change Energy Storage: Materials and Application". Energy Conversion and Management Volume 45, Issues 9–10, June 2004, Pages 1597-1615

12. Belen Zalba, Jose M Marin, Luisa F. Cabeza, Harald Mehling. "Review On Thermal th Phase Change: Materials, lysis And Applications". 11 Oct 2002. Applied Thermal Engineering Volume 23, Issue 3, February 2003, Pages 251-283

13. M. Medrano, M.O. Yilmaz, M. Nagues. I. Martorell, Joan Roca, Luisa F. Cabeza. "Experimental Evaluation of Commercial Heat Exchanger for Use as PCM Thermal Storage System". 13 Jan 2009. Applied Energy Volume 86, Issue 10, October 2009, Pages 2047-2055

14. Jinjia Wei, Yasuo Kawaguchi, Satoshi Hirano, Hiromi Takeuchi. "Study on A PCM Heat Storage System for Rapid Heat Supply". 25Feb 2005. Applied Energy 112 (2013) 1222–1232

15. Prabhu P. A, Shinde N. N, Prof. Patil P. S. "Review Of Phase Change Materials for Thermal Energy Storage Applications". International journal of engineering research and application (IJERA) Issue Vol.2, Issue 3, May-June 2012.

16. Mithat Akgun, Orhan Aydin, Kamil Kaygusuz. "Thermal Energy Storage Performance of Paraffin in a Novel Tube in Shell System". 27 May 2007. Applied Thermal Engineering Volume 28, Issues 5–6, April 2008, Pages 405-413

17. Zhenya Liu, Yuanteng Yao, Huiying. "Numerical Modelling For Solid Liquid Phase Change Phenomena in Porous Medium: Shell

and Tube Type Latent Heat Thermal Energy Storage". 5 Feb 2013. Applied Energy 112 (2013) 1222–1232

18. S. Jegadheeswaran, S. D. Pohekar. "Energy And Exergy Analysis Of Particle Dispersed Latent Heat Storage System". Vol.1, Issue 3,2010 Pp 445-458.

19. A.Andreozzi, Buonomo, O. Manca, P. Mesolella, S. Tamburrino. "Numerical Investigation Sensible Thermal Energy Storage with Porous Media for High Temperature Solar Systems". 29-81031. Applied Thermal Engineering Volume 71, Issue 1, 5 October 2014, Pages 130-141

20. Mehmet Esen, Aydin Durmus and Ayla Durmus. "Geometric Design of Solar Aided Latent Heat Store Depending On Various Parameters and Phase Change Materials". Solar Energy Vol.62, 10 Sep 1997, Elsevier science.

21. D. Laing, T. Bauer, W. D. Steimann, D. Lehmann. "Advanced High Temperature Latent Heat Storage System: Designand Test Results". 38-40, 70569. Molten Salts Chemistry from Lab to Applications 2013, Pages 415–438

22. R. Meenakshi Reddy, N. Nallusamy and K. Hemachandra Reddy. "Experimental Studies on Phase Change Material-Based Thermal tem for Solar Water Heating rnal of Fundamentals of Renewable Energy and Applications Vol.2 (2012) article Id R120314, Ashdin publishing.

23. Petrone G, Cammarata G. "Simulation of PCM Melting Process in a Differentially Heated Enclosure". Department Of Industrial Engineering-University of Catania Viale A. Doria, 6,95125 Catania, Italy. Energy Procedia Volume 45, 2014, Pages 1337-1343

24. Arthur E Bergles. "High-Flux Processes through Enhanced Heat Transfer". Experimental Thermal and Fluid Science Volume 26, Issues 2–4, June 2002, Pages 335-344

25. Francisco Colellaa, Adriano Seiacovellia, Vittorio Verda. "Numerical Analysis Of A Medium Scale Latent Energy Storage Unit For District Heating System". Doi: 10.4303/jfrea/R120314. Energy Volume 45, Issue 1, September 2012, Pages 397-406

26. Abduljalil, A. Al-Abidin, Sohif Binmat, K. Sopian, M. Y. Sulaiman, C,H. Lim, Abdul Rahman. "Review of Thermal Energy Storage for Air Conditioning System". Solar Energy Research Institute. Renewable and Sustainable Energy Reviews Volume 16, Issue 8, October 2012, Pages 5802-5819

27. V. Mittal, Ks. Kasana, Ns Thakur. "The Study of Solar Absorption Air Conditioning System".

28. Amirtham Valan Arasu, Agus P. Sasmito, and Arun S. Mujumdar. “Numerical Performance Study Of Paraffin Wax Dispersed With Alumina In A Concentric Pipe Latent Heat Storage System”. THERMAL SCIENCE: Year 2013, Vol. 17, No. 2, pp. 419-430..

Nomenclatures:

C_p	Specific heat capacity
H	enthalpy
k	thermal conductivity
L	latent heat
P	pressure
Q	heat energy charged/discharged
t	time
T	temperature
U	velocity vector
β	liquid fraction
$\eta_{exchanger}$	exchanger efficiency
$\eta_{overall}$	overall efficiency
μ	dynamic viscosity
ρ	density
λ	volumetric expansion coefficient

用红霉素作为 PCM 的潜热蓄热系统的数值和实验研究

V. MAYILVELNATHAN, A. VALAN ARASU

热能储存提高了热效率，并减少了能源供应和工业和太阳能应用的能源需求之间的不匹配。从不同类型的热能储存中，相变材料（PCM）热能储存由于其高储存容量和恒定的热能而表现出更高的效率。在这项工作中，实验和数值分析的目的是研究在壳管式换热器充放电过程中赤藓糖醇作为 PCM 的热行为和传热特性。进行实验以研究在恒定入口温度下增加传热流体（HTF）的质量流率对熔化和凝固过程的影响。数值计算基于有限体积数学建模程序，该程序结合了用于模拟相变概念的单域焓公式。利用数值模拟分析了不同温度过程中的熔融锋面。实验结果表明，通过将传热流体的质量流量从 30kg / hr 增加到 90kg / hr，充放电过程的实验效率分别从 21.22％提高到 35.45％，数值从 23.01％提高到 34.59％。

Research Paper

BIODIESEL PRODUCTION AND OPTIMIZATION FROM *PROSOPIS JULIFERA* OIL – A THREE STEP METHOD

M. Rajeshwaran[1], K. Raja[2,], P.Marimuthu[3]and M.D. Duraimurugan alias Saravanan[4]

Address for Correspondence

[1]Department of Mechanical Engineering, Mohamed Sathak Engineering College, Kilakarai, Ramanathapuram 623 806, Tamil Nadu, India.

[2]Department of Mechanical Engineering, Anna University, University college of Engineering Dindigul - 624005, Tamil Nadu, India.

[3]Principal, Syed Ammal Engineering College, Ramanathapuram-623502, Tamil Nadu, India,

[4]Department of Chemical Engineering, National Institute of Technology, Tiruchirappalli – 620015, Tamil nadu, India.

ABSTRACT

The production of Biodiesel by the method of transesterification has been admired in the recent years due to the anxiety in the conservation of fossil fuels and due to the price hike in conventional fuel. *Prosopis Julifera* is a non edible feedstock found in the arid and semi-arid regions. Oil from *Prosopis Julifera* was extracted by the method of solvent extraction. The present work mainly concentrates on the three step process of biodiesel production from *Prosopis Julifera* oil .Initially the acid value of *Prosopis Julifera* oil was reduced below 1% from 21.85% (43.7 mg KOH/gm) by the two step pretreatment process using acid catalyst 1% v/v H_2SO_4. The second step is the esterification process of the product obtained from pretreatment using alkaline catalyst. The parameters such as methanol to *Prosopis Julifera* oil molar ratio, amount of catalyst used, reaction time and reaction temperature were studied. For the efficient conversion of *Prosopis Julifera* oil to methyl ester gas chromatography was used to analyse the Fatty acid methyl esters. The optimum reaction conditions of Methanol/oil molar ratio of 9:1v/v, reaction temperature of 60^0C, reaction time of 2 hrs and 1% w/v of NaOH usage were determined. In the acid transesterification process, the main objective for process optimization was the reduction of acid value. The process optimization was done using Response surface Methodology technique (RSM). The methyl ester obtained from the previous step was refined to produce biodiesel in the third step. The fuel properties of *Prosopis Julifera* methyl ester (PJME) such as viscosity, cetane number, flash point, acid value, etc were determined. The values thus found experimentally were compared according to the ASTM standards.

KEYWORDS: *Prosopis Julifera*; Acid Esterification; Transesterification; Process optimization.

1. INTRODUCTION

As there is the increase in population, there is the rapid increase in the energy demand. The depletion of fossil fuel reserves and conventional energy sources has stimulated the interest in the alternative energy sources. While considering the environmental concerns, the alternative fuel source must be eco friendly in nature [8].This led the researchers to propose biodiesel to be the ideal choice among all the alternative fuels. In the recent years, world market for biodiesel has expanded rapidly. Though various research works, evaluations, tests and certifications from large number of countries, researchers have confirmed as clean alternative fuel having self combustion properties with lower carbon emission, no sulfur and no aromatics [9].Wide ranges of traditional oil seed crops such as ground nut, mustard, rape seed, sunflower, safflower, linseed, soybean, palm etc were used for the biodiesel production [29]. Though there is the production of large volume of oils, India is not self sufficient in producing edible oils [7]. If the edible oils were used for biodiesel production, then there will be the world food crisis [8].Human rights activists and social reformers have called for a ban on the production of biodiesel from food crops for several years and hence resolved the food versus fuel conflict. Waste cooking oil, Tallow and animal fat have replaced the edible oils in the production of Biodiesel [30].Though they can be afforded at the lowest price, the disposal of these materials constitutes a major problem.

For the production of biodiesel, non edible vegetable oil sources have become more attractive now a day. Thus the dependence of biodiesel production non iced to a greater extent [18]. toxic components in the non suitable for having as food. btained from the plants grown Non edible oils like Jatropha obacco[14], Rubber seed[21], *sativa* [25], Rice bran [10] etc. are found to be the cheapest feedstock for biodiesel production.

Prosopis Julifera is one such cheapest feedstock which acts as a source of fuel, vegetative fence for protection and increased fertility to the arid and semi arid zones of India. The shrubs of drought resistant *Prosopis Julifera* can grow in highly saline areas, alkaline soils, areas near sea, and corrupted grasslands [4].

The species *Prosopis Julifera* is widespread all over the world. It consists of 44 species, having mostly thorny trees and shrubs. Different species of *Prosopis Julifera* and *Acacia Nilotica* have been predicted to occupy some 3.1million sq.km in the world [1].India covers an area of about 3.29 million sq.km. Over 40% of the country's total land surface constitutes the arid and semi-arid regions. Nearly it covers 10 states of India (DFID). Prosopis Julifera grow up abundantly in India [1].It is commonly known as Mesquite in English, Algarroba in Spanish. In India it is called as Vilayati babul, Vilayati khejra, Gando baval, Vilayati kikar. The genus *Prosopis Julifera* seems to be originated before the separation of the African and South African continents, approximately about the million years ago. The history of the first introduction of *Prosopis Julifera* into India is about 130 years old [1].

According to the Department of land resources (DOLR), GOI about 63.9 million hectare of land is lying waste in India. Since these lands are unsuitable for cultivation, they are termed as "Waste lands". Waste lands are said to be characterized by sandy soils, rocky soils, saline soils etc [5]. About 23 million hectare land (10 million hectare salt affected region and 13 hectare arid and semi arid region) is found to be lying waste [45] in India. The current strategy is cultivation of Jatropha, sweet sorghum, and castor, Pongamia in these waste lands [32]. The oils obtained from these plants are non-edible oils. Though these plants grow in diverse agro-climate conditions, withstand pest attack and drought, the

yield of the seed, oil content and nutrient requirements are found to be critical. This leads to the less chance for plantation of these plants in the waste lands [6].

Hence the afforestation of the waste lands can be done with *Prosopis Julifera, Acacia Nilotica* etc. These species require only less amount of water and is found to be more suitable for dry and arid waste lands.

Prosopis Julifera has been recommended as the "Wonder tree" for dry saline areas. *Prosopis Julifera* is found to be abundantly used in various fields and new research is going on in making new drugs and pesticides from the same [1]. Oils obtained from non edible feedstock can be converted into Biodiesel using four standard techniques namely blending, Pyrolysis, Transesterification and micro-emulsification [24].Among these four methods, Transesterification resolves the problem of oils having high viscosity. This process has the advantage of reducing the viscosity of oil thereby increasing the fuel properties [36]. Transesterification is a chemical reaction to produce mono ester by reacting triglycerides with short chain alcohol in the presence of catalysts. Methanol, ethanol, propanol, butanol are the commonly used short chain alcohols. Methanol is widely used alcohol due to its lowest price [10].The triglyceride in the vegetable oil or animal fat react with alcohol to form a mixture of glycerol and fatty acid methyl ester called biodiesel [19].

Transesterification reaction can be a carried out with the help of one or more than one catalyst. Depending on the FFA content, the reaction is either one step or two step process. When comparing edible oils with non-edible oils, edible oils are found to contain large amount of FFA [11, 13, 23]. Base catalysed transesterification of non edible oils produces high quality biodiesel in a shorter reaction time. This usage of base catalyst has the disadvantage of reduction in the yield of biodiesel due to soap formation [35]. NaOH and KOH are the catalysts used in most of the processes. The use of acid catalyst in the transesterification process has the advantage of tolerance and less sensitivity towards high FFAs. However the rate of reaction using acid catalyst is slow. Commonly used acid catalysts are H_2SO_4 and [10, 21] .The advantages of both acid and base catalysts are combined to form 2 step acid (acid/base) process for production of biodiesel from non edible oils having high FFA content [28]. In the first step, the FFA value was reduced below 1% using acid catalysed transesterification. In the next step, biodiesel of *Prosopis Julifera* is produced using an alkaline catalyst[25].This two step transesterification is influenced by reaction time, reaction temperature, and quantity of catalyst [14,25].In acid catalysed and base catalysed reactions,to get the faster yield of FAME, methanol was used as the alcohol when compared with ethanol [6].

nvolving factors affecting the onse surface methodology uitable tool. Comparing RSM information obtained is very shorter time period. The main e Methodology is to identify n be thought of as a surface over the variables experimental space. The explanatory variables use an experimental design like central-composite design CCD to fit full second-order polynomial model. In general, a CCD coupled with a full second-order polynomial model, is considered to be a very powerful combination providing an adequate representation of most continuous response surfaces. For the investigation of complex processes, RSM is proved to be the effective statistical technique giving enough information in the reduced number of experimental runs. Most of the research regarding optimization of Biodiesel production is carried out by RSM only [21].In the present study, RSM was used to optimize and to study the maximum biodiesel conversion of Prosopis Julifera.

The literatures from the recent years show that non-edible oil is the best for the production of biodiesel when compared with the edible oils. In some of the review papers, authors have suggested different techniques to reduce the FFA content of non edible oils using acid and base catalysed transesterification [6, 10]. The high viscosity found in the non edible vegetable oil creates serious problem if it is used directly used in the diesel engines [33].The transesterification process makes biodiesel as a suitable fuel for CI engine [34].

Based on the above literature, there is no detailed work regarding the extraction of oil from the non edible feedstock-*Prosopis Julifera* oil which has a huge potential for biodiesel Production. Also optimization of the oil extracted from *Prosopis Julifera* was not yet reported so far.

The main aim of this paper is to discover a new and powerful non edible feedstock that produces biodiesel for the future use. Also, the transesterification processes, and optimization techniques are taken much care for the improvement of FAME.

2. MATERIALS AND METHODS

2.1 Materials

The genus *Prosopis Julifera* fit into the Botanical family Leguminosae (Fabaceae), sub-family Mimosoideae [1]. The form of the tree and its size vary between the species. *Prosopis Julifera* normally reaches a maximum height of 12m and can also reach upto 20m.The wood of *Prosopis Julifera* is diffusely porous in structure[3]. The tree has thorns which vary in number and size. It may be present in some branches or may be absent.

The size of the leaflets varies greatly, 2.5-23 mm long and 1-7 mm wide [1]. The flowers are small which are densely gathered together on cylindrical, spike-like inflorescences. Flowers are 4-6mm long and are generally straw yellow in colour [2]. The plant flowers almost any time of the year except from hot summer to mid rainy season.

The pods of *Prosopis Julifera* are flattened and straight. The pods are 6-30cm long, 5-16mm wide and 4-9mm thick. The aged pods will swell and become pulpy and will look yellowish brown in colour. The number of pods produced per inflorescence will vary with 1-16 fruit per inflorescence. Seeds are upto 6.5mm long and weigh approximately 0.25 to 0.3g (25000-30000 seed/kg) [1].The production of pods approximately vary from 5 kg to 40 kg/tree depending on the climatic conditions and habitat[44]. Also, 2300 Kg/ha pods

can be produced with *Prosopis Julifera* planted with a density of 20 Kg/tree [45].

The dried fruits of *Prosopis Julifera* were gathered from the waste lands of Ramnad district in Tamil Nadu. Prosopis Julifera collected during the seasonal period were then cleaned and dried for removal of moisture content. The dried pods are crushed and powdered. From the powdered pods, PJO was extracted using the soxhlet apparatus. Polar and non-polar solvents such as Petroleum Ether (68.7^{0}C), n-Pentane (35-37^{0}C), Ethyl acetate (76-78^{0}C), Iso-propanol (81-83^{0}C), Hexane (60-80^{0}C), Methanol (65^{0}C), and Ethanol (78.36^{0}C) were used and the amount of oil extracted with these solvents ranged from 10-37%. Since, maximum oil yield was obtained with methanol, oil from *Prosopis Julifera* was extracted using methanol as the solvent.

The unrefined oil of *Prosopis Julifera* oil was dark brown in colour. Gas chromatography analysis was made and the fatty acid composition of *Prosopis Julifera* oil was found. Based on Triglycerides, the vegetable oil has different grades of Fatty acid and variation in fatty acid is based on hydrocarbon chain length and number of double bonds. Percentage compositions of fatty acids differ based on the flora species and growth conditions. Table [1] provides the properties of oils produced from non edible feedstock.

The saturated (palmitic, stearic) fatty acids and unsaturated (oleic, linoleic) fatty acids present in PJO was 23% and 68% respectively. The PJO had an acid value of about (39-43.7) mg KOH/gm, which corresponds to a fatty acid value of 21.85%.For the agreeable transesterification reaction using acid catalyst, the FFA value should be 1%.Since the FFA value obtained was far away from the limits, the transesterification process became complicated forming soap .The formation of soap prevented the separation of Biodiesel from Glycerin. Hence, the FFAs were initially converted into ester in a pre-treatment process, using an acid catalyst like 1% (v/v) H_2SO_4.In this pretreatment process, the acid value of PJO can be reduced below a FFA value of 1%.

TABLE 1. PROPERTIES OF OIL PRODUCED FROM NON-EDIBLE FEEDSTOCKS

properties	Jatropha oil [6][23]	Rubber seed oil [11][21]	Rice Bran oil[10]	Mahua oil [15][28]	Karanja oil[12]	*Camelina Sativa* oil[25]	Waste cooking oil[29]	Tobacco oil[14]	*Prosopis Julifera* oil(PJO)
Density, Kg/m^3	913	910	922	960	909	910	920	923	967-971
Viscosity at 40^{0}C(mm^2/sec)	40.4	76.4	43.5	24.9	27.84	14.03	28.8	27	38-41.2
Calorific value(MJ/kg)	38.65	37.5	--	36	--	44.5	44.44	--	38-41
Flash point(^{0}C)	240	198	316	232	232	--	--	--	202-212
Acid value (mg KOH/g of oil)	28	34	40	38	12.27	3.163	17.41	36.6	39-43.7
Saponification value (mg KOH/g of oil)	195	206	--	--	165.5	193.31	166.3	--	180-186
Iodine value (I_2g100/g of oil)	101	135.3	108	--	89	--	--	130.2	102-112

2.2 Apparatus

Fig [1], the apparatus used for transesterification consists of constant temperature water bath, reaction flask with condenser and digital rpm. Digital rpm is used for controlling the Mechanical stirrer. The agitation speed of the mechanical stirrer was maintained as 600rpm for all the transesterification processes. The glass reactor consists of three necks, one for stirrer, and others for condenser. The volume of the glass reactor measured 500ml.The reaction temperature was measured using a temperature indicator.

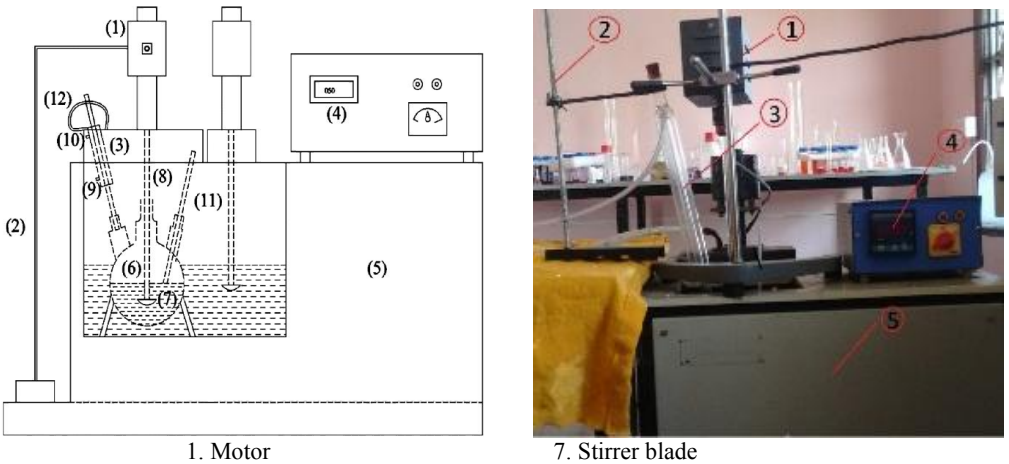

1. Motor
2. Motor stand
3. Lie beg condenser
4. Temperature controller
5. Constant temperature Water bath
6. Three neck round bottom flask
7. Stirrer blade
8. Stirrer rod
9. Water in
10. Water out
11. Thermocouple
12. Tube

hematic diagram and photographic view of constant temperature water bath

oil obtained from *Prosopis* wo steps. The influence of methanol /oil molar ratio,(3,5,6,7and 9) v/v, and reaction time (0.5,0.75,1,1.25,1.5,2,2.5 hours) on the acid value of PJO in each step of pretreatment were

studied. In this pretreatment process, whatever may be the methanol/oil molar ratio and reaction time, the amount of H_2SO_4 used was 1% v/v only [10]. 100gm of PJO was taken and poured into a flask which was kept in a water bath. The water bath was retained hot by keeping at the temperature 110^0C for 30 minutes to eliminate moisture and the PJO was preheated [18].To this preheated oil, sulfuric acid methanol solution was added and the mixture was stirred at the same rate for few minutes. After the completion of this reaction, the end product was poured into a separating funnel to separate the excess methanol. The excess methanol along with H_2SO_4 and impurities moved to the top surface and it was then removed .Using standard ASTM method, the acid value of the product separated at the bottom surface was measured at standard intervals. In a minimum reaction time, the product having an acid value of 8.6mg KOH/gm and very little amount of methanol was utilized as raw material for the second step. For to investigating the influences of methanol/oil molar ratio and reaction times and the acid value of the raw material obtained the same experimental procedure as above was repeated. For the transesterification reaction, the product having 2.7mgKOH/gm and with lowest amount of methanol in minimum reaction time was used. Rubber seed oil having acid values of 35mgKOH/gm was reduced to 3.8mg KOH/gm and 40mg KOH/gm was reduced to 0.9mg KOH/gm in Rice bran oil [10]. Similarly in Jatropha oil an acid value of 28mg KOH/gm was reduced to 2mg KOH/gm [17]. The final reaction mixture was poured into a separating funnel. The mixture was separated by centrifugal process was then washed with distilled water and then dried with anhydrous sodium sulphate and was used for additional processing.

2.4 Transesterification

The experimental setup for this process was the same as utilized in the pretreatment process using acid as catalyst. Before starting the reaction, PJO was preheated to the desired temperature to maintain the catalytic activity and to avoid the moisture absorbance, NaOH-methanol solution was prepared newly. The methanolic solution was then added to the already present PJO in the reaction flask and from that point, time was noted. The product obtained after transesterification was poured into a separating funnel. The esters present in the lower aqueous glycerol were then separated by gravity. The esters thus separated were then washed twice with distilled water. In a rotary evaporator, the washed esters were dried under vacuum and were stored for further analysis.

Fatty acid methyl ester composition of *Prosopis Julifera* oil was analysed by means of Gas chromatography attached with a flame ionization detector (GC FID). Gas chromatography analysis was performed in Central Electrochemical Research Institute (CECRI) - CSIR Lab, located at Karaikudi, in Tamil nadu. Gas Chromatograph used was Agilent Technologies, model 7980A with split-spiltless injector. This Gas chromatograph used a capillary column of dimension (30 x 250µm x0.25 µm) Helium was used as a carrier gas at velocity of 36.445 cm/s .The split ratio was maintained at 1:10.The initial temperature of the oven was kept at 50^0C for 1 minute then, 10^0C for 1minute to 300^0C for 3minutes and the run time as a total of 28 minutes. The lipids and other components composed in extracted oils were quantitatively and qualitatively analyzed using AOAC norms. Methyl esters obtained from *Prosopis Julifera* contain 16% saturated fatty acids like Palmitic and stearic acids. Table [2] shows the fatty acid composition of *Prosopis Julifera* oil. The percentage of unsaturated fatty acids such as Oleic, Linoleic and linolenic acids present in oil was 78.1% .The proportion of fatty acid present in the Biodiesel extracted from *Prosopis Julifera* pods is as follows: Palmitic acid (10.6%), oleic acid (34.7%), linoleic acid (43.4%), Lauric acid (0.2%), Myristic acid (0.1%), Arachidice acid (0.13%), Behenic acid (0.1%) and Stearic acid (5.2%).

TABLE 2. FATTY ACID COMPOSITION OF PROSOPIS JULIFERA OIL

Fatty Acids	Formula	Systematic name	Structure	Net (%)
Lauric acid	$C_{12}H_{24}O_2$	Dodecanoic acid	C_{12}	0.2
Myristic acid	$C_{14}H_{28}O_2$	Tetradecanoic acid	C_{14}	0.1
Palmitic acid	$C_{16}H_{32}O_2$	Hexadecanoic acid	C_{16}	10.6
Stearic acid	$C_{18}H_{38}O_2$	Octadecanoic acid	C_{18}	5.2
Oleic acid	$C_{18}H_{34}O_2$	Cis-9- Octadecanoic acid	$C_{18:1}$	34.7
Linoleic acid	$C_{18}H_{32}O_2$	Cis-9-cis12-Octadecanoic acid	$C_{18:2}$	43.4
Arachidice acid	$C_{20}H_{40}O_2$	Eicosanoic acid	C_{20}	0.13
Behenic acid	$C_{22}H_{44}O_2$	Docosanoic acid	C_{22}	0.1

3. RESULTS AND DISCUSSION

3.1. Pretreatment

Pretreatment is found to be the best method for the reduction of acid values below 1mg KOH/gm as all the non-edible oils have an acid values in the range 20 to 45mgKOH/gm[10,11,17].Important variables which affect the acid value were type of feedstock and alcohol, alcohol: oil molar ratio, concentration of catalyst, reaction time and reaction temperature. From figure [2], it can be seen that the reaction was and became very slow in the research, the rate of reaction ratio and reaction time. With atio, the acid value decreased ion rate were found to be ce due to the effect of water terification of FFA, the supplementary reaction may be put off and the reaction rate was nearly identical [14]. If the FFA should be 1mgKOH/gm after the second pretreatment step, then FFA of 5mgKOH/gm should be obtained in the first step [11, 15].The optimum condition of 9:1v/v methanol/oil ratio and 2 hours minimum reaction time was selected for reducing the acid value from 43.7mg KOH/gm to 8.6mgKOH/gm. In the second step pretreatment also, the same tendency was followed similar to the first step. This can be shown from the figure [3].The combination of 9:1v/v methanol/oil molar ratio and reaction time of 2 hours was found to be optimum value which reduced acid value from 8.6mgKOH/gm to 2.7mg KOH/gm. With the increase in the Methanol/oil ratio and the reaction time, there was a decrease in the acid value.

Transesterification of PJO with methanol was performed after this pre-treatment process.

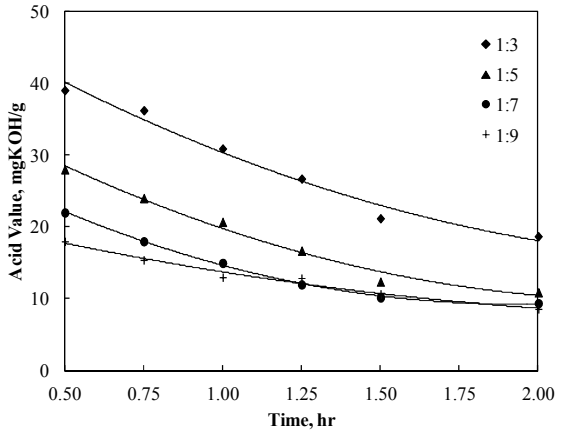

Fig. 2 Effect of methanol /oil molar ratio and reaction time on reduction of acid value of PJO during the first step pretreatment of biodiesel production. Initial acid value was 43.7mg KOH/g of oil.

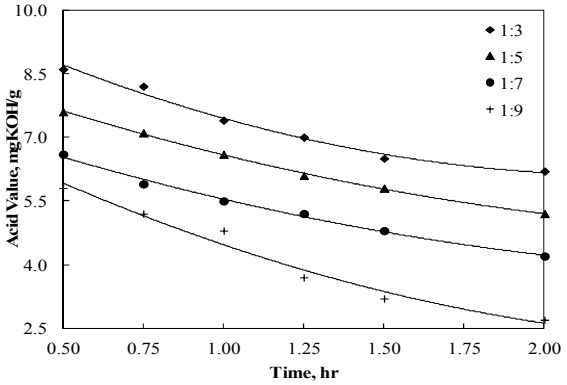

Fig. 3 Effect of methanol /oil molar ratio and reaction time on reduction of acid value of PJO during the second step pretreatment of biodiesel production. Initial acid value was 8.6mg KOH/g of oil.

3.2. Alkaline catalysed transesterification

The reaction product obtained from acid catalyzed pretreatment was used for this alkali catalysed transesterification. The experiments were carried out at different molar ratios, catalyst amount, reaction temperature and reaction time and optimum condition was noted down.

3.2.1 Effect of molar ratio on conversion efficiency

Three moles of alcohol and one mole of triglyceride reacts to yield 3 moles of fatty acid alkyl esters and one mole of glycerol [35].Methanol to oil ratio is an important parameter in the conversion of fatty acid alkyl esters [22]. Surplus amount of alcohol is needed to impel reaction products to right side of equilibrium reactions.

In the present work molar ratios of 3:1, 5:1, 7:1, 9:1, 12:1 v/v were used. From the test, it was found that the molar/oil ratio had no effect on acid, peroxide, saponification and iodine values of methyl ester [10]. Figure [4] shows the conversion efficiency at different molar ratios. With the increase in the addition of methanol, the conversion efficiency showed proportional increase in the initial stage and

rsion efficiency was very less molar ratio was above 9:1v/v. fered with the separation of creased solubility. Amount of he solution drove the reaction t side of equilibrium, and thus of low amount of esters. An optimum value of methanol was chosen carefully. From the literatures, the methanolysis reaction of non-edible oils was carried out with the molar ratio from 6:1 to 18:1 for both the steps irrespective of the catalyst. The molar ratio increased from 3:1 to 6:1, showed improved results on the ester yield. In the first step, when the methanol/oil molar ratio increased, the acid value reduced stridently, then slowly decreased and was constant at the final step [24]. More amount of triglycerides would be produced if the molar ratio was increased further and the reaction will also be incomplete if the molar ratio is less than 6:1.Aslo mixing of the reactants during transesterification will be insufficient for molar ratio < 6:1. The end product will be diluted if the molar ratio is greater than 6:1 and if it is increased further than 6:1, the methanol added will not have any effect on the yield of esters [35].

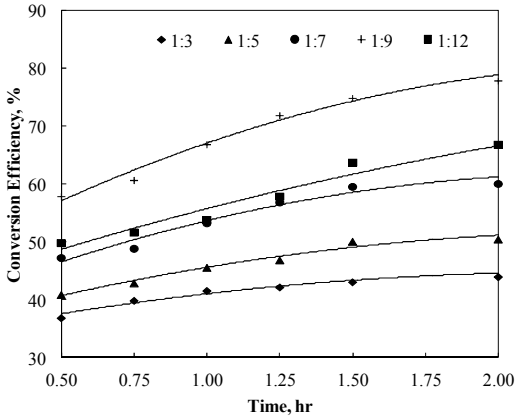

Molar Ratio Vs Time

Fig 4. Influence of molar ratio (methanol /oil) on the yield of PJME (NaOH 1%, temperature 60^{0}C, rate of stirring 600 rpm).

The present study revealed that the better yield of methyl esters of about 81% was at an optimum methanol/oil molar ratio of 9:1.Also, it was inferred that the yield of methyl esters gradually increased from 42 % to 81%.This gradual increase was noticed for the ratios from 3:1 to 9:1.After that methyl ester yield decreased. The transparency of biodiesel and the oil yield decreases if the molar ratio is increased from 7:1 to11:1. Abundant quantity of methanol used for the reaction leads to the difficulty in the separation of glycerol from biodiesel [22]. For the molar ratio above 13:1, unreacted methanol in the top level, ester in the middle level and glycerin at the bottom will be obtained [20].

3.2.2 Effect of catalyst amount on conversion efficiency

A set of experiments were conducted by changing the amount of NaOH from 0.25%to 1.5% w/v figure [5] shows the conversion efficiency with different catalyst amounts. The maximum yield of ester was obtained during the esterification of PJO with the catalyst 1% w/v NaOH. It was observed that the lowest catalytic concentration (0.25%) was not sufficient to complete the reaction. Increasing the amount of catalyst above 1.25%w/v did not increase the conversion efficiency. With the enhancement in the concentration of catalyst beyond 1.25%w/v, the methyl ester yield diminished and the quality of ester yield was based on the formation of glycerol and soap. The ester yield efficiency reduced with the increase in the amount of catalyst added. Excess amount of catalyst used led to the formation of

emulsion which increased the viscosity and formation of gels and at last the reaction ceased. From the experimental work, it was found that, for an efficient transesterification reaction, 1%w/v of NaOH was the optimum amount of catalytic concentration. The yield of methyl ester for Rapseed oil, Tobacco seed oil and *Pongamia pinnata* was 95-96% ,98% and 97-98% using 1%NaOH[6].Catalytic concentration of 1.33% yielded 89.9% of Karanja oil and 86.2% *Jatropha curcas* oil was obtained using 1% NaOH [24].

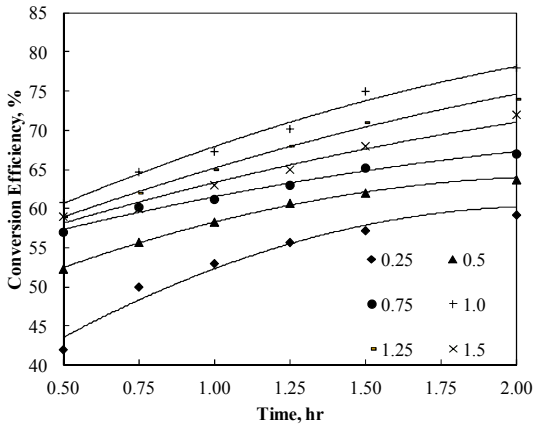

Catalyst Vs Reaction Time

Fig.5 Influence of NaOH concentration on the yield of PJME (methanol /oil molar ratio 9:1, temperature 60^{0}C, rate of stirring 600 rpm).

3.2.3 Effect of reaction temperature on conversion efficiency

The influence of reaction temperature on conversion efficiency is shown in the figure [6] keeping 9:1 molar ratio and 1%w/v NaOH catalytic concentration. For the yield of esters, reaction temperatures of 55^{0}C, 60^{0}C, 65^{0}C, 70^{0}C were used. The conversion efficiency was 71% for the temperature of 55^{0}C and at the reaction temperature of 60^{0}C, and 2.5 hrs, maximum ester yield of 81% was obtained. Similar results have been reported by earlier researchers using non edible oils [20]. In general for the base catalysed transesterification reaction, the temperature was set based on the type of alcohol used [24]. The methyl ester yield efficiency reduced when there was the rise in temperature. When the temperature was further increased from 65^{0}C -70^{0}C, PJ biodiesel yield and purity was decreased. At the high reaction temperature, loss of methanol accelerates saponification of glycerol by alkaline catalyst and the ester yield will be attained earlier than the completion of alcoholysis. Bubbles produced due to the vaporization of methanol obstructed the alcoholysis reaction though condensation system was used in the experiment. Hence the reaction temperature must not exceed the boiling point of methanol (65^{0}C) and reaction at higher temperature must be avoided. The findings from the experimental results of most of the researchers conclude that almost all the experiments were conducted near the boiling point of methanol

er yield was observed in the om 50 to 60^{0}C.95- 99% of ıed for Jatropha oil, Mahua ın oil [10], *Pongamia pinnata* ılepia syiraca* oil[40] ,*croton* reaction temperature of 60^{0}C

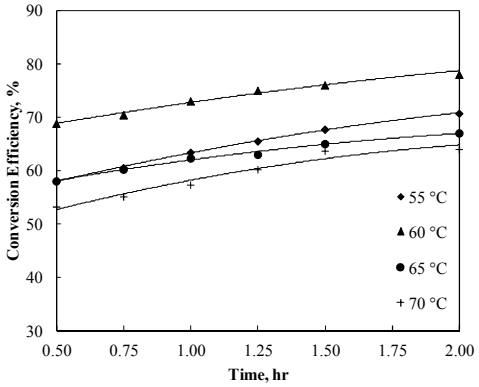

Reaction Temperature Vs Time

Fig 6. Influence of Reaction Temperature on the yield of PJME (methanol /oil) 9:1, Catalyst NaOH 1%, rate of stirring 600 rpm).

3.2.4 Effect of reaction time on conversion efficiency

The ester conversion was carried out at the reaction time such as 0.5, 0.75, 1, 1.25, 1.5, 1.75,2 and 2.5 hours keeping 9:1v/v molar ratio, 1%w/v NaOH catalytic concentration and 60^{0}C reaction temperature. The conversion efficiency can be improved by stirring the chemical reagents and oil at constant rate [11]. drawn between the biodiesel yield and reaction time, it was observed that reaction time extremely influenced the yield of esters. When the reaction time was enhanced from 1.5 to 2.5 hrs, there was the rise in the conversion efficiency of PJME. The conversion procedure is considered to be the best if it achieves maximum conversion within a shortest time period. The data obtained from the current experiments indicate that the reaction time of 2 hours was sufficient for the completion of the reaction and also it was found to be the optimum value. The ester conversion of *Prosopis Julifera* oil with this time was found to be 81%. If the oil is kept too long under the reaction time than the optimal value, the appearance of the oil becomes dark in colour. The yield of Jatropha biodiesel was 95% and 98% for Soybean and castor oil for a reaction time of 2 hours[42].In general, on edible oils can be analysed by further increasing the reaction time above 2 hours. Neem oil when reacted at 6.5to 8 hrs yielded 88 to 94% biodiesel[43] and Mahua oil produced 99% of ester yield after undergoing a chemical reaction of 3hours[15].

3.2.5 Fuel Properties of Methyl esters of *Prosopis Julifera* oil

Based on the Biodiesel ASTM standards, the fuel properties of Methyl esters *Prosopis Julifera* oil are summed up in Table 3. Most of the properties of Prosopis Julifera Biodiesel match the values as prescribed in the ASTM standard D6751-02.

Oxygen content present in Biodiesel helps in complete combustion. The calorific value of *Prosopis Julifera* Biodiesel was lower than that of diesel and that is due to the presence of oxygen content in Biodiesel. The Cetane number was found to be slightly greater than the regular diesel fuel. Also viscosity value was noticed to be a little bit greater than diesel. This implies that the biodiesel is having good ignition properties and there is the need to do slight engine modification. Density was very much greater than the diesel. The flash point and cloud point observed was confined as per the ASTM D6751-02 and DIN EN 14214 standards.

TABLE 3. PROPERTIES OF BIODIESEL PRODUCED FROM NON-EDIBLE FEEDSTOCKS

Properties	Test Procedure	Biodiesel-standard ASTM D6751-02	DIN EN 14214	Diesel	Diesel Prosopis Julifera oil-Biodiesel(PJME)
Density, Kg/m^3	ASTM D4052	875-900	860–900	847	893
Viscosity at $40^0C(mm^2/sec)$	ASTM D445	1.9–6.0	3.5–5.0	2.85	4.9
Calorific value(MJ/kg)	ASTM D240			43.4	39
Cetane number	D613	47 min	51 min	46	49
Flash point(^0C)	ASTM D4052	>130	>120	68	120
Cloud point (^0C)	ASTM D2500	-3 to 12	--	--	4
Acid value (mg KOH/g of oil)	ASTM D4052	>0.8	>0.50	0.35	2.7
Saponification value (mg KOH/g of oil)	--	--	--	--	92
Iodine value (I_2g100/g of oil)	--	--	--	--	87

3.2.6 Optimization of transesterification process

To evaluate the effect of process parameters on acid value in the first step of Transesterification, Central composite design (CCD) was used. The model significance and suitability was tested by analysis of variance (ANOVA) based on the alkaline value (response).The process parameters level for the optimization of transesterification process is given in Table no[4].The statistical analysis of experimental data was done using Deign expert 7.1.5 trial software.

3.2.7 Optimization of alkaline-esterification process parameters

After reducing the FFA value of the *Prosopis Julifera* oil by Acid transesterification process, Biodiesel was produced by Alkaline Transesterification.

Analysis of variance was then carried out to test the model significance. The ANOVA table is given in Table no [6].

TABLE 4. PROCESS PARAMETERS LEVEL FOR THE OPTIMIZATION OF TRANSESTERIFICATION PROCESS

Factors	Process Parameters	Lower level(-1)	Middle level (0)	Upper level (+1)	Std. Dev.
A	Methanol/oil (v/v)	3:1	6	9:1	2.32379
B	NaOH (w/v)	0.25	0.8583	1.5	0.470741
C	Extraction temperature (deg C)	55^0C	62.5^0C	70^0C	5.809475
D	Extraction time (min)	30	75	120	34.85685

TABLE 5. EXPERIMENTAL DESIGN WITH PROCESS DATA AND THE RESPONSE FOR TRANSESTERIFICATION PROCESS MODEL

Std	Run	Methanol/ (v/v)	NaOH (w/v)	Temperature deg C	Time (min)	Yield of Methyl Ester (%)
1	1	3	0.25	55	30	42
2	2	9	0.25	55	30	51
3	3	3	1.5	55	30	43.7
4	4	9	1.5	55	30	53
9	5	3	0.25	55	120	59.1
10	6	9	0.25	55	120	79.9
11	7	3	1.5	55	120	61.4
12	8	9	1	55	120	81
21	9	6	0.875	55	75	60.3
17	10	3	0.875	62.5	75	52
18	11	9	0.875	62.5	75	72.5
19	12	6	0.25	62.5	75	57.4
20	13	6	1.5	62.5	75	62.5
23	14	6	0.875	62.5	30	44.7
24	15	6	0.875	62.5	120	77.2
25	16	6	0.875	62.5	75	62
26	17	6	0.875	62.5	75	62
27	18	6	0.875	62.5	75	62
28	19	6	0.875	62.5	75	62
29	20	6	0.875	62.5	75	62
30	21	6	0.875	62.5	75	62
5	22	3	0.25	70	30	43.2
	23	9	0.25	70	30	55
	24	3	1.5	70	30	60.3
	25	9	1.5	70	30	58
	26	3	0.25	70	120	57
	27	9	0.25	70	120	76
	28	3	1.5	70	120	54
	29	9	1.5	70	120	73
22	30	6	0.875	70	75	62.3

TABLE 6. ANOVA RESULT FOR METHYL ESTER YIELD BY TRANSESTERIFICATION METHOD

Source	Sum of Squares	df	Mean Square	Value	p-value Prob > F	
Model	2867.982	10	286.7982	20.11568	< 0.0001	Significant
A-Methanol/oil (v/v)	862.0208	1	862.0208	60.46111	< 0.0001	
B-NaOH	33.40525	1	33.40525	2.343004	0.1423	
C-Temperature	4.226698	1	4.226698	0.296456	0.5924	
D-Time	1518.303	1	1518.303	106.492	< 0.0001	
AB	13.81237	1	13.81237	0.968783	0.3374	
AC	5.950516	1	5.950516	0.417362	0.5260	
AD	149.384	1	149.384	10.47762	0.0043	
BC	3.29608	1	3.29608	0.231183	0.6361	
BD	41.28586	1	41.28586	2.895741	0.1051	
CD	135.1723	1	135.1723	9.480824	0.0062	
Residual	270.8914	19	14.25744			
Lack of Fit	242.6781	14	17.33415	3.071978	0.1107	not significant
Pure Error	28.21333	5	5.642667			
Cor Total	3138.874	29				

The investigation of process parameters methanol/oil volume ratio (factor A), amount of sodium hydroxide (factor B), reaction temperature (factor C) and reaction time (factor D) with respect to methyl ester yield(Y) was analysed with the help of the following equation.

$$Y = +60.24 + 6.97 * A + 1.44 * B + 0.48 * C + 9.24 * D - 0.96 * A * B - 0.62 * A * C + 3.08 * A * D + 0.46 * B * C - 1.67 * B * D - 2.93 * C * D$$

The model using Response surface methodology with central-composite design (CCD) for the methyl ester yield had an F-value of 20.65 and a p-value of 0.0001 which show that the model is significant with a chance of 0.01% and the Model-F value happened due to noise. In this RSM model, methanol/oil volume ratio (factor A) was the important resolving factor in the Biodiesel yield and the main aim is to increase the yield. This was validated by the high F-value of 109.44 for factor A. Other than this, the parameters like amount of alkaline catalyst, sodium hydroxide (factor B) also had significant impact on the biodiesel yield and the effect of temperature has not much deviation in the methyl ester yield. The two process variable namely methanol/oil volume ratio (factor A) and amount of sodium hydroxide (factor B) had an interactive effect as observed from the p-value of 0.3417 which was less than 0.05. R squared & adj R squared values found using RSM were 0.915744 and 0.8714 respectively is shown in Table [7].Figure [a] shows the normal distribution of the data which help to confirm the ANOVA results. The RSM based predicted and actual methyl ester yield and perturbation chart is shown in the figure [b] and [c].

The Perturbation chart showed a negative non-linear steep curvature for methanol/oil volume ratio and the methyl ester yield. The chart also depicts that the (factor A) was the most important process parameter when compared with other variables. The other process parameters such as sodium hydroxide, time and temperature showed a plateau shaped curves in the Perturbation chart indicating their less odiesel yield. The response ester yield comparing (factors in figure [d] and the other kept at middle level. The ximum when the methanol/oil ot minimum 3:1v/v and the d were also minimum.

The percentage of yield can be given by the empirical formula

Yield Of Methyl Ester = - 17.14458 + 2.77394 * Methanol/oil(v/v) + 3.74168 * NaOH + 0.79556 * Temperature + 0.66313* Time - 0.50977 * Methanol/oil (v/v) * NaOH-0.027478 * Methanol/oil (v/v) * Temperature + 0.022820* Methanol/oil (v/v) * Time + 0.097240* NaOH * Temperature - 0.059318* NaOH * Time - 8.68369E - 003 * Temperature * Time

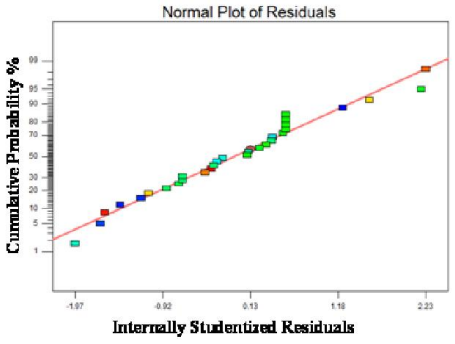

Fig (a) Normal Probability Plot of Residuals

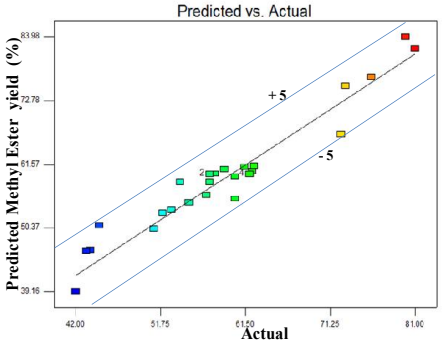

Fig(b) Predicted and Actual Methyl Ester Yield (%)

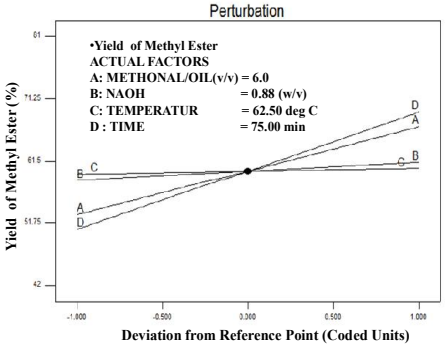

Fig (c) Perturbation of Transesterification for Percentage Yield of Methyl Ester

Table 7. R-squared results for methyl ester yield

Factor	Optimum value	Factor	Optimum value
Std. Dev.	3.726169	R-Squared	0.915744
Mean	60.28333	Adj R-Squared	0.871399
C.V. %	6.181094	Pred R-Squared	0.679232
PRESS	1004.313	Adeq Precision	19.84067

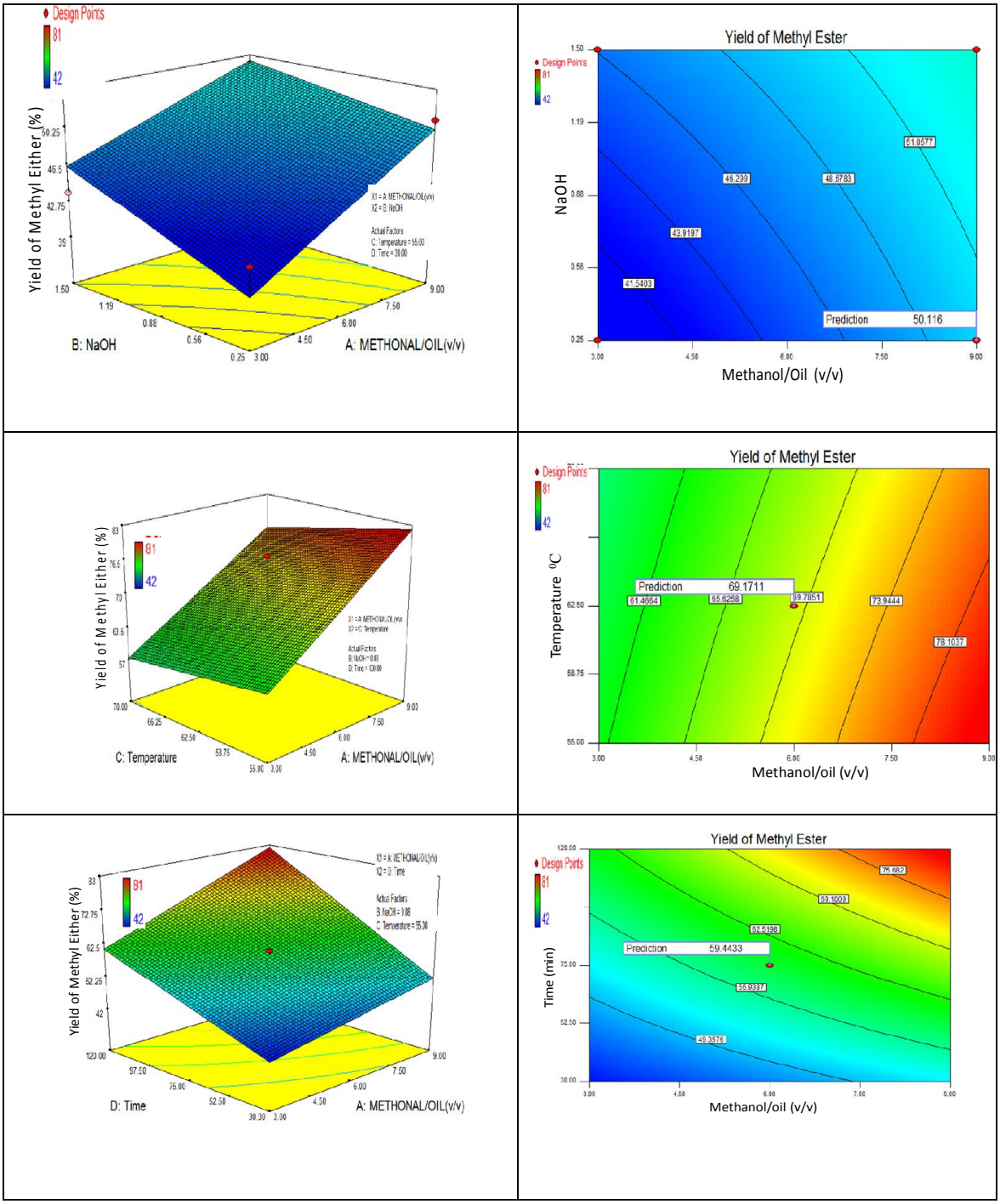

Fig (d) Response Surface and contour plots of methyl ester as function relationship of AB, AC, AD base on the second order polynomial equation.

4. Conclusion

There is 10 million hectare of salt affected land and 13 million hectare of arid and semi-arid zones which are suitable for the growth of trees like *Prosopis* Hence, 23 million hectare of for the plantation of *Prosopis* amount of 6.3 million litres an be produced from about 1 ion of *Prosopis Julifera.* By *rosopis Julifera* oil to methyl amount of 5 million litres of biodiesel can be produced. Hence, the species Prosopis Julifera found abundant in our country can do wonders if utilized in a useful manner.

Biodiesel from *Prosopis Julifera* oil was obtained by acid catalysed transesterification reaction using various catalyst concentration, methanol/oil molar ratios, reaction temperature and reaction time. The following points are concluded from the present work.

- In a two step acid esterification process using 1% v/v H_2SO_4 and9:1v/v methanol/oil ratio and 2 hours minimum reaction time, the FFA level of *Prosopis Julifera* oil was decreased from

43.7mgKOH/gm to 8.6mgKOH/gm and then finally it was reduced to 2.7mgKOH/gm.

- The optimum condition for transesterification was found to be using NaOH as catalyst, 1%w/v catalytic concentration, 9:1v/v molar ratio,60^{0}C reaction temperature and 2 hours reaction time.
- The ester conversion efficiency with these parameters is 81%.
- Using Response surface methodology, optimum conditions of 9:1v/v methanol/oil molar ratio, 1% w/v sodium hydroxide, at an extraction temperature of 55^{0}C and an extraction time of 120 min produced 82.27% of methyl ester yield.
- The properties of refined biodiesel such as cetane number, kinematic viscosity, Acid value, calorific value after transesterification agrees well with the ASTM standards.
- The biodiesel obtained in this process could be the best suitable alternative fuel for direct injection diesel engines.

REFERENCES

1. Pragnesh N. Dave, International Journal of Chemical Studies, 2321-4902.
2. Controlling and/or using *Prosopis Julifera* in spate irrigation system.
3. "A Technical manual on Managing *prosopis Julifera*", Department or International development, Foretsry Research programme.
4. P. Felker," Review of Applied aspects of *Prosopis*", Center for semi-Arid Forest Resources,Texas A&M University,Kingsville,Texas78363,U.S.A.
5. Deepak Rajagpoal, " Rethinking current strategies for biofuel Production in India".
6. E. Atabani., Non-edible Vegetable Oils: A Critical Evolution of Oil Extraction, Fatty Acid Compositions, Biodiesel Production, Characteristics, Engine Performance and Emission Production. Renewable and Sustainable Energy Reviews 18: (2013); 211-245.
7. Mambully Chandraekaran Gopinathan, Biofuels: Opportunities and Challenges in India, Springer-In vitro cell. Dev. Biol-plant 45 ;(2009):350-371.
8. Palligarnai T. Vasudevan, Bioiesel production-current state of the art and challenges. Springer-J Ind Microbiol Biotechnol 35;(2008):421-430.
9. Bryan R. Moser ,Biodiesel production, properties and feed stocks, Springer-In vitro cell. Dev. Biol-. plant 45; (2009):229-266.
10. Lin Lin., Dong Ying., Sumpun Chaitep., Saritporn Vittayapaung., Biodiesel production from crude rice bran oil and properties as fuel, Applied energy 86;(2009):681-688.
11. A. S. Ramadhas, S. Jayaraj, C. Muraleedharan Biodiesel production from high FFA rubber seed oil, Fuel 84; (2005):335–340.
12. Junhua Zhang , Lifeng Jiang Acid-catalyzed esterification of *Zanthoxylum bungeanum* seed oil with high free fatty acids for biodiesel production, Bioresource Technology 99 ;(2008): 8995–8998.
13. Hanny Johanes Berchmans a, Shizuko Hirata b, Biodiesel production from crude *Jatropha curcas* L. seed oil with a high content of free fatty acids, Bioresource Technology 99; (2008): 1716–1721.
14. V.B. Veljkovic, S. H. Lakic´evic, O.S. Stamenkovic, Z. B. Todorovic, M.L. Lazic Biodiesel production from tobacco (*Nicotiana tabacum* L.) seed oil with a high content of free fatty acids, Fuel 85; (2006): 2671–2675.
15. Shashikant Vilas Ghadge, Hifjur Raheman Biodiesel production from mahua (*Madhuca indica*) oil having high free fatty acids, Biomass and Bioenergy 28;(2005):601–605.
16. gadaravi, J. Nandagopal, P. '. Sathya Selva Bala, S. Sivanesan, sterification of karanja (*Pongamia* high free fatty acids for biodiesel 3;(2012): 1–4.
17. ri, Akhilesh Kumar, Hifjur Raheman tion from jatropha oil (*Jatropha* h free fatty acids: An optimized and Bioenergy 31; (2007):569–575.
18. Rui Wang, Wan-Wei Zhou , Milford A. Hanna , Yu-Ping Zhang , Pinaki S. Bhadury , Yan Wanga, Bao-An Song , Song Yang. Biodiesel preparation, optimization, and fuel properties from non-edible feedstock, *Datura stramonium* L. Fuel 91; (2012): 182–186.
19. Venu Babu Borugadda, Vaibhav V. Goud Biodiesel production from renewable feedstocks: Status and opportunities, Renewable and Sustainable Energy Reviews 16 ;(2012): 4763–4784.
20. B.K. Venkanna, C. Venkataramana Reddy, Biodiesel production and optimization from *Calophyllum inophyllum linn oil* (honne oil) – A three stage method, Bioresource Technology 100 ;(2009): 5122–5125.
21. D.F. Melvin Jose, R. Edwin Raj, B. Durga Prasad, Z. Robert Kennedy, A. Mohammed Ibrahim A multi-variant approach to optimize process parameters for biodiesel extraction from rubber seed oil, Applied Energy 88; (2011):2056–2063.
22. Mehdi Atapour, Hamid-Reza Kariminia, Characterization and transesterification of Iranian bitter almond oil for biodiesel production, Applied Energy 88;(2011):2377–2381.
23. Feng Guo, Zhen Fang , Xiao-Fei Tian, Yun-Duo Long, Li-Qun Jiang, ''One-step production of biodiesel from Jatropha oil with high-acid value in ionic liquids'' Bioresource Technology 140;(2013):447–450.
24. Ivana B. Bankovi´ c´-ll', Olivera S. Stamenkovi´, Vlada B. Veljkovi´, Biodiesel production from non-edible plant oils, Renewable and Sustainable Energy Reviews 16;(2012):3621– 3647.
25. Patil P, Gude VG, Deng S. Biodiesel production from *Jatropha curcas*, waste cooking and *Camelina sativa oils*. Ind Eng Chem Res 48; (2009): 8:10850–6.
26. Tiwari AK, Kumar A, Raheman H. Biodiesel production from jatropha oil (*Jatropha curcas*) with high free fatty acids: an optimized process. Biomass Bioenergy 31 ;(2007):569–75.
27. Naik M, Meher LC, Naik SN, Das LM. Production of biodiesel from high free fatty acid karanja (*Pongamia pinnata*) oil. Biomass Bioenergy 32 ;(2008):354–7.
28. Ghadge SV, Raheman H. Biodiesel production from mahua (*Madhuca indica*) oil having high free fatty acids. Biomass Bioenergy 28 ;(2005):601–5.
29. Mustafa Balat. Potential alternatives to edible oils for biodiesel production – A review of current work. Energy Conversion and Management 52; (2011): 1479–1492.
30. Singh D, Singh SP. Low cost production of ester from non edible oil of *Argemone mexicana*. Biomass Bioenergy 2010; 34:545–9.
31. Phan AN, Phan TM. Biodiesel production from waste cooking oils. Fuel 87 ;(2008):3490–6.
32. Pradip Kumar Biswas, Sanjib Pohit, RajeshKumar. Biodiesel from jatropha: Can India meet the 20% blending target?. Energy Policy 38 ;(2010):1477–1484.
33. Raheman H, Ghadge S V. Performance of diesel engine with biodiesel at varying compression ratio and ignition timing Fuel, 87(12); (2008): 2659–66.
34. Anand K, Sharma R ,Mehta P S. Experimental investigations on combustion, performance and emissions characteristics of neat karanji biodiesel and its methanol blend in a diesel engine. Biomass and Bioenergy 35(1);2011: 533–41.
35. Umar Rashid, Farooq Anwar, Gerhard Knothe. Evalution of biodiesel obtained from cotton seed oil. Fuel processing Technology 90; (2009):1157-1163.
36. Mustafa Balat , Havva Balat. Progress in biodiesel processing. Applied Energy 87 ;(2010): 1815–1835.
37. Mustafa Balat , Havva Balat. Progress in biodiesel processing. Applied Energy 87; (2010): 1815–1835.
38. Parlak A, Karabas H, Ayhan V, Yasar H, Soyhan HS, Ozsert I. Comparison of the variables affecting the yield of tobacco seed oil methyl ester for KOH and NaOH catalysts. Energy Fuels 23 ;(2009):1818–24.
39. Kamath HV, Regupathi I, Saidutta MB. Optimization of two step karanja biodiesel synthesis under microwave irradiation. Fuel Process Technology 92 ;(2011):100–5.
40. Wang R, Hanna MA, Zhou WW, Bhadury PS, Chen Q, Song BA, et al. Production and selected fuel properties of biodiesel from promising non-edible oils: *Euphorbia lathyris* L., *Sapium sebiferum* L. and *Jatropha curcas* L. Bioresour Technol 102;(2011):1194–9.
41. Pinzi S, Garcia IL, Gimenez FJL, Castro MDL, Dorado G, Dorado MP. The ideal vegetable oil-based biodiesel

composition: a review of social, economical and technical implications. Energy & Fuels 23; (2009): 2325–41.
42. Kafuku G, Mbarawa M. Biodiesel production from Croton megalocarpus oil and its process optimization. Fuel 89(9);(2010): 2556–60.
43. Barbosa DC, Serra TM, Meneghetti SMP, Meneghetti MR. Biodiesel production by ethanolysis of mixed castor and soybean oils. Fuel 89 ; (2010): 3791–4.
44. Barbosa DC, Serra TM, Meneghetti SMP, Meneghetti MR. Biodiesel production by ethanolysis of mixed castor and soybean oils. Fuel 89;2010: 3791–4.
45. Nabi MdN, Hustad JE, Kannan D. First generation biodiesel production from non-edible vegetable oil and its effect on diesel emissions. In: Proceedings of the 4th BSME–ASME international conference on thermal engineering, 2008.
46. L. N. Harsh and J. C. Tewari, Prosopis in the arid regions of India: some important aspect of research and development - central Arid Zone research Institute, Jodhpur, India.
47. Saxena, S.K and J. Venkateswaralu, Mesquite: an ideal tree for desert reclamation and fuel wood production 41 ;(1991):15-21.

A TEXT BOOK ON MARINE ENGINEERING

VOLUME - II
(Stability of Ships, Ship Construction, Ship Performance)

With Best wishes
K. R

K. Ramaraj,
B.E (MECH.), M.SC ENGG (MECH), D.M.M, M.E.O.CL.I
Chief Mechanical Engineer (Retrd.), Chennai Port Trust.;
Professor, Marine, Sri Venkateswara College of Engineering, Chennai;
Director, Chidhambaram Institute of Maritime Technology, Chennai;
Professor and Head of the Department, Mohamed Sathak Engineering Colle
Kilakarai, Ramnad.

ESWAR PRESS®
THE SCIENCE & TECHNOLOGY BOOK PUBLISHERS
"Archana Arcade", No. 27, Natesan Street, T.Nagar, Chennai - 600 017, INDIA.
Ph. : 044 - 2432 5902, 4286 7431, 2432 3659
il: yempeyes@gmail.com, eswarpress@airtelmail.in

ESWAR PRESS
"ARCHANA ARCADE",
No. 27, Natesan Street,
T.Nagar, Chennai - 600 017.
Ph. : 044 - 2432 5902, 4286 7431, 2432 3659
E-mail: yempeyes@gmail.com, eswarpress@airtelmail.in

ISBN : 81-7874-099-0

Published by M. Periyasamy for Eswar Press,
No. 27, Natesan Street, T.Nagar, Chennai - 600 017.

Printed by Novena Printers, Chennai.